Cenozoic Geology of Idaho

Editors
Bill Bonnichsen
Roy M. Breckenridge

STATE OF IDAHO

Idaho State Board of Land Commissioners

Governor and President of State Board of Land Commissioners ..... John V. Evans

Secretary of State ..... Pete T. Cenarrusa

Attorney General ..... David H. Leroy

State Auditor ..... Joe R. Williams

State Superintendent of Public Instruction ..... Jerry L. Evans

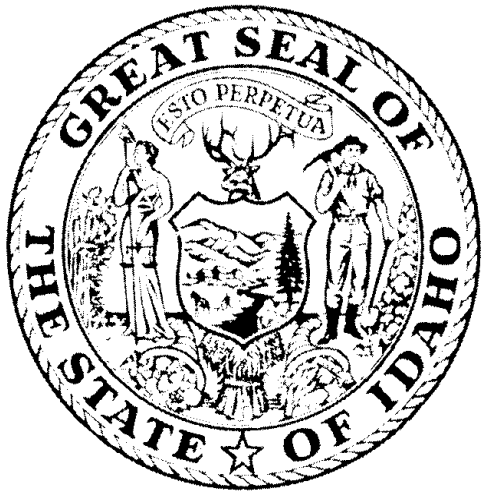

Department of Lands

Director ..... Gordon C. Trombley

Bureau of Mines and Geology

Chief ..... Maynard M. Miller

Publication Staff

Editor ..... Roger C. Stewart

Editorial Assistants ..... Sue Buckle, Pamela Peterson, Serena Smith

Layout ..... Sue Buckle, Pamela Peterson

Typography ..... Idaho Bureau of Printing Services

Cover Design ..... Leo Ames, Creative Director, UI Publications Design

Printer ..... North Country Book Express, Moscow

Cenozoic Geology of Idaho

Cenozoic Geology of Idaho

Edited by
Bill Bonnichsen
Roy M. Breckenridge

The Idaho Bureau of Mines and Geology
will become the Idaho Geological Survey
at the University of Idaho on July 1, 1984

Idaho Department of Lands
Bureau of Mines and Geology
Moscow, Idaho 83843

Contents

Page

Foreword ix

Preface xi

Chapter 1—Challis Volcanic Field, Central Idaho 1

Stratigraphic and Structural Framework of the Challis Volcanics in the Eastern Half of the Challis 1° x 2° Quadrangle, Idaho, by D. H. McIntyre, E. B. Ekren, and R. F. Hardyman 3

Temporal Evolution of the Thunder Mountain Caldera and Related Features, Central Idaho, by B. F. Leonard and R. F. Marvin 23

Early Tertiary-Age Kamiah Volcanics, North-Central Idaho, by R. W. Jones 43

Chapter 2—Columbia River Basalt Group, Western Idaho 53

Columbia River Basalt in Idaho: Physical and Chemical Characteristics, Flow Distribution, and Tectonic Implications, by V. E. Camp, P. R. Hooper, D. A. Swanson, and T. L. Wright 55

Stratigraphy of the Grande Ronde Basalt, Columbia River Basalt Group, From the Lower Salmon River and Northern Hells Canyon Area, Idaho, Oregon, and Washington, by S. P. Reidel 77

Geology and Basalt Stratigraphy of the Weiser Embayment, West-Central Idaho, by J. F. Fitzgerald 103

Structural Model for the Columbia River Basalt Near Riggins, Idaho, by P. R. Hooper 129

Chapter 3—General Features of the Snake River Plain 137

Geophysics and Tectonics of the Snake River Plain, Idaho, by D. R. Mabey 139

Development of the Snake River Plain-Yellowstone Plateau Province, Idaho and Wyoming: An Overview and Petrologic Model, by W. P. Leeman 155

Chapter 4—Volcanic Rock Groups, Snake River Plain 179

Olivine Tholeiitic Basalts of the Snake River Plain, Idaho, by W. P. Leeman 181

Evolved and Hybrid Lavas From the Snake River Plain, Idaho, by W. P. Leeman 193

Rhyolites of the Snake River Plain-Yellowstone Plateau Province, Idaho and Wyoming: A Summary of Petrogenetic Models, by W. P. Leeman 203

Chapter 5—Volcanic Rocks, Snake River Plain and Owyhee Uplands, Southwestern Idaho 213

Cenozoic Stratigraphy of Western Owyhee County, Idaho, by E. B. Ekren, D. H. McIntyre, E. H. Bennett, and R. F. Marvin 215

The Bruneau-Jarbidge Eruptive Center, Southwestern Idaho, by Bill Bonnichsen 237

The Cougar Point Tuff, Southwestern Idaho and Vicinity, by Bill Bonnichsen and G. P. Citron 255

Rhyolite Lava Flows in the Bruneau-Jarbidge Eruptive Center, Southwestern Idaho, by Bill Bonnichsen 283

Pre-Cougar Point Tuff Volcanic Rocks Near the Idaho-Nevada Border, Owyhee County, Idaho, by John Bernt and Bill Bonnichsen 321

Chapter 6—Rhyolitic Volcanism, Eastern Snake River Plain and Vicinity 331

Preliminary Stratigraphic Framework of the Pliocene and Miocene Rhyolite, Eastern Snake River Plain, Idaho, by G. F. Embree, L. A. McBroome, and D. J. Doherty 333

Late Cenozoic Volcanism of the Island Park Area, Eastern Idaho, by R. L. Christiansen 345

Geology of the Magic Reservoir Area, Snake River Plain, Idaho, by W. P. Leeman 369

The Geology and Geothermal Setting of the Magic Reservoir Area, Blaine and Camas Counties, Idaho, by D. W. Struhsacker, P. W. Jewell, Jon Zeisloft, and S. H. Evans, Jr. 377

The Geology of Big Southern Butte, Idaho, by D. B. Spear and J. S. King 395

Chapter 7—Basaltic Volcanism, Eastern Snake River Plain and Vicinity 405

The Style of Basaltic Volcanism in the Eastern Snake River Plain, Idaho, by Ronald Greeley 407

The Great Rift and the Evolution of the Craters of the Moon Lava Field, Idaho, by M. A. Kuntz, D. E. Champion, E. C. Spiker, R. H. Lefebvre, and L. A. McBroome 423

Selected Volcanic Features of the South-Central Snake River Plain, Idaho, by J. S. King 439

Phreatic Eruptions of the Eastern Snake River Plain of Idaho, by M. B. Womer, Ronald Greeley, and J. S. King 453

Mineralogy and Petrology of Tertiary-Quaternary Volcanic Rocks in Caribou County, Idaho, by D. W. Fiesinger, W. D. Perkins, and B. J. Puchy 465

Chapter 8—Stratigraphy and Structural Relationships, Southeastern Idaho 489

Cenozoic Stratigraphy and Tectonic Evolution of the Raft River Basin, Idaho, by P. L. Williams, H. R. Covington, and K. L. Pierce 491

Sequence of Late Cenozoic Deformation in the Blackfoot Mountains, Southeastern Idaho, by R. W. Allmendinger 505

Chapter 9—Stratigraphy of Lacustrine Sediments, Western Snake River Plain 517

Fish Biostratigraphy of Late Miocene to Pleistocene Sediments of the Western Snake River Plain, Idaho, by G. R. Smith, Krystyna Swirydczuk, P. G. Kimmel, and B. H. Wilkinson 519

Volcanic Ash Beds as Stratigraphic Markers in the Glenns Ferry and Chalk Hills Formations From Adrian, Oregon, to Bruneau, Idaho, by Krystyna Swirydczuk, G. P. Larson, and G. R. Smith 543

Stratigraphy, Age, and Tectonic Setting of the Miocene-Pliocene Lacustrine Sediments of the Western Snake River Plain, Oregon and Idaho, by P. G. Kimmel 559

Chapter 10—Stratigraphy and Paleontology, American Falls Area 579

Revised Quaternary Stratigraphy and Chronology in the American Falls Area, Southeastern Idaho, by W. E. Scott, K. L. Pierce, J. P. Bradbury, and R. M. Forester 581

Paleontology of the Lacustrine Member of the American Falls Lake Beds, Southeastern Idaho, by R. C. Bright 597

Chapter 11—Pleistocene Lava Dams and Canyon History 615

The Yahoo Clay, a Lacustrine Unit Impounded by the McKinney Basalt in the Snake River Canyon Near Bliss, Idaho, by H. E. Malde 617

Canyon-Filling Lavas and Lava Dams on the Boise River, Idaho, and Their Significance for Evaluating Downcutting During the Last Two Million Years, by K. A. Howard, J. W. Shervais, and E. H. McKee 629

Chapter 12—Mountain Glaciation 643

Glacial Reconnaissance of the Selway-Bitterroot Wilderness Area, Idaho, by C. M. Dingler and R. M. Breckenridge 645

Glaciation of the Pioneer Mountains: A Proposed Model for Idaho, by E. B. Evenson, J. F. P. Cotter, and J. M. Clinch 653

Chapter 13—Pleistocene Flood Deposits and Gravels 667

Late Cenozoic Gravels in Hells Canyon and the Lewiston Basin, Washington and Idaho, by G. D. Webster, M. J. P. Kuhns, and G. L. Waggoner 669

Pleistocene Episodes of Alluvial-Gravel Deposition, Southeastern Idaho, by K. L. Pierce and W. E. Scott 685

Chapter 14—Loess Deposits, Southeastern Idaho 703

Distribution and Character of Loess and Loess Soils in Southeastern Idaho, by G. C. Lewis and M. A. Fosberg 705

Loess Deposits of Southeastern Idaho: Age and Correlation of the Upper Two Loess Units, by K. L. Pierce, M. A. Fosberg, W. E. Scott, G. C. Lewis, and S. M. Colman 717

Contents by Author

Allmendinger, R. W., 505

Bennett, E. H., 215
Bernt, John, 321
Bonnichsen, Bill, 237, 255, 283, 321
Bradbury, J. P., 581
Breckenridge, R. M., 645
Bright, R. C., 597

Camp, V. E., 55
Champion, D. E., 423
Christiansen, R. L., 345
Citron, G. P., 255
Clinch, J. M., 653
Colman, S. M., 717
Cotter, J. F. P., 653
Covington, H. R., 491

Dingler, C. M., 645
Doherty, D. J., 333

Ekren, E. B., 3, 215
Embree, G. F., 333
Evans, S. H., Jr., 377
Evenson, E. B., 653

Fiesinger, D. W., 465
Fitzgerald, J. F., 103
Forester, R. M., 581
Fosberg, M. A., 705, 717

Greeley, Ronald, 407, 453

Hardyman, R. F., 3
Hooper, P. R., 55, 129
Howard, K. A., 629

Jewell, P. W., 377
Jones, R. W., 43

Kimmel, P. G., 519, 559
King, J. S., 395, 439, 453
Kuhns, M. J. P., 669
Kuntz, M. A., 423

Larson, G. P., 543
Leeman, W. P., 155, 181, 193, 203, 369
Lefebvre, R. H., 423
Leonard, B. F., 23
Lewis, G. C., 705, 717

Mabey, D. R., 139
Malde, H. E., 617
Marvin, R. F., 23, 215
McBroome, L. A., 333, 423
McIntyre, D. H., 3, 215
McKee, E. H., 629

Perkins, W. D., 465
Pierce, K. L., 491, 581, 685, 717
Puchy, B. J., 465

Reidel, S. P., 77

Scott, W. E., 581, 685, 717
Shervais, J. W., 629
Smith, G. R., 519, 543
Spear, D. B., 395
Spiker, E. C., 423
Struhsacker, D. W., 377
Swanson, D. A., 55
Swirydczuk, Krystyna, 519, 543

Waggoner, G. L., 669
Webster, G. D., 669
Wilkinson, B. H., 519
Williams, P. L., 491
Womer, M. B., 453
Wright, T. L., 55

Zeisloft, Jon, 377

FOREWORD

The Idaho Bureau of Mines and Geology by its statutory mission is the lead agency for the coordinated investigation, assembly, and interpretation of scientific information on the geologic resources of the state. This publication on Idaho's Cenozoic geology is the first such comprehensive effort since our agency began in 1919. It brings together a compendium of Tertiary and Quaternary knowledge of significance and value.

The work provides a multidiciplinary view of the dynamic sequence of tectonic, volcanic, geomorphic, hydrologic, glaciologic, and climatic events that have shaped the rock and landform character of this region. Comprising much of the middle and northern Rocky Mountains and extending for nearly 600 miles from its southeast corner to its northwest edge, the state also involves accretionary terranes on a diastrophically active margin of the North American continent. As such it embraces a fugue of endogenetic and exogenetic processes during the Cenozoic Era which are globally significant.

In recent years, Idaho's population has grown rapidly, and the U. S. Census Bureau forecasts a 50 percent increase by the end of the first decade of the twenty-first century. Accompanying this growth, the state's economy is diversifying from one dominated by agriculture, lumbering, and mining to one that includes increased tourism and recreational use of the land, the construction and utilization of facilities for food processing, light manufacturing, high-tech electronics industries, commercially applied scientific research, transportation, and power generation. Accompanying these changes, a leveling off or reduction is possible in the forest products and minerals-based industries; with foreign markets agriculture should expand. Nevertheless all of these enterprises will continue to stress the state's natural resources.

Many of these resources because they involve the soils, lakes and rivers, ground water, rock formations for construction aggregates as well as nonfuel minerals, phosphate ore for fertilizers, recreational areas and wilderness, plus even the cherished open spaces, are all or partly in the geologic realm. Thus the potential for a progressive use of our resources, or for premature destruction or unwitting waste, will be governed by their accurate identification and scientific interpretation. From this then can stem responsible and appropriate planning for wise use, for conservation, and for protection in the interest of coming generations.

In light of these prospects, the importance of this volume is to provide a needed descriptive and scientific background. Specific groups who will draw upon this new geologic knowledge include university and high-school teachers as well as the public at large. There will be value as well to the geologic and allied professions in the state exploring for minerals, energy resources, and construction materials.

The value to agriculture and forest industries is patent, as it is to future urban and rural planners who will strive for balance in the use and conservation of limited ground-water sources, in better control of soil erosion, and in planning and zoning decisions that best fit the geologic framework of the land. This significance is highlighted by the fact that nearly all of Idaho's population resides in or obtains livelihood from areas underlain by volcanic rock and sedimentary formations of Cenozoic Age.

Basic information in this volume will also help in identifying and predicting geologic hazards, such as faults that have the potential for dangerous earthquakes, areas with potential for slope failure, and floods or volcanicity based on previous patterns in recent geologic time. During the Cenozoic Era, Idaho has been repeatedly affected by major climatic changes controlling the character of its water resources, and it has been one of the most active earthquake and volcanic sectors of our Earth.

This volume gives us scientific reasons to suspect that this geologic activity has not diminished over the brief span of man's historic occupation of the state. In fact, much of this book deals directly with the volcanism and tectonism which have occurred in Idaho during the Cenozoic Era.

Not to be taken lightly is the aesthetic value of the book's contents through its contribution to the better understanding of our planet. This is relevant to Idaho's citizens and to visitors interested in knowing how, why, and when the beautiful scenery and other facets of the Gem State's geologic endowment came to be formed. Most of the papers in this volume describe not only the geologic character but also the origin of surface features that form our landscape. Many of the studies relate to areas of great scenic attractiveness visited by large numbers of people each year.

This information will also be significant to the private and public portions of our state's economy. To geologists engaged in further enquiry in the northwestern United States, these ideas and references should be invaluable. This compendium is a baseline of knowledge from which the next generation of geologists can identify new areas of basic and applied scientific enquiry to be pursued for the further betterment of the citizens and economy of Idaho.

The Idaho Bureau of Mines and Geology has a key role to play as a clearinghouse for geologic and mineral resource information for the state. The publication of the *Cenozoic Geology of Idaho* furthers that role and befits our mission within the government of Idaho.

As noted in more detail in the editors' preface, we have benefitted from a large number of excellent professional contributions by geologists of the U. S. Geological Survey and from academic scientists with various university affiliations. The volume is, therefore, a successful product of a major combined effort and represents the best in informal state-federal-university cooperation at the personal and individual scientist level. To each of these authors, we are deeply indebted and grateful.

Our own Idaho Bureau of Mines and Geology staff has gone more than the extra lap to sustain professional quality and to release this information in a timely fashion. To be noted, too, are the considerable financial resources that have been involved in the preparation stages. It is clearly amazing that such an enormous task has been accomplished so well by so few in such a limited time. Particularly to be thanked for extraordinary effort are the two scientific editors, Drs. Bonnichsen and Breckenridge, and our superb and dedicated professional editor, Roger Stewart, together with his proficient editorial staff.

Maynard M. Miller
Chief—Idaho Bureau of Mines and Geology
Dean—College of Mines and Earth Resources,
University of Idaho

PREFACE

The Cenozoic Era was a time of dramatic display of geologic forces. Landscapes and life forms have come and gone in this span of time called "the age of mammals." The *Cenozoic Geology of Idaho* provides a scientific look into the last 65 million years of Earth's history in the area that is now our state. In Idaho, we can trace a nearly complete record of both ordinary and spectacular geologic events right up to the present. Here at the edge of an active continental margin, this land of Idaho has undergone large-scale tectonic uplift and faulting, gigantic volcanic eruptions as large as anywhere on Earth, glaciation of both alpine and continental scale, and two floods unrivaled on this planet. Indeed, some of Idaho's geologic features are being used as analogs to guide investigations into the geologic past of other planets. To study Idaho's young geologic terrane in both a physical and scientific sense is especially exciting.

In recent years Idaho's population has grown rapidly, a trend likely to continue into the next century. An accurate descriptive and interpretive scientific understanding of Idaho's geology is fundamental to making sound decisions for conserving the state's natural resources in the future. Providing this information to the public is an important purpose of this volume. For it, the Idaho Bureau of Mines and Geology has brought together an array of geologic research papers on the Cenozoic Era. Much of Idaho especially the more heavily populated parts of the state, is underlain by geologic formations and materials that had their origin during this portion of geologic time.

We have organized this volume into fourteen chapters on particular aspects of the Cenozoic geology of the state. In general, the papers on volcanism and tectonic events are in the first eight chapters, and the papers on sedimentary materials and geomorphology are in the last six. As a practical function, the chapters are generally arranged in a sequence progressing from papers on older deposits and phenomena at the beginning of the book to papers on younger materials and events in the latter part. Within the chapters where it has been possible, the articles have been arranged from the more general studies to the more specific.

This volume of papers is the outgrowth of numerous geologic research programs in Idaho supported by several sponsors: agencies of the U. S. government, including the U. S. Geological Survey, the Department of Energy, the National Aeronautics and Space Administration, and the National Science Foundation; the University of Idaho and many other colleges and universities around the country; the National Geographic Society; several companies; and the Idaho Bureau of Mines and Geology.

As editors, we take great pleasure in acknowledging our gratitude to the many individuals and organizations whose efforts have contributed to the geological knowledge collected here. First of all we thank the authors for their full cooperation in getting the manuscripts into final edited form and for their patience as the volume progressed through an extensive editorial process before taking its published form. We wish also to express our special appreciation for the fine papers from various scientists with the U. S. Geological Survey, an agency whose research has contributed much over the years to the knowledge of Idaho's geology.

We are indebted to the following individuals for their expertise in anonymously reviewing various manuscripts: Richard W. Allmendinger, Earl H. Bennett, Robert C. Bright, Gary P. Citron, Harry R. Covington, Donald W. Fiesinger, David G. Frey, William B. Hall, Peter R. Hooper, Robert W. Jones, John S. King, Eugene P. Kiver, Mel A. Kuntz, William P. Leeman, Don R. Mabey, Harold E. Malde, Brainerd E. Mears, Jr., Lisa A. McBroome, David H. McIntyre, Steve S. Oriel, Kurt L. Othberg, Kenneth L. Pierce, Susan M. Price, William E. Scott, John A. Sharp, C. Jack Smiley, Gerald R. Smith, Dallas B. Spear, Debra W. Struhsacker, and Paul L. Williams.

We are especially grateful to the publication staff of the Idaho Bureau of Mines and Geology for their diligence and care. Production of the volume was efficiently managed by Roger C. Stewart, the bureau's editor, and he was capably assisted by Susan Buckle. Additional support was provided by Pamela Peterson and Serena Smith. Finally, we would like to express our appreciation to Maynard M. Miller, the chief of the bureau, for his guidance, and to Earl H. Bennett, the associate chief, for his understanding, as other important bureau projects were put aside so that this volume might be completed.

Bill Bonnichsen
Roy M. Breckenridge

Chapter 1

Challis Volcanic Field Central Idaho

Stratigraphic and Structural Framework of the Challis Volcanics in the Eastern Half of the Challis 1° x 2° Quadrangle, Idaho

by

D. H. McIntyre[1], E. B. Ekren[1], and R. F. Hardyman[1]

ABSTRACT

Volcanism in the eastern half of the Challis 1° x 2° quadrangle, Idaho, began about 51 million years ago with voluminous eruptions of intermediate lava from numerous centers and lasted until approximately 40 million years ago. At about 48.4 million years ago, explosive volcanism began in the Van Horn Peak cauldron complex with an eruption of rhyodacite ash-flow tuff, and it continued intermittently until about 45 million years ago, when alkali-rhyolite ash-flow tuffs were erupted from the Twin Peaks caldera, the youngest part of the cauldron complex. The emplacement of small intrusive masses of rhyodacite south of Challis at about 40 million years brought volcanic activity to a close. The volcanic rocks are cut by northwest-trending faults with right-lateral horizontal slip components and by northeast-trending faults with left-lateral slip components. The northeast-trending Custer and Panther Creek grabens were formed during volcanism in the cauldron complex.

INTRODUCTION

The principal aim of this paper is to provide a broad overview of the Challis Volcanics and its structural setting in the eastern half of the Challis 1° x 2° quadrangle, Idaho. Geologic map coverage of the area is not yet complete, but enough is known to draw a fairly clear picture of the regional relations.

The volcanic rocks within the area fall into two categories: The first is the lavas and volcaniclastic rocks of intermediate to mafic composition (rhyodacite to MgO-rich basalt) that are the products of small-volume, chiefly nonexplosive eruptions from numerous widely scattered vents. These eruptions occurred from at least 51 to about 47 million years ago, with one small vent area active as late as 40 million years ago. The aggregate volume is large. These rocks generally correspond to the latite-andesite member of Ross (1937), but some were also included in a unit called basalt by Ross (1937, plate 1). The second category is the rhyolite lavas and domes and the rhyodacitic to alkali rhyolitic ash-flow tuff and tephra derived from a cauldron complex in the northern part of the area from about 48.4 to about 45 million years ago. These rocks occur as intracauldron fill in the northern part of the area and as outflow, both subaqueous and subaerial, in the southern part. In addition, ash-flow tuff and tephra locally are present that were derived from sources west and southeast of the map area. All the tuffaceous rocks and the rhyolite lava were included by Ross (1937) in the Germer Tuffaceous Member and the Yankee Fork Rhyolite Member.

Several reversals of magnetic polarity are recorded by the volcanic rocks. The polarities of several volcanic units are shown in Table 1.

The volcanic rocks are broken by northwest- and northeast-trending faults. Displacements commonly are oblique, with left-lateral horizontal slip components on northeast-trending faults and right-lateral slip components on northwest-trending faults.

INTERMEDIATE AND MAFIC ROCKS

Intermediate and mafic lavas and associated volcaniclastic rocks predominate in the southern part of the area, where they rest upon a rugged, high-relief

[1]U. S. Geological Survey, Denver, Colorado 80225.

McIntyre, D. H., E. B. Ekren, and R. F. Hardyman, 1982, Stratigraphic and structural framework of the Challis Volcanics in the eastern half of the Challis 1° x 2° quadrangle, Idaho, *in* Bill Bonnichsen and R. M. Breckenridge, editors, Cenozoic Geology of Idaho: Idaho Bureau of Mines and Geology Bulletin 26, p. 3-22.

Table 1. Magnetic polarities for several Challis Volcanic stratigraphic units shown in Figure 5. Polarities determined in field with fluxgate magnetometer.

Unit	Magnetic Polarity
Tuff of Red Ridge	Reversed
Tuff of Challis Creek	Normal
Tuff of Table Mountain	Reversed
Tuff of Ninemile Creek	Reversed
Tuff of Pennal Gulch	Reversed
Tuff of Eightmile Creek	Reversed
Tuff of Herd Lake	Reversed
Latite and K-rich andesite lavas	Reversed
Tuff of Ellis Creek	Reversed
Dacite of Anderson Spring	Reversed
Rhyolite of Mill Creek Summit	Reversed
Lavas of Block Creek	Normal
Rhyodacite and K-rich andesite	Normal and reversed
Quartz latite ash-flow tuff in Sage Creek-Jerry Peak area	Normal

surface carved on Precambrian and Paleozoic sedimentary rocks. Locally, the pre-Tertiary rocks were much broken by high-angle faults prior to deposition of the volcanic rocks (Hobbs and others, 1975; Hays and others, 1978; McIntyre and Hobbs, 1978). The volcanic rocks were erupted from numerous centers scattered throughout the area. About a dozen such centers are known or confidently inferred within the map area, and many undoubtedly remain to be discovered (Figure 1). The amount of material erupted from any single center was small in most places. Where mapping has been sufficiently detailed to discriminate between products of adjacent centers, the diameter of each deposit was found to be less than about 8 kilometers. Nevertheless, the total volume of these rocks is large, because of the large area they cover.

Products of all these eruptions vary widely in composition and mineralogy. During the brief eruptive history of a single center, however, there was little variation in composition. The K_2O-SiO_2 variation in these rocks is shown in Figure 2. Table 2 lists analyses for numbered large points on Figure 2; the numbers on Figure 2 refer to correspondingly numbered analyses in Table 2.

The indermediate and mafic rocks are readily divided into two groups on the basis of their appearance: (1) light-colored rocks with prominent phenocrysts of plagioclase, pyroxene, or amphibole and biotite, and (2) dark, crystal-poor, "basaltlike" rocks with phenocrysts of pyroxene or olivine and plagioclase. Chemical analyses show that the light-colored rocks are best called dacite and rhyodacite. The dark "basaltlike" rocks include potassium-rich andesite, andesite, and latite, in addition to minor volumes of MgO-rich basalt and potassium-rich basalt. Comparisons of phenocryst contents with whole-rock chemical analyses show that rock classifications based solely on phenocryst mineralogy are misleading and generate considerable confusion when applied to these rocks.

DACITE AND RHYODACITE

Rocks in this range of composition (Figure 2 and Table 2) form a network of marginally overlapping lava accumulations that surround the many vents in the central part of the area (Figure 1). These accumulations take the form of small stratovolcanoes and dome complexes. Many phenocryst assemblages differ among the accumulations. Intermediate plagioclase, always present, is accompanied by various combinations of mafic phenocrysts including biotite, amphibole, clinopyroxene, orthopyroxene, and altered olivine. Assemblages in apparent equilibrium include (1) plagioclase, amphibole, and minor biotite, and (2) plagioclase, clinopyroxene, orthopyroxene, and biotite. Disequilibrium assemblages are common, most showing a reaction between amphibole and pyroxenes. Some rocks contain minor xenocrystic quartz.

The oldest and the youngest rocks in the area belong to this group of nonexplosive dacite and rhyodacite. The oldest (51.1 million years; Table 3) is a dacite lava; the youngest (39.7 million years; Table 3) is an intrusive rhyodacite. Table 4 compares the major element composition of the 40-million-year-old intrusive rocks with the composition of the older (49 million years) eruptive rocks of the same area. Both sequences of rocks have the same phenocryst assemblage (plagioclase, orthopyroxene, clinopyroxene, biotite), but the younger rocks have slightly higher MgO and CaO contents and lower K_2O contents as would be expected for products of later partial melting of the same parent material that yielded the older rocks.

POTASSIUM-RICH BASALT, ANDESITE, AND MgO-RICH BASALT

Potassium-rich basalt and andesite commonly occur together and are often indistinguishable without chemical analyses. The MgO-rich basalt, a local variant of the potassium-rich basalt, on the other hand, is readily identified in thin section. These three rock types occur most commonly as flows in and east of the Warm Springs Creek graben (Figure 1) and as discordant and concordant intrusive masses farther west; this distribution of extrusive versus intrusive masses is probably a function of depth of erosion.

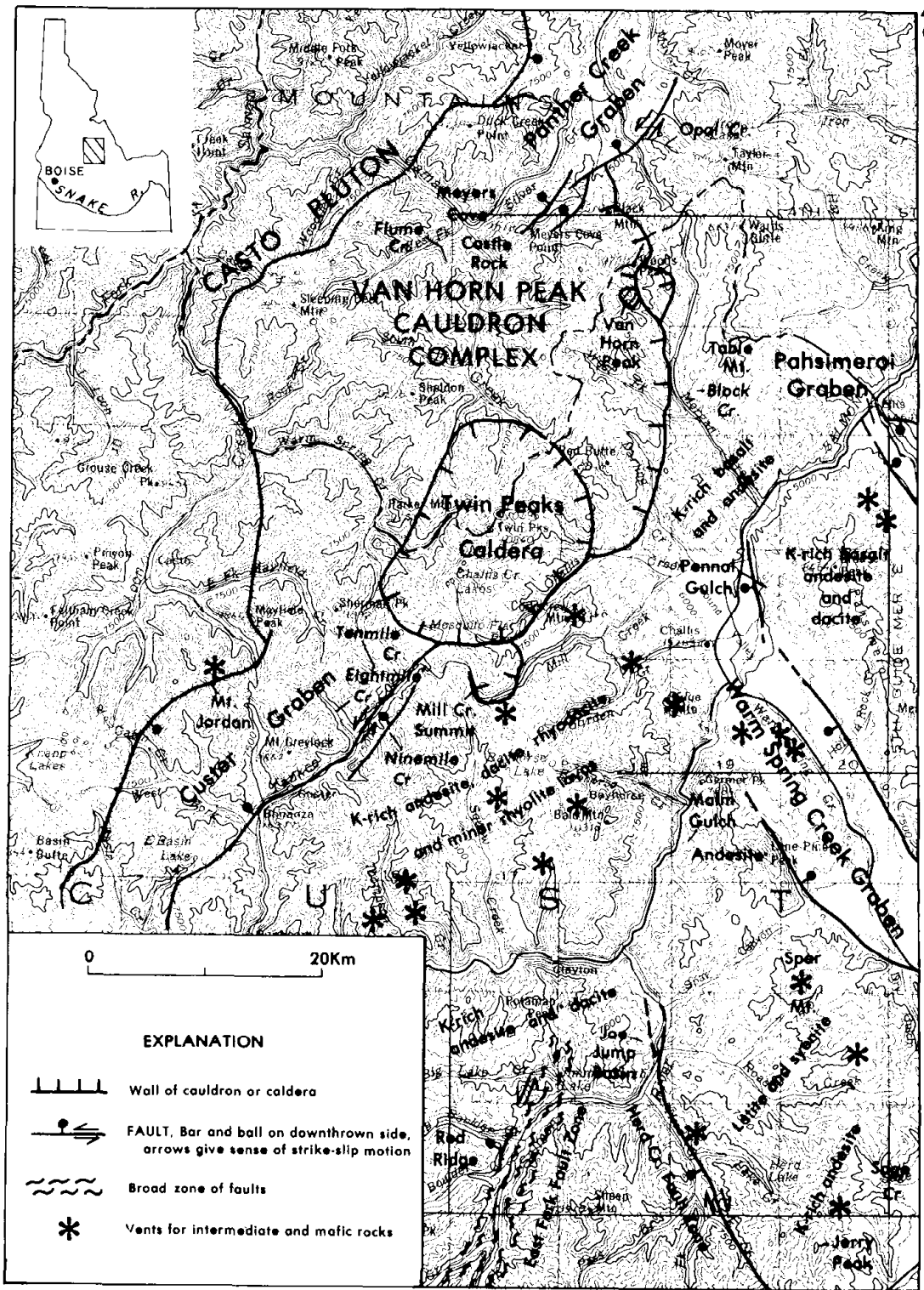

Figure 1. Map showing principal volcanic and tectonic features in eastern half of Challis 1° x 2° quadrangle, Idaho. Lava compositions prevalent in various parts of the area are labeled; other rocks, including pre-Tertiary, are also present in these areas. Data from unpublished mapping by the authors and from Siems and others (1979), Hays and others (1978), Hobbs and others (1975), McIntyre and Hobbs (1978), and F. Foster (unpublished data).

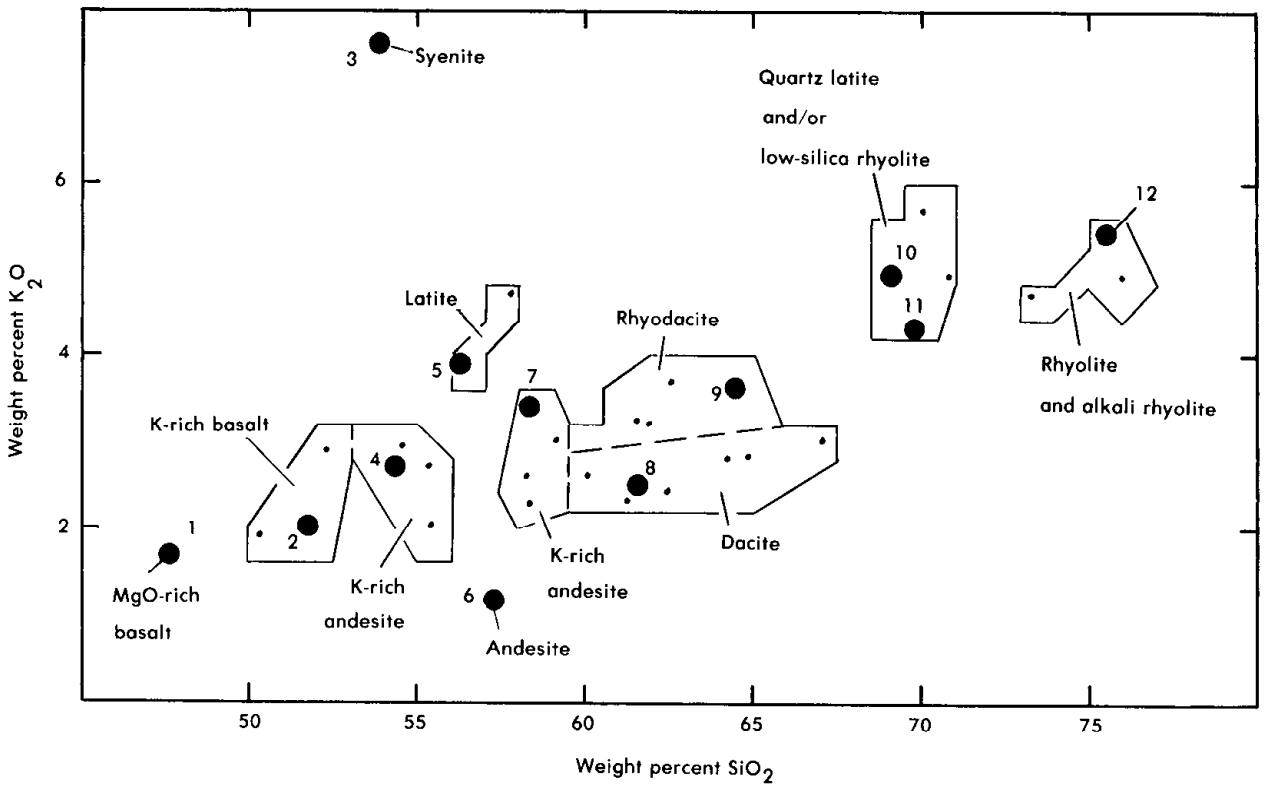

Figure 2. K_2O-SiO_2 diagram for analyses of volcanic rocks from the eastern half of the Challis 1° x 2° quadrangle, Idaho. Many points represent averages of two or more analyses from a single map unit. Numbered points are those for analyses shown in Table 2. Total data set is 61 analyses.

The flows commonly weather brown to reddish brown and are dark gray, greenish gray, and black where fresh. They are crystal-poor rocks containing small phenocrysts of olivine, clinopyroxene, orthopyroxene, and plagioclase in any combination. Orthopyroxene, clinopyroxene, and plagioclase are prominent in some of the potassium-rich andesites, which also locally contain olivine phenocrysts. Quartz xenocrysts with rims of finely granular clinopyroxene or clots consisting entirely of clinopyroxene after quartz are common although minor constituents in some flows. In flows with well-crystallized matrices, minute crystals of brown mica may occur together with the usual plagioclase, clinopyroxene, and opaque oxides. The MgO-rich basalt is characterized by sparse olivine and clinopyroxene microphenocrysts, commonly in a glassy matrix, with little or no plagioclase. These crystal-poor, commonly glassy rocks lack cumulophyric textures.

Most of the intrusive masses west of the Warm Springs Creek graben are clustered in a belt that trends southeastward for about 25 kilometers from Mill Creek Summit. The masses include dikes, plugs, and irregular sills, many of which are bordered by prominent zones of glassy, fused tuff in the vitric tuffs they transect. The mineralogy of these intrusive rocks is identical to that of the flows described above.

The oldest rocks in this group are the 50.3-million-year-old potassium-rich andesite lavas that are intimately associated with rhyodacite lavas south of Challis (Table 3). The bulk of this sequence, however, falls in the approximate age range of 47 to 46 million years. Andesite lavas in this age range that are exposed in the northeastern part of the area rest upon the tuff of Ellis Creek, which has been dated at 48.4 million years (Table 3). These lavas are, in turn, overlain by a sequence of pyroclastic flows capped by the tuff of Challis Creek, which has a potassium-argon age of 45 million years.

The intrusive masses west of Warm Springs Creek graben cut rocks as young as the rhyolite flows at Mill Creek Summit, which have been dated at 48.5 million years. We suspect that this group of intrusive rocks has essentially the same age as the lavas exposed to the east.

LATITE AND SYENITE

Latite lavas, potassium-rich andesite lavas, and a spatially associated intrusive mass of syenite occur in

Table 2. Average chemical analyses (weight percent) and CIPW norms for volcanic rocks in the eastern half of the Challis 1° x 2° quadrangle. [All analyses by U. S. Geological Survey analysts: J. Baker, G. Chloe, P. Elmore, J. Glenn, Z. Hamlin, J. Kelsey, H. Kirshenbaum, P. Klock, B. Lai, H. Moore, H. Smith, J. Taggart, and J. Wahlberg]

	1	2	3	4	5	6	7	8	9	10	11	12
						Chemical analyses						
SiO_2	47.60	52.20	53.85	54.30	56.30	57.20	58.40	61.50	64.50	69.10	69.70	75.55
Al_2O_3	9.30	12.90	16.05	14.00	14.00	16.50	14.90	16.70	15.73	14.30	15.00	12.40
Fe_2O_3	2.20	3.00	3.05	3.50	1.09	3.20	3.20	3.10	1.56	1.30	1.62	1.05
FeO	7.90	4.70	2.50	5.60	5.80	3.05	3.80	1.80	1.52	0.84	1.53	0.52
MgO	17.70	9.80	2.45	6.80	5.51	3.40	3.40	2.10	1.75	0.66	0.55	0.09
CaO	8.70	7.60	4.95	7.30	6.59	6.15	6.20	4.90	3.77	2.20	1.77	0.37
Na_2O	1.30	2.00	2.25	3.10	2.10	3.45	2.40	4.10	2.65	2.85	3.25	3.10
K_2O	1.70	2.90	7.55	2.70	3.88	1.20	3.40	2.50	3.56	4.90	4.34	5.40
H_2O+	0.39	1.20	2.25	1.10	0.73	3.55	0.79	0.80	1.80	1.10	0.70	1.07
H_2O-	0.38	1.30	0.85	0.81	0.67	0.74	1.11	0.81	1.10	1.02	0.43	0.25
TiO_2	0.70	0.83	0.99	1.00	0.80	0.80	0.86	0.56	0.56	0.33	0.39	0.17
P_2O_5	0.26	0.39	0.53	0.39	0.43	0.33	0.36	0.24	0.18	0.11	0.00	0.03
MnO	0.19	0.11	0.11	0.12	0.12	0.10	0.89	0.08	0.83	0.03	0.02	0.02
CO_2	0.82	0.09	2.56	0.08	0.69	0.10	0.01	0.03	0.01	0.00	0.23	0.00
Sum	99.14	99.02	99.94	100.88	98.69	99.77	98.92	99.22	98.70	98.73	99.52	100.01

	1	2	3	4	5	6	7	8	9	10	11	12
						CIPW Norms						
q	0.00	1.35	5.99	2.43	8.07	15.75	14.99	16.20	26.12	29.38	30.32	36.49
c	0.00	0.00	2.45	0.00	0.00	0.00	0.00	0.00	1.16	0.59	2.32	0.87
or	10.21	17.75	46.06	16.13	23.55	7.43	20.70	15.13	21.96	29.97	26.07	32.33
ab	11.18	17.53	19.65	26.52	18.26	30.57	20.93	35.54	23.40	24.96	27.95	26.58
an	14.76	18.29	5.07	16.49	17.80	27.22	20.45	20.26	18.23	10.55	7.42	1.66
di-wo	9.23	7.32	0.00	7.11	3.52	0.76	3.66	1.19	0.00	0.00	0.00	0.00
di-en	6.62	5.48	0.00	4.85	2.06	0.56	2.48	1.02	0.00	0.00	0.00	0.00
di-fs	1.79	1.12	0.00	1.71	1.30	0.12	0.90	0.00	0.00	0.00	0.00	0.00
hy-en	12.16	19.80	6.30	12.27	12.03	8.30	6.25	4.33	4.55	1.69	1.38	0.21
hy-fs	3.28	4.05	0.66	4.32	7.58	1.79	2.27	0.00	0.66	0.00	0.88	0.00
ol-fo	18.24	0.00	0.00	0.00	0.00	0.00	0.00	0.00	0.00	0.00	0.00	0.00
ol-fa	5.42	0.00	0.00	0.00	0.00	0.00	0.00	0.00	0.00	0.00	0.00	0.00
mt	3.24	4.51	4.57	5.13	1.63	4.86	4.78	4.55	2.36	1.91	2.39	1.26
hm	0.00	0.00	0.00	0.00	0.00	0.00	0.00	0.04	0.00	0.03	0.00	0.19
il	1.35	1.63	1.94	1.92	1.56	1.59	1.68	1.09	1.10	0.65	0.75	0.33
ap	0.63	0.96	1.30	0.93	1.03	0.82	0.88	0.58	0.44	0.27	0.00	0.07
cc	1.90	0.21	6.01	0.18	1.61	0.24	0.02	0.07	0.02	0.00	0.53	0.00

1. MgO-rich basalt, 1 analysis.
2. K-rich basalt lava, 2 analyses.
3. Syenite sill, 2 analyses.
4. K-rich andesite flows, interbedded with flows of Table 4, analysis 1, 2 analyses.
5. Latite lavas, 4 analyses.
6. Andesite flows, 2 analyses.
7. K-rich andesite flows of Table Mountain SE of Challis, 3 analyses.
8. Dacite flows NE of Challis, 2 analyses.
9. Tuff of Ellis Creek, 3 analyses.
10. Tuff of Eightmile Creek, 2 analyses.
11. Tuff in Van Horn Peak vent, 2 analyses.
12. Tuff of Challis Creek, 2 analyses.

the southeastern part of the quadrangle (Figure 1). Lavas of similar character may extend as far to the west as the Red Ridge area, but no chemical analyses are available yet to confirm this conjecture. Ross (1937) mapped all these lavas as basalt, justifiably so because there are few clues in outcrop or thin section that indicate their true composition. Most flows are brown and reddish brown, weathering gray to black. For the most part, they contain only sparse phenocrysts of clinopyroxene. Some flows contain minor plagioclase and a few contain olivine phenocrysts. These lavas and associated pyroclastic breccias form an overlapping series of shieldlike accumulations surrounding several vents. Locally exposed thicknesses commonly exceed 400 meters. The youngest lavas in this sequence, exposed at Spar Mountain (Figure 1), are black glassy rocks containing conspicuous altered olivine in addition to clinopyroxene and minor plagioclase. Devitrification produced spherulites as much as 2 centimeters in diameter. The Spar Mountain rocks are markedly more potassic than those lower in the sequence; an average of three K_2O analyses is 4.75 percent.

The syenite, first described by Ross (1937), forms an irregular, sill-like mass, as much as 120 meters thick southeast of Spar Canyon, that intrudes volcanic mudstones, sandstones, and mudflow conglomerates (Hays and others, 1978). Pink alkali feldspar crystals as much as 2 centimeters long, biotite as much as 1 centimeter, and clinopyroxene as much as 5 millimeters are the most conspicuous constituents; chlorite and carbonate locally replace the mafic minerals or occupy voids. Calcite veins several centimeters in width traverse some outcrops. The northeast and southwest margins of the mass are fringed by a dark basaltlike rock that contains altered olivine phenocrysts. Thin sections of this rock show that the altered olivine phenocrysts are set in a fine, holocrystalline groundmass of alkali feldspar and biotite, indicating that this rock is a fine-grained, more mafic marginal variant of the syenite.

No potassium-argon age data are available for these rocks. Biotite in the syenite is sufficiently altered to cast doubt on its suitability for potassium-argon determinations. The latite lavas occupy about the same levels in the regional stratigraphic sequence as the potassium-rich andesite, suggesting that they may be similar in age (48-47 million years).

CAULDRON-RELATED VOLCANIC ROCKS

Cauldron-related activity started with the eruption of the tuff of Ellis Creek about 48.4 million years ago and ended with the ash eruptions and collapse of the Twin Peaks caldera about 45 million years ago. Available potassium-argon ages and stratigraphic relations show that by the time the ash eruptions started the relatively quiescent nonexplosive dacite and rhyodacite outpourings described earlier were on the wane. Eruptions of potassium-rich basalt, an-

Table 3. Potassium-argon ages of volcanic rocks in the eastern half of the Challis 1° x 2° quadrangle. [Data from Armstrong (1975), Marvin and Dobson (1979), McIntyre and others (1976), and R. F. Marvin (written communication, 1980). Ages from Armstrong (1975) recalculated using currently accepted constants: $^{40}K/K_{Total} = 1.167 \times 10^{-4}$; $\lambda_\epsilon = 0.581 \times 10^{-10}$/yr; $\lambda_\beta = 4.962 \times 10^{-10}$/yr (Steiger and Jager, 1977).]

Unit	Rock type	Location		Published age (million years)	Recalculated age (million years)
	Dacite lava	44°24.6′N,	114°23.1′W	49.9±1.7 (biotite)	51.1±1.7
	K-rich andesite lava	44°29′15″N,	114°19′15″W	49.0±1.5 (whole rock)	50.3±1.5
Rhyodacite of Blue Mountain	Rhyodacite lava	44°27′20″N,	114°18′35″W	48.0±1.4 (feldspar)	49.3±1.4
Rhyodacite of upper Second Creek	Rhyodacite lava	44°19′42″N,	114°25′42″W	49.2±1.2 (biotite)	
Block Creek	Rhyodacite lava	44°59′18″N,	114°25′12″W	48.6±1.7 (biotite)	
Rhyolite flows at Mill Creek Summit	Rholite lava	44°27′24″N,	114°29′06″W	48.5±1.2 (biotite)	
Tuff of Ellis Creek	Rhyodacitic ash-flow tuff	44°56′18″N,	114°27′18″W	48.4±1.6 (biotite)	
	K-rich basalt	44°21′30″N,	114°15′30″W	46.9±1.4 (whole rock)	48.2±1.4
Tuff of Eightmile Creek	Quartz latite ash-flow tuff	44°27′54″N,	114°35′14″W	46.9±1.6 (biotite)	
Tuff of Challis Creek	Rhyolitic ash-flow tuff	44°30′30″N,	114°14′05″W	43.8±1.3 (feldspar)	45.0±1.3
	Rhyodacite intrusion	44°26′00″N,	114°11′50″W	38.7±1.2 (plagioclase)	39.7±1.2

Table 4. Chemical analyses (weight percent) and CIPW norms for 49-million-year-old rhyodacite flows and 40-million-year-old rhyodacite intrusions south of Challis. [All norms recalculated to 100 percent, H_2O-free]

	1	2	3	4
Chemical analyses				
SiO_2	61.70	62.40	63.84	63.68
Al_2O_3	15.80	15.50	16.35	15.82
Fe_2O_3	3.40	1.70	0.00	0.00
FeO	1.60	3.30	4.82	4.93
MgO	2.70	3.10	2.79	3.17
CaO	4.50	5.10	4.66	5.20
Na_2O	3.00	3.60	3.10	3.68
K_2O	3.20	2.40	3.31	2.45
H_2O+	2.00	1.80	0.00	0.00
H_2O-	1.60	0.80	0.00	0.00
TiO_2	0.70	0.76	0.72	0.77
P_2O_5	0.32	0.23	0.33	0.23
MnO	0.08	0.07	0.08	0.07
CO_2	0.05	0.04	0.00	0.00
Sum	100.65	100.80	100.00	100.00

	1	2	3	4
CIPW norms				
q	19.96	17.16	16.38	15.13
c	0.10	0.00	0.00	0.00
or	19.48	14.44	19.56	14.48
ab	26.15	31.02	26.23	31.14
an	20.52	19.39	20.92	19.41
di-wo	0.00	1.91	0.02	2.04
di-en	0.00	1.23	0.01	1.00
di-fs	0.00	0.56	0.01	1.00
hy-en	6.93	6.63	6.94	6.89
hy-fs	0.00	3.03	7.80	6.91
mt	3.49	2.51	0.00	0.00
hm	1.09	0.00	0.00	0.00
il	1.37	1.47	1.37	1.46
ap	0.78	0.55	0.78	0.54
cc	0.12	0.09	0.00	0.00

1. 49-million-year-old flows, average of 4 analyses.
2. 40-million-year-old intrusions, average of 3 analyses.
3. Analysis 1 oxides recalculated to 100 percent, volatile-free, with total iron as FeO.
4. Analysis 2 oxides recalculated as in 3 above.

desite, and latite, however, continued well into the period of cauldron-related, ash-flow tuff volcanic activity.

ROCKS OF VAN HORN PEAK CAULDRON COMPLEX

The Van Horn Peak cauldron complex, exclusive of whatever parts were destroyed or obfuscated by the Casto pluton (see discussion in *Tuff of Ellis Creek*), occupies an elliptical subsided area about 34 kilometers by 48 kilometers (22 miles by 30) miles within Figure 1. Van Horn Peak intracauldron rocks are also found west of the Casto pluton, west of the area shown in Figure 1. The cauldron complex, including the youngest major structure of the complex, the Twin Peaks caldera (Hardyman, 1981), is the source of nearly all the ash-flow tuffs exposed in the eastern part of the Challis 1° x 2° quadrangle. The complex is named after Van Horn Peak, a major ash-flow tuff vent on a ring-fracture zone near the northeastern boundary of the complex (Ekren, 1981; Figure 1). We use the term "cauldron complex" to denote a volcanic terrane within which numerous related cauldrons occur. Although the cauldrons originally were basin-shaped topographic depressions (calderas) that were more or less bounded by arcuate faults, subsequent events have greatly modified them. In fact, the cauldron complex, at present, is both structurally and topographically high compared with most of the adjacent outflow terrane.

Most rocks within the cauldron complex have been hydrothermally altered. Many of these altered volcanic rocks were included by Ross (1934) in the unit he named "Casto Volcanics." Geologic mapping and petrographic studies (Rahn, 1979; Wagstaff, 1979; unpublished mapping by the authors, 1979-1981; McIntyre and Foster, 1981) have shown conclusively that all these rocks are part of the Challis Volcanics. We concur with the conclusion of Cater and others (1973) that the term "Casto Volcanics" be abandoned.

Tuff of Ellis Creek

The caldera cycle started with the massive eruptions of the tuff of Ellis Creek. This tuff is known to extend for several kilometers north of 45°00' N. latitude and as far south as 44°20'—a distance of about 80 kilometers. Its extent east to west probably was similar, and these dimensions because of deep post-tuff erosion are minimum values. The westerly extent can never be accurately determined because it has been completely removed by deep erosion.

Outside the cauldron complex, the tuff of Ellis

Creek is a green-gray, densely welded rock that tends to weather to smooth outcrops which deceptively suggest partial welding (Figure 3). The tuff is as much as 400 meters thick near the eastern cauldron boundary from whence it thins gradually eastward. It is as much as 150 meters thick along U. S. Highway 93 near the mouth of Hat Creek (Figure 1) at a distance of about 25 kilometers from the ring-fracture zone, and it probably originally extended several kilometers beyond this point. In this eastern area, however, it probably never constituted a continuous thick prism of tuff because of extremely rugged underlying paleotopography. This paleosurface was developed on a variety of pre-Tertiary and Tertiary strata (McIntyre and Hobbs, 1978). High areas that probably were never blanketed by the tuff existed in close proximity to the cauldron boundary. Within the caldron, the tuff of Ellis Creek is more faulted, sheared, and hydrothermally altered than it is outside; but the consanguinity of the tuffs in the two areas is readily apparent on the basis of characteristics of pumice and other fragments, mineralogy, and color. The tuff is exposed in a broad belt between Duck Creek Point and Sleeping Deer Mountain (Figure 1). In this belt, which lies entirely within the cauldron complex, the tuff is as much as 1,300 meters thick, and where the tuff adjoins the Casto pluton or other intrusive rocks of Tertiary age, the tuff is very dark gray and black. The black color is due to abundant magnetite dust in the groundmass and in the ferromagnesian minerals. The dark tuff weathers massive and closely resembles intrusive rock of dioritic composition. Recent mapping by Ekren and Gordon May (unpublished data, 1981-1982) has shown that dark intracauldron Ellis tuff with the "intrusive dioritic" appearance occurs also on the west side of the Middle Fork of the Salmon River about 20 kilometers west of Middle Fork Peak (Figure 1). The best exposures there are in the vicinity of Shellrock Peak where the tuff adjoins the west flank of the Casto pluton. The tuff (probably at least 60 meters thick near Shellrock Peak) dips toward the west. In contrast, the thick tuff on the east side of the pluton in the belt extending from Duck Creek Point through Sleeping Deer Mountain dips toward the east or southeast. The suggestion is strong, therefore, that the pluton emplaced itself into deeply buried tuffs of the cauldron complex and, in doing so, it arched the tuffs into a broad anticlinorium. The western boundary of the Van Horn Peak cauldron complex filled by Ellis tuff lies just west of Shellrock Peak and is cut there by later cauldrons.

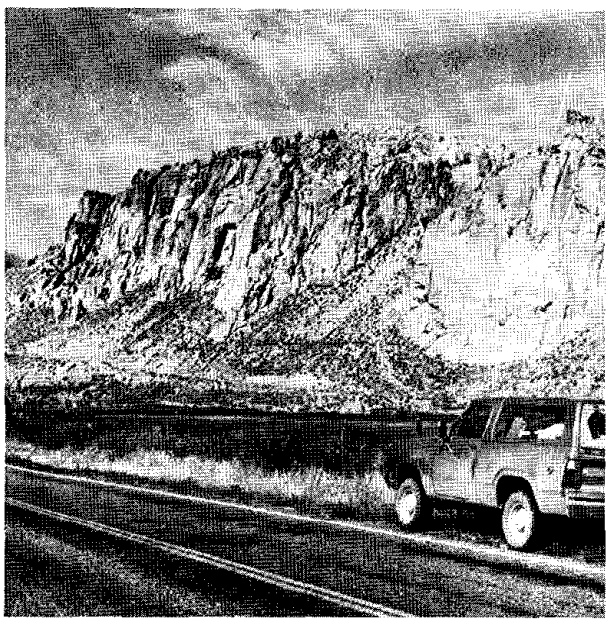

Figure 3. Tuff of Ellis Creek; view to northeast along U. S. Highway 93 north of Ellis, Idaho. In this area the tuff rests on intermediate lava and is overlain by a few tens of meters of tuffaceous sedimentary rocks and a sequence of intermediate lavas.

The presence of a segment of the Van Horn Peak cauldron complex lying west of the Casto pluton indicates that the cauldrons to the east and those to the west of the pluton (Leonard and Marvin, 1982 this volume) are not separate and distinct complexes that, having formed, were then further separated by the emplacement of the Casto pluton. Instead, the Challis Volcanics and volcanic centers in both areas are parts of a single large volcanic field, the central part of which contains numerous cauldrons. If the Casto pluton had not been emplaced, and had the original calderas remained intact without deformation or deep erosion, the vast central part would have resembled a lunar landscape with some craters cross-cutting others. It appears to us, therefore, at this stage of our knowledge that the Van Horn Peak cauldron complex is merely the eastern or southeastern part of the vast cauldron-riddled source terrane of Challis Volcanics, and that the Thunder Mountain caldera and related cauldrons compose the western part of the same source terrane. Without doubt, some cauldrons or cauldron segments await discovery on both sides of the Casto pluton.

The area that subsided or collapsed as a direct result of the eruptions of the tuff of Ellis Creek, which is the most widespread tuff in the Challis Volcanics, is as yet incompletely known. Outcrops of the tuff of Ellis Creek that are 150 meters thick and are at least 25 kilometers from the eastern cauldron rim suggest that the volume of erupted material was enormous. The occurrence of intracauldron tuff of Ellis Creek near Shellrock Peak indicates the possibility exists that a circular cauldron about 60 kilometers in

diameter may have formed as a direct result of the massive eruptions of the tuff of Ellis Creek. For reasons discussed on later pages, this area did not include the grabens at either end of the Van Horn Peak complex (Figure 1).

The tuff of Ellis Creek is a multiple-flow compound cooling unit and is rhyodacite in composition (Table 2). It is characterized by (1) abundant phenocrysts that locally constitute as much as 50 percent of the volume of the rock and (2) abundant mafic phenocrysts consisting of subequal biotite and hornblende that together make up as much as 32 percent of the total phenocrysts. The tuff does not contain alkali feldspar phenocrysts, which distinguish it from the overlying tuff of Eightmile Creek (Table 2) and most of the younger ash-flow tuffs within the cauldron complex. Exclusive of phenocrysts in some cognate and pumice clasts, the plagioclase phenocrysts range in size from about 2 to 5 millimeters; the quartz grains are as much as 4 millimeters or slightly larger in diameter and most show considerable resorption. The plagioclase phenocrysts, where unaltered, show conspicuous oscillatory zoning.

The tuff of Ellis Creek typically contains well-flattened pumice fragments darker than the matrix. These are commonly 3 centimeters long in the outflow tuff and as much as 1 meter long in the intracauldron tuff (Figure 4). The tuff also contains cognate fragments that are not appreciably flattened. These last, which must have been solidified when ejected, together with some typical pumice fragments, commonly contain phenocrysts 1.5 to 3 times larger than those in the enclosing matrix. Both intracauldron and outflow rocks contain these distinctive cognate and pumice clasts.

Although the tuff of Ellis Creek is characterized by pumice fragments darker than the matrix, it does contain layers a few meters to several tens of meters thick in which pumice fragments are lighter than the matrix. There are no obvious mineralogic differences between the light and dark pumice fragments or between the fragments and the matrix, but the light and dark fragments probably came from different parts or levels of the magma chamber.

The tuff of Ellis Creek shows no systematic mineralogic variations from base to top, although zones of bedded tuff and zones of partial welding indicate multiple ash flows and a complex cooling history. Our sampling thus far shows the rock to be rhyodacite throughout. The lack of mineralogic and chemical changes from base to top suggests that the tuff of Ellis Creek, like certain tuffs in Owyhee County (see Ekren and others, 1982 this volume), was erupted from a magma chamber that did not contain a high-silica rhyolite roof zone which appears to characterize high-level magma chambers. The hydrous mafic mineral assemblage of the tuff of Ellis Creek shows, however, that its magma chamber probably was positioned at higher levels of the crust than were the Owyhee chambers. This level was sufficiently shallow so that the partial exhaustion of the Ellis Creek chamber during the early phases of Ellis Creek eruptions was immediately followed by cauldron collapse. Eruptions of the tuff of Ellis Creek continued, however, after collapse began because the tuff is so much thicker within the complex than it is outside. Stated another way, subsidence and tuff eruptions occurred concurrently.

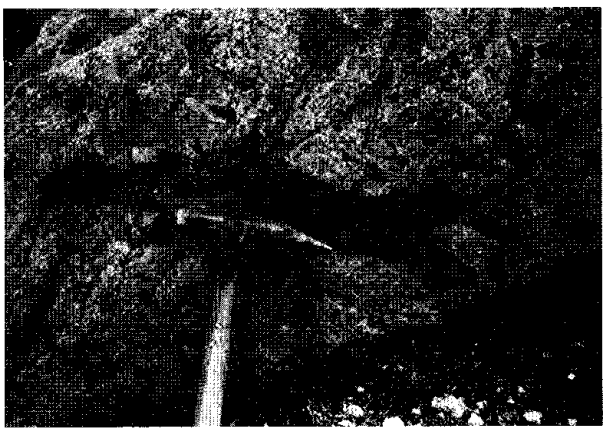

Figure 4. View of large flattened pumice fragment in intracauldron tuff of Ellis Creek near Sleeping Deer Mountain, Idaho.

Tuff of Eightmile Creek

The eruptions of the rhyodacitic tuff of Ellis Creek were followed by the eruption of a quartz latite tuff which has been variously named or mapped but which probably everywhere is the same unit. In the Custer graben it has been called the tuff of Eightmile Creek (Tables 2 and 3 and Figure 5; McIntyre, unpublished mapping, 1976). In the Challis quadrangle (McIntyre and Hobbs, 1978) the unit is thin and discontinuous and was mapped, in places, with the underlying tuff of Ellis Creek, or in other places with the overlying tuff of Pennal Gulch. At Meyers Cove near the northern end of the cauldron complex, the tuff may be about 800 meters thick (Ekren, unpublished mapping, 1979) and was included in the tuff of Camas Creek, unit A by Rahn (1979). In the Meyers Cove area it probably comprises more than one cooling unit as it does in the Custer graben. At Mount Jordan in the Custer graben (Figure 1), the tuff may be as much as 600 meters thick (F. Foster, unpublished mapping, 1980). The large thicknesses at Meyers Cove and Mount Jordan suggest that an elongate area extending from a few kilometers north

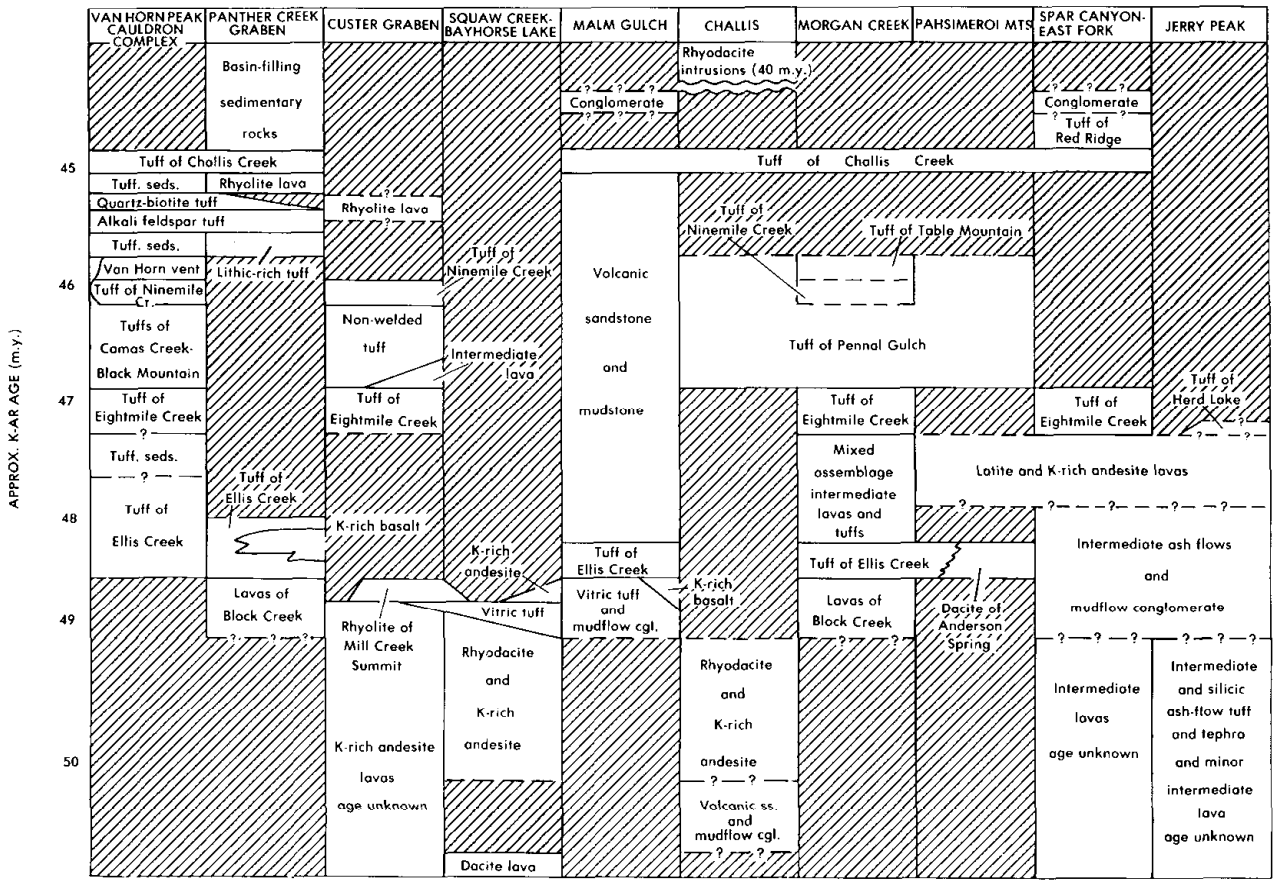

Figure 5. Correlation of principal stratigraphic units, eastern half of Challis 1° x 2° quadrangle, Idaho. [Potassium-argon ages made available after this manuscript was prepared (R. F. Marvin, written communication, February 2, 1982) now provide age control for two units in the Jerry Peak area. Biotite in vitrophyre from the tuff of Herd Lake has an age of 48.1 ± 1.7 million years. Biotite from the unit labelled "intermediate ash flows and mudflow conglomerate" has an age of 49.0 ± 1.8 million years. Hornblende from the same sample has an age of 49.0 ± 2.9 million years. Both stratigraphic units are older than we guessed they might be at the time this figure was constructed.]

of Meyers Cove through the Custer graben probably subsided during the eruption of the tuff. This subsidence may have been a function of both magma withdrawal and concomitant crustal rifting (see discussion in *Rocks and Faults of Custer Graben*).

The tuff is green gray and light gray and, like the tuff of Ellis Creek, contains thick zones in which the pumice is darker than the matrix and thinner zones in which the pumice is lighter than the matrix. The degree of welding varies from very dense with extremely flattened pumice to partial welding with pumice showing only slight flattening. Two thin sections—one from Meyers Cove, the other from Custer graben—each contained nearly 45 percent phenocrysts. The bulk of the rock examined thus far, however, contained fewer than 40 percent phenocrysts. Of these, quartz constitutes from 2 to 22 percent, alkali feldspar from 3 to 25 percent, plagioclase from 35 to 65 percent, and mafic minerals from 10 to 23 percent. The mafic phenocrysts consist of biotite and hornblende in ratios of about 3:1. Sparse clinopyroxene and orthopyroxene that rarely constitute more than 1 percent of the total phenocrysts were observed in the least altered rocks. The pyroxene and most of the biotite and hornblende are altered in exposures on Mount Jordan and at Meyers Cove. The freshest rock in the region occurs near Eightmile Creek and especially around Tenmile Creek where a sample containing fresh biotite yielded a potassium-argon age of 46.9 million years (Table 3). The tuff in nearly all thin sections contains abundant zircon and apatite and trace amounts of allanite.

Tuffs of Camas Creek, Black Mountain, and Pennal Gulch

Several cooling units of ash-flow tuff, exposed in the Meyers Cove area, rest on the tuff of Eightmile Creek and are overlain by tuffs that postdate the

initial collapse of the Van Horn Peak cauldron complex (see discussion in *Rocks and Faults of Panther Creek Graben*). These various cooling units are all genetically related and were included in the tuffs of Camas Creek by Rahn (1979). They correlate outside the cauldron complex with part of the tuff of Pennal Gulch (McIntyre and Hobbs, 1978). We refer to the intracauldron rocks of this suite as the tuffs of Camas Creek-Black Mountain because of the excellent exposures in these two localities, and we continue to refer to the outflow tuffs as the tuff of Pennal Gulch. We do this because most of the tuffs in this suite did not spill over the cauldron rim and have no counterparts in Pennal Gulch or elsewhere outside the complex. Those that did, with a few exceptions, cannot be correlated precisely with their thicker counterparts within the complex. The intracauldron rocks are at least 3,000 meters thick; the outflow units, on the other hand, including interbedded tuffaceous sandstones and ash-fall tuffs between the thin cooling units, exceed about 300 meters in thickness in only a few places.

The intracauldron tuffs are mostly red, red-brown, or reddish gray where hydrothermal alteration is relatively mild. Most of the various cooling units are only a few tens of meters thick and tend to be densely welded. They are separated from each other by thin zones of bedded tuff and sandstone. Some cooling units show zones of weak or moderate welding at their bases in which pumice clasts (mostly darker than the enclosing matrices) show only slight to moderate flattening. These basal zones grade upward within a few meters into rocks in which the pumice is commonly flattened into thin delicate wisps. Such zones are well exposed at Meyers Cove and also on the north face of Black Mountain (Fitzgerald, 1977) where the densely welded rocks are dark brownish gray, dark gray, and in places black. Pumice is extremely obscure in the dark gray and black rocks whose colors in most places are a function of intense silicification and abundant magnetite dust. One or more of these intracauldron tuffs in the Camas Creek and Black Mountain areas is flow layered and easily confused with lavas. Most of the cooling units contain sparse to abundant small volcanic lithic fragments, which are gray and crystal poor. A few fragments are composed of siltstone and quartzite.

Both the intracauldron and outflow tuffs are characterized by small phenocrysts. The most conspicuous of these, plagioclase, averages less than 2 millimeters in length. The amount of phenocrysts is highly variable. Some tuffs (mostly poorly welded) contain as little as 5 percent phenocrysts; others contain as much as 48 percent. Mostly they contain about 20 percent within the cauldron complex and about 10 percent outside where the rocks are weakly welded. Typically these tuffs contain no quartz phenocrysts or only trace amounts. Plagioclase is ubiquitous and exceeds alkali feldspar. The abundance of the latter is extremely erratic. Some cooling units contain none, others trace amounts; and in others, alkali feldspar may constitute as much as 30 percent of the total phenocrysts. The abundance of mafic phenocrysts ranges from about 4 percent to 30 percent of the total phenocrysts. Biotite is nearly ubiquitous and, in a few rocks at or near the base of the sequence, is the sole or principal mafic phenocryst. Hornblende is common but never dominant. Some rocks that crop out both near the base and near the top of the sequence within the cauldron complex contain altered pyroxene as nearly the sole mafic constituent. Pseudomorphs after pyroxene in these rocks include two different combinations of propylitic alteration products, which suggests that two chemically different pyroxenes were originally present.

The distribution and descriptions of the tuff of Pennal Gulch east and southeast of the cauldron complex are shown on the map of McIntyre and Hobbs (1978). The distribution of the tuffs of Camas Creek-Black Mountain within the cauldron complex is not as well known. The thick sequence in the Meyers Cove area (Rahn, 1979) gradually wedges out westward toward Sleeping Deer Mountain (Figure 1), apparently as a result of both internal thinning and deep erosion that preceded the deposition of the overlying quartz-biotite tuff and rhyolitic tuff of Challis Creek (Ekren, unpublished mapping, 1980). The tuff is not present in the Panther Creek graben, which postdates the Camas-Black Mountain sequence.

In the Custer graben a thin cooling unit, which occurs above the tuff of Eightmile Creek, is called informally the tuff of Ninemile Creek (McIntyre, unpublished mapping, 1976). The lithology of this tuff reveals that it is definitely part of the Camas-Black Mountain sequence. Furthermore, this rock can be correlated with reasonable certainty with a cooling unit at Meyers Cove (unit C of Rahn, 1979) and with a cooling unit in the tuff of Pennal Gulch at Table Mountain (Figure 5; McIntyre and Hobbs, 1978).

The caprock at Table Mountain can also be correlated with tuff within the cauldron complex. This caprock is a densely welded ash-flow tuff that was fed from the vent at Van Horn Peak (Figure 6; Ekren, 1981). The rocks in both vent and sheet are distinctive because they contain plagioclase as the sole felsic phenocryst and biotite and altered pyroxene as mafic constituents. The tuff is characterized in the vent and the outflow sheet by delicate fiamme and extremely thin-walled shards.

Figure 6. Van Horn Peak, Idaho, viewed from north. Dark, pluglike mass is densely welded vent tuff that correlates with the tuff of Table Mountain.

ROCKS AND FAULTS OF CUSTER GRABEN

The Custer graben (Figure 1) is a southwest-trending linear depression that formed in response to both crustal rifting and magma withdrawal. Available data suggest that rifting and volcanism began later in the Custer graben than in the adjoining cauldron complex. The Panther Creek graben to the northeast (Figure 1) formed still later.

A potassium-rich andesite lava sequence (andesite of Bonanza Peak of Siems and others, 1979) crops out both within and outside the graben and probably predates graben subsidence. A fault within the graben displaces this andesite at least 750 meters. This displacement probably was greatly exceeded by movement along the graben-bounding faults. The extrusive rocks that are chiefly confined to the graben consist of rhyolite lavas, quartz latitic ash-flow tuff, and tephra.

The oldest rock of the intra-graben sequence is a series of rhyolite lava flows having a minimum thickness of 400 meters. Most of the rhyolites are crystal poor and contain plagioclase, biotite, amphibole, and locally, quartz. Both black vitrophyric and pink, devitrified, finely flow-laminated rocks are present. Lavas of this sequence are exposed for at least 13 kilometers along a southwest trend within the graben. In the Mill Creek Summit area, a quartz-bearing flow unit of local extent is also present. These quartz-bearing rocks yielded a potassium-argon age of 48.5 million years (Table 3).

The previously described tuff of Eightmile Creek overlies the rhyolite lavas. This unit is 200 meters thick in several localities within the graben, and as mentioned earlier, may be 600 meters thick on Mount Jordan (F. Foster, written communication, 1980). It is overlain locally by a thin flow of intermediate lava and in some other local areas by a crystal-poor rhyolite vitrophyre. In most areas, however, the tuff of Eightmile Creek is overlain by crystal-poor, nonwelded tuff as much as 120 meters thick, which in turn is overlain by the previously described tuff of Ninemile Creek, which was recognized at Meyers Cove and beneath the tuff of Table Mountain. The lack of Ellis tuff in the Custer graben indicates that the graben did not form as a result of the voluminous eruptions of Ellis tuff. The lack of Ellis tuff also indicates that the graben did not exist as a topographic low when the Ellis tuff was erupted.

Rocks within the graben are cut by numerous northeast-trending faults in addition to those at its margin. A left-lateral horizontal component of movement is evident on some; the best documented example is one described by Anderson (1949). Many of these faults were invaded by rhyolite dikes, irregular plugs, stocklike masses, and extrusive domes. Several of the rhyolite masses have been fractured by renewed fault movements; these fractured zones were favorable loci for epithermal silver-gold mineralization. The silver-gold mineralization near the southeast graben margin (Lucky Boy, General Custer) is localized by faults and fractures in andesite that forms the roof of a complex intrusion. The intrusion ranges in composition from tonalite to granite (Anderson, 1949; McIntyre, unpublished data).

A few basaltic dikes also are present. At one locality, lat 44°28′23″N., long 114°40′41″W., a composite basalt and rhyolite dike contains a 9-meter-wide zone of mixed basalt and rhyolite. Thin sections show that the two liquids intermingled and thus were injected simultaneously.

ROCKS AND FAULTS OF PANTHER CREEK GRABEN

The Panther Creek graben at the northeastern end of the cauldron complex is a counterpart of the Custer graben, but as mentioned earlier it apparently started to form at a later date than either the Custer graben or the main cauldron complex. This conclusion is based on the fact that the extremely thick intracauldron tuffs of Camas Creek-Black Mountain do not occur in the graben north of the buried north boundary of the main complex (Figure 1). In this part of the graben, tuffs younger than the Camas Creek-Black Mountain sequence rest directly on the tuff of Ellis Creek or on potassium-rich basalt that is intercalated or intruded in the Ellis Creek. Apparently the caldera, whose north boundary is now mostly

hidden, was filled completely with flat-lying Camas Creek-Black Mountain tuffs before the first graben tuffs swept over the area, because there is no angular unconformity between the Camas Creek-Black Mountain rocks and the graben-filling strata near the cauldron wall. If any Camas Creek rocks were emplaced in the graben area, they had been removed by erosion prior to graben development. The present dip of the strata within both the graben and the complex is due to eastward tilting that is probably related to intrusion of the Tertiary Casto pluton. The fact that the youngest strata in the Panther Creek graben dip less steeply than the oldest indicates tilting was contemporaneous with graben development. The graben is actually a tilted block whose bounding faults on the southeast side have great aggregate displacement (probably about 4,000 meters), and whose bounding fault on the northwest side has only a few hundred or a few tens of meters of displacement.

The bounding fault on the west side either merges with the cauldron boundary (Figure 1) or abuts it. The fault does not cut the cauldron wall. The bounding fault on the southeast side, in contrast, cuts the cauldron boundary. This fault zone was locally intruded by crystal-poor, flow-laminated rhyolite. Subsequent fault movements fractured the rhyolite masses, and, like the rhyolite counterparts in the Custer graben, the fractured masses were favorable loci for silver and gold mineralization, in particular at the Singheiser and Rabbits Foot mines.

In addition to the volcanic strata described below, the Panther Creek graben contains a great thickness of postvolcanic, poorly consolidated, poorly sorted conglomerate and tuffaceous sandstone. Much of this material actually slid into place during the evolution of the graben. The material remains unstable, and landslides are commonplace. Some of these slides periodically dam Panther Creek. Locally, the graben-filling material is well stratified, and in places, for example near Moyer Creek (Figure 1), it contains considerable carbonaceous debris. The graben-filling material near Opal Creek and the two forks of Moyer Creek (Figure 1) is mantled with a considerable amount of glacial debris derived from deep valley glaciers that flowed westward from Taylor Mountain. Glacial striae high on the walls of these valleys (E. B. Ekren, unpublished mapping, 1979) suggest an ice thickness that requires an ice cap on Taylor Mountain itself.

The oldest volcanic rocks in the Panther Creek graben consist of rhyodacite lavas that we have correlated mineralogically with the lavas of Block Creek of McIntyre and Hobbs (1978). Biotite from lava at the top of the rhyodacite sequence in the Panther Creek graben yielded a potassium-argon age of 48.6 million years (Table 3). The rhyodacite lava sequence in the Panther Creek graben averages no more than a few tens of meters thick. It rests directly on the Yellowjacket Formation of Proterozoic or Precambrian Y age and is overlain by the tuff of Ellis Creek. The tuff of Ellis Creek, in turn, is overlain by a sequence of quartz latite and rhyolite tuffs that from oldest to youngest include a lithic-rich tuff sequence as much as 300 or 400 meters thick, a flow-layered tuff with conspicuous alkali feldspar phenocrysts that is also 300 or 400 meters thick, a quartz and biotite-rich tuff about 400 meters thick, a flow-layered red rhyolite lava(?), and tuffs related to and including the tuff of Challis Creek.

Lithic-Rich Tuffs

Three or more resistant, mostly vitrophyric, ash-flow tuff cooling units that are characterized by abundant lithic fragments crop out just above the tuff of Ellis Creek or its interfingering potassium-rich basalt for a distance of about 15 kilometers in the western part of the graben. The vitrophyric tuffs pinch out both southward and northward from the central part. The vitrophyric and lithic-rich character of these rocks suggests that they are the distal ends of sheets erupted from sources outside the graben. These sources presumably lay to the west because of a general lack of Tertiary volcanic rocks in terranes east of the graben.

The rocks are densely welded and form distinct hogbacks. Where devitrified, they show stretched, locally lamellar pumice fragments. In vitrophyric parts, the pumice is shiny, black, and well-flattened; the vitric matrix is brown, brownish gray, or reddish gray.

The lithic-rich tuffs are typically crystal-poor rocks containing 2 to 10 percent phenocrysts, which are principally plagioclase less than 2 millimeters long. The basal cooling unit is fairly rich in mafic phenocrysts; the other two contain only trace amounts. Two thin sections of the lowest unit contained 3 percent and 6.5 percent phenocrysts consisting respectively of 73 and 78 percent plagioclase, 10 percent and 18 percent nonpleochroic orthopyroxene, and trace amounts of hornblende, biotite, alkali feldspar, and quartz, in order of decreasing abundance. Magnetite composed 3 percent of the phenocrysts in both thin sections of the lowest unit. The lithic fragments that characterize all three cooling units consist mostly of small (1-4 centimeters) fragments of lava having virtually the same mineralogy as the enclosing tuff. They probably were torn from the walls of the vent during the eruption of the tuffs. Other fragments include crystal-poor tuffs and sparse quartzite and siltite.

Alkali Feldspar Tuff

The alkali feldspar tuff, so called because of its readily visible alkali feldspar phenocrysts, together with the next overlying quartz-biotite tuff forms a distinct hogback above the tuffs of Camas Creek-Black Mountain within the cauldron complex. It forms ledgey outcrops (locally a hogback) for a short distance within the Panther Creek graben where the tuff crops out above the lithic-rich tuffs previously described. The tuff has been mapped from the southern part of the Panther Creek graben southwestward for a distance of about 30 kilometers, nearly to Sleeping Deer Mountain (Figure 1). Throughout this area the tuff occurs in a series of repetitious fault blocks, every block tilted to the southeast and bounded by normal faults that dip toward the northwest.

The alkali feldspar tuff is flow layered from base to top and is another example of ash-flow tuff that coalesced in large part to liquid before final emplacement and cooling (see Ekren and others, 1982 this volume). Shards and pumice are intact, however, in a few scattered localities in the basal vitrophyre, and they also occur in local zones within the devitrified interior of the compound cooling unit. The alkali feldspar tuff is at least 300 meters thick in exposures near Flume Creek between Sleeping Deer Mountain and Meyers Cove (Figure 1). Throughout these exposures it tends to weather platy and hackly because of the pronounced flow layering. In places the devitrified rock is extremely spherulitic, and the basal vitrophyre is everywhere coral pink and perlitic. The rock is hydrothermally altered throughout its area of exposure and varicolored in shades of gray, yellow, pink, and red-brown. It is phenocryst poor; seven thin sections from widely spaced localities contained from 4 to 10 percent crystals. The alkali feldspar is less abundant than plagioclase in all but one thin section, but it is far more conspicuous in outcrop because it escaped intense alteration. The plagioclase, in contrast, in most localities is extremely altered and obscure in hand specimen. The plagioclase makes up 40 to 66 percent of the phenocrysts, alkali feldspar 30 to 55 percent, and altered mafic minerals less than 1 to 10 percent. The preexisting mafic minerals were apparently pyroxene and a trace amount of biotite.

The source of the alkali feldspar, flow-layered tuff probably was the central cauldron complex. The Panther Creek graben was not well expressed at this time, possibly because of basin filling by the lithic-rich tuffs.

Quartz-Biotite Tuff

The quartz-biotite tuff, so called because of its conspicuous quartz and biotite phenocrysts, is distributed farther to the north and west than the alkali feldspar tuff. It extends for a short distance north of the north boundary of the Challis 1° x 2° quadrangle, and it overlaps the alkali feldspar tuff just east of Sleeping Deer Mountain. Like the alkali feldspar tuff, the quartz-biotite tuff probably was erupted from a source within the central cauldron complex.

The quartz-biotite tuff attains its maximum thickness near Flume Creek (Figure 1) within the cauldron complex. In places there and also near lower Silver Creek, the tuff consists of two cooling units that are locally flow layered and flow brecciated. The lowest cooling unit possibly is quite local in areal extent. It is commonly separated from the alkali feldspar tuff by about 20 meters of biotite-rich tuffaceous sandstones and even-bedded lacustrine siltstones and from the overlying cooling unit by a thinner sequence of similar strata. It is thin (30 meters) near the Silver Creek-Camas Creek junction and possibly pinches out both to the north and west.

The quartz-biotite tuff, whether consisting of one or two cooling units, is predominately light gray or light green-gray in its more northern and western exposures. Near Silver Creek and as far to the west as Flume Creek (Figure 1), it is red or reddish brown except where bleached by hydrothermal solutions. Mostly the unit contains pumice fragments darker than the matrix. This is true whether the matrix is light gray or reddish brown. Where the matrix is gray, the fragments commonly are brown or green-brown. The size and character of these well-flattened brown pumice fragments set in a gray matrix are startlingly similar to those in both the tuff of Ellis Creek and the tuffs of Camas Creek-Black Mountain, thereby suggesting a common magmatic source for all these rocks.

The quartz-biotite tuff contains 20 to 38 percent phenocrysts, principally quartz, alkali feldspar, and plagioclase in subequal amounts. These felsic crystals, however, vary considerably in relative abundance; in some outcrops quartz is the most abundant, and in others alkali feldspar or plagioclase is dominant. The quartz is as much as 4 millimeters (in a few places as much as 6 millimeters) in diameter and commonly quite smoky; in places it is as dark as the biotite. Some of the alkali feldspar is chatoyant. Mafic phenocrysts, principally biotite, constitute 4 to 18 percent of the total phenocrysts. Where the mafic content is low, the quartz-biotite tuff is not easily distinguished from the overlying tuff of Challis Creek which in places also contains smoky quartz and chatoyant alkali feldspar. In twenty-three thin sections from outcrops extending from the north border of the quadrangle to Sleeping Deer Mountain (Figure 1), biotite was found to be always dominant, and in

places it is the sole mafic. Hornblende is commonly present and in the more mafic-rich zones constitutes as much as 4 percent of the total phenocrysts. Sparse altered mafic pseudomorphs after pyroxene(?) occur in most rocks.

Quartz and some alkali feldspar phenocrysts are slightly to extensively resorbed. The quartz in some rocks is optically anomalous, having an optic angle of as much as 15 or 20 degrees. Grains yielding the abnormal 2V's are not strained, and they do not show inclusions. Like the tuffs of Camas Creek-Black Mountain, the quartz-biotite tuff contains abundant accessory zircon, and most thin sections contain a few grains of allanite.

Flow-Layered Red Rhyolite

The flow-layered red rhyolite is entirely confined to the Panther Creek graben. It forms a gentle hogback extending from just north of Silver Creek to slightly north of the Challis quadrangle boundary, a distance of about 10 kilometers. No conclusive evidence was found to indicate that this unit is a flow-layered welded tuff. We presume it is rhyolite lava, which in at least one locality consists of two cooling units having the same phenocryst mineralogy. The lower unit is only a few tens of meters thick and sandwiched between two flows of potassium-rich basalt. The lower of the two basalts appears to rest directly on the quartz-biotite tuff. The higher cooling unit of red rhyolite is as much as 400 meters thick.

The rhyolite typically contains 10 percent phenocrysts consisting of 80 to 95 percent euhedral alkali feldspar as long as 6 millimeters, a trace to 3 percent quartz, a trace to 5 percent plagioclase, and 1 to 12 percent pseudomorphs after pyroxene(?). The rock contains flattened vugs that are partly filled with opal and vapor-phase crystals of tridymite and alkali feldspar. The sparse plagioclase phenocrysts in this rhyolite are commonly cloaked with alkali feldspar.

The flow-layered red rhyolite, being confined to the Panther Creek graben, probably was fed from a vent in the graben. The extrusion of this thick and widespread unit (for a lava) was immediately followed by rapid subsidence of the graben as indicated by thick accumulations of bedded tuffs and nonwelded ash-flow tuffs, all of rhyolitic compositions.

Tuff of Challis Creek in the Panther Creek Graben and Northern Cauldron Complex

The tuff of Challis Creek forms conspicuous and in places spectacular outcrops north and west of the caldera source for this unit, the Twin Peaks caldera. At least six cooling units of the tuff of Challis Creek are preserved at and near Castle Rock. The Castle Rock monolith is formed by two thick cooling units of densely welded red tuff that are separated by two, thin units of red tuff. These units overlie a slope-forming nonwelded red tuff that, in turn, overlies the quartz-biotite tuff. The upper, capping tuff of the monolith is overlain by at least one more red cooling unit in exposures east of the monolith. The entire sequence is at least 500 meters thick. The overall phenocryst content ranges from 14 to 20 percent and consists of 24 to 52 percent quartz, 43 to 70 percent alkali feldspar, and a trace to 4 percent of plagioclase. The lower four units at Castle Rock contain sparse flakes of biotite. The upper units appear to contain only clinopyroxene having a small to moderate optic angle and less abundant hypersthene. Quartz grains in all cooling units are bipyramidal and tend to be smokey. Alkali feldspar is weakly to strongly chatoyant in all the cooling units near Castle Rock.

In exposures extending throughout the length of the Panther Creek graben, the occurrences of soft, punky, varicolored ash-flow tuff and associated ash-fall tuff weather to a vast variety of red, orange, and pink hoodoos and monoliths. The punky rock exhibits a mineralogy typical of the tuff of Challis Creek, but it is not clear how the punky units correlate with the cooling units at Castle Rock, nor is it clear how the units at Castle Rock correlate in detail with the rocks exposed in the Twin Peaks caldera.

ROCKS AND GENERALIZED STRUCTURE OF TWIN PEAKS CALDERA

The Twin Peaks caldera is a roughly circular collapse structure about 20 kilometers in diameter (Figure 1) that formed about 45 million years ago as a result of the eruptions of the tuff of Challis Creek (R. F. Hardyman, 1981 and unpublished mapping, 1979-1981). The subsided block consists primarily of two thick, dense, cooling units, each 300 to 400 meters thick, separated by variable thicknesses of nonwelded pyroclastic debris. These two thick cooling units are overlain locally by several thin rhyolite ash-flow tuffs that are nearly confined to the subsided cauldron. The extreme variations in thickness of these units suggest the possible breakup of the initial collapsed block. The outflow sheet is thin, exceeding 30 to 40 meters in only a few places. Erosional remnants of the tuff of Challis Creek are found as far as 40 kilometers from the caldera margins.

The main ring-fracture zone forms a moderately well-defined topographic low around the western and southern boundaries of the caldera. Various intrusive

rocks together with several thick deposits of caldera wall-slump debris are localized along this ring-fracture zone. A latite intrusive mass and accompanying outflow lava form the east margin of the caldera. The northern margin is not well defined topographically but is marked by a series of rhyolite dikes and eroded domes that separate the thick intracaldera tuff of Challis Creek from older volcanic rocks outside the caldera.

The tuff of Challis Creek is alkali rhyolite in composition (Table 2, analysis 12). It is red, reddish brown, and orange (in a few places light gray) and, in most exposures within and outside the caldera, the tuff is densely welded. Like other ash-flow tuffs erupted from the cauldron complex, the tuff of Challis Creek contains zones in which all the pumice clasts (as long as 10 centimeters) are darker than the matrix and other zones in which the clasts are lighter than the matrix. The two principal ash-flow cooling units are not separable solely by mineralogy, although the higher unit tends to have smokier quartz phenocrysts and apparently more conspicuously chatoyant alkali feldspar. Typically, the tuff has from 25 to 35 percent phenocrysts consisting of 29 to 50 percent bipyramidal quartz, 49 to 69 percent alkali feldspar, a trace of plagioclase, and a trace to 2 percent pyroxene—clinopyroxene and subordinate hypersthene. A trace of biotite occurs locally. In most samples the pyroxenes have been destroyed. Most of this destruction probably occurred during the devitrification process and is not due to hydrothermal alteration. Zircon is an abundant accessory, and allanite is fairly common. We have not been able to distinguish the various cooling units on the basis of their mineralogy.

The tuff of Challis Creek is a widespread regional stratigraphic marker, as Figure 5 shows. At Challis, east of Round Valley, and near Grandview Canyon, a single, densely welded cooling unit rests on an irregular erosion surface carved on the underlying tuff of Pennal Gulch. To the southwest, at Joe Jump Basin, a single, densely welded cooling unit, 55 meters thick, is overlain by 90 meters of nonwelded ash-flow tuff with the same phenocryst mineralogy. In Spar Canyon, at least two densely welded cooling units are present, each about 30 meters thick and separated by about 35 meters of nonwelded tuff.

ROCKS FROM SOURCES OUTSIDE THE AREA

Two separate ash-flow tuff sheets in the area that have not been previously discussed were derived from sources outside the area of Figure 1. In addition, a sequence of quartz latitic or rhyolitic ash-flow tuff and tephra, at the base of the local sequence exposed in the southeast corner of the map area, was also derived from a source outside the area.

Tuff of Herd Lake

One of the rhyolitic ash-flow tuff sheets, the tuff of Herd Lake, occurs as erosional remnants capping ridges over an area of about 25 square kilometers in the southeastern part of the area. It locally attains a thickness of about 150 meters near Herd Lake, where it consists of two cooling units. The rock is a low-silica, high-alkali rhyolite containing sparse 1-millimeter phenocrysts of plagioclase, biotite, and clinopyroxene. Most exposures consist of devitrified, red-purple or red-brown, locally lithophysal rock with fine flow laminae; these rocks show no trace of relict pumice or vitroclastic textures. An exposure on the ridge 3.7 kilometers south of Jerry Peak reveals a marginal vitrophyre rich in shards. This exposure, the sheetlike aspect of the deposit, and an iron-titanium oxide equilibration temperature in excess of 1000°C, indicate that the unit was emplaced as a very hot ash flow that coalesced and moved like a lava prior to final chilling.

The distribution of the tuff of Herd Lake and the lack of a possible source within the area of Figure 1 suggest a source toward the southeast, most probably in or near the White Knob Mountains.

The tuff of Herd Lake rests on latite and potassium-rich andesite and probably is older than the tuff of Challis Creek.

Tuff of Red Ridge

A second rhyolitic ash-flow tuff sheet with a source outside the area is exposed principally as erosional remnants on ridgecrests in the area of Big Lake Creek, Boulder Creek, and Red Ridge (Motzer, 1978). Farther east in the Spar Canyon area, discontinuous remnants of the unit occur interbedded with volcanic sandstone, mudstone, and conglomerate, in close association with remnants of the tuff of Challis Creek. The rhyolitic ash-flow tuff, the tuff of Red Ridge, is a grayish purple and reddish brown, crystal-poor, pumice-poor rock as much as 140 meters thick with crystals of anorthoclase, amphibole, and clinopyroxene less than 1 millimeter in size. The shard-rich matrix is readily seen in all samples examined to date. A partial chemical analysis for alkalis and alumina shows that the rock borders on the peralkaline; the agpaitic index is 0.93. No other rock unit so far discovered in the area resembles the tuff of Red Ridge in phenocryst mineralogy or chemistry.

The distribution of the unit and the orientation of flow-deformed lithophysae at one locality near Big Lake Creek indicate a source to the west, most likely

one associated with the Sawtooth pluton. The ash flow probably traveled eastward, skirting the north end of the White Cloud Peaks (concealed beneath explanation on Figure 1) and then moved southward into a depression along their eastern flank.

No potassium-argon age is available for this unit. Its close stratigraphic association with the tuff of Challis Creek suggests that the tuff of Red Ridge is of about the same age or slightly younger, that is, about 45 million years. Potassium-argon ages for the Sawtooth pluton (Armstrong, 1975) are 45.7 million years and 44.9 million years, indicating that an association of the tuff of Red Ridge with the pluton is permitted by available potassium-argon age data.

Tuff Sequence in Sage Creek-Jerry Peak Area

A sequence at least 300 meters thick of dacitic to quartz latitic tuff and tephra is exposed locally beneath the potassium-rich andesite and latite lavas in the southeastern part of the quadrangle. The quartz latitic ash-flow tuffs commonly contain alkali feldspar, plagioclase, and biotite; the dacitic rocks contain only plagioclase. Toward the south, a few thin flows of pyroxene and amphibole-bearing lavas are intercalated within the tuff sequence. Conglomerate rich in cobbles and boulders of gray quartzite underlies these rocks. The entire sequence is extensively broken by faults and distinctly more deformed than the overlying sequence of lavas. The distribution of these rocks suggests that they were erupted from sources southeast of the map area.

YOUNGER GRANITIC INTRUSIVE ROCKS

CASTO PLUTON

The Casto pluton (Cater and others, 1973, p. 26) was intruded into the north-central part of the Challis volcanic field, beginning about 46.6 million years ago (R. F. Marvin, written communication, 1982). The batholith was first mapped and described by Ross (1934) who noted that the principal rock type was pink granite composed of about 28 percent quartz, 48 percent microperthite, 13 percent oligoclase, 7 percent biotite, and 3 percent hornblende. He noted that the quartz content ranged from as little as 10 percent to as much as 50 percent and also that in some rocks hornblende exceeded biotite. Thin sections show that rocks with low quartz and high hornblende contents are adamellites, according to the classification of Johannsen (1948). Although the granite is predominantly pink in color, the freshest rock locally tends to be light gray or light pinkish gray. Quartz in all thin sections examined thus far shows slight to moderate straining.

The Casto pluton "intrudes its own ejecta" as pointed out by Cater and others (1973). The pluton actually occupies the central (axial) part of a northeast-trending regional anticline whose southeastern limb includes the Van Horn Peak cauldron complex and whose northwestern limb includes the Thunder Mountain caldera and associated volcanic fields (Leonard in Cater and others, 1973; Leonard and Marvin, 1982 this volume).

INTRUSIVE PORPHYRIES

Ross (1934, p. 60-63) described various porphyritic rocks that he believed were, in large part, border facies of the "pink granite." In addition to these, in and adjacent to the Challis volcanic field are abundant dikes and irregular-shaped intrusive masses that in aggregate, are comparable in volume to the "pink granite." The most important of these rocks are a "pink porphyry" that is characterized by phenocrysts of smoky quartz and a "gray porphyry" characterized by phenocrysts of euhedral white plagioclase.

Pink Porphyry

The pink porphyry in most localities corresponds to the "pink granophyre" of Ross (1934). The rock typically contains bipyramids of smoky quartz about 4 millimeters in diameter; subequal alkali feldspar and plagioclase as large as 8 millimeters, and sparse flakes of biotite. These phenocrysts are set in a micrographic groundmass that varies in grain size from nearly a graphic texture to one that can be seen only with a petrographic microscope. In a few localities, for example, near the Yellowjacket mine, the pink porphyry is extremely coarse grained, with quartz phenocrysts as large as 1 centimeter, and both alkali feldspar and plagioclase as large as 5 centimeters. A large, single alkali feldspar crystal (sanidine) yielded a potassium-argon age of 44.4 ± 1.0 million years. The pink porphyry everywhere forms discordant intrusive masses.

Gray Porphyry

The gray porphyry contains 35-50 percent phenocrysts of plagioclase as large as 1 centimeter and abundant mafic phenocrysts consisting of varying proportions of pyroxene, hornblende, and biotite. The gray porphyry is everywhere somewhat hydrothermally altered. In contrast to the everywhere

discordant pink porphyry, the gray porphyry is commonly concordant. Several masses of gray porphyry in the central part of the Van Horn Peak cauldron complex north of the Twin Peaks caldera are clearly sill-like and other masses whose bases are not exposed probably resemble laccoliths. The gray porphyry in a few localities contains sparse phenocrysts of quartz.

REGIONAL CENOZOIC STRUCTURE

The pre-Tertiary rocks southeast of the cauldron complex are cut by northwest- and north-trending high-angle faults, many of which do not displace the volcanic rocks (Hobbs and others, 1975; Hays and others, 1978). Several of these faults bound horst blocks of pre-Tertiary rocks that form the positive elements of the rugged topography upon which the volcanic rocks were deposited. This block faulting with a dominant northwest trend appears to be restricted to the areas south and southeast of the cauldron complex. Major postvolcanic movement on the northwest-trending faults produced the Pahsimeroi graben and Warm Springs Creek graben (Antelope Flat-Round Valley graben of Baldwin, 1951, p. 898) and affected other areas of volcanic rocks. Movement on these northwest-trending faults has continued into the Quaternary.

Conspicuous faults of northeast trend, as well as northwest, cut the volcanic rocks in the area southeast of the cauldron complex. Faults of both trends commonly show evidence of lateral or oblique slip. The northwest-trending faults have right-lateral horizontal components of slip, the northeast-trending faults, left-lateral. This pattern is remarkably consistent over the entire area. A well-documented exception is near the mouth of Basin Creek, where faults trending N. 55° E. to N. 70° E. have right-lateral displacement (Choate, 1962; McIntyre, unpublished mapping, 1981).

Within the volcanic rocks of the cauldron complex, in marked contrast to the area to the southeast, the dominant fault trend is northeast. Faulting and graben subsidence were concurrent with volcanism. The northeast-trending Custer and Panther Creek grabens have no pronounced topographic expression today. It does not appear likely that significant postvolcanic subsidence affected the Custer graben; rather, it seems likely that the cessation of subsidence coincided with the cessation of associated volcanism. Evidence cited earlier shows that the Custer graben is older than the Panther Creek graben, which does contain thick basin-filling deposits that postdate the tuff of Challis Creek, indicating that, in the Panther Creek graben, subsidence did continue for a time following volcanism.

The pattern of lateral movement on northwest- and northeast-trending faults suggests a component of north-south compression (Figure 1). Concurrent subsidence of the Panther Creek and Custer grabens suggests a right-lateral couple operating in a north-south direction.

Current earthquake activity reveals that a component of north-south extension is present, at least in the western part of the area. A focal mechanism solution for an earthquake there on September 11, 1963, indicated normal faulting on an east-trending, steep fault plane (Sbar and others, 1972). Thus, the present tectonic regime in the area is different from that during the volcanism, when a component of north-south compression apparently was present. Our mapping has delineated a group of east-trending, high-angle faults in the epicentral area of this earthquake. Obliquely raking slickensides on one exposed fault plane indicate a left-lateral component during some past event.

SUMMARY AND DISCUSSION

Volcanism in the eastern half of the Challis 1° x 2° quadrangle began with the eruption of intermediate lavas over a broad area from numerous vents. This activity, which commenced about 51 million years ago, lasted for roughly 2 million years. Toward the north, the mode of eruption abruptly changed to predominantly explosive, with accompanying cauldron collapse. It should be noted that this change of mode was not accompanied by or a direct consequence of change in bulk magma composition. The first regionally extensive explosive product, the tuff of Ellis Creek, still was of intermediate composition, not greatly different from rhyodacite lavas that had erupted earlier. Subsequent explosive products of the cauldron complex became progressively more silicic and potassic with time, ranging from the initial rhyodacite through quartz latite to rhyolite and finally to alkali rhyolite. This activity took place from 48.4 to 45.0 million years ago.

Cauldron subsidence partly preceded and was then accompanied by the formation of two northeast-trending, linear volcano-tectonic depressions, the Custer graben and the Panther Creek graben, that were the loci of numerous rhyolite intrusions, extrusive domes and flows, and epithermal silver-gold mineralization. The Casto pluton was intruded along the northwest margin of the Panther Creek graben during the formation of the graben and at about the same time as alkali rhyolite was erupted from the

Twin Peaks caldera at the southeast margin of the cauldron complex.

Toward the south, eruption of potassium-rich andesite and latite lavas took place during the time that the cauldron complex was active. The lava eruptions ended sometime before explosive eruptions to the north had ceased.

Small flows of potassium-rich olivine basalt, intercalated throughout the sequence of ash-flow tuffs in the cauldron complex, indicate the constant availability of mafic magma while the more silicic magmas were erupting. In the Custer graben, a composite rhyolite-basalt dike with a broad zone of mixing demonstrates the contemporaneity of the two magmas during the waning phase of activity in that area. A comparable bimodality of composition locally is evident in the older sequence of intermediate lavas where potassium-rich andesite, with phenocrysts of olivine, clinopyroxene, and plagioclase locally accompanied the eruption of rhyodacite. In one place, potassium-rich andesite and rhyodacite lavas from adjacent vents are interbedded, proving that both materials were available at about the same time and place. Both the early intermediate magmas erupted as lavas, and the later, explosively erupted, intermediate to silicic magmas associated with cauldron subsidence probably were produced by partial melting of crustal rocks. The associated more mafic rocks probably are closely related to mantle-derived mafic magmas that rose into the crust and provided the heat that accomplished the melting. The potassium-rich andesites and latites toward the south probably are directly evolved from mantle-derived mafic rocks.

The sequence of events described above is not universal within the Challis volcanic field. The presence of quartz latitic ash-flow tuffs exposed beneath the potassium-rich andesite and latite lavas in the southeast part of the quadrangle shows that an explosive eruption at some center southeast of the map area began with more silicic compositions than those initially available in the Van Horn Peak cauldron complex. The sequence of events deduced for the Thunder Mountain area (Leonard and Marvin, 1982 this volume) differ somewhat from that outlined here. Similar differences in the sequence of volcanic events may become clear elsewhere in the region as more data become available.

ACKNOWLEDGMENTS

Most of the data reported here are the results of the U. S. Geological Survey's Challis CUSMAP and Jerry Peak projects, still in progress, and earlier work from the Challis Volcanics project and the Bayhorse project. We are indebted to many of our Geological Survey colleagues for discussion and support, especially F. S. Fisher, S. W. Hobbs, W. H. Hays, W. E. Hall, B. F. Leonard, R. F. Marvin, and C. M. Tschanz. Various aspects of the geology of the region also have been discussed with H. J. Prostka, P. L. Siems, R. W. Jones, E. H. Bennett, and B. Bonnichsen. We especially appreciate the technical reviews of this paper by F. S. Fisher and B. F. Leonard.

REFERENCES

Anderson, A. L., 1949, Silver-gold deposits of the Yankee Fork district, Custer County, Idaho: Idaho Bureau of Mines and Geology Pamphlet 83, 37 p.

Armstrong, R. L., 1975, The geochronometry of Idaho: Isochron West, no. 14, p. 1-50.

Baldwin, E. M., 1951, Faulting in the Lost River Range area of Idaho: American Journal of Science, v. 249, p. 884-902.

Cater, F. W. and others, 1973, Mineral resources of the Idaho Primitive Area and vicinity, Idaho: U. S. Geological Survey Bulletin 1304, 431 p.

Choate, Raoul, 1962, Geology and ore deposits of the Stanley area: Idaho Bureau of Mines and Geology Pamphlet 126, 121 p.

Ekren, E. B., 1981, Van Horn Peak—a welded tuff vent in central Idaho, *in* Montana Geological Society Field Conference and Symposium Guidebook to Southwest Montana, p. 311-315.

Ekren, E. B., D. H. McIntyre, E. H. Bennett, and R. F. Marvin, 1982, Cenozoic Stratigraphy of western Owyhee County, Idaho, *in* Bill Bonnichsen and R. M. Breckenridge, editors, Cenozoic Geology of Idaho: Idaho Bureau of Mines and Geology Bulletin 26.

Fitzgerald, J. F., 1977, Geology of Woods Peak area, Black Mountain quadrangle, Idaho: University of Idaho M.S. thesis.

Hardyman, R. F., 1981, Twin Peaks Caldera of central Idaho, *in* Montana Geological Society Field Conference and Symposium Guidebook to Southwest Montana, p. 317-322.

Hays, W. H., D. H. McIntyre, and S. W. Hobbs, 1978, Geologic map of the Lone Pine Peak quadrangle, Custer County, Idaho: U. S. Geological Survey Open-File Report 78-1060.

Hobbs, S. W., W. H. Hays, and D. H. McIntyre, 1975, Geologic map of the Clayton quadrangle, Custer County, Idaho: U. S. Geological Survey Open-File Report 75-76.

Johannsen, Albert, 1948, A Descriptive Petrography of the Igneous Rocks: University of Chicago Press, Chicago, 318 p.

Leonard, B. F. and R. F. Marvin, 1982, Temporal evolution of the Thunder Mountain caldera and related features, central Idaho, *in* Bill Bonnichsen and R. M. Breckenridge, editors, Cenozoic Geology of Idaho: Idaho Bureau of Mines and Geology Bulletin 26.

Marvin, R. F. and S. W. Dobson, 1979, Radiometric ages: Compilation B, U. S. Geological Survey: Isochron West, no. 26, p. 3-32.

McIntyre, D. H. and Fess Foster, 1981, Pre-Tertiary volcanic rocks in central Idaho—a reappraisal: Isochron West, no. 30, p. 3.

McIntyre, D. H. and S. W. Hobbs, 1978, Geologic map of the Challis quadrangle, Custer County, Idaho: U. S. Geological Survey Open-File Report 78-1059.

McIntyre, D. H., S. W. Hobbs, R. F. Marvin, and H. H. Mehnert, 1976, Late Cretaceous and Eocene ages for hydrothermal alteration and mineralization, Bayhorse district and vicinity, Custer County, Idaho: Isochron West, no. 16, p. 11-12.

Motzer, W. E., 1978, Volcanic stratigraphy of an area southeast of the White Cloud Peaks, Sawtooth National Recreation Area, Custer County, Idaho: University of Idaho M.S. thesis.

Rahn, J. E., 1979, The geology of the Meyers Cove area, Lemhi County, Idaho: University of Idaho M.S. thesis, 111 p.

Ross, C. P., 1934, Geology and ore deposits of the Casto quadrangle, Idaho: U. S. Geological Survey Bulletin 854, 135 p.

———, 1937, Geology and ore deposits of the Bayhorse region, Custer County, Idaho: U. S. Geological Survey Bulletin 877, 161 p.

Sbar, M. L., M. Barazangi, J. Dorman, C. H. Scholz, and R. B. Smith, 1972, Tectonics of the Intermountain seismic belt, western United States, micro-earthquake seismicity and composite fault plane solutions: Geological Society of America Bulletin, v. 83, p. 13-28.

Siems, P. L., D. F. Albers, R. W. Malloy, V. E. Mitchell, and P. C. Perley, 1979, Uranium potential and geology of the Challis Volcanics of the Basin Creek-Yankee Fork area, Custer County, Idaho: U. S. Departmentof Energy Report GJBX-33(79), 200 p.

Steiger, R. H. and E. Jager, 1977, Subcommission on geochronology: Convention on the use of decay constants in geo- and cosmochronology: Earth and Planetary Science Letters, v. 36, p. 359-362.

Wagstaff, D. A., 1979, The geology of the southwest quarter of the Meyers Cove quadrangle, Lemhi County, Idaho: University of Idaho M.S. thesis, 101 p.

Temporal Evolution of the Thunder Mountain Caldera and Related Features, Central Idaho

by

B. F. Leonard[1] and R. F. Marvin[1]

ABSTRACT

The eruption of latite ash flows 50 million years ago began an episode of volcanic activity that lasted about 7 million years. Ash flows and minor lava flows, first latitic, then rhyolitic, built the Thunder Mountain field of Challis Volcanics to a height of 1,500 meters before subsidence of a nearly circular cauldron block 60-65 kilometers in diameter. Subsidence of the Quartz Creek cauldron, dated at 47 million years, was accompanied by development of the Cougar Basin caldera, within which the Sunnyside rhyolitic ash flow (an informal, locally recognized unit) was erupted from a central vent 46-47 million years ago. The eruption of the Sunnyside rhyolite was attended by development of the Thunder Mountain caldera, to which most of the Sunnyside was confined. The caldera was filled to shallow depth with volcaniclastic sediments containing plant remains of Eocene age. The caldera floor was tilted, perhaps by diapiric(?) emplacement of the Casto pluton about 44 million years ago. A minor vent near the caldera edge spilled latite lava across the tilted caldera floor. The highest latite flow has a date of about 43 million years; younger dates obtained from the flow very likely reflect argon loss from glass. The outpouring of latite lava is the last volcanic event recorded in the caldera. The dates of the earliest intrusives (47-million-year-old dikes of the cauldron margin) and of the latest (37-million-year-old dike of the Little Pistol swarm) indicate that intrusive activity began within the explosive stage of local volcanism and apparently ceased some few million years after extrusion of the youngest lavas of the field. Within this interval, the eastern margin of the cauldron was invaded by the Casto pluton, and myriad small stocks and dikes of rhyolite and latite were emplaced, mainly along the margins of the cauldron and its nested calderas. Twenty-eight new potassium-argon dates document the history summarized here.

[1]U. S. Geological Survey, Denver, Colorado 80225.

INTRODUCTION

The Thunder Mountain caldera is the central feature of an irregular field of Challis Volcanics (Figure 1) that formed during the Eocene at the geographic center of the Idaho batholith. The caldera is old, has been deformed repeatedly almost from its inception to the present, and is virtually indistinguishable topographically from the jumbled fault blocks of the Salmon River Mountains in which it lies. Nevertheless, the caldera has evolved in much the same way as the better exposed and better studied calderas of Oligocene to Pleistocene age in the western United States. We present here a geologic sketch of the local volcanic field and an outline of the temporal evolution of the Thunder Mountain caldera and related features. The main conclusions of this report were given earlier as an abstract (Leonard and Marvin, 1975).

Formality requires the naming of two subsidence features that were glossed over in the abstract. The Thunder Mountain caldera nests within a larger caldera, here named the Cougar Basin caldera (Figure 1). The northern and eastern sectors of the Cougar Basin caldera are hard to reach and poorly known, and our attempts to date the subsidence of the caldera isotopically have been frustrated by the difficulty of preparing suitable mineral separates. For these reasons, the Cougar Basin caldera receives little more than its name in this report. Both calderas are outlined by remnants of their wall rocks, but part of the subcircular outline of the calderas is now masked by a northeast-trending linear structure, too complex to be labeled a medial graben, that passes through the calderas and ends near the north margin of the cauldron. The cauldron—the large volcanic subsidence structure that delimits the Challis Volcanics of the Thunder Mountain field—is here named the Quartz Creek cauldron (Figure 1). The northern sector of the cauldron nearly coincides with the principal trough of the 1,800-gamma contour of the aeromagnetic map of Cater and others (1973, plate 1). The southwest sector coincides approximately with the

Leonard, B. F. and R. F. Marvin, 1982, Temporal evolution of the Thunder Mountain caldera and related features, central Idaho, *in* Bill Bonnichsen and R. M. Breckenridge, editors, Cenozoic Geology of Idaho: Idaho Bureau of Mines and Geology Bulletin 26, p. 23-41.

smoothed 1,600-gamma contour of an aeromagnetic map kindly made available by Don R. Mabey, U. S. Geological Survey.

Principal place names used in the text are shown on published topographic maps of the U. S. Geological Survey, chiefly on the Big Creek and Yellow Pine 15-minute quadrangles and the Challis and Elk City 2-degree quadrangles. The name Land Monument Mesa is not shown on published maps. The name is for the mesa 1.7 kilometers north-northeast of the Dewey mine, Thunder Mountain district. Most of the sample locations (Figure 2) are referred to maps available when the fieldwork was done. Since then, new maps have replaced or supplemented some of the old ones. As anyone who wishes to visit the sample sites will soon find only the newer maps available, the principal changes are noted here. The former 15-minute quadrangles have been subdivided into the Wolf Fang Peak, Big Creek, Edwardsburg, Profile Gap, Yellow Pine, Stibnite, Big Chief Creek, and Chilcoot Peak 7½-minute quadrangles; the Monument, Safety Creek, and Rainbow Peak 7½-minute quadrangles now supplement the 2-degree quadrangles for the area northeast and east of Thunder Mountain. The elevations of sample sites are reported in feet because elevations are so shown on the topographic maps of the region. Horizontal distances have been converted from English to metric units. Plate 1 of Cater and others (1973) shows reconnaissance geologic information for all but the western part of the area treated in our report.

GEOLOGIC SKETCH

The Quartz Creek cauldron that delimits the Thunder Mountain field is crudely circular in plan, 60-65 kilometers in diameter, bounded on the west and northwest by a system of ring faults and an attendant swarm of dikes, and along its eastern sector invaded by the Eocene Casto pluton (Figure 1). Radial faults and subsidiary ring fractures dissect the cauldron block, but their pattern is largely obscured by a host of younger faults produced by regional rotational stress and by recent regional and local subsidence. Within the cauldron block, vertical displacement along major subsidence faults exceeds several kilometers, causing plutonic Precambrian intrusives, low- to high-grade Precambrian metamorphic rocks, and various facies of the Cretaceous Idaho batholith to lie in disarray against one another and against the Challis Volcanics.

The Challis Volcanics of the Thunder Mountain field comprise (1) two units of regional extent, (2) a pyroclastic and volcaniclastic filling unit, confined to the Thunder Mountain caldera and its environs, and (3), as a minor part of the filling unit, late flows confined to the caldera but separated from other components of the caldera filling by an erosion surface of at least local extent.

The units of regional extent are a lower, latitic unit and an upper, rhyolitic unit. Both are largely ash-flow tuffs and their welded equivalents. The lower unit of latite tuff and breccia is 400-500 meters thick. It rests on rocks of the Idaho batholith and older metamorphic complexes, locally contains consolidated mudflow debris rich in blocks of batholithic granodiorite and grus derived therefrom, contains at least two thin flows of latite, and in composition ranges without evident order from latite to quartz latite. The latitic unit is exposed only at the cauldron edge and at the periphery of the main area of Challis Volcanics; its extent throughout the field is conjectural. The upper unit of rhyolite tuff and welded tuff is 1,000-1,100 meters thick. It rests on the latite unit but laps onto the adjacent plutonic and metamorphic terrane. In addition to the predominant rhyolitic pyroclastics, the upper, rhyolitic unit contains one or more thin flows of rhyolite, two or more of andesite, and a few lenses of volcanic sandstone and granodiorite-bearing mudflow debris. The disposition of the two units of regional extent (Figure 1) indicates that they were formed before major subsidence of the cauldron, but the vent or vents from which they issued have not been identified.

The filling unit, confined to the Thunder Mountain caldera and its environs, has three subunits. The lowest is the Sunnyside rhyolite.

The informal name Sunnyside rhyolite is adopted in this report for a subunit of local interest in the Challis Volcanics of the Thunder Mountain field. Mining men and geologists familiar with the Thunder Mountain district customarily use the name Sunnyside rhyolite, and it is appropriate to accede to their custom. The informal name Sunnyside rhyolite corresponds to the equally informal rhyolite of Sunnyside (Leonard, *in* Cater and others, 1973, p. 46) and to the Sunnyside rhyolite crystal tuff, Sunnyside rhyolite tuff, Sunnyside tuff, and Sunnyside welded tuff of Shannon and Reynolds (1975).

The Sunnyside rhyolite is a crystal-rich tuff, evidently the product of a single ash flow more than 200 meters thick, that is dominantly a single cooling unit with local, thin cooling units near the top. The major cooling unit is thought to have a thin, basal vitrophyre (seen only as slivers along faults), a thick medial zone of welded tuff with discontinuous vapor-phase zones near its upper contact, and a capping of nonwelded tuff, perhaps 10-20 meters thick, that thickens northeastward toward the distal end of the flow. The distribution of pumice fragments and biotite flakes in

the Sunnyside rhyolite suggests that the ash flow issued from a vent near Thunder Mountain, at the center of the volcanic field.

Current work by E. B. Ekren and Gordon May (oral communication, 1982) leads them to conclude that the Sunnyside rhyolite of Leonard's usage comprises deposits from two major ash flows, and that multiple cooling units may be present in the lower ash flow. Thus our treatment of the Sunnyside rhyolite in this report may be too simple.

The Sunnyside rhyolite is overlain by the Dewey beds. The informal name Dewey beds is adopted in this report for a subunit of local interest in the Challis Volcanics of the Thunder Mountain field. Mining men and geologists familiar with the Thunder Mountain district customarily use the name Dewey beds, and their name for the subunit is conveniently adoptable here. The name corresponds to the volcaniclastic subunit of Leonard (*in* Cater and others, 1973) and to the Dewey beds, Dewey conglomerate, Dewey conglomerates, Dewey strata, Dewey unit, Dewey volcaniclastic beds, and Dewey volcaniclastics of Shannon and Reynolds (1975).

The Dewey beds consist of water-laid volcanic conglomerate, volcanic sandstone, mudstone, carbonaceous shale, a little lignite, and at one place lake beds of laminated carbonaceous mudstone and airfall(?) tuff. This largely volcaniclastic subunit, rich in material eroded from the Sunnyside rhyolite, is well exposed only at the Dewey mine, where its drilled thickness exceeds 90 meters. The outcrop, near site 5 of Figure 2, is too small to show on Figure 1. Fragmentary plant fossils from the volcaniclastic subunit are Eocene (J. A. Wolfe, written communication, 1967; oral communication, 1968, 1981). Associated with the volcaniclastic rocks is a black, carbonaceous breccia of uncertain stratigraphic position and irregular distribution, interpreted as ancient mudflow debris. Carbonaceous mudstone, perhaps representing an ancient swamp deposit, was exposed by mining in 1981, after fieldwork for this report was finished.

An angular unconformity of a few degrees separates the Dewey beds from a pair of thin, vesicular-topped, anomalously young-looking latite flows derived from a small volcanic center within the caldera at Lookout Mountain, 10 kilometers northeast of Thunder Mountain. The flows are indicated on Figure 1 as flows of Lookout Mountain.

The part of the filling unit below the latite flows is economically significant, for the upper part of the Sunnyside rhyolite, undetermined parts of the Dewey beds, and some of the black breccia contain the low-grade gold deposits of the Sunnyside and Dewey mines (Leonard, *in* Cater and others, 1973, p. 45-52).

Much younger than the Tertiary filling unit is water-laid Pleistocene gravel that may once have formed a thin veneer on the southern half of the caldera floor. The gravel is now found only as relics along minor faults that dissect the complex graben of the Thunder Mountain district.

Deposition of the gravel marked the end of the caldera as a topographic depression. Most of the former sump is now a high, rolling upland, a few hundred meters lower than the fringing alpine peaks and mostly separated from them by canyons formed in narrow grabens. The caldera floor is perched 1,500 meters above the main drainage from the Thunder Mountain district.

Tertiary intrusives of the area comprise dikes, stocks, and a plutonic mass of batholithic dimensions—the Casto pluton—which dominates the southeast sector of the cauldron. The dikes range in width from less than 1 meter to more than 100 meters, and in length from a few meters to more than 1 kilometer. Most of the dikes stand vertically. They are dominantly rhyolitic or latitic in composition, and commonly they are porphyritic, but their fabric varies widely. The dikes, if counted, would surely number several thousand, most of them concentrated in swarms, and most of them external to the two calderas. Two swarms, Smith Creek and Little Pistol, are labeled on Figure 1, but they are merely parts of larger arrays of dikes that extend beyond the limits of the illustration. Locally within these swarms the dikes lie side by side, without intervening relics of country rock, yet no dike is seen to cut its neighbors.

A few stocks are present within the dike swarms, but many more are clustered within the Challis Volcanics between the margins of the Thunder Mountain and Cougar Basin calderas, at sites 12 kilometers southwest and 15 kilometers northeast of Thunder Mountain (Figure 1). The stocks are nonequant in shape, seldom more than a few hundred meters in mean diameter, variable in fabric, commonly fault bounded, locally riddled by dikes, and—like the dikes—dominantly rhyolitic or latitic in composition. A few stocks, dikes, and less simple intrusives are dioritic or quartz dioritic.

The dikes, stocks, and pluton are related to structural settings or events in ways that make it desirable to treat the intrusives individually or as geographic and chronologic groups, according to the problems they present rather than as the class of all intrusives.

Two great silicified zones within the cauldron block but outside the Cougar Basin caldera contain many of the gold, silver, antimony, and tungsten deposits of the region. The silicified zones are some kilometers long and tens or hundreds of meters wide. The western zone is in part coextensive with the Smith Creek dike swarm and in part peripheral to the western margin of the cauldron. The eastern zone is

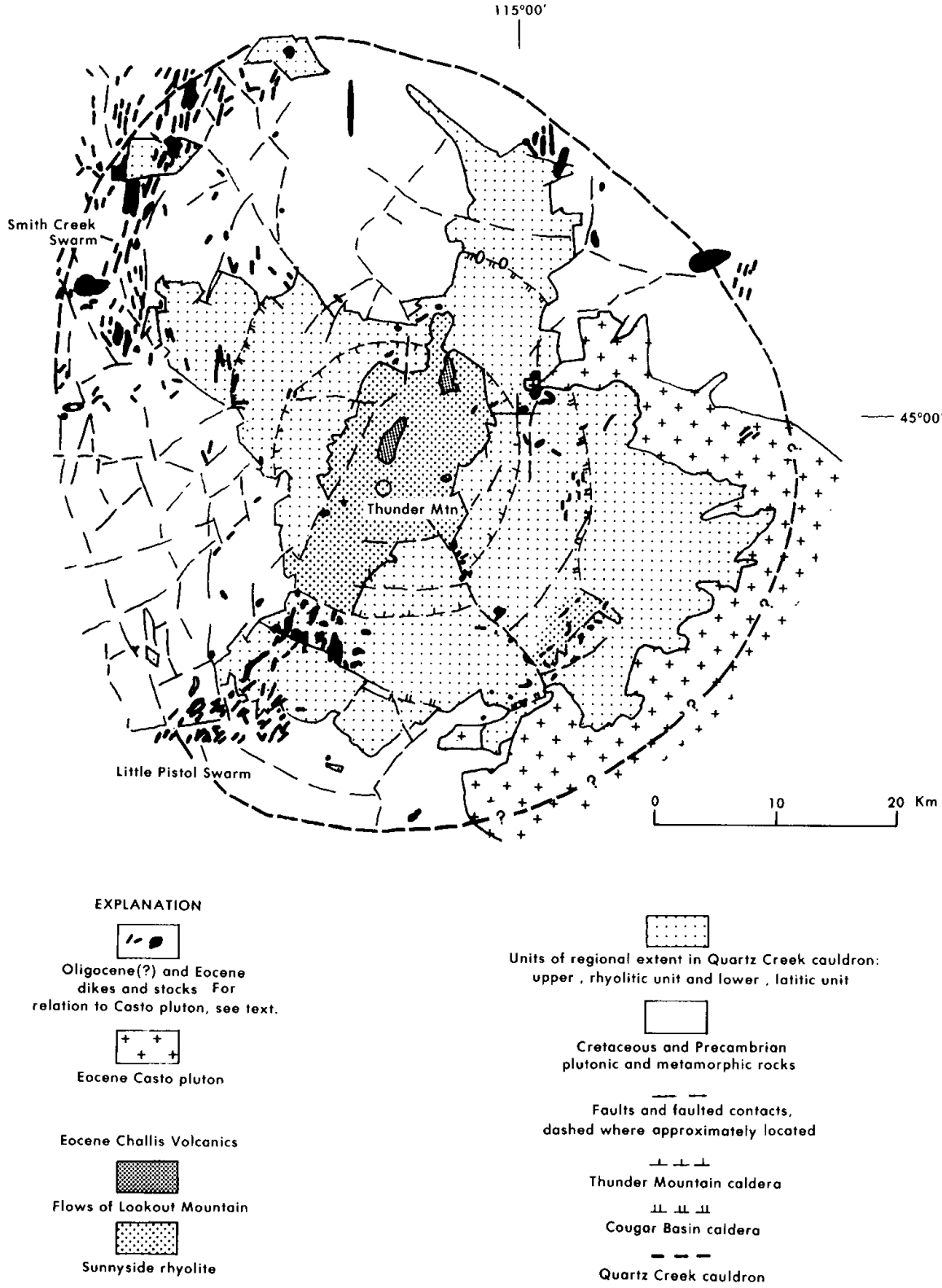

Figure 1. Geologic sketch of Thunder Mountain caldera and related features. Compiled by B. F. Leonard from mapping at various scales by Cater and others (1973, plate 1), B. F. Leonard (unpublished), and J. G. Brophy and Gordon May (unpublished).

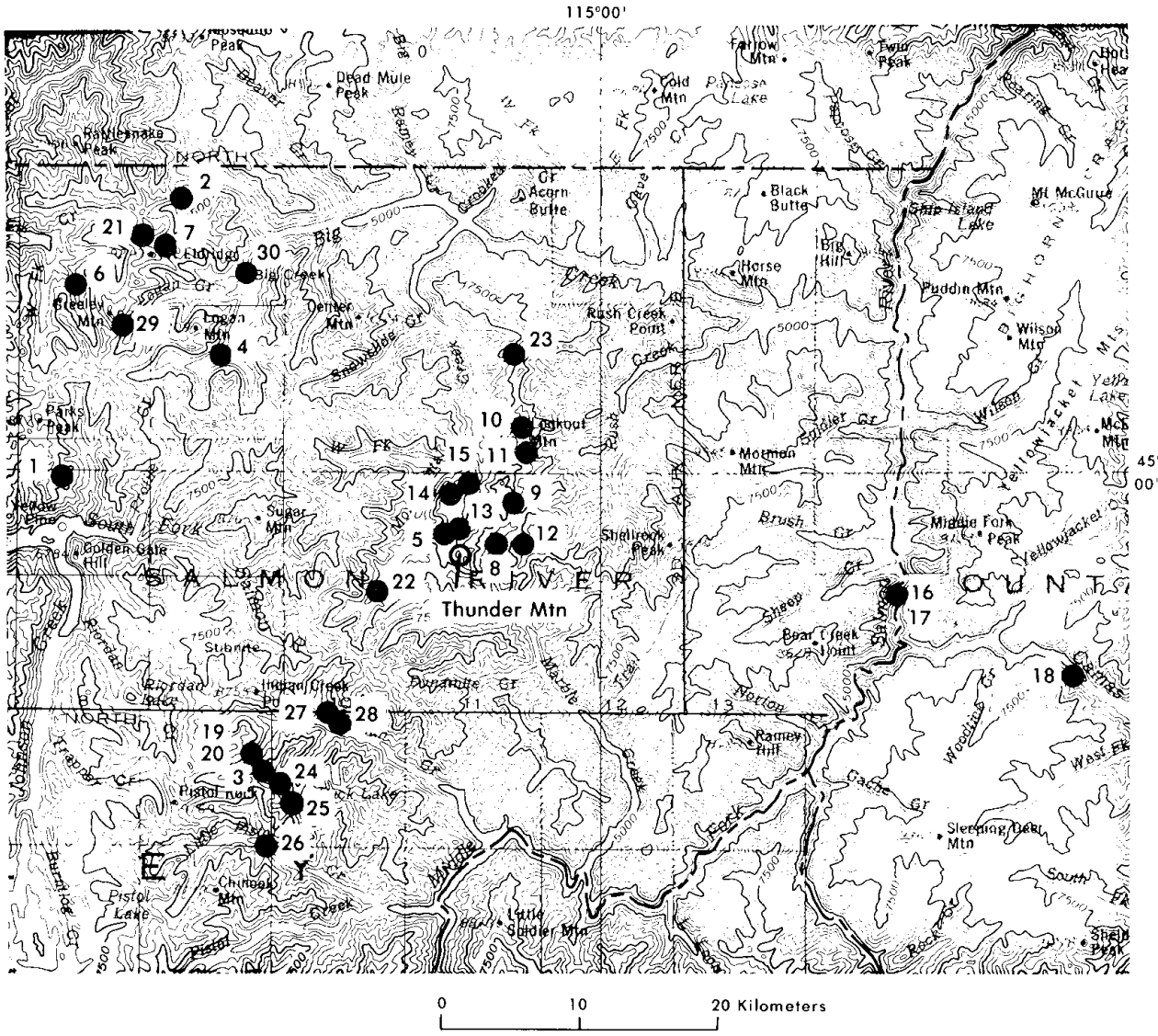

Figure 2. Location of samples. Base from topographic map of the state of Idaho, U. S. Geological Survey, scale 1:500,000.

associated with ring fractures of the Cougar Basin caldera (see subsequent discussion of the stocks of upper Indian Creek). The silicified zones and their mineral deposits receive scant attention in this report because they have not been adequately dated.

DATING OF VOLCANIC FEATURES

The radiometric dates of thirty samples, including two dates from the literature, are given in Tables 1 and 2 and discussed according to geologic occurrence. The radiometric dates approximately fix the main stages of cauldron and caldera development and attendant intrusive activity. There are still too few dates, because rock minerals well suited for dating are sparse. Some dates are anomalous.

PRESUBSIDENCE STAGE

Lower, Latitic Unit

Samples 1 and 2 (Table 1) are from the lowest part of the latitic unit. Sample 1, from welded tuff that rests on granodiorite of the Idaho batholith at the west edge of the cauldron, was collected within a few meters of the contact. The rock is unusual in having a little phenocrystic sanidine (8.84 weight percent K_2O)

Table 1. Potassium-argon dates of Challis Volcanics and Tertiary intrusives of the Quartz Creek cauldron and Thunder Mountain caldera. [Calculated according to decay constants recommended by Steiger and Jager (1977).]

Sample Number	Rock unit	Rock type	Date, million years ± 2σ				
			biotite	hornblende	plagioclase	sanidine	whole rock
		Presubsidence stage of cauldron					
	Challis Volcanics						
1	Lower, latitic unit	Latite tuff, welded			47.1±5.6	50.8±1.7	
2	do.	do.			50.3±3.1		46.4±1.5
3	do.	Latite, amygdaloidal		72.4±12.8	43.5±3.0		
4	do.	Augite-hornblende latite		48.3±2.8			43.3±1.4
5	?	Rhyolite tuff, welded					50.3±2.0
		Subsidence stage of cauldron					
6	Dike, cauldron margin	Quartz diorite	47.1±1.6				
7	Dike, outer ring-fracture zone	Hornblende latite		47.3±1.3			
		Caldera filling stage					
	Challis Volcanics						
8	Sunnyside rhyolite	Rhyolite tuff, nonwelded				46.3±1.0	
9	do.	Rhyolite tuff, welded	47.7±1.6			46.3±1.1	
10	Flows of Lookout Mountain	Latite					43.4±1.4
11	do.	Latite					41.0±1.4
[For numbers 12, 13, 14, and 15, see Table 2]							
		Intrusives, mainly of postsubsidence stage					
	Casto pluton						
16	Core	Granite	47.8±1.9				
17	do.	Granite	43.8±2.8				
18	Roof facies	Granite, miarolitic	[1]41.6±1.8				
	Upper Indian Creek stocks						
19	Stock	Granite porphyry, miarolitic				46.9±1.6	
20	do.	Quartz diorite		44.4±1.8			
	Profile-Smith Creek swarm						
21	Dike	Rhyolite, granophyric				45.7±1.6	
	Stocks in and near Thunder Mountain caldera						
22	Century Creek stock	Rhyolite				44.6±1.5	
23	Paint Creek stock	Rhyolite, feldspathized	47.1±1.6				
	Little Pistol swarm						
24	Dike	Rhyolite				45.2±1.5	
25	do.	do.				42.4±1.5	
26	do.	Hornblende latite		36.7±1.5			
	Middle Indian Creek stocks						
27	Stock	Rhyolite, miarolitic					[2]39.8±0.9
28	do.	Rhyolite				[3]41.1±0.9	
	Logan Creek stock						
29	Stock	Granite, miarolitic	38.7±1.3				
	Dike, The Hogback						
30	Dike	Rhyolite	20.7±0.7			46.3±1.1	

[1]Mostly septechlorite
[2]Groundmass
[3]Nearly pure potassium feldspar

Table 1. continued.

Sample Number	Field Number	Laboratory Number	Location
1	L-73-1	D2364	Summit of Van Meter Hill, Elev. 8,119 ft, SW¼ sec. 9, T. 19 N., R. 8 E., Yellow Pine 15-min quadrangle, Valley County, Idaho. 45°00′ N., 115°30′ W.
2	L-73-5	D2366	Lip of block stream northwest of Smith Creek, 0.8 km N. 45° W. of BM 6681, Big Creek 15-min quadrangle, Valley County, Idaho. 45°11′ N., 115°23′ W.
3	L-72-2	D2363	Hump 8052, Big Baldy Ridge, north of Springfield Creek, Yellow Pine 15-min quadrangle, Valley County, Idaho. 44°48′ N., 115°20′ W.
4	L-73-2	D2365	Knoll 150 m northwest of culvert of Big Creek stream, NW¼ sec. 15, T. 20 N., R. 9 E., Big Creek 15-min quadrangle, Valley County, Idaho.
5	--	R0411	Near Dewey mine, Thunder Mountain district, Valley County, Idaho. Dated by Geochron Laboratories (Axelrod, 1966, p. 499).
6	L-73-19	D2933	Talus, 150 m southwest of trail ford near Elev. 6,200 ft, South Fork of Elk Creek, Big Creek 15-min quadrangle, Valley County, Idaho. 45°07.2′ N., 115°29.2′ W.
7	L-71-4	D2234	Elk Summit road, near head of South Fork Smith Creek, Elev. 7,825, 107 m east of creek, Big Creek 15-min quadrangle, Valley County, Idaho. 45°08.5′ N., 115°24′ W.
8	TM-71-2	D2235	East side of Marble Creek, ~300 m southeast of ruins of Belleco mill, Thunder Mountain district, Safety Creek quadrangle, Valley County, Idaho. 44°52′ N., 115°02′ W.
9	L-74-7	D2934	Lookout Mountain Ridge, Elev. ~8,000 ft, 0.5 km southwest of junction of Lookout Mountain and Holy Terror Creek trails, Safety Creek quadrangle, Valley County, Idaho. 44°58.9′ N., 115°05.0′ W.
10	L-74-5	D2410	180 m south-southwest of Lookout Mountain lookout, Monument quadrangle, Valley County, Idaho. 45°01.9′ N., 115°04.3′ W.
11	L-74-6	D2411	1.24 km south-southeast of Lookout Mountain lookout. 45°01.3′ N., 115°04.0′ W.
[For samples 12, 13, 14, and 15, see Table 2]			
16	FWC-6-67	D2121	Rock cut, Middle Fork Salmon River, mouth of Aparejo Creek, Aparejo Point quadrangle, Lemhi County, Idaho. 44°55.25′ N., 114°43.7′ W.
17	FWC-6-67L	--	As above. Dated by R. L. Armstrong (Armstrong, 1974, p. 13).
18	L-71-1	D2232	Talus, north side of Camas Creek. ~430 m upstream from Anvil Creek, Yellowjacket quadrangle, Lemhi County, Idaho. 44°52.5′ N., 114°33.75′ W.
19	L-73-12	D2932	Indian Creek Elev. ~6,750 ft, 1.3 km upstream from meadow, Yellow Pine 15-min quadrangle, Valley County, Idaho. 44°48.5′ N., 115°19.5′ W.
20	L-73-11	D2517	Talus, north side of Indian Creek, Elev. ~6,700 ft, 1.3 km upstream from meadow, Yellow Pine 15-min quadrangle, Valley County, Idaho. 44°48.4′ N., 115°19.5′ W.
21	L-73-22	D2963	240 m northwest of Elk Summit, Wolf Fang Peak quadrangle, Valley County, Idaho. 45°09.09′ N., 115°25.42′ W.
22	L-74-11	D2965	Spur, Elev. 6,660 ft, ~0.5 km northeast of mouth of Century Creek and ~0.25 km east of Monumental Creek road, Rainbow Peak quadrangle, Valley County, Idaho. 44°55.98′ N., 115°12.02′ W.
23	L-75-MCD	D2966	Divide north of Paint Creek, Elev. ~8,100 ft, near peak 8123, Monument quadrangle, Valley County, Idaho. 45°04.7′ N., 115°05.2′ E.
24	L-72-1	D2362	Big Baldy Ridge, 0.6 km west-southwest of peak 8966, Yellow Pine 15-min quadrangle, Valley County, Idaho. 44°48′ N., 115°18′ W.
25	L-73-15	D2962	Stevens Creek-Savage Creek divide, Elev. ~7,500 ft, 75 m east of crest and ~0.8 km northwest of forks of Savage Creek, Big Chief Creek quadrangle, Valley County, Idaho. 44°46.4′ N., 115°17.7′ W.
26	L-73-18	D2518	Elev. 6,500±50 ft, ~0.8 km southeast of mouth of Winchester Creek, Yellow Pine 15-min quadrangle, Valley County, Idaho. 44°45.6′ N., 115°18.5′ W.
27	L-73-8	D2516	East side of Little Indian Creek, at mouth; Yellow Pine 15-min quadrangle, Valley County, Idaho. 44°50.6′ N., 115°15.3′ W.
28	L-73-9	D2961	Indian Creek, below trail, 1 km downstream from mouth of Little Indian Creek, Big Baldy quadrangle, Valley County Idaho. 44°50.3′ N., 115°14.5′ W.
29	L-71-2	D2233	Elev. 7,500-7,650 ft, west of Logan Creek, azimuth 280° from Moore Point, Big Creek 15-min quadrangle, Valley County, Idaho. 45°06′ N., 115°26′ W.
30	L-74-14	D2935	South end of The Hogback, Elev. 5,900 ft, 500 m southeast of Big Creek Lodge, Big Creek 15-min quadrangle, Valley County, Idaho. 45°07.4′ N., 115°19.25′ W.

and some glass. There is no evidence that the analyzed sanidine fraction contains admixed orthoclase from the granodiorite, though small inclusions of that rock are present locally in the welded tuff. The sanidine date is preferable to the plagioclase date, owing to slight alteration of the plagioclase and to low K_2O content (0.26 weight percent), but analytical uncertainty makes the two dates indistinguishable.

Sample 2, from welded tuff that rests on Precambrian syenite and quartzite near the northwest end of the cauldron, was collected within 10-100 meters of the contact. Plagioclase (0.75 weight percent K_2O) was the only mineral suitable for analysis. There is no evidence that the plagioclase fraction contains antiperthite from the underlying syenite, though inclusions of syenite as well as quartzite are locally present in the welded tuff. Mafic phenocrysts are sparse and altered; mafic minerals in the aphanitic groundmass are perhaps chloritized but too fine grained for microscopic study. The whole-rock date is a minimum for the welded tuff. The date was determined as a guide to interpreting other whole-rock dates from the area.

Sample 3 is from a slightly amygdaloidal lava flow near the base of the unit. The depositional contact of the Challis Volcanics is not exposed at the sample site. The radiometric dates obtained on phenocrysts of "hornblende" (0.14 weight percent K_2O) and plagioclase (0.43 weight percent K_2O) differ widely. The analytical error is large for "hornblende," owing to low K_2O content and small sample size. The "hornblende" is a green amphibole that forms perfect monocrystalline pseudomorphs after orthopyroxene, of which no trace except the relict cleavage remains. Accordingly, we regard the "hornblende" date as invalid. Fresh, abundant plagioclase has yielded a date that we are inclined to doubt because it differs so much from that of the "hornblende." The processes that converted orthopyroxene to amphibole and formed the microscopic amygdules of chlorite, quartz, and calcite have apparently disturbed isotopic equilibrium sufficiently to make the rock unsuitable for dating.

Sample 4 is from a thin lava flow low in the section, probably within 100 meters of the base of the lower, latitic unit. Hornblende from the holocrystalline flow is notably fresh, contains 0.91 weight percent K_2O, and yields a date that we cannot question in spite of the small size of the pure separate. The whole-rock date, determined for comparison, is

Table 2. Potassium-argon dates of latite flows of Lookout Mountain. Age decrease vs. size and quantity of glass patches.

Sample Number	Potassium-argon Date (R) m.y. ± 2σ	ΔAge[1]	Glass Volume Percent V	Glass Patch size, mm s ± σ	V^s		ΔAge vs. s	ΔAge vs. V^s
10	43.4 ± 1.4	--	[2]	--	--			
11	41.0 ± 1.4	--	[2]	--	--			
12	40.3 ± 1.8	1.9	3.2	0.022 ± 0.010	1.026	r	0.950	0.996
13	29.1 ± 1.1	13.1	63.1	0.039 ± 0.010	1.175	r^2	0.902	0.992
14	27.5 ± 0.9	14.7	55.5	0.043 ± 0.014	1.118			
15	17.0 ± 0.6	25.2	33.9	0.089 ± 0.014	1.368			

Whole-rock K_2O = 2.50-3.46, mean 3.10 wt. percent
[1]Accepting mean of (43.4 + 41.0) = 42.2 as base
[2]Mostly devitrified

Sample Number	Field Number	Laboratory Number	Location
10, 11			See Table 1.
12	L-74-8	D2412	150 m east of Black Pole, east side of Marble Creek, Thunder Mountain district, Safety Creek quadrangle, Valley County, Idaho. 44°57.38′ N., 115°04.75′ W.
13	AAS-262	D1649	South end Land Monument Mesa, 1 km northeast of Dewey mine, Thunder Mountain district, Rainbow Peak quadrangle, Valley County, Idaho. 44°58′ N., 115°08′ W.
14	L-74-13	D2414	West edge Land Monument Mesa, 53 m northeast of Land Monument No. 5A, Thunder Mountain district, Rainbow Peak quadrangle, Valley County, Idaho. 44°58.72′ N., 115°08.50′ W.
15	L-74-12	D2413	Northeast spur Land Monument Mesa, Elev. 7,830 ft, Thunder Mountain district, Rainbow Peak quadrangle, Valley County, Idaho. 44°59.48′ N., 115°07.58′ W.

substantially younger. The K_2O content of the rock is 3.08 weight percent, more than three times that of the hornblende. Presumably, some of the radiogenic argon produced by potassium of the fine-grained groundmass has been lost by diffusion.

Three of the four mineral samples (1, 2, and 4) from the lower, latitic unit adequately date this part of the Challis Volcanics at 48.3 to 50.8 million years, mean 49.8 ± 1.3 (1σ) or 49.8 ± 2.6 (2σ).

Upper, Rhyolitic Unit

We have not attempted to date the upper, rhyolitic unit, owing to the scarcity of feldspar phenocrysts, the scarcity of nonwelded tuffs, and the prevalence of glass (much of it devitrified) in the welded tuffs. Axelrod (1966) reported a whole-rock date of 49.0 ± 2.0 million years (50.3 million years, recalculated according to 1977 decay constants) for welded rhyolite tuff that he thought overlay the plant-bearing volcaniclastic rocks of the Dewey mine, Thunder Mountain district. Leonard's mapping of this intimately block-faulted district fails to show evidence for the existence of any welded tuff above the plant-bearing beds. The sample may have come from the upper, rhyolitic unit of the Challis Volcanics or from the Sunnyside rhyolite, both of which are stratigraphically lower than the plant-bearing beds and are exposed close to the Dewey mine in one or another of the nearby fault blocks. Because the stratigraphic position of the Axelrod sample is indeterminate, we do not know how to interpret the published whole-rock date.

STAGE OF MAJOR SUBSIDENCE

Major subsidence, as used here, refers to the stage following ash-flow eruptions of regional extent and preceding eruption of the Sunnyside ash flow into the Thunder Mountain caldera. Major subsidence presumably involved much or all of the cauldron block and very likely produced a large central depression, the Cougar Basin caldera, within which the Thunder Mountain caldera formed later. The original shape, areal extent, and depth of the Cougar Basin caldera are not adequately known. Until they are known, we look to the cauldron margins to date the stage of major subsidence. Here, draped or interfingering volcanic or volcaniclastic deposits that might provide direct geologic evidence of subsidence have not been found. However, the outer ring-fracture zones of the cauldron contain abundant dikes parallel or subparallel to the ring fractures. Assuming that some of the dikes might represent magma that rose while the cauldron block—the piston—was sinking, we have proceeded to date several dikes. The soundness of the assumption is open to question, though the assumption has often been made by students of cauldron complexes.

The largest intrusive along the cauldron edge in the western sector of the cauldron is an isolated body of quartz diorite porphyry that forms the ridge west of the upper reaches of the South Fork of Elk Creek. For convenience, this body is called the Elk Creek quartz diorite porphyry intrusive, an informal name. Dikes of the Profile-Smith Creek swarm are in part coextensive with the ring-fracture zone next inward from the cauldron edge. We infer that dikes of the swarm may have been emplaced at widely different times, though all are effectively restricted to rhyolite and latite in composition and none shows crosscutting relations with its neighbors. The work of dating these dikes has just begun.

The Elk Creek intrusive cuts granodiorite of the Idaho batholith. The porphyry, showing 12 percent phenocrysts of plagioclase, hornblende, and biotite in the proportions 6:3:1, looks dioritic in hand specimen but contains in the groundmass 15 percent quartz, 5 percent orthoclase, and a little clinopyroxene and orthopyroxene in addition to abundant plagioclase and some hornblende and biotite. It is one of the few rocks intermediate between the rhyolites and latites that dominate the Tertiary suite of the region. Biotite (Table 1, sample 6; 6.255 weight percent K_2O), mostly from the matrix of the porphyry, gives the date 47.1 ± 1.6 million years. A pure concentrate of hornblende from the porphyry could not be obtained.

Hornblende (Table 1, sample 7; 0.847 weight percent K_2O) from the phenocrysts of an unaltered granophyric latite dike of the Profile-Smith Creek swarm gives the date 47.3 ± 1.3 million years. The dike was selected because it is a few hundred meters distant from other dikes and from a major silicified zone. Rock contacts are not visible in the small meadow where the dike crops out, but mapping of the environs suggests that the dike was emplaced in alaskite of the Idaho batholith.

The 47.1- and 47.3-million-year dates are identical within the limits of measurement, and they are reasonable dates for cauldron subsidence if, by analogy with better-studied cauldrons, subsidence closely followed regional pyroclastic eruption. However, if the usual statistical tests are applied, these two dates cannot be distinguished from the group of dates for the lower Challis Volcanics, or from the dates for the Sunnyside ash flow of the caldera filling, or from the date of the dike to be discussed next. That the dates of samples 6 and 7 fall where they do may be a happy accident.

By taking one too many samples, we have complicated the interpretation of cauldron subsidence while

apparently confirming the inference that dikes of the Profile-Smith Creek swarm may not all be coeval. Phenocrystic sanidine (Table 1, sample 21; 6.00 weight percent K_2O) from a granophyric rhyolite dike well within the swarm gives the date 45.7 ± 1.6 million years. This date is not distinguishable at 2σ from the 47.3-million-year date of the latite dike, sample 7. If the dates are averaged, they yield a number so close to the dates for the Sunnyside rhyolite that one could infer simultaneity or close overlap in subsidence of the Quartz Creek cauldron, lubricated by magma along the outer ring fractures, and collapse of the Thunder Mountain caldera. But if the dates are indeed different, though not assertably so from the analytical results, one could infer that magma invaded the ring-fracture zone more than once. Both inferences are plausible, and a choice between them cannot now be made. The requirement for an approximate chronology of intrusives of the region is satisfied without bias by placing the 45.7-million-year date where the reader finds it in Table 1.

CALDERA FILLING STAGE

Sunnyside Rhyolite

The gross structure of the Thunder Mountain district, as mapped, requires the Sunnyside rhyolite to overlie one or more local ash flows of the regionally distributed upper, rhyolitic unit of the Challis Volcanics. Parts of the Sunnyside contain fragments of stony rhyolite and rhyolite welded tuff, both crystal poor, identical in appearance to rhyolites of the regional unit, but the depositional contact of the Sunnyside has not been seen in outcrops or drill cores. Fault contacts alone are mappable.

One dated sample of Sunnyside rhyolite (Table 1, sample 8) comes from the nonwelded top of the ash flow, from one of the few sites where the nonwelded tuff is well exposed and, to the unaided eye, little altered. Phenocrysts (26 percent) of biotite, hornblende(?), quartz, and feldspars lie in an ashy matrix of mineral fragments and devitrified glass whose nearly equant particles are 2-12μm in diameter. Some quartz of the matrix has been coarsened and recrystallized; however, most of the matrix is remarkably unchanged for a rhyolitic tuff of the district. The mafic phenocrysts, totaling 4 percent, are completely altered to chlorite and opaque material, but the feldspar phenocrysts are mostly fresh. Some sanidine phenocrysts contain small inclusions of altered biotite and patches of epidote; these were removed to make a tolerably pure separate of fresh sanidine whose K_2O content is 13.53 weight percent. The date of the sanidine separate is 46.3 ± 1.0 million years.

A second sample of Sunnyside rhyolite comes from the welded interior of the ash flow. It represents the widespread gray facies of welded tuff, here brownish gray and crystal rich, with sparse, moderately to highly flattened inclusions of white pumice and welded tuff 1-2 centimeters long. The matrix of partly welded ash and abundant, densely welded, barely devitrified pumice fragments, locally axiolitic, encloses phenocrysts of fresh biotite, murky hornblende, quartz, and fresh sanidine and plagioclase. The phenocryst content of 46 ± 1 percent, including 1.5 percent mafic minerals, is nearly twice that of the nonwelded Sunnyside rhyolite, but the chemical composition of the two rocks is nearly identical: essentially 71 (weight) percent SiO_2, 14 percent Al_2O_3, 1 percent CaO, 3 percent Na_2O, and 5 percent K_2O. Phenocrystic sanidine from the welded tuff gives the date 46.3 ± 1.1 million years (Table 1, sample 9; 10.30 weight percent K_2O). Phenocrystic biotite gives the date 47.7 ± 1.6 million years (sample 9; 6.285 weight percent K_2O). The dates are indistinguishable at 2σ, and the sanidine date of this sample of welded tuff is identical with the sanidine date of sample 8, which represents the nonwelded upper part of the ash flow.

The three dates are consistent with the geologic occurrence; the Sunnyside rhyolite is the youngest ash flow in the Challis that belongs to the Thunder Mountain volcanic field, and the age of the Sunnyside is accepted as 46-47 million years.

Crystal-rich welded tuff of the Norton Ridge area has not been dated (Norton Ridge is at the head of Norton Creek, Figure 2). The tuff of Norton Ridge resembles the Sunnyside rhyolite of the Thunder Mountain caldera and is so shown on Figure 1. According to E. B. Ekren (oral communication, 1981), the tuff of Norton Ridge also resembles the quartz-biotite tuff unit assigned by McIntyre and others (1982 this volume) to the Van Horn Peak cauldron complex southeast of the Casto pluton. Presumably the welded tuff of Norton Ridge is a far-traveled outflow unit from one volcanic center or the other, but we do not know which.

Volcaniclastic Subunit

Diamond drilling of the Sunnyside group of claims by Homestake Mining Company in 1973 confirmed that the Dewey beds overlie the Sunnyside rhyolite. Some of the silty felsic laminae in varvelike lake beds assigned to the volcaniclastic subunit may represent air-fall tuff, and laminae of similar appearance interbedded with coarse volcaniclastic debris may represent reworked air-fall tuff. The impossibility of distinguishing this fine felsic material from ash of the Sunnyside rhyolite, and the likelihood that younger ash would be contaminated with products of the

Sunnyside, has deterred us from attempting to date the Dewey beds radiometrically.

The geologic age of the Dewey beds, based on fragmentary plant fossils, is a matter of some dispute. Plant fossils collected in 1967 by Helmut Ehrenspeck, then of the U. S. Geological Survey, were examined by Jack A. Wolfe of the Survey. Mr. Wolfe reported (written communication, 1967):

> *Your collection from Dewey mine contains*: Equisetum *sp.*, Osmunda *sp.*, Picea *sp.*, Pinus *spp.*, Sequoia affinis *Lesq.*, Comptonia columbiana *Penh.*, [*and*] *cf.* Viburnum? *n. sp.*
>
> *Most of the above items are not stratigraphically diagnostic.* Sequoia affinis *indicates a Paleogene age.* Comptonia columbiana *has a known age range of late Eocene (Princeton, B.C., and Republic, Washington, floras), but conceivably this species could have a longer range. The determination of* Viburnum? *n. sp. is based on a specimen that is not well preserved; this specimen appears conspecific with* Viburnum? *n. sp. from the Princeton flora. It is probable that your material is of late Eocene age, but a middle Eocene age cannot be excluded.*

Mr. Wolfe recently stated (oral communication, 1981) that the Princeton and Republic floras are now regarded as middle Eocene in age. The uneasy shifts of meaning of middle and late, applied to informal subdivisions of the Eocene, lead us to abandon both adjectives in the discussion that follows.

Mr. Wolfe's conclusion that the fossil plants are of Eocene age is consistent with our 46.3 ± 1.0-million-year date for the upper part of the Sunnyside rhyolite. If one accepts that radiometric date, the flora is at most about 46 million years old. (For another opinion, see Axelrod, 1966. He based his opinion on the 50-million-year date obtained on a sample whose stratigraphic position we regard as indeterminate.) We hesitate to set a younger limit on the age of the flora because the range of dates obtained on overlying latite flows is susceptible of several interpretations. (See below.)

Erosional Hiatus

An erosional unconformity separates the Dewey beds from overlying latite flows. The erosion surface cut on the volcaniclastic rocks initially had a gentle southwest dip or was tilted southwestward, perhaps as a result of emplacement of the Casto pluton discussed below.

Latite Flows of Lookout Mountain

A minor volcanic center at Lookout Mountain produced latite cinders and bombs interbedded with latite flows. The number of flows is indeterminate. In this account, we deal with the lowest flow, recognized only near the vent, and with the two uppermost flows. The two uppermost flows spread southwestward 8 kilometers across the caldera floor, ramping slightly near the Dewey mine but sending fingers some distance farther southward. One flow, thought to be the highest in the section, is exposed at Black Pole, where it shows an angular unconformity of about 10 degrees against the underlying volcanic sandstone. The flows look young, resembling more nearly the Columbia River Basalt Group and the Snake River Group than basalts in the type area of the Challis Volcanics, and the beds of cinders and bombs resemble those found at Pleistocene and Holocene cinder cones. We emphasize the field aspect of the flows because it does not fit the results of radiometric dating.

The latite of flows from the Lookout Mountain center is black, aphanitic, without megascopic phenocrysts, and all samples contain glassor devitrified glass. Microphenocrysts and patches of glass are too small to be separated from finely crystalline parts of the matrix. Six samples from the flows yield whole-rock dates that range from 43.4 to 17.0 million years (Table 1, samples 10 and 11; Table 2, samples 10-15). Sample 11 is from the lowest flow exposed in the section. All other samples are from the highest flow.

The lowest flow, dated at 41.0 ± 1.4 million years, is 5 meters thick. It is underlain by a bed of orange latite breccia that is rich in volcanic bombs. The breccia bed is at least 6 meters thick; its base is not exposed. Overlying the lowest flow is 90 meters of breccia—mixed blocks, lapilli, cinders, and bombs—interlayered with many thin flows. Capping the breccia are the two principal flows of the Lookout Mountain area. The first of these, 9 meters thick, is highly vesicular. The second, the highest flow in the section, is slightly more than 6 meters thick, lies directly on the first, and is distinguished from it by having fewer vesicles. The highest flow gives a date of 43.4 ± 1.4 million years where sampled (sample 10) almost vertically above the sample site in the lowest flow (sample 11). The dates do not match the stratigraphic order, but they are indistinguishable at 2σ of analytical error. It is possible that neither date indicates an age of extrusion, but the pair of dates differs significantly and in the right sense from the 46 to 47-million-year age of the Sunnyside rhyolite (Table 1, samples 8 and 9).

Table 2 shows that samples 12 to 15, dated at 40.3 to 17.0 million years, contain fresh glass and are therefore prime candidates for argon loss. Disregarding the absolute age of samples 10 and 11, from which some argon may have been lost before devitrification

of the glass, we may take the mean of their two dates as a base against which to compare the remaining dates from the highest flow. When this is done, we see that there is no correlation between decrease in age and volume of glass (V), a good correlation between decrease in age and mean diameter of glass patches (s), and a nearly perfect correlation between decrease in age and the exponential function V^s. The coefficients of correlation and determination remain the same if the base is taken as 43.4 or 41.0 million years, instead of 42.3. The correlation between decrease in age and the function V^s is so good, and attempted correlations between decrease in age and other features such as geographic position, distance from the eruptive center, vesicularity, size of microphenocrysts or groundmass plagioclase, and position of a hypothetical resurgent intrusive are so poor, that we attribute the misfit dates of samples 12 through 15 to argon loss from glass. The best date for the highest flow is accepted as 43.4 ± 1.4 million years, and the published date of 28.4 million years (Cater and others, 1973, p. 29; there-undesignated sample AAS-262, which is sample 13 in our Table 2) is set aside as having been based on inadequate data. This leaves the anomalously young appearance of the flow and other products of the Lookout Mountain center unexplained. The 41.0-million-year date for the lowest flow is suspect.

The true age of the highest flow may not be 43.4 million years, but we accept the date provisionally in conjunction with the geologic relations discussed in a subsequent section on the Casto pluton.

DATING OF INTRUSIVES, MAINLY OF POSTSUBSIDENCE STAGE

Intrusive bodies varying widely in size and fabric but having mostly the bimodal latite-rhyolite compositions of the Challis Volcanics were emplaced in and near the Thunder Mountain field as the cauldron evolved. Intrusives of Tertiary but pre-Challis age have not been found. Dikes of the major subsidence stage have already been discussed. Intrusives mainly of the postsubsidence stage are now considered, primarily according to their spatial or geologic relations and secondarily according to the apparent chronologic age of the geographic or geologic examples.

Casto Pluton

The Casto or Middle Fork pluton is the large northeast-trending body of biotite-microperthite granite that trends diagonally across the Idaho batholith and separates the Challis Volcanics of the Thunder Mountain field from the Challis Volcanics of the Van Horn Peak cauldron complex southeast of the Middle Fork of the Salmon River. The Casto pluton bowed up the Challis Volcanics to form a major anticline (Ross, 1934, plate 1). The thermal effects of the pluton locally hornfelsed the Challis weakly, modifying the generally latitic volcanics enough so that Ross assigned these rocks of "paleo aspect" to another formation, the Casto Volcanics. The term Casto Volcanics has since been abandoned (Cater and others, 1973). Rocks formerly assigned to the Casto are now part of the Challis. The emplacement of the Casto pluton in the lower, latitic part of the Challis Volcanics, the readjustment of the terrane during episodes of block faulting, and the deep erosion of the roof of the pluton have left the geologic relation of the pluton to the upper, rhyolitic part of the Challis uncertain. The dates reported below do little to resolve the pluton-rhyolite problem, but some structural evidence sheds light on it.

Three dates for the pluton are available (Table 1, samples 16, 17, and 18). The problem posed by these dates baffles the geologist and the analyst. The geologist, alarmed by the wide range in dates, mistrusts all three but supposes that the mean of the dates might be credible if the core of the pluton (samples 16 and 17) crystallized much earlier than the fluorite-rich, miarolitic roof facies (sample 18). The analyst, observing that the dates decrease sympathetically with the K_2O content of the biotite samples (6.04, 3.91, and 1.875 weight percent for samples 16, 17, and 18, respectively), cautions against averaging dates that may not be of comparable reliability; samples 17 and 18 are deficient in K_2O, relative to most biotites.

Samples 16 and 17 (Table 1) represent massive granite from the interior of the pluton, 1,200 to 2,500 meters below the restored roof. The discrepancy between the dates of 47.8 million years (this report) and 43.8 million years (Armstrong, 1974; date recalculated according to 1977 decay constants) is unexplained. Both dates were obtained on F. W. Cater's samples from a single site. Except that the biotite of our sample contained minute inclusions of primary molybdenite before cleaning, the biotite is typical of the dark green variety commonly found in the pluton. The 47.8-million-year date may represent the time of crystallization of the core of the pluton, but not the time of emplacement of the pluton (see subsequent discussion).

Sample 18, collected at the southeast edge of the pluton, is from what we interpret to be a volatile-enriched, near-roof facies that may have crystallized somewhat later than the core. However, the 41.6-million-year date reported for the sample (Table 1) is

probably invalid. We now know, from X-ray diffraction analysis and more detailed optical study of a split of the analyzed sample, that the "biotite" which looked so clean in thin section and in minus 60-, plus 80-mesh concentrates is an intimate mixture of (1) a septechlorite, unusually coarse, strongly birefringent, strongly pleochroic from greenish brown to very dark brownish green, and optically indistinguishable from biotite in thin section and in crushed particles larger than 200 mesh; (2) biotite; and (3) a common green chlorite. The proportions of (1), (2), and (3) are roughly 75:20:5. The low proportion of biotite makes us skeptical of the date obtained from the mixture. Since we could not initially tell the difference between the biotite-septechlorite intergrowth of this sample and the usual biotite, similar in pleochroism, found in Tertiary rhyolites and granites of the region, it is clear that the identification of micaceous minerals from these rocks deserves more than usual care.

Radiometric evidence that the pluton is a postsubsidence intrusive, rather than one temporally related to subsidence or to presubsidence volcanism, is equivocal. The 47.8-million-year date given by sample 16 is indistinguishable at 2σ from the mean date of the lower, latitic unit of the Challis Volcanics, from the dates of dikes of the cauldron subsidence stage (samples 6 and 7), and from the dates of the Sunnyside rhyolite (samples 8 and 9). The 43.8-million-year date given by sample 17 is distinguishable only from the mean date of the lower, latitic unit. The moot status of the 43.8-million-year date makes inadvisable an averaging of the 47.8- and 43.8-million-year dates to give a number that would fit the geologic argument next to be developed.

Some event imparted a regional slope to the floor of the Thunder Mountain caldera, for the highest flows from the Lookout Mountain center spilled southwestward 8 kilometers and more from the center. Flow direction is established unequivocally by the absence of the latite flows north of the center, by the present regional dip, by vesicle elongation in the flows, and by local ramp structures. The only event likely to impart a regional tilt of this extent at the right time is the emplacement of the Casto pluton. The geologic maps of Ross (1934, plate 1) and of Cater and others (1973, plate 1) show, facing the Thunder Mountain caldera, gentle northwest dips off the main part of the Casto pluton and southwest dips off the northwest lobe of the pluton. Local structures of younger age complicate this relation, but its existence at the margins of the pluton is clear. The dips, if originally of regional extent, define a broad syncline whose axis plunges gently westward and passes across the caldera at the latitude of the most southerly remnants of the latite flows. The north limb of the syncline provided a gentle slope down which the flows could move, and the south limb of the caldera wall effectively kept the flows from spreading farther. According to this reasoning, the caldera floor had to exist before the pluton was emplaced, and the floor had to be deformed before the latite flows were erupted onto it. Deformation of the caldera floor by the pluton seems geologically reasonable but is beyond proof. The sum of the evidence seems to us to favor postsubsidence emplacement of the pluton, and the position of the pluton seems clearly to have been determined by the shape and extent of the Quartz Creek cauldron. The pluton occupies what was formerly the eastern sector of the outer ring-fracture zone of that cauldron, or it occupies disputed territory between the neighboring Quartz Creek and Van Horn Peak cauldrons.

How the pluton got there, is a puzzle. Presumably the edges of the Quartz Creek and Van Horn Peak cauldrons provided a zone of weakness that the ascending pluton could make use of. But the pluton is large. Its thermal aureole is not. The metamorphic effect on the adjacent Challis Volcanics is slight, and the effect on the Precambrian Yellowjacket Formation in the Yellowjacket district seems negligible. The variety and style of mineral deposit that might be expected to accompany a fluorite-bearing, potassium-rich granite have not been reported from the area. Perhaps the deposits have not been found; perhaps they are lacking. These strange attributes of the pluton, as well as the odd assortment of rocks within it, might be comprehensible if the pluton in large part rose to its present level of exposure diapirically, borne upward by ascending magma that locally consolidated to form the many small intrusives which penetrate the pluton, and dragging or rafting with it tracts of the pre-Challis terrane—rocks of the Idaho batholith suite, Precambrian schists and migmatites, and bodies of mafic plutonic rock whose assignment to the Tertiary now seems questionable. The distribution of these exotic tracts within the Casto pluton is well shown on plate 1 of Ross (1934). Nonmagmatic ascent of the pluton to its present level of exposure is a working hypothesis to account for strange geologic facts that bothered Mr. Ross as well as us. The 47.8-million-year date obtained from the pluton is consistent with the hypothesis. The date may represent the time of magmatic crystallization of the pluton, not the time of emplacement of the pluton into its present environment. Radiometric dating of minor intrusives within the pluton thus becomes critical for testing the hypothesis that ascending magma, which locally produced the minor intrusives, bore the pluton en masse into its present environment.

We regard the Casto pluton as a postsubsidence feature structurally and an enigmatic feature petrologically. As a structural feature, the pluton is

reasonably interpreted as having developed after the eruption of the Sunnyside rhyolite and before the effusion of the flows of Lookout Mountain, within the time span represented by the 46 to 47-million-year dates of the Sunnyside and the estimated 43-million-year date of the highest flow from the Lookout Mountain center. As a petrologic feature, the pluton remains little known and insufficiently dated and thus inappropriate for discussion here.

Stocks of Upper Indian Creek

Two stocks are present at the south end of the silicified zone that extends southward from the Meadow Creek mine near Stibnite, Yellow Pine 15-minute quadrangle. The silicified zone, described in reports by Cater and others (1973) and by Curtin and King (1974), occupies part of the ring-fracture zone that bounds the west side of the Cougar Basin caldera. The stocks are of granite porphyry and quartz diorite porphyry. Their relative geologic ages are indeterminate, but according to isotopic dating the granite porphyry is older.

The granite porphyry is almost wholly concealed by fan debris and alluvium that merge at the valley bottom. The rock contains small miarolitic cavities, sparse phenocrysts of quartz and feldspar, and abundant, vaguely subhedral patches of coarser micropegmatite set in a finer, nearly equigranular matrix of quartz, alkali feldspars, and sparse micropegmatite. The matrix particles, which have an average diameter of 0.4 ± 0.1 millimeter, are distinctly coarser than the 0.02-0.06 millimeter matrix particles of intrusive rhyolites of the region. Sanidinelike alkali feldspar (9.41 weight percent K_2O) of the matrix of the granite porphyry gives the date 46.9 ± 1.6 million years (Table 1, sample 19).

The quartz diorite porphyry stock, locally mylonitized and bounded by faults, intrudes mainly the metamorphic-rock component of an area of mixed rocks—metamorphic rocks invaded by sheets and small discordant bodies of alaskite of the Idaho batholith. Small inclusions of Precambrian amphibolite, hornfelsed metavolcanics, and quartzite are present in the porphyry, along with rare inclusions of alaskite. A single inclusion of slightly hornfelsed rhyolitic crystal tuff, presumably of the Challis Volcanics, was observed. The foregoing features, the gross aspect of the stock, and its microscopic features are appropriate for a Tertiary stock. The puzzling feature of the stock is that dikes of aplite—locally pegmatitic, locally vuggy—cut it. These dikes, some almost a meter wide but seen only in large blocks of talus, look in the field and under the microscope exactly like aplite or fine-grained alaskite of the Idaho batholith. For this reason, the stock was originally interpreted as an atypical and early facies of the batholith and was not shown by separate symbol on Cater's map of the Idaho Primitive Area (Cater and others, 1973, plate 1). Leonard has reexamined the stock twice after mapping it but has found no additional evidence bearing on the misfit age relations of quartz diorite porphyry and aplite. The contradictory evidence on relative age is here interpreted to mean that the magma giving rise to the porphyry stock was of Tertiary age, that it mechanically incorporated some batholithic alaskite, and that locally it remelted some alaskite, which then intruded the cooler parts of the consolidating porphyry body. The hypothesis that the aplite is remelted or directly intruded granite porphyry like that of sample 19 cannot be eliminated. The contrast between the interlocking fabric of the aplite and the micropegmatitic fabric of the granite porphyry merely seems to speak against that hypothesis if one is familiar with the range of microscopic fabrics shown by aplites, alaskites, and granite porphyries of the region.

A homogeneous sample of quartz diorite porphyry was selected for radiometric dating. The rock is a hornblende-pyroxene quartz diorite or granodiorite containing 8 percent quartz, 15.5 percent potassium feldspar, and a little micropegmatite and biotite, in addition to abundant plagioclase with subordinate hornblende and pyroxene. The microscopic fabric is intergranular, like that of a diabase; mafic minerals, accompanied by subordinate quartz, potassium feldspar, plagioclase, and micropegmatite, are interstitial to plagioclase laths several millimeters long. Sparse phenocrysts of plagioclase, together with mafics that are microscopically intergranular and clustered but megascopically phenocrystlike, make hand specimens of the rock look distinctly "porphyritic." Hornblende, the dominant mafic, gives the date 44.4 ± 1.8 million years (Table 1, sample 20; 0.935 weight percent K_2O).

The 46.9- and 44.4-million-year dates obtained from the two stocks on upper Indian Creek overlap at 2σ but are discrete at 1σ. Suppose, for the moment, that the individual dates are acceptable at face value. The 46.9-million-year date is close to the 47.1- and 47.3-million-year dates that we have related to cauldron subsidence; the date is consistent with the interpretation that the Cougar Basin caldera collapsed along the Meadow Creek fault zone at nearly the same time that the cauldron block subsided. The 44.4-million-year date nearly matches that obtained from the Century Creek stock, discussed below as sample 22, and is thus consistent with the interpretation that more than one stock grew within the cauldron block about 44 million years ago. The interpretations are geologically reasonable, but we remain skeptical of too much refinement.

Dating the quartz diorite porphyry does little to guide our thinking about the age of the silicified zone that extends southward from the Meadow Creek mine. The silicified zone (Leonard, *in* Curtin and King, 1974) ends at the quartz diorite porphyry stock, but a fault or a zone of faults separates the two units, and inclusions of one have not been found in the other. Thin veinlets of vuggy chalcedonic quartz do cut the porphyry seen in a few talus blocks. However, several generations of quartz are represented in the silicified zones of the region. Thus the assumption that a quartz veinlet in the quartz diorite porphyry has a temporal or genetic connection with the bulk of the quartz in the local silicified zone is unwarranted.

Stocks Within and Close to the Thunder Mountain Caldera

Stocks and dikes within the Thunder Mountain caldera are rare. In contrast, they occur in clusters at the caldera edge near the middle reaches of Monumental and Marble Creeks, where they have been seen to cut the wall rocks but not the caldera filling. Dates for one intracaldera stock (Century Creek) and one peripheral stock (Paint Creek) are given here.

The *Century Creek stock* is one of two small stocks exposed near Thunder Mountain. All contacts with the surrounding Sunnyside rhyolite and buff rhyolite tuff (part of the upper, rhyolitic unit of the Challis Volcanics) are faults. The stock lies within the Thunder Mountain caldera, but it may have intruded the wall zone of a minor, unnamed caldera within the Thunder Mountain caldera. Much of the stock is highly altered to limonite and replaced by tridymite. The highly altered rock was mentioned in an earlier report (Cater and others, 1973, p. 47).

Fresh rock is dark green. Phenocrysts of ferrohedenbergite (1 percent) and bipyramidal quartz, sanidine, and plagioclase (24 percent, taken together) are embedded in an aphanitic matrix of the same minerals and a little primary(?) chlorite. Granules consisting of orange chlorophaeite(?) and a yellowish, fibrous amphibole represent pseudomorphs, surely in part after ferrohedenbergite, though most of the pyroxene is fresh, but perhaps in part after fayalite, of which no relic has been found. The rock is a ferrohedenbergite rhyolite porphyry, and the Century Creek stock is the sole occurrence of it known in this region.

Phenocrystic sanidine from fresh rock gives the date 44.6 ± 1.5 million years (Table 1, sample 22; 8.355 weight percent K_2O). At 2σ, the date overlaps the sanidine dates of the Sunnyside rhyolite; at 1σ, it does not. Lack of overlap is consistent with the geologic interpretation reached in the field: though the Century Creek stock is now bounded by faults, it probably intruded the Sunnyside, as well as the buff rhyolite tuff. That interpretation is also consistent with the occurrence of small bodies of rhyolite intruding the Sunnyside along Monumental and Telephone Creeks. However, neither the isotopic data nor the field relations eliminate the possibility that the Century Creek stock and the buff tuff, behaving as a unit, were faulted against the Sunnyside rhyolite.

The intrusive body here termed the *Paint Creek stock* is peculiar. It has fresh phenocrysts in an altered groundmass. The stock, exposed on the divide between Paint Creek and Deer Creek, intrudes the upper, rhyolitic unit of the Challis Volcanics just north of a downfaulted mass of Sunnyside rhyolite. The area about the stock and its host rock is incorrectly shown as Yellowjacket Formation on plate 1 of Cater and others (1973).

The stock is a composite body of granite porphyry and quartz latite porphyry. A small body of granite porphyry, possibly an apophysis of the stock, is exposed about 300 meters east of the stock, and several latite dikes hold up the sharp topographic spur southwest of the stock. The latite dikes of the spur, taken together with some porphyry dikes that cut the composite stock, seem to radiate from the stock, but the relation may be fortuitous.

Our sample of granite porphyry from the composite stock is better termed rhyolite porphyry, but one needs a microscope to see that the matrix is indeed extremely fine grained. Abundant phenocrysts of biotite, hornblende, quartz, plagioclase (weakly zoned sodic oligoclase to strongly zoned andesine), and sanidine—all perfectly fresh—are set in a matrix of chalcedony and adularia, instead of quartz and two alkali feldspars, the common matrix assemblage for intrusive rhyolites of the region. The chalcedony-adularia matrix consists of a net of extremely fine material enveloping abundant, roundish areas of slightly coarser material. The roundish areas are 0.2-0.8 millimeter in diameter, and it is their size that makes the matrix look "crystalline" to the unaided eye. Some of the roundish areas have thin rims of adularia, and patches of colloform adularia are scattered throughout the net. Most of the adularia particles are rhombuses less than or equal to 10 μm in length; the chalcedony particles are generally smaller than those of adularia. A few lenticular aggregates of rather coarse chalcedony and adularia are present, as well as rare lenticles of colloform stuff that may be opal or almost submicroscopic bands of alternating chalcedony and adularia. A few discontinuous replacement veinlets of chalcedony, mostly confined to the matrix, locally cut phenocrysts of plagioclase.

A genetic interpretation of the chalcedony-adularia matrix cannot be made with assurance. The absence of sodic plagioclase in the matrix suggests that

chalcedony and adularia have formed essentially by replacement of a preexisting aggregate of quartz and two alkali feldspars, not by a simple recrystallization of the primary groundmass. If so, the process would have some resemblance to the potassic alteration that locally affects mineralized stocks. Without careful study of the Paint Creek stock, one cannot know whether the alteration process has been confined to the rhyolite porphyry of a composite intrusive, or has converted parts of a simple quartz latite porphyry to a rock now classifiable as rhyolite porphyry.

Phenocrystic biotite from the rhyolite porphyry gives the date 47.1 ± 1.6 million years (Table 1, sample 23; 7.89 weight percent K_2O). Neither phenocrystic sanidine nor groundmass adularia could be made suitably pure for dating. The 47.1-million-year date of the biotite can be interpreted several ways. (1) It means what it says; the stock, so dated, intruded the upper, rhyolitic unit of the Challis Volcanics and is coeval with dikes of the cauldron subsidence stage or with the Sunnyside rhyolite. (2) The date is suspect because the stock is composite and its quartz latite porphyry has not been dated, owing to lack of suitable material. (3) The date needs to be viewed against the background provided by paired biotite and sanidine dates from the Sunnyside rhyolite (Table 1, sample 9)—47.7 million years for biotite, but 46.3 for sanidine. So viewed, biotite from the Paint Creek stock appears younger than biotite from the Sunnyside rhyolite. Thus it is reasonable to suppose that the stock was emplaced after the Sunnyside was erupted and, quite likely, after the Sunnyside collapsed into the Thunder Mountain caldera. We prefer interpretation (3) because it gives more weight to relative values than to absolute ones.

Dikes of Little Pistol Swarm

Dikes of the Little Pistol swarm (Leonard, 1965) cut plutonic rocks and Challis Volcanics along the southern sector of the cauldron. C. P. Ross (oral communication, 1957) thought that dikes of this swarm were broadly contemporaneous with the Casto pluton. Because the dikes occupy extension fractures related to great shear zones that cut the cauldron block, Leonard has supposed that the dikes were considerably younger than the Challis Volcanics. The three radiometric dates obtained on dikes from the swarm indicate that dikes of several ages are present.

Phenocrystic sanidine from a rhyolite dike that cuts the lower, latitic unit of the Challis Volcanics has a date of 45.2 ± 1.5 million years (Table 1, sample 24; 9.48 weight percent K_2O). This date is younger than the more reliable of the dates reported for the lower, latitic unit and falls within the time span that we think is appropriate for the diapiric(?) emplacement of the Casto pluton. The rise of the pluton, the development of extension fractures in the Little Pistol area, and the intrusion of the first dikes of the Little Pistol swarm may be closely related, both structurally and temporally.

Another rhyolite dike cuts Challis Volcanics (undivided) and alaskite of the Idaho batholith, the latter containing inclusions of Precambrian Hoodoo Quartzite. Phenocrystic sanidine from this dike gives the date 42.4 ± 1.5 million years (Table 1, sample 25; 6.56 weight percent K_2O). At 2σ, this date barely overlaps the 45.2 ± 1.5-million-year date of dike 24.

Phenocrystic hornblende from a latite dike that cuts plutonic rocks 1 kilometer south of the nearest exposure of Challis Volcanics has a date of 36.7 ± 1.5 million years (Table 1, sample 26; 0.785 weight percent K_2O). Plutonic rocks at the sample site are an agmatite of Precambrian quartzite and hornfelsed biotitic metavolcanic rock in a matrix of alaskite of the Idaho batholith. The 36.7-million-year date for latite dike 26 differs little from the date of one of the middle Indian Creek stocks, next described, but is substantially and reliably younger than the date for rhyolite dike 25. Dikes 24, 25, and 26 are but three of the hundreds mapped within the Little Pistol swarm. They represent the two common compositional types, but we are not prepared to believe that rhyolite dikes of the swarm are of one age and latite dikes of another. Unfortunately, two other latite dikes of the swarm failed to yield mineral separates pure enough for dating.

Stocks of Middle Indian Creek

A group of small stocks at the mouth of Little Indian Creek is the westernmost expression of a 5-kilometer-wide cluster of rhyolite and latite stocks that extends at least 8 kilometers down Indian Creek. The stocks are densely studded along the southern ring-fracture zone of the Cougar Basin and Thunder Mountain calderas, approximately at the contact between the Sunnyside rhyolite and lower units of the Challis Volcanics.

Two rhyolite stocks were dated. Both contain phenocrysts of biotite, bipyramidal quartz, sanidine, and plagioclase. These make up less than 10 percent of one stock and 37 percent of the other. Both stocks contain a trace of accessory fluorite.

The first stock east of the mouth of Little Indian Creek is sparsely porphyritic, slightly miarolitic rhyolite that intrudes tuff of the upper, rhyolitic unit of Challis Volcanics close to its fault contact with granodiorite-bearing mudflow debris of the same unit. Neither phenocrystic biotite nor sanidine was recoverable as a suitably clean mineral concentrate, so we used the separated groundmass of very fine-

grained alkali feldspars, quartz, and a trace of biotite and opaque minerals. The mean date of two groundmass samples is 39.8 ± 0.9 million years (Table 1, sample 27; 4.955 weight percent K_2O).

A nearby stock is flanked by narrow fault blocks of Challis Volcanics and laminated siltite-argillite of the Precambrian Yellowjacket Formation. Slightly turbid, faintly mottled, phenocrystic potassium feldspar from the stock resembles the sanidine commonly found in other rhyolites but is nearly pure "orthoclase" (15.425 weight percent K_2O). This feldspar gives the date 41.1 ± 0.9 million years (Table 1, sample 28).

At 2σ, the 39.8- and 41.1-million-year dates do not overlap, but the analyst regards the first date as a minimum. The first date is close to that of the far-distant Logan Creek stock, whose size and setting are different (see description of sample 29, below). The second date is close to that of a rhyolite dike of the Little Pistol swarm (sample 25). The dated rhyolite stocks on the middle reaches of Indian Creek are petrographically distinct, separate but close in space, and close but perhaps separate in age. We conclude that these two stocks were emplaced several million years after the development of the ring-fracture zone of the Cougar Basin and Thunder Mountain calderas.

Logan Creek Stock

A stock of coarsely miarolitic, fluorite-bearing granite cuts across the outer ring-fracture zone of the western sector of the cauldron. The stock, about 1 kilometer wide and 6 kilometers long, is the largest stock west of the Casto pluton. Biotite from the stock gives a date of 38.7 ± 1.3 million years (Table 1, sample 29; 4.18 weight percent K_2O). The date is consistent with the local geology and indicative of the continuation of intrusive activity long after major subsidence of the cauldron block.

Dike of The Hogback, Big Creek

Small dikes of rhyolite and latite are scattered throughout the cauldron block without a detectable relation to major structural features. The dike in andalusite phyllite of the Precambrian Yellowjacket at The Hogback is an example. Except for its lack of alteration, this dike is identical in general character to rhyolite dikes of the Little Pistol and Profile-Smith Creek swarms. Biotite from the dike gives the date 20.7 ± 0.7 million years; sanidine gives the date 46.3 ± 1.1 million years (Table 1, sample 30; 5.295 weight percent K_2O for biotite, 13.465 for sanidine). The discrepancy between the biotite and sanidine dates is large and unexplained. Sample 30 is the third one that we have collected and dated from this site. All three samples show the same discrepancy in dates, yet the biotite and sanidine—both phenocrystic—are the least altered of any we have seen in Tertiary rocks of the region. The dike is holocrystalline and shows no xenoliths, nothing in thin section looks xenocrystic, and no other Tertiary intrusive is exposed within 500 meters of the sample site. Does the biotite date point to a thermal event whose source or effects we have not recognized elsewhere in the region? Was biotite alone affected, or was sanidine affected too? We do not know how to interpret the discrepant dates.

Dates obtained earlier on samples of The Hogback dike were extrapolated (Leonard, 1965) as a guide to the age of dikes in the Little Pistol swarm. The extrapolation was inadvisable.

CONCLUSION

The eruption of latite ash flows 50 million years ago began an episode of volcanic activity that lasted about 7 million years. Ash flows and minor lava flows, first latitic, then rhyolitic, built the Thunder Mountain field of Challis Volcanics to a height of perhaps 1500 meters before the subsidence of a nearly circular cauldron block having a diameter of 60-65 kilometers. Major subsidence, dated at 47 million years, was accompanied by development of the Cougar Basin caldera, within which the Sunnyside rhyolitic ash flow was erupted from a central vent 46-47 million years ago. Eruption of the Sunnyside ash flow was attended by development of the Thunder Mountain caldera, to which most of the Sunnyside ash flow was confined. Collapse of the Thunder Mountain caldera cannot be precisely dated. An upper limit is either the 47-million-year date of cauldron subsidence or more likely, we think, the 46 to 47-million-year date of eruption of the Sunnyside rhyolite. A likely lower limit is the 44.6-million-year date of the Century Creek stock, a small intrusive nearly central to the caldera. Water-laid volcaniclastic debris, derived mainly from the Sunnyside rhyolite, was spread thinly over the floor of the collapsed Thunder Mountain caldera, trapping plant remains of Eocene age. The floor of the Thunder Mountain caldera was tilted gently southwestward, perhaps by diapiric emplacement of the Casto pluton. A minor vent 8 kilometers northeast of the center of the caldera erupted latite cinders, bombs, and lava of the Lookout Mountain unit. Thin flows from this vent spread southwestward across the caldera floor. The highest latite flow has a date of about 43 million years; younger dates obtained from the flow very likely reflect argon loss from glass. The outpouring of latite lava is the last volcanic event recorded in the caldera, whose evolution extended from middle Eocene to late

Eocene time. (The informal designations of Eocene time are keyed to the preferred radiometric dates, recalculated according to 1977 decay constants, of Harland and others, 1971.) During the Pleistocene, part of the defunct caldera again served as a depositional site, this time for gravels carried in by meltwater from small alpine glaciers of the bordering highlands.

At present levels of exposure, the earliest indication of Tertiary intrusive activity is given by quartz diorite and latite dikes of the outer ring-fracture zone of the Quartz Creek cauldron. The dikes have a date of 47 million years. The latest indication of intrusive activity is given by a latite dike, dated at 37 million years, from the Little Pistol dike swarm. Thus the evidence points to a beginning of intrusive activity during the explosive stage of local volcanism and a cessation some few million years after extrusion of the youngest lavas of the Thunder Mountain field. Between the extremes of 47 and 37 million years, the eastern margin of the cauldron was invaded by the Casto pluton, and myriad small stocks and dikes were emplaced along the margins of the cauldron and its nested calderas. Small rhyolite stocks grew near the center of the Thunder Mountain caldera.

The Casto pluton presents a special problem, different from that of the stocks and dikes. The most reliable date, analytically, for the pluton is 47.8 million years. That date may represent the time of crystallization of the core of the pluton at some considerable depth beneath the cover rocks. The pluton did not, we think, ascend to invade the cauldron margin till much later, perhaps 44-45 million years ago.

The dates of the Challis Volcanics of the Thunder Mountain field do not differ significantly from the dates reported by Armstrong (1974) for the Challis Volcanics of the type area near the town of Challis: about 43-50 million years for the former and about 45-50 million years (recalculated) for the latter. The comparison excludes dates of ours that we have discussed as aberrant and dates of Armstrong's for which he expressed some reservations. However, the Challis Volcanics extend far beyond the areas whose rocks have been radiometrically dated in our study and in Armstrong's. Within the large expanse of the Challis Volcanics of central Idaho there are, we believe, at least seven major caldera-related volcanic fields whose extrusive products, similar in composition and locally lapping over from one field to another, may be nearly contemporaneous but not rigidly so. Until the local sequences have been established and dated, appropriate limits for "Challis time" are only approximately definable. Meanwhile, it is worth noting that although a good many Tertiary intrusives in central Idaho are coeval with the Challis Volcanics as currently datable, some intrusives are younger. The 37-million-year date of hornblende latite from the Little Pistol dike swarm, for example, is an Oligocene date if referred to Harland and others' (1971) preferred date of 38 million years (39 million years, recalculated) for the base of the Oligocene, and is statistically excludable from the set of 43 to 50-million-year dates that represent reliably dated Challis Volcanics.

ACKNOWLEDGMENTS

We thank these members of the U. S. Geological Survey for their contributions to our work: Jack A. Wolfe for examination of plant fossils; H. H. Mehnert and V. M. Merritt for assistance with potassium-argon analyses; and Alan J. Busacca, Bruce T. Brady, G. T. Cebula, Ezekiel Rivera, and Michael Sekulich for mineral separations. Mr. Busacca and former field associates Neil Dale, Stephen J. Reynolds, and John Schloderer helped collect the rock samples. Don R. Mabey provided supplementary geophysical data. E. Bartlett Ekren and David H. McIntyre examined a suite of thin sections. Mr. McIntyre and Frederick S. Fisher reviewed the report. Melvin and Jim Ed Biggers, Sweet, Idaho; Lafe Cox, Yellow Pine, Idaho; and Larry Rowe, Caldwell, Idaho, efficiently managed pack strings and provided support in base camps. Eleanor Leonard and Ruth Leonard O'Neil kindly served as unpaid camp cooks.

REFERENCES

Armstrong, R. L., 1974, Geochronometry of the Eocene volcanic-plutonic episode in Idaho: Northwest Geology, v. 3, p. 1-15.

Axelrod, D. I., 1966, Potassium-argon ages of some western Tertiary floras: American Journal of Science, v. 264, p. 497-506.

Cater, F. W., D. M. Pinckney, W. B. Hamilton, R. L. Parker, R. D. Weldin, T. J. Close, and N. T. Zilka, 1973, Mineral resources of the Idaho Primitive Area and vicinity, Idaho, with a section on the Thunder Mountain district by B. F. Leonard, and a section on aeromagnetic interpretation by W. E. Davis: U. S. Geological Survey Bulletin 1304, 431 p.

Curtin, G. C. and H. D. King, 1974, Antimony and other metal anomalies south of Stibnite, Valley County, Idaho, with a section on Geology by B. F. Leonard: U. S. Geological Survey Open-File Report 74-111, 54 p.

Harland, W. B., E. H. Francis, and P. Evans, 1971, The Phanerozoic time-scale—a supplement: Geological Society of London Special Publication 5, 356 p.

Leonard, B. F., 1965, Tertiary dike swarm on Little Pistol Creek, Yellow Pine quadrangle, central Idaho (abstract): Geological Society of America Special Paper 82, Abstracts for 1964, p. 336-337.

Leonard, B. F. and R. F. Marvin, 1975, Temporal evolution of the Thunder Mountain caldera, central Idaho: Geological Society of America, Abstracts with Programs, v. 7, no. 5, p. 622-623.

McIntyre, D. H., E. B. Ekren, and R. F. Hardyman, 1982, Stratigraphic and structural framework of the Challis Volcanics in the eastern half of the Challis 1° x 2° quadrangle, Idaho, *in* Bill Bonnichsen and R. M. Breckenridge, editors, Cenozoic Geology of Idaho: Idaho Bureau of Mines and Geology Bulletin 26.

Ross, C. P., 1934, Geology and ore deposits of the Casto quadrangle, Idaho: U. S. Geological Survey Bulletin 854, 135 p.

Shannon, S. S., Jr., and S. J. Reynolds, 1975, A brief geological survey of the east Thunder Mountain mining district, Valley County, Idaho: Idaho Bureau of Mines and Geology Information Circular 29, 13 p.

Steiger, R. H. and E. Jager, 1977, Subcommission on geochronology: convention on the use of decay constants in geo- and cosmochronology: Earth and Planetary Science Letters, v. 36, p. 359-362.

Early Tertiary-Age Kamiah Volcanics, North-Central Idaho

by

Robert W. Jones[1]

ABSTRACT

The Kamiah Volcanics form Kamiah Buttes, a group of kipukas rising 1,000 feet above the Clearwater plateau, 7 miles southwest of Kamiah in Idaho County, Idaho. The outcrop area is about 22 square miles. The Kamiah Volcanics rest unconformably on granites of the Cretaceous-age Idaho batholith and are overlain by, and protrude through, lava flows of the Columbia River Basalt Group of Miocene age. The stratigraphic relations suggest correlation with the Challis Volcanics of Eocene age.

The Kamiah Volcanics are flat-lying and consist of two units. The upper unit of about 1,000 feet of andesite consists of a number of thin lava flows and a subordinate amount of pyroclastic deposits. In outcrop and hand specimen, the andesite lava flows could be confused with basalt flows of the Columbia River Basalt Group. In thin section, obvious differences are the lower color index (10-20) and strongly alined groundmass plagioclases of the andesite. The lower unit of the Kamiah Volcanics is at least 300 feet of quartz latite that contains one or more thick, vitrophyric lava flows and a small amount of pyroclastic rocks. Four chemical analyses show that the rocks are typical andesites and quartz latites. Petrology and chemistry support, but do not prove, correlation with the Challis Volcanics.

Along with the volcanic rocks at Potato Hill near Deary, 45 miles to the north, the Kamiah Volcanics may be either remnants of a once much larger Challis Volcanic field or isolated centers of Challis-age volcanism.

INTRODUCTION

The Kamiah Buttes are kipukas of older Tertiary volcanic rocks surrounded by Miocene lava flows of the Columbia River Basalt Group. The Kamiah Volcanics consist of an upper andesite unit about 1,000 feet thick which lies on a lower quartz latite unit that is 300 or more feet thick. The andesites of the upper unit resemble the basalts and could be confused with them in the field, but the quartz latites of the lower unit are distinctive. The purpose of my report is to describe the rocks of the Kamiah Volcanics, to explain how to tell the andesites from the basalts, and to discuss the possible correlation of the Kamiah Volcanics with the Challis Volcanics of east-central Idaho.

The original northern and western limits of the Challis Volcanics field are uncertain because of the removal of the rocks by erosion, the lack of detailed mapping, and the substantial cover by the Columbia River Basalt Group. Armstrong (1974) has presented evidence that igneous activity of Challis age was widespread beyond the present limits of the Challis Volcanics field. It is possible that the original Challis Volcanics field extended into the area now covered by the Columbia River Basalt Group or that isolated volcanic centers were active in that area during Challis time. The Kamiah Volcanics could be a remnant of the original field or one of the isolated centers.

LOCATION AND ACCESS

The Kamiah Buttes rise as much as 1,000 feet above the general level of the Clearwater embayment of the Columbia Plateau in Idaho County, Idaho (Anderson, 1930; Ross and Forrester, 1958; Bond, 1963). The two larger buttes are Big Butte, elevation 3,382 feet, to the north (Figure 1), and Twin Buttes, elevation 3,745 feet, to the south. A small, isolated butte, locally known as "Lone Butte," is about 3 miles east of Big Butte. The buttes may be reached from Kamiah by Idaho Highway 62 and from Nezperce or Grangeville by Idaho Highway 7. County roads and farm roads provide convenient access within the area. The area is within the U. S. Geological Survey's

[1]Department of Geology, University of Idaho, Moscow, Idaho 83843.

Jones, R. W., 1982, Early Tertiary-age Kamiah Volcanics, north-central Idaho, *in* Bill Bonnichsen and R. M. Breckenridge, editors, Cenozoic Geology of Idaho: Idaho Bureau of Mines and Geology Bulletin 26, p. 43-52.

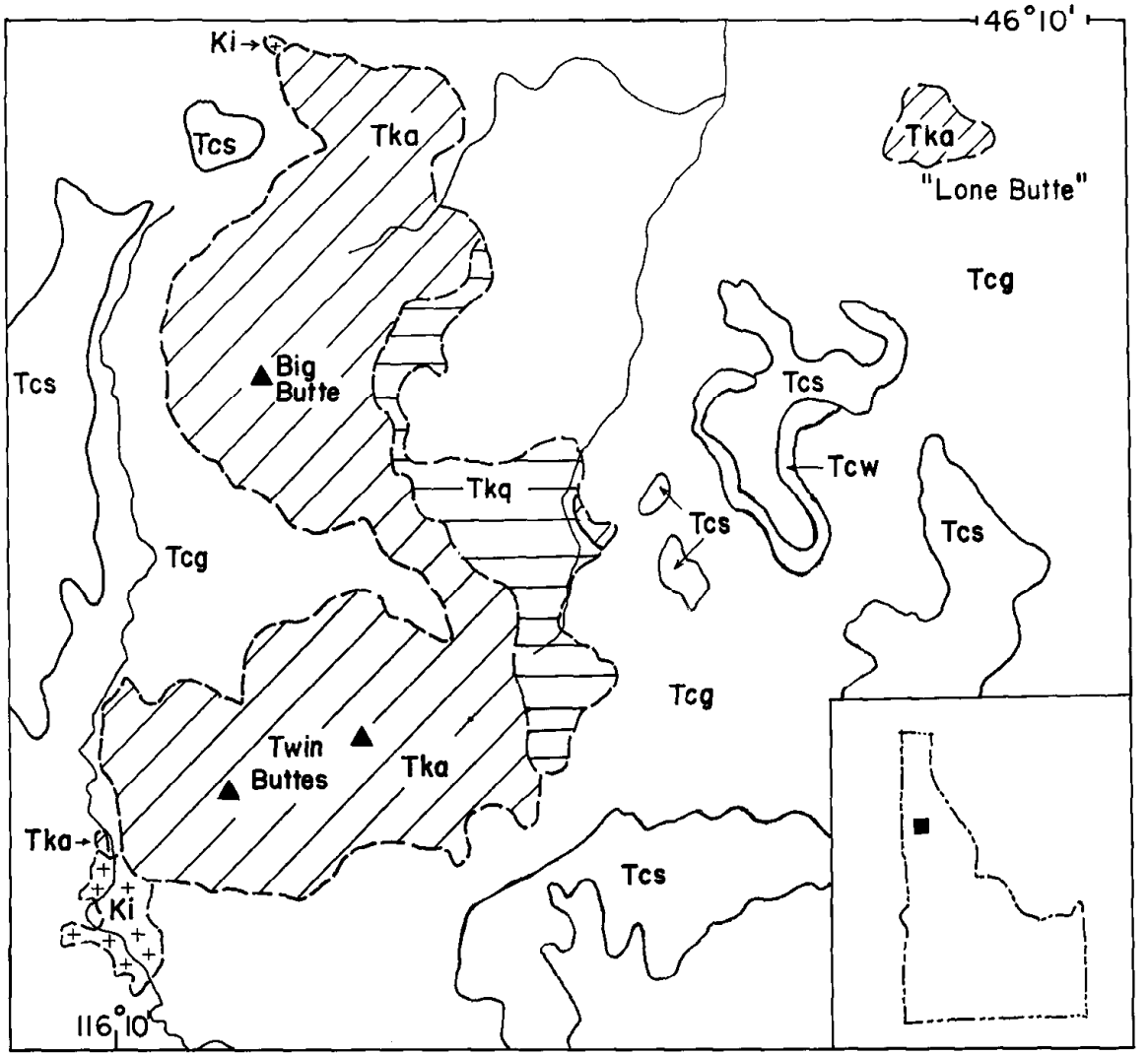

Kamiah Volcanics and Idaho batholith? by R.W. Jones (1974). Columbia River Basalt Group from Geologic Map of the Pullman quadrangle (Rember and Bennett, 1979).

Columbia River Basalt Group

Miocene

Tc — Tcs Saddle Mountain Basalt; Tcw Wanapum Basalt; Tcg Grande Ronde Basalt

Kamiah Volcanics

Eocene

Tka — Andesite

Tkq — Quartz latite

Idaho batholith?

Cretaceous

Ki — Granite

Explanation

▲ Peak

Approximate contact

Creek

0 1 2 miles

N

Figure 1. Geology of the Kamiah Buttes area, Idaho County, Idaho.

Nezperce, Nezperce SW, Nezperce SE, and Kamiah 7½-minute quadrangles.

PREVIOUS STUDIES

Anderson (1930, p. 24) recognized that the Kamiah Buttes are partially buried hills of older volcanic rocks which protrude through the Columbia River Basalt Group. He stated that two rock types are present, andesite and quartz latite, and suggested a correlation with the Challis Volcanics of east-central Idaho. Bond (1963) recognized that "Lone Butte" is also underlain by Kamiah Volcanics.

STRATIGRAPHIC UNITS

PALOUSE FORMATION

Loess of the Pleistocene-age Palouse Formation is the youngest geologic unit in the area. It mantles most of the flatter areas of the Clearwater plateau, forms an apron around the base of the buttes, and extends up onto some of the flatter areas, especially on Twin Buttes.

COLUMBIA RIVER BASALT GROUP

The next youngest unit is the Columbia River Basalt Group, a widespread sequence of subaerial basalt flows and sedimentary interbeds that are mostly Miocene in age. Columbia River basalt flows crop out in gulches and stream valleys on all sides of the buttes. The basalts are essentially flat-lying and rest unconformably on the erosion surface cut into the Kamiah Volcanics. The actual contact is mostly covered by loess. A flat-lying contact is exposed along the upper reaches of Thorn Creek on the northern part of Big Butte (SW¼SW¼ sec. 32, T. 33 N., R. 3 E.). A steeply dipping contact cuts across a gulch north of the county road along the southwest corner of Twin Buttes (SW¼SW¼ sec. 24, T. 32 N., R. 2 E.). In general, the contacts are the steeply dipping sides of hills of flat-lying Kamiah Volcanics around which flowed flat-lying lavas of the Columbia River Basalt Group.

The stratigraphic nomenclature of the Columbia River Basalt Group has been worked out by Swanson and others (1979) and is reviewed by Camp and others (1982 this volume). The basalts of the Clearwater embayment were first mapped in detail by Bond (1963). The basalt units shown in Figure 1 were taken from the geologic map of the 1° x 2° Pullman quadrangle (Rember and Bennett, 1979). The units present are Saddle Mountains Basalt, Wanapum Basalt, and Grande Ronde Basalt. The Imnaha Basalt does not crop out in the map area, but is present elsewhere in the Clearwater embayment.

KAMIAH VOLCANICS

Anderson (1930, p. 24) named the Kamiah Volcanics, assigned them formational rank, and gave the type area as Kamiah Buttes. He recognized that two major rock groups—the andesite of Kamiah Buttes and the quartz latite of Kamiah Buttes—are present. Anderson suggested correlating the Kamiah Volcanics with the Challis Volcanics because of position in the stratigraphic sequence and similarity in lithology. No radiometric ages are available for the Kamiah Volcanics, but many dates of 40 to 50 million years have been obtained from the Challis Volcanics (Armstrong, 1974; Leonard and Marvin, 1982 this volume; McIntyre and others, 1982 this volume). The nearest recognized Challis Volcanics are at Thunder Mountain, about 90 miles southeast of Kamiah Buttes (Leonard, 1975; Leonard and Marvin, 1982 this volume).

The stratigraphically higher part of the andesite of Kamiah Buttes may be studied on the southwest side of Big Butte, along a bearing southwesterly from the Winona benchmark, elevation 3,879 feet, downhill to about elevation 3,200 feet, where the rocks become covered by loess. The lower part may be studied on the west side of Twin Buttes, from about elevation 2,800 feet near Yellow Bull Spring along a northeasterly bearing uphill to about elevation 3,350 feet. Representative exposures of the quartz latite of Kamiah Buttes are scattered on the east side of the buttes; the most accessible outcrop is near milepost 15 on Idaho Highway 62. Several others are east of Mt. Zion Cemetery, on the east side of Twin Buttes.

The contact between the andesite of Kamiah Buttes and the quartz latite of Kamiah Buttes is not exposed. A break in slope at about elevation 3,080 feet seems to coincide with the contact along the east side of Twin Buttes. This contact has been provisionally extended north, along the east slopes of Big Butte (Figure 1). The Kamiah Volcanics rest on an erosion surface cut in granitic rocks that probably are related to the Idaho batholith. The actual contact was not seen, but is close to the surface in several places, such as about 100 feet south of Yellow Bull Spring (NE¼SE¼ sec. 23, T. 32 N., R. 2 E). The minimum thickness of the Kamiah Volcanics is about 1,500 feet.

IDAHO BATHOLITH

The granitic rocks exposed at the southwest end of Twin Buttes are medium-grained granites to granodiorites. Similar rocks make up the nearest exposures of the main Idaho batholith at Lowell, about 30 miles east of Kamiah Buttes. Other granites exposed in the Clearwater embayment are assigned to the Idaho batholith by Rember and Bennett (1979).

ANDESITE OF KAMIAH BUTTES

Anderson (1930, p. 25) described the andesites of Kamiah Buttes as mostly grayish and vesicular with some being reddish. He reported up to 18 percent phenocrysts, mostly andesine plus a little augite, set in a microcrystalline matrix of andesine laths, glass, and magnetite. He stated that some rocks show flow structures that may not be obvious in hand specimen but that are pronounced in thin section. My studies confirm most of Anderson's observations but show that the plagioclase is labradorite rather than andesine, and that olivine, bronzite, and pigeonite phenocrysts are present in addition to augite. I also found pyroclastic deposits that Anderson did not mention. The minimum thickness of the andesite sequence is about 1,080 feet.

LAVA FLOWS

The andesite lava flows are poorly exposed so that individual flows cannot be traced for any distance. Overall, the layering is nearly horizontal but individual flows are made up of numerous thin flow units that are mutually unconformable and change in appearance laterally.

Platy joints, spaced 5 to 20 millimeters apart, are common. These partings cause the rocks to split into slabs of equal thicknesses. Their attitudes characteristically vary markedly within distances of a few feet and have no simple relationship to the overall horizontal attitude of the flows. Steeply dipping platy structures are more common than those with shallow dips, probably because the shallow dipping surfaces were more easily covered by the loess. The platy structures are thought to follow the shear zones along which these fairly viscous lavas moved.

Columnar joints were seen in only one outcrop, a roadcut on the northwest side of Big Butte (NW¼NE¼ sec. 36, T. 33 N., R. 2 E.). The columns are vertical and about 6 inches in diameter. The outcrop resembles an outcrop of Wanapum Basalt, but thin section study shows the rock to be the andesite of Kamiah Buttes.

Open-textured rocks are common and include very vesicular zones and flow breccias. Flow breccias and related rocks are very well displayed at Red Rock Butte (NW¼SW¼ sec. 23, T. 32 N., R. 2 E.). The lower slopes of the west side of Twin Buttes have a high proportion of units that are open-textured throughout. Elsewhere, open textures typically occur in flow-top and flow-bottom breccias that make up about 10 percent of the thickness of the sequence.

Hand Specimen Appearance

Much of the andesite consists of dense, aphanitic, holocrystalline rock that contains 5 to 20 percent plagioclase phenocrysts up to 2 millimeters long. Some rocks contain fresh pyroxene phenocrysts up to 1 millimeter in length, and some contain 1 to 15 percent of red, red-brown, or brown iddingsite which pseudomorphs olivine or orthopyroxene. Fresh olivine is not generally visible in hand specimens.

The fresh dense rock is dark to medium dark gray, or olive gray. Some of the dense rocks are mottled with thin, lenticular yellowish gray zones. Where platy structure is present, the mottled lenticles commonly are elongate parallel to the joints. Some of the mottling is irregular in shape and shows no relation to platy structure. Oxidized phases of the dense rock are yellowish brown or pale red or dark red.

The dense, platy to massive rocks probably formed in the interiors of flow units, whereas the open-textured rocks probably formed at flow tops and bottoms and in zones of internal inconsistency. The open-textured rocks range from moderately vesicular to scoriaceous, and some exhibit various slaggy or brecciated structures. The slaggy rocks commonly consist of partially rounded clasts, generally about an inch across, with or without a matrix of fine-grained to glassy lava. In a few places, the matrix has been autointruded between the clasts. The open-textured rocks are similar in color to the dense rocks, but tend to be more brown or red.

Mineralogy and Petrography

I studied fifteen thin sections of the andesite of Kamiah Buttes in detail; an additional thirty-three sections were scanned for fabrics and mafic mineral identification. Most of the specimens are from the dense rocks on Big Butte and Twin Butte; a few are from the open-textured rocks. Two are dense specimens from Lone Butte, and one is from a dike that cuts the quartz latite of Kamiah Buttes.

All contain plagioclase and pyroxene in a ratio of about 5 plagioclase to 1 pyroxene. About half contain

olivine, which generally is at least partly altered to iddingsite. Other minerals present are groundmass opaques and alteration products of glass and plagioclase. Traces of biotite were found in one specimen. Glass is common in the open-textured rocks and is present in a few of the dense rocks. Modes of the holocrystalline rocks are plagioclase, 70 to 80 percent; pyroxenes, 10 to 20 percent; olivine and iddingsite, 0 to 15 percent; and opaques, 1 to 5 percent. Fabrics are seriate prophyritic with plagioclase laths up to 1.5 millimeters long, and pyroxene and olivine phenocrysts up to 1 millimeter across. Matrix grains are about 0.1 to 0.3 millimeter in diameter. Most of the specimens are holocrystalline; five contain glass in amounts of 1 to 20 percent.

The plagioclase grains are subhedral tabular with width to length ratios ranging from 1:3 to 1:10. The grains are moderately to strongly alined in forty-one of the forty-eight specimens examined. In a few specimens, two directions of alinement are present, with most of the grains alined in one direction, and narrow zones of grains with a different alinement cutting across the main trend. The alinements probably resulted from flow in moderately viscous lava, and the cross-cutting zones probably were caused by later flow regime changes. Both phenocryst and matrix plagioclase grains show albite twins. In a few specimens, combined Carlsbad-albite twins are common. Most of the phenocrysts show combined normal and oscillatory zoning. Anorthite contents of phenocrysts range from An_{50} to An_{70} and that of the matrix grains range from An_{50} to An_{60}.

Both the phenocryst and matrix pyroxenes are colorless and range from crudely columnar to rounded anhedral. The type of pyroxene was determined for nineteen specimens. Both clinopyroxene and orthopyroxene are present in thirteen. Most contain both augite and pigeonite. Some contain only clinopyroxene or clinopyroxene plus orthopyroxene, but none contain only orthopyroxene. Most of the specimens that contain orthopyroxene do not contain olivine; these minerals occur together in only four specimens. The pyroxenes are generally fresh, although orthopyroxene cores occur in iddingsite grains in a few rocks.

The clinopyroxenes have optic angles of 40 to 60 degrees, and in many the optic planes are at an angle to the (110) cleavage trace, indicating they are pigeonites. Some grains have different optic angles in different places, suggesting that they are zoned augite and pigeonite. The orthopyroxenes are optically positive and generally have optic angles of 70 to 90 degrees, or locally in the 60 to 70 degree range, suggesting that most are bronzites and the rest are hypersthenes.

Unaltered olivine is colorless in the andesite but it is rare; all of the olivine grains are fresh in only three of the sections studied. In the rest, the olivine is more or less altered, commonly to iddingsite. The fresh olivine grains and iddingsite pseudomorphs normally exhibit anhedral, more or less rounded shapes but euhedral grains locally are present. Optic angles are between 80 and 90 degrees, and both positive and negative optic signs were obtained indicating that the olivine is magnesium-rich.

Most of the opaque grains are black in obliquely incident reflected light. Most are 0.01 to 0.03 millimeter in diameter and confined to the groundmass; in a few specimens they are as large as 0.4 millimeter. Most of the grains are anhedral and rounded, but some with diamond, square, or rectangular shapes indicate an octahedral mineral, probably magnetite. In a few specimens the edges of the grains are red, suggesting hematite, and in others the opaques have been oxidized to red or brown iron oxides. Opaque grains with elongate shapes suggestive of ilmenite occur in only two of the thin sections.

With the exception of olivine and orthopyroxene, most of the minerals in the andesites are fresh. Red, red-brown, or brown pseudomorphs of weakly pleochroic to nonpleochroic iddingsite replacing olivine or orthopyroxene phenocrysts are conspicuous in twenty-one of the specimens studied. In thirteen, cores of olivine or orthopyroxene are present. Olivine cores are far more abundant than those of orthopyroxene. Iddingsite was not seen in the groundmass. According to Wilshire (1958), iddingsite may form from olivine or orthopyroxene either by deuteric alteration or by weathering. Because the other minerals are not altered, the iddingsite is considered to be a weathering product. Olivine also is locally altered to pale brown, pale yellow brown, or pale green micaceous minerals with moderate birefringences and normal interference colors that may be clay minerals of the smectite group.

Some specimens from the southwestern slopes of Twin Buttes have altered plagioclases, but fresh pyroxenes. The outer more sodic zones are fresh, but the inner more calcic zones have been replaced by a pale brown mineral with a micaceous habit and moderate, normal interference colors. This also may be a smectite group mineral.

PYROCLASTIC DEPOSITS

Pyroclastic rocks are exposed several places within the andesite of Kamiah Buttes. Most of the exposures are in the lower part of the sequence, suggesting that the eruptions began with pyroclastic activity and then changed to lava-flow activity.

A bedded, well-sorted lapillistone crops out for 300 feet along the east bank of the creek followed by a county road in NW¼SE¼ sec. 14, T. 32 N., R. 2 E., on the west edge of Twin Butte. The base of this exposure is covered by alluvium, and the pyroclastics are overlain by a flow of dense, platy andesite; the exposed thickness is about 30 feet. The clasts are very vesicular and range from 2 to 10 millimeters in diameter; many are 2 to 5 millimeters. The colors are light gray or light to dark brown or yellowish brown, contrasting with the darker colors of the andesite flows. The one thin section studied shows the clasts to be very fine grained to glassy. Many contain plagioclase microlites; a few contain small phenocrysts of pyroxene.

Another exposure on the northeast part of Big Butte (NW¼NW¼ sec. 29, T. 33 N., R. 3 E.) is about 1,000 feet long and 12 feet thick. The rocks are lapillistones and tuff breccias that contain a few bombs of dense andesite; the base is covered by loess. Many of the clasts are lapilli-size, are very finely vesicular, and are light to dark gray to red.

On the south edge of Twin Buttes (NW¼ sec. 20 and SW¼ sec. 19, T. 32 N., R. 2 E.), road cuts and drainage ditches show some poor exposures of poorly- to well-sorted volcaniclastic and epiclastic rocks.

DIKES

Two nearly vertical dikes of andesite cut across the quartz latite of Kamiah Buttes in a road cut at milepost 15 on Idaho Highway 62 (SW¼SW¼ sec. 4, T. 32 N., R. 3 E.). The southern dike is about 12 feet wide; the northern dike is at least 15 feet wide, but its northern edge is covered.

The dike rocks are typical, massive, grayish-brown weathering andesite. The fresh rock is medium dark gray and is sprinkled with a few rounded white phenocrysts about 1 millimeter in diameter. The rock contains 20 percent plagioclase phenocrysts and 1-2 percent pyroxene phenocyrsts in a microcrystalline matrix that is mostly plagioclase. The plagioclase phenocrysts are fresh, subhedral-tabular, and show a continuous range of lengths from 0.4 to 2.0 millimeters; many are 0.4 to 0.8 millimeter. The pyroxenes are augite, pigeonite, and bronzite in about equal amounts; most are columnar and 0.5 to 1 millimeter in length.

Although the color index is very low, the dikes are sufficiently similar to the andesite of Kamiah Buttes to be correlated to it. These dikes and perhaps others probably fed the extrusions of the andesite of Kamiah Buttes.

COMPARISON OF THE ANDESITE OF KAMIAH BUTTES WITH THE COLUMBIA RIVER BASALT

Basalt units in the vicinity of Kamiah Buttes belonging to the Columbia River Basalt Group include the Saddle Mountains Basalt, Wanapum Basalt, and Grande Ronde Basalt. The Imnaha Basalt crops out nearby (Rember and Bennett, 1979). The properties described in this section for the basalts are those exhibited in the vicinity of Kamiah Buttes; they may not apply to the Columbia River Basalt Group elsewhere.

In outcrop, the andesites commonly show well-developed platy joints spaced at 5 to 20 centimeters; attitudes on the platy partings change greatly over short distances. In the basalts, such joints are less common and more widely spaced, with attitudes that change gradually. Columnar joints are rare in the andesites and common in the basalts. Flow breccias are common in the andesites and are rare in the basalts. Although their overall outcrop colors are similar, the andesites tend to be more gray and the basalts more brown. Air-fall pyroclastics are a significant phase of the andesites and are absent in the basalts.

In hand specimen, the andesites contain 5 to 20 percent plagioclase phenocrysts plus 1 to 2 percent pyroxene phenocrysts or iddingsite pseudomorphs after olivine or pyroxene. Most of the phenocrysts are about 1 millimeter in diameter; the largest are 2 millimeters. In the basalts, phenocrysts are absent in the Grande Ronde Basalt, but the Wanapum Basalt and the Saddle Mountains Basalt may contain olivine and plagioclase phenocrysts. The phenocrysts can be larger than those in the andesites; plagioclase may be as much as 10 millimeters in length. The Imnaha Basalt typically contains a sprinkling of plagioclase phenocrysts up to 4 centimeters long.

The weathered color of the andesite tends to be olive gray, whereas the basalts tend to weather to some shade of brown. Some parts of the Wanapum Basalt weather to a light gray that resembles the weathered color of the andesites. The fresh colors of the andesites and the basalts overlap considerably; both commonly are dark gray or dark brown. However, some of the andesites are reddish browns that do not occur in the basalts, and some of the basalts are yellowish browns, blue grays, or blue blacks that do not occur in the andesites.

The differences between the andesites and the basalts are most obvious in thin section. The most diagnostic characteristic is color index; that of the andesites generally ranges from 10 to 20 and seldom exceeds 30 whereas that of the basalts generally is

greater than 40. Another striking difference is that many of the andesites have strongly alined groundmass plagioclase laths whereas the groundmass of the basalts nearly always is directionless. Olivine phenocrysts or pseudomorphs of iddingsite after olivine or orthopyroxene are common in the andesites. They are absent in the Grande Ronde Basalt, but may occur in the other three basalt units. Both augite and pigeonite are common as phenocrysts in the andesites, and about half of them have phenocrysts of orthopyroxene. In the basalts, pyroxenes do not form phenocrysts and orthopyroxenes are absent.

QUARTZ LATITE OF KAMIAH BUTTES

According to Anderson (1930, p. 25), a flow of quartz latite crops out extensively along the southeast margin of Kamiah Buttes. He described the rock as light gray with a flow structure shown by widely spaced glassy layers, and containing a few phenocrysts of andesine, quartz, and biotite set in a groundmass of orthoclase, oligoclase, and much glass. I could not confirm the presence of orthoclase in the groundmass.

My studies suggest that the quartz latites mostly were vitrophyric lava flows that are now largely devitrified. I also found air-fall pyroclastics that seem to be related to the quartz latites. The base and the top of the unit are covered. Assuming the layering is horizontal, the minimum thickness is about 300 feet. I did not find any internal contacts within the unit and do not know if it is only one flow or composed of several flows.

LAVA FLOWS

Outcrop and Hand Specimen Appearance

Natural outcrops of the quartz latite of Kamiah Buttes are few and small. The most accessible exposures of fresh vitrophyre are in a roadcut and in nearby natural exposures at milepost 15 on Idaho Highway 62 (SW¼SW¼ sec. 4, T. 32 N., R. 3 E.). The vitrophyre is grayish black where fresh and weathers yellowish brown with patches of yellowish gray. Plagioclase phenocrysts make up 20 percent of the rock; they are clear, glassy to slightly translucent, subhedral, and 1 to 2 millimeters long. Flow structure is absent but perlitic structure is weakly developed. Near the dikes of the andesite of Kamiah Buttes, weathering accentuates local color contrasts in the quartz latite. These may represent shear which took place during emplacement of the dikes.

Another exposure is in a roadcut 0.6 mile south of milepost 15 at the junction of Idaho Highway 62 and two county roads (NW¼SW¼ sec. 9, T. 32 N., R. 3 E.). The rock here is fully devitrified and weathers pale yellowish brown; the fresh color is brownish gray. Flow layering is prominent and shows as streaks, layers, and lenses of pinkish gray. This is the only outcrop in which this type of quartz latite was seen. The more typical devitrified rock is exposed in small outcrops, such as in the ditches along the county road south from the junction. The fresh rock is light gray, grayish red, or dark red. Flow structure shows as alternating lighter and darker layers that pinch and swell and range from several millimeters to a centimeter in thickness.

Mineralogy and Petrography

I studied nine thin sections of the quartz latite of Kamiah Buttes. Three are fresh vitrophyres, two are devitrified but not altered, and four had been devitrified and altered in different amounts. All contain 10 to 20 percent plagioclase phenocyrsts up to 2 millimeters in length. About half contain 1 to 2 percent of greenish brown to brown hornblende. Traces of pyroxene are present in a few, but no potassium feldspar crystals were recognized.

About half of the specimens show flow layering, such as differences in color, or layers of spherulitic devitrification alternating with layers of granophyric devitrification, or stringers of partially collapsed pumice. Crystals do not show preferred orientation. Incipient perlitic structure is common in the specimens with fresh glass. Most of these rocks have a sprinkling of crystallites in the matrix. Devitrification has most commonly resulted in spherulitic structure, but axiolitic structures also are present. Granophyric devitrification has occurred in a few specimens.

The plagioclase phenocrysts show albite twins and are weakly zoned. Anorthite contents range from An_{37} to An_{50}. In one specimen, the plagioclase phenocrysts contain abundant inclusions of glass. In about half of the specimens, the plagioclase is strongly altered to clay minerals.

In most of the specimens, quartz is not present as phenocrysts. In several devitrified specimens, quartz is present in granophyric intergrowths with feldspar or in lenses of small crystals lying parallel to the flow layering.

Phenocrysts of mafic minerals are so scarce that little data could be obtained. The hornblendes are subhedral to euhedral, greenish brown to brown, and have negative optic angles of about 70 degrees. Pyroxenes are colorless; both optically positive and optically negative forms are present, suggesting that both clinopyroxene and orthopyroxene are present.

PYROCLASTIC DEPOSITS

Pyroclastic and epiclastic rocks that probably are related to the quartz latite of Kamiah Buttes crop out at the northwest edge of Big Butte, near the barns and at the loading areas at the base of the grain storage bins at the Gille ranch in SW¼SW¼ sec. 19, T. 33 N., R. 3 E. These deposits consist of light-colored, bedded and nonbedded tuffs and lapillistones. Fresh, transparent, pale gray glass in rounded grains up to 10 millimeters in diameter forms cores of some of the lapilli. Clasts of nonvolcanic rocks, such as quartzites and granites, are present as well as clasts of the andesite of Kamiah Buttes.

In one part of the exposure, a nonbedded tuff is overlain by an epiclastic conglomerate containing granitic and volcanic clasts. This conglomerate is overlain by a flow of the andesite of Kamiah Buttes that, in turn, is overlain by colluvium. In another part of the exposure, the andesite seems to have intruded the pyroclastic-epiclastic sequence. A buried soil zone is present within the pyroclastic-epiclastic sequence in another part of the exposure. Deeply weathered granitic rock crops out within a few feet of the pyroclastic-epiclastic exposures, but the contact is not exposed. The above observations indicate that an interval of erosion and sediment deposition occurred between extrusion of the quartz latite and the andesite of Kamiah Buttes.

CHEMISTRY

Analyses of four samples from the Kamiah Volcanics (Table 1) confirm Anderson's (1930) petrographic classifications of the rocks. The two andesites are typical andesites and the two quartz latites are typical as the term was used in Anderson's time. In the International Union of Geological Sciences classification (Streckeisen, 1979), the quartz latites would be classed as rhyolites.

Correlation of the Kamiah Volcanics with the Challis Volcanics on major element chemistry cannot yet be done because the range of chemical compositions of the Challis Volcanics is unknown. At least some of the andesites of the Challis Volcanics contain significantly more K_2O than those of the Kamiah Volcanics, but low-K_2O andesites also are present in the Challis (Ross, 1962; Buffa, 1976; McIntyre and others, 1982 this volume). Rocks with chemistries very similar to the quartz latites of Kamiah Buttes are present in the Challis Volcanics (R. W. Jones and T. E. Smith, unpublished analyses). The available data indicate that the correlation of the two units is possible, but does not confirm the correlation.

Table 1. Chemical analyses of rocks from the Kamiah Volcanics. [Analyzed by Frank Fenne, at the Department of Geology, Washington State University, using pressed-powder samples in a Philips X-ray fluorescence instrument. Analyses are normalized to a 100 percent sum on a volatile-free basis. Fe_2O_3 and FeO are calculated from the total iron by the method of Irvine and Barringer (1971).]

	1	2	3	4
SiO_2	58.12	55.63	73.11	73.33
Al_2O_3	17.83	19.29	13.68	13.55
Fe_2O_3	2.46	2.66	1.84	1.97
FeO	4.85	4.62	0.84	1.64
MgO	2.87	3.12	0.44	0.55
CaO	7.28	7.87	2.12	1.59
Na_2O	3.35	3.40	2.91	3.20
K_2O	1.95	1.90	4.49	3.49
TiO_2	0.96	1.16	0.34	0.47
P_2O_5	0.25	0.27	0.14	0.13
MnO	0.09	0.09	0.08	0.08
CIPW NORMS				
q	10.97	6.98	34.19	37.16
c			0.51	1.93
or	11.52	11.22	26.54	20.62
ab	28.33	28.74	24.63	27.08
an	27.87	31.79	9.60	7.04
wo	2.76	2.3		
en	7.14	7.76	1.10	1.37
fs	5.45	4.53		0.76
mt	3.56	2.85	1.98	2.86
hm			0.47	
il	1.82	2.20	0.65	0.89
ap	0.59	0.64	0.33	0.31

1. Andesite of Kamiah Buttes, southwest side of Big Butte, about 500 feet southwest of Winona benchmark (SW¼NW¼ sec. 1, T. 32 N., R. 2 E.)
2. Andesite of Kamiah Buttes, southwest side of Big Butte, about 1,800 feet southwest of Winona benchmark (SW¼NW¼ sec. 1, T. 32 N., R. 2 E.)
3. Fresh vitrophyre of quartz latite of Kamiah Buttes, road cut at milepost 15 on Idaho Highway 62 (SW¼SW¼ sec. 4, T. 32 N., R. 3 E.)
4. Devitrified and altered quartz latite of Kamiah Buttes, roadcut at mile 15.6 on Idaho Highway 62 (NW¼SW¼ sec. 9, T. 32 N., R. 3 E.)

DISCUSSION

By about mid-Eocene time, the granitic rocks of the Cretaceous-age Idaho batholith had been uplifted and eroded. More than 300 feet of the quartz latite of Kamiah Buttes was extruded and probably subjected to an interval of erosion and weathering. Dikes of the andesite of Kamiah Buttes then cut through the

quartz latites and served as feeders for eruption of the andesites. Some of the vents are probably within the present outcrop area of the Kamiah Volcanics and are represented by the poorly sorted pyroclastic deposits of the andesite. More than 1,000 feet of flat-lying andesite was extruded, but the lateral extent of the field is not known. These eruptive events probably took place during the same time interval as the eruption of the Challis Volcanics to the east and south.

A new event of erosion carved out the buttes and removed most of the volcanic deposits. A surface with more than 1,000 feet of relief formed. In Miocene time, Columbia River basalt flows covered the Clearwater embayment and lapped up onto the flanks of the buttes. Renewed erosion cut deep canyons into the basalts. The area was blanketed with loess during Pleistocene(?) time.

Several other buttes of older rocks protrude through the basalts in the Clearwater embayment (Rember and Bennett, 1979). However, they are composed of granitic rocks of the Idaho batholith or metasedimentary and metamorphic rocks of the Seven Devils Group of Permian and Triassic age. The metavolcanic rocks of the Seven Devils Group do not resemble the Kamiah Volcanics.

Near Deary, about 45 miles north-northwest of Kamiah Buttes, Potato Hill is underlain by probable older Tertiary-age volcanic rocks (Bitten, 1951). The volcanic rocks of Potato Hill resemble the Kamiah Volcanics in that dark-colored lava flows overlie light-colored lava flows. They have broadly the same stratigraphic relations in that the volcanic rocks of Potato Hill rest on an erosion surface cut into the granitic rocks of the Idaho batholith. Flows of the Columbia River Basalt Group rest in turn on an erosion surface cut into the volcanic rocks of Potato Hill. However, the kinds of volcanic rock differ at Kamiah Buttes and Potato Hill. The dark-colored flows at Potato Hill are heterogenous, polylithologic flow breccias unlike anything at Kamiah Buttes. The felsic rocks of Potato Hill do not resemble the quartz latites of Kamiah Buttes in that they are much less glassy, have fewer phenocrysts, and have closely spaced flow layering. Bitten (1951) reported that features indicative of pyroclastic-flow origin are present in some of the felsic rocks of Potato Hill. I did not see any such features in the felsic rocks at Kamiah Buttes.

The two sequences resemble each other in that an event of felsic volcanism was followed by an event of more mafic volcanism during the broad span of geologic time that followed the uplift and erosion of the Idaho batholith, but preceded the extrusion of the Columbia River Basalt Group.

Both the Kamiah Volcanics and the volcanic rocks of Potato Hill probably once were more extensive than they are now. They might be the remnants of a once continuous field of Challis-age volcanic rocks that covered this part of northern Idaho and linked up with the main field to the south and east. On the other hand, they might be isolated centers of Challis-age volcanism. Other, as yet unrecognized, older Tertiary-age volcanic rocks may be present in northern Idaho.

ACKNOWLEDGMENTS

The Idaho Bureau of Mines and Geology furnished field support, thin sections, and assistance in preparation of the manuscript. The X-ray fluorescence instrument was made available by the Geology Department of Washington State University. Frank Fenne, then a graduate student at the University of Idaho, did the analyses. Appreciation is expressed to the land owners of the Kamiah Buttes area for permitting me to enter their property and for providing useful information on access.

REFERENCES

Anderson, A. L., 1930, The geology and mineral resources of the region about Orofino, Idaho: Idaho Bureau of Mines and Geology Pamphlet 34, 63 p.

Armstrong, R. L., 1974, Geochronometry of the Eocene volcanic-plutonic episode in Idaho: Northwest Geology, v. 3, p. 1-15.

Bitten, B. I., 1951, Age of the Potato Hill volcanic rocks near Deary, Latah County, Idaho: University of Idaho M.S. thesis, 65 p.

Bond, J. G., 1963, Geology of the Clearwater embayment, Idaho: Idaho Bureau of Mines and Geology Pamphlet 128, 83 p.

Buffa, J. W., 1976, Geology of the SW¼ Twin Peaks quadrangle, Custer County, Idaho: University of Idaho M.S. thesis, 74 p.

Camp, V. E., P. R. Hooper, D. A. Swanson, and T. L. Wright, 1982, Columbia River basalt in Idaho: physical and chemical characteristics, flow distribution, and tectonic implications, *in* Bill Bonnichsen and R. M. Breckenridge, editors, Cenozoic Geology of Idaho: Idaho Bureau of Mines and Geology Bulletin 26.

Irvine, T. N. and W. R. A. Barringer, 1971, Guides to chemical classification of common volcanic rocks: Canadian Journal of Earth Science, v. 8, p. 523-548.

Leonard, B. F., 1975, Temporal evolution of the Thunder Mountain caldera, central Idaho: Geological Society of America, Abstracts with Programs, v. 6, no. 5, p. 622-623.

Leonard, B. F. and R. F. Marvin, 1982, Temporal evolution of the Thunder Mountain caldera and related features, central Idaho, *in* Bill Bonnichsen and R. M. Breckenridge, editors, Cenozoic Geology of Idaho: Idaho Bureau of Mines and Geology Bulletin 26.

McIntyre, D. H., E. B. Ekren, and R. F. Hardyman, 1982, Stratigraphic and structural framework of the Challis Volcanics in the eastern half of the Challis 1° x 2° quadrangle, Idaho, *in* Bill Bonnichsen and R. M. Breckenridge, editors, Cenozoic Geology of Idaho: Idaho Bureau of Mines and Geology Bulletin 26.

Rember, W. C. and E. H. Bennett, 1979, Geologic map of the Pullman quadrangle, Idaho: Idaho Bureau of Mines and Geology Geologic Map Series, scale 1:250,000.

Ross, C. P., 1962, Stratified rocks in south-central Idaho: Idaho Bureau of Mines and Geology Pamphlet 125, 126 p.

Ross, C. P. and J. D. Forrester, 1958, Outline of the geology of Idaho: Idaho Bureau of Mines and Geology Bulletin 15, 74 p.

Streckeisen, Albert, 1979, Classification and nomenclature of volcanic rocks, lamprophyres, carbonatites, and melilitic rocks: recommendations and suggestions of the IUGS Subcommission on the systematics of igneous rocks: Geology, v. 7, p. 331-335.

Swanson, D. A., T. L. Wright, P. R. Hooper, and R. D. Bentley, 1979, Revisions in stratigraphic nomenclature of the Columbia River Basalt Group: U. S. Geological Survey Bulletin 1457-G, 59 p.

Wilshire, H. G., 1958, Alteration of olivine and orthopyroxenes in basic lavas and shallow intrusions: American Mineralogist, v. 43, p. 120-147.

Chapter 2

Columbia River Basalt Group Western Idaho

Columbia River Basalt in Idaho: Physical and Chemical Characteristics, Flow Distribution, and Tectonic Implications

by

Victor E. Camp[1], Peter R. Hooper[2],
Donald A. Swanson[3], and Thomas L. Wright[4]

ABSTRACT

Flows of the Columbia River Basalt Group were extruded in Miocene time, forming an extensive plateau between the active Cascade chain of calcalkaline volcanic rocks to the west and the rising mountains of Cretaceous to early Tertiary rocks of the Idaho batholith and Challis Volcanics to the east. That part of the plateau extending into western Idaho represents the easternmost encroachment of basalt as it thins and pinches out against the western flank of the Rocky Mountains.

Most of the plateau has now been mapped at reconnaissance scale, and a coherent stratigraphy has been developed from chemical, petrographic, paleomagnetic, and field criteria. The Columbia River Basalt Group is divided into five formations, the Imnaha, Grande Ronde, Picture Gorge, Wanapum, and Saddle Mountains Basalts, of which all but the Picture Gorge Basalt occur in the Idaho portion of the plateau. We describe the chemical and physical properties of each of these formations and their distribution in Idaho. Flow distribution was influenced by (1) the location of feeder dikes, (2) the erosional topography and drainage pattern during and before extrusion, (3) the volume of flows, and (4) the deformation during the eruptive episode. The origin of all structural elements in the southeast part of the plateau can be attributed to a combination of (1) the regional westward tilting of the plateau during and after basalt extrusion, (2) the presence of a regional stress regime having a horizontal north to north-northwest axis of maximum compression and a horizontal west to west-northwest axis of minimum compression, and (3) the reactivation of an older northwest-southeast and northeast-southwest structural grain in the pre-Miocene basement.

The uplifted and deeply dissected eastern margin of the Columbia Plateau in Idaho exposes some of the earliest members of the Columbia River Basalt Group. This situation provides an opportunity to examine not only the relations between basalt and older, deeply eroded prebasalt topography but also the effects of the encroaching basalt flows on Miocene streams draining the Rocky Mountain highlands to the east. Lava dams are evident along the margin of the plateau, and repeated damming is responsible for the deposition of detritus now preserved as sediments intercalated with Columbia River basalt. The basalt-prebasalt interface is marked by numerous flows invasive into sediment, resulting in the formation of pillows, hyaloclastite, palagonite tuff, and peperite.

INTRODUCTION

Eruption of the Columbia River Basalt Group began about 17 million years ago (McKee and others, 1981) with extrusion from north- to north-northwest-trending fissures now preserved as dikes. Lava flows encroached on a rugged terrain produced by the uplift and erosion of older rocks that began in the Oligocene (Axelrod, 1968). This topography allowed the development of three lobes extending eastward from the main body of the Columbia Plateau; from south to north the lobes are the Weiser embayment, the Clearwater embayment, and the much smaller St. Maries embayment (Figure 1). Of these, the Clearwater embayment contains the most representative and complete section of the group. This paper emphasizes the basalt stratigraphy in the Clearwater embayment (Figure 1) together with the physical and chemical properties, flow

[1]c/o Directorate General of Mineral Resources, P.O. Box 5219, Jeddah, Saudi Arabia.
[2]Department of Geology, Washington State University, Pullman, Washington 99164.
[3]U. S. Geological Survey, 345 Middlefield Road, Menlo Park, California 94025.
[4]U. S. Geological Survey, 959 National Center, Reston, Virginia 22092.

Camp, V. E., P. R. Hooper, D. A. Swanson, and T. L. Wright, 1982, Columbia River basalt in Idaho: physical and chemical characteristics, flow distribution, and tectonic implications, *in* Bill Bonnichsen and R. M. Breckenridge, editors, Cenozoic Geology of Idaho: Idaho Bureau of Mines and Geology Bulletin 26, p. 55-75.

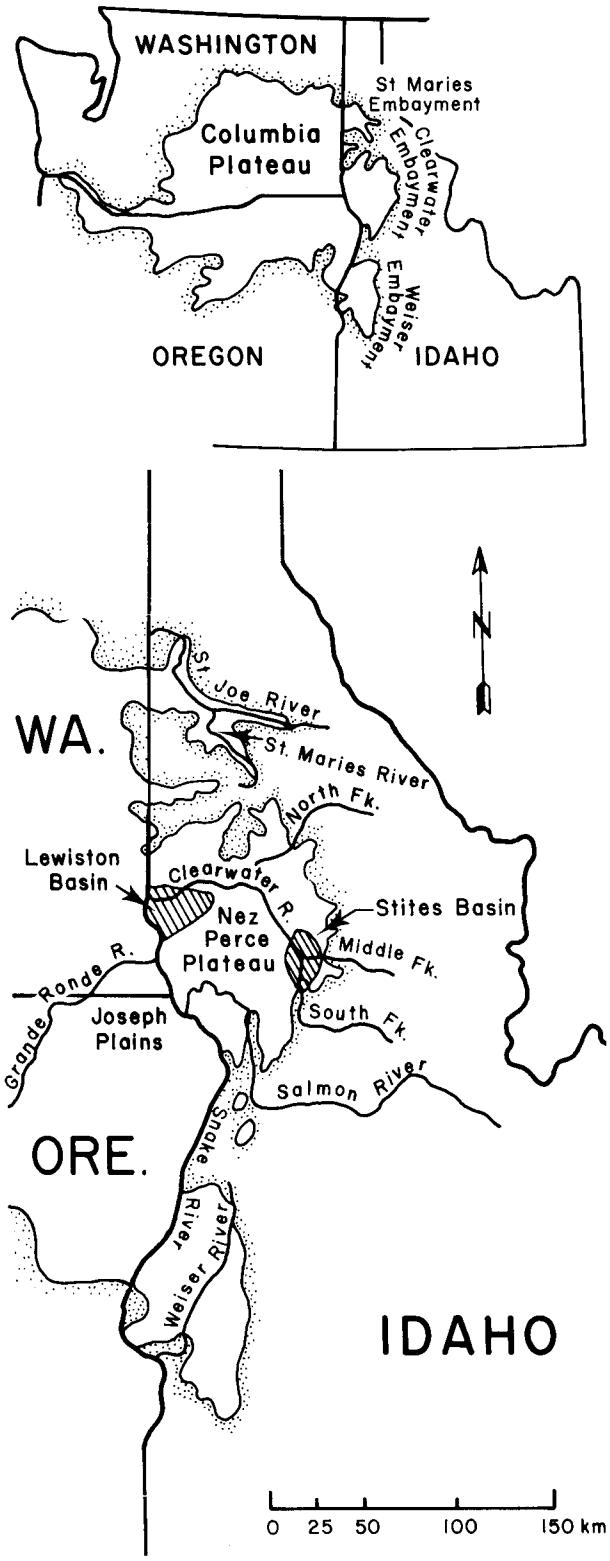

Figure 1. Location and physiographic maps of the eastern margin of the Columbia Plateau in Idaho and parts of Washington and Oregon.

distribution, and tectonic implications of basalt along the eastern margin of the Columbia Plateau.

GENERAL STRATIGRAPHIC RELATIONS

Although a relatively small flood basalt province (about 300,000 cubic kilometers), the Columbia Plateau covers most of central and eastern Washington, north-central and northeastern Oregon, and a large part of western Idaho (Figure 1). For years the plateau was thought to be composed of a monotonous sequence of indistinguishable flows, each having limited extent. The key to mapping the plateau came with the realization that the province contains individual flows or sequences of flows that can be identified and traced for great distances. The concept that the plateau contains mappable units came slowly. An initial plateau-wide subdivision of the Columbia River Basalt Group into the older Picture Gorge Basalt and the younger Yakima Basalt was made by Waters (1961). His subdivision, based on stratigraphic, petrographic, and chemical criteria, also included a late textural and mineralogic variant of the Yakima Basalt, which he called the late Yakima petrographic-type. Several late Yakima flows were recognized in the central and western part of the plateau and traced by Laval (1956), Mackin (1961), Bingham and Grolier (1966), and Schmincke (1967a, 1967b).

In Idaho, Bond (1963) divided the Columbia River basalt in the Clearwater embayment into the "lower" and "upper" basalt on the basis of field appearance and stratigraphic position. The "lower" basalt resembles the coarse-grained Picture Gorge Basalt; Bond (1963, p. 13) suggested their correlation. However, studies by Wright and others (1973), Hooper (1974), Nathan and Fruchter (1974), and Kleck (1976) show significant chemical differences between the two. These differences prompted Hooper (1974) to adopt W. H. Taubeneck's suggestion that the name Imnaha Basalt be applied to Bond's "lower" basalt, which is well-exposed along the Imnaha River in northeastern Oregon.

Wright and others (1973) expanded the work of Waters (1961) by defining a four-unit informal stratigraphy for the plateau, from oldest to youngest: (1) the "lower" (Imnaha) basalt of Bond (1963) and the Picture Gorge basalt, (2) the lower Yakima basalt, (3) the middle Yakima basalt, and (4) the upper Yakima basalt. The stratigraphic nomenclature for the Columbia River Basalt Group has since been revised and formalized by Swanson and others (1979c). The stratigraphic column is shown in Figure 2. Of the five formations now recognized in the

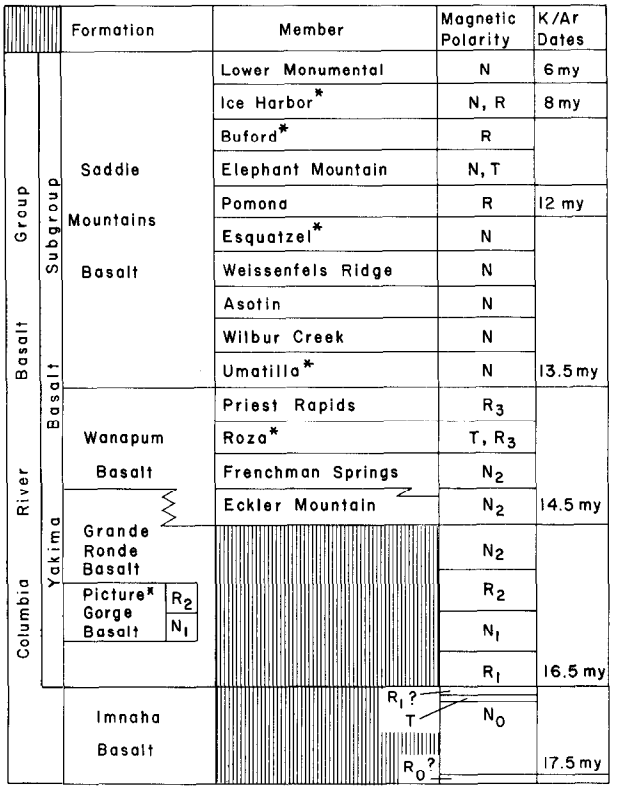

Figure 2. Stratigraphy of the Columbia River Basalt Group (modified after Swanson and others, 1979c). Asterisks denote basalt units which have not been found in Idaho. R= reversed, N= normal, and T= transitional polarity (numerical subscripts refer to magnetic sequence without a physical break).

Columbia River Basalt Group, the Imnaha, Grande Ronde, Wanapum, and Saddle Mountains Basalts occur in Idaho, while the Picture Gorge Basalt is restricted to an isolated basin in north-central Oregon. Each formation contains flows whose average thickness is between 15 and 30 meters, but some flows may be more than 120 meters thick where they have ponded in structural basins or stream channels. The maximum thickness of the group in any one place is about 1,500 meters (Waters and others, 1979), but the total thickness obtained by adding the maximum thickness recorded for each formation is closer to 2,500 meters (Hooper, 1980).

Several flows have hand specimen and field characteristics enabling them to be recognized and traced, but only in the last decade have units been defined by rapid, precise chemical analyses using X-ray fluorescence and by field measurements of magnetic polarity using a portable fluxgate field magnetometer. These techniques have enabled researchers to "fingerprint" units which otherwise would appear nondistinctive. The integration of chemical and magnetic information with hand specimen identification, visual field characteristics, and general stratigraphic position has established the current routine for mapping the thick basalt pile underlying the Columbia Plateau.

These techniques have proven especially useful in mapping the eastern part of the Columbia Plateau in western Idaho, northeast Oregon, and southeast Washington. This area has been uplifted to nearly 2,000 meters, resulting in deep canyon erosion by the Snake, Salmon, Clearwater, Grande Ronde, Imnaha, and St. Joe River systems (Griggs, 1976; Camp and Hooper, 1981, p. 665). Erosion has exposed the base of the Columbia River Basalt Group, providing a series of excellent cross-sections, up to nearly 1,200 meters thick, exposed through the earliest known flows of the Columbia River Basalt Group.

Bond (1963) laid the foundation for all future work in the southeast part of the plateau. Without the use of many current techniques, he mapped the contact between the Imnaha (lower) and Grande Ronde (upper) Basalt in the Clearwater embayment of Idaho. He also mapped remnants of the stratigraphically highest flow in the embayment, the Lolo flow, which he distinguished primarily by hand specimen identification. The Lolo flow remnants have since been identified as several different units within the Wanapum and Saddle Mountains Basalts (Camp, 1981).

By employing chemical and paleomagnetic techniques, the 1970s saw a revitalization of interest in the Columbia River basalt. The work of Bond (1963) was followed by several detailed studies of the Columbia River Basalt Group in Idaho (Hoffer, 1970; Holden, 1974; Hooper, 1974; Camp, 1976; Griggs, 1976; Holden and Hooper, 1976; Lynch, 1976; McNary, 1976; Bard, 1977; Reidel, 1978, 1982 this volume) and adjacent Washington and Oregon (Price, 1974, 1977; Kleck, 1976; Ross, 1978; Shubat, 1979). Parts of these studies have been summarized in Hooper and others (1976, 1979), Vallier and Hooper (1976), Camp and others (1978), Swanson and Wright (1978), Swanson and others (1980), and Swanson and Wright (1980).

The Columbia Plateau is presently being mapped at 1:250,000 scale. Preliminary maps of the Columbia River Basalt Group in Washington, northern Idaho, and northern Oregon (Swanson and others, 1979a, 1980, 1981) are now available.

LOCATION OF FEEDER DIKES

Most flows of the Columbia River Basalt Group were fed from dikes in the southeast and east part of the plateau. These fissure-filling dikes are remarkable

for their consistent north to north-northwest trend. Waters (1961) emphasized the concentration of dikes in three limited areas (Figure 3): the Monument dike swarm, feeding only the Picture Gorge Basalt (Fruchter and Baldwin, 1975); the Grande Ronde dike swarm in the lowest reaches of the Grande Ronde River on the eastern extremity of the Oregon-Washington border; and the Cornucopia dike swarm on the southeast side of the Wallowa Mountains. Taubeneck (1970) emphasized that there is no discernible break between the dikes comprising Waters' (1961) Grande Ronde and Cornucopia swarms. He therefore suggested that all dikes exposed in the southeast part of the plateau be classified as members of a single major swarm: the Chief Joseph dike swarm (Figure 3).

Although dikes may be concentrated in certain areas, they occur across a vast expanse of the Columbia Plateau. Swanson and others (1975b) documented a series of north-northwest-trending dike and vent systems, mostly concentrated on the eastern third of the plateau where many others have subsequently been found. They also demonstrated the presence of dikes as far west as the Pasco Basin in Washington. It is probable that many more are buried beneath the central parts of the Columbia Plateau where subsidence has prevented deep erosion. Camp (1981) has demonstrated that linear dike systems and source areas occur along the eastern extremity of the Columbia Plateau in the Clearwater embayment of Idaho. The recognition of dikes depends greatly on the depth of erosion, the nature of exposure, and a trained eye. What can definitely be said is that eruptions occurred episodically across at least the eastern two-thirds of the Columbia Plateau.

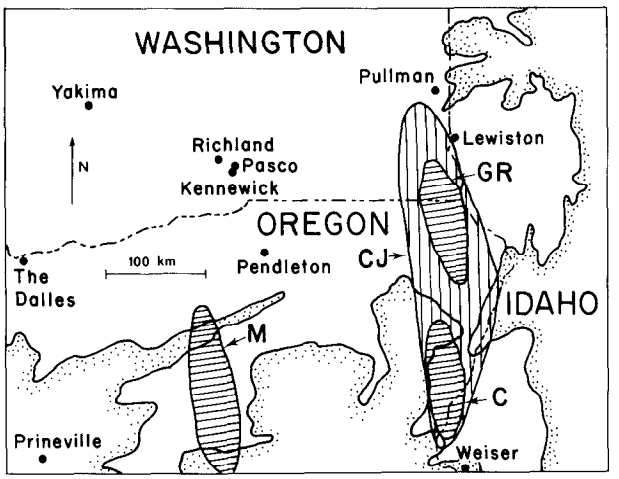

Figure 3. Location of major dike swarms feeding the Columbia River Basalt Group. M = monument swarm, GR = Grande Ronde swarm, C = Cornucopia swarm, CJ = Chief Joseph swarm.

AGE AND ACCUMULATION RATES

Columbia River basalt volcanism occurred over an 11.0-million-year interval (17.0 to 6.0 million years ago), on the basis of presently available radiometric dates. The timing and accumulation rate of the Imnaha, Grande Ronde, Wanapum, and Saddle Mountains Basalts are shown in Figure 4. Volcanism began in the southeast part of the province about 17.0 million years ago (McKee and others, 1981) with the eruption of Imnaha Basalt. After filling ancient valleys at least 600 meters deep, Imnaha Basalt was followed without a break by the voluminous (greater than 200,000 cubic kilometers) Grande Ronde Basalt from 16.5 to about 14.5 million years ago (Watkins and Baksi, 1974). Grande Ronde and Wanapum Basalt are interbedded in places (Figure 2) and may overlap in time by as much as a few hundred thousand years. Volcanism during Wanapum time was short, from about 14.5 to 13.5 million years ago. Saddle Mountains Basalt followed with intermittent extrusions over a 7.5-million-year interval ending with the Lower Monumental Member filling the Clearwater and Snake River canyons near Lewiston and farther west about 6.0 million years ago (McKee and others, 1977).

The accumulation rate was highest during the extrusion of Grande Ronde Basalt when rates were equivalent to those at Kilauea and Mauna Loa; the accumulation rate diminished rapidly during the intermittent extrusion of Saddle Mountains Basalt. This pattern is evident from both paleomagnetic information and field relations. The presence of a few flows with transitional polarity between thick sequences of different polarity (Choiniere and Swanson, 1979; Hooper and others, 1979) suggests that the initial seven polarity epochs, from R_30 to R_3

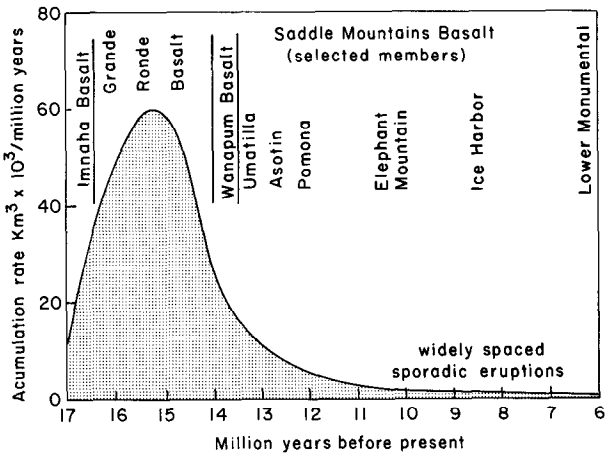

Figure 4. Accumulation rate with time for the Columbia River Basalt Group (modified from Hooper, 1980).

(Figure 2), are consecutive. This covers an approximately 3.5-million-year interval (17.0 to 13.5 million years ago) during which the Imnaha, Grande Ronde, and Wanapum Basalts were extruded. The eruption of Saddle Mountains Basalt during the waning period of activity (13.5 to 6.0 million years ago) was sporadic, with increasingly longer periods between eruptions, so that many polarity epochs are unrepresented in the sequence. Short intervals between eruptions are suggested by the near absence of erosional or depositional contacts between flows of Imnaha and Grande Ronde Basalt (Kleck, 1976; Camp, 1976; Holden and Hooper, 1976; Reidel, 1978, 1982 this volume). Longer time intervals between eruptions are suggested by the Wanapum Basalt, flows of which commonly overlie sedimentary interbeds and erosion surfaces of low relief (Camp, 1976, 1981; Ross, 1978; Swanson and others, 1979c). However, the issue is complicated by the possible effects of tectonism during this period. Hooper and Camp (1981) argue that the most probable model based on the present evidence involves continuous deformation throughout the Columbia River basalt eruption. The time between eruptions of Saddle Mountains Basalt was generally quite long, hundreds of thousands of years or even longer as suggested by potassium-argon dates and by the development of deeply dissected canyons of the ancestral Snake and Clearwater River systems between successive eruptions of Saddle Mountains flows (Swanson and others, 1975a; McKee and others, 1977; Camp, 1981).

PHYSICAL AND CHEMICAL PROPERTIES

IMNAHA BASALT

The first eruptions of the Columbia River volcanic event were Imnaha Basalt. The magma flowed from fissures in the southeast extremity of the Columbia Plateau to form thick units that filled valleys in the deeply dissected prebasalt topography; flows commonly backfilled the westerly draining valleys to the east, and the consequent ponding of the lava resulted in the formation of unusually thick units. The most complete exposures occur along the Snake River and its immediate tributaries north and south of Hells Canyon on the Idaho-Oregon border. Here over twenty individual flows can be recognized with a maximum exposed thickness of 700 meters in the vicinity of Oxbow Dam.

All but a few flows of Imnaha Basalt are characterized by abundant and large phenocrysts of plagioclase and smaller phenocrysts of olivine. Imnaha Basalt flows may be classified into the American Bar and the Rock Creek chemical types (Table 1). The two types interdigitate stratigraphically, but the American Bar dominates in the lower part of the succession and the Rock Creek dominates in the upper part. In the field the American Bar is characterized by its finer grained matrix and fewer phenocrysts, and the Rock Creek by an exceptionally coarse matrix and abundance of large plagioclase phenocrysts (Hoffer, 1970; Hooper, 1974).

Waters (1961) and Bond (1963) both emphasized the difference in the weathering aspects of the Imnaha and Grande Ronde Basalts. Imnaha Basalt breaks down more easily to form relatively gentle canyon slopes covered in a drusy debris, in contrast to the sharp, occasionally vertical, cliffs of the finer grained Grande Ronde Basalt. The very coarse flows of Rock Creek type lie immediately below flows of Grande Ronde Basalt; this results in a sharp break in slope along the canyon walls for many miles (Waters, 1961, Plate 1).

Almost the whole of the Imnaha Basalt succession has normal polarity (Figure 2), including the lowest exposed flows in the Snake River canyon. W. Taubeneck, D. Swanson, and D. Nelson (written communication, 1977) have recorded flows at the base and at the top of the Imnaha Basalt succession, on the west side of the Wallowa Mountains, which give reversed polarity on a fluxgate magnetometer. The same is true for many of the top Imnaha flows found in the Clearwater embayment north of the Salmon River. The top two flows in the Snake-Imnaha Rivers area (the Fall Creek and Log Creek flows) register reversed polarities on the fluxgate magnetometer, but the removal of the unstable magnetic components of drilled cores indicate both have transitional polarity (Hooper and others, 1979). At the mouth of the Grande Ronde River, the top four flows of Imnaha Basalt have transitional polarity, as do the lowest two flows of Grande Ronde Basalt (Hooper and others, 1979).

Dikes of both Imnaha chemical types have been recorded from the Imnaha River canyon and south-southeast to the Weiser-Huntington areas on either side of the Snake River (Taubeneck, 1970; Kleck, 1976; Fitzgerald, 1982 this volume; Hooper, unpublished data). This and the lack of evidence for Imnaha Basalt flows northwest of the Blue Mountains ridge in southeast Washington suggest that the Imnaha Basalt eruption was confined to the southeast part of the plateau.

All Imnaha Basalt may be classified as tholeiite on its normative mineralogy (hypersthene and quartz in norm). The American Bar type is more siliceous and displays an olivine-liquid reaction

typical of tholeiitic basalt. Classification of the Rock Creek type is more ambiguous; it lacks the olivine-liquid reaction and it contains both an iron-rich olivine and a calcium clinopyroxene zoned to a high-titanium outer rim (Hooper, 1974).

There is a sharp break in chemical composition between the Imnaha and Grande Ronde types reflected in their distinctive petrographies. Imnaha Basalt contains much more olivine and more calcic plagioclase. Imnaha Basalt has lower SiO_2 (less than 52.5 percent) and generally lower K_2O than Grande Ronde Basalt (Table 1). It is also characterized by higher Al_2O_3, MgO, and CaO than the Grande Ronde Basalt. The American Bar type, with higher SiO_2 than the Rock Creek type, displays a progressive increase in incompatible elements (for

Table 1. Average major-element compositions for chemical types in the Columbia River Basalt Group (6-31 from Swanson and others, 1979c). Analyses are in weight percent. Rounding during normalization accounts for those analyses that do not add up to 100 percent.

Chemical Type	1	2	3	4	5	6	7	8	9	10	11	12	13	14	15
Oxide	(11)[2]	(14)	(72)	(8)	(16)	(8)	(4)	(13)	(13)	(8)	(10)	(9)	(20)	(4)	(8)
SiO_2	51.51	51.53	50.20	51.11	50.15	50.36	51.46	51.57	53.78	55.94	54.37	50.01	52.13	54.80	52.29
Al_2O_3	15.56	14.17	16.25	16.25	16.82	16.81	15.54	15.39	13.87	14.45	14.04	15.28	17.08	15.41	13.86
"FeO"[1]	11.74	14.01	12.08	11.04	11.15	11.25	12.46	12.28	11.35	11.77	9.46	10.01	10.66	13.32	14.38
MgO	5.93	4.52	5.97	5.47	6.61	6.68	4.86	4.44	5.25	3.36	5.91	7.84	5.92	2.84	4.04
CaO	10.33	8.39	9.05	9.41	9.84	10.67	9.45	8.12	9.07	6.88	9.79	11.01	10.18	6.48	7.90
Na_2O	2.56	2.78	2.79	2.71	2.52	2.95	3.29	3.36	2.83	3.14	2.80	2.44	3.00	3.18	2.67
K_2O	0.37	1.06	0.76	0.75	0.49	0.57	0.74	2.02	1.05	1.99	0.77	0.27	0.68	1.87	1.41
TiO_2	1.60	2.96	2.43	2.25	2.02	1.56	1.79	2.71	1.78	2.27	1.17	1.00	1.48	2.46	3.17
P_2O_5	0.19	0.37	0.30	0.26	0.23	0.22	0.33	1.39	0.28	0.43	0.29	0.19	0.35	0.93	0.71
MnO	0.20	0.21	0.18	0.18	0.18	0.20	0.23	0.24	0.19	0.19	0.16	0.14	0.19	0.26	0.22

Chemical Type	16	17	18	19	20	21	22	23	24	25	26	27	28	29	30	31
Oxide	(35)	(15)	(55)	(13)	(11)	(6)	(3)	(2)	(12)	(30)	(41)	(8)	(12)	(13)	(8)	(24)
SiO_2	51.19	50.27	50.09	54.70	54.41	50.72	52.12	49.75	54.16	51.88	51.08	54.46	47.45	48.73	47.50	50.44
Al_2O_3	14.07	13.69	14.31	14.10	14.51	16.23	14.33	15.26	13.84	14.88	13.54	14.29	13.84	13.88	12.50	14.07
"FeO"[1]	13.91	15.04	13.78	12.63	11.07	9.64	11.64	11.82	12.60	10.55	14.75	11.05	15.22	14.41	17.53	13.78
MgO	4.39	4.29	5.18	2.71	4.51	8.19	5.58	7.10	3.91	6.96	4.28	4.85	5.99	5.88	4.41	5.01
CaO	8.48	8.31	8.88	6.14	8.32	10.70	9.64	10.13	7.71	10.67	8.34	8.54	9.71	9.72	8.80	8.67
Na_2O	2.72	2.67	2.57	3.20	2.69	2.22	2.69	2.32	2.66	2.36	2.45	2.75	2.31	2.42	2.44	2.79
K_2O	1.22	1.16	1.07	2.68	1.77	0.51	0.87	0.46	1.70	0.64	1.25	1.39	0.72	0.73	1.23	1.47
TiO_2	3.13	3.55	3.15	2.80	1.95	1.45	2.48	2.42	2.82	1.62	3.52	2.17	3.62	3.30	3.79	2.90
P_2O_5	0.67	0.81	0.78	0.88	0.56	0.18	0.49	0.55	0.41	0.25	0.59	0.35	0.91	0.73	1.54	0.66
MnO	0.23	0.21	0.19	0.17	0.21	0.17	0.17	0.21	0.19	0.17	0.20	0.15	0.23	0.20	0.27	0.21

[1]FeO + 0.9 Fe_2O_3
[2]Number of analyses used in computing average

1. American Bar (low incompatible elements)
2. American Bar (high incompatible elements)
3. Rock Creek (average of all analyses)
4. Rock Creek (Fall Creek Flow)
5. Rock Creek (Log Creek Flow)
6. High-Mg Picture Gorge (Wright and others, 1973)
7. Low-Mg Picture Gorge (Wright and others, 1973)
8. Prineville (recalculated from Uppuluri, 1974)
9. High-Mg Grande Ronde (one flow)
10. Low-Mg Grande Ronde (one flow)
11. Very high-Mg Grande Ronde (one flow)
12. Robinette Mountain
13. Dodge
14. Shumaker Creek
15. Frenchman Springs (one flow)
16. Roza
17. Rosalia
18. Lolo
19. Umatilla
20. Wilbur Creek
21. Asotin
22. Slippery Creek
23. Lewiston Orchards
24. Esquatzel
25. Pomona
26. Elephant Mountain
27. Buford
28. Basin City
29. Martindale (Ice Harbor 1)
30. Goose Island (Ice Harbor 2)
31. Lower Monumental

example, K, Ti, P) from the base of the succession upwards (Kleck, 1976). Local ponding of some Rock Creek flows has resulted in some settling of plagioclase and olivine phenocrysts, as in the Salmon River-Rocky Canyon area west of Grangeville, Idaho.

GRANDE RONDE BASALT

Grande Ronde Basalt comprises over 85 percent of the estimated volume of the Columbia River Basalt Group (Swanson and others, 1979b). At its type section near the mouth of the Grande Ronde River in southeast Washington, near the Oregon-Idaho border, the formation is 800 meters thick and contains thirty-five basalt flows (Camp and others, 1978). The formation consists overwhelmingly of aphyric to slightly phyric fine-grained basalt. Individual flows are difficult to map over large distances, and field mapping of magnetic polarity is the only reliable means of providing a regional stratigraphic breakdown of the Grande Ronde Basalt. Four magnetostratigraphic units have been defined within the Grande Ronde Basalt, from oldest to youngest, R_1, N_1, R_2, N_2 (Figure 2), where R means reversed and N normal polarity (Swanson and Wright, 1976; Hooper and others, 1976; Swanson and others, 1979c).

Dikes of Grande Ronde chemical type (Swanson and others, 1979c) are abundant in the Chief Joseph dike swarm but are scarce east of the Snake River in Idaho. In addition, many more thin flows of R_1 are observed in the lower Grande Ronde River area than to the south and east, suggesting that during early Grande Ronde time volcanic activity was concentrated west of Idaho.

Grande Ronde Basalt flows are relatively siliceous quartz tholeiites. They fall within a continuous range of chemical composition defined as the Grande Ronde chemical type (Swanson and others, 1979c). Reidel (1978, 1982 this volume) has shown that individual Grande Ronde flows can be correlated over limited distances using major and trace element compositions and discriminant analysis of flow sequences. This procedure is complicated by the character of many individual Grande Ronde flows, which pinch out after spreading laterally only a few kilometers or tens of kilometers from their source, and by the difficulty in detailed sampling of very thick basalt sections. The Grande Ronde Basalt does, however, contain groups of flows which can be readily correlated over tens of kilometers by chemical and mineralogical composition. Flows within these groups fall into subtypes of Grande Ronde chemistry as illustrated by the high-Mg, low-Mg, and very high-Mg Grande Ronde flows given in Table 1.

Chemical subtypes are recognized in the Clearwater embayment of Idaho and adjacent Washington and Oregon, where Grande Ronde Basalt can be divided into a sequence of low-Si flows overlain by a sequence of high-Si flows. The contact between the two may be gradational in places, but it consistently occurs one or two flows below the R_1-N_1 contact and has been traced throughout much of the east and southeast part of the plateau (Reidel, 1975, 1978, 1982 this volume; Camp, 1976; Holden and Hooper, 1976; Price, 1977; Camp and others, 1978). The lower group of flows averages 0.7 percent higher in MgO and 2 percent lower in SiO_2 than the upper group (Camp and others, 1978). Many flows of the low-Si group are plagioclase-phyric, whereas only a few flows of the high-Si group exhibit small plagioclase phenocrysts. The low-Si group contains all plagioclase phenocrysts. The low-Si group contains common groundmass olivine and rare pigeonite, whereas the high-Si group contains common groundmass pigeonite and rare olivine (Reidel, 1975, 1978, 1982 this volume; Camp, 1976; Camp and others, 1978).

The top of the Grande Ronde Basalt throughout the plateau is generally marked by a residual soil (saprolite) or a sedimentary interbed separating the formation from the overlying Wanapum or Saddle Mountains Basalt. The contact is also marked by a chemical break, labeled the "TiO_2 discontinuity" by Siems and others (1974), above which the flows have much higher TiO_2 values than those below. Throughout most of the plateau the "TiO_2 discontinuity" occurs between flows of Grande Ronde chemistry and flows of Frenchman Springs, Rosa, Rosalia, and Lolo chemical types (Table 1). A prominent saprolite mantles the surface of the Grande Ronde Basalt in southeast Washington (Swanson and others, 1980) and adjacent Idaho (Camp, 1976, 1981) and Oregon (Ross, 1978). In Idaho the saprolite can be readily seen near the top of the Lewiston and Kendrick grades (Figure 5) and along U. S. Highway 12 about 11 kilometers east of Lewiston. The saprolite progressively thickens eastward from Devils Canyon along the Snake River in central Washington to the eastern margin of the plateau in Idaho. It is an excellent marker for mapping the Grande Ronde-Wanapum contact in the Clearwater and St. Maries embayments of Idaho. The zone is not recognized in the Weiser embayment, where units younger than Grande Ronde Basalt (Wanapum Basalt and Saddle Mountains Basalt) have not been documented (Fitzgerald, 1982 this volume).

Figure 5. Saprolite developed on Grande Ronde R_1 near the top of Kendrick grade on the Troy-Kendrick road. Overlying flow is the Priest Rapids Member.

WANAPUM AND SADDLE MOUNTAINS BASALTS

Volumetrically, the Wanapum Basalt (less than 10,000 cubic kilometers) and Saddle Mountains Basalt (about 2,000 cubic kilometers) make up much less than 10 percent of the Columbia River Basalt Group (Swanson and others, 1979b). They are extensively exposed, however, covering the upper surface of most of the Columbia Plateau. They differ from the Grande Ronde Basalt in that they are composed of flows or sequences of flows that can be combined into members by their distinctive chemistry and generally identifiable hand specimen and field appearance. Wright and others (1973) and Swanson and others (1979c) have defined several chemical types from the two formations (Table 1). The chemical differences, combined with field and magnetic criteria, have enabled Swanson and others (1979c) to divide the Wanapum Basalt into four members (Eckler Mountain, Frenchman Springs, Roza, Priest Rapids) and the Saddle Mountains Basalt into ten (Umatilla, Wilbur Creek, Asotin, Weissenfels Ridge, Esquatzel, Pomona, Elephant Mountain, Buford, Ice Harbor, Lower Monumental). Most of these members occur in Idaho (Figure 2).

The petrography, field appearance, and chemistry for each of these members is well documented. For more detailed information regarding the physical and chemical properties of individual units, the reader is referred to Schmincke (1967a), Wright and others (1973), Camp (1976, 1981), Price (1977), Ross (1978), Swanson and others (1979c), and Shubat (1979).

Camp (1981) identified and described several new units of the Columbia River Basalt Group in the Clearwater embayment of Idaho. Of these, the Onaway Member is designated as a formal member of the Wanapum Basalt, and the Swamp Creek, Grangeville, Icicle Flat, and Craigmont Members are designated as formal members of the Saddle Mountains Basalt. In addition, four units have been mapped and given informal designations: from oldest to youngest, the basalt of Feary Creek in the Frenchman Springs Member, the basalt of Potlatch in the Onaway Member, the basalt of Lapwai in the Wilbur Creek Member, and the basalt of Weippe in the Pomona Member. The relative age of these new members and informal units to the formalized Wanapum and Saddle Mountains Basalt stratigraphy of Swanson and others (1979c) is illustrated in Figure 6. The average major element composition and physical properties of the new members and informal basalt units are given in Tables 2 and 3, respectively. For further information on these units, the reader is referred to Camp in Swanson and others (1979a) and Camp (1981).

Most Wanapum and Saddle Mountains members had their source in the southeast part of the Columbia Plateau. Of the Wanapum units, the

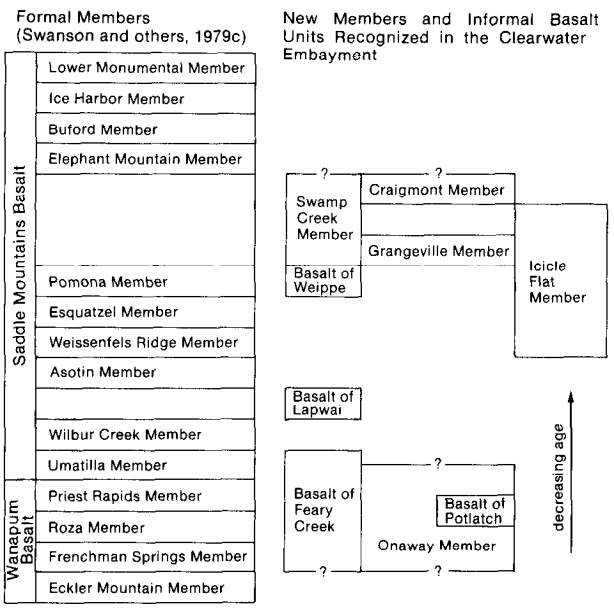

Figure 6. Relative age range for new members and informal basalt units in the Clearwater embayment with respect to the formalized stratigraphy of Wanapum and Saddle Mountains Basalts (after Camp, 1981). Vertical position indicates relative age based on field observations.

Priest Rapids and Onaway Members had their source in the Clearwater embayment. The same is true for at least seven Saddle Mountains units: the Wilbur Creek, Asotin, Pomona, Swamp Creek, Grangeville, Icicle Flat, and Craigmont Members. The Weissenfels Ridge and Lower Monumental Members occur in the Lewiston basin of Washington and Idaho and may also have had local sources in the embayment (Camp, 1976; Price, 1977; Swanson and others, 1979c). Relations in the St. Maries embayment indirectly suggest that some Priest Rapids flows erupted there, as did at least one flow in the Eckler Mountain Member (Swanson and others, 1979a, 1979c).

Table 2. Average major element compositions for the new Wanapum and Saddle Mountains Members and informal units found in the Clearwater embayment (modified from Camp, 1981).

	CM (7)[2]	IF (6)	GV (4)	SC (6)	PL[1] (6)	WE (29)	LA (9)	FC (6)
SiO_2	52.57	52.22	53.06	51.17	48.25	51.41	52.64	51.56
Al_2O_3	14.37	15.19	16.04	14.43	16.58	15.41	15.54	14.10
"FeO"[3]	13.86	10.93	8.73	13.82	12.83	10.99	10.76	14.21
MgO	3.48	5.06	6.21	4.54	4.97	6.31	5.61	4.03
CaO	7.29	10.01	10.89	8.62	7.84	10.33	9.25	7.79
Na_2O	2.30	2.89	2.38	2.68	3.21	2.36	2.34	2.64
K_2O	1.88	0.78	0.72	1.27	1.69	0.46	1.40	1.73
TiO_2	2.93	1.45	1.36	2.69	3.69	1.76	1.71	3.20
P_2O_5	0.47	0.32	0.19	0.35	0.59	0.23	0.37	0.35
MnO	0.20	0.25	0.17	0.23	0.17	0.19	0.17	0.20

Note: CM, Craigmont Member; IF, Icicle Flat Member; GV, Grangeville Member; SC, Swamp Creek Member; PL, basalt of Potlatch; WE, basalt of Weippe; LA, basalt of Lapwai; FC, basalt of Feary Creek. XRF analyses by P. R. Hooper. They are weight percent and normalized to 100 percent.

[1]The basalt of Potlatch is the only mappable unit within the Onaway Member and the only unit which displays consistent chemistry within a defined field.
[2]Number of analyses used in computing average.
[3]FeO + 0.9 Fe_2O_3.

Table 3. Physical Properties for the new Wanapum and Saddle Mountains Members and informal basalt units found in the Clearwater embayment (modified from Camp, 1981).

Unit	Groundmass Size[1]	Groundmass Olivine	Phenocryst phase[2]	Number of flows	Magnetic polarity
Craigmont	f-mg	rare	plg (≤10 mm), rare	one	normal
Icicle Flat	m-cg	abundant	plg (≤15 mm), abundant olv (≤5 mm)	one	normal
Grangeville	m-cg	common	plg (≤7.5 mm), rare	one	reverse
Swamp Creek	m-cg	abundant	olv (≤10 mm), common plg (≤5 mm), rare	one	normal
Weippe	m-cg	abundant	olv (≤5 mm) plg (≤5 mm)	one	reverse
Lapwai	f-mg	common	plg (<5 mm) rare	one	normal
Feary Creek	f-mg	common	plg (≤10 mm)	two or three	normal
Onaway[3]	m-cg	none	plg (≤10 mm), common	several	normal

[1]based on average length of plagioclase laths in the matrix, where fine- to medium-grained (f-mg) ≤0.3 mm ≤ medium- to coarse-grained (m-cg)
[2]plg, plagioclase; olv, olivine
[3]petrographic information is for the basalt of Potlatch

FLOW DISTRIBUTION AND TECTONIC IMPLICATIONS

Reconnaissance mapping of the plateau (Swanson and others, 1979a, 1980) shows that the distribution of units within the Columbia River Basalt Group is controlled by four factors: (1) the location of source areas, (2) paleotopography, (3) the volume of flows, and (4) deformation before and during the eruptive episode. The location of source dikes and vents is discussed above, and more specific information can be obtained from Price (1974, 1977), Swanson and others (1975b, 1979c), Ross (1978), and Camp (1981). Paleotopography controlled the initial distribution of Columbia River basalt flows, as Imnaha and early Grande Ronde flows filled deep canyons eroded into prebasalt rocks in the southeast part of the province. Erosion during the interval between eruptions was controlled by the tectonic uplift of the southeast part of the plateau; it had a signigicant effect on the distribution of Saddle Mountains flows (Swanson and others, 1975a, 1975b, 1979c; Camp, 1976, 1981), which were extruded during a period of waning volcanism. It had less effect on Imnaha and Grande Ronde flows, which were extruded during a period when the rate of eruption was more rapid (Figure 4). Even if the rate and intensity of deformation were continuous throughout the eruptive period, structures controlling flow distribution would have had more time to develop when accumulation rates diminished.

WEISER EMBAYMENT

The thickest sequences of Imnaha Basalt occur in the extreme southeast part of the basalt province, where some of the oldest flows of the Columbia River Basalt Group occur. Fitzgerald (1982 this volume) has demonstrated that Grande Ronde R_1 thickens from northeast Oregon into the Weiser embayment. Here, there are very few Grande Ronde N_1 flows, and flows which may be younger than Grande Ronde Basalt are of uncertain affinity. The increased thickness of Imnaha and Grande Ronde R_1 flows in the Weiser embayment probably reflects the lower elevation of that area during the early stage of volcanism. The apparent absence or scarcity of younger flows probably reflects uplift of the area during and after middle Grande Ronde time, when adjacent northeastern Oregon was uplifted (Camp and Hooper, 1981).

ST. MARIES EMBAYMENT

In contrast to the Weiser embayment, the St. Maries embayment contains no Imnaha or early Grande Ronde flows. Swanson and others (1979a) mapped a small amount of R_2 and a thin sequence of Grande Ronde N_2 flows along the east and west sides of Coeur d'Alene Lake. Wanapum Basalt (Eckler Mountain and Priest Rapids Members) occurs above Grande Ronde N_2 west of St. Maries, Idaho (Griggs, 1976), and continues east and southeast of St. Maries within the St. Joe and St. Maries River valleys, where it overlies prebasalt rocks. A representative of the Eckler Mountain Member, the basalt of Dodge, appears to have a local vent in the St. Maries River valley about 7 kilometers northwest of Clarkia, Idaho (Swanson and others, 1979a). Similarly, the Priest Rapids Basalt appears to have a local source in the headwaters of the St. Joe River, although no vent areas or dikes have been found. Nonpillowed Priest Rapids intracanyon flows occur far up the river valley, suggesting that the Priest Rapids was erupted from an upstream vent that dammed the river and allowed the basalt to flow down a nearly dry canyon (Swanson and others, 1979b). A Priest Rapids source in this area would lie along the projected north-northwest trend of Priest Rapids feeder dikes in the Clearwater embayment about 30 kilometers to the south (Camp, 1981). The well-known fossil leaf locality near Clarkia (Smiley and Rember, 1979) is within a sedimentary sequence, locally invaded by a flow of the Priest Rapids Member. Our mapping suggests that the sediments were deposited in a lake dammed by lava flows of either latest Grande Ronde or early Wanapum age. If so, the sediments and included fossil leaves are about 15 million years old. However, Smiley and Rember (1979, p. 6) note that floral and paleoclimatic evidence suggests they may be 20 million years or older. This would make the sediments older than any known Columbia River basalt, and another mechanism would be required to explain the Miocene damming and consequent creation of Clarkia Lake.

The northeastern part of the Columbia Plateau (east-central Washington and the St. Maries embayment, Idaho) remained relatively stable throughout the extrusive period, allowing (1) Grande Ronde N_2 flows to advance across the nearly horizontal Columbia Plateau to its eastern edge and (2) Priest Rapids Basalt to flow westward across the entire northern portion of the plateau (Swanson and others, 1979a) unimpeded by structurally controlled topography. Present-day dips of flows in the embayment probably approximate primary dips but may be slightly steeper owing to regional westward tilting of the area between the Idaho batholith and the Cascade Range.

CLEARWATER EMBAYMENT

The Clearwater embayment contains parts of the Snake, Salmon, and Clearwater River systems (Figure 1), which have eroded numerous canyons that cut through the entire basalt section in several places. The embayment lies adjacent to the eastern margin of the Chief Joseph dike swarm (Figure 3) and contains several sources for Wanapum and Saddle Mountains flows found throughout the plateau (Camp, 1981). It has been tectonically active during and after the eruptive period. Flow distribution in the embayment has been controlled by the location of source areas, by tectonic activity during extrusion, and by volumes of erupted material.

The Imnaha Basalt, erupted mostly from the Chief Joseph swarm, advanced eastward into the Clearwater embayment, thinning to the east upon a highly irregular prebasalt surface. This contrasts with the eastward thickening of Imnaha Basalt into the Weiser embayment (Fitzgerald, 1982 this volume) and may be attributed simply to the lower elevation of the Weiser embayment during the initial phases of basalt extrusion.

Grande Ronde Basalt thins gradually to the northeast across the Clearwater embayment from 800 meters at its type section to its pinch-out along the eastern margin of the embayment in Idaho. Each Grande Ronde magnetostratigraphic unit thins eastward as well (Reidel, 1982 this volume). Each successive unit pinches out farther west than the preceding unit, indicating a continuous westward tilting of this part of the plateau during the eruption of Grande Ronde Basalt (Figure 7). This is consistent, on a regional scale, with evidence of a westward-dipping paleoslope across most of the plateau during the eruption of late Grande Ronde Basalt (Swanson and others, 1979b).

In addition to regional westward tilting, the Clearwater embayment was subjected to significant deformation during Grande Ronde time, particularly during its late stage. N_1 thickens abruptly near the confluence of the middle and south forks of the Clearwater River near Kooskia, Idaho. A small "island" of R_2 exists in this area as well (Figure 7). The thickening of N_1 and the occurrence of R_2 in this area resulted from the initiation of the Stites basin (Figure 1) during N_1 time. Camp and Hooper (1981) suggest that the deepening of the basin resulted from vertical movement along reactivated north-trending prebasalt faults, much like those in the Riggins area to the south (Hamilton, 1962).

The Limekiln fault (Figure 7) represents a major northeast- to southwest-trending structure across the Clearwater embayment. The fault merges into monoclinal flexures along both its northeast and southwest projections. Grande Ronde N_2 pinches out along the southwest monoclinal projection of the Limekiln fault in northeastern Oregon, adjacent to the Clearwater embayment (Figure 7). S. Reidel (1977, personal communication) and Camp and Hooper (1981) thus propose that initial movement along the Limekiln fault occurred near the end of R_2 time, before extrusion of Grande Ronde N_2. This movement had a significant effect on the distribution of all younger flows in the Clearwater embayment and adjacent northeast Oregon. A large tectonic block, the Nez Perce plateau (Figures 1 and 8), was uplifted southeast of the fault. The downthrown side of the fault-monocline complex marks the southeast boundary of the present Lewiston basin (Figure 1) in Idaho and of the Troy basin in Oregon. By the end of Grande Ronde time the physiography of the Clearwater embayment was dominated by the Stites and Lewiston basins separated by the uplifted Nez Perce plateau.

While Grande Ronde N_2 and early Wanapum flows were being extruded in adjacent Washington and Oregon, only minor volcanism occurred in northern Idaho. During this interval the Clearwater embayment was undergoing a period of weathering, which formed a residual soil thicker in the east where it had begun to form earlier on older Grande Ronde flows (Figure 5). In places, the soil, now preserved as a saprolite, is thin or nonexistent, apparently the result of erosion as the rocks weathered.

Volcanism in the Clearwater embayment during late Wanapum time was dominated by extrusion of the voluminous Priest Rapids Member. After erupting from a linear system of north- to northwest-trending dikes passing through Orofino, Idaho (Camp, 1981), the Priest Rapids flowed down a westward-dipping slope across an irregular plateau mantled by a residual soil. It advanced from the Clearwater and St. Maries embayments to cover the northern half of the Columbia Plateau. The only other Wanapum Basalt flows in the Clearwater embayment are the locally derived Onaway Member and the basalt of Feary Creek, both of limited extent.

Wanapum Basalt occurs in the Clearwater embayment and adjacent northeastern Oregon (Figure 8a). It is evident that the Joseph Plains and Nez Perce plateau (the areas uplifted by the Limekiln fault and monocline in Oregon and Idaho) were isolated from Wanapum volcanism; Wanapum Basalt accumulated in the Troy basin in Oregon (Ross, 1978) and the low-lying areas of the Clearwater embayment including the Lewiston and Stites basins.

The distribution of Saddle Mountains Basalt was

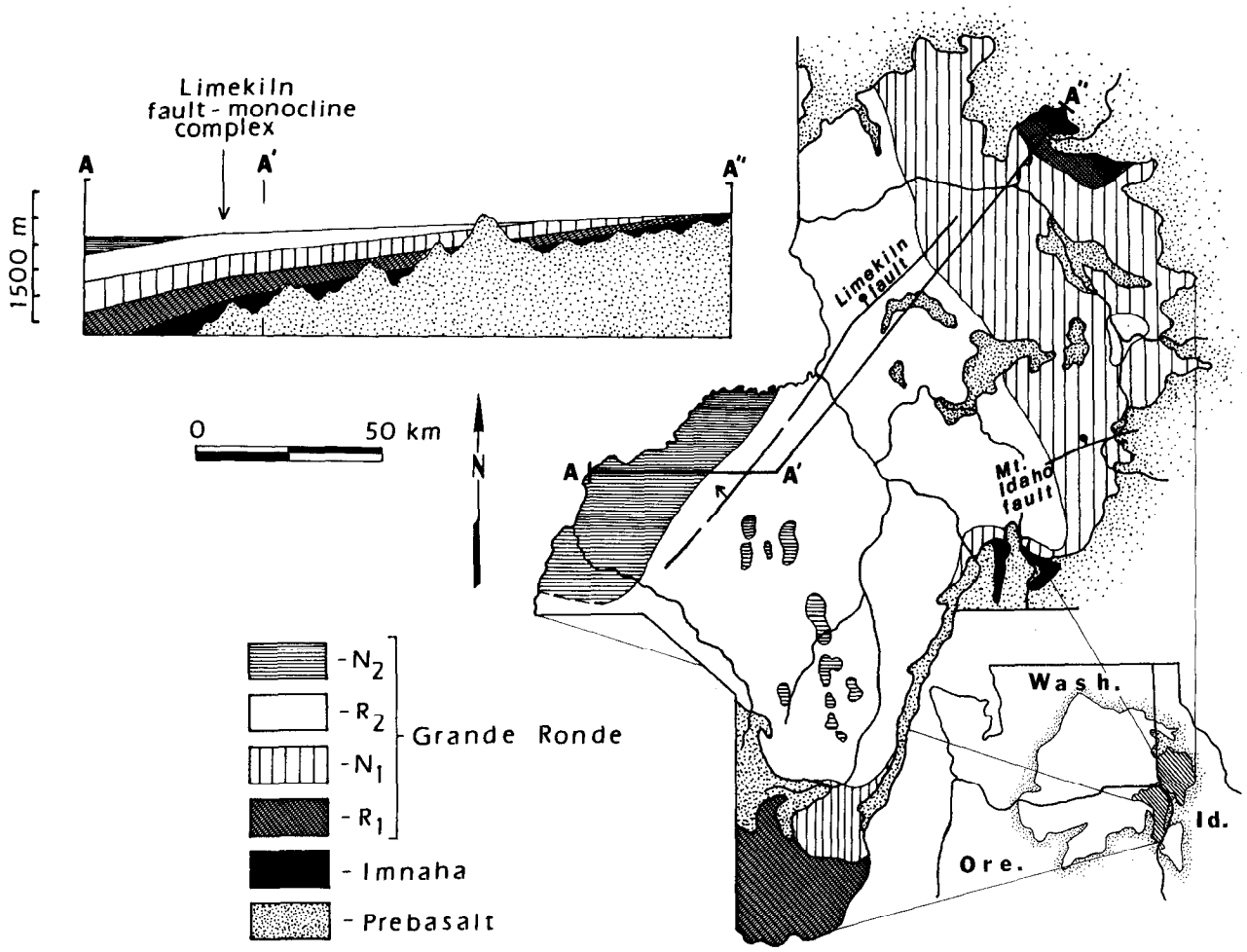

Figure 7. Map view and cross-section of the Clearwater embayment and adjacent northeast Oregon immediately after extrusion of Grande Ronde Basalt (after Camp and Hooper, 1981). Refer to Figure 1 for place names and topographic features.

similarly restricted (Figure 8b). Some Saddle Mountains units occur on the Nez Perce plateau, but they are attributed to extrusion from dikes that broke the surface of the plateau rather than incursion of flows onto the plateau surface from a more distant source.

Most Saddle Mountains flows in the Clearwater embayment were extruded from sources in the upper North Fork of the Clearwater River (Figure 1). Because of long intervals between eruptions and high rates of erosion on the southeast part of the plateau, canyons formed during different stages of development of the ancestral Snake (Swanson and others, 1975a, 1980; Camp, 1976) and Clearwater (Camp, 1981) River systems. These ancient drainages significantly affected the distribution of Saddle Mountains flows. Some Saddle Mountains units extruded from the upper North Fork were trapped in ancestral Clearwater River canyons and transported westward to the Lewiston basin. The more voluminous units buried the ancestral canyons and flowed south along irregular plateau surfaces to the Stites basin as well as west to the Lewiston basin. In contrast to Wanapum Basalt, the distribution of Saddle Mountains Basalt was largely controlled by the drainage systems developed during volcanism and by older deformation that had occurred during late Grande Ronde time.

Deformation continued in the Clearwater embayment after volcanism ceased about 6.0 million years ago (McKee and others, 1977). The most obvious post-Columbia River basalt deformation in the embayment is reflected in the east- to west-trending Lewiston structure (Camp, 1975, 1976; Camp and Hooper, 1981) which forms the present northern boundary of the Lewiston basin.

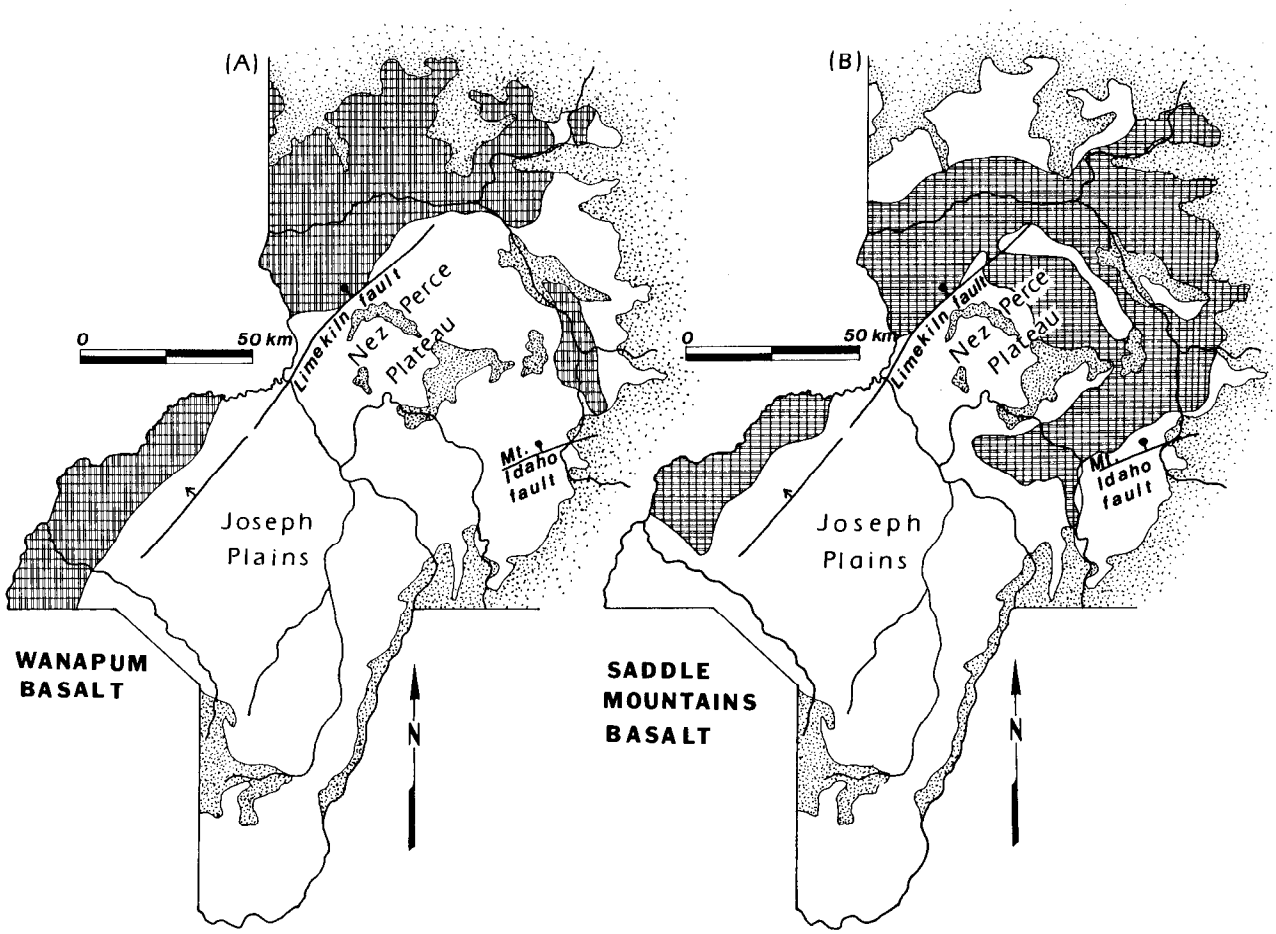

Figure 8. Distribution maps for (A) Wanapum Basalt and (B) Saddle Mountains Basalt in the Clearwater embayment and adjacent northeast Oregon (after Camp and Hooper, 1981). Pattern indicates extent of each formation. For general location refer to inset in Figure 7.

TECTONIC MODEL

The geologic map of Idaho (Bond, 1978) reveals a northwest-southeast and northeast-southwest fault pattern in the prebasalt rocks of western Idaho. In expanding the tectonic model of Ross (1978) in the Troy basin, Hooper and Camp (1981) argue that if a stress regime having a horizontal north-northwest south-southeast axis of maximum compression and east to west regional tilting is imposed on basalt overlying this older structural grain, then most of the structural elements in the east and southeast part of the plateau can be accounted for. These structural elements, developed during and after basalt extrusion, include (1) folds with east-west axes and associated reverse faults also striking east-west, (2) faults displaying a predominantly vertical displacement with northwest-southeast, northeast-southwest, and to a lesser extent north-south trends, and (3) the vertical basalt feeder dikes which are remarkable for their consistent north to north-northwest trend. The orientation of these structural elements in relation to the stress regime proposed by Hooper and Camp (1981) is illustrated in Figure 9b.

The offlap of progressively younger basalt units (Imnaha through Grande Ronde N_2) from prebasalt topographic highs is illustrated in Figure 9c. Progressive westward tilting away from the prebasalt margin of the plateau is most likely the result of relative uplift of lighter prebasalt rocks due to isostatic adjustment (Hooper and Camp, 1981). This uplift continued at least through Grande Ronde time (Figure 7). Most Wanapum and Saddle Mountains Basalts in the east and southeast part of the plateau flowed west, suggesting that a westward-dipping paleoslope persisted throughout volcanism.

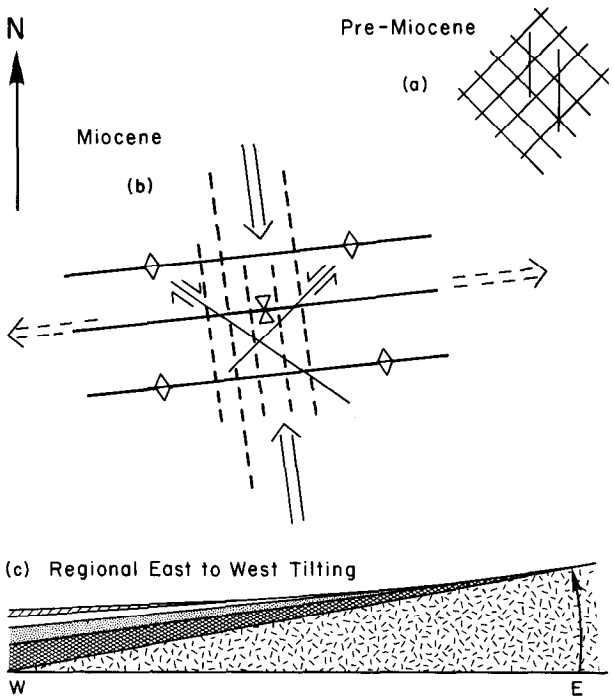

Figure 9. Diagram illustrating (a) the structural grain in the pre-Miocene rocks of northern Idaho, (b) the orientation of the principal structural elements in the southeast and east part of the Columbia Plateau and the stress field responsible [dashed lines represent dike trend; double-lined arrows represent the direction of maximum compression (solid) and maximum tension (dashed)], and (c) the offlap of progressively younger basalt units from the rising prebasalt topographic highs (after Hooper and Camp, 1981).

NOTE ON SEDIMENT RELATIONS

The occurrence of lacustrine and fluvial strata interbedded and lying upon Columbia River basalt along the eastern margin of the plateau has been well-documented by several earlier researchers (Lindgren, 1898; Russell, 1902; Washburne, 1911; Pardee and Bryan, 1926; Kirkham and Johnson, 1929; Kirkham, 1931; Wheeler and Cook, 1954; Bond, 1963; Gray and Kittleman, 1967; Griggs, 1976). The Latah Formation was defined by Kirkham and Johnson (1929) to include all sedimentary interbeds in the northeast corner of the plateau: from Grande Coulee, Washington, to the north and throughout the St. Maries and Clearwater embayments in Idaho to the east. Griggs (1976) suggested that the Latah Formation be restricted geographically to those sedimentary rocks associated with the Columbia River Basalt Group within the Spokane River drainage, as originally defined by Pardee and Bryan (1926). In the extreme southeast corner of the plateau the Payette Formation is interbedded with Columbia River basalt that is, in turn, overlain by the relatively undeformed Idaho Formation (Kirkham, 1931; Wheeler and Cook, 1954). Disregarding stratigraphic terminology, it is evident that several local basins of deposition existed along the eastern margin of the plateau throughout the 11-million-year interval of basalt extrusion. Most sedimentary rocks along the basalt-prebasalt interface are not part of a single continuous unit but rather are isolated pockets produced by a successive damming of ancestral drainages by periodic encroachment of basalt. These sedimentary interbeds are thickest near the eastern margin of the plateau and thin westward away from the basalt-prebasalt contact (Bond, 1963; Griggs, 1976; Camp, 1981). Some of the sediments marginal to the plateau, such as the White Bird Lake sediments (Bond, 1963; Gray and Kittleman, 1967) and the Idaho Lake sediments (Idaho Formation of Wheeler and Cook, 1954), may have resulted from deformation and associated erosion after Grande Ronde time. However, most interbedded sediments along the eastern margin of the plateau appear to have been deposited as a result of advancing flows damming Miocene rivers. Such sediments include the fossiliferous sedimentary rocks near Grande Coulee, Washington (Gray and Kittleman, 1967), the Latah Formation as geographically restricted by Griggs (1976), the sediments of Clarkia Lake (Smiley and Rember, 1979) in the present St. Maries River valley, the Whiskey Creek interbed (Bond, 1963) and most interbeds of the Clearwater embayment, and the Payette Formation (Kirkham, 1931; Wheeler and Cook, 1954) of the Weiser embayment.

Field evidence supporting the previous existence of lava dams along the plateau margin in the Clearwater embayment have been documented (Camp, 1981). In addition to thick sedimentary sequences, the criteria include the existence of (1) remnants of canyon-filling flows overlying gravel of ancient streams eroded into both basalt and prebasalt rocks, (2) pillows along the top of several Grande Ronde and younger flows (Figure 10), formed as streams were dammed and water spilled onto the top of the advancing flow, and (3) a widespread, thick (about 30 meters) hyaloclastite in the North Fork area along the top of Imnaha Basalt (Figure 11), formed in much the same way but with greater violence between the diverted stream or streams and the hot fluid basalt invading its channels.

Dike- and sill-like bodies that intrude sediments marginal to the plateau have been suggested as possible feeders for local flows interbedded with the Latah Formation in and around Spokane (Pardee and Bryan, 1926), in the Clarkia Lake sediments south of St. Maries (Smiley and Rember, 1979), and

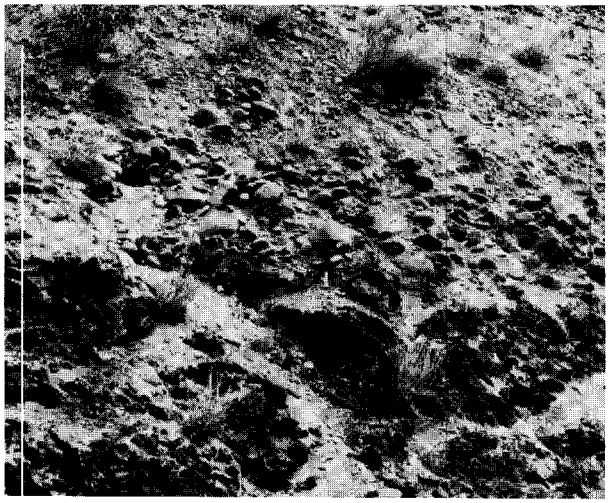

Figure 10. Pillows along the top of the Lower Monumental Member in the Lewiston basin near the confluence of the Snake and Clearwater Rivers, north of Lewiston; bottom of member (not shown) is massive. Pillows formed when an ancestral Clearwater River was diverted along the top of the flow that invaded its channel. Overlying cobbles were deposited by the ancestral Clearwater River upon the Lower Monumental Member immediately after basalt invaded its channel. Similar relations are observed in R_1 flows near the margin of the embayment east of Orofino. For scale note hammer in center of photograph.

in the Whiskey Creek interbed northeast of Orofino (Bond, 1963; McNary, 1976). However, recent investigations (Griggs, 1976; Swanson and others, 1979a; Camp, 1981) have shown these intrusive bodies to be apophyses of flows that have bulldozed their way into the then soft, unconsolidated sediments. The lateral intrusion of dense basalt into lighter, unconsolidated sediments was common in structural basins where sediment was accumulating in the interior of the plateau (Schmincke, 1967b; Camp, 1976) and in basins of deposition along the northwest plateau margin (Byerly and Swanson, 1978). In Idaho the basalt-sediment relations of these invasive flows can be most easily observed in (1) Saddle Mountains Basalt units throughout the Lewiston basin (Camp, 1976), (2) R_1 (Figure 12) and Priest Rapids units in Orofino and Whiskey Creeks, northeast of Orofino, and (3) scattered exposures of the Priest Rapids Member between Troy and Bovill. Many invasive flows continue beneath sediments for several kilometers but can be traced into subareal flows out of basins (for example, the Asotin member in the Lewiston basin; Camp, 1976). The tops of invasive flows are nonvesicular or only slightly vesicular, with glassy (generally palagonitized) selvages where basalt chilled abruptly against the cooler, overlying sediments. Lenses or wisps of sediment are sometimes

Figure 11. Hyaloclastite overlying Imnaha Basalt along the North Fork of the Clearwater River about 5 kilometers north of Dent, Idaho. The rock contains highly shattered glassy basalt fragments, small broken pillows of Imnaha Basalt, palagonite, and in places medium- to coarse-grained fluvial clastics.

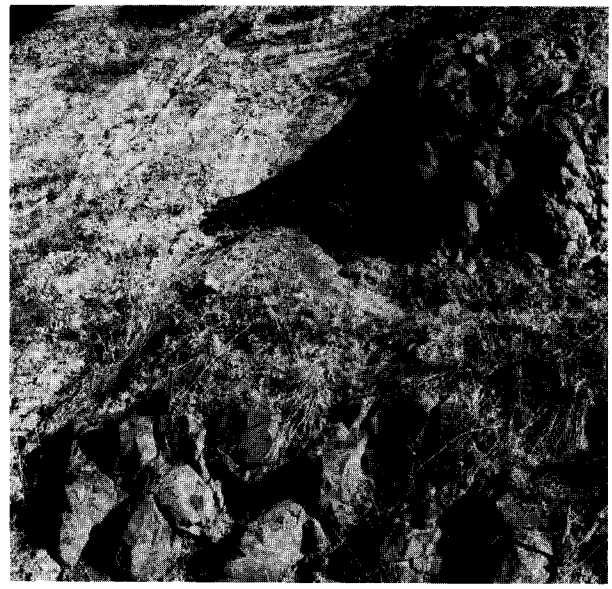

Figure 12. Invasive Grande Ronde R_1 flow with chilled upper contact against overlying Whiskey Creek interbed, about 5 kilometers northeast of Orofino. Large pillow incorporated in sediment belongs to underlying flow. For scale note hammer at sediment-basalt contact.

incorporated in the upper part of an invasive flow, and apophyses, blocks, and pillows may be incorporated in the lower part of the sedimentary unit (Figure 12); the sediment, however, is generally only slightly disturbed. Peperites (Schmincke, 1967b), a mixture of fragmented, glassy or palagonitized lava and broken and shattered sedimentary rock, is not uncommon along the basalt-sediment interface. The occurrence of peperite, pillows, or hyaloclastite is the logical result of hot, fluid lava invading wet, unconsolidated sediments.

ORIGIN AND EVOLUTION OF THE COLUMBIA RIVER BASALT

The petrochemical data collected during the studies of the Columbia River basalt, along with the now well-defined volcanic-tectonic evolution of the province, provides an excellent basis for an analysis of the origin and evolution of the Columbia River basalt magma. Such an analysis is currently in progress, but no well-defined model has yet been achieved.

All plateau basalts are significantly more siliceous than their ocean floor counterparts and tend to have lower Mg/Fe ratios and Ni and Cr abundances, implying that they are more evolved (less primitive) than an original partial melt formed from a mantle source. Traditionally, these chemical characteristics of plateau basalts have been ascribed in part to sialic contamination of the basalt magma as it penetrated the continental crust. Evidence from the Columbia Plateau does not substantiate this view. $^{87}Sr/^{86}Sr$ ratios do increase with time during the 11.0 million years of eruption (McDougall, 1976; Nelson and others, 1980), but attempts to correlate this with chemical changes such as increasing SiO_2 or K_2O percentages have been notably unsuccessful with the exception of the very last few percent of the erupted material (Saddle Mountains Basalt) for which a case for significant assimilation of crustal rocks has been made (Helz, 1979; Nelson and others, 1980).

Shaw and Swanson (1970) and Swanson and others (1975b) have emphasized the very rapid eruption rate of the Columbia River basalt and the physical problems this poses for any model that includes low pressure crystal fractionation or extensive crustal assimilation in magma chambers within the crust. Various authors (Goles and Leeman, 1976; Wright and others, 1976; Wright and Helz, 1979) stress the apparent inability of fractionation of lower pressure phases to account for the compositional differences between the many chemical types represented on the plateau. In the most general way, the present evidence points to the individual basalt members representing separate partial melts, probably associated with crystal fractionation at depth after separation from the residual mantle (to account for the low Mg/Fe ratios and Ni and Cr abundances). Some melts may have been modified locally by low pressure fractionation (as in the Imnaha Basalt) and crustal assimilation (as in some of the Saddle Mountains Basalt members). The small variations in the $^{87}Sr/^{86}Sr$ ratio and the ratios of incompatible elements may be explained by heterogeneities in the mantle source (Wright and others, 1979).

SUMMARY

The application of new field and laboratory techniques (whole rock chemistry and magnetic polarity measurements) has produced a reconnaissance geologic map of most of the Columbia Plateau (Swanson and others, 1979a) and a detailed stratigraphy for the Columbia River Basalt Group. No other flood basalt province has yet been mapped in such detail. Mapping along the eastern margin of the plateau in Idaho gives geologists a rare opportunity to investigate geologic processes along the edge of a flood basalt province where canyon-cutting has resulted in excellent exposures of the stratigraphic section. These exposures allow an evaluation of (1) the role of prebasalt structural or erosional paleotopography, or both, in influencing flow distribution, (2) the relationship between present structures and reactivated prebasalt structures, and (3) the development of lava dams and the ensuing relations between encroaching basalt and marginal basins of deposition. A summary of the geologic history along the eastern margin of the plateau follows.

Columbia River basalt volcanism began 17.0 million years ago in the Weiser embayment, Idaho, and adjacent northeast Oregon with extrusion of Imnaha Basalt from dikes in the extreme southeast corner of the plateau (Figure 2). The youngest Imnaha flows advanced into the Clearwater embayment during late N_0 and possibly early R_1 time. Uplift of the eastern margin of the plateau is evident throughout Grande Ronde time. Grande Ronde magnetostratigraphic units thin and progressively pinch out to the east in the Clearwater embayment and adjacent northeast Oregon and southeast Washington. Only a thin wedge of Grande Ronde R_2 occurs in the Clearwater embayment; Grande Ronde N_2 is absent (Figure 7). The northeast corner of the plateau was exempt from regional tilting during Grande Ronde time as implied by the occurrence of Grande Ronde N_2 throughout the area covered by the Spokane 1° x 2° quadrangle in Washington and in the St. Maries embayment, Idaho.

Deformation near the end of Grande Ronde time resulted in uplift of the Nez Perce plateau in Idaho (Clearwater embayment) and the Joseph Plains in Oregon along the northeast-trending Limekiln fault. This uplift effectively isolated the Weiser embayment and most of northeast Oregon from further volcanism generated from dikes in the northern part of the Chief Joseph swarm (Figures 3, 7, and 8). By the end of Grande Ronde volcanism in the Clearwater embayment, uplift along the Limekiln and Mt. Idaho faults had led to the development, or

enhancement, of the Lewiston and Stites structural basins (Camp and Hooper, 1981).

After a late Grande Ronde-early Wanapum period of soil formation in the Clearwater embayment, the Priest Rapids Member was extruded from a north-northwest-trending linear system of dikes extending through Orofino, Idaho. Because of the regional paleoslope, the Priest Rapids Member flowed to the west across an irregular surface mantled by residual soil (saprolite). The Priest Rapids Member was restricted to the Lewiston and Stites structural basins and low-lying areas of the Clearwater embayment, which resulted from deformation during late Grande Ronde time. In addition, several flows of the Priest Rapids Member were probably extruded from a dike along the northern extension of the linear system that cut the present St. Joe River valley. These flows presumably flowed down the valley to cover the St. Maries embayment. From the Clearwater and St. Maries embayments, the Priest Rapids Member continued to flow to the west eventually covering about one-half of the Columbia Plateau, making it one of the most voluminous members in the Columbia River Basalt Group (Swanson and others, 1979c).

Most Saddle Mountains Basalt members had their source in the southeast part of the plateau, and several were erupted from centers in the Clearwater embayment (Camp, 1981). No known Saddle Mountains Basalt occurs in the Weiser or St. Maries embayments. The Wilbur Creek, Lapwai, Asotin, Weippe (Pomona), and Swamp Creek Members were erupted in and around the North Fork of the Clearwater River west of Headquarters, Idaho. The Grangeville, Icicle Flat, and Craigmont Members were erupted from dikes cutting the Nez Perce plateau west and northwest of Grangeville, Idaho. The Lewiston Orchards and Lower Monumental Members were probably erupted from local sources in the Lewiston basin.

The distribution of Saddle Mountains Basalt in the Clearwater embayment and adjacent Washington and Oregon was significantly affected by the previous late Grande Ronde-early Wanapum deformation that uplifted the Nez Perce plateau and downdropped the Lewiston and Stites structural basins. The only Saddle Mountains flows occurring on the Nez Perce plateau are those whose dikes apparently cut the plateau. All other Saddle Mountains units in the Clearwater embayment are restricted to areas from which they erupted and to the low-lying areas which surround the Nez Perce plateau, including the Lewiston and Stites basins.

Erosion between successive eruptions of Saddle Mountains Basalt also had a strong influence on flow distribution. Those Saddle Mountains flows that erupted in the North Fork area poured into canyons of the ancestral Clearwater River during different stages of its development (Camp, 1981). The Wilbur Creek and Lapwai Members were restricted to these canyons which acted as conduits for transport westward to the Lewiston basin. The Asotin and Weippe Members filled and, in part, buried the ancestral canyons and flowed south to the Stites basin as well as west to the Lewiston basin. Several Saddle Mountains members left the Lewiston basin via ancestral canyons of both the Snake River and Union Flat Creek (Swanson and others, 1975a, 1975b, 1979c, 1980; Camp, 1976). Ancestral drainages allowed several members to travel remarkable distances across the plateau, as exemplified by the Weippe (Pomona) which, after erupting from the eastern extremity of the plateau, flowed west along ancestral drainages of the Clearwater, Snake, and Columbia Rivers, as far as the Oregon coast (Snavely and others, 1973; Swanson and others, 1975a, 1980; Beeson, 1979; Choiniere and Swanson, 1979; Anderson, 1980; Camp, 1981; Hooper, 1982).

The consistent north to north-northwest trend for dikes in the Monument and Chief Joseph swarms, together with the same trend for other dikes of Grande Ronde, Wanapum, and Saddle Mountains flows, implies that a consistent and definitive stress regime existed across most of the plateau throughout the middle and late Miocene. Compressional deformation during and after basalt eruption can be explained by a north-northwest horizontal axis of maximum compression, and fissure development with consequent dike injection can be explained by a complementary west-southwest horizontal axis of maximum tension (Figure 9; Hooper and Camp, 1981). The northwest and northeast structural grain of the prebasalt rocks underlying the plateau along its eastern margin (Figure 9a) was used to accommodate the regional stress regime, and this resulted in a similar fault pattern throughout the eastern part of the overlying plateau. That the stress regime has continued to exist through the Pliocene-Pleistocene and Holocene is evident from (1) approximately east-trending folds and associated reverse faults of post-Columbia River basalt age in the tri-state area (includes the Lewiston structure; Camp, 1975, 1976), (2) similar folding and faulting in the Yakima fold belt, some of which is Holocene in age (Bingham and others, 1970; Campbell and Bentley, 1980), (3) many small east-west reverse faults that cut gravel younger than the Lower Monumental Member in the Lewiston basin (Kuhns, 1980), and (4) composite focal mechanisms from low magnitude events, indicating that the central Columbia Plateau is under a general north-south compression today (Malone and others, 1975).

ACKNOWLEDGMENTS

Geologic mapping on which this paper is based was performed under U. S. Geological Survey-U. S. Department of Energy interagency agreement EY-78-1-06-1078. The mapping is part of the regional geologic studies of the Basalt Waste Isolation Project by Rockwell Hanford Operations for the U. S. Department of Energy. The manuscript was reviewed by S. Reidel, M. Ross, and S. Price. The authors wish to dedicate this paper to the memory of Jim Fitzgerald, who died in the May 18, 1980, eruption of Mount St. Helens.

REFERENCES

Anderson, J. L., 1980, Pomona Member of the Columbia River Basalt Group: an intracanyon flow in the Columbia River Gorge, Oregon: Oregon Geology, v. 42, no. 12, p. 195-199.

Axelrod, D. I., 1968, Tertiary floras and topographic history of the Snake River basin, Idaho: Geological Society of America Bulletin, v. 79, p. 713-734.

Bard, C. E., 1977, Mineralogy and chemistry of pyroxene from the Imnaha and lower Yakima Basalts of west-central Idaho: Washington State University M.S. thesis, 75 p.

Beeson, M. H., 1979, The origin of the Miocene basalts of coastal Oregon and Washington: an alternative hypothesis: Oregon Geology, v. 41, no. 10, p. 159-166.

Bingham, J. W. and M. J. Grolier, 1966, The Yakima Basalt and Ellensburg Formation of south-central Washington: U. S. Geological Survey Bulletin 1224-G.

Bingham, J. W., C. J. Londquist, and E. H. Baltz, 1970, Geologic investigation of faulting in the Hanford region, Washington: with a section on the occurrence of microearthquakes by A. M. Pitt: U. S. Geological Survey Open-File Report.

Bond, J. G., 1963, Geology of the Clearwater embayment: Idaho Bureau of Mines and Geology Pamphlet 128, 83 p.

———, 1978, Geologic map of Idaho: Idaho Bureau of Mines and Geology, Moscow, Idaho.

Byerly, Gary and D. A. Swanson, 1978, Invasive Columbia River basalt flows along the northwestern margin of the Columbia Plateau, north-central Washington: Geological Society of America, Abstracts with Programs, v. 10, no. 3, p. 98.

Camp, V. E., 1975, Structure and basalt stratigraphy of the "Lewiston Downwarp," Idaho-Washington: Geological Society of America, Abstracts with Programs, v. 7, no. 3, p. 300.

———, 1976, Petrochemical stratigraphy and structure of the Columbia River basalt, Lewiston basin area, Idaho-Washington: Washington State University Ph.D. dissertation, 201 p.

———, 1981, Geologic studies of the Columbia Plateau: Part II, Upper Miocene basalt distribution reflecting source locations, tectonism, and drainage history in the Clearwater embayment, Idaho: Geological Society of America Bulletin, v. 92, p. 669-678.

Camp, V. E. and P. R. Hooper, 1981, Geologic studies of the Columbia Plateau: Part I, Late Cenozoic evolution of the southeast part of the Columbia River Basalt Province: Geological Society of America Bulletin, v. 92, p. 659-668.

Camp, V. E., S. M. Price, and S. P. Reidel, 1978, Descriptive summary of the Grande Ronde Basalt type section, Columbia River Basalt Group: Rockwell Hanford Operations Document, RHO-BWI-LD-15, Richland, Washington, 26 p.

Campbell, Newell and R. D. Bentley, 1980, Late Quaternary faulting, Toppenish Ridge—south-central Washington: Geological Society of America, Abstracts with Programs, v. 12, no. 3, p. 101.

Choiniere, S. R. and D. A. Swanson, 1979, Magnetostratigraphy and correlation of Miocene basalts of the northern Oregon coast and Columbia Plateau, southeast Washington: American Journal of Science, v. 279, no. 7, p. 755-777.

Fitzgerald, J. F., 1982, Geology and basalt stratigraphy of the Weiser embayment, west-central Idaho, *in* Bill Bonnichsen and R. M. Breckenridge, editors, Cenozoic Geology of Idaho: Idaho Bureau of Mines and Geology Bulletin 26.

Fruchter, J. S. and S. F. Baldwin, 1975, Correlations between dikes of the Monument swarm, central Oregon, and Picture Gorge Basalt flows: Geological Society of America Bulletin, v. 86, p. 514-516.

Goles, G. G. and W. P. Leeman, 1976, Petrogenesis of Picture Gorge Basalt: a preliminary report: Geological Society of America, Abstracts with Programs, v. 8, no. 3, p. 376.

Gray, Jane and L. R. Kittleman, 1967, Geochronometry of the Columbia River basalt and associated floras of eastern Washington and western Idaho: American Journal of Science, v. 265, p. 257-291.

Griggs, A. B., 1976, The Columbia River Basalt Group in the Spokane quadrangle, Washington, Idaho, and Montana: U. S. Geological Survey Bulletin 1413, 39 p.

Hamilton, Warren, 1962, Late Cenozoic structure of west-central Idaho: Geological Society of America Bulletin, v. 73, p. 511-516.

Helz, R. T., 1979, Chemical and experimental study of the Ice Harbor Member of the Yakima Basalt subgroup; evidence for intracrustal storage and contamination: Abstract, American Geophysical Union, Northwest Meeting.

Hoffer, J. M., 1970, Plagioclase mineralogy of the Rock Creek flow, Columbia River basalt, *in* E. H. Gilmour and Dale Stradling, editors, Proceedings Second Columbia River Basalt Symposium: Eastern Washington State College Press, p. 51-53.

Holden, G. S., 1974, Chemical and petrographic stratigraphy of the Columbia River basalt in the lower Salmon River canyon, Idaho: Washington State University M.S. thesis, 97 p.

Holden, G. S. and P. R. Hooper, 1976, Petrology and chemistry of a Columbia River basalt section, Rocky Canyon, west-central Idaho: Geological Society of America Bulletin, v. 87, p. 215-255.

Hooper, P. R., 1974, Petrology and chemistry of the Rock Creek flow, Columbia River basalt, Idaho: Geological Society of America Bulletin, v. 85, p. 15-20.

———, 1980, The role of magnetic and chemical analyses in establishing the stratigraphy, tectonic evolution and petrogenesis of the Columbia River basalt, *in* K. V. Subbarao and R. N. Sukheswala, editors, Deccan Volcanism and Related Basalt Provinces in Other Parts of the World: Memoir Geological Society of India, 3, p. 362-376.

Hooper, P. R., 1982, The Columbia River basalts: Science, v. 215, p. 1463-1468.

Hooper, P. R. and V. E. Camp, 1981, Deformation of the southeast part of the Columbia Plateau: Geology, v. 9, p. 323-328.

Hooper, P. R., V. E. Camp, W. D. Kleck, S. P. Reidel, and C. E. Sundstrom, 1976, Magnetic polarity and stratigraphy of the southeastern part of the Columbia River Basalt Plateau: Geological Society of America, Abstracts with Programs, v. 8, no. 3, p. 383.

Hooper, P. R., C. R. Knowles, and N. D. Watkins, 1979, Magnetostratigraphy of the Imnaha and Grande Ronde Basalts in the southeast part of the Columbia Plateau: American Journal of Science, v. 279, p. 737-754.

Kirkham, V. R. D., 1931, Revision of the Payette and Idaho Formations: Journal of Geology, v. 39, p. 193-239.

Kirkham, V. R. D. and M. M. Johnson, 1929, The Latah Formation in Idaho: Journal of Geology, v. 39, p. 483-504.

Kleck, W. D., 1976, Chemistry, petrography, and stratigraphy of the Columbia River Group in the Imnaha River Valley region, eastern Oregon and western Idaho: Washington State University Ph.D. dissertation, 208 p.

Kuhns, M. J., 1980, Late Cenozoic deposits of the lower Clearwater valley, Washington State University M.S. thesis.

Laval, W. N., 1956, Stratigraphy and structural geology of portions of south-central Washington: University of Washington Ph.D. dissertation, 208 p.

Lindgren, Waldemar, 1898, The canyons of the Salmon and Snake Rivers, Idaho: Science, v. 7, p. 71-72.

Lynch, M. B., 1976, Remnant paleomagnetism in the Miocene basalts of north Idaho: University of Idaho M.S. thesis, 150 p.

Mackin, J. H., 1961, A stratigraphic section in the Yakima Basalt and Ellensburg Formation in south-central Washington: Washington Division of Mines and Geology Report of Investigation 19, 45 p.

Malone, S. D., G. H. Rothe, and S. W. Smith, 1975, Details of microearthquake swarms in the Columbia Basin, Washington: Seismological Society of America Bulletin, v. 65, p. 855-864.

McDougall, Ian, 1976, Geochemistry and origin of basalt of the Columbia River Group, Oregon and Washington: Geological Society of America Bulletin 87, p. 777-792.

McKee, E. H., P. R. Hooper, and W. D. Kleck, 1981, Age of Imnaha Basalt-oldest basalt flows of the Columbia River Basalt Group, northwest United States: Isochron West, no. 31, p. 31-33.

McKee, E. H., D. A. Swanson, and T. L. Wright, 1977, Duration and volume of Columbia River basalt volcanics, Washington, Oregon, and Idaho: Geological Society of America, Abstracts with Programs, v. 9, p. 463.

McNary, S. W., 1976, Petrographic and field studies of late Cenozoic basalt flows and intrusions in the Orofino-Elk River area, Idaho: University of Idaho M.S. thesis, 135 p.

Nathan, Simon and J. S. Fruchter, 1974, Geochemical and paleomagnetic stratigraphy of the Picture Gorge and Yakima Basalts (Columbia River Group) in central Oregon: Geological Society of America Bulletin, v. 85, p. 63-76.

Nelson, D. O., J. D. Cocker, and E. J. Dasch, 1980, Strontium and oxygen isotopic studies of radiogenic basalts of the Saddle Mountains Basalt: Geological Society of America, Abstracts with Programs, v. 12, no. 3, p. 144.

Pardee, J. T. and Kirk Bryan, 1926, Geology of the Latah Formation in relation to the lavas of the Columbia Plateau near Spokane, Washington: U. S. Geological Survey Professional Paper 140-A, 17 p.

Price, S. M., 1974, A geochemical classification of dikes of the Grande Ronde swarm, Columbia River basalt: Atlantic Richfield Hanford Company, U. S. Atomic Energy Commission Report ARH-SA-202, 29 p.

———, 1977, An evaluation of dike-flow correlations indicated by geochemistry, Chief Joseph swarm, Columbia River basalt: University of Idaho Ph.D. dissertation, 320 p.

Reidel, S. P., 1975, Pyroxene composition and subdivision of the lower Yakima Basalt of the Columbia River Group in the Snake and Salmon River canyons of Washington, Oregon, Idaho: Geological Society of America, Abstracts with Programs, v. 7, no. 3, p. 364-365.

———, 1978, The stratigraphy and petrogenesis of the Grande Ronde Basalt in the lower Salmon and adjacent Snake River canyons: Washington State University Ph.D. dissertation, 415 p.

———, 1982, Stratigraphy of the Grande Ronde Basalt, Columbia River Basalt Group, from the lower Salmon River and northern Hells Canyon area, Idaho, Oregon, and Washington, *in* Bill Bonnichsen and R. M. Breckenridge, editors, Cenozoic Geology of Idaho: Idaho Bureau of Mines and Geology Bulletin 26.

Ross, M. E., 1978, Stratigraphy, structure and petrology of the Columbia River basalt in a portion of the Grande Ronde-Blue Mountains area of Oregon and Washington: University of Idaho Ph.D. dissertation, 407 p.

Russell, I. C., 1902, Geology and water resources of the Snake River plains of Idaho: U. S. Geological Survey Bulletin 199, 192 p.

Schmincke, H. U., 1967a, Stratigraphy and petrography of four upper Yakima Basalt flows in south-central Washington: Geological Society of America Bulletin, v. 78, p. 1385-1422.

———, 1967b, Fused tuff and peperites in south-central Washington: Geological Society of America Bulletin, v. 78, p. 319-330.

Shaw, H. R. and D. A. Swanson, 1970, Eruption and flow rates of flood basalts, *in* E. H. Gilmour and Dale Stradling, editors, Proceedings of the Second Columbia River Basalt Symposium: Eastern Washington State College Press, p. 271.

Shubat, M. A., 1979, Stratigraphy, petrochemistry, petrography and structural geology of the Columbia River basalt in the Minam-Wallowa River area, northeast Oregon: Washington State University M.S. thesis, 156 p.

Siems, B. A., J. H. Bush, and J. W. Crosby, 1974, TiO_2 and geophysical logging criteria for Yakima Basalt correlation, Columbia Plateau: Geological Society of America Bulletin, v. 85, p. 1061-1068.

Smiley, C. J. and W. C. Rember, 1979, Guidebook and road log to the St. Maries River (Clarkia) fossil area of northern Idaho: Idaho Bureau of Mines and Geology Information Circular 33, 27 p.

Snavely, P. D., Jr., N. S. MacLoed, and H. C. Wagner, 1973, Miocene tholeiitic basalts of coastal Oregon and Washington and their relations to coeval basalts of the Columbia Plateau: Geological Society of America Bulletin, v. 84, no. 2, p. 387-424.

Swanson, D. A., James Anderson, R. D. Bentley, G. R. Byerly, V. E. Camp, J. N. Gardner, and T. L. Wright, 1979a, Reconnaissance geologic map of the Columbia River Basalt Group in eastern Washington and northern Idaho: U. S. Geological Survey Open-File Report 79-1363, scale 1:250,000.

Swanson, D. A., J. L. Anderson, V. E. Camp, P. R. Hooper, W. H. Taubeneck, and T. L. Wright, 1981, Reconnaissance geologic map of the Columbia River Basalt Group, northern Oregon and western Idaho: U. S. Geological Survey Open-File Report 81-797, scale 1:250,000.

Swanson, D. A., R. D. Bentley, G. R. Byerly, J. N. Gardner, and T. L. Wright, 1979b, Preliminary reconnaissance geologic maps of the Columbia River Basalt Group in parts of eastern Washington and northern Idaho, U. S. Geological Survey Open-File Report 79-534, scale 1:250,000.

Swanson, D. A. and T. L. Wright, 1976, Magnetostratigraphic units in the Yakima Basalt, southeast Washington: Geological Society of America, Abstracts with Programs, v. 8, no. 3, p. 413-414.

———, 1978, Bedrock geology of the northern Columbia Plateau and adjacent areas, *in* V. R. Baker and Dag Nummedal, editors, The Channeled Scabland: NASA, Washington, D.C.

———, 1980, The regional approach to the Columbia River Basalt, *in* K. V. Subbarao and R. N. Sukheswala, editors, Deccan Volcanism and Related Basalt Provinces in Other Parts of the World: Memoir Geological Society of India, 3, p. 58-80.

Swanson, D. A., T. L. Wright, V. E. Camp, J. N. Gardner, R. T. Helz, S. M. Price, S. P. Reidel, and M. E. Ross, 1980, Reconnaissance geologic map of the Columbia River Basalt Group, Pullman and Walla Walla quadrangles, southeast Washington and adjacent Idaho: U. S. Geological Survey Miscellaneous Geologic Investigations Map I-1139, scale 1:250,000.

Swanson, D. A., T. L. Wright, and R. Clem, 1975a, Intracanyon flows of Yakima Basalt along the Snake River, southeast Washington: Geological Society of America, Abstracts with Programs, v. 7, no. 5, p. 645.

Swanson, D. A., T. L. Wright, and R. T. Helz, 1975b, Linear vent systems and estimated rates of magma production and eruption for the Yakima Basalt on the Columbia Plateau: American Journal of Science, v. 275, p. 877-905.

Swanson, D. A., T. L. Wright, P. R. Hooper, and R. D. Bentley, 1979c, Revisions in stratigraphic nomenclature of the Columbia River Basalt Group: U. S. Geological Survey Bulletin 1457-G, 54 p.

Taubeneck, W. H., 1970, Dikes of the Columbia River basalt in northeastern Oregon, western Idaho and southeastern Washington, *in* E. H. Gilmour and Dale Stradling, editors, Proceedings of the Second Columbia River Basalt Symposium: Eastern Washington State College Press, p. 73-96.

Uppuluri, V. R., 1974, Prineville chemical type: a new basalt type in the Columbia River Group: Geological Society of America Bulletin, v. 85, p. 1315-1318.

Vallier, T. L. and P. R. Hooper, 1976, Geologic guide to Hells Canyon, Snake River: Geological Society of America, Cordilleran Section Meeting, Pullman, Washington, 1976, Field Guide No. 5, 38 p.

Washburne, C. W., 1911, Gas and oil prospects near Vale, Oregon and Payette, Idaho: U. S. Geological Survey Bulletin 431, p. 56-57.

Waters, A. C., 1961, Stratigraphic and lithologic variations in the Columbia River basalt: American Journal of Science, v. 259, p. 583-611.

Waters, A. C., C. W. Myers, D. J. Brown, and R. K. Ledgerwood, 1980, Columbia Plateau with special emphasis on the basalt stratigraphy of the Pasco Basin, *in* K. V. Subbarao and R. N. Sukheswala, editors, Deccan Volcanism and Related Basalt Provinces in Other Parts of the World: Memoir Geological Society of India, 3, p. 19-44.

Watkins, N. D. and A. K. Baksi, 1974, Magnetostratigraphy and oroclinal folding of the Columbia River, Steens, and Owyhee basalts in Oregon, Washington, and Idaho: American Journal of Science, v. 274, p. 148-189.

Wheeler, H. E. and E. F. Cook, 1954, Structural and stratigraphic significance of the Snake River capture, Idaho-Oregon: Journal of Geology, v. 62, p. 525-536.

Wright, T. L., M. J. Grolier, and D. A. Swanson, 1973, Chemical variation related to the stratigraphy of the Columbia River basalt: Geological Society of America Bulletin, v. 84, p. 371-386.

Wright, T. L. and R. T. Helz, 1980, Generation of the tholeiitic basalt: a comparative study of three interplate provinces, *in* K. V. Subbarao and R. N. Sukheswala, editors, Deccan Volcanism and Related Basalt Provinces in Other Parts of the World: Memoir Geological Society of India, 3, p. 419-421.

Wright, T. L., D. A. Swanson, and John Fruchter, 1976, Petrogenesis of Yakima Basalt in southeast Washington: Geological Society of America, Abstracts with Programs, v. 8, no. 3, p. 422.

Wright, T. L., D. A. Swanson, and R. T. Helz, 1979, Generation of continental tholeiite of the Yakima Basalt subgroup: geological and chemical constraints: Abstracts, Hawaiian Symposium on Interplate Volcanism and Submarine Volcanism, Hilo, Hawaii, p. 51.

Stratigraphy of the Grande Ronde Basalt, Columbia River Basalt Group, From the Lower Salmon River and Northern Hells Canyon Area, Idaho, Oregon, and Washington

by

Stephen P. Reidel[1]

ABSTRACT

The Grande Ronde Basalt is the most voluminous formation (85 percent) of the Columbia River Basalt Group. The thickest exposed section (about 800 meters) occurs near the confluence of the Grande Ronde and Snake Rivers and consists of three magnetostratigraphic units (R_1, N_1, R_2) and thirty-five flows.

The Imnaha Basalt underlies the Grande Ronde Basalt and was erupted into a mountainous terrain consisting of Triassic and Jurassic metasedimentary and metavolcanic rocks. One flow of the Saddle Mountains Basalt overlies the Grande Ronde Basalt near the confluence of the Snake and Grande Ronde Rivers.

Detailed mapping of the magnetostratigraphic units and physically distinct flows combined with chemical analyses of basalt flows from sixteen measured and sampled stratigraphic sections permit the refinement of the Grande Ronde Basalt stratigraphy. The thickness of the R_1 magnetostratigraphic unit remains relatively constant across the area, but the number of flows decreases to the east. Both the N_1 and R_2 magnetostratigraphic units thin eastward, with a corresponding decrease in the number of flows. The physical characteristics of several flows are distinctive; thus these flows can be easily traced throughout the area. Most Grande Ronde flows, however, are physically similar and cannot be traced far. Plagioclase-phyric flows and those with thick entablatures are the most easily recognized.

Chemical stratigraphy is by far the most useful and reliable technique for recognizing and correlating flows. Although the variation in chemical composition among most flows is small, many flows or groups of flows have one or more chemically distinct elements that allow them to be easily recognized. The flows of the R_1 magnetostratigraphic unit are all comparatively lower in SiO_2 and higher in MgO with several flows that are easily distinguished by their high MgO contents. Flows of the N_1 magnetostratigraphic unit are generally characterized by lower MgO and TiO_2 and higher SiO_2 than the R_1 flows. Several N_1 flows stand out with low TiO_2 contents. Flows of the R_2 magnetostratigraphic unit have high SiO_2 and incompatible element contents but generally are low in MgO.

Analysis of flow distributions indicates two types of flows: those of limited extent that pinch out within the area, and those of a much greater extent. The primary source was from the west, but a secondary source is present east of the area. Volume is the primary factor controlling the flow distribution, but of secondary importance is a westward-dipping paleoslope.

The structural evolution of the area is reflected by the distribution of flows. Two main fault directions occur in the area: northeast (as evidenced by the Limekiln fault, which was active in Grande Ronde time) and north-northwest. The parallelism of the dike trend, of the trend of the Snake River prebasalt ridge, and of the northwest fault trend suggests basement control on the prebasalt topography.

The petrographic characteristics of the flows are generally similar. The older R_1 flows are slightly coarser grained and contain more olivine and plagioclase phenocrysts. Plagioclase and augite are ubiquitous to the basalt; olivine, orthopyroxene, and accessory minerals are minor in abundance but important to the paragenesis.

Discriminant analysis was used to evaluate the characterization of a flow using only the chemical composition of a sample. It was found that 67 percent of the samples do indeed best characterize the flow from which they came. Of the 33 percent incorrectly

[1]Department of Geology, Washington State University, Pullman, Washington 99164.

Reidel, S. P., 1982, Stratigraphy of the Grande Ronde basalt, Columbia River Basalt Group, from the lower Salmon River and northern Hells Canyon area, Idaho, Oregon, and Washington, *in* Bill Bonnichsen and R. M. Breckenridge, editors, Cenozoic Geology of Idaho: Idaho Bureau of Mines and Geology Bulletin 26, p. 77-101.

reclassified by the technique, 46 percent were stratigraphically within one flow of the correct flow, 63 percent were within two flows, and 75 percent were within three flows. Calculated posterior probabilities provide a method of evaluating correlations with samples from unknown flows. Higher probabilities are generally associated with correctly classified samples, whereas low probabilities are associated with misclassified samples.

INTRODUCTION

The Columbia River basalt consists of a series of tholeiitic basalt flows that cover nearly 200,000 square kilometers of Idaho, Oregon, and Washington (Figure 1). It is the only Phanerozoic flood basalt province in North America having erupted between 17 and 6 million years ago (Watkins and Baksi, 1974; McKee and others, 1977). The Columbia River basalt encroached upon the Rocky Mountain highlands of Idaho in three places (Figure 1): the St. Maries embayment (Swanson and others, 1979b), the Clearwater embayment (Bond, 1963; Camp, 1981; Camp and others, 1982 this volume), and the Weiser embayment (Fitzgerald, 1982 this volume).

Recently, Swanson and others (1979a) have revised the Columbia River basalt nomenclature and subdivided it into five formations (Figure 2). The Grande Ronde Basalt is by far the most voluminous, constituting nearly 85 percent of the total volume (Reidel and others, 1982), even though it erupted over a relatively short time from about 16.5 to 14.5 million years ago (Watkins and Baksi, 1974). At least 800 meters of Grande Ronde Basalt is exposed in the deep canyons cut by the Salmon and Snake Rivers in the southeast part of the plateau (Camp and others, 1978).

Waters (1961) first recognized the main stratigraphic elements of the Columbia River basalt and produced the first reconnaissance geologic map of the plateau. Bond (1963) laid the groundwork for the present studies in the Clearwater embayment. He recognized two basic units, the upper and lower basalts, and several subdivisions of these units which he was able to map. The lower basalt was tentatively correlated with the Picture Gorge Basalt of Waters (1961), whereas the upper basalt was correlated with the Yakima Basalt. In the Clearwater embayment, the bulk of the upper basalt is Grande Ronde Basalt with lesser amounts of Wanapum and Saddle Mountains Basalt. The lower basalt was renamed the Imnaha Basalt by Hooper (1974) after a suggestion by Taubeneck.

Generally, the Wanapum and Saddle Mountains

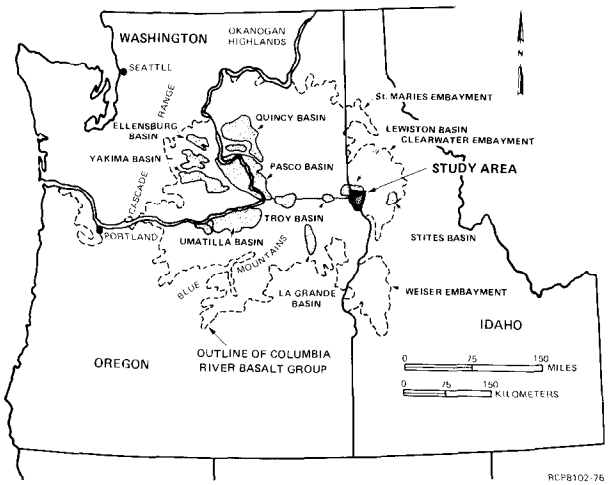

Figure 1. Extent of the Columbia River basalt in Idaho, Washington, and Oregon. Location of the area considered in this paper is shown on the east side of the plateau.

Basalts are easily recognized in the field, since most flows have distinct physical appearances. Chemical compositions, however, provide a means to easily verify identification, because many flows can be assigned to distinct chemical types (Wright and others, 1973; Swanson and others, 1979a). The Imnaha Basalt has received considerably less attention, but several detailed studies (Holden, 1974; Hooper, 1974; Holden and Hooper, 1976; Kleck, 1976; Reidel, 1978 and unpublished data) have shown that many distinct flows can be easily recognized throughout the area.

The Grande Ronde Basalt provides the most challenging stratigraphic problem of the Columbia River basalt. Wright and others (1973) and Swanson and others (1979a) were able to recognize only three distinct Grande Ronde chemical types on the plateau: the high-Mg, the low-Mg, and the very high-Mg, in spite of the overall dominance of the Grande Ronde Basalt. Swanson and Wright (1976) recognized four paleomagnetic reversals in the Grande Ronde Basalt from which a regional subdivision can be made. The magnetostratigraphic units are time units, however, and provide no information as to how many flows are present and if basalt flows from two different parts of the plateau are the same, or if they are entirely different ones erupted from different vents. Questions such as these are important to petrogenetic considerations and, ultimately, to the origin of the plateau.

The purpose of this paper is to present the results of a detailed study of the Grande Ronde Basalt stratigraphy from the lower Salmon River and northern Hells Canyon area. A detailed stratigraphy is developed using major, minor, and trace elements, paleomagnetism, and physical features of Grande Ronde Basalt flows from sixteen closely spaced

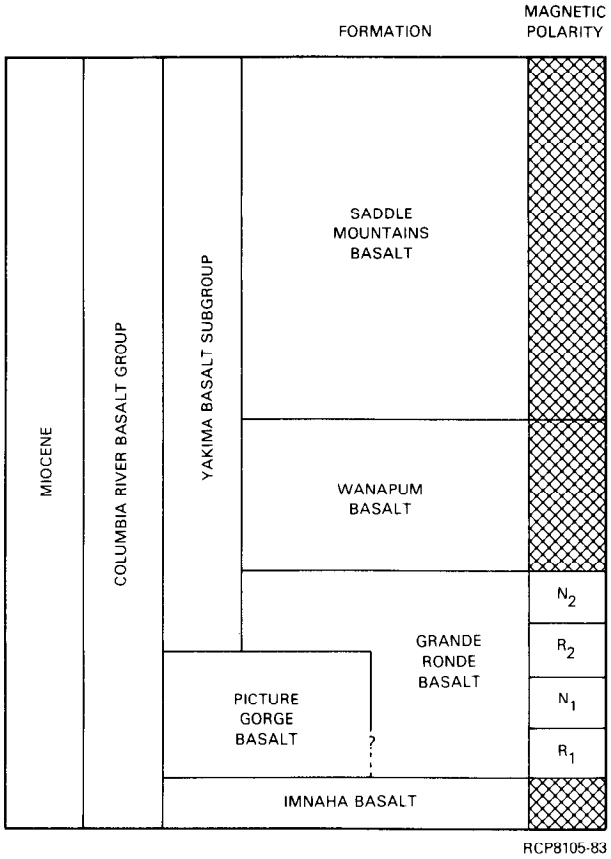

Figure 2. Generalized stratigraphy of the Columbia River Basalt Group. Nomenclature is based upon revision by Swanson and others (1979a).

stratigraphic sections. These data are then used to describe the general physical and chemical characteristics and the lateral extent of the flows. The implications these data have on developing a tectonic history of the area are also discussed. Finally, a method is provided for extending this stratigraphy elsewhere.

STUDY AREA

The area investigated covers over 1,000 square kilometers of deep canyon country in Idaho and adjacent parts of Oregon and Washington on the Snake River (Figure 3). This area makes up a portion of the western Clearwater embayment (Bond, 1963) and lies within the Chief Joseph dike swarm (Waters, 1961; Taubeneck, 1970).

Four units lie within the map area: the Permian, Triassic, and Jurassic metavolcanic, metasedimentary, and plutonic rocks that form the basement complex (Vallier, 1974, 1977), the Imnaha Basalt, the Grande Ronde Basalt, and the Saddle Mountains Basalt.

PERMIAN, TRIASSIC, AND JURASSIC METAMORPHIC ROCKS AND PREBASALT TOPOGRAPHY

Bond (1963) described the prebasalt Clearwater embayment as a rugged, mountainous terrain with a well-developed system of valleys and ridges. These ridges are composed of faulted and folded metasedimentary and metavolcanic rocks, which include the Seven Devils Group, and have been described by Vallier (1974, 1977).

Two major ridges existed prior to the Miocene volcanism, one along the present course of the Snake River (Figure 4) and one to the east, of which Cottonwood Butte is part. Both ridges had over a thousand meters of relief, the eastern one having the greatest.

The lower Salmon River area represented an intermontane basin at this time and was part of the Miocene Oregon drainage system of Bond (1963). Both Bond (1963) and Holden (1974) concluded that the system had a southwest gradient from the present highlands of Idaho.

IMNAHA BASALT

The Imnaha Basalt underlies the Grande Ronde Basalt and reaches a thickness of over 425 meters (Reidel, 1978) in the area, although the base of the section is not exposed in the lower Salmon River canyon. The Imnaha Basalt consists of ten exposed flows in the area. The prominent Eagle Creek interbed (Bond, 1963) occurs above the lowest exposed flow and makes an excellent marker bed in the lower Salmon River area.

Average flow thickness for the Imnaha Basalt in the area is about 60 meters. Ponding of flows against ridges and in valleys is common as evidenced by flows in excess of 100 meters thick; for example, at Downy Gulch, one flow reaches a thickness of 137 meters (Reidel, 1978).

The uppermost Imnaha flow in the lower Salmon River area is a plagioclase-phyric flow with phenocrysts up to several centimeters in size. This flow is over 70 meters thick at China Creek. Two to three flows below is the Rock Creek flow of Bond (1963), which Hooper (1974) described in detail from the Whitebird area. Throughout much of the lower

Salmon River area, the Rock Creek flow is over 100 meters thick and makes a prominent weathering horizon. Near Eagle Creek, a thick hyaloclastite-pillow complex is developed at the base of the flow.

Interbedded sediments with abundant plant fossils commonly occur between the flows, and pillowed, hyaloclastic zones are not uncommon, indicating that major rivers were flowing from the highlands to the east through the canyons at this time.

The prebasalt ridges formed significant barriers for many of the Imnaha flows. As the basalt flows began accumulating to great thicknesses, however, the topography was gradually submerged and flows were able to spread throughout the area.

SADDLE MOUNTAINS BASALT

One flow of the Saddle Mountains Basalt occurs in the northwest part of the area, north of the Grande Ronde River in the Lewiston basin (Camp and

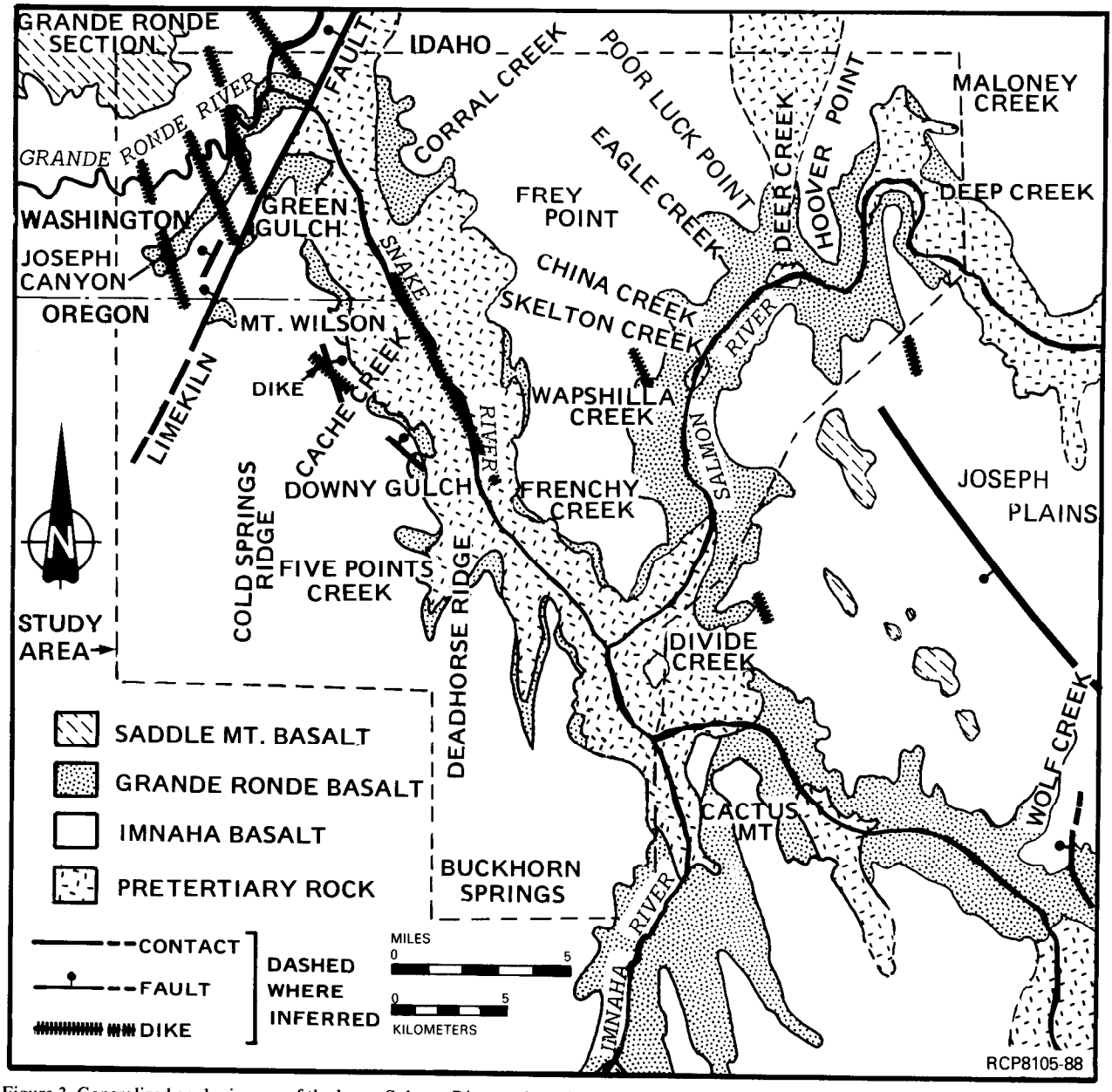

Figure 3. Generalized geologic map of the lower Salmon River and northern Hells Canyon area (generalized from Reidel, 1978; surrounding area generalized from Swanson and others, 1979b; Kleck, 1976; and Camp, 1981).

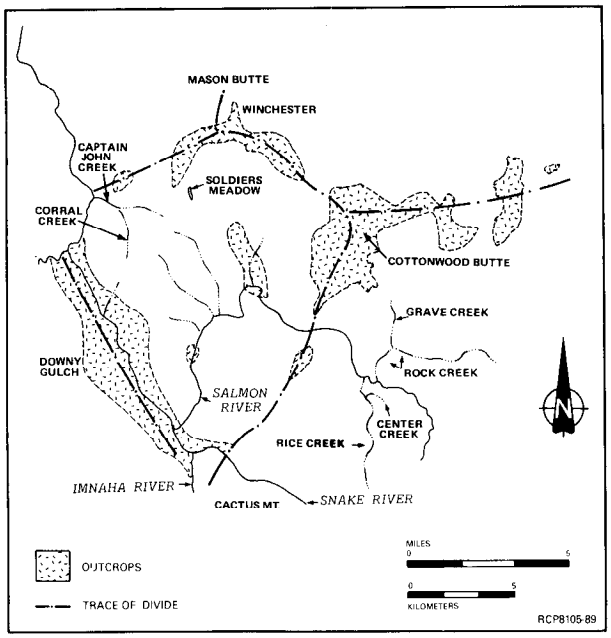

Figure 4. Exposures of metasedimentary, metavolcanic, and plutonic rocks older than Columbia River basalt in the lower Salmon River and northern Hells Canyon area. Trace of prebasalt ridges from Bond (1963).

others, 1978). This is the Slippery Creek flow of the Weissenfels Ridge Member. A flow of the Saddle Mountains Basalt also occurs on the Joseph Plains to the east but pinches out before reaching the area (Camp, 1981). Several dikes of Saddle Mountains Basalt composition are exposed on the canyon walls but did not erupt at the surface (Reidel, 1978). A dike near Cache Creek in the Snake River canyon has been identified as being of the Elephant Mountain chemical type, and a dike near Wapshilla Creek in the lower Salmon River canyon is similar chemically, yet distinct, to flows of the Saddle Mountains Basalt near Grangeville that have been mapped by Camp (1981).

GRANDE RONDE BASALT

The thickest sequence of the Grande Ronde Basalt exposed on the plateau (greater than 800 meters) occurs near the confluence of the Snake and Grande Ronde Rivers (Figures 3 and 5). Here the Grande Ronde Basalt consists of thirty-five flows, which vary from 30 to 75 meters in thickness, but the entire sequence of Grande Ronde Basalt thins eastward (Bond, 1963; Figure 5, this study). Grande Ronde Basalt flows stand out in marked contrast to the much thicker flows of the Imnaha Basalt. No sedimentary units occur between the Grande Ronde Basalt flows in this area.

Seventeen complete or partial sections of Grande Ronde Basalt from the area were measured and sampled for chemical composition and paleomagnetism (natural remanent magnetization). Seven sections were measured along the north wall of the Salmon River canyon, six in the Snake River canyon, three in Joseph Canyon, and one in the Imnaha River canyon. The Mt. Wilson section in Joseph Canyon is faulted in several places, so it was of limited use.

Of the four magnetostratigraphic units observed in the Grande Ronde Basalt by Swanson and Wright (1976) three are present in the area: the R_1, N_1, and R_2 (R [reversed] refers to the magnetic north pole being oriented opposite of the present earth field and N [normal] refers to it being oriented similar to the present field). Swanson and Wright's (1976) N_2 unit does not occur in the study area but pinches out about 20 kilometers to the west (Price, 1977; Ross, 1978) except for several isolated cones of the Joseph Volcanics in the Imnaha River area (Kleck, 1976; Camp and Hooper, 1980). The lower part of Grande Ronde Basalt along the Snake River north of the area was sampled and analyzed by Hooper and others (1979) for the inclination and declination of the paleomagnetic poles. They found that the lower two flows of the R_1 unit are transitional rather than reversed as indicated by a fluxgate magnetometer.

A total of 327 samples from the measured sections were collected and analyzed for major, minor, and trace elements using X-ray fluorescence (XRF) tech-

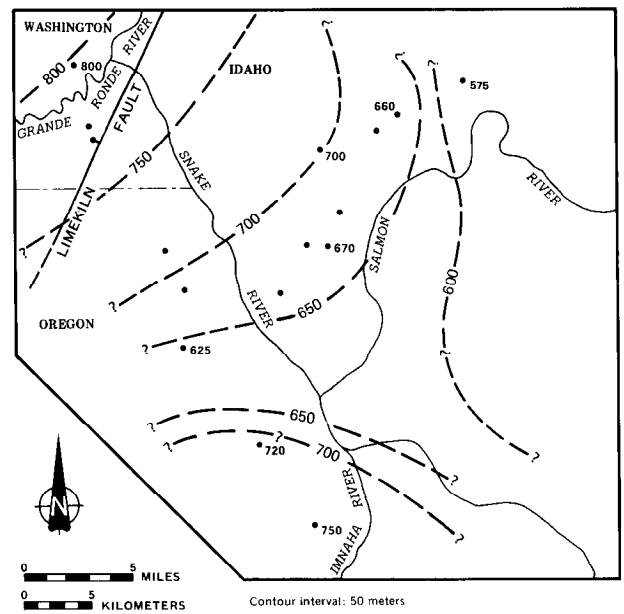

Figure 5. Isopach map of the Grande Ronde Basalt from the lower Salmon River and northern Hells Canyon area. Dots show locations of measured sections. Areas of thinning on paleotopographic highs omitted.

niques. In addition, 100 of these samples were analyzed for trace elements using instrumental neutron activation analysis techniques. These analyses were used to further identify and characterize flows. The analytical and total precision (Table 1) have been discussed by Reidel (1978).

THE R_1 MAGNETOSTRATIGRAPHIC UNIT

The R_1 magnetostratigraphic unit is the oldest subdivision of the Grande Ronde Basalt. Its thickness remains relatively uniform (about 300 meters, Figure 6) throughout much of the area, except where flows onlap the prebasalt ridges. There are thirteen flows near the Grande Ronde River and twelve flows in the Imnaha River valley. The number of flows, however, decreases to the east, with ten occurring near China Creek and seven at Hoover Point (Figure 3).

The fewer number of flows in the east than in the west, in contrast to the uniform thickness of the R_1 unit in the area, suggests that individual flow volume was one of the principal factors that controlled the lateral extent of the flows. Flows of less volume were confined to the west near the vent area, and flows having greater volume were able to move eastward into the valleys where they ponded and filled them to a uniform level.

Holden (1974) described several sections of Grande Ronde Basalt from the Rice Creek area, 20 kilometers farther east (Figure 4). Here the R_1 magnetostratigraphic unit is about 280 meters thick and has seven to eight flows (Holden and Hooper, 1976) with even less total thickness and fewer flows farther east near Whitebird (Camp and Hooper, 1980).

Table 1. Instrumental and total precision of X-ray fluorescence data.

	Total Precision		Instrumental Precision		
	1σ	(N)	1σ	(%)	(N)
SiO_2	0.28	(13)	0.27	(0.5)	(31)
Al_2O_3	0.16	(13)	0.04	(0.24)	(34)
TiO_2	0.03	(13)	0.02	(0.71)	(25)
FeO	0.18	(13)	0.09	(0.63)	(26)
MnO	0.005	(13)	0.002	(0.71)	(18)
CaO	0.11	(13)	0.05	(0.55)	(28)
MgO	0.08	(13)	0.08	(1.07)	(44)
K_2O	0.015	(13)	0.01	(0.004)	(28)
Na_2O	0.19	(13)	0.19	(5.48)	(24)
P_2O_5	0.007	(13)	0.004	(1.21)	(24)
Zr	8.8	(15)	3.51	(1.63)	(28)
Sr	5.5	(8)	7.0	(2.03)	(21)
Rb	2.3	(15)	4.0	(3.06)	(21)
Ba	14.4	(15)	43.3	(1.48)	(23)
V	14.5	(8)	16.0	(3.0)	(28)
Ni	4.5	(15)	7.5	(4.10)	(26)
Co	4.5	(15)	11.2	(-)	(25)
Cu	4.5	(7)	4.3	(3.03)	(27)
Sc	1.1	(15)	1.6	(1.47)	(26)
Cr	5.9	(15)			

Total precision (one standard deviation = 1σ) estimated for oxides from 13 sets of 3 beads; for trace elements, N number of beads of Grande Ronde Basalt prepared for each rock used. Instrumental precision for all elements from N number of replicate analyses. Instrumental precision is given as one standard deviation (1σ) relative to actual weight percent and percent of mean concentration percent, since several beads with concentrations much different from Grande Ronde Basalt were used, (Reidel, 1978).

THE N_1 MAGNETOSTRATIGRAPHIC UNIT

The N_1 magnetostratigraphic unit (Figure 7) is the second oldest subdivision of the Grande Ronde Basalt. Its thickness decreases from 300 meters at the Grande Ronde River to about 270 meters near Buckhorn Springs in the Imnaha River valley. The

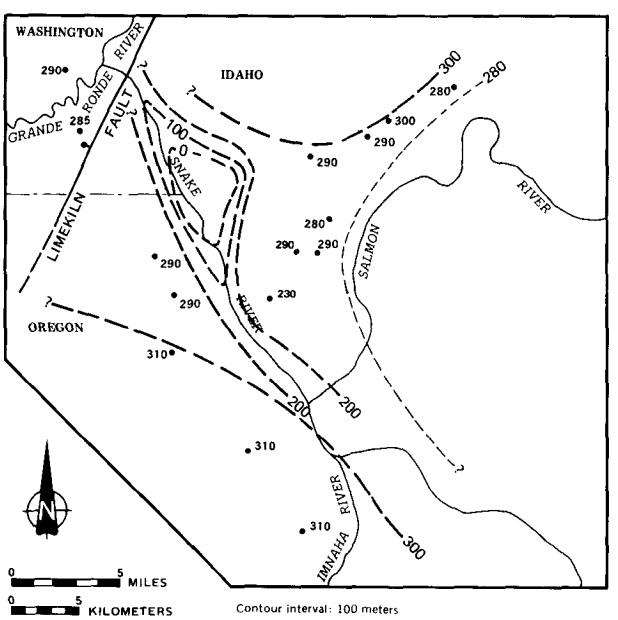

Figure 6. Isopach map of the R_1 magnetostratigraphic unit of the Grande Ronde Basalt from the lower Salmon River and northern Hells Canyon area. Thinning of basalt onto the prebasalt topographic high in the Snake River canyon is shown but near Hoover Point (Figure 3) thinning is not shown due to the size of the area of thinning. Dots show locations of measured sections.

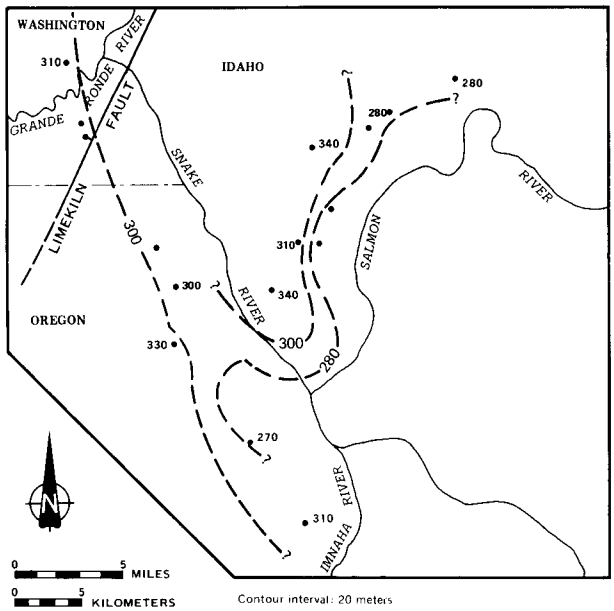

Figure 7. Isopach map of the N_1 magnetostratigraphic unit of the Grande Ronde Basalt from the lower Salmon River and northern Hells Canyon area. Thinning in the Snake River canyon is not shown due to lack of control and thinning near Hoover Point is not shown due to the size of the area of thinning. Dots show locations of measured sections.

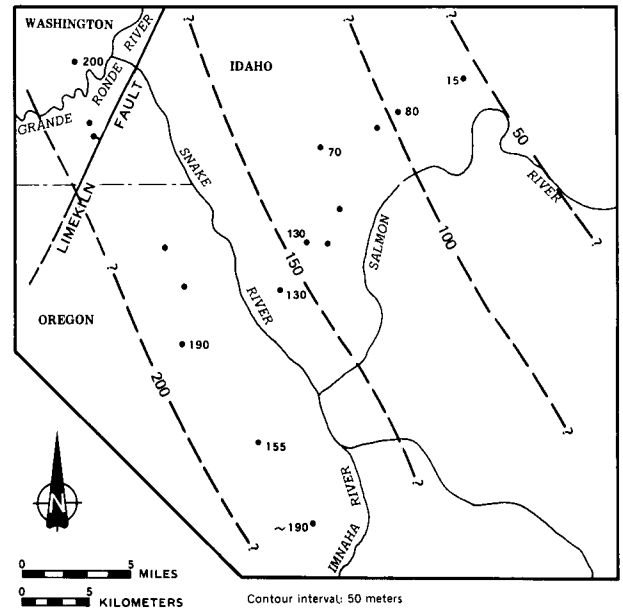

Figure 8. Isopach map of the original inferred thickness of the R_2 magnetostratigraphic unit of the Grande Ronde Basalt from the lower Salmon River and northern Hells Canyon area. Dots show locations of measured sections with actual measured thicknesses. Inferred thicknesses based upon estimation of amount of erosion.

thickness remains relatively constant as far east as China Creek but decreases to 260 meters at Maloney Creek, 15 kilometers farther east. The number of flows decreases from thirteen at the Grande Ronde River to about ten or eleven at Buckhorn Springs and to about nine flows at Maloney Creek.

Near Rice Creek, east of the study area (Figure 4), the N_1 magnetostratigraphic unit is about 220 meters thick and consists of five flows (Holden, 1974; Holden and Hooper, 1976). The eastward thinning of the N_1 magnetostratigraphic unit and the fewer number of flows suggest that flow volume and probably a westward-dipping paleoslope (Camp and Hooper, 1980) influenced the lateral extent of these flows.

THE R_2 MAGNETOSTRATIGRAPHIC UNIT

The R_2 magnetostratigraphic unit is the youngest unit exposed in the area (Figure 8). There are eight to nine R_2 flows with a total thickness of 185 meters extending from the Grande Ronde River south to the Imnaha River. This decreases eastward to one or two flows, a total of 15 meters thick near Hoover Point. Erosion has removed probably one flow from the eastern portion of the area and perhaps as many as two at Maloney Creek, and one or two flows have been eroded from the Buckhorn Springs section. Isolated remnants of R_2 have been found north of Rock Creek (Camp, in Swanson and others, 1979b); these are the farthest east of known R_2 flows.

Ross (1978) and Price (1977) show that the R_2 thickness remains relatively constant as far west as Troy, Oregon, but it thickens farther west into the Pasco Basin (Packer and Petty, 1979). Flows of the overlying N_2 magnetostratigraphic unit, which pinch out eastward near Troy, also thicken into the Pasco Basin (Packer and Petty, 1979; Taylor, 1976) supporting the concept that a westward-dipping paleoslope influenced the distribution of the R_2 and N_2 units.

GENERAL FLOW CHARACTERISTICS

There are three general parts (Figure 9) to a typical basalt flow in the area: a colonnade, an entablature, and a flow top. The colonnade and entablature are distinguished primarily by the size and regularity of jointing of the columns. The proportions of these parts vary in most flows. The average flow is 30 to 50 meters thick and has a well-developed colonnade, thin entablature, and thin, scoriaceous flow top. Most flows fall into Long's (1978) type 1 and type 3 flows. Type 1 flows have stubby, irregular columns that lack a well-defined entablature; type 3 flows have both well-defined entablatures and colonnades with a

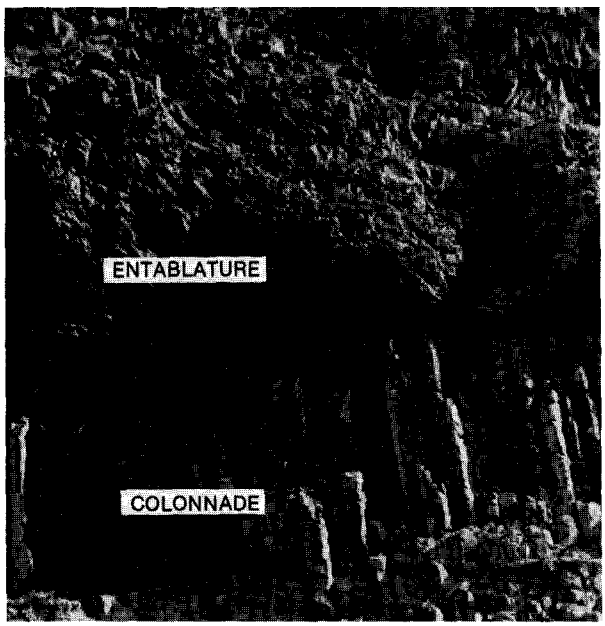

Figure 9. Exposure of Grande Ronde Basalt from the Pasco Basin having well-developed colonnade and entablature.

sharp break separating the two. Type 1 flows predominate over type 3 flows. Only rare examples of type 2 flows, multi-tiered (colonnade and entablature equal one tier) flows, are present; these are more common in the Imnaha Basalt.

Variations in the physical characteristics tend to be the rule, rather than the exception. Several flows, including the Center Creek and Johns Creek flows of Bond (1963), are composed almost entirely of entablature with little or no colonnade and minor flow-top scoria, and fit Long's (1978) type 3 classification. This makes them relatively easy to trace throughout much of the area. This characteristic varies slightly across the area but is best developed on the east side of the area where ponding occurred away from the vent. Flow-top breccias are present but not abundantly common. The breccias developed in the thicker flows and can be up to 40 percent of a 100-meter-thick flow. Flow-top breccia tends to vary in thickness along the length of the flow. They are most common in the west near the vent area, but become thinner and disappear eastward. Only the lowermost flows appear to be exceptions. They have thick flow-top breccias at the east side of the area but none at the west. Within thick flow-top breccias, commonly large pods of fine-grained, glassy basalt up to several meters in diameter occur.

Hyaloclastites are rare in the Grande Ronde Basalt from this area. In one location near China Creek, a small stream valley cut into Imnaha Basalt is filled with pillowed basalt and hyaloclastic material from the lowermost Grande Ronde flow. Nowhere is an extensive hyaloclastic deposit present that might be associated with a major river in the canyon. This is also supported by the absence of sedimentary interbeds.

FLOW CORRELATIONS BASED ON PHYSICAL AND PETROGRAPHIC APPEARANCE

Most Grande Ronde Basalt flows have a similar physical appearance, so few flows can be traced throughout the area with a high degree of confidence. Older flows generally have more distinguishing characteristics than younger flows; many are plagioclase-phyric, some contain olivine phenocrysts, and others are coarser grained.

A prominent plagioclase-phyric flow (P0, Figure 10) occurs near the base of the section. It is the second flow above the Imnaha-Grande Ronde contact in the lower Salmon River area and can be easily traced to Downy Gulch in the Snake River canyon and possibly to Buckhorn Springs in the Imnaha River canyon. Positive identification cannot be made farther north along the Snake River, but Camp (1976) has described the occurrence of many flows which are plagioclase-phyric in the lower part of the section near Lewiston. This flow is 30 meters thick in the Snake River canyon but 50 meters thick near Poor Luck Point. Generally it is a type 1 flow with a colonnade, a poorly developed entablature, and thin scoriaceous flow top. In the Salmon River area, where it reaches 50 meters in thickness, it has a well-developed entablature and is a type 3 flow.

Two plagioclase-phyric flows (P1 and P2) occur in the Grande Ronde section and have been informally named the Rogersburg flows (Camp and others, 1978). These have been traced south and east from the Grande Ronde section (Figure 10). Both flows occur in the western part of the area, but only the upper, more phyric flow (P2) occurs in the Salmon River canyon. This upper flow can be correlated farther east with a plagioclase-phyric flow near Rocky Canyon that Holden (1974) described. These flows are probably present in the sequence of plagioclase-phyric flows in the Lewiston basin described by Camp (1976). They are present as far west as the Umatilla dike near Puffer Butte in the Grande Ronde River valley (Price, 1977), but their westward extent is unknown. They vary from 10 to 60 meters in thickness, with the upper flow reaching its greatest thickness at Buckhorn Springs where it has a flow-top breccia. Throughout this area, these flows lie from 100 to 170 meters above the Imnaha Basalt-

Grande Ronde Basalt contact.

Bond (1963) and Holden (1974) described a plagioclase-phyric flow in the Rock Creek-Rice Creek area (Figure 4) that occurs three to four flows below the Center Creek flow. On the basis of their descriptions and its relative stratigraphic position, the flow is probably correlative with the upper Rogersburg flow (P2). Kleck (1976) also described a plagioclase-phyric flow in a similar stratigraphic position near Imnaha (Figure 3) in the Imnaha River valley which is probably also correlative.

Bond (1963) was able to trace three Grande Ronde flows throughout much of the southern Clearwater embayment: the Grave Creek, the Center Creek, and the Johns Creek flows. On the basis of his description, the Center Creek and Johns Creek flows were traced through much of the area, but the identification of the Grave Creek flow was more tenuous. The Grave Creek flow is the lowest stratigraphically, and in the study area the flows at that position do not fit Bond's (1963) description from the type area at Grave Creek (Figure 4). Flow B (Figure 10) is in the correct stratigraphic position but is not typical of the Grave Creek flow.

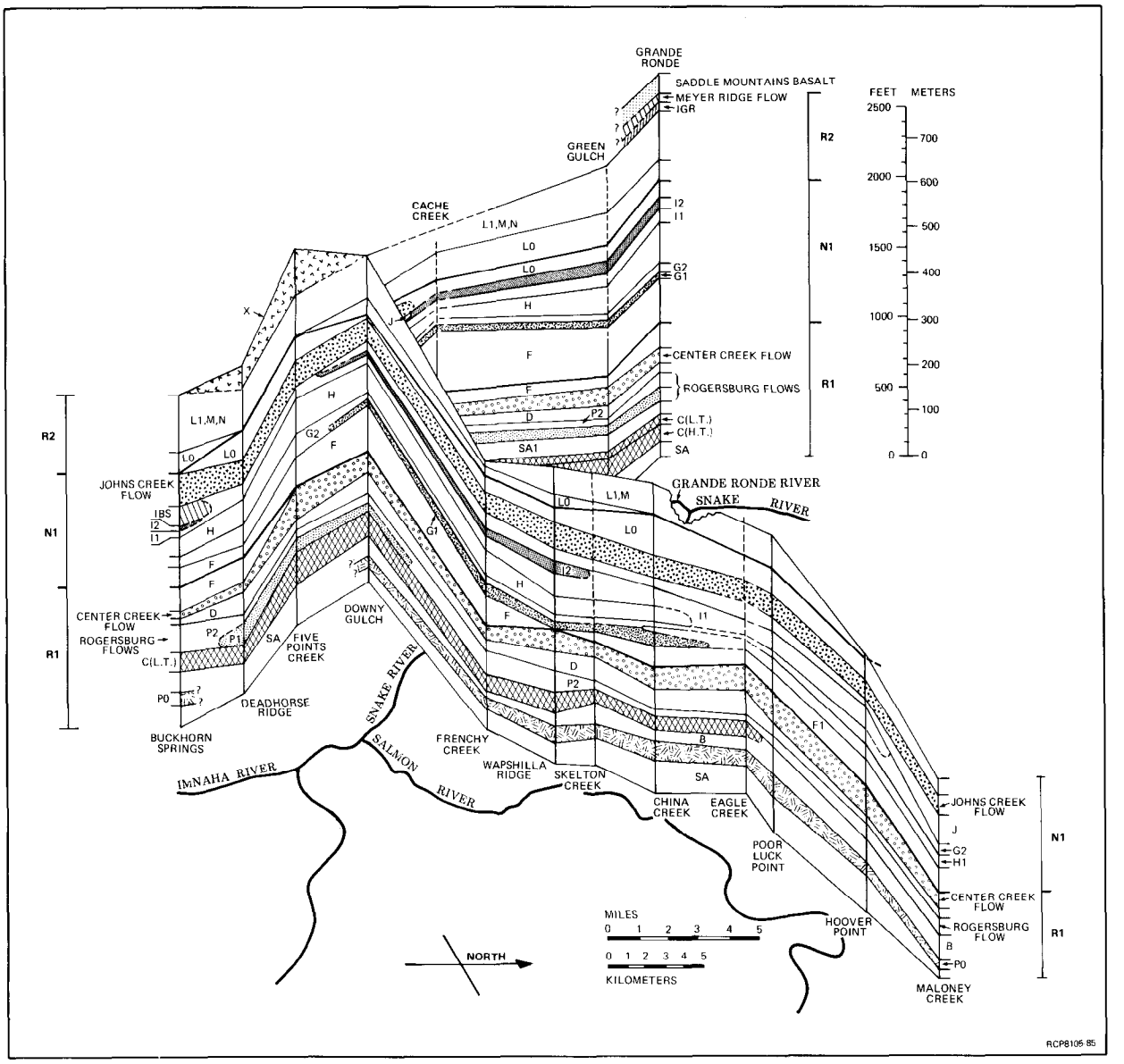

Figure 10. Fence diagram of the Grande Ronde Basalt showing the distribution and thickness of flows in the lower Salmon River and northern Hells Canyon area. Datum is Imnaha Basalt-Grande Ronde Basalt contact; prebasalt topographic highs are omitted.

The Center Creek flow (Figure 10) occurs near the top of the R_1 magnetostratigraphic unit and lies approximately 200 to 250 meters above the Imnaha Basalt-Grande Ronde Basalt contact. It varies in thickness from a maximum of 60 meters to a minimum of 15 meters in the Snake River canyon. Almost 80 percent of the flow is entablature near the east side of the area, but this decreases to less than 50 percent in the Snake River canyon. It is this thick entablature that sets it off from other flows. Locally, several flow lobes comprising the flow can be observed. The amount of scoria and flow-top breccia increases closer to the main dike occurrence. Holden (1974) recognized and mapped the Center Creek flow throughout the Rocky Canyon area east of the study area. There it occurs at the top of the R_1 magnetostratigraphic unit and physically resembles the flow in the area of this study. In the lower Salmon River canyon, the Center Creek flow also occurs at the top of the R_1 magnetostratigraphic sequence and forms a prominent bench, but in the Snake River canyon, several R_1 flows lie above it. No interbed or weathering zone was observed at the upper contact, suggesting that the bench results from the resistance of this flow to weathering.

The Johns Creek flow lies near the top of the N_1 magnetostratigraphic unit and occurs from 160 to 250 meters above the Center Creek flow. Near Poor Luck Point, almost 90 percent of the flow is entablature, which gives way westward to a thick flow-top breccia. On the western margin of the area, the Johns Creek flow is mapped as three similar-appearing flows which probably represent pulses of the same eruption. The flow can be traced east, but it apparently did not spread as far north as the present Grande Ronde River (Figure 10). Bond (1963) and Holden (1974) have traced the Johns Creek flow throughout much of the area to the east. At Rocky Canyon it occurs three flows below the top of the N1 magnetostratigraphic unit.

Other flows can be traced between sections, but the characteristics used to identify them are local. Many of these flows can be traced less than 15 kilometers and, in most places, only 5 to 7 kilometers. The inability of a Grande Ronde flow to retain physical characteristics over a great distance appears to be the rule, rather than the exception.

CHEMICAL STRATIGRAPHY

Waters (1961, 1962) first presented evidence for chemical differences among basalt flows of the Yakima Basalt. Wright and others (1973) subdivided the Yakima Basalt and described three chemical types within the Grande Ronde Basalt (formerly lower Yakima Basalt): the high-Mg, the low-Mg, and the very high-Mg. The Grande Ronde Basalt from the lower Salmon River and northern Hells Canyon area primarily falls within the low-Mg chemical type, although some flows are of the high-Mg chemical type. Camp (1976) divided the Grande Ronde Basalt flows from the Lewiston basin into a high SiO_2 group and an underlying and gradational low SiO_2 group. This subdivision can be extended into the area and generally corresponds to the base of the Center Creek flow, but is not a distinct break and has limited usefulness.

The chemical composition of the Grande Ronde Basalt is mostly gradational between flows. The differences discussed in this section are relative, and as Tables 2 and 3 show, there is considerable overlap between many flows for many oxides and elements. There are, however, many horizons that are distinct enough to be recognized with confidence throughout the area. These chemically distinct flows, combined with the physically recognizable flows and magnetostratigraphic units, were used to produce the fence diagram (Figure 10) for the lower Salmon River and northern Hells Canyon area. This diagram represents the best possible breakdown of flow stratigraphy based upon available data. Table 4 summarizes the number of flows or flow lobes for each group at each stratigraphic section.

CHEMICAL COMPOSITION OF FLOWS OF THE R_1 MAGNETOSTRATIGRAPHIC UNIT

The most chemically distinct group of flows is the group C flows (Figure 10). This group is characterized (Tables 2 and 3) by high CaO (about 9.0 weight percent) and MgO (about 5.0 weight percent). These flows also have low P_2O_5, K_2O, Na_2O, Zr, Rb, Ba, La, and FeO contents and high Cr and Cu contents. This group can be further subdivided using TiO_2; one group (H.T.) has a high TiO_2 composition (about 2.40 weight percent) while the other (L.T.) has a low TiO_2 composition (about 1.96 weight percent). The high TiO_2 flows occur only within the northern part of the area and pinch out before reaching Downy Gulch, but they are apparently present at Camp's (1976) Moses Siding section in the Lewiston basin. The low TiO_2 flows occur stratigraphically above the high TiO_2 flows but are more extensive. They can be traced as far east as Eagle Creek but pinch out to the north before reaching the Moses Siding section of Camp (1976). They are apparently present in Kleck's (1976) Imnaha section based on chemical analyses that he reported. This group is not present in the

Rocky Canyon section of Holden (1974). The overall composition of this group is actually more similar to the high-Mg Grande Ronde chemical type than to the low-Mg chemical type.

Below this horizon, the flows have been combined into one group, the SA group (Figure 10). The only distinct marker in this group is the lowest plagioclase-phyric flow (P0) discussed previously. This group has low SiO_2 (51-53.5 weight percent; Table 2), lower CaO and MgO than group C, but higher FeO, Sr, and Ba (Table 3), and is not greatly different from other flows of the R_1 magnetostratigraphic unit. Group SA has two subdivisions labeled A1 and B in the eastern part of the area because there the lower plagioclase-phyric flow makes a distinct marker. Flow B can be traced throughout the lower Salmon River area and is compositionally gradational to SA but has slightly higher SiO_2, Ba, and Th.

Flow group A1 consists of two flows present only at China Creek and represents a local subdivision of the SA group. Group A1 was separated because it has lower P_2O_5, Zr, and Ba yet higher TiO_2, CaO, and MgO than the SA group. Group A1 also has lower TiO_2, Zr, and Ba yet higher MgO and CaO than flow B. The chemical composition of the A1 group is not unlike flow P0, but the flows are not plagioclase-phyric.

The lower plagioclase-phyric flow, P0, and the two Rogersburg flows (P1 and P2) are all relatively similar in composition. They have higher than normal Ni contents (Table 3), but most flows, except the SA group of the R_1 magnetostratigraphic unit, have higher Ni, Cr, Sr, and Eu contents than those of the N_1 and R_2 magnetostratigraphic units.

Group SA1 lies below the Rogersburg flows and above the group C flows but is only present in the northern Snake River canyon. It is distinct from group C flows, but its composition is gradational with the Rogersburg flows.

Flow D is constrained stratigraphically by the upper Rogersburg flow (P2) below it and the Center Creek flow (CC) above it. The chemical composition of D is similar to both P2 and CC but has slightly higher SiO_2 and lower MgO than P2.

CHEMICAL COMPOSITION OF FLOWS FROM THE N_1 MAGNETOSTRATIGRAPHIC UNIT

The F and F1 groups are a series of similar flows both physically and chemically that occur at or above the transition from R_1 to N_1. They are constrained by the Center Creek flow below and above by several flows with distinct chemical compositions, the G group, that occur everywhere except on the eastern side of the area. Group F is confined largely to the Snake River canyon and group F1 to the lower Salmon River canyon; the distinction is made only because continuity between the two groups cannot be shown. Both groups have an overall compositional similarity to the Center Creek flow, but this is misleading because the flows within the F group have a great range which is reflected in the large dispersion (Tables 2 and 3).

Most flows of the N_1 magnetostratigraphic unit are generally characterized by TiO_2 contents lower than R_1 flows, but are compositionally distinct and can be traced throughout the area.

The group G flows (G1 and G2) are two flows with no major distinguishing physical characteristics. Their most significant feature is a lower than average TiO_2 content (Table 2) which is covariant with low P_2O_5, Zr, Ba, La, Sm, and Hf. They lie above the F group and below the H group, both of which have significantly higher TiO_2 than the G group. The oldest flow of the H sequence has a well-developed entablature and an extremely thick, scoriaceous flow-top breccia (up to 60 meters) that permits it to be traced in the southwestern part of the area. In the lower Salmon River canyon, however, a single flow of relatively higher TiO_2 (H1) intercalates with the group G flows at China Creek, within 5 kilometers of where the lower flow (G1) pinches out. The compositions of both H and H1 are variable as shown by the dispersion (Tables 2 and 3) which, for the case of H, is due to a greater range of values as in group F.

Two flows chemically similar to the G group, the I group, lie above the H group. They are also characterized by low TiO_2, P_2O_5, Zr, Ba, La, Sm, and Hf and are present throughout much of the area. The upper flow (I2) pinches out south of Downy Gulch and east of Wapshilla Ridge. There are two I group flows at Buckhorn Springs, however, which suggest that either the area between Downy Gulch and Buckhorn Springs is a local pinchout or the upper flow (I2) at Buckhorn Springs is a flow different from I2 along the lower Salmon River (Figure 10). The lower flow (I1) pinches out east of Hoover Point. The I group is overlain by flow J, which is chemically similar to the I group but confined to the lower Salmon River area. Flow J pinches out within a few kilometers to the north and south of Downy Gulch. It has higher Eu and lower Ni, Ta, and Cs than the group I flows. Two flows (IBS) at Buckhorn Springs lie in a stratigraphically similar position to flow J but have distinctly different compositions (Tables 2 and 3). They have higher TiO_2, FeO, K_2O, Rb, V, and P_2O_5 and lower SiO_2, MgO, and Sr and are compositionally similar to the overlying Johns Creek group, but with higher TiO_2 and P_2O_5.

The Johns Creek flow is traceable throughout the

lower Salmon River area, but on the west side it cannot be distinguished from several other flows or flow lobes, all of which have the same composition and are grouped together as the Johns Creek flow. A basaltic tuff is intercalated with the upper flow of the Johns Creek group in the Buckhorn Springs area and is compositionally the same. This suggests the presence of avent and the possibility that these flows are pulses of the Johns Creek flow. The Johns Creek flow has slightly lower CaO and higher FeO, La, Sm, and Hf (Tables 2 and 3) than the G, I, and J groups.

CHEMICAL COMPOSITION OF FLOWS OF THE R_2 MAGNETOSTRATIGRAPHIC UNIT

The L0 group, which overlies the Johns Creek flow, varies from one to five flows and occurs both above and below the transition from N_1 to R_2. It is typical of the R_2 flows (Tables 2 and 3) in that it has higher TiO_2, FeO, K_2O, Na_2O, P_2O_5, Ba, V, Sm, Th, and Ta and lower CaO, MgO, Sc, Cr, and Hf than typical N_1 flows. This is the first set of high TiO_2

Table 2. Chemical composition of flows and flow groups. [Individual analyses were determined using XRF techniques and normalized to 100 percent on a volitile free basis prior to calculating the mean $\bar{X}$ and one standard deviation 1σ. N indicates number of samples used to calculate general statistics.].

Flow	SA		A1		P0		B		C(L.T.)		C(H.T.)		SA1		P1	
Number of Samples	N=13		N=2		N=9		N=14		N=12		N=5		N=5		N=6	
Mean ($\bar{X}$), One std. dev. (1σ)	$\bar{X}$	1σ	$\bar{X}$	1σ	$\bar{X}$	1σ	$\bar{X}$	1σ	$\bar{X}$	1σ	$\bar{X}$	1σ	$\bar{X}$	1σ	$\bar{X}$	1σ
SiO_2	52.85	0.40	52.82	0.21	52.82	0.68	53.27	0.44	53.03	0.41	52.06	0.59	53.43	0.35	53.36	0.39
Al_2O_3	14.73	0.25	14.88	0.05	14.75	0.24	14.64	0.23	15.04	0.31	14.96	0.32	14.76	0.22	14.64	0.21
FeO	12.86	0.31	11.76	0.02	12.18	0.53	12.42	0.27	11.57	0.52	12.16	0.47	12.47	0.54	12.06	0.33
MnO	0.23	0.02	0.20	0.00	0.20	0.00	0.20	0.00	0.20	0.01	0.22	0.01	0.22	0.02	0.20	0.02
CaO	8.20	0.32	8.73	0.12	8.65	0.56	8.06	0.26	9.15	0.37	9.23	0.22	8.02	0.16	8.40	0.32
MgO	4.45	0.15	4.88	0.03	4.55	0.47	4.14	0.18	5.05	0.35	5.06	0.20	4.17	0.04	4.45	0.24
K_2O	1.15	0.13	1.44	0.02	1.32	0.24	1.59	0.11	0.98	0.13	1.11	0.14	1.38	0.07	1.40	0.03
TiO_2	2.21	0.10	2.34	0.00	2.43	0.11	2.46	0.09	1.96	0.07	2.40	0.06	2.32	0.09	2.28	0.06
P_2O_5	0.39	0.03	0.31	0.01	0.33	0.01	0.34	0.01	0.27	0.03	0.32	0.02	0.34	0.01	0.33	0.02
Na_2O	2.89	0.24	2.61	0.05	2.72	0.14	2.81	0.22	2.76	0.22	2.46	0.03	2.82	0.07	2.82	0.20

Flow	P2		D		Center Creek		F		F1		G1		H1		G2	
Number of Samples	N=13		N=16		N=20		N=23		N=10		N=5		N=6		N=10	
Mean ($\bar{X}$), One std. dev. (1σ)	$\bar{X}$	1σ	$\bar{X}$	1σ	$\bar{X}$	1σ	$\bar{X}$	1σ	$\bar{X}$	1σ	$\bar{X}$	1σ	$\bar{X}$	1σ	$\bar{X}$	1σ
SiO_2	53.58	0.59	54.11	0.64	54.47	0.42	54.67	0.90	54.94	0.77	55.01	0.72	55.62	1.41	54.66	0.74
Al_2O_3	14.65	0.24	14.71	0.23	14.78	0.23	14.67	0.33	14.90	0.37	15.14	0.34	14.73	0.12	15.09	0.21
FeO	12.16	0.56	12.07	0.67	11.96	0.54	12.09	0.85	12.01	0.69	11.08	1.07	11.66	1.01	11.22	0.61
MnO	0.20	0.01	0.19	0.01	0.20	0.01	0.20	0.01	0.20	0.01	0.19	0.01	0.21	0.03	0.21	0.02
CaO	8.13	0.42	7.82	0.44	7.66	0.27	7.63	0.39	7.43	0.52	8.23	0.72	7.09	0.71	8.24	0.72
MgO	4.21	0.34	4.09	0.38	4.02	0.26	3.84	0.35	3.73	0.43	4.45	0.63	3.58	0.45	4.38	0.61
K_2O	1.55	0.15	1.54	0.13	1.59	0.22	1.68	0.23	1.59	0.25	1.44	0.28	1.85	0.41	1.42	0.27
TiO_2	2.30	0.10	2.21	0.11	2.10	0.09	2.11	0.10	2.08	0.06	1.72	0.38	2.16	0.08	1.82	0.24
P_2O_5	0.33	0.02	0.32	0.03	0.32	0.03	0.31	0.04	0.30	0.03	0.25	0.03	0.33	0.03	0.25	0.02
Na_2O	2.85	0.22	2.87	0.21	2.84	0.16	2.70	0.30	2.76	0.22	2.41	0.11	2.71	0.31	2.65	0.12

flows above the low TiO_2 flows of the N_1 magnetostratigraphic unit. It is apparent in Figure 10 that flows of the L0 group in R_2 magnetostratigraphic unit are primarily in the Snake River area both north and south of the Deadhorse Ridge-Five Points Creek area, whereas L0 flows in the underlying N_1 magnetostratigraphic unit are more widespread.

The L0-3 group is a subgroup consisting of three flows or flow lobes of group L0 and occurs only at China Creek between the Johns Creek flow and group L0. It is distinguished by significantly lower TiO_2. Group L0-3 is shown as undivided from L0 on Figure 10 because of its local extent and because the combined thickness of L0-3 and L0 at China Creek are nearly similar to the thickness of L0 in nearby stratigraphic sections.

The L1 flow group lies directly above the L0 group and contains from two to five flows. The L1 flow group also has high TiO_2 (Table 2) but differs in that the flows have higher SiO_2, P_2O_5, Zr, Rb, Ba, La, Th, Hf, and Eu and lower CaO, MgO, Sc, and Cr (Tables 2 and 3) than L0. This group (L1) has been further divided into the M and N subgroups. In the M and N subgroups, CaO, V, and Sc are slightly higher and Sr

Table 2. continued.

Flow	H		I1		I2		J		IBS		Johns Creek		L0-3	
Number of Samples	N=17		N=15		N=9		N=7		N=2		N=17		N=3	
Mean ($\bar{X}$), One std. dev. (1σ)	$\bar{X}$	1σ	$\bar{X}$	1σ	$\bar{X}$	1σ	$\bar{X}$	1σ	$\bar{X}$	1σ	$\bar{X}$	1σ	$\bar{X}$	1σ
SiO_2	54.11	0.93	54.19	1.06	55.26	0.65	54.14	0.37	53.87	0.14	54.47	0.75	54.20	0.78
Al_2O_3	14.69	0.26	15.08	0.37	15.04	0.40	14.95	0.41	14.90	0.04	15.02	0.38	14.65	0.34
FeO	12.63	0.68	11.79	0.62	11.76	0.84	11.71	0.83	12.67	0.31	12.17	0.61	12.03	1.19
MnO	0.21	0.01	0.20	0.01	0.20	0.01	0.20	0.00	0.22	0.01	0.20	0.01	0.26	0.07
CaO	7.75	0.51	8.16	0.38	8.20	0.51	8.40	0.71	7.59	0.21	7.70	0.58	8.12	0.58
MgO	3.90	0.39	4.41	0.35	4.33	0.51	4.59	0.66	3.93	0.06	4.20	0.34	4.09	0.16
K_2O	1.47	0.20	1.35	0.14	1.33	0.36	1.26	0.17	1.52	0.07	1.35	0.10	1.51	0.17
TiO_2	2.09	0.16	1.81	0.10	1.90	0.24	1.79	0.23	2.14	0.04	1.88	0.09	1.93	0.09
P_2O_5	0.33	0.05	0.27	0.04	0.30	0.07	0.28	0.06	0.36	0.03	0.29	0.04	0.32	0.02
Na_2O	2.76	0.23	2.69	0.18	2.62	0.24	2.62	0.23	2.76	0.09	2.67	0.40	2.85	0.32

Flow	L0		L1		N		M		X		IGR		MRF	
Number of Samples	N=27		N=26		N=10		N=9		N=8		N=1		N=1	
Mean ($\bar{X}$), One std. dev. (1σ)	$\bar{X}$	1σ	$\bar{X}$	1σ	$\bar{X}$	1σ	$\bar{X}$	1σ	$\bar{X}$	1σ	$\bar{X}$	1σ	$\bar{X}$	1σ
SiO_2	54.21	0.89	54.73	0.81	54.11	0.83	54.24	1.11	54.27	0.89	53.44		52.94	
Al_2O_3	14.78	0.28	14.81	0.31	14.75	0.26	14.84	0.47	14.60	0.24	15.08		14.94	
FeO	12.60	0.67	12.42	1.19	12.63	0.81	12.16	1.26	12.66	0.84	12.33		10.28	
MnO	0.21	0.01	0.20	0.05	0.20	0.00	0.21	0.01	0.20	0.00	0.28		0.19	
CaO	7.49	0.52	6.93	0.33	7.26	0.46	7.49	0.33	7.33	0.34	8.63		10.18	
MgO	3.73	0.38	3.30	0.30	3.61	0.28	3.63	0.25	3.60	0.27	4.18		6.0	
K_2O	1.55	0.26	1.88	0.19	1.78	0.18	1.78	0.19	1.68	0.16	1.21		0.95	
TiO_2	2.26	0.10	2.44	0.20	2.41	0.15	2.40	0.20	2.27	0.07	1.80		1.61	
P_2O_5	0.37	0.03	0.44	0.05	0.38	0.02	0.41	0.04	0.40	0.02	0.28		0.26	
Na_2O	2.86	0.15	2.79	0.16	2.82	0.20	2.78	0.15	2.95	0.13	2.82		2.64	

Table 3. Trace element composition of flows and flow groups.

Flow	SA			A1			P0			B			C(L.T.)			C(H.T.)		
Element	N	$\bar{X}$	1σ	N	$\bar{X}$	1σ	N	$\bar{X}$	1σ	N	$\bar{X}$	1σ	N	$\bar{X}$	1σ	N	$\bar{X}$	1σ
Zr	13	220.74	15.28	2	204.80	6.64	9	219.15	9.18	14	232.94	7.55	12	183.77	8.10	5	201.89	9.70
Sr	13	310.09	17.19	2	352.15	3.04	9	354.11	10.02	14	342.87	13.99	12	352.89	34.32	5	356.45	11.21
Rb	13	35.52	3.58	2	44.80	4.10	9	40.07	4.02	14	43.28	3.14	12	38.13	1.79	5	35.30	6.20
Ba	13	463.08	38.99	2	427.86	3.81	9	451.86	46.94	14	504.78	31.88	12	348.49	35.61	5	495.21	100.60
V	13	405.77	18.39	2	358.05	67.24	9	346.36	23.07	14	362.17	11.45	12	325.36	31.72	5	370.12	21.21
Ni	13	41.58	26.89	2	19.02	10.55	9	30.39	18.16	14	35.90	27.77	12	54.50	23.85	5	80.80	35.10
Sc	13	42.40	2.11	2	37.40	1.41	9	36.90	2.76	14	37.02	1.61	12	40.41	1.93	5	37.61	1.93
Cu	13	131.02	29.88	2	38.33	2.94	9	56.03	18.48	14	62.93	42.63	5	123.31	43.64	5	107.50	56.67
Cr	13	42.35	14.53	2	69.10	19.09	9	75.40	36.31	14	42.35	17.65	5	97.82	47.20	5	85.61	28.10
La	5	22.74	2.67	1	24.61		1	23.21		2	21.30	3.30	5	19.74	1.43	2	21.04	1.78
Sm	5	7.66	2.22	1	7.85		1	13.12		2	7.26	2.19	4	6.11	0.31	3	5.76	0.46
Eu	5	2.27	0.13	1	2.13		2	2.31	0.24	2	2.13	0.45	5	2.02	0.14	3	2.14	0.14
Tb	2	0.98	0.21	1	N.D.		2	N.D.		1	0.90		1	1.51		2	1.03	0.16
Hf	5	5.01	0.51	1	4.72		2	5.09	1.48	2	4.79	1.49	5	4.01	0.60	3	4.30	0.53
Th	5	2.38	0.12	1	4.26		2	4.45	0.67	2	3.98	0.82	5	3.02	0.50	3	3.70	0.74
Ta	5	1.27	0.56	1	1.77		2	1.38	0.43	2	1.85	0.14	5	1.11	0.41	3	1.22	0.41
Cs	2	0.78	0.13	1	1.30		2	1.35	0.61	1	2.15		2	0.75	0.12	3	N.D.	

Flow	SA1			P1			P2			D			Center Creek			F		
Element	N	$\bar{X}$	1σ	N	$\bar{X}$	1σ	N	$\bar{X}$	1σ	N	$\bar{X}$	1σ	N	$\bar{X}$	1σ	N	$\bar{X}$	1σ
Zr	5	220.66	13.66	6	220.28	4.70	13	227.44	13.44	16	228.93	14.54	20	218.76	13.01	23	216.63	17.18
Sr	5	334.14	17.08	6	345.85	18.34	13	333.37	26.00	16	331.35	27.01	20	348.19	30.87	23	322.47	14.58
Rb	5	39.10	3.46	6	38.96	3.84	13	44.22	4.91	16	43.48	4.96	20	44.17	4.64	23	44.07	4.45
Ba	5	475.17	93.78	6	550.45	117.29	13	527.95	56.52	16	534.86	80.21	20	559.46	49.59	23	604.37	79.31
V	5	362.00	22.74	6	354.83	40.63	13	343.53	34.22	16	350.89	26.78	20	347.62	25.21	23	371.81	40.17
Ni	5	34.09	26.27	6	70.59	29.74	13	41.51	16.35	16	38.73	26.78	20	26.06	16.41	23	40.02	18.40
Sc	5	38.02	2.53	6	36.40	0.38	13	35.88	1.45	16	36.73	1.67	20	35.81	1.83	23	36.43	2.31
Cu	5	112.02	64.73	6	163.17	31.14	13	123.48	44.28	16	97.11	40.79	20	85.05	49.87	23	110.52	161.39
Cr	5	34.68	19.59	6	47.28	5.09	13	49.84	23.96	16	56.09	39.53	20	33.66	17.60	23	22.36	16.85
La	4	22.63	2.19	2	24.64	1.37	3	22.45	2.85	4	21.24	0.94	4	23.49	2.99	10	26.80	13.69
Sm	4	6.71	0.33	2	6.89	1.04	3	6.30	1.42	4	7.38	1.31	4	6.53	1.29	10	8.13	3.38
Eu	4	2.20	0.06	2	2.12	0.10	3	2.03	0.04	4	2.02	0.23	4	2.13	0.28	10	2.09	0.14
Tb	4	0.81	0.65	2	1.01	0.48	2	0.89	0.20	2	1.27	0.20	3	1.08	0.12	4	1.06	0.21
Hf	4	4.64	0.93	2	4.61	0.03	3	4.39	0.48	4	4.78	0.69	4	4.56	0.97	10	4.47	0.45
Th	4	3.44	0.79	2	3.72	0.59	3	3.80	0.83	4	4.17	1.12	4	3.93	0.79	10	3.93	0.64
Ta	4	1.15	0.30	2	1.22	0.02	3	1.04	0.30	4	1.31	0.35	4	1.35	0.66	10	1.31	0.40
Cs	1	0.39		2	0.40	0.56	2	1.09	0.42	2	1.30	0.01	4	0.73	0.24	10	1.40	0.14

Zr through Cr determined using XRF and La through Cs determined using INAA, values in ppm

Table 3. continued.

Flow	F1			G1			H1			G2			H			I1		
Element	N	$\bar{X}$	1σ	N	$\bar{X}$	1σ	N	$\bar{X}$	1σ	N	$\bar{X}$	1σ	N	$\bar{X}$	1σ	N	$\bar{X}$	1σ
Zr	10	218.72	12.76	5	192.16	25.69	6	228.11	35.21	10	195.19	22.56	17	195.92	15.94	15	177.24	9.67
Sr	10	338.81	28.48	5	340.36	29.41	6	330.14	18.09	10	343.39	21.97	17	322.36	13.93	15	329.98	10.56
Rb	10	46.40	4.16	5	41.14	21.44	6	48.83	9.90	10	42.81	5.26	17	41.12	4.81	15	43.76	3.15
Ba	10	607.34	63.44	5	454.31	81.90	6	685.08	183.31	10	506.54	84.07	17	557.73	58.63	15	451.66	54.00
V	10	345.88	34.27	5	325.36	51.29	6	342.31	56.16	10	311.20	26.67	17	348.18	46.91	15	320.38	30.01
Ni	10	24.74	12.41	5	45.56	37.09	6	22.19	15.55	10	25.91	24.17	17	33.73	22.48	15	22.41	17.83
Sc	10	36.65	2.55	5	36.40	1.76	6	35.89	3.61	10	37.35	1.64	17	38.22	1.11	15	39.37	1.91
Cu	10	64.37	40.00	5	71.99	52.75	6	46.71	18.04	10	57.23	31.68	17	54.49	29.56	15	50.77	31.70
Cr	10	39.86	17.25	5	30.32	19.88	6	45.56	16.55	10	38.60	12.74	17	29.39	17.95	15	33.60	23.87
La	1	23.10		2	22.30	2.15	1	24.76		3	21.37	2.55	6	21.83	2.04	2	18.50	0.36
Sm	1	7.71		2	6.55	1.37	1	7.75		3	6.33	0.76	6	6.53	0.98	2	5.71	0.02
Eu	1	2.24		2	1.99	0.26	1	2.32		3	1.86	0.08	6	1.94	0.14	3	1.82	0.19
Tb	1	N.D.		2	0.87	0.15	1	1.34		1	0.96		2	1.19		1	0.67	
Hf	1	5.07		2	4.30	0.84	1	5.73		3	4.02	0.56	6	4.32	0.69	3	3.80	0.29
Th	1	4.79		2	4.45	0.25	1	6.41		3	3.99	1.19	6	4.06	0.41	3	3.53	0.31
Ta	1	1.75		2	2.16	0.33	1	1.78		3	1.40	0.40	5	1.26	0.25	3	1.06	0.07
Cs	1	1.87		0	N.D.			2.03		3	1.15	0.44	5	0.74	0.24	2	0.94	0.16

Flow	I2			J			IBS			Johns Creek			L0-3			L0		
Element	N	$\bar{X}$	1σ	N	$\bar{X}$	1σ	N	$\bar{X}$	1σ	N	$\bar{X}$	1σ	N	$\bar{X}$	1σ	N	$\bar{X}$	1σ
Zr	9	185.80	19.78	7	176.84	20.76	2	176.30	17.39	17	186.90	12.03	3	194.10	8.20	27	198.20	17.81
Sr	9	335.88	17.80	7	334.65	10.22	2	314.15	8.69	17	324.60	20.13	3	333.73	22.47	27	340.57	19.99
Rb	9	39.36	5.75	7	43.22	2.36	2	49.94	1.76	17	43.49	3.85	3	42.73	5.91	27	42.35	5.85
Ba	9	472.22	115.92	7	438.80	113.80	2	521.36	26.72	17	494.14	58.09	3	592.42	52.40	27	620.57	107.70
V	9	323.11	37.32	7	311.05	37.72	2	389.00	37.75	17	335.53	46.74	3	365.80	31.96	27	366.04	27.34
Ni	9	33.08	28.85	7	16.41	13.44	2	14.89	0.38	17	23.65	15.79	3	6.84	5.45	27	25.17	23.58
Sc	9	39.48	1.05	7	39.24	1.27	2	40.10	0.42	17	39.57	1.22	3	39.03	0.47	27	37.78	2.44
Cu	9	49.84	39.58	7	76.42	58.06	2	29.48	7.91	17	66.16	44.31	3	49.50	14.40	27	46.94	36.19
Cr	9	31.98	17.88	7	32.72	13.26	2	50.85	2.19	17	45.64	19.32	3	36.63	20.59	27	35.01	15.01
La	2	20.57	3.29	2	19.14	6.83	2	21.43	2.44	4	22.35	1.33	3	22.85	2.53	9	22.69	2.46
Sm	2	5.78	0.02	2	5.61	1.11	2	7.26	1.62	4	6.65	0.52	3	7.91	0.53	9	7.64	3.90
Eu	2	1.71	0.22	2	2.03	0.31	2	1.99		4	1.91	0.12	3	1.90	0.05	9	2.14	0.12
Tb	1	0.96		1	1.12		2	N.D.		4	N.D.		3	N.D.		3	1.28	0.15
Hf	2	4.08	0.59	2	3.38	0.21	2	4.06	0.77	4	4.47	0.59	3	4.37	0.18	9	4.09	0.61
Th	2	3.63	0.02	2	3.20	0.61	2	3.58	0.26	4	3.52	0.97	3	3.40	0.26	9	4.31	1.38
Ta	2	1.31	0.43	2	0.82	0.12	2	1.02	0.28	4	0.95	0.27	3	1.16	0.12	9	1.20	0.41
Cs	2	1.07	0.04	1	0.76		2	0.92	0.33	4	0.96	0.49	3	1.05	0.42	9	0.87	0.36

Zr through Cr determined using XRF and La through Cs determined using INAA, values in ppm

Table 3. continued.

Flow	LI			N			M			X			IGR			Meyer Ridge		
Element	N	$\bar{X}$	1σ	N	$\bar{X}$	1σ	N	$\bar{X}$	1σ	N	$\bar{X}$	1σ	N	$\bar{X}$	1σ	N	$\bar{X}$	1σ
Zr	26	232.32	17.65	10	216.78	10.51	9	218.82	21.14	8	218.43	15.04	1	173.90		1	162.70	
Sr	26	339.96	24.41	10	328.60	18.96	9	345.60	31.29	8	330.83	17.45	1	339.60		1	346.60	
Rb	26	48.52	5.83	10	45.51	3.60	9	47.25	5.27	8	46.63	3.53	1	36.10		1	34.50	
Ba	26	791.71	117.02	10	695.46	74.33	9	783.15	156.19	8	697.60	68.52	1	569.08		1	349.68	
V	26	345.87	31.81	10	380.74	31.60	9	372.14	29.60	8	350.67	13.59	1	281.60		1	307.70	
Ni	26	20.53	17.21	10	35.95	28.60	9	28.06	13.88	8	33.56	21.92	1	66.46		1	118.17	
Sc	26	35.86	1.71	10	36.47	2.15	9	37.58	1.89	8	37.60	2.02	1	40.00		1	44.60	
Cu	26	34.99	15.64	10	52.61	27.89	9	80.71	51.27	8	54.98	17.88	1	195.44		1	173.05	
Cr	26	24.01	15.32	10	26.59	14.41	9	25.40	16.83	8	34.55	21.18	1	70.50		1	145.00	
La	6	27.17	2.62	4	24.32	3.23	4	29.55	5.09				1	25.09		1	19.38	
Sm	6	9.55	3.87	4	6.37	0.81	4	7.74	1.45				1	6.27		1	5.05	
Eu	6	2.26	0.15	4	2.04	0.26	4	2.35	0.25				1	1.88		1	1.71	
Tb	2	1.38	0.13	2	0.14	0.04	1	1.09					1	1.01		1	N.D.	
Hf	6	4.52	0.62	4	4.17	0.40	4	4.97	0.15				1	3.56		1	3.19	
Th	6	4.96	0.69	4	4.32	1.07	4	5.17	0.69				1	3.36		1	3.19	
Ta	6	1.05	0.26	4	1.16	0.45	4	1.59	0.44				1	1.16		1	1.43	
Cs	4	1.21	0.26	4	1.13	0.54	4	1.26	0.32				1	N.D.		1	0.53	

Zr through Cr determined using XRF and La through Cs determined using INAA, values in ppm

Table 4. Number of flows or flow lobes present in each stratigraphic section.

Flow or Flow Group	SA	A1	P0	B	CLT	CHT	SA1	P1	P2	D	C*C	F	F1	G1	H1	G2	H	I1	I2	J	IBS	J**CF	L0-3	L0	L1	N	M	X	IGR	M***RF
Section																														
Grande Ronde	2	0	0	0	1	2	1	1	1	1	1	7	0	1	0	1	1	1	1	0	0	0	0	4	1	1	3	0	1	1
Green Gulch	2	0	0	0	2	1	2	1	1	1	1	3+																		
Cache Creek	3	0	?	0	2	1	1	1	1	1	1	5+																		
Downy Gulch	4	0	1	0	1	0	1	1	1	2	1	5	0	1	0	1	2	1	1	1	0	2	0	3	1	2	1	0?	0	0
Five Points Creek	4	0	0	1	2	0	1	1	1	2	1	3	0	0	0	1	1	1	0	0	0	3	0	1	1	2	1	8	0	0
Deadhorse Ridge	4	0	0	0	1	0	0	1	2?	1	1	3	0	0	0	1	1	1	0	0	0	4	0	4	3	2	1	3+	0	0
Buckhorn Springs	2	0	1	0	2	0	0	0	1	1	1	4	0	0	0	1	1	1	1	0	0	3	0	2	3	2	?	0	0	0
Frenchy Creek	1	0	1	1	3	0	0	0	1	2	1	4	0	1	0	1	1	1	1	1	0	2	0	2	1+	?	?	0	0	0
Wapshilla Creek/Ridge	1	0	1	2	2	0	0	0	1	2	1	0	0	1	0	1	2	2	1	1	0	3	0	2	2	?	?	0	0	0
Skelton Creek	1	1	1	3	2	0	0	0	1	2	2	0	1	1																
China Creek	1	1	1	2	2	0	0	0	1	1	2	0	1	1	1	1	2	1	0	1	0	1	3	2	2	0	1	0	0	0
Eagle Creek	1	0	1	1	2	0	0	0	1	2	2	0	1+																	
Poor Luck Point	1	0	1	1	0	0	0	0	1	1	1	0	2	0	1	1	0	1	0	1	0	1	0	3	4	0	1	0	0	0
Hoover Point	1	0	1	2	0	0	0	0	1	1	1	0	2	0	1	1	0	1	0	1	0	1	0	2	1+	0	?	0	0	0
Maloney Creek	1	0	1	2	0	0	0	0	1	1	1	0	2	0	1	1	0	0	0	0	0	1	0	2	?	0	?	0	0	0

*Center Creek flow
**Johns Creek flow
***Meyer Ridge flow

and La (N only), and Sm are lower. The two subgroups generally differ, in that M is stratigraphically higher and has higher La while N has lower Ba, Eu, Hf, and Th. Subgroup N is recognized only in the Snake River canyon, while subgroup M can be recognized in both canyons.

In the Salmon River canyon near Downy Gulch, a sequence of thin flow lobes interpreted to be pulses of the same eruption are identified as group X. These flows are similar to group L1 but have lower Ba and TiO_2. They might extend south into the Imnaha Canyon or north beyond Downy Gulch, but they definitely pinch out before reaching the Grande Ronde section. Erosion in the area north of Downy Gulch and the lack of exposure near Buckhorn Springs prevents further estimates of this group's limits.

The youngest Grande Ronde flows in the area, IGR and Meyer Ridge flow (MRF, Camp, 1976), occur only in the Grande Ronde section and cannot be traced south across the Limekiln fault. This suggests that the Limekiln fault was probably active, thus preventing these flows from leaving a subsiding Lewiston basin. These flows are characterized (Tables 2 and 3) by low TiO_2, P_2O_5, Zr, Rb, Hf, and Th. The two differ in that the Meyer Ridge flow has significantly higher CaO, MgO, Cr, and Ni and lower La, Ba, and Sm. The Meyer Ridge flow, like group C, is compositionally closer to the high-Mg rather than the low-Mg chemical type.

DISTRIBUTION OF GRANDE RONDE BASALT FLOWS

It is apparent from Figure 10 that most flows are concentrated on the west side of the area. The thickness of the magnetostratigraphic units remains relatively constant along the strike of the dikes, as does the number of flows, but the entire section thins to the east. From the Grande Ronde area to Rocky Canyon, there is a loss of twenty-two flows. The main source for the flows was from the west, but a less important source at Rocky Canyon (Price and others, 1973) and a possible vent there described by Holden (1974) and Holden and Hooper (1976) could have fed some flows. The flows of the F1 and H1 groups and flow J are the most likely ones to have erupted east of the area. The eastward loss of flows is also reflected in the stratigraphic variations in chemical composition. Holden and Hooper (1976) recognized a distinct "SiO_2 break" at Rocky Canyon which occurs at the base of the flow below the Center Creek flow. This break is a local feature and is due to the absence of flows that constitute part of the complete gradational sequence observed farther west.

The Imnaha flows formed a relatively level surface within the steep-walled canyons and allowed the Grande Ronde Basalt flows to easily spread throughout the paleodrainage system. The thickening of R_1 flows to the east suggests a certain amount of ponding, possibly due to ramparts that built up along the dikes and blocked drainages to the east, but most flows moved unhindered from drainage to drainage. The lack of hyaloclastites and pillow complexes in the Grande Ronde Basalt demonstrates that the Imnaha Basalt had previously rerouted the canyon-cutting rivers and, at that time, only minor streams were flowing from the highlands into the canyons. If the rivers were still flowing in the area at this time, flows that erupted in the west and flowed east would have developed extensive hyaloclastic deposits as they moved up the river valleys.

The relatively consistent thicknesses of the R_1 and N_1 units, but with fewer flows in the east than in the west, suggest something about the volume of the flows. Many flows probably had insufficient volume to spread too far beyond the vent. Other flows were of sufficient volume to spread throughout the area and fill the canyons to a uniform level. It is these flows that had the greatest chance of reaching the Pasco Basin (Figure 1) and points west.

The analysis of flow distribution for this area thus suggests that two types of flows are present: those that are of a limited extent and those that are of a much greater extent, possibly as great as some of the flows of the Wanapum Basalt and Saddle Mountains Basalt. The flows of limited extent apparently outnumber those of much greater extent, but additional detailed studies similar to this will be necessary before a clearer idea of the regional distribution of Grande Ronde Basalt flows emerges.

Two other factors must be considered when dealing with the regional Grande Ronde Basalt relationships. First, a very gentle westward-dipping paleoslope that was forming in Grande Ronde time (Camp and Hooper, 1980) should have caused some eastward thinning. This is interpreted to be reflected in the total, gradual eastward thinning of the magnetostratigraphic units as shown on the isopach maps. These maps suggest that the slope could have been no more than 1 to 2.5 meters per kilometer in this area which is comparable to that determined by Long and others (1980) for the Pasco Basin. The second factor is the possibility that many flows on the western end of the study area are actually flow lobes, as in the case of the Johns Creek flow. The present distribution is probably a combination of all three but was most heavily influenced by flow volumes.

STRUCTURE

The structural evolution of an area on the Columbia Plateau is reflected by the distribution and thickness variations in the basalt flows. This was demonstrated by Reidel and others (1980) for the tectonic evolution of the Pasco Basin and by Camp and Hooper (1980) for the tectonic evolution of the Clearwater embayment.

The structural elements of the area are shown in Figure 11. Two fault directions have been observed in the area, one trending northeast that is marked by the Limekiln fault, and one trending N. 10-20° W. The Limekiln fault trends northeast along the northern boundary of the area and separates the Craig Mountain-Cold Springs Ridge area from the Lewiston basin. It is a normal fault with over 600 meters of displacement where the Snake River cuts it, but offset decreases both east (Bond, 1963; Camp, 1976) and west (Reidel, 1978). The N. 10-20° W. trend parallels the main dike trend and the Miocene Snake River ridge. These faults show primarily vertical movement, although horizontal slickensides found on other faults to the east by Holden (1974) and to the west by Ross (1978) suggest that some might have a component of horizontal movement. This is compatible with the tectonic model proposed by Ross (1978) for the Troy basin in Oregon and expanded by Camp and Hooper (1980) for the southeast plateau. This model is based upon a north-northwest-trending axis of maximum horizontal compression.

One of the primary questions concerning the tectonic history of the plateau is the timing of deformation. In this area, the distribution of late Grande Ronde Basalt flows (R_2) reveals that the Limekiln fault was active at this time. This is evidenced by the Meyer Ridge flow and the next youngest (IGR, Figure 10) which were prevented from crossing it and flowing south. This suggests that the Lewiston basin was subsiding by at least late Grande Ronde time. By N_2 Grande Ronde time and through Saddle Mountains time, it was an effective barrier preventing flows from crossing into the area. The Limekiln fault was probably active during much of the time the Columbia River basalt was being erupted. Similar conclusions were reached by Camp and Hooper (1980) for the southeast plateau.

It is difficult to estimate the rate at which the Limekiln fault was growing. Owing to the presence of a nearly representative sequence of flows through time in the Pasco Basin, rates of uplift have been determined for structures there (Reidel and others, 1980). Reidel and others (1980) have determined a relatively slow rate of uplift and subsidence (40 to 80 meters per million years) which is on the same order

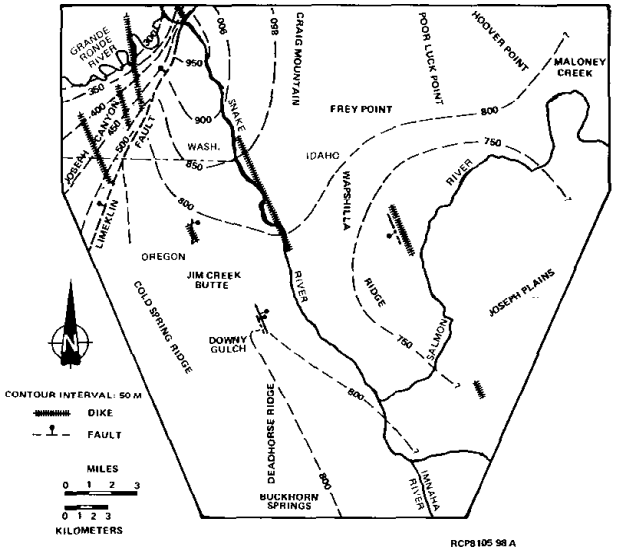

Figure 11. Structural contour map of the Imnaha Basalt-Grande Ronde Basalt contact in the lower Salmon River and northern Hells Canyon area. Contour interval is 50 meters and measured from sea level. Ball on fault indicates downthrown side.

of magnitude as present strain rates indicate (Savage and others, 1981). This has led Caggiano and others (1980) to suggest a relatively constant rate of uplift for those structures.

If the Limekiln fault and similar structures were growing at comparable rates, then deformation would be difficult to observe in the Grande Ronde Basalt since only 80 to 160 meters of offset would have occurred while over 800 meters of basalt were accumulating. The offset would probably be reflected in a minor thinning of flows at this time across the zone of deformation.

The parallel trend between the dikes, the northwest faults, the Snake River ridge, and the present course of the Snake River through the area suggests that a northwest fault direction has played an important role in the structural evolution of the area from before the Columbia River basalt was erupted (Reidel, 1978). As noted by Camp and Hooper (1980), the dominant structural trends throughout the southeast part of the plateau are coincident with those found in the prebasalt structural trends of northern Idaho.

MINERALOGY AND PETROGRAPHY

The mineralogy and petrography of the Grande Ronde Basalt from areas within the Clearwater embayment have been described by many individuals (Bond, 1963; Holden, 1974; Camp, 1976; Kleck, 1976;

Reidel, 1978; and Bard, 1978). This discussion is directed toward summarizing the mineralogy and petrography of the stratigraphic subdivisions for the Grande Ronde Basalt from the study area. First to be discussed will be the mineralogy, next followed by the distribution of mineral phases in flows, and finally the paragenetic sequence.

The Grande Ronde Basalt is generally fine grained and aphyric in hand specimen. Except for the presence of several coarser grained and plagioclase-phyric flows in the R_1 magnetostratigraphic unit, most flows have few diagnostic petrographic features. In thin section, clinopyroxene and plagioclase dominate the mineralogy. Although they are the predominant mineral phases, olivine, orthopyroxene, pigeonite, and accessory apatite, magnetite, ilmenite, and iron and copper sulfides are important to the paragenesis.

Textures range from intergranular to intersertal and occasionally are hyalo-ophitic. Intergranular textures are most commonly found in the colonnades, whereas intersertal textures occur in both the colonnade and entablature. Samples from the entablature have higher glass contents than those from the colonnade, with percentages of glass ranging from a few percent in the colonnade to greater than 50 percent in the entablature and flow tops. Samples from chilled margins and scoriaceous flow tops are commonly hyalo-ophitic.

OLIVINE

Olivine is a minor constituent of the Grande Ronde Basalt. The R_1 flows contain an average of 1.3 percent modal olivine, with no more than 3.0 percent in any one flow; the N_1 and R_2 flows average only 0.42 percent and 0.19 percent modal olivine, respectively. The greatest percent modal olivine occurs in the group C flows with as much as 6 percent olivine in some samples.

A little olivine occurs in the flows as subhedral crystals within the groundmass. Only one flow group, C, has subhedral olivine phenocrysts which occur intergrown with sparse plagioclase phenocrysts. Electron microprobe analysis of the phenocrysts yields an average core of Fo_{67} and rim of Fo_{47}. No liquid-crystal reaction rim was observed in any flow, but all crystals show some alteration (iddingsite?).

PLAGIOCLASE

Plagioclase occurs both as subhedral to euhedral crystals in the groundmass and as phenocrysts and microphenocrysts. It most commonly occurs in the groundmass, ranging in length from 0.1 to 0.5 millimeter, but plagioclase phenocrysts (5 to 10 millimeters in length) are common in many R_1 flows. A few phenocrysts occur in some of the N_1 and R_2 flows. Core to margin variations range from An_{69} to An_{52}, respectively (Reidel, 1978), and zoning is generally oscillatory with an overall normal trend.

PYROXENES

Three varieties of pyroxene occur in the Grande Ronde Basalt. These are augite, pigeonite, and bronzite-hypersthene. Augite is the most common clinopyroxene and occurs as both microphenocrysts and in the groundmass. The crystals are honey-yellow to clear, and most have a 2V of 42 to 50 degrees. Pigeonite is a common accessory phase of N_1 and R_2 flows but is less common in R_1 flows. Pigeonite most commonly occurs as distinct grains in the groundmass or as the core of a composite microphenocryst with an augite rim. As phenocrysts it commonly has optical zoning (Figure 12). Orthopyroxenes normally occur as unzoned phenocrysts or microphenocrysts (Figure 12) that possess a pale-pink/green pleochroism when the composition is hypersthene. The optic angle (2V = 55 to 70 degrees) places the composition of the orthopyroxenes as bronzite to hypersthene, and electron microprobe studies confirm this (Reidel, 1978 and unpublished data). In every sample, the orthopyroxene is mantled by pigeonite or less commonly by augite in a reaction relationship, and every orthopyroxene crystal shows some degree of resorption (Figure 12). Commonly orthopyroxene and plagioclase phenocrysts are intergrown.

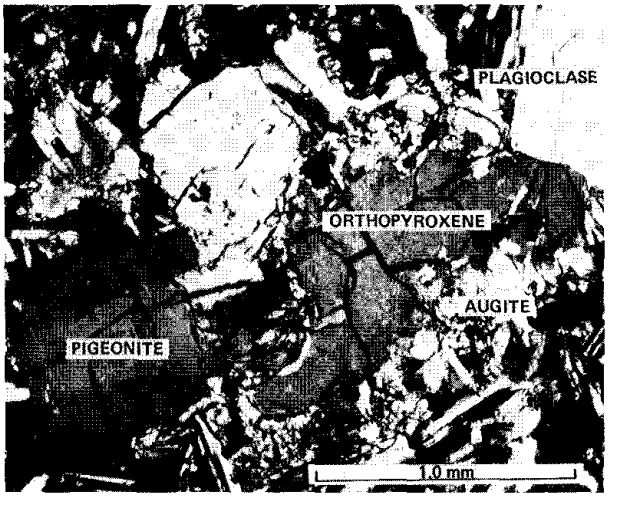

Figure 12. Photomicrograph of resorped orthopyroxene crystal with reaction rim of clinopyroxene. The orthopyroxene is intergrown with a plagioclase microphenocryst and an optically zoned microphenocryst of pigeonite.

OPAQUES

Titaniferous magnetite and sulfides (pyrite, pyrrhotite, and chalcopyrite) are present in minor amounts. A distinction between magnetite and ilmenite has been made based upon morphology, although the chemical compositions for samples from the area have not been determined. Octahedral, equant crystals are classed as magnetite, and elongate crystals are classed as ilmenite. Most opaque oxides from Grande Ronde Basalt in the Pasco Basin, however, are titaniferous magnetite (Noonan and others, 1980) and contain 28 to 32 percent TiO_2, so the distinction between magnetite and ilmenite in this study is probably morphological rather than chemical.

STRATIGRAPHIC VARIATION OF MINERALS

The important mineral phases, other than ubiquitous groundmass augite and plagioclase, are summarized for each flow group in Figures 13 and 14. Flows of the R_1 magnetostratigraphic unit are coarser grained than the N_1 and R_2 flows and contain more olivine, plagioclase phenocrysts, ilmenite, and less pigeonite. Pigeonite and bronzite-hypersthene are minor components in the R_1 flows. The flows of group C (Figures 13 and 14) have the most modal olivine, followed by the two Rogersburg flows. The silicic flows of the N_1 and R_2 units have more pigeonite and less olivine than R_1 flows; there is also less ilmenite and more orthopyroxene in these flows.

The mineralogy is independent of the stratigraphy as shown in Figures 13 and 14. Augite and plagioclase are present in every flow, but the pyroxene/plagioclase ratio is variable both within a flow at one location and laterally within a single flow (Reidel, 1978). The less abundant minerals vary greatly between stratigraphic sections; for instance in Figure 13, olivine is present in the Center Creek flow at China Creek, Downy Gulch, and Hoover Point, yet

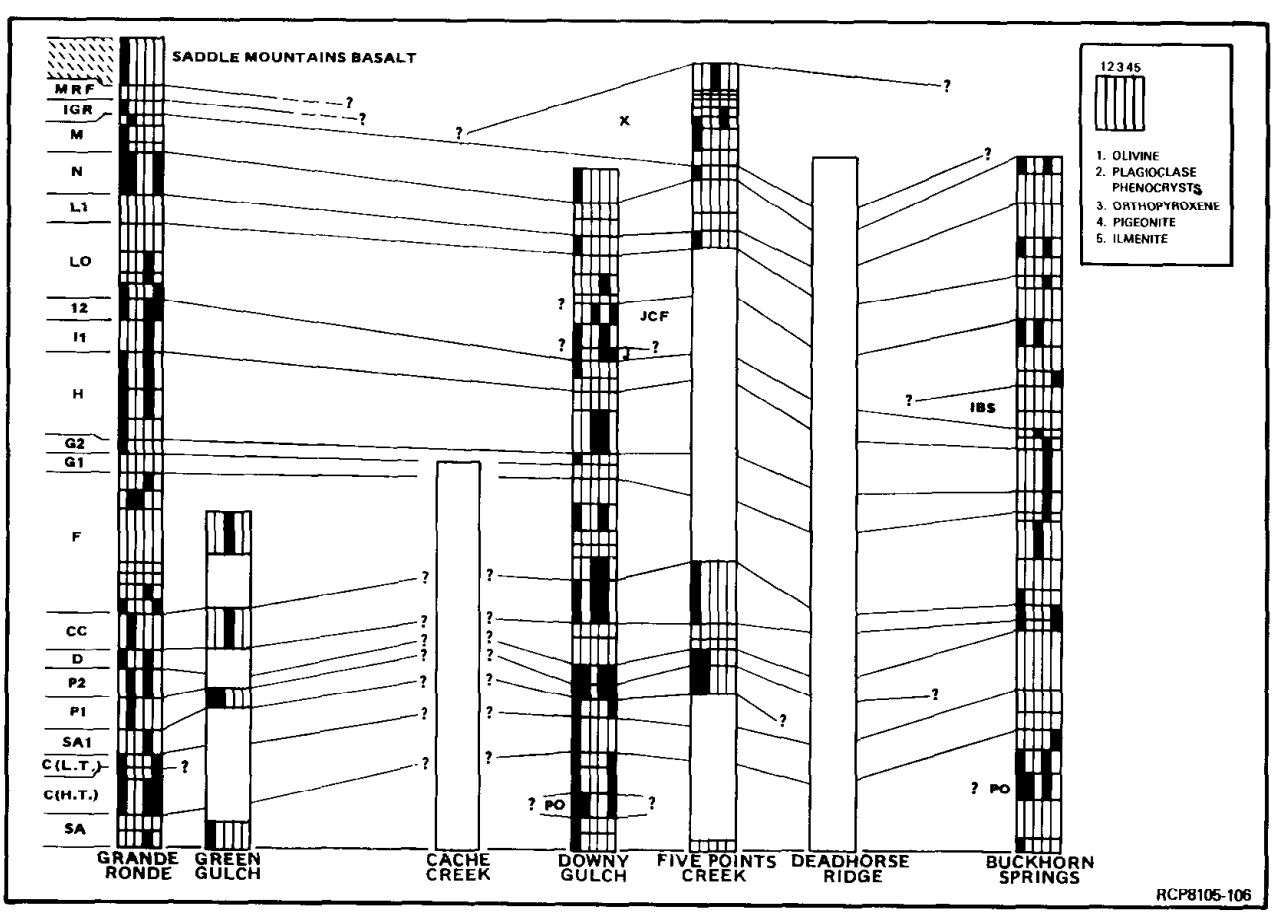

Figure 13. Summary of mineral phases present in the Grande Ronde Basalt flows from the Snake River canyon. Black indicates presence of mineral phase, white absence. Where flows were not examined, areas are left blank.

was not observed elsewhere.

PARAGENETIC SEQUENCE

Textural evidence suggests that the first crystallizing phases of the Grande Ronde Basalt were orthopyroxene, plagioclase, and possibly olivine. They probably crystallized simultaneously in a crustal storage chamber (Reidel, 1978). The sporadic nature of orthopyroxene and the presence of resorption in every crystal argues for low pressure instability. This suggests that the final stage of ascent for most flows was rapid, followed by rapid cooling at the surface. The observed reaction relation between orthopyroxene → pigeonite → augite (Reidel, 1978), however, suggests that, for some flows, the final ascent might have occurred with several stages of intermediate storage. Upon eruption, olivine, augite, and plagioclase were joined by titaniferous magnetite and apatite.

DISCRIMINANT ANALYSIS AS A METHOD OF EXTENDING FLOW CORRELATIONS

One of the major problems in correlating Grande Ronde Basalt flows throughout the deep canyon country of Idaho lies in the terrain. Because it is impractical to walk out flows, detailed stratigraphic sections must be measured and even this must be supplemented with chemical analyses. Measuring closely spaced sections can involve considerable expense, especially when chemical analyses are also involved. Since many flows have overlapping chemical compositions, random samples from a section still leave many uncertainties in making correlations. One method of correlating widely spaced sections or random samples is the multivariant statistical procedure of discriminant analysis.

Discriminant analysis has been successfully applied to the classification of igneous rocks (Chayes, 1976,

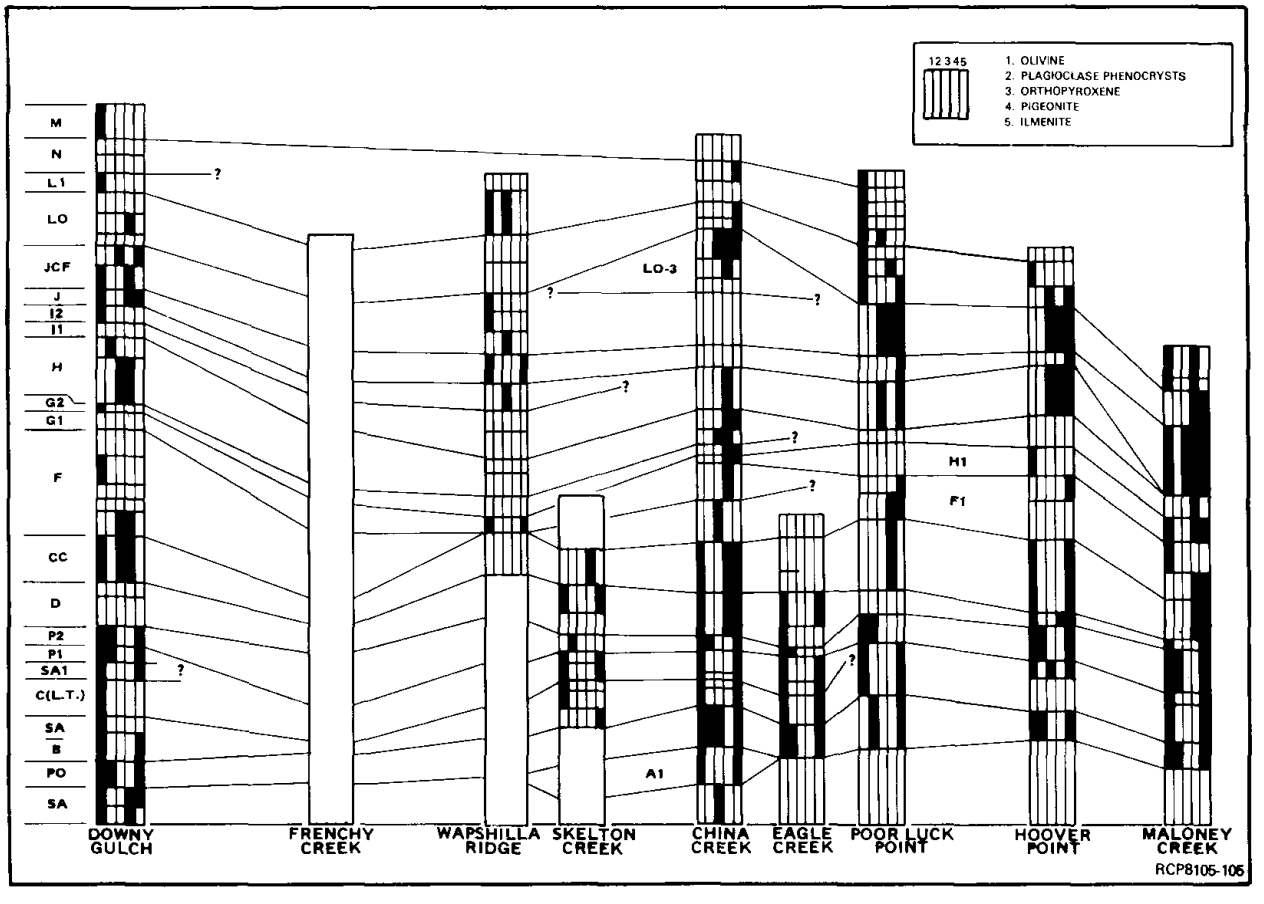

Figure 14. Summary of the mineral phases present in the Grande Ronde Basalt from the lower Salmon River canyon. Black indicates presence of mineral phase, white absence. Where flows were not examined, areas are left blank.

1980), and its use in this area is a natural extension of this work. Discriminant analysis is a multivariant statistical procedure where knowledge about the relationship between samples is used to establish a classification system employing those variables that comprise the samples. Individual samples comprising the classifications were used to test the probability of correctly identifying a particular flow using chemical analysis.

The procedure of Barr and others (1976) was used to calculate the statistical classification criterion. The discriminant function is based upon the generalized square distance between classification groups using a pooled covariance matrix. Prior probabilities, which were set to be equal for each group, were taken into account in the calculations. The posterior probabilities for classification in each group are calculated for each sample based upon the statistical classification criterion. The posterior probabilities indicate the probability of each sample belonging to each group. These probabilities were used to evaluate the flow classification and the probability of correctly identifying a flow using chemical composition alone.

Discriminant analysis was found to give a reasonable estimate of the probability of placing a sample within its proper flow using chemical composition alone. The results, using XRF-determined major and trace elements for flows of this study (Reidel, 1978), are summarized in Table 5 and show that over 67 percent of the samples were correctly classified by the

Table 5. Summary table of discriminant analysis results.

Flow or Flow Group	Total Number of Samples	Samples Classified Correct by Technique	Samples Reclassified by Technique	Range of Posterior Probabilities	Average Posterior Probability
SA	13	13	0	0.85-1.00	0.98
A1	2	2	0	0.75-0.99	0.87
P0	9	6	3	0.81-0.99	0.93
B	14	13	1	0.53-0.95	0.76
C(L.T.)	12	11	1	0.66-1.00	0.92
C(H.T.)	5	5	0	0.65-0.99	0.93
SA1	5	3	2	0.56-0.96	0.77
P1	6	4	2	0.56-0.98	0.62
P2	13	10	3	0.35-0.92	0.60
D	18	10	8	0.31-0.92	0.45
Center Creek	20	14	6	0.27-0.94	0.69
F	23	16	7	0.27-0.98	0.67
F1	10	7	3	0.33-0.92	0.47
G1	5	4	1	0.71-0.98	0.88
H1	6	3	3	0.74-1.00	0.90
G2	10	3	7	0.24-0.98	0.55
H	17	7	10	0.30-0.82	0.51
I1	15	6	9	0.41-0.90	0.52
I2	9	1	8	----	0.92
IBS	2	2	0	----	0.99
J	7	5	2	0.66-0.78	0.69
Johns Creek	17	10	7	0.37-0.99	0.73
L0-3	3	1	2	----	1.00
L0	27	16	11	0.50-0.97	0.71
L1	26	20	6	0.38-0.99	0.80
N	10	6	4	0.61-0.99	0.84
M	8	5	3	0.38-0.97	0.68
X	9	9	0	0.45-0.81	0.60
IGR	1	1	0	----	1.00
MRF	1	1	0	----	1.00

technique. Table 5 shows the number of samples for each flow or flow group that was used, the number of correctly classified samples according to posterior probabilities, those reclassified based upon posterior probabilities, and the average and range of posterior probabilities for those that were not reclassified by the technique. It is apparent that those flows or flow groups with the least number of reclassifications are those with distinct chemical compositions such as groups SA, C, and X although there are still some reclassified samples because of similarities with other groups. Flows or flow groups with a greater number of reclassified samples generally do not have distinct compositions. Reclassification of samples is usually due either to a high dispersion in the composition of the flow or to several flows with nearly identical chemical compositions. A good example of the latter is flows G1, G2, I1, I2, J, and the Johns Creek flow which are compositionally similar. The samples comprising these flows have lower probabilities for the correct flow because the similarities of the chemical composition of flows or groups cause the posterior probabilities to be split between them, thus lowering probabilities for all groups and resulting in many reclassifications.

This study shows that chemical composition of a flow can be used to characterize a flow from a specified stratigraphic position and that confidence can be placed in correlations based upon chemistry. Reidel and Long (1980) have had similar success with Grande Ronde Basalt flows from core holes in the Pasco Basin. Tests (Reidel, 1978; Reidel and Long, 1980) show that samples which are correctly classified using this technique also have very high posterior probabilities for the correct flow, whereas low posterior probabilities result from samples incorrectly classified or from several flows with nearly identical compositions. This provides a method for evaluating the correlations produced by this technique and a means of estimating the level of confidence.

SUMMARY

By combining the mapping of physical characteristics and magnetostratigraphic units with chemical analyses from detailed stratigraphic sections, a detailed stratigraphy of the Grande Ronde Basalt has been deduced for the lower Salmon River canyon and northern Hells Canyon area. The Grande Ronde Basalt here as elsewhere on the plateau is the most voluminous formation of the Columbia River Basalt Group and thus is a major key to understanding the petrogenesis and tectonics of the Columbia River Plateau. Estimates of the volume and lateral extent of each flow and flow group undoubtedly will provide significant constraints on petrogenetic and tectonic models that might be proposed.

Three magnetostratigraphic units of the Grande Ronde Basalt are present in the area. The thickness and number of flows in each unit decreases from west to east. Several physically distinct flows have been traced throughout the area, but most flows have few physical characteristics that make them easily recognized. However, chemical analyses of basalt flows from detailed stratigraphic sections have provided a method for resolving the details of the Grande Ronde Basalt stratigraphy. Many flows or groups of flows have distinct concentrations of one or more oxides or elements that have allowed them to be recognized throughout the area, even though considerable overlap occurs in the chemical composition between many adjacent flows.

Only a few flows have distinct petrographic features that allow them to be recognized throughout the area. The presence of plagioclase phenocrysts is the most useful feature, and the habit of olivine is characteristic of some flows.

The analysis of flow distributions details what reconnaissance studies show using the thickness of magnetostratigraphic units. Detailed studies also show two general types of flows, those with apparently limited lateral extent which pinch out within the area and those of much greater lateral extent which show no evidence of pinching out in or near the area. Flows of local extent appear to dominate.

Flow distributions also reflect the tectonic history of the area. In particular, they were affected by the regional paleoslope and demonstrate that the Limekiln fault was probably active and the Lewiston basin subsiding in Grande Ronde time.

Due to the impracticality of walking out flows in the deep canyon country and the costs involved in collecting and analyzing many basalt samples from closely spaced sections, the multivariant statistical technique of discriminant analysis is proposed as a method to extend this Grande Ronde Basalt stratigraphy beyond this area using limited data. This method also would provide an estimate of the probability of these correlations being correct.

ACKNOWLEDGMENTS

This study was supported in part by a National Science Foundation grant GA-39802 to P. R. Hooper. The manuscript was reviewed by V. E. Camp, R. D. Landon, M. R. Knight, and P. R. Hooper whose comments and suggestions were greatly appreciated. I would especially like to thank Bill Bonnichsen for

critically reviewing the manuscript and making many valuable suggestions which greatly improved it. R. W. Cross and W. H. Crowley, Jr., provided much of the graphic support; the manuscript was typed by Barbara Chapple.

REFERENCES

Bard, C. S., 1978, Mineralogy and chemistry of pyroxenes from the Imnaha and lower Yakima basalts of west central Idaho: Washington State University M.S. thesis, 75 p.

Barr, A. J., J. H. Goodnight, J. P. Sall, and J. T. Halwig, 1976, A user's guide to SAS76: Raleigh, North Carolina SAS Institute, Inc., 329 p.

Bond, J. G., 1963, Geology of the Clearwater embayment: Idaho Bureau of Mines and Geology Pamphlet 128, 83 p.

Caggiano, J. A., K. R. Fecht, S. M. Price, S. P. Reidel, and A. M. Tallman, 1980, A preliminary assessment of the relative rate of deformation in the Pasco Basin, south-central Washington: Geological Society of America, Abstracts with Programs, v. 12, no. 7, p. 397.

Camp, V. E., 1976, Petrochemical stratigraphy and structure of the Columbia River basalt, Lewiston basin area, Idaho-Washington: Washington State University Ph.D. dissertation, 200 p.

———, 1981, Geologic studies of the Columbia Plateau, Part II: Upper Miocene basalt distribution reflecting source locations, tectonism, and drainage history in the Clearwater embayment, Idaho: Geological Society of America Bulletin, v. 92, p. 669-678.

Camp, V. E. and P. R. Hooper, 1980, Tectonic evolution of the southeastern part of the Columbia River Basalt Plateau: Geological Society of America, Abstracts with Programs, v. 12, no. 3, p. 100-101.

Camp, V. E., P. R. Hooper, D. A. Swanson, and T. L. Wright, 1982, Columbia River basalt in Idaho: physical and chemical characteristics, flow distribution, and tectonic implications, *in* Bill Bonnichsen and R. M. Breckenridge, editors Cenozoic Geology of Idaho: Idaho Bureau of Mines and Geology Bulletin 26.

Camp, V. E., S. M. Price, and S. P. Reidel, 1978, Descriptive summary of the Grande Ronde Basalt type section, Columbia River Basalt Group: RHO-BWI-LD-15, Rockwell Hanford Operations, Richland, Washington, 23 p.

Chayes, Felix, 1976, Characterizing the consistency of current usage of rock names by means of discriminant functions: Carnegie Institution of Washington Yearbook, v. 75, p. 782-784.

———, 1980, Partitioning by discriminant analysis: a measure of consistency in the nomenclature and classification of volcanic rocks: *in* H. S. Yoder, editor, The Evolution of the Igneous Rocks: Princeton University Press, Princeton, New Jersey, p. 521-532.

Fitzgerald, J. F., 1982, Geology and basalt stratigraphy of the Weiser embayment, west-central Idaho, *in* Bill Bonnichsen and R. M. Breckenridge, editors, Cenozoic Geology of Idaho: Idaho Bureau of Mines and Geology Bulletin 26.

Holden, G. S., 1974, Chemical and petrographic stratigraphy of the Columbia River basalt in the lower Salmon River canyon, Idaho: Washington State University M.S. thesis, 97 p.

Holden, G. S. and P. R. Hooper, 1976, Petrology and chemistry of a Columbia River basalt section, Rocky Canyon, west-central Idaho: Geological Society of America Bulletin, v. 87, p. 215-225.

Hooper, P. R., 1974, Petrology and chemistry of the Rock Creek flow, Columbia River basalt, Idaho: Geological Society of America Bulletin, v. 85, p. 15-26.

Hooper, P. R., C. R. Knowles, and N. D. Watkins, 1979, Magnetostratigraphy of the Imnaha and Grande Ronde Basalts in the southeast part of the Columbia Plateau: American Journal of Science, v. 279, p. 737-754.

Kleck, W. D., 1976, Chemistry, petrography, and stratigraphy of the Columbia River Group in the Imnaha River Valley region, eastern Oregon and western Idaho: Washington State University Ph.D. dissertation, 202 p.

Long, P. E., 1978, Characterization and recognition of intraflow structures, Grande Ronde Basalt: RHO-BWI-LD-10, Rockwell Hanford Operations, Richland, Washington, 74 p.

Long, P. E., R. K. Ledgerwood, C. W. Myers, S. P. Reidel, R. D. Landon, and P. R. Hooper, 1980, Chemical stratigraphy of Grande Ronde Basalt, Pasco Basin, south-central Washington: Geological Society of America, Abstracts with Programs, v. 12, no. 3, p. 117.

McKee, E. H., D. A. Swanson, and T. L. Wright, 1977, Duration and volume of Columbia River basalt volcanism, Washington, Oregon, and Idaho: Geological Society of America, Abstracts with Programs, v. 9, no. 4, p. 463.

Noonan, A. F., Kurt Fredriksson, and Joseph Nelen, 1980, Phase chemistry of the Umtanum basalt, a reference repository host in the Columbia Plateau: RHO-BWI-SA-77, Rockwell Hanford Operations, Richland, Washington.

Packer, D. R. and M. H. Petty, 1979, Magnetostratigraphy of the Grande Ronde Basalt, Pasco Basin, Washington: RHO-BWI-C-46, Rockwell Hanford Operations, Richland, Washington, 43 p.

Price, S. M., 1977, An evaluation of dike-flow correlation indicated by geochemistry, Chief Joseph dike swarm, Columbia River basalt: University of Idaho Ph.D. dissertation, 320 p.

Price, W. H., C. R. Knowles, and J. G. Bond, 1973, Columbia River basalt dikes of the Camas Prairie area, Idaho: Geological Society of America, Abstracts with Programs, v. 5, no. 7, p. 773.

Reidel, S. P., 1978, Stratigraphy and petrogenesis of the Grande Ronde Basalt in the lower Salmon and adjacent Snake River canyons: Washington State University Ph.D. dissertation, 425 p.

Reidel, S. P., P. E. Long, C. W. Myers, and Jack Mase, 1982, New evidence for greater than 3.2 km of Columbia River basalt beneath the central Columbia Plateau: Transactions of the American Geophysical Union (EOS), v. 63, no. 8, p. 173.

Reidel, S. P., R. K. Ledgerwood, C. W. Myers, M. G. Jones, and R. L. Landon, 1980, Rate of deformation in the Pasco Basin as determined by distribution of Columbia River basalt flows: Geological Society of America, Abstracts with Programs, v. 12, no. 3, p. 149.

Reidel, S. P. and P. E. Long, 1980, Discriminant analysis as a method of flow identification and correlation in layered basalt provinces: Geological Society of America, Abstracts with Programs, v. 12, no. 7, p. 507.

Ross, M. E., 1978, Stratigraphy, structure and petrology of the Columbia River basalt in a portion of the Grande Ronde-Blue Mountains area of Oregon and Washington: University of Idaho Ph.D. dissertation, 407 p.

Savage, J. C., M. Lisowski, and W. H. Prescott, 1981, Geodetic strain measurements in Washington: Journal of Geophysical Research, v. 86, no. B6, p. 4929-4940.

Swanson, D. A. and T. L. Wright, 1976, Magnetostratigraphic units in the Yakima Basalt, southeast Washington: Geological Society of America, Abstracts with Programs, v. 8, no. 3, p. 413-414.

Swanson, D. A., T. L. Wright, P. R. Hooper, and R. D. Bentley, 1979a, Revision of Columbia River basalt nomenclature: U. S. Geological Survey Bulletin 1457-G, 59 p.

Swanson, D. A., J. L. Anderson, R. D. Bentley, G. R. Byerly, V. E. Camp, J. N. Gardner, and T. L. Wright, 1979b, Reconnaissance geologic map of the Columbia River Basalt Group in eastern Washington and northern Idaho: U. S. Geological Survey Open-File Report 79-1363, 12 sheets.

Taubeneck, W. H., 1970, Dikes of the Columbia River basalt in northeastern Oregon, western Idaho and southeastern Washington, *in* E. H. Gilmour and Dale Stradling, editors, Proceedings of the Second Columbia River Basalt Symposium: Eastern Washington State College Press, p. 73-96.

Taylor, T. L., 1976, The basalt stratigraphy and structure of the Saddle Mountains of south-central Washington: Washington State University M.S. thesis, 116 p.

Vallier, T. L., 1974, A preliminary report of the geology of part of the Snake River canyon, Oregon, Idaho: GMS-6, Department of Geology and Mineral Industries, State of Oregon, 15 p., 1 map.

———, 1977, The Permian and Triassic Seven Devils Group, eastern Oregon and western Idaho: U. S. Geological Survey Bulletin 1437, 58 p.

Waters, A. C., 1961, Stratigraphy and lithologic variations in the Columbia River basalt: American Journal of Science, v. 259, p. 583-611.

———, 1962, Basalt magma types and their tectonic associations: Pacific Northwest of the United States, *in* The Crust of the Pacific Basin: American Geophysical Union Monograph 6, p. 158-170.

Watkins, N. D. and A. K. Baksi, 1974, Magnetostratigraphy and oroclinal folding of the Columbia River, Steens, and Owyhee basalts in Oregon, Washington, and Idaho: American Journal of Science, v. 274, p. 148-189.

Wright, T. L., M. J. Grolier, and D. A. Swanson, 1973, Chemical variation related to the stratigraphy of the Columbia River basalt: Geological Society of America Bulletin, v. 84, p. 371-386.

Geology and Basalt Stratigraphy of the Weiser Embayment, West-Central Idaho

by

James F. Fitzgerald[1]

ABSTRACT

The Weiser embayment in west-central Idaho is the southeasternmost extension of the Columbia Plateau. It is made up of rocks of the Columbia River Basalt Group. Field mapping and X-ray fluorescence chemical analysis of numerous samples resulted in a geologic map and the delineation of both regional and localized Columbia River basalt units in the embayment.

Subbasalt rocks consist of Permian to Jurassic metavolcanic and metasedimentary lithologies, Mesozoic schists and gneisses, and Mesozoic and Cenozoic granodiorite to quartz diorite intrusive complexes. Prior to basalt extrusion, basement rocks were eroded into a relatively mature topography with considerable local relief.

Regional Imnaha and Grande Ronde Basalt sequences are present in the Weiser embayment. Over 700 meters of Imnaha Basalt first spread over lowlands and filled canyons to establish the general configuration of the embayment. The overlying Grande Ronde Basalt sequence was more constrained in extent. A thickness of 150 to 300 meters accumulated in the northwestern part of the embayment; progressively thinner accumulations occur to the south and east. A few thin, ashy interbeds occur locally within both the Imnaha and Grande Ronde sequences.

Minor warping of the Grande Ronde surface preceded extrusion of the localized Weiser Basalt units and accumulation of the associated pyroclastic and fluvial sediments. Four distinct units were identified within the Weiser Basalt sequence: the Cambridge member, the Sugarloaf member, the Star Butte member, and the basalt of Black Canyon. These units were defined by physical, chemical and remanent magnetic characteristics, and by stratigraphic position. Common to each is a relatively high (generally above 16 percent) Al_2O_3 content when compared to the regional units. Two vents and related pyroclastic accumulations exposed at the top of the Weiser Basalt are included in that sequence, although they could not be correlated with any specific unit. Additional localized basalt units may also occur in the embayment.

The geographically isolated basalt of Cuddy Mountain could not be chemically or stratigraphically correlated with Imnaha, Grande Ronde, or Weiser Basalts. Field relations suggest it may actually consist of both pre- and post-Grande Ronde Basalt flows.

Following the Weiser Basalt eruptive episode, structural activity became pronounced. Basement blocks were uplifted and tilted into fault-blocks and horst and graben structures, generally along preexisting zones of weakness. Three major fault patterns developed in the embayment. These are (1) the Long Valley fault system—a north-trending block-fault pattern along the eastern margin of the embayment, (2) the Paddock Valley fault system—a northwest-trending open-fold and block-fault pattern in the south-central and southwestern portion of the embayment, and (3) the Snake River fault system—a northeast-trending block-fault pattern in the northwestern portion of the embayment. All three systems extend beyond the embayment and are regional in perspective. Other structural activity includes continued

[1]Editors' note: James F. Fitzgerald was a graduate student at the University of Idaho in 1977 when he embarked on the research reported in this article. It was his intention to submit the completed research to the University of Idaho to fulfill the requirements for his Ph.D. degree in geology. Toward that end he spent the summers of 1978 and 1979 in the field and the remainder of his time in classroom and laboratory studies at the University of Idaho and Washington State University. Unfortunately, he was never able to complete the research, due to his untimely death in the May 18, 1980, cataclysmic eruption of Mount St. Helens in Washington. By the time of his death he had nearly completed the field and laboratory research upon which this report is based. It is important to note that the final field work, much of the interpretation of the field and laboratory investigations, and the preparation of the written account were completed by his friends and associates. In large part, credit for completion of the project is due to the diligent efforts of John G. Bond and John D. Kauffman of Geoscience Research Consultants, and their associates William C. Rember and Donna J. Shieveler, all of Moscow, Idaho. Not only did the fine work of these people make it possible for this article to be completed, but their efforts in completing the research also made it possible for Jim Fitzgerald to be granted posthumously, in May 1981, the Ph.D. degree in geology from the University of Idaho.

Fitzgerald, J. F., 1982, Geology and basalt stratigraphy of the Weiser embayment, west-central Idaho, *in* Bill Bonnichsen and R. M. Breckenridge, editors, Cenozoic Geology of Idaho: Idaho Bureau of Mines and Geology Bulletin 26, p. 103-128.

downwarping of the central embayment area and uplifting of the Seven Devils area connected by the south-dipping Seven Devils homocline, plus doming and anticlinal-synclinal warping southwest of Cuddy Mountain. Postbasalt terrigenous sediments accumulated in basins and along the southern margin of the embayment; these remain relatively undeformed.

INTRODUCTION

The eastern part of the Columbia Plateau consists of three major lobes of basalt which protrude into Idaho. From north to south these are called the Benewah, Clearwater, and Weiser embayments (Figure 1). The northern and central basalt lobes were mapped by Bishop (1969) and Bond (1963), respectively. Subsequently, these were mapped and studied in additional detail by Camp (in Swanson and others, 1979a, 1981; Camp, 1981; Camp and Hooper, 1981; Camp and others, 1982 this volume). The southernmost lobe, the Weiser embayment, however, has been the subject of only localized mapping by the U. S. Geological Survey (McIntyre, 1976a, 1976b) and a number of theses by students mainly from the University of Idaho and Oregon State University (Breeser, 1972; Fankhauser, 1968; Juras, 1973; King, 1971; Nakai, 1979; Paris, 1969; Shah, 1966, 1968; Skurla, 1969; Slater, 1969). The Columbia River Basalt Group in the Weiser embayment has not been previously studied and mapped in a regional stratigraphic format.

This study examines in detail these basalt flows of the Weiser embayment in order to (1) determine the interrelations of observations and findings from prior field projects conducted in scattered parts of the embayment, (2) complete the mapping of previously unmapped regions of the embayment, (3) establish a stratigraphic framework for Weiser embayment basalt flows and correlate it with the chemical-magnetostratigraphic framework established by Swanson and others (1979b) for Columbia River Basalt Group units of the Columbia Plateau, and (4) determine the current structural setting of the embayment and fit this pattern into the volcanic history and postextrusion structural evolution of the Columbia Plateau.

The full results of this study have been incorporated in the plateauwide investigation being compiled by the U. S. Geological Survey. The results are also reported in Rockwell Hanford Operations Basalt Waste Isolation publication RHO-BWI-SA-217p, (1982). All preserved field notes, basalt samples, and analytical data are on file with the Rockwell Hanford Operations Basalt Waste Isolation project at Richland, Washington.

LOCATION AND GEOMORPHIC SETTING

The Weiser embayment is the southeastern lobe of the Columbia River Basalt Group at the eastern edge of the Columbia Plateau in west-central Idaho (Figure 1). It is bounded on the east by the Salmon River Mountains, and on the west by the deep canyon of the Snake River. It is bounded on the north by the Seven Devils Mountains, and on the south by the Snake River Plain. The embayment is roughly delta-shaped, approximately 130 kilometers from north to south, and 75 kilometers wide near the Snake River Plain; it covers about 7,500 square kilometers. The map area, including the main geographical locations and features, is shown in Figure 2.

Topographic relief is greatest near the northwestern and eastern mountainous margins of the delta-shaped area. These uplifted areas, with elevations over 2,135 meters (7,000 feet), are separated by a broad, topographically subdued, southerly plunging synclinal depression with elevations below 915 meters (3,000 feet). Local relief around the periphery of the embayment is as much as 1,525 meters (5,000 feet). Local relief within the central Indian Valley synclinal portion of the area ranges between 90 and 185 meters (300 and 600 feet), except where block faulting has occurred along the flanking limbs or where stream dissection is marked.

The Weiser River drainage system dissects the interior of the embayment. Deep, youthful canyons of the Weiser system include Crane Creek canyon

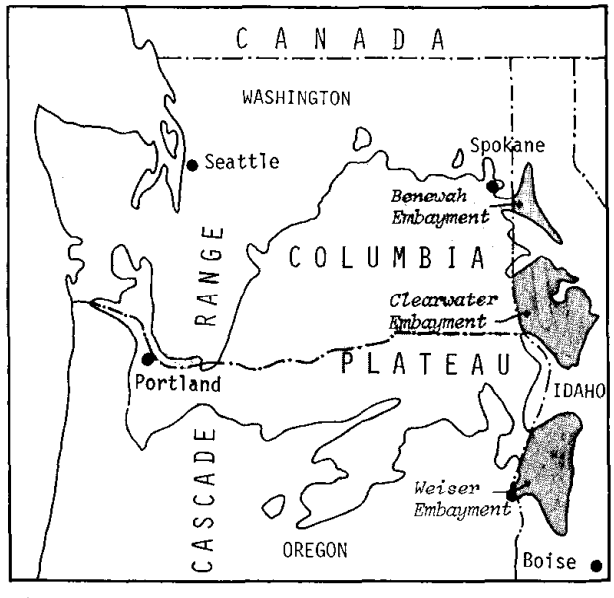

Figure 1. Location map of Columbia Plateau and major basalt embayments in Idaho (after Waters, 1961; Swanson and others, 1979b).

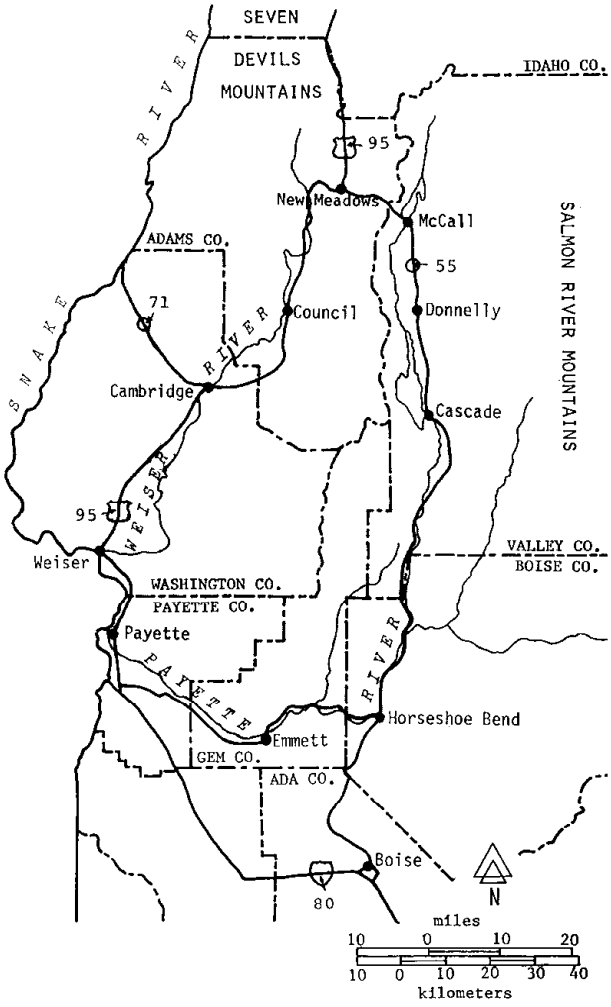

Figure 2. Location map of the Weiser embayment, Idaho.

east-northeast of Weiser and the main Weiser River canyon north of Council and south of Cambridge. These canyons generally have walls cut 250 meters (800 feet) or more in Columbia River basalt flows. The Snake River and its tributaries of the western border area and those of the Payette River on the east have cut through the basalt to expose subbasalt rock units.

STUDY METHODS

Field work in the Weiser embayment consisted of a reconnaissance and planning inspection in 1977, detailed mapping and sampling of the central and southern portions of the area in the summer and fall of 1978, and detailed mapping and sampling of the northern portion and other incompletely mapped localities in the summer and fall of 1979.

The basalt flows were grouped into stratigraphic units by using lithologic and hand-specimen characteristics, lateral correlation of sampled and described canyon sections, and paleomagnetic properties.

For geochemical characterization, major oxide abundances for approximately 280 basalt samples were determined by X-ray fluorescence at the department of geology, Washington State University, during the winter and spring following the two major field seasons. The report was prepared while at the department of geology, University of Idaho.

PREVIOUS INVESTIGATIONS

COLUMBIA PLATEAU FLOOD BASALT UNITS

Until the mid-1950's, most geologists regarded the Columbia Plateau of Idaho, Washington, and Oregon (Figure 1) as composed of a monotonous, uninteresting sequence of flood basalts. During the last twenty years, however, the areal distribution, physical and chemical properties, and petrogenesis of individual basalt flows have been the subjects of intensive scientific investigations.

Waters (1961) was the first to divide Columbia River basalt flows (after the Columbia basalt and Columbia River basalt of Russell, 1893 and 1901, respectively) into three formal, regional stratigraphic types—Picture Gorge Basalt, Yakima Basalt (after Yakima basalt of Smith, 1901) and Late Yakima Basalt. Using Waters' oldest-to-youngest stratigraphic framework and Mackin's (1961) flow-by-flow field identification approach, such subsequent workers as Grolier (1965), Bingham and Walters (1965), Schmincke (1967), Swanson (1967), and Lefebvre (1970) were able to delimit accurately the continuity of individual flows and sequences of flows over several tens of kilometers in western and central portions of the Columbia Plateau. Similarly, broad-area stratigraphic correlations were made by Bond (1963) and Bishop (1969) for basalt flows of the Columbia Plateau that extended eastward into northern Idaho. These various studies from throughout the Columbia Plateau demonstrated the viability of a regional stratigraphic framework.

Waters' initial three-unit stratigraphic classification was subsequently modified by Wright and others (1973), who further divided Columbia River basalt flows into chemical types and suggested a four-unit, oldest-to-youngest stratigraphic grouping—Picture Gorge, lower Yakima, middle Yakima, and upper Yakima Basalts. This framework was refined more recently (Swanson and others, 1979b) with the establishment of a Columbia River Basalt Group

which has been subdivided into one subgroup—the Yakima Basalt, five formations—the Imnaha, Picture Gorge, Grande Ronde, Wanapum, and Saddle Mountains Basalts, and fourteen members (Figure 3). Chemical analysis data were important parameters in developing these units, which have become the working nomenclature of the basalt sequences of the Columbia Plateau (Camp and others, 1982 this volume).

Findings from the Weiser embayment demonstrate that the regional Imnaha and Grande Ronde Basalts persist into the southern Columbia Plateau area of Idaho. In addition, a younger, relatively unmapped and previously unnamed Weiser Basalt sequence occurs in the embayment and is added to the established stratigraphic framework (Figure 4).

WEISER EMBAYMENT STRATIGRAPHY

Lindgren (1898), the first geologist to report on that portion of Idaho including the Weiser embayment, noted that unconformable relations exist between the flood basalts of the area and the underlying granite, and also between the sequence of basalt flows and the overlying sedimentary Idaho Formation. Later, Kirkham (1930, 1931), who studied the southern part of the embayment from the Snake River west of Weiser to Horseshoe Bend near the eastern margin, noted that "a series of terrestrial deposits and lake beds exists in the Columbia River basalt" and that "a series of terrestrial deposits and lake beds, in places several thousand feet thick, overlies the Columbia River basalt and Owyhee rhyolite" (1931, p. 201), which he redefined as the Payette and Idaho Formations respectively. By his definition, the Payette Formation includes all sediments interbedded with Columbia River basalt flows; the Idaho Formation applies to all sediments overlying these basalt flows. Anderson (1934) extended the basalt discussion of Kirkham into the Pearl area east of Horseshoe Bend, noting the existence of two types of basalt—olivine free and olivine rich—in this very distal portion of the

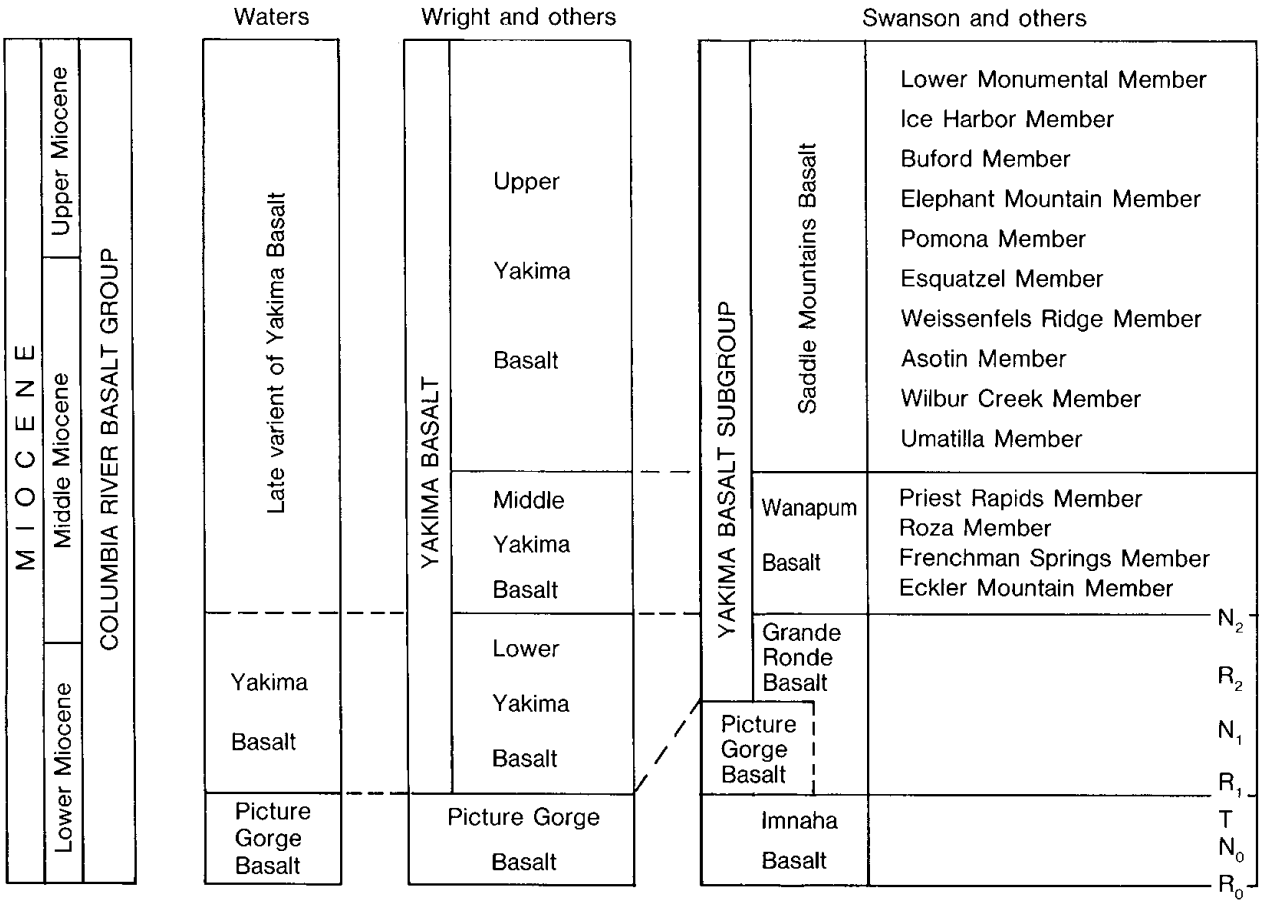

Figure 3. Sequential development of Columbia River Basalt Group stratigraphic nomenclature (after Waters, 1961; Wright and others, 1973; Swanson and others, 1979b).

Columbia Plateau. Two comparable mineralogical types of basalt were noted by Savage (1958, 1961) as occurring in the southern portion of the embayment. After conducting a paleontological study of the sediments associated with basalt of the southern embayment margin, Shah (1966, 1968) concluded that the oldest Columbia River basalt flows in that region were to the west along the Snake River.

Most recent field investigations which have touched on basalt stratigraphy of the Weiser embayment generally have been either (1) very localized geothermal or mineral-resource studies of parts of the southern and western portion of the embayment, or (2) highway-corridor studies concerned with general surficial mapping and engineering needs in the central and northern portion of the embayment.

Young and Whitehead (1975) and McIntyre (1976b) analyzed hot springs in Crane Creek canyon in the south-central part of the embayment and mapped areas surrounding them. A photogeologic map of the general Cambridge-Council area also was prepared by McIntyre (1976a). McIntyre concluded that most of the sediments of the Payette Formation appeared to overlie the main body of lava and that most of the lava flows exposed in Crane Creek canyon compositionally were andesites rather than basalts. Nakai (1979), in a study of hydrocarbon-storage potential of the Payette Formation, identified several basalt flows interlayered with sediments in four measured sections east of Weiser.

Previous studies in the western and northern portions of the embayment, in particular, reflect the changes in basalt nomenclature that occurred elsewhere on the Columbia Plateau during the 1960's and 1970's. For example, mineral deposit studies in the Sturgill Peak-Cuddy Mountain area, conducted by Fankhauser (1968), Slater (1969), and King (1971), subdivided the then "Columbia River Basalt" into phyric "Picture Gorge" and aphyric "Yakima" sequences after the stratigraphic framework established by Waters (1961) for the basalt flows to the west.

About the same time Hoover (1968) used a "Lower" (phyric) and "Upper" (aphyric) basalt stratigraphic nomenclature in his U. S. Highway 95 corridor study,

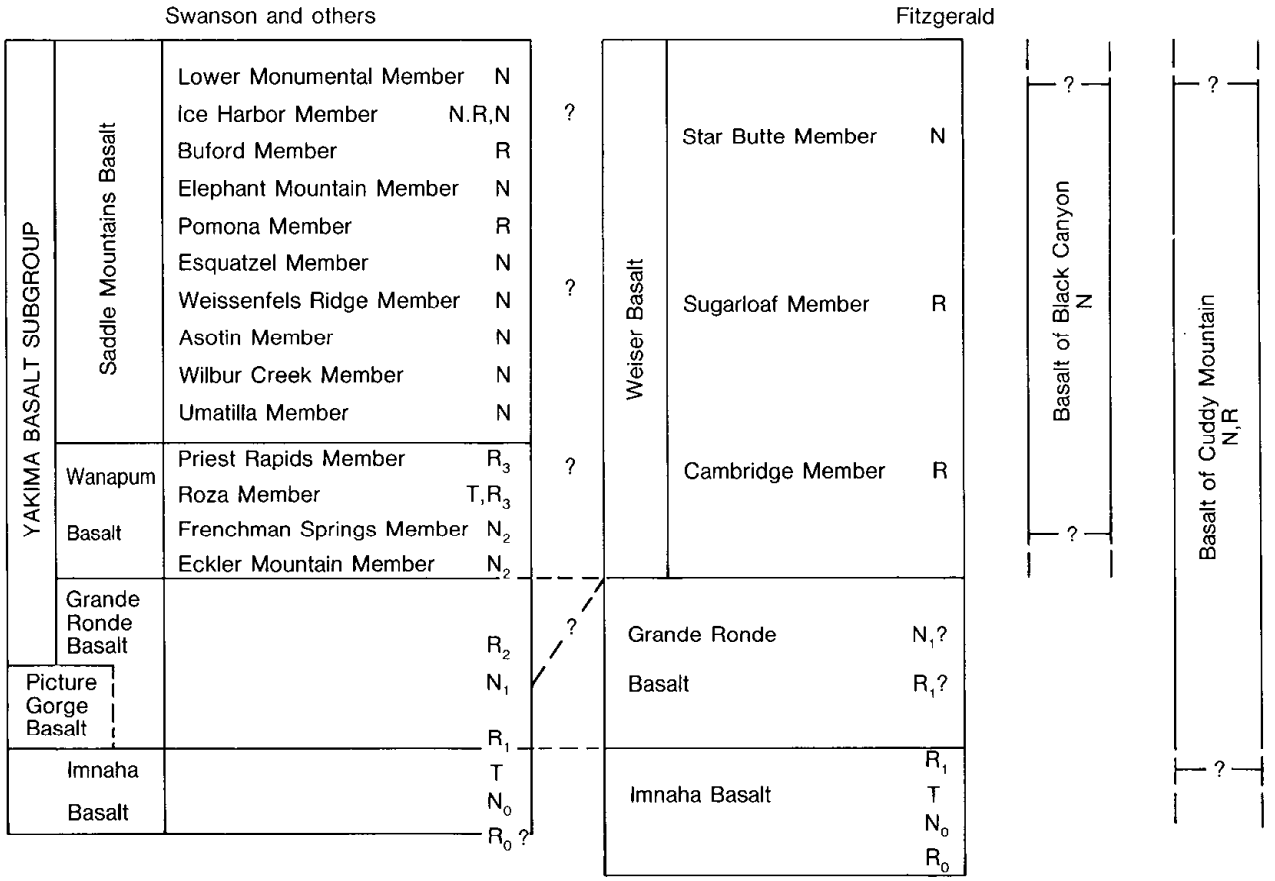

Figure 4. Comparison of regional Columbia River Basalt Group stratigraphic sequence, on left, with Weiser embayment basalt sequence, on right. Correlation of Weiser Basalt to Wanapum Basalt and Saddle Mountains Basalt is uncertain (after Swanson and others, 1979b; Fitzgerald, 1982).

similar to that estabished by Bond (1963) to the north. The presence of younger local vent rock and near-vent flows also was recognized by Hoover in the Cambridge area. Later, Breeser (1972) and Vallier and Hooper (1976) used the terms Imnaha and Yakima to designate the same or correlative sequences of phyric and aphyric, older and younger basalt units.

In summary, geologists previously working with the Weiser embayment generally approached dividing basalt flows and associated sediments into mappable stratigraphic units by using local field and hand-specimen relationships. Investigators in the southern portion of the embayment commonly used Payette Formation interbeds as the breaks between selected map units. In contrast, investigators working to the west and north used broad-area phyric-aphyric basalt flow associations for older and younger (now Imnaha and Grande Ronde) map-unit boundaries. Post-Yakima Basalt units (Weiser Basalt), where recognized, were considered to be near-source, Pliocene(?) flows.

For further overviews or extensions of current basalt stratigraphic associations into nearby areas, the reader is referred to Bond (1978), Gaston and Bennett (1979), Mitchell and Bennett (1979a, 1979b), Strowd (1978), Myers and others (1979), Camp (1981), Camp and Hooper (1981), Hooper (1982), Camp and others (1982 this volume), and Reidel (1982 this volume).

GENERAL GEOLOGY

SUBBASALT ROCKS AND CONDITIONS

Based on data sources previously cited and the field observations of this study, rocks older than the Columbia River Basalt Group in the vicinity of the Weiser embayment, from oldest to youngest, include Permian to Jurassic metavolcanic and metasedimentary lithologies, Mesozoic schists and gneisses, and Mesozoic to Cenozoic granodiorite to quartz diorite intrusive bodies. These basement rocks are exposed locally above plateau level as ancestral highlands and steptoes and below plateau surface elevations where they have become exposed by erosion.

Subbasalt rocks were eroded into a relatively mature topography prior to extrusion of the Columbia River Basalt Group in middle Miocene time. The Peck Mountain, Cuddy Mountain, and Sturgill Peak steptoes and nearby exhumed basement surfaces, plus erosional exposures of basement-basalt contacts in the Snake River canyon, demonstrate that more than 915 meters of relief characterized western Idaho in the early Miocene. Well-developed westerly to southwesterly flowing drainage systems existed at that time. Contact relations between basalt flows and older rocks along the eastern border of the embayment show that the subcropping basement paleotopography was youthful to mature. Here, thick sections of basalt, as on Squaw Butte, give way easterly in less than 10 kilometers to markedly unconformable basalt-basement contacts and basement uplands.

BASALT DISTRIBUTION

The eruption of fluid Miocene Columbia River lavas approximately 17 to 14 million years ago (McKee and others, 1981) consisted of sheets of Imnaha Basalt followed by those of Grande Ronde Basalt that spread westerly into and through the lowlands and valleys of the embayment. At least 700 meters of Imnaha Basalt spread over many low-lying areas. The Imnaha, the principal sequence of flows to spread almost completely across the area, established the general configuration of the embayment. The overlying Grande Ronde sequence was more limited areally; its thickest portion of 150 to 300 meters was toward the northwest, and it progressively thinned to the south and east. The southeastern wedge-edge margin of initial Grande Ronde Basalt distribution was near Squaw Butte.

During quiescent periods between eruptive episodes in Imnaha and Grande Ronde time, fine- to medium-grained sediments from adjoining upland areas were deposited on the transient, constructional plateau, particularly near its margins. Ashy layers and weathered soil zones also formed on the plateau surface and were preserved as volcaniclastic and saprolitic interbeds by succeeding flows. Together, these scattered, relatively thin interbeds can most appropriately be categorized as "lower" Payette Formation. They are not extensively exposed in the embayment.

By the end of the Imnaha and Grande Ronde volcanism, the broad plateau of the Weiser embayment, excluding basement steptoes, covered the older terrain east of its current erosional margin, as shown by basalt remnants overlying Idaho batholith rocks at many localities east of Payette River canyon. At the end of Grande Ronde volcanism the Weiser embayment locally merged northward with the Clearwater embayment through saddles between the Seven Devils steptoes. The plateau surface also extended southward into the area now down-dropped and filled by terrigenous deposits of the late Cenozoic Snake River Plain. Basement steptoes remained above plateau

level in the Seven Devils Mountains area in the north, at Peck Mountain, Cuddy Mountain, and Sturgill Peak in the west, in the McCall-Payette River area in the east, and locally elsewhere.

Prior to major deformation and erosion, and penecontemporaneous with early downwarping of the central part of the embayment, sediments from eastern upland areas accumulated on the plateau surface. These fluvial sediments were deposited by streams from preexisting upland drainage systems as they ponded and spilled generally westward across the plateau toward the Pacific Ocean.

Concurrently with downwarping, sporadic local volcanism commenced within the embayment, perhaps as early as Grande Ronde time in the Cuddy Mountain area. However, most of this volcanism, the Weiser volcanic episode, followed the accumulation and initial warping of the Grande Ronde Basalt. Weiser volcanism is recorded by localized accumulation of lava flows and associated near-vent ejecta and coarse-grained pyroclastic debris. This sequence now forms the bulk of the basalt exposed in the structurally depressed south-central portion of the embayment.

Locally, up to 350 meters of Weiser Basalt accumulated in a nearly flow-on-flow sequence. Intercalation of sediments, ash layers, pyroclastic units, and basalt flows commonly occurred during the Weiser eruptive interval so that stratigraphic sections vary from 100 percent sediments and ash to nearly 100 percent lava flows and associated pyroclastic accumulations. The sediments and ashy material associated with Weiser Basalt flows and pyroclastic layers are aptly called "upper" Payette Formation.

The greatest thickness of Weiser Basalt and associated sediments accumulated in the downwarped Indian Valley trough in the central part of the embayment. However, flows, pyroclastic units, ash layers, and associated sediments of the Weiser Basalt sequence, with the exception of the basalt of Cuddy Mountain, extend as far north as Mesa, as far east as Montour near the Payette River, as far west as Warm Springs Creek northwest of Weiser, and at least as far south as the northern edge of the Snake River Plain.

In the southeastern part of the embayment, poorly sorted, coarse-grained arkoses are exposed locally near the basalt-basement contact and also in association with flows of the Weiser Basalt. These sediments generally reflect the composition of nearby granitic basement, show only short transport, are moderately lithified, and typically dip less than 10 degrees. They are principally of Weiser Basalt age and have resulted from the influx of abundant basement detritus. Some postdate Weiser Basalt units and are relatively undeformed.

The general characteristics of the various basalt units in the Weiser embayment are summarized in Table 1, and the geographic distribution of the main units are indicated in Figure 5.

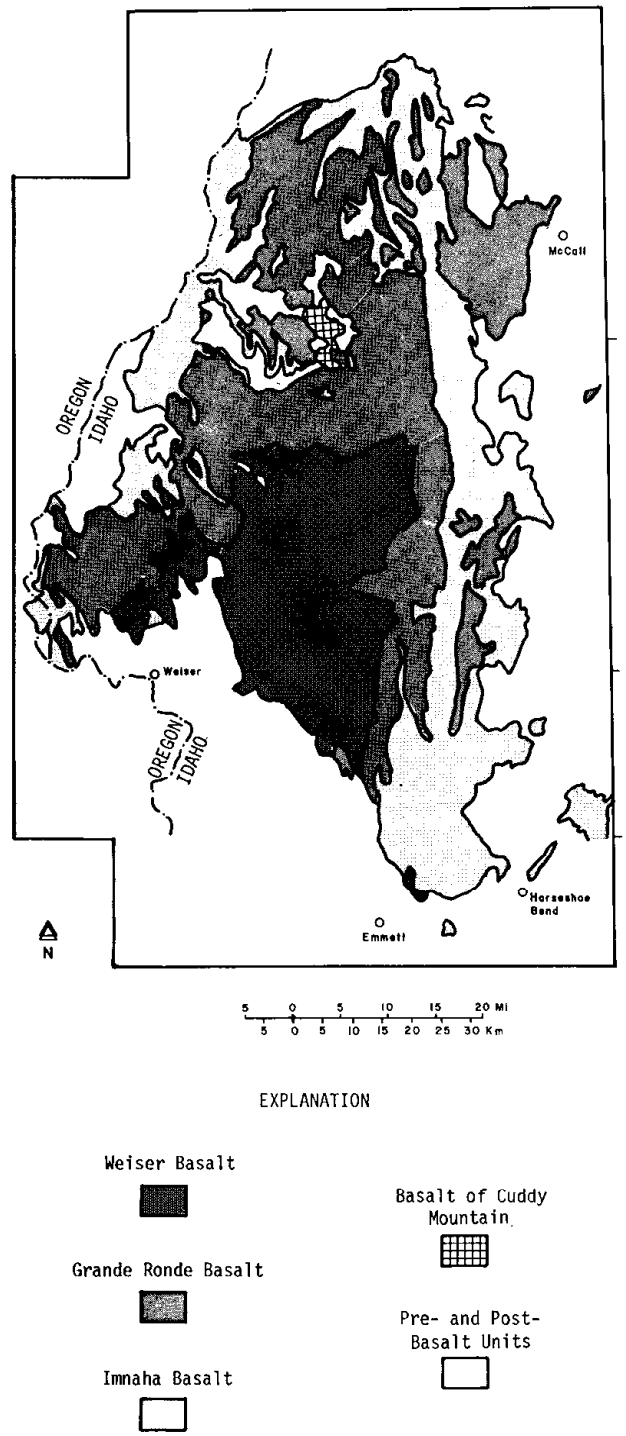

Figure 5. Generalized geologic map of the Weiser embayment showing basalt distribution.

POSTBASALT CONDITIONS

Following the Weiser episode of Miocene-age volcanism, structural activity became pronounced in the eastern and western parts of the embayment, as granitic and metamorphic basement blocks were jostled and uplifted into a series of tilted fault blocks and imperfect horst and graben structures. Movement commonly occurred along preexisting zones of weakness. Sediments continued to accumulate on the plateau, particularly in down-dropped and downwarped areas of the central and southern portion of the embayment. At the same time the Snake River took its present course south of the embayment and west of the Seven Devils steptoe flowing northward to the Columbia River. The postbasalt terrigenous sediments which accumulated at that time and still remain relatively undeformed are primarily associated with the embayment's southern margin, the Snake River Plain. They are most aptly categorized as Idaho Formation.

Following volcanism, three major fault patterns developed or continued to develop in different portions of the embayment. These are (1) a north-

Table 1. Summary of physical characteristics of Weiser embayment basalt units.

Vent and pyroclastic material in the Weiser Basalt

Near-vent units appear as low hummocky slopes and mounds; pumice-laden tuffs form coarsely "etched" surfaces. Hand specimens consist of volcaniclastic material. Bombs and other ejecta occur near vents. Lapilli tuff with abundant pumice is common. Pyroclastic material is associated with the Cambridge, Sugarloaf, and Star Butte members of the Weiser Basalt and is abundant in the Stockton Ranch and Weiser River vents.

Star Butte member of the Weiser Basalt

Paleomagnetically normal. Locally forms columnar-jointed massive cliffs; weathers black. Overlies a tuffaceous interbed in most areas. Hand specimens are aphyric to slightly phyric with small plagioclase phenocrysts visible in some samples. Unit consists of 2 to 4 flows.

Sugarloaf member of the Weiser Basalt

Paleomagnetically reverse. Forms cliffs along canyons; commonly weathers to subrounded boulders 0.5 to 2.0 meters in diameter. Sooty appearance common on weathered outcrops. Hand specimens have a grainy appearance and are phyric, with plagioclase and minor olivine and pyroxene phenocrysts visible on most surfaces. Finely vesicular to microvesicular; a resinous appearance is common. Unit probably contains 15 to 20 flows of basalt to basaltic andesite.

Cambridge member of the Weiser Basalt

Paleomagnetically reverse. Forms cliffs on steep slopes; weathers dark brown. Scoriaceous, rubbly, purple and pinkish purple flow tops are prominent in road cuts south of Cambridge. Hand specimens are sparsely phyric to phyric with plagioclase and minor olivine and pyroxene phenocrysts. Dark gray to black, glassy, and microvesicular. Unit consists of 12 to 14 flows.

Basalt of Black Canyon member of the Weiser Basalt

Paleomagnetically normal. Forms massive, bulbous cliffs; is very dark colored; has extremely hackly jointing and little or no internal structure. Hand specimens are aphyric, very dense, black, and glassy. Rocks are characterized by numerous joints intersecting at acute angles. Occurs as a thick valley- or canyon-filling flow near Black Canyon Dam. The stratigraphic position of this unit relative to the other members of the Weiser Basalt has not been determined due to its geographic isolation.

Basalt of Cuddy Mountain

Both normal and reverse paleomagnetic determinations were obtained. Unit appears to consist of more than one flow or sequence of flows. A highly phyric, nonvesicular type is common in the Pyramid Peak area of Cuddy Mountain. Elsewhere, a sparsely phyric, nearly nonvesicular nature appears to be characteristic. Coarsely phyric type forms columnar-jointed (columns 10 to 16 centimeters across) ledges; sparsely phyric type forms massive outcrops. Locally, phyric type forms prominent cliffs with talus slopes at base; several tiers occur in the thick accumulation on Cuddy Mountain. Hand specimens vary from coarsely phyric (abundant pyroxene crystals 0.3 to 2.5 centimeters long) to nearly aphyric. Rocks are black, dense, and nonvesicular at most exposures. Weathering forms pits in pyroxene-rich flows (coarsely phyric), to give a vesicular appearance. The stratigraphic position of this unit has not been determined from field relationships; it may be as old as Imnaha Basalt or as young as part of the Weiser Basalt.

Grande Ronde Basalt

Reverse paleomagnetism is most common, but normal paleomagnetism readings have been recorded locally within the reverse sequences. The upper flow or flows have normal paleomagnetism in the southeast portion of the embayment and perhaps elsewhere. Where dipping 10 degrees or less, rubbly flow tops or basal columns form intermittent low-relief ledges on slopes; where dipping more steeply, cliffs are more pronounced. Light reddish brown residual soil and weathered flow-top surfaces typify the unit and are most pronounced in low-dip areas. Hand specimens generally are aphyric, but narrow plagioclase laths are scattered in some flows. A sugary texture is common. Medium dark gray; weathered specimens show yellowish green mottling on freshly broken surfaces in most samples.

Imnaha Basalt

Normal paleomagnetism (probably the N_0 magnetostratigraphic epoch) occurs in most stratigraphic sections, except in the southeastern portion of the embayment. A stratigraphically lower, paleomagnetically reverse (probably the R_0 magnetostratigraphic epoch) section has been documented only on the east side of Squaw Butte. The unit may have one or more paleomagnetically transitional or reverse (perhaps the early part of the R_1 magnetostratigraphic epoch) flows at the tops of some sections. Commonly forms steep cliffs from basal columns and retreating slopes from upper portions of flows in rugged areas. Dip slopes tend to have patchy irregular outcrops. Columns weather dark brown to sooty or resinous in appearance. Flow tops are rubbly and pinkish purple to purple, particularly in the south. Hand specimens are sparsely phyric to extremely phyric. Phenocrysts are mostly plagioclase laths 0.5 to 3.0 centimeters long, but some olivine and pyroxene phenocrysts are present. Rocks are black (sooty to resinous) in appearance, with a microvesicular to diktytaxitic texture in many flows. Sparsely phyric flows commonly are more dense and glassy. Unit contains as many as 19 flows in a single exposed sequence; its base is not exposed.

trending block-fault pattern along the eastern margin of the embayment referred to as the Long Valley fault system (after Capps, 1941), (2) a northwest-trending open-fold and block-fault pattern in the south-central and southwestern portion of the embayment called the Paddock Valley fault system, and (3) a northeast-trending block-fault pattern in the northwestern portion of the embayment called the Snake River fault system (after Newcomb, 1970) (Figure 7). All of these fault systems extend beyond the Weiser embayment and are regional in perspective.

Other postbasalt structural activity included the continued broad downwarping of the central embayment Indian Valley trough, a synclinal depression, and upwarping of the Seven Devils area. Doming and weak anticlinal-synclinal folding along northwesterly axes that parallel the Paddock Valley fault system became more pronounced at this time southwest of Cuddy Mountain through the Sturgill Peak area to Dead Indian Ridge. This style of deformation has continued to contribute to the late Cenozoic topographic development of major geographic features in the western part of the embayment.

IMNAHA BASALT

Eruption of Imnaha Basalt flows began approximately 17 million years ago (McKee and others, 1981) during the R_0 paleomagnetic epoch. Imnaha flows covered nearly all of the Weiser embayment (Figure 5) by the end of the N_0 paleomagnetic epoch or early during the R_1 epoch. These flows apparently were extruded during several separate eruptive events from numerous feeder dikes west of the embayment and along its western margin.

In the southeastern corner of the embayment, near the distal margin of the original Columbia Plateau, over 400 meters of Imnaha Basalt accumulated during the R_0 and the succeeding N_0 paleomagnetic epochs. There, at least nineteen flows, aggregating 400 meters of R_0 and N_0 basalt, occur in a single stratigraphic section at Squaw Butte (sec. 26, T. 8 N., R. 1 W.). A minimum of twelve flows, aggregating 200 meters of N_0 Imnaha Basalt, is exposed at the nearby Big Willow Creek section (sec. 28, T. 9 N., R. 1 W.).

A minimum thickness of 700 meters of N_0 Imnaha Basalt accumulated in ancestral lowland portions of the western Weiser embayment near known sources. This thickness is continuously exposed in the canyons of the Snake River and its major tributaries northwest of Cuddy Mountain. In this portion of the embayment, fourteen flows of N_0 basalt occur in a single section at Wildhorse Canyon (sec. 23, T. 18 N., R. 4 W.). If intraformational chemical breaks can be used for lateral correlations (see discussion below), a minimum of twenty-five N_0 flows of Imnaha Basalt, aggregating 900 meters, can be recognized in a composite section at Oxbow Dam and Wildhorse Canyon.

No subbasalt rocks are exposed below the lowest outcrops in any of the thick Imnaha Basalt sections previously discussed in either the southeastern or northwestern embayment areas; therefore, a greater overall thickness undoubtedly is present.

The Imnaha sequence of flows changes upward from a very phyric lower portion to a nearly aphyric central portion to a coarsely phyric upper portion. The phyric flows generally have large phenocrysts of plagioclase and olivine that measure as much as 1 to 2 centimeters and 0.5 to 1 centimeter in length, respectively. Imnaha flows generally range in thickness from 20 to 60 meters. Flow-top breccia is present in a few flows.

The phyric, coarse-grained nature of most flows, along with their intergranular glass content, makes the Imnaha Basalt relatively susceptible to surficial weathering. The basalt commonly disaggregates into grus, particularly in the middle and upper portions of a flow, forming canyon walls that consist of a series of relatively subdued slopes developed from the upper parts of flows and nearly vertical cliffs developed from basal colonnades. Generally, isolated exposures of Imnaha Basalt are readily recognizable by their characteristic weathering into spalled columns and rounded boulders.

Relative concentrations of major oxides in the Imnaha sequences (Table 2) show ranges of composition characteristic of that unit elsewhere in the Columbia Plateau (Wright and others, 1973; Hooper and others, 1976; Reidel and others, 1981; Camp and others, 1982 this volume). The typical lower silica and higher alumina contents, when compared with Grande Ronde (lower Yakima) concentrations (Wright and others, 1973), can be recognized in Imnaha samples from the Weiser embayment.

At least two chemical basalt types occur in the Imnaha sequence in the northwestern part of the embayment as determined from the Wildhorse Canyon section (sec. 23, T. 18 N., R. 4 W.). An upper unit of at least eleven flows consists of moderately high SiO_2 (greater than 50.4 percent) and intermediate Al_2O_3 (less than 16.0 percent) contents. These flows overlie a group of at least six flows of lower SiO_2 (less than 50.2 percent) and higher Al_2O_3 (greater than 16.1 percent) contents. Neither the base of the Imnaha section nor its contact with the overlying Grande Ronde is exposed in the Wildhorse Canyon section; all flows in this section are of N_0 paleomagnetism.

This older group of lower silica flows in the

Table 2. Characteristic ranges in chemical composition of Weiser embayment basalt units (weight percent).

	IMNAHA 145 analyses	GRANDE RONDE 20 analyses	CUDDY MOUNTAIN 7 analyses	CAMBRIDGE 25 analyses	SUGARLOAF 31 analyses	STAR BUTTE 34 analyses	BLACK CANYON 1 analysis
SiO_2	48.05-53.13	52.73-56.04	44.24-47.45	49.43-53.21	52.22-58.09	47.82-51.95	57.64
Al_2O_3	14.21-18.33	14.25-15.98	13.83-15.97	16.17-17.80	15.92-19.03	15.42-17.94	16.08
FeO*	9.52-14.61	10.68-13.16	12.42-14.25	9.40-11.08	9.21- 9.93	10.05-13.04	11.38
MgO	3.63- 7.91	2.37- 4.83	4.00-11.93	3.39- 9.53	3.04- 5.96	3.41- 8.83	2.27
CaO	7.89-10.26	6.36- 8.21	9.71-11.81	7.41-10.94	7.30- 9.96	7.67-10.15	5.53
Na_2O	1.96- 3.40	2.30- 3.10	0.36- 3.17	2.07- 3.47	2.45- 3.33	2.13- 3.14	2.68
K_2O	0.33- 1.75	1.19- 2.44	0.86- 2.14	0.47- 1.86	0.87- 2.43	0.51- 1.80	1.82
TiO_2	1.48- 3.33	1.90- 2.52	2.70- 3.58	1.24- 1.94	0.73- 1.44	1.26- 3.06	1.73
P_2O_5	0.19- 0.45	0.27- 0.48	0.34- 1.73	0.30- 0.85	0.31- 0.51	0.27- 0.80	0.65
MnO	0.13- 0.25	0.17- 0.27	0.15- 0.32	0.15- 0.21	0.17- 0.23	0.17- 0.30	0.22

* FeO + Fe_2O_3

Wildhorse Canyon section is similar to the Rock Creek chemical type recognized by Brock and Grolier (1973) for some lower basalt (Imnaha) flows in the Little Salmon River section of Breeser (1972). This Little Salmon River vertical section (sec. 27, T. 22 N., R. 1 E.) is located east of the Seven Devils Mountains approximately 15 kilometers north of Pollock Mountain and the northern erosional margin of the Weiser embayment.

The overlying group of higher silica Imnaha flows in the Wildhorse Canyon section corresponds closely in chemical composition to the high-TiO_2 Picture Gorge (Imnaha) chemical type of Brock and Grolier sampled by Breeser near the base of the Little Salmon River stratigraphic section.

An Imnaha stratigraphic section near Oxbow Dam (sec. 17, T. 19 N., R. 4 W.), 16 kilometers northwest of the Wildhorse Canyon section, is in contact with the overlying Grande Ronde Basalt. In this Imnaha section the lower portion is of a high silica/intermediate alumina character similar to the upper portion of the Wildhorse Canyon section. This suggests the upper part of the Oxbow section is stratigraphically higher than the Wildhorse Canyon section. Silica is relatively high (greater than 50.5 percent) and alumina is intermediate (less than 16.2 percent) in the lower part of the Oxbow section. Above this is a lower SiO_2 (less than 49.9 percent) and higher Al_2O_3 (greater than 16.2 percent) group of at least three flows. This same separation into two chemical groups of flows also occurs in the upper Lick Creek section (sec. 31, T. 21 N., R. 1 W.) about 30 kilometers northeast of Oxbow.

The upper group of lower silica and higher alumina flows at Oxbow and Lick Creek are directly below the Grande Ronde contact. It is significant that they could not be distinguished from the underlying group of Imnaha flows near river level at the base of the Wildhorse Canyon section. This suggests that, even though chemically recognizable Imnaha flow groups can be laterally correlated in the western part of the embayment, the chemical variation is the result of intermittent eruption of different magma batches from various sources and feeder systems, rather than magma from a single source which evolved chemically by subsurface differentiation processes. Multiple sources of magma that erupted through different feeder systems may also explain why the lower SiO_2 (less than 49.0 percent) and lower Al_2O_3 (less than 15.9 percent) Little Salmon chemical type (Brock and Grolier, 1973) was not identified in the northern Weiser embayment southwest of the Little Salmon River section.

Other chemical groups occur in the thick Squaw Butte section (sec. 26, T. 8 N., R. 1 W.) in the southeast part of the embayment where both R_0 and younger N_0 Imnaha flows occur. In the upper part of the Squaw Butte section, at least eleven flows of relatively low SiO_2 (less than 50.6 percent) and high Al_2O_3 (greater than 16.7 percent, with greater than 17 percent typical) contents make up the paleomagnetically normal series. These are slightly different from the low silica Imnaha flows near the bottom of the Wildhorse Canyon section, many kilometers to the northwest by being consistently higher in alumina by about 1.0 percent and generally lower in both FeO and TiO_2 by that amount. The Squaw Butte N_0 flows are also higher in alumina than the uppermost N_0 low-silica flows of the Oxbow section.

At Big Willow Creek (sec. 28, T. 9 N., R. 1 W.), approximately 10 kilometers northwest of the Squaw Butte section, the lowermost flow exposed is Imnaha of the N_0 magnetostratigraphic epoch. This flow is chemically and magnetically similar to the low silica-

high alumina upper flows of the Squaw Butte section. Above this flow at Big Willow Creek are seven to nine N_0 flows of higher SiO_2 (greater than 51.2 percent) and lower Al_2O_3 (less than 16.2 percent) contents. If these are part of a chemical unit stratigraphically above the N_0 flows at Squaw Butte, an additional 200 meters of Imnaha Basalt can be added to the 400 meters of continuous section exposed at Squaw Butte to give a minimum of 600 meters of Imnaha Basalt in the southeastern portion of the embayment.

The older R_0 Imnaha flows at Squaw Butte differ from the overlying N_0 flows by having a lower Al_2O_3 content (less than 16.9 percent, with less than 16.7 percent typical) below the paleomagnetic break in at least ten flows. Chemical compositions in the R_0 series, however, do not show as consistent a grouping as in the N_0 series at Squaw Butte and other sections to the northwest. Intermixed intermediate and low silica Imnaha flows appear to be present in the Squaw Butte R_0 sequence. Detailed sampling and analyses might separate these into chemically distinguishable units. The interlayering of possibly different Imnaha R_0 chemical types at Squaw Butte is similar to the mixed pattern of the Little Salmon section (Brock and Grolier, 1973), again suggesting multiple, intermittent magma sources.

GRANDE RONDE BASALT

Eruption of Grande Ronde Basalt within the Columbia Plateau began in the R_1 magnetostratigraphic epoch about 14.7 million years ago (Watkins and Baksi, 1973) and continued through the N_1, R_2, and N_2 epochs. However, only one reverse paleomagnetic sequence is found in the Weiser embayment. Along Big Willow Creek, in the southeastern part of the area, a normal paleomagnetic flow or thin sequence of flows has been recorded, apparently resting on Imnaha flows. At other locations in the northwestern portion of the embayment a few normal flows overlie reverse Grande Ronde flows. Because no paleomagnetic continuum of R_1 through N_2 could be found, it is not possible to determine conclusively which reverse and normal sequences are present. Tentative correlation with units mapped to the northwest in Oregon and to the north in Idaho (Camp and Hooper, 1981; Camp, 1981) would place the Weiser embayment-Imnaha sequence in the R_1 and N_1 epochs. This interpretation requires a westward regional tilting of the transcient Columbia Plateau surface after early Grande Ronde Basalt extrusions and confinement of later Grande Ronde flows to Oregon, Washington, and northern Idaho as proposed by Camp and Hooper (1981). It is conceivable, however, that the reverse sequence could be R_2 and the normal N_2, or the reverse sequence R_1 and the normal N_2. Until specific Grande Ronde units are traced laterally northwestward into areas where the complete magnetostratigraphic sequence is exposed, the magnetostratigraphic position of the Weiser embayment Grande Ronde sequence will remain in question.

Grande Ronde Basalt spread as far southeast as present-day Squaw Butte (Figure 5). It covered about three-quarters of the earlier Imnaha surface in the southern portion of the embayment, and also spread eastward to the outer margin of the initial Imnaha surface and into canyons of the ancestral Salmon River Mountains. This is east of the present location of Long Valley south of McCall.

Grande Ronde Basalt in the embayment ranges from scattered phyric at the base of the exposed sequence of flows to sparsely phyric in the middle to medium-grained aphyric at the top. The weakly phyric units are principally in the reverse epoch, while aphyric flows occur at the top of the reverse and in the normal intervals.

In contrast with flows of the underlying Imnaha sequence, most Grande Ronde units have a flow-top breccia, are thinner at 10 to 20 meters, and are relatively resistant to weathering. As a result, they are more continuously exposed on steep erosional slopes as layered dark bands. Their debris is angular and forms prominent talus slopes.

Highly oxidized flow tops and scattered, very thin, oxidized, and layered ashy interbeds characterize the Grande Ronde in the embayment. Residual soils and weathered surfaces on Grande Ronde flows have a reddish cast rather than the darker colors typical of weathered Imnaha flows in the northwest, or the blues, pinks, and purples of Imnaha flow contacts in the southeast.

At least seven paleomagnetically reverse Grande Ronde flows occur in the northwest part of the embayment, where about 200 meters of this unit is exposed in canyons northwest of Cuddy Mountain (T. 17 N., R. 4 W.). There, the lowermost flow is thickest and appears to consist of a number of flow units. Paleomagnetically normal flows occur above this, northeastward toward the Seven Devils.

The flows mapped as Grande Ronde (Table 2) show major oxide abundances typical of Grande Ronde flows from elsewhere in the Columbia Plateau (Wright and others, 1973); they have relatively high SiO_2 (greater than 52.7 percent) and relatively low Al_2O_3 (less than 16.0 percent) concentrations. This also is about the same as the aphyric, oxidized Yakima flows identified by Brock and Grolier (1973) in the Little Salmon River section of Breeser (1972). It also agrees with Brock and Grolier's separate

sampling of five sequential post-Imnaha flows on the Seven Devils homocline in the Grouse Creek area (sec. 10, T. 19 N., R. 2 E.). These units were considered part of the (lower) Yakima chemical stratigraphic unit and informally called "Weiser River Basalt" (Breeser, 1972), to distinguish them from the underlying, highly porphyritic Imnaha sequence. The Grande Ronde chemistry of this study suggests that one of McIntyre's (1976b) samples from the Weiser Hot Springs area was also from the Grande Ronde sequence.

WEISER BASALT

The post-Grande Ronde basalt flows in the Weiser embayment are collectively referred to as the Weiser Basalt. Individual flows of this unit are much more restricted areally than those of the older Imnaha and Grande Ronde Basalts. Extrusion of the Weiser Basalt was accompanied by the eruption of large volumes of pumice breccia, scoria, volcaniclastic debris, and ash. These pyroclastic materials are an integral part of the unit.

No single or contiguous series of outcrops in the embayment exhibits a complete stratigraphic sequence for the Weiser Basalt. Stratigraphic position within that sequence is based on overlapping units and flow-on-flow relationships exposed in scattered canyons and scarps. Thus, the post-Grande Ronde stratigraphy is largely a floating stratigraphy based on relative positions and probable lateral correlations of flows but with no fixed position in post-Grande Ronde time.

Four distinct members of Weiser Basalt have been defined by a combination of outcrop characteristics and unconformable relations with underlying Imnaha and Grande Ronde flows. Three of these occur in succession in Crane Creek canyon near its confluence with the Weiser River. From oldest to youngest, these are the basalts of Cambridge, Sugarloaf, and Star Butte (Figure 4). The fourth member, the basalt of Black Canyon, is geographically isolated and thus has not been placed in relative stratigraphic position with the other three.

Additional chemically distinct, local basalt units, similar to the basalt of Black Canyon, may have gone unrecognized in the southern part of the embayment. For example, five of the eleven samples from near Weiser Hot Springs analyzed by McIntyre (1976b) could not be correlated with any of the basalt units discussed in this study.

This four-part subdivision of the Weiser Basalt is not all-inclusive; other post-Grande Ronde volcanic rocks with andesitic to rhyolitic compositions occur at scattered localities in the embayment (McIntyre, 1976b, and analyses gathered for this study). In addition, the local basalt unit at Cuddy Mountain does not show a clear stratigraphic relationship or a chemical similarity to either the Weiser Basalt or to the older Imnaha and Grande Ronde Basalts; thus, in this study, it has been treated as a separate unit.

CAMBRIDGE MEMBER

The Cambridge member contains twelve to fourteen basalt flows that spread across much of the south-central portion of the embayment (Figure 6). Northward thinning remnants of the Cambridge flows overlie the Grande Ronde in low areas northeast and northwest of Cambridge. The unit extends as far east as Indian Valley and westward to Warm Springs Creek valley northwest of Weiser. A pumice breccia tuff commonly occurring at the base of the unit extends northwestward beyond the headwaters of Rock Creek into the Rock Creek syncline. Cambridge flows were traced as far south as Weiser Cove near the edge of the Snake River Plain; south of this location, sediments of the younger Idaho Formation cover all older units.

The Cambridge flows were erupted during a paleomagnetically reverse epoch. The amount of structural deformation which followed Grande Ronde accumulation but preceded the Cambridge eruptions suggests that this reverse epoch is of post-R_2-N_2 time.

Cambridge flows typically are from 10 to 15 meters thick. Individual flows, as those well exposed in Weiser River canyon (sec. 15, T. 14 N., R. 3 W.) south of Cambridge, consist of basal columnar colonnades and rubbly, brecciated tops. Similar characteristics can be seen in the multi-flow exposures along Mann Creek north of Mann Creek Reservoir and at the bottom of Crane Creek canyon near its juncture with Weiser River canyon. Rolled-in portions of vesicular crust and ashy material commonly occur, particularly within the upper portions of flows and near basal contacts. Cambridge flows typically are oxidized and altered to variegated purple and pink shades in vesicular and rubbly zones. Columnar outcrops and hand specimens are dark gray to black and nearly aphyric. Textures commonly are microvesicular or diktytaxitic, giving a grainy appearance to fresh surfaces.

The lower silica and higher alumina contents generally distinguish Cambridge flows from the underlying Grande Ronde units, as do the lower FeO and TiO_2 and higher MgO and CaO contents. Cambridge units have lower silica contents than Sugarloaf or Black Canyon flows, but have higher silica contents than Star Butte or Cuddy Mountain flows. Cam-

bridge basalt can also generally be distinguished from the directly overlying Sugarloaf flows by its higher FeO and TiO_2 content. As in comparisons of the older Imnaha Basalt flows, where a wide range of chemical compositions is involved, the identification of Cambridge flows must rely on field relations, hand-specimen characteristics, and remanent magnetization in addition to chemical composition.

SUGARLOAF MEMBER

Sugarloaf basalt was one of the first chemical-stratigraphic units within the Weiser Basalt to be recognized (Fitzgerald, 1980); it occurs primarily in the southern portion of the Indian Valley trough (Figure 6). No exposures north of Midvale are known, and only scattered outcrops occur north of Crane Creek Reservoir. Mann Creek is the approximate western limit of Sugarloaf distribution, and Four Mile Creek is the eastern limit. The east-west segment of Big Willow Creek southeast of Weiser is about the southern limit. As with Cambridge flows, the southernmost exposures are at the northern margin of the Snake River Plain, so it is probable that the unit extends farther south beneath the Idaho Formation. Nine Sugarloaf member flows are exposed in Crane Creek canyon (sec. 9, T. 11 N., R. 3 W.), where 150 meters of basalt rests on an ignimbrite layer separating the Sugarloaf and Cambridge members.

The Sugarloaf member is paleomagnetically reverse and may have been erupted during a continuation of the reverse epoch of Cambridge basalt extrusion. The confinement of the Sugarloaf to the Indian Valley trough suggests that post-Cambridge basining partly controlled its distribution. The spatial association of the Sugarloaf with the north-northwest trending Paddock Valley fault system suggests that a fault-controlled vent system also may be a significant factor in the unit's distribution.

Sugarloaf flows typify the Weiser Basalt by being relatively thin (10 to 20 meters) and by having abundant ash and other pyroclastic material associated with top and bottom contacts. Sugarloaf flows are generally distinguishable from other Weiser Basalt units in the field by their abundant plagioclase phenocrysts with 0.5 to 1.0 centimeter lengths.

Sugarloaf basalt is distinguishable chemically from other Weiser Basalt units by its high SiO_2 (greater than 52.2 percent and as great as 58.1 percent) and low FeO (less than 10.0 percent) contents (Table 2).

STAR BUTTE MEMBER

Basalt flows of the Star Butte member occur primarily as remnant caps in the Indian Valley trough (Figure 6). The unit is not as widely distributed as the two underlying Weiser Basalt members. Most exposures occur between the Little Weiser River on the north and Paddock Valley Reservoir on the south, and between the South Fork of Crane Creek on the east and Middle Valley and the main Weiser River on the west.

About 25 meters of Star Butte basalt overlies the Sugarloaf member in the Crane Creek area. Four thin flows occur at the top of the Crane Creek canyon section (sec. 4, T. 11 S., R. 3 W.). Individual flows typically are 5 to 7 meters thick. As with the other Weiser Basalt members, pyroclastic material and ashy interbeds form part of the Star Butte unit. Outcrops typically are small knobs or patches of rounded or vesicular, blocky boulders. Hand samples are aphyric or contain only scattered small plagioclase phenocrysts, in contrast to the abundant large plagioclases in the underlying Sugarloaf unit. Fresh surfaces of Star Butte basalt typically have a grainy appearance.

Star Butte basalt is chemically similar to the Cambridge member, but slightly richer in iron and titanium (Table 2). It is much lower in silica than the Sugarloaf member. Star Butte basalt is paleomagnetically normal, in contrast to the reverse paleomagnetic character of the Cambridge and Sugarloaf units.

BASALT OF BLACK CANYON

The basalt of Black Canyon is located at the southeastern margin of the embayment where the Payette River goes through Black Canyon. The unit apparently consists of a single very massive flow, up to 100 meters thick, with no indications of flow-on-flow emplacement. It very likely filled a preexisting valley or canyon. A vertical basalt rib on the south side of Black Canyon Reservoir near the western margin of the unit's distribution may be a feeder remnant. The basalt of Black Canyon is paleomagnetically normal. It unconformably overlies westward-dipping and faulted Imnaha flows.

The basalt of Black Canyon has a hackly to blocky appearance in outcrop. Its color ranges from black to dark gray on fresh surfaces to rusty brown on weathered surfaces. The rock is aphyric with a very fine-grained to glassy texture and in places, contains abundant vesicles. Joint and fracture intersections are very acute, reflecting the dense, glassy texture of the rock.

The Black Canyon basalt is distinct with a very high SiO_2 content (greater than 57.6 percent) and very low MgO (less than 2.3 percent) and CaO (less than 5.5 percent) contents, when compared with other basalts in the embayment (Table 2).

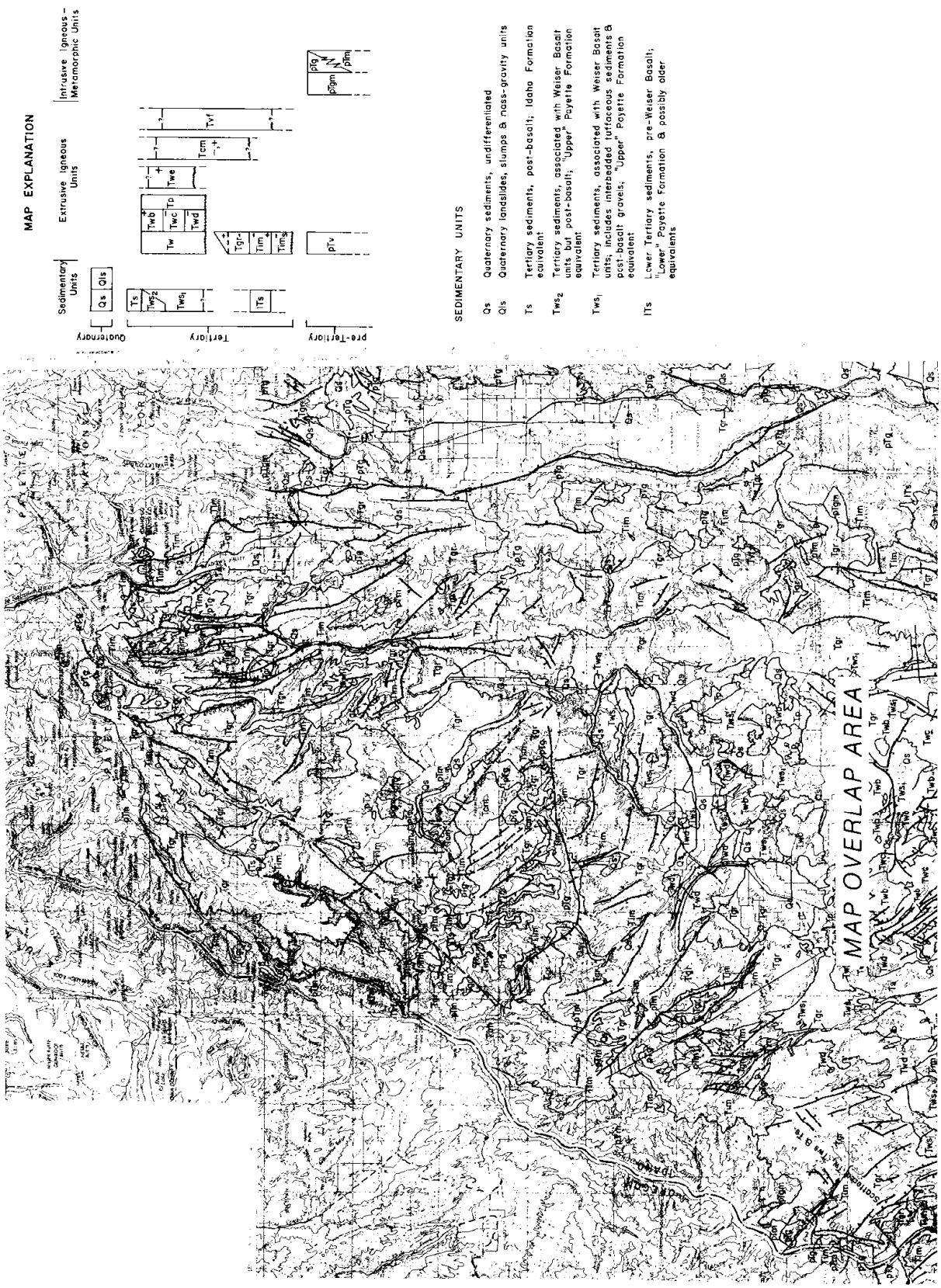
MAP EXPLANATION
Sedimentary Units
Extrusive Igneous Units
Intrusive Igneous-Metamorphic Units
Quaternary
Tertiary
pre-Tertiary
Qs
Qls
Ts
Tws2
Tws1
Tw
Twb
Twc
Tp
Twd
Twe
Tcm
Tvf
Tgr
Tim
Tims
ITs
pTv
pTg
pTgm
pTm
SEDIMENTARY UNITS
Qs Quaternary sediments, undifferentiated
Qls Quaternary landslides, slumps & mass-gravity units
Ts Tertiary sediments, post-basalt; Idaho Formation equivalent
Tws2 Tertiary sediments, associated with Weiser Basalt units but post-basalt; "Upper" Payette Formation equivalent
Tws1 Tertiary sediments, associated with Weiser Basalt units; includes interbedded tuffaceous sediments & post-basalt gravels; "Upper" Payette Formation equivalent
ITs Lower Tertiary sediments, pre-Weiser Basalt; "Lower" Payette Formation & possibly older equivalents
MAP OVERLAP AREA
Idaho
Oregon

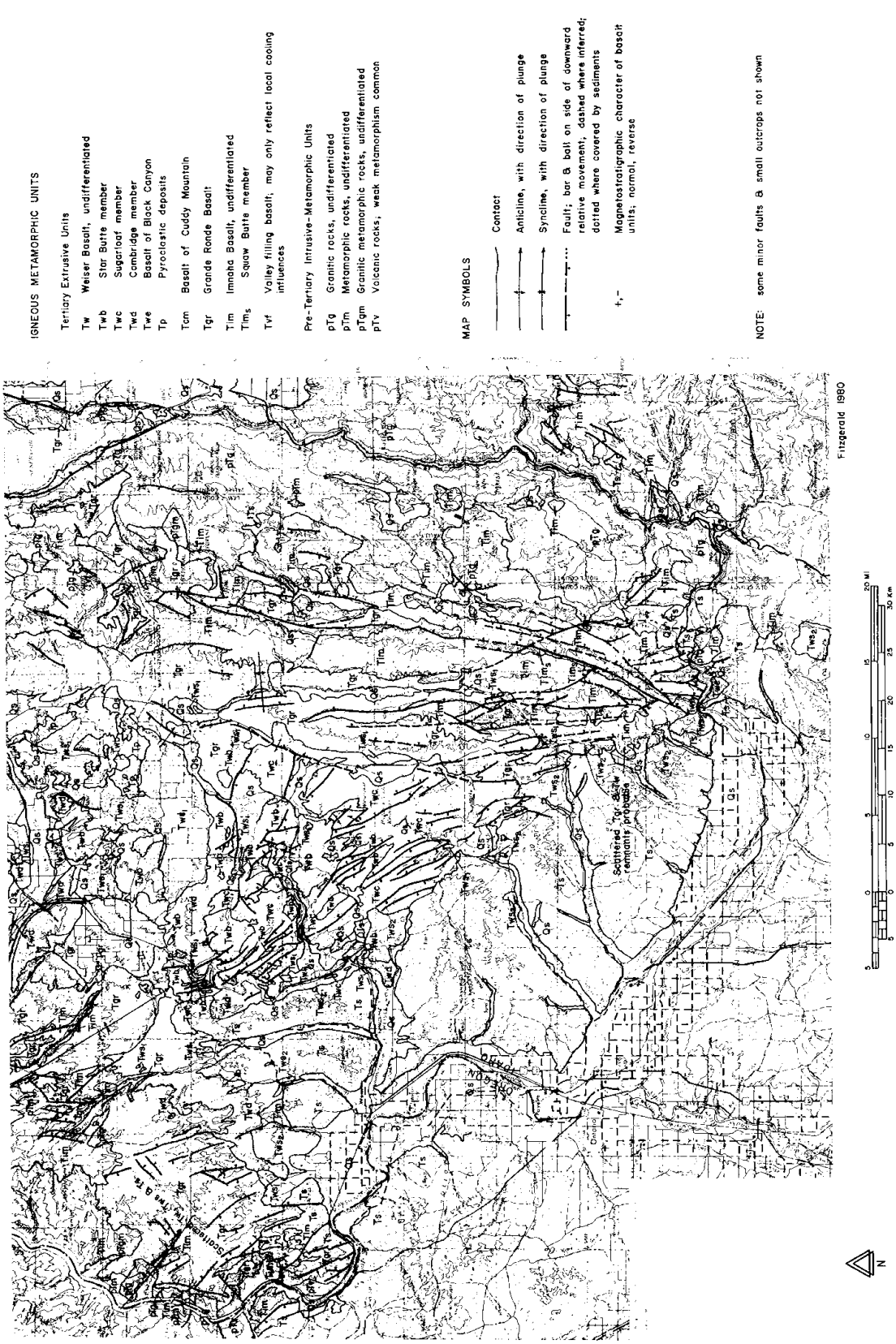

Figure 6. Geologic map of the Weiser embayment. (Many geologic contacts are generalized because of small map scale.)

Cascade fault
Long Valley fault
Mountain fault
Little Salmon fault
Mud Creek fault zone
Lost Creek fault zone
Seven Devils lineament
Lost Creek fault
Calamity Meadows fault zone
Horse Creek fault
Kinnikinnick
Cordy
Pine Creek anticline
Pine Creek fault zone
Stargill fault
Stargill Peak anticline
Manns Creek fault zone
SNAKE RIVER FAULT
MAP OVERLAP AREA

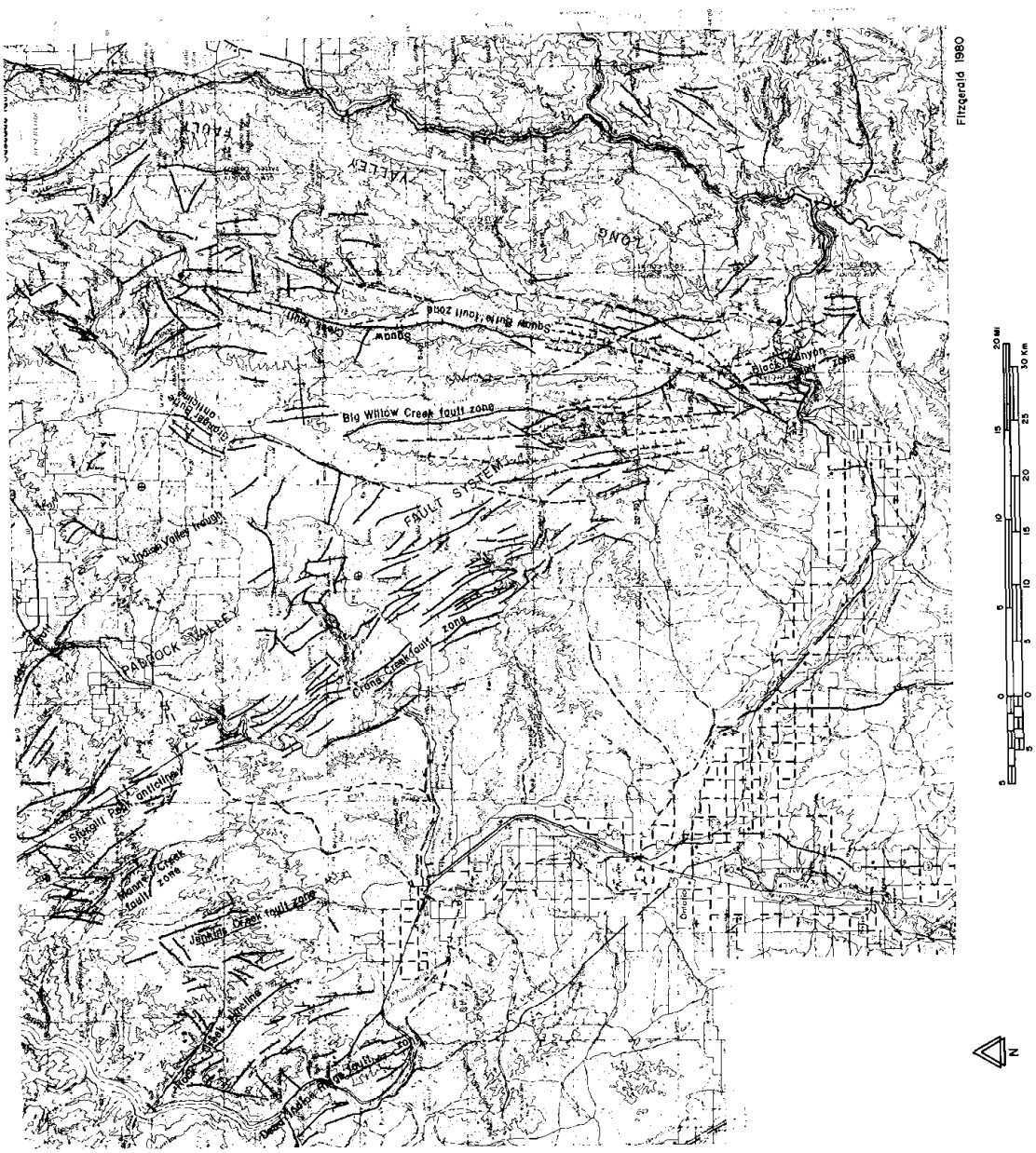

Figure 7. Structural map of the Weiser embayment.

VENTS

Two large vent areas are preserved in the southern half of the embayment. They are the result of some of the last volcanic eruptions in the area and thus are relatively young in the Weiser Basalt sequence. Both vents are accompanied by abundant pyroclastic deposits that have modified the local topography. Basalt on both vents is paleomagnetically reverse, as are adjacent flows.

One, the Stockton Ranch vent, is located 18 kilometers east of Cambridge. Hoover (1968) recognized its post-flood-basalt stratigraphic position and suggested it was Pliocene in age. It also was partially described by McIntyre (1976a). The other, the Weiser River vent, located 7 kilometers south of Midvale, was previously defined by Fitzgerald (1979).

The Stockton Ranch vent area consists of several small, gently sloping hills composed of pyroclastic material that surrounds and partially covers four aphyric dikes. Basaltic ash, pumice, lapilli, and occasional fragments up to 4 centimeters across are present. This pyroclastic deposit extends 10 kilometers from the source and is at least 30 meters thick in places. It could not be correlated with other Weiser Basalt units from its physical and chemical properties. The pyroclastic debris generally is well layered with each layer less than 14 centimeters thick; the layers terminated eastward in the Lava Flats area on a series of small bluffs covered by lacustrine deposits of Weiser Basalt age. The pyroclastic deposits dip gently toward their source but lie beneath younger Weiser Basalt lava flows that have a horizontal attitude. This is interpreted as an initial depositional dip.

The Weiser River vent overlooks the Weiser River from the east. It is a partially dissected cinder cone that consists of two distinct circumferential zones. The outer zone consists of pinkish to orangish red, poorly welded, scoriaceous, well-layered pyroclastic material that is impregnated with numerous volcanic bombs up to 30 centimeters in length. The inner zone is highly welded pyroclastic material with a few lithic fragments; it appears to be a drain-back zone containing mainly welded spatter.

The pyroclastic apron of the Weiser River vent is much less developed than that of the Stockton Ranch vent to the east. It was recognized no more than 1 kilometer in any direction from the source.

As with the Stockton Ranch vent, the Weiser River vent cannot be physically correlated to any flow of the Weiser Basalt. Chemical data, likewise, do not make diagnostic associations between vent material and individual flows. The two vent units, therefore, also demonstrate the local nature of some eruptive features within the Weiser Basalt.

BASALT OF CUDDY MOUNTAIN

The basalt of Cuddy Mountain is exposed mainly along the eastern edge of the Cuddy Mountain uplift. Small isolated exposures also occur a few kilometers to the west on Cuddy Mountain. The basalt of Cuddy Mountain has not been included in the Weiser, Grande Ronde, or Imnaha Basalts because definitive stratigraphic relations have not been found, and the Cuddy Mountain unit differs chemically from any of the other units (Table 2). Both paleomagnetically normal and reverse flows have been found in the basalt of Cuddy Mountain.

Two textural varieties of Cuddy Mountain basalt were found: (1) a slightly phyric unit, and (2) a highly phyric, pyroxene- and plagioclase-rich unit with pyroxene phenocrysts as large as 2 centimeters in length. Based on major element chemistry of seven samples, the two types are indistinguishable (Table 2).

The slightly phyric type appears to be the more widely distributed. It underlies a Grande Ronde Basalt flow in an isolated exposure on the southwestern part of Cuddy Mountain. Other exposures, however, lie directly on pre-Tertiary rocks of the Cuddy Mountain steptoe. The slightly phyric variety is commonly massive and nonvesicular or only locally vesicular, and contains scattered small plagioclase, pyroxene, and olivine phenocrysts set in a fine-grained, glassy groundmass.

The highly phyric type occurs only near Pyramid Point and at the southeasternmost limit of the basalt of Cuddy Mountain. In the southeastern part of Cuddy Mountain the highly phyric type appears to overlie Grande Ronde Basalt, although a clearcut contact was not located. The phyric type is massive or displays well-developed, thin columns 10 to 20 centimeters in diameter. Weathered surfaces of the highly phyric variety are strongly pitted because of differential weathering of pyroxene and plagioclase phenocrysts. Fresh rock contains abundant and large pyroxene and plagioclase phenocrysts and scattered olivine phenocrysts in a black, glassy groundmass.

The basalt of Cuddy Mountain shows low SiO_2 (less than 47.5 percent) and generally low Al_2O_3 (less than 15.9 percent) contents and generally high FeO (greater than 12.4 percent), CaO (greater than 9.7 percent), and TiO_2 (greater than 2.7 percent) contents when compared with the Weiser Basalt (Table 2). There appear to be two chemical types of Cuddy Mountain flows as defined by low MgO (less than 7.4 percent), and high MgO (greater than 9.5 percent) contents. However, the chemical types do not correspond to the slightly and highly phyric textural types. Additional detailed mapping and sampling will be

required to further resolve the age relationships between the chemical and textural varieties of the basalt of Cuddy Mountain.

STRUCTURE

The principal structural features within the Weiser embayment include the north-south aligned Long Valley fault system (Capps, 1941) on the east, the north-northwest-trending Paddock Valley fault system in the southern and south-central portions of the area, and the northeast-trending Snake River fault system (Newcomb, 1970) on the west (Figure 7). Other major structural features with marked topographic expressions include the Seven Devils homocline which forms the south flank of the Seven Devils arched uplift in the north, the Cuddy Mountain uplift on the northwest, the Sturgill Peak uplift (anticlinal warp) on the west, Dead Indian Ridge on the southwest, and the broad south-plunging Indian Valley synclinal trough underlying the central and southern lowlands of the embayment. Virtually all structural features at the south margin of the embayment are truncated or down-dropped by the younger Snake River Plain.

NORTH-TRENDING BLOCK FAULTS—LONG VALLEY FAULT SYSTEM

The Long Valley fault system is a belt of north-trending, high-angle normal faults at the eastern margin of the Weiser embayment and in the adjacent western margin of the Idaho batholith (Anderson, 1934; Capps, 1941; Hamilton, 1962). This system extends along and north of the 165-kilometer-long eastern border of the embayment; it is up to 30 kilometers wide. This fault system is responsible for the alternating north- and south-flowing rivers in the area—South Fork of the Salmon, Payette, Little Salmon, and upper Weiser—and for the deep, elongate valleys and tilted fault-block ridges which characterized the eastern margin of the embayment.

Relative movement across the fault planes typically is east-side down with steep fault scarps on the eastern slopes of the fault-block mountains and 5 to 20 degree dip slopes on the western sides of the tilted blocks. This east-side down character is most pronounced where the Idaho batholith makes up the bulk of exposed bedrock.

Numerous individual faults and parallel sets of faults (fault zones) make up the Long Valley fault system. Examples (Figure 7) include Bally Mountain fault, Little Salmon fault, Mud Creek fault zone, and Lost Creek fault zone in the northeast, Long Valley fault in the east, and Squaw Creek fault, Big Willow Creek fault zone, and Squaw Butte fault zone in the southeast.

The Long Valley fault system consists primarily of dip-slip faults which are straight to slightly curvilinear or sinuous in plan view. Several faults branch or splay; this is most common in the northeastern and southeastern portions of the fault system where it intersects the Snake River and Paddock Valley fault systems respectively. Subordinate to the north-trending faults of the Long Valley fault system are short, linear to slightly arcuate faults that trend at acute angles to the major north-trending traces. A cluster of these occurs at the headwaters of the Little Weiser River west of Long Valley. These faults generally have northwesterly and northeasterly orientations and appear to be a conjugate set of the Long Valley fault system.

The offset along the major faults of the Long Valley system exceeds 900 meters at many localities, as documented by the displacement of particular Imnaha and Grande Ronde Basalt flows from uplifted fault blocks to adjoining valleys. Council Mountain, Snowbank Mountain, and Squaw Butte demonstrate 1,000 meters of displacement relative to adjoining down-dropped areas. Major postbasalt structural movement within the Long Valley fault system is also demonstrated by the homoclinal dip slopes of Imnaha Basalt flows on Tripod Peak, Indian Mountain, and Timber Butte that plunge beneath the Grande Ronde in adjacent downslope areas.

Columbia River Basalt Group flows that discordantly overlie older metamorphic and plutonic rocks in the fault blocks are themselves offset and tilted. This indicates that tectonism has long been persistent and that faulting, in its latest episodes, is less than 14 million years old. Youthful consequent and antecedent drainage patterns within the area, when considered along with the discordance between the Grande Ronde and overlying Weiser Basalts, suggest that movement of the Long Valley fault system commenced shortly after the Grande Ronde eruptive interval and has continued, at least intermittently, nearly to the present.

NORTHWEST-TRENDING BLOCK FAULTS AND FOLDS—PADDOCK VALLEY FAULT SYSTEM

In the south-central portion of the embayment, the basalt units and overlying sediments have been folded and faulted along northwesterly trends (Kirkham, 1928, 1931; McIntyre, 1976b). This is the Paddock

Valley fault system of northwest-trending block faults and open folds; it extends from the Big Willow Creek area north of Emmett to near the Snake River canyon between Cuddy Mountain and Olds Ferry (Figure 7). The belt is approximately 80 kilometers wide in the southeast to 50 kilometers wide in the northwest. Faults within this system are nearly parallel to the trend of the structural belt except in the Sturgill Peak uplifted block and near Dead Indian Ridge, where fault orientations are variable and cross faults occur. This zone of variable orientations occurs where the Paddock Valley system intersects the northeast-trending Snake River fault system.

The Paddock Valley fault system, in contrast to the Long Valley system, does not show a consistent down-to-the-east or down-to-the-west pattern. Displacements, particularly in the southern and central areas, appear to have responded to local structural adjustments in the Indian Valley synclinal trough, the Sturgill Peak plunging anticline, the Rock Creek syncline, and the Dead Indian Ridge uplift (Figure 7).

Displacements across faults in the Paddock Valley system typically range from 10 to 100 meters in areas of high fault density in the southeast. This amount of deformation appears to have partly accommodated minor late Cenozoic folding and gravity faulting. Displacements also were probably in response to slumping and sliding of Weiser Basalt flows on shallow interbed units throughout much of the southern Paddock Valley fault system.

Greater displacements occur to the northwest and west, near Sturgill Peak and Dead Indian Ridge, where offsets across major faults have exposed subbasalt rocks at numerous localities and juxtaposed Imnaha and Grande Ronde units. Displacements on faults and fault zones of the Paddock Valley system are at least 700 meters in the Cuddy Mountain and Sturgill Peak areas and over 300 meters at Dead Indian Ridge. Part of the vertical movement in the Cuddy Mountain-Sturgill Peak area was due to postbasalt localized uplift which occurred largely along established faults of the Paddock Valley system.

Many individual faults and fault zones make up the Paddock Valley fault system (Figure 7). In the northwest these include the Pine Creek fault zone, the Cambridge fault, the Sturgill Peak fault, and the Mann Creek fault zone. The northwest-trending western portion of the Cuddy Mountain fault probably also belongs to the Paddock Valley system. This northwest-trending fault system also manifests itself as the Calamity Meadows fault zone on the Cuddy Mountain uplift and the Hornet Creek fault northeast of Cuddy Mountain. The Crane Creek fault zone, in the center of the Paddock Valley fault system and near the center of the embayment, is where fault density is greatest but displacements are lowest. The Black Canyon fault zone south of Squaw Butte appears to be a southeasterly extension of the Paddock Valley system within an area dominated by the Long Valley system.

Individual fault traces in the Crane Creek and Black Canyon fault zone segments of the Paddock Valley system range from 3 to 15 kilometers and average about 6 kilometers in length. An average length of 8 to 10 kilometers occurs to the northwest where the belt widens to about 50 kilometers and the fault density decreases. This change probably reflects both differences in magnitude of deformation and the response of the different basalt units to stresses in the two areas. In the southeast the near-surface units are the less competent Weiser Basalt flows and interbedded and abutting sediments, whereas in the northwest the near-surface units are the more competent flow-on-flow Grande Ronde and Imnaha sequences.

Faulting and folding in the Paddock Valley system occurred before and after the deposition of Idaho Formation sediments (Kirkham, 1928; McIntyre, 1976b). Folds, such as the Sturgill Peak anticline, are open and plunge gently to the southeast (Kirkham, 1928). The age, style, and location of these northwest-trending structures suggest they formed during the downwarping and faulting of the western Snake River Plain (Kirkham, 1931; Hamilton, 1962; McIntyre, 1976b). The northwestward continuation of the fault system into Oregon (Newcomb, 1970) also supports the interpretation that the Paddock Valley system is associated with the evolution of the western Snake River Plain. The geographic relationship of the Paddock Valley system to the Weiser Basalt flows suggest that dip-slip disruption provided pathways for magma ascent and volcanic eruptions.

NORTHEAST-TRENDING HIGH-ANGLE FAULTS-SNAKE RIVER FAULT SYSTEM

Pre-Tertiary northeast-trending faults of the Snake River fault system occur along the northwestern margin of the embayment, generally parallel to the Snake River canyon (Figure 7). Some high-angle dip-slip faults of this belt offset Columbia River basalt flows, attesting to recurring and postextrusion movement (Cook, 1954; Hamilton, 1962; Brooks and Vallier, 1967; Vallier, 1977).

The Snake River system forms a belt up to 25 kilometers wide, much of which lies west of the Weiser embayment. The system extends into the Clearwater embayment to the north, where it intersects the Long Valley system. Faults of the Snake River system strike dominantly N. 30-45° E.; movement is nearly vertical and of block-fault character.

In Idaho, offsets generally are west-side-down, so that the Oregon portion of the Columbia Plateau next to the Weiser embayment is lower in elevation.

Many youthful northeastward-aligned streams along the western border of the embayment and nearby in Oregon follow the Snake River system. Vertical uplift along these faults accounts for much of the northward elevation increase from Olds Ferry to the Seven Devils in western Idaho.

Fault density, as mapped during this study and compiled from previous work (Bond, 1978; Mitchell and Bennett, 1979a, 1979b), is less than in the Long Valley or Paddock Valley systems. However, because much Snake River system deformation is in basement rocks west of the area mapped, the fault abundance is not well represented on Figure 7. Fault offsets are as great as in the Long Valley system and far greater than in the Paddock Valley system. The vertical displacement of the Cuddy Mountain-Sturgill Peak area relative to Oregon is well over 1,000 meters, as demonstrated by the offset of Imnaha and Grande Ronde Basalt units. Similar displacement occurs in the Seven Devils area, where remnants of Imnaha Basalt are at 2,440 meters (8,000 feet) elevation, compared with exposures in the adjacent Snake River canyon at 1,220 meters (4,000 feet) elevation.

Major individual faults and fault zones in the Snake River system that offset Columbia River basalt flows within the embayment include (Figure 7) the Indian Creek fault, the Wildhorse Creek fault zone, and the Lick Creek fault (including the latter's extension southwestward to Sturgill Peak).

The Snake River system deformation is clearly both pre- and post-Columbia River Basalt Group in age. The northeasterly alignment of the Sturgill Peak, Cuddy Mountain, and Seven Devils blocks or domal structures (Hamilton, 1962) along the same trend also attests to the long activity of this structural belt. These areas were structural highs prior to Columbia River basalt extrusion and became steptoes when the Weiser embayment was formed. Their present-day elevated condition and the tilted basalt remnants they contain demonstrate postbasalt movement.

UPLIFTED BLOCKS AND INTERVENING COMPLEX GRABEN

The Sturgill Peak, Cuddy Mountain, and Seven Devils uplifts are dome-shaped blocks of pre-Tertiary rocks capped by remnants of Columbia River basalt. Cook (1954) reported that the lowest basalt unit at Cuddy Mountain was draped over the subbasalt structure, suggesting postbasalt doming. Fankhauser (1968) noted that flow thicknesses do not markedly vary from the flanks to the top of Cuddy Mountain, also indicating that uplift occurred, or recurred, after the basalt accumulated. Similarly, Cook (1954) reported that Columbia River basalt occurs at 2,485 meters (8,150 feet) elevation in the Seven Devils Mountains. This is the northernmost erosional remnant of Weiser embayment flows. These remnants are mainly Imnaha flows, suggesting Grande Ronde units may have been eroded so that more structural than topographic relief occurs.

The uplifted blocks have a northeast-trending alignment which, as noted before, parallels the Snake River fault system (Figure 7). Cook (1954) suggested that the uplifts were squeezed up between preexisting northeast-trending structures when the Columbia Plateau was regionally folded along east-west axes. Hamilton (1962) stated that the domal blocks are dominantly bounded by northwest-trending normal faults; that is, the Paddock Valley fault system.

The Sturgill Peak block is uplifted on the east and northeast by the north- to northwest-trending dip-slip Sturgill Peak fault and Pine Creek fault zone of the Paddock Valley fault system. The southwestern margin of the uplift generally coincides with the down-to-the-southwest offset across the Mann Creek fault zone. The southeast-plunging Sturgill Peak anticline records postbasalt deformation within the block, as does the central uplift and flank step-faulting in the Paddock Valley fault system along the southeastward projection of the anticlinal axis.

The Cuddy Mountain block is largely bounded by dip-slip faults. On its southwestern and northeastern sides the faults trend northwestward and belong to the Paddock Valley system. The faults bounding the southwest (Cuddy Mountain fault) and northeast sides (Hornet Creek fault) trend approximately N. 45° W. The nearly east-west segment of the Cuddy Mountain fault forms the southern boundary. These offsets, together with offsets across faults of the Snake River system to the northwest, give the uplift a horst configuration.

The south flank of the Seven Devils uplift is primarily a basalt dip slope that is tilted rather uniformly toward the Weiser River valley. This southward-dipping slope extends from the northernmost erosional basalt remnants near Smith Peak and Pollock Mountain to near Mesa in the middle of the embayment. This dip slope, the Seven Devils homocline, is cut by numerous faults of the Snake River system on the west and the Long Valley system on the east. The north-dipping Doumecq homocline of the Clearwater embayment is the mirror-image dip slope on the north flank of the Seven Devils Mountains and demonstrates the arching of that uplifted block.

A complex graben, the Pine Creek graben, separates Cuddy Mountain from Sturgill Peak. It is drained by Pine Creek and several subparallel trib-

utaries of the Weiser River. The graben trends N. 30-50° W. in the northwest and about N. 90° E. at the east end where it widens and parallels the east-west Cuddy Mountain fault and merges with the central synclinal region of the embayment.

The Pine Creek graben widens southeastward from about 6 kilometers near the Snake River to about 30 kilometers east of Cambridge between the Little Weiser River and the southern side of Cuddy Mountain. The southwestern boundary of the graben steps up to the southwest on the flank faults of Sturgill Peak. These subparallel splay faults generally dip northeast to east. Several northwest-trending faults occur near the middle of the Pine Creek graben where the trend of the graben axis changes from northwest to east-west. Subsidiary northwest-trending horst and graben fault-sets trend southeastward into the graben from the south-dipping faults at the southern boundary of the Cuddy Mountain uplift.

CENTRAL SYNCLINAL REGION—INDIAN VALLEY TROUGH

The Indian Valley trough at the center of the embayment is a south-plunging syncline or complex basin bounded by the fault systems and other structures discussed above (Figure 7). Although this region has poorly defined margins, it is characterized by roughly centripetal drainage of tributaries to the Middle Weiser River and Crane Creek. Many of the large alluvial valleys in the embayment and much of the Weiser Basalt and associated sediments, as well as younger Tertiary sediments, are in this central depression.

A strong structural pattern is not evident between the Paddock Valley and Long Valley fault systems. Minor dip-slip faults with generally east-west trends are the main faults in this area. North and south of Crane Creek Reservoir, south-dipping faults form discontinuous parallel east-west structural breaks. Faults with this trend also form the eastern boundary of the Pine Creek graben where it meets the Indian Valley trough.

Faults within the Indian Valley trough are irregularly distributed, less abundant, and have less displacement than in the surrounding regions. In part, this reflects the higher concentration of late Cenozoic, relatively unconsolidated sediments overlying the Columbia River basalt in that area.

Minor flexures in the Indian Valley trough can be seen where the basalt is not covered by younger sediments. For example, Granger Butte, near the east side of the trough, is a doubly plunging anticline that formed when Grande Ronde Basalt was weakly folded along a north-northeast axis; this structure has about 150 meters of relief.

LATE CENOZOIC GEOLOGIC HISTORY

The evolution of structures formed since Imnaha time (16 million years ago) in the Weiser embayment has been fairly well established from field relationships between basalt units, sedimentary units, fault displacements, and stream patterns. The important events are summarized below in chronologic order.

(1) A youthful to mature topography with a relief exceeding 1,500 meters existed in west-central Idaho in Miocene time. Higher elevations existed near the Idaho-Oregon border where the present-day Seven Devils Mountains, Peck Mountain, Cuddy Mountain, and Sturgill Peak occur. The bedrock in this area consisted mostly of Seven Devils metavolcanic units and younger Mesozoic intrusive bodies. The area had achieved its topographic relief by structural uplift. The general elevations also were higher to the east in central Idaho where the Idaho batholith and metamorphic rocks were exposed in the ancestral Salmon River Mountains.

(2) The eruption of Imnaha Basalt began in eastern Oregon and in Idaho near the present-day Snake River canyon during the R_0 magnetostratigraphic epoch. At least twenty-five Imnaha flows, totaling more than 700 meters, had spread eastward into Idaho by the end of N_0 time. Extrusion of Imnaha flows may have continued into the paleomagnetic transition at the beginning of R_1 time. When the Imnaha eruptions stopped, basalt had spread as far southeast as Horseshoe Bend, as far east as Council Mountain, and had joined the Clearwater embayment on the north. This basalt field probably defined the eastern and northern margin of the ancestral drainage basin for Miocene streams flowing westward from the Salmon River Mountains. Imnaha Basalt also probably flowed southward into the present-day western Snake River Plain toward the ancestral Owyhee Mountains in southwestern Idaho.

(3) Eruption of Grande Ronde Basalt began in R_1 time in Oregon and Washington. Major accumulations formed north and northwest of the Weiser embayment during the R_1 and N_1 magnetostratigraphic intervals. During R_1 and N_1 time the initial Weiser embayment underlain by Imnaha Basalt appears to have been tilted slightly downward to the northwest, perhaps by the initial regional basining toward the center of the Columbia Plateau. Several reverse and locally a few normal flows, probably of the R_1 and N_1

magnetostratigraphic epochs, spread into and across the embayment from the west or northwest or both, to as far south as Squaw Butte and as far east as Long Valley. The thickest Grande Ronde accumulations of up to 200 meters were in the northwest, and the sequence thinned and wedged out to the south and east. This southeasterly thinning may have been partly or entirely due to the basining of the Columbia Plateau to the northwest, or partly or entirely due to the primary dip effects of the southeastward-spreading Grande Ronde flows.

During this same interval a local minor eruption of lava may have occurred within the embayment, as suggested by the position of the sparsely phyric unit of Cuddy Mountain basalt, possibly beneath Grande Ronde flows on the southwestern margin of Cuddy Mountain.

(4) Grande Ronde Basalt eruptions continued during the R_2 and N_2 magnetostratigraphic epochs with most, if not all, of the basalt accumulating to the north and northwest as regional westward tilting and central plateau basining continued.

(5) Following Grande Ronde Basalt accumulation within the Weiser embayment, major deformation of the embayment surface began with incipient expression of the Sturgill Peak anticline, the Indian Valley trough, probably the Rock Creek syncline, and the regional southward homoclinal tilting southward from the Seven Devils. Streams from the Salmon River Mountains carried basement-derived sediments onto the embayment margin and into slightly subsiding areas south of the Seven Devils. Mixing of basalt detritus from the incipient Seven Devils homocline with prebasalt detritus from the east led to the deposition of heterolithologic conglomerates on the Grande Ronde Basalt in the Indian Valley trough southward from near Mesa, and on the Imnaha Basalt near Big Willow Creek. Consequent drainages, such as the Weiser River, flowed southward as they developed on the embayment surface down the incipient Seven Devils homocline. The interplay between accumulating sediments and shallow structures controlled many stream courses in the lowlands during this interval. The Weiser River may have been displaced westward and was constrained to flow along the base of the east flank of the growing Sturgill Peak anticline by post-Grande Ronde Indian Valley conglomeratic fill from the east.

(6) Activation and reactivation of faulting along the preexisting Long Valley and Snake River systems followed formation of the trough and fold structures; this probably was concurrent with regional tilting and continued movement of the local warps. Most of the present-day fault blocks in the area began to show topographic expression prior to Weiser Basalt extrusion. The north-south aligned drainages controlled by the Long Valley fault system developed during this early fault-block movement. This event diverted much of the easterly derived detritus from the embayment interior.

(7) Eruption of Weiser Basalt flows and pyroclastic deposits commenced as locally derived sediments continued to accumulate within the Indian Valley trough. The concentration of eruptive conduits for the Weiser Basalt within the Paddock Valley fault system suggest that this fault system, as well as the associated northeastern margin of the Snake River Plain, was active by the time of Weiser Basalt volcanism. Structural uplifts, such as the Squaw Butte fault block, the Sturgill Peak anticline (or "domal" block), and the Seven Devils homocline had developed sufficiently by then to confine the Weiser Basalt and associated sediments to the present-day lowlands. One possible exception is the phyric type of the basalt of Cuddy Mountain which occurs on the east flank of Cuddy Mountain near Pyramid Point. Its occurrence on an uplifted block within the Paddock Valley fault system permits interpretations of local extrusion of basalt on an upland area, or of posteruption uplift.

The Weiser Basalt initially extended eastward to the margin of the Long Valley fault system, northward to the base of the Seven Devils homocline south of Mesa, northwestward as if wrapped around the southeast-plunging Sturgill Peak anticline, and westward to the general area of the Rock Creek syncline. Distinctive local units accumulated at Black Canyon south of Squaw Butte and possibly at Cuddy Mountain. Angular relationships between all Weiser Basalt units and the underlying Grande Ronde and Imnaha Basalt units document interformational structural movement. Continued movement during this time is suggested by the distribution patterns of the individual Weiser Basalt members. During this period consequent streams, such as Crane Creek and Rock Creek, began to drain local basins, and the Weiser River made a midsegment course change near the northern margin of the Weiser Basalt.

(8) Structural growth of present-day features continued following the eruption of the Weiser Basalt. A new cycle of stream development began as basins and uplands became more pronounced. Continued movement of the Paddock Valley fault system left the Weiser River in an antecedent position across structural features, such as the Cambridge fault, while its tributaries developed in consequent and subsequent positions, as in the up-dip Pine Creek graben. Crane Creek, developing primarily in post-Weiser Basalt time from runoff gathered in the Indian Valley trough, became incised across the developing step-fault blocks of the Paddock Valley fault system. Weiser Basalt units near Mann Creek Reservoir were

slightly uplifted as the Sturgill Peak block and anticline continued to rise. This is indicated by the incision of the Weiser River course across the Sturgill Peak anticline and adjacent Weiser Basalt units southeast of Shoe Peg Valley.

(9) Development of the present-day topography and structures formed primarily by continued movement of the major faults, by the development of subsequent streams along fault zones, and by the development of consequent streams on dip slopes and in depressions. A thick accumulation of Idaho Formation sediments was deposited along the southern margin of the embayment and similar sediments partially filled fault-block troughs of the Long Valley fault system. The basement-derived arkosic composition of these sediments suggests that the drainage system and structural controls at the eastern margin of the embayment were well developed by the Pliocene, so that most post-Miocene structural activity was a continuation of an already established pattern.

ACKNOWLEDGMENTS

This research was supported principally by a Northwest College and University Association for Science (NORCUS—University of Washington) grant under contract E4-76-5-06-225 with the U. S. Department of Energy. For this assistance and for that provided by Rockwell Hanford Operations in the form of field equipment, materials, geochemical analyses, and a vehicle, a very sincere thank you is due.

Acknowledgments and thanks are also given to numerous geologists and personnel active in the discipline of basalt stratigraphy. Many are currently with the Idaho Bureau of Mines and Geology and the University of Idaho, Moscow, Idaho; with Washington State University, Pullman, Washington; with the U. S. Geological Survey at Denver, Colorado, and Menlo Park, California; and with Rockwell Hanford Operations at Richland, Washington.

REFERENCES

Anderson, A. L., 1934, Geology of the Pearl-Horseshoe Bend gold belt, Idaho: Idaho Bureau of Mines and Geology Pamphlet 41, 36 p.

Bingham, J. W. and K. L. Walters, 1965, Stratigraphy of the upper part of the Yakima Basalt in Whitman and eastern Franklin Counties, Washington: U. S. Geological Survey Professional Paper 525-C, p. C87-C90.

Bishop, D. T., 1969, Stratigraphy and distribution of basalt, Benewah County, Idaho: Idaho Bureau of Mines and Geology Pamphlet 140, 22 p.

Bond, J. G., 1963, Geology of the Clearwater embayment: Idaho Bureau of Mines and Geology Pamphlet 128, 83 p.

———, 1978, Geologic map of Idaho: Idaho Bureau of Mines and Geology, scale 1:500,000.

Breeser, P. J., 1972, General geology and highway realignment considerations in the Pinehurst-New Meadows-Tamarack area, west-central Idaho: University of Idaho M.S. thesis, 103 p.

Brock, M. R. and M. J. Grolier, 1973, Chemical analyses of 305 basalt samples from the Columbia River Plateau, Washington, Oregon, and Idaho: U. S. Geological Survey Open-File Report 73-33, 35 p.

Brooks, H. C. and T. L. Vallier, 1967, Progress report of the geology of part of the Snake River canyon, Oregon and Idaho: The Ore Bin, v. 29, no. 12, p. 233-266.

Camp, V. E., 1981, Geologic studies of the Columbia Plateau: Part II. Upper Miocene basalt distribution, reflecting source locations, tectonism, and drainage history in the Clearwater embayment, Idaho: Geological Society of America Bulletin, v. 92, p. 669-678.

Camp, V. E. and P. R. Hooper, 1981, Geologic studies of the Columbia Plateau: Part I. Late Cenozoic evolution of the southeast part of the Columbia Plateau basalt province: Geological Society of America Bulletin, v. 92, p. 659-668.

Camp, V. E., P. R. Hooper, D. A. Swanson, and T. L. Wright, 1982, Columbia River basalt in Idaho: physical and chemical characteristics, flow distribution, and tectonic implications, *in* Bill Bonnichsen and R. M. Breckenridge, editors, Cenozoic Geology of Idaho: Idaho Bureau of Mines and Geology Bulletin 26.

Capps, S. R., 1941, Faulting in western Idaho—its relation to the higher placer deposits: Idaho Bureau of Mines and Geology Pamphlet 56, 20 p.

Cook, E. F., 1954, Mining geology of the Seven Devils region: Idaho Bureau of Mines and Geology Pamphlet 97, 22 p.

Fankhauser, R. E., 1968, Geology and mineralization of the southern Cuddy Mountains, Washington County, Idaho: Oregon State University M.S. thesis, 138 p.

Fitzgerald, J. F., 1979, An examination of two vents in the Columbia River basalts, Weiser embayment, Idaho (abstract): Geological Society of America, Abstracts with Programs, Rocky Mountain Section, 32nd Annual Meeting, v. 11, no. 6., p. 272.

———, 1980, A possible new unit in the Columbia River basalts, Weiser embayment, Idaho (abstract):

Northwest Science Program and Abstracts, 53rd Annual Meeting, University of Idaho, Moscow, Idaho, p. 33.

———, 1982, Geology and basalt stratigraphy of the Weiser embayment, west-central Idaho: Rockwell Hanford Operations RHO-BWI-SA-217p.

Gaston, M. P. and E. H. Bennett, 1979, Geologic map of the Grangeville quadrangle, Idaho: Idaho Bureau of Mines and Geology Geologic Map Series (2° quadrangle), scale 1:250,000.

Grolier, M. J., 1965, Geology of part of the Big Bend area in the Columbia Plateau, Washington: Johns Hopkins University Ph.D. dissertation.

Hamilton, Warren, 1962, Late Cenozoic structure of west-central Idaho: Geological Society of America Bulletin, v. 73, p. 511-515.

Hooper, P. R., 1982, The Columbia River basalts: Science, v. 215, p. 1463-1468.

Hooper, P. R., S. P. Reidel, J. C. Brown, G. S. Holden, W. D. Kleck, C. E. Sundstrum, and T. L. Taylor, 1976, Major element analysis of Columbia River basalt, part I: Open-File Report (revised 1981), Basalt Research Group, Washington State University, 59 p.

Hoover, L., 1968, Geologic map in the Tamarack-Cambridge area along U. S.Highway 95, Idaho: unpublished manuscript for the Idaho Department of Highways.

Juras, D. S., 1973, Pre-Miocene geology of the northwest part of Old's Ferry quadrangle, Washington County, Idaho: University of Idaho M.S. thesis, 82 p.

King, J. R., 1971, The geology of the southeastern Cuddy Mountain district, Idaho: Oregon State University M.S. thesis, 78 p.

Kirkham, V. R. D., 1928, Brief papers on geologic field work in Idaho during 1927: Idaho Bureau of Mines and Geology Pamphlet 29, 15 p.

———, 1930, Old erosion surfaces in southwestern Idaho: Journal of Geology, v. 38, p. 652-653.

———, 1931, Revision of the Payette and Idaho Formations: Journal of Geology, v. 39, no. 3, p. 193-239.

Lefebvre, R. H., 1970, Columbia River basalts of the Grande Coulee area, *in* E. H. Gilmour and D. Stradling, editors, Proceedings of the Second Columbia River Basalt Symposium: Eastern Washington State College Press, Cheney, Washington, p. 1-38.

Lindgren, Waldemar, 1898, The mining districts of the Idaho Basin and the Boise Ridge, Idaho: U. S. Geological Survey 18th Annual Report, part III, p. 617-736.

Mackin, J. H., 1961, A stratigraphic section in the Yakima Basalt and the Ellensburg Formation in south-central Washington: Report of Investigation No. 19, Washington Division of Mines and Geology, 45 p.

McIntyre, D. H., 1976a, Photogeologic map of the Cambridge quadrangle and western half of the Council quadrangle, western Idaho: U. S. Geological Survey Open-File Report 76-857, scale 1:62,500.

———, 1976b, Reconnaissance geologic map of the Weiser geothermal area, Washington County, Idaho: U. S. Geological Survey Miscellaneous Field Studies Map MF-745, scale 1:62,500.

McKee, E. H., P. R. Hooper, and W. D. Kleck, 1981, Age of Imnaha Basalt—oldest basalt flows of the Columbia River Basalt Group, northwest United States: Isochron West, no. 31, p. 31-33.

Mitchell, V. E. and E. H. Bennett, 1979a, Geologic map of the Baker quadrangle, Idaho: Idaho Bureau of Mines and Geology Geologic Map Series (2° quadrangle), scale 1:250,000.

———, 1979b, Geologic map of the Boise quadrangle, Idaho: Idaho Bureau of Mines and Geology Geologic Map Series (2° quadrangle), scale 1:250,000.

Myers, C. W. and others, 1979, Geologic studies of the Columbia Plateau, a status report: Rockwell Hanford Operations, RHO-BWI-ST-4, Richland, Washington.

Nakai, T. S., 1979, Stratigraphy of the Payette Formation, Washington County, Idaho: University of Idaho M.S. thesis, 187 p.

Newcomb, R. C., 1970, Tectonic structure of the main part of the basalt of the Columbia River Group, Washington, Oregon and Idaho: U. S. Geological Survey Miscellaneous Geologic Investigations Map I-587, scale 1:500,000.

Paris, Gabriel, 1969, Geology of the east-central part of Mineral quadrangle, Washington County, Idaho: University of Idaho M.S. thesis, 106 p.

Reidel, S. P., 1982, Stratigraphy of the Grande Ronde Basalt, Columbia River Basalt Group, from the lower Salmon River and northern Hells Canyon area, Idaho, Oregon, and Washington, *in* Bill Bonnichsen and R. M. Breckenridge, editors, Cenozoic Geology of Idaho: Idaho Bureau of Mines and Geology Bulletin 26.

Reidel, S. P., V. E. Camp, and M. E. Ross, 1981, Major element analysis of Columbia River basalt, part II: Open-File Report, Basalt Research Group, Washington State University, 90 p.

Russell, I. C., 1893, Geologic reconnaissance in central Washington: U. S. Geological Survey Bulletin 108, 108 p.

———, 1901, Geology and water resources of Nez Perce County, Idaho: U. S. Geological Survey Water-Supply Papers 53 and 54, 141 p.

Savage, C. N., 1958, Geology and mineral resources of Ada and Canyon Counties: Idaho Bureau of Mines and Geology County Report 3, 94 p.

———, 1961, Geology and mineral resources of Gem and Payette Counties: Idaho Bureau of Mines and Geology County Report 4, 50 p.

Schmincke, H. V., 1967, Flow directions in Columbia River basalt flows and paleocurrents of interbedded sedimentary rocks, south-central Washington: Geologische Rundschau, v. 56, p. 992-1020.

Shah, S. M. I., 1966, Stratigraphy and paleobotany of the Weiser area, Idaho: University of Idaho M.S. thesis, 191 p.

———, 1968, Stratigraphic paleobotany of the Weiser area, Idaho: University of Idaho Ph.D. dissertation, 189 p.

Skurla, S. J., 1974, Geology of the Sturgill Peak area, Washington County, Idaho: Oregon State University M.S. thesis, 98 p.

Slater, M. N., 1969, Geology and mineral deposits of the western Cuddy Mountain district, western Idaho: Oregon State University M.S. thesis.

Smith, G. O., 1901, Geology and water resources of a portion of Yakima County, Washington: U. S. Geological Survey Water-Supply Paper 55, p. 68.

Strowd, William, 1978, Bibliography of geologic studies, Columbia Plateau (Columbia River basalt) and adjacent areas in Idaho: Rockwell Hanford Operations, RHO-BWI-C-44, 204 p.

Swanson, D. A., 1967, Yakima basalt of the Tieton River area, south-central Washington: Geological Society of America Bulletin, v. 78, p. 1077-1110.

Swanson, D. A., J. L. Anderson, R. D. Bentley, G. R. Byerly, V. E. Camp, J. N. Gardner, and T. L. Wright, 1979a, Reconnaissance geologic map of the Columbia River Basalt Group in eastern Washington and northern Idaho: U. S. Geological Survey Open-File Report 79-1363, scale 1:250,000.

Swanson, D. A., J. L. Anderson, V. E. Camp, P. R. Hooper, W. H. Taubeneck, and T. L. Wright, 1981, Reconnaissance geologic map of the Columbia River Basalt Group, northern Oregon and western Idaho: U. S. Geological Survey Open-File Report 81-797, scale 1:250,000.

Swanson, D. A., T. L. Wright, P. R. Hooper, and R. D. Bentley, 1979b, Revisions in stratigraphic nomenclature of the Columbia River Basalt Group: U. S. Geological Survey Bulletin 1457-G, 59 p.

Vallier, T. L., 1977, The Permian and Triassic Seven Devils Group, western Idaho and northeastern Oregon: U. S. Geological Survey Bulletin 1437, 58 p.

Vallier, T. L. and P. R. Hooper, 1976, Geologic guide to Hells Canyon, Snake River: Geological Society of America, Cordilleran Section Meeting, Field Trip Guide No. 5, Pullman, Washington, 38 p.

Waters, A. C., 1961, Stratigraphic and lithologic variations in the Columbia River basalts: American Journal of Science, v. 259, p. 583-611.

Watkins, N. D. and A. K. Baksi, 1974, Magnetostratigraphy and oroclinal folding of the Columbia River, Steens and Owyhee basalts in Oregon, Washington and Idaho: American Journal of Science, v. 274, p. 148.

Wright, T. L., M. J. Grolier, and D. A. Swanson, 1973, Chemical variations related to the stratigraphy of the Columbia River basalt: Geological Society of America Bulletin, v. 84, p. 371-386.

Young, H. W. and R. I. Whitehead, 1975, Geothermal investigations in Idaho, Part 3, an evaluation of thermal water in the Weiser area, Idaho: Idaho Department of Water Resources Information Bulletin 30, 35 p.

Structural Model for the Columbia River Basalt Near Riggins, Idaho

by

P. R. Hooper[1]

ABSTRACT

Imnaha Basalt and Grande Ronde Basalt (R_1) of the Columbia River Basalt Group form a small synclinal basin immediately west of Riggins, Idaho. The displacement of the margins of the basalt outcrop, of the synclinal axis, and of a dike of Saddle Mountains(?) Basalt define a pattern best explained by a model of west-northwest to east-southeast and north-northwest to south-southeast dextral strike-slip faults and east-northeast to west-southwest sinistral strike-slip faults. The development of the syncline, downthrow on the east side of the easterly dipping Riggins fault, and the strike-slip displacement are regarded as broadly contemporaneous. Regional implications of significant west-northwest strike-slip movement in the Riggins area and the possible displacement of the Columbia River dike swarm by such a movement farther west is noted.

INTRODUCTION

The Riggins 30-minute quadrangle includes parts of the western margin of the Idaho batholith and the eastern edge of the Columbia River basalt province, as mapped and described by Hamilton (1962, 1963a, 1963b, 1969, 1976; Onasch, 1977). The marginal facies of the batholith include the Riggins Group, a highly metamorphosed and sheared sequence, thrust westward over the Seven Devils Group on the Rapid River thrust (Hamilton, 1963a). The Seven Devils Group is an island arc assemblage of Permian-Triassic age thought to have been accreted to the North American Plate in late Permian to Cretaceous time (Hamilton, 1976; Davis and others, 1978). In the Riggins area the suture zone between the accreted island arc and the earlier western boundary of the North American Plate corresponds to a broad synformal trough that extends from the Clearwater embayment in the north through Meadows Valley and the Payette Valley to the south. Isolated outcrops of Columbia River basalt are exposed in this trough between the Clearwater and Weiser embayments (see Figure 1 in Camp and others, 1982 this volume).

Reconnaissance mapping of the small areas of basalt near Riggins, undertaken by the writer during 1980, was designed to locate the stratigraphic divisions of the Columbia River basalt recognized in the main part of the Columbia Plateau (Swanson and others, 1979). The most obvious stratigraphic horizon in the Riggins area is the contact between the coarsely phyric Imnaha Basalt and the overlying aphyric flows of the Grande Ronde Basalt. The contact is easily traced across the area west of Riggins (Figure 1). Whereas the present work is significantly less comprehensive than that of Hamilton, mapping the contact has made it possible to clarify the type and sequence of deformation which has affected the basalt in the last 17 million years.

STRATIGRAPHY AND STRUCTURE

Two main outcrops of basalt are present (Hamilton, 1969). The slightly larger outcrop occurs along the bottom and sides of the Little Salmon River canyon, 3 to 35 kilometers south of Riggins. This is composed almost entirely of Imnaha Basalt (Ti) with one or two flows of Grande Ronde Basalt (Tgr_1) forming only the highest exposures west of the canyon. The smaller basalt outcrop, the subject of this paper, lies immediately west of Riggins (Figure 1) and is some 17 kilometers long from north to south and 8 kilometers wide. It includes 500 meters of Imnaha Basalt (Ti) conformably overlain by 335 meters of Grande Ronde Basalt of the oldest magne-

[1]Department of Geology, Washington State University, Pullman, Washington 99164.

Hooper, P. R., 1982, Structural model for the Columbia River basalt near Riggins, Idaho, *in* Bill Bonnichsen and R. M. Breckenridge, editors, Cenozoic Geology of Idaho: Idaho Bureau of Mines and Geology Bulletin 26, p. 129-136.

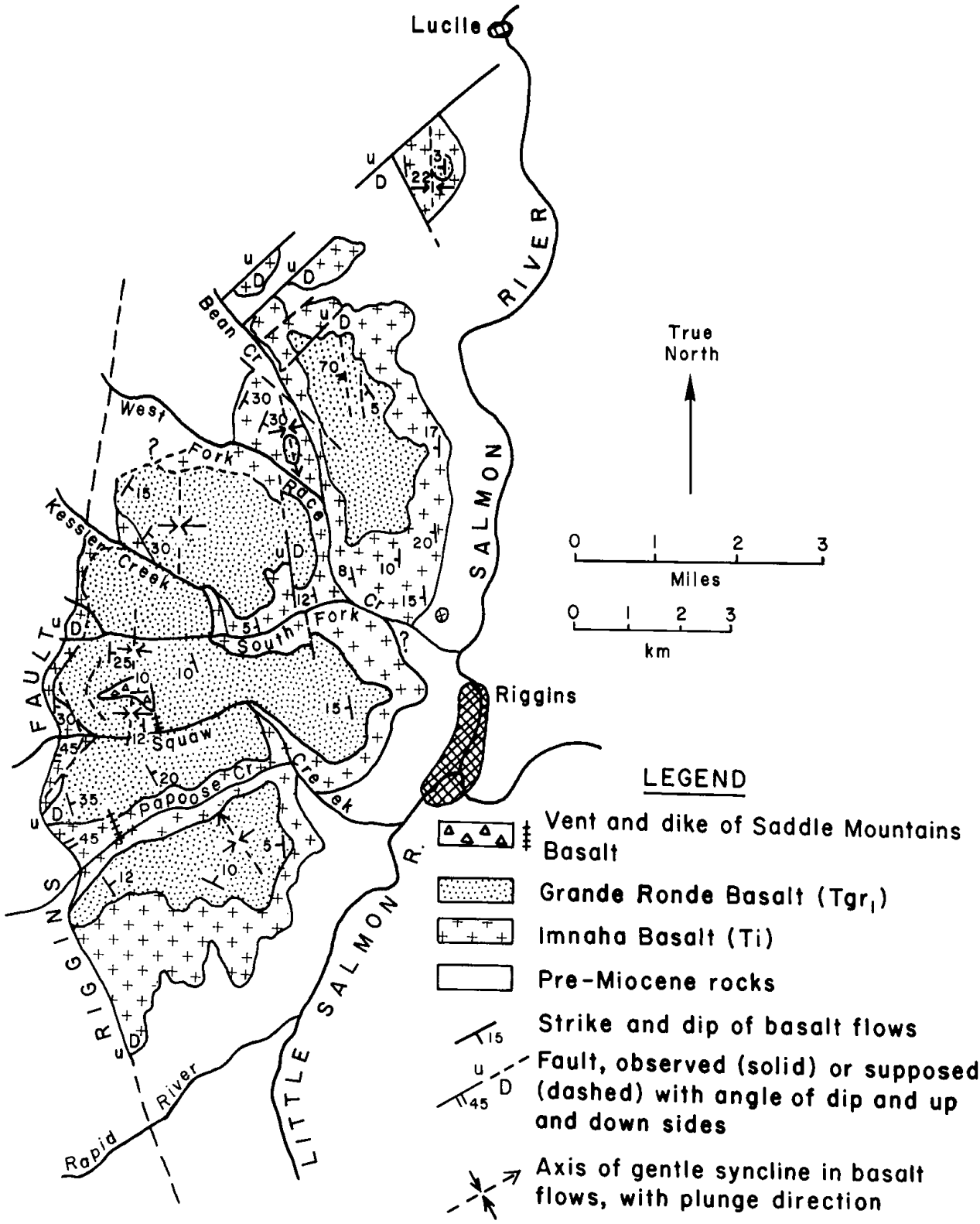

Figure 1. Geologic map of the Columbia River basalt near Riggins, Idaho.

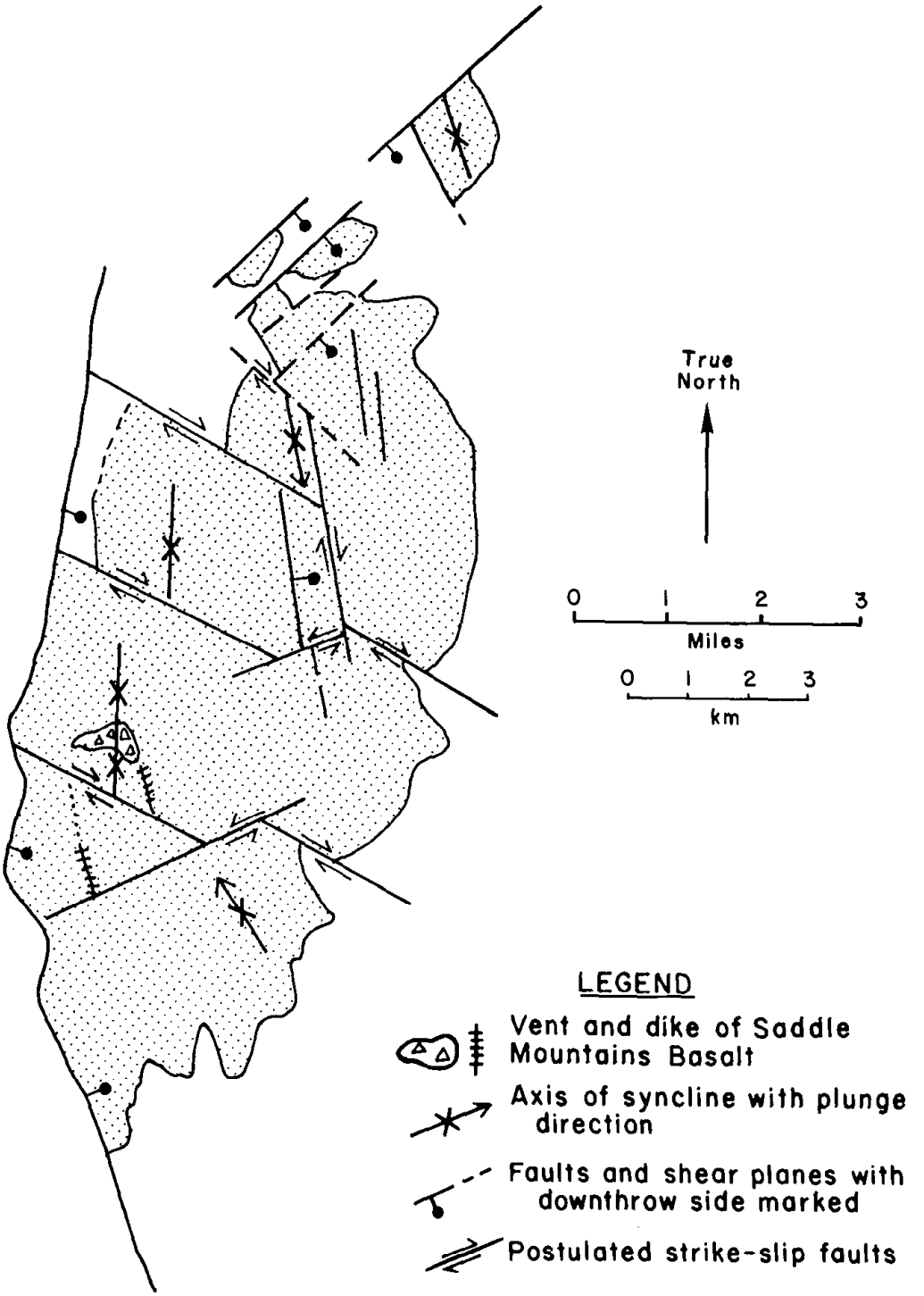

Figure 2. Structural model of the Columbia River basalt near Riggins, Idaho.

tic unit (Tgr_1; see Swanson and others, 1979, for full Columbia River Basalt Group stratigraphy).

At least thirteen individual flows of Imnaha Basalt are present in this outcrop. All but the lowest one have been correlated with flow types recognized in the Snake, Imnaha, and lower Salmon River canyons (Hooper and others, 1979; Hooper and others, in preparation), and they lie in the same stratigraphic sequence (Table 1). The easily recognizable highest flows in the type Imnaha Basalt area, however, the Fall Creek, Log Creek, and associated American Bar types, are missing from the Riggins area.

The contact between Imnaha and Grande Ronde Basalts is recognizable in the field, and its disposition clarifies the structural history. The flows form a gentle synclinal basin elongated north-south. They consistently dip inward from the contact with the surrounding pre-Tertiary metamorphic rocks. The dip increases as the contact is approached (Figure 1), and small sympathetic normal faults commonly occur near the contact. On the east side, the base of the basalt sequence is clearly unconformable; the lava appears to have filled a deep valley, and younger flows overlap the valley side to the east. The west side of the basalt outcrop is bounded by the

Table 1. Major element analyses of Columbia River basalt west of Riggins, Idaho. (Analyses by XRF, normalized on a weight percent volatile-free basis with Fe_2O_3 set at 2.00%).

	SiO_2	Al_2O_3	TiO_2	Fe_2O_3	FeO	MnO	CaO	MgO	K_2O	Na_2O	P_2O_5	Comments
I. Saddle Mountains vent, flow and dike (Squaw Peak)												
PH80037	49.63	14.90	2.37	2.00	10.29	0.20	10.54	6.96	0.52	2.09	0.49	dike[1]
PH80041	48.86	14.61	2.59	2.00	10.26	0.20	10.95	6.94	0.62	2.41	0.55	flow
PH80044	50.32	15.02	2.36	2.00	10.11	0.20	10.07	6.56	0.60	2.28	0.48	dike[2]
II. Typical Grande Ronde Basalt flows (Tgr_1)												
PH80003	55.20	14.93	1.73	2.00	9.41	0.21	7.72	4.25	1.38	2.94	0.23	
PH80004	54.53	14.53	2.31	2.00	10.80	0.21	6.98	3.44	1.84	3.00	0.37	
PH80005	54.27	14.60	2.39	2.00	10.50	0.21	7.54	3.55	1.59	2.96	0.38	
III. Lowest Grande Ronde Basalt flow (?Grave Creek flow)												
PH80026	52.99	15.05	2.24	2.00	10.13	0.21	8.58	4.80	0.98	2.70	0.33	
PH80006	53.29	15.09	2.28	2.00	10.47	0.21	8.09	4.31	1.05	2.84	0.36	
PH80036	53.31	14.95	2.24	2.00	10.06	0.21	8.41	4.65	1.05	2.77	0.34	
IV. Imnaha Basalt flows in stratigraphic sequence												
PH80 024[3] 025	51.13	14.75	3.04	2.00	11.64	0.22	8.39	4.57	1.02	2.85	0.43	AB-7[4] top
PH80 020 023	49.30	16.42	2.69	2.00	10.95	0.18	9.50	5.50	0.85	2.60	0.36	RC-1
PH80019	52.62	14.89	2.58	2.00	10.43	0.21	8.76	4.61	0.70	2.82	0.38	AB-5
PH80 017 018	52.11	16.13	1.91	2.00	9.50	0.20	9.80	4.80	0.45	2.77	0.29	AB-3/4
PH80 014 016	51.65	15.50	1.62	2.00	9.55	0.21	10.35	5.80	0.26	2.71	0.21	AB-2
PH80013	48.85	14.11	1.56	2.00	8.82	0.28	14.11	4.80	1.39	3.67	0.42	? bottom

[1] Squaw Creek
[2] Papoose Creek
[3] average analysis of sample numbers given
[4] flow types from P. R. Hooper, W. D. Kleck, C. R. Knowles, and S. P. Reidel, in preparation

Riggins fault (Hamilton, 1969) which has been traced north to Whitebird and has a downthrow to the east of over 600 meters (Hooper, in Swanson and others, 1981). In the Riggins area the fault plane dips to the east at angles as low as 45 degrees and is accompanied by many parallel faults within the basalt which juxtapose Imnaha Basalt against Grande Ronde Basalt in many places. The easterly dip of the flows increases to as much as 35 degrees as the Riggins fault is approached, at which point the less competent flow tops are sometimes used as small fault planes.

The whole basalt outcrop is cut by small faults, and the systematic orientation of the creeks suggests many more. Observed faults include a set of northeast-southwest faults in the north part of the outcrop at the head of Bean Creek (Figure 1). Vertical displacement with downthrow to the southeast is evident. Vertical cliffs form the east side of the ridge between Bean Creek and the Salmon River canyon and result from major N. 10° W.-trending planes of shattered rock, apparently dipping west at about 70 degrees. No displacement along the zones was observed. Another fault of similar trend near the middle of the basalt outcrop shows significant vertical displacement with the downthrow to the east, and a part of Race Creek follows the same trend (Figure 1). Less direct evidence of faulting can be found in the stepped nature of the northwest and southeast boundaries of the basalt outcrop and in the apparent displacement of the axis of the syncline and of a well-defined dike (Figure 2). In many places, these apparent displacements lie along west-northwest to east-southeast-trending valleys, and all suggest dextral strike-slip movement. Another dominant drainage direction has an east-northeast to west-southwest trend.

Hamilton's map (1969) shows three sharp steps in the northwest part of the basalt boundary with 90 degree reentrant angles occurring across Kessler Creek, West Fork of Race Creek, and Bean Creek. Whereas exposures are notably poor in the critical areas and more detailed work is required to draw the contact precisely, the writer's current mapping has confirmed this unusual form. The most obvious explanation is a set of faults with west-northwest trends parallel to the valleys along which a component of dextral strike-slip movement has occurred. Evidence in support of this explanation can be found in the displacement of the axis of the syncline (Figure 1). Hamilton (1969) drew this axis as a sinuous line, and because the syncline is a shallow one, the exact position of the axis is not easy to define. Nevertheless, it is quite clear in the field that the axis is offset across the West Fork of Race Creek and Kessler Creek and that the size of the offset is approximately that required to displace the basalt contact by dextral strike-slip (Figure 2).

Additional evidence of dextral strike-slip movement occurs further south between Squaw Creek and Papoose Creek. A prominent peak, the Squaw triangulation station on the north side of Squaw Creek, is a deeply dissected volcanic vent composed predominantly of pyroclastic and lahar materials dipping and thinning away from a central point capped by a thin lava flow. A roadcut in Squaw Creek below the vent reveals a wide dike with prominent and unusual cooling joints (Figure 3). Chemical analyses of the flow and the dike reveal a similar chemical composition which is distinguishable from either Imnaha or Grande Ronde chemical types (Table 1). The vent is later than the Grande Ronde Basalt on which it stands and appears to lie on or near the axis of the basalt syncline. Its chemical composition most closely resembles that of the Sprague Lake and Lewiston Orchards flow of northeast Washington (Wright and others, 1980).

Another dike outcrop of similar width, vertical dip, petrography, and chemical composition and with the same unusual joint pattern occurs on the north side of Papoose Creek. No other dike of the Columbia River Basalt Group has been observed in this area, and the evidence strongly suggests that they are two parts of the same feeder dike. As the two exposures are clearly not on trend, the explanation must lie in en echelon emplacement or in the presence of a dextral strike-slip fault. Of the many dikes of Columbia River basalt this writer has mapped, only a few display en echelon emplacement, in which the separation is a few meters at most. Thus, it is probable that a plane of strike-slip movement of between 1 and 2 kilometers is present. Topographic expression of such a fault plane is not obvious; however, a west-northwest line connecting local evidence of faulting west of Squaw Peak and passing through saddles in the ridge between Squaw and Papoose Creeks may be the trace of the fault. In this southern part of the basalt outcrop the predominant drainage trend is east-northeast to west-southwest (upper Squaw Creek and Papoose Creek); the synclinal axis is displaced to the east along this drainage, and on the south side it plunges gently northward from the southern contact (Figure 1). A plausible but as yet unverified model to account for these trends and displacements includes a second set of strike-slip faults with sinistral displacement in the east-northeast to west-southwest direction (Figure 2).

A significant obstacle to a model including a set of major west-northwest to east-southeast dextral strike-slip faults is the obvious failure of the faults to cross

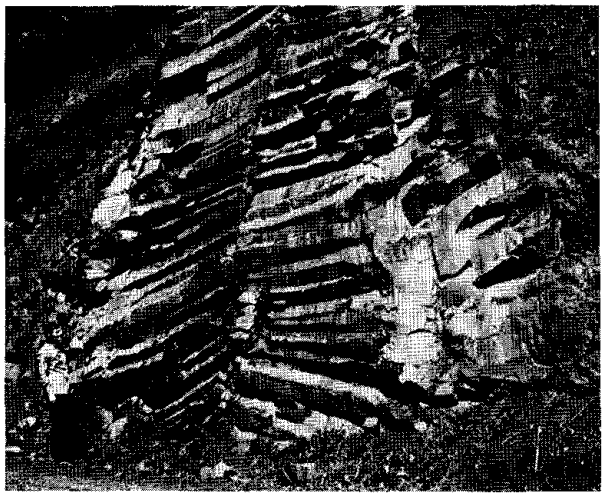

Figure 3. Photograph of Saddle Mountains Basalt dike feeding the Squaw vent.

the entire basalt outcrop. The West Fork of Race Creek, Kessler Creek, and indeed both upper Squaw Creek and Papoose Creek are sharply truncated at their eastern ends by a north-northwest-trending valley (Figure 1), to the east of which the west-northwest to east-southeast trend is not present. The lower reaches of both Race Creek and Squaw Creek do, however, display a west-northwest to east-southeast orientation with evidence of dextral strike-slip displacement of the basalt contact (Figure 1). Clearly, if these are the same dextral strike-slip faults that displace the northwest basalt contact, they must themselves have been displaced by strike-slip movement either along the north-northwest trend (dextral) or along the east-northeast to west-southwest trend (sinistral). On the evidence available from this reconnaissance field work, no unique solution is possible. One model is suggested in Figure 2 in which the syncline formed first and was followed by the Saddle Mountains Basalt vent along its axis and then by the west-northwest to east-southeast dextral strike-slip faults that were later displaced by both the north-northwest to south-southeast and east-northeast to west-southwest strike-slip movements. The normal, approximately north-south, Riggins fault was the last event. Such a time sequence is probably misleading. For example, there is almost certainly some association between the development of the syncline and the uplift along the Riggins fault, which clearly increased the dip on the western limb of the syncline. It also seems inevitable that, in a deformation pattern such as illustrated in Figure 2, the movement in one plane must be accompanied by movement in the other planes, resulting in an overall east-west extension and north-south shortening. The apparent time sequence most probably represents the order of the most recent movements in each direction.

DISCUSSION

The north-south suture zone along the western margin of the Idaho batholith has been tectonically active in the last 17 million years. The Stites basin, a northern extension of this zone in the Clearwater embayment, was active during early Grande Ronde Basalt eruption (Camp, 1981), and the thickness of both Imnaha and lower Grande Ronde (Tgr_1) Basalt units near Riggins suggests that this area was already a topographic low separating the batholith from the Seven Devils Mountains at the time of their eruption. Since Grande Ronde time, both the Seven Devils Mountains and the Nez Perce plateau on the west have risen relative to the suture zone primarily by vertical movement along the Riggins fault (Camp and Hooper, 1981). The north-south syncline displayed by the basalt near Riggins is probably a result of the drag caused by this movement.

The deformation model proposed (Figure 2) to explain the present features of the basalt involves west-northwest to east-southeast dextral, east-northeast to west-southwest sinistral, and north-northwest to south-southeast dextral strike-slip movement. Of these, the dextral faults appear to show the greatest displacement. The total effect is a shortening in a north-south direction, an extension in the east-west direction, and a distortion of an originally north-south or north-northwest to south-southeast long axis of the outcrop into a north-northeast to south-southwest long axis and a possible slight rotation of the synclinal axis in a clockwise direction.

Evidence of strike-slip displacement in the southeast part of the Columbia River basalt province has been presented by Ross (1978), Price and others (1973), and Shubat (1979), but the horizontal disposition of the flows has made it difficult to ascertain the number and significance of such faults in the southeast part of the Columbia Plateau. More recently, dextral strike-slip movement close to the Olympic-Wallowa lineament has been postulated by Farooqui (1980), Kienle and Hamill (1980), and Gehrels and others (1980). Hooper and Camp (1981) have suggested that the Olympic-Wallowa lineament marks a rough boundary separating an area to the southwest, where dextral shear predominates, from an area to the northeast where the shear component is less evident but where north-south shortening and east-west extension have resulted in north-northwest basalt feeder dikes and east-west folds modified

locally by older basement structures. The basalt outcrop west of Riggins provides evidence of an unusually detailed deformation pattern well to the northeast of the eastern extension of the Olympic-Wallowa lineament. It is clear that the structural development of this critical zone needs more detailed study.

The probability of more extensive west-northwest to east-southeast dextral strike-slip movement in this area than had hitherto been proposed may have some interesting consequences in interpreting the evolution of the Columbia Plateau to the north and west. For example, the concentrations of feeder dikes at the mouth of the Grande Ronde River and at Cornucopia, Oregon, are significantly greater than in adjacent areas. Yet these two concentrations are not on trend with each other. The relatively few dikes in the deeply eroded Imnaha and Snake River canyons make it clear that this is not simply a matter of more dikes occurring in the more deeply dissected areas. Although Taubeneck (1970) and Swanson and others (1979) have emphasized the presence of dikes outside the Grande Ronde and Cornucopia swarms, yet the greater concentration of dikes within these originally named swarms has become increasingly apparent with more detailed mapping. It is interesting to speculate that dextral strike-slip movement within a broad zone that includes the extension of the Olympic-Wallowa lineament, with a cumulative effect of about 35 kilometers (20 miles) of displacement, would place the two areas of maximum dike concentration in line with each other.

ACKNOWLEDGMENTS

I am grateful to V. E. Camp, D. A. Swanson, and C. B. Hole for their helpful reviews of the manuscript. The geologic mapping was undertaken under U. S. Geological Survey/U. S. Department of Energy Interagency Agreement EV-78-1-06-1078. The mapping is part of the regional geologic studies of the Basalt Waste Isolation Project operated by Rockwell Hanford Operations for the U. S. Department of Energy.

REFERENCES

Camp, V. E., 1981, Geologic studies on the Columbia Plateau: Part II, Wanapum and Saddle Mountains volcanism of the Columbia River Basalt Group in the Clearwater embayment of western Idaho: Geological Society of America Bulletin, v. 92, p. 669-678.

Camp, V. E. and P. R. Hooper, 1981, Geologic studies on the Columbia Plateau: Part I, Late Cenozoic evolution of the southeast part of the Columbia River basalt province: Geological Society of America Bulletin, v. 92, p. 659-678.

Camp, V. E., P. R. Hooper, D. A. Swanson, and T. L. Wright, 1982, Columbia River basalt in Idaho: physical and chemical characteristics, flow distribution, and tectonic implications, *in* Bill Bonnichsen and R. M. Breckenridge, editors, Cenozoic Geology of Idaho: Idaho Bureau of Mines and Geology Bulletin 26.

Davis, G. A., J. W. H. Monger, and B. C. Burchfiel, 1978, Mesozoic construction of the Cordilleran "collage," central British Columbia to central California, *in* D. G. Howell and K. A. McDougall, editors, Mesozoic Paleogeography of the Western United States: Society of Economic Paleontologists and Mineralogists, Pacific Section, Pacific Coast Paleogeography Symposium 2, p. 1-32.

Farooqui, S. M., 1980, Analysis of the Wallula fault, Columbia Plateau, southeastern Washington: Geological Society of America, Abstracts with Programs, v. 12, no. 3, p. 106.

Gehrels, G. E., R. R. White, and G. A. Davis, 1980, The La Grande pullapart basin, northeastern Oregon: Geological Society of America, Abstracts with Programs, v. 12, no. 3, p. 107.

Hamilton, Warren, 1962, Late Cenozoic structure of west-central Idaho: Geological Society of America Bulletin, v. 73, no. 5, p. 511-516.

———, 1963a, Metamorphism in the Riggins region, western Idaho: U. S. Geological Survey Professional Paper 436, 95 p.

———, 1963b, Columbia River basalt in the Riggins quadrangle, western Idaho: U. S. Geological Survey Bulletin 1141-L, 37 p.

———, 1969, Reconnaissance geological map of the Riggins quadrangle, west-central Idaho: U. S. Geological Survey Map I-579.

———, 1976, Tectonic history of west-central Idaho: Geological Society of America, Abstracts with Programs, v. 8, no. 3, p. 378-379.

Hooper, P. R. and V. E. Camp, 1981, Deformation of the southeast part of the Columbia Plateau: Geology, v. 9, p. 323-328.

Hooper, P. R., C. R. Knowles, and N. D. Watkins, 1979, Magnetostratigraphy of the Imnaha and Grande Ronde Basalts in the southeast part of the Columbia Plateau: American Journal of Science, v. 279, p. 737-754.

Hooper, P. R., W. D. Kleck, C. R. Knowles, and S. P. Reidel, (in preparation), Imnaha Basalt, Columbia River Group.

Kienle, C. F. and N. L. Hamill, 1980, Strike-slip faulting of post-middle Miocene age in the Blue Mountains of NE Oregon: Geological Society of America, Abstracts with Programs, v. 12, no. 3, p. 115.

Onasch, C. M., 1977, Structural evolution of the western margin of the Idaho batholith in the Riggins, Idaho, area: Pennsylvania State University Ph.D. dissertation, 196 p.

Price, W. H., C. R. Knowles, and J. G. Bond, 1973, Columbia River basalt dikes of the Camas Prairie area, Idaho: Geological Society of America, Abstracts with Programs, v. 5, no. 7, p. 773.

Ross, M. E., 1978, Stratigraphy, structure and petrology of the Columbia River basalt in a portion of the Grande Ronde-Blue Mountains area of Oregon and Washington: University of Idaho Ph.D. dissertation, 407 p.

Shubat, M. A., 1979, Stratigraphy, petrochemistry, petrography and structural geology of the Columbia River basalt in the Minam-Wallowa River area, northeast Oregon: Washington State University M.S. thesis, 156 p.

Swanson, D. A., J. L. Anderson, V. E. Camp, P. R. Hooper, W. H. Taubeneck, and T. L. Wright, 1981, Reconnaissance geologic map of the Columbia River Basalt Group, northern Oregon and western Idaho: U. S. Geological Survey Open-File Report 81-797, scale 1:250,000.

Swanson, D. A., T. L. Wright, P. R. Hooper, and R. D. Bentley, 1979, Revisions in stratigraphic nomenclature of the Columbia River Basalt Group: U. S. Geological Survey Bulletin 1457G, 59 p.

Taubeneck, W. H., 1970, Dikes of the Columbia River basalt in northeastern Oregon, western Idaho and southeastern Washington, *in* E. H. Gilmour and Dale Stradling, editors, Proceedings, Second Columbia River Basalt Symposium: Eastern Washington State College Press, p. 73-96.

Wright, T. L., K. N. Black, D. A. Swanson, and T. O'Hearn, 1980, Columbia River basalt: 1978-1979 sample data and chemical analyses: U. S. Geological Survey Open-File Report 80-921, 99 p.

Chapter 3

General Features of the Snake River Plain

Geophysics and Tectonics of the Snake River Plain, Idaho

by

Don R. Mabey[1]

ABSTRACT

Although the regional surface geology of the Snake River Plain in Idaho is well known and many shallow and a few deep holes have been drilled on the plain, major uncertainties remain concerning the structure of the plain. Seismic refraction profiles have revealed that under the plain a thin upper crust overlies a lower crust which is thicker than that under the Basin and Range province to the south. The large Bouguer gravity high over the plain reflects this thin upper crust, but in the central and western plain it also indicates a dense layer at intermediate depth. Superimposed on the gravity high is a low produced by low-density sedimentary and volcanic rocks that partly fill the depression of the plain, which is in approximate isostatic equilibrium with the adjoining highlands. The regional magnetic anomaly over the central and western plain reflects a layer of strongly magnetized rock that is probably volcanic and, in the east, an upper crust made up of a complex of magnetized bodies. Near-surface heat flow is lower over the axis of the plain than along the margins, but this may or may not reflect the deep heat flow. A large negative P-wave delay anomaly lies along the northwest edge of the eastern plain.

The western and central segments of the Snake River Plain appear to be a fault-bounded depression containing a layer of dense, strongly magnetized rock that may be Miocene basalt overlain by silicic volcanic rocks and interbedded basalt flows and sediments. Rocks typical of the upper crust of continents may not occur under the axis of this part of the plain. The eastern Snake River Plain is more likely a downwarp containing a complex of calderas with a great thickness of silicic volcanic rocks overlain by interbedded basalt flows and sediments. Fissures, along which the younger basalts have been erupted, parallel trends of the basin and range structures to the north and south of the eastern plain and may be extensions of these structures. Although typical upper crustal rocks may underlie the eastern plain, the geologic structure in these rocks appears to be different from the adjoining regions. The evolution of the eastern Snake River Plain appears to have consisted of a northeastward-moving center of volcanism that is now at Yellowstone National Park and of an increase in the density of the crust by a corresponding thinning of the upper crust and the resulting subsidence. Current deformation of the eastern plain is a southwest extension, parallel to the plain.

INTRODUCTION

The Snake River Plain, which extends in a 600-kilometer arc across southern Idaho, is the most prominent Cenozoic feature in the state (Figure 1). The plain is distinguished from the surrounding terrain by lower elevation and lower surface relief and by a complete cover of Cenozoic sedimentary and volcanic rocks. Well-defined topographic features form the boundary of the Snake River Plain throughout most of its length except in the southern part of the arc of the plain, where the moderately dissected surface of the plain rises to merge with the mountains to the south. This segment of the boundary has commonly been drawn as an arc connecting the well-defined segments to the northwest and east. However, the gravity and magnetic data suggest that the subsurface structure of the plain extends farther south, and the boundary suggested by the geophysical data will be used in this report.

The regional surface geology of the Snake River Plain has been known for many years, and in recent years, much of the surface geology has been studied in moderate detail. Added to the surface information are data from thousands of water wells, several deep oil and geothermal exploration wells, and a wide variety of geophysical surveys. Yet the Snake River Plain remains one of the least understood geologic structures in the United States. The data on the plain have been interpreted in very divergent ways by different investigators. The Snake River Plain has been described as a depression, downwarp, graben, rift, and lateral rift. In addition, several volcanic or thermal events have been used to explain the forma-

[1]U. S. Geological Survey, Salt Lake City, Utah 84101.

Mabey, D. R., 1982, Geophysics and tectonics of the Snake River Plain, Idaho, *in* Bill Bonnichsen and R. M. Breckenridge, editors, Cenozoic Geology of Idaho: Idaho Bureau of Mines and Geology Bulletin 26, p. 139-153.

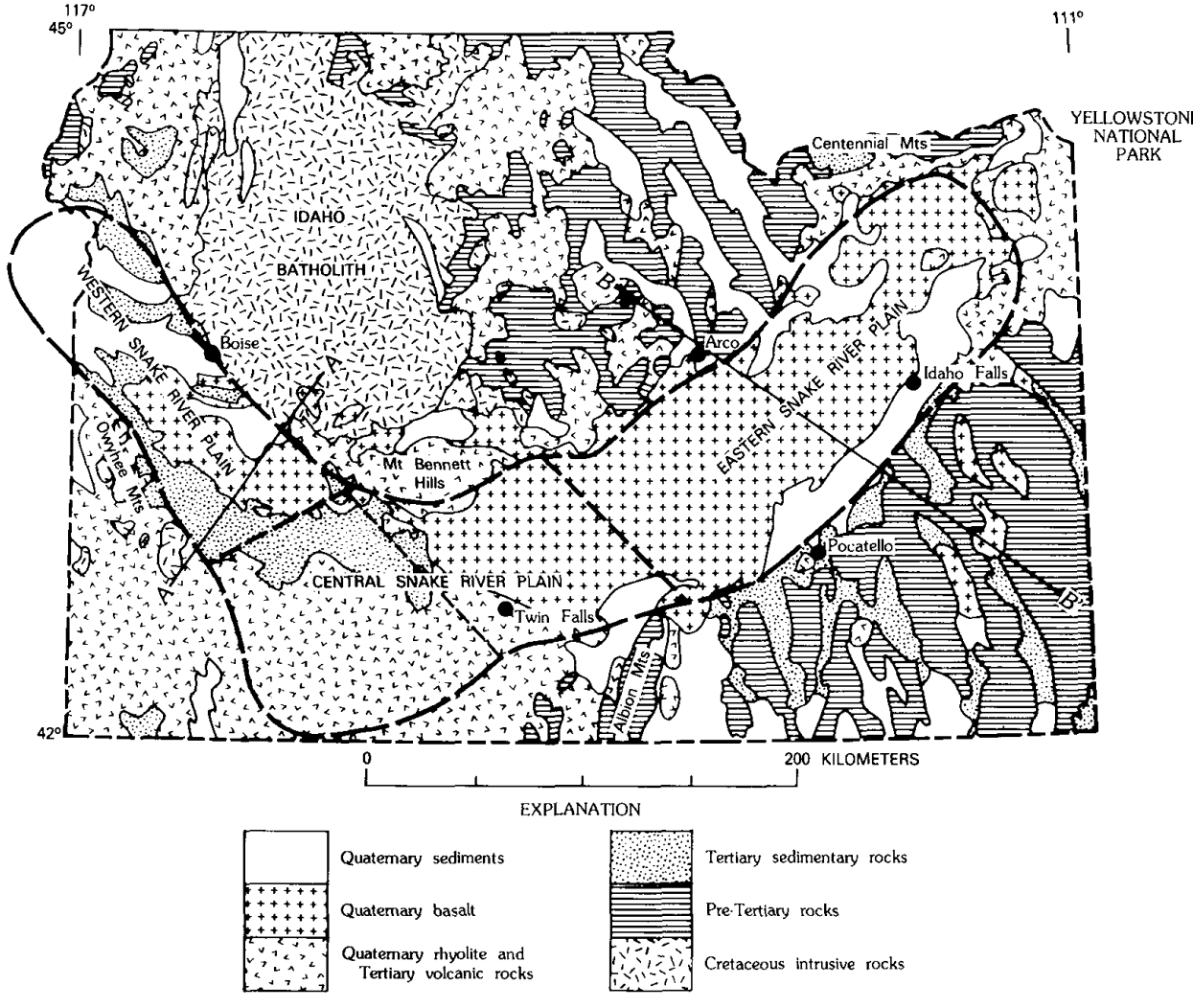

Figure 1. Geologic map of southern Idaho showing the Snake River Plain and location of profiles. Heavy dashed lines indicate major divisions of the plain. Narrow dashed line is lineament defined by the geophysical data. Geology generalized from geologic map of the United States (King and Beikman, 1974).

tion of the plain, and the plain has been tied to several plate tectonic models. Although the Snake River Plain is a continuous arc across southern Idaho, major differences exist between the surface geology and the geophysical anomalies in the western, central, and eastern parts of the plain. It is, therefore, convenient to discuss the plain as three units: the northwest-trending western Snake River Plain, the northeast-trending eastern Snake River Plain, and the central Snake River Plain between them (Figure 1).

WESTERN SNAKE RIVER PLAIN

The western Snake River Plain is 50 to 70 kilometers wide, trends northwest, and is generally considered to be a fault-bounded depression with normal faults forming major segments of both edges of the plain (Malde, 1965). Much of the northwestern part of the western Snake River Plain is covered by Quaternary alluvium. To the southeast, the surface rocks are primarily Tertiary and Quaternary lacustrine sediments and basalt flows, and the land surface and the rocks generally dip gently toward the axis of the plain. Southwest of the plain are the Owyhee Mountains with a core of metamorphic rocks and Cretaceous granitic rock overlain by Tertiary volcanic rock. To the northeast are the Cretaceous granitic rocks of the Idaho batholith locally overlain by Tertiary volcanic rock.

Several oil and geothermal test wells have been

drilled on the western Snake River Plain to depths as great as 4,300 meters. These wells have revealed lacustrine sediments several hundred meters thick underlain by 1,000 to 2,000 meters of basalt flows with some interbedded sediments. The two deepest holes, Chevron Highland No. 1 and Halbouty James No. 1, had reportedly bottomed in interbedded silicic volcanic rocks, lacustrine sediments, and basalt. To the southeast, one deep drill hole, 22 kilometers southeast of Mountain Home, Bostic No. 1-A, penetrated about 2,300 meters of interbedded basalt and sediment and bottomed in silicic volcanic rock (Arney and others, 1980). A drill hole about 70 kilometers south of Boise, Anschutz Federal No. 1, penetrated basalt and sediment to a depth of 800 meters and then predominately silicic volcanic rock to 3,400 meters, where granite was found (McIntyre, 1979).

The major sets of geophysical data available in the western and central Snake River Plain are regional gravity and magnetic surveys (Mabey and others, 1974; Zietz and others, 1979), a seismic refraction profile (Hill and Pakiser, 1966), and numerous thermal-gradient and heat-flow measurements (Brott and others, 1976). More detailed geophysical studies have been made in local areas, particularly near some of the deep drill holes.

The Bouguer[1] gravity high over the Snake River Plain, which was first reported by Bonini and Lavin (1957), has been studied by several investigators. The maximum amplitude of the high, which is about 100 milligals, is over the western Snake River Plain (Figure 2). Here the crest of the high trends a few degrees more westerly than the axis of the plain and has one major offset. Steep gradients associated with the gravity high show that at least part of the anomaly is produced by a positive mass anomaly within the upper crust, but part has a deeper source. The Bouguer gravity high is approximately coincident with the topographic low. Because the isostatic compensation for the plain is unusually local, the value of isostatic anomalies computed for gravity stations on or near the plain are highly dependent on the model assumed in computing the anomaly. The free-air and Faye anomalies over southwestern Idaho average slightly positive, and those over the axis of the gravity high on the plain are more positive than the average for southwestern Idaho (Figure 3). Although the plain in the area of the crest of the gravity high may not be in complete isostatic equilibrium, the western plain as a unit appears to be in approximate isostatic equilibrium with the adjoining regions, and the relative depression of the plain probably reflects an isostatic response to the large positive mass anomaly underlying the plain.

The gravity anomaly over the western Snake River Plain can be interpreted in several ways, but most interpretations involve a combination of dense basalt and a thinning of the upper crust that underlies the plain. At least three mass anomalies contribute in a major way to the gravity anomaly over the western Snake River Plain: a thin upper crust, low-density sediment with interbedded basalt, and massive dense basalt flows. The thinning of the upper crust, indicated by the refraction data, is a large positive mass anomaly and could produce most of the gravity high. Sedimentary rocks with some interbedded basalt cover much of the western plain and in some areas are over 1 kilometer thick. The average density of these rocks is low and their effect is to reduce the Bouguer anomaly over the plain. Three drill holes (Chevron Highland No. 1, Halbouty James No. 1, and Bostic No. 1-A) on the western Snake River Plain have penetrated 2 to 3 kilometers of basalt, but the bulk density of this basalt has not been determined. The dry bulk density of forty-nine samples of basalt flows of the Quaternary Snake River Group on the eastern Snake River Plain averaged 2.55 grams per cubic centimeter, and seven samples of basalt flows of the Miocene Columbia River Basalt Group north of the plain averaged about 2.9 grams per cubic centimeter. Two and one-half kilometers of the denser basalt would produce a 25-milligal anomaly, about one-fourth of the measured high. Three of the deep holes (Halbouty James No. 1, Bostic No. 1-A, and Anschutz Federal No. 1) found thick sequences of other volcanic rocks that, on the average, are probably less dense than the average crustal rocks.

Residual magnetic intensity over the western Snake River Plain is generally higher than over the areas to the north and south, but no magnetic feature coincides

[1]Bouguer gravity anomalies include a correction for the elevation of the point of observation relative to a reference datum (usually sea level). Included is a correction for the attraction of the material between the point and the reference datum. The Bouguer anomalies reflect all mass anomalies below the reference datum as well as variations from the density assumed in correcting for the material above the datum. Free-air anomalies include the correction for the elevation but not for the material above the reference datum. If a region is in isostatic equilibrium, the material above the reference datum will be compensated by an equal mass deficiency at depth. The gravity effect of the two masses at an observation point are approximately equal and opposite in sign, and the free-air is near zero. However, local relief on the Earth's surface is not compensated, and in areas of considerable local relief, free-air anomalies are strongly dependent upon the elevation of the observation point. The Faye anomaly includes a correction to the free-air anomaly for the difference between the elevation of the observation point and the average surrounding elevation. The Faye anomaly, which is a special type of isostatic anomaly, is approximately equal to the free-air anomaly that would be measured at a point with an elevation equal to the average surrounding elevation. Faye anomalies are designed to be used in areas of considerable local relief to reveal subsurface massanomalies that are not isostatically compensated and regional departures from isostatic equilibrium. See Mabey, 1966.

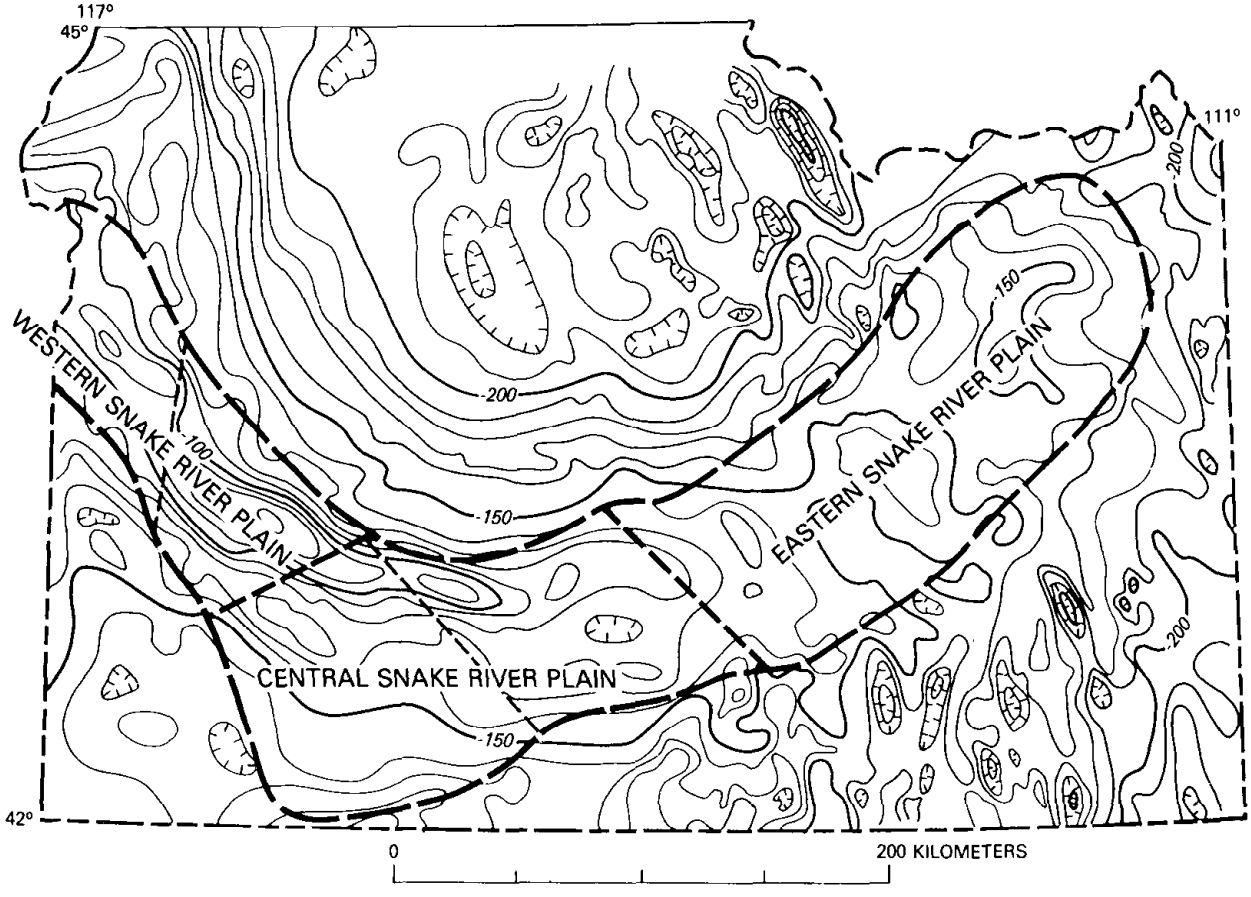

Figure 2. Bouguer gravity contour map of southern Idaho generalized from Mabey and others (1974). Heavy dashed lines indicate major divisions of the plain. Narrow dashed lines are lineaments defined by the geophysical data. Contour interval is 10 milligals.

with the axis of the plain or the gravity high (Figure 4). The most prominent feature of the total-intensity magnetic field is a high along the south side of the plain with a less conspicuous low along the north edge. Lower amplitude highs and lows, which generally do not correlate with surface geologic features, occur over the central part of the western plain. The magnetic field can be modeled in a variety of ways, but the high along the south edge of the plain and the low along the north edge, along with the extent of the associated gradients, strongly suggests that the plain is underlain, at a depth of a few kilometers, by a layer of rock strongly magnetized in the approximate present direction of the Earth's magnetic field. At one location on the southwest side of the plain, an appendage of the magnetic high extends beyond the plain. Underlying this appendage is the only extensive body of Eocene volcanic rock exposed south of the plain.

Shot points along the seismic-refraction profile that extends south across the plain from near Boise were at Lucky Peak Reservoir north of the plain, at C. J. Strike Reservoir near the axis of the plain, and at Mountain City south of the plain. In addition, underground nuclear tests on the Nevada Test Site were recorded. Several interpretations have been made of the data obtained, and although interpretations differ in detail, they agree that the total crust under the plain is over 40 kilometers thick, which is about 10 kilometers thicker than in central Nevada, and that the upper crust is thin under the axis of the plain (Hill and Pakiser, 1966).

Heat-flow measurements in southwestern Idaho have defined a heat-flow high along the margins of the plain and a relative heat-flow low over the plain (Figure 5). Brott and others (1978) conclude that a large heat source underlies the plain and that the heat-flow values measured in the near surface result from thermal refraction in the sedimentary and volcanic rocks underlying the plain and from the low heat generation of the rocks in the upper crust under the plain.

The gravity, magnetic, and seismic data have been combined to produce an interpreted profile across the

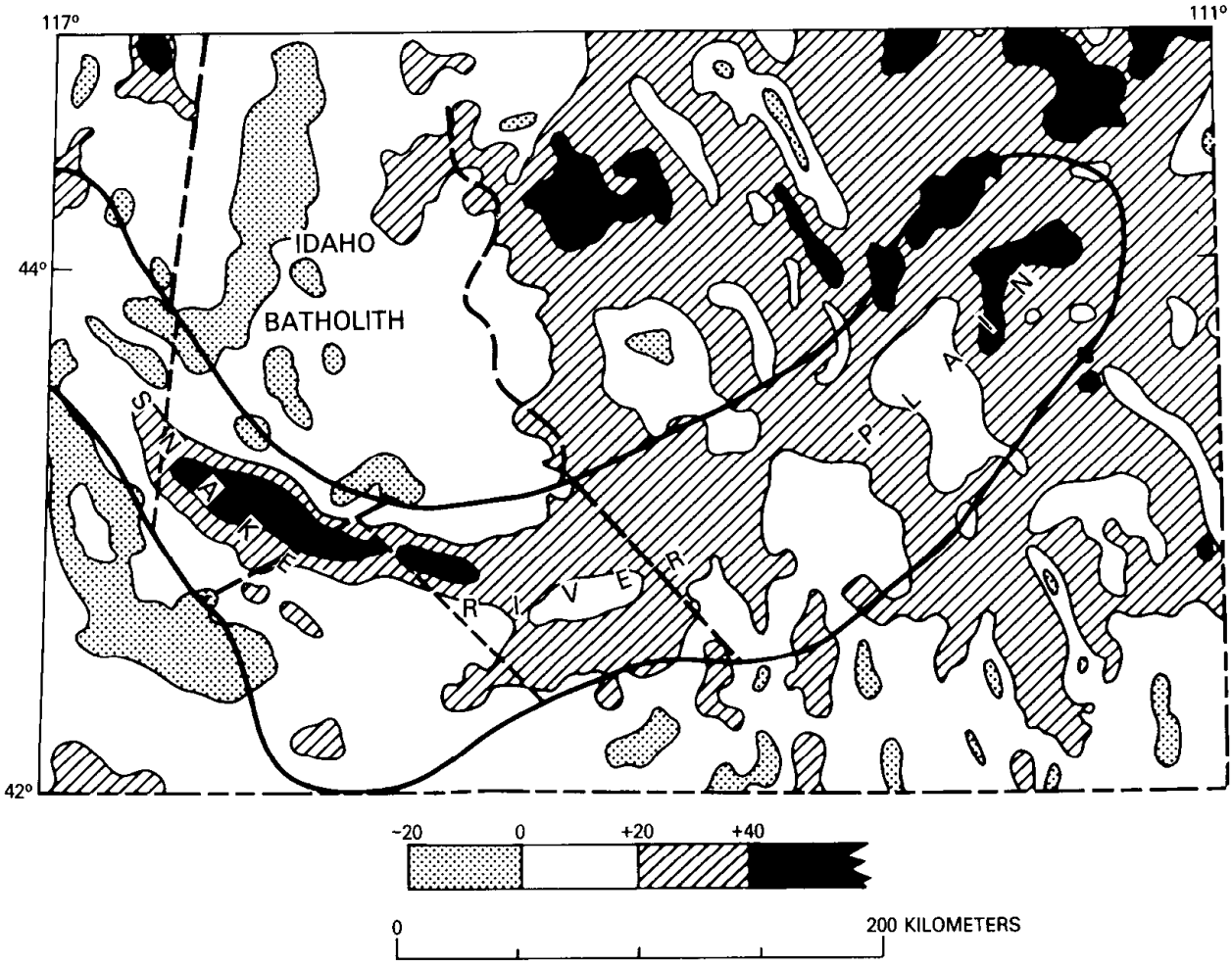

Figure 3. Faye gravity anomaly map of southern Idaho. Contour interval is 20 milligals. Heavy dashed lines indicate major divisions of the plain. Narrow dashed lines are lineaments defined by the geophysical data and approximate extent of the Idaho batholith. The Faye anomaly is the free-air anomaly corrected for the difference between the elevation of the gravity station and the average elevation surrounding the station. For this map the elevations were averaged over an area 64 kilometers in radius.

western Snake River Plain. The extent of the flanks of the gravity high beyond the plain require that a part of the positive mass either extends across the borders of the plain or lies at depths greater than 10 kilometers below the surface of the plain. Thus, the anomaly is not produced entirely by dense rock underlying the plain at depths of less than 10 kilometers. Very likely, the part of the anomaly with a deep source relates to the thinning of the upper crust as indicated by the refraction data. The steepest gravity gradients associated with the high, however, require a source above 10 kilometers. Some of these steep gradients can be attributed to variations in the thickness of the low-density sedimentary and silicic volcanic rocks, but a high-density mass above 10 kilometers is also indicated. If the magnetic anomaly over the plain is assumed to reflect a layer of dense, strongly magnetized rock, the magnetic data can be used with the gravity data to infer the depth and extent of this unit. The near-surface anomalies can be attributed to variations in the thickness and density of overlying low-density rocks and the remaining gravity anomaly attributed to the thinning in the upper crust. Such a model is shown in Figure 6. Large variations in this model are possible (for example, see Mabey, 1976), but good evidence exists for the approximate position and size of the major units.

Southwest of Boise, the crest of the gravity high along the axis of the plain is offset about 30 kilometers in a right-lateral sense (dashed line, Figure 2). This offset may reflect displacement upon a north-trending strike-slip fault. Such an offset is consistent with the magnetic data and the configuration of the southwest margin of the plain. North of the plain, the

trend of the offset projects along the linear western margin of the exposed part of the Idaho batholith. If the two highs reflect a geologic unit that has been offset, the offset probably occurred after most of the mass anomalies underlying the plain were emplaced but before part of the relative subsidence of the plain that produced the present topography occurred.

All of the geological and geophysical evidence is consistent with major segments of the western Snake River Plain being bounded by normal faults, although these faults may not have been the fundamental structure that formed the plain. A thick sequence of volcanic and sedimentary rock underlies the plain, but what, if any, pre-Cenozoic basement underlies the plain is not known. The large Bouguer gravity high and the approximate isostatic equilibrium of the plain relative to the adjoining highlands is in marked contrast to the basin and range structures to the south. With the basin and range structures, gravity highs do not occur over the basins; isostatic balance does not exist between the basins and the ranges; and the bounding faults do not appear to extend deep into the crust (Mabey, 1966). In contrast, the structure of the western Snake River Plain extends deep into and perhaps through the crust. If the term graben is used to describe the western Snake River Plain, a qualifying statement should be included noting that pre-Cenozoic rocks similar to those exposed north and south of the plain are not known to be downfaulted under the plain.

The western Snake River Plain has been described by Warner (1975) as a lateral rift, and by several others as a rift. Warner cites several lines of evidence to prove that 80 kilometers of left-lateral displacement has occurred along the Snake River Plain, mostly since early Pleistocene time. He also infers some separation across the western Snake River Plain. Yet, Warner's evidence for lateral movement does not appear to have been generally accepted by investigators of the plain. The trend of the western Snake River Plain is approximately parallel to the San Andreas and related faults southwest of the plain, but no evidence of the right-lateral movement of this system along the plain has been reported. Although the geophysical data do not establish that lateral movement has not occurred along the western Snake River Plain, lateral movement does not appear to be a likely cause of the major geophysical anomalies associated with the plain.

Several investigators have inferred a relationship

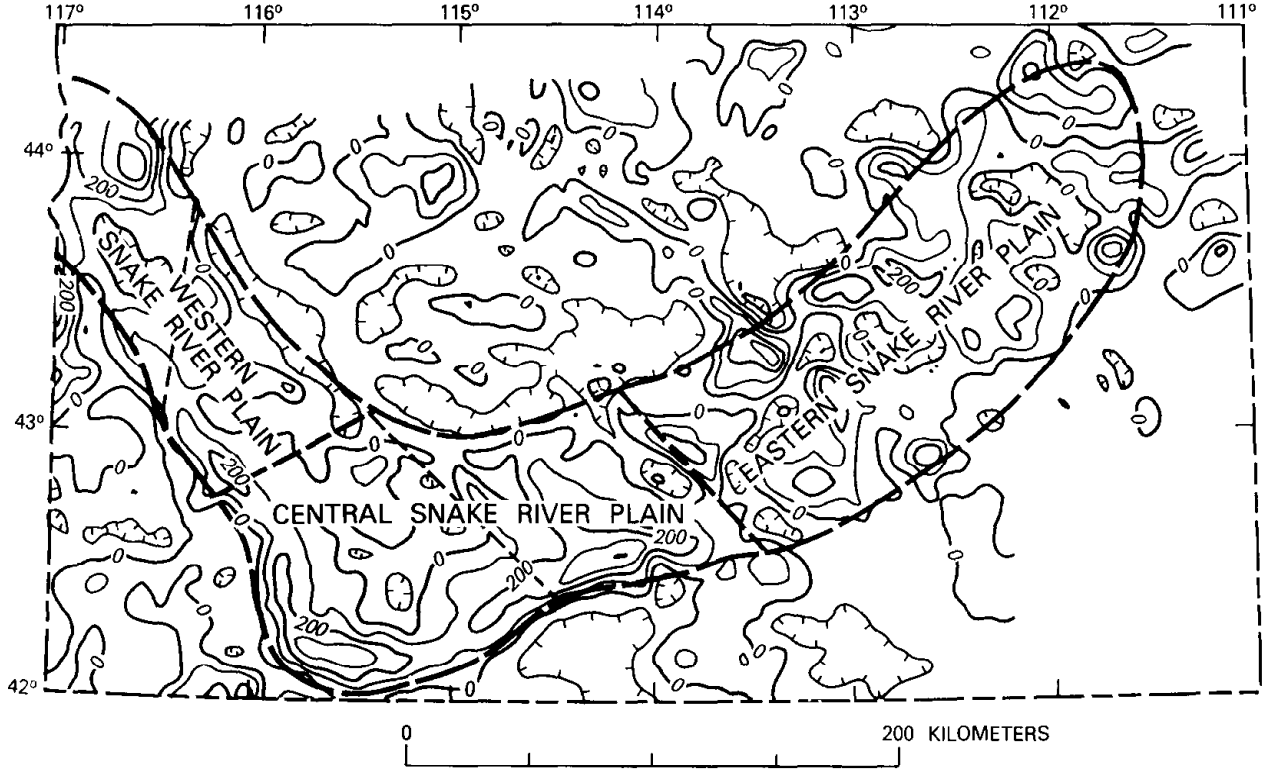

Figure 4. Residual total intensity magnetic map of southern Idaho at 3.8 kilometers above sea level. Heavy dashed lines indicate major divisions of the plain. Narrow dashed lines are lineaments defined by the geophysical data. Contour interval is 100 gammas. Map from Bhattacharyya and Mabey (1980).

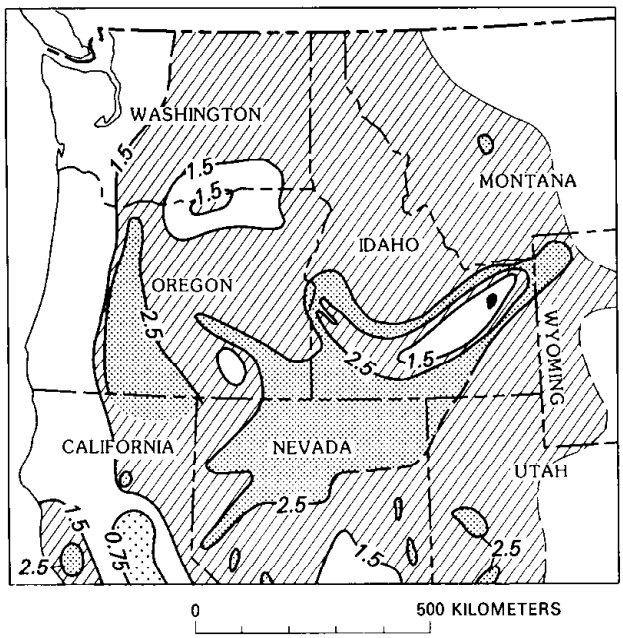

Figure 5. Contour map of heat flow in Idaho and adjacent areas. Map modified from Lachenbruch and Sass (1980). Values are heat-flow units.

between the western Snake River Plain and a better exposed but narrower rift of parallel trend in northern Nevada (Christiansen and McKee, 1978; Zoback and Thompson, 1978; Mabey, 1976). The rift in Nevada, which is Miocene in age, consists of a swarm of basalt dikes overlain by a graben, filled with basalt flows and sediments. Christiansen and McKee suggest that the rift in Nevada and the western Snake River Plain developed as a continuous rift about 17 million years ago. They postulate that the two structures were offset in a right-lateral sense by a transform fault coincident with the eastern Snake River Plain and the Brothers fault zone and related fault zones in Oregon.

If a rift is defined as an elongate rupture of the entire thickness of the lithosphere under tension, such an origin of the western Snake River Plain appears consistent with most of the geological and geophysical evidence. The upper crust apparently was thinned or pulled apart as major extension began about 17 million years ago, and the resulting depression was filled with upwelling basalt and debris from the adjoining highlands. The only major inconsistencies are the cuttings of granitic rock reported from the bottom of the deep drill hole 70 kilometers south of Boise (McIntyre, 1979) and the suggestion given by the magnetic high over Eocene volcanic rocks south of the plain that the magnetic high under the plain may relate to Eocene volcanic rocks. The presence of granitic basement at the bottom of the drill hole overlain by a section of volcanic and sedimentary rocks that were not strongly magnetized is not consistent with the measured magnetic anomaly, which requires strongly magnetized rock at depth. Perhaps, the granite is a relatively thin slide block, a floored intrusive unit, or a narrow sliver. The possibility that a thick sequence of pre-Miocene volcanic rock may underlie the western Snake River Plain has not been evaluated.

The western Snake River Plain appears to be a rift. However, the western Snake River Plain differs significantly from typical modern continental rifts such as the Rio Grande rift in Colorado and New Mexico and the Dead Sea and east African rifts. One

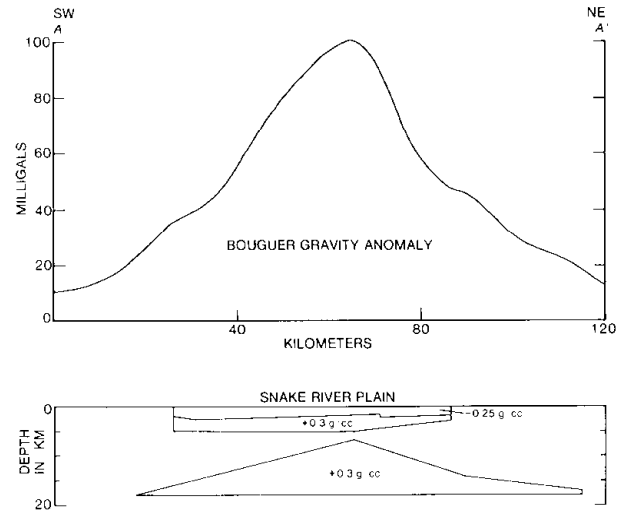

Figure 6. Interpreted gravity profile A-A', across the western Snake River Plain, Idaho. Location of profile shown in Figure 1.

prominent difference is that the other rifts coincide with gravity lows produced by low-density sediments within the rift. Although the sediments underlying the western Snake River Plain produce a gravity low, the low is much smaller than the larger gravity highs with approximately the same extent produced by deeper mass anomalies. The gravity anomaly is similar to that in the Salton Trough or the mid-continent gravity high.

Two primary structures can explain the heat-flow pattern in the western Snake River Plain. Brott and others (1978) propose the emplacement of a large heat source under the plain about 20 million years ago and the development of an overlying crust with low thermal conductivity and low heat-generating capacity. The resulting model would account for the measured high heat flow along the margins of the plain and the low values on the plain. An alternate explanation would involve the continued extension concentrated along the margins of the plain and

continued subsidence as the plain seeks isostatic balance. Either thermal model is consistent with the formation of the western Snake River Plain in Miocene time as a tension rift.

CENTRAL SNAKE RIVER PLAIN

The boundary between the western and central Snake River Plain is here taken as an east-northeast line extending across the Snake River Plain from the south end of the Owyhee Mountains at Poison Creek to the southern flank of the Mount Bennett Hills (Figure 1). Southeast of this line the plain widens as the southwest margin of the plain loses topographic expression and bends to the south and as the northeast margin curves to the east and also becomes a less prominent topographic feature. The prominent magnetic high that lies along the southwest margin of the western plain bends to the south and continues to near the Idaho-Nevada border (Figure 4). Here, the high makes a bend of about 90 degrees to the east, and generally corresponds to the margin of the Bruneau-Jarbidge eruptive center (Bonnichsen, 1982 this volume). A less prominent gravity gradient is coincident with the magnetic anomaly. The margin of the Snake River Plain in this segment has no well-defined topographic or surface geologic expression and is here assumed to coincide with the south edge of the subsurface mass indicated by the magnetic high and the gravity gradient.

Silicic volcanic rocks extend southwest of the plain into northern Nevada and southeast Oregon. South of the plain silicic volcanic rocks lap onto a highland in northern Nevada with a core of pre-Tertiary sedimentary and intrusive igneous rocks and onto the Albion Mountains with a core of Precambrian gneiss domes. On the north are the Tertiary silicic volcanic rocks of the Mount Bennett Hills and further north, beyond the west-trending Camas Prairie, is the Idaho batholith.

The Tertiary sedimentary rocks that cover much of the surface of the western Snake River Plain extend into the northwest part of the central plain, but most of the central plain is covered by volcanic rocks. In the west and south, the volcanic rocks are Miocene and Pliocene rhyolite overlain by Pliocene and Quaternary basalt and, in the east, Quaternary basalt. Faults trending north to northwest are common in the older volcanic rocks. No data from deep holes are available from this part of the plain, but Bonnichsen (1982 this volume) has suggested that calderas are beneath this area, buried within the Bruneau-Jarbidge eruptive center.

Although the gravity and magnetic features along the north edge of the western Snake River Plain generally parallel its margin, the magnetic low is interrupted where this margin of the plain begins the eastward arc. Patterns in both the gravity and the magnetic data can be interpreted to indicate a structure across the plain on a projection of the linear northeast border of the western plain (Figures 2, 3, and 4). A northwest grain in the magnetic data is apparent to the east of this projection.

The amplitude of the gravity high over the central segment of the plain is about 75 milligals, contrasted with 100 milligals over the western plain. The crest of the gravity high lies near the north edge of the plain, and in two places to the south (Figure 2), closed gravity highs trend parallel to this main gravity crest. Although the amplitude of the gravity high over the central plain is lower than over the western plain, the plain and the total gravity high are broader and the cross-sectional area of the positive mass underlying the central plain is as large or larger than that under the western plain.

The magnetic pattern over the central Snake River Plain is similar to that over the western plain but the amplitude of the high along the south edge is greater. A northwest grain to the magnetic anomalies is also more prominent, particularly in the eastern part.

No deep seismic-refraction data are available across the central Snake River Plain, but the gravity anomaly suggests a thinning of the upper crust. The thinning, distributed over a greater width than under the western plain or shallower positive mass anomalies, may cause the greater width of the gravity high. As in the western plain, a layer of dense, strongly magnetized material appears to be overlain by less dense and less strongly magnetized rock.

The heat-flow pattern over the central plain is similar to the west except that high heat flow on the southwest is continuous with the large area of high heat flow in northern Nevada (Figure 5). The model of Brott and others (1981) for the western plain also applies to the western part of the central plain, but to the east an area of low heat flow related to the horizontal movement of ground water in volcanic aquifers extends into the central plain.

The similarity between the geophysical anomalies and the geology in the western and central Snake River Plain suggests that these two parts of the plain have a similar origin. One explanation is that they both developed during extension in response to regional tension approximately normal to the trend of the present western Snake River Plain. Southwest of the edge of the Idaho batholith, the extension and the resulting thinning of the upper crust and subsidence of the surface may have been concentrated in a narrow zone, thus producing the structure of the western Snake River Plain. Southeast of the batholith,

the extension may have been distributed over a wider zone producing the structure of the central Snake River Plain. If the crest of the gravity high reflects the zone of maximum thinning of the upper crust, the eastward arcing of the crest of the gravity high suggests a greater south component of movement of the block south of the Idaho batholith. Perhaps the block south of the plain was rotated clockwise.

EASTERN SNAKE RIVER PLAIN

The magnetic and gravity patterns change abruptly on the east at a zone that trends northwest across the plain from the northeast end of the Albion Mountains (dashed line, Figure 1). Southwest of this zone, a pronounced single or compound gravity high trends subparallel to the plain. Northeast of the zone, the Bouguer gravity anomaly is generally higher than over adjoining areas but consists of a complex pattern of highs and lows with the largest closed gravity high elongated approximately normal to the axis of the plain. No continuous magnetic high lies along the south edge of the eastern plain. Over the plain instead is a series of magnetic highs and lows with high amplitude and a grain normal to the plain. Thus, no evidence exists of a dense, strongly magnetized layer underlying the eastern Snake River Plain. The land surface along most of the axis of the eastern plain is higher than the margins, indicating greater recent subsidence of the margins.

Southeast of the eastern plain are basin and range structures trending approximately normal to the plain. The ranges are primarily folded pre-Tertiary sedimentary rock, and the valleys commonly are underlain by thick accumulations of Cenozoic sediments. Pliocene and Quaternary volcanic rock occur in several areas. Northwest of the eastern plain is a zone of basin and range structures flanked on the southwest by the Pioneer and White Knob Mountains and on the northeast by the east-trending Centennial Mountains. Folded pre-Tertiary sedimentary rocks are the most common rocks in the ranges north of the eastern plain, but Eocene extrusive and intrusive igneous rocks are abundant. Geologic mapping north and south of the plain has not revealed any evidence of lateral movement parallel to the axis of the plain (S. S. Oriel, oral communication, 1980).

Most of the eastern Snake River Plain is covered by Quaternary basalt flows. The younger flows appear to have erupted along fissures normal to the plain approximately parallel to and in some places along extensions of basin and range structures to the north and south. Rhyolite domes ranging in age from 0.3 to 1.5 million years rise above the surface of the basalt in the central part of the eastern plain (Kuntz and Dalrymple, 1979; Spear and King, 1982 this volume). Rhyolite ash flows are common around the margins of the plain, and rhyolite has been found in all of the deeper drill holes on the plain. Cenozoic sediments are abundant in the surface and shallow subsurface near the margins of the plain. Although cracks and fissures with trends generally normal to or parallel to the axis of the plain are common, evidence of displacement along them is rare.

The structure of segments of the margins of the eastern Snake River Plain appear to differ. The linearity and steep gravity gradient parallel to the margin of the plain east of Arco suggest a normal fault near the plain margin. Along the south edge of the plain west of Pocatello, the ranges appear to dip under the margins of the plain but the gravity data suggest they are terminated in the subsurface a few kilometers to the north. East of Idaho Falls, a segment of the margin of the plain is coincident with the edge of the Rexburg caldera complex (Embree and others, 1982 this volume).

Although the eastern Snake River Plain extends into the Intermountain seismic belt, there are few earthquakes under the plain. Apparently, whatever deformation is occurring does not involve large-scale brittle failure of rocks underlying the plain.

Northeast of the eastern Snake River Plain lie the large Island Park and Yellowstone caldera complexes. Another large caldera complex, the Rexburg caldera complex, has been identified on the eastern Snake River Plain, and the existence of several others has been inferred (Embree and others, 1982 this volume). A northeast decrease in age of the silicic volcanic rocks in and adjacent to the plain has been noted from southwestern Idaho to Yellowstone National Park (Armstrong and others, 1975). This large-scale progression has been interpreted as indicating that the central and eastern Snake River Plain coincides with the track of a northeastward-moving center of silicic volcanism (Christiansen and McKee, 1978).

Only one deep hole has been drilled on the eastern Snake River Plain. This hole, which is on the Idaho National Engineering Laboratory about 30 kilometers east of Arco, was 3,155 meters deep and was bottomed in a rhyodacite porphyry. The rock in the lower part of the hole, which has been dated at 11.2 million years (McBroome, 1981), may be an ash-flow tuff or a high-level intrusive rock. Doherty and others (1979) suggest that this hole was drilled into a caldera. Drilling and resistivity soundings (Zohdy and Bisdorf, 1980) suggest that Quaternary basalt is generally less than 1 kilometer thick on the eastern plain, although in part of the area it may be thicker.

Extensive seismic-refraction profiling has been done in the eastern Snake River Plain and Yellow-

stone National Park. Preliminary reports on the interpretation of these data suggest that the velocity structure of the crust under the eastern Snake River Plain is similar to that of the western plain with a thin upper crust and a thick lower crust and suggests that the total crust thickens northeastward toward Yellowstone National Park (Braile and Smith, 1979).

The regional gravity high centered over the eastern Snake River Plain extends well beyond the plain (Figure 7). This high apparently reflects the thinning of the upper crust toward the center of the plain indicated by the refraction data, and the thinning appears to extend well beyond the plain. Superimposed on this high are two gravity lows produced by the Cenozoic sedimentary and volcanic rocks underlying the margins of the plain. The maximum thickness of these Cenozoic rocks has not been determined, but it is likely to be several kilometers.

The source of most of the more extensive magnetic highs on the eastern Snake River Plain is uncertain. The basalt flows in the near surface of the plain are strongly magnetized with both normal and reversely magnetized flows, but the more extensive magnetic highs have been interpreted as having a deeper source (Bhattacharyya and Mabey, 1980). Some of the highs on the plain near the south edge are over uplifted blocks of Cenozoic rock and can be inferred to relate to underlying Cenozoic intrusive rocks. Eaton and others (1975) and Mabey and others (1978) have pointed out that the eastern Snake River Plain is part of a northeast-trending magnetic zone: the Humboldt zone, that extends through Yellowstone National Park. To the northeast of Yellowstone, this zone is reflected in Precambrian rocks. Although the source of the deeper magnetic anomalies over the eastern Snake River Plain is not known, the crust under the plain is composed of more strongly magnetized units

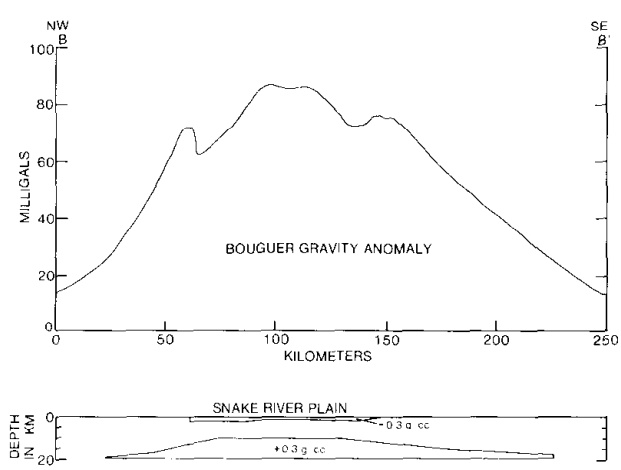

Figure 7. Interpreted gravity profile B-B′, across the eastern Snake River Plain, Idaho. Location of profile shown in Figure 1.

than adjoining areas.

Deep conductivity data are available in the eastern Snake River Plain from magnetotelluric (Stanley and others, 1977) and magnetic variometer soundings (Fitterman, 1979; Wier, 1979). Published interpretations of the magnetotelluric data indicate a conductive layer in the crust at depths of from 12 to 22 kilometers, but neither technique reveals a deep conductive anomaly coincident with the plain.

A delay of up to 1.5 seconds in teleseismic P-wave arrivals suggests that a low-velocity zone extends to depths of over 200 kilometers under the northwest edge of the eastern Snake River Plain (Evans, 1981). This anomaly is a westward continuation of the P-wave delay anomaly underlying Yellowstone National Park. Thus, the Snake River Plain appears to be offset from the low-velocity zone in the mantle. Shear wave velocities of the crust and upper mantle are lower under the eastern Snake River Plain than in the Basin and Range province to the south (Greensfelder and Kovach, 1980). Both low-velocity anomalies might reflect high-temperature zones.

Although the surface relief across the eastern Snake River Plain is about equal to that of the plain farther west, the gravity and magnetic anomalies suggest a somewhat different crustal anomaly. Rather than an abrupt thinning or perhaps complete parting of the upper crust, as appears to have occurred in the western plain with an outpouring of large volumes of basalt, the thinning of the crust under the eastern plain is a broader feature; no evidence of large early eruption of basalt is apparent. Instead, a complex of silicic volcanic rocks and related intrusive bodies appear to underlie most of the eastern plain.

The heat-flow pattern over the eastern plain is also similar to that in the west. Over most of the eastern plain, the near-surface heat flow is disturbed by the southwestward movement of ground water down the plain in the volcanic aquifer that underlies most of the eastern plain. Brott and others (1981) believe that this movement of water is the cause of the low heat flow measured over the interior of the plain and that the heat flow under the aquifer is very high. However, the thermal data from the three holes drilled through the aquifer in the INEL area of the plain do not confirm that the thermal gradients below the aquifer are higher than those along the margins of the plain.

The free-air gravity anomaly indicates that the eastern part of the Snake River Plain, like its central and western segments, is in approximate isostatic equilibrium with the adjoining highlands. The thinning of the upper crust under the plain represents a positive mass anomaly that is the compensation for the low surface elevation of the plain. The relative thinning of the upper crust could result from extension normal to the plain, from lateral mass transfer

related to igneous activity, or a combination of the two. Extension normal to the plain would account for the thinned upper crust, and the concentration of the thinning near the margins could explain the apparent subsidence and high heat flow there. However, the evidence of northwest regional extension in this part of the western United States in late Tertiary and Quaternary time is unconvincing. The average density of the crust can also be increased by the ejection of lower density material in volcanic eruptions; however, there is no evidence of the very large eruptions that would be required to remove the volume of upper crustal material necessary to produce the density decrease indicated by the gravity anomaly.

In its simplest form, the thermal model suggests a heat source propagating northeast relative to the surface from southwest Idaho to a current position under Yellowstone National Park. Brott and others (1981) propose a quantitative model with a 120-kilometer-wide heat source plane normal to the Snake River Plain moved through a 42-kilometer-thick slab of lithosphere at a velocity of 35 millimeters a year. The model combines the heating and cooling in this thermal event with a density increase under the plain, which they believe could be caused by extension, dispersion of granitic material, extrusion of ash flows, or erosion. In this model, the major subsidence of the plain is caused by isostatic adjustment of the density increase. In their model, the continued subsidence is caused by contraction due to cooling, as is the development of rifts and the elevation decrease of the plain toward the southwest. Morgan (1972) had earlier suggested that the Snake River Plain is the track of a mantle plume over which the continent moved in Cenozoic time, whereas Smith and Christiansen (1980) suggest a mantle hot spot. Blackwell (1978) has suggested that the heat source is related to magma developed over a subducted slab. Others have suggested that the Snake River Plain is a zone of extension or a propagating fracture (Hamilton and Myers, 1966; Lachenbruch and Sass, 1978; Smith, 1977, 1978; Furlong, 1979). In these models, a mechanical process is the primary cause of the structure and the thermal events. Numerous combinations of thermal and mechanical processes are possible. A further complication is that the low-velocity zone in the mantel indicated by the P-wave delay anomaly, which is probably related to a deep heat source, lies north of the plain.

Numerous fractures extend inward from the margins of the eastern Snake River Plain. From segments of these fractures, large volumes of basalt have erupted; other are open fissures in basalt flows (Kuntz and others, 1982 this volume; King, 1982 this volume). These fractures must be tensional features related to extension parallel to the axis of the plain; the fact that basalt is erupted through them suggests that they extend to great depth. The model of Brott and others (1981) suggests that cooling and related contraction at depth could account for the opening of the rifts normal to the axis of the plain. However, these rifts may reflect a more regional extension suggested by the basin and range structures to the north and south.

The most prominent volcanic rift on the eastern Snake River Plain is the Great Rift along which the Craters of the Moon lava field occurs. On the north, this rift is coincident with an aeromagnetic anomaly that extends across the edge of the plain and for 100 kilometers north of the plain. To the north this anomaly is coincident with a zone which contains several Cenozoic plutons. On the plain, the rift arcs to the south to parallel basin and range structures south of the plain. Thus, the rift appears to be related to structures that extend beyond the plain.

The apparent relationship between the rifts on the eastern Snake River Plain and the basin and range faults to the north and south suggests they represent different responses to extension of the crust approximately parallel to the axis of the plain. Normal faults south of the plain, and presumably those north of the plain, appear to be controlled by old structures, many related to overthrusting; many of the normal faults flatten at depth to merge with major thrust faults. Movement along these faults results in a thinning of a surface layer that appears to generally correspond to the allochthonous unit involved in the thrusting. The underlying layer appears to extend by ductile flow without the development of major normal faults. Although the belt of overthrusting probably initially extended across the area of the Snake River Plain, subsequent igneous activity along the plain and perhaps extension normal to the plain have disrupted the thrust faults. Current extension of the upper layer on the plain is not accommodated along preexisting thrust faults but rather occurs by the opening of vertical fractures to the depth at which extension is by ductile flow. The greater subsidence of the margins of the plain could occur under tension parallel to the margins, if the ductile layer is thicker there, or it may reflect the development of more local isostatic balance.

Although the entire Snake River Plain appears to be in approximate isostatic equilibrium with the area to the north and south, a more regional isostatic anomaly is apparent on the Faye or average free-air anomaly map of southern Idaho (Figure 3). Over most of southern Idaho, the average free-air anomaly values are positive, as contrasted with near-zero values in Nevada (Mabey, 1966). However, the southeastern Idaho values are even more positive with most of the area higher than +20 milligals. The isostatic equilibrium of the plain relative to adjacent areas superimposed on a more regional isostatic

disequilibrium suggests that the compensation of the plain occurs at relatively shallow depths but that a much larger region apparently centered northeast of the Snake River Plain is undercompensated. Perhaps, deep dynamic forces account for a part of the high elevation of this large region.

CONCLUSIONS

Geophysical data and deep drilling have been used to obtain information on several aspects of the deep structure of the Snake River Plain. Major problems addressed are: (1) What regional anomalies in the crust and upper mantle are associated with the plain? (2) What is the nature of the stress fields and thermal events that have formed the plain? (3) What is the age of the plain? (4) What is the primary structure of the major segments of the plain? (5) What rocks underlie the plain at depths greater than the deeper drill holes? (6) Do structural patterns adjacent to the plain extend onto the plain?

The entire Snake River Plain appears to be underlain by a thicker crust than the Basin and Range province to the south. The Snake River Plain crust consists of a thin upper crust and thick lower crust. P-wave delays and shear-wave velocities indicate that the mantle underlying the region of at least the eastern Snake River Plain is also anomalous. The velocity structure of the eastern Snake River Plain has been studied intensely in recent years, and an analysis of the data obtained will provide a velocity model of this part of the plain. More refraction data are needed to define the velocity structure of the central and western plains. The anomalous crust and upper mantle very likely are directly related to the formation of the plain and probably preceded or accompanied the formation of the plain. The thin upper crust can be explained by extension, but the cause of thick lower crust is not obvious. Brott and others (1981) postulate that magma above a subducting slab coalesced under the Snake River Plain in the manner that salt flows laterally into an initial perturbation. A mantle hot spot or plume may have thickened the lower crust as it moved under the plain. The Snake River Plain-Yellowstone crust and upper mantle appear to be a unique intraplate anomaly, and the events in its development are not yet understood. Regardless of how the crustal and upper mantle anomaly under the Snake River Plain formed, the structure of the upper crust underlying the plain appears to have developed in a regional stress pattern that is much more extensive than the plain.

The Snake River Plain is a major feature in the crust. Active volcanism, open fissures, and evidence of continued subsidence show that the plain is an active structure that continues to develop. A suggestion exists in the magnetic data that the eastern Snake River Plain may be part of a northeast trend reflected in Precambrian rocks to the northeast, but no evidence has been reported to suggest that the plain existed before Miocene time. Several lines of evidence do suggest that the development of the plain may coincide with the large-scale extension of the Basin and Range province to the south, which began about 17 million years ago.

The western and central Snake River Plain appears to be, at least in part, a down-faulted block. It may be termed a graben or a rift but differs from typical continental grabens and rifts. It probably developed in Miocene time in response to west-southwest regional extension, and perhaps clockwise rotation of the block south of the plain, which greatly thinned or completely parted the upper crust. The gravity and magnetic data suggest that a thick layer of dense strongly magnetized rocks formed within the resulting depression. The plain has continued to subside perhaps because of cooling, continued tension, loading of sediment, and isostatic adjustment due to the large positive mass under the plain.

The eastern Snake River Plain appears to have a more complex history than the western plain. The eastern plain is basically a downwarp containing numerous calderas. Extension normal to the plain is a possible explanation for the thinned upper crust under the plain and the high thermal flux indicated by the intense volcanic activity. Alternately, the plain may represent the track of a thermal anomaly now centered under Yellowstone National Park that moved northeastward across southern Idaho producing a complex of calderas that are now largely obscured by younger basalt flows on the Snake River Plain. Such a thermal event can be used to explain the formation of the eastern Snake River Plain only if some mechanism for the development of a large positive mass anomaly under the plain is also involved. The current tectonics of the eastern plain appear to be extension parallel to the axis of the plain.

The gross structure of the central Snake River Plain combines elements of both the western plain and the eastern plain. There is evidence of a down-faulted block filled with dense, strongly magnetized rock, but the current deformation appears to be downwarping. This segment of the plain probably formed with the western plain but has an overprint of the structure of the eastern plain.

What rocks and structures underlie the Snake River Plain at great depth remains unknown. One of the deep drill holes on the western Snake River Plain apparently bottomed in granite, which could be part

of an extensive Cretaceous mass of granite that makes up the Idaho batholith north of the plain and is present south of the plain in less extensive outcrops in southwestern Idaho and northern Nevada. However, the very large gravity and magnetic anomalies over the western plain suggest that the crust under the plain is drastically different from adjoining areas. Thus, it appears unlikely that the pre-Tertiary rocks north and south of the western plain make up the bulk of the crust under the plain. The magnetic anomaly and particularly the gravity anomaly over the eastern plain are not as profound as over the western plain. The upper crust under the eastern plain is composed of more magnetic units than are adjoining areas, indicating a greater abundance of igneous rocks in the crust under the plain. The response of the eastern plain to the regional stress is very different from areas to the north and south. This suggests that the structure and perhaps the lithology are different. The average density of the upper crust under the eastern plain is probably not greatly different from the adjoining areas, but intense igneous activity in Cenozoic time has probably produced major changes in the lithology and destroyed most of the older structures. The basin and range structures north and south of the eastern Snake River Plain either terminate at the margin of the plain or extend only a few kilometers onto the plain. However, the pattern of volcanic rifts on the plain suggests that they may be related to the basin and range structures.

Concealed beneath a complete cover of Cenozoic sediments and volcanic rocks, several fundamental aspects of the deep structure of the Snake River Plain remain uncertain despite the acquisition of considerable regional geophysical data and the drilling of several holes to depths of over 3 kilometers. More geophysical data and creatively combined interpretations of all of the available data will continue to add to our understanding of the area, but many critical data can be obtained only by drilling very deep holes and taking continuous core samples.

REFERENCES

Armstrong, R. L., W. P. Leeman, and H. E. Malde, 1975, K-Ar dating, Quaternary and Neogene volcanic rocks of the Snake River Plain, Idaho: American Journal of Science, v. 275, p. 225-251.

Arney, B. H., J. H. Boyer, D. B. Simon, F. B. Tonani, and R. B. Weiss, 1980, Hot dry rock geothermal site evaluation, western Snake River Plain, Idaho: Geothermal Resources Council Transactions, v. 4, p. 197-200.

Bhattacharyya, B. K. and D. R. Mabey, 1980, Interpretation of magnetic anomalies over southern Idaho using generalized multibody models: U. S. Geological Survey Open-File Report 80-475, 48 p., 9 figs.

Blackwell, D. D., 1978, Heat flow and energy loss in the western United States, *in* R. B. Smith and G. P. Eaton, editors, Cenozoic Tectonics and Regional Geophysics of the Western Cordillera: Geological Society of America Memoir 152, p. 175-208.

Bonini, W. E. and P. M. Lavin, 1975, Gravity anomalies in southern Idaho and southwestern Montana: Geological Society of America Bulletin, v. 68, p. 1702.

Bonnichsen, Bill, 1982, The Bruenau-Jarbidge eruptive center, southwestern Idaho, *in* Bill Bonnichsen and R. M. Breckenridge, editors, Cenozoic Geology of Idaho: Idaho Bureau of Mines and Geology Bulletin 26.

Braile, L. W. and R. B. Smith, 1979, The structure of the crust in the Yellowstone-Snake River Plain area and adjacent provinces and the implications for crustal evolution: EOS, American Geophysical Union, v. 60, no. 46, p. 941.

Brott, C. A., D. D. Blackwell, and J. C. Mitchell, 1976, Geothermal investigations in Idaho, Part 8, Heat flow study of the Snake River Plain, Idaho: Idaho Department of Water Resources Water Information Bulletin 30, 195 p.

———, 1978, Tectonic implications of the heat flow of the western Snake River Plain: Geological Society of America Bulletin, v. 89, p. 1697-1707.

Brott, C. A., D. D. Blackwell, and J. P. Ziago, 1981, Thermal and tectonic implications of heat flow in the eastern Snake River Plain, Idaho: Journal of Geophysical Research, v. 86, p. 11709-11734.

Christiansen, R. L. and E. H. McKee, 1978, Late Cenozoic volcanic and tectonic evolution of the Great Basin and Columbia Intermontane regions, *in* R. B. Smith and G. P. Eaton, editors, Cenozoic Tectonics and Regional Geophysics in the Western Cordillera: Geological Society of America Memoir 152, p. 283-312.

Doherty, D. J., L. A. McBroome, and M. A. Kuntz, 1979, Preliminary geological interpretation and litholigic log of the exploratory geothermal test well (INEL-1), Idaho National Engineering Laboratory, eastern Snake River Plain, Idaho: U. S. Geological Survey Open-File Report 79-1248, 10 p.

Eaton, G. P., R. L. Christiansen, H. M. Iyer, A. M. Pitt, D. R. Mabey, H. R. Blank, Isidore Zietz, and M. E. Gettings, 1975, Magma beneath Yellowstone National Park: Science, v. 188, p. 787-796.

Embree, G. F., L. A. McBroome, and D. J. Doherty, 1982, Preliminary stratigraphic framework of the Pliocene and Miocene rhyolites, eastern Snake River Plain, Idaho, *in* Bill Bonnichsen and R. M. Breckenridge, editors, Cenozoic Geology of Idaho: Idaho Bureau of Mines and Geology Bulletin 26.

Evans, J. R., 1981, Compressional-wave velocity structure of the upper 350 km under the eastern Snake River Plain near Rexburg, Idaho: Journal of Geophysical Research, v. 87, p. 2654-2670.

Fitterman, D. V., 1979, Geomagnetic induction study across the eastern Snake River Plain, Idaho: EOS, American Geophysical Union, v. 60, no. 46, p. 944.

Furlong, K. P., 1979, An analytic stress model applied to the Snake River Plain: Tectonophysics, no. 58, p. 11-15.

Greensfelder, R. W. and R. L. Kovach, 1980, Shear wave velocities beneath the eastern Snake River Plain, Idaho: EOS, American Geophysical Union, v. 61, no. 46, p. 1026.

Hamilton, Warren and W. B. Myers, 1966, Cenozoic tectonics of the western United States: Reviews of Geophysics, v. 4, p. 509-550.

Hill, D. P. and L. C. Pakiser, 1966, Crustal structure between the Nevada Test Site and Boise, Idaho, from seismic-refraction measurements, *in* J. S. Steinhard and T. J. Smith, editors, The Earth Beneath the Continents: American Geophysical Union, Geophysics Monograph 10, p. 391-419.

King, J. S., 1982, Selected volcanic features of the south-central Snake River Plain, Idaho, *in* Bill Bonnichsen and R. M. Breckenridge, editors, Cenozoic Geology of Idaho: Idaho Bureau of Mines and Geology Bulletin 26.

King, P. B. and H. M. Beikman, 1974, Geologic map of the United States: U. S. Geological Survey, scale 1:2,500,000.

Kuntz, M. A. and H. R. Covington, 1979, Do basalt structures and topographic features reflect buried calderas in the eastern Snake River Plain?: EOS, American Geophysical Union, v. 60, no. 46, p. 945.

Kuntz, M. A. and G. B. Dalrymple, 1979, Geology, geochronology and potential volcanic hazards in the Lava Ridge-Hells Half Acre area, eastern Snake River Plain, Idaho: U. S. Geological Survey Open-File Report 79-1657, 66 p.

Kuntz, M. A., D. E. Champion, E. C. Spiker, R. H. Lefebvre, and L. A. McBroome, 1982, The Great Rift and the evolution of the Craters of the Moon lava field, Idaho, *in* Bill Bonnichsen and R. M. Breckenridge, editors, Cenozoic Geology of Idaho: Idaho Bureau of Mines and Geology Bulletin 26.

Lachenbruch, A. H. and J. H. Sass, 1978, Models of an extending lithosphere and heat flow in the Basin and Range province, *in* R. B. Smith and G. P. Eaton, editors, Cenozoic Tectonics and Regional Geophysics of the Western Cordillera: Geological Society of America Memoir 152, p. 209-250.

_____, 1980, Heat flow and energetics of the San Andreas fault zone: Journal of Geophysical Research, v. 85, p. 6185-6222.

Mabey, D. R., 1966, Relation between Bouguer gravity anomalies and regional topography in Nevada and the eastern Snake River Plain, Idaho: in U. S. Geological Survey Professional Paper 550-B, p. B108-B110.

_____, 1976, Interpretation of a gravity profile across the western Snake River Plain, Idaho: Geology, v. 4, p. 53-55.

_____, 1978, Regional gravity and magnetic anomalies in the eastern Snake River Plain, Idaho: U. S. Geological Survey Journal of Research, v. 6, no. 5, p. 553-562.

Mabey, D. R., D. L. Peterson, and C. W. Wilson, 1974, Preliminary gravity map of southern Idaho: U. S. Geological Survey Open-File Report 74-78.

Mabey, D. R., Isidore Zietz, G. P. Eaton, and M. D. Kleinkopf, 1978, Regional magnetic patterns in part of the Cordillera in the western United States, *in* R. B. Smith and G. P. Eaton, editors, Cenozoic Tectonics and Regional Geophysics of the Western Cordillera: Geological Society of America Memoir 152, p. 93-106.

Malde, H. E., 1965, Snake River Plain, *in* H. E. Wright, Jr. and D. G. Frey, editors, The Quaternary of the United States: Princeton University Press, p. 255-263.

McBroome, L. A., 1981, Stratigraphy and origin of Neogene ash-flow tuffs on the north-central margin of the eastern Snake River Plain, Idaho: University of Colorado M.S. thesis, 74 p.

McIntyre, D. H., 1979, Preliminary description of Anschutz Federal No. 1 drill hole, Owyhee County, Idaho: U. S. Geological Survey Open-File Report 79-651, 14 p.

Morgan, W. J., 1972, Convection plumes and plate motions: American Association of Petroleum Geologists Bulletin, v. 56, p. 203-213.

Smith, R. B., 1977, Intraplate tectonics of the western North American Plate: Tectonophysics, no. 37, p. 323-336.

_____, 1978, Seismicity, crustal structure, and intraplate tectonics of the interior of the western Cordillera, *in* R. B. Smith and G. P. Eaton, editors, Cenozoic Tectonics and Regional Geophysics of the Western Cordillera: Geological Society of America Memoir 152, p. 111-144.

Smith, R. B. and R. L. Christiansen, 1980, Yellowstone Park as a window on the Earth's interior: Scientific American, v. 242, p. 104-117.

Spear, D. B. and J. S. King, 1982, Geology of Big Southern Butte, Idaho, *in* Bill Bonnichsen and R. M. Breckenridge, editors, Cenozoic Geology of Idaho: Idaho Bureau of Mines and Geology Bulletin 26.

Stanley, W. D., J. E. Boehl, F. X. Bostick, and H. W. Smith, 1977, Geothermal significance of magnetotelluric soundings in the eastern Snake River Plain-Yellowstone region: Journal of Geophysical Research, v. 82, p. 2501-2514.

Warner, M. M., 1975, Special aspects of Cenozoic history of southern Idaho and their geothermal implications: Geological Society of America, Abstracts with Programs, v. 7, no. 5, p. 649-650.

Wier, Stuart, 1979, Geomagnetic variation anomalies on the central Snake River Plain: EOS, American Geophysical Union, v. 60, no. 46, p. 944.

Zietz, Isidore, F. P. Gilbert, and J. R. Kirby, Jr., 1979, Aeromagnetic map of Idaho—color coded intensities: U. S. Geological Survey Geophysical Investigations Map GP-920, scale 1:1,000,000.

Zoback, M. L. and G. A. Thompson, 1978, Basin and range rifting in northern Nevada—clues from a mid-Miocene rift and its subsequent offsets: Geology, v. 6, p. 111-116.

Zohdy, A. A. R. and R. J. Bisdorf, 1980, Deep Schlumberger sounding for geothermal exploration at INEL, Snake River Plain, Idaho: Geophysics, v. 45, no. 4, p. 583-584.

Development of the Snake River Plain-Yellowstone Plateau Province, Idaho and Wyoming: An Overview and Petrologic Model

by

William P. Leeman[1]

ABSTRACT

The Snake River Plain-Yellowstone Plateau province is anomalous, compared with neighboring regions, in style and age progression of volcanism, crustal structure and other geophysical characteristics, and geological and structural evolution. Its development has been attributed to several general processes including (a) northerly extension coupled with crustal thinning (rifting), (b) migration of the continent over a stationary, deeply rooted melting anomaly (or hot spot), (c) propagation of a lithospheric fracture, possibly localized along a preexisting zone of weakness, or (d) passive deformation due to the cessation of subduction along the California coast and a reorientation of intraplate stresses.

A brief summary is given of the general geology, constraints on the stress field orientation, geophysical characteristics, and petrochemistry of volcanic rocks associated with the province. In combination with geological information, such features as (a) anomalously high $^3He/^4He$ ratios, (b) apparent transient uplift, (c) seismic wave attenuation characteristics, and (d) high heat flow associated with the Yellowstone Plateau suggest that this volcanic area is a focal point of large-scale magmatism in the underlying mantle and crust. The documented northeastward migration of bimodal basalt-rhyolite volcanic centers along the Snake River Plain at an apparent average rate of 3 to 4 centimeters per year, the inferred orientations of regional and local stress fields, and the geophysical evidence for large-scale reconstitution of the crust favor an origin of the province as the result of the North American plate passing over a stationary Yellowstone-like magmatic focus (hot spot) which is rooted at least several hundred kilometers below the surface. A petrologic model is presented to account for the general temporal and spatial progression of volcanism and crustal deformation and modification. The available evidence is not considered consistent with formation of the province as a typical crustal rift, although its westernmost physiographic arm (northwest trending) may have developed as a riftlike basin in response to southwesterly extension beginning in Miocene time. Sparse information on characteristics of crustal deformation and orientation of regional stresses seems less consistent with propagating fracture than hot spot models to account for development of the province.

[1]Department of Geology, Rice University, Houston, Texas 77001.

INTRODUCTION

The Snake River Plain is an arcuate depression of low topographic relief that extends more than 500 kilometers across southern Idaho and conspicuously truncates structural and geologic outcrop trends of the Basin and Range province and the northern Rocky Mountains. Geologic relationships and recent radiometric dating have demonstrated that since middle Miocene time the Snake River Plain-Yellowstone Plateau province has been characterized by voluminous bimodal rhyolite and basalt volcanism that has progressed eastward with time from the Owyhee Plateau (Ekren and others, 1982 this volume) and is now focused at Yellowstone National Park (Figure 1). It was early recognized that the physiographic western Snake River Plain is a grabenlike structure bounded by northwest-trending en echelon normal faults (Malde, 1959, 1965), although part of the southwest margin is apparently downwarped (McIntyre, 1972). The central and northeast-trending eastern Snake River Plain has been interpreted as a structural downwarp (Kirkham, 1931a) based on inward dipping attitudes of volcanic and sedimentary rocks along its margins and the paucity of evidence for bounding faults. In contrast to the apparent subsidence of the Snake River Plain proper, signif-

Leeman, W. P., 1982, Development of the Snake River Plain-Yellowstone Plateau province, Idaho and Wyoming: an overview and petrologic model, *in* Bill Bonnichsen and R. M. Breckenridge, editors, Cenozoic Geology of Idaho: Idaho Bureau of Mines and Geology Bulletin 26, p. 155-177.

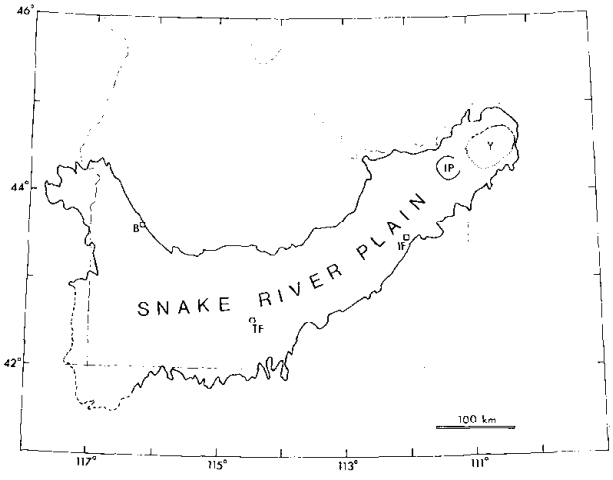

Figure 1. Index map for the Snake River Plain-Yellowstone Plateau province showing locations of Boise (B), Twin Falls (TF), Idaho Falls (IF), Yellowstone caldera (Y), and Island Park caldera (IP) for reference. The province boundary is broadly interpreted to include known or likely source areas for rhyolitic and basaltic volcanism characteristic of the province. The Owyhee Plateau (Ekren and others, 1982 this volume) is thus included.

icant uplift is occurring today in the vicinity of Yellowstone (Reilinger and others, 1977; Pelton and Smith, 1979, 1982). The nature and origin of this apparently anomalous region has long been a subject of debate.

Considering the apparent eastward propagation of volcanism and general increase in elevation toward Yellowstone, a number of authors (for example, Morgan, 1972; Smith and Sbar, 1974; Suppe and others, 1975) have suggested that at least the eastern Snake River Plain is the track of a deep mantle plume (or hot spot) over which the continent has migrated at a steady rate. It has also been proposed that the Snake River Plain is a zone of crustal extension (Hamilton and Myers, 1966) or an eastwardly propagating fracture (for example, Smith, 1977; Furlong, 1979) that may be localized by a zone of preexisting weakness in the crust (Eaton and others, 1975). Christiansen and McKee (1978) interpreted the Snake River Plain essentially as a "leaky transform" boundary that accommodates differential strain on either side and localizes the ascent of magma. The problem boils down to a choice between two general classes of models: (a) forceful upwelling of mantle material (and derivative partial melts) or (b) crustal extension accompanied by more passive upwelling of mantle material as the lithosphere is thinned (see Lachenbruch and Sass, 1978). The former process implies, as a driving force, some form of upward convective flow within the asthenosphere or deeper mantle, whereas the latter process more directly reflects the interactions between lithospheric plates.

Although it is difficult to resolve this dilemma, geological, geophysical, and petrological data provide useful constraints on the proposed hypotheses. This paper assesses the available observational data and discusses their implications for the origin and development of the Snake River Plain-Yellowstone Plateau province. In this paper it is assumed that the entire region characterized by post middle Miocene volcanism (as outlined in Figure 1) comprises a coherent petrologic-tectonic province. It is noted that this usage is broader than traditional views which have restricted discussion to the physiographic (topographically defined) Snake River Plain proper and its adjacent margins.

GENERAL GEOLOGY

Miocene and younger volcanic rocks of southern Idaho rest unconformably upon deformed or tilted sedimentary and plutonic rocks ranging in age from Precambrian to Mesozoic and upon faulted remnants of middle to late Eocene "calcalkalic" volcanic rocks (Ross, 1962; Axelrod, 1968; Armstrong, 1975; Armstrong and Hills, 1967). The presence of high-grade metamorphic rocks of Precambrian age beneath at least marginal parts of the Snake River Plain is inferred by the occurrence of such rocks as xenoliths in certain Snake River Plain lavas (Leeman, 1979, 1980). Continuation of the Idaho batholith beneath the western part of the plain was suggested by similar structural orientations of contact facies rocks exposed both north and south of the plain (Taubeneck, 1971). However, paleomagnetic data (Basham and Larson, 1978) for such rocks in southwest Idaho show that they have been tectonically rotated in a clockwise sense, in which case it is possible that they have been displaced horizontally by crustal rifting (see Hamilton and Myers, 1966).

The structural grain produced during Laramide mountain building and mid-Cenozoic basin and range block faulting is approximately north-south, nearly perpendicular to the axis of the Snake River Plain (Figure 2). Where older structures plunge beneath the plain on both sides, they show no evidence of deflection. Thus, there is no conclusive evidence that the Snake River Plain existed as a structural feature prior to Miocene time. A gap in the stratigraphic record in southern Idaho, lasting from late Eocene through early Miocene time, conspicuously separates Snake River Plain tectonic evolution from the earlier geologic history of the region. Further discussion is focused on middle Miocene and younger events. In

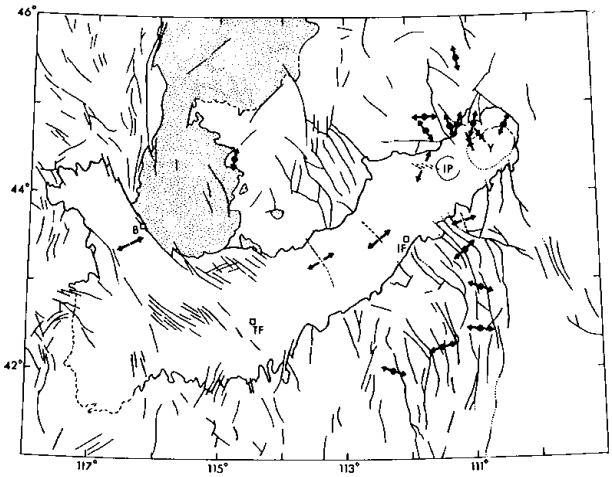

Figure 2. Major faults and inferred directions of extension based on fault-plane solutions (←●→) and orientations of rift zones (← →). Extension direction for western Snake River Plain is taken from Zoback and Thompson (1978), but components of Pliocene or younger horizontal slip deformation cannot be excluded (see Lawrence, 1976). Fault distribution is from the geologic map of the United States (U. S. Geological Survey). Major outcrops of Idaho batholith equivalent granitoid rocks are shown by stippled pattern.

all cases, chronostratigraphic assignments of Berggren (1972) are used.

WESTERN SNAKE RIVER PLAIN

In southwestern Idaho, middle Miocene (about 15-16 million years old) rhyolites (locally mineralized) and alkali basalts occur in the Owyhee Mountains (Pansze, 1972; Ekren and others, 1981, 1982 this volume). These rocks are dissimilar to those of the Snake River Plain in chemical and isotopic compositions (Leeman, unpublished data) and are probably more closely related to time-correlative volcanic rocks of the Oregon-Nevada Lineament (Stewart and others, 1975; Zoback and Thompson, 1978). Early members of the Columbia River Basalt Group (Swanson and others, 1979) are also time-correlative, but they are chemically distinct from basaltic rocks both from the Owyhee Mountains and the Snake River Plain province (for example, Powers, 1960). North and northwest of Boise, Columbia River basalt intertongues with lacustrine, volcaniclastic, and other sedimentary deposits of the Payette Formation which was deposited in a basin underlying part of the northwest-trending arm of the western Snake River Plain (Kirkham, 1931b).

Rhyolitic tuffs and ash flows, clastic sediments, and minor basaltic flows unconformably overlie the locally mineralized volcanic rocks and older rocks in highlands north and south of the Snake River Plain. Similar rocks are locally exposed along the Snake River canyon and its tributaries. The widely dispersed ash-flow tuffs likely were erupted from calderas that are now buried beneath younger deposits in the western Snake River Plain (Bonnichsen and others, 1975; Bonnichsen, 1982a this volume; Ekren and others, 1981, 1982 this volume). They range in age from about 15 to 11 million years (Armstrong and others, 1975, 1980; McKee and others, 1976). A complex stratigraphic sequence of fluvial and lacustrine sediments, locally containing abundant volcanic ash and interbedded basaltic lavas, was deposited in a subsiding basin. These units were named the Idaho Group by Malde and Powers (1962) who subdivided them into the Poison Creek Formation, Banbury Basalt, Chalk Hills Formation, Glenns Ferry Formation, and Bruneau Formation in ascending stratigraphic sequence. Detailed stratigraphic studies within the sediments (for example, Malde, 1972; Neville and others, 1979; Kimmel, 1979, 1982 this volume; Swirydczuk, 1980; Swirydczuk and others, 1982 this volume) supplemented by potassium-argon dating of interbedded ash layers and basalt flows (Armstrong and others, 1975, 1980; McKee and others, 1976; Evernden and others, 1964; Kimmel, 1979; J. D. Obradovich, quoted in Neville and others, 1979) indicate that these stratigraphic units are in part time-transgressive. Samples of Banbury Basalt from southwestern Idaho and northern Nevada and from the Mount Bennett Hills north of the Snake River Plain range in age from about 8 to 11 million years. Some of these basalts overlie the Poison Creek Formation, which in turn overlies Idavada ash-flow tuffs dated at about 11 million years. Basalt and two ash layers interbedded in the Chalk Hills Formation have been dated at 8.4, 8.7, and 7.0 million years, respectively. Uncertainties on all of these ages are about ±1 million years. Glenns Ferry basalts and ash layers yield potassium-argon ages that are somewhat discordant, but the most reliable values fall between 3 and 4 million years and are consistent with vertebrate fossil age assignments and paleomagnetic stratigraphy (Neville and others, 1979). Detailed sediment facies studies (see Swirydczuk, 1980; Swirydczuk and others, 1982 this volume) and correlations of distinctive interbedded ash layers indicate the time equivalence of upper Poison Creek-lower Chalk Hills and upper Chalk Hills-lower Glenns Ferry strata and a southward transgression of sediment facies which suggests progressive subsidence of the southwestern edge of the western Snake River Plain basin. A number of basalts assigned to the Banbury Formation in the Hagerman-Glenns Ferry area (see Malde and others,

1963; Malde and Powers, 1972) yielded potassium-argon ages in the range of those in the Glenns Ferry Formation. If these age determinations are accurate, it appears that the Banbury Formation is also eastwardly time-transgressive and may span most of Idaho Group time. The Bruneau Formation consists largely of lake and stream sediments and intercalated basalt flows. This unit accumulated after an erosional gap and deposition of the Tuana Gravel (Malde and Powers, 1962). Several of the basalts yielded consistent potassium-argon ages of about 1.4 million years, and all are characterized by reversed magnetic polarity (Cox and others, 1965; Armstrong and others, 1975). A large number of Bruneau-age shield volcano vents occur near the southern front of the Mount Bennett Hills from Mountain Home to the Twin Falls area and in the graben of Camas Prairie north of the Mount Bennett Hills. This apparently marks a northward shift of major basaltic vent activity as pre-Bruneau vents are concentrated south of the Snake River (Malde and others, 1963). Basaltic lavas and sediments assigned to the Bruneau Formation in the eastern Mount Bennett Hills and Bellevue areas (Schmidt, 1961; Malde and others, 1963; Smith, 1966) are probably somewhat younger than those to the southwest as a number of the lavas are characterized by normal magnetic polarity and intertongue with glacial outwash sediments (Leeman, 1982d this volume).

Deposition of the Snake River Group, a sequence that includes a number of upper Pleistocene formations (Stearns and others, 1938; Malde and Powers, 1962; Malde, 1971a), followed another break in the stratigraphic record of the western Snake River Plain marked by erosion, deposition of the Black Mesa Gravel, and renewed downcutting. All of the basaltic lavas in this unit are very young, and most are characterized by normal magnetic polarity. Potassium-argon and carbon-14 dating reveal that virtually all of these lavas are less than 0.7 million years old (Armstrong and others, 1975; Kuntz and Dalrymple, 1979; Kuntz and others, 1980a, 1980b, 1982 this volume). Vents for these basalts are nearly all located east of longitude 114° W (near Twin Falls); however, small isolated lava flows have issued from vents along the southern margin of the Idaho batholith and from numerous vents in a small lava field (Smith Prairie) along the Boise River (Howard and Shervais, 1973). The bulk of Snake River Group volcanism was concentrated in the eastern Snake River Plain.

Volumes of volcanic rocks in the western Snake River Plain are difficult to assess due to limited deep exposures and complex lateral variations in thickness. Oil and geothermal test wells penetrated several hundred meters of sediment which was underlain by up to 2 kilometers of interbedded basalt flows and sediments. Some deep holes (for example, Griffith "Bostic 1-A") bottomed in silicic volcanic rocks at depths near 3 kilometers (Malde, 1959; Arney and others, 1980), and one (Anschutz "6013 Federal"), 70 kilometers south of Boise, reached granitic basement at a depth of 3.4 kilometers (McIntyre, 1979). At the surface silicic volcanic rocks are more voluminous than basaltic lavas in this part of the plain (Ekren and others, 1982 this volume; Bonnichsen, 1982 this volume), but quantitative volume estimates are not available.

EASTERN SNAKE RIVER PLAIN

Older volcanic rocks of the eastern Snake River Plain are exposed locally in highlands along its margins. These rocks have been studied in detail along the southern and eastern boundaries (Mansfield, 1927; Carr and Trimble, 1963; Trimble, 1976; Trimble and Carr, 1976; Prostka and Embree, 1978; Williams and others, 1982 this volume; Embree and others, 1982 this volume), in extrusive dome complexes within the Snake River Plain (Kuntz, 1978; Kuntz and Dalrymple, 1979; Spear, 1979; Spear and King, 1982 this volume), in the Idaho National Engineering Laboratory site (near Arco), and in the Island Park-Yellowstone areas (Stearns and others, 1939; Hamilton, 1965; Christiansen and Blank, 1972; Christiansen, 1982 this volume, in press).

Silicic volcanic sequences (Starlight and Salt Lake Formations) are similar to those in the western Snake River Plain but are somewhat younger and not as steeply dipping into the plain. The oldest dated rhyolitic tuffs and domes between Twin Falls and Idaho Falls are about 10 million years old, and the youngest widespread ash flow (Walcott Tuff) is about 6.2 million years old. Minor basalt flows are interbedded with Starlight Formation tuffs near American Falls, and basalts from the Massacre Volcanics (Carr and Trimble, 1963) are dated as about 6.3 million years old (Armstrong and others, 1975). Somewhat younger tuffs (less than 5 million years old) along the eastern and northern margins of the Snake River Plain apparently were derived from the Rexburg caldera complex (Prostka and Embree, 1978; Embree and others, 1982 this volume), and highlands at the northeast end of the Snake River Plain are blanketed by deposits of the Yellowstone Tuffs (major eruptions at about 2, 1.2, and 0.6 million years ago).

The Island Park caldera and Yellowstone Plateau are volcanic highlands consisting largely of rhyolite welded tuffs and flows with only minor basaltic lavas. Major ash-flow tuff eruptions at the aforementioned times were associated with caldera collapse events

and were subsequently followed by extrusion of massive rhyolite flows, the youngest only 0.07 million years ago (J. D. Obradovich, in Christiansen and Blank, 1972).

As noted earlier, most basaltic lavas in the eastern Snake River Plain and Yellowstone Plateau largely are correlative with the Snake River Group in the west-central plain. Vents for these lavas are widely distributed (LaPoint, 1977); however, a constructional topographic high that is more or less axial symmetric to the eastern Snake River Plain (Stone, 1969) may represent a zone of especially voluminous eruptive activity. Locally, the thickness of Pleistocene and younger basalts (with minor interbedded sediments) exceeds 1 kilometer as inferred from drilling (see Walker, 1964; Doherty and others, 1979; Kuntz and others, 1980b) and electrical sounding methods (Zohdy and Stanley, 1973).

In summary, geological and geochronological data document an eastward transgression of Snake River Plain volcanism as illustrated in Figure 3. The facies concept outlined by Armstrong and others (1975) holds in a general way as follows. An early silicic volcanic facies, consisting of volcaniclastic sediments, air-fall and ash-flow rhyolite tuffs, rhyolite flows, and subordinate basaltic flows and pyroclastic deposits, marks the inception of volcanic activity. This facies is typified today by the Yellowstone-Island Park volcanic field where the silicic volcanic rocks are clearly associated with large calderas. A younger facies composed of basaltic lavas with some interbedded sediment and a few rhyolite flows and domes overlaps the early facies everywhere in the Snake River Plain proper. Contemporary examples of this facies are found from Twin Falls to the Rexburg area. An uppermost facies consists of continental sediments with subordinate basaltic lavas and distal rhyolitic ash-flow or air-fall deposits; rhyolite flows and domes are distinctly lacking. This facies is represented mainly in the western Snake River Plain. From earlier discussion, it is clear that these generalized facies are time-transgressive toward the east. However, the transgression is not smooth. Rather, the "volcanic front" appears to have shifted eastward in irregular jumps, but these are not well quantified owing to uncertainties in the locations of source areas for many of the dated rocks (especially ash-flow tuffs). Despite these uncertainties, an average eastward shift of silicic volcanic centers is estimated at about 3 to 4 centimeters per year.

Finally, there appear to be significant differences in the history of the western and eastern parts of the Snake River Plain. In the west there is an elongate topographic low: (a) that has a northwesterly trend somewhat analogous to trends for the Northern Nevada Rift and Columbia River basalt feeder dikes (Zoback and Thompson, 1978); (b) that is bounded by pronounced northwest-trending normal fault zones (Figure 2); (c) that was a structural basin as early as middle Miocene time (about 15 million years ago) and has accommodated cumulative subsidence probably in excess of 3 kilometers (Malde, 1959; Stone, 1967); and (d) that contains a great thickness of continental sediment, silicic volcanic rocks, and subordinate basalt. South of this basin (the physiographic Snake River Plain), on the Owyhee Plateau, is a northward tilted block of mainly Miocene-Pliocene silicic volcanic rocks which rest in places on older basement rocks. Several calderas have been inferred in this part of the petrologic province. Little basalt is present in this area (Ekren and others, 1982 this volume). The eastern Snake River Plain (a) trends northeasterly, (b) exhibits only minor fault control along its margins, (c) has subsided little compared

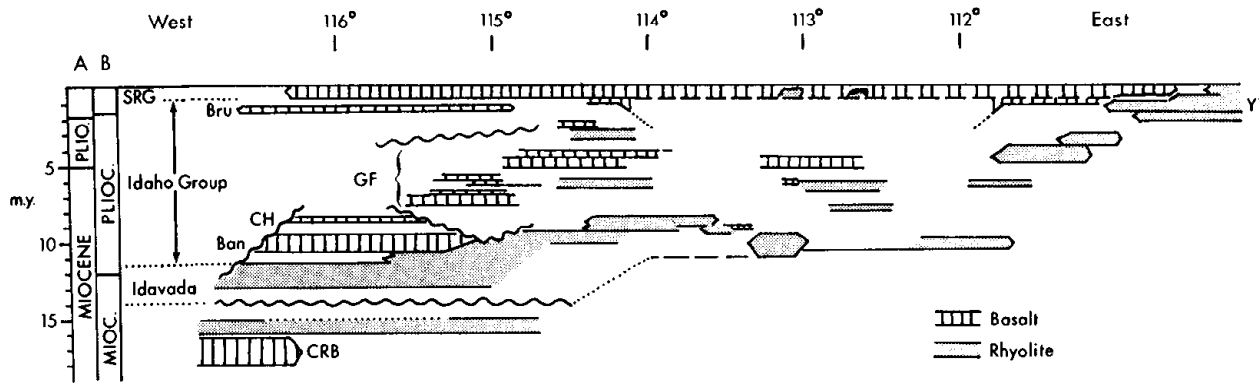

Figure 3. Potassium-argon ages of volcanic rocks as a function of each sample's longitudinal position (after Armstrong and others, 1975, with updates as noted in text). This figure gives a simplified view of stratigraphic relations and time-transgressive history of volcanic events. For reference, two stratigraphic scales are shown, namely those of (A) Berggren (1972) and (B) Evernden and others (1964). Selected stratigraphic units are indicated as follows: Snake River Group (SRG), Bruneau (Bru), Glenns Ferry (GF), Chalk Hills (CH), and Banbury (Ban) Formations, Yellowstone Tuff (YT), and Columbia River basalt age-equivalent rocks (CRB).

with the topographic basin of the western Snake River Plain and is actually rising near its eastern tip, and (d) contains a substantial volume of silicic and basaltic volcanic rocks with relatively minor sediment, except along its margins where drainages emerge from the neighboring highlands.

SEISMICITY AND FAULTING

Studies of contemporary seismicity and faulting provide useful constraints on present-day stress orientations and on possible modes of deformation associated with the Snake River Plain-Yellowstone Plateau province. Virtually all recorded seismicity in the region is concentrated west and northwest of Yellowstone caldera along an east-west (Centennial) zone, and south of the caldera along a north-south (Teton) zone (Trimble and Smith, 1975; Smith and others, 1977). Maximum focal depths and frequency of earthquakes decrease markedly within the caldera. Fault plane solutions indicate general north-south extension immediately west of the caldera, possible radial compression near the western caldera rim, and northeast to southeast extension at different localities south of the caldera (Figure 2). Many of the recorded earthquakes appear to be spatially related to known faults, some of which appear to be reactivated older structures (for example, Teton fault; Love and others, 1972) that predate Yellowstone Plateau volcanism. Fault plane solutions for other earthquakes in the region are compatible with generally east-west extension in the northern Rocky Mountains and Intermountain seismic belt of southeastern Idaho (Smith and Sbar, 1974; Trimble and Smith, 1975; Friedline and others, 1976; Smith, 1977; Smith and Lindh, 1978). Thus the stress field near and west of Yellowstone is somewhat anomalous and probably is related to recent uplift in that area (Reilinger and others, 1977). Radial compression near Yellowstone caldera may be associated with ongoing rapid uplift within the caldera (Pelton and Smith, 1979) that probably reflects shallow movement of magma. The Snake River Plain proper appears to be aseismic at present (Pennington and others, 1974). If deformation is occurring there, it must be accommodated by essentially ductile flow or creep strain.

Estimates of stress orientations within the Snake River Plain can be obtained only indirectly. Although no major faults have been recognized in the central and eastern plain, Recent basaltic rift zones trend nearly perpendicular to its axis (Prinz, 1970; Kuntz and others, 1980a, 1980b, 1982 this volume; Kuntz and Dalrymple, 1979; LaPoint, 1977). Assuming that such rifts manifest dikelike feeder conduits, Weaver and others (1979) and Zoback and Zoback (1980) inferred that the direction of maximum extension must parallel the axis of the plain (Figure 2). If this inference is valid the modern extension direction (roughly northeasterly) is consistent with that associated with the mid-Miocene Northern Nevada Rift (Zoback and Thompson, 1978). It is not coincident with the inferred extension direction (northwesterly) for the Basin and Range province during latest Cenozoic time (Zoback and Thompson, 1978; Wright, 1976) but seemingly is consistent within uncertainties with the regional fault plane solution data summarized above.

The volcanic rift zones commonly are oriented along extensions of range front faults in areas adjoining the eastern Snake River Plain and in some cases (for example, areas near Craters of the Moon, Rexburg, and Island Park) along inferred caldera structures (Stone, 1969; Kuntz, 1977, 1979; Kuntz and Dalrymple, 1979). If rift orientations are indeed controlled in part by such older structures, it remains likely that a significant component of east-west extension is still required to reactivate the old structures. Displacements of this sense that are contemporaneous with or younger than development of the Snake River Plain have been documented for range front faults north and south of the eastern plain (Malde, 1971b; Cline and Niccum, 1978; Allmendinger, 1979). The latter two references also document small dip-slip displacements on cross-range faults that parallel margins of the eastern Snake River Plain; these faults may accommodate minor subsidence of the plain. However, there is no evidence for alignment of volcanic vents parallel to the margins. Finally, in some parts of the western Snake River Plain (for example, the Magic Reservoir and Bruneau-Jarbidge areas), basaltic vents conform to a pattern of northwest-trending en echelon faults that is also consistent with northeasterly extension (Stone, 1969). No evidence exists in the western Snake River Plain for control by transverse subjacent structures. It is tentatively concluded that the least principal stress direction has remained roughly southwest-northeast for the Snake River Plain and adjacent areas since the inception of the Snake River Plain-Yellowstone Plateau province and at least as far back as about 17 million years ago when the Northern Nevada Rift formed.

GEOPHYSICAL CHARACTERISTICS

Geophysical characteristics of the Snake River Plain-Yellowstone Plateau province are reviewed by Mabey (1982 this volume), so only a brief summary

of relevant observations is given here. Of particular importance are the structure and composition of the underlying crust. Seismic refraction studies reveal that the entire Snake River Plain is underlain by anomalously thick (about 40 kilometers) crust compared with that beneath the northern Basin and Range and Colorado Plateau provinces (see Figure 4). The lower crust layer is anomalously thick, whereas the upper crust is everywhere anomalously thin beneath the plain. In detail, it appears that upper crustal rocks thicken eastward toward Yellowstone at the expense of the lower crustal layer (Figure 4). P-wave velocities in the underlying mantle are slightly low (about 7.9 to 8.0 km/sec) compared with those for typical subcontinental mantle (for example, Hill and Pakiser, 1967; Braile and others, 1982; Sparlin and others, 1982), and S-wave velocities in the deep crust and upper mantle beneath the eastern Snake River Plain and Yellowstone Plateau are also anomalously low (Greensfelder and Kovach, 1982; Priestley and Orcutt, 1982; Daniel and Boore, 1982). Teleseismic P-wave delay studies (Hadley and others, 1976; Iyer, 1979; Evans, 1982) show that the easternmost Snake River Plain and Yellowstone Plateau are underlain by anomalously low-velocity mantle to depths of about 250 kilometers; attenuation of P-waves is greatest (5-15 percent) below Yellowstone Plateau but is still appreciable (about 3 percent) beneath the northeastern Snake River Plain.

Gravity and aeromagnetic data for the Snake River Plain-Yellowstone Plateau province further indicate the anomalous nature of the underlying crust

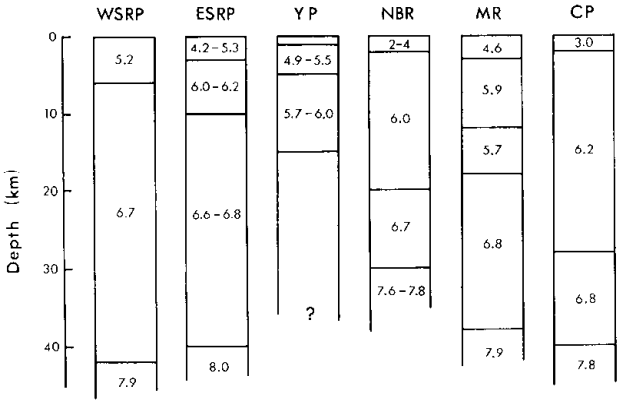

Figure 4. Comparative crustal structure for western Snake River Plain (WSRP), eastern Snake River Plain (ESRP), Yellowstone Plateau (YP), northern Basin and Range province (NBR), Middle Rocky Mountains (MR), and Colorado Plateau (CP). Mean P-wave velocities inferred for layers are given in kilometers per second. References are as follows: WSRP and NBR (Hill and Pakiser, 1967), ESRP (Akermann, 1979; Olsen and others, 1979; Smith and others, 1979), YP (Schilly and others, 1979), MR (Braile and others, 1974), CP (Keller and others, 1975).

and mantle (Mabey, 1976, 1978, 1982 this volume; Eaton and others, 1975; Smith and others, 1977). The overall positive Bouguer gravity high over the Snake River Plain reflects the thinned upper crust. Yellowstone Plateau is characterized by a negative Bouguer gravity anomaly and apparently is not isostatically compensated (Eaton and others, 1975); this anomaly may be related in part to the presence of a low-density magma body at shallow crustal depths. This conclusion is supported by recent seismic studies in the vicinity of Yellowstone National Park (Lehman and others, 1982; Schilly and others, 1982).

The geophysical data further emphasize a distinction between the eastern and western Snake River Plain. Several positive Bouguer anomaly ridges roughly parallel the axis of the grabenlike western Snake River Plain and suggest thick accumulations of dense lavas or intrusive rocks in the upper crust. Subsidence of this area seems required to account for its approximate isostatic equilibrium (Mabey, 1976, 1982 this volume). A large magnetic intensity high is localized along the southwest margin of this basin. This feature apparently reflects a subsurface accumulation of igneous rocks having high magnetic susceptibilities. However, the magnetic and gravity highs are not superimposed. The magnetic anomaly has been attributed to a thick subsurface accumulation of Columbia River basalt (Mabey, 1976), Eocene Challis Volcanics basement (Mabey, 1982 this volume), or mid-Miocene volcanic rocks related to the Northern Nevada Rift (Zoback and Thompson, 1978). Also, stratigraphic and structural evidence is compatible with subsidence of the southwest margin of the physiographic western Snake River Plain where basaltic feeder vents and flows may be localized. Present data are inadequate to resolve the source of the magnetic anomaly.

The eastern Snake River Plain is characterized by a complex configuration of gravity and magnetic highs and lows most likely related to variations in the thickness and distribution of volcanic rocks, sediments, and underlying basement rocks. Pronounced short-wavelength gravity or magnetic anomalies like those in the western plain are not observed. However, a broad axial Bouguer gravity high over the eastern plain, coupled with apparent isostatic equilibrium of this area, indicates the presence of dense compensating material (mafic intrusions?) at deep crustal levels (Mabey, 1978). Gravity and magnetic signatures characteristic of adjoining structural provinces are not observed over the plain. If pre-Snake River Plain crustal rocks underlie the eastern plain they apparently have been thinned or disrupted.

Several lines of evidence, other than obvious volcanism, indicate a marked thermal disturbance beneath the Snake River Plain-Yellowstone Plateau

province. Near-surface heat flow typically exceeds normal continental values in and adjacent to the Snake River Plain (particularly when heat loss to the Snake River Plain aquifer is considered), and it is exceptionally high at Yellowstone where convective heat transfer is associated with ongoing magmatism and hydrothermal activity (Brott and others, 1978, 1981; Morgan and others, 1977; Fournier and others, 1976). Regional circulation of cold ground water in shallow aquifers within the Snake River Plain apparently reduces near-surface geothermal gradients, so heat flow measurements there probably represent lower limit values. Accordingly, the observed high regional heat flow represents a significant thermal perturbation within the crust and upper mantle. Assuming that emplacement of large heat sources (mafic intrusions) beneath the Snake River Plain caused the perturbation and that such intrusive events propagated eastward toward Yellowstone with time, Brott and others (1978, 1981) have shown that the predicted heating and cooling effects in the crust are consistent with changes in regional elevation and with available heat flow data. In their model, initial intrusion promoted thermal expansion of mantle and crustal rocks and caused topographic uplift analogous to that near Yellowstone (Suppe and others, 1975; Reilinger and others, 1977; Pelton and Smith, 1979, 1982). Also, aseismic subsidence of the Snake River Plain can be interpreted as a thermal contraction phenomenon.

Anomalously high geothermal gradients beneath the eastern Snake River Plain and Yellowstone Plateau are revealed by other geophysical investigations. Magnetotelluric and magnetic variometer soundings (Stanley and others, 1977; Fitterman, 1979; Wier, 1979) suggest an eastward-shoaling conductive layer beneath the eastern Snake River Plain and Yellowstone Plateau. Stanley and others (1977) estimate depths to the 900° C isotherm of about 35 kilometers beneath the east-central Snake River Plain and about 25 kilometers below Yellowstone Plateau. Although these estimates are somewhat model dependent, they are qualitatively supported by estimates of depth to the Curie isotherm (about 570° C) of about 5 to 13 kilometers below Yellowstone caldera and about 20 kilometers outside the caldera (Bhattacharyya and Leu, 1975; Smith and others, 1977).

PETROCHEMISTRY OF SNAKE RIVER PLAIN-YELLOWSTONE PLATEAU VOLCANIC ROCKS

In any given area, Snake River Plain-Yellowstone Plateau volcanism was initiated with voluminous eruptions of pyroclastics, ash-flow tuffs, domes and lava flows of high-silica peraluminous rhyolite, and only minor interbedded basaltic lavas. With time the rhyolitic volcanism declined in intensity and was followed by sporadic outpourings of olivine tholeiitic basalt flows and pyroclastics. Intermediate composition volcanic rocks are notably rare, except for local and volumetrically minor occurrences of mixed rhyolite-basalt lavas (for example, Fenner, 1938, 1944; Wilcox, 1944) and strongly differentiated or contaminated hybrid lavas. Petrologic details of the olivine tholeiites, hybrid lavas, and rhyolites are summarized elsewhere in this volume (Bonnichsen, 1982b; Bonnichsen and Citron, 1982; Christiansen, 1982; Ekren and others, 1982; Leeman, 1982a, 1982b, 1982c).

The basaltic lavas are classified as olivine tholeiites on the basis of their normative compositions (ol- and hy-bearing); yet in certain other respects (for example, alkali-silica relationships and compositions of groundmass pyroxenes) they may be considered transitional between tholeiitic and mildly alkaline basalts (Leeman and Vitaliano, 1976), and a few samples actually contain small amounts of normative nepheline (Stout and Nicholls, 1977; Leeman, unpublished data). Collectively, the basalts are relatively uniform in composition compared with those from many other flood basalt provinces. However, they display significant ranges in certain element contents (especially trace elements) that reflect the roles of varied degrees of partial melting and fractional crystallization in their petrogenesis. A minor variant of these basalts is relatively high in Al_2O_3, MgO, and CaO and low in TiO_2 and K_2O; these rocks not only are most commonly associated with early rhyolitic volcanism but also are found among the youngest phases of basaltic activity. Worldwide, Snake River Plain-Yellowstone Plateau basalts most closely resemble certain olivine basalts from Iceland, the Hebridian province of Britain, and the Afar triangle (see Leeman, 1982a this volume). In detail, however, no exact analogs are known for the Snake River Plain-Yellowstone Plateau basalts; for example, their systematically high P_2O_5 contents (average 0.6 weight percent) are distinctive.

The rhyolites appear to be remarkably similar in major-element composition, particularly when highly porphyritic variants are excluded. This fact is emphasized by the compositional uniformity of obsidians, crystal-poor vitrophyres, and glasses from more crystal-rich samples (Leeman, 1982c this volume). These data are compatible with the derivation of the rhyolitic magmas as so-called "minimum melts" (as in the quartz-albite-orthoclase system, Tuttle and Bowen, 1958) of crustal source rocks (Wyllie, 1977) or with the homogenization of these

magmas in crustal reservoirs. Given their wide temporal and spatial distribution, a reproducible set of mechanisms seems required to produce the rhyolitic magmas. In detail, the petrogenesis of these magmas must be complex. Isotopic and trace element studies (Doe and others, 1982; Leeman, unpublished data) show that at Yellowstone a number of factors are involved, including vapor/crystal/liquid fractionation, interaction between the magmas and crustal wall rocks or hydrothermal fluids, and complexities of the partial melting process (varied source rock compositions and degrees of melting, for example). In addition, density- and diffusion-controlled stratification (see Hildreth, 1979; Rice, 1981), magma mixing, and perhaps other processes are probably important within the crustal magma chambers and conduits. Volume relations between erupted rhyolite and basalt and the petrochemical data for these rocks seemingly preclude a derivation of the rhyolitic magmas from basaltic parental magmas (for example, by crystal fractionation or silicate liquid immiscibility). Various lines of evidence, including lead and strontium isotopic data, indicate distinct sources for the two magma types (Leeman and Manton, 1971; Doe and others, 1982; Leeman, unpublished data). It is likely that the rhyolite parental magmas formed by crustal anatexis as a consequence of the emplacement of large volumes of basaltic magma into the crust (see Lachenbruch and others, 1976; Eichelberger and Gooley, 1977; Baker and others, 1977; Duffield and others, 1980; Christiansen, in press).

The hybrid lavas (Leeman and others, 1976; Leeman, 1982b this volume) are demonstrably formed in part as the result of rather extreme degrees of fractional crystallization of more mafic parental magmas—probably of olivine tholeiite composition. On the basis of textural and isotopic evidence, and the presence of crustal xenoliths in some cases, it is suggested that such magmas were contaminated to varied degrees by crustal material. In this paper, the hybrid magmas are viewed as the consequence of complicated evolution of tholeiitic magmas that ascended slowly through, and perhaps stagnated within, the crust. Under conditions envisaged to attain in the crust during Snake River Plain-Yellowstone Plateau magmatism, the mixing of magmas derived by both mantle and crustal anatexis and subsequent crystallization and contamination of such magmas seems inevitable.

In summary, Snake River Plain-Yellowstone magmatism is considered to be "fundamentally basaltic" (Christiansen and Lipman, 1972) in that the injection of massive volumes of basaltic magma seemingly can explain the general sequence of magmatic events. The following section presents a conceptual model for development of the Snake River Plain-Yellowstone Plateau province. This model is an attempt to unify the petrologic, geologic, and geophysical evidence presented earlier.

PETROLOGIC-GEOLOGIC MODEL

A schematic time-lapse view is given in Figure 5 for a typical cross-section perpendicular to the Snake River Plain-Yellowstone Plateau axis. Panels A through D, respectively, may be considered roughly correlative with the area immediately northeast of Yellowstone Plateau (A and B?), Yellowstone Plateau proper (C), and the eastern Snake River Plain (D). The western Snake River Plain is considered to have passed through all four stages and is now characterized by waning stages of basaltic volcanism and advanced stages of subsidence as isostatic compensation is approached. The model resembles aspects of similar models proposed by Gill (1973), Eichelberger and Gooley (1977), Fedotov (1975, 1981), and Cox (1980), among others. It is essentially based on the concept that magmas ascend primarily due to bouyancy effects which are influenced by lithostatic load (that is, density structure of crust and mantle).

STAGE A—INCIPIENT BASALT ASCENT

Regardless of its origin, primitive (picritic?) basaltic magma formed in the mantle will tend to ascend because it is less dense (2.8-3.0 g/cc or less, after the method of Bottinga and Weill, 1970) than mantle rocks (peridotites, pyroxenites, eclogites). Whether such magma erupts at the surface depends on several factors including the density structure of crust and mantle, depth to the zone of magma segregation, and mode of ascent. Because basaltic magma is denser than continental upper crustal rocks, the magma column must extend to sufficient mantle depths to provide adequate hydrostatic pressure for it to reach the surface. Alternatively, ascent of magma in the form of discrete blebs would lead to its stagnation at depths where the wall rocks had comparable densities—for example, at the base of or within the lower crust (Gill, 1973; Fedotov, 1975). Neglecting the magma pressure required to develop feeder conduits (that is, yield strength of crustal and mantle rocks) and assuming a reasonable density structure for either the western Snake River Plain or the middle Rocky Mountains (Figure 4), the minimum depth of segregation for magma with a density of 3.0 g/cc is at least 65 kilometers in order for such magma to reach the surface. Consideration of yield

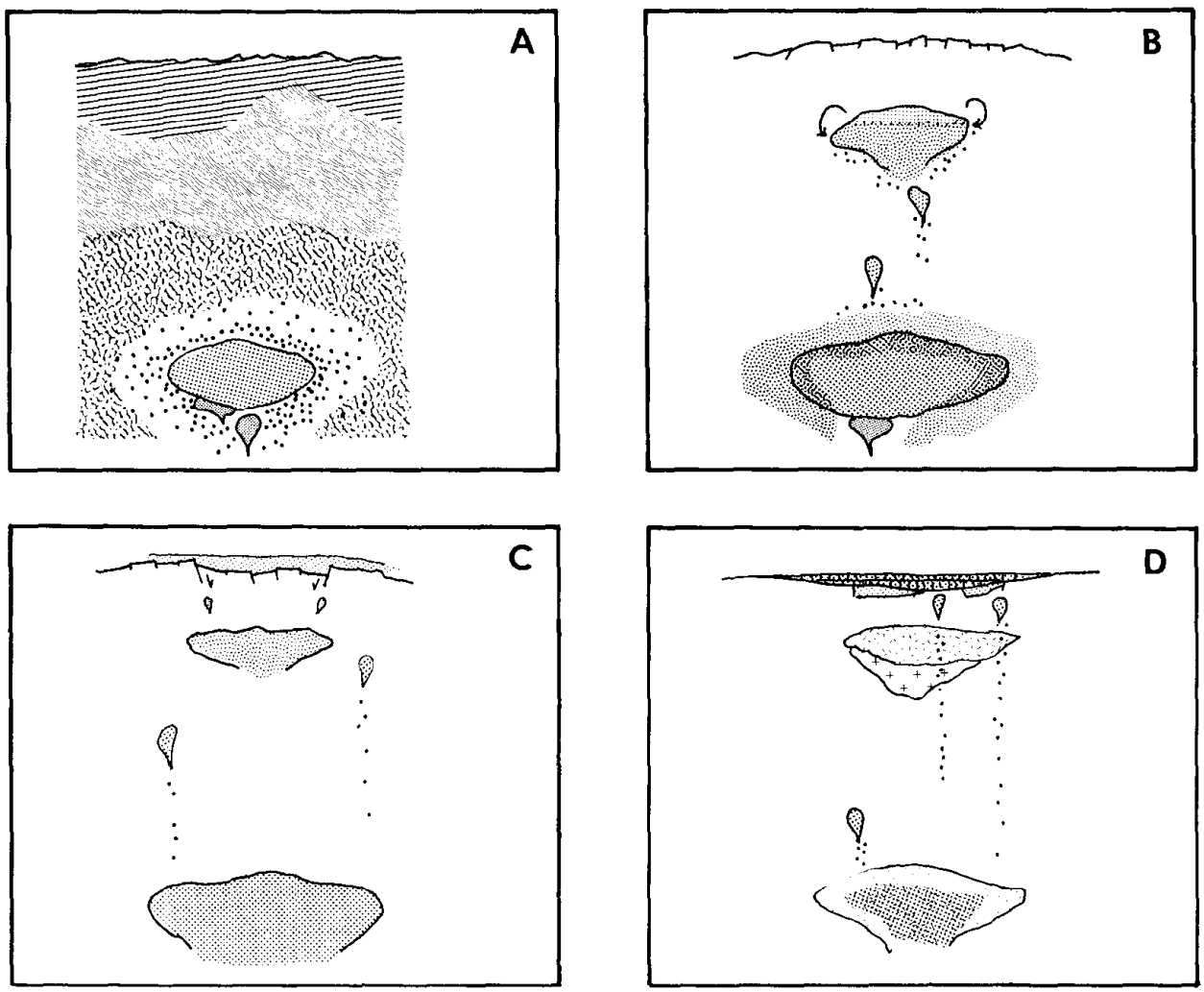

Figure 5. Cartoon of proposed petrologic model for the Snake River Plain-Yellowstone Plateau province. A. Incipient basalt ascent and stagnation in the deep crust where anatexis occurs (dotted zone around stippled magma body); B. Formation and segregation of crustal anatectic melts (fine stippling) to form vertically zoned high-level silicic magma body, with tumescence of crust, and possible hydrothermal circulation (arrows); C. Predominantly rhyolitic volcanism fed from high-level magma body, with ash-flow tuff eruptions associated with caldera collapse, and minor basalt extrusion peripheral to silicic volcanic centers; D. Predominantly basaltic volcanism fed from deep-crustal or upper mantle magma bodies; magmas ascend through solidified silicic plutons; deep magma body progressively solidifies and crust gradually subsides as it moves away from principle melting anomaly. See text for further details. Scale is not given, but depths of about 40 kilometers and 10 kilometers to the mafic and silicic magma bodies, respectively, seem reasonable. Horizontal scale for mafic magma body and its anatectic aureole may be about 100 kilometers. Patterned layers in panel (A) are intended only to represent schematically from bottom to top: (1) lower crust igneous and metamorphic rocks, (2) crystalline basement rocks of the upper crust, and (3) chiefly sedimentary and volcanic rocks of the upper crust. For clarity such layers are not indicated in the other panels.

strength would require a greater minimum depth of segregation, but this factor is offset to some degree if lower magma densities are assumed (Figure 6).

In a given area, initial basaltic magmas probably stagnate in the deep crust because of hydrostatic, structural, or thermal factors (see Cox, 1980). However, repeated influx of basaltic magma leads to the development of a large lenticular magma chamber or perched sill-like bodies. In this manner the lower crust could be gradually thickened (under- or intraplating). Progressive solidification of these intrusions would form layers of dense cumulate rocks and more fractionated residual basalt magma. At the same time conductive and convective transfer of heat to the wall rocks would promote their partial fusion. Under favorable conditions (for example, high initial temperature of wall rocks), as much as one part anatectic melt could form for each part of basaltic magma

intruded (Hodge, 1974; Younker and Vogel, 1975).

STAGE B—SEGREGATION OF CRUSTAL MELTS

The aureole of partly fused wall rocks would enlarge with time and continued influx of mafic magma. Partial melts (intermediate to silicic magma) of deep crustal rocks (mafic to silicic granulites; amphibolites at shallower depths) expectedly would be more felsic and less dense than basaltic magmas or refractory residual restites and would tend to coalesce and ascend higher in the crust to form high-level magma chambers. Intermediate to silicic composition magmas in these chambers would further differentiate and interact with upper crustal wall rocks and possibly with hydrothermal fluids in upper apophyses. A plexus of magma reservoirs and feeder conduits could characterize much of the crust at this stage, and opportunities for magma mixing, polybaric crystallization, and crustal contamination could be rife. Ascending magmas gradually elevate crustal temperatures, and the resulting thermal expansion causes regional uplift that is not isostatically compensated. Also, continued influx of basaltic magma and partial melting gradually modify the composition of the deep crust, making it more mafic and more dense.

STAGE C—PREDOMINANTLY RHYOLITIC VOLCANISM

Vigorous rhyolitic volcanism is inferred to be associated with the development and evolution of shallow silicic magma bodies like those postulated to exist below Yellowstone. The relative compositional uniformity of Snake River Plain-Yellowstone Plateau rhyolites could be attributed to homogenizing convection processes occurring in high-level reservoirs (see R. L. Smith, 1979). On the other hand, individual Snake River Plain-Yellowstone Plateau ash-flow tuffs display compositional zoning (Hildreth and others, 1980; Christiansen, in press) analogous to, though less pronounced than, that in the Bishop Tuff and other ignimbrites (Hildreth, 1979; R. L. Smith, 1979). Accordingly, the high-level reservoirs probably developed some degree of compositional stratification. It is noteworthy that ash-flow tuffs in the Bruneau-Jarbidge and Owyhee Plateau areas apparently do not display significant compositional zoning (Bonnichsen, personal communication, 1982). Explosive eruptions of voluminous ash-flow tuffs, accompanied by caldera collapse and followed by

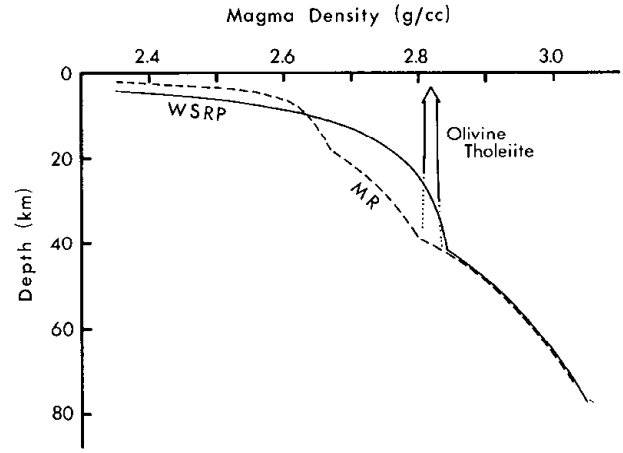

Figure 6. Curves showing minimum required depths to magma sources versus magma density for the case where lithostatic load drives magma to the surface. Curves are shown for two extreme crustal density structures: Western Snake River Plain (WSRP) and Middle Rocky Mountains (MR) from Figure 4.

resurgent doming, may be repeated numerous times (as at Yellowstone) before the shallow silicic magma chambers are largely solidified. Judging from trace element data (see Leeman, 1982c this volume), comparatively small rhyolite domes, extruded long after the dominant rhyolite phase (as in the eastern Snake River Plain), apparently represent highly residual dregs of the original silicic magma bodies.

The paucity of erupted basalt during this stage has been attributed to the presence of high-level silicic magma bodies (Christiansen, in press). The latter bodies, while largely molten, would effectively "quench" higher temperature basaltic magmas. Furthermore, it would be difficult to propagate conduit dikes or fissures through such bodies, as fluids cannot sustain deviatoric stresses. Notably, basaltic vents at Yellowstone are confined to areas outside the dominant eruptive centers for silicic magmas. The trapping of mafic magmas below the silicic magma reservoirs would provide a substantial heat flux that would tend to prolong cooling and help maintain convective stirring of the reservoirs (see Lachenbruch and others, 1976).

As the deep crust becomes depleted in its low-temperature melting components (for example, at temperatures of at least 950-1000° C; see Hildreth and others, 1980) and becomes more refractory, the supply of intermediate to silicic magmas (parental to rhyolite) decreases. Gradual solidification of the high-level silicic magma bodies follows, and rhyolitic volcansim wanes in a given area. Later phases of silicic magmatism shift northeastward following propagation of the Snake River Plain-Yellowstone Plateau melting anomaly.

STAGE D—PREDOMINANTLY BASALTIC VOLCANISM

The last stage of volcanism is characterized by eruptions of olivine basalt and local hybrid lavas. Petrochemical evidence shows that most of these rocks represent more or less fractionated magmas, rather than truly primitive liquids. Hydrostatic considerations suggest that basaltic magmas (with densities of about 2.8 g/cc) could be driven by lithostatic pressure from reservoirs as shallow as 20 to 40 kilometers, given a reasonable density structure for the western Snake River Plain. Less dense hybrid magmas could be derived from even shallower reservoirs (Figure 6). Recall that these are minimal depth estimates. The ascent of these magmas to the surface presumably is possible because high-level silicic magma bodies have largely solidified by this stage.

It is not clear why sporadic basaltic eruptions span such a large time interval (about 10 million years in the western Snake River Plain). Either some fraction of the postulated early massive influx of mafic magmas can remain partly molten for such long times, or there has been repeated influx of fresh magma. The latter possibility seems more reasonable because relatively unfractionated basaltic magma was available for eruption over the last 10 million years. Unfortunately, there are no good estimates of magma influx rates. Nor could reliable estimates be derived from careful field studies, because a large volume fraction of the available magmas was never erupted.

However, it is instructive to consider implications of the model as they pertain to crustal structure. Here it is assumed that initially the crust beneath southern Idaho resembled that beneath the middle Rocky Mountains (see Figure 4) and that systematic differences in the structures beneath Yellowstone Plateau and the eastern and western Snake River Plain have resulted entirely from magmatic processes as outlined in the model. The net change in lower crustal structure is transient thickening by approximately 3 to 5 percent per million years relative to an initial (assumed) thickness of 20 kilometers (Figure 7). For comparison, this rate would correspond to an increase in thickness of the lower crust by nearly 1 kilometer per million years. It is difficult to convert these figures to volume, but assuming a length of 600 kilometers and width of 100 kilometers for the affected area, approximately 0.5 x 10^6 cubic kilometers of added material is suggested. This figure corresponds to a mean influx rate of about 35 x 10^6 cubic meters per year, if the thickening of the lower crust is attributed entirely to an addition of basaltic magma. This influx rate is lower than estimates for active Hawaiian volcanoes or for the Columbia River

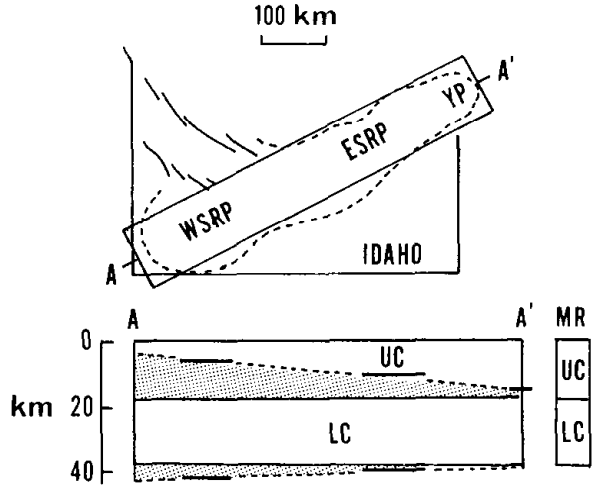

t_{lc} (km)	36	30	~23	20
$\dot{t}_{lc}$ (km/m.y.)	1.1	1.0	~1	-

Figure 7. Crustal profile for Snake River Plain-Yellowstone Plateau province with map view showing location of profile and area used in calculations discussed in text. Shaded areas in profile show extent of anomalous thickening of lower crust (LC) relative to a standard Middle Rocky Mountains (MR) crust (see Figure 4). Note lateral thinning of upper crust (UC). Table give values for thickness of lower crust (t_{lc}) and average rate of thickening ($\dot{t}_{lc}$).

Plateau (Swanson and others, 1975), but it falls well within Fedotov's (1981) regime of "continuously active" volcanoes.

The estimated Snake River Plain-Yellowstone Plateau mean magma influx rate is approximate at best because of uncertainties in the initial crustal structure and in the lag time (neglected here) between initial magma influx and incipient volcanism. It is possible that initially the lower crust was anomalously thick beneath the Snake River Plain, in which case lower influx rates would be necessary. Conversely, an initial crustal structure like that for the Basin and Range province would lead to improbably high influx rates, and in any event is unlikely because the Basin and Range crust has thinned in Cenozoic time (Eaton, 1982). Although the validity of the model may be questioned, the seemingly systematic lateral changes in crustal structure strongly suggest that these changes are indeed related to magmatic processes attending the development of the Snake River Plain-Yellowstone Plateau province. It should be noted that the model appears to be qualitatively consistent with other geophysical observations. Low magnetic intensity and lack of prominent positive Bouguer gravity anomalies in the eastern part of the province can be

attributed to high crustal temperatures and the likelihood that significant proportions of crustal magma bodies are still molten.

Another important aspect of the model is the apparent thinning of the upper crust with time. Thinning may be effected by lateral extension or removal of material. Inasmuch as regional extension appears to be subparallel to the axis of the province, except in the western Snake River Plain graben, it is doubtful that extension alone can account for much of the upper crustal thinning, nor could it account for complementary thickening of the lower crust. Assuming the geometry shown in Figure 7, about 4×10^5 cubic kilometers of upper crustal rocks have been displaced. For comparison, Christiansen (1982 this volume) estimates that the three Yellowstone Tuff eruptions alone constitute a minimum volume of about 4×10^3 cubic kilometers (about 1 percent of the displaced crustal rocks). It is suggested that a significant portion though certainly not all of the "missing upper crust" can be accounted for by wind and water dispersal of pyroclastic and volcaniclastic material. A simple mass balance approach is not realistic, however, because geophysical properties of the upper and lower crust beneath the Snake River Plain are not typical of cratonic crust elsewhere. It is perhaps more reasonable to consider the intermediate crust as a zone of transient magma injection (basalt) and partial melting (rhyolite parental magmas) in which the proportions of mafic intrusions and crustal restite are not known.

TECTONIC INTERPRETATION AND ORIGIN OF THE SNAKE RIVER PLAIN-YELLOWSTONE PLATEAU PROVINCE

As outlined earlier, the Snake River Plain-Yellowstone Plateau province has been interpreted as either a hot-spot trace or the locus of a propagating crack. Available evidence, though fragmentary, provides useful constraints on genetic interpretations. Specific features that require explanation include the following: (a) unusually thick lower crust and lateral gradations in overall crustal structure, (b) high heat flow, (c) eastward progression of volcanic activity, (d) production of voluminous bimodal basaltic and rhyolitic magma, (e) specific geochemical features of the volcanic rocks (especially isotopic evidence that both basalts and rhyolites are derived from ancient but different protoliths), and (f) structural and tectonic characteristics of the province.

The latter characteristics may be quite restrictive and deserve further comment in the context of regional tectonics. Thompson (1977) and Christiansen and McKee (1978) interpret the Snake River Plain as a transformlike northern boundary to the Basin and Range province. However, roughly southwestward Basin and Range style extension has continued to Recent time north of the Snake River Plain, even though strain rates are possibly lower there than in the Great Basin region. In fact, the limited data available suggest that during the late Cenozoic much of southern Idaho has behaved as a relatively coherent crustal block; within this area deformation is limited mainly to southwestward regional extension approximately parallel to the absolute motion vector for the North American plate (Minster and others, 1974) and to early mid-Miocene extension of the back-arc style Northern Nevada Rift (Zoback and Thompson, 1978).

The northwest-trending western physiographic arm of the Snake River Plain is grabenlike and has certain characteristics of rift zones, including axial subsidence and accumulation of voluminous sediments and prominent positive axial gravity anomalies (see Neumann and Ramberg, 1978). However, its early development (contemporaneous with the Northern Nevada Rift), its orientation approximately normal to the inferred late Cenozoic extension direction, and the asymmetry of magnetic anomalies there suggest that this structure developed in a different manner than the eastern Snake River Plain. Vent areas for some of the earliest Snake River Plain rhyolites (flows and tuffs) and basalts are concentrated along a southwestward extension of the eastern Snake River Plain (Ekren and others, 1978, 1982 this volume; Bonnichsen and others, 1975, 1982 this volume; Malde and others, 1963), and it is this area where seismic refraction studies confirm the presence of anomalously thick and atypical crust. For this reason I interpret the Snake River Plain-Yellowstone Plateau magmatic province as extending in a near linear trace into southwestern Idaho (Figure 7). The grabenlike western Snake River Plain physiographic feature is thus viewed as the consequence of southwestward extension. Its location coincides closely with the $^{87}Sr/^{86}Sr$ boundary delimited by Armstrong and others (1977) and subsequently corroborated by strontium and lead isotopic data for Cenozoic volcanic rocks (Leeman, unpublished data). Higher $^{87}Sr/^{86}Sr$ (and $^{207}Pb/^{206}Pb$) ratios east of this north-south trending boundary were attributed to the presence of an ancient cratonic crust, whereas lower ratios to the west coincide with a crustal regime composed of accreted Phanerozoic oceanic and island-arc terranes (Armstrong and others, 1977). If this interpretation is correct, post-17-million-year-old rifting associated with the Northern Nevada Rift-western Snake River Plain was apparently localized at the

suture zone between very different crustal terranes, and much of southern Idaho may be underlain by a relatively coherent cratonic crustal block. It is noteworthy that Snake River lavas from widespread localities contain xenoliths of Archean high-grade metamorphic rocks (Leeman, 1982b this volume; Leeman and others, 1976).

Whereas available indicators (as previously discussed) suggest roughly southeasterly extension across much of southern Idaho from Miocene to Recent time, a clockwise rotation of the regional extension direction occurred in the northern Basin and Range province and attained a northwest orientation by at least 6 million years ago (Zoback and Thompson, 1978; Dockery and Oldow, unpublished data). A northwestward propagation of silicic volcanism across southeastern Oregon since about 15 million years ago (MacLeod and others, 1976) was associated with northwesterly regional extension there. A number of authors (Smith, 1977; Christiansen and McKee, 1978) have cited difficulties in relating the contemporaneous bifurcating propagation of silicic volcanism in southeastern Oregon and the Snake River Plain. It is particularly difficult to explain these trends with a hot-spot model alone; however, Oldow and Leeman (unpublished data) suggest that the Oregon trend is unrelated to the Snake River Plain and can be explained in terms of late Cenozoic plate interactions and resultant deformation—for example, clockwise rotation of the Cascade block (Magill and Cox, 1981; Magill and others, 1981) and shear-coupling between the Pacific and North American plates (see Wright, 1976).

The southwest-oriented regional extension inferred for southern Idaho is inconsistent with major extension normal to the axis of the Snake River Plain-Yellowstone Plateau magmatic province (Hamilton and Myers, 1966) or with the analytical model of Furlong (1979) which assumes a northwest-directed extensional stress field. It also appears to be inconsistent with simple stress models for propagation of a magma-filled dike (see Bhattacharji and Koide, 1978) which, for high aspect (length to width) ratios, would predict a significant component of extension normal to the axis of intrusion.

On the other hand, analytical stress models for diapiric intrusion into an elastic plate subjected to regional extension (see Odé, 1957; Muller and Pollard, 1979) predict stress fields that are in reasonable qualitative agreement with stress indicators (faults and volcanic rifts) for the Snake River Plain-Yellowstone Plateau province. Such models roughly approximate conditions associated with the migration of southern Idaho over a stationary hot spot (that is, diapiric intrusion) of low aspect ratio. According to such theoretical models, radial compression (as documented northwest of Yellowstone Park by Smith and others, 1977) would be superimposed on a regional field of southwestward extension, which becomes progressively more dominant with distance from the magmatic (hot spot) focus. This interpretation can account for the linear trace of the province, the age progression for initial volcanism, the transient uplift of the focal area, and many of the geophysical observations. Anomalously high $^3He/^4He$ ratios measured at Yellowstone (Craig and others, 1978) resemble only those measured at Hawaii and Iceland and suggest an analogy with these presumed hot spots. Magmatism associated with a hot spot may account for the thickening of the lower crust, the inferred volumes of magma, and the observed heat flow.

If a hot-spot model is accepted, there still remains the problem of explaining where and how magmas are produced and why there is no manifestation of this feature prior to about 15 million years ago. Theoretical analysis (Lachenbruch and Sass, 1978) suggests that decompression of upwelling mantle material cannot by itself readily explain the mass and heat balance constraints for large magmatic systems, like that at Yellowstone, unless large-scale advective processes are involved. Other means of heat generation, mechanical or radiogenic, have been suggested (see Christiansen and McKee, 1978), but it is not clear whether these mechanisms are capable of generating the required large volumes of magma. Some insight into the scale and thermal structure of the hot spot is obtained from studies of P- and S-wave delays near Yellowstone (see Iyer, 1979; Iyer and others, 1981) which suggest that a partial melt zone may extend to depths of 250 to 300 kilometers. Curiously, these studies do not reveal significant velocity anomalies at greater depths. If basaltic magmas form by decompression melting of upwelling deep-mantle diapirs, it is possible that seismic velocity attenuation marks the depths at which fusion occurs or primitive magmas segregate from their protolith. The nature of the protolith is difficult to assess because it is difficult to identify primitive magmas (if such are ever erupted at the surface). However, lead and strontium isotopic studies of Snake River Plain-Yellowstone Plateau basalts suggest that these magmas for the most part form by partial melting of ancient subcontinental lithospheric mantle (Leeman, 1977; Doe and others, 1981). The isotopic data seemingly preclude the derivation of the erupted basalts by fusion of asthenospheric mantle similar to that which is assumed to produce young oceanic basalts. It is possible that the lithospheric mantle is partially melted as a result of its intrusion by hot diapiric asthenospheric mantle or by partial melts from asthenospheric mantle. Paucity at the surface of magmas originating in the asthenosphere may reflect their greater density, for example.

Initial manifestation of the postulated Yellowstone hot spot roughly 15 million years ago may be attributed either to its inception at about that time (for example, associated with formation of the Northern Nevada Rift) or to the possibility that it existed earlier but left no surficial trace, possibly due to its deflection by the subducted Farallon plate. Cross and Pilger (1978) note that the initiation of basaltic volcanism and extensional deformation in the Basin and Range province was indeed contemporaneous with Farallon subduction, and the presence of a coherent subducted slab beneath the continent may be implied. The ascent of a preexisting deep-mantle diapir, or magmas derived therefrom, would be favored by the disruption of the subducted slab in response to an inferred clockwise rotation of oceanic-continental plate convergence directions (see Cross and Pilger, 1978) and the inception of Basin and Range deformation.

Alternatively (or perhaps in conjunction with the demise of the Farallon plate), the initiation of a new melting anomaly about 17 million years ago may have been triggered by passive mantle diapirism in a region of pronounced extension and volcanism near the present-day intersection of the Oregon-Idaho-Nevada state lines (for example, Smith, 1977; Christiansen and McKee, 1978; Cross and Pilger, 1978). Subsequent thermal feedback mechanisms may have led to the establishment of a large, stable melting anomaly extending to sublithospheric depths (see Christiansen and McKee, 1978).

CONCLUSIONS

AN OVERVIEW

Compared with nearby regions, the Snake River Plain-Yellowstone Plateau province is strikingly distinct in its voluminous bimodal basalt-rhyolite volcanism, its anomalous crustal structure and other geophysical characteristics, and its geological evolution. Such features as (a) northeastward migration of silicic volcanic centers with time at an apparent rate of 3 to 4 centimeters a year, (b) anomalous $^3He/^4He$ ratios measured at Yellowstone, (c) apparent transient uplift associated with the focus of volcanism, (d) inferred orientations of regional and local stress fields, (e) seismic wave attenuation beneath Yellowstone Plateau, and (f) inferred large-scale reconstitution of the crust favor an origin of the province as the result of passage of the North American plate over a stationary melting anomaly rooted at least several hundred kilometers below the surface. The exact nature of the melting anomaly remains unclear.

A petrologic model is proposed for the upper mantle and crust, in which primitive basaltic magmas are derived from the subcontinental lithospheric mantle and ascend to depths near the Moho or in the lower crust. There, advective heat transfer leads to extensive partial fusion of the deep crust. The crustal anatectic melts ascend to form high-level silicic magma bodies that feed silicic volcanic centers and inhibit the ascent of basaltic magmas to the surface. With protracted solidification of these magma bodies, silicic volcanism wanes. Basaltic volcanism becomes dominant at this stage because of favorable hydrostatic factors (increased density of the crust and decreasing density of differentiating basaltic magma bodies in the deep crust) coupled with solidification of the high-level silicic magma bodies.

Over time intervals of a few million years at any given area within the Snake River Plain-Yellowstone Plateau province, the lower crust increases in thickness due to injection of basaltic magma. Subsequently, the lower crust becomes more dense due to the solidification of basalt to form gabbroic and ultramafic cumulate lenses and the transfer of silicic crustal anatectic melt components to the upper crust. Once the continental plate migrates past the melting anomaly, the crust begins to subside due to thermal contraction as well as its increased density. The entire process is time-dependent, so a lateral facieslike shift is effected.

The proposed model in a general way explains many geological and geophysical observations but does not in itself explain some features, such as volumetrically minor basaltic volcanism since late Miocene time in the western-most Snake River Plain. However, considering the development of the province in the context of regional tectonics, it seems likely that westward extension has occurred across the province since at least the mid-Miocene, and this deformation may have resulted in complicated surficial expressions of volcanism and deformation. The control of older crustal structures on the localization of volcanism and faulting is evident locally.

REMAINING PROBLEMS AND FUTURE STUDIES

It should be evident from the review presented here that we have only a sketchy idea of how the Snake River Plain-Yellowstone Plateau formed. A number of areas for future research easily come to mind. First, much more detailed information is desirable concerning crustal structure and the significance of some of the existing geophysical data. Further seismic refraction and reflection profiling along and across the volcanic axis would be profit-

able, particularly in the western parts of the province (Owyhee Plateau and the basin of the physiographic western arm of the Snake River Plain). Such information would enhance our understanding of gravity and magnetic data for that area. Deep drilling and extensive coring (for example, in the vicinity of some of the magnetic and gravity anomalies) would complement seismic studies and add important stratigraphic information. Secondly, there remain many uncertainties in stratigraphic correlations and timing of volcanic activity. Further mapping is required in many areas to solve these problems and to identify volcanic centers. This effort would benefit from geochronological and geochemical studies of stratigraphically defined volcanic units. Thirdly, our understanding of current tectonics and past deformation is weak and could be improved by continued studies of seismicity, fault-plane solutions for earthquakes, detailed analysis of fault patterns, and geodetic and releveling studies. Paleomagnetic studies of basement rocks and careful mapping along margins of the province may help resolve modes and extent of crustal deformation north and south of the Snake River Plain. For example, are there significant components of extension across the plain or of transcurrent faulting along its margins? Fourthly, the petrologic model presented herein is considered to be a working hypothesis at best. Much additional work is necessary to establish a systematic petrologic and geochemical data base for the volcanic rocks. Such a framework, based on stratigraphic studies, is needed to fully appreciate the petrologic evolution of this magmatic province. Finally, theoretical studies of the thermal and mass transfer processes postulated herein are obviously desirable to test their viability.

ACKNOWLEDGMENTS

This work reflects a long, though intermittent, involvement in studies of the Snake River Plain-Yellowstone Plateau province. In this work I have benefited from interactions with R. L. Christiansen, B. R. Doe, M. A. Kuntz, D. R. Mabey, J. S. Oldow, and S. S. Oriel, among many others, none of whom deserve blame for my liabilities. Funding for this work was provided by National Science Foundation Graduate Fellowships and the U. S. Geological Survey and by grants from the National Geographic Society and National Science Foundation (EAR 80-18580). Manuscript preparation was immeasurably enhanced by the cheerful assistance of A. Elsweiler and A. Walters. Finally, I wish to thank Bill Bonnichsen and an anonymous reviewer for their many constructive comments on the manuscript.

REFERENCES

Akermann, H. D., 1979, Velocity structure to 3000 meter depth at the Idaho National Engineering Laboratory, eastern Snake River Plain: EOS, v. 60, p. 942.

Allmendinger, R. W., 1979, Late Cenozoic deformation and the age of Basin and Range faulting in the Blackfoot Mountains, southeastern Idaho: Geological Society of America, Abstracts with Programs, v. 11, no. 5, p. 65.

Armstrong, R. L., 1975, Precambrian (1500 m.y. old) rocks of central Idaho—the Salmon River Arch and its role in Cordilleran sedimentation and tectonics: American Journal of Science, v. 275-A, p. 437-467.

Armstrong, R. L., J. E. Harakal, and W. M. Neill, 1980, K-Ar dating of Snake River Plain volcanic rocks: new results: Isochron West, v. 27, p. 5-10.

Armstrong, R. L. and F. A. Hills, 1967, Rubidium-strontium and potassium-argon geochronologic studies of mantled gneiss domes, Albion Range, southern Idaho, U. S.: Earth and Planetary Science Letters, v. 3, p. 114-124.

Armstrong, R. L., W. P. Leeman, and H. E. Malde, 1975, K-Ar dating, Quaternary and Neogene volcanic rocks of the Snake River Plain, Idaho: American Journal of Science, v. 275, p. 225-251.

Armstrong, R. L., W. H. Taubeneck, and P. O. Hales, 1977, Rb-Sr and K-Ar geochronometry of Mesozoic granitic rocks and their Sr isotopic composition, Oregon, Washington, and Idaho: Geological Society of America Bulletin, v. 88, p. 397-411.

Arney, B. H., J. H. Boyer, D. B. Simon, F. B. Tonani, and R. B. Weiss, 1980, Hot dry rock geothermal site evaluation, western Snake River Plain, Idaho: Geothermal Resources Council Transactions, v. 4, p. 197-200.

Axelrod, D. I., 1968, Tertiary floras and topographic history of the Snake River basin, Idaho: Geological Society of America Bulletin, v. 79, p. 713-734.

Baker, B. H., G. G. Goles, W. P. Leeman, and M. M. Lindstrom, 1977, Geochemistry and petrogenesis of a basalt-benmoreite-trachyte suite from the southern part of the Gregory Rift, Kenya: Contributions to Mineralogy and Petrology, v. 64, p. 303-332.

Basham, W. L. and E. E. Larson, 1978, Paleomagnetic evidence for clockwise rotation in western Idaho, eastern Oregon, and northern Nevada: Geological Society of America, Abstracts with Programs, v. 10, no. 5, p. 210.

Berggren, W. A., 1972, A Cenozoic time-scale—some implications for regional geology and paleobiogeography: Lethaia, v. 5, p. 195-215.

Bhattacharji, Somder and H. Koide, 1978, The origin and evolution of rifts and rift valley structures: a mechanistic interpretation, *in* I. B. Ramberg and E. R. Neumann, editors, Tectonics and Geophysics of Continental Rifts: Reidel Publishing Company, Boston, p. 29-37.

Bhattacharyya, B. K. and L. -K. Leu, 1975, Analysis of magnetic anomalies over Yellowstone National Park: mapping of Curie point isothermal surface for geothermal reconnaissance: Journal of Geophysical Research, v. 80, p. 4461-4465.

Bonnichsen, Bill, 1982a, The Bruneau-Jarbidge eruptive center, southwestern Idaho, *in* Bill Bonnichsen and R. M. Breckenridge, editors, Cenozoic Geology of Idaho: Idaho Bureau of Mines and Geology Bulletin 26.

———, 1982b, Rhyolite lava flows in the Bruneau-Jarbidge eruptive center, southwestern Idaho, *in* Bill Bonnichsen and R. M. Breckenridge, editors, Cenozoic Geology of Idaho: Idaho Bureau of Mines and Geology Bulletin 26.

Bonnichsen, Bill and G. P. Citron, 1982, The Cougar Point Tuff, southwestern Idaho and vicinity, *in* Bill Bonnichsen and R. M. Breckenridge, editors, Cenozoic Geology of Idaho: Idaho Bureau of Mines and Geology Bulletin 26.

Bonnichsen, Bill, W. B. Travers, and G. P. Citron, 1975, Rhyolitic volcanism and structural evolution of the Snake River Plain: Geological Society of America, Abstracts with Programs, v. 7, no. 5, p. 589-590.

Bottinga, Yan and D. F. Weill, 1970, Densities of liquid silicate systems calculated from partial molar volumes of oxide components: American Journal of Science, v. 269, p. 169-182.

Braile, L. W., R. B. Smith, Jorg Ansorge, M. R. Baker, M. A. Sparlin, Claus Prodahl, M. M. Schilly, J. H. Healy, Stephan Mueller, and K. H. Olsen, 1982, The Yellowstone-Snake River Plain seismic profiling experiment: crustal structure of the eastern Snake River Plain: Journal of Geophysical Research, v. 87, p. 2597-2610.

Braile, L. W., R. B. Smith, G. R. Keller, R. M. Welch, and R. P. Meyer, 1974, Crustal structure across the Wasatch Front from detailed seismic refraction studies: Journal of Geophysical Research, v. 79, p. 2669-2677.

Brott, C. A., D. D. Blackwell, and J. C. Mitchell, 1978, Tectonic implications of the heat flow of the western Snake River Plain, Idaho: Geological Society of America Bulletin, v. 89, p. 1697-1707.

Brott, C. A., D. D. Blackwell, and J. P. Ziagos, 1981, Thermal and tectonic implications of heat flow in the eastern Snake River Plain, Idaho: Journal of Geophysical Research, v. 86, p. 11709-11734.

Carr, W. J. and D. E. Trimble, 1963, Geology of the American Falls quadrangle, Idaho: U. S. Geological Survey Bulletin 1121-G, 44 p.

Christiansen, R. L., 1982, Late Cenozoic volcanism of the Island Park area, eastern Idaho, *in* Bill Bonnichsen and R. M. Breckenridge, editors, Cenozoic Geology of Idaho: Idaho Bureau of Mines and Geology Bulletin 26.

———, in press, Quaternary and Pliocene volcanism of the Yellowstone rhyolite plateau region of Wyoming, Idaho, and Montana: U. S. Geological Survey Professional Paper 729.

Christiansen, R. L. and H. R. Blank, Jr., 1972, Volcanic stratigraphy of the Quaternary rhyolite plateau in Yellowstone National Park: U. S. Geological Survey Professional Paper 729-B, 18 p.

Christiansen, R. L. and P. W. Lipman, 1972, Cenozoic volcanism and plate-tectonic evolution of the western United States, II. Late Cenozoic: Royal Society of London Philosophical Transactions, v. 271, p. 249-284.

Christiansen, R. L. and E. H. McKee, 1978, Late Cenozoic volcanic and tectonic evolution of the Great Basin and Columbia intermontane regions: Geological Society of America Memoir 152, p. 283-311.

Cline, K. M. and M. R. Niccum, 1978, Mid-late Cenozoic faulting in central Idaho north of the Snake River Plain: Geological Society of America, Abstracts with Programs, v. 10, no. 5, p. 213.

Cox, Allen, R. R. Doell, and G. B. Dalrymple, 1965, Quaternary paleomagnetic stratigraphy, *in* H. E. Wright, Jr., and D. G. Frey, editors, The Quaternary of the United States: Princeton University Press, Princeton, New Jersey, p. 817-829.

Cox, K. G., 1980, A model for flood basalt volcanism: Journal of Petrology, v. 21, p. 629-650.

Craig, Harmon, J. E. Lupton, J. A. Welhan, and Robert Poreda, 1978, Helium isotope ratios in Yellowstone and Lassen Park volcanic gases: Geophysical Research Letters, v. 5, p. 897-900.

Cross, T. A. and R. H. Pilger, Jr., 1978, Constraints on absolute motion and plate interaction inferred from Cenozoic igneous activity in the western United States: American Journal of Science, v. 278, p. 865-902.

Daniel, R. G. and D. M. Boore, 1982, Anomalous shear wave delays and surface wave velocities at Yellowstone caldera, Wyoming: Journal of Geophysical Research, v. 87, p. 2731-2744.

Doe, B. R., W. P. Leeman, R. L. Christiansen, and C. E. Hedge, 1982, Lead and strontium isotopes and related trace elements as genetic tracers applied to the Quaternary rhyolite-basalt association of the Yellowstone Plateau volcanic field, U.S.A.: Journal of Geophysical Research, v. 87, p. 4785-4806.

Doherty, D. J., L. A. McBroome, and M. A. Kuntz, 1979, Preliminary geological interpretation and lithologic log of the geothermal exploration well (INEL-1), Idaho National Engineering Laboratory, eastern Snake River Plain, Idaho: U. S. Geological Survey Open-File Report 79-1248, 7 p.

Duffield, W. A., C. R. Bacon, and G. B. Dalrymple, 1980, Late Cenozoic volcanism, geochronology, and structure of the Coso Range, Inyo County, California: Journal of Geophysical Research, v. 85, p. 2381-2404.

Eaton, G. P., 1982, The Basin and Range province: origin and tectonic significance: Annual Reviews of Earth and Planetary Sciences, v. 10, p. 409-440.

Eaton, G. P., R. L. Christiansen, H. M. Iyer, A. M. Pitt, D. R. Mabey, H. R. Blank, Jr., Isidore Zietz, and M. E. Gettings, 1975, Magma beneath Yellowstone National Park: Science, v. 188, p. 787-796.

Eichelberger, J. D. and Ronald Gooley, 1977, Evolution of silicic magma chambers and their relationship to basaltic volcanism: American Geophysical Union Monograph 20, p. 57-77.

Ekren, E. B., D. H. McIntyre, and E. H. Bennett, 1981, Preliminary geologic map of the west half of Owyhee County, Idaho: U. S. Geological Survey Miscellaneous Investigations Map I-1256.

Ekren, E. B., D. H. McIntyre, E. H. Bennett, and R. F. Marvin, 1982, Cenozoic stratigraphy of western Owyhee County, Idaho, *in* Bill Bonnichsen and R. M. Breckenridge, editors, Cenozoic Geology of Idaho: Idaho Bureau of Mines and Geology Bulletin 26.

Embree, G. F., L. A. McBroome, and D. J. Doherty, 1982, Preliminary stratigraphic framework of the Pliocene and Miocene rhyolites, eastern Snake River Plain, Idaho, *in* Bill Bonnichsen and R. M. Breckenridge, editors, Cenozoic Geology of Idaho: Idaho Bureau of Mines and Geology Bulletin 26.

Evans, J. R., 1981, Compressional-wave velocity structure of the upper 350 km under the eastern Snake River Plain near Rexburg, Idaho: Journal of Geophysical Research, v. 87, p. 2654-2670.

Evernden, J. F., D. E. Savage, G. H. Curtis, and G. T. James, 1964, Potassium-argon dates and the Cenozoic mammalian chronology of North America: American Journal of Science, v. 262, p. 145-198.

Fedotov, S. A., 1975, Mechanism of magma ascent and deep feeding channels of island arc volcanoes: Bulletin Volcanologique, v. 39, p. 241-259.

———, 1981, Magma rates in feeding conduits of different volcanic centres: Journal of Volcanology and Geothermal Research, v. 9, p. 379-394.

Fenner, C. N., 1938, Contact relations between rhyolite and basalt on Gardiner River, Yellowstone Park, Wyoming: Geological Society of America Bulletin, v. 49, p. 1441-1483.

———, 1944, Rhyolite-basalt complex on Gardiner River, Yellowstone Park, Wyoming: Geological Society of America Bulletin, v. 55, p. 1081-1096.

Fitterman, D. V., 1979, Geomagnetic induction study across the eastern Snake River Plain, Idaho: EOS, v. 60, p. 944.

Fournier, R. O., D. E. White, and A. H. Truesdell, 1976, Convective heat flow in Yellowstone National Park, *in* Proceedings, 2nd United Nations Symposium on the Development and Use of Geothermal Resources, San Francisco, California, May 20-29, 1975, v. 1: Berkeley, California, Lawrence Berkeley Laboratory, University of California, p. 731-739.

Friedline, R. O., R. B. Smith, and D. D. Blackwell, 1976, Seismicity and contemporary tectonics of the Helena, Montana area: Seismological Society of America Bulletin, v. 60, p. 81-96.

Furlong, K. P., 1979, An analytic stress model applied to the Snake River Plain (northern Basin and Range province, U.S.A.): Tectonophysics, v. 58, p. 11-15.

Gill, R. C. O., 1973, Mechanism for the salic magma bias of continental alkaline provinces: Nature Physical Science, v. 242, p. 41-42.

Greensfelder, R. W. and R. L. Kovach, 1982, Shear wave velocities and crustal structure of the eastern Snake River Plain, Idaho: Journal of Geophysical Research, v. 87, p. 2643-2653.

Hadley, D. M., G. S. Stewart, and J. E. Ebel, 1976, Yellowstone: seismic evidence for a chemical mantle plume: Science, v. 191, p. 1237-1239.

Hamilton, W. B., 1965, Geology and petrogenesis of the Island Park caldera of rhyolite and basalt, eastern Idaho: U. S. Geological Survey Professional Paper 504-C, 37 p.

Hamilton, W. B. and W. B. Myers, 1966, Cenozoic tectonics of the western United States: Reviews of Geophysics, v. 4, p. 509-549.

Hildreth, E. W., 1979, The Bishop Tuff: evidence for the origin of compositional zonation in silicic magma chambers: Geological Society of America Special Paper 180, p. 43-85.

Hildreth, E. W., R. L. Christiansen, and J. R. O'Neil, 1980, Catastrophic isotopic modification of rhyolitic magma by creation of the Yellowstone caldera: Geological Society of America, Abstracts with Programs, v. 12, no. 3, p. 111.

Hill, D. P. and L. C. Pakiser, 1967, Seismic-refraction study of crustal structure between the Nevada Test Site and Boise, Idaho: Geological Society of America Bulletin, v. 78, p. 685-704.

Hodge, D. S., 1974, Thermal model for origin of granitic batholiths: Nature, v. 251, p. 297-299.

Howard, K. A. and J. W. Shervais, 1973, Geologic map of Smith Prairie, Elmore County, Idaho: U. S. Geological Survey Miscellaneous Geological Investigations Map I-818.

Iyer, H. M., 1979, Deep structure under Yellowstone National Park, U.S.A.: a continental "hot spot": Tectonophysics, v. 56, p. 165-197.

Iyer, H. M., J. R. Evans, George Zandt, R. M. Stewart, J. M. Coakley, and J. N. Roloff, 1981, A deep low-velocity body under the Yellowstone caldera, Wyoming: Delineation using teleseismic P-wave residuals and tectonic interpretation: Geological Society of America Bulletin, v. 91, p. 792-798.

Keller, G. R., R. B. Smith, and L. W. Braile, 1975, Crustal structure along the Great Basin-Colorado Plateau transition from seismic refraction studies: Journal of Geophysical Research, v. 80, p. 1093-1098.

Kimmel, P. G., 1979, Stratigraphy and paleoenvironments of the Miocene Chalk Hills Formation and Pliocene Glenns Ferry Formation in the western Snake River Plain, Idaho: University of Michigan Ph.D. thesis.

_____, 1982, Stratigraphy, age, and tectonic setting of the Miocene-Pliocene lacustrine sediments of the western Snake River Plain, Oregon and Idaho, *in* Bill Bonnichsen and R. M. Breckenridge, editors, Cenozoic Geology of Idaho: Idaho Bureau of Mines and Geology Bulletin 26.

Kirkham, V. R. D., 1931a, Snake River downwarp: Journal of Geology, v. 39, p. 456-482.

_____, 1931b, Igneous geology of southwestern Idaho: Journal of Geology, v. 39, p. 564-591.

Kuntz, M. A., 1977, Rift zones of the Snake River Plain, Idaho, as extensions of Basin-Range and older structures: Geological Society of America, Abstracts with Programs, v. 9, no. 7, p. 1061-1062.

_____, 1978, Geologic map of the Arco-Big Southern Butte area, Blaine and Bingham Counties, Idaho: U. S. Geological Survey Open-File Report 78-302.

_____, 1979, Do basalt structures and topographic features reflect buried calderas in the eastern Snake River Plain?: EOS, v. 60, p. 945.

Kuntz, M. A., D. E. Champion, E. C. Spiker, R. H. Lefebvre, and L. A. McBroome, 1982, The Great Rift and the evolution of the Craters of the Moon lava field, Idaho, *in* Bill Bonnichsen and R. M. Breckenridge, editors, Cenozoic Geology of Idaho: Idaho Bureau of Mines and Geology Bulletin 26.

Kuntz, M. A. and G. B. Dalrymple, 1979, Geology, geochronology, and potential volcanic hazards in the Lava Ridge-Hells Half Acre area, eastern Snake River Plain, Idaho: U. S. Geological Survey Open-File Report 79-1657, 66 p.

Kuntz, M. A., G. B. Dalrymple, D. E. Champion, and D. J. Doherty, 1980a, An evaluation of potential volcanic hazards at the Radioactive Waste Management Complex, Idaho National Engineering Laboratory, Idaho: U. S. Geological Survey Open-File Report 80-388, 68 p.

Kuntz, M. A., R. H. Lefebvre, D. E. Champion, L. A. McBroome, D. R. Mabey, W. D. Stanley, H. R. Covington, John Ridenour, and R. B. Stotelmeyer, 1980b, Geological and geophysical investigations, and mineral resources potential of the proposed Great Rift Wilderness area, Idaho: U. S. Geological Survey Open-File Report 80-475, 54 p.

Lachenbruch, A. H. and J. H. Sass, 1978, Models of an extending lithosphere and heat flow in the Basin and Range province: Geological Society of America Memoir 152, p. 209-250.

Lachenbruch, A. H., J. H. Sass, R. J. Munroe, and T. H. Moses, Jr., 1976, Geothermal setting and simple heat conduction models for the Long Valley caldera: Journal of Geophysical Research, v. 81, p. 769-784.

LaPoint, P. J. I., 1977, Preliminary photogeologic map of the eastern Snake River Plain, Idaho: U. S. Geological Survey Map MF-850.

Lawrence, R. D., 1976, Strike-slip faulting terminates the Basin and Range province in Oregon: Geological Society of America Bulletin, v. 87, p. 846-850.

Leeman, W. P., 1977, Comparison of Rb/Sr, U/Pb, and rare earth characteristics of sub-continental and sub-oceanic mantle regions: Oregon Department of Geology and Mineral Industries Bulletin 96, p. 149-168.

_____, 1979, Primitive lead in deep crustal xenoliths from the Snake River Plain, Idaho: Nature, v. 281, p. 365-366.

_____, 1980, Deep crustal xenoliths from the Snake River Plain: EOS, v. 60, p. 945.

_____, 1982a, Olivine and tholeiitic basalts of the Snake River Plain, Idaho, *in* Bill Bonnichsen and R. M. Breckenridge, editors, Cenozoic Geology of Idaho: Idaho Bureau of Mines and Geology Bulletin 26.

_____, 1982b, Evolved and hybrid lavas from the Snake River Plain, Idaho, *in* Bill Bonnichsen and R. M. Breckenridge, editors, Cenozoic Geology of Idaho: Idaho Bureau of Mines and Geology Bulletin 26.

_____, 1982c, Rhyolites of the Snake River Plain-Yellowstone Plateau province, Idaho and Wyoming: a summary of petrogenetic models, *in* Bill Bonnichsen and R. M. Breckenridge, editors, Cenozoic Geology of Idaho: Idaho Bureau of Mines and Geology Bulletin 26.

———, 1982d, Geology of the Magic Reservoir area, Snake River Plain, Idaho, *in* Bill Bonnichsen and R. M. Breckenridge, editors, Cenozoic Geology of Idaho: Idaho Bureau of Mines and Geology Bulletin 26.

Leeman, W. P. and W. I. Manton, 1971, Strontium isotopic composition of basaltic lavas from the Snake River Plain, southern Idaho: Earth and Planetary Science Letters, v. 11, p. 420-434.

Leeman, W. P. and C. J. Vitaliano, 1976, Petrology of McKinney Basalt, Snake River Plain, Idaho: Geological Society of America Bulletin, v. 87, p. 1777-1792.

Leeman, W. P., C. J. Vitaliano, and Martin Prinz, 1976, Evolved lavas from the Snake River Plain: Craters of the Moon National Monument, Idaho: Contributions to Mineralogy and Petrology, v. 56, p. 35-60.

Lehman, J. A., R. B. Smith, and M. M. Schilly, 1982, Upper crustal structure of the Yellowstone caldera from seismic delay time analyses and gravity observations: Journal of Geophysical Research, v. 87, p. 2713-2730.

Love, J. D., J. C. Reed, R. L. Christiansen, and J. R. Stacy, 1972, Geologic block diagram and tectonic history of the Teton region, Wyoming-Idaho: U. S. Geological Survey Miscellaneous Investigations Map I-730.

Mabey, D. R., 1976, Interpretation of a gravity profile across the western Snake River Plain, Idaho: Geology, v. 4, p. 53-55.

———, 1978, Regional gravity and magnetic anomalies in the eastern Snake River Plain, Idaho: U. S. Geological Survey Journal of Research, v. 6, p. 553-562.

———, 1982, Geophysics and tectonics of the Snake River Plain, Idaho, *in* Bill Bonnichsen and R. M. Breckenridge, editors, Cenozoic Geology of Idaho: Idaho Bureau of Mines and Geology Bulletin 26.

MacLeod, N. S., G. W. Walker, and E. H. McKee, 1976, Geothermal significance of eastward increase in age of upper Cenozoic rhyolitic domes in southeastern Oregon, *in* Proceedings, 2nd United Nations Symposium on the Development and Use of Geothermal Resources, San Francisco, California, May 20-29, 1975, v. 1: Berkeley, California, Lawrence Berkeley Laboratory, Univeristy of California, p. 465-474.

Magill, James and Allen Cox, 1981, Post-Oligocene tectonic rotation of the Oregon western Cascade Range and the Klamath Mountains: Geology, v. 9, p. 127-131.

Magill, James, Allen Cox, and R. A. Duncan, 1981, Tillamook Volcanic Series: further evidence for tectonic rotation of the Oregon Coast Range: Journal of Geophysical Research, v. 86, p. 2953-2970.

Malde, H. E., 1959, Fault zone along northern boundary of western Snake River Plain, Idaho: Science, v. 130, p. 272.

———, 1965, Snake River Plain, *in* H. E. Wright, Jr., and D. G. Frey, editors, The Quaternary of the United States: Princeton University Press, Princeton, New Jersey, p. 255-263.

———, 1971a, History of the Snake River canyon indicated by revised stratigraphy of the Snake River Group near Hagerman and King Hill, Idaho: U. S. Geological Survey Professional Paper 644-F, 21 p.

———, 1971b, Geologic investigation of faulting near the National Reactor Testing Station, Idaho: U. S. Geological Survey Open-File Report, 167 p.

———, 1972, Stratigraphy of the Glenns Ferry Formation from Hammett to Hagerman, Idaho: U. S. Geological Survey Bulletin 1331-D, 19 p.

Malde, H. E. and H. A. Powers, 1962, Upper Cenozoic stratigraphy of western Snake River Plain, Idaho: Geological Society of America Bulletin, v. 73, p. 1197-1220.

———, 1972, Geologic map of the Glenns Ferry-Hagerman area, west-central Snake River Plain, Idaho: U. S. Geological Survey Miscellaneous Geological Investigations Map I-696.

Malde, H. E., H. A. Powers, and C. H. Marshall, 1963, Reconnaissance geologic map of the west-central Snake River Plain, Idaho: U. S. Geological Survey Miscellaneous Geological Investigations Map I-373.

Mansfield, G. R., 1927, Geography, geology, and mineral resources of part of southeastern Idaho: U. S. Geological Survey Professional Paper 152, 448 p.

McIntyre, D. H., 1972, Cenozoic geology of the Reynolds Creek experimental watershed, Owyhee County, Idaho: Idaho Bureau of Mines and Geology Pamphlet 151, 115 p.

———, 1979, Preliminary description of Anschutz Federal No. 1 drill hole, Owyhee County, Idaho: U. S. Geological Survey Open-File Report 79-651, 14 p.

McKee, E. H., A. L. Tarshis, and R. F. Marvin, 1976, Summary of radiometric ages of Tertiary volcanic and selected plutonic rocks in Nevada, Part V: northeastern Nevada: Isochron West, no. 16, p. 15-27.

Minster, J. B., T. H. Jordan, Peter Molnar, and Eldon Haines, 1974, Numerical modelling of instantaneous plate tectonics: Geophysical Journal of the Royal Astronomical Society, v. 36, p. 541-576.

Morgan, Paul, D. D. Blackwell, R. E. Spafford, and R. B. Smith, 1977, Heat flow measurements in Yellowstone Lake and the thermal structure of

the Yellowstone caldera: Journal of Geophysical Research, v. 82, p. 3719-3732.

Morgan, W. J., 1972, Deep mantle convection plumes and plate motions: American Association of Petroleum Geologists Bulletin, v. 56, p. 203-213.

Muller, O. H. and D. D. Pollard, 1979, The stress state near Spanish Peaks, Colorado, determined from a dike pattern: Paleogeophysics, v. 115, p. 69-86.

Neumann, E. R. and I. B. Ramberg, 1978, Paleorifts—concluding remarks, *in* I. B. Ramberg and E. R. Neumann, editors, Tectonics and Geophysics of Continental Rifts: Reidel Publishing Company, Boston, p. 409-424.

Neville, Colleen, N. D. Opdyke, E. H. Lindsay, and N. M. Johnson, 1979, Magnetic stratigraphy of Pliocene deposits of the Glenns Ferry Formation, Idaho, and its implications for North American mammalian biostratigraphy: American Journal of Science, v. 279, p. 503-526.

Odé, Helmer, 1957, Mechanical analysis of the dike pattern of the Spanish Peaks area, Colorado: Geological Society of America Bulletin, v. 68, p. 567-576.

Olsen, K. H., E. F. Homuth, J. N. Stewart, R. N. Felch, T. G. Handel, and P. A. Johnson, 1979, Upper crustal structure beneath the eastern Snake River Plain interpreted from seismic refraction measurements near Big Southern Butte, Idaho: EOS, v. 60, p. 941.

Pansze, A. J., 1972, K-Ar ages of plutonism, volcanism, and mineralization, Silver City region, Owyhee County, Idaho: Isochron West, no. 4, p. 1-4.

Pelton, J. R. and R. B. Smith, 1979, Recent crustal uplift in Yellowstone National Park: Science, v. 206, p. 1179-1182.

_____, 1982, Contemporary vertical surface displacements in Yellowstone National Park: Journal of Geophysical Research, v. 87, p. 2745-2761.

Pennington, W. D., R. B. Smith, and A. B. Trimble, 1974, A microearthquake survey of parts of the Snake River Plain and central Idaho: Seismological Society of America Bulletin, v. 64, p. 307-312.

Powers, H. A., 1960, A distinctive chemical characteristic of Snake River basalts of Idaho: U. S. Geological Survey Professional Paper 400-B, p. 298.

Priestley, Keith and John Orcutt, 1982, Extremal travel time inversion of explosion seismology data from the eastern Snake River Plain, Idaho: Journal of Geophysical Research, v. 87, p. 2634-2642.

Prinz, Martin, 1970, Idaho rift system, Snake River Plain, Idaho: Geological Society of America Bulletin, v. 81, p. 941-947.

Prostka, H. J. and G. F. Embree, 1978, Geology and geothermal resources of the Rexburg area, eastern Idaho: U. S. Geological Survey Open-File Report 78-1009, 15 p.

Reilinger, R. E., G. P. Citron, and L. D. Brown, 1977, Recent vertical crustal movements from precise leveling data in southwestern Montana, western Yellowstone National Park, and the Snake River Plain: Journal of Geophysical Research, v. 82, p. 5349-5359.

Rice, Alan, 1981, Convective fractionation: a mechanism to provide cryptic zoning (macrosegregation), layering, crescumulates, banded tuffs and explosive volcanism in igneous processes: Journal of Geophysical Research, v. 86, p. 405-417.

Ross, C. P., 1962, Stratified rocks in south-central Idaho: Idaho Bureau of Mines and Geology Pamphlet 125, 126 p.

Schilly, M. M., R. B. Smith, L. W. Braile, and Jorg Ansorge, 1982, The 1978 Yellowstone-eastern Snake River Plain seismic profiling experiment: data and upper crustal structure of the Yellowstone region: Journal of Geophysical Research, v. 87, p. 2692-2704.

Schmidt, D. L., 1961, Quaternary geology of the Bellevue area in Blaine and Camas Counties, Idaho: University of Washington Ph.D. thesis, 125 p.

Smith, C. L., 1966, Geology of eastern Mount Bennett Hills, Camas, Gooding, and Lincoln Counties, Idaho: University of Idaho Ph.D. thesis, 129 p.

Smith, R. B., 1977, Intraplate tectonics of the western North American plate: Tectonophysics, v. 37, p. 323-326.

Smith, R. B. and A. G. Lindh, 1978, Fault-plane solutions of the western United States, a compilation: Geological Society of America Memoir 152, p. 107-109.

Smith, R. B. and M. L. Sbar, 1974, Contemporary tectonics and seismicity of the western United States with emphasis on the Intermountain seismic belt: Geological Society of America Bulletin, v. 85, p. 1205-1218.

Smith, R. B., R. T. Shuey, J. R. Pelton, and J. P. Bailey, 1977, Yellowstone hot-spot, contemporary tectonics and crustal properties from earthquake and aeromagnetic data: Journal of Geophysical Research, v. 82, p. 3665-3676.

Smith, R. L., 1979, Ash-flow magmatism: Geological Society of America Special Paper 180, p. 5-27.

Sparlin, M. A., L. W. Braile, and R. B. Smith, 1982, Crustal structure of the eastern Snake River Plain determined from ray trace modeling of seismic refraction data: Journal of Geophysical Research, v. 87, p. 2619-2633.

Spear, D. B., 1979, The geology of Big Southern Butte and the surrounding area: State University of New York at Buffalo Ph.D. thesis, 136 p.

Spear, D. B. and J. S. King, 1982, Geology of Big Southern Butte, Idaho, *in* Bill Bonnichsen and R. M. Breckenridge, editors, Cenozoic Geology of Idaho: Idaho Bureau of Mines and Geology Bulletin 26.

Stanley, W. D., J. E. Boehl, F. X. Bostick, and H. W. Smith, 1977, Geothermal significance of magnetotelluric sounding in the eastern Snake River Plain-Yellowstone region: Journal of Geophysical Research, v. 82, p. 2501-2514.

Stearns, H. T., L. L. Bryan, and Lynn Crandall, 1939, Geology and water resources of the Mud Lake region, Idaho, including the Island Park area: U. S. Geological Survey Water Supply Paper 818, 125 p.

Stearns, H. T., Lynn Crandall, and W. G. Steward, 1938, Geology and groundwater resources of the Snake River Plain in southeastern Idaho: U. S. Geological Survey Water Supply Paper 774, 268 p.

Stewart, J. H., G. W. Walker, and F. J. Kleinhampl, 1975, Oregon-Nevada lineament: Geology, v. 3, p. 265-268.

Stone, G. T., 1967, Petrology of upper Cenozoic basalts of the Snake River Plain: University of Colorado Ph.D. thesis, 392 p.

———, 1969, Structural implications of Quaternary lava-dome distribution in the Snake River Plain, Idaho: Geological Society of America, Abstracts with Programs, v. 1, no. 7, p. 217-218.

Stout, M. Z. and Jim Nicholls, 1977, Mineralogy and petrology of Quaternary lavas from the Snake River Plain, Idaho: Canadian Journal of Earth Science, v. 14, p. 2140-2156.

Swanson, D. A., T. L. Wright, and R. T. Helz, 1975, Linear vent systems and estimated rates of magma production and eruption for the Yakima Basalt on Columbia Plateau: American Journal of Science, v. 275, p. 877-905.

Swanson, D. A., T. L. Wright, P. R. Hooper, and R. D. Bently, 1979, Revisions in stratigraphic nomenclature of the Columbia River Basalt Group: U. S. Geological Survey Bulletin 1457-G, 59 p.

Suppe, John, Christine Powell, and Robert Berry, 1975, Regional topography, seismicity, Quaternary volcanism, and the present-day tectonics of the western United States: American Journal of Science, v. 275-A, p. 397-436.

Swirydczuk, Krystyna, 1980, Sedimentology of the Pliocene Glenns Ferry oolite and its stratigraphic setting in the western Snake River Plain: University of Michigan Ph.D. thesis, 247 p.

Swirydczuk, Krystyna, G. P. Larsen, and G. R. Smith, 1982, Volcanic ash beds as stratigraphic markers in the Glenns Ferry and Chalk Hills Formations from Adrian, Oregon, to Bruneau, Idaho, *in* Bill Bonnichsen and R. M. Breckenridge, editors, Cenozoic Geology of Idaho: Idaho Bureau of Mines and Geology Bulletin 26.

Taubeneck, W. H., 1971, Idaho batholith and its southern extension: Geological Society of America Bulletin, v. 82, p. 1899-1928.

Thompson, R. N., 1977, Columbia/Snake River-Yellowstone magmatism in the context of western U.S.A. Cenozoic geodynamics: Tectonophysics, v. 39, p. 621-636.

Trimble, A. B. and R. B. Smith, 1975, Seismicity and contemporary tectonics of the Hebgen Lake-Yellowstone Park region: Journal of Geophysical Research, v. 80, p. 733-741.

Trimble, D. E., 1976, Geology of the Michaud and Pocatello quadrangles, Bannock and Power Counties, Idaho: U. S. Geological Survey Bulletin 1400, 88 p.

Trimble, D. E. and W. J. Carr, 1976, Geology of the Rockland and Arbon quadrangles, Power County, Idaho: U. S. Geological Survey Bulletin 1399, 15 p.

Tuttle, O. F. and N. L. Bowen, 1958, Origin of granite in the light of experimental studies in the system $NaAlSi_3O_8$-$KAlSi_3O_8$-SiO_2-H_2O: Geological Society of America Memoir 74, 153 p.

Walker, E. H., 1964, Subsurface geology of the National Reactor Testing Station, Idaho: U. S. Geological Survey Bulletin 1133-E, 22 p.

Weaver, C. S., A. M. Pitt, and D. P. Hill, 1979, Crustal spreading direction of the Snake River Plain-Yellowstone system: EOS, v. 60, p. 946.

Wier, Stuart, 1979, Geomagnetic variation anomalies on the central Snake River Plain: EOS, v. 60, p. 944.

Wilcox, R. E., 1944, Rhyolite-basalt complex on Gardiner River, Yellowstone Park, Wyoming: Geological Society of America Bulletin, v. 55, p. 1047-1079.

Williams, P. L., H. R. Covington, and K. L. Pierce, 1982, Cenozoic stratigraphy and tectonic evolution of the Raft River Basin, Idaho, *in* Bill Bonnichsen and R. M. Breckenridge, editors, Cenozoic Geology of Idaho: Idaho Bureau of Mines and Geology Bulletin 26.

Wright, Lauren, 1976, Late Cenozoic fault patterns and stress fields in the Great Basin and westward displacement of the Sierra Nevada block: Geology, v. 4, p. 489-494.

Wyllie, P. J., 1977, Crustal anatexis, an experimental review: Tectonophysics, v. 43, p. 41-71.

Younker, L. W. and Tom Vogel, 1975, Role of mantle derived magmas in the production of crustal melts: EOS, v. 56, p. 473-474.

Zoback, M. L. and G. A. Thompson, 1978, Basin and Range rifting in northern Nevada, clues from a

mid-Miocene rift and its subsequent offsets: Geology, v. 6, p. 111-116.

Zoback, M. L. and Mark Zoback, 1980, State of stress in the conterminous United States: Journal of Geophysical Research, v. 85, p. 6113-6156.

Zohdy, A. A. R. and W. D. Stanley, 1973, Preliminary interpretation of electrical sounding curves obtained from the Snake River Plain from Blackfoot to Arco, Idaho: U. S. Geological Survey Open-File Report.

Chapter 4

Volcanic Rock Groups Snake River Plain

Olivine Tholeiitic Basalts of the Snake River Plain, Idaho

by

William P. Leeman[1]

ABSTRACT

Basalts of the Snake River Plain-Yellowstone Plateau province are dominantly olivine tholeiites that can be distinguished into two groups—variably fractionated (for example, differentiated) lavas (Group I) and relatively primitive low-K lavas (Group II). Although none of these rocks may represent true primary magmas, those of Group II probably have been modified least during ascent. Compositional variations within Group I are attributed to formation of these magmas by different degrees of partial melting of relatively uniform spinel peridotite source rocks, and to subsequent low-pressure (less than 10 kilobars) fractionation of olivine and plagioclase during their ascent and stagnation in crustal reservoirs. Strontium and lead isotopic data for these basalts are believed to reflect magma genesis via partial melting of aged (about 2.5 billion years old) subcontinental lithospheric mantle. There is little evidence to indicate that these magmas were significantly contaminated by crustal material, nor is there an indication of substantial contributions of magma from asthenospheric (or deeper) mantle sources such as have produced oceanic basalts.

Lithospheric mantle rocks may have partially melted as the continent migrated over a stationary sublithospheric heat source, such as an upwelling diapir of asthenospheric mantle. In the absence of significant crustal extension, basaltic magmas accumulated near the base of the crust which led to thickening of the mafic lower crust and to crustal anatexis that produced associated rhyolitic magmas.

INTRODUCTION

The Snake River Plain-Yellowstone Plateau province has been characterized by bimodal basalt-rhyolite volcanism during the past 15 million years. As outlined by Leeman (1982a this volume), this volcanism has occurred in two general phases beginning in any given area with the early extrusion of rhyolitic lavas and tuffs and minor intercalated basaltic lavas. Subsequent volcanism was predominantly basaltic and continued sporadically over much of the province until Recent time. The focus of most intense volcanism migrated northeasterly with time and is now located at Yellowstone. An influx of mafic magmas from the upper mantle into the crust caused extensive crustal anatexis whereby the rhyolitic magmas (or their parental magmas) formed (Christiansen and McKee, 1978; Leeman, 1982a this volume; Christiansen, in preparation). Thus, Snake River Plain-Yellowstone Plateau magmatism is fundamentally basaltic in character. This paper is concerned with the petrology and geochemistry of basaltic lavas from the Snake River Plain and the problems of magma genesis and evolution.

The present account is based on studies of basaltic lavas mainly from the western and central Snake River Plain where flow units covering the widest possible age range (about 13 million years to Holocene) could be sampled. In addition, representative lavas from the eastern Snake River Plain were studied to provide a wide geographic coverage for units from about 6 million years old to Holocene in age. This work is complemented by several other important studies. Stone (1967) provided detailed petrographic descriptions and analyses of basalts from the west-central Snake River Plain, where stratigraphic control was established by Malde and Powers (1962, 1963, 1972). One flow unit in this area (McKinney Basalt) was investigated in detail by Leeman (1976) and Leeman and Vitaliano (1976), who provided major and trace element analyses and petrographic, mineralogic, and experimental data bearing on its origin. A reconnaissance study of Holocene basaltic lavas from the east-central Snake River Plain (Stout and Nicholls, 1977) and several other studies (Leeman, 1974; Spear, 1979; Karlo and Clemency, 1980; Trimble and Carr, 1976) provide

[1]Department of Geology, Rice University, Houston, Texas 77001.

Leeman, W. P., 1982, Olivine tholeiitic basalts of the Snake River Plain, Idaho, *in* Bill Bonnichsen and R. M. Breckenridge, editors, Cenozoic Geology of Idaho: Idaho Bureau of Mines and Geology Bulletin 26, p. 181-191.

additional petrologic and analytical data. Leeman and Manton (1971) and Leeman (1977) discussed results of lead and strontium isotopic analyses of many representative units, and additional isotopic data are available (Muehlenbachs and Stone, 1973; Leeman and Whelan, in preparation; Leeman, unpublished data). Finally, experimental phase equilibria studies at one atmosphere and higher pressures have been carried out on a few Snake River Plain basaltic lavas (Tilley and Thompson, 1970; Thompson, 1972, 1975; Leeman, 1974).

PETROGRAPHY AND MINERALOGY

Snake River Plain basalts are characteristically vesicular and commonly have well-developed diktytaxitic macroscopic texture. Flows are generally thin (less than 5 to 10 meters thick) and extensive in comparison with their volume, which suggests that they were relatively fluid upon eruption. Depositional relationships are complex in many areas along the Snake River, where flows repeatedly accumulated in deep channels (in excess of 100 meters in some places) and formed lava dams (Stearns and others, 1938; Carr and Trimble, 1963; Malde, 1972). In such occurrences glassy pillow lavas are common.

Microscopic textures in Snake River Plain basalts are varied from subophitic or ophitic in slowly cooled flow interiors to variolitic, hyaloophitic, hyalopilitic, or intersertal in more rapidly cooled portions of flows.

Basalts of the Snake River Plain are remarkably similar in mineralogy. Typically these rocks are porphyritic and contain up to 20 volume percent of combined olivine and plagioclase phenocrysts, with the feldspar dominant. In addition, spinel occurs in most of these rocks as inclusions in the silicate phenocrysts and as sparse microphenocrysts. Rare clinopyroxene phenocrysts have been observed in only a few samples. Olivine is commonly found in the groundmass of these basalts along with plagioclase, clinopyroxene, magnetite, and ilmenite and minor apatite, glass, rutile, and oxidation products. A few samples contain cristobalite which occurs as vesicle linings. Plagioclases commonly grade serially from phenocrysts (up to 1 centimeter long in some samples) to groundmass microlites and display normal zoning. Oscillatory zoning and sievelike inclusions of olivine, opaques, and trapped glass are observed in plagioclases from some samples.

Analyses of constituent phenocrysts have been reported by Stone (1967), Leeman (1974), Leeman and Vitaliano (1976), and Stout and Nicholls (1977). Olivine phenocrysts in these basalts range in composition from Fo_{85} to Fo_{60} (core compositions from more than thirty different lava flows). Groundmass olivines are more iron-rich (about Fo_{50} to Fo_{40}). Zoning in olivines is common and quite pronounced in some samples. A fairly good correlation exists between maximum Fo content of olivine phenocrysts and MgO content of the whole rock samples. Plagioclases range in composition from about An_{80} to An_{60} for phenocrysts and to more sodic compositions in the groundmass (about An_5 in several samples). A moderate correlation exists between maximum An and Fo contents of plagioclase and olivine phenocrysts, respectively. Groundmass clinopyroxenes (augites) commonly are zoned toward more iron-rich compositions. The most magnesium-rich pyroxenes in many of the samples are similar in composition (about $Wo_{41}En_{43}Fs_{16}$). Inclusions of spinel in olivine phenocrysts and cores of spinel microphenocrysts contain high contents of Cr, Mg, and Al. The microphenocrysts are strongly zoned and have rims of normal titanomagnetite which approach groundmass magnetites in composition. Compositions of coexisting groundmass ilmenite and magnetite indicate crystallization of these minerals at temperatures near 1000°C and at oxidation conditions between the quartz-fayalite-magnetite and Ni-NiO solid buffer assemblages. Plagioclase- and olivine-liquid geothermometers (for example, Drake, 1976; Leeman and Scheidegger, 1977) yield near-liquidus temperature estimates of about 1200°C for some pillow lavas. These estimates are supported by experimental crystallization studies (Tilley and Thompson, 1970; Leeman and Vitaliano, 1976).

Interstitial glass in the basalts is typically rich in SiO_2 and approaches rhyolitic compositions in some samples (Leeman and Vitaliano, 1976; Stout and Nicholls, 1977). However, these glasses do not closely resemble Snake River Plain rhyolites in composition.

CHEMICAL ANALYSES

There are now well over two hundred major element analyses of Snake River Plain basalts, many of which are unpublished. In addition, Leeman (1974) presented some sixty trace element analyses for representative samples. These and published data from sources given in the introduction establish that there two major variants of basaltic lavas—an olivine tholeiite basalt suite and a group of lavas that are best described as highly evolved. Many of the latter lavas are clearly hybrid in origin and reflect a complicated petrogenesis involving extreme

crystal fractionation of olivine tholeiite(?) parental magmas coupled with varied degrees of crustal contamination (see Leeman, 1982b this volume for further discussion). The former suite constitutes the vast majority of basaltic lavas in the Snake River Plain. Within the olivine basalt suite itself, it is possible to distinguish at least two subgroups.

Group I lavas are somewhat diverse in composition (Figure 1) but display trends that are consistent with fractionation of observed phenocryst assemblages (olivine + plagioclase ± spinel). Compositional variations in McKinney Basalt, which is representative of these lavas, are nearly as great as those for the entire Group I suite. This unit is interpreted to include numerous individual flows that differed in phenocryst content and composition as they successively tapped a zoned or inhomogeneous magma reservoir (Leeman and Vitaliano, 1976). Average analyses are given in Table 1 (analysis 10) for seventy-eight Group I lavas. They are characterized by relatively high K_2O, P_2O_5, and TiO_2 contents and display a tendency toward iron enrichment with relatively constant SiO_2 as MgO decreases (that is, a tholeiitic differentiation trend somewhat like that for the Skaergaard intrusion; Wager and Brown, 1967). Most of the olivine basalts studied fall into Group I.

Group II lavas differ from the first group in having lower contents of TiO_2, K_2O, and P_2O_5 and higher contents of CaO and Al_2O_3 (Table 1, analysis 11). These rocks contain phenocryst assemblages like those in Group I, but the olivines and plagioclases are slightly more refractory (that is, richer in MgO and CaO, respectively). Group II lavas are less common than those of Group I and typically appear among the early lavas (that is, Banbury Formation) of the western Snake River Plain (Mark and others, 1975; Bonnichsen, personal communication, 1982). They also occur among younger lavas of the eastern Snake River Plain (for example, at Island Park and near Arco), so there is no obvious pattern to their distribution in space or time.

Molecular (or CIPW) norms for both groups of lavas generally contain both olivine and hypersthene; none contain quartz, but a few Group I lavas have small amounts of nepheline. According to the scheme of Yoder and Tilley (1962) most of these rocks are classified as olivine tholeiites. In the normative basalt tetrahedron (Yoder and Tilley, 1962) these rocks define olivine- and plagioclase-control lines (Figure 2), and for McKinney Basalt normative compositions display significant correlations with contents of various major and trace elements (Figure 3). These trends are consistent with magmatic differentiation by removal (or addition) of olivine and plagioclase.

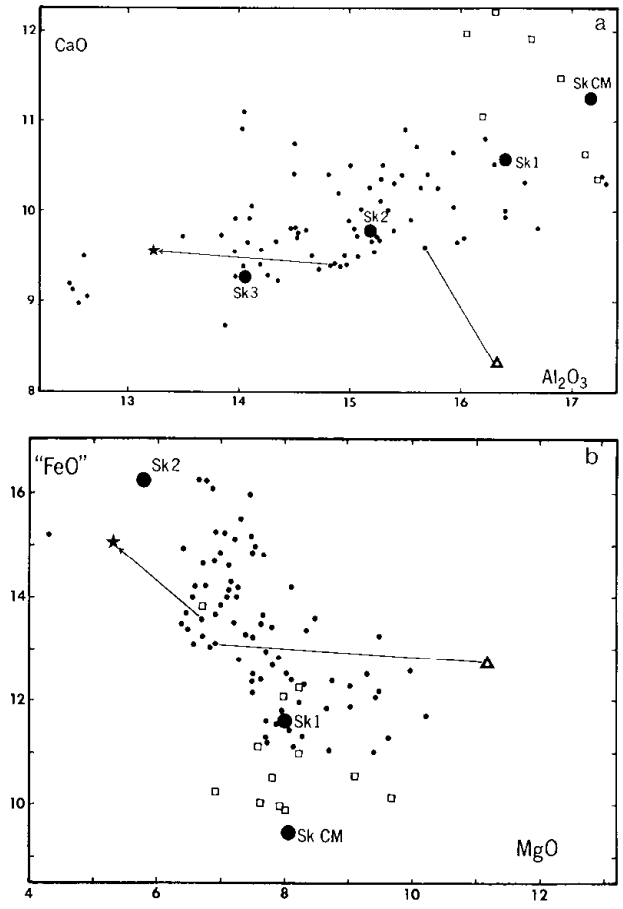

Figure 1. CaO-Al_2O_3 (a) and FeO-MgO (b) variation diagrams for Group I (solid dots) and Group II (open squares) olivine basalts. Solid lines connect troctolite xenolith (triangle), pillow lava glass (star), and intermediate composition whole-rock samples, all from McKinney Basalt (Tilley and Thompson, 1970; Leeman and Vitaliano, 1976). Large solid circles represent compositions of chilled margin gabbro (SkCM) and estimated successive liquids (Sk 1 to Sk 3) of the Skaergaard intrusion (Wager and Brown, 1967). Trend for McKinney Basalt lavas and pillow glass is consistent with fractionation of two parts plagioclase (~An_{70}) and one part olivine (~Fo_{80}). Analyses are taken from Leeman (1974), Trimble and Carr (1976), and Bonnichsen (personal communication, 1982). Note: five Group II lavas have more than 17.5 percent Al_2O_3 and plot off diagram (a).

Table 2 presents averaged trace element data for Group I and Group II basalts contrasted with those for McKinney Basalt (Leeman, 1974 and unpublished data). Frequency distributions for selected trace elements and $^{87}Sr/^{86}Sr$ ratios for these rocks are shown in Figure 4. The observed ranges in these data require a complicated petrogenesis for the basalts involving varied conditions of crystallization or partial melting. No patterns in major or trace element composition are apparent with age or location, except that potassium and rubidium contents

are higher among the Holocene Snake River Group lavas (Group I) and that their average potassium/rubidium ratios are significantly lower (Table 2).

Group II lavas (four samples) are distinct from those of Group I in trace element contents. They are characterized by relatively high Cr/Ni ratios and lower contents of magmaphile trace elements (Th, Hf, Ta, Rb, Zr) in addition to phosphorus, potassium, and titanium. They have lower rare earth element (REE) abundances and REE profiles that are only slightly fractionated (light REE enriched) relative to chondrites (Figure 5). Compared with these rocks Group I lavas have greater absolute REE contents and display greater enrichment of the light REE.

Strontium isotopic ratios in both Groups I and II basalts are indistinguishable and suggest a common source. These ratios are systematically higher (0.7055-0.7075) for the Snake River Plain olivine tholeiites than for mid-ocean ridge and most oceanic island basalts (Hofmann and Hart, 1978), although comparable values have been measured for basalts from a few islands (Peterman and Hedge, 1971). These high ratios have been attributed to derivation of Snake River Plain basaltic magmas from an ancient subcontinental mantle source rather than to crustal contamination (Leeman and Manton, 1971; Leeman, 1977; Doe and others, 1982).

ORIGIN OF SNAKE RIVER PLAIN OLIVINE THOLEIITES

Detailed petrologic and experimental studies of McKinney Basalt and other Snake River Plain olivine tholeiites (Leeman, 1976; Leeman and Vitaliano, 1976; Thompson, 1975; Stout and Nicholls, 1977) have provided several lines of evidence that the corresponding magmas were ultimately derived by partial melting of a spinel peridotite mantle source within the continental lithosphere at depths of perhaps 60 to 90 kilometers. Subsequent analysis of the development of the Snake River Plain province suggests a modified interpretation (Leeman, 1982a this volume). Whatever the ultimate mode of magma genesis there is a high probability that mafic magmas tend to stagnate within the upper mantle or lower crust where hydrostatic equilibrium with wall rocks would be attained. Under such circumstances, these magmas would likely experience some degree of high-pressure crystallization and possible equilibration with wall rocks at depth. If this were the case, it may be difficult to unravel the history of these magmas in detail. We must therefore consider two extreme cases: (a) the Snake River Plain basaltic magmas ascended more or less directly from the depths at which they formed, and (b) their ascent

Table 1. Averaged major element compositions of major basalt types in the northwest United States[1].

	1	2	3	4	5	6	7	8	9	10	11
SiO_2	49.70	48.64	49.50	50.36	54.37	51.19	47.45	48.73	47.50	47.04	47.84
TiO_2	1.54	1.29	2.31	1.56	1.17	3.13	3.62	3.30	3.79	2.70	1.07
Al_2O_3	17.93	17.54	16.61	15.54	15.28	14.07	13.84	13.88	12.50	15.11	16.35
FeO	9.79	10.12	12.14	11.25	9.46	13.91	15.22	14.41	17.53	13.51	10.18
MnO	0.14	0.18	0.17	0.20	0.16	0.23	0.23	0.20	0.27	0.20	0.18
MgO	6.99	8.09	4.95	6.68	5.91	4.39	5.99	5.88	4.41	7.65	9.66
CaO	10.02	10.61	9.02	10.67	9.79	8.48	9.71	9.72	8.80	10.06	12.34
Na_2O	2.91	2.83	3.57	2.95	2.80	2.72	2.31	2.42	2.44	2.54	2.09
K_2O	0.73	0.46	1.26	0.57	0.77	1.22	0.72	0.73	1.23	0.61	0.17
P_2O_5	0.26	0.23	0.47	0.22	0.29	0.67	0.91	0.73	1.54	0.58	0.18
Mg no.	56.0	58.8	42.1	51.4	52.7	36.0	41.2	42.1	31.0	50.2	62.8

[1]All analyses are adjusted to total 100 weight percent with volatiles excluded and all iron as FeO.

Sources of data presented:

1. Oregon Plateau, high-alumina basalts (n = 21); Waters (1962)
2. Diamond Craters, southeast Oregon (n = 10); L. C. Rowan (personal communication, 1974)
3. Steens Mountain basalts (n = 63); Gunn and Watkins (1970)
4. High-Mg Picture Gorge Basalt (n = 8); Swanson and others (1979)
5. Very high-Mg Grand Ronde Basalt (n = 10); Swanson and others (1979)
6. Roza basalt (n = 35); Swanson and others (1979)
7. Basin City basalt (n = 12); Swanson and others (1979)
8. Martindale basalt (n = 13); Swanson and others (1979)
9. Goose Island basalt (n = 8); Swanson and others (1979)
10. Snake River Plain olivine basalt (n = 78); Leeman and Manton (1971)
11. Low-K Snake River Plain basalt (sample 72-24, this study; location in roadcut 18 miles southwest of Arco on U.S. Highway 93)

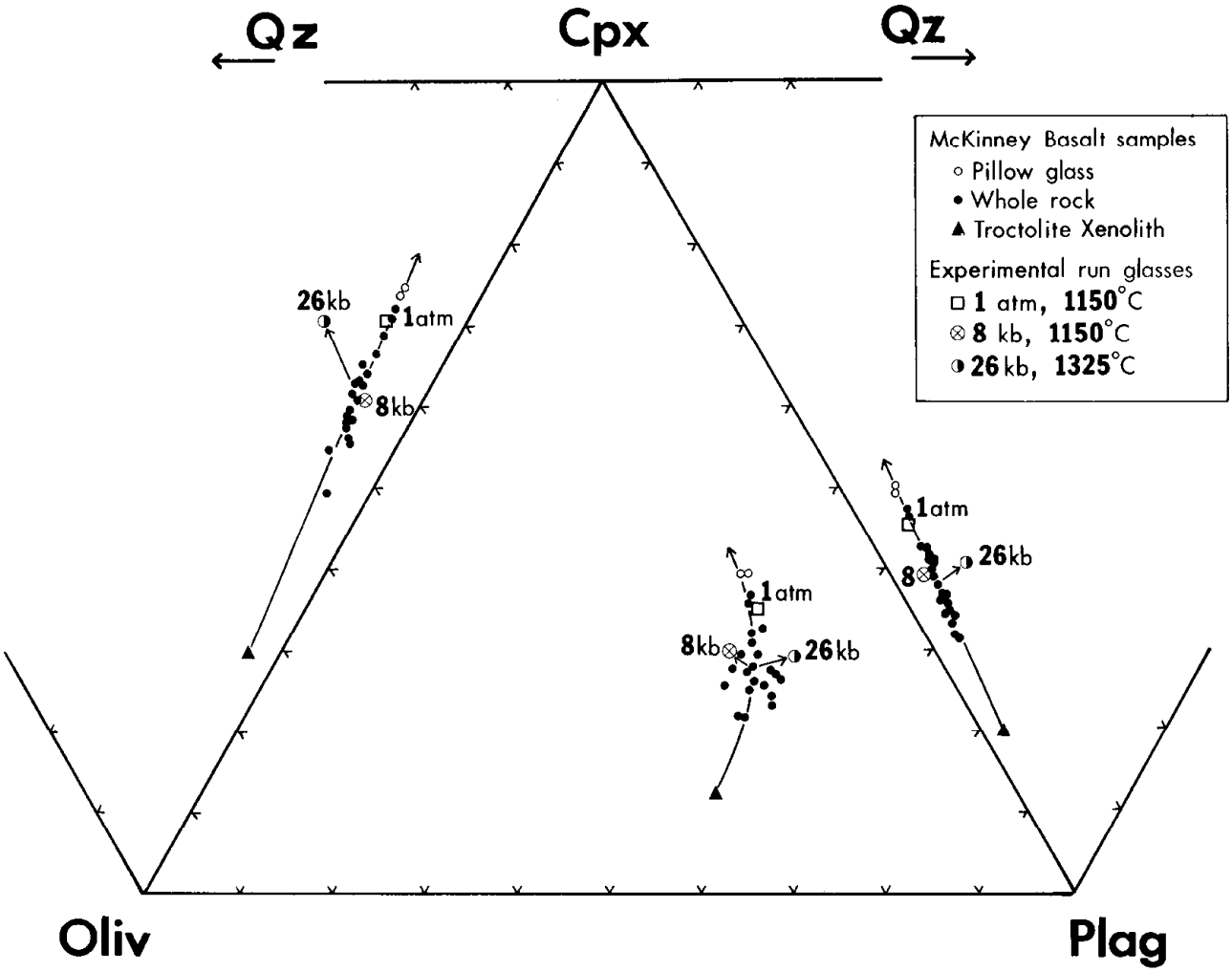

Figure 2. Expanded view of the normative basalt tetrahedron showing projected analyses of McKinney Basalt samples and liquids produced experimentally from one of these samples at different pressures. The observed differentiation trends are consistent with low pressure fractionation of mainly plagioclase and olivine.

was interrupted by stagnation at one or more levels, at which they may have evolved away from the compositions of the parental magmas.

The phenocrystic nature of most Snake River Plain basalts, the relatively evolved compositions of their olivine and plagioclase phenocrysts, and the diversity and iron-rich nature of whole-rock compositions all attest that most of these magmas evolved to some degree either during ascent or within relatively shallow reservoirs. The virtual absence of clinopyroxene phenocrysts and results of experimental studies by Thompson (1975) suggest that significant differentiation occurred at depths shallower than 30 kilometers (that is, within the crust). It is also evident that lithostatic pressure at such depths would be sufficient to drive olivine tholeiite magmas to the surface (Leeman, 1982a this volume). The absence of high-pressure phenocrysts or xenolith inclusions in Snake River Plain basalts nevertheless restricts penultimate differentiation to relatively shallow depths. We can rule out case (a) for direct ascent of the magmas, with the possible exceptions of certain nonporphyritic lavas (see Stout and Nicholls, 1977). The latter magmas apparently ascended at sufficiently high rates that they did not appreciably crystallize.

These nonporphyritic lavas (Leeman, 1974; Stout and Nicholls, 1977) are rather similar in major and trace element compositions to other contemporaneous Group I lavas. Accordingly, it may be argued that shallow differentiation of the porphyritic magmas did not induce significant compositional modifications, particularly for magmaphile elements such as the REE. In support of this view, Leeman

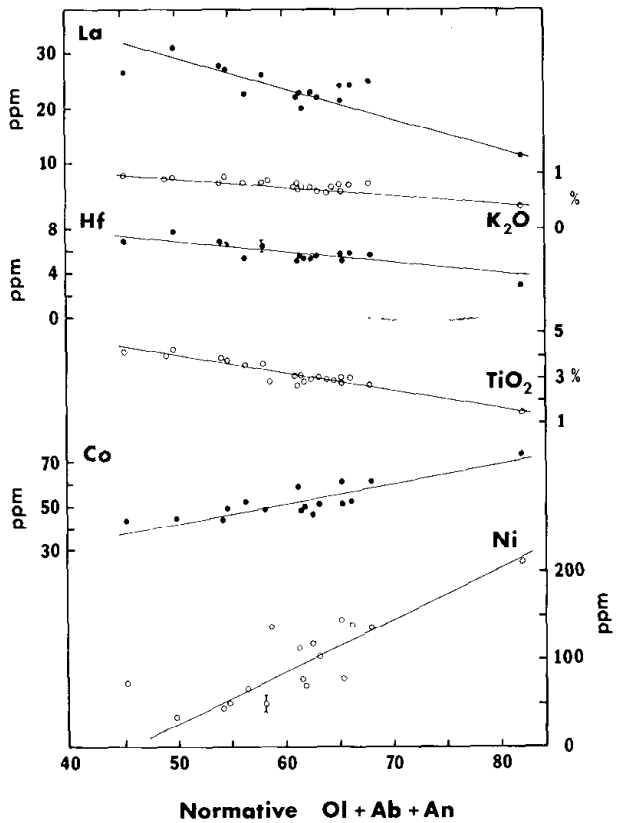

Figure 3. Variation diagram showing covariance of several major and trace elements with an index of normative olivine plus plagioclase for McKinney Basalt samples. Isolated point on right is troctolite xenolith. Representative error bars are shown where analytical uncertainty exceeds size of the symbols.

Table 2. Element statistics for minor elements in Snake River Plain olivine tholeiites.

Element	Group I[a]	Group II[a]	McKinney Basalt[b]
Ni	106.	76.	87.
Co	51.	49.	51.
Sc	31.	40.	31.
Cr	246.	287.	215.
Ba	399.	162.	380.
Sr	293.	209.	321.
Rb	10.	4.	17.
K	4990.	2390.	6640.
Zr	255.	84.	278.
La	24.	6.8	24.
Ce	55.	16.	54.
Sm	8.1	3.1	7.6
Eu	2.6	1.1	2.6
Tb	1.4	0.65	1.2
Yb	3.4	2.3	3.4
Lu	0.58	0.41	0.56
$^{87}Sr/^{86}Sr$	0.7062	0.7061	0.7065

[a]Data from Leeman (1974)
[b]Average of 14 samples, excluding troctolite xenolith and glass separates, from Leeman and Vitaliano (1976)

(1976) pointed out that relatively large degrees of crystallization are required to produce significant changes in the contents of these elements.

Assuming a uniform mantle source for most Snake River Plain olivine tholeiites, the range in REE contents observed in these lavas (Figure 5) seemingly reflects differing degrees of partial melting of that source. Because Group II lavas have the lowest REE contents, they could have formed by higher degrees of melting than Group I magmas or by further melting of previously depleted mantle. As an example, lanthanum (La) is strongly enriched in silicate melts relative to all significant mantle phases. Thus, La contents in magmas derived from a uniform source must vary inversely with degree of partial melting. Group I basalts display La enrichments up to about 150 relative to chondrites, whereas some Group II basalts are enriched to a lesser extent (about 15 times chondrites). If we assume a uniform source composition, the tenfold range in La enrichment would ideally correspond to a tenfold

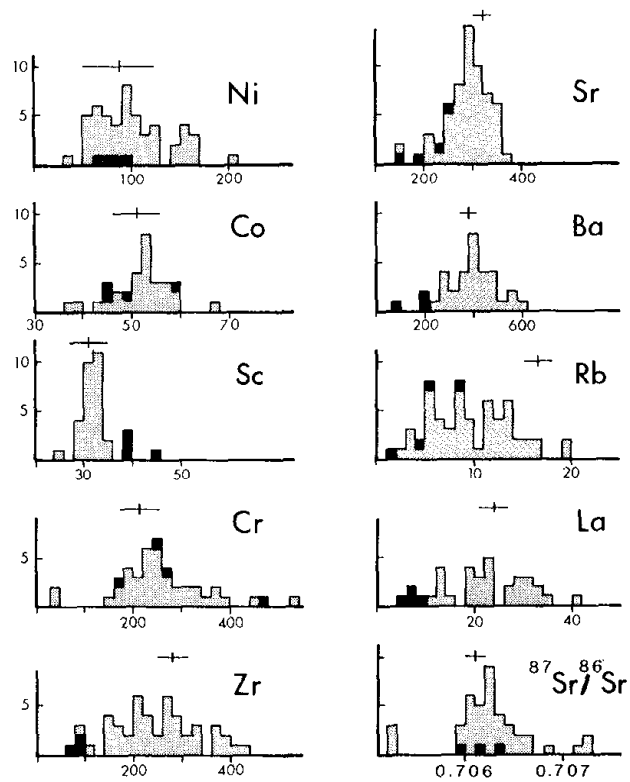

Figure 4. Histograms of contents of several trace elements and $^{87}Sr/^{86}Sr$ ratios in Snake River Plain olivine basalts. Cross above each histogram shows the mean and standard deviation for these parameters in McKinney Basalt samples (which are excluded from the histograms). Number of samples is shown at left and concentrations in parts per million are shown at base for the indicated trace elements. Group II lavas are shown by dark pattern.

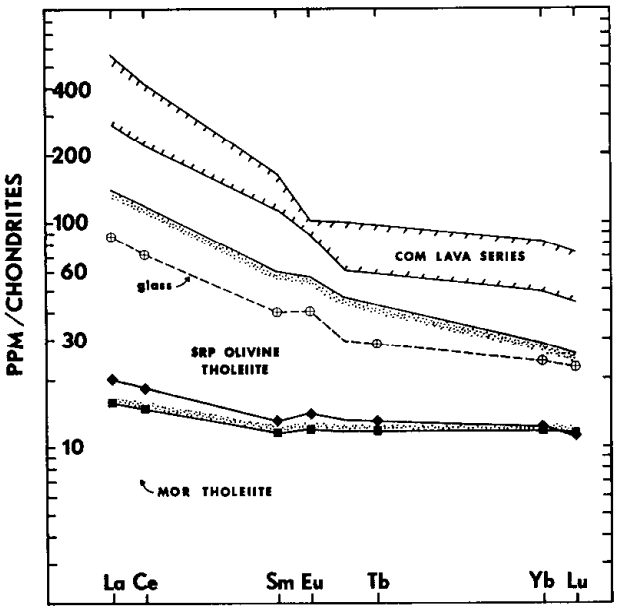

Figure 5. Comparative REE profiles for Snake River Plain olivine basalts (between stippled boundaries), evolved lavas from Craters of the Moon (COM) lava series (Leeman and others, 1976; Leeman, 1982b this volume), and mid-ocean ridge (MOR) tholeiites (Kay and others, 1970). Individual profiles are shown for two Group II low-K basalts (■, ◆) and glass from McKinney Basalt pillow lava (⊕).

difference in the degree of fusion. Crystal fractionation alone would require about 90 percent solidification to account for the same degree of La enrichment! Other major and trace element data are consistent with these possibilities. Exact estimates of the degree of melting required to produce Group I or II magmas depend on actual REE contents of the source, which are not known (see Leeman, 1976, for further discussion). Of course, some of the variance in REE patterns could reflect nonuniformity of source materials.

Shapes of the REE profiles also provide some constraints on the mineralogical nature of the source material. The consistently small fractionation of heavy REE suggests that the magmas did not equilibrate with source rocks containing appreciable garnet (which strongly incorporates the heavy REE). Accordingly, Leeman (1976) inferred that garnet-free peridotite is a reasonable source material. For case (a), this inference would imply a maximum depth of melting (about 60 kilometers) defined by the lower pressure stability of garnet in the mantle. For case (b), it would be necessary to postulate that if primitive Snake River Plain basaltic magmas formed at greater depths they must have ascended to shallow mantle depths where they stagnated and reequilibrated with garnet-free wall rocks.

Isotopic studies of the olivine tholeiites provide further constraints on their origin. Oxygen isotopic analyses (Muehlenbachs and Stone, 1973; Leeman and Whelan, in preparation) of fresh samples and their plagioclase phenocrysts yield $\delta^{18}O$ between 5 and 6 per mil; these $\delta^{18}O$ values are identical with data for fresh oceanic basalts and are consistent with a mantle origin. Strontium isotopic ratios (Leeman and Manton, 1971) are high relative to most oceanic basalts, and range between 0.7055 to 0.7075. The lack of any correlation between strontium contents and $^{87}Sr/^{86}Sr$ ratios is believed to be inconsistent with significant contamination by crustal material.

Lead isotopic compositions (Leeman, 1977; Doe and others, 1982; Leeman and Doe, in preparation) are quite varied and define a linear array in $^{207}Pb/^{204}Pb$—$^{206}Pb/^{204}Pb$ space (Figure 6). This array could be interpreted in two ways. It could be a mixing line for mantle and crustal components of lead. However, there is no correlation between lead contents and isotopic compositions, nor is it probable that such a linear array would result from mixing between two reservoirs each of which is likely to be heterogeneous in isotopic and elemental composition. The favored interpretation is that the array is a secondary isochron whose slope corresponds to an age of about 2.5 billion years. In the secondary isochron model, this age corresponds to the source materials that were partially melted to form the basaltic magmas. According to this model the mantle source must have been a closed system since 2.5 billion years ago (that is, part of the continental tectosphere); in other words, it was isotopically homogenized at the time of major crustal development but retained small heterogeneities in its uranium/lead (also rubidium/strontium) elemental ratio. Subsequently, these heterogeneities, coupled with decay of radioactive uranium and rubidium isotopes, led to lead and strontium isotopic heterogeneities in the present-day subcontinental mantle. Partial melts of this aged mantle terrain thus sampled the continuum of its present-day isotopic compositions.

Further evidence that the isotopic data do not reflect crustal contamination is provided by a comparison between the olivine tholeiites and the evolved and hybrid lavas described by Leeman (1982b this volume). Figure 7 contrasts strontium and lead isotopic ratios for these rocks. Clearly-contaminated lavas from the Craters of the Moon and King Hill suites are characterized by elevated $^{87}Sr/^{86}Sr$ ratios which are strongly correlated with $^{206}Pb/^{204}Pb$ ratios. The correlation trends project toward fields outlining known crustal compositions. The olivine tholeiites display no such correlations, although they contain comparable strontium and lower lead contents, and should be at least as

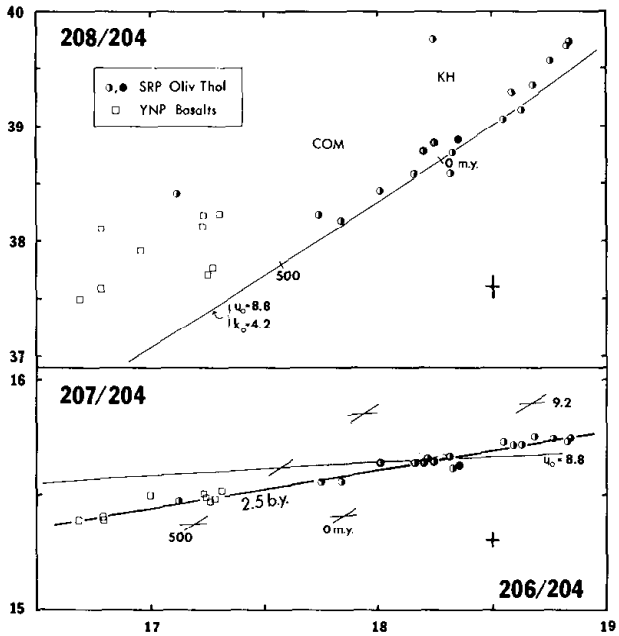

Figure 6. $^{208}Pb/^{204}Pb$ and $^{207}Pb/^{204}Pb$ versus $^{206}Pb/^{204}Pb$ in basalts from the Snake River Plain-Yellowstone National Park (SRP-YNP) province. Growth curves for lead isotope evolution in the mantle source rocks are estimated for the given values of $^{238}U/^{204}Pb$ (μ_o) and $^{232}Th/^{238}U$ (κ_o). A least-squares fit isochron, corresponding to an age of 2.5 billion years for the source rocks, is shown in the lower panel. Stippled areas show fields of lead isotopic compositions for evolved lavas from Craters of the Moon (COM) and King Hill (KH) lava suites.

susceptible to crustal contamination.

The data discussed in this section seemingly are consistent with derivations of Snake River Plain basaltic magmas by different degrees of partial melting of relatively homogeneous spinel peridotite source rocks. The isotopic data further show that the source rocks are located within the aged subcontinental lithospheric mantle rather than in the asthenospheric (or deeper) mantle that presumably gives rise to oceanic volcanic rocks. Few if any of the erupted lavas are considered to represent primary magmas because textural and geochemical characteristics indicate that they are somewhat fractionated. However, Group II lavas have magnesium numbers [100 x Mg/(Mg + Fe), atomic ratio] consistent with their equilibration with ultra mafic rocks containing olivines (Fo_{85}) typical of some upper mantle rocks (see Roder and Emslie, 1970). Of all the basalts studied, those of Group II are judged to be the most primitive in the sense that they have undergone the least degree of differentiation during ascent. Most Group I lavas seem to represent magmas that evolved to differing extents as they ascended, and possibly stagnated, at deep crustal or upper mantle levels. On the basis of available data, crustal contamination is considered negligible for most of these basalts.

None of the lavas studied seems to record evidence supporting an origin or evolution at mantle depths greater than 90 to 100 kilometers, although such evidence could have been obscured by subsequent evolutionary processes. Evidence for the massive influx of such magmas into a crustal regime that is not characterized by significant degrees of extension, and the inferred northeastward propagation of magmatism with time (Leeman, 1982a this volume), suggest that melting of the subcontinental lithospheric mantle occurred in response to the migration of the continent over a stationary heat source. The nature of the heat source is poorly constrained, but it could be related to diapirically upwelling asthenospheric mantle. It is not known whether partial melts derived from such a diapir contribute significantly to Snake River Plain-Yellowstone Plateau magmatism. With the exception of helium isotopic anomalies observed at Yellowstone (Craig and others, 1978), no other isotopic data appear to reflect substantial involvement of asthenospheric partial melts. This aspect of the magmatism deserves further examination.

COMPARATIVE PETROLOGY

Magmatism contemporaneous with that of the Snake River Plain-Yellowstone Plateau province has characterized much of the Pacific Northwest. An in-depth discussion is beyond the scope of this paper, but it is important to stress that basaltic lavas from nearby provinces generally are distinct from those in the Snake River Plain (Powers, 1960). Table 1 presents averaged analyses of basalts from southeastern Oregon and from the Columbia River Plateau. The southeastern Oregon basalts comprise distinct high-alumina and mildly alkalic series (Table 1; analyses 1 to 3) that developed in a region of pronounced extension as the Cascades structural block rotated clockwise toward the west (Magill and Cox, 1981; Oldow and Leeman, in preparation). The underlying crust consists of accreted oceanic and island arc terranes of late Paleozoic and younger age. It is, therefore, no surprise that strontium and lead isotopic ratios in the young basalts from this region are characteristic of primitive oceanic mantle source rocks (Leeman, 1982c; McKee and others, in press).

Columbia River Plateau lavas include numerous distinctive groups erupted mainly between 16 and 8 million years ago from several different vent areas in

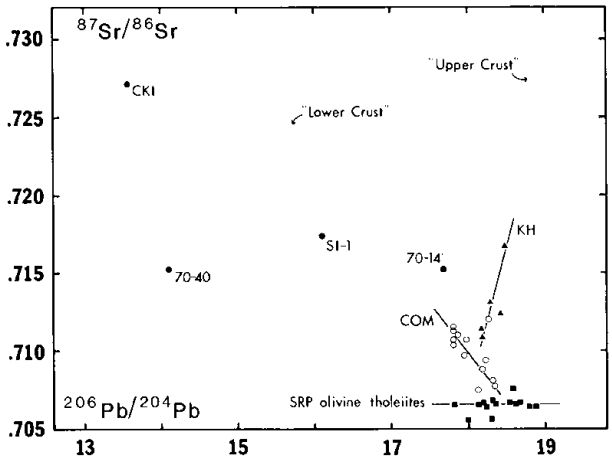

Figure 7. $^{87}Sr/^{86}Sr$ versus $^{206}Pb/^{204}Pb$ in Snake River Plain olivine tholeiites and evolved lavas from King Hill (KH) and Craters of the Moon lava field (COM). Stippled areas show typical range in isotopic compositions for lower and upper crustal rocks. Data points within lower crust field represent analyses of xenoliths (CKI, SI-1, 70-40) from Craters of the Moon lavas. Sample 70-14 is a quartz monzonite from the southern Idaho batholith.

north-central and northeastern Oregon, southeastern Washington, and west-central Idaho (Swanson and others, 1979). The early most voluminous variants have been attributed to some form of back-arc rifting, which is characteristic of a structural zone that extends to north-central Nevada (Stewart and others, 1975; Christiansen and McKee, 1978). Leeman (1982a this volume) suggests that rifting was localized along the "suture zone," between accreted oceanic terranes to the west and a stable cratonic block on the east, that acted as a zone of weakness. Younger variants are confined to vent areas mainly in southeastern Washington that may be underlain by crust of a transitional nature (see Armstrong and others, 1977). Analyses of these lava groups (Table 1, analyses 4 to 9) all differ from the Snake River Plain basalts. Notably, most of these lavas have low magnesium numbers and appear to be relatively fractionated. Only the high-Mg Picture Gorge and Grande Ronde variants have magnesium numbers comparable with average Group I basalts from the Snake River Plain, yet they differ in other important respects. Strontium and lead isotopic composition of Columbia River basalts differ according to location of their vent areas (see summaries of Leeman, 1977, 1982c). Only the Picture Gorge (westernmost vents) and a few early Grande Ronde basalts have oceaniclike isotopic compositions. All others are characterized by elevated $^{87}Sr/^{86}Sr$ ratios which approach or even exceed values for Snake River Plain basalts, and lead isotopic ratios in the youngest (Saddle Mountains Basalt) define a 2.5 billion year secondary isochron like that for the Snake River Plain (S. E. Church, personal communication, 1976). Thus, some Columbia River basaltic magmas may have been derived from old mantle source rocks, but it is not yet possible to rule out their contamination by old crustal rocks (Carlson and others, 1981).

In summary, the tectonic settings, age relationships, and compositions of basaltic lavas differ between the Snake River Plain and other provinces discussed. It is likely that the magmas from these areas formed and evolved in different ways. Unlike in the other provinces, basaltic magmatism in the Snake River Plain does not appear to be related to significant crustal extension. Furthermore, the association of voluminous rhyolitic volcanism there seemingly is a consequence of the interaction between basaltic magmas and initially thick sialic cratonic crust, which is not present to any great extent beneath the provinces to the west (Leeman, 1982a this volume).

CONCLUSIONS

Snake River Plain basaltic lavas can be distinguished into two compositional groups—relatively primitive low-K (II) and more fractionated (I) olivine tholeiites. Compositional variants of these lavas can be attributed to the formation of magmas by varied degrees of partial melting of relatively uniform spinel peridotite source rocks, and to subsequent low pressure (10 kilobars or less) olivine and plagioclase fractionation during ascent and stagnation in deep crustal reservoirs. Strontium and lead isotopic data do not show significant contamination of these magmas by crustal material. Rather, they imply the derivation of the magmas via partial melting of aged subcontinental lithospheric mantle. There is no indication in the isotopic data of significant direct contributions of magma from asthenospheric mantle sources such as have produced most oceanic basalts.

Lithospheric mantle rocks were partially melted as the continent migrated over a stationary sublithospheric heat source. The nature of the postulated heat source is poorly constrained but may be an upwelling diapir of asthenospheric mantle.

The thickening of the mafic lower crust and the association of voluminous rhyolitic magmatism in the Snake River Plain are interpreted as consequences of the influx of large volumes of basaltic magma, much of which stagnated at crustal levels, where fractionation and crustal anatexis occurred, in the absence of significant crustal extension. Con-

temporaneous magmatism in nearby parts of Oregon and Washington differed from that in the Snake River Plain largely as a result of different tectonic regimes (extension) and different crustal structures.

ACKNOWLEDGMENTS

This work was made possible by grant support from the National Geographic Society and National Science Foundation (EAR80-18580). I thank A. Elsweiler and A. Walters for assistance with manuscript preparation, and Bill Bonnichsen for his thoughtful editorial comments.

REFERENCES

Armstrong, R. L., W. H. Taubeneck, and P. O. Hales, 1977, Rb-Sr and K-Ar geochronometry of Mesozoic granitic rocks and their Sr isotopic composition, Oregon, Washington, and Idaho: Geological Society of America Bulletin, v. 88, p. 397-411.

Carlson, R. W., G. W. Lugmair, and J. D. Macdougall, 1981, Columbia River volcanism: the question of mantle heterogeneity or crustal contamination: Geochimica et Cosmochimica Acta, v. 45, p. 2483-2499.

Carr, W. J. and D. E. Trimble, 1963, Geology of the American Falls quadrangle, Idaho: U. S. Geological Survey Bulletin 1121-G, 44 p.

Christiansen, R. L., in preparation, Quaternary and Pliocene volcanism of the Yellowstone rhyolite plateau region of Wyoming, Idaho, and Montana: U. S. Geological Survey Professional Paper 729.

Christiansen, R. L. and E. H. McKee, 1978, Late Cenozoic volcanic and tectonic evolution of the Great Basin and Columbia intermontane regions: Geological Society of America Memoir 152, p. 283-311.

Craig, H., J. E. Lupton, J. A. Welhan, and Robert Poreda, 1978, Helium isotope ratios in Yellowstone and Lassen Park volcanic gases: Geophysical Research Letters, v. 5, p. 897-900.

Doe, B. R., W. P. Leeman, R. L. Christiansen, and C. E. Hedge, 1982, Lead and strontium isotopes and related trace elements as genetic tracers applied to the Quaternary rhyolite-basalt association of the Yellowstone Plateau volcanic field, U.S.A.: Journal of Geophysical Research, v. 87, p. 4785-4806.

Drake, M. J., 1976, Plagioclase-melt equilibria: Geochimica et Cosmochimica Acta, v. 40, p. 457-465.

Gunn, B. M. and N. D. Watkins, 1970, Geochemistry of the Steens Mountain Basalts, Oregon: Geological Society of America Bulletin, v. 81, p. 1497-1516.

Hofmann, A. W. and S. R. Hart, 1978, Assessment of local and regional isotopic equilibrium in the mantle: Earth and Planetary Science Letters, v. 38, p. 44-62.

Karlo, J. F. and C. V. Clemency, 1980, Picrite xenoliths from the eastern Snake River Plain, Idaho: Contributions to Mineralogy and Petrology, v. 73, p. 173-178.

Kay, Robert, N. J. Hubbard, and P. W. Gast, 1970, Chemical characteristics and origin of oceanic ridge volcanic rocks: Journal of Geophysical Research, v. 75, p. 1585-1613.

Leeman, W. P., 1974, Petrology of basaltic lavas from the Snake River Plain, Idaho (Part I); experimental determination of partitioning of divalent cations between olivine and basaltic liquid (Part II): University of Oregon Ph.D. thesis, 337 p.

———, 1976, Petrogenesis of McKinney (Snake River) olivine tholeiite in light of rare-earth element and Cr/Ni distributions: Geological Society of America Bulletin, v. 87, p. 1582-1586.

———, 1977, Comparison of Rb/Sr, U/Pb, and rare earth characteristics of sub-continental and sub-oceanic mantle regions: Oregon Department of Geology and Minerals Industry Bulletin, v. 96, p. 149-168.

———, 1982a, Development of the Snake River Plain-Yellowstone Plateau province, Idaho and Wyoming: an overview and petrologic model, *in* Bill Bonnichsen and R. M. Breckenridge, editors, Cenozoic Geology of Idaho: Idaho Bureau of Mines and Geology Bulletin 26.

———, 1982b, Evolved and hybrid lavas from the Snake River Plain Idaho, *in* Bill Bonnichsen and R. M. Breckenridge, editors, Cenozoic Geology of Idaho: Idaho Bureau of Mines and Geology Bulletin 26.

———, 1982c, Tectonic and magmatic significance of strontium isotopic variations in Cenozoic volcanic rocks from the western United States: Geological Society of America Bulletin, v. 93, p. 487-503.

Leeman, W. P. and W. I. Manton, 1971, Strontium isotopic composition of basaltic lavas from the Snake River Plain, southern Idaho: Earth and Planetary Science Letters, v. 11, p. 420-434.

Leeman, W. P. and K. G. Scheidegger, 1977, Olivine/liquid distribution coefficients and a test for crystal-liquid equilibrium: Earth and Planetary Science Letters, v. 35, p. 247-257.

Leeman, W. P. and C. J. Vitaliano, 1976, Petrology of McKinney Basalt, Snake River Plain, Idaho: Geological Society of America Bulletin, v. 87, p. 1777-1792.

Leeman, W. P., C. J. Vitaliano, and Martin Prinz, 1976, Evolved lavas from the Snake River Plain: Craters of the Moon National Monument, Idaho: Contributions to Mineralogy and Petrology, v. 56, p. 35-60.

Magill, James and Allen Cox, 1981, Post-Oligocene tectonic rotation of the Oregon western Cascade Range and the Klamath Mountains: Geology, v. 9, p. 127-131.

Malde, H. E., 1972, Stratigraphy of the Glenns Ferry Formation from Hammett to Hagerman, Idaho: U. S. Geological Survey Bulletin, 1331-D, 19 p.

Malde, H. E. and H. A. Powers, 1962, Upper Cenozoic stratigraphy of western Snake River Plain, Idaho: Geological Society of America Bulletin, v. 73, p. 1197-1220.

———, 1972, Geologic map of the Glenns Ferry-Hagerman area, west-central Snake River Plain, Idaho: U. S. Geological Survey Miscellaneous Geologic Investigations Map I-696.

Malde, H. E., H. A. Powers, and C. H. Marshall, 1963, Reconnaissance geologic map of the west-central Snake River Plain, Idaho: U. S. Geological Survey Miscellaneous Geologic Investigations Map I-373.

Mark, R. K., C. Lee-Hu, H. R. Bowman, Frank Asaro, E. H. McKee, and R. R. Coats, 1975, A high $^{87}Sr/^{86}Sr$ mantle source for low alkali tholeiite, northern Great Basin: Geochimica et Cosmochimica Acta, v. 39, p. 1671-1678.

McKee, E. H., W. A. Duffield, and R. J. Stern, in press, Late Miocene and early Pliocene basaltic rocks and their implications for crustal structure, northeastern California and south-central Oregon: Geological Society of America Bulletin.

Muehlenbachs, Karlis and G. T. Stone, 1973, Oxygen isotope compositions of some basaltic lavas from the Snake River Plain: Carnegie Institute of Washington Yearbook 72, p. 598-601.

Peterman, Z. E. and C. E. Hedge, 1971, Related strontium isotopic and chemical variations in oceanic basalts: Geological Society of America Bulletin, v. 82, p. 493-500.

Powers, H. A., 1960, A distinctive chemical characteristic of Snake River basalts of Idaho: U. S. Geological Survey Professional Paper 400-B, p. 298.

Roeder, P. L. and R. F. Emslie, 1970, Olivine-liquid equilibrium: Contributions to Mineralogy and Petrology, v. 29, p. 275-289.

Spear, D. B., 1979, The geology of Big Southern Butte and the surrounding area: State University of New York at Buffalo Ph.D. thesis, 136 p.

Stearns, H. T., Lynn Crandall, and W. G. Steward, 1938, Geology and ground-water resources of the Snake River Plain in southeastern Idaho: U. S. Geological Survey Water Supply Paper 774, 268 p.

Stewart, John, G. W. Walker, and F. J. Kleinhampl, 1975, Oregon-Nevada lineament: Geology, v. 3, p. 265-268.

Stone, G. T., 1967, Petrology of upper Cenozoic basalts of the Snake River Plain: University of Colorado Ph.D. thesis, 392 p.

Stout, M. Z. and Jim Nicholls, 1977, Mineralogy and petrology of Quaternary lavas from the Snake River Plain, Idaho: Canadian Journal of Earth Science, v. 14, p. 2140-2156.

Swanson, D. A., T. L. Wright, P. R. Hooper, and R. D. Bentley, 1979, Revisions in stratigraphic nomenclature of the Columbia River Basalt Group: U. S. Geological Survey Bulletin 1457-G, 59 p.

Thompson, R. N., 1972, The 1-atmosphere melting patterns of some basaltic volcanic series: American Journal of Science, v. 272, p. 901-932.

———, 1975, Primary basalts and magma genesis, II. Snake River lavas at pressures up to 35 Kb: Contributions to Mineralogy and Petrology, v. 52, p. 213-232.

Tilley, C. E. and R. N. Thompson, 1970, Melting and crystallization relations of the Snake River basalts of southern Idaho, U.S.A.: Earth and Planetary Science Letters, v. 8, p. 79-92.

Trimble, D. E. and W. J. Carr, 1976, Geology of the Rockland and Arbon quadrangles, Power County, Idaho: U. S. Geological Survey Bulletin 1399, 115 p.

Wager, L. R. and G. M. Brown, 1967, Layered Igneous Rocks: Freeman and Company, San Francisco, 588 p.

Waters, A. C., 1962, Basalt magma types and their tectonic associations: Pacific Northwest of the United States: American Geophysical Union Monograph 6, p. 158-170.

Yoder, H. S. and C. E. Tilley, 1962, Origin of basalt magmas: an experimental study of natural and synthetic rock systems: Journal of Petrology, v. 3, p. 343-532.

Evolved and Hybrid Lavas from the Snake River Plain, Idaho

by

William P. Leeman[1]

ABSTRACT

Numerous suites of evolved or hybrid lavas from the Snake River Plain-Yellowstone Plateau province are briefly described in this paper. Despite that such rocks are widely dispersed in time and space throughout the province, they display remarkable coherence in their major element compositional variations from one place to another. In addition, these rocks typically have anomalous strontium, lead, and oxygen isotopic compositions compared with the associated more voluminous olivine tholeiites. Where sufficient data exist, the isotopic compositions in the lavas trend toward typical crustal values with increasing differentiation. This observation suggests that the magmas evolved at crustal levels where they were progressively contaminated by interactions with crustal wall rocks. However, crystal-liquid fractionation is considered to be the dominant factor in their evolution. Available petrochemical and experimental data support this view and reveal that the evolved lavas initially developed by high-pressure (about 8-10 kilobars) crystallization of olivine tholeiitic magmas.

INTRODUCTION

Lavas of an evolved or hybrid nature occur as isolated flows or in lava fields of small volume in numerous localities within the Snake River Plain-Yellowstone Plateau province. With few exceptions they have received little study and relatively little is known about their petrogenesis and their relation to the more voluminous olivine tholeiites. The purpose of this paper is to call attention to their unusual mineralogical and compositional features. At present only tentative conclusions can be drawn as to how they formed, but it is apparent that they have certain characteristics in common.

[1]Department of Geology, Rice University, Houston, Texas 77001.

OCCURRENCES AND DESCRIPTIONS

Locations of known occurrences of evolved lavas are shown in Figure 1 and brief comments concerning each are given in Table 1 with pertinent references. Representative chemical analyses of lavas from these localities are given in Table 2. The best characterized example is that at Craters of the Moon lava field (Figure 1, location E). These rocks have been discussed in some detail by Leeman and others (1976) and have recently been remapped (Kuntz and others, 1980, 1982 this volume). Most of the lavas are aphyric to slightly porphyritic. Their compositions range from ferrobasalt (Table 2, analyses 1 and 2) to ferrolatite (analysis 5) with essentially complete compositional gradation between these extremes. The entire series is characterized by high contents of P_2O_5 and K_2O. The mineralogy of these rocks has been discussed in several papers (Thompson, 1972, 1975a, 1975b; Leeman and others, 1976; Stout and Nicholls, 1977). The mafic lavas contain phenocrysts of olivine, plagioclase, magnetite, and apatite. In lavas containing greater than about 56 percent SiO_2, olivine and apatite are sparse and traces of clinopyroxene appear on the liquidus. The phenocryst compositions reflect the evolution of the lava series. With increasing whole-rock SiO_2 contents, (a) the rocks display strong iron enrichment (Mg Number [= 100 x Mg/(Mg + Fe)] ranges from 0.29 to 0.04), progressive enrichment in such magmaphile elements as Rb, Cs, Th, Ba, and Zr, and depletion in transition metal contents; (b) olivine cores range in composition from Fo_{72} to Fo_{10}; and (c) plagioclase cores range in composition from An_{62} to An_{38}. Variation diagrams for Craters of the Moon lavas reveal a high degree of coherence between most elemental contents (see Leeman and others, 1976). Correlation coefficients for representative oxide components (Table 3) illustrate this coherence. However, covariation trends for oxide pairs are not perfectly linear

Leeman, W. P., 1982, Evolved and hybrid lavas from the Snake River Plain, Idaho, *in* Bill Bonnichsen and R. M. Breckenridge, editors, Cenozoic Geology of Idaho: Idaho Bureau of Mines and Geology Bulletin 26, p. 193-202.

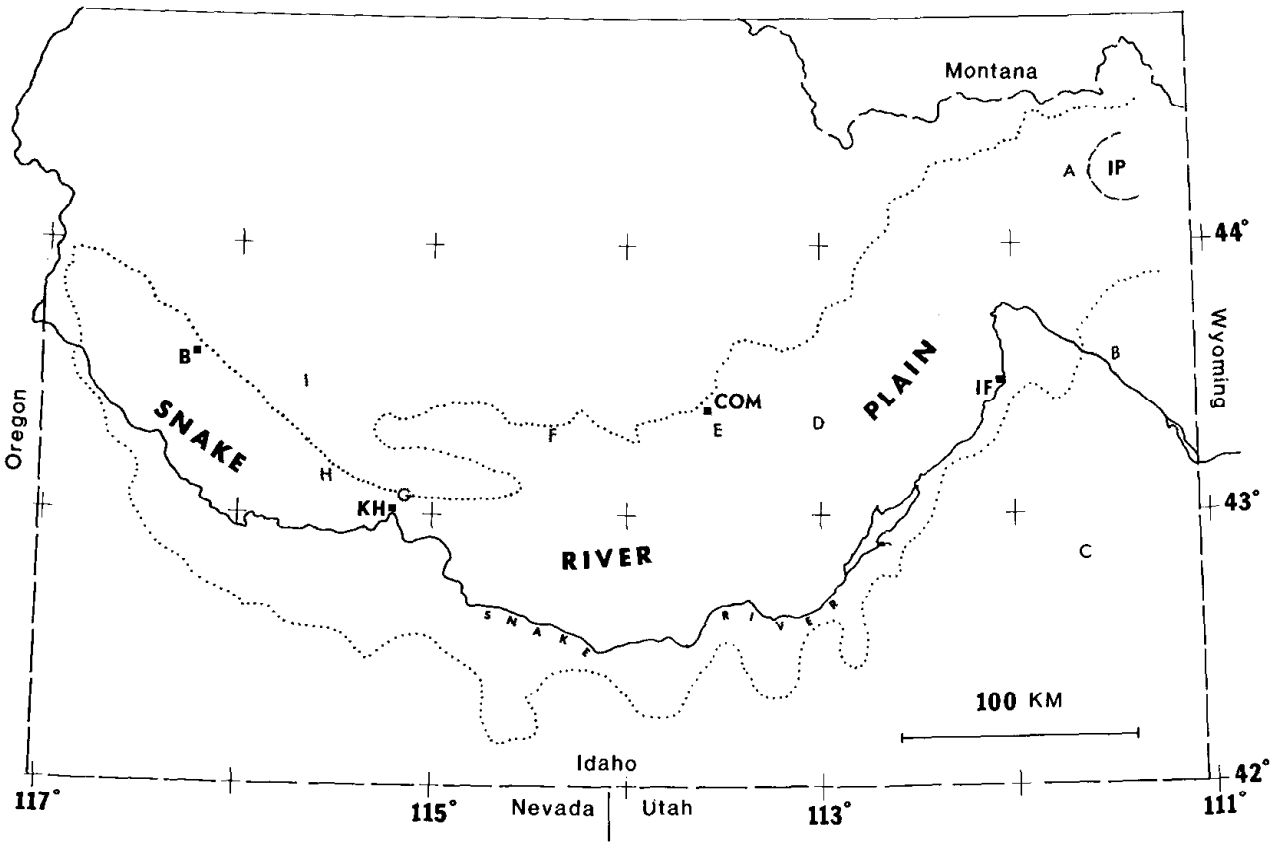

Figure 1. Map showing locations where evolved or hybrid lavas occur in and peripheral to the Snake River Plain, Idaho. See Table 1 and text for brief descriptions. Geographic localities shown for reference are Boise (B), King Hill (KH), Craters of the Moon National Monument (COM), Idaho Falls (IF), and Island Park (IP).

but display changes in slope that correspond to changes in the phenocryst assemblages.

Least-squares mixing calculations (Leeman and others, 1976) show that the observed range in composition for these lavas can be explained quantitatively by fractional crystallization of observed phenocryst phases. Experimental studies at one atmosphere (Thompson, 1972, 1975a; Leeman and others, 1976) are consistent with this hypothesis. However, strontium, lead, and oxygen isotopic studies (Leeman and others, 1976; Leeman, 1974 and unpublished data; Leeman and Whelan, in preparation) reveal that assimilation of crustal material is required, in addition to fractional crystallization, to explain the evolution of these lavas. For example, $^{87}Sr/^{86}Sr$ ratios increase from 0.7075 to 0.7113 with increasing SiO_2 content, and reach 0.7120 in one intermediate sample. Textural evidence (embayed quartz and potassium-feldspar xenocrysts) and the occurrence of deep-crustal xenoliths (granulite gneiss and granitic rocks) attest to some form of crustal contamination as these magmas evolved in crustal reservoirs.

Lavas similar to those at Craters of the Moon occur elsewhere (Table 1), but generally only a few flows are present and at any given locality their ranges in composition are more restricted. Because the characterization of these rocks is less advanced, they will not be discussed in detail. The lavas at King Hill (Powers, 1960; Stone, 1967; Thompson, 1975b) and near Magic Reservoir (Schmidt, 1961) are noteworthy because some are exceptionally rich in xenocrystic material and, in some flows, crustal xenoliths.

As an example, one lava flow (Table 4, sample 69-63) contains an unusual mineral assemblage including three distinct clinopyroxene compositional populations (Table 4, Px-1 to Px-3), olivine (Fo_{35}-Fo_{21}), apatite, anorthoclase ($An_{22}Ab_{60}Or_{18}$, possibly xenocrystic), plagioclase (An_{46}-An_{30}), titanomagnetite, and quartz (xenocrystic) in a glassy groundmass. A basaltic flow (Table 2, analysis 16) from the same locality lacks crustal xenocrysts but contains sparse phenocrysts(?) of moderately aluminous orthopyroxene (Table 4, Px-4) with olivine reaction rims. This latter pyroxene is interpreted as possibly having crystallized at high

pressure from the host magma or a more primitive precursor magma because its composition (up to 5 percent Al_2O_3) is similar to those of orthopyroxenes crystallized from olivine tholeiite compositions at pressures above 18 kilobars (Green and Ringwood, 1967). Furthermore, the orthopyroxene is intergrown with large labradorite phenocrysts and magnetite; these glomeroporphs are distinct from disaggregated xenocrysts derived from crustal xenoliths. In general, these rocks display textural evidence for incorporation of crustal material and for polybaric crystallization. Without exception they are characterized by

Table 1. Brief summary of occurrences of hybridized (contaminated) lavas, Snake River Plain, Idaho.

Map Symbol	Locality	Age (million years)	Comments	References
A	Island Park-Spencer rift zone	<<0.6	Early cinder cone vents and flows of transitional basalt (hawaiite?), many containing crustal xenoliths or xenocrysts, and minor ferrolatite (Antelope Flat-High Point vent). Later or contemporaneous olivine tholeiite flows from fissure or shield vents are apparently uncontaminated.	1, 4, 5
B	Area southeast of Idaho Falls	<~2.3	Isolated flows (for example, Ririe damsite) of transitional and ferrolatite composition. These have not been studied in detail.	1, 9
C	Blackfoot Reservoir area	<~1-2	Transitional lavas associated with olivine tholeiite and rhyolite domes in Blackfoot lava field and along fault zones in nearby valleys. Many flows contain quartz xenocrysts and some of the youngest (less than 0.05 million years old) contain xenoliths of rhyolite and crustal rocks.	1, 10, 11, 16, 19
D	Southeast of Big Southern Butte	<~0.4	Cedar Butte and Cerro Grande lavas (ferrobasalt to ferrolatite) resemble Craters of the Moon lavas in composition. They are associated with olivine tholeiite lavas from numerous fissure and shield vents.	5, 6, 7, 18
E	Craters of the Moon lava field	<0.02	Contaminated and differentiated lavas ranging from ferrobasalt to ferrolatite (44 to 63 percent SiO_2). Some flows contain common xenoliths of granitic to gneissic crystalline rocks, silicic volcanic clasts, and alkali feldspar and quartz xenocrysts. $^{87}Sr/^{86}Sr$ ranges from 0.7075 to 0.7120.	1, 2, 3
F	Magic Reservoir area	~5	Extensive flows of Square Mountain Basalt contain common crustal xenoliths and xenocrysts of quartz and alkali feldspar. A few analyses indicate ferrolatite composition but the flows are probably variable in composition. $^{87}Sr/^{86}Sr$ is 0.714 in one flow. Recent lava of Black Crater is transitional in composition suggesting slight contamination; $^{87}Sr/^{86}Sr$ is 0.7075.	1, 15, 16
G	King Hill Basalt	~2-3	A sequence of three isolated flows ranging from transitional basalt to ferrolatite, with significant internal variability in composition, containing xenocrysts of quartz, alkali feldspar; high pressure (?) glomeroporphs of moderately aluminous orthopyroxene and plagioclase are common in one flow. $^{87}Sr/^{86}Sr$ ranges from 0.7104 to 0.7167.	1, 13, 14, 17
H	Mountain Home area	~1-2	Numerous lavas of Bruneau age (for example, Basalts of Berry Ranch, McGinness Ranch, and Hammett) contain quartz xenocrysts and some have slightly anomalous compositions relative to associated olivine tholeiites. Lavas of Cold Springs Creek Basalt range in composition from normal olivine tholeiite to ferrobasalt and ferrolatite; the latter contains rare crustal xenoliths.	1, 12, 13, 17
I	Smith Prairie-Boise River area	<<0.7	Intracanyon lavas of mainly olivine tholeiite, but some flows of more siliceous lava contain common xenoliths of granitic and gneissic crystalline rocks. No data available on chemical compositions or radiometric ages.	8

References: 1. Leeman (unpublished data); 2. Leeman and others (1976); 3. Kuntz and others (1980); 4. Hamilton (1965); 5. LaPoint (1977); 6. Kuntz (1978); 7. Spear (1979); 8. Howard and Shervais (1973); 9. H. J. Prostka (personal communication, 1975, 1979); 10. Mansfield (1927); 11. Armstrong (1969); 12. Stone (1967); 13. Malde and Powers (1962); 14. Powers (1960); 15. Schmidt (1961); 16. Leeman (Table 2, this study); 17. Stone (1970); 18. Fountain and Spear (1979); 19. Fiesinger and others (1982 this volume).

elevated $^{87}Sr/^{86}Sr$ ratios compared with olivine tholeiites of the province (Table 1; Leeman and Manton, 1971).

In addition to obviously contaminated lavas, numerous flows (for example, locations A, C, H, I) contain sparse quartz xenocrysts. Some of these flows have slightly anomalous compositions, but in general they simply appear to be more fractionated variants of the olivine tholeiite suite. However, as Bowen (1928) pointed out, the heat consumed in assimilating crustal material by a given magma is in part provided by crystallization of near liquidus phases. Hence, the resulting hybrid magmas would appear to be derivitives of less fractionated (and uncontaminated) parental magma. Strontium isotope ratios in the analyzed lavas containing quartz xenocrysts are not markedly different from those in the olivine tholeiites, so it appears that the degree of contamination has not been large for these lavas.

Slightly to moderately porphyritic lavas of hawaiite to mugearite composition are abundant in a few places (locations A, B, C, D). These lavas commonly contain large plagioclase phenocrysts (up to 5 centimeters long), and some contain clinopyroxene-orthopyroxene-plagioclase cumulate xenoliths (for example, Swan Butte, location A). These lavas are typically associated with large cinder cone vents, so it appears that the corresponding magmas may have been relatively rich in volatiles. Some contain deep-crustal xenoliths (granulite facies metamorphic rocks) and have elevated $^{87}Sr/^{86}Sr$ ratios, features that are indicative of crustal contamination. Coexisting plagioclase and groundmass from two such samples (Swan Butte and Crystal Butte, location A) display

Table 2. Major element analyses (weight percent) of representative hybrid lavas from the Snake River Plain, Idaho.

Sample	1 69-28	2 CM-1	3 CM-3	4 CM-2	5 62P-81	6 72S-15A	7 HAM-4	8 72S-25	9 73-106G	10 72S-22	11 DS-CB
SiO_2	45.1	46.04	50.07	56.75	62.86	48.16	61.33	49.22	51.9	52.11	61.62
TiO_2	3.21	3.11	2.68	1.29	0.59	2.82	0.72	3.51	3.07	2.28	0.86
Al_2O_3	14.3	13.91	13.74	14.51	14.56	15.38	16.34	13.63	13.9	16.93	13.68
FeO	15.24	16.39	15.45	12.78	8.39	12.65	7.61	15.35	13.7	10.68	9.21
MnO	0.27	0.30	0.28	0.25	0.19	0.23	0.19	0.24	0.25	0.22	0.28
MgO	6.26	3.89	3.01	1.12	0.21	3.51	0.47	3.84	3.65	2.55	0.36
CaO	9.55	7.45	6.80	4.56	3.05	8.01	2.48	7.86	7.31	7.40	3.14
Na_2O	2.55	3.45	3.51	4.02	4.16	3.42	4.44	2.73	3.13	4.16	4.67
K_2O	1.21	1.88	2.14	3.32	4.72	1.65	4.27	1.44	1.95	1.71	4.09
P_2O_5	2.08	2.28	1.65	0.63	0.15	1.67	0.19	1.04	1.13	1.14	0.20
H_2O+	0.20	0.74	0.21	0.15	0.40	0.62	0.56	0.51	-	0.18	1.2
H_2O-	0.09	0.13	0.04	0.03	0.06	0.12	0.56	0.06	-	0.04	-
CO_2	0.05	0.02	0.01	0.01	0.01	0.01	0.00	0.02	-	0.02	0.03

Sample	12 70-34	13 P-87	14 59P276	15 59P311	16 OB-32	17 CP-41	18 SMB-1B	19 SRV72-9	20 H871	21 H344	22 AVG-OT
SiO_2	52.2	49.86	47.97	56.56	47.17	60.38	59.9	46.26	60.07	54.18	46.59
TiO_2	2.15	2.58	3.47	1.09	4.15	1.44	1.95	2.64	1.53	1.97	2.77
Al_2O_3	16.3	13.34	13.76	16.22	13.34	14.20	14.8	14.36	14.22	13.74	14.80
FeO	10.8	15.54	14.40	10.33	15.22	9.15	9.06	12.88	9.99	12.48	13.51
MnO	0.17	0.24	0.25	0.24	0.23	0.15	0.20	0.18	0.26	0.30	0.20
MgO	4.72	2.96	3.76	1.13	4.42	1.22	0.35	8.52	1.39	2.42	7.71
CaO	7.68	7.41	7.17	3.96	7.68	3.25	3.19	9.84	4.35	6.34	9.69
Na_2O	2.56	3.00	3.36	4.49	3.40	3.89	4.05	2.88	4.02	3.46	2.44
K_2O	1.61	2.05	2.54	4.52	2.00	4.21	4.67	0.78	2.75	1.85	0.63
P_2O_5	0.75	1.77	1.80	0.52	1.39	0.56	0.19	0.91	0.60	1.30	0.58
H_2O+	0.88	0.64	0.72	0.20	0.33	0.30	-	0.19	0.67	1.40	0.40
H_2O-	0.14	0.49	0.07	0.13	0.15	0.40	-	0.23	0.06	0.26	0.41
CO_2	0.03	0.03	0.01	0.00	0.04	0.01	-	-	-	-	0.03

differences in $^{87}Sr/^{86}Sr$, so it is clear that these lavas have not attained isotopic equilibrium; the ratios are higher in the groundmass (approximately 0.709) than in the plagioclases (approximately 0.708). It appears not only that the respective magmas are contaminated but also that the contamination of the liquids continued after crystallization of the phenocrysts was well established.

No systematic relations are apparent in the temporal or spatial distribution of hybrid lavas, except that they are most commonly exposed near margins of the province. It is tempting to conclude that this distribution reflects the proximity of the parental magmas to crustal wall rocks along the province boundaries. However, hybrid lavas are found near the axis of the Snake River Plain near Big Southern Butte (location D; Spear, 1979), and other occurrences well within the plain may be obscured by the voluminous tholeiitic lava flows deposited there. No occurrences are known to be associated with early rhyolite facies volcanism, but in some places hybrid lavas appear to be localized near known or suspected caldera structures (for example, locations A, B, D, F). Others (for example, locations C, E, I) are quite late in the eruptive history for their localities. Finally, xenoliths of hybrid lavas are found in the young rhyolite of East Butte (about 20 kilometers east of locality D).

PETROGENESIS

Despite differences in the age, location petrographic and chemical features, and abundance (or absence) of xenocrystic or xenolithic crustal material, there are notable similarities among the hybrid lava suites. For example, MgO variation diagrams (Figure 2) for the analyses given in Table 2 are relatively coherent and for most elements closely parallel the liquid line of descent defined by lavas from Craters of the Moon. This is all the more remarkable considering that the analyses were selected at random, the only criteria being that they were of high quality and that they covered the spectrum of compositions at each locality. Furthermore, $^{87}Sr/^{86}Sr$ ratios for these rocks are quite varied, so the degree of strontium contamination is apparently different from one place to another. It therefore seems that, insofar as the isotopic data reflect bulk contamination, this process is probably not the dominant control on magma compositions. This same conclusion was drawn for the Craters of the Moon lavas, from a more detailed study (Leeman and others, 1976).

Compositional fields are also shown in Figure 2 for olivine tholeiites and cognate cumulate xenoliths from the province. In general, the hybrid lavas define rather clear extensions of the tholeiite data.

Table 2. continued.

Sources of chemical analyses[a]

1.	(69-28)	Fissure flow at southeastern margin, Craters of the Moon lava field (Leeman and others, 1976)
2.	(CM-1)	Sunset Cone northwest flow (Thompson, 1972) (0.04% Cl; 0.20% F)
3.	(CM-3)	Devils Orchard flow (Thompson, 1972) (0.04% Cl; 0.16% F)
4.	(CM-2)	Indian Tunnel flow (Thompson, 1972) (0.06% Cl; 0.13% F)
5.	(62P-81)	Highway flow (Stone, personal communication, 1973) (0.06% Cl; 0.11% F)
6.	(72S-15A)	Crystal Butte (Stone, personal communication, 1976)
7.	(HAM-4)	Antelope Flat latite (Hamilton, 1965) (0.03% Cl; 0.02% F)
8.	(72S-25)	Ririe damsite, capping flow (Stone, personal communication, 1976)
9.	(73-106G)	Groundmass, lava from Swan Butte
10.	(72S-22)	Porphyritic basalt xenolith, in rhyolite of East Butte (Stone, personal communication, 1976)
11.	(DS-CB)	Cedar Butte latite (Spear, 1979)
12.	(70-34)	Basalt along Chippy Creek, southeast of Wayan
13.	(P-87)	Intracanyon flow along Blackfoot River near Wapello (Prinz, personal communication, 1970)
14.	(59P276)	Cold Springs Creek lava (Stone, personal communication, 1976)
15.	(59P311)	Cold Springs Creek lava (Stone, personal communication, 1976)
16.	(OB-32)	King Hill (Stone, 1967; Thompson, 1975b; Powers, 1960)
17.	(CP-41)	King Hill (Stone, 1967; Powers, 1960)
18.	(SMB-1B)	Square Mountain Basalt
19.	(SRV72-9)	Black Crater flow (Stout and Nicholls, 1977)
20.	(H871)	Marscoite, Skye (Wager and others, 1965)
21.	(H344)	Ferrodiorite, Skye (Wager and others, 1965)
22.	(AVG-OT)	Average of 37 "normal" olivine tholeiites (Stone, 1967)

[a]Where no reference is given, analyses are new. All iron is reported as FeO to facilitate comparisons as degree of oxidation is varied.

Table 3. Least-squares regression coefficients for Craters of the Moon lava series.

x	y	r	a	b
MgO	SiO_2	-0.959	-3.71	62.75
Do.	TiO_2	0.938	0.60	0.57
Do.	Al_2O_3	-0.470	-0.43	15.12
Do.	FeO	0.863	1.74	8.86
Do.	CaO	0.978	1.13	3.06
Do.	Na_2O	-0.833	-0.21	4.16
Do.	K_2O	-0.933	-0.675	4.54
Do.	P_2O_5	0.916	0.48	0.01
K_2O	SiO_2	0.981	5.49	37.83
Do.	TiO_2	-0.963	-0.88	4.58
Do.	P_2O_5	-0.903	-0.71	3.25

Notes: 1. All iron treated as FeO
2. Linear regression of data for 37 samples.
3. Coefficients a and b define best-fit line: y = ax + b
4. Correlation coefficient (r) values greater than 0.53 are significant at the 99.95 percent confidence limit.

However, relative to the tholeiites the Craters of the Moon lavas display breaks in the SiO_2 and P_2O_5 trends, whereas for the other hybrid lavas variation trends for these elements are more coherent. Several factors could produce such inflections or discontinuities in the variation trends: (a) the hybrid magmas were not derived from a parental tholeiitic magma; (b) they may be derivative, but are related to the tholeiites by fractional crystallization at different pressures; (c) contamination involving different crustal rocks from one place to another leads to differences in the overall compositional trends; or (d) some combination of (b) and (c).

In support of case (b) experimental studies (Thompson, 1975a, 1975b) show that hybrid lavas from the Snake River Plain have quite different near-liquidus phenocryst assemblages at different pressures. On the basis of these experiments, it appears possible to derive mafic variants of the hybrid lavas via intermediate pressure (about 10 kilobars) crystallization of olivine tholeiite magma. At this pressure moderately aluminous clinopyroxene is a liquidus phase on the tholeiitic magma; its crystallization leads to iron enrichment and slight silica depletion in residual liquids. Actual compositional trends may vary from one suite to another due to differences in the proportions or compositions of phenocryst phases as a result of differences in the pressure and temperature conditions attending crystallization. There is evidence in support of high-pressure crystallization in the form of sparse aluminous clinopyroxene-plagioclase-olivine glomeroporphs in the Lava Creek flow at Craters of the Moon (Leeman, unpublished data). As noted earlier, aluminous orthopyroxene phenocrysts occur in some of the King Hill lavas (location G), and two pyroxene-plagioclase cognate xenoliths are found at Swan Butte (location A). None of Thompson's (1975b) high-pressure experiments on Snake River Plain lavas produced orthopyroxene as a near-liquidus phase, but it is a common near-liquidus phase in moderately high-pressure experiments on slightly different olivine tholeiitic compositions (see Green and Ringwood, 1967).

Least-squares mixing calculations, using major element analyses of minerals from Thompson's (1975b) 8-kilobar experiments, are crudely compatible with case (b) for mafic lavas from Craters of the Moon and suggest that such lavas could result from roughly 20 to 40 percent crystallization of olivine, plagioclase, and augite from an olivine tholeiite parental magma at that pressure (Figure 3A). However, enrichments of magmaphile elements (such as Rb, K, and Th) in the ferrobasalts seemingly require even greater degrees of crystallization (65 to 85 percent), if they are derived from typical olivine tholeiite magmas (Leeman and others, 1976). However, both of these approaches to estimate the extent of crystallization are very approximate as they depend heavily on the composition of the hypothetical parental magma, which is very poorly constrained, and on the unlikely assumption that closed system crystallization was attained.

The more evolved ferrolatite and intermediate lavas seemingly can be produced by extensive (at least 70 percent) low-pressure crystallization of

Table 4. Compositions (weight percent) of groundmass and pyroxenes in King Hill hybrid lava 69-63.

	Rock[b]	Groundmass	Px-1	Px-2	Px-3	Px-4[a]
SiO_2	60.9	65.6	48.9	50.0	49.7	50.8
TiO_2	1.26	0.83	0.40	0.39	0.85	0.61
Al_2O_3	15.0	14.3	1.42	1.58	2.89	4.11
FeO[c]	8.50	5.83	29.2	24.3	13.3	17.1
MnO	0.14	0.01	0.53	0.40	0.20	0.24
MgO	1.06	0.67	11.6	16.2	14.0	23.7
CaO	3.78	3.02	7.13	6.06	16.0	2.01
Na_2O	4.01	4.18	0.27	0.28	0.34	0.14
K_2O	4.57	5.31	-	-	-	-
P_2O_5	0.65	0.23	-	-	-	-

[a]Aluminous orthopyroxene ($Wo_{4.2}$ $En_{68.2}$ $Fs_{27.6}$) xenocryst (or megacryst) with olivine (Fo_{56} to Fo_{51}) reaction rim from sample 70-9.

[b]Rock contains (in ppm): Ba, 2930; Zr, 800; La, 113; Hf, 22; Rb, 79; Sr, 331; $^{87}Sr/^{86}Sr$, 0.7163 (Leeman, unpublished data).

[c]All iron reported as FeO.

All analyses were carried out by electron microprobe as described by Leeman and others (1976).

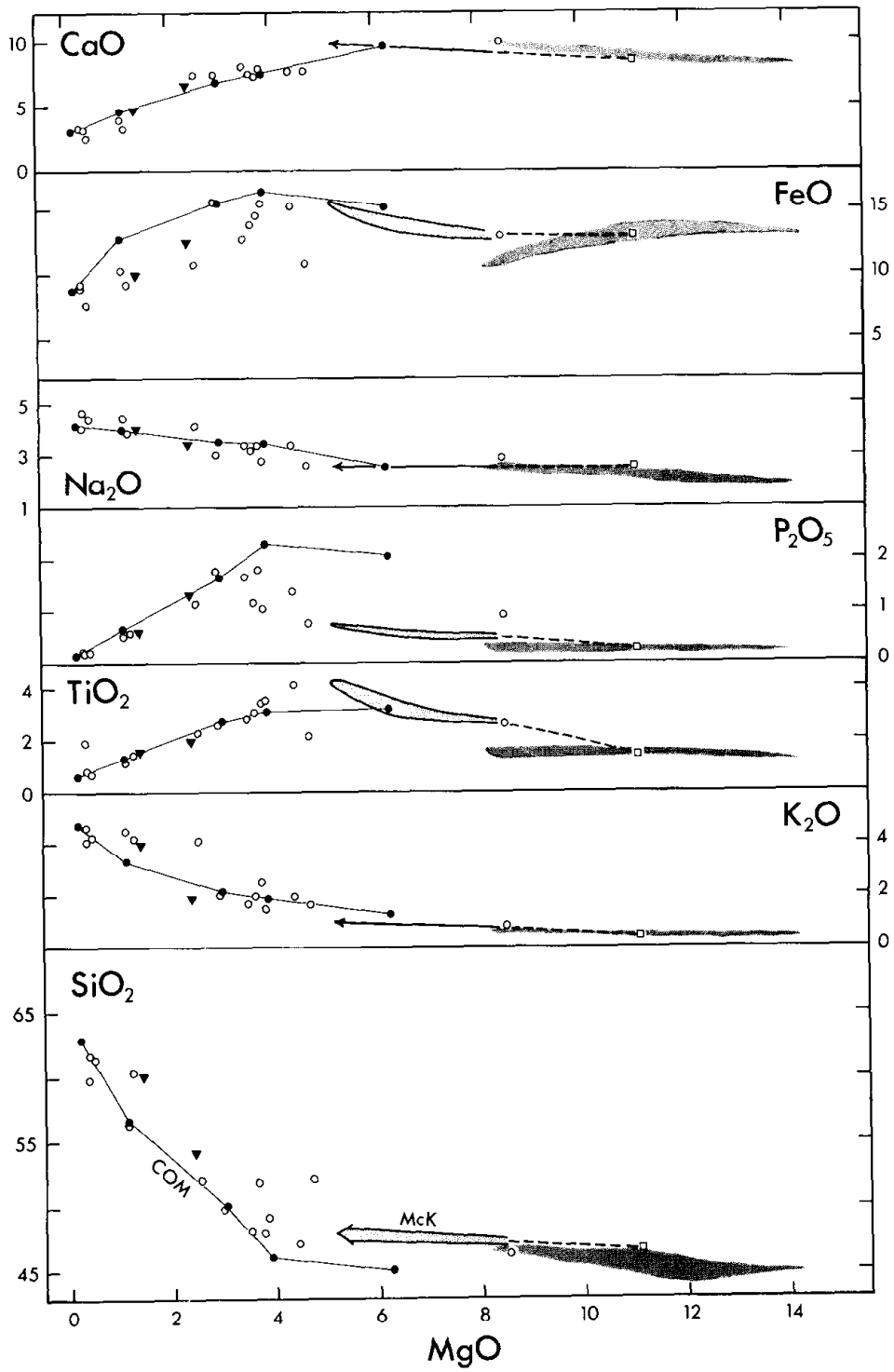

Figure 2. MgO variation diagram for evolved and hybrid lavas from the Snake River Plain, Idaho. Individual data points represent analyses given in Table 2. Solid line connects representative Craters of the Moon lavas. Arrows and light-stippled fields show compositional range for McKinney Basalt samples (Leeman and Vitaliano, 1976), which are representative of many olivine tholeiites of the plain. Dark-stippled fields on the right show the compositional range for cognate xenoliths found in Snake River Plain tholeiites (Leeman and Vitaliano, 1976; Karlo and Clemency, 1980); open square is troctolite xenolith from McKinney Basalt. Solid triangles show compositions of ferrodiorite and marscoite from Skye (Wager and others, 1965).

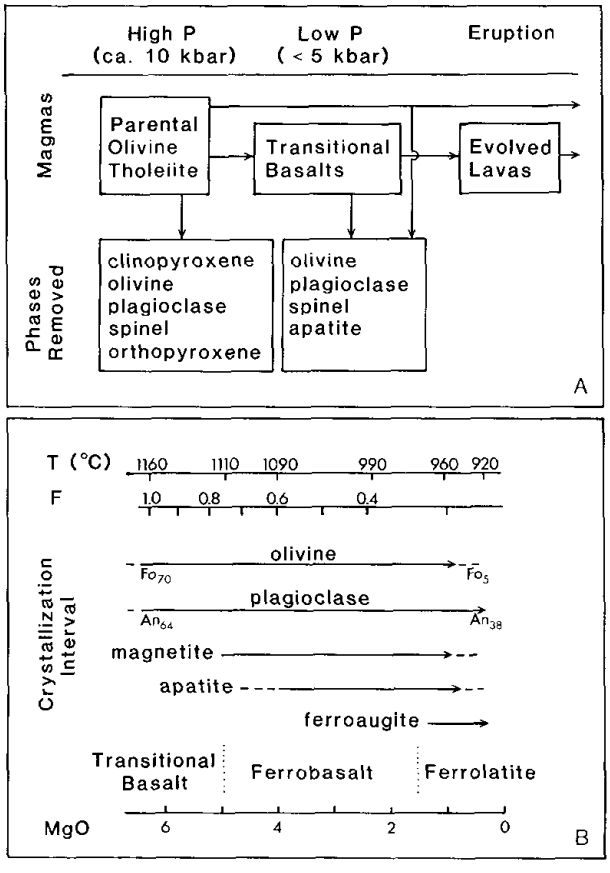

Figure 3. (A) Schematic model for derivation of ferrobasalt parental magmas by high pressure crystallization of olivine tholeiite magma. (B) Schematic diagram illustrating low pressure crystallization models for the Craters of the Moon lava series as a function of MgO content, inferred liquidus temperatures (Leeman, unpublished data), and the fraction (F) of original liquid remaining, assuming all lavas were derived from a common parent having about 6.2 percent MgO (see Leeman and others, 1976).

ferrobasalt precursor magmas, based on experimental studies at one atmosphere pressure, least-squares mixing models using major element data, and models of magmaphile trace element behavior (Leeman and others, 1976). Changes in the phenocryst assemblages, as liquid compositions change and temperature decreases, account for inflections in the Craters of the Moon variation trends in Figure 2. The phenocryst assemblages as a function of MgO content in the rocks and estimated liquidus temperatures (Leeman, unpublished data) are illustrated in Figure 3B.

In summary, a polybaric fractionation scheme appears to reasonably account for most major and trace element variations within the Craters of the Moon lava series. Presumably the same can be said for the other suites of hybrid lavas, but small compositional differences between suites reveal that the conditions attending their crystallization or the compositions of the respective parental magmas differ somewhat. Also the processes and extent of crustal contamination likely differ from one place to another. Considering the varied factors that can affect the compositions of such derivative magmas, it is perhaps remarkable that they appear so similar.

Evolved and hybrid rocks similar to those from the Snake River Plain occur locally in the British Tertiary volcanic province. On the Isle of Skye such rocks occur as intrusive bodies intimately associated with high-level granitic intrusions of the Western Red Hills complex. Wager and others (1965) described two variants known as ferrodiorite and marscoite. The former rocks appear to be extreme differentiates of basaltic magmas, whereas the latter are clearly hybrid rocks that contain xenocrysts derived from both the associated ferrodiorites and the epigranites. These rocks resemble many of the Snake River Plain ferrolatites in xenocryst/phenocryst mineralogy, major element compositions (Figure 2), and even strontium isotopic ratios (Moorbath and Thompson, 1980). The hybrid rocks of the Snake River Plain are probably extrusive analogs for the ferrodiorite-marscoite association, and the latter rocks may provide further insight into origin of the former.

Wager and others (1965) proposed a model for Skye magmatism that is similar to the model for the Snake River Plain-Yellowstone Plateau province (Leeman, 1982 this volume). They suggested that influx of basaltic magma led to crustal anatexis and the formation of high-level silicic magma bodies. Protracted crystallization of the mafic magmas was believed to eventually produce residual ferrodiorite liquids, although details of this crystallization model were not specified. Because of the density contrast between these and granitic liquids, the mixing of the two magmas was thought to be limited to the interface between the respective reservoirs where convective stirring produced the hybrid marscoites. This model may apply generally to the Snake River Plain wherein similar processes may operate at moderate depths in the crust—that is near the base of high-level silicic magma bodies like those beneath Yellowstone. The exact depths of differentiation are not well constrained by the few available experimental data. Evidence for high-pressure (about 8-10 kilobars) crystallization of olivine tholeiite liquids to produce ferrobasalts suggests that differentiation occurs at crystal depths on the order of 30 kilometers. However, there is likely to be some latitude

in the depths at which individual hybrid magma suites evolve. In addition, differences in strontium, lead, and oxygen isotopic characteristics of individual suites (Leeman and Manton, 1971; Muchlenbachs and Stone, 1973; Leeman, 1977; Leeman and Whelan, in preparation) apparently reflect differences in the age or composition of crustal wall rocks with which these magmas interact. Because the respective isotopic ratios in the Snake River Plain hybrid lavas systematically approach values for typical crystal rocks with increasing differentiation, their evolution clearly involves varied degrees of assimilation of crustal material. Wager and others (1965) postulated that evolved rocks at Skye may represent partial melts of some unusual protolith, but recent isotopic studies of these rocks (Moorbath and Thompson, 1980) show that they too have been contaminated by crustal material.

CONCLUSIONS

Evolved and hybrid lavas from the Snake River Plain are widely dispersed in space and time, yet they display surprisingly systematic compositional relations to one another. Some may have originated by high-pressure crystallization of olivine tholeiitic magmas, although details of this process are obscure. Subsequently, mafic variants of these lavas (ferrobasalts) evolved further via lower pressure crystallization to produce ferrolatite magmas. The most extreme ferrolatite differentiates at Craters of the Moon lava field may reflect 90 percent or more crystallization of an olivine tholeiite parental magma. At any given locality, there is a systematic variation in strontium, lead, and oxygen isotopic compositions which trend toward crustal values concurrently with progressive differentiation. The isotopic data show that even the most mafic evolved lavas have interacted with crustal rocks. Therefore, the evolution of these magmas is envisaged to occur largely within the crust, but may take place over a range of depths. Accordingly, differences in isotopic characteristics between specific suites of evolved lavas are thought to reflect differences in the nature of the crustal rocks with which the magmas interact. Despite often remarkable enrichment in $^{87}Sr/^{86}Sr$, for example, it appears that contamination may not exert dominant control upon the magma compositions. Rather, crystal-liquid fractionation is believed to be more important as this process can more readily account for the similarities in differentiation trends between individual suites of evolved lavas.

ACKNOWLEDGMENTS

This work was made possible by grant support from the National Geographic Society and National Science Foundation (EAR80-18580) and by field support from the U. S. Geological Survey. I thank A. Walters and A. Elsweiler for assistance with manuscript preparation and Bill Bonnichsen for very helpful suggestions for improving it.

REFERENCES

Armstrong, F. C., 1969, Geologic map of the Soda Springs quadrangle, southeastern Idaho: U. S. Geological Survey Miscellaneous Geologic Investigations Map I-557.

Bowen, N. L., 1928, The Evolution of the Igneous Rocks: Princeton University Press, Princeton, New Jersey, 332 p.

Fiesinger, D. W., W. D. Perkins, and B. J. Puchy, 1982, Mineralogy and petrology of Tertiary-Quaternary volcanic rocks in Caribou County, Idaho, *in* Bill Bonnichsen and R. M. Breckenridge, editors, Cenozoic Geology of Idaho: Idaho Bureau of Mines and Geology Bulletin 26.

Fountain, J. C. and D. B. Spear, 1979, Geochemistry of ferrobasalt, ferrolatite, and rhyolite lavas from the Cedar Butte area, eastern Snake River Plain, Idaho: Geological Society of America, Abstracts with Programs, v. 11, no. 6, p. 272-273.

Green, D. H. and A. E. Ringwood, 1967, The genesis of basaltic magmas: Contributions to Mineralogy and Petrology, v. 15, p. 103-190.

Hamilton, W. B., 1965, Geology and petrogenesis of the Island Park caldera of rhyolite and basalt, eastern Idaho: U. S. Geological Survey Professional Paper 504-C, 37 p.

Howard, K. A. and J. W. Shervais, 1973, Geologic map of Smith Prairie, Elmore County, Idaho: U. S. Geological Survey Miscellaneous Geological Investigations Map I-818.

Karlo, J. F. and C. V. Clemency, 1980, Picrite xenoliths from the eastern Snake River Plain, Idaho: Contributions to Mineralogy and Petrology, v. 73, p. 173-178.

Kuntz, M. A., 1978, Geologic map of the Arco-Big Southern Butte area, Blaine and Bingham Counties, Idaho: U. S. Geological Survey Open-File Report 78-302.

Kuntz, M. A., D. E. Champion, E. C. Spiker, R. H. Lefebvre, and L. A. McBroome, The Great Rift and the evolution of the Craters of the Moon lava field, Idaho, *in* Bill Bonnichsen and R. M. Breckenridge, editors, Cenozoic Geology of Idaho: Idaho Bureau of Mines and Geology Bulletin 26.

Kuntz, M. A., R. H. Lefebvre, D. E. Champion, L. A. McBroome, D. R. Mabey, W. D. Stanley, H. R. Covington, John Ridenour, and R. B. Stotelmeyer, 1980, Geological and geophysical investigations, and mineral resources potential of the proposed Great Rift Wilderness Area, Idaho: U. S. Geological Survey Open-File Report, 80-475, 54 p.

LaPoint, P. J. I., 1977, Preliminary photogeologic map of the eastern Snake River Plain, Idaho: U. S. Geological Survey Map MF-850.

Leeman, W. P., 1977, Comparison of Rb/Sr, U/Pb, and rare earth characteristics of sub-continental and sub-oceanic mantle regions: Oregon Department of Geology Mineral Industry Bulletin 96, p. 149-168.

———, 1982, Development of the Snake River Plain-Yellowstone Plateau province, Idaho and Wyoming: an overview and petrologic model, *in* Bill Bonnichsen and R. M. Breckenridge, editors, Cenozoic Geology of Idaho: Idaho Bureau of Mines and Geology Bulletin 26.

Leeman, W. P. and W. I. Manton, 1971, Strontium isotopic composition of basaltic lavas from the Snake River Plain, southern Idaho: Earth and Planetary Science Letters, v. 11, p. 420-434.

Leeman, W. P. and C. J. Vitaliano, 1976, Petrology of McKinney Basalt, Snake River Plain, Idaho: Geological Society of America Bulletin, v. 87, p. 1777-1792.

Leeman, W. P., C. J. Vitaliano, and Martin Prinz, 1976, Evolved lavas from the Snake River Plain: Craters of the Moon National Monument, Idaho: Contributions to Mineralogy and Petrology, v. 56, p. 35-60.

Malde, H. E. and H. A. Powers, 1962, Upper Cenozoic stratigraphy of western Snake River Plain, Idaho: Geological Society of America Bulletin, v. 73, p. 1197-1220.

Mansfield, G. R., 1927, Geography, geology, and mineral resources of part of southeastern Idaho: U. S. Geological Survey Professional Paper 152, 448 p.

Moorbath, Stephen and R. N. Thompson, 1980, Strontium isotope geochemistry and petrogenesis of the early Tertiary lava pile of the Isle of Skye, Scotland, and other basic rocks of the British Tertiary province: an example of magma-crust interaction: Journal of Petrology, v. 21, p. 295-321.

Muehlenbachs, Karlis and G. T. Stone, 1973, Oxygen isotope compositions of some basaltic lavas from the Snake River Plain: Carnegie Institution of Washington Yearbook 72, p. 598-601.

Powers, H. A., 1960, Alkalic lava flow, with fluidity of basalt, in the Snake River Plain, Idaho: U. S. Geological Survey Professional Paper 400-B, p. 297.

Schmidt, D. L., 1961, Quaternary geology of the Bellevue area in Blaine and Camas Counties, Idaho: University of Washington Ph.D. thesis, 125 p.

Spear, D. B., 1979, The geology of Big Southern Butte and the surrounding area: State University of New York at Buffalo Ph.D. thesis, 136 p.

Stone, G. T., 1967, Petrology of upper Cenozoic basalts of the Snake River Plain: University of Colorado Ph.D. thesis, 392 p.

———, 1970, Highly evolved basaltic lavas in the western Snake River Plain, Idaho: Geological Society of America, Abstracts with Programs, v. 2, no. 7, p. 695-696.

Stout, M. Z. and Jim Nicholls, 1977, Mineralogy and petrology of Quaternary lavas from the Snake River Plain, Idaho: Canadian Journal of Earth Science, v. 14, p. 2140-2156.

Thompson, R. N., 1972, The 1-atmosphere melting patterns of some basaltic volcanic series: American Journal of Science, v. 272, p. 901-932.

———, 1975a, The 1-atmosphere liquidus oxygen fugacities of some tholeiitic intermediate, alkalic and ultra-alkalic lavas: American Journal of Science, v. 275, p. 1049-1072.

———, 1975b, Primary basalts and magma genesis, II. Snake River lavas at pressures up to 35 kb: Contributions to Mineralogy and Petrology, v. 52, p. 213-232.

Wager, L. R., E. A. Vincent, G. M. Brown, and J. D. Bell, 1965, Marscoite and related rocks of the Western Red Hills complex, Isle of Skye: Philosophical Transactions Royal Society of London, v. A-257, p. 273-307.

Rhyolites of the Snake River Plain-Yellowstone Plateau Province, Idaho and Wyoming: A Summary of Petrogenetic Models

by

William P. Leeman[1]

ABSTRACT

Rhyolitic lava flows, domes, and tuffs comprise a significant volume of eruptive products within the Snake River Plain-Yellowstone Plateau province, particularly in its initial development at any given area. Typically, these rocks are intimately associated with basaltic lava flows, and together they form a bimodal basalt-rhyolite association. The origin of this association is considered on the basis of geologic, petrologic, and geochemical data. These data provide strong constraints against a cogenetic-relation between the two magma types. The most reasonable model for origin of the rhyolites involves the formation of silicic to intermediate precursor magmas by crustal anatexis due to the injection of mantle-derived mafic magmas into the deep crust. The former magmas further evolve by a combination of crystal fractionation, wall-rock and hydrothermal fluid interactions, and probably other less well-defined processes as they ascend the stagnate in high-level reservoirs.

INTRODUCTION

Rhyolitic ash-flow tuffs, lava flows, and domes dominantly represent early phases of magmatism in the Snake River Plain, and almost wholly constitute the volcanic deposits at Yellowstone, notwithstanding the presence of minor volumes of intercalated basaltic lava flows. Comparatively minor domes and flows of rhyolite were extruded locally in association with younger, predominantly basaltic phases of magmatism in the east-central Snake River Plain. Mixed rhyolite-basalt lavas are known in the Gardiner River complex at Yellowstone (Fenner, 1938, 1944; Wilcox, 1944). All of these occurrences attest to the close spatial and temporal association of bimodal basalt and rhyolite magmas during development of the Snake River Plain-Yellowstone Plateau province. Intermediate composition lavas are notably absent with the exception of minor occurrences of highly evolved differentiates discussed by Leeman (1982a this volume).

A number of hypotheses have been presented to account for such bimodal basalt-rhyolite associations, which are common in many anorogenic continental settings. It has been suggested that (1) the silicic magmas may be derived from parental basaltic magmas by means of fractional crystallization (for example, Bowen, 1928) or silicate liquid immiscibility (for example, Fenner, 1938; Roedder and Weiblen, 1971; Yoder, 1973); (2) rhyolites and basalts may be derived from independent parental magmas (Bunsen, 1851), perhaps produced by fractional fusion of the same source material (Presnall, 1969; Yoder, 1973); or (3) injection of mantle-derived basaltic magma into the crust may provide sufficient heat to form anatectic rhyolitic magma (Holmes, 1931; Wager and others, 1965; Blake and others, 1965; Hodge, 1974). The merits of these models have been discussed by Yoder (1973) for the general case of bimodal magma associations. Combinations of these models are certainly possible, and additional complexities may arise as the result of magmatic differentiation or mixing, wall-rock contamination, convective circulation, and internal diffusion in magmas during their ascent (compare Hildreth, 1979).

This paper focuses on petrologic and geochemical characteristics of Snake River Plain rhyolites in an attempt to evaluate these models for their origin. However, because rhyolites of the Yellowstone Plateau have been studied in far greater detail (Boyd, 1961; Hamilton, 1965; Christiansen and Blank, 1972; Christiansen, in preparation; Doe and others, 1982), data for these rocks strongly influence the conclusions that can be drawn at present. Limited pub-

[1]Department of Geology, Rice University, Houston, Texas 77001.

Leeman, W. P., 1982, Rhyolites of the Snake River Plain-Yellowstone Plateau province, Idaho and Wyoming: a summary of petrogenetic models, *in* Bill Bonnichsen and R. M. Breckenridge, editors, Cenozoic Geology of Idaho: Idaho Bureau of Mines and Geology Bulletin 26, p. 203-212.

lished data elsewhere within the Snake River Plain and Owyhee Plateau (Bonnichsen, 1982; Trimble and Carr, 1976; Ekren and others, 1982 this volume) generally support the contention that rhyolitic rocks from the entire province are quite similar in major element compositions and mineralogy.

CHARACTERISTICS OF THE RHYOLITIC ROCKS

Rhyolite units of the eastern Snake River Plain-Yellowstone Plateau province are strikingly uniform both in mineralogy and in major element composition (Figure 1). Microprobe analyses of glasses from vitrophyric rhyolite samples from the east-central and western Snake River Plain show similar compositions to those from Yellowstone (Leeman, unpublished data). The small range in composition observed can be attributed inpart to variations in the content and nature of phenocryst phases and to varied degrees of hydration and alkali metasomatism particularly in the older units. Representative analyses of selected whole-rock samples of rhyolite lava flows, domes, and ash-flow tuffs are given in Table 1. An analysis of silicified Jarbidge Rhyolite is included to illustrate the effects of SiO_2-enrichment and alkali exchange (preferential incorporation of K_2O at the expense of Na_2O) that commonly accompanies hydrothermal alteration. On a water-free basis, all analyzed samples contain more than 70 percent SiO_2, and most are high-SiO_2 rhyolite (74 to 77 percent SiO_2) with peraluminous character (molar Al exceeds total alkalies). The survey (noted above) of major element compositions of glasses in some 100 rhyolite samples revealed that they are even more uniform than the whole-rock samples. Thus there appears to be little compositional variation with space or time for the province as a whole.

Within individual eruptive centers subtle compositional variations may be discerned. At Yellowstone a slightly more calcic variant of rhyolite occurs in certain flows and domes, such as those associated with the resurgence of the youngest caldera (Upper Basin Member of Christiansen, in preparation); these rhyolite units have slightly lower SiO_2 (about 70 percent) and higher CaO (about 1 percent) contents than the majority of rhyolite units there, contain more abundant sodic plagioclase, and ap-

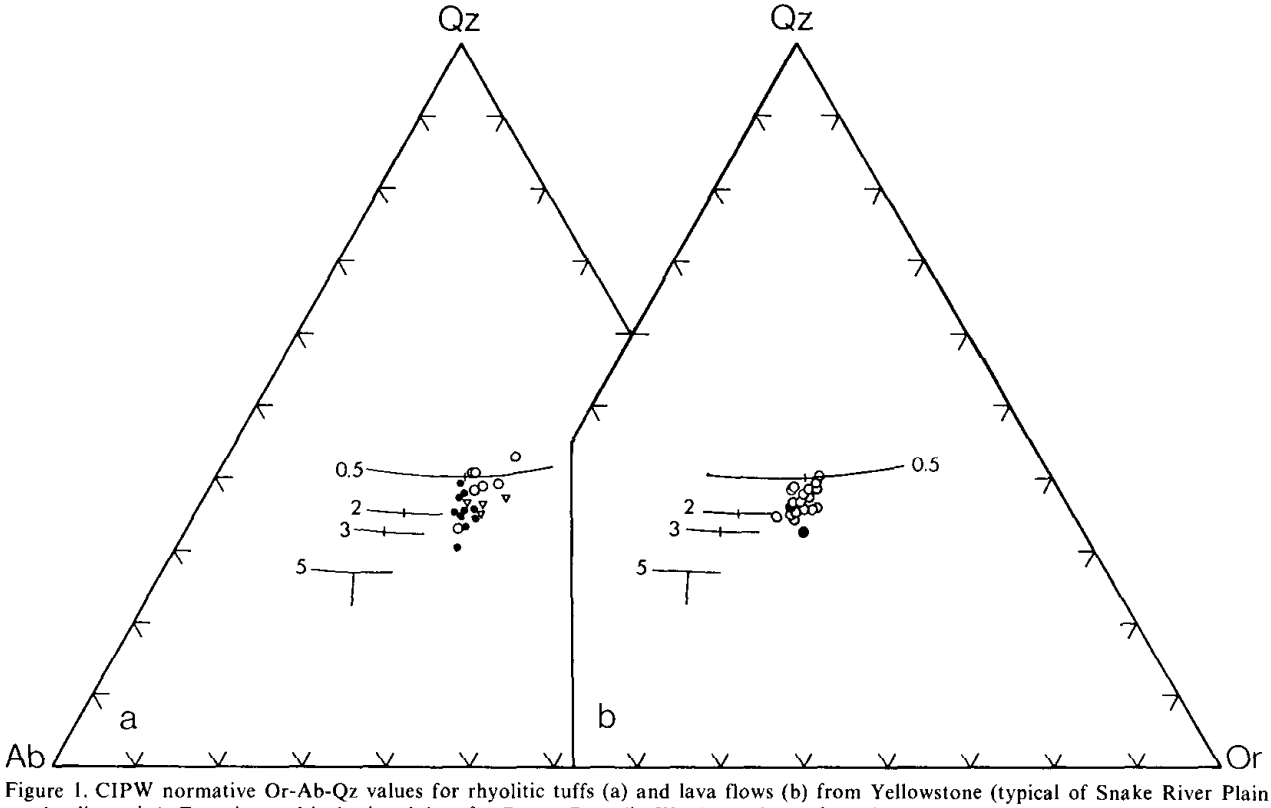

Figure 1. CIPW normative Or-Ab-Qz values for rhyolitic tuffs (a) and lava flows (b) from Yellowstone (typical of Snake River Plain rhyolite units). Experimental isobaric minima for $P_{H_2O} = P_{Total}$ (in Kbar) are shown for reference (Tuttle and Bowen, 1958; Luth and others, 1964). Symbols are as follows: in (a), (filled circles) Huckleberry Ridge Tuff, (open inverted deltas) Mesa Falls Tuff, (open circles) Lava Creek Tuff, and in (b), (filled circles) high-Ca and (open circles) low-Ca rhyolites. Data are from Doe and others (1982).

parently represent somewhat higher temperature (about 900-950° C), less evolved magmas (Hildreth and others, 1980). The small observed range in compositions of Yellowstone rhyolite units likely reflects varied degrees of differentiation within the magma reservoir (Christiansen, in preparation; Leeman, unpublished data). Vertical compositional zoning is evident in the ash-flow tuff units at Yellowstone but is most apparent with respect to trace element and mineralogical compositions (Hildreth and others, 1980; Doe and others, 1982). The latter evidence indicates that the ash-flow tuffs are derived from reservoirs that are compositionally zoned (compare Smith, 1979).

Phenocryst mineralogy of the rhyolite units typically consists of ubiquitous quartz, sanidine or sodic plagioclase, and small amounts of ferromagnesian minerals (typically ferroaugite, fayalitic olivine, orthopyroxene, and iron-titanium oxides). However, sanidine is rare or absent in many rhyolitic rocks from the western Snake River Plain. Hydrous minerals such as amphibole and mica are absent in most, but amphibole is present in a few units (for example, member B of the Lava Creek Tuff; Christiansen, in preparation). Accessory zircon, sphene, monozite, allanite, apatite, and chevkinite occur in many units. The anhydrous phenocryst assemblages in most of these rocks suggest relatively high temperatures and low H_2O contents for the corresponding magmas. Geothermometry using coexisting iron-titanium oxides, orthopyroxene and clinopyroxenes, or plagioclase-alkali feldspar pairs corroborate high liquidus temperatures in the range of 800 to 950° C (Hildreth and others, 1980; Leeman, unpublished data). Thus it is unlikely that most Snake River Plain-Yellowstone Plateau rhyolite magmas formed by fusion of hydrous source rocks; they cannot represent H_2O-saturated granitic minimum melts (compare Tuttle and Bowen, 1958) even though their normative compositions lie close to the low pressure ternary minima in the Qz-Ab-Or system (see Figure 1).

Trace element compositions are also relatively uniform for most analyzed rhyolite samples, although analyses are not numerous. For example, Figure 2 displays rare earth element (REE) data, normalized to chondritic values, for samples from the east-central Snake River Plain. The majority of analyzed samples of ash-flow tuffs and lava flows, including those from Yellowstone, have similar REE profiles and range in absolute concentrations by only a factor of two. The extreme range for sixteen typical ash-flow tuff samples is given in Figure 2a. However, it is notable that late-stage domes (for example, East, Wedge, and Big Southern Buttes) commonly deviate from the norm (Figure 2b). REE

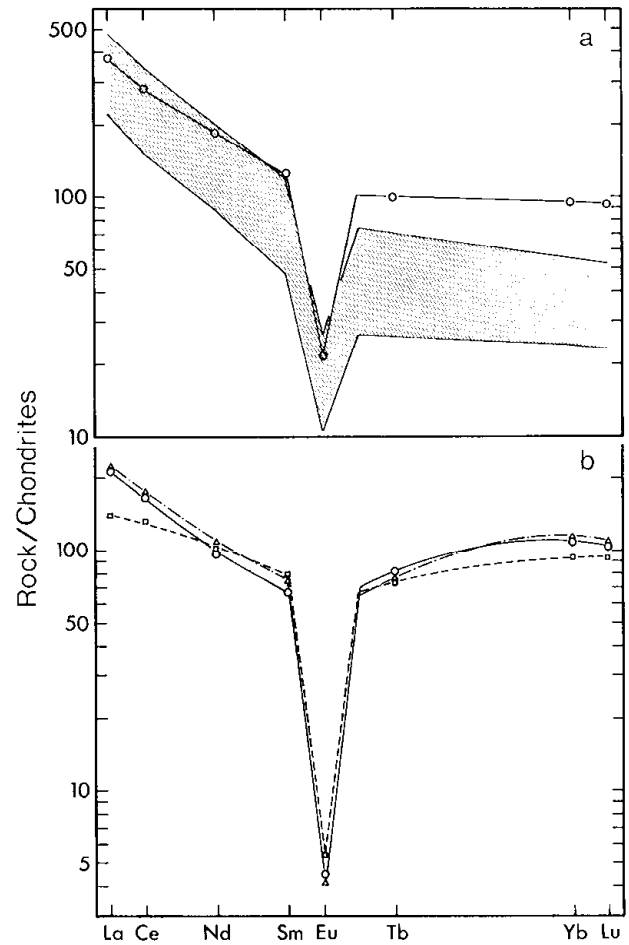

Figure 2. Chondrite-normalized REE profiles for Snake River Plain rhyolites: (a) patterned field represents sixteen individual analyses; (open circles) represents rhyolite of East Butte; (b) profiles for three samples of evolved rhyolite—(open circles, open deltas) Big Southern Butte, (open squares) Wedge Butte. Units show enrichment of each REE in rock relative to its concentration in Leedey chondrite.

profiles for these latter rhyolite domes are relatively depleted in Eu, are enriched in heavy REE, and may even display relative depletion of light REE as was noted by Noble and others (1979). These features are paralleled by strong depletions of strontium, calcium, and magnesium (Table 1) and seemingly reflect pronounced differentiation to produce the samples in question. Normally, fractional crystallization, involving the removal of the observed phenocrysts (quartz, feldspars, ferromagnesian minerals), would lead to steady enrichment of all the REE (compare Hanson, 1978). If the rhyolitic magmas formed by such a process, either trace element partition coefficients for the typical phenocrysts changed markedly as crystallization proceeded, or additional phases which preferentially incorporate light over heavy REE must have been removed in significant

Table 1. Complete major element analyses of selected Snake River Plain rhyolite samples (weight percent).

	69-9 WR[a]	74-11 WR	74-23 Obs	74-54 WR	74-57 WR	74-60 WR	74-77 WR	74-80 WR	74-83 Obs
SiO_2	71.31	75.57	74.76	73.44	74.31	74.67	75.85	79.21	74.30
TiO_2	0.39	0.22	0.11	0.42	0.23	0.10	0.33	0.22	0.36
Al_2O_3	12.49	12.38	12.28	11.93	12.61	12.57	12.74	11.24	12.18
Fe_2O_3	1.73	1.22	0.72	2.89	2.20	1.53	0.44	0.36	0.91
FeO	1.03	0.24	1.16	0.49	0.44	0.26	0.47	0.39	1.45
MnO	0.049	0.021	0.045	0.048	0.049	0.034	0.013	0.012	0.037
MgO	0.31	0.16	0.04	0.20	0.09	0.02	0.13	0.04	0.16
CaO	0.99	0.57	0.47	0.77	0.83	0.70	0.97	0.03	0.86
Na_2O	3.16	3.15	4.33	3.21	3.34	3.94	3.14	0.34	3.00
K_2O	5.07	5.30	4.67	4.90	5.17	4.91	5.08	7.19	5.51
P_2O_5	0.06	0.04	0.02	0.07	0.04	0.14	0.06	0.03	0.05
H_2O+	2.53	0.21	0.36	0.32	0.10	0.10	0.29	0.77	0.22
H_2O-	0.56	0.09	0.16	0.46	0.08	0.04	0.24	0.13	0.08
Cl	<0.05	<0.05	0.2	<0.05	<0.05	<0.05	<0.05	<0.05	<0.05
F	0.04	0.05	0.29	<0.01	0.21	0.42	0.05	<0.01	0.29
Subtotal	99.72	99.22	99.62	99.15	99.70	99.43	99.80	99.96	99.41
Less 0	0.02	0.02	0.12	0.00	0.09	0.17	0.02	0.00	0.12
Total	99.70	99.20	99.50	99.15	99.61	99.26	99.78	99.96	99.29

	74-81 WR	74-87 WR	74-144 Obs	A98-3 WR	E2248 WR	E2250 WR	E2251 WR	E2252 WR
SiO_2	74.74	74.90	74.93	73.71	70.99	72.86	76.45	69.70
TiO_2	0.31	0.32	0.17	0.14	0.49	0.23	0.22	0.56
Al_2O_3	12.07	11.96	12.31	11.84	12.81	12.05	12.14	12.77
Fe_2O_3	2.38	1.89	0.60	0.76	2.13	1.54	0.71	1.93
FeO	0.31	0.57	1.19	1.09	0.65	0.29	0.54	1.71
MnO	0.029	0.033	0.046	0.027	0.04	0.04	0.04	0.06
MgO	0.11	0.12	0.20	0.05	0.28	0.16	0.12	0.29
CaO	0.39	0.55	0.60	0.68	1.24	0.57	0.53	1.64
Na_2O	2.89	3.07	3.80	2.90	2.92	2.91	3.37	2.71
K_2O	5.44	5.48	4.97	5.44	5.22	5.40	5.29	5.16
P_2O_5	0.05	0.05	0.02	0.02	0.07	0.02	0.01	0.10
H_2O+	0.44	0.12	0.23	2.44	2.36	3.04	0.11	2.69
H_2O-	0.26	0.08	0.13	0.49	0.26	0.35	0.04	0.26
Cl	<0.05	<0.05	<0.05	<0.05	—	—	—	—
F	<0.01	<0.02	0.12	0.15	0.10	0.10	0.12	0.09
Subtotal	99.42	99.16	99.32	99.74	99.56	99.56	99.69	99.67
Less 0	0.00	0.01	0.05	0.06	0.04	0.04	0.05	0.04
Total	99.42	99.15	99.27	99.68	99.52	99.52	99.64	99.63

Analyses performed by U. S. Geological Survey under direction of L. C. Peck (E-series samples only) and B. P. Fabbi (all other samples).

[a]Material analyzed indicated by WR (whole rock) or Obs (obsidian).

Table 1. Continued.

69-9	ash-flow tuff, crystal rich, Ammon quarry (4.1 ± 0.1 m.y.)
74-11	flow-banded rhyolite, Juniper Hills (~3 m.y.?)
74-23	obsidian, Big Southern Butte (0.3 m.y.)
74-54	ash-flow tuff, crystal-rich vitrophyre (Picabo B Tuff), Picabo Hills
74-57	rhyolite, Moonstone Mountain
74-60	rhyolite, Wedge Butte dome (3.0 m.y.)
74-77	rhyolite, near Twin Peaks, Owyhee Mountains (~15-16 m.y.)
74-80	Jarbidge Rhyolite, near Jarbidge, Nevada (~16 m.y.)
74-83	obsidian, Cougar Point Tuff (~13 m.y.), along East Fork of the Jarbidge River
74-81	devitrified ash-flow tuff, Cougar Point tuff } different cooling units
74-87	devitrified ash-flow tuff, Cougar Point tuff } different cooling units
74-144	obsidian chips in Wolverine Creek tuff, near Kelly Mountain, east of Heise
A98-3	Silver City Rhyolite, near Silver City, Owyhee Mountains (15.6 m.y.)
E2248	vitrophyre, Starlight Formation, near American Falls (6.5 ± 0.1 m.y.)
E2250	vitrophyre, Ammon quarry (same unit as 69-9 above)
E2251	vitrophyre, Lost River Range, near Howe
E2252	pumiceous rhyolite, Picabo Hills

Note: detailed sample descriptions and discussion of age relations are beyond the intent of the present paper and will appear elsewhere (Leeman, in preparation).

proportions. The latter rhyolites are significantly enriched in halogens (Table 1), so it is possible that vapor phase fractionation of REE may have played an important role in magma evolution in addition to normal liquid-crystal fractionation.

Isotopic compositions of strontium, lead, and oxygen have been measured in selected rhyolite units, predominantly from Yellowstone (Leeman and Manton, 1971; Doe and others, 1982; Leeman, unpublished data). Briefly, $^{87}Sr/^{86}Sr$ ratios are high and range between 0.709 and 0.713 for Snake River Plain rhyolite units. At Yellowstone (Doe and others, 1982), most intracaldera rhyolite lava flow and ash-flow tuff samples fall into this range. However, the calcic rhyolite units and some extracaldera lava flows have $^{87}Sr/^{86}Sr$ ratios between 0.714 and 0.718. Even higher ratios are observed in some samples of Huckleberry Ridge Tuff, which exhibits a large range in $^{87}Sr/^{86}Sr$ (0.711 to 0.726). Figure 3 shows temporal variations in $^{87}Sr/^{86}Sr$ at Yellowstone.

Oxygen isotopic compositions ($\delta^{18}O$) in a few eastern Snake River Plain rhyolite units average about 6 per mil (Leeman and Whelan, in preparation). At Yellowstone, Friedman and others (1974) observed temporal variations in $\delta^{18}O$ (Figure 3) that they interpreted as reflecting varied degrees of preeruptive magma-meteoric water interaction. The highest $\delta^{18}O$ values (7.0 to 7.5 per mil) were observed in extra caldera obsidian flows (Taylor, 1968); these values appear to be normal for rhyolitic rocks elsewhere. Values for all other post-2.0-million-year-old rhyolite and tuff units are relatively depleted in ^{18}O, with calcic rhyolite samples of the Upper Basin Member showing extreme depletion (Hildreth and others, 1980).

Lead isotopic compositions of eastern Snake River Plain-Yellowstone Plateau rhyolite units range considerably but define a crudely linear array in $^{206}Pb/^{204}Pb$—$^{207}Pb/^{204}Pb$ space that reflects their derivation from an ancient (about 2.5 billion year old) source, or possibly contamination of the parental magmas by such ancient crustal rocks. At Yellowstone, intracaldera rhyolite flows and tuffs display a progressive increase in $^{206}Pb/^{204}Pb$ with decreasing age (Main Trend, Figure 3). Superimposed on this trend are large variations in $^{206}Pb/^{204}Pb$ in the compositionally zoned Huckleberry Ridge Tuff. Upper Basin Member calcic rhyolite samples are enriched, and extracaldera obsidian flows are depleted in $^{206}Pb/^{204}Pb$ relative to the Main Trend.

From Figure 3 it appears that all three isotopic parameters in the intracaldera rhyolite flows and tuffs (excluding Huckleberry Ridge Tuff Member C) are time dependent. Figure 4 shows the covariance between $\delta^{18}O$ and $^{206}Pb/^{204}Pb$. From this diagram it appears that the rhyolite units define a trend toward the composition field of meteoric waters (Leeman and others, 1977). On the basis of such observations, Doe and others (1982) suggest that isotopic compositions of oxygen, lead, and strontium reflect some form of interaction between the rhyolitic magmas and hydrothermal fluids and the hydrothermally altered wall rocks. Some extracaldera obsidian flows (OB, Figure 4) display little evidence for such interaction, and their lead and strontium isotopic compositions may be more representative of

their parental magmas. However, the strong compositional zoning observed in Huckleberry Ridge Tuff raises the possibility that isotopic compositions may also be modified due to magma-crust interactions or other processes associated with the shallow-level magma chamber. Strontium isotopic compositions are particularly susceptible to modification because most Yellowstone rhyolites have very low strontium contents (less than 10 to 20 ppm).

Although there is some uncertainty as to how well the available isotopic data represent parental rhyolitic magmas, it is apparent at Yellowstone that hydrothermal processes not only reduce $\delta^{18}O$ but also tend to reduce $^{87}Sr/^{86}Sr$ and increase $^{206}Pb/^{204}Pb$ as well (compare Leeman and others, 1977). Comparison with associated basaltic lavas therefore leads to the conclusion that these two magma types are characterized by significantly distinct isotopic characteristics (Table 2). Figure 5 contrasts REE data for basalt and rhyolite units from Yellowstone. These and other petrochemical and geological constraints can be used to evaluate models for origin of the bimodal basalt-rhyolite association of the Snake River Plain-Yellowstone Plateau province.

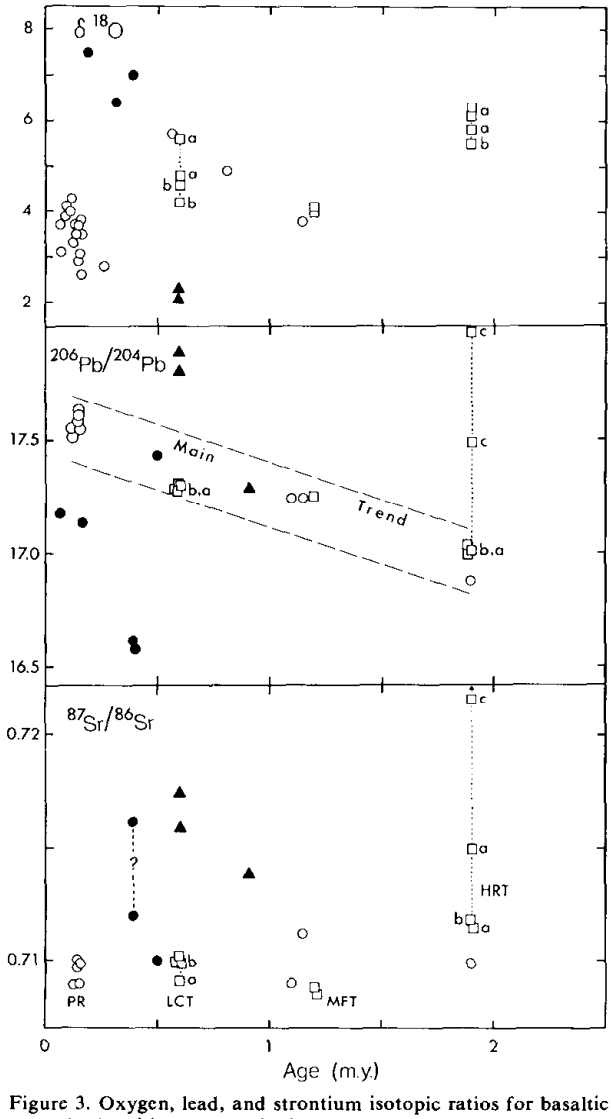

Figure 3. Oxygen, lead, and strontium isotopic ratios for basaltic and rhyolitic rocks of Yellowstone Plateau shown as a function of their age (from Doe and others, 1982): (open circles) intracaldera flows, (open squares) ash-flow tuffs (lower case letters refer to eruptive member), (filled circles) extracaldera flows, and (filled deltas) high-Ca rhyolite units. Plateau Rhyolite units (PR), Lava Creek Tuff (LCT), Mesa Falls Tuff (MFT), and Huckleberry Ridge Tuff (HRT) are denoted.

PETROLOGIC MODELS FOR RHYOLITE GENESIS

DIFFERENTIATION OF BASALTIC PARENTAL MAGMAS

Derivation of high-silica rhyolitic magmas by extreme differentiation of basaltic magmas is considered unlikely in the Snake River Plain-Yellowstone Plateau province judging from geological and geochemical evidence. The predominance of

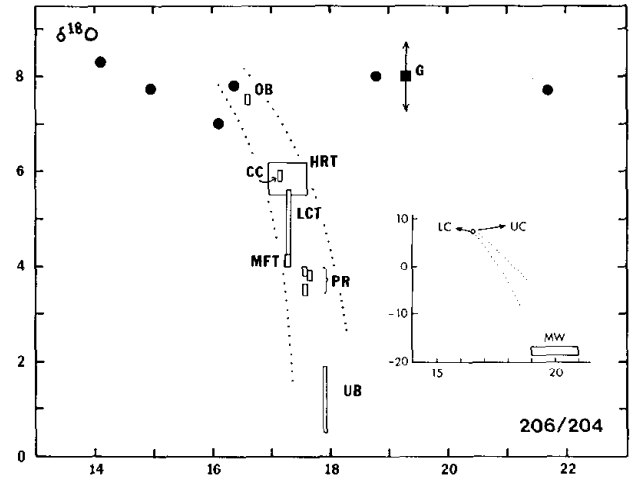

Figure 4. Oxygen and lead isotopic covariance in Yellowstone rhyolite units. Rectangles show ranges in composition for Obsidian Cliff (OB) and Cougar Creek (CC) extracaldera flows, ash-flow tuffs (HRT, MFT, LCT as in Figure 3), intracaldera Plateau Rhyolite samples (PR), and Upper Basin Member (UB). Inset shows inferred range for meteoric (hydrothermal) water (MW) and arrows point toward upper crust (UC) and lower crust (LC) compositional fields. Analyses of granulite xenoliths (filled circles) from Snake River Plain hybrid lava flows (Leeman, unpublished data) and a sample of granitic gneiss (G) from Yellowstone Park ($\delta^{18}O$ inferred for this sample) are shown for comparison.

Table 2. Comparison of isotopic characteristics between most primitive Yellowstone basalt and rhyolite magmas.

	Basalt	Rhyolite
$^{87}Sr/^{86}Sr$	<0.707	>0.712
$^{206}Pb/^{204}Pb$	16.1-17.3	<17.0
$^{207}Pb/^{204}Pb^{a}$	15.9	16.0
$^{208}Pb/^{204}Pb^{a}$	~37.8	≥38.0
$\delta^{18}O$	~6.0	≥7.0

[a]Lead isotopic ratios interpolated from covariance trends with $^{206}Pb/^{204}Pb$ at a value of $^{206}Pb/^{204}Pb$ = 17.0. This comparison is intended to illustrate differences in $^{207}Pb/^{204}Pb$ and $^{208}Pb/^{204}Pb$ ratios in basalts and rhyolites having similar $^{206}Pb/^{204}Pb$ ratios.

Estimates from Doe and others (1982); see that reference for full discussion.

rhyolite over basalt (95:5 ratio at Yellowstone Plateau) and the virtual absence of intermediate composition magmas argue against a cogenetic relationship between these magma types as do the differences in their isotopic compositions (Table 2). Although the mafic lavas commonly contain high-silica residual glass in their mesostasis (Table 3), this material represents a very small fraction of the original liquid, and compositions of these glasses are typically enriched in TiO_2, Al_2O_3, MnO, and K_2O relative to most of the rhyolite samples. Trace element data (Figure 5; Leeman, in preparation) provide arguments against both crystal fractionation and silicate liquid immiscibility. For example, evolved mafic and intermediate lavas, which are considered to be differentiates of olivine tholeiitic magmas (Leeman 1982a this volume), commonly display enrichments in REE and other magmaphile trace elements that exceed contents of these elements in rhyolite even though the evolved lavas have much lower SiO_2 contents. Also, the partitioning of REE elements between the basaltic and rhyolitic magmas does not mimic that produced in experimentally derived immiscible mafic and silicic melts. Watson (1976) and Ryerson and Hess (1978) have demonstrated the strong preference of REE, P_2O_5, Th, and other high field-strength cations for the more mafic conjugate liquids in such experiments, yet Snake River Plain-Yellowstone Plateau rhyolite units are relatively enriched in many of these elements compared with associated olivine tholeiite.

FRACTIONAL FUSION OF A COMMON SOURCE

The origin of Snake River Plain-Yellowstone Plateau rhyolites and basalts by fractional fusion of a common mantle source is considered unlikely for many of the reasons stated above—for example, the distinction in isotopic compositions of the basaltic and rhyolitic units. Geologic evidence for coexistence

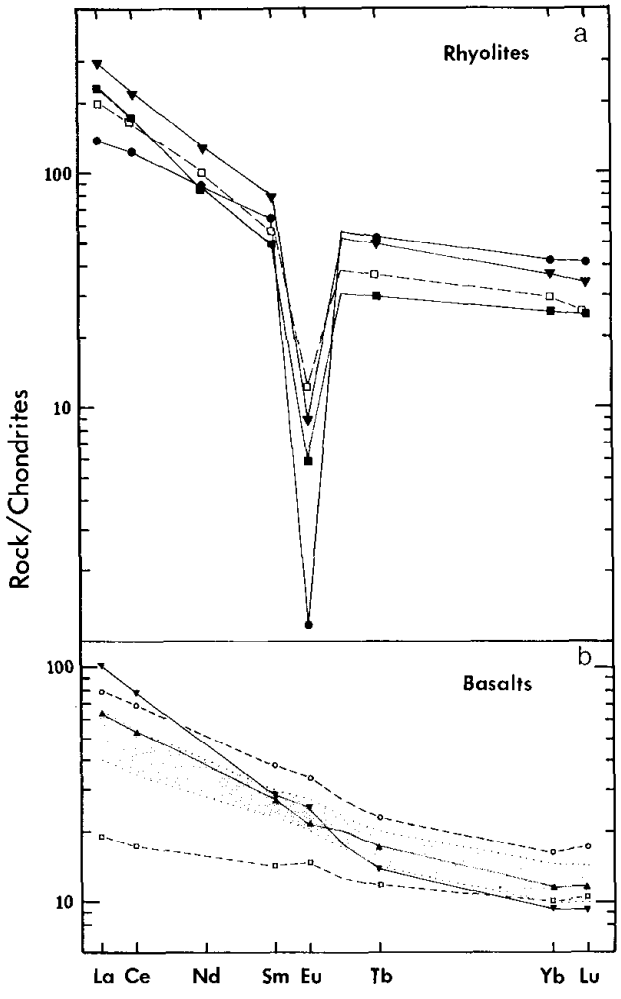

Figure 5. Chondrite-normalized REE profiles for representative basalt and rhyolite samples from Yellowstone. Analyses were selected to show extreme ranges for lava flows. Units represented are as follows: in (a), (open squares) Gardiner River rhyolite, (filled circles) Gibbon River flow, (filled squares) Cougar Creek dome, and (filled inverted deltas) West Yellowstone flow; in (b), (open squares) Gerrit Basalt, Island Park, (filled deltas) Gardiner River basalt, (filled inverted deltas) basalt of The Narrows, (open circles) basalt of Fall Creek, and (stippled area) eight other Yellowstone basalts of similar composition.

of mafic and silicic magmas at early stages of development of Snake River Plain-Yellowstone Plateau volcanic centers is particularly difficult to reconcile with the fractional fusion model (see Yoder, 1973) which predicts initial production of silicic magma at a relatively low-temperature "invariant" point for the source material. In this model, mafic magmas would form only after segregation of the silicic magma had occurred and temperatures were elevated to the point where relatively refractory residual source material could partially melt, perhaps at a higher temperature invariant point.

Fractional fusion of distinct sources is more probable, with rhyolitic magmas derived from a crustal source.

Table 3. Compositions[a] of residual glasses in Snake River Plain mafic lavas compared with typical Snake River Plain rhyolites.

	1	2	3	4	5	6	7
	70-22G	V-31G	59P160G	Rhy-Avg	69-45	74-83	74-23
SiO_2	73.1	66.2	71.0	74.6	69.7	75.2	75.8
TiO_2	1.03	0.56	0.93	0.4	0.74	0.36	0.11
Al_2O_3	13.7	13.3	14.4	12.8	14.1	12.3	12.5
FeO	2.13	8.03	1.55	2.3	4.12	2.34	1.88
MnO	--	0.18	0.17	0.2	0.08	0.04	0.05
MgO	0.08	0.19	0.15	0.5	0.79	0.16	0.04
CaO	0.78	2.86	0.79	3.4	2.16	0.87	0.48
Na_2O	3.74	3.38	4.33	4.0	3.31	3.04	4.39
K_2O	5.23	5.29	6.56	4.4	4.81	5.58	4.74
P_2O_5	0.17	0.11	0.12	0.3	0.14	0.05	0.02

1. Residual glass in groundmass (<1 volume %), Craters of the Moon-type ferrobasalt.
2. Residual glass in groundmass (~40 volume %), Craters of the Moon ferrolatite (Leeman and others, 1976).
3. Residual glass in groundmass (<1 volume %), troctolite xenolilth, McKinney Basalt (Leeman and Vitaliano, 1976).
4. Average Snake River Plain rhyolite (Leeman and others, 1976, Table 5).
5. Shoshone Falls vitrophyric tuff (sample with lowest SiO_2 value measured).
6. Cougar Point tuff, obsidian.
7. Big Southern Butte, obsidian.

[a]All analyses recalculated to a sum of 100 weight percent, excluding H_2O, F, and Cl.

CRUSTAL ANATEXIS DUE TO INJECTION OF HIGH-TEMPERATURE MAFIC MAGMAS

The formation of rhyolitic magmas by crustal anatexis is developed in some detail for the Snake River Plain-Yellowstone Plateau province by Leeman (1982b this volume) as it appears most consistent with available information. In this model, a dual source configuration is envisaged to produce basaltic and rhyolitic precursor magmas. Isotopic data strongly support derivation of the silicic magmas from an ancient crustal source that is characterized by relatively high Rb/Sr and $\delta^{18}O$ and by relatively low U/Pb. Deep crustal granulites or amphibolites commonly display such characteristics (for example, Moorbath and others, 1969; Black and others, 1973; Leeman, 1979), and such rocks could produce tonalitic to rhyolitic magmas upon partial fusion (Wyllie, 1977). Also, thermal modelling demonstrates the feasibility of producing large volumes of silicic anatectic magma by the injection and cooling of mantle-derived mafic magmas in the lower crust (Hodge, 1974). The local contemporaneity of mafic and silicic magmas observed in the Snake River Plain-Yellowstone Plateau province lends strong support to this model.

CONCLUSIONS—A REASONABLE COMPROMISE

Origin of the rhyolites by crustal anatexis is considered most reasonable in its general aspects. However, the juxtaposition of mafic magmas and intermediate to silicic crustal anatectic magmas and their potential interaction with one another and with crustal wall rocks undoubtedly leads to a very complicated petrogenesis. In modeling isotopic data for Tertiary granites from Skye, Moorbath and others (1969) and subsequent authors have noted the likely derivation of such rocks from ancient deep crustal rocks. However, REE data for these granites cannot easily be modeled in terms of direct fusion of typical crust (Thorpe and others, 1977). Condie and Hunter (1976) propose a two-stage petrogenesis for Archean granitic rocks from South Africa which involves partial fusion of granulitic crustal rocks to produce tonalitic magmas, which in turn evolve via fractional crystallization to rhyolitic (granitic) compositions. REE profiles for their samples (for example, Sicanusa-type plutons) are essentially equivalent to those for Snake River Plain-Yellowstone Plateau rhyolites. Additional processes, including interactions of silicic magmas with upper crustal wall rocks, hydrothermally altered sediments and volcanic or plutonic rocks, and possibly hydrothermal fluids are indicated by isotopic data for Yellowstone rhyolite units (Doe and others, 1982). Finally, diffusion and other poorly understood processes may play important roles in the development of high-silica rhyolitic magmas within high-level crustal reservoirs (Hildreth, 1979; Smith, 1979). Accumulating evidence suggests that the development and evolution of Snake River Plain-Yellowstone Plateau rhyolitic magmas followed a complicated scenario involving most of the aforementioned processes to varying degree. However, the ultimate source for these magmas most likely was the deep crust. The associated basaltic magmas are not considered to be cogenetic in a strict sense, but they constitute an essential complement to the silicic magmatic systems.

ACKNOWLEDGMENTS

This work has benefitted from my interactions with numerous colleagues, notably B. R. Doe, R. L. Christiansen, and C. E. Hedge, to whom I am grateful. Portions of this work were supported by the U. S. Geological Survey during the tenure of a National Research Council Fellowship and by National Science Foundation Grant EAR80-18580. I am also indebted to A. Elsweiler and A. Walters for their skilled assistance with manuscript preparation.

REFERENCES

Black, L. P., Stephen Moorbath, R. J. Pankhurst, and R. B. Windley, 1973, $^{207}Pb/^{206}Pb$ whole rock age of the Archean granulite facies metamorphic event in West Greenland: Nature, v. 244, p. 50-53.

Blake, D. H., R. W. D. Elwell, I. L. Gibson, R. R. Skelhorn, and G. P. L. Walker, 1965, Some relationships resulting from the intimate association of acid and basic magmas: Quarterly Journal of the Geological Society of London, v. 121, p. 31-50.

Bonnichsen, Bill, 1982, Chemical composition of the Cougar Point Tuff and rhyolite lava flows from the Bruneau-Jarbidge eruptive center, Owyhee County, Idaho: Idaho Bureau of Mines and Geology Open-File Report 82-1, 22 p.

Bowen, N. L., 1928, The Evolution of the Igneous Rocks: Princeton University Press, Princeton, New Jersey, 332 p.

Boyd, F. R., 1961, Welded tuffs and flows in the rhyolite plateau of Yellowstone Park, Wyoming: Geological Society of America Bulletin, v. 72, p. 387-426.

Bunsen, R., 1851, Uber die Pro-esse der vulkanischen Gesteinbildungen Islands: Annals of Physical Chemistry, v. 83, p. 171-197.

Christiansen, R. L., in preparation, Quaternary and Pliocene volcanics of the Yellowstone rhyolite plateau region of Wyoming, Idaho, and Montana: U. S. Geological Survey Professional Paper.

Christiansen, R. L. and H. R. Blank, Jr., 1972, Volcanic stratigraphy of the Quaternary rhyolite plateau in Yellowstone National Park: U. S. Geological Survey Professional Paper 729-B, 18 p.

Condie, K. D. and D. R. Hunter, 1976, Trace element geochemistry of Archean granitic rocks from the Barberton region, South Africa: Earth and Planetary Science Letters, v. 29, p. 389-400.

Doe, B. R., W. P. Leeman, R. L. Christiansen, and C. E. Hedge, 1982, Lead and strontium isotopes and related trace elements as genetic tracers in Quaternary rhyolite-basalt association of the Yellowstone Plateau volcanic field, U.S.A.: Journal of Geophysical Research, v. 87, p. 4785-4806.

Ekren, E. B., D. H. McIntyre, E. H. Bennett, and R. F. Marvin, 1982, Cenozoic stratigraphy of western Owyhee County, Idaho, *in* Bill Bonnichsen and R. M. Breckenridge, editors, Cenozoic Geology of Idaho: Idaho Bureau of Mines and Geology Bulletin 26.

Fenner, C. N., 1938, Contact relations between rhyolite and basalt on Gardiner River, Yellowstone Park, Wyoming: Geological Society of America Bulletin, v. 49, p. 1441-1483.

———, 1944, Rhyolite-basalt complex on Gardiner River, Yellowstone Park, Wyoming: Geological Society of America Bulletin, v. 55, p. 1081-1096.

Friedman, Irving, P. W. Lipman, J. D. Obradovich, and J. D. Gleason, 1974, Meteoric water in magmas: Science, v. 184, p. 1069-1072.

Hamilton, W. B., 1965, Geology and petrogenesis of the Island Park caldera of rhyolite and basalt, eastern Idaho: U. S. Geological Survey Professional Paper 504-C, 37 p.

Hanson, G. N., 1978, The application of trace elements to the petrogenesis of igneous rocks of granitic composition: Earth and Planetary Science Letters, v. 38, p. 26-43.

Hildreth, E. W., 1979, The Bishop Tuff: evidence for the origin of compositional zonation in silicic magma chambers: Geological Society of America Special Paper 180, p. 43-75.

Hildreth, E. W., R. L. Christiansen, and J. R. O'Neil, 1980, Catastrophic isotopic modification of rhyolitic magma by creation of the Yellowstone caldera: Geological Society of America, Abstracts with Programs, v. 12, no. 3, p. 111.

Hodge, D. S., 1974, Thermal model for origin of granitic batholiths: Nature, v. 251, p. 297-299.

Holmes, Arthur, 1931, The problem of the association of acid and basic rocks in central complexes: Geological Magazine, v. 68, p. 241-255.

Leeman, W. P., 1979, Primitive lead in deep crustal xenoliths from the Snake River Plain, Idaho: Nature, v. 281, p. 365-366.

———, 1982a, Evolved and hybrid lavas from the Snake River Plain, Idaho, *in* Bill Bonnichsen and R. M. Breckenridge, editors, Cenozoic Geology of Idaho: Idaho Bureau of Mines and Geology Bulletin 26.

———, 1982b, Development of the Snake River Plain-Yellowstone Plateau province, Idaho and Wyoming: an overview and petrologic model, *in* Bill Bonnichsen and R. M. Breckenridge, editors, Cenozoic Geology of Idaho: Idaho Bureau of Mines and Geology Bulletin 26.

Leeman, W. P. and W. I. Manton, 1971, Strontium isotopic composition of basaltic lavas from the Snake River Plain, southern Idaho: Earth and Planetary Science Letters, v. 11, p. 420-434.

Leeman, W. P., B. R. Doe, and Joseph Whelan, 1977, Radiogenic and stable isotope studies of hot-spring deposits in Yellowstone National Park and their genetic implications: Geochemical Journal, v. 11, p. 65-74.

Leeman, W. P. and C. J. Vitaliano, 1976, Petrology of McKinney Basalt, Snake River Plain, Idaho: Geological Society of America Bulletin, v. 87, p. 1777-1792.

Leeman, W. P., C. J. Vitaliano, and Martin Prinz, 1976, Evolved lavas from the Snake River Plain: Craters of the Moon National Monument, Idaho: Contributions to Mineralogy and Petrology, v. 56, p. 35-60.

Luth, W. C., R. H. Jahns, and O. F. Tuttle, 1964, The granite system at pressures of 4 to 10 kilobars: Journal of Geophysical Research, v. 69, p. 759-773.

Moorbath, Stephen, H. Welke, and N. H. Gale, 1969, The significance of lead isotope studies in ancient, high-grade metamorphic basement complexes, as exemplified by the Lewisian rocks of northwest Scotland: Earth and Planetary Science Letters, v. 6, p. 245-256.

Noble, D. C., W. L. Rigot, and H. R. Bowman, 1979, Rare-earth element content of some highly differentiated ash-flow tuffs and lavas: Geological Society of America Special Paper 180, p. 77-85.

Presnall, D. C., 1969, The geometrical analysis of partial fusion: American Journal of Science, v. 267, p. 1178-1194.

Roedder, Edwin and P. W. Weiblen, 1971, Petrology of silicate melt inclusions, Apollo 11 and Apollo 12 and terrestrial equivalents: Proceedings of the Second Lunar Science Conference, Geochimica et Cosmochimica Acta, Supplement 1, v. 1, p. 507-528.

Ryerson, F. J. and P. C. Hess, 1978, Implications of liquid-liquid distribution coefficients to mineral-liquid partitioning: Geochimica et Cosmochimica Acta, v. 42, p. 921-932.

Smith, R. L., 1979, Ash-flow magmatism: Geological Society of America Special Paper 180, p. 5-27.

Taylor, H. P., 1968, The oxygen isotope geochemistry of igneous rocks: Contributions to Mineralogy and Petrology, v. 19, p. 1-71.

Thorpe, R. S., P. J. Potts, and M. B. Sbarre, 1977, Rare earth evidence concerning the origin of granites of the Isle of Skye, northwest Scotland: Earth and Planetary Science Letters, v. 36, p. 111-120.

Trimble, D. E. and W. J. Carr, 1976, Geology of the Rockland and Arbon quadrangles, Power County, Idaho: U. S. Geological Survey Bulletin 1399, 115 p.

Tuttle, O. F. and N. L. Brown, 1958, Origin of granite in the light of experimental studies in the system $NaAlSi_3O_8$-$KAlSi_3O_8$-SiO_2-H_2O: Geological Society of America Memoir 74, 153 p.

Wager, L. R., E. A. Vincent, G. M. Brown, and J. D. Bell, 1965, Marscoite and related rocks of the western Red Hills complex, Isle of Skye: Philosophical Transactions of the Royal Society of London, v. A-257, p. 273-307.

Watson, E. B., 1976, Two-liquid partition coefficients: experimental data and geochemical implications: Contributions in Mineralogy and Petrology, v. 56, p. 119-134.

Wilcox, R. E., 1944, Rhyolite-basalt complex on Gardiner River, Yellowstone Park, Wyoming: Geological Society of America Bulletin, v. 55, p. 1047-1079.

Wyllie, P. J., 1977, Crustal anatexis: an experimental review: Tectonophysics, v. 43, p. 41-71.

Yoder, H. S., Jr., 1973, Contemporaneous basaltic and rhyolitic magmas: American Mineralogist, v. 58, p. 153-171.

Chapter 5

Volcanic Rocks Snake River Plain and Owyhee Uplands Southwestern Idaho

Cenozoic Stratigraphy of Western Owyhee County, Idaho

by

E. B. Ekren[1], D. H. McIntyre[1], E. H. Bennett[2], and R. F. Marvin[1]

ABSTRACT

The Cenozoic rocks of western Owyhee County, Idaho, are principally lavas and welded tuffs that range in age from Eocene to Pleistocene. The Eocene lavas and tuffs are intermediate in composition, as much as 1,000 meters thick, and restricted to a small area in the eastern part of the Owyhee Mountains. Volcanic rocks of Oligocene age are also restricted areally and form a local accumulation as much as 1,160 meters thick in the northern Owyhee Mountains. The Oligocene rocks are lavas that contain olivine or pyroxene phenocrysts or both. The Oligocene and Eocene volcanic rocks and the Cretaceous granitic rocks form the eroded basement surface upon which widespread olivine basalts and dark gray latite and quartz latite lavas of Miocene age were deposited. These younger rocks of basalt to latite composition are at least 1,000 meters thick. They are overlain by thick, widespread rhyolite tuffs and lavas that are the principal subject of this paper. The rhyolites, in turn, are overlain by basalt lavas that are 8-10 million years old on the Owyhee Plateau but as young as Pleistocene on the Snake River Plain.

The rhyolitic rocks were erupted from vents in and adjacent to the Owyhee Mountains and Owyhee Plateau from 16 to about 10 million years ago. They are mainly welded tuffs that, regardless of their source, have one feature in common: namely, internal characteristics indicating *en masse* viscous lavalike flowage. On the basis of the tabular nature of the rhyolitic deposits, their broad areal extent, and the local preservation of pyroclastic textures at the bases, tops, and distal ends of some of the deposits, we have concluded that the rocks were emplaced as ash flows at extremely high temperatures and that they coalesced to liquids before final emplacement and cooling.

The rhyolites generally are crystal poor. Those that were erupted from the Silver City Range about 16 million years ago commonly contain fewer than 3 percent phenocrysts consisting of quartz, plagioclase, and alkali feldspar; most of these rocks contain sparse flakes of biotite and are the only rhyolites in the study area that do. Rocks that are 14 million years to about 10 million years old contain only pyroxenes, chiefly ferriferous and intermediate pigeonites, as mafic constituents. Rhyolites erupted from the Owyhee Plateau include two sequences that were mapped over areas having diameters of about 100 kilometers. These two sheets are the 13.8-million-year-old tuff of Swisher Mountain, which was erupted from the Juniper Mountain volcanic center, and the 10-million-year-old tuff of Little Jacks Creek which is inferred to have been erupted from a source on the part of the Owyhee Plateau that lies just east of the study area. The two inferred source areas are expressed as gentle domes without structural features indicative of cauldron subsidence.

Iron-titanium oxide determinations reveal that both the tuff of Swisher Mountain and the tuff of Little Jacks Creek were erupted at a minimum temperature of 1090° C. We conclude that both tuffs formed in water-deficient levels of the crust, probably at depths as great as 15-25 kilometers, and that the tuffs were erupted from these great depths.

INTRODUCTION

Owyhee County, Idaho, west of 116° longitude (Figure 1), was mapped at a scale of 1:125,000 during the summers of 1977 and 1978 (Ekren and others, in press, 1981) as part of the U. S. Geological Survey's investigation of potential geothermal areas. The present report briefly summarizes the results of this investigation. The reader interested in more detailed descriptions of the rocks or more complete discussion of rock chemistry and petrogenesis should consult the references noted above. The mapping and associated stratigraphic studies focussed on the voluminous rhyolitic rocks exposed in the Silver City Range (Owyhee Mountains) and the Owyhee Plateau of extreme southwestern Idaho because these strata underlie the principal recharge area and are the

[1]U. S. Geological Survey, Denver, Colorado 80225.
[2]Idaho Bureau of Mines and Geology, Moscow, Idaho 83843.

Ekren, E. B., D. H. McIntyre, E. H. Bennett, and R. F. Marvin, 1982, Cenozoic stratigraphy of western Owyhee County, Idaho, *in* Bill Bonnichsen and R. M. Breckenridge, editors, Cenozoic Geology of Idaho: Idaho Bureau of Mines and Geology Bulletin 26, p. 215-235.

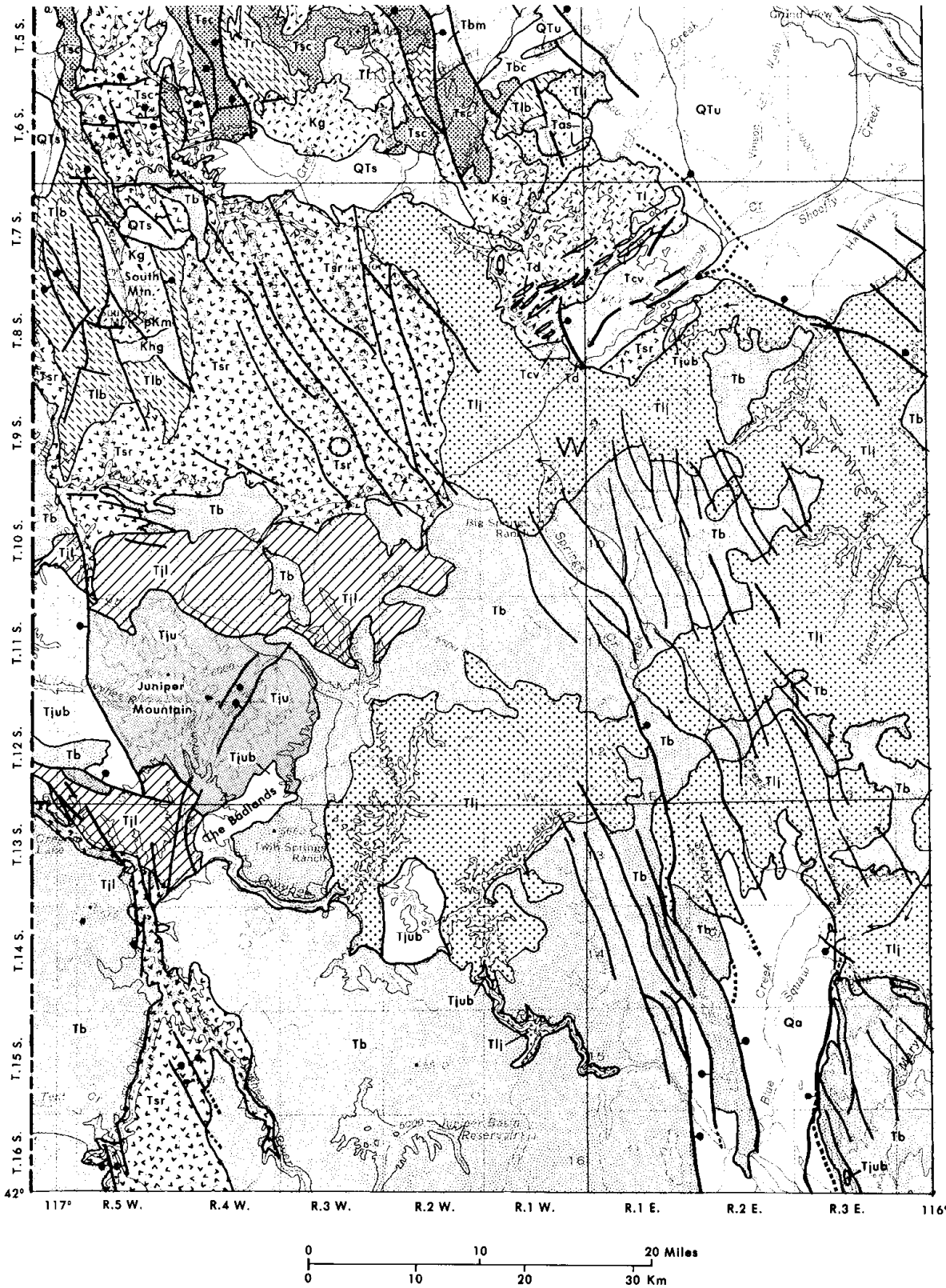

Figure 1. Generalized geologic map of western Owyhee County, Idaho (modified from Ekren and others, 1981).

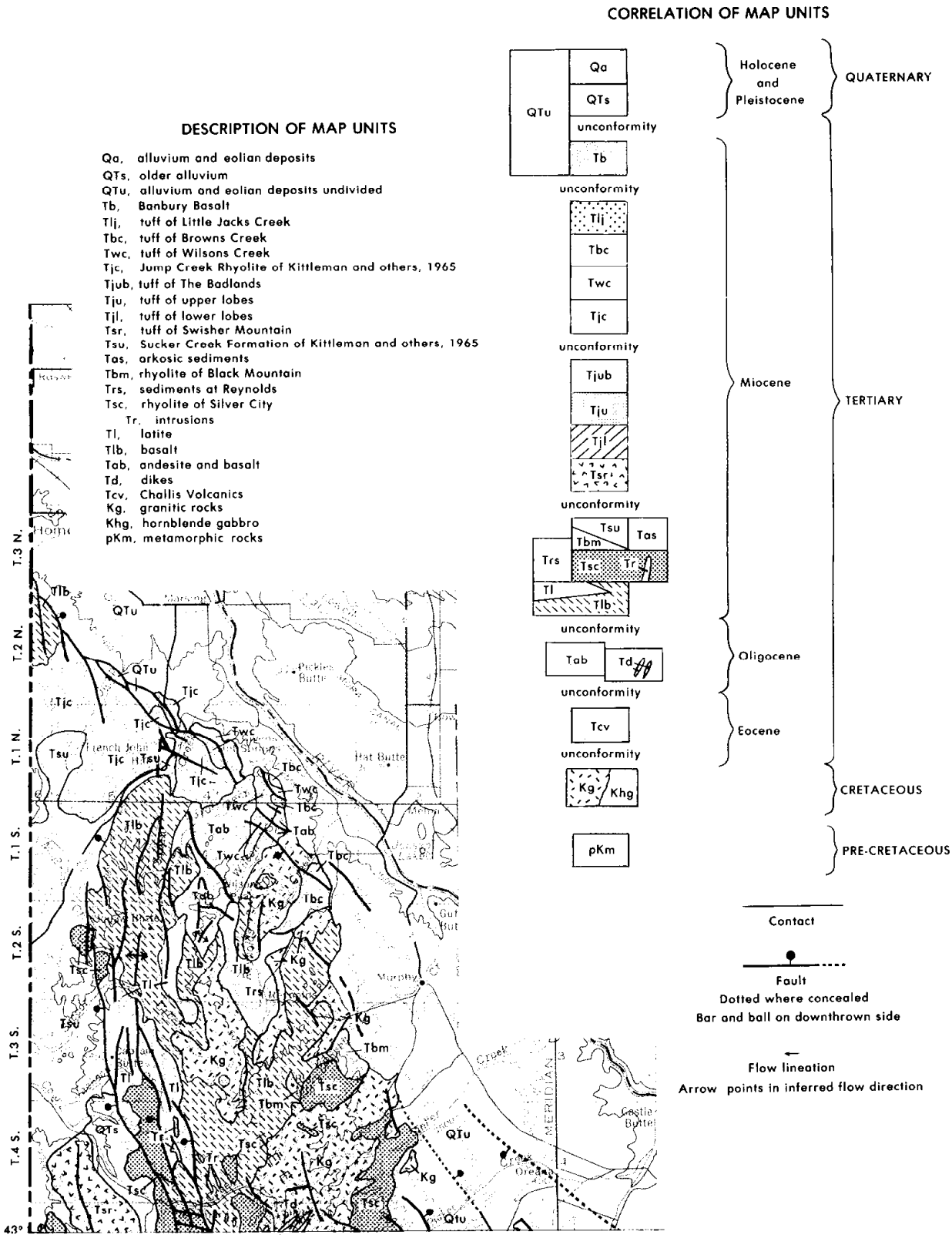

Figure 1. continued.

principal thermal reservoir rocks of the Bruneau-Grand View geothermal area (Young and Whitehead, 1975).

STRATIGRAPHY OF ROCKS OTHER THAN RHYOLITE

The northern mountainous part of Owyhee County, variously called the Owyhee Mountains or the Silver City Range, is underlain by Cretaceous granitic rocks and by a variety of Tertiary volcanic rocks from Eocene to Miocene in age. The granitic rocks are chiefly granodiorite and quartz monzonite, but they include large masses of granite and porphyritic diorite or granodiorite. Near South Mountain (Figure 1), the granitic rocks are bordered by Cretaceous hornblende gabbro and are roofed by pre-Cretaceous metasedimentary rocks (Sorenson, 1927; Bennett, 1976). We concur with Taubeneck (1971) and earlier researchers (for example, Lindgren, 1900) that the granitic rocks are an integral part of the Idaho batholith.

Rhyodacite and quartz latite lava flows and ash-flow tuffs of Eocene age that correlate with the Challis Volcanics (Axelrod, 1968) are locally exposed 38 kilometers east of South Mountain and are 500-1,000 meters thick. One of these ash-flow tuff units yielded a potassium-argon age of 44.7 ± 0.8 million years (Armstrong and others, 1980).

Rocks of Oligocene age consist of a local accumulation of olivine basalt and andesite lavas as much as 1,160 meters thick that are chemically dissimilar to the overlying Miocene volcanic rocks (Table 1). The Oligocene rocks contain olivine or pyroxene phenocrysts or both, and a whole-rock analysis yielded a potassium-argon age of 30.6 million years.

The Oligocene rocks and the Cretaceous granitic rocks are unconformably overlain by widespread Miocene volcanic rocks at least 1,000 meters thick. These consist of interbedded olivine basalt and dark gray latite and quartz latite (Table 1). A basalt from this sequence collected by Pansze (1975) yielded a whole-rock potassium-argon age of 17 million years. The basalt-latite sequence is overlain and intruded by rhyolitic rocks, the major subject of this paper.

The rhyolitic rocks, in turn, are overlain in many places on the Owyhee Plateau by widespread olivine basalts and interbedded sedimentary rocks that correlate with the Banbury Basalt of Malde and others (1963). The sequence locally exceeds 300 meters in thickness, and potassium-argon dates from nearby exposures to the east and south range from about 8 to 10.5 million years (Armstrong and others, 1975). The sedimentary rocks interbedded with the basalts include a large variety of conglomeratic tuffaceous sandstones and conglomerates containing well-rounded pebbles and cobbles of dark gray chert and brown quartzite, both of which were apparently derived from sources in northern Nevada west of the Jarbidge Mountains. Local accumulations of flat-bedded lacustrine siltstone and diatomite indicate intermittent ponding of drainages during the basalt eruptions.

Table 1. Chemical analyses and CIPW norms for some prerhyolite mafic and intermediate volcanic rocks, western Owyhee County, Idaho (modified from Table 1 of Ekren and others, in press).

	1	2	3	4	5
	Chemical Analyses				
SiO_2	48.30	56.60	47.60	54.69	66.31
Al_2O_3	15.94	17.28	15.58	15.15	13.60
Fe_2O_3	3.33	4.03	3.23	1.92	1.63
FeO	6.67	2.22	8.25	7.75	3.38
MgO	7.47	3.97	8.04	4.81	1.85
CaO	8.42	6.48	9.89	7.30	3.27
Na_2O	3.48	4.27	2.75	2.90	2.69
K_2O	1.13	1.80	0.43	1.68	4.05
H_2O+	1.30	0.71	0.73	1.17	1.77
H_2O-	0.79	1.00	0.71	0.60	0.57
TiO_2	2.05	0.96	1.87	1.77	0.65
P_2O_5	0.71	0.42	0.27	0.34	0.12
MnO	0.15	0.10	0.18	0.16	0.00
CO_2	0.22	0.04	0.12	0.04	0.03
Sum	99.96	99.88	99.65	100.28	99.92
	CIPW Norms				
q	0.00	7.91	0.00	7.44	25.17
c	0.00	0.00	0.00	0.00	0.00
or	6.82	10.83	2.59	10.08	24.52
ab	30.08	36.80	23.69	24.91	23.33
an	25.06	23.08	29.42	23.71	13.40
di-wo	4.78	2.76	7.50	4.40	0.93
di-en	3.27	2.38	4.73	2.32	0.49
di-fs	1.12	0.00	2.30	1.94	0.41
hy-en	6.72	7.69	8.83	9.83	4.23
hy-fs	2.31	0.00	4.29	8.23	3.47
ol-fo	6.31	0.00	4.78	0.00	0.00
ol-fa	2.39	0.00	2.56	0.00	0.00
mt	4.93	4.79	4.77	2.83	2.42
hm	0.00	0.80	0.00	0.00	0.00
il	3.98	1.86	3.62	3.41	1.27
ap	1.72	1.01	0.65	0.82	0.29
cc	0.51	0.09	0.28	0.09	0.07

1. Oligocene K-rich olivine basalt.
2. Oligocene andesite; average of 3 analyses.
3. Miocene basalt; average of 2 analyses.
4. Miocene basaltic andesite; average of 2 analyses.
5. Miocene quartz latite; average of 2 analyses.

Lacustrine sedimentary rocks and intercalated basalt units of Pleistocene age on the Snake River Plain at the northern boundary of Owyhee County were not examined in detail during this study, but are currently being mapped by H. E. Malde of the U. S. Geological Survey (written communication, 1980).

STRATIGRAPHY OF PRINCIPAL RHYOLITE UNITS

HISTORICAL REVIEW

The rhyolite of the Owyhee Mountains and Plateau has puzzled geologists for many years. The main problem has been whether the bulk of the rocks are flow-layered welded tuffs or rhyolite lava flows. Lindgren (1900) did not concern himself with this problem because the concept of ash flow had not as yet been developed. Later geologists found themselves in a predicament in correctly identifying the rocks, because in most places the rocks displayed features indicative of lava flows, but in other places they showed some textures suggestive of welded tuffs as described by Smith (1960). The later geologists included Littleton and Crosthwaite (1957), Asher (1968), McIntyre (1972), Pansze (1975), Bennett and Galbraith (1975), Neill (1975), and Bennett (1976). Most, but not all, of these authors concluded that the rocks must be welded tuffs, primarily on the basis of their widespread areal extents.

We infer that most of the rhyolite units in the Owyhee area were emplaced as ash flows that coalesced to liquids before final emplacement and cooling on the basis of the following features: (1) the broad areal extent and tabular nature of the flows; (2) local presence of pumice and shards at the base, top, and sides of some of the units, and also within the interiors of some cooling units; (3) ubiquitous internal flowage features indicative of liquid flow; (4) the presence of flow breccia locally at the base of nearly every unit; and (5) the presence of flow-alined incipient microlites in glassy zones which shows that liquefaction in these zones was complete.

RHYOLITE UNITS OF SILVER CITY RANGE AND ADJACENT AREAS

Flow-layered rhyolites, which for the most part contain only a small percentage of small phenocrysts (Figure 2), form the backbone of the Silver City Range and large parts of the downdropped eastern and western flanks of the range. These rocks are the principal hosts for the silver-gold veins of the Silver City district. Isotopic data (Table 2; Armstrong, 1975; Pansze, 1975; Dalrymple, written communication, 1977) show that the rocks are about 16 million years old and that the associated silver-gold mineralization is about 16-15.2 million years old (Armstrong and others, 1980).

Field relations show that some of the Silver City

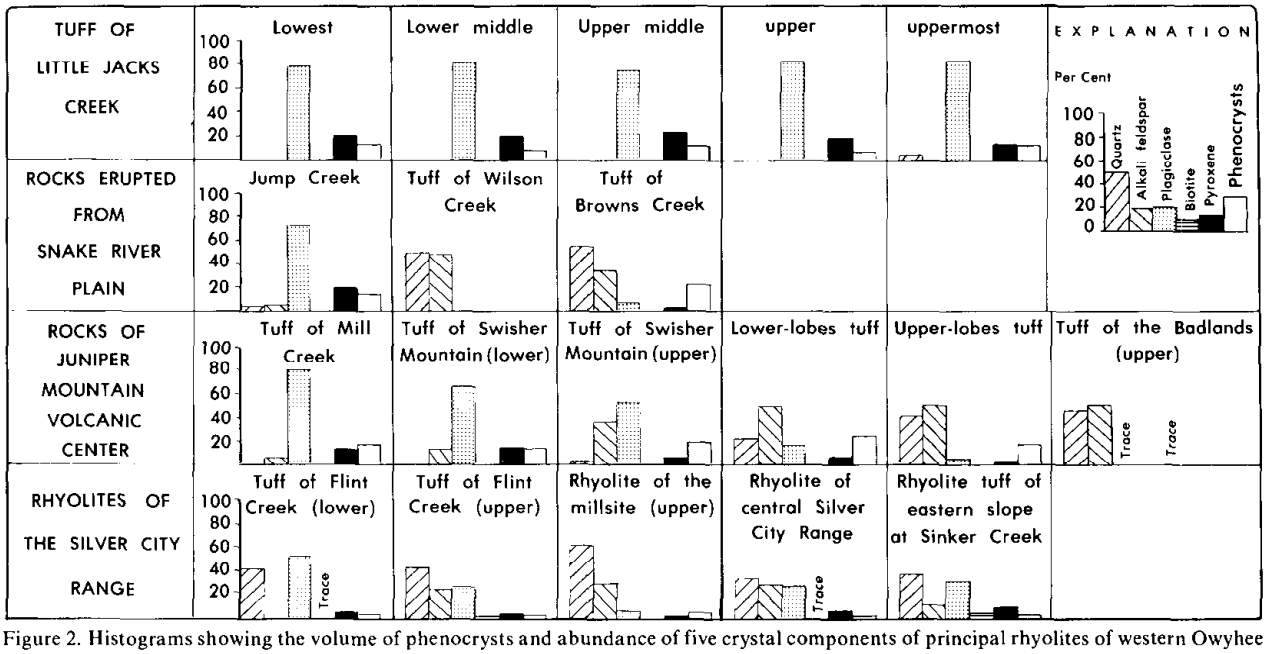

Figure 2. Histograms showing the volume of phenocrysts and abundance of five crystal components of principal rhyolites of western Owyhee County, Idaho.

Table 2. Potassium-argon ages for volcanic rock units from western Owyhee County referred to in this report. [For more complete data see Ekren and others (in press). Sources of data: (A) Armstrong and others (1980); (B) Armstrong (1975), recalculated using currently accepted constants (see Steiger and Jager, 1977); (C) Ekren and others (in press).]

Unit	K-Ar age (m.y.)	Source
Jump Creek Rhyolite	11.1 ± 0.2	A
Tuff of Browns Creek (average of 2 analyses)	11.2 ± 0.65	A
Tuff of The Badlands	12.0 ± 0.2	A
Tuff of upper lobes	13.9 ± 0.5	C
Tuff of lower lobes	13.8 ± 0.5	C
Tuff of Swisher Mountain	13.5 ± 0.2	A
Do.	14.2 ± 0.4	A
Rhyolite of Black Mountain	15.7 ± 0.5	C
Rhyolite of Silver City Range (average of 6 analyses)	16.1 ± 0.3	B, C
Andesite (Figure 1, Tab)	30.6 ± 1.0	C
Challis Volcanics (22 miles southwest of Grand View)	44.7 ± 0.8	A

rhyolite units grade laterally from near-source rocks, flow layered from base to top, to classic densely welded tuffs within a distance of a few kilometers. Most units were probably erupted from vents in and adjacent to the present Silver City Range, which is characterized by numerous feeder dikes, plugs, and extrusive domes of rhyolite (Pansze, 1975; Piper and Laney, 1926; Bennett and Galbraith, 1975). Many of the dikes were intruded after extensive north- to northwest-trending normal faulting, especially in the De Lamar area, had occurred, thereby dating the start of normal faulting of that trend before 16 million years.

Rhyolite Units of the Western Flank

Numerous rhyolite masses on the western flank of the Silver City Range that were mapped and described by us (Ekren and others, 1981, in press) are too restricted areally to warrant description in this short review. However, two fairly widespread units in and adjacent to the open-pit mine at De Lamar are typical of the rhyolite units of the western flank. These units are the tuff of Flint Creek, which rests directly on basalt and latitic lava flows of Miocene age, and the next overlying rhyolite, which we term the rhyolite of the millsite. Both of these units are included with the rhyolite of the Silver City Range on the accompanying geologic map (Figure 1).

Tuff of Flint Creek. Two genetically related ash-flow tuff cooling units, each from 30 meters to as much as 90 meters thick (Figure 2), are exposed in the canyon of Flint Creek (Figure 1) in the central part of T. 6 S., R. 4 W. Both units at Flint Creek grade upward from partially welded gray tuff at the base into flow-layered, purplish gray or reddish brown tuff at the top, in which pumice clasts are so flattened and stretched that they resemble laminations in rhyolite lava. In outcrops to the north near De Lamar, closer to the presumed source, all vitroclastic textures have been destroyed. There the rock is conspicuously flow layered from base to top and tends to weather to thin plates; it is gray, hydrothermally altered, and not easily distinguished from underlying gray crystal-poor latite lava flows. Distinction was made on the presence of sparse, fine (mostly 1 millimeter) grains of quartz in the rhyolite and on the lack of quartz in the latite.

The lower unit of the tuff of Flint Creek (Table 3) is principally a plagioclase-pyroxene tuff that contains a little quartz and little or no alkali feldspar and only trace amounts of biotite. It probably contains less SiO_2 and alkali metals than the upper unit, which has considerably more alkali feldspar and quartz phenocrysts (Figure 2).

Rhyolite of the millsite. Flow-layered rhyolite, overlying the tuff of Flint Creek but locally resting directly on the basalt and latite sequence, is relatively rich in phenocrysts compared with other rhyolite units of the Silver City-De Lamar area; it is exposed mainly near the millsite of the De Lamar open-pit mine. Flow layering in the rock in the vicinity of the millsite, as seen on aerial photographs, defines a broad whorl that is about 1.6 kilometers in diameter. This whorl possibly marks the vent of the rhyolite. Exclusive of the whorl, the rhyolite is at least 50 meters thick.

The rhyolite of the millsite, like the tuff of Flint Creek, contains little or no alkali feldspar in its basal part but grades upward to rock that is rich with phenocrysts of alkali feldspar (Figure 2) as large as 4 millimeters. The rock is pinkish gray and white and characterized from base to top by abundant vug-filling vapor-phase crystals. In places, large (about 15 centimeters) spherulites are present in the rock and conspicuously abundant on weathered slopes.

In exposures just south of the Flint Creek Mining District, the unit is separated from the underlying upper cooling unit of the tuff of Flint Creek by a zone of nonwelded, soft, yellowish gray tuff several meters thick. The soft tuff is overlain by aphyric flow-layered rhyolite that is highly altered. We inferred that this rock without phenocrysts is the rhyolite of the millsite. No pumice was noted in the flow-layered rhyolite in the Flint Creek area or in any other outcrop as far north as the northernmost exposures about 6.4 kilometers northwest of De Lamar and

Jordan Creek. The distribution of the rhyolite, therefore, is known with reasonable certainty to extend from about 6.4 kilometers northwest of Jordan Creek on the north to Flint Creek on the south, a distance of about 21 kilometers. Although no conclusive evidence was found during the course of this study to show that the rhyolite of the millsite is a welded tuff, its distribution suggests that it may be.

Table 3. Chemical analyses and CIPW norms for rhyolitic rocks, western Owyhee County, Idaho. [Modified from Tables 4, 5, and 8, of Ekren and others, in press.]

	1	2	3	4	5	6	7	8	9	10	11	12
Chemical analyses												
SiO_2	70.44	76.50	74.98	71.27	70.77	72.97	76.27	75.00	68.89	74.02	75.11	72.13
Al_2O_3	13.75	12.71	12.80	13.94	13.09	12.56	11.78	12.68	13.82	11.99	11.91	12.42
Fe_2O_3	2.49	0.69	1.24	2.33	1.94	1.79	1.42	1.63	1.28	1.17	1.16	1.88
FeO	0.79	0.36	0.54	0.12	1.07	0.40	0.16	0.42	1.67	0.13	0.43	1.30
MgO	0.29	0.01	0.03	0.02	0.24	0.00	0.06	0.04	0.33	0.13	0.06	0.13
CaO	1.94	0.67	1.40	1.28	1.20	0.63	0.61	0.79	1.77	0.90	0.80	1.22
Na_2O	3.75	3.10	3.11	3.44	2.98	2.80	3.12	2.94	3.32	3.46	2.96	2.76
K_2O	4.05	5.16	4.97	5.06	5.51	6.01	5.35	5.61	4.89	5.01	5.31	5.21
H_2O+	0.45	0.30	0.16	0.31	1.70	1.57	0.30	0.90	2.86	0.54	1.35	1.15
H_2O-	0.54	0.23	0.34	0.57	0.44	0.57	0.37	0.38	0.16	0.44	0.27	0.42
TiO_2	0.70	0.21	0.33	0.58	0.52	0.32	0.19	0.28	0.53	0.11	0.20	0.46
P_2O_5	0.18	0.04	0.06	0.10	0.09	0.05	0.16	0.07	0.13	0.04	0.06	0.09
MnO	0.05	0.04	0.03	0.02	0.04	0.03	0.02	0.03	0.10	0.00	0.02	0.04
CO_2	0.03	0.08	0.06	0.07	0.03	0.05	0.02	0.37	0.01	0.18	0.22	0.07
Sum	99.45	100.10	100.05	99.11	99.62	99.75	99.83	101.14	99.76	98.12	99.83	99.28
CIPW Norms												
q	29.58	37.76	35.32	30.26	30.52	33.41	37.07	35.93	27.26	34.33	37.18	34.50
c	0.17	1.09	0.04	0.90	0.34	0.55	0.18	1.36	0.19	0.00	0.48	0.41
or	24.31	30.62	29.50	30.57	33.40	36.38	31.88	33.20	29.87	30.48	31.95	31.51
ab	32.23	26.34	26.43	29.76	25.87	24.27	26.62	24.91	29.04	38.14	25.50	23.90
an	8.39	2.57	6.20	5.37	5.31	2.54	1.86	1.12	8.13	2.46	2.27	5.14
di-wo	0.00	0.00	0.00	0.00	0.00	0.00	0.00	0.00	0.00	0.29	0.00	0.00
di-en	0.00	0.00	0.00	0.00	0.00	0.00	0.00	0.00	0.00	0.25	0.00	0.00
di-fs	0.00	0.00	0.00	0.00	0.00	0.00	0.00	0.00	0.00	0.00	0.00	0.00
hy-en	0.73	0.03	0.08	0.05	0.61	0.00	0.15	0.10	0.85	0.08	0.15	0.33
hy-fs	0.00	0.00	0.00	0.00	0.00	0.00	0.00	0.00	1.36	0.00	0.00	0.15
ol-fo	0.00	0.00	0.00	0.00	0.00	0.00	0.00	0.00	0.00	0.00	0.00	0.00
ol-fa	0.00	0.00	0.00	0.00	0.00	0.00	0.00	0.00	0.00	0.00	0.00	0.00
mt	0.68	0.69	0.89	0.00	2.13	0.46	0.04	0.64	1.92	0.10	0.88	2.79
hm	2.06	0.22	0.63	2.38	0.52	1.52	1.40	1.19	0.00	1.13	0.57	0.00
il	1.35	0.40	0.63	0.29	1.01	0.62	0.36	0.53	1.04	0.22	0.39	0.89
ap	0.43	0.10	0.14	0.24	0.22	0.12	0.38	0.17	0.32	0.10	0.13	0.22
cc	0.07	0.18	0.14	0.16	0.07	0.12	0.05	0.84	0.02	0.42	0.50	0.16

1. Tuff of Flint Creek, lower unit.
2. Rhyolite of the Silver City Range; average of 3 analyses.
3. Rhyolite of Black Mountain.
4. Tuff of Mill Creek.
5. Tuff of Swisher Mountain; average of 2 analyses.
6. Tuff of lower lobes; average of 3 analyses.
7. Tuff of upper lobes; average of 2 analyses.
8. Tuff of The Badlands; average of 2 analyses.
9. Quartz latite, Jump Creek rhyolite of Kittleman and others, 1965.
10. Tuff of Wilson Creek.
11. Tuff of Browns Creek; average of 2 analyses.
12. Tuff of Little Jacks Creek; average of 7 analyses.

Rhyolite of the Central Silver City Range

Flow-layered and hydrothermally altered white and light gray rhyolite caps both the Silver City Range on Florida Mountain and a broad area south of War Eagle Mountain (Figure 1). In places, this capping rhyolite is at least 300 meters thick. Most of the exposed rock contains only 1-2 percent phenocrysts (Figure 2) that rarely exceed 1 millimeter in length. Three locally preserved vitrophyre layers at the base, middle, and top of the rhyolite section indicate breaks or partial breaks in cooling but show no mineralogic breaks. The vitrophyres differ modally from cooling units of the tuff of Flint Creek (see histograms, Figure 2) exposed along the western flank of the range, and their fewer and smaller phenocrysts preclude correlation with the rhyolite of the millsite. The three vitrophyres appear to be representative of most of the rhyolite section in the central Silver City Range, as we observed no rocks in our reconnaissance that were obviously different. No samples were collected from the mostly highly altered rhyolite on Florida Mountain which, according to Pansze (1975, p. 30), includes welded tuff breccias.

Rhyolite of the Eastern Flank

Phenocryst-poor, extensively flow-layered rhyolite crops out along the eastern flank of the Silver City Range from the south line of T. 6 S. to the north line of T. 4 S. (Figure 1). This sequence, which is at least 250 meters thick, was not sampled in its entirety, but several thin sections, mostly from exposures along creek beds, strongly suggest that most of the rocks are the same as those that cap the central Silver City Range. In contrast to the latter, the rocks along the eastern flank are mostly fresh and pale red, brownish gray, or reddish gray. Apache tears from the basal rhyolite in T. 6 S., R. 2 W. (Figure 1), yielded a potassium-argon age of 16.0 ± 0.3 million years (Table 2; G. B. Dalrymple, written communication, 1979). This age indicates the rocks along the eastern flank to be coeval with those on the western flank and at Silver City (Table 2; Panzse, 1975; Armstrong and others, 1980).

Several outcrops were found that confirm an ash-flow tuff origin for some of the eastern flank rhyolite units. One of these outcrops is along the Sinker Creek-Silver City road in NW¼, T. 4 S., R. 2 W., where the lowest rhyolite unit in the section rests directly on granite and the contact locally is nearly vertical. The foliation is defined by well-flattened pumice fragments in the basal vitrophyre, and thin sections show that these fragments are enclosed in a matrix of shards. The devitrified rock above the basal vitrophyre at this locality is extensively flow layered, and all vitroclastic textures have been destroyed. In the Pickett Creek drainage in sec. 16, T. 5 S., R. 2 W. (Figure 1), rhyolite in about the middle of the rhyolite sequence consists of brown, thin-bedded, welded air-fall tuff (agglutinate) about 15 meters thick, overlain by flow-layered and laminated, partly devitrified rhyolite that looks like typical lava. A thin section of the basal part of the "typical lava," however, shows a matrix of strung-out, highly deformed shards. The Pickett Creek locality is inferred to be close to a vent because of the occurrence of the extremely hot air fall. The vent first gave rise to airborne ash that retained sufficient heat to weld when it settled on the ground. It then gave rise to avalanching ash flows that retained sufficient heat not only to weld but also to coalesce to liquid before final emplacement and cooling.

At Sinker Creek, near an old abandoned homestead in sec. 15, T. 4 S., R. 2 W., rhyolite is exposed that is correlative mineralogically with the sequence at Pickett Creek. The rhyolite at the old homestead, however, rests directly on granite. Despite this rhyolite being flow layered and contorted, strung-out shards are preserved in some laminae within the interior of the unit (Figure 3).

ROCKS OF THE JUNIPER MOUNTAIN VOLCANIC CENTER

Juniper Mountain is a gentle structural dome about 30 kilometers in diameter that rises as a low eminence above a broad northeast-plunging depression that extends from at least 70 kilometers west of the mapped area in Oregon to the Snake River Plain about 70 kilometers east of the mapped area. The depression is virtually filled with rocks of the Juniper Mountain center and the Little Jacks center (Figure 4). The structural depression, in turn, lies within a linear, east-northeast-trending rifted region that includes the eastern Snake River Plain (Ekren and others, in press; Mabey and others, 1978; Bonnichsen and others, 1975; Christiansen and Lipman, 1972). We believe that the structural low is due to both crustal rifting along the eastern Snake River Plain trend and to magma withdrawal during the massive eruptions at the two centers.

At least five rhyolite tuff sheets were erupted within a brief interval from a buried vent complex centered near Juniper Mountain. From oldest to youngest the rocks are the tuff of Mill Creek, the tuff of Swisher Mountain, the tuff of lower lobes, the tuff

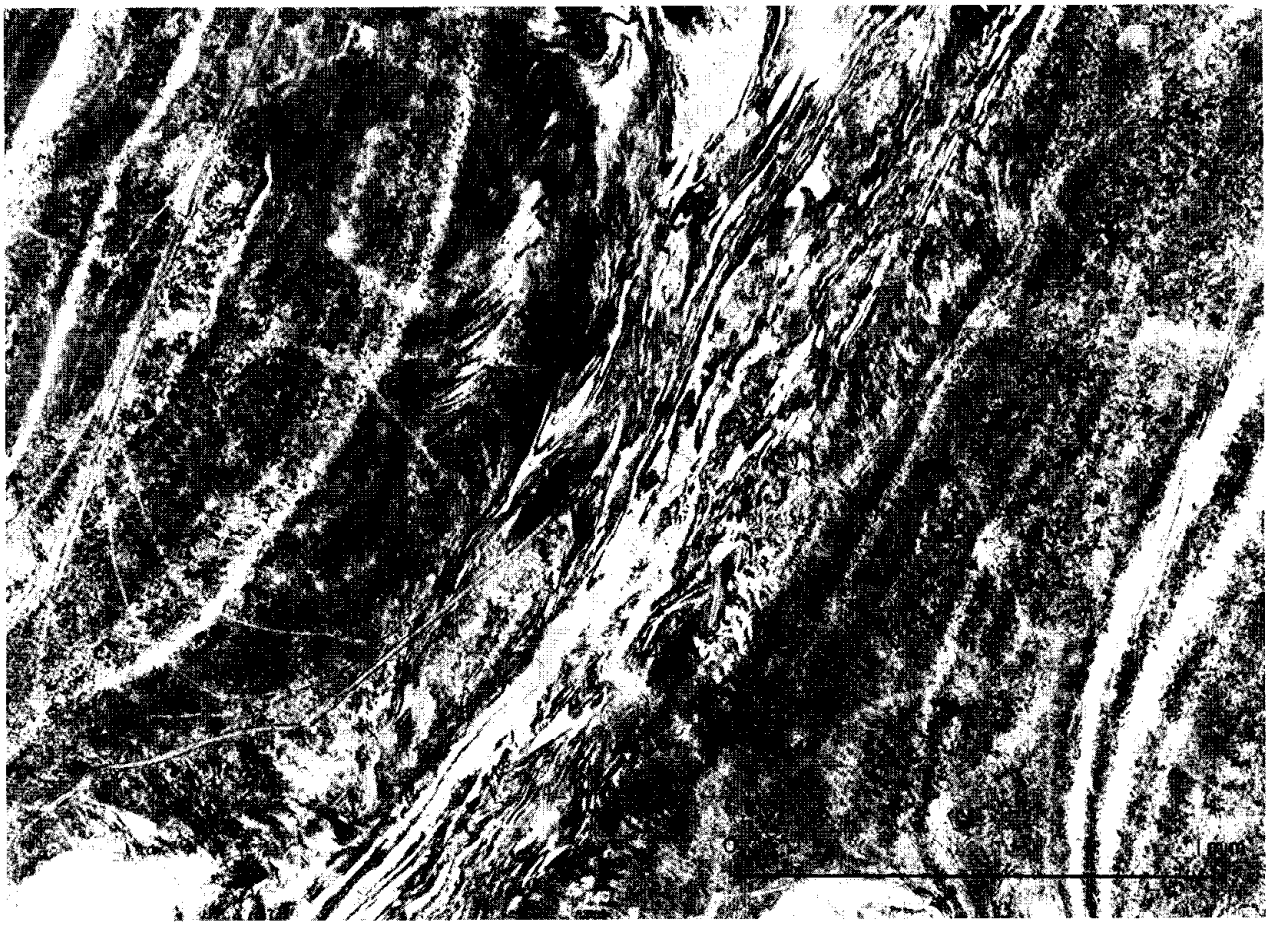

Figure 3. Photomicrograph of preserved shards in rhyolite at Sinker Creek on the eastern flank of the Silver City Range.

of upper lobes, and the tuff of The Badlands. The Juniper Mountain volcanic center is not bounded by arcuate faults indicative of cauldron collapse. We believe that the lack of cauldron collapse can best be explained by an eruption from a magma chamber located at unusually great depth, perhaps 15 kilometers or more below the surface.

Tuff of Mill Creek

The tuff of Mill Creek is the least understood of the units of the Juniper Mountain center because most canyons in the area have not been cut to sufficient depth to expose this unit. The tuff is exposed only in the canyons of Boulder Creek and its tributaries east and northeast of South Mountain (Ekren and others, 1981), but it may also be exposed in the Owyhee River canyon in Oregon (Figure 4), where two collected samples are modally similar either to the tuff of Mill Creek or to the basal part of the tuff of Swisher Mountain (Figure 4, locality 638). The two units can be distinguished from each other with certainty only by their magnetic polarity, which was not determined in the Owyhee River outcrops or in any other exposure in Oregon.

The tuff of Mill Creek is over 30 meters thick, reddish gray or brown, and flow layered from base to top. The basal vitrophyre in the Mill Creek area, a tributary of Boulder Creek, is conspicuously columnar-jointed at the base. Owing to highly irregular paleotopography, the columns dip at diverse angles, commonly horizontal, and in places they display nearly vertical internal flow banding. At several localities, flattened pumice fragments are visible in the basal vitrophyre (Ekren and others, in press).

The tuff of Mill Creek has smaller phenocrysts, contains less alkali feldspar, and has reversed magnetic polarity in comparison with the tuff of Swisher Mountain.

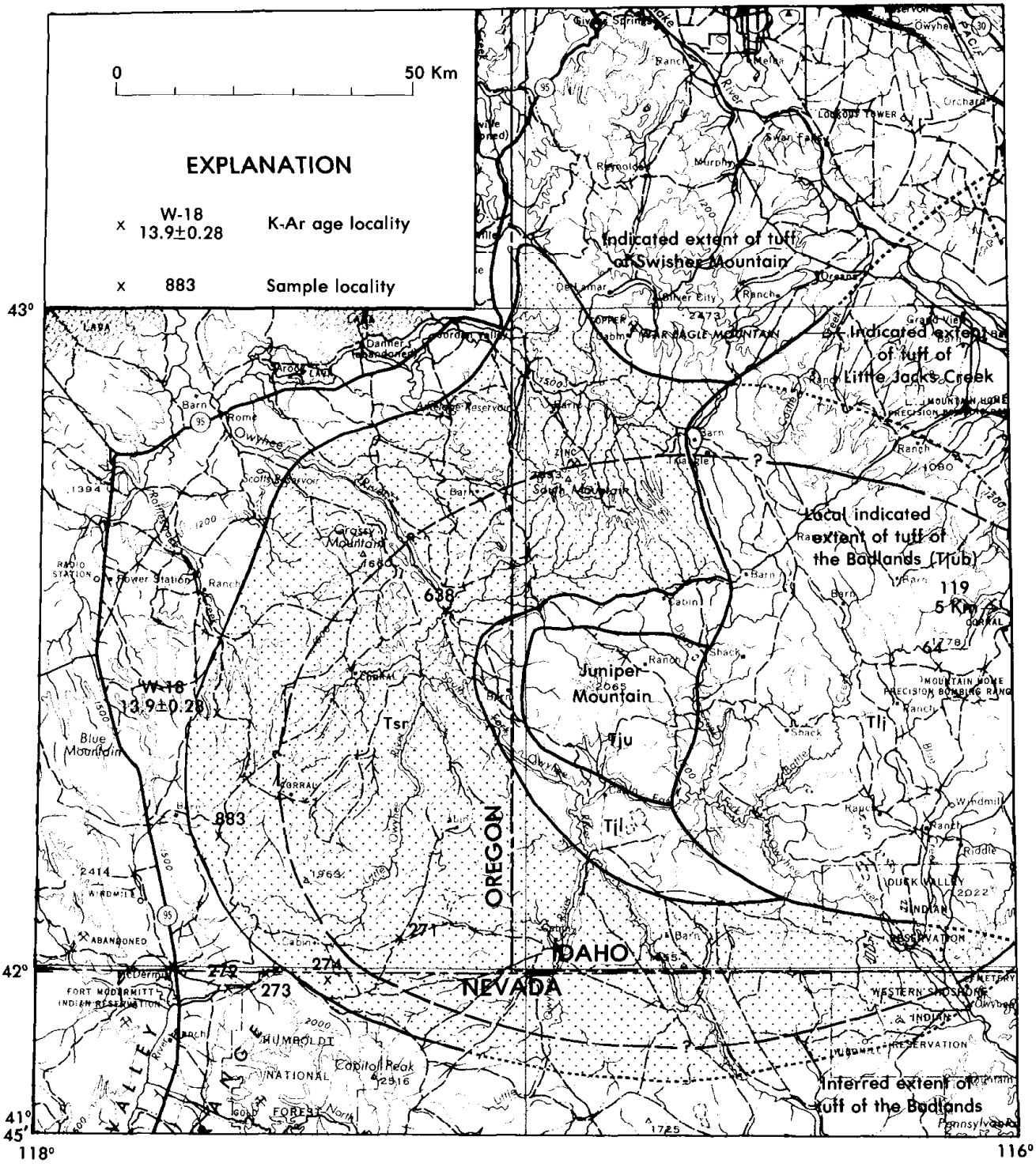

Figure 4. Map showing inferred distribution of tuffs of the Juniper Mountain volcanic center and the tuff of Little Jacks Creek within Owyhee County, Idaho, west of 116° west longitude. For explanation of letter symbols see Figure 1.

Tuff of Swisher Mountain

The tuff of Swisher Mountain is as much as 200 meters thick in the vicinity of Juniper Mountain. It is reddish gray, brown, and brick red and in most localities is flow layered from base to top. In several places it displays well-developed flow breccia at its base. In exposures west of De Lamar (Figure 4), at the extreme north end of Swisher Mountain, it consists entirely of flow breccia. Farther south, however, the unit, although flow layered, is not brecciated everywhere, and flattened pumice fragments are preserved locally in the basal vitrophyre and elsewhere in the unit. Where pyroclastic textures are obscure or have been destroyed in the tuff of Swisher Mountain, thin sections show the development of tiny feldspar microlites that we regard as proof that the ash flow achieved a liquid state (Figure 5) before final emplacement. In several localities the microlites show a more pronounced flow alinement than is apparent in this figure. That the microlites formed after the ash avalanched from the eruption column rather than before is indicated by various thin sections that show incipient microlites in stretched pumice lumps but not in the enclosing matrix. We believe that the occurrence of microlites in the lumps and not in the matrix of these particular rocks is due to the presence of more volatiles trapped in the pumice. Furthermore, had the microlites formed in the magma chamber prior to eruption many undoubtedly would have been smashed during the explosive eruption process. Microlites of various sizes and shapes should have ensued. This does not seem to be the case. In most rocks containing microlites, the tiny crystals are strikingly similar in size and shape; in some rocks they are all virtually crystallites.

On Swisher Mountain, the tuff is generally less than 50 meters thick and appears to be a densely welded simple cooling unit with a vitrophyre at the base and one at the top. Southward toward Juniper Mountain, the unit thickens and shows several partial or complete cooling breaks that are marked by black vitrophyres, most of which show flattened pumice fragments. Some of the black vitrophyres are flow brecciated. Nevertheless, without evidence of erosion beneath the vitrophyres or the presence of bedded tuffs at these lithologic breaks, it is impossible to be certain whether the cooling breaks were complete. Westward in Oregon, if correlations made during a raft trip are correct (Ekren and others, in press), two or more separate cooling units are present in the tuff of Swisher Mountain in the Owyhee River canyon. The phenocryst mineralogy elsewhere in Oregon—for example, at traverse localities 271 through 274 and at locality 883 (Figure 4)—can be matched precisely with various thin sections from Swisher Mountain

Figure 5. Photomicrograph showing incipient feldspar microlites in basal glass of tuff of Swisher Mountain (crossed polarizers). Sample taken from outcrop a few kilometers south of Swisher Mountain, Idaho (in NW¼, T. 6 S., R. 5 W.).

and from localities east and south of South Mountain (Figure 4). A sample collected and analyzed by Dalrymple and others (reported in Laursen and Hammond, 1978) and recalculated using constants of Table 2 yielded a potassium-argon sanidine age of 13.9 ± 0.28 million years (Figure 4, sample locality W-18). This is virtually the same age as the average of two dates for samples collected by Neill (1975) at Poison Creek (Ekren and others, 1981) where the tuff of Swisher Mountain is directly overlain by the tuff of Little Jacks Creek.

As mentioned earlier, the basal part of the tuff of Swisher Mountain is not easily distinguished from the tuff of Mill Creek—both are for the most part plagioclase-pyroxene rhyolites (Figure 2). However, the tuff of Swisher Mountain upward from the base shows increasing amounts of alkali feldspar, and in places toward the top it contains nearly as much alkali feldspar as plagioclase. Quartz occurs sporadically throughout the unit; most samples from widely scattered localities contain none. In general, quartz is most apt to be found in the upper one-third of the unit; locally, in the top vitrophyre, it may make up as much as 3 percent of the total phenocrysts, which

constitute about 17 percent of the volume of the rock. The pyroxene in the tuff of Swisher Mountain is principally intermediate pigeonite (C. Knowles, written communication, 1980), but a few grains of hypersthene and a few grains of clinopyroxene with a large 2V are generally present per thin section. The upper vitrophyre commonly displays abundant pumice in outcrop (Figure 6), and a thin section of this rock shows a matrix of shards.

The tuff of Swisher Mountain is magnetically normal on Swisher Mountain and in several localities near Juniper Mountain; however, we never methodically measured it from base to top in areas of maximum thickness.

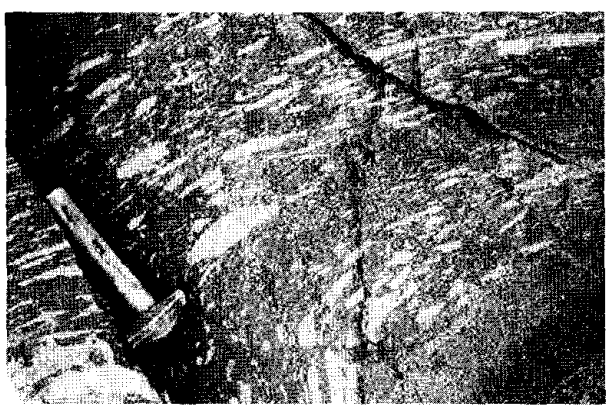

Figure 6. Pumice-rich vitrophyric top of tuff of Swisher Mountain at an outcrop a few kilometers north of Juniper Mountain, Idaho. Tuff exposed a few centimeters below this outcrop is flow layered, contorted, and devitrified, and all pumice fragments and shards have been destroyed.

Tuff of Lower Lobes

Juniper Mountain and surrounding benches are formed by two rhyolite cooling units that on high-altitude, infrared photographs and Landsat images have the appearance of two congealed masses of viscous molasses (Figure 7). Flowage of both units resulted in the formation of concentrically ridged flow lobes; as a consequence, the two units are informally called the tuff of lower lobes and the tuff of upper lobes of Juniper Mountain. A startling feature of both units is that without the lobate appearance of the units and the well-defined flowage structures visible on aerial photographs, an experienced volcanologist would not hesitate to call both units ash-flow tuffs on the basis of sparse occurrences of well-flattened pumice fragments within and at the bases of both units. We infer that both are ash-flow tuffs which coalessed in large part to viscous liquids.

The tuff of lower lobes is about 200 meters thick in the vicinity of Juniper Mountain. The basal vitrophyre is brecciated in most exposures, but the breccia clasts commonly show well-defined, well-flattened pumice fragments. The overlying devitrified and partly devitrified rock is red, flow-layered, and contorted to an exceptional degree. The tuff contains more phenocrysts and a more rhyolitic phenocryst assemblage than the tuff of Swisher Mountain (compare histograms, Figure 2). The pyroxene is intermediate pigeonite, like that in the Swisher Mountain but the modal abundance of pyroxene is considerably less.

The tuff of lower lobes is magnetically reversed, and it is 13.8 ± 0.5 million years old based on potassium-argon analyses of sanidine from an outcrop north of Juniper Mountain (Figure 4).

Tuff of Upper Lobes

The tuff of upper lobes forms the crest of Juniper Mountain and a series of high benches more or less radially arranged around its summit (Figures 1 and 4). Unlike the tuff of lower lobes, the tuff of upper lobes does not have a brecciated basal vitrophyre. Instead, the basal part locally consists of alternating, partially welded and moderately welded tuff that grades upward into densely welded tuff and thence upward into flow-layered tuff in which nearly all pyroclastic textures have been destroyed. Exposures of partially welded tuff at the base are confined to the eastern and southeastern flanks of Juniper Mountain. The partially welded tuff apparently thins northward and westward and possibly pinches out entirely in those directions. In the northern and western exposures, the contact between the upper lobes and lower lobes is everywhere covered by thick talus, or it is hidden by the overlapping tuff of The Badlands (Figure 1). In several places along the north flank, however, the covered interval is so thin that any hidden, intervening, partially welded, nonflow-layered tuff in the vicinity of the lower lobes-upper lobes contact would necessarily be thin or absent.

On the east flank, the partially welded tuff is at least 100 meters thick and consists of alternating weakly welded and moderately welded pink, red, and reddish brown tuff that contains abundant, conspicuous pumice lapilli generally darker than the enclosing matrix. We infer that this interval includes a number of ash flows emplaced with sufficient time lapses between eruptions to cause compound cooling. At a few localities in the Beaver Creek drainage in T. 12 S., R. 4 W., the partially welded tuff can be seen to grade upward into densely welded tuff in which the pumice clasts are lighter colored than the matrix, and these show increasing degrees of flattening upward until, in a vertical distance of about 10 meters, they

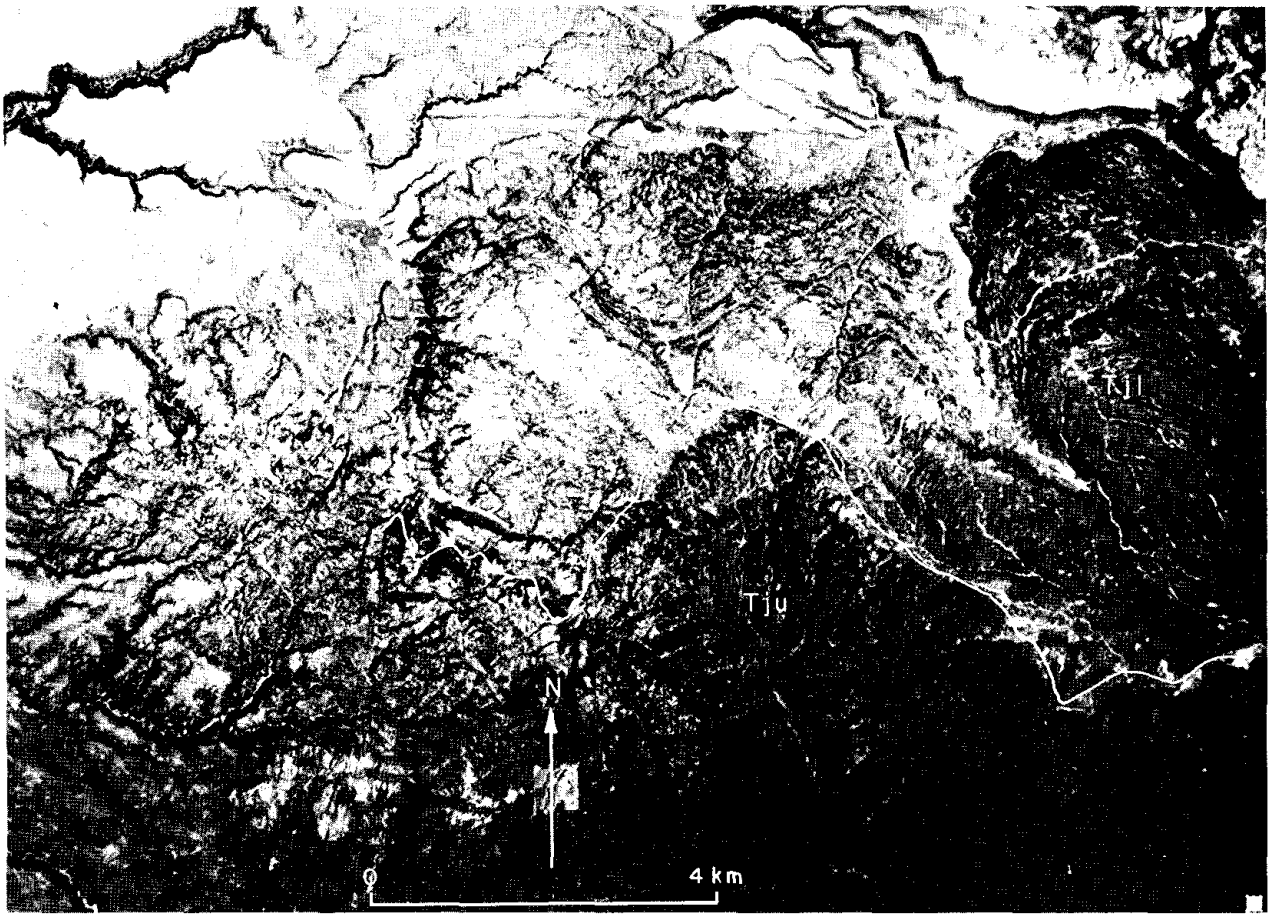

Figure 7. High-altitude infrared photograph of the north flank of Juniper Mountain, Idaho, showing distal parts of the tuff of lower lobes (Tjl) and tuff of upper lobes (Tju).

become so stretched as to be nearly unrecognizable as pumice (Figure 8). Above this zone, the rock becomes flow-layered and contorted, and stretched pumice fragments are preserved only locally. The flow-layered rocks form the lobate masses so conspicuous on aerial photographs.

The outcrops show that the welded tuff did not simply become flow layered at the top because of laminar flowage (Walker and Swanson, 1968); the flow lobes reveal that the extremely hot particles in the ash flow or flows coalesced to form a viscous liquid. The difference between the tuff of lower lobes and the tuff of upper lobes is merely that the initial ash flows of the upper tuff were colder.

The gradational nature of the contact between unequivocal welded tuff and the flow-layered rock which gave rise to flow lobes precludes the possibility that the rock is hybrid, formed in part from ash flows and in part from liquid lava. Had the vent switched from spewing ash to liquid, there would necessarily have been a time lapse between the rapidly emplaced ash flows and the slowly emplaced viscous flows, and some disruption of the underlying ash would surely have occurred; none is evident. In all likelihood, the slow-moving viscous lava would have formed a flow breccia, and none is evident. We infer, instead, that the evidence of denser welding upwards in the tuff of upper lobes is due to gradually increasing emplacement temperatures as eruptions proceeded, and that the last flows were emplaced at such high temperatures that the extremely hot ash coalesced to form a liquid. The relatively restricted areas of distribution of both the lobate tuffs (about 56 kilometers in diameter for the lower lobes) suggest that their eruption columns were not nearly as high as the columns which gave rise to the widespread tuffs of Swisher Mountain and Little Jacks Creek (see later pages). The smaller columns may have been somewhat analogous to fire fountains—a possibility that was first suggested by R. L. Christiansen (oral communication, 1977).

The tuff of upper lobes typically contains 7-10

Figure 8. Stretched pumice fragments in transitional zone of tuff of upper lobes between flow-layered lobate rock above and densely welded tuff with flattened, but not stretched, pumice fragments below.

percent phenocrysts in the lower partially-welded basal part and as much as 26 percent in the upper flow-layered part (Figure 2). Except for a few sparse and poorly exposed layers at and near the top of Juniper Mountain that contain phenocrysts as large as those in the tuff of The Badlands, the relative proportions and sizes of phenocrysts remain virtually the same from base to top.

The tuff of upper lobes has normal magnetic polarity and is 13.9 ± 0.5 million years old based on potassium-argon analyses of sanidine from outcrops on the northeast flank of Juniper Mountain (Table 2).

Tuff of The Badlands

Tuff of The Badlands is the name that we informally apply to the youngest cooling unit of the Juniper Mountain volcanic center. It forms the rugged topography at The Badlands (Figure 1) where its flow-brecciated, black basal vitrophyre rests directly on red welded tuff of the upper lobes. The tuff of The Badlands was distributed over a broader area than the tuff of upper lobes. On the southern and western flanks, the tuff of The Badlands rests directly on the tuff of lower lobes, and at Poison Creek, at the extreme northeastern edge of its distribution pattern, it rests directly on the tuff of Swisher Mountain (Figure 1, T. 8 S., R. 1 E.).

The tuff of The Badlands shows more extreme mineralogic variations internally than the other units of the Juniper Mountain center display among one another. The lower part, as much as 200 meters thick, is reddish gray and weathers brown. It locally contains the largest phenocrysts found in any of the Juniper Mountain rocks. The upper part, also as much as 200 meters thick, contains perhaps the smallest phenocrysts. The unit bridges the lithologies of the tuffs of lower and upper lobes: The lower part of the tuff of The Badlands is a virtual repeat of the tuff of lower lobes, and the upper part is a repeat of the tuff of upper lobes.

In exposures on The Badlands and in the Owyhee River canyon, except for the large mass of rock exposed between Deep Creek and Battle Creek (Figure 1), the tuff of The Badlands consists only of the large-phenocryst lower part. In places in the canyon south of Lambert Table, the large-phenocryst rock is vitrophyric at the base and also at the top. The presence of the vitrophyre at the top, which is directly overlain by sedimentary rocks associated with the Banbury Basalt, show that the lower, large-phenocryst part of the tuff of The Badlands and the upper, small-phenocryst part are not a continuous simple cooling unit. Instead, the two parts are at least separated by a partial cooling break, and in the canyon exposures south of Lambert Table the upper part either was removed by erosion prior to the deposition of Banbury Basalt and related sedimentary rocks or was never deposited there.

In several exposures the tuff of The Badlands contains quartz phenocrysts as large as 8 millimeters and alkali feldspar and plagioclase phenocrysts as large as 1 centimeter. If these large phenocrysts were consistently present laterally and vertically throughout the unit, they would provide a useful criterion to distinguish the unit from the tuff of lower lobes; unfortunately they are not. Where the large grains are present, however, they are spectacular because they are so extensively resorbed. Commonly, they are completely riddled with holes and show as virtual sieves in thin section. The degree of resorption of the crystals, however, is nearly matched by resorption of the crystals in the tuff of lower lobes.

Between Deep Creek and Battle Creek, the large outcrop labeled "Tjub" (Figure 1) consists entirely of the upper lithology of the tuff of The Badlands. The contact with the lower lithology, the large phenocryst tuff, is not exposed. The exposed rock is pink, flow layered, and characterized by intense vapor-phase crystallization, but nevertheless it shows stretched pumice fragments in nearly all exposures. The rock in these exposures is as thick as 200 meters.

Elsewhere, the tuff of The Badlands is typically flow layered from base to top, and the basal vitrophyre commonly is extensively flow brecciated. In most exposures, the lower as well as the upper part

displays unequivocal stretched pumice, and thin sections from widely scattered localities display highly deformed shards. If the correlation of the unit (Figure 4) as far east as the Duck Valley Indian Reservation and to the west as far as Tent Creek in Oregon is correct, the unit is second only to the tuff of Swisher Mountain in the areal extent of units erupted from the Juniper Mountain center.

Both parts of the tuff of The Badlands are magnetically normal. Armstrong and others (1980) reported a potassium-argon date of 12.0 ± 0.2 million years on sanidine from an outcrop sampled by Neill (1975) at Poison Creek (Figure 1).

TUFF OF WILSON CREEK

The tuff of Wilson Creek occurs as a tabular sheet, much broken by minor faults, along the Snake River Plain margin and as a paleocanyon-filling tongue extending parallel to Wilson Creek. It is a simple cooling unit that locally reaches a thickness of more than 170 meters. Toward the northwest, it overlies the Jump Creek Rhyolite and toward the southeast it underlies the rhyolite tuff of Browns Creek (Figure 1). For descriptions of these units see Ekren and others (1981). The tuff of Wilson Creek must be about 11 million years old because potassium-argon ages established for both the underlying and overlying units are approximately 11 million years. The unit has reversed magnetic polarity.

The tuff of Wilson Creek is a grayish red to grayish red-purple, crystal-poor, devitrified rhyolite containing fewer than 5 percent crystals, smaller than 2 millimeters in size, of quartz and sanidine in subequal amounts, together with rare clinopyroxene. The sparse vitrophyric rocks in this unit contain a few crystals of xenocrystic(?) biotite and plagioclase. Lithic inclusions sparsely scattered throughout the unit are mostly plagioclase-rich andesites that occur in the surrounding area and, locally, directly beneath the tuff of Wilson Creek. Most outcrops of the tuff of Wilson Creek are devitrified, lithophysal, and finely flow layered. In places near the Snake River Plain margin, the flow layering is thrown into broad folds. Toward the southwest the folding disappears, and at the southwesternmost end of the paleocanyon fill, flow layering is mostly horizontal except where it steepens to meet the lateral margins of the paleocanyon.

The only known exposures of vitrophyre in the tuff of Wilson Creek are along the paleocanyon margins at the southwest end of the canyon fill. Some of this glassy material is as flow layered as the devitrified rock. However, exposures at Wilson Bluff, at the southwestern extremity of the paleocanyon fill, show abundant collapsed pumice fragments, as large as 2 by 6 centimeters, and similar-size lithic inclusions in a shard matrix in the marginal vitrophyre. Continuous exposures allow the vitrophyre to be traced upward and channelward into patchily devitrified rock, which locally preserves pumice outlines, and then into steeply flow-layered lithophysal rock in which all traces of pyroclastic character have been erased. Continuing away from the margin, the steep flow layering flattens and merges with the layering in the inner part of the flow. No discontinuities interrupt the transition from pumice-rich vitrophyre at the paleocanyon margin to devitrified, flow-layered, lithophysal rock in the interior of the paleocanyon fill. These exposures provide firm evidence that the tuff of Wilson Creek is a welded ash flow or flows, whose fragmental texture has at most places been completely obliterated by homogenization and the formation of lithophysae. The preservation of vitroclastic texture at the paleocanyon margins appears to be due to rapid chilling.

Geologic mapping shows that the paleocanyon occupied by the tuff of Wilson Creek could not have extended much farther southwest than where it is presently filled by the southwesternmost end of the tonguelike sheet. No possible source for the unit exists to the west or south; the tuff must have been erupted from a source to the northeast now buried beneath the Snake River Plain. Detailed study in the highlands to the southwest (McIntyre, 1972) shows that streams draining the highlands flowed toward the Snake River Plain during the time when the tuff of Wilson Creek was emplaced. Thus, the tuff of Wilson Creek must have flowed up-canyon during its emplacement, additional evidence that the unit moved as an ash flow and not as a viscous lava.

TUFF OF LITTLE JACKS CREEK

A compositionally distinctive sequence of dark, flow-layered rhyolite tuff that for the most part contains only plagioclase and ferriferous pigeonite phenocrysts (determined with microprobe by C. Knowles, written communication, 1980) is well exposed throughout a large part of the eastern Owyhee Plateau. The best exposures are in Little Jacks Creek Canyon about 35 kilometers south of Grand View, where at least four and possibly as many as six cooling units are exposed (Figures 1 and 9). This sequence is referred to in this report as the tuff of Little Jacks Creek. It corresponds to the tuff of Antelope Ridge of Bennett (1976) and the rhyolite of Owyhee Plateau of Neill (1975), who obtained potassium-argon dates of 9.6 ± 2.0 million years and 10.0 ±

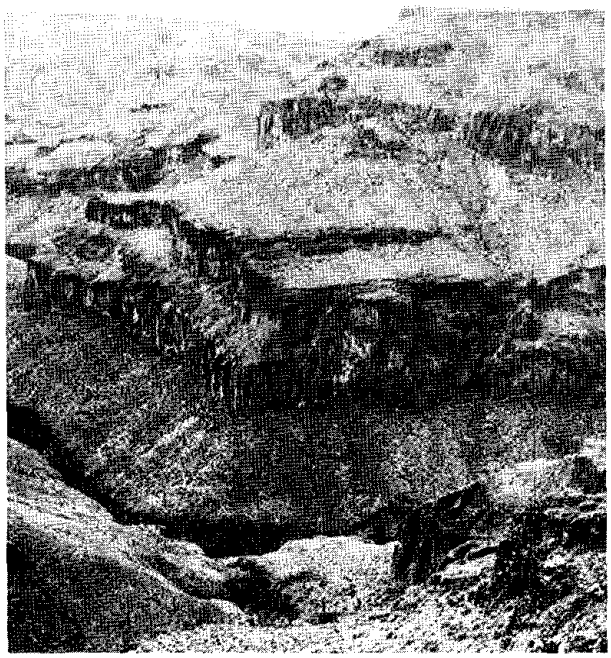

Figure 9. Tuff of Little Jacks Creek, Idaho, in Little Jacks Creek canyon about 8 kilometers above mouth. Note tabular appearance of these ledge-forming, flow-layered cooling units. Four cooling units are inferred at this locality: an upper, mesa-capping unit at skyline, which is about 15 meters thick; an upper middle unit about 100 meters thick that forms two distinct ledges; a lower middle unit, also about 100 meters thick, that also forms two distinct ledges; and an incompletely exposed lower unit. The four cooling units are indistinguishable on the basis of phenocryst mineralogy (Figure 2). Soft zones between cooling units consist mostly of yellow-brown tuffaceous sandstone and reworked ash-fall tuff.

1.5 million years from plagioclase separates from outcrops in Little Jacks Creek canyon (Armstrong and others, 1980).

The various cooling units in the tuff of Little Jacks Creek, although internally flow layered and contorted, are exceptionally tabular where exposed in the deep canyons (Figure 9). The basal vitrophyres are mostly flow brecciated, but the degree of development of the basal breccia varies considerably. In places, only the lower 2 meters or so shows incipient brecciation (Figure 10); elsewhere the basal breccia may be 10 meters or more thick. The lower part above the breccia may be either massive (Figure 10) or extensively flow folded (Figure 11). The devitrified rhyolite in the interior of the various cooling units is gray to purplish gray on fresh surfaces and dark purple or purplish gray on weathered surfaces; rarely it weathers deep red. Because of its well-developed flow layering, the tuff weathers into flagstones that, in most areas, completely cover intervening zones of soft tuff. The soft tuff zones show maximum thickness along the east border of the mapped area (Figure 1), which we infer is near the source area (see Bonnichsen, 1982a this volume).

The various cooling units in at least 95 percent of the outcrops have all the features indicative of lava flows and none of the characteristics of ash-flow tuffs. In a few outcrops, however, well-flattened pumice fragments are preserved, and thin sections show that the fragments are enclosed in shard-rich groundmass (Figure 12). Several thin sections of tuff of Little Jacks Creek show the development of tiny feldspar microlites like those in the tuff of Swisher Mountain (Figure 5). A few thin sections show a virtual felt of these tiny microlites, and many thin sections show them in pronounced flow alinement. The microlites must have formed after the flow coalesced to a dense, fluid mass but before the mass had come to rest.

The tuff of Little Jacks Creek displays a remarkably consistent mineralogy from base to top (Figure 2). The tuff contains from 3 to 15 percent phenocrysts consisting of 75-85 percent plagioclase that are 2-4 millimeters long; 10-20 percent pale brown or brown-

Figure 10. Base of Little Jacks Creek cooling unit near Big Jacks Creek, Idaho. Note the incipient development of basal breccia. Rhyolite rests on tuffaceous sandstone and reworked crystal-poor ash-fall tuff.

Figure 11. Flow fold at base of a Little Jacks Creek cooling unit at mouth of Little Jacks Creek canyon, Idaho. Fold is about 2 meters high.

Figure 12. Photomicrograph of thick-walled undeformed shards in basal glass of lower middle cooling unit (See Figure 9) of tuff of Little Jacks Creek.

ish green ferriferous pigeonite (C. Knowles, written communication, 1980) 1 millimeter and smaller; and from 2 percent to as much as 9 percent small Fe-Ti oxide crystals that are less than 1 millimeter. The plagioclase crystals include many that are considerably resorbed and a few that are poikilitic, containing very fine grains of pigeonite and Fe-Ti oxide. Several thin sections of tuff of Little Jacks Creek contain a few crystals of ferrohypersthene, and a few thin sections contain an occasional grain of clinopyroxene that has a large axial angle.

In a few localities in the eastern part of the area, for example at localities 64 and 119 (Figure 4), the uppermost rhyolite contains a few small phenocrysts of quartz per thin section or, less commonly, of both quartz and alkali feldspar. This rock resembles the tuff of Little Jacks Creek so closely in outcrop and thin section that genetic affinity to the Little Jacks Creek plagioclase tuff seems a valid assumption. We infer that the quartz-bearing unit constitutes one of the last products of the Little Jacks eruptive center and that the center lies just east of the eastern boundary of Figure 1. We base this conclusion on the fact that the tuff of Little Jacks Creek is thickest in this general region and that flow lineation trends (Figure 1) converge in this area. The source probably is centered a few kilometers northeast of localities 64 and 119 (Figure 4) in Townships 9, 10, and 11 S.; Ranges 4, 5, and 6 E. This area, when viewed from vantage points on the Snake River Plain, stands in gentle relief with the configuration of an inverted saucer or a flat-topped domical area. This area was mapped in reconnaissance by Malde and others (1963), and it is obvious from their map and from Landsat images that no caldera complex bounded by arcuate faults is present in the inferred source area. We believe that a lack of cauldron collapse in this area, like that at Juniper Mountain, is due to eruption from depths that precluded such development.

CHEMISTRY AND PETROLOGY

Chemical analyses and CIPW norms for the rhyolitic rocks described in this report and for others described in Ekren and others (1981) are shown in Table 3. Comparing an average of twenty of these with the average of twenty-four calc-alkalic rhyolites compiled by Nockolds (1954) shows that Owyhee rocks are normal calc-alkaline eruptives. Thus, their high fluidity is not a function of abnormal chemistry. The rocks from the Juniper Mountain center and the Little Jacks center (Table 3), however, are richer in iron than Nockolds' average, and according to R. L. Smith and G. A. Izett (oral communication, 1978 and 1979), they are considerably richer in iron than are most rhyolites that have been described from the western United States. The abundance of iron in these rocks, however, was obviously not a critical factor that accounted for high fluidity because several of the equally fluid rhyolite tuffs from the Silver City Range (Table 3, column 2) have relatively low iron values—values that are less than Nockolds' average.

The rhyolites, whether erupted from the western Snake River Plain (Table 3, analyses 9, 10, and 11), the Silver City Range and vicinity (Table 3, analyses 1, 2, and 3), Juniper Mountain (Table 3, analyses 4 through 8), or the Little Jacks center (Table 3, analysis 12), are characterized by low Ca and exceedingly low Mg contents. According to Noble (1972, p. 143-144; oral communication, 1979), rhyolites with this chemistry are fairly typical of areas of bimodal

basalt-rhyolite volcanism, and the low Ca and exceedingly low Mg values represent their highly differentiated states. Whether the low values of the Owyhee rocks represent end stages of a differentiation process or whether they reflect early products of partial melting a moot.

The analyses of the rocks erupted from the Juniper Mountain center (Table 3, analyses 4 through 8) show that little differentiation took place during the time span of eruptive activity, which may have been as long as 2 million years. Even less took place in the Little Jacks center (Ekren and others, in press). The data show that the early eruptive products of a single eruptive cycle tend to be more mafic than later products. This is the opposite of the well-known compositional zonation of ash-flow tuffs produced during caldera-forming eruptions; in those tuffs the early erupted products are more silicic than those that follow. This has been attributed to progressive tapping, from the roof down, of a magma chamber with a zone of more silicic magma at the roof. This zonation appears to be a common characteristic of ash-flow tuffs associated with caldera-forming eruptions from magma chambers located at shallow depths (Lipman and others, 1966; Byers and others, 1976; Hildreth, 1979). Chemical variation in the Owyhee chambers, the opposite of this, surely is attributable to some as yet unknown set of conditions or mechanisms.

Recent laboratory experiments by Whitney (1975) using high temperatures and pressures and low water contents provide some approximate limits to the conditions under which crystallization of the Owyhee rocks may have taken place (Ekren and others, in press). In brief, Whitney's data for a synthetic granite melt show that the crystallization sequence of plagioclase plus liquid to plagioclase plus quartz, a sequence occurring in the uppermost parts of the tuff of Little Jacks Creek, takes place only at temperatures greater than 1000°C, at very high pressure (8 Kb), and at extremely low water contents (2 weight-percent water or less). At lower pressures, but probably not much lower than 8 Kb, the field "plagioclase plus quartz plus liquid" disappears. Therefore, those rocks in the highest unit of the tuff of Little Jacks Creek that contain phenocrysts of plagioclase and quartz and that lack alkali feldspar must have crystallized under conditions similar to those defined by Whitney's experiments. A reasonable conclusion is that a pressure of 6-8 Kb probably prevailed during eruption of both the plagioclase-quartz cooling units of the tuff of Little Jacks Creek, whose crystallization conditions are closely constrained by the Whitney data, and the plagioclase-only tuff. These pressures suggest a depth of about 20-25 kilometers, which is within the lower crust in this region as defined by Hill and Pakiser (1966).

The inferred temperature is corroborated by analyses of iron-titanium oxides in the tuff of Little Jacks Creek and the tuff of Swisher Mountain. Equilibration temperatures for these minerals in both units are 1090°C or higher (Ekren and others, in press). The very low water content and high temperature called for also are reflected in the anhydrous mineral assemblage that characterizes these rocks.

The experimental data of Whitney (1975) cannot be used to define the pressure prevalent during crystallization of the tuff of Swisher Mountain because alkali feldspar always is present and quartz is sparse. We infer that pressures were less than those in the Little Jacks Creek magma chamber in order to account for the marked differences in phenocryst assemblages between the two tuffs. The anhydrous phenocryst assemblage in the tuff of Swisher Mountain suggests low water contents comparable with the tuff of Little Jacks Creek and, by inference, with the derivation of the magma from similar, water-deficient source materials. The magma chambers at both centers were at depths so great that subsidence above the chambers accompanying magma withdrawal was expressed as gentle downwarping rather than as fault-bounded cauldron collapse.

No stable magma chamber could exist for long at the temperatures indicated for the times of eruption. Walls of the chamber would be under active attack by the magma. Where other evidence suggests the presence of a stable chamber the extremely high temperatures must have been limited to the time immediately prior to eruption; indeed, such eruptions may have been triggered by a sudden temperature rise. Repetition of phenocryst characteristics and chemical zonation of the tuff of lower lobes and tuff of upper lobes within a later, single cooling unit, the tuff of The Badlands, suggests that a stable magma chamber existed under Juniper Mountain that was capable of repeatedly supplying the same material. In units like the tuff of Swisher Mountain that contain enormous volumes of material within each cooling unit, it is difficult to imagine such volumes being available for eruption without storage in some kind of magma chamber, at least for a short time. In units that show only a narrow range of variation in phenocryst characteristics and chemistry, and moderate volume within each cooling unit, such as the tuff of Little Jacks Creek, there is no evidence that a stable magma chamber ever existed. There is a distinct possibility that rocks such as these were erupted directly from their depths of origin without detectable residence time in a magma chamber at moderate to shallow depth.

Many authors now believe that the most likely source of heat for producing rhyolite magmas in

regions of crustal extension is the injection of basaltic magma (Hildreth, 1979; Lachenbruch and Sass, 1978; Leeman, 1982 this volume; and Bonnichsen, 1982b this volume). Heat transfer from basaltic magma is also believed to be a common mechanism for triggering the eruption of rhyolitic rocks (Sparks and others, 1977). Heat transfer from basalt likely was involved in the generation and eruption of the Owyhee rocks because we can imagine no other way to raise these rhyolitic magmas to the eruption temperatures typical of basalt. Why this process should have operated in such a unique way in the Owyhee region remains a puzzle.

PROBABLE ORIGIN

The first comprehensive descriptions of the zones and geologic relations of welded ash-flow tuffs (Smith, 1960; Ross and Smith, 1961) showed that these rocks, in general, have features and properties that are so unlike those of typical lava flows that little room seemed to exist for possible confusion in distinguishing the two rock types. Later studies showed that many welded tuffs, in fact, exhibit features that are borderline with those of lavas (Hoover, 1964; Walker and Swanson, 1968; Anderson, 1970; Ekren and others, 1974). These borderline rocks, nevertheless, all have one feature in common: Their basal parts show unmistakable, flattened pumice fragments, and thin sections from various parts of the cooling units commonly show shard matrices, although most shards are so strung out as to be nearly unrecognizable. Our studies show that the Owyhee rocks are a step still farther removed from typical welded tuffs because they only locally display preserved flattened pumice fragments and shards even in their lowest parts and, to further confound matters, they commonly display flow-brecciated basal vitrophyres.

Our studies show that the southwestern Idaho tuffs were erupted at extremely high temperatures—1090°C and higher according to iron-titanium oxide compositions. At these extreme temperatures, particles within the interiors of the eruption columns and the avalanches that gave rise to the ash flows may have more closely resembled liquid droplets than rigid, angular glass shards. Perhaps, the only rigid shards and pumice fragments that existed were at the cooler tops, bases, and sides of each ash flow. These may be what we see locally preserved at the margins of and, in some tuffs, within a cooling unit containing several ash flows. We infer that in the final stages of ash-flow movement the various particles, whether rigid, semi-rigid, or liquid, coalesced in the main body of the sheet to form a nearly homogeneous viscous liquid. This liquid, then, moved sufficiently far to develop extensive flow layering and flow folds. The distance involved need not have been large—perhaps, no farther than a few hundred meters. Much of the flowage could well have been internal and could have resulted from final adjustments of the liquid to underlying topography. At this stage there may have been very little advancement of the molten sheet. The movement that occurred was completely analogous to flowage of a rhyolite lava flow.

Is it misleading or inappropriate to call the Owyhee rocks "ash-flow tuffs" when a possibility exists that most of the particles in the flows were not glass fragments but liquid droplets instead? We think not, because of the small differences in physical properties of white-hot shards and liquid droplets and because the resulting sheetlike deposits, extending 50 kilometers or more from their sources, certainly must have been emplaced in much the same way as ordinary ash flows.

REFERENCES

Anderson, R. E., 1970, Ash-flow tuffs of Precambrian age in southeast Missouri: Missouri Division Geological Survey and Water Resources Report of Investigations 46, 50 p.

Armstrong, R. L., 1975, The geochronometry of Idaho: Isochron West, no. 14, 50 p.

Armstrong, R. L., J. E. Harakal, and W. M. Neill, 1980, K-Ar dating of Snake River Plain (Idaho) volcanic rocks—new results: Isochron West, no. 27, p. 5-10.

Asher, R. R., 1968, Geology and mineral resources of a portion of the Silver City region, Owyhee County, Idaho: Idaho Bureau of Mines and Geology Pamphlet 138, 106 p.

Axelrod, D. I., 1968, Tertiary floras and topographic history of the Snake River basin, Idaho: Geological Society of America Bulletin, v. 79, p. 713-734.

Bennett, E. H., 1976, Reconnaissance geology and geochemistry of the South Mountain-Juniper Mountain region, Owyhee County, Idaho: Idaho Bureau of Mines and Geology Pamphlet 166, 68 p.

Bennett, E. H. and J. H. Galbraith, 1975, Reconnaissance geology and geochemistry of the Silver City-South Mountain region, Owyhee County, Idaho: Idaho Bureau of Mines and Geology Pamphlet 162, 88 p.

Bonnichsen, Bill, 1982a, The Bruneau-Jarbidge eruptive center, southwestern Idaho, *in* Bill Bonnichsen and R. M. Breckenridge, editors, Cenozoic Geology of Idaho: Idaho Bureau of Mines and Geology Bulletin 26.

———, 1982b, Rhyolite lava flows in the Bruneau-Jarbidge eruptive center, southwestern Idaho, *in* Bill Bonnichsen and R. M. Breckenridge, editors, Cenozoic Geology of Idaho: Idaho Bureau of Mines and Geology Bulletin 26.

Bonnichsen, Bill, W. B. Travers, and G. P. Citron, 1975, Rhyolitic volcanism and structural evolution of the Snake River Plain (abstract): Geological Society of America, Abstracts with Programs, v. 7, p. 589-590.

Byers, F. M., Jr., W. J. Carr, P. P. Orkild, W. D. Quinlivan, and K. A. Sargent, 1976, Volcanic suites and related cauldrons of Timber Mountain-Oasis Valley caldera complex, southern Nevada: U. S. Geological Survey Professional Paper 919, 70 p.

Christiansen, R. L. and P. W. Lipman, 1972, Cenozoic volcanism and plate-tectonic evolution of the western United States. II. Late Cenozoic: Philosophical Transactions of the Royal Society of London, v. A271, p. 249-284.

Ekren, E. B., D. H. McIntyre, and E. H. Bennett, in press, High-temperature, large-volume, lavalike ash-flow tuffs without calderas in southwestern Idaho: U. S. Geological Survey Professional Paper 1272.

Ekren, E. B., D. H. McIntyre, E. H. Bennett, and H. E. Malde, 1981, Geologic map of Owyhee County, Idaho, west of longitude 116° W.: U. S. Geological Survey Miscellaneous Geologic Investigations Map I-1256.

Ekren, E. B., W. D. Quinlivan, R. P. Snyder, and F. J. Kleinhampl, 1974, Stratigraphy, structure, and geologic history of the Lunar Lake caldera of northern Nye County, Nevada: U. S. Geological Survey Journal of Research, v. 2, no. 5, p. 599-608.

Hildreth, Wes, 1979, The Bishop Tuff: evidence for the origin of compositional zonation in silicic magma chambers: Geological Society of America Special Paper 180, p. 43-75.

Hill, D. P. and L. C. Pakiser, 1966, Seismic-refraction study of crustal structure between the Nevada test site and Boise, Idaho: Geological Society of America Bulletin, v. 78, p. 685-704.

Hoover, D. L., 1964, Flow structures in a welded tuff, Nye County, Nevada, *in* Abstracts for 1963: Geological Society of America Special Paper 76, p. 83.

Kittleman, L. R., A. R. Green, A. R. Hagood, A. M. Johnson, J. M. McMurray, R. G. Russell, and D. A. Weeden, 1965, Cenozoic stratigraphy of the Owyhee region, southeastern Oregon: University of Oregon Museum of Natural History Bulletin 1, 45 p.

Lachenbruch, A. H. and J. H. Sass, 1978, Models of an extending lithosphere and heat flow in the Basin and Range province: Geological Society of America Memoir 152, p. 209-250.

Laursen, J. M. and P. E. Hammond, 1978, Summary of radiometric ages of Oregon rocks, Supplement 1, July 1972 through December 1976: Isochron West, no. 23, p. 3-28.

Leeman, W. P., 1982, Development of the Snake River Plain-Yellowstone Plateau province, Idaho and Wyoming: an overview and petrologic model, *in* Bill Bonnichsen and R. M. Breckenridge, editors, Cenozoic Geology of Idaho: Idaho Bureau of Mines and Geology Bulletin 26.

Lindgren, Waldemar, 1900, The gold and silver veins of Silver City, De Lamar, and other mining districts in Idaho: U. S. Geological Survey 20th Annual Report, Part IIIc, p. 77-189.

Lipman, P. W., R. L. Christiansen, and J. T. O'Connor, 1966, A compositionally zoned ash-flow sheet in southern Nevada: U. S. Geological Survey Professional Paper 524-F, 47 p.

Littleton, R. T. and E. G. Crosthwaite, 1957, Ground water geology of the Bruneau-Grand View area, Owyhee County, Idaho: U. S. Geological Survey Water-Supply Paper 1460-D, p. 147-198.

Mabey, D. L., Isidore Zietz, G. P. Eaton, and M. D. Kleinkopf, 1978, Regional magnetic patterns in part of the Cordillera in the western United States: Geological Society of America Memoir 152, p. 93-106.

Malde, H. E., H. A. Powers, and C. H. Marshall, 1963, Reconnaissance geologic map of west-central Snake River Plain, Idaho: U. S. Geological Survey Miscellaneous Geologic Investigations Map I-373.

McIntyre, D. H., 1972, Cenozoic geology of the Reynolds Creek experimental watershed, Owyhee County, Idaho: Idaho Bureau of Mines and Geology Pamphlet 151, 115 p.

Neill, W. M., 1975, Geology of the southeastern Owyhee Mountains and environs, Owyhee County, Idaho: Stanford University M.S. thesis, 59 p.

Noble, D. C., 1972, Some observations on the Cenozoic volcanic-tectonic evolution of the Great Basin, western United States: Earth and Planetary Science Letters, v. 17, p. 142-150.

Nockolds, S. R., 1954, Average chemical composition of some igneous rocks: Geological Society of America Bulletin, v. 65, p. 1007-1032.

Pansze, A. J., Jr., 1975, Geology and ore-deposits of the Silver City-De Lamar-Flint region, Owyhee County, Idaho: Idaho Bureau of Mines and Geology Pamphlet 161, 79 p.

Piper, A. M. and F. B. Laney, 1926, Geology and metalliferous resources of the region about Silver City, Idaho: Idaho Bureau of Mines and Geology Bulletin 11, 165 p.

Ross, C. S. and R. L. Smith, 1961, Ash-flow tuffs; their origin, geologic relations, and identification:

U. S. Geological Survey Professional Paper 366, 81 p.

Smith, R. L., 1960, Ash flows: Geological Society of America Bulletin, v. 71, p. 795-842.

Sorenson, R. E., 1927, The geology and ore deposits of the South Mountain mining district, Owyhee County, Idaho: Idaho Bureau of Mines and Geology Pamphlet 22, 47 p.

Sparks, R. S. J., Haraldur Sigurdson, and Lionel Wilson, 1977, Magma mixing: a mechanism for triggering acid explosive eruptions: Nature, v. 267, p. 315-318.

Steiger, R. H. and E. Jager, 1977, Subcommission on geochronology: convention on the use of decay constants in geo- and cosmochronology: Earth and Planetary Science Letters, v. 36, p. 359-362.

Taubeneck, W. H., 1971, Idaho batholith and its southern extension: Geological Society of America Bulletin, v. 82, p. 1899-1928.

Walker, G. W. and D. A. Swanson, 1968, Laminar flowage in a Pliocene soda rhyolite ash-flow tuff, Lake and Harney Counties, Oregon, *in* Geological Survey Research, 1968: U. S. Geological Survey Professional Paper 600-B, p. B37-B47.

Whitney, J. A., 1975, History of granodioritic and related magma systems—an experimental study: Journal of Geology, v. 83, p. 1-31.

Young, H. W. and R. L. Whitehead, 1975, An evaluation of thermal water in the Bruneau-Grand View area, southwest Idaho, with a section on a reconnaissance audio-magnetotelluric survey, by D. B. Hoover and C. L. Tippens, *in* Geothermal Investigations in Idaho, Part 2: Idaho Department of Water Resources Water Information Bulletin 30, 126 p.

The Bruneau-Jarbidge Eruptive Center, Southwestern Idaho

by

Bill Bonnichsen[1]

ABSTRACT

The Bruneau-Jarbidge eruptive center in southwestern Idaho is a 95-by-55-kilometer structural basin on line with and southwest of the eastern Snake River Plain. During the middle and late Miocene, a sequence of nine or more welded ash-flow tuff cooling units (the Cougar Point Tuff), eight to twelve large to enormous rhyolite lava flows, and a succession of olivine tholeiite basalt flows from forty or more shield volcanoes were erupted from the region now occupied by this basin. The Bruneau-Jarbidge eruptive center does not now have the physiographic form of a caldera, although much of the subsidence of its interior is believed to have occurred, perhaps between 11 and 10 million years ago, during or just after the eruption of the voluminous Cougar Point Tuff. The resulting basin was subsequently filled by the rhyolite lava flows, basalt flows, and lacustrine and fluvial sediments, so that the only remaining topographic vestige of its original physiographic form is the Grasmere escarpment along the west side of the eruptive center. However, the eruptive center may contain one or more buried calderas.

Along its southern margin, the boundary zone of the eruptive center is denoted at several localities by a combination of down-to-the-north faults of small displacement, a moat zone filled with sediments and basalt, and lateral transitions from welded ash-flows on the south to rhyolite lava flows on the north. The eastern and northern margins of the eruptive center are buried beneath younger geologic units, primarily basalt flows. The extent of the eruptive center has been partly defined on the basis of aeromagnetic anomalies. During the latter part of the silicic volcanism in the Bruneau-Jarbidge eruptive center it appears that the original basin was nearly filled by very large rhyolite flows and was disrupted by accompanying northeastward rifting and subsidence to the north, generally associated with the progressive eastward shifting of silicic volcanism associated with the southwestern margin of the western Snake River Plain.

INTRODUCTION

The Bruneau-Jarbidge eruptive center is an area in eastern Owyhee County, Idaho, from which numerous rhyolite ash-flow and lava-flow units and basalt flows erupted during Miocene and possibly early Pliocene time. It is a structural basin about 95 kilometers long located southwest of, and in line with, the northeast-trending eastern Snake River Plain (Figure 1). The eruptive center lies between 115° and 116° west longitude. Its southern margin is a few kilometers north of the Idaho-Nevada boundary near 42° north latitude, and its western margin follows the Grasmere escarpment northward to about 42°40′ north latitude (Figure 2). The southern and western margins of the eruptive center have been defined by geologic mapping. The northern and eastern margins, however, are covered by later basalt flows, but their positions have been inferred from the regional aeromagnetic pattern and other indirect evidence.

The area underlain by the Bruneau-Jarbidge eruptive center is a virtually unpopulated plateau, generally ranging in elevation from 1,100 meters in the north to 1,800 meters in the south. It is dissected by the canyon of the Bruneau River, which flows northward to join the Snake River, and by the canyons of its principal tributaries, the Jarbidge River, Sheep Creek, and Clover Creek (Figure 2). These canyons commonly exceed 300 meters in depth, and their steep to vertical walls provide excellent exposures of the volcanic units underlying the area. The climate is semiarid. Sagebrush and various grasses are the principal forms of vegetation on the plateau, and juniper trees occur at the bottom of many of the canyons.

The Bruneau-Jarbidge region constitutes the southwestern part of the central Snake River Plain (Figure

[1]Idaho Bureau of Mines and Geology, Moscow, Idaho 83843.

Bonnichsen, Bill, 1982, The Bruneau-Jarbidge eruptive center, southwestern Idaho, *in* Bill Bonnichsen and R. M. Breckenridge, editors, Cenozoic Geology of Idaho: Idaho Bureau of Mines and Geology Bulletin 26, p. 237-254.

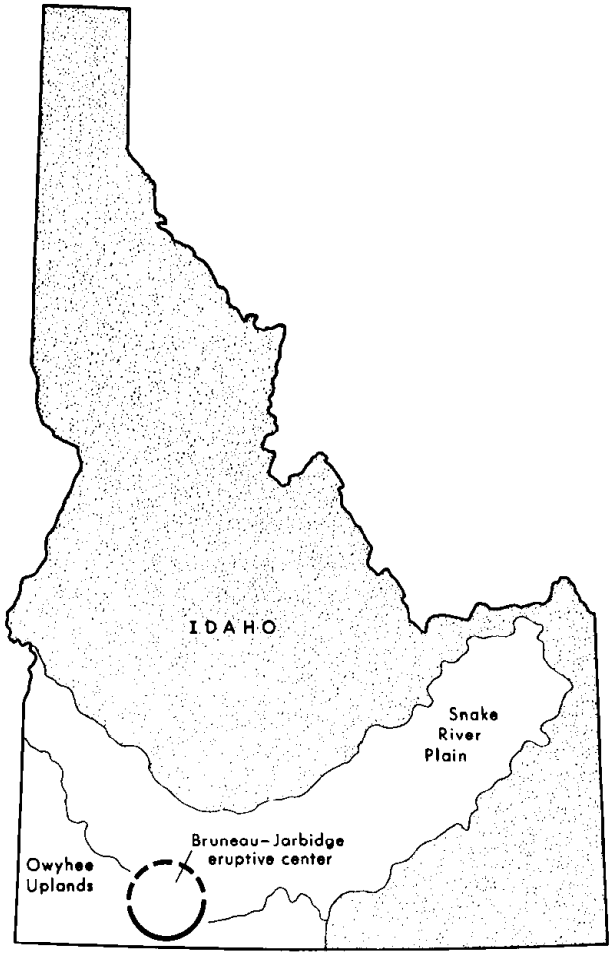

Figure 1. Index map showing the location of the Bruneau-Jarbidge eruptive center in southwestern Idaho.

1; also Figure 1 in Mabey, 1982 this volume). The region contains a large and complex bimodal basalt-rhyolite volcanic system that is part of the Snake River Plain volcanic province. Because the area is dissected by several deep canyons and has undergone only minimal structural adjustment since volcanism, much unequivocal stratigraphic and descriptive information has been developed for the volcanic units. In contrast to the Island Park-Yellowstone National Park region at the northeastern end of the volcanic province (Christiansen, 1982 this volume), where volcanic processes may still be in progress, it appears that the progression of volcanic events has run its course in the Bruneau-Jarbidge region. Geologic studies of the Bruneau-Jarbidge region have provided a better understanding of the evolution of the Snake River Plain volcanic province, and such studies can improve our interpretation of the genesis of the bimodal basalt-rhyolite association.

The principal geologic units in and adjacent to the eruptive center are noted in Figure 3, which has been generalized from my unpublished mapping and from the compilations by Malde and others (1963), Hope and Coats (1976), and Rember and Bennett (1979). These units include an older group of rhyolitic welded ash-flow and lava-flow units and a younger group of basalt flows. Continental clastic sediments and buried soil horizons occur between many of the volcanic units and are especially abundant around the periphery of the eruptive center.

The rhyolite units associated with forming and filling the eruptive center are part of the Idavada Volcanics; these were succeeded by flows of the Banbury Basalt. The Idavada Volcanics and the Banbury Basalt, which were named by Malde and Powers (1962), have by subsequent usage become fairly broad in meaning. They include most of the rhyolitic units and many of the basaltic units in the central Snake River Plain as well as some basalt units from farther west. In the Bruneau-Jarbidge area the Idavada Volcanics include an older group of highly welded ash-flow tuff units known as the Cougar Point Tuff and a younger group of rhyolite lava flows.

Southeast, south, and southwest of the Bruneau-Jarbidge eruptive center, the Cougar Point Tuff lies on volcanic rocks of Miocene age (Jarbidge Rhyolite—Coats, 1964; and pre-Cougar Point Tuff rhyolite units in the upper Sheep Creek drainage—Bernt and Bonnichsen, 1982 this volume) and Eocene age (Bieroth volcanics—Bushnell, 1967; and Bernt and Bonnichsen, 1982 this volume). These in turn were deposited on Paleozoic marine sediments and Cretaceous granitic rocks, such as the Cottonwood Creek pluton (Coats and McKee, 1972). To the northeast in the central Snake River Plain the rhyolite units are covered by the Banbury Basalt and younger sedimentary and basaltic units. To the northwest, the rhyolite in the eruptive center is juxtaposed against other Miocene rhyolite units (tuff of Little Jacks Creek—Ekren and others, 1981, 1982 this volume). Although the tuff of Little Jacks Creek overlaps the rhyolite units in the eruptive center in age, the unit-by-unit stratigraphic details between the two groups have yet to be resolved.

The following discussion outlines the nature and the boundaries of the eruptive center and the stratigraphic relations among the volcanic units that erupted from it in order to set the stage for the detailed stratigraphic, descriptive, petrographic, and chemical discussions of the rhyolitic units that follow in this volume (Bonnichsen and Citron, 1982; Bonnichsen, 1982b). The basalt flows that partially cover the eruptive center are also briefly discussed.

THE BRUNEAU-JARBIDGE ERUPTIVE CENTER

DEFINITION AND EXTENT OF THE ERUPTIVE CENTER

The Bruneau-Jarbidge eruptive center is named for the two principal rivers and their canyons that cut across eastern Owyhee County (Figure 2). The term "eruptive center," as I have used it, does not have a specific genetic or physiographic significance; it is only meant to refer to the geographic region from which were erupted the numerous volcanic units that are discussed in this and the following two articles (Bonnichsen and Citron, 1982; Bonnichsen, 1982b). Based on the observations noted in the following discussion of its boundaries, the Bruneau-Jarbidge eruptive center encompasses the specific region indicated in Figure 2.

It would be misleading to refer to the Bruneau-Jarbidge eruptive center as a caldera, because it does not have the required form of a large crater or physiographic basin. Subsidence of the region within the eruptive center did occur during volcanism, however; in this sense the region has evolved in a fashion similar to that of many calderas, caldera complexes, and cauldrons. The Bruneau-Jarbidge eruptive center encloses several times more area than most calderas, and it may contain one or more buried calderas or a caldera complex, but this has not been proven.

The Bruneau-Jarbidge eruptive center subsided during or following the time in which the Cougar Point Tuff was erupted. It is not yet known if the subsidence was a single event or many separate ones, but separate events seem more probable in view of the numerous Cougar Point Tuff cooling units that were erupted. None of the rhyolite units that issued from the eruptive center are known to have produced a volcano or other sort of constructional vent structure; presumably the eruptions came through fissures which are now buried. The later basaltic volcanism which partially covered the eruptive center, however, formed many relatively small shield volcanoes.

Along its northern and eastern margins the Bruneau-Jarbidge eruptive center merges into the rest of the central Snake River Plain. Thus the eruptive center is part of the even larger, structurally downdropped, central Snake River Plain volcanic system. Although the stratigraphic relations among the rhyolite units and the timing of volcanic events throughout this larger system are not fully known, it is clear that volcanism was occurring elsewhere in the central Snake River Plain during the same time as in the Bruneau-Jarbidge eruptive center. The central Snake River Plain might be thought of as a very large cauldron or a cauldron complex, in a sense similar to that used by Smith and Bailey (1968) or by McIntyre and others (1982 this volume). In terms of its size, general complexity, and volcanic products, the Bruneau-Jarbidge eruptive center seems quite similar to the caldera complex, described by Christiansen (1982 this volume), in the Island Park-Yellowstone National Park region at the northeastern end of the Snake River Plain volcanic province.

BOUNDARIES OF THE ERUPTIVE CENTER

The Bruneau-Jarbidge eruptive center is bounded on the south and west by a series of faults and accompanying lateral lithologic changes, but its northern and eastern margins are covered by later units. Circumstantial evidence suggests the eruptive center was a coherent structural basin that formed semi-independently from the rest of the central Snake River Plain.

I have used geologic observations and the regional aeromagnetic pattern (U. S. Geological Survey, 1978) to outline the Bruneau-Jarbidge eruptive center as an oval region 95 kilometers long from northwest to southeast and 55 kilometers wide. It encloses approximately 4,100 square kilometers (Figures 2 and 4). The eruptive center margin follows the curved intense positive aeromagnetic anomaly along its southern and western sides, and I have drawn the boundary to include the two relatively modest negative anomalies in its northeastern part (see Mabey, 1982 this volume, for a more regional view of these anomalies). A comparison of Figures 2 and 4 with Figure 1 of this article or Figure 4 in Mabey (1982 this volume) shows that the eruptive center is approximately the same width as, and on line with, the eastern Snake River Plain to the northeast.

Along its southern and western margins, the eruptive center boundary forms the transition zone between welded tuff exposures to the south and west, outside of the eruptive center, and rhyolite lava flow exposures to the north and east, inside the eruptive center. Abundant postrhyolite terrestrial sediments are trapped along this boundary (Figure 3); greater thicknesses occur in and near the margin than to either side because the zone was a moatlike topographic depression that followed the periphery of the eruptive center. Small-displacement faults, consistently down to the north or east, help mark this boundary zone, and past and present hot spring activity is concentrated there. Additionally, in the Cougar Point Tuff units, the thickness and intensity of welding variations and the distribution of primary

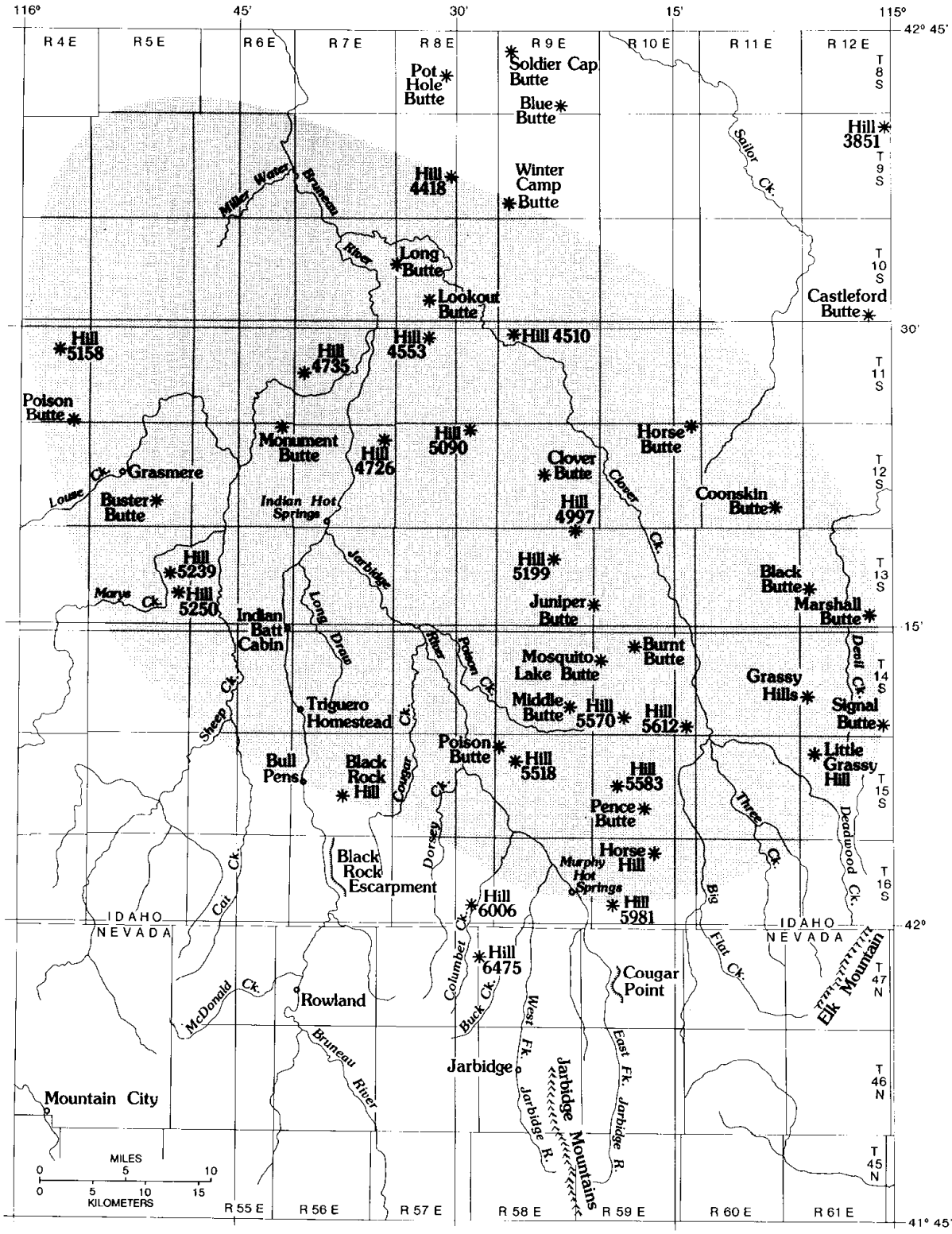

Figure 2. Geographic reference map of eastern Owyhee County, Idaho, and vicinity. The Bruneau-Jarbidge eruptive center is indicated by the shaded area.

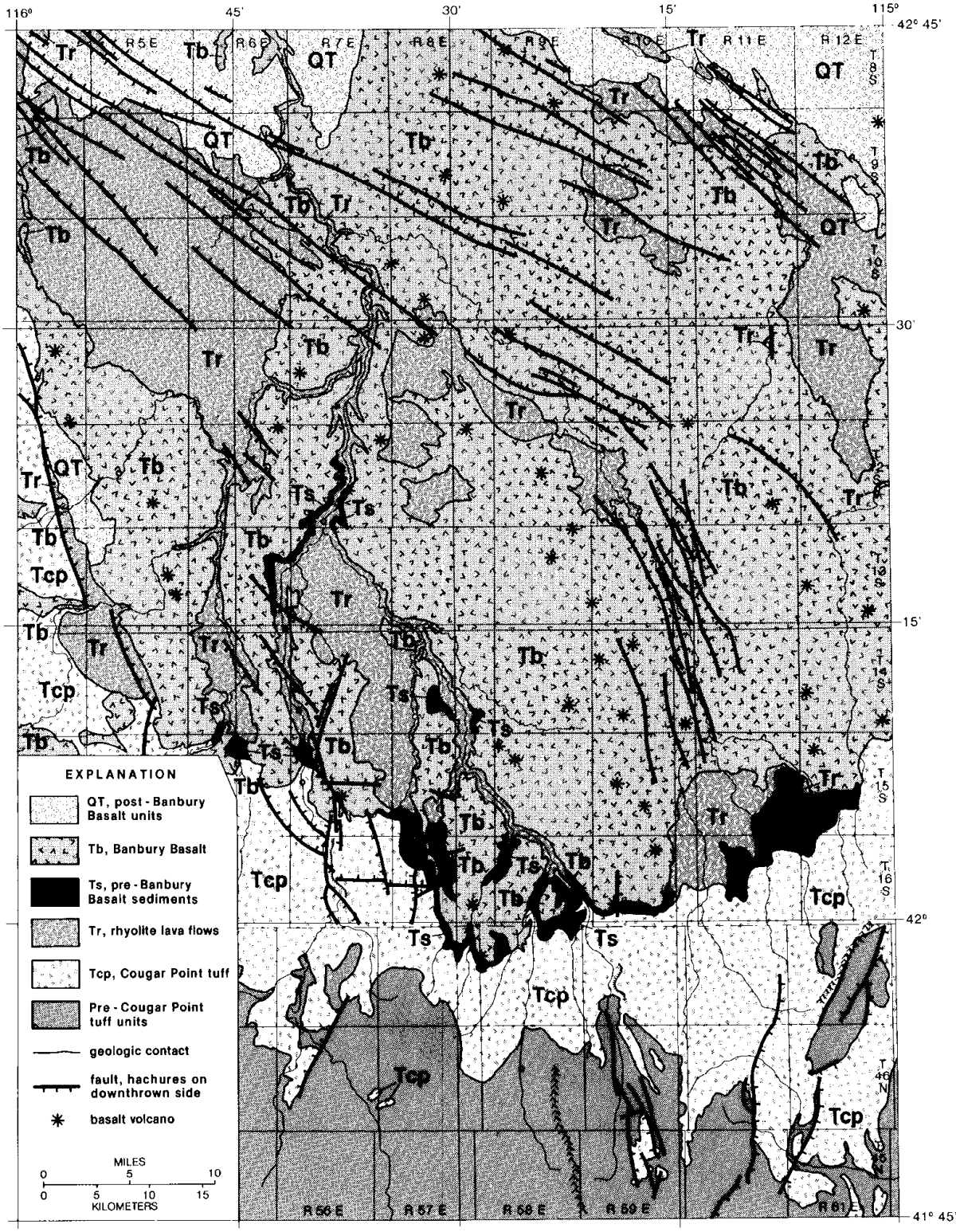

Figure 3. Generalized geologic map of eastern Owyhee County, Idaho, and vicinity.

flow marks (see Figure 20, Bonnichsen and Citron, 1982 this volume) imply that those units were erupted from the eruptive center, north of where they are exposed.

In the following discussion, I have made note of a number of specific geologic relations that show the nature and location of the boundary zone of the eruptive center. The discussion is arranged so as to progress counterclockwise around the eruptive center periphery, starting from its west side.

In T. 10 S., R. 4 E., the boundary zone is a basalt-covered plain that lies between the west end of the topographically higher Sheep Creek rhyolite on the east side (Figure 5) and the rhyolite units which have been assigned by Ekren and others (1981, 1982 this volume) to the tuff of Little Jacks Creek on the west. The basalt in this zone evidently came from vents such as Hill 5158 and Poison Butte in T. 11 S., R. 4 E. (Figure 2), and flowed northward into the moat zone, being constrained laterally by the topographically higher rhyolite units on either side.

To the south of this, in T. 11-14 S., R. 4-5 E., the boundary zone follows the base of the Grasmere escarpment. This east-facing escarpment has up to 200 meters of relief and extends north-northwestward for 43 kilometers. The key relationship here is that the rhyolite unit to the west, which forms the escarpment (the rhyolite of Grasmere escarpment), is older, but topographically higher, than the Marys Creek rhyolite flow that laps up against the eastern base of the escarpment. This relationship is established in T. 13-14 S., R. 4-5 E., just south of Marys

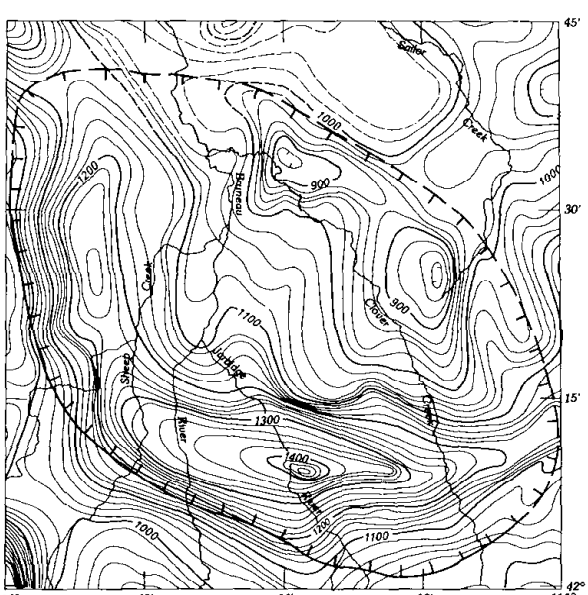

Figure 4. Outline of the Bruneau-Jarbidge eruptive center superimposed on a portion of the U. S. Geological Survey's (1978) aeromagnetic map of Idaho. Contour interval is 20 gammas.

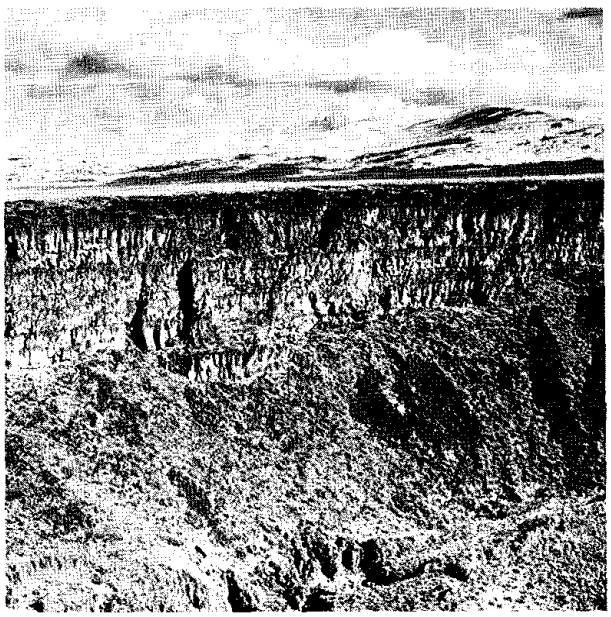

Figure 5. Looking eastward across Big Jacks Creek canyon at the basalt-filled moat zone along the west side of the Bruneau-Jarbidge eruptive center from sec. 4, T. 10 S., R. 4 E. The unit below the basalt is one of the rhyolite units within the tuff of Little Jacks Creek, and the distant hills, within the eruptive center, are part of the Sheep Creek rhyolite flow.

Creek, where a former valley of post-escarpment, but pre-Marys Creek rhyolite age, permitted the Marys Creek rhyolite to flow out of the eruptive center on top of the rhyolite of Grasmere escarpment.

To the southeast, the boundary zone crosses Sheep Creek near the mouth of Cat Creek in the south part of T. 14 S., R. 6 E. In Sheep Creek canyon in sections 32 and 33, the boundary is marked by a gap filled with sediments 1 kilometer across between the southernmost rhyolite lava flow exposures and the northernmost welded tuff exposures. About 100 meters of sediments is exposed in the canyon in this gap. A similar situation exists further southeast in Cat Creek canyon in sec. 4, T. 15 S., R. 6 E. The sediments in the Cat Creek-Sheep Creek area, although poorly exposed, contain deposits of jasper, opal, and diatomite. The diatomite is silicified. The opal and jasper, especially, are indicative of extensive paleo-hot springs activity.

Turning eastward, the boundary zone crosses Bruneau Canyon in the Bull Pens area in T. 15 S., R. 7 E. At this locality (Figure 6) the upper flow of the Cougar Point Tuff (unit XV) is exposed at the surface to the south. It is down-dropped about 100 meters to the north along a west-northwest trending fault. Northward from this boundary fault, the uppermost Cougar Point Tuff unit is exposed in the canyon for nearly 3 kilometers inside the eruptive center

before it drops out of sight below the lowermost rhyolite lava flows (Triguero Homestead and Indian Batt flows). Extensive slumping of the canyon walls has occurred north of this boundary fault (Figure 6). This slumping is a consequence of a thick accumulation of only partially consolidated sedimentary and volcanic ash deposits which occur below and between the lava flows lying above the Cougar Point Tuff. These sediments evidently do not extend south of the boundary fault, as there is no canyon-wall slumping to the south of the Bull Pens area (Figure 6); this suggests the sediments were ponded against a preexisting escarpment within the moat zone.

Just east of Bruneau Canyon, still within T. 15 S., R. 7 E., a prominent basalt shield volcano—Black Rock Hill—lies on the boundary zone. The west-northwest trending fault, noted above to mark the south side of the Bull Pens area, strikes directly toward this basaltic vent. Farther east, in T. 15-16 S., R. 8-9 E., the boundary zone is situated in the shallow canyons of Cougar, Dorsey, and Columbet Creeks, between occurrences of the Dorsey Creek rhyolite to the north and exposures of Cougar Point Tuff unit XV to the south. A considerable quantity of sediment (locally up to 100 meters is exposed) was trapped in this area within the moat zone created by the southwest edge of the Dorsey Creek flow and the top of the northward-dipping Cougar Point Tuff.

Further to the east the eruptive center boundary crosses the West Fork of Jarbidge Canyon in secs. 15, 16, and 21, T. 16 S., R. 9 E. There, about 150 meters of moat-zone sediment is exposed beneath a cap of Banbury Basalt (Figure 7). The sediment-filled gap marking the boundary zone in that area is nearly 3 kilometers across between exposures of the Cougar Point Tuff to the southwest and those of the Dorsey Creek rhyolite to the northeast.

The eruptive center boundary zone crosses the East Fork of the Jarbidge River at Murphy Hot Springs in the NW¼ of sec. 24, T. 16 S., R. 9 E. Here, the con-

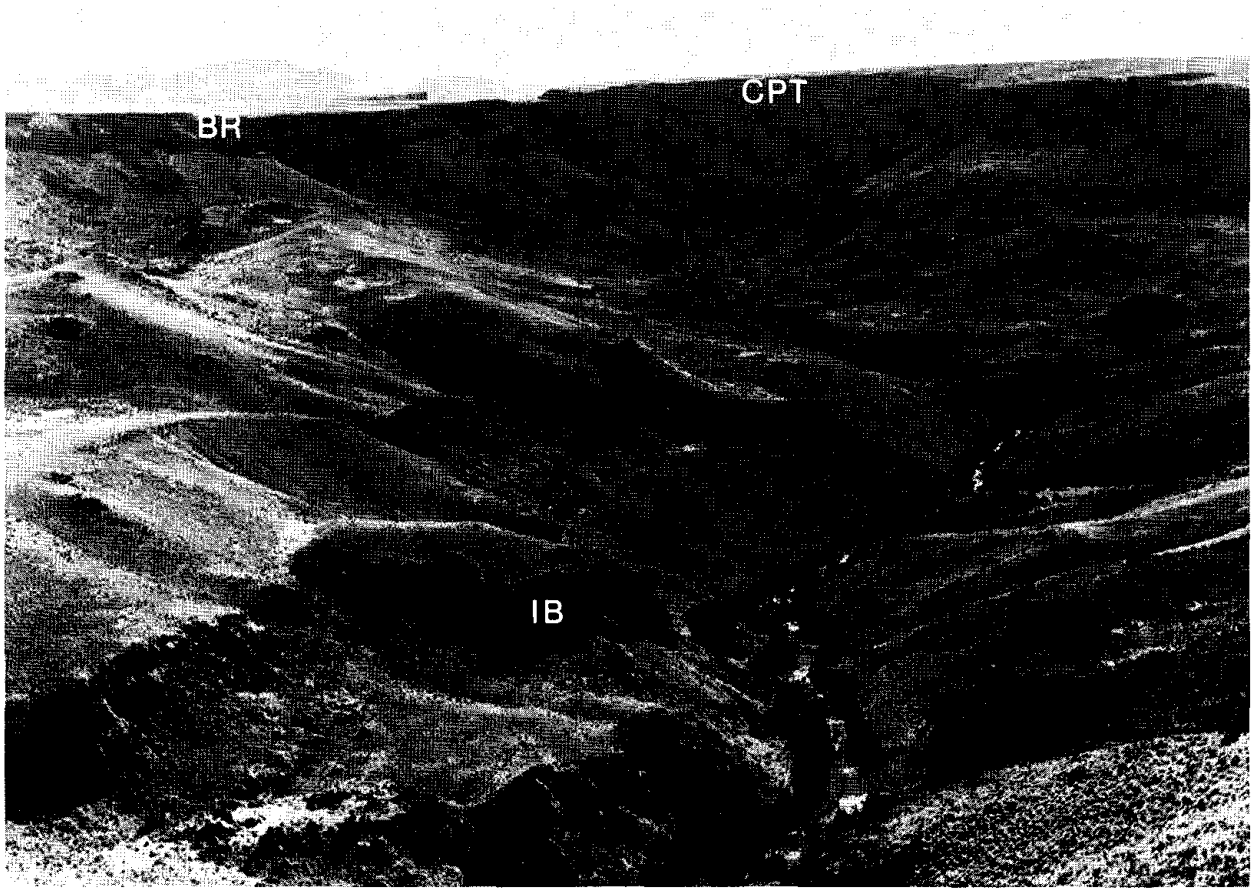

Figure 6. Looking southward in Bruneau Canyon from sec. 7, T. 15 S., R. 7 E., at the Cougar Point Tuff (CPT) where it plunges beneath the southern margins of the Triguero Homestead and Indian Batt (IB) rhyolite flows. The Black Rock basalt (BR) forms the eastern canyon rim. The fault marking the eruptive center boundary crosses the canyon where it abruptly widens. Note the extensive debris flows on this side of the boundary fault. The distant hill on the left side is Black Rock escarpment.

Figure 7. Looking southwestward, up the West Fork of Jarbidge Canyon, from near the confluence of the East and West Forks of the Jarbidge River. The Dorsey Creek rhyolite flow occurs in the canyon in the foreground. It is overlain by a thick section of sedimentary materials filling the moat zone of the eruptive center, which in turn is capped by Banbury Basalt flows. The Cougar Point Tuff, which dips toward the observer, plunges beneath the canyon floor at about where the canyon turns in the distance.

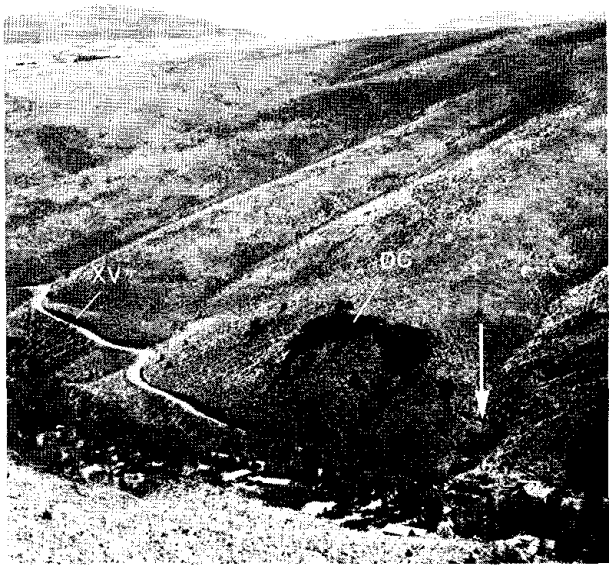

Figure 8. View of Murphy Hot Springs on the East Fork of the Jarbidge River. The southern end of the Dorsey Creek (DC) rhyolite flow is the prominent rock outcrop on the right, just above where the road goes out of view. Small exposures of the uppermost unit (XV) of the Cougar Point Tuff occur just upstream from this. It is inferred that a deep-seated fault is covered by the end of the Dorsey Creek rhyolite below the position of the arrow, where a large hot spring is located.

tact between the uppermost Cougar Point Tuff unit and the southern edge of the Dorsey Creek rhyolite flow is nearly exposed beneath about 150 meters of unconsolidated sedimentary material (Figure 8). The fashion in which the welded-tuff unit and the somewhat younger lava flow abut suggests that a post-Cougar Point Tuff, but pre-lava flow, paleo-escarpment is buried beneath the end of the Dorsey Creek rhyolite. The position of a fairly large hot spring about 0.2 kilometer north of the end of the Dorsey Creek flow further suggests this (Figure 8). The existence of the hot spring implies that a fault extending to considerable depth is buried beneath the end of the Dorsey Creek flow. Erosion along such a fault before the Dorsey Creek rhyolite was emplaced could easily have formed a north-facing escarpment against which the rhyolite flow was emplaced from the north. The existence of a buried, fault-line scarp at Murphy Hot Springs is further suggested by the local occurrence of unconsolidated sediment cobbles enclosed in a matrix of other unconsolidated sediment beneath the end of the Dorsey Creek rhyolite flow (Figure 9).

East of Jarbidge Canyon, in T. 16 S., R. 10 E., the boundary zone is drawn through a small basalt shield volcano (Hill 5981). East of this in T. 16 S., R. 11 E., and T. 15 S., R. 12 E., the boundary trends northeastward between occurrences of the Three Creek rhyolite flow and the overlying Banbury Basalt to the north, and occurrences of the Cougar Point Tuff to the south. Extensive, generally unconsolidated, sediments occur in the vicinity of the boundary zone in this region (Figure 3), apparently filling a moat zone in the same fashion as further west.

The boundary zone has been drawn northward, east of Devil Creek, through T. 15 to 12 S., R. 12 E., so as to cross two basalt shield volcanoes—Signal Butte and Marshall Butte (Figure 2). In this eastern region, and to the north and northwest, the boundary crosses surface rocks of mainly Banbury Basalt. The older rhyolite units and any structural relations that might be like those noted for the western and southern sides of the eruptive center are buried.

To the northwest of T. 12 S., R. 12 E., I have drawn the boundary zone between the two negative magnetic anomalies within the eruptive center (Figure 4) and the large region underlain by rhyolite northeast of the eruptive center (partially shown in the upper right-hand part of Figure 3). The exposures of rhyolite in this northeastern region, which is approximately 50 kilometers long from southeast to northwest by 30 kilometers wide, suggests that this area is

Figure 9. Cobbles of unconsolidated sedimentary material enclosed in a matrix of unconsolidated sediment and volcanic ash at Murphy Hot Springs on the east side of the bottom of Jarbidge Canyon. This exposure is located where a buried paleo-escarpment, marking the margin of the eruptive center, is proposed to exist at the south end of the Dorsey Creek rhyolite flow.

structurally elevated relative to the region to the southwest which has been included within the eruptive center.

Farther to the northwest, in T. 9 S., R. 8-9 E., the boundary zone has been drawn to pass through two more basalt shield volcanoes—Winter Camp Butte and Hill 4418. West of this, the boundary zone crosses Bruneau Canyon in T. 9 S., R. 6 E., just north of Miller Water, so as to include the northernmost rhyolite lava flow exposures in the canyon, occurring at Miller Water, within the eruptive center.

Generally, from T. 12 S., R. 12 E., at the eastern side of the eruptive center to the crossing of Bruneau Canyon in the northwestern part, the boundary zone has been drawn parallel to the northwest-trending faults in that region. At the northwestern end of the eruptive center, however, between Bruneau Canyon and the moat zone in T. 10 S., R. 4 E., where this description of boundary zone commenced, the boundary zone crosses the northwest-trending faults. If an arcuate boundary zone ever existed through this northwestern region as I have drawn it, it has since been buried by a large rhyolite flow (Sheep Creek rhyolite) and further obscured by the development of the northwest-trending faults. Thus, the original nature of the northwest end of the eruptive center remains unknown.

RHYOLITE UNITS

The first rhyolitic magmas erupted from the Bruneau-Jarbidge eruptive center were emplaced as a sequence of welded ash-flow tuff cooling units known as the Cougar Point Tuff. The name, Cougar Point welded tuff, was first proposed by Coats (1964) for the excellent exposures at Cougar Point in the East Fork of Jarbidge Canyon in northernmost Nevada (Figure 2). Coats (1964, p. M13-M14) regarded the Cougar Point area as the type locality and noted that similar rhyolitic rocks in the margins of the Snake River Plain from as far east as the Goose Creek area in Cassia County to as far west as western Owyhee County and as far north as the Mount Bennett Hills near Mountain Home on the north side of the Snake River Plain were to be included in the Cougar Point welded tuff. However, the name Idavada Volcanics, which earlier had been applied to the same rhyolitic rocks in this wide region by Malde and Powers (1962), has been used by most geologists.

The meaning of the term, Cougar Point Tuff, as it has been used in this paper, in the accompanying paper (Bonnichsen and Citron, 1982 this volume), and in two previous reports (Bonnichsen, 1981 and 1982a), is more restricted than the usage of Coats (1964). The definition used here is that *the Cougar Point Tuff refers specifically to those Miocene-age rhyolitic welded-tuff units that were erupted from the Bruneau-Jarbidge eruptive center.* Thus, I consider the Cougar Point Tuff to be a subdivision of the Idavada Volcanics. As noted in the accompanying paper (Bonnichsen and Citron, 1982 this volume) the Black Rock escarpment area on the east side of Bruneau Canyon in T. 16 S., R. 7 E. (Figure 2), is recommended as the best reference section for the Cougar Point Tuff; it is a more complete section than the one at Cougar Point.

The Cougar Point Tuff consists of several cooling units separated by layers of sediment and unconsolidated tuff. The units found so far have been given the Roman numeral designations of III, V, VII, IX, X, XI, XII, XIII, and XV. The basis of this current nomenclature system, and the previous ones, is discussed in Bonnichsen (1981) and Bonnichsen and Citron (1982 this volume). The individual cooling units in both the Jarbidge Canyon and Bruneau Canyon areas are listed in stratigraphic order in Figure 10, and their magnetic polarities, as determined by fluxgate magnetometer measurements, are noted in Table 1. These units are exposed on both sides of the Idaho-Nevada border between 115° and 116° longitude (Figure 3). The Cougar Point Tuff also extends east of 115° longitude, but since unit-by-unit stratigraphic studies are incomplete in that

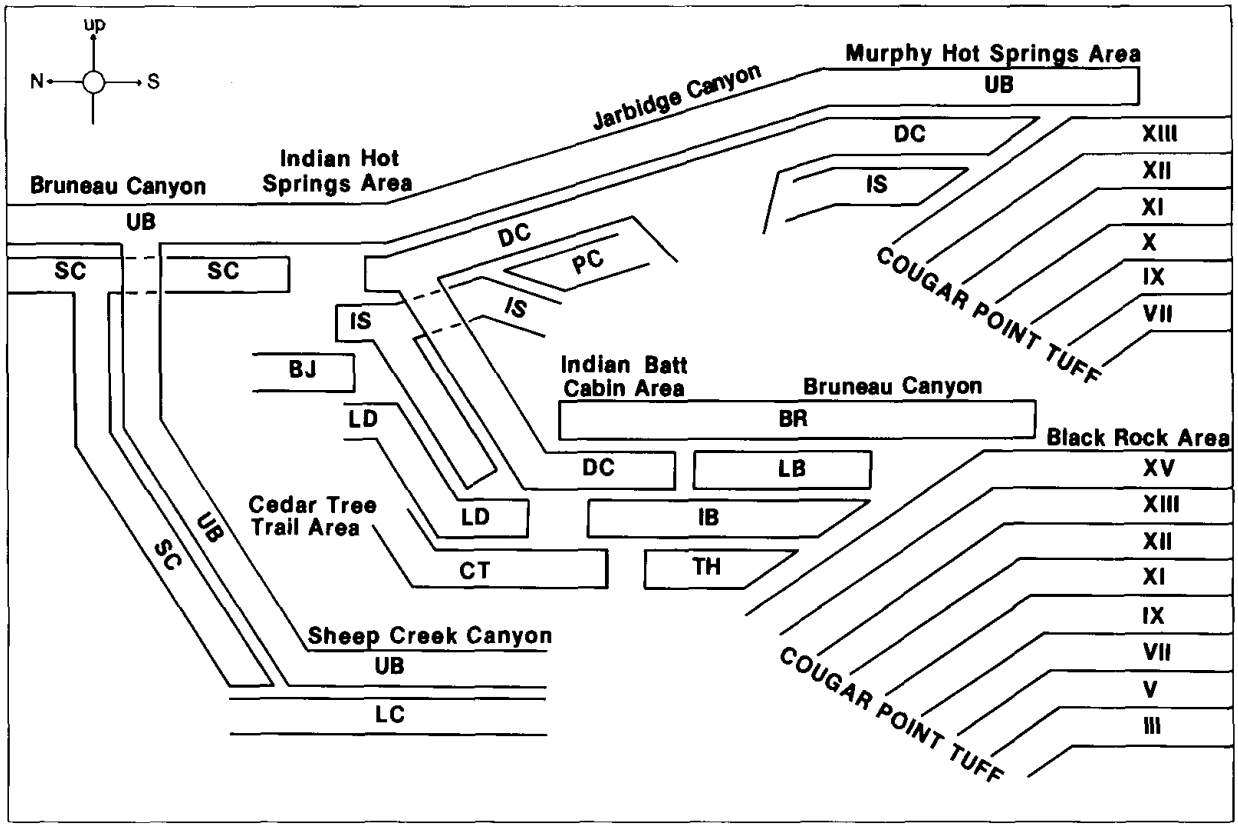

Figure 10. Schematic fence diagram showing the stratigraphic succession and lateral distribution of volcanic units exposed in canyon walls in the Bruneau-Jarbidge eruptive center (BJ—Bruneau Jasper rhyolite, BR—Black Rock basalt, CT—Cedar Tree rhyolite, DC—Dorsey Creek rhyolite, IB—Indian Batt rhyolite, IS—Indian Springs basalt, LB—lower basalt at Triguero Homestead, LC—lower rhyolite at Louse Creek, LD—Long Draw rhyolite, PC—lower rhyolite at Poison Creek, SC—Sheep Creek rhyolite, TH—Triguero Homestead rhyolite, UB—undivided flows of the Banbury Basalt; Roman numerals—cooling units of the Cougar Point Tuff). Note orientation diagram at upper left.

region, the discussion here and in Bonnichsen and Citron (1982 this volume) considers only the relationships west of 115° longitude. Each of the Cougar Point Tuff units is described in Bonnichsen and Citron (1982 this volume).

West of the Bruneau River, mainly between Sheep Creek and Cat Creek (Figure 2), Bernt (1982) has mapped a sequence of welded ash-flow units within the Cougar Point Tuff. These Cougar Point Tuff units were assigned numbers by Bernt ranging from unit 8 for the youngest to unit 1 for the oldest. Most of the units noted by Bernt have an equivalent at Black Rock and farther east. These probable correlations are discussed further in Bonnichsen and Citron (1982 this volume). However, at least one of Bernt's units—unit 5—evidently does not extend as far east as Black Rock. This unit has not yet been assigned a designation in the Roman numeral nomenclature scheme.

Two older welded-tuff units in the area between Sheep Creek and Cat Creek—the Whiskey Draw rhyolite and the Rattlesnake Draw tuff—have been identified (Bernt and Bonnichsen, 1982 this volume); they are petrologically and chemically similar to the lowest Cougar Point Tuff units which overlie them. At present, it is not clear if these units should be assigned to the Cougar Point Tuff, or if they had a source outside the Bruneau-Jarbidge eruptive center.

A large rhyolite unit is exposed on Grasmere escarpment for many kilometers along the western side of the eruptive center. This unit is referred to as the rhyolite of Grasmere escarpment, and it probably consists of one, or locally more, welded ash-flow tuff cooling units; but it has been examined in only a cursory fashion. It has been traced westward into the multi-flow rhyolite unit, referred to as the tuff of Little Jacks Creek (Ekren and others, 1981 and 1982 this volume), and southeastward into the Cougar Point Tuff. The rhyolite of Grasmere escarpment has been included as part of the Cougar Point Tuff in Figure 3; it occurs in T. 11-14 S., R. 4-5 E., along the left-hand side of the figure.

At most localities, the rhyolite of Grasmere escarpment is a dense lithoidal unit generally 100 to 200 meters thick. At some localities, its upper part is vitrophyre containing abundant flow streaks, folded flow bands, and sheeting joints. The local presence of vitrophyre in the middle of the unit suggests that it may be a compound cooling unit. The unit has reverse magnetic polarity (Table 1).

To the southeast, the rhyolite of Grasmere escarpment merges into the Cougar Point Tuff, but it has not yet been established which, if any, of the units described in Bonnichsen and Citron (1982 this volume) might be equivalent to it. If the rhyolite of Grasmere escarpment is the same as any of the units exposed at Black Rock, its reverse magnetic polarity would restrict the choice to units XI, VII (Table 1), or perhaps III.

To the north, the rhyolite of Grasmere escarpment has been shown by Dan Kauffman (personal communication) to be near the base of a sequence of about ten rhyolite units that constitute the tuff of Little Jacks Creek in the canyons of Big Jacks Creek and Little Jacks Creek.

The rhyolite of Grasmere escarpment very likely formed from voluminous quantities of rhyolitic magma from the Bruneau-Jarbidge eruptive center, although this has not yet been firmly established. Further investigations are needed to clarify the exact stratigraphic position of this unit before the stratigraphic relationship between the individual units forming the Cougar Point Tuff and the tuff of Little Jacks Creek can be resolved.

Situated to the north of and lying stratigraphically above the Cougar Point Tuff are several large rhyolite lava flows. Geologic mapping along the southern and western margins of the eruptive center has shown that these flows are almost totally confined to the interior of the eruptive center where they originated. Some were limited in their areal distribution by topographically elevated regions around the periphery of the eruptive center, which probably developed as a result of regional subsidence during and after the eruption of the Cougar Point Tuff but before most of the lava flows were emplaced. The stratigraphic positions of the individual rhyolite flows are shown in Figure 10, and their magnetic polarities are listed in Table 1. These flows are described and discussed in detail in the accompanying paper (Bonnichsen, 1982b).

BASALT FLOWS

More than half of the eruptive center is covered by the Banbury Basalt (compare Figures 2 and 3). It is more abundant and thicker in the eastern part than in the west. The basalt was erupted from a large number of shield volcanoes, many of which have been identified. Altogether, about forty basalt volcanoes are known to occur within the eruptive center (Figures 2

Table 1. Magnetic polarities of volcanic units associated with the Bruneau-Jarbidge eruptive center.

Volcanic Unit	Number of Stations	Number of Deflection Measurements +	-	other	Apparent Magnetic Polarity
Black Rock basalt	7	17	6	0	Normal
Three Creek rhyolite	4	6	0	0	Normal
Dorsey Creek rhyolite	6	18	0	0	Normal
Lower rhyolite at Poison Creek	1	4	0	0	Normal
Sheep Creek rhyolite	6	18	1	0	Normal
Indian Springs basalt	3	0	12	1	Reverse
Bruneau Jasper rhyolite	4	0	6	1	Reverse
Indian Batt rhyolite	5	2	7	2	Reverse
Lower rhyolite at Louse Creek	2	4	0	0	Normal
Long Draw rhyolite	2	6	0	0	Normal
Cedar Tree rhyolite	2	6	0	0	Normal
Triguero Homestead rhyolite	5	8	0	0	Normal
Marys Creek rhyolite	10	16	2	1	Normal
Cougar Point Tuff, unit XV	7	16	2	3	Normal
Cougar Point Tuff, unit XIII	2	12	0	0	Normal
Cougar Point Tuff, unit XII	2	11	0	2	Normal
Cougar Point Tuff, unit XI	4	0	12	2	Reverse
Cougar Point Tuff, unit IX	4	10	0	9	Normal
Cougar Point Tuff, unit VII	3	0	13	0	Reverse
Cougar Point Tuff, unit V	3	8	0	1	Normal
Rhyolite of Grasmere escarpment	9	3	16	7	Reverse

and 3), including some along the boundary zone and two just to the south (Hills 6006 and 6475) that fed flows into the eruptive center. A few additional volcanoes undoubtedly contributed basalt to the area, but either they are such inconspicuous hills that they are unrecognizable as vents, or they have been partially to completely buried by later flows.

Most of the basalt volcanoes within the eruptive center fall into one of three generally north-northwest trending zones. Nearly half are within a 10-kilometer-wide band stretching across the eruptive center from Hill 5981 (T. 16 S., R. 10 E.) on the south side to Hill 4418 (T. 9 S., R. 8 E.) on the north. A second concentration occurs in the east, from Signal Butte and Little Grassy Hill on the south to Horse Butte on the north; and a third concentration is near the western margin from Hill 5250 on the south to Hill 5158 on the north. Only a few basalt volcanoes do not occur in one of these bands or elsewhere on the eruptive center margin.

One basalt unit, the Indian Springs basalt, is intercalated within the succession of rhyolite lava flows in the eruptive center. It occurs beneath the Dorsey Creek rhyolite (Figure 10; Figure 8 in Bonnichsen, 1982b this volume) and the lower rhyolite at Poison Creek, and above the Bruneau Jasper and Long Draw rhyolite flows, so that it is part of the Idavada Volcanics. Nevertheless, the Indian Springs basalt seems to be chemically and petrographically like the younger Banbury Basalt units that cover the eruptive center. Other basalt flows in the eruptive center may also be older than some of the rhyolite flows, but the direct stratigraphic evidence by which to evaluate this is lacking. The lower basalt unit in the Triguero Homestead area of Bruneau Canyon (LB in Figure 10, and in Figure 2 of Bonnichsen, 1982b this volume) is a good candidate because it occurs beneath nearly 100 meters of pre-Black Rock basalt sediments.

The basalt volcanoes in the Bruneau-Jarbidge eruptive center are notably inconspicuous, because they have very low profiles (Figure 11 is a good example). This is true even though the vents have undergone minimum dissection because of erosion. Many have craters preserved at their tops, and all essentially have their original outline and form preserved. All of the basalt volcanoes associated with the eruptive center are low-profile shields. Many are approximately circular in plan and have smooth profiles, but a few are somewhat elongate (typically along a northwest-trending axis) and others have irregular to complex forms and are characterized by multiple vents.

Margi Jenks (personal communication) has recently measured the height, average diameter, and side slope for most of the basalt volcanoes in the Bruneau-Jarbidge eruptive center. She has found that for thirty-six of the volcanoes the height ranges from 20 to 100 meters, with an average of 50 meters, and the diameter ranges from 1.5 to 7.3 kilometers, with an average of 3.2 kilometers. The side slopes vary from 2 to 7 percent, and the average side slope for the thirty vents for which she was able to make reliable measurements is 4.5 percent. These relatively small sizes and low profiles for the basaltic vents in the Bruneau-Jarbidge eruptive center indicates that the basaltic volcanism there was similar to the "plains" style of volcanism proposed to characterize the eastern Snake River Plain by Greeley (1982 this volume).

For most of the individual basalt units, a definite geomorphic distinction can be made between the basaltic outflow sheet and the shield constructed over the zone where basalt was erupted. Most of the outflow sheets consist of one to several, but rarely more than about ten, basalt flows deposited in a flow-on-flow arrangement with no intervening sedimentary interbeds. No evidence has been found to suggest that any of the volcanoes erupted basaltic lava at widely spaced intervals in time. Rather, it appears that each basaltic shield and accompanying outflow sheet resulted from the injection of a batch of magma into the upper crust and the eruption of part of that material as a single flow, or as a succession of flows closely spaced in time. The proximity of some volcanoes suggests that in some instances more than one volcano was formed during the extrusion of lava from different parts of the same shallow magma chamber.

Lava tubes are essentially absent from the many kilometers of canyon-rim basalt throughout the region and few situations suggest that even localized channelization occurred as the basaltic lava spread, except near the margins of the outflow sheets. Much of the basalt evidently spread as thin sheets constrained primarily by preexisting topographic irregularities and by the regional tilt of the land. Several of the outflow sheets are elongate, mainly northwards from their sources, following the regional tilt of the landscape that existed when they erupted. The lack of lava tubes and the scarcity of narrow channelization features (lava rivers and other distributaries) within individual flows probably resulted from a combination of relatively rapid effusion rate and low viscosity so that sheet-flow resulted. In this respect, the flows within the Bruneau-Jarbidge eruptive center differ from many of those in the eastern Snake River Plain, where geologists have noted many extensive lava tube systems (Greeley, 1982 this volume; King, 1982 this volume; Kuntz and others, 1982 this volume).

Although the various basalt outflow sheets have yet to be completely mapped, it is clear that some are

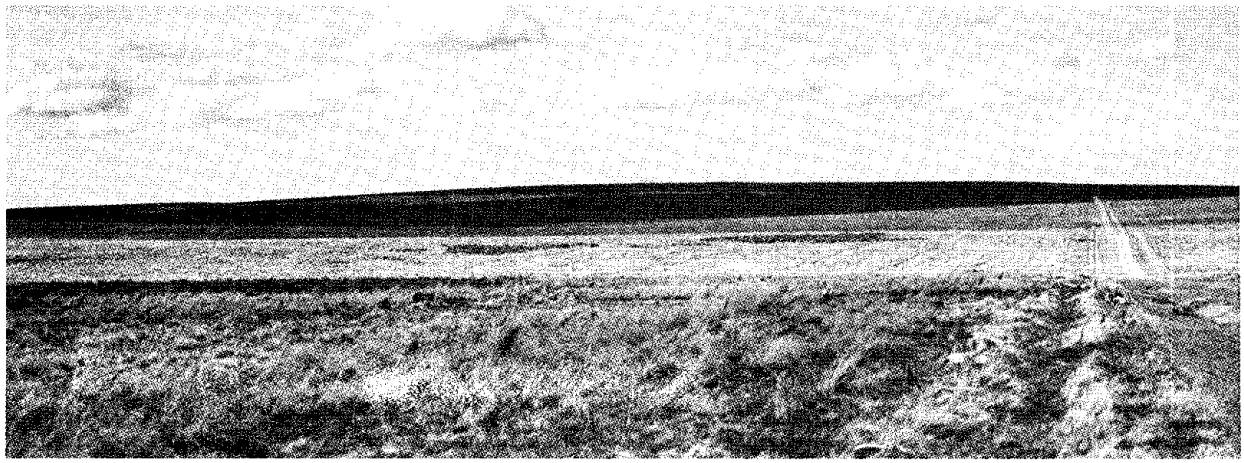

Figure 11. Looking northward at Clover Butte in T. 12 S., R. 9 E. This is an example of a low-profile basaltic shield volcano in the interior of the Bruneau-Jarbidge eruptive center.

moderately large. Several have been traced for more than 20 kilometers from their source, and some may extend 30 kilometers or farther.

Individual flows within an outflow sheet can, at most locations, be easily discerned by their variably vesicular and slightly oxidized tops, commonly with ropey surfaces, that contrast with the much more massive basalt and pipe vesicles at the flow bases. Virtually all of the basalt in the eruptive center is of the pahoehoe type. The individual flows typically range from 2 to 10 meters in thickness. Even thinner flows are common on the basaltic vents (Margi Jenks, personal communication). Locally, thicker flows have been found, and they very likely represent situations where the lava became ponded in some sort of topographic depression. Shallow enclosed depressions, generally irregular in outline and up to about a half kilometer across, are a common feature near the margins of several of the outflow sheets; these probably resulted where late-stage draining away of lava occurred after the top of the flow had crusted over.

In hand sample the basalt ranges from dark gray or brown to nearly black, and from massive to quite vesicular. Scoriaceous basalt is restricted mainly to the upper parts of the shield volcanoes. The basalt is typically quite fresh, except for the common weathered surfaces that normally are less than a millimeter thick.

In thin section most basalt samples have a distinct groundmass—representing the lava that crystallized after emplacement—and distinct phenocrysts—representing intertelluric crystals carried from depth. The groundmass varies in texture and carries plagioclase, a single clinopyroxene (probably subcalcic augite), and opaque oxides. Interstitial very dark glass and small olivine grains are also common. Neither hypersthene nor pigeonite has been observed in the groundmass, although the latter would closely resemble the Ca pyroxene and could easily escape detection.

The phenocryst minerals are plagioclase and olivine. In addition, small, equant opaque grains, presumably Cr-Al spinels, occur in some rocks. Most basalt units contain both olivine and plagioclase phenocrysts, although the grains may be widely scattered and their relative abundances vary markedly from flow to flow. Some, however, have only one of the minerals, and a few flows are aphyric, or practically so. Olivine phenocrysts typically are subhedral, but other forms occur, including embayed grains and multiple-grain clots. Olivine phenocrysts commonly have thin to prominent oxidized rims. Presumably this oxidation occurred during the time of surface flowage. Plagioclase phenocrysts typically are laths, and loose clusters of laths occur in a few units. The plagioclase typically is seriate, with all sizes of grains ranging from tiny groundmass crystals to the largest phenocrysts occurring together. Olivine, however, rarely shows a seriate texture. The opaque microphenocrysts may be dispersed in the groundmass, but more typically they occur attached to the surface of the olivine phenocrysts or embedded within them. The collective petrographic characteristics of the basalt units in the Bruneau-Jarbidge eruptive center are very much like other Snake River Plain basalt units, such as those described by Stone (1967) or reviewed by Leeman (1982b this volume).

The chemical compositions of four basalt samples from the Bruneau-Jarbidge eruptive center, selected from about forty available, are presented in Table 2. These analyses illustrate the range of basalt compositions in the eruptive center, and show that a single, multi-flow basalt unit erupted from one vent can vary nearly as widely in its chemical composition as the variation noted among all of the flows in the region.

Analyses 1 and 4 in Table 2 are at opposite ends of the compositional range for basalt in the eruptive center. Note that analysis 4 is considerably enriched in iron, TiO_2, K_2O, and P_2O_5 and impoverished in Al_2O_3, CaO, and MgO compared with analysis 1. Analyses 2 and 3 show a difference similar to that between 1 and 4, although 2 and 3 are compositionally a little closer together than are 1 and 4. Both 2 and 3 are from the Black Rock basalt; 2 is from an early erupted flow which travelled a long distance whereas 3 is from a small diabase plug in the throat of the vent (Black Rock Hill), and which presumably represents the very last lava erupted.

Leeman (1982b this volume) has suggested that the basalt associated with the Snake River Plain can be divided into two intergradational categories. Most analyses, which he refers to as Group I, have compositions similar to those illustrated by analyses 3 and 4 of Table 2, or are slightly enriched in Al_2O_3, CaO, and MgO and slightly impoverished in iron, TiO_2, K_2O, and P_2O_5, so as to have compositions generally intermediate between 2 and 3. Leeman notes that a few analyses, compared with his Group I type, have more abundant CaO and Al_2O_3, and are impoverished in TiO_2, P_2O_5, and K_2O; he refers to these as the Group II type. Analyses 1 and 2 in Table 2 clearly fall within Leeman's Group II category.

The basalt composition represented by analyses 1 and 2 of Table 2 also clearly falls in the high-alumina basalt category recognized by Kuno (1968), a basalt type that in some aspects of its chemistry (sum of K_2O and Na_2O for a given SiO_2 content) is intermediate between alkali olivine basalts and tholeiites, and that for aphyric rocks is characterized by more than 16.5 percent of Al_2O_3. The analyzed samples of the Group II type of basalt from the Bruneau-Jarbidge eruptive center (1 and 2 of Table 2, and a few additional unreported analyses) typically are practically aphyric, generally with less than 1 percent of phenocrysts.

Table 2. Chemical composition (weight percent) of basalt samples from the Bruneau-Jarbidge eruptive center. Analyzed by X-ray fluorescence, Washington State University, June 1980.

	1	2	3	4
SiO_2	48.45	48.47	47.44	47.58
Al_2O_3	17.59	17.37	15.74	14.78
TiO_2	0.99	1.14	2.36	2.82
Fe_2O_3*	10.96	11.58	13.63	15.33
MnO	0.17	0.19	0.20	0.21
CaO	11.17	10.44	9.83	9.46
MgO	7.95	7.74	7.10	5.92
K_2O	0.11	0.11	0.31	0.43
Na_2O	2.45	2.76	2.94	3.02
P_2O_5	0.16	0.20	0.45	0.45

(Analyses have been normalized to a sum of 100 percent)

*Total Fe reported as Fe_2O_3.

1. Sample I-961, unnamed basalt flow, NW¼NW¼ sec. 22, T. 15 S., R. 8 E.; probably erupted from Hill 6475, northern Nevada.
2. Sample I-438, Black Rock basalt, SW¼NW¼ sec. 14, T. 14 S., R. 6 E.; erupted from Black Rock Hill, T. 15 S., R. 7 E.
3. Sample I-858, small diabasic basalt plug, NW¼SE¼ sec. 21, T. 15 S., R. 7 E., in throat of Black Rock Hill volcano.
4. Sample I-971, unnamed basalt flow, NW¼NW¼ sec 22, T. 15 S., R. 8 E.; source vent is not known.

In classifying the Bruneau-Jarbidge eruptive center basalts by their C.I.P.W. normative constituents in the quartz-olivine-nepheline-clinopyroxene "basalt tetrahedron" of Yoder and Tilley (1962), all of my unpublished basalt analyses from the eruptive center plot within the hypersthene-olivine-plagioclase-clinopyroxene portion of the tetrahedron, if relatively high FeO/Fe_2O_3 ratios, such as 4 or more, are assumed. Stone (1967), for example, shows that western Snake River Plain basalt FeO/Fe_2O_3 ratios typically are greater than 4 and may range above 10. This hypersthene-olivine normative behavior indicates that the Bruneau-Jarbidge area basalt is olivine tholeiite. In this respect, the basalt is like that elsewhere in the Snake River Plain (for example, see Leeman, 1982b this volume). No hybridized or evolved basaltic rocks, similar to those that Leeman (1982c this volume) has described from various Snake River Plain localities, have so far been found in the Bruneau-Jarbidge eruptive center.

I believe that most of the compositional variation in the Bruneau-Jarbidge region basalt flows resulted from the selective extraction of olivine and plagioclase crystals within crustal magma chambers, perhaps as a result of crystal settling. This explanation is consistent with the common occurrence of those two minerals as phenocrysts, and is in accord with the interpretation of others (see Leeman, 1982b for example) for the diversity of basalt compositions elsewhere in the Snake River Plain. If this is the case, then the least differentiated (or most primitive) magmas known to exist in the Bruneau-Jarbidge eruptive center are represented by analyses 1 and 2 of Table 2, and are typical high-alumina basalts. Fractional crystallization and separation of the early formed olivine and plagioclase crystals from various magma batches have resulted in marked enrichment of iron, TiO_2, P_2O_5, and K_2O, slight to moderate enrichment of MnO and Na_2O, and impoverishment of Al_2O_3, CaO, and MgO in the residual magmas, while little change, or a slight decrease, in the silica content has occurred. This iron-enrichment differentiation trend is typical of basalts from throughout the Snake River Plain-Yellowstone National Park area (see Leeman, 1982b and 1982c this volume).

GEOLOGIC HISTORY

Three temporally overlapping stages of volcanism occurred during the evolution of the Bruneau-Jarbidge eruptive center. The first stage was the eruption of several large silicic ash flows to form the Cougar Point Tuff cooling units. The second was the eruption of several additional silicic magma batches as rhyolite lava flows. The third was the eruption of numerous batches of basaltic magma.

During the formation of the Cougar Point Tuff, sufficient time elapsed between the eruption of the individual cooling units for sedimentary interbeds to be deposited and, in some cases, for the Earth's magnetic field to reverse its polarity (Table 1). The time at which the ash-flow eruptions began, although not known precisely, was about 12 million years ago. The available radiometric dates suggesting this (Table 3) are the (minimum) age of 11.3 million years for Cougar Point Tuff unit VII and the age of 11.22 million years for the rhyolite of Grasmere escarpment. As noted previously, the rhyolite of Grasmere escarpment is thought to be part of the Cougar Point Tuff, even though its exact stratigraphic position has not been determined.

It is unclear if the 12.5-million-year age (Table 3) of the Cougar Point welded tuff sample from near Mountain City, Nevada, reported by Coats (1968) is relevant to dating the Cougar Point Tuff volcanism, as the unit has been redefined in this article to include only those cooling units with the Bruneau-Jarbidge eruptive center as their source. Since Coats (1964) considered the Cougar Point welded tuff to be a unit of broad regional extent and since the location of the dated sample he reports is considerably west and south of the main Cougar Point Tuff area, there is no assurance that the material which provided the 12.5-million-year age came from the Bruneau-Jarbidge eruptive center. It easily could have come from some other location, probably to the west.

The second stage of volcanism commenced with the general change from ash-flow eruptions to the extrusion of rhyolite lava flows. This was not an abrupt change but was gradational, as it has been established that rhyolite lava flows are intercalated in the upper part of the Cougar Point Tuff sequence (Bonnichsen and Citron, 1982 this volume; Bonnichsen, 1982b this volume). In all probability, the eruptive center had developed as a structural and topographic basin by the end of the ash-flow volcanism. The virtual confinement of the later rhyolite lava flows to its interior, and the downfaulting of the upper Cougar Point Tuff units at its margin (Figures 6 and 8) support this interpretation. The form of the southern and western parts of the eruptive center when the ash-flow volcanism ceased was probably much like it is today, except that the later volcanic and sedimentary materials had yet to be deposited. It would have been a pronounced topographic basin at that time, but has since been practically filled. About the only vestige of this former topographic basin remaining is the Grasmere escarpment, which formed its west side.

The sequence of events during the evolution of the eruptive center that led to its completed form by the end of Cougar Point Tuff volcanism has not been resolved entirely, because the uppermost ash-flow units and succeeding volcanic units cover nearly all the terrain in the region. Its very large size suggests that the eruptive center probably evolved to its final form by a series of subsidences rather than forming

Table 3. Radiometric age (K-Ar) determinations for rhyolite units from the Bruneau-Jarbidge eruptive center and vicinity.

Unit	Age in m.y.	Sample Location	Material Dated	Reference and Sample
Cougar Point welded tuff	*12.5±0.8	NE¼SE¼ sec. 8, T. 46 N., R. 53 E., Nevada	sanidine	Coats, 1968 (62NC51)
Cougar Point Tuff, unit VII	11.3±2.0	SW¼NE¼ sec. 28, T. 47 N., R. 58 E., Nevada	whole rock (basal vitrophyre)	Bonnichsen and Citron, 1982 this volume (I-841)
Rhyolite of Grasmere escarpment	11.22±0.52	border sec. 21, 22, 27, 28, T. 13 S., R. 4 E., Idaho	whole rock	Hart and Aronson, in press (H-9-15A)
Tuff of Little Jacks Creek (next to top unit)	9.6±2.0	42°43′14″ N., 116°07′05″ W.	plagioclase	Armstrong and others, 1980 (JK-B)
Tuff of Little Jacks Creek (top of section)	10.0±1.5	42°43′14″ N., 116°07′05″ W.	plagioclase	Armstrong and others, 1980 (JK-A)
Sheep Creek rhyolite	9.88±0.46	sec. 6, T. 10 S., R. 5 E., Idaho	whole rock	Hart and Aronson, in press (H-9-11)
Dorsey Creek rhyolite	8.22±0.38 8.00±0.38	SE¼ sec. 14, T. 16 S., R. 9 E., Idaho	whole rock	Hart and Aronson, in press (H-9-6C)

*Recalculated to new decay constants using the tables of Dalrymple (1979); the age was initially reported as 12.2±0.8 m.y.

during a single catastrophic collapse at the end of ash-flow volcanism.

The absolute time by which the eruptive center had completed its subsidence is not well established, but it may have been between 11 and 10 million years ago, based on the 11.3-million-year radiometric date for Cougar Point Tuff unit VII and the 9.88-million-year date for the Sheep Creek rhyolite (Table 3). Stratigraphically, however, the time of subsidence appears to be tightly bracketed between the deposition of Cougar Point Tuff unit XV, which (as shown in Figure 6) is cut by boundary zone faults, and the emplacement of the Triguero Homestead rhyolite lava flow, which postdates the faulting. As indicated elsewhere (Bonnichsen, 1982b this volume) unit XV and the Triguero Homestead flow appear to be part of the same cycle of volcanism and both probably were erupted during the same paleomagnetically normal time interval (Table 1).

The stratigraphic time limit for the subsidence at the eruptive center margin is not nearly as tightly constrained to either the west, along the Grasmere escarpment, or to the east, in the Jarbidge River and Clover Creek drainages, as it is in the Bruneau Canyon area where unit XV is juxtaposed against the Triguero Homestead flow. No direct evidence is available to indicate whether the subsidence in these widely separated areas was synchronous or occurred at different times.

During the second stage of volcanism the size of the rhyolite flows appears to have changed from large (10 cubic kilometers or greater) to enormous (as large as 200 cubic kilometers). As noted in Bonnichsen (1982b this volume) the older rhyolite lava flows (Figure 10) for which the volume has been estimated (Triguero Homestead rhyolite, Cedar Tree rhyolite, Indian Batt rhyolite, and Long Draw rhyolite) seem smaller than the later units (Sheep Creek rhyolite, Dorsey Creek rhyolite, and the rhyolite of the Juniper-Clover area).

This eruption-volume change suggests that about 10 million years ago major northwest-oriented faulting, probably accompanying northeastward extension perpendicular to the faults, was initiated across the middle and northeastern part of the eruptive center. The extrusion of the voluminous Sheep Creek and Dorsey Creek flows, and the rhyolite of the Juniper-Clover area accompanied this postulated rifting. At the same time, the structural integrity of the eruptive center was disrupted, especially in its northeastern part, where further down-dropping to the north may have occurred.

These very large rhyolite flows are on line with, and southeast of, the northwest-southeast trending southwestern margin of the western Snake River Plain (Figure 1; and see Figures 1-4 in Mabey, 1982 this volume; Figure 2 in Leeman, 1982a this volume; Figure 1 in Ekren and others, 1982 this volume). The southwestern margin of the western Snake River Plain is a zone that underwent extensive faulting and probable northeastward extension during the development and subsidence of that part of the Snake River Plain. Rhyolitic magmas probably were erupted from that marginal zone as extension occurred to form some of the rhyolite units that Ekren and others (1982 this volume) have described in the northwestern part of Owyhee County.

As indicated in Table 3, the age of the Sheep Creek rhyolite seems very close to that of two units of the tuff of Little Jacks Creek (Ekren and others, 1982 this volume) situated just west of the northwestern part of the Bruneau-Jarbidge eruptive center. These units within the tuff of Little Jacks Creek also lie along the southwestern margin of the western Snake River Plain and appear to be part of the group of rhyolite flows which erupted from that northwest-southeast trending zone. Rhyolitic volcanism along the southwestern margin of the western Snake River Plain and extending southeastward from that zone into the Bruneau-Jarbidge eruptive center evidently lasted to about 8 million years ago, since that is the approximate age of the Dorsey Creek rhyolite flow (Table 3). It may have lasted even longer if the undated rhyolite of the Juniper-Clover area or if the Three Creek rhyolite flow are younger. Thus, taking into account the ages that Armstrong and others (1980) report for some of the later rhyolite units which Ekren and others (1982 this volume) describe in northwestern Owyhee County (tuff of Browns Creek, 11.0 ± 0.7 m.y. and 11.4 ± 0.6 m.y.; Jump Creek rhyolite, 11.1 ± 0.2 m.y.; and the tuff of Little Jacks Creek, Table 3) it appears that, as time passed, the location of silicic volcanic eruptions shifted eastward from the southwestern margin of the western Snake River Plain to its southeastward extension into the Bruneau-Jarbidge eruptive center. This shift is consistent with previous observations that silicic volcanism generally has migrated eastward in the Snake River Plain (Armstrong and others, 1975; Armstrong and others, 1980; Leeman, 1982a this volume; Hart and Aronson, in press).

The third major episode of volcanism in the evolution of the Bruneau-Jarbidge eruptive center was basaltic. The change from the extrusion of rhyolite lava flows to the extrusion of basalt flows was gradual, as shown by the occurrence of the Indian Springs basalt beneath the Dorsey Creek rhyolite and beneath the lower rhyolite at Poison Creek (Figure 10); but most of the basalt in the area postdates the rhyolitic volcanism.

The thinness of the basalt flows in most parts of the eruptive center shows that the basaltic volcanism had little effect on the nature of the terrain, except to

fill in low-lying areas such as the moat zone in the northwestern part (Figure 5) and to cover much of the area with a veneer of basalt. By the time many of the basalt flows erupted, the terrain over the eruptive center had acquired a gentle northward slope toward the Snake River. This is indicated by the elongate northward trend established by the outflow sheets of many of the basalt units that erupted within the eruptive center. The outflow sheet for the Black Rock basalt, which extends for at least 20 kilometers north of its vent at Black Rock Hill, is a good example. The eruption of the numerous batches of basaltic magma apparently finished the volcanic evolution of the eruptive center.

As discussed in Bonnichsen (1982b this volume), this final basaltic volcanic episode probably was a continuation of a long sequence of injections of basaltic magma into the crust which earlier had caused the melting of the rhyolite magmas from buried crustal rocks. By the time of basaltic volcanism, however, the underlying crustal zone had been extensively fractured and generally depleted of its less dense rhyolitic fraction, and probably had undergone considerable vertical subsidence, so that the later batches of basaltic magma were able to rise to the surface.

ACKNOWLEDGMENTS

I would like to thank Nancy Wotruba, Steve Devine, Ivan Herrick, and Peter Hooper for their assistance with the chemical analyses that are reported, and I am pleased to thank Margi Jenks for her helpful review of the manuscript. I take pleasure in thanking Serena Smith for her help and patience during the typing of many versions of this and all my other manuscripts in this volume. The drawings for this and my other articles in the volume were capably drafted by Gibb Johnson and Drew Harvey. Finally, it is a great pleasure to me to thank Roger Stewart for his expert editorial assistance during the preparation of this and my other articles in this volume.

REFERENCES

Armstrong, R. L., J. E. Harakal, and W. M. Neill, 1980, K-Ar dating of Snake River Plain (Idaho) volcanic rocks—new results: Isochron West, no. 27, p. 5-10.

Armstrong, R. L., W. P. Leeman, and H. E. Malde, 1975, K-Ar dating, Quaternary and Neogene volcanic rocks of the Snake River Plain, Idaho: American Journal of Science, v. 275, p. 225-251.

Bernt, John, 1982, Geology of the southern J-P Desert, Owyhee County, Idaho: University of Idaho M.S. thesis, 73 p.

Bernt, John and Bill Bonnichsen, 1982, Pre-Cougar Point Tuff volcanic rocks near the Idaho-Nevada border, Owyhee County, Idaho, *in* Bill Bonnichsen and R. M. Breckenridge, editors, Cenozoic Geology of Idaho: Idaho Bureau of Mines and Geology Bulletin 26.

Bonnichsen, Bill, 1981, Stratigraphy and measurements of magnetic polarity for volcanic units in the Bruneau-Jarbidge eruptive center, Owyhee County, Idaho: Idaho Bureau of Mines and Geology Open-File Report 81-5, 75 p.

_____, 1982a, Chemical compositions of the Cougar Point Tuff and rhyolite lava flows from the Bruneau-Jarbidge eruptive center, Owyhee County, Idaho: Idaho Bureau of Mines and Geology Open-File Report 82-1, 22 p.

_____, 1982b, Rhyolite lava flows in the Bruneau-Jarbidge eruptive center, southwestern Idaho, *in* Bill Bonnichsen and R. M. Breckenridge, editors, Cenozoic Geology of Idaho: Idaho Bureau of Mines and Geology Bulletin 26.

Bonnichsen, Bill and G. P. Citron, 1982, The Cougar Point Tuff, southwestern Idaho and vicinity, *in* Bill Bonnichsen and R. M. Breckenridge, editors, Cenozoic Geology of Idaho: Idaho Bureau of Mines and Geology Bulletin 26.

Bushnell, Kent, 1967, Geology of the Rowland quadrangle, Elko County, Nevada: Nevada Bureau of Mines Bulletin 67, 38 p.

Christiansen, R. L., 1982, Late Cenozoic volcanism of the Island Park area, eastern Idaho, *in* Bill Bonnichsen and R. M. Breckenridge, editors, Cenozoic Geology of Idaho: Idaho Bureau of Mines and Geology Bulletin 26.

Coats, R. R., 1964, Geology of the Jarbidge quadrangle, Nevada-Idaho: U. S. Geological Survey Bulletin 1141-M, 24 p.

_____, 1968, The Circle Creek rhyolite, a volcanic complex in northern Elko County, Nevada: Geological Society of America Memoir 116, p. 69-106.

Coats, R. R. and E. H. McKee, 1972, Ages of plutons and types of mineralization, northwestern Elko County, Nevada, *in* Geological Survey Research 1972: U. S. Geological Survey Professional Paper 800-C, p. C165-168.

Dalrymple, G. B., 1979, Critical tables for conversion of K-Ar ages from old to new constants: Geology, v. 7, p. 558-560.

Ekren, E. B., D. H. McIntyre, E. H. Bennett, and H. E. Malde, 1981, Geologic map of Owyhee County, Idaho, west of 116° West longitude: U. S.

Geological Survey Miscellaneous Investigations Series Map I-1256, scale 1:125,000.

Ekren, E. B., D. H. McIntyre, E. H. Bennett, and R. F. Marvin, 1982, Cenozoic stratigraphy of western Owyhee County, Idaho, *in* Bill Bonnichsen and R. M. Breckenridge, editors, Cenozoic Geology of Idaho: Idaho Bureau of Mines and Geology Bulletin 26.

Greeley, Ronald, 1982, The style of basaltic volcanism in the eastern Snake River Plain, Idaho, *in* Bill Bonnichsen and R. M. Breckenridge, editors, Cenozoic Geology of Idaho: Idaho Bureau of Mines and Geology Bulletin 26.

Hart, W. K. and J. L. Aronson, in press, K-Ar ages of rhyolite from the western Snake River Plain area, Oregon, Idaho, and Nevada: Isochron West, no. 36, p. 17-19.

Hope, R. A. and R. R. Coats, 1976, Preliminary geologic map of Elko County, Nevada: U. S. Geological Survey Open-File Report 76-779, scale 1:100,000.

King, J. S., 1982, Selected volcanic features of the south-central Snake River Plain, Idaho, *in* Bill Bonnichsen and R. M. Breckenridge, editors, Cenozoic Geology of Idaho: Idaho Bureau of Mines and Geology Bulletin 26.

Kuno, Hisashi, 1968, Differentiation of basalt magmas, *in* H. H. Hess and Arie Poldervaart, editors, Basalts, the Poldervaart Treatise on Rocks of Basaltic Composition, Volume 2: Interscience Publishers, p. 623-688.

Kuntz, M. A., D. E. Champion, E. C. Spiker, R. H. Lefebvre, and L. A. McBroome, 1982, The Great Rift and the evolution of the Craters of the Moon lava field, Idaho, *in* Bill Bonnichsen and R. M. Breckenridge, editors, Cenozoic Geology of Idaho: Idaho Bureau of Mines and Geology Bulletin 26.

Leeman, W. P., 1982a, Development of the Snake River Plain-Yellowstone Plateau province, Idaho and Wyoming: an overview and petrologic model, *in* Bill Bonnichsen and R. M. Breckenridge, editors, Cenozoic Geology of Idaho: Idaho Bureau of Mines and Geology Bulletin 26.

———, 1982b, Olivine tholeiitic basalts of the Snake River Plain, Idaho, *in* Bill Bonnichsen and R. M. Breckenridge, editors, Cenozoic Geology of Idaho: Idaho Bureau of Mines and Geology Bulletin 26.

———, 1982c, Evolved and hybrid lavas from the Snake River Plain, Idaho, *in* Bill Bonnichsen and R. M. Breckenridge, editors, Cenozoic Geology of Idaho: Idaho Bureau of Mines and Geology Bulletin 26.

Mabey, D. R., 1982, Geophysics and tectonics of the Snake River Plain, Idaho, *in* Bill Bonnichsen and R. M. Breckenridge, editors, Cenozoic Geology of Idaho: Idaho Bureau of Mines and Geology Bulletin 26.

Malde, H. E. and H. A. Powers, 1962, Upper Cenozoic stratigraphy of the western Snake River Plain, Idaho: Geological Society of America Bulletin, v. 73, p. 1197-1210.

Malde, H. E., H. A. Powers, and C. E. Marshall, 1963, Reconnaissance geologic map of west-central Snake River Plain, Idaho: U. S. Geological Survey Miscellaneous Geologic Investigations Map I-373, scale 1:125,000.

McIntyre, D. H., E. B. Ekren, and R. F. Hardyman, 1982, Stratigraphic and structural framework of the Challis Volcanics in the eastern half of the Challis 1° x 2° quadrangle, Idaho, *in* Bill Bonnichsen and R. M. Breckenridge, editors, Cenozoic Geology of Idaho: Idaho Bureau of Mines and Geology Bulletin 26.

Rember, W. C. and E. H. Bennett, 1979, Geologic map of the Twin Falls quadrangle, Idaho: Idaho Bureau of Mines and Geology Geologic Map Series, Twin Falls 2° quadrangle, scale 1:250,000.

Smith, R. L. and R. A. Bailey, 1968, Resurgent cauldrons: Geological Society of America Memoir 116, p. 613-662.

Stone, G. T., 1967, Petrology of upper Cenozoic basalts of the western Snake River Plain, Idaho: University of Colorado Ph.D. dissertation, 392 p.

U. S. Geological Survey, 1978, Aeromagnetic map of Idaho: U. S. Geological Survey Geophysical Investigations Map GP-919, scale 1:500,000.

Yoder, H. S., Jr., and C. E. Tilley, 1962, Origin of basalt magmas: an experimental study of natural and synthetic rock systems: Journal of Petrology, v. 3, p. 342-532.

The Cougar Point Tuff, Southwestern Idaho and Vicinity

by

Bill Bonnichsen[1] and Gary P. Citron[2]

ABSTRACT

The Cougar Point Tuff is a sequence of densely welded, rhyolitic ash-flow tuff cooling units that erupted from the Bruneau-Jarbidge eruptive center during late Miocene time. By the end of Cougar Point Tuff volcanism, the eruptive center had developed into a large structural and physiographic basin. The exposed part of the Cougar Point Tuff consists of outflow-facies rocks that extend beyond the margins of the eruptive center. Thicker intracaldera facies of the welded tuff units may be hidden beneath younger rhyolite and basalt lava flows and sediments which fill the basin.

The Cougar Point Tuff is best exposed in the canyons of the Bruneau River and the East and West Forks of the Jarbidge River near the Idaho-Nevada border. At Black Rock escarpment in Bruneau Canyon, eight units are exposed and have an aggregate thickness of 400-475 meters. At Cougar Point in the East Fork of Jarbidge Canyon, six of the units are exposed with a thickness of about 250 meters.

The various Cougar Point Tuff units are quite similar in composition and in the temperature and mode of eruption. Where relatively thick, all are simple cooling units, but some, traced into areas where they are thin, change into compound cooling units or even bifurcate into composite sheets. In a vertical section through a unit, the typical zones from base to top consist of (1) a basal layer of thinly bedded air-fall ash, (2) a vitrophyre layer at the base of the ash-flow cooling unit, (3) a massive, relatively thick, lithoidal central zone of the ash-flow sheet in which most structures have been obliterated by matrix crystallization, and (4) an upper zone of the ash-flow sheet with abundant primary flow marks and secondary folds.

Quartz, sanidine, plagioclase, augite, pigeonite, fayalite, magnetite, and ilmenite are the principal phenocryst minerals, and are accompanied by accessory zircon, monazite(?), and apatite. Hornblende and biotite are essentially absent, suggesting that the magmas were relatively hot and dry. The absence of hypersthene and the presence of pigeonite, the high-temperature Ca-poor pyroxene, in nearly every unit mean that the magmas were hotter than the pigeonite-hypersthene inversion boundary. Plagioclase-clinopyroxene-opaque oxide cumulophyric aggregates occur in most units; these are interpreted to be fragments of the rocks melted to form the magmas.

Chemically analyzed samples from locations many kilometers apart in each unit reveal that each has a relatively narrow compositional range. Overall, the Cougar Point Tuff becomes increasingly femic upwards, but local reversals in the trend exist. The tuff has been divided into three compositional cycles based on these local reversals. In each cycle the composition became increasingly femic upwards, as successive magma batches were erupted. The emplacement of each unit was a distinct volcanic event, separated by the deposition of sedimentary layers. In some cases sufficient time elapsed between eruptions for Earth's magnetic field to reverse its polarity.

A potassium-argon age of 11.3 million years is reported for one of the lower Cougar Point Tuff units. Initial strontium isotope ratios indicate a predominantly, if not exclusively, crustal origin for the Cougar Point Tuff, being similar in that respect to other rhyolitic rocks in the Snake River Plain-Yellowstone Plateau volcanic province. In all probability, the Cougar Point Tuff magmas originated in deep crustal rocks that were partially melted as successive large batches of basaltic magma were injected into the crust. The silicic magmas that gave rise to the ash-flow units are interpreted to have been relatively hot and dry as they rose through the crust, so that the disruptive vesiculation which propelled hot ash high into the atmosphere during their eruption occurred at comparatively shallow depths.

INTRODUCTION

The Cougar Point Tuff is a sequence of densely welded ash-flow tuff cooling units that were erupted

[1]Idaho Bureau of Mines and Geology, Moscow, Idaho 83843.
[2]Amoco Production Company, P.O. Box 50879, New Orleans, Louisiana 70150.

Bonnichsen, Bill and G. P. Citron, 1982, The Cougar Point Tuff, southwestern Idaho and vicinity, *in* Bill Bonnichsen and R. M. Breckenridge, editors, Cenozoic Geology of Idaho: Idaho Bureau of Mines and Geology Bulletin 26, p. 255-281.

from the Bruneau-Jarbidge eruptive center (Bonnichsen, 1982b this volume) during late Miocene time. The eruption of the Cougar Point Tuff was the first volcanic phase in the evolution of the Bruneau-Jarbidge eruptive center. By the end of Cougar Point Tuff volcanism, the eruptive center had developed as a large structural and physiographic basin. The subsequent extrusion of several large rhyolite lava flows nearly filled the basin, however. As now exposed, the Cougar Point Tuff consists only of outflow-facies rocks which escaped from the eruptive center. Presumably more voluminous portions of the individual units are buried within their source areas (calderas?) beneath the younger rhyolite lava flows, basalt flows, and sedimentary deposits.

Our main objective in this paper is to describe the internal features of the units that constitute the Cougar Point Tuff, and their stratigraphic, chemical, and general petrographic relations. This paper is a companion to others in this volume that describe the Bruneau-Jarbidge eruptive center and the rhyolite lava flows within it (Bonnichsen, 1982b, 1982c); thus, extensive reference has been made to figures and tables in these accompanying papers. The final section of this article discusses how the rhyolitic magmas behaved during their eruption and once they reached their final resting place. For a discussion of how the rhyolitic magmas may have been formed, the reader is referred to the final section of the following paper by Bonnichsen (1982c). Also of possible interest in that article is a comparative discussion of the chemical and physical features of the Cougar Point Tuff with the rhyolite lava flows in the Bruneau-Jarbidge eruptive center.

The general distribution of the Cougar Point Tuff in Idaho and northern Nevada is noted in Figure 3 of Bonnichsen (1982b this volume). The detailed distribution of the Cougar Point Tuff is known for some parts of northern Nevada (Rowland 15-minute quadrangle—Bushnell, 1967; Jarbidge 15-minute quadrangle—Coats, 1964; Elk Mountain 15-minute quadrangle—Mathias, 1959, Fifer, 1960, and Higgs, 1960); but for much of that region the unit has been lumped with Miocene welded-tuff units from other source areas (Hope and Coats, 1976; Stewart and Carlson, 1976, 1978).

Some of the Cougar Point Tuff units exposed in Jarbidge Canyon extend eastward into southwestern Twin Falls County. It has yet to be determined, however, if any of these correlate with the sequence of similar welded ash-flow tuff units east of Salmon Falls Creek Reservoir in southern Twin Falls County described by Alief (1962).

The Cougar Point Tuff occupies about the same stratigraphic position as the tuff of Little Jacks Creek (Ekren and others, 1981, 1982 this volume) which occurs west of 116° longitude, west and northwest of the area underlain by the Cougar Point Tuff. The stratigraphic and genetic relationship between the Cougar Point Tuff and the tuff of Little Jacks Creek has yet to be established. The extensive rhyolite unit which connects the two is referred to as the rhyolite of Grasmere escarpment (Bonnichsen, 1982b this volume), from its exposures along the east-facing escarpment west of Grasmere that forms the western margin of the Bruneau-Jarbidge eruptive center (Figures 2 and 3, Bonnichsen, 1982b this volume). As discussed elsewhere (Bonnichsen, 1982b this volume), the rhyolite of Grasmere escarpment is considered to be part of the Cougar Point Tuff even though its exact stratigraphic position relative to the units with Roman numeral designations has yet to be resolved.

The best places to examine the Cougar Point Tuff are in the canyons of the Bruneau River, Jarbidge River, and Sheep Creek. In the canyon of the East Fork of the Jarbidge River, the tuff is exposed southward from Murphy Hot Springs past Cougar Point to the Robinson Hole area where it unconformably overlies the Jarbidge Rhyolite (see Figures 2 and 3 in Bonnichsen, 1982b this volume). In the canyon of the West Fork of the Jarbidge River, it is exposed southward from about 0.6 kilometer north of the mouth of Buck Creek to about 2 kilometers south of the mouth of Jack Creek, where it overlies the Jarbidge Rhyolite. In Bruneau Canyon, the Cougar Point Tuff is exposed southward from the Bull Pens area to about 2 kilometers north of the mouth of McDonald Creek, where it unconformably laps onto the older Bieroth volcanics. In Sheep Creek canyon, units of the Cougar Point Tuff are exposed southwestward from 1.6 kilometers upstream from the mouth of Cat Creek to a few kilometers north of the Idaho-Nevada border, where they overlie the older volcanic units discussed by Bernt and Bonnichsen (1982 this volume). The extent and nature of the Cougar Point Tuff in the Sheep Creek drainage have recently been investigated by Bernt (1982).

UNITS WITHIN THE COUGAR POINT TUFF

The best exposed and most complete section of the Cougar Point Tuff is at Black Rock escarpment on the east side of Bruneau Canyon just north of the Idaho-Nevada border (see Figure 2 in Bonnichsen, 1982b this volume). The Black Rock escarpment (Figure 1) should be considered the principal reference locality for the Cougar Point Tuff. Eight cooling units are exposed there. The Cougar Point Tuff is named for its well-exposed occurrence in the canyon

of the East Fork of the Jarbidge River near Cougar Point (Figure 2, Bonnichsen, 1982b this volume), and was called the Cougar Point welded tuff by Coats (1964). Six cooling units are exposed at Cougar Point (Figure 2); however, neither the lowest nor the highest part of the sequence is exposed there. At Black Rock escarpment the exposed portion of the Cougar Point Tuff ranges from 400 to 475 meters in thickness, whereas in Jarbidge Canyon the exposed portion is about 250 meters thick. It is not known what lies immediately below the Cougar Point Tuff in either canyon.

Based on the succession of units in the Bruneau and Jarbidge Canyons, geologic mapping, petrography, chemical composition, and magnetic polarity measurements, it is clear that the Cougar Point Tuff contains nine or more cooling units. Except in distal areas or where thin, each is a simple cooling unit (Smith, 1960) formed from one or a sequence of ash-flow emplacements closely spaced in time, probably during a virtually continuous eruption. A system of Roman numerals is used to designate the various units. Units that have been recognized on canyon walls are shown in Figures 1 and 2. The Roman numeral nomenclature system supercedes two previous designation systems, as discussed by Bonnichsen (1981). At the present time we know that the Cougar Point Tuff consists of the following cooling units: III, V, VII, IX, X, XI, XII, XIII, and XV. Units that would correspond to Roman numerals I, II, IV, VI, VIII, XIV, or XVI and higher are not known to exist, but further studies east and west of the region considered in this report might recognize additional units that could be designated by these numbers.

UNIT III

Unit III is exposed in the bottom of Bruneau Canyon (Figure 1) between the fault-controlled gully in the southwestern part of sec. 9, T. 16 S., R. 7 E., and the Rowland, Nevada, area where it pinches out against the older Bieroth volcanics (Figure 3). It is the oldest unit assigned, so far, to the Cougar Point Tuff. It is in the correct stratigraphic position to be the same as unit 1 of Bernt (1982) in Cat Creek along the Idaho-Nevada border and in Cottonwood Creek southwest of the Bruneau-Jarbidge eruptive center, but this possible correlation is not firm. Erosion at Jarbidge Canyon is not deep enough to determine if unit III extends that far to the east. In Bruneau Canyon, the unit ranges from 50 meters to 90 meters in thickness.

Unit III is lighter in color than any of the overlying units. It contains numerous lithophysae generally concentrated in subhorizontal zones. At some localities the unit displays considerable internal contortions. The rocks of unit III appear somewhat altered and bleached, perhaps from vapor-phase crystallization.

Unit III contains phenocrysts of quartz, sanidine, and magnetite. Plagioclase has not been observed, but only two thin sections were studied. Small plagioclase crystal fragments do occur, however, in the airfall ash at the base of the unit. Sanidine is more abundant than quartz. The sanidine crystals are as much as several millimeters across and are conspicuously larger than those in any of the overlying units. Quartz occurs as dipyramids 0.1-0.3 millimeter in diameter and as irregular to anhedral equant grains, commonly more than a millimeter across, suggesting that both phenocrysts and xenocrysts are present.

An analysis of the basal vitrophyre from unit III (Table 1) reveals that the unit is more silicic than any of the overlying units; this is confirmed by several additional analyses of the unit (Bonnichsen, 1982a and unpublished data). The magnetic polarity of unit III has not been determined.

UNIT V

Unit V forms a comparatively low cliff in Bruneau Canyon (Figure 1). The unit typically ranges from 10 meters to 40 meters in thickness, and generally thickens northward. At some localities where it is thin, the unit contains medial vitrophyre layers, clearly indicating that it is a compound cooling unit. Like the underlying unit III, unit V is observed to pinch out southwards against the older Bieroth volcanics in the Rowland, Nevada, area (Figure 3). Unit V is exposed in the Jarbidge River drainage only at the bottom of the West Fork canyon about 1.3 kilometers north of the mouth of Deer Creek (sec. 21, T. 47 N., R. 58 E.). At this locality the entire thickness of the unit is exposed and is seen to be only about 5 meters thick. Unit V is at the proper stratigraphic position to be equivalent to Bernt's (1982) unit 2, farther west, but this correlation is considered as only tentative. The unit has normal magnetic polarity (see Table 1, Bonnichsen, 1982b this volume).

Examination of two thin sections indicates that unit V contains phenocrysts of quartz, sanidine, plagioclase, augite, and magnetite. One grain of hematized biotite was found. Sanidine is more abundant than plagioclase which, in turn, is more abundant than quartz. Chemical analyses of unit V (Bonnichsen, 1982a and unpublished data) indicate a composition more femic than the underlying unit III, but less femic than VII, the overlying unit, and reveal that V is generally quite similar to units IX, XI, and XIII which occur stratigraphically higher.

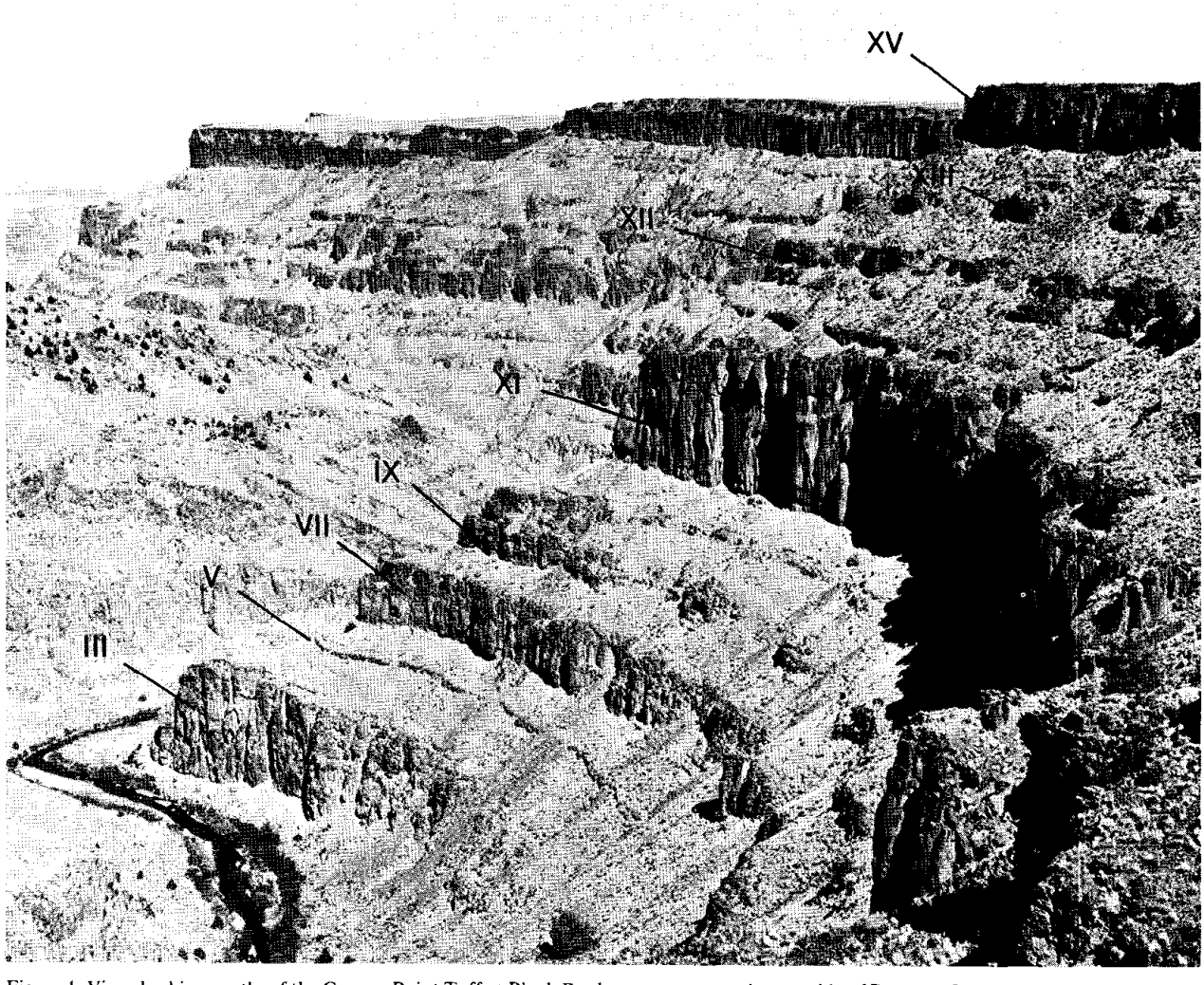

Figure 1. View, looking north, of the Cougar Point Tuff at Black Rock escarpment on the east side of Bruneau Canyon. The various units are indicated by Roman numerals.

UNIT VII

Unit VII forms a prominent cliff near the bottom of both Bruneau and Jarbidge Canyons (Figures 1 and 2). The unit is thicker in Bruneau Canyon, where it typically ranges from 40 meters to nearly 100 meters in thickness; it seems to thicken northward. In Jarbidge Canyon, it generally ranges from 20 and 40 meters in thickness and is the lowest unit there that can be continuously traced (Figure 2). Based on its similar chemical composition, reverse magnetic polarity, and stratigraphic position, unit 3 of Bernt (1982) to the west in the Cat Creek-Sheep Creek area is probably part of unit VII.

The multiple-step cliff formed by unit VII in Bruneau Canyon (see Figure 16 in Bonnichsen, 1981) suggests that the unit resulted from a sequence of ash-flow emplacements spaced closely enough in time to form a simple cooling unit. In both canyons, unit VII pinches out southward against older topography (Figure 3). Unit VII has reverse magnetic polarity (Table 1, Bonnichsen, 1982b this volume). In Bruneau Canyon, the upper part of VII is highly contorted, with curved sheeting joints that range from horizontal to vertical or overturned within a few meters.

The phenocryst minerals in unit VII are plagioclase, sanidine, quartz, pigeonite, augite, and magnetite. The average abundance of phenocrysts for seven modal analyses from the Jarbidge Canyon area is 10.7 percent. The approximate proportions of the various phenocryst minerals are shown in Figures 4, 5, and 6. Plagioclase is the most abundant; it com-

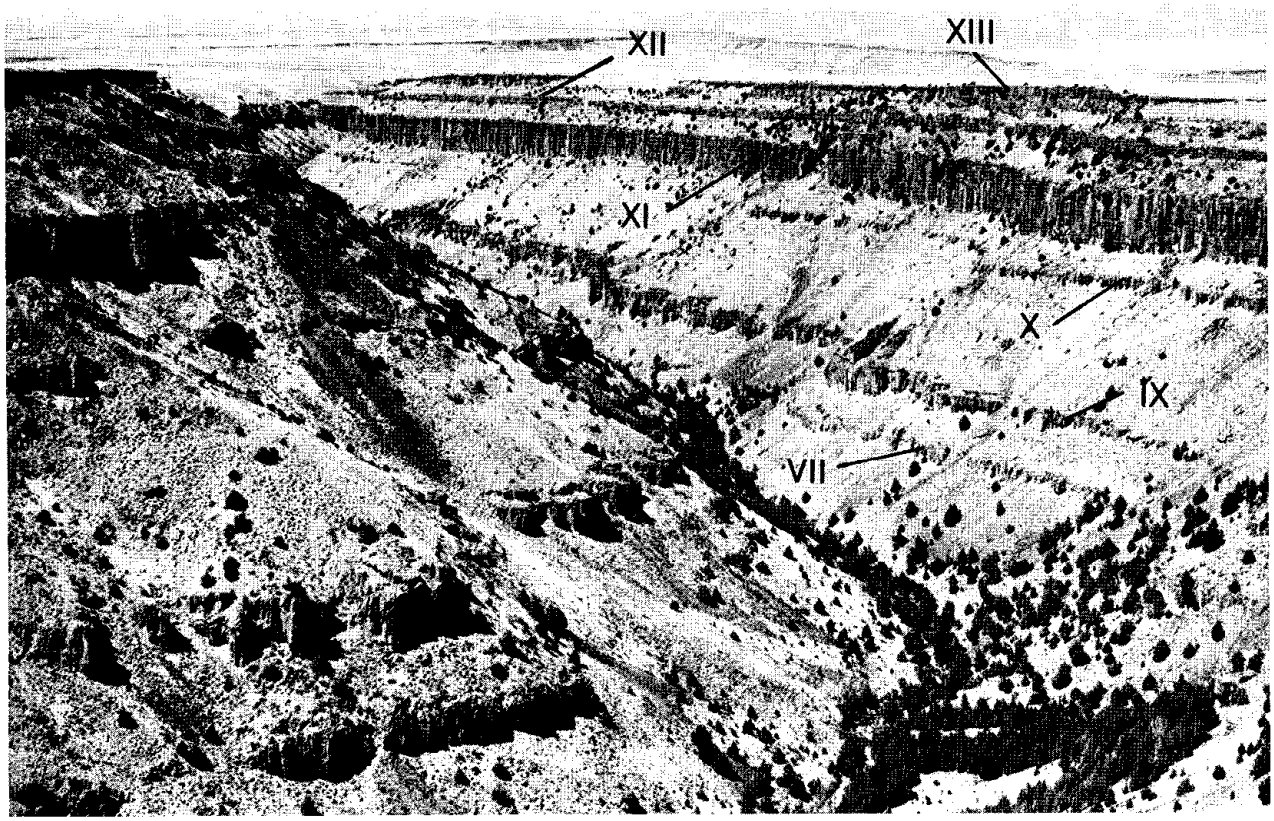

Figure 2. View, looking north-northeast from Cougar Point, of the Cougar Point Tuff exposed in East Fork Jarbidge River canyon. The various units are indicated by Roman numerals.

monly accounts for nearly 40 percent of the total phenocrysts (Figure 6). Sanidine is second in abundance (Figure 4), and quartz occurs in most rocks but is sparce (Figures 4 and 5). Pigeonite commonly is more abundant than augite. Fayalite has not been detected in unit VII. Magnetite occurs in all thin sections examined, and possible ilmenite tablets occur in two of eleven sections. Magnetite and clinopyroxene occur in approximately equal amounts (Figure 5). Traces of biotite and hornblende occur in a few thin sections as overgrowths on pyroxenes, or as alteration products, but not as independent phenocrysts. Plagioclase-clinopyroxene-opaque oxide cumulophyric aggregates are common in unit VII.

An analysis of the basal vitrophyre of unit VII (Table 1) indicates a composition more femic than several of the other Cougar Point Tuff units. This is confirmed by eight additional analyses from the unit (Bonnichsen, 1982a and unpublished data).

A potassium-argon age determination* of 11.3±2.0 million years was obtained from a unit VII sample from near the bottom of Deer Creek grade in the West Fork of the Jarbidge River canyon.

*The material dated was a whole-rock sample (I-841) of the basal vitrophyre of unit VII from the SW¼NE¼, sec. 28, T. 47 N., R. 58 E., Elko County, Nevada. The analysis was performed by Professor Daniel Krummenacher, Department of Geological Sciences, San Diego State University, San Diego, California. Analytical data from the determination include: weight percent K=4.81%; moles per gram of $^{40}Ar_{rad}$=9.48 x 10^{-11}; and $^{40}Ar_{atm}$=90%. Constants used for age calculation are λ_β=4.962 x 10^{-10} per year, λ_ϵ=0.581 x 10^{-10} per year, and percent ^{40}K of total K=0.01167. This age determination should be considered a minimum age, in view of the ever-present possibility of argon leakage from somewhat hydrated volcanic glass, although less hydration for the dated sample than for most other Cougar Point Tuff vitrophyres is suggested by the relatively high sum of the major oxides (99.01%) (no. 2, Table 1) in comparison with other analyses in Table 1, and in Bonnichsen (1982a).

Figure 3. View of the lower Cougar Point Tuff units (Roman numerals) pinching out against the older Bieroth volcanics (BV) near the confluence of McDonald Creek and the Bruneau River in northern Nevada.

UNIT IX

Unit IX is exposed in both Bruneau and Jarbidge Canyons (Figures 1, 2, 3, and 7). In Jarbidge Canyon it forms a prominent horizontally layered cliff below 50 meters or more of nonresistant material (covered slope in Figure 2). In Bruneau Canyon unit IX forms a conspicuously layered cliff tightly sandwiched between the thicker and more massive units VII, below, and XI, above (Figures 1, 3, and 7). Its layered nature clearly shows that unit IX resulted from a sequence of emplacements. In some areas the unit appears to be a simple cooling unit, but at other places it might better be thought of as a compound cooling unit. Like the units beneath it, IX pinches out southward against older topography in the Rowland, Nevada, area (Figure 3). In Bruneau Canyon, unit IX typically is 40 to 50 meters thick, whereas in Jarbidge Canyon its resistant part generally is 30 to 40 meters thick. Unit IX has normal magnetic polarity (Table 1, Bonnichsen, 1982b this volume).

In its Bruneau Canyon exposures, unit IX characteristically contains fairly abundant small, generally angular, devitrified and probably cognate volcanic rock clasts in its lower part. The welding does not extend completely to the base of the ash flow at some locations in Bruneau Canyon. The unit also contains veins and segregations of jasper in its upper portions in Bruneau Canyon, suggesting post-eruption interaction with water.

Unit IX contains phenocrysts of plagioclase, sanidine, quartz, augite, pigeonite, and magnetite. The average phenocryst abundance is 8.6 percent in eleven Jarbidge Canyon samples for which modal analyses are available. In most, sanidine is more abundant than plagioclase, which in turn is more abundant than quartz (Figure 4). Clinopyroxene, magnetite, and quartz occur in approximately equal proportions (Figure 5). Sanidine and quartz generally account for half or more of the phenocrysts; plagioclase accounts for 10 to 25 percent, and the mafic minerals for 20 to 40 percent (Figure 6). Locally, fragments of quartz-sanidine micrographic intergrowths occur, but they are much less abundant than in units XI and XIII. Plagioclase-clinopyroxene-opaque oxide cumulophyric aggregates are common, and hornblende rims on augite grains were noted in a few samples from Jarbidge Canyon.

Chemical analyses (Bonnichsen, 1982a and unpublished data) reveal unit IX to be similar in composition to the thick overlying unit XI, but not as femic as the underlying unit VII.

UNIT X

Unit X is well exposed only in the canyon of the East Fork of the Jarbidge River. It is 20 to 25 meters thick in the Cougar Point area of that canyon (Figure 2). Scattered outcrops of what probably is the same unit also occur in the east wall of the West Fork of Jarbidge Canyon near the mouth of Deer Creek (sec. 27, T. 47 N., R. 58 E.); but there the unit is only a few meters thick and does not form a traceable ledge. Unit X has not been found in Bruneau Canyon. The limited distribution of this relatively thin unit suggests that it is not as voluminous as the other Cougar Point

Table 1. Chemical analyses and CIPW norms for representative samples of the Cougar Point Tuff.

Unit	1 III	2 VII	3 XI	4 XII	5 XIII	6 XV	7 XV	8 XV
				Major oxides in weight percent				
SiO_2	74.87	72.24	73.16	72.97	74.25	73.58	72.05	72.04
Al_2O_3	12.34	12.83	12.00	12.64	12.26	12.14	11.04	12.53
TiO_2	0.14	0.48	0.30	0.52	0.29	0.40	0.36	0.40
Fe as Fe_2O_3	1.40	3.27	2.32	3.36	2.26	3.47	4.54	2.84
MnO	0.02	0.05	0.02	0.05	0.02	0.04	0.04	0.04
CaO	0.64	1.32	0.82	1.21	0.86	0.77	0.86	0.80
MgO	0.21	0.37	0.12	0.34	0.20	0.22	0.26	0.21
K_2O	5.47	5.67	5.76	5.48	5.64	6.08	5.84	6.03
Na_2O	2.76	2.69	2.92	2.88	2.90	2.33	2.31	2.26
P_2O_5	0.02	0.09	0.03	0.10	0.03	0.06	0.08	0.06
Total	97.87	99.01	97.45	99.55	98.71	99.09	100.27	97.21
				Minor elements in parts per million				
Rb	307	213	233	194	209	--	--	--
Sr	13	83	35	65	55	--	--	--
Zr	229	528	455	571	497	--	--	--
Pb	49	40	38	33	43	--	--	--
Zn	73	80	79	74	99	--	--	--
Th	51	44	48	38	50	--	--	--
Mo	8	12	10	7	7	--	--	--
				CIPW norms				
qz	34.56	29.68	31.02	30.18	31.81	32.75	33.76	32.52
or	33.55	34.55	35.55	33.20	34.35	37.20	36.50	37.50
ab	25.75	24.90	27.35	26.50	26.85	21.65	21.95	21.35
an	3.15	6.15	2.75	5.50	3.90	3.55	2.65	3.80
co	0.87	0.09	-0-	0.01	-0-	0.53	-0-	1.11
px	1.26	2.34	1.83	2.22	1.65	2.12	1.38	1.76
mt	0.60	1.41	1.01	1.44	0.97	1.50	2.22	1.26
hm	-0-	-0-	-0-	-0-	-0-	-0-	0.86	-0-
il	0.20	0.68	0.44	0.74	0.42	0.58	0.52	0.58
ap	0.05	0.19	0.05	0.21	0.05	0.13	0.16	0.13

Notes:

Except as noted below, the samples were analyzed for major oxides by a combination of X-ray fluorescence and atomic absorption at Washington State University (XRF) and at the Idaho Bureau of Mines and Geology (AA) and for minor elements by X-ray fluorescence at the Research and Development Department of Conoco, Inc.

For samples in which only the total iron was analyzed, the CIPW norms were calculated by assigning 40 atom percent of the Fe to Fe_2O_3 and 60 atom percent to FeO.

1. Sample I-569, basal vitrophyre of Cougar Point Tuff unit III; NW¼NE¼, sec. 28, T. 16 S., R. 7 E., Owyhee County, Idaho.
2. Sample I-841, basal vitrophyre of Cougar Point Tuff unit VII; SW¼NE¼, sec. 28, T. 47 N., R. 58 E., Elko County, Nevada.
3. Sample I-463, basal vitrophyre of Cougar Point Tuff unit XI; NW¼SW¼, sec. 9, T. 16 S., R. 7 E., Owyhee County, Idaho.
4. Sample I-799, basal vitrophyre of Cougar Point Tuff unit XII; SE¼NE¼, sec. 28, T. 16 S., R. 7 E., Owyhee County, Idaho.
5. Sample I-461, basal vitrophyre of Cougar Point Tuff unit XIII; SE¼SW¼, sec. 9, T. 16 S., R. 7 E., Owyhee County, Idaho.
6. Sample I-76, vitrophyre from Cougar Point Tuff unit XV; SE¼NW¼, sec. 24, T. 16 S., R. 9 E., Owyhee County, Idaho. In Bonnichsen (1982a), this sample was erroneously assigned to unit XIII. The revision to unit XV has also been made in Figure 21.
7. Sample I-76, same description and location as given in 6. Analyzed by K. Ramlal at the University of Manitoba, 1972, by methods described in Wilson and others, 1969. The total includes 2.98 percent H_2O, 0.04 percent CO_2, 0.01 percent S, and Fe reported as 3.18 percent Fe_2O_3 and 1.22 percent FeO.
8. Sample S-193, vitrophyre from Cougar Point Tuff unit XV; SE¼SW¼, sec. 21, T. 16 S., R. 9 E., Owyhee County, Idaho.

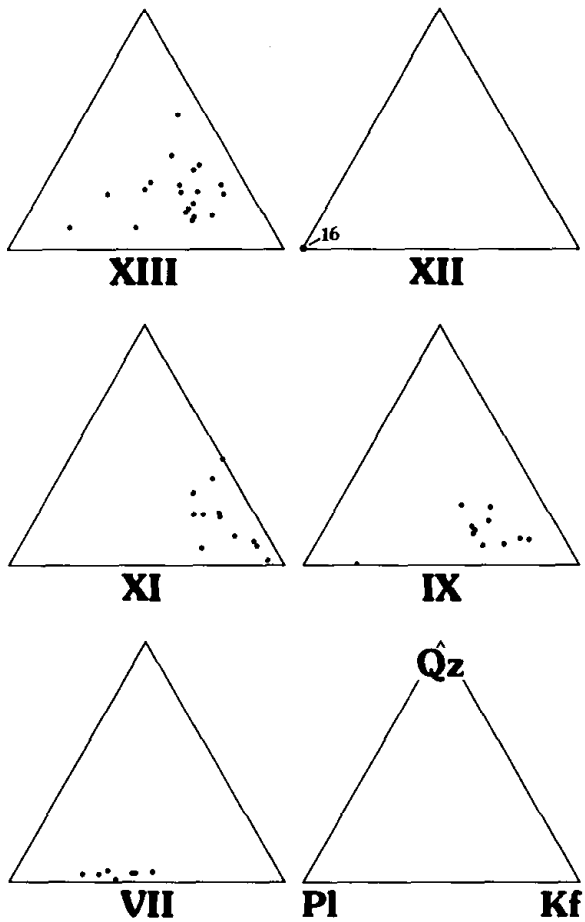

Figure 4. Proportions of quartz, plagioclase, and sanidine in several Cougar Point Tuff units (see Citron, 1976, for modal analyses). Small numerals indicate the number of analyses having identical proportions.

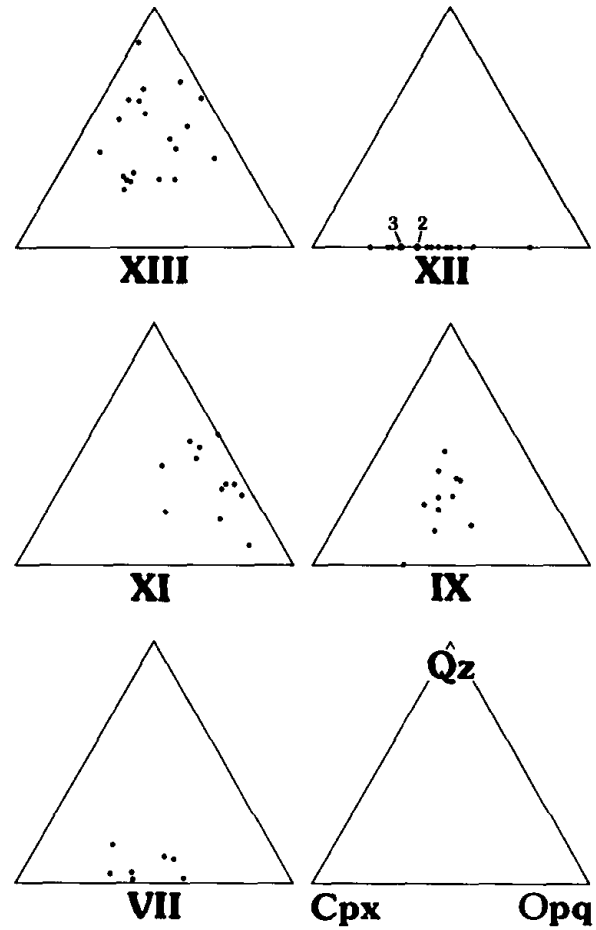

Figure 5. Proportions of quartz, clinopyroxene, and opaque oxide minerals in several Cougar Point Tuff units (see Citron, 1976, for modal analyses). Small numerals indicate the number of analyses having identical proportions.

Tuff units.

The one thin section from unit X that has been examined contains phenocrysts of sanidine, plagioclase, and quartz with proportions similar to those in unit XI, and phenocrysts of magnetite and oxidized pyroxenes. A chemical analysis (Bonnichsen, 1982a) of X indicates a composition similar to the underlying unit, IX, and overlying unit, XI.

UNIT XI

Unit XI is one of the most voluminous and complex units in the Cougar Point Tuff. In Bruneau Canyon (Figures 1, 3, and 7), it forms a high cliff in about the middle of the section and ranges from 90 to probably more than 100 meters in thickness. In Jarbidge Canyon it ranges from 30 to more than 50 meters in thickness and is the thickest unit in that area (Figure 2). In both canyons the internal horizontal layering clearly shows that it resulted from a sequence of ash-flow emplacements. Where it is thick, unit XI forms a simple cooling unit. However, where XI has been mapped across northern Nevada between Bruneau and Jarbidge Canyons, it appears to bifurcate into thinner separate cooling units. This composite sheet behavior (Smith, 1960) probably is the result of overall southward thinning of the unit onto preexisting topographic irregularities distal from the unit's source.

Unit XI's distribution east of Jarbidge Canyon in northern Nevada has yet to be explored in detail, but it very likely extends as far east as Elk Mountain (see Figures 2 and 3, Bonnichsen, 1982b this volume). West of Bruneau Canyon, the unit which Bernt (1982) designated as unit 6 in the Sheep Creek area very likely is, at least in part, the same as unit XI.

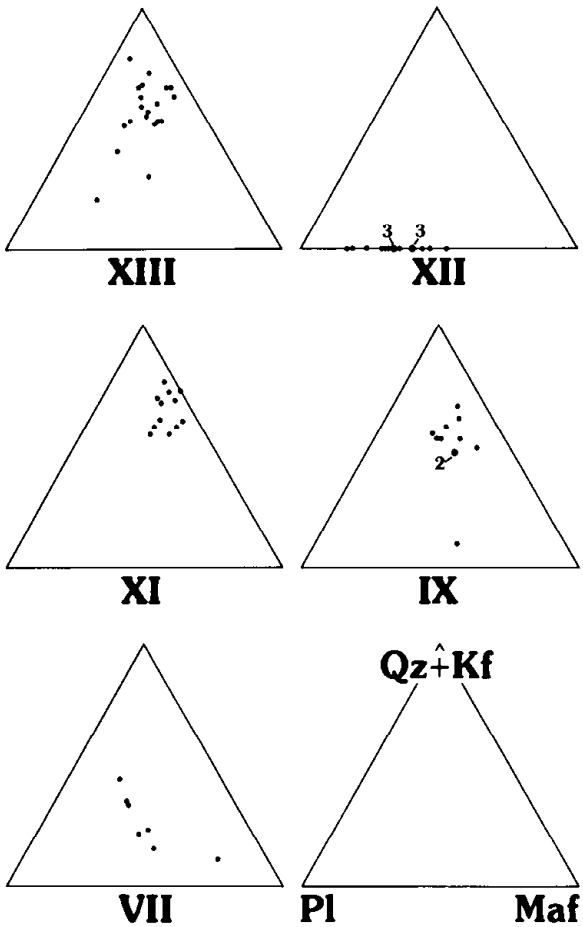

Figure 6. Proportions of quartz plus sanidine, plagioclase, and mafic minerals in several Cougar Point Tuff units (see Citron, 1976, for modal analyses). Small numerals indicate the number of analyses having identical proportions.

In both Bruneau and Jarbidge Canyons, unit XI is characterized by many picturesque erosional pillars, as can be seen in Figures 7 and 8. In the West Fork of Jarbidge Canyon near Deer Creek grade, the upper part of the unit contains many flattened pumice inclusions, some as much as a meter long (Figure 9). Unit XI has reverse magnetic polarity (Table 1, Bonnichsen, 1982b this volume).

Unit XI contains sanidine, quartz, plagioclase, magnetite, ilmenite, augite, pigeonite, and fayalite phenocrysts. The average phenocryst abundance for twelve samples from the Jarbidge River drainage area is 5.5 percent. The overall proportion of quartz and sanidine generally ranges from 55 to 75 percent, that of plagioclase from 0 to 20 percent, and that of the mafic minerals from 20 to 35 percent (Figure 6). Sanidine is the most abundant; in most samples it exceeds quartz in abundance and is twice or more as plentiful as plagioclase (Figure 4). Generally, quartz is more abundant than plagioclase. In the Jarbidge Canyon area the proportion of quartz and plagioclase relative to sanidine increases upwards through the unit. Locally, quartz and plagioclase are absent or very sparse (Figure 4). Most of the quartz occurs as tiny dipyramids, although larger rounded to irregular quartz xenocrysts have been noted in a few rocks. In most unit XI samples a few sanidine grains have partial rims of quartz-sanidine micrographic intergrowths; fragments of these intergrowths also occur. Unit XI is similar only to unit XIII in its abundance of these intergrowths.

Magnetite is the most common mafic mineral (Figure 5), followed by augite. In the Jarbidge Canyon area, the augite is accompanied by minor fayalite, whereas in the Black Rock area of Bruneau Canyon and in northern Nevada between the Bruneau and Jarbidge Rivers, pigeonite occurs instead of fayalite. Fayalite and pigeonite have not been observed together in the same sample. A few plagioclase-clinopyroxene-opaque oxide cumulophyric aggregates occur in most unit-XI thin sections. Many of these consist predominantly of granoblastic plagioclase containing inclusions of pyroxene and magnetite. The presence in most thin sections of a few small elongate laths of probable ilmenite distinguishes unit XI from all other units except XIII.

An analysis of typical basal vitrophyre material from unit XI (Table 1) indicates a composition quite similar to that of IX and XIII, and not as femic as units VII, XII, and XV. Additional analyses of XI (Bonnichsen, 1982a and unpublished data) generally confirm this.

UNIT XII

Unit XII is widely distributed but not as extensive as the units below (XI) and above (XIII). Its most prominent exposures are in the walls of the East and West Forks of Jarbidge Canyon (Figure 2) where it generally ranges from 30 to 40 meters in thickness. Unit XII has been traced east of Jarbidge Canyon, through the Jarbidge and Elk Mountain, Nevada, 15-minute quadrangles, to as far east as 115 degrees longitude (right side of Figures 2 and 3, Bonnichsen, 1982b this volume). The unit has been traced westward in northern Nevada to the Black Rock escarpment on the east side of Bruneau Canyon (Figures 1 and 7). It is thin and discontinuous there, indicating that the area is near its western margin. Unit XII was not reported farther west, in the area recently mapped by Bernt (1982). Unit XII has normal magnetic polarity (Table 1, Bonnichsen, 1982b this volume).

Unit XII contains phenocrysts of plagioclase,

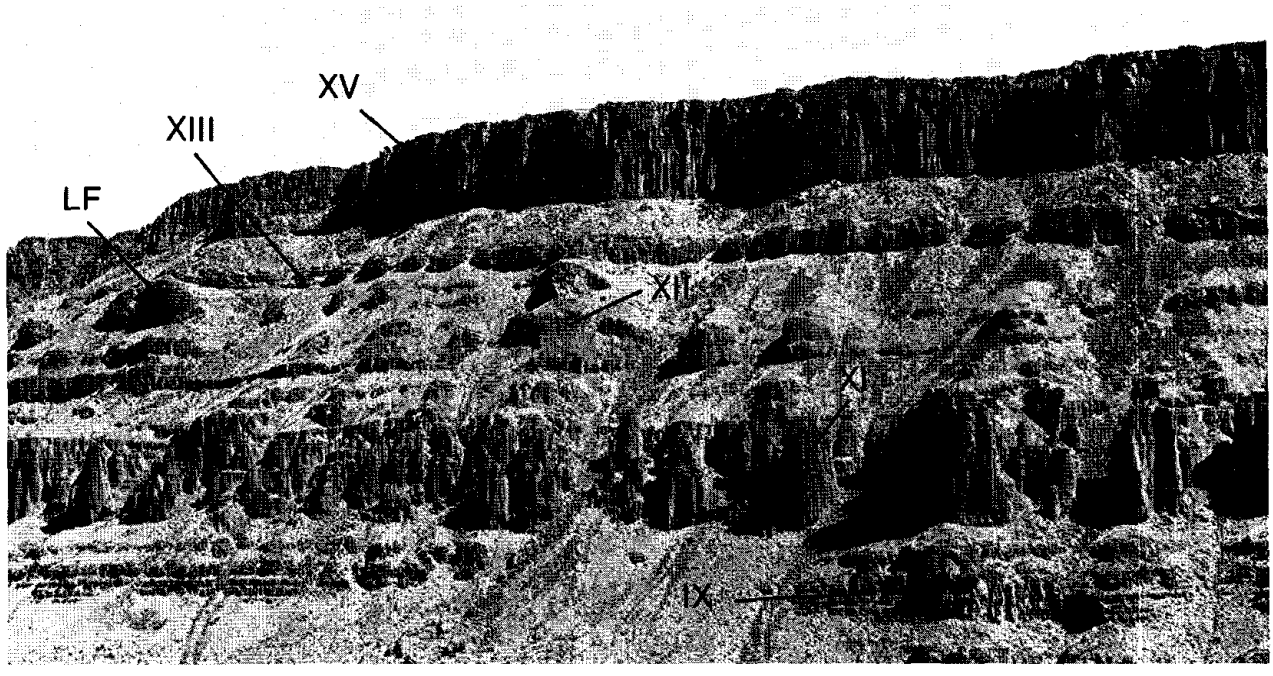

Figure 7. View of the upper Cougar Point Tuff units (Roman numerals) at the north end of Black Rock escarpment in Bruneau Canyon. Note the bulbous unnamed rhyolite lava flow (LF) between XII and XIII and the conspicuous layering within IX and XI.

augite, pigeonite, and magnetite. Modal analyses of sixteen samples indicate an average phenocryst abundance of 10.9 percent. Plagioclase is the most abundant, followed by pyroxenes and magnetite (Figures 4, 5, and 6). Quartz and sanidine normally do not occur in the unit; in the few sections in which they have been noted, their habit suggests they are xenocrysts. Their absence distinguishes unit XII from all the other Cougar Point Tuff units. In most samples clinopyroxene is more abundant than magnetite (Figure 5), and generally pigeonite is more abundant than augite. Plagioclase-clinopyroxene-opaque oxide cumulophyric aggregates are common in unit XII, more so than in most other units.

An analysis of a unit XII basal vitrophyre sample (Table 1) shows that XII is one of the most femic units, along with VII and XV. Two additional analyses of XII (Bonnichsen, 1982a and unpublished data) are almost identical to the one reported.

UNIT XIII

Unit XIII is one of the most widespread of the Cougar Point Tuff units. It has been traced 65 kilometers along the southern margin of the Bruneau-Jarbidge eruptive center and its eastern limit has yet to be determined. It is the uppermost unit in most of the Jarbidge River drainage area, occurring at the canyon rim (Figure 2) where it ranges in thickness from 20 to 45 meters. In Bruneau Canyon (Figures 1 and 7) it ranges from less than 30 meters to 40 meters in thickness. It extends west of Bruneau Canyon into Sheep Creek canyon, where it pinches out westward (Bernt, 1982, unit 7) in the northwestern part of T. 15 S., R. 6 E. Unit XIII extends an undetermined distance east of 115 degrees longitude in Idaho and is widely distributed in the northern parts of the Contact, Elk Mountain, Jarbidge, and Rowland 15-minute quadrangles in northern Nevada.

Although it is a simple cooling unit, XIII has a horizontal layered appearance at some localities suggesting it may have resulted from a sequence of ash-flow emplacements. A characteristic feature of unit XIII throughout most of its distribution area is a thin (generally 1 to 2 meters) horizontal lithophysal zone (Figure 10) about two-thirds of the way up from its base. Unit XIII has normal magnetic polarity (Table 1, Bonnichsen, 1982b this volume).

Unit XIII contains plagioclase, sanidine, quartz, augite, fayalite, magnetite, and ilmenite phenocrysts. The average phenocryst abundance for twenty modal analyses of samples from the Jarbidge River drainage is 8.9 percent. Generally, sanidine is more abundant than either quartz or plagioclase (Figure 4), and the unit shows a greater variation in the ratio of feldspars to quartz than any of the other units for which modal data are available (Figures 4, 5, and 6). In general, sanidine decreases upwards in the unit relative to plagioclase and quartz. The proportions of quartz

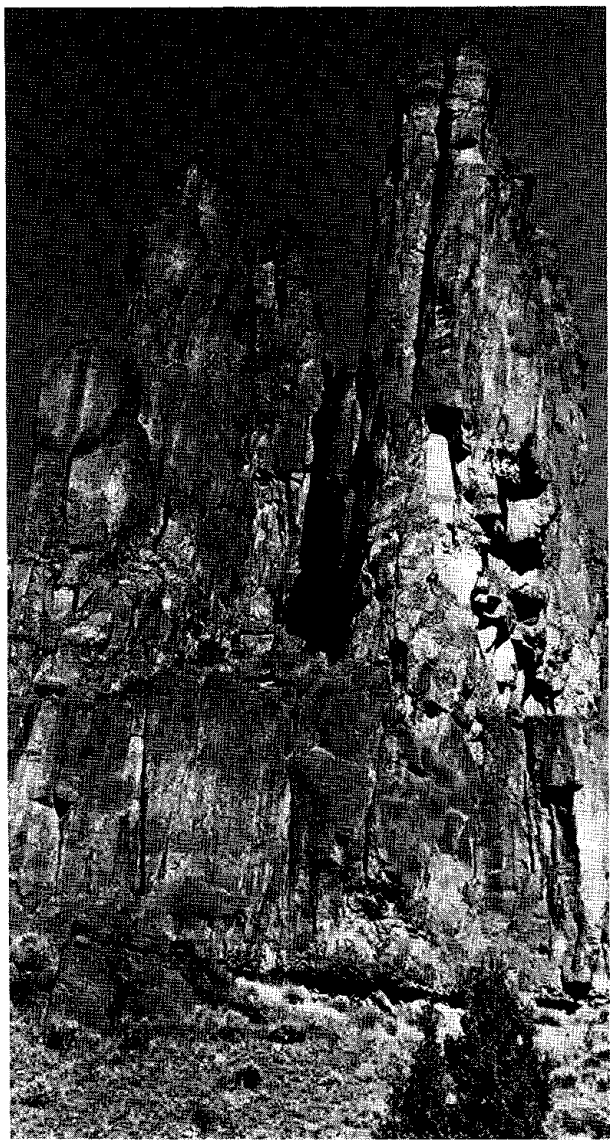

Figure 8. Erosional pillars in the massive central zone of Cougar Point Tuff unit XI in West Fork Jarbidge River canyon. The horizontal break about one-third of the way up from the cliff base is a boundary between successive ash emplacements. A lithophysal zone occurs just below this break. The basal vitrophyre is exposed in the alcove eroded at the base of the cliff.

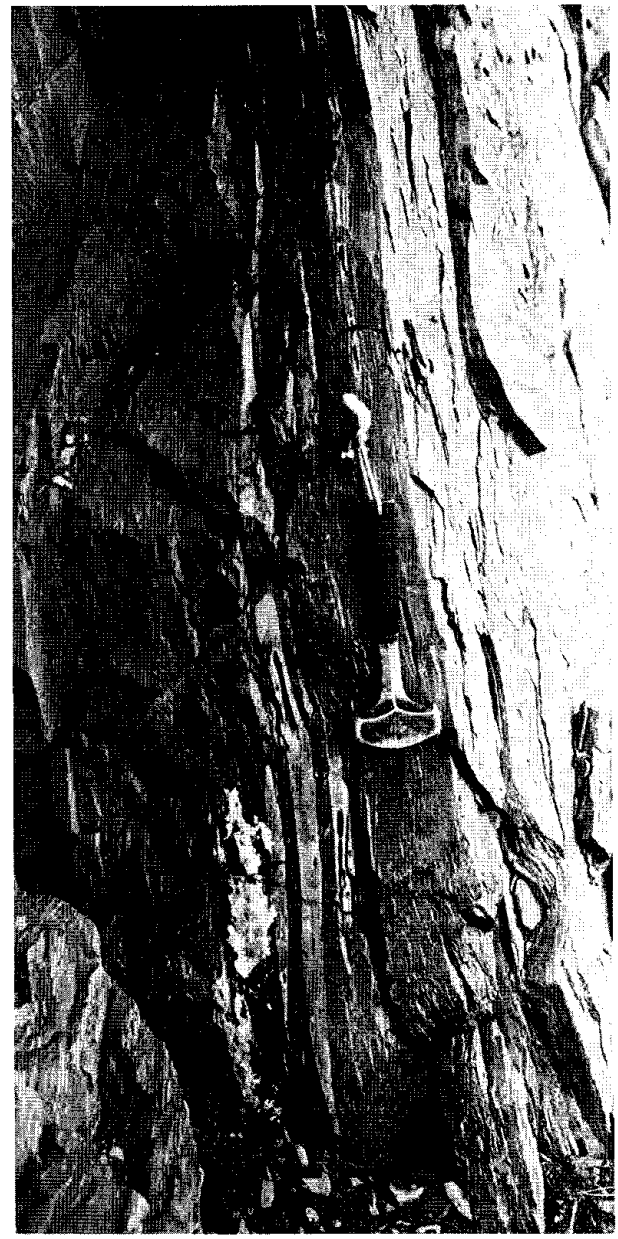

Figure 9. Flattened pumice fragments within the upper zone of Cougar Point Tuff unit XI, from Deer Creek grade in West Fork Jarbidge River canyon. Post-compaction movement within the unit has rotated the previously horizontal lenses to nearly vertical. For scale, the hammer is 28 centimeters long.

and plagioclase vary widely in XIII (Figure 4), but no vertical trend has been noted. Quartz generally is more abundant than pyroxene or opaque minerals (Figure 5), and the ratio of magnetite to pyroxene varies more than for other units. Mafic minerals normally constitute 15 to 35 percent of the phenocrysts, plagioclase 5 to 40 percent, and quartz and sanidine together 50 to 75 percent (Figure 6).

Quartz occurs both as small dipyramidal grains, and as larger rounded and deeply embayed grains with undulatory extinction considered to be xenocrysts. Quartz-sanidine micrographic intergrowths occur as partial rims on some sanidine grains and as fragments in most thin sections. The only pyroxene identified is a clinopyroxene with an optic angle of about 60 degrees; it probably is subcalcic ferroaugite. No pigeonite grains have been found in XIII; evidently it is absent, and fayalite takes its place as

Figure 10. The distinctive lithophysal zone in Cougar Point Tuff unit XIII, from near Murphy Hot Springs in East Fork Jarbidge River canyon. This zone occurs about two-thirds of the way above the base of XIII and has been traced for tens of kilometers. At many locations the gas cavities are equant, but at others, such as shown here, they are elongate. For scale, the knife is 24 centimeters long.

the calcium-poor mafic mineral. Plagioclase-augite-opaque oxide cumulophyric aggregates occur in several of the thin sections from unit XIII. Elongate laths of probable ilmenite are sparse, occurring in only about half of the thin sections examined.

An analysis of the basal vitrophyre of unit XIII (Table 1) indicates the unit is one of the most silicic and compositionally is very much like units V, IX, and XI. Several additional analyses (Bonnichsen, 1982a and unpublished data; Bernt, 1982) confirm this.

UNIT XV

The uppermost unit (XV) occurs most prominently along the rim of Bruneau Canyon (Figures 1 and 7) in the Black Rock escarpment area, where it ranges from 30 to nearly 100 meters in thickness. The dark appearance of the thick part of unit XV, especially as seen from the north and west in morning shadows or on cloudy days, is the reason the topographically high escarpment on the east side of Bruneau Canyon is called Black Rock.

In the Bruneau Canyon area unit XV thins southward into Nevada along the rim of Deep Creek, and pinches out a few kilometers south of the state line. However, it continues to the north and is downfaulted to a level below the Triguero Homestead rhyolite in the Bull Pens area (see Figure 6 in Bonnichsen, 1982b this volume). Unit XV occurs at the surface from Dorsey Creek and westward to about as far west as the Three Forks area of Sheep Creek in the southeastern part of T. 15 S., R. 5 E., where it pinches out (Bernt, 1982). In the canyon of Cat Creek between Bruneau Canyon and Sheep Creek, unit XV is 50 to 75 meters thick, and it thins and bifurcates into two separate cooling units both to the north and south to form a composite sheet (Bernt, 1982, unit 8). At all other localities the unit is observed to be a simple cooling unit.

East of Dorsey Creek, unit XV is discontinuously exposed as far east as the grade on the east side of Jarbidge Canyon at Murphy Hot Springs. Unit XV generally is less than 5 meters thick at all localities east of Dorsey Creek and consists mainly of vitrophyre.

In the thick part of the unit in the Black Rock area, the basal part of the unit contains abundant, generally small, greatly flattened pumice fragments. Unit XV has normal magnetic polarity (Table 1, Bonnichsen, 1982b this volume).

The phenocryst minerals in unit XV are plagioclase, sanidine, quartz, augite, pigeonite, fayalite, and magnetite. In general, plagioclase is considerably more abundant than either quartz or sanidine. Quartz is not present in all thin sections that have been examined, and sanidine occurs in only about half. Both augite and pigeonite occur in most of the thin sections examined. In sections from the Murphy Hot Springs area in the East Fork of Jarbidge Canyon, which probably is the location farthest removed from the source of the ash flow, fayalite takes the place of pigeonite. Cumulophyric aggregates of plagioclase, pyroxenes, and opaque oxides are common throughout the unit.

Analyses of two basal vitrophyre samples (Table 1) show unit XV to be one of the more femic Cougar Point Tuff units, along with VII and XII. This is confirmed by several additional analyses (Bonnichsen, 1982a and unpublished data; Bernt, 1982).

INTERNAL FEATURES OF THE UNITS

Although each has its distinctive internal physical characteristics, the various Cougar Point Tuff units are quite similar in magma composition, temperature and mode of eruption, and nature of the landscape each was deposited upon. Where relatively thick, as in Bruneau and Jarbidge Canyons, they are simple cooling units in the sense of Smith (1960), and each unit can be divided into a vertical succession of distinct internal zones. Some units, when traced laterally into areas where they are thin, change into compound cooling units or even bifurcate into composite sheets. Units V, IX, XI, and XV exhibit this style of behavior, as noted in the preceding section. The internal zones are discussed below in relation to the simple cooling units, ignoring complications that arise where they are compound or split into composite sheets.

In this report rocks with a crystallized groundmass, regardless if due to devitrification alone or to vapor-phase crystallization as well (in the sense of Ross and Smith, 1961) are referred to as lithoidal. All relationships between glassy and lithoidal rocks in the Cougar Point Tuff can logically be interpreted as the result, or the lack, of crystallization and oxidation of the groundmass in the short time immediately after emplacement. None of the glassy-lithoidal relationships observed have resulted from subsequent reheating, structural processes, or groundwater-induced situations. Weathering has seldom caused devitrification of a thickness of more than a centimeter adjacent to exposed rock surfaces. More commonly, weathered zones (other than hydration of the glasses) are less than a millimeter thick. The introduction of meteoric water after the deposition of the ash flows may have hydrated some of the vitrophyres, however. Furthermore, the introduction of meteoric water probably caused the late-stage precipitation of local opal, chalcedony, and jasper near the tops of the cooling units, and may also have induced minor groundmass crystallization there.

Lithoidal rocks with crystallized groundmasses generally have red, orange, tan, or lavender colors, in marked contrast to the black or gray tones that characterize most glassy rocks. Some of the steeply dipping joint surfaces in lithoidal rhyolite in the upper zones of units, and some of the crumbly joint surfaces in lithoidal rhyolite in the massive central zones, have a distinctive red or reddish brown glazed appearance, generally brighter in appearance than fresh rock adjacent to the joints and fractures. This condition probably is the result of a greater amount of oxidation along fractures which formed during the cooling of the units. This characteristic tends to give the Cougar Point Tuff units an appearance that is more reddish from a distance than is the color of freshly broken rock surfaces.

Where it has occurred, groundmass crystallization has resulted in the partial to usually complete destruction of shards or other identifiable particles inherited from the ash-flow portion of a unit's history. However, larger, extremely flattened fragments of what probably was pumice, and rare small rock chips (Figures 9 and 11) are preserved in the lithoidal portions of some units. The flattened pumice fragments appear as small discoid inclusions with length-to-height ratios generally between 10 and 100.

In a typical vertical section through a simple cooling unit of the Cougar Point Tuff basically four distinctive zones exist that differ in the manner of emplacement, cooling rate, amount of compaction, and thickness. Typical zones, from base to top, are (1) a basal layer of thinly bedded, principally air-fall ash, (2) a thoroughly welded vitrophyre layer which is the base of the ash-flow tuff, (3) a massive, relatively thick, lithoidal central zone in which most precrystallization structures have been obliterated, and (4) an upper zone where stretched vesicles, flow marks, and secondary folds are common and where vitrophyre may occur.

Figure 11. Flattened pumice fragments and small lithic inclusions within Cougar Point Tuff unit XI, from Deer Creek grade in West Fork Jarbidge River canyon. For scale, the jackknife is about 11 centimeters long.

BASAL BEDDED ASH ZONES

At the base of each cooling unit is a bedded air-fall volcanic ash layer that generally is between 1 and 3 meters thick (Figure 12). Typically, this material varies from white or tan to gray or nearly black. These ash deposits are characterized by numerous laminations and thin beds, arising from color and particle size variations. The layers typically vary from light colored and almost unconsolidated at the base to dark colored and hard at the top where fused by the overlying ash flow (Figure 12).

Nearly all of the material has a particle size of less than 2 millimeters. Only a minor proportion of lapilli-sized particles (2-64 millimeters) has been found, and nearly all fragments are less than a centimeter across. No volcanic blocks or bombs have been found. Ninety percent or more of the bedded ash is a mixture of shards, more or less equant to flattened glass particles, and glassy dust. Phenocrysts are generally present; typically they are the same minerals as in the overlying ash-flow portions of units. Feldspar phenocrysts are mainly crystal fragments, thus tending to be smaller than the intact phenocrysts in the ash-flow portion of a unit. Most commonly the volcanic rock inclusions are less than 2 millimeters across and range from angular to rounded, from glassy to lithoidal, and from pumiceous to devoid of vesicles. Rock fragments from nonvolcanic sources are exceedingly rare in these bedded ash deposits.

Much of the bedding in the basal bedded ash zones is the result of particle size variation. Graded beds with upwards-decreasing average particle size are common, and other, more complex particle size variations have also been noted. Massive ash zones up to 20-30 centimeters thick, which occur locally in the bedded ash layers, may be small ash flows. Locally, thin intervals within the basal ash zones are cross-bedded, generally with dips of less than 10 degrees and with cross-bedded sections comonly only a few centimeters thick. Whether these cross-beds resulted from base-surge deposition, water or aeolian deposition, or from some other origin is unknown.

The bedded ash zones are poorly exposed, because they are not resistant and because they become covered with rocks falling from the overlying cliffs. Local exposures do reveal that the ash was deposited on tan-colored, generally structureless, silt-sized material which probably represents old soil layers. In other places, however, the material under the bedded ash has been found to be white clay-sized laminated sedimentary material, probably of lacustrine origin, or coarse-grained sandstone composed principally of materials derived from underlying volcanic units and probably deposited in a fluvial or deltaic environment. Such features, along with local lithophysal zones near the bases of the overlying welded ash flows, suggest that in some places ash fell and ash flows erupted into shallow water.

The upper parts of basal ash zones commonly have been fused or welded to such an extent as to resemble

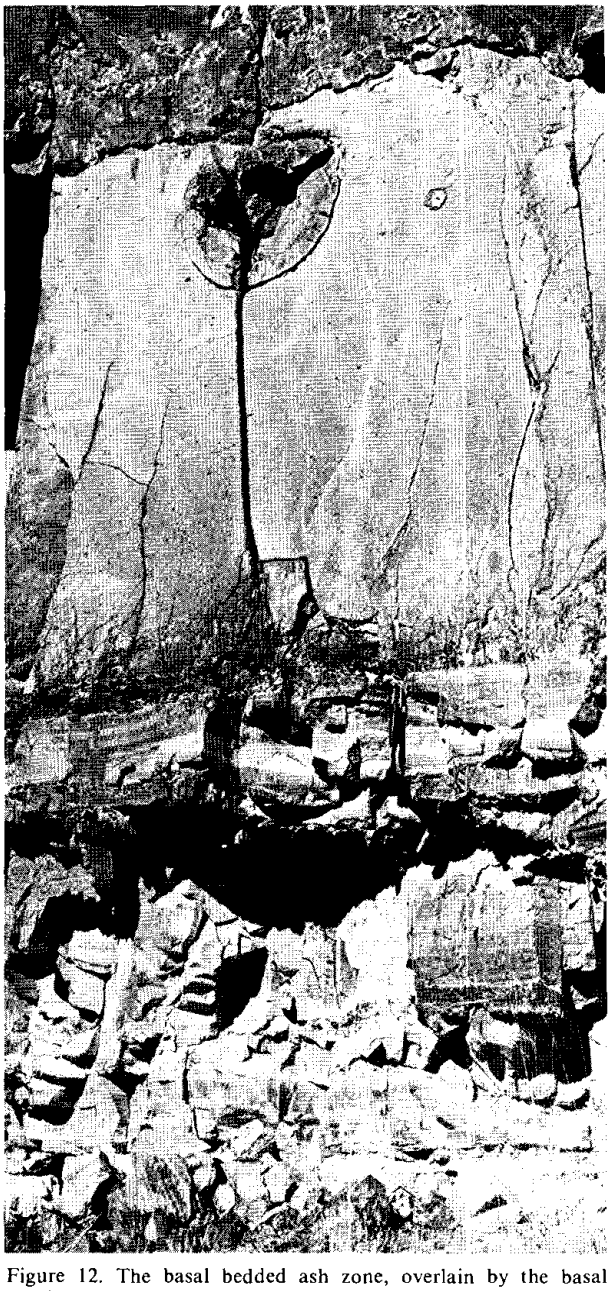

Figure 12. The basal bedded ash zone, overlain by the basal vitrophyre, of Cougar Point Tuff unit XV at Black Rock escarpment. Note that the upper part of the bedded ash zone is darker in color and more resistant where it has been thoroughly fused. The large spherulite in the basal vitrophyre in just below the bottom of the devitrified massive central zone. For scale, note the hammer immediately below the top of the basal bedded ash zone.

the dark-colored overlying basal vitrophyre zone (Figure 12). The basal ash, however, retains its bedded character, whereas the overlying basal vitrophyre is massive. Wherever observed, the contacts between the two zones are sharp and subhorizontal. The boundaries between the fused and nonfused portions of the basal bedded ash zones always are gradational, generally through an interval from 0.5 meter to 1.5 meters thick. Locally, beneath particularly thick units, the fusing has extended completely through the basal bedded ash zone and into the underlying sedimentary material.

BASAL VITROPHYRE ZONES

A vitrophyre layer occurs at the base of the ash-flow portion of each Cougar Point Tuff unit. These layers are black to dark gray and generally 1 to 3 meters thick (Figure 12). Thicker vitrophyre zones occur where the units are thin in their distal portions. Only locally did welding not extend to the base of the ash-flow portion of a unit to entirely fuse the particles into continuous glass, as at the base of IX at Black Rock.

The boundaries between basal vitrophyre layers and central lithoidal zones are sharp, slightly undulating, subhorizontal planes separating the reddish lithoidal rhyolite from the underlying dark-colored vitrophyre (Figure 13). The undulations result from convex-downward lithoidal growth surfaces that merged together at the frozen front of downward-progressing groundmass crystallization.

Red-colored spherulites are common in the basal vitrophyre zones (Figures 14 and 15). Their spacing varies from several meters apart to crowded so closely together that only patches of vitrophyre remain. Spherulites tend to be most abundant in the upper parts of the basal vitrophyre zones (Figure 12). Most spherulites are less than 15 centimeters across, although individuals may exceed one-half meter (Figure 15). Typically, all but the smallest have interior shrinkage cavities. Some cavities contain deposits of jasper, opal, chalcedony, carbonate minerals, zeolites, and possibly other minerals, but the quantity of material is generally minor. The shrinkage cavities typically are angular (Figures 12 and 15); star-shaped cross sections of 3 to 6 points are common. Ghosts of spherulites locally can be seen at the bottoms of the central lithoidal zones (Figure 13), as indicated by the angular shrinkage cavities.

MASSIVE CENTRAL ZONES

The massive central zone constitutes most of a typical cooling unit of the Cougar Point Tuff. These zones are completely welded lithoidal rhyolite, compacted to such an extent that virtually no pore space exists. It is primarily these zones which form the

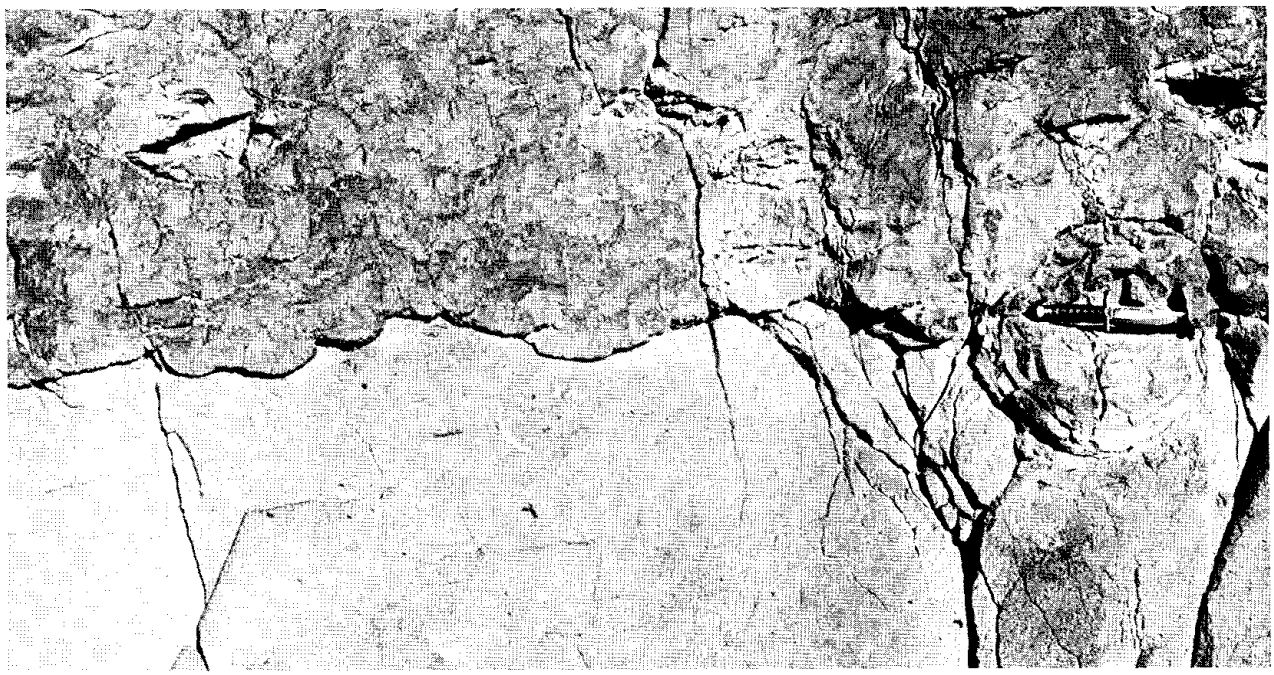

Figure 13. The contact between the basal vitrophyre zone (below) and devitrified rhyolite (above) at the bottom of the central massive zone in Cougar Point Tuff unit XV at Black Rock escarpment. Note the flattened pumice fragments within the basal vitrophyre and the ghosts of spherulites within the devitrified rhyolite.

Figure 14. Small spherulites enclosed within vitrophyre in Cougar Point Tuff unit XV where the unit is only a few meters thick near Murphy Hot Springs, East Fork Jarbidge River canyon.

prominent cliff exposures of the units (Figure 16), and which may weather to hoodoo-like vertical pinnacles (Figure 8). Only where a unit is thin does the massive central zone become subordinate in thickness to the basal vitrophyre and the upper zone. Where cooling units are less than about 10 meters thick, the massive zone may be absent, leading to poor exposures.

Most rhyolite in the massive central zones has only weakly developed, closely spaced, subhorizontal jointing (sheeting), but is characterized by fairly well-developed, widely spaced, vertical joints. Vertical joints are most conspicuously developed where the massive zones are thickest (Figures 1, 7, 8, and 16). The massive central zones characteristically are cut by numerous closely spaced irregular fractures that vary in orientation. This causes rock surfaces to be crumbly and leads to the rounding of pinnacles and other angular protuberances on cliffs (Figure 16). At the upper and lower margins of massive central zones, closely spaced, subhorizontal sheeting joints may be prominent (Figures 16 and 17). Such sheeting also tends to be more abundant where massive central zones are thin. The relatively abrupt upward increase in abundance of such sheeting marks the gradational transition between the central and upper zones in a unit.

Figure 15. Large spherulites in the basal vitrophyre zone of Cougar Point Tuff unit XV at Black Rock escarpment. Note the shrinkage cracks and minor encrustations of secondary minerals in the spherulites, and the flattened pumice fragments within the vitrophyre.

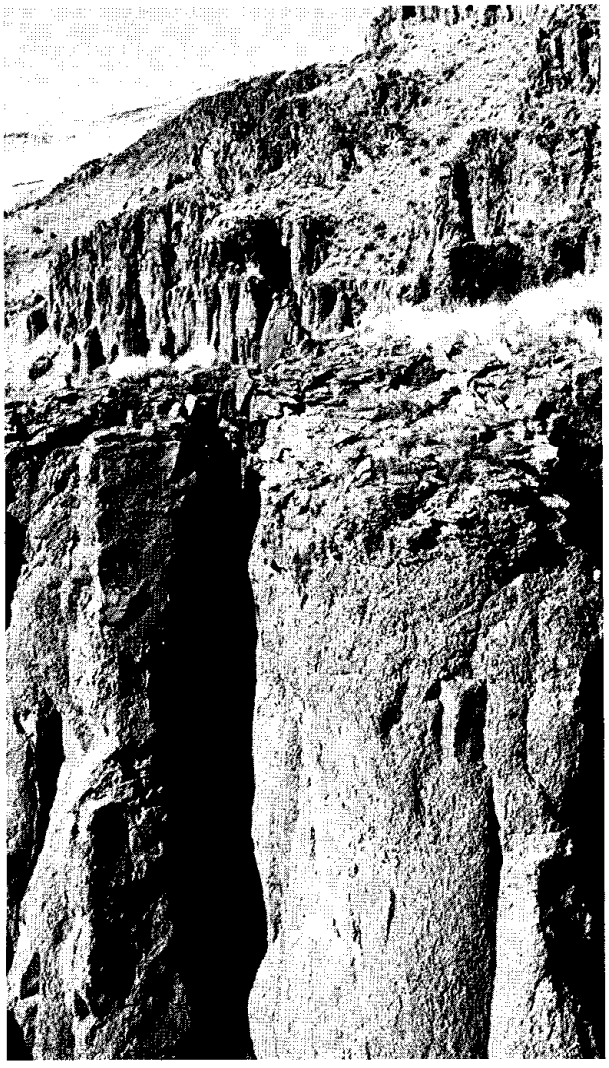

Figure 16. The upper part of the massive central zone in Cougar Point Tuff unit XI at Black Rock escarpment. Note how the upper 1 to 2 meters of the cliff has pronounced subhorizontal sheeting joints, marking the boundary between the massive central and upper zones.

UPPER ZONES

The upper zones consist mainly of lithoidal rhyolite which characteristically is quite variable in structure and appearance. Most upper-zone rhyolite is cut by well-developed, closely spaced, subparallel sheeting joints which commonly are contorted into foldlike forms (Figure 18). The upper zones contain local ramp structures and chaotically jointed areas where the sheeting varies from subhorizontal to steeply dipping within a few meters or less. Downward toward the massive central zones the sheeting becomes less pronounced and is confined to more nearly horizontal attitudes. The upper zone generally constitutes from less than one fourth to more than one half of a unit, depending on its thickness. Thinner units have a greater proportion of upper-zone material.

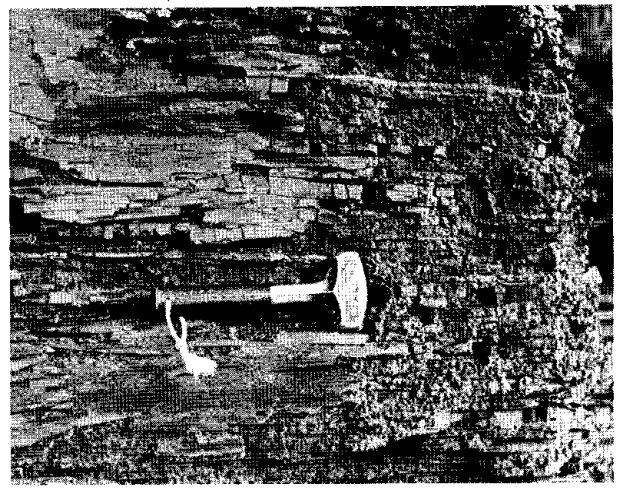

Figure 17. Well-developed subhorizontal sheeting joints near the base of the massive central zone of Cougar Point Tuff unit XII along Deer Creek grade, West Fork Jarbidge River canyon.

The rhyolite in the upper zones commonly contains vesicles. Most commonly these are elongate parallel to one another, and were partially to completely flattened to flow marks (Figure 19) after they were formed. Lithophysal horizons and zones of spherulites also occur locally in the upper zones.

A zone of vitrophyre has been observed at the very top of some units. At most locations, however, the tops of units are poorly exposed, or not exposed at

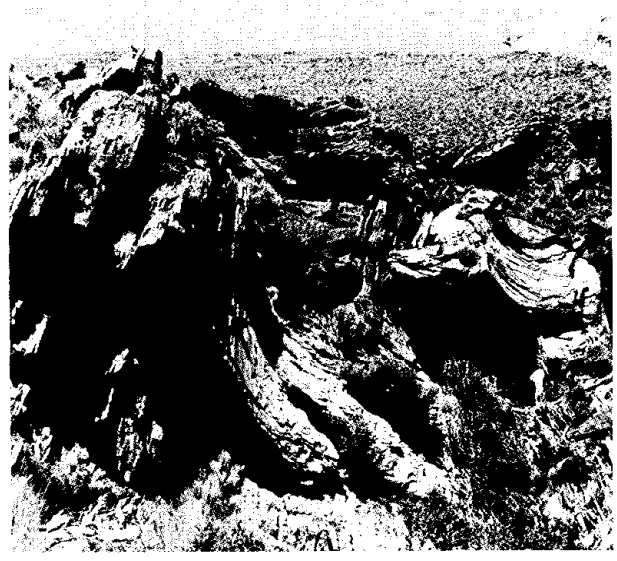

Figure 18. Curved sheeting joints indicating flow-folding in the upper zone of Cougar Point Tuff unit XV, at the rim of Black Rock escarpment, Bruneau Canyon.

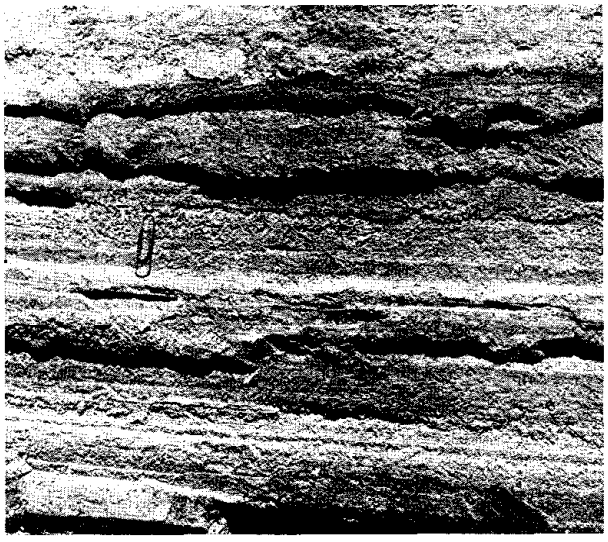

Figure 19. Prominent flow marks developed on a subhorizontal surface in the upper zone of Cougar Point Tuff unit XV. Note paper clip for scale.

all, because they are porous and easily eroded or have become covered by scree that has fallen down canyon walls from the overlying units; thus, not much is known of detailed relations at unit tops. The best exposure of an original cooling-unit top that has been found is in unit XV along the lower part of the grade leading out of Jarbidge Canyon on the road from Murphy Hot Springs to Rogerson in sec. 24, T. 16 S., R. 9 E. The ash flow is only a few meters thick here, and consists mainly of vitrophyre containing centimeter-sized spherulites but very few vesicles in its central part (Figure 14). In the upper meter of the unit the vitrophyre changes upwards from a dense black glass to a friable gray vitric ash, which, at the very top of the unit, is so weak that it can be hand-crushed. The upper contact is sharp and overlain by brown silty sediment, probably loess, containing fragments of the underlying gray ash.

LITHOPHYSAL ZONES

Lithophysal zones containing numerous angular to spherical gas cavities occur in most of the Cougar Point Tuff units. These zones vary from rather local features with limited lateral continuity to subhorizontal layers that have been traced for tens of kilometers, but they are not considered to be major subdivisions of the ash-flow units in the same fashion as the basal, central, and upper zones. Lithophysal zones most commonly are within a few meters of the upper or lower boundaries of the massive central zones of the units in which they occur. They range from about a meter to several meters thick. The spacing of individual gas cavities in these zones varies from widely separated to closely packed (Figure 10). Individual lithophysae may be nearly solid, resembling spherulites, but more commonly they are hollow vugs. Individual lithophysae in such zones generally are a few centimeters across and are essentially undeformed, commonly having irregular outlines but being equant overall. In other instances they may be flattened or somewhat elongate, indicating they formed before compaction and local lateral motion of the rhyolite had ended (Figure 10).

Some lithophysal zones were probably formed when successive ash emplacements were deposited closely enough in time to trap the last of the volatiles being expelled from the one below. This may be the origin of the thin, areally extensive zones such as the one in unit XIII. Other lithophysal zones, especially those locally near the base of a unit, very likely have resulted from the ash flow having come to rest above a moisture-laden zone. The lithophysae in some zones are associated with inclusions of what probably were pumice fragments, suggesting the gas cavities resulted from water initially trapped in the inclusions. In fact, some lithophysae contain marginal crusts of what may have been pumice.

In one place (upper zone of unit XI on Deer Creek grade, West Fork of Jarbidge Canyon), a horizontal lithophysal zone of undeformed gas cavities has been observed to cut across a zone of steeply inclined flattened pumice fragments and sheeting. This relationship establishes that those particular lithophysal cavities formed later than the sheeting and folding, and very likely shows lithophysal zones to be relatively late structures. The most common cause for lithophysal zones to form in the Cougar Point Tuff units is probably the entrapment of the last gasses that were expelled, as in this example.

ELONGATE VESICLES AND FLOW MARKS

The rhyolite in the upper zones of the units is variably vesicular, with scattered small vesicles to abundant vesicles more than a centimeter across. The amount of vesicularity generally increases upwards and towards the distal ends of the flows, but varies markedly on a local scale. Most vesicles are greatly stretched parallel to one another. Elongations with lengths of 10 to 100 times the diameters are normal. Most vesicles are subhorizontal, but some plunge at various angles, having been deflected by the same forces that formed and deformed the sheeting joints.

Parallel streaks or flow marks are locally numerous in lithoidal rhyolite of most of the Cougar Point Tuff units. These marks vary considerably in appearance

and size. Some are merely color variations on joint surfaces. Others, probably most, are shallow parallel grooves on subhorizontal sheeting-joint planes (Figure 19), and others are elongate vesicles which have not been completely flattened. Flow marks range from a millimeter to several centimeters wide and from about a centimeter to many meters long. It is common for streaks of various widths and lengths to occur in proximity to one another. The flow marks are considered to have been gas cavities that became extremely stretched in the direction the ash was flowing at the time of its final emplacement, and that then were flattened. Both the flow marks and stretched gas cavities are considered to be primary flow lineations in the sense of Chapin and Lowell (1979).

Linear streaks and elongate vesicles are most abundant in the upper zones of units, but have also been found near the bases of some massive central zones. Most flow marks occur in lithoidal rhyolite. Where elongate features occur in vitrophyre, they generally are seen to be open vesicles rather than completely flattened streaks.

The elongation directions of many flow marks and linear vesicles have been measured. At a given locality (perhaps tens of meters across) all generally are within 10 or 20 degrees of one another. Throughout much larger areas (a kilometer or more across) the streaks and vesicles tend to be subparallel, generally with azimuths approximately perpendicular to the margin of the Bruneau-Jarbidge eruptive center. All available flow marks and elongate vesicle orientations for units XV and XIII are plotted in Figure 20, where the azimuths can be seen to generally converge toward the interior of the eruptive center. Figure 20 also shows some areas where preexisting topographic obstructions may have caused local deviations in the flow-mark azimuths.

Flow-mark and elongate-vesicle azimuths have been measured in all the other Cougar Point Tuff units except X and III. The pattern for units XII and XI is essentially the same as shown for units XV and XIII in Figure 20. In general, the flow azimuths for the units below XI suggest that their source may have been somewhat west of the source region indicated for the upper units, but not enough measurements are available to be sure. If the marks do reveal a more westerly source, it would be consistent with the lower units being thicker in Bruneau Canyon to the west, than in Jarbidge Canyon.

PETROGRAPHY

PHENOCRYST MINERALOGY

Quartz, sanidine, plagioclase, augite, pigeonite, fayalitic olivine, magnetite, and ilmenite are the principal phenocryst minerals in the Cougar Point Tuff. Accessory minerals are zircon, monazite(?), and apatite. Notably absent are phenocrysts of hornblende, biotite, and hypersthene. The phenocryst

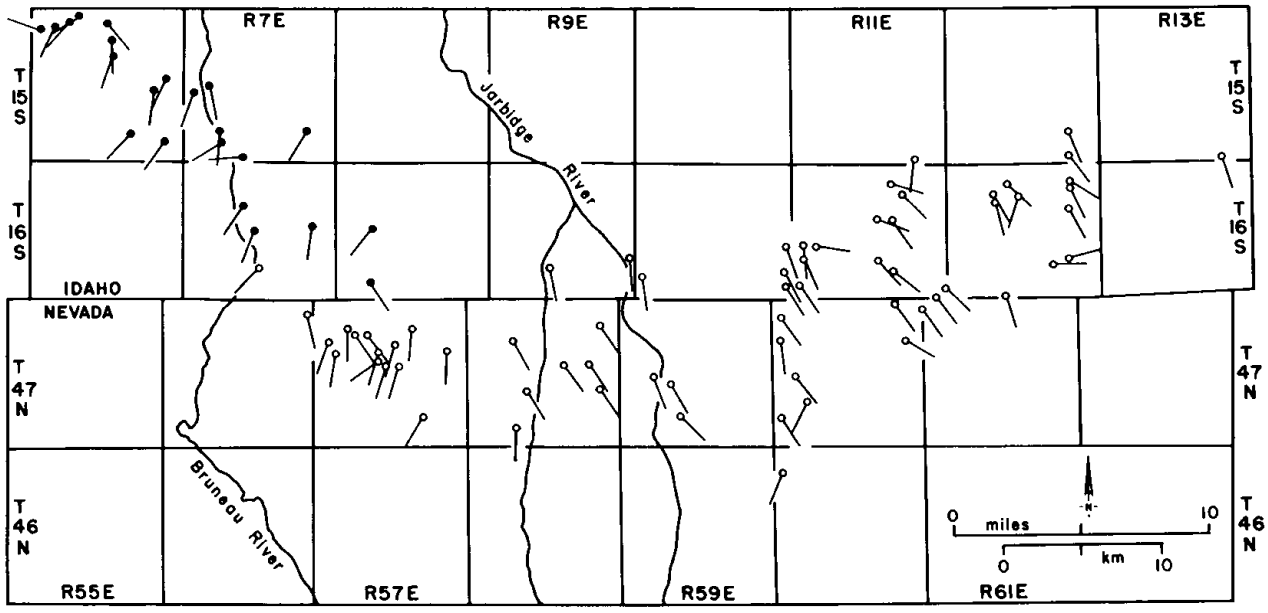

Figure 20. Regional distribution of flow azimuths, as measured from flow marks and elongate vesicles in Cougar Point Tuff units XV (solid symbols) and XIII (open symbols). The measurements are by Citron (1976), Bernt (1982), and Bonnichsen (unpublished data). The tails on the symbols indicate the inferred directions of flow away from the Bruneau-Jarbidge eruptive center.

assemblage suggests that the Cougar Point Tuff magmas were comparatively hot as they rose through the crust and that they apparently had relatively low water contents. Also notable is the occurrence of plagioclase-pyroxene-opaque oxide cumulophyric aggregates, commonly with metamorphic textures, within most of the Cougar Point Tuff units. These are most abundant in the more femic (VII, XII, and XV) and upper units, and are interpreted as fragments of protolithic material carried up from the magma source area.

The various Cougar Point Tuff units are mineralogically fairly homogeneous. Vertical zonation involving the loss or addition of a phenocryst phase has not been documented at any particular site. Slight vertical variations in the ratios of phenocryst minerals, however, do exist in some units. The principal lateral variation noted is the substitution of fayalite for pigeonite in thinner, probably more distal portions of some units. The total abundance of phenocrysts is greater in the more femic units (VII, XII, and XV) than in the other units. The abundance of phenocrysts decreases generally but sporadically away from the Bruneau-Jarbidge eruptive center in many of the cooling units.

Quartz occurs mainly as small, dipyramidal grains, nearly always between 0.05 and 0.3 millimeter across. These vary from euhedral to rounded and may be embayed; they probably crystallized from the magma, and then locally were partially resorbed by it. In some units, larger rounded to irregular quartz grains occur in addition; these probably are xenocrysts.

Sanidine occurs as euhedral to subhedral grains with only modest local zoning at crystal margins, and more commonly as crystal fragments. Unbroken grains range from 0.5 millimeter to 3 millimeters in length. Some sanidines are partially resorbed, with rim embayments and interior zones of isolated glass inclusions. The sanidine crystals tend to be more abundant and larger in the more silicic units. In some of these units sanidine has also locally overgrown and has partially replaced plagioclase or has formed micrographic intergrowths with quartz. The micrographic intergrowths occur as partial rims attached to sanidine crystals, and as broken fragments.

Plagioclase is abundant, and various textural types commonly are seen together in individual thin sections. Plagioclase compositions are mainly in the An_{30} to An_{55} range, with the higher anorthite contents occurring in the more femic units. Single plagioclase crystals, generally subhedral tablets or laths, and fragments broken from such grains, are common; these mainly are 0.5 and 2.0 millimeters long, but locally are as much as 4 or 5 millimeters long.

In many rocks some of the plagioclases have ordinary combined albite-Carlsbad twinning and weakly to strongly developed, normal or oscillatory concentric zoning. Such individuals are interpreted as phenocrysts which crystallized from the magma during ascent. Others have characteristics suggesting they are refractory protolithic material which was not entirely melted when the magma was generated. These include anhedral grains, grain fragments, and clots with annealed textures, patchy, irregular, or negligible zoning, and anhedral equant inclusions of pyroxene and opaque oxide minerals.

Cumulophyric aggregates of plagioclase, augite, pigeonite, magnetite, and perhaps ilmenite in variable proportions are common. These aggregates have internal textures ranging from plutonic igneous with subhedral crystal forms to metamorphic with anhedral grains arranged as in a granulite or as in refractory rocks from which substantial quantities of interstitial melt have been extracted. Individual aggregates are similar in size to the larger feldspar grains, ranging from a millimeter to about 4 millimeters across.

The plagioclases in the cumulophyric aggregates show little or no zoning or have patchy, irregular, or local domain zoning. Part of the plagioclase grains in many rocks show minor to extensive embaymentation, and contain small brown glass inclusions commonly arranged in internal zones, whereas adjacent grains may be unsieved. Although it may not be entirely evident in an individual thin section, it is hard to escape the conclusion that in most Cougar Point Tuff units the plagioclase phenocrysts are a mixture of crystals which grew from the magma and of grains inherited from the protolith.

The pyroxenes are a mixture of augite and pigeonite. No hypersthene has been observed. Augite occurs in all units and pigeonite in most, but pigeonite is absent in rocks containing fayalite. Pigeonite and augite are texturally identical, but their ratio varies with more pigeonite than augite in some rocks and the reverse in others. The pyroxenes occur as rounded equant to subhedral prismatic single crystals and as equant to irregular anhedral crystals in the cumulophyric aggregates. Some pyroxene grains are wholly enclosed within plagioclase, and pyroxene grains locally enclose rounded magnetite grains in some aggregates. Pyroxene crystals typically are 0.1 to 0.75 millimeter long, and few exceed this size. Rare poikilitic pyroxenes have been found, with groundmass material filling the holes rather than any mineral, suggesting a former included mineral was melted from the pyroxene during magma formation or ascent. Pyroxenes in glassy rocks commonly are fresh, but pyroxenes in lithoidal rhyolite are partially to completely oxidized.

Fayalitic olivine occurs in parts of units XI and XV and is ubiquitous in XIII. The olivine is texturally very similar to the pyroxenes but it generally occurs as isolated crystals; however, in a few rocks the olivine grains are attached to augite or magnetite. It is likely that most, if not all, of the olivine crystallized from the enclosing magma rather than representing part of the protolith. Olivine grains commonly are partially oxidized, primarily to opaque material (probably magnetite). They are preserved best in vitrophyre samples.

Opaque oxides occur in all of the Cougar Point Tuff units. Both magnetite and ilmenite probably are present, but systematic polished-section confirmations have yet to be made. Most of this material occurs as small (generally less than 0.25 millimeter) anhedral to euhedral equant, probably octahedral, grains, believed to be magnetite. Locally, irregular grains and groups of equant to irregular grains occur. Small plates of what is believed to be ilmenite occur in some units. These plates are most abundant in two of the least femic units (XI and XIII). Opaque oxide grains in the cumulophyric aggregates range in shape from anhedral equant to irregular. Some of the opaque grains in these aggregates may be ilmenite rather than magnetite, as is the case in some of the rhyolite lava flows in the Bruneau-Jarbidge eruptive center (Bonnichsen, 1982c this volume).

Accessory minerals identified in the Cougar Point Tuff are apatite, monazite(?), and zircon. Zircon probably is the most abundant. These minerals are most commonly associated with pyroxene and opaque oxide grains, especially those within the cumulophyric aggregates. Single crystals of zircon and monazite(?) have been noted, however, and apatite occurs as elongate grains enclosed within plagioclase in some rocks.

The Cougar Point Tuff is virtually free of hydrous phenocryst phases. The principal occurrences are in some of the lower units, where brown hornblende and biotite sporadically occur as partial rims on pyroxene. One partially hematized biotite grain was found as a free-floating phenocryst in unit V. No independent hornblende grains have been observed in numerous thin sections from the region around Bruneau and Jarbidge Canyons, but Bernt (1982) reported a single grain from unit XV in the Cat Creek-Sheep Creek area.

THE GROUNDMASS

The groundmass varies from wholly glassy to devitrified. Where glassy, it commonly is gray glass containing abundant microlites or brown glass with few, if any, microlites. The glass occurring in embayments and as inclusions in plagioclase, sanidine, and other minerals tends to be brown and free of crystallites. At the bases of the thicker units, the gray glass may contain wispy darker layers that probably represent squashed pumice fragments, but it generally shows little evidence of shard preservation. At the tops of the units and in the basal vitrophyres of thin units, however, shards are well preserved and vary in shape depending on their amount of compaction. The glass in shards commonly is brown and free of crystallites. Where shards are preserved it is also common to find small, variably compacted, angular to rounded, lumps of pumice and of less-vesicular layered glass of variable gray to brown color. Such fragments commonly are less than 2 millimeters across.

Where devitrified, the groundmass commonly is too fine-grained for its mineralogy to be readily distinguished. In the interior of the thick units, however, cooling evidently was prolonged enough so that groundmass quartz grew epitaxially from the surfaces of quartz phenocrysts to yield, in crossed polarizers, snowflake-like micrographic intergrowths with other groundmass constituents.

Where the rhyolite has been devitrified, it is common for the mafic minerals to have been partially to completely oxidized. In fact, the devitrification process generally involved strong oxidation, so as to impart a definite red color to most devitrified rocks, and to generate abundant very fine-grained hematite, and perhaps rutile, in the groundmass. In some rocks with partially crystallized groundmasses in which only a little compaction has occurred, some individual glass particles contained delicate dendritic growths of red opaque material, probably hematite.

This oxidation, although not understood in detail, seems to have strongly affected all of the Cougar Point Tuff units, but only some of the associated younger rhyolite lava flows to the same extent (Bonnichsen, 1982c this volume). The fact that the oxidation is generally restricted to the lithoidal portions of the rhyolite units but is rare in the glassy parts argues that the oxidation occurred during cooling of the flows, and is not an unrelated later feature.

Vesicles are common in the upper part of the Cougar Point Tuff units. All filling material has been identified as tridymite. Most vesicles are only partially filled, and some have no filling at all. No other vapor-phase mineral has been noted, although local quartz and calcite of probable secondary origin have been observed in a few vesicles.

CHEMICAL COMPOSITION OF THE COUGAR POINT TUFF

The major oxide analyses, norms, and abundances of some minor elements for a few Cougar Point Tuff samples are presented in Table 1. The major oxide abundances of these samples have been determined two or more times. The Table 1 values combine the available X-ray fluorescence and atomic absorption data and are thought to be more accurate, especially for Na_2O and MgO, than previously reported values for the same rocks (Bonnichsen, 1982a). The analyses in Table 1 were prepared in the same manner as those of the associated rhyolite lava flows (Table 1, Bonnichsen, 1982c this volume) and older volcanics from the region (Table 1, Bernt and Bonnichsen, 1982 this volume); thus, the three data sets can readily be compared.

For the Cougar Point Tuff units, samples that were analyzed from localities many kilometers apart reveal that each unit has a compositional range considerably narrower than the group as a whole (Figures 21 and 22; for details regarding individual samples see Bonnichsen, 1982a). Nearly all of the analyses used for Figures 21 and 22 are of basal vitrophyres. Some units have a composition easily distinguishable from that of adjacent units (for example, compare XI with XII), but other pairs (for example, compare VII with XII or XI with XIII) cannot easily be distinguished.

Some units are distinctly more femic than others. Inspection of the variation from unit to unit in Figures 21 and 22 reveals that a femic group of constituents (Fe_2O_3, MgO, CaO, TiO_2, MnO, P_2O_5, Sr, and Zr) varies in a coherent fashion with stratigraphic position, whereas a salic group (SiO_2, K_2O, Rb, Th, and Pb) shows opposing trends. Triangular variation diagrams showing the femic or salic behavior of some of the elements are also presented in Bonnichsen (1982a and 1982c this volume, Figure 34). The variation exhibited by Al_2O_3, Na_2O, Zn, and Mo is not distinctive enough to conclusively assign them to either group.

The Cougar Point Tuff generally becomes increasingly femic upwards (Figures 21 and 22); however, there are local reversals. Units VII, XII, and XV are the three most femic. The two reversals in this overall trend (between units VII and IX and between units XII and XIII) suggest that the Cougar Point Tuff consists of three cycles (separated by the horizontal dashed lines in Figures 21 and 22) and that in each cycle the magma became increasingly femic as successive batches were erupted. The lower cycle consists of units III, V, and VII; the middle cycle of units IX, X, XI, and XII; and the upper cycle of units XIII and XV. The two lava flows, the Triguero Homestead rhyolite (TH) and the Indian Batt rhyolite (IB) that directly overlie unit XV in Bruneau Canyon (Bonnichsen, 1982b and 1982c this volume), appear to continue the upward increase in femic constituents of this upper cycle.

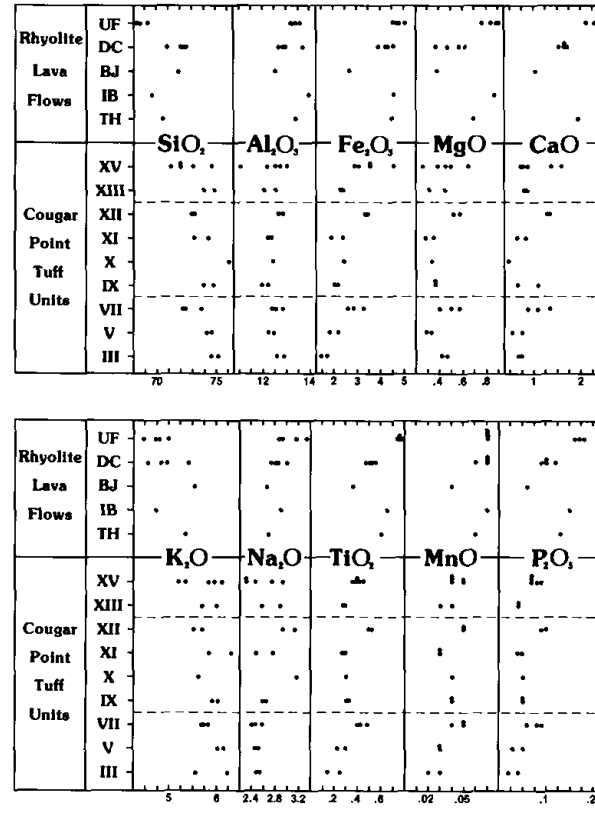

Figure 21. Weight percent of major oxides versus stratigraphic position of the Cougar Point Tuff units and of some rhyolite lava flows. The analyses plotted are from Tables 2, 3, and 4 in Bonnichsen (1982a). (BJ—Bruneau Jasper rhyolite, DC—Dorsey Creek rhyolite, IB—Indian Batt rhyolite, TH—Triguero Homestead rhyolite, UF—unnamed flows from the eastern part of the region.)

The subdivision of the Cougar Point Tuff into these compositional cycles should be considered as descriptive and not meant to imply any particular genetic relationship among successive magma batches. The eruption of each unit was a distinct volcanic event, separated from the eruption of the other units by sufficient time for complete cooling and the deposition of sediment layers between units. In many cases sufficient time elapsed for Earth's magnetic field to reverse its polarity (Bonnichsen, 1981 and Table 1, 1982b this volume). The overall chemical similarity of the Cougar Point Tuff units suggests a similar source and mode of formation for all.

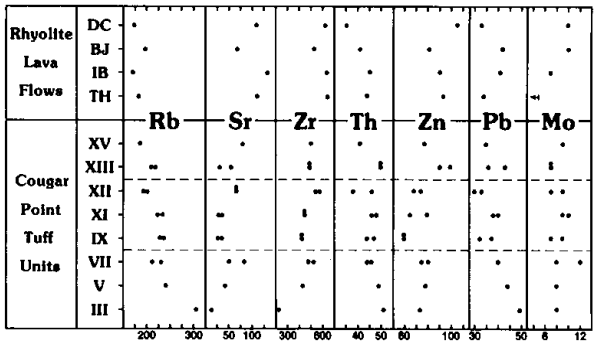

Figure 22. Abundance of minor elements (parts per million) versus stratigraphic position of the Cougar Point Tuff units and of some rhyolite lava flows. The analyses plotted are from Table 5 in Bonnichsen (1982a). Abbreviations used for the rhyolite lava flows are identified in the caption of Figure 21.

INITIAL STRONTIUM ISOTOPE RATIOS

The initial $^{87}Sr/^{86}Sr$ ratios for four Cougar Point Tuff units and one rhyolite lava flow, reported in Table 2, are calculated using alternate assumptions of a 12 million-year-old and a 9 million-year-old age. Although few radiometric dates are available for the Cougar Point Tuff and lava flows in the Bruneau-Jarbidge eruptive center (see Table 3, Bonnichsen, 1982b this volume), these assumed ages probably are sufficient to bracket the true Cougar Point Tuff age range, since unit VII was noted earlier to have an age of about 11.3 million years.

The strontium isotope ratios in Table 2 strongly suggest that the ash flows and lava flows in the Bruneau-Jarbidge eruptive center had a predominantly, if not exclusively, crustal origin, and are similar to other rhyolites in the Snake River Plain-Yellowstone Plateau volcanic province in their strontium isotope ratios, such as those reported by Leeman (1982 this volume), Leeman and Manton (1971), and Doe and others (1982).

DISCUSSION

The conditions and processes that led to the formation of many of the physical features that characterize the Cougar Point Tuff ash-flow units are discussed below. These features generally are discussed in the sequence in which they are believed to have formed, as the rhyolitic magmas erupted, flowed across the surface, came to rest, and were cooled and compacted.

Each Cougar Point Tuff unit formed from one or a succession of pyroclastic eruptions that blew hot vesiculated magma particles high into the atmosphere. The 1 to 3 meters of bedded ash at the base of each unit suggests that the pyroclastic eruptions began with large volumes of vesiculated magma being propelled to great enough heights so that the ash could be buoyed by air currents and transported through the atmosphere for long distances. Gravitational collapse of these eruption columns imparted high velocities to the hot ash and permitted it to flow long distances along the surface. The great lateral extent and uniformity of the units and the planar nature of their bases and internal layering suggests the hot ash flowed away from the venting areas over a terrain of low relief (Figures 1 and 2).

The large volumes of the units and their rapid eruption implies that subsidence probably occurred over the magma chambers (see Bonnichsen, 1982b this volume). Extensive younger rocks and the shallow erosion level do not permit knowing for sure whether such subsidence formed calderas. Taken collectively, however, the series of subsidences accompanying the ash-flow eruptions formed the Bruneau-Jarbidge eruptive center. The exposed portions of all of the Cougar Point Tuff units have been interpreted as outflow-facies rocks, rather than intracaldera-facies rocks; thicker deposits of the latter may be buried within the eruptive center.

The pyroclastic eruptions require that the magmas contained sufficient water for disruptive vesiculation to occur when the confining lithostatic pressure became sufficiently low, during their ascent through the upper crust. Much of the vesiculation may have occurred at relatively shallow depths, in comparison with the situation for ash flows in many other regions. Suggesting shallow vesiculation is the near absence of accidental xenoliths in the units. Evidently the magmas had little opportunity to incorporate wall-rock material as they rose, either below or above the level of vesiculation. Aside from the plagioclase-clinopyroxene-opaque oxide cumulophyric aggregates, which we have interpreted as protolithic fragments of the zone of melting rather than xenoliths from the zone of high-level intrusion, the only other common lithic inclusions are small angular to subrounded fragments of Cougar Point Tuff-type volcanic rocks. These very likely were obtained from earlier units at shallow depths, perhaps of a kilometer or less, or from the surface during flow of the ash away from the venting areas. The subsequent extrusion of the rhyolite lava flows that are petrologically similar to the Cougar Point Tuff (Bonnichsen, 1982c this volume), but with so little water that disruptive vesiculation did not occur, additionally suggests that the water contents of the Cougar Point Tuff magmas were

relatively low, restricting vesiculation to shallow depths.

The abundant vesicles, flow marks, and fold structures preserved in most of the units, the very dense nature of the massive central zones, and the fusing of the underlying bedded ash zones suggest that emplacement temperatures for the ash flows were high. This is confirmed by temperatures ranging from about 900° to more than 1000° C, as determined by electron microprobe analysis of iron-titanium oxides (Hildreth, 1981, Figure 3). Such high temperatures are in accord with the anhydrous nature of the phenocryst assemblage and the occurrence of pigeonite rather than hypersthene. They also point out the general similarity of the Cougar Point Tuff to other southwestern Idaho rhyolite units. Ekren and others (1982 this volume) also report very high emplacement temperatures which they determined by means of the coexisting oxide-mineral geothermometer.

The internal features of the cooling units suggest that, once erupted, each had a similar evolution. After gravitational collapse of the eruption columns, we believe the eruptive material consisted primarily of particles (mainly shards, some pumice, and a few lithic fragments) traveling at high speed away from the site of eruption as a dense cloud buoyed up by hot gases, possibly some of which were still being exsolved from the hot glass particles. This conventional glowing avalanche, or fluidized bed, flowage style seems plausible as the way the flows were transported the large distances from their sources, especially since shards and flattened pumice fragments are preserved in many units.

As the hot ash flowed away from its source it slowed down and eventually came to rest, after losing most of the gases which suspended the hot particles during flowage and making local structural adjustments while the hot masses compacted and cooled. Using the terminology of Chapin and Lowell (1979), the flowage away from the source, and the structures preserved from that part of a unit's history, are termed *primary*. Later motion and structures which formed after primary motion had ceased are termed *secondary*.

By this classification, the elongate vesicles and flow marks (Figures 19 and 20) in the units are primary structures, whereas the sheeting joints and folds defined by them, and the variety of compaction features, are secondary. This sequential age relation between the flow marks and sheeting is indicated by the observation that the elongate vesicles and flow marks have commonly been rotated to steeply dipping attitudes where they follow around the folds in the sheeting.

The existence of the flow marks and elongate vesicles shows that the ash flows had partly, if not largely, coalesced to viscous liquid similar to that in a rhyolitic lava flow before the cessation of primary motion. Such coalescence to a silicate melt before flowage was complete is termed primary welding by Chapin and Lowell (1979). Only in this way could have the elongate vesicles and flow marks been formed and preserved, since a liquid medium was necessary to contain the gas bubbles.

The later secondary flowage is manifested mainly by structures preserved in the upper zones of the

Table 2. Strontium isotope ratios for rhyolite units from the Bruneau-Jarbidge eruptive center.

Sample Number	Geologic Unit	Sample Location	Rb(ppm)	Sr(ppm)	Present Day $^{87}Sr/^{86}Sr$	Initial $^{87}Sr/^{86}Sr$ calculated for: 9 m.y. age	12 m.y. age
I-529	Dorsey Creek rhyolite	NE¼SW¼ sec. 3, T. 16 S., R. 9 E. Owyhee County, Idaho	117 ± 4	108 ± 1.3	0.71283 ± 0.00003	0.71223 ± 0.00004	0.71204 ± 0.00004
I-459	Cougar Point Tuff - XV	SE¼SW¼ sec. 9, T. 16 S., R. 7 E. Owyhee County, Idaho	190 ± 3	79 ± 1.7	0.71047 ± 0.00001	0.70958 ± 0.00003	0.70928 ± 0.00005
X-37	Cougar Point Tuff - XIII	NW¼ sec. 20, T. 47 N., R. 59 E. Elko County, Nevada	211 ± 4	29 ± 1.4	0.71234 ± 0.00004	0.70965 ± 0.00016	0.70875 ± 0.00020
I-841	Cougar Point Tuff - VII	SW¼NE¼ sec. 28, T. 47 N., R. 58 E. Elko County, Nevada	218 ± 3	82 ± 2.2	0.71165 ± 0.00003	0.71067 ± 0.00005	0.71034 ± 0.00005
I-569	Cougar Point Tuff - III	NW¼NE¼ sec. 28, T. 16 S., R. 7 E. Owyhee County, Idaho	306 ± 5	14.7 ± 0.1	0.71922 ± 0.00003	0.71152 ± 0.00016	0.70896 ± 0.00019

Analyzed at Geochronology Laboratory, Conoco, Inc. Research and Development Department, Ponca City, Oklahoma. All rubidium and strontium analyses and calculations are by Lois Jones using TEFA (tube excited X-ray fluorescence), except that strontium for sample I-569 was analyzed by James Rathman by isotope dilution. Each analysis is an average of six determinations and ± values are for a standard deviation of 2 σ. The interlaboratory strontium carbonate standard is NBS-987, with $^{87}Sr/^{86}Sr$ of 0.71036 ± 0.00002. All $^{87}Sr/^{86}Sr$ values are normalized to $^{86}Sr/^{88}Sr$ of 0.11940. Initial ratios were calculated using the ^{87}Rb decay constant of 1.42×10^{-11} yr^{-1}. All samples are vitrophyres from the bases of their units.

units. Secondary and probably primary structures as well, which may have formed in the central massive zones, very likely were destroyed by the essentially complete compaction which occurred later as the final step of secondary flowage and by the complete crystallization of those zones. Formation and folding of the sheeting joints, the compaction which occurred throughout the units as most of the remaining gases were expelled, and the freezing of devitrification fronts around spherulites and at the bases of the units are the most conspicuous of the secondary structures.

The near lack of secondary flowage structures that penetrate down through the units probably is the result of the flat topography on which they were deposited, rather than the lack of any capacity of the coalesced silicate liquids to undergo mass flowage like that in a rhyolite lava flow. Mass flowage could more easily occur if the material moved down a slope, such as would occur in an area of uneven topography.

The scarcity of flow banding in the vitrophyric portions of the units probably also suggests that the silicate liquids had nowhere to flow once they had been emplaced and coalesced to a viscous mass, rather than indicating any incapacity to flow had a slope been available. Flow banding is common in the vitrophyric parts of the rhyolite lava flows in the eruptive center and is thought (Bonnichsen, 1982c this volume) to have been caused mainly by mass flowage within a unit, rather than by simple compaction. After coalescence, the ash-flow sheets would have been nearly enough like the rhyolite lava flows, so that if mass flowage had occurred, one would expect flow-banding to commonly be preserved; it is rare, however.

Sheeting joints evidently formed and were deformed during secondary flowage, probably concurrent with, or shortly following, the onset of devitrification. Sheeting joints are restricted to lithoidal rhyolite in the Cougar Point Tuff units and in the rhyolite lava flows in the Bruneau-Jarbidge eruptive center; they do not occur in the glassy rocks (Figures 12-15, and see the discussion of sheeting joints and related structures in Bonnichsen, 1982c this volume). Parallel sheeting joints, the type most common in the upper zones of the cooling units, may have followed flow bands that were established in the coalesced flows immediately after the end of primary flowage, while gasses were still being expelled from the silicate liquid. Such gas would have been in bubbles which might have become concentrated into parallel planes, along which most of the shear during flowage of the coalesced silicate liquid was occurring. Such bubble layers would have become planes of weakness along which the sheeting joints would ultimately form, once devitrification and the concomitant shrinkage were to occur.

The end-stage of sheeting-joint formation may very well have coincided with the final compaction within the units, as the pattern typical of some, as depicted in Figure 17, is to outline elongate lensoidal fragments which may have undergone slight lateral slip relative to one another.

The "pencil" type of jointing locally found in lithoidal parts of most rhyolite lava flows in the Bruneau-Jarbidge eruptive center (Bonnichsen, 1982c this volume), where the intersection of two or more closely spaced sheeting-joint sets has formed elongate fragments, are virtually nonexistent in the Cougar Point Tuff units. This, again, may be due to the general lack of mass flowage of great enough thicknesses to develop sufficient internal stresses for this type of joint pattern to form.

Sheeting joints are not known to occur in any of the vitrophyres in the Cougar Point Tuff units and are rare and imperfectly developed in vitrophyres of the rhyolite lava flows in the eruptive center. In fact, it has been shown that sheeting joints in lithoidal rhyolite die out as they abut against adjacent vitrophyres in the lava flows (Bonnichsen, 1982c this volume, Figure 27). Both the ash-flow and lava-flow vitrophyres are characterized by jointing which is entirely different from the type in lithoidal rhyolite (compare Figures 12, 13, 14, and 15 with Figures 9, 16, 17, and 18). These observations strongly suggest that the crystallization and oxidation, or devitrification, of the ash flows commenced before the sheeting joints were formed. Very likely the shrinkage which accompanied devitrification was influential in promoting the formation of the sheeting. Devitrification may have commenced at temperatures as high as 950-1000° C (see Tuttle and Bowen, 1958, Figures 26-28, which show the increasing crystallization temperature and lowered content of water that can be dissolved in synthetic granite as the total pressure is decreased).

The basal vitrophyre zones were prevented from crystallizing because of the much more rapid cooling of the magma at the flow bases than within the flow interiors. The sharp, cuspate nature of the contacts between the basal vitrophyre zones and devitrified rock above them (Figure 13), imply that the crystallization fronts were moving downward until low temperatures froze them in place. The spherulitic ghosts within the devitrified rocks and the overall planar nature of these vitrophyre-lithoidal rock contacts attest to the lack of mass flowage or other lateral motion in the flow bases at any time since their formation.

As the ash-flow sheets devitrified and cooled further, they underwent a small percentage of shrinkage. Evidence that such shrinkage accompanied the devitrification process is indicated by the irregular open

cavities within many spherulites, especially large ones (Figure 15) that are enclosed within glassy rhyolite. The gases, which kept the shrinkage cavities in the spherulites inflated, very likely were the last bits of water dissolved in the silicate melts. They were released as the groundmass crystallized to an essentially anhydrous mixture of largely quartz and feldspars.

The last gases exsolved in the interior parts of the units are also believed to have been responsible for the generation of some of the lithophysal zones. Some lithophysal zones may have resulted from relatively complex cooling situations such as would arise along the boundary of successive ash flows in the same cooling unit. The little-deformed or nondeformed shapes of the gas cavities in these zones imply they formed late, and it is not unlikely that some may have formed during devitrification.

The bulk shrinkage that resulted from degasing, devitrification, and cooling would first have been accommodated by compaction. Later, during post-devitrification cooling, after compaction of the flows was complete, the prominent vertical joints that characterize the massive central zones formed. This essentially ended the development of the welded ash-flow sheets.

ACKNOWLEDGMENTS

The writers take pleasure in thanking John Bernt, Dale Conover, Falma Moye, and Maura Weathers Bird for their assistance during the field work; Nancy Wotruba, Steve Devine, Ivan Herrick, and Peter Hooper for their assistance with the X-ray fluorescence analyses; and Fred Hutchison for performing the atomic absorption analyses. We also are pleased to thank Bill Rehrig and Bob Wilson for making the arrangements with Conoco, Inc., to provide the minor element analyses, the strontium isotope analyses, and the potassium-argon age date. Finally, we would like to thank Bob Christiansen, Dave McIntyre, and Margi Jenks for their very helpful reviews of our manuscript.

REFERENCES

Alief, M. H., 1962, Variation in SiO_2, Al_2O_3, Fe_2O_3, CaO, MgO, Na_2O, K_2O and H_2O in some ignimbrites in southern Twin Falls County, Idaho: University of Idaho M.S. thesis, 60 p.

Bernt, John, 1982, Geology of the southern J-P Desert, Owyhee County, Idaho: University of Idaho M.S. thesis, 73 p.

Bernt, John and Bill Bonnichsen, 1982, Pre-Cougar Point Tuff volcanic rocks near the Idaho-Nevada border, Owyhee County, Idaho, *in* Bill Bonnichsen and R. M. Breckenridge, editors, Cenozoic Geology of Idaho: Idaho Bureau of Mines and Geology Bulletin 26.

Bonnichsen, Bill, 1981, Stratigraphy and measurements of magnetic polarity for volcanic units in the Bruneau-Jarbidge eruptive center, Owyhee County, Idaho: Idaho Bureau of Mines and Geology Open-File Report 81-5, 75 p.

———, 1982a, Chemical composition of the Cougar Point Tuff and rhyolite lava flows from the Bruneau-Jarbidge eruptive center, Owyhee County, Idaho: Idaho Bureau of Mines and Geology Open-File Report 82-1, 22 p.

———, 1982b, The Bruneau-Jarbidge eruptive center, southwestern Idaho, *in* Bill Bonnichsen and R. M. Breckenridge, editors, Cenozoic Geology of Idaho: Idaho Bureau of Mines and Geology Bulletin 26.

———, 1982c, Rhyolite lava flows in the Bruneau-Jarbidge eruptive center, southwestern Idaho, *in* Bill Bonnichsen and R. M. Breckenridge, editors, Cenozoic Geology of Idaho: Idaho Bureau of Mines and Geology Bulletin 26.

Bushnell, Kent, 1967, Geology of the Rowland quadrangle, Elko County, Nevada: Nevada Bureau of Mines Bulletin 67, 38 p.

Chapin, C. E. and G. R. Lowell, 1979, Primary and secondary flow structures in ash-flow tuffs of the Gribbles Run paleovalley, central Colorado, *in* C. E. Chapin and W. E. Elston, editors, Ash-Flow Tuffs: Geological Society of America Special Paper 180, p. 137-154.

Citron, G. P., 1976, Idavada ash-flows in the Three Creek area, southwestern Idaho, and their regional significance: Cornell University M.S. thesis, 83 p.

Coats, R. R., 1964, Geology of the Jarbidge quadrangle, Nevada-Idaho: U. S. Geological Survey Bulletin 1141-M, 24 p.

Doe, B. R., W. P. Leeman, R. L. Christiansen, and C. E. Hedge, 1982, Lead and strontium isotopes and related trace elements as genetic tracers applied to the Quaternary rhyolite-basalt association of the Yellowstone Plateau volcanic field, U.S.A.: Journal of Geophysical Research, v. 87, p. 4785-4806.

Ekren, E. B., D. H. McIntyre, E. H. Bennett, and H. E. Malde, 1981, Geologic map of Owyhee County, Idaho, west of 116° West longitude: U. S. Geological Survey Miscellaneous Investigations Series Map I-1256, scale 1:125,000.

Ekren, E. B., D. H. McIntyre, E. H. Bennett, and R. F. Marvin, 1982, Cenozoic stratigraphy of western Owyhee County, Idaho, *in* Bill Bonnichsen and R. M. Breckenridge, editors, Cenozoic

Geology of Idaho: Idaho Bureau of Mines and Geology Bulletin 26.

Fifer, H. C., Jr., 1960, Geology of a portion of the Jarbidge 1 quadrangle, Elko County, Nevada: University of Oregon M.S. thesis, 48 p.

Higgs, N. B., 1960, The geology of the southeastern part of the Jarbidge 1 quadrangle, Elko County, Nevada: University of Oregon M.S. thesis, 100 p.

Hildreth, Wes, 1981, Gradients in silicic magma chambers: implications for lithospheric magmatism: Journal of Geophysical Research, v. 86, p. 10153-10192.

Hope, R. A. and R. R. Coats, 1976, Preliminary geologic map of Elko County, Nevada: U. S. Geological Survey Open-File Report 76-779.

Leeman, W. P., 1982, Rhyolites of the Snake River Plain-Yellowstone Plateau province, Idaho and Wyoming: a summary of petrogenetic models, *in* Bill Bonnichsen and R. M. Breckenridge, editors, Cenozoic Geology of Idaho: Idaho Bureau of Mines and Geology Bulletin 26.

Leeman, W. P. and W. I. Manton, 1971, Strontium isotopic composition of basaltic lavas from the Snake River Plain, southern Idaho: Earth and Planetary Science Letters, v. 11, p. 420-434.

Mathias, D. E., 1959, The geology of the northern part of the Elk Mountains, Elko County, Nevada: University of Oregon M.S. thesis, 73 p.

Ross, C. S. and R. L. Smith, 1961, Ash-flow tuffs: their origin, geologic relations, and identification: U. S. Geological Survey Professional Paper 366, 81 p.

Smith, R. L., 1960, Zones and zonal variations in welded ash flows: U. S. Geological Survey Professional Paper 354-F, p. 149-159.

Stewart, J. H. and J. E. Carlson, 1976, Cenozoic rocks of Nevada: Nevada Bureau of Mines and Geology Map 52.

———, 1978, Geologic map of Nevada: U. S. Geological Survey, scale 1:500,000.

Tuttle, O. F. and N. L. Bowen, 1958, Origin of granite in the light of experimental studies in the system $NaAlSi_3O_8$-$KAlSi_3O_8$-SiO_2-H_2O: Geological Society of America Memoir 74, 153 p.

Wilson, H. D. B., L. C. Kilburn, A. M. Graham, and Ken Ramlal, 1969, Geochemistry of some Canadian nickeliferous ultrabasic intrusions, *in* H. D. B. Wilson, editor, Magmatic Ore Deposits—A Symposium: Economic Geology Monograph 4, p. 294-309.

Rhyolite Lava Flows in the Bruneau-Jarbidge Eruptive Center, Southwestern Idaho

by

Bill Bonnichsen[1]

ABSTRACT

In the Bruneau-Jarbidge eruptive center in southwestern Idaho, eight to twelve large rhyolite lava flows were erupted into and generally fill the structural and topographic basin left after the eruption of the Cougar Point Tuff. Several of the rhyolite flows are about 100 meters thick and contain minimum volumes of about 10 cubic kilometers each. Two and perhaps three are much larger; the largest (Sheep Creek rhyolite) exceeds 250 meters in thickness and contains 200 cubic kilometers or more of rhyolite.

The flows have massive lithoidal central zones cut by vertical shrinkage joints. Where well exposed in canyons, these zones occur as double cliffs separated by a medial slope. The margins of the flows typically consist of flow lobes separated by structurally complex zones of sheeted and brecciated rhyolite similar to that in the upper zones. The flow bases may be massive or brecciated glassy rhyolite. Brecciated vitrophyre generally occurs in marginal areas, and massive vitrophyre occurs in the flow interiors. The upper zones of the flows typically are a mixture of glassy and lithoidal rhyolite and are complicated by various types of breccia, and by complex jointing and folding patterns. The interior parts of some flows contain large gas cavities in their upper zones.

The rhyolite contains phenocrysts of plagioclase, augite, pigeonite, and opaque oxides. Some flows contain quartz, and a few contain sanidine as well as quartz. None of the flows contains hypersthene, in contrast to several flows in areas contiguous to the eruptive center that do. Like the earlier Cougar Point Tuff units, the rhyolite flows contain plagioclase-pyroxene-opaque oxide cumulophyric aggregates. These have been interpreted to be fragments of the crustal rocks that were being melted in the zone where the rhyolitic magmas formed.

All of the flows except one have fairly uniform chemical compositions. They differ from one another primarily in their proportions of SiO_2 and the femic group of constituents (Fe, Mg, Ca, Ti, Al, P, Mn). Collectively, the rhyolite flows compositionally overlap with the Cougar Point Tuff units, but extend to more femic compositions.

The rhyolite flows are considered to be closely related in origin to the Cougar Point Tuff units. Both groups of units are thought to have resulted from the injection of numerous successive large-volume batches of basaltic magma into quartz- and alkali feldspar-rich crustal rocks. A substantial portion of the crustal rocks underlying the eruptive center is thought to have been melted under relatively anhydrous conditions. As time passed, the crustal zone became dehydrated and depleted in its least refractory constituents, resulting in the general trend of the later rhyolitic magmas becoming more femic, and containing so little water that the later magmas erupted from fissures as lava flows rather than ash flows.

INTRODUCTION

Several large rhyolite lava flows occur within the Bruneau-Jarbidge eruptive center in the eastern part of Owyhee County, southwestern Idaho (see Figures 1-3, Bonnichsen, 1982b this volume for location and geologic map). They lie beneath a partial cover of Banbury Basalt and local accumulations of lacustrine, fluvial, and fanglomeratic sediments and above the Cougar Point Tuff, which previously had been erupted from the same volcanic center.

The principal objectives of this paper are to describe the stratigraphic relations and the physical, petrographic, and chemical characteristics of the rhyolite lava flows, to compare them to the related but earlier Cougar Point Tuff, and to discuss the manner in which the rhyolitic magmas may have originated. This paper is a companion to others in this volume that describe the Bruneau-Jarbidge eruptive center (Bonnichsen, 1982b) and the Cougar Point Tuff (Bonnichsen and Citron, 1982); thus extensive reference has been made to figures and tables in these

[1]Idaho Bureau of Mines and Geology, Moscow, Idaho 83843.

Bonnichsen, Bill, 1982, Rhyolite lava flows in the Bruneau-Jarbidge eruptive center, southwestern Idaho, *in* Bill Bonnichsen and R. M. Breckenridge, editors, Cenozoic Geology of Idaho: Idaho Bureau of Mines and Geology Bulletin 26, p. 283-320.

accompanying papers.

Rhyolite lava flows are an integral part of the silicic volcanism in the Snake River Plain volcanic province. The occurrence and nature of such flows or of volcanic domes elsewhere in the province are noted in this volume by Bernt and Bonnichsen (1982), Christiansen (1982), Ekren and others (1982), Leeman (1982a, 1982b, and 1982c), Spear and King (1982), and Struhsacker and others (1982). The features within the rhyolite lava flows discussed in this paper are probably a good guide to the nature of other rhyolite lava flows exposed or buried elsewhere in the volcanic province. The excellent exposures of the rhyolite lava flows in the canyons of the Bruneau River and its tributaries makes the eastern part of Owyhee County a unique area within the volcanic province in which to examine the characteristics of the Snake River Plain-type of rhyolite lava flows in three dimensions.

THE RHYOLITE LAVA FLOWS

The individual rhyolite flows will be described in ascending stratigraphic order, although the exact positions of some have not been established. The relative stratigraphic position of most of the flows, and of the Cougar Point Tuff units and some of the basalt units within the Bruneau-Jarbidge eruptive center, is summarized in Figure 10 of Bonnichsen (1982b this volume). The apparent magnetic polarities and the number of determinations upon which these polarities are based for most of the rhyolite flows are summarized in Table 1 of that paper.

One or more chemical analyses are available for all of the rhyolite units discussed below. A few are presented in Table 1, and others have been published previously (Bonnichsen, 1982a). Most of the analyses available for the rhyolite flows, however, have yet to be published. To indicate the chemical variability within the group of rhyolite flows from the Bruneau-Jarbidge eruptive center, partial analyses of thirty-five samples from within the eruptive center and six rhyolite flows from the area northeast of the eruptive center are summarized in Figure 1 and in a later illustration (Figure 33) that compares the compositions of the rhyolite lava flows and the Cougar Point Tuff.

Twelve different flows are discussed below. For a few of them (the lower rhyolites at Poison Creek and Louse Creek, the rhyolite of the Juniper-Clover area, and possibly the Three Creek rhyolite), it has yet to be clearly established if they are separate units, or if they are parts of other flows. Thus the number of post-Cougar Point Tuff rhyolite lava flows known in the eruptive center is between eight and twelve. Some of the principal features of the rhyolite lava flows within the eruptive center, noted in the following discussion, have been summarized for easy reference in Table 2.

All of the rhyolite lava flows discussed below are younger than the Cougar Point Tuff. Two additional rhyolite lava flows are known to be intercalated within the Cougar Point Tuff between units XII and XIII in the Black Rock escarpment area of Bruneau Canyon. One is visible at the north end of the escarpment (Figure 7, Bonnichsen and Citron, 1982 this volume). These older flows seem the same in their physical and petrologic characteristics as the ones discussed in this article. Their existence suggests that additional older rhyolite lava flows may be buried in the eruptive center, and points out that not all of the rhyolite flows within the eruptive center postdate the Cougar Point Tuff.

Rhyolite flows, similar to those within the Bruneau-Jarbidge eruptive center, occur in adjacent areas. One, the Johnstons Camp rhyolite, occurs in the upper Sheep Creek area a few kilometers southwest of the eruptive center. This one has been shown by Bernt and Bonnichsen (1982 this volume) to be older than the Cougar Point Tuff. It apparently erupted from a local center of Snake River Plain-type silicic volcanism in the upper Sheep Creek area before the establishment of the Bruneau-Jarbidge eruptive center. Other flows very similar to those in the Bruneau-Jarbidge eruptive center occur in a 30 by 50 kilometer zone a few kilometers northeast of the eruptive center. Six rhyolite samples from that region have been included in Figure 1 for comparison with the flows from within the eruptive center. The rhyolite in that area is discussed briefly at the end of this section.

TRIGUERO HOMESTEAD RHYOLITE

The Triguero Homestead rhyolite is exposed for more than 12 kilometers in Bruneau Canyon between the southeast part of sec. 1, T. 14 S., R. 7 E., on the north, to the north edge of sec. 18, T. 15 S., R. 7 E., on the south (see Figure 2, Bonnichsen, 1982b this volume, for location). The unit is named for the Frank Triguero Homestead in Bruneau Canyon. The Triguero Homestead rhyolite lies below the Indian Batt rhyolite (Figure 2). At the southern end of its exposure, it overlies unit XV of the Cougar Point Tuff. The Triguero Homestead rhyolite is also exposed beneath the Indian Batt rhyolite near the confluence of Cat Creek with Sheep Creek, about 8 kilometers west of Bruneau Canyon. The Triguero

Homestead rhyolite does not extend as far north in Bruneau Canyon as reported earlier (Bonnichsen, 1981). Petrography and chemical analyses show that the lower rhyolite flow in the canyon north of Indian Batt Cabin is unlike the Triguero Homestead rhyolite. The unit to the north has been named the Cedar Tree rhyolite, and is discussed next.

The phenocryst minerals in the Triguero Homestead rhyolite are plagioclase, augite, pigeonite, and opaque oxides; no quartz or sanidine was detected in the four thin sections examined. A chemical analysis of one sample from the unit is included in Table 1 (no. 1). Four chemical analyses (Figure 1, symbol TH) indicate that the Triguero Homestead rhyolite is intermediate in composition compared with the other flows. The unit has normal magnetic polarity (Table 1, Bonnichsen, 1982b this volume).

Near Triguero Homestead, where the base of the unit is exposed, the flow is seen to approximately 100 meters thick. In that area, the basal vitrophyre contains remarkably well-developed columnar joints (Figure 3). Also occurring beneath the Triguero Homestead rhyolite in that area (Figure 2), but not well exposed, are tens of meters of volcanic ash, which contains pumice fragments, vitrophyre blocks, and locally disrupted (slumped?) bedding. These ash occurrences suggest that the vent or fissure through which the rhyolite was erupted may be hidden nearby. At its north end, the marginal breccia zone of the flow is exposed. This breccia consists of poorly stratified to nonstratified ash containing vitrophyre blocks (Figure 4). Based on its exposed dimensions, the Triguero Homestead rhyolite is estimated to have a volume of 10 cubic kilometers or more.

CEDAR TREE RHYOLITE

The Cedar Tree rhyolite is exposed beneath the Indian Batt and Long Draw rhyolite units for about 6 kilometers in Bruneau Canyon, from just north of Indian Batt Cabin in sec. 36, T. 13 S., R. 6 E., northward to the mouth of Long Draw at the north edge of sec. 18, T. 13 S., R. 7 E., where it disappears beneath the Long Draw rhyolite. Previously, the Cedar Tree rhyolite was considered to be part of the Triguero Homestead rhyolite (Bonnichsen, 1981), but its chemical composition and phenocryst assemblage have shown it to be a separate flow. Its age, relative to the Triguero Homestead rhyolite, is not known. It has been named for the Cedar Tree trail on the west side of Bruneau Canyon in secs. 12 and 13, T. 13 S., R. 6 E. The unit appears to be about 100 meters thick in Bruneau Canyon.

The Cedar Tree rhyolite (Figure 1, symbol CT) is more silicic than many of the rhyolite flows in the Bruneau-Jarbidge eruptive center. The unit contains phenocrysts of quartz, sanidine, plagioclase, augite, pigeonite, and opaque oxides (four thin sections). The quartz grains are typically equant dipyramids with rounded corners, but they are not embayed. They range to a maximum diameter of about 0.5 millimeter. The unit has normal magnetic polarity (Table 1, Bonnichsen, 1982b this volume).

LONG DRAW RHYOLITE

The Long Draw rhyolite is named for Long Draw, a tributary which joins Bruneau Canyon near Indian Hot Springs (Figure 2, Bonnichsen, 1982b this volume). The Long Draw rhyolite is exposed for more than 6 kilometers upstream in Bruneau Canyon from the Indian Hot Springs area and at the bottom of Jarbidge Canyon for about 4 kilometers upstream from the mouth of the Jarbidge River. At its northernmost exposure, about a kilometer downstream from Indian Hot Springs, the unit disappears beneath the Bruneau Jasper rhyolite. Near the mouth of Long Draw, where its base is exposed, the Long Draw rhyolite is about 100 meters thick.

In the Indian Hot Springs area and upstream in Bruneau and Jarbidge Canyons, the Long Draw rhyolite is overlain by the Indian Springs basalt. To the southwest in Bruneau Canyon the original southern margin of the flow, which consists of a sequence of flow lobes (Figure 5), is exposed in the northeastern part of sec. 13, T. 13 S., R. 6 E. Here, the Long Draw rhyolite is sandwiched between the Dorsey Creek flow (above) and the Cedar Tree flow (below), so that it is at the same stratigraphic level as the Indian Batt rhyolite flow which occurs about 4 kilometers farther south in Bruneau Canyon. It is doubtful if these two flows are time equivalents, however, because their magnetic polarities appear to be different.

Two chemical analyses of the Long Draw rhyolite (Figure 1, symbol LD) show that the unit is less silicic and more iron-rich than many of the other flows in the eruptive center. The unit contains phenocrysts of plagioclase, augite, pigeonite, and opaque oxides, but quartz and sanidine have not been found (four thin sections). The Long Draw rhyolite has normal magnetic polarity (Table 1, Bonnichsen 1982b this volume).

The similarities in chemical composition, phenocryst assemblage, and magnetic polarity of the Long Draw rhyolite with the lower rhyolite at Louse Creek (discussed next) in Sheep Creek canyon a few kilometers to the west, suggest that the two may be part of the same flow. If the lower rhyolite at Louse Creek is part of the Long Draw flow, the areal dimensions

Table 1. Chemical analyses and CIPW norms for representative samples of rhyolite lava flows from the Bruneau-Jarbidge eruptive center and vicinity.

Unit	1 TH	2 JB	3 DC	4 DC	5 DC	6 UF	7 UF
			Major oxides in weight percent				
SiO_2	70.61	68.97	72.74	70.90	72.00	69.18	68.45
Al_2O_3	13.18	13.90	13.62	12.66	12.75	13.53	13.26
TiO_2	.60	.66	.55	.51	.52	.77	.74
Fe as Fe_2O_3	4.40	4.53	4.47	4.24	4.24	4.76	4.59
MnO	.06	.06	.07	.06	.07	.07	.07
CaO	1.88	2.36	1.65	1.67	1.62	2.27	2.12
MgO	.46	.75	.38	.37	.32	.83	.84
K_2O	5.29	4.86	4.78	4.53	5.36	4.93	4.71
Na_2O	2.82	2.92	3.07	2.74	2.84	3.04	2.92
P_2O_5	.12	.14	.09	.12	.09	.16	.16
Total	99.42	99.15	101.42	99.61	99.81	99.54	100.02
			Minor elements in parts per million				
Rb	182	170	--	--	173	--	--
Sr	110	133	--	--	109	--	--
Zr	642	642	--	--	623	--	--
Pb	34	41	--	--	33	--	--
Zn	93	90	--	--	105	--	--
Th	44	45	--	--	35	--	--
Mo	<5	7	--	--	10	--	--
			CIPW norms				
qz	27.49	25.51	29.66	32.08	29.05	25.04	26.53
or	32.15	29.55	28.45	28.05	32.45	29.85	29.05
ab	26.05	26.95	27.80	25.80	26.15	28.00	27.35
an	7.90	10.78	7.65	7.85	6.38	8.93	9.58
co	0	0	.68	.58	0	0	0
px	3.40	4.01	2.90	2.62	3.21	4.69	3.87
mt	1.89	1.95	1.89	2.01	1.83	2.04	2.19
hm	0	0	0	0	0	0	0
il	.86	.96	.78	.74	.74	1.10	1.08
ap	.27	.29	.19	.27	.19	.35	.35

Notes

Except as noted below, the samples were analyzed for major oxides by a combination of X-ray fluorescence and atomic absorption at Washington State University (XRF) and the Idaho Bureau of Mines and Geology (AA) and for minor elements by X-ray fluorescence at the Research and Development Department of Conoco, Inc.

For samples in which only the total iron was analyzed the CIPW norms were calculated by assigning 40 atom percent of the Fe to Fe_2O_3 and 60 atom percent to FeO.

1. Sample I-448, vitrophyre from the Triguero Homestead rhyolite flow from SE¼NW¼ sec. 30, T. 14 S., R. 7 E., Owyhee County, Idaho.

2. Sample I-445, basal vitrophyre from the Indian Batt rhyolite flow from SE¼NW¼ sec. 30, T. 14 S., R. 7 E., Owyhee County, Idaho.

Table 1. continued

3. Sample I-84, lithoidal rhyolite from the base of the Dorsey Creek rhyolite flow from NE¼SE¼ sec. 10, T. 16 S., R. 9 E., Owyhee County, Idaho.

4. Sample I-84, same description and location as given in 3. Analyzed by K. Ramlal at the University of Manitoba, 1972, by methods described in Wilson and others, 1969. The total includes 1.96 percent H_2O, 0.08 percent CO_2, 0.01 percent S, and Fe reported as 1.84 percent Fe_2O_3 and 2.16 percent FeO.

5. Sample I-529, basal vitrophyre of the Dorsey Creek rhyolite flow from NE¼SW¼ sec. 3, T. 16 S., R. 9 E., Owyhee County, Idaho.

6. Sample I-15, basal vitrophyre from an unnamed rhyolite lava flow near Balanced Rock, NE¼ sec. 20, T. 10 S., R. 13 E., Twin Falls County, Idaho.

7. Sample I-15, same description and location as given in 6. Analyzed by K. Ramlal at the University of Manitoba, 1972, by methods described in Wilson and others, 1969. The total includes 2.42 percent H_2O and Fe reported as 2.01 percent Fe_2O_3 and 2.32 percent FeO.

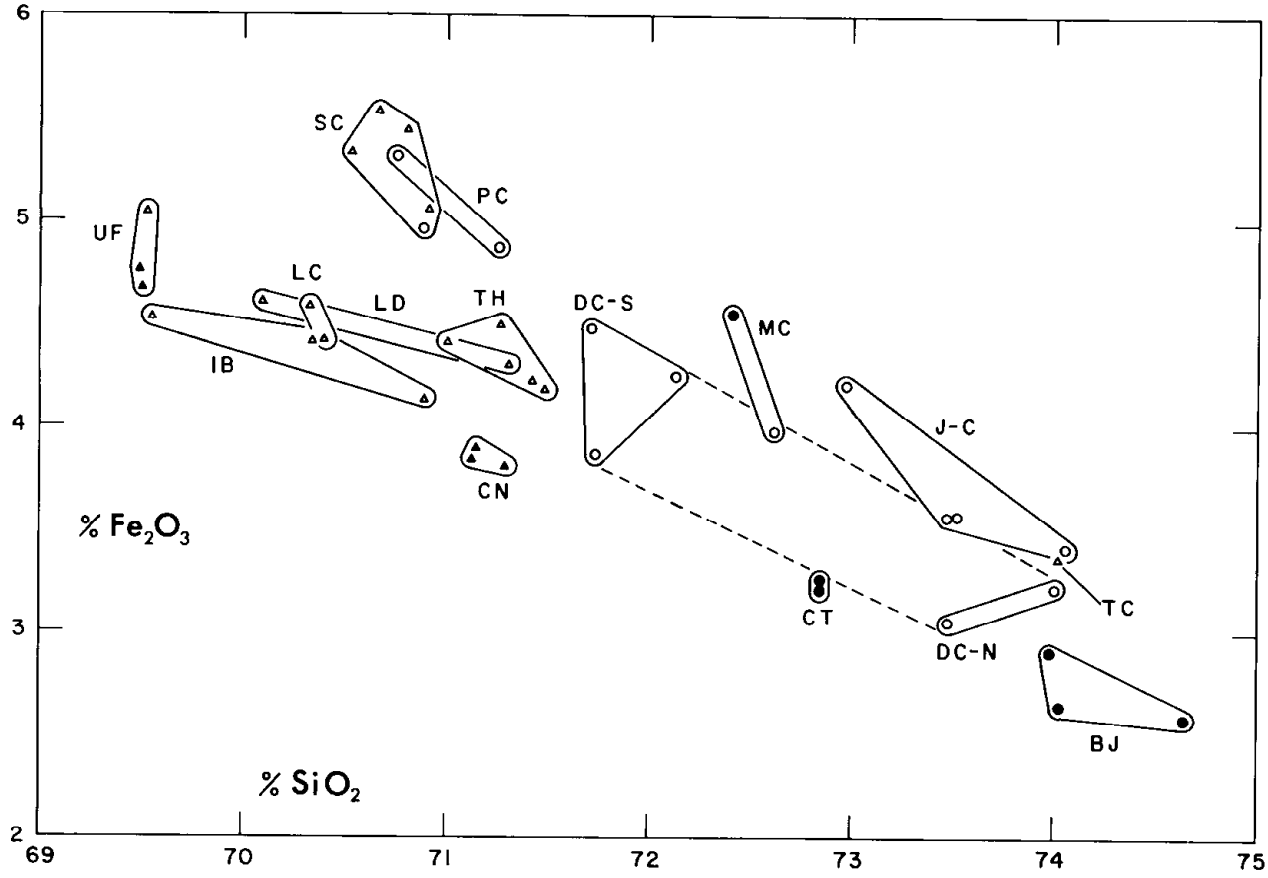

Figure 1. Plot of Fe_2O_3 versus SiO_2 for rhyolite lava flows in and northeast of the Bruneau-Jarbidge eruptive center. Filled circles are samples with phenocrysts of quartz and sanidine; open circles are samples with phenocrysts of quartz but no sanidine; open triangles are samples with no quartz or sanidine phenocrysts; and filled triangles are samples with hypersthene instead of, or in addition to, pigeonite, but no quartz or sanidine. The SiO_2 and Fe_2O_3 values are unpublished X-ray fluorescence analyses (weight percentages) done at Washington State University; Fe_2O_3 represents the total iron, and the SiO_2 values have been normalized to a sum of 100 percent for the ten major oxides. Abbreviations used for the flows are: BJ—Bruneau Jasper rhyolite, CN—unnamed rhyolite flow in the Crows Nest area, CT—Cedar Tree rhyolite, DC-N—north part of the Dorsey Creek rhyolite, DC-S—south part of the Dorsey Creek rhyolite, IB—Indian Batt rhyolite, J-C—rhyolite of the Juniper-Clover area, LC—lower rhyolite at Louse Creek, LD—Long Draw rhyolite, MC—Marys Creek rhyolite, PC—lower rhyolite at Poison Creek, SC—Sheep Creek rhyolite, TC—Three Creek rhyolite, TH—Triguero Homestead rhyolite, and UF—unnamed flows from northeast of the eruptive center.

and thickness indicate a volume that probably exceeds 10 cubic kilometers.

LOWER RHYOLITE AT LOUSE CREEK

An unnamed rhyolite flow occurs beneath the Sheep Creek rhyolite near the mouth of Louse Creek in T. 12 S., R. 6 E. (Figure 2, Bonnichsen, 1982b this volume). This flow is exposed for a few kilometers to the south in the bottom of Sheep Creek canyon, but its full extent and stratigraphic relationship to the Indian Batt rhyolite farther south in that canyon are unknown. Only the upper part of the lower rhyolite at Louse Creek is exposed, so the unit's thickness is not known.

Two analyses of the lower rhyolite of Louse Creek show that the unit is less silicic and more iron-rich than most of the flows in the eruptive center (Figure 1, symbol LC). Phenocryst minerals which have been found in the unit are plagioclase, augite, pigeonite, and opaque oxides (two thin sections). No quartz or sanidine has been found. Based on limited data, the lower rhyolite at Louse Creek is considered to have normal magnetic polarity (Table 1, Bonnichsen, 1982b this volume).

On the basis of its chemical composition, phenocryst assemblage, and apparent magnetic polarity, it is possible that the lower rhyolite at Louse Creek is part of the Long Draw flow, as was noted above. However, until further field and laboratory investigations are conducted, this should be considered as only tentative.

INDIAN BATT RHYOLITE

The Indian Batt rhyolite is exposed for about 16 kilometers in Bruneau Canyon from about 2 kilometers north of Indian Batt Cabin, for which the flow is named, southwards to the Bull Pens area (see

Table 2. Summary of features for the rhyolite lava flows in the Bruneau-Jarbidge eruptive center.

Unit	Magnetic Polarity	Phenocrysts[1]	Nature of Quartz Phenocrysts	Greatest Observed Thickness (meters)	Estimated Minimum Volume (cubic kilometers)	Comments
Marys Creek rhyolite	normal	quartz and sanidine	embayed, commonly more than 1 mm across	--	large	stratigraphic position not known
rhyolite of the Juniper-Clover area	unknown	quartz	small and equant	--	very large	stratigraphic position not known
Three Creek rhyolite	normal	quartz	small and equant, sparse	--	10	stratigraphic position not known
Dorsey Creek rhyolite	normal	quartz	euhedral to rounded, less than 0.5 mm across	more than 200	75	composition varies from north to south
lower rhyolite at Poison Creek	normal	quartz	equant and sparse, less than 0.3 mm across	about 100	--	might be equivalent to Sheep Creek rhyolite
Sheep Creek rhyolite	normal	quartz	small and equant, very sparse	about 250	200	quartz found in only 2 of 14 thin sections
Bruneau Jasper rhyolite	reverse	quartz and sanidine	deeply embayed, commonly 1 to 3 mm across	about 150	--	replacement of plagioclase by sanidine
Indian Batt rhyolite	reverse	(none)	--	100 or more	12	--
lower rhyolite at Louse Creek	normal	(none)	--	--	--	might be part of the Long Draw rhyolite
Long Draw rhyolite	normal	(none)	--	about 100	10	volume estimate includes lower rhyolite at Louse Creek
Cedar Tree rhyolite	normal	quartz and sanidine	rounded and equant, less than 0.5 mm across	100 or more	--	--
Triguero Homestead rhyolite	normal	(none)	--	about 100	10	--

[1]Phenocrysts in addition to plagioclase, augite, pigeonite, and opaque oxides.

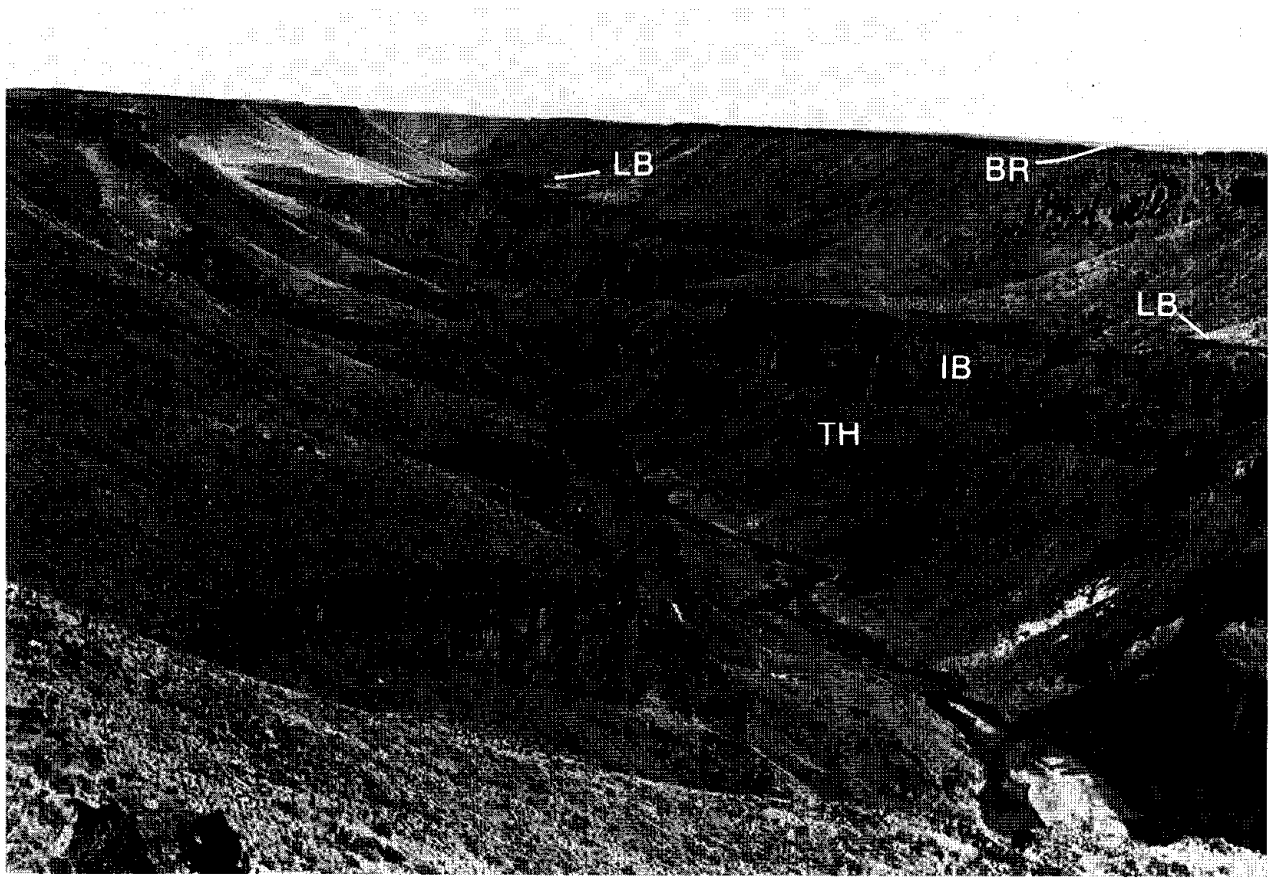

Figure 2. Looking northward in Bruneau Canyon at the Indian Batt rhyolite (IB) overlying the Triguero Homestead rhyolite (TH). The rim unit is the Black Rock basalt (BR). An unnamed lower basalt unit (LB) lies just above the Indian Batt rhyolite. The white zone at the right below the Triguero Homestead rhyolite is a thick accumulation of volcanic ash. View is from the northeastern part of sec. 25, T. 14 S., R. 6 E., in the Triguero Homestead area.

Figure 2, Bonnichsen, 1982b this volume, for locations). The original northern margin of the flow is exposed between the Cedar Tree rhyolite (below) and the Dorsey Creek rhyolite (above). The Indian Batt rhyolite overlies the Triguero Homestead rhyolite (Figure 2) for the length of the latter in Bruneau Canyon and overlies Cougar Point Tuff unit XV at its southern end. The Indian Batt rhyolite is 100 meters thick or slightly more throughout much of its extent in Bruneau Canyon, but is thinner at its north and south ends and in Sheep Creek.

The Indian Batt rhyolite is well exposed to the west in Sheep Creek canyon, for several kilometers northward from the mouth of Cat Creek. The Indian Batt rhyolite is at the same stratigraphic level as the Long Draw rhyolite and the overlying Indian Springs basalt, which are exposed a few kilometers farther north in Bruneau Canyon, but its age relative to these units is not known.

Three analyses show that the Indian Batt rhyolite has about the same iron content as some of the other flows, but contains less silica than most (Figure 1, symbol IB). One analysis is included in Table 1 (no. 2). Phenocryst minerals in the unit are plagioclase, augite, pigeonite, and opaque oxides (four thin sections). No quartz or sanidine has been found. The unit is now believed to have reverse magnetic polarity (Table 1, Bonnichsen, 1982b this volume), although as suggested earlier, it is possible the unit is transitional in magnetic characteristics (Bonnichsen, 1981).

Near its southern end the basal vitrophyre of the Indian Batt rhyolite has been observed to lie directly on a baked buried soil horizon (Figure 6) with no intervening layer of volcanic ash. At its north end, however, a layer of volcanic ash a few centimeters thick has been observed, and at one locality there the flow has been devitrified all the way to its base. These observations suggest that the fissure or vent through which the unit erupted may be near the north end of the unit. Perhaps it is near, or buried beneath, a relatively thick portion of the flow in the vicinity of Indian Batt Cabin in sec. 36, T. 13 S., R. 6 E.

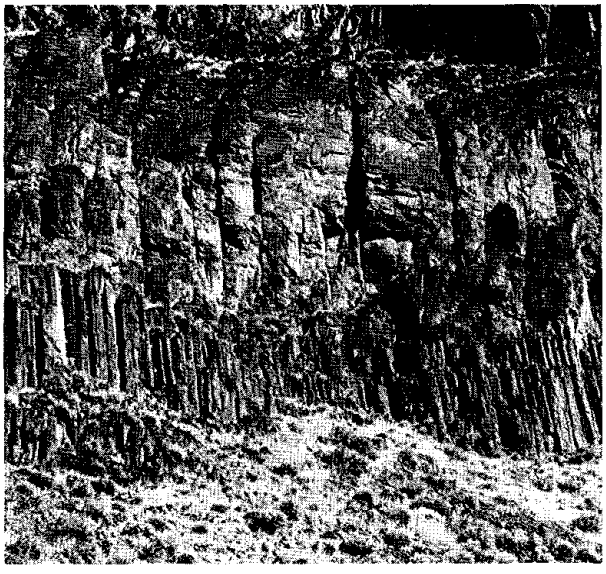

Figure 3. The lower part of the Triguero Homestead rhyolite near Triguero Homestead in Bruneau Canyon. The basal vitrophyre zone is cut by the vertical columnar joints, and the overlying lower portion of the lithoidal central zone contains subhorizontal sheeting joints and widely spaced vertical shrinkage fractures. Note that the individual joints in the two vertical fracture sets show no interpenetration.

Based on its exposed areal extent and thickness, the Indian Batt rhyolite would appear to have a volume of at least 12 cubic kilometers, and perhaps quite a bit more, depending on how far eastward it extends beneath the Dorsey Creek rhyolite.

BRUNEAU JASPER RHYOLITE

The Bruneau Jasper rhyolite is exposed for nearly 8 kilometers in the bottom of Bruneau Canyon from the Indian Hot Springs area northward to about a kilometer south of the mouth of Stiff Tree Draw (see Figure 2, Bonnichsen, 1982b this volume, for location). The southern limit of this unit is exposed near Indian Hot Springs in the northern part of sec. 33, T. 12 S., R. 7 E., and is the original margin of the flow. Here the Bruneau Jasper rhyolite lies below the Indian Springs basalt and above the Long Draw rhyolite. At the northern limit of its exposure the Bruneau Jasper rhyolite is overlain by the Sheep Creek rhyolite. At that locality the Bruneau Jasper rhyolite drops to an elevation lower than the bottom of Bruneau Canyon so that its northward extent is unknown (see Figure 8, Bonnichsen, 1981). The Bruneau Jasper rhyolite is named for a well-known jasper deposit in secs. 28 and 33, T. 12 S., R. 7 E., near its southern margin. This flow is nearly 150 meters thick where both its base and top are exposed in section 28.

The Bruneau Jasper rhyolite has the highest silica and lowest iron content of any of the flows in the eruptive center (Figure 1, symbol BJ). The Bruneau Jasper rhyolite contains phenocrysts of quartz, sanidine, plagioclase, augite, pigeonite, and opaque oxides (four thin sections). The quartz phenocrysts typically are 1 to 3 millimeters across and are deeply embayed. They distinguish this unit from all the other rhyolite lava flows by their greater abundance and size, and the amount of embaymentation. Also distinctive is the partial replacement of some plagioclase grains by sanidine. The Bruneau Jasper rhyolite is characterized by reverse magnetic polarity (Table 1, Bonnichsen, 1982b this volume).

SHEEP CREEK RHYOLITE

The Sheep Creek rhyolite is exposed for about 30

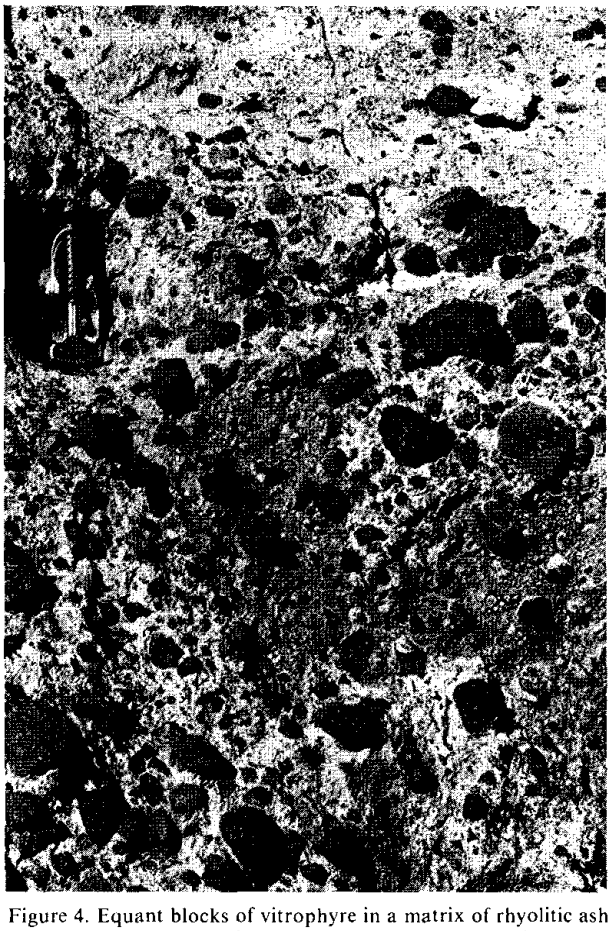

Figure 4. Equant blocks of vitrophyre in a matrix of rhyolitic ash at the north margin of the Triguero Homestead rhyolite, about 1.3 kilometers south of Indian Batt Cabin in Bruneau Canyon. This is interpreted as a crumble-breccia type of flow-margin deposit.

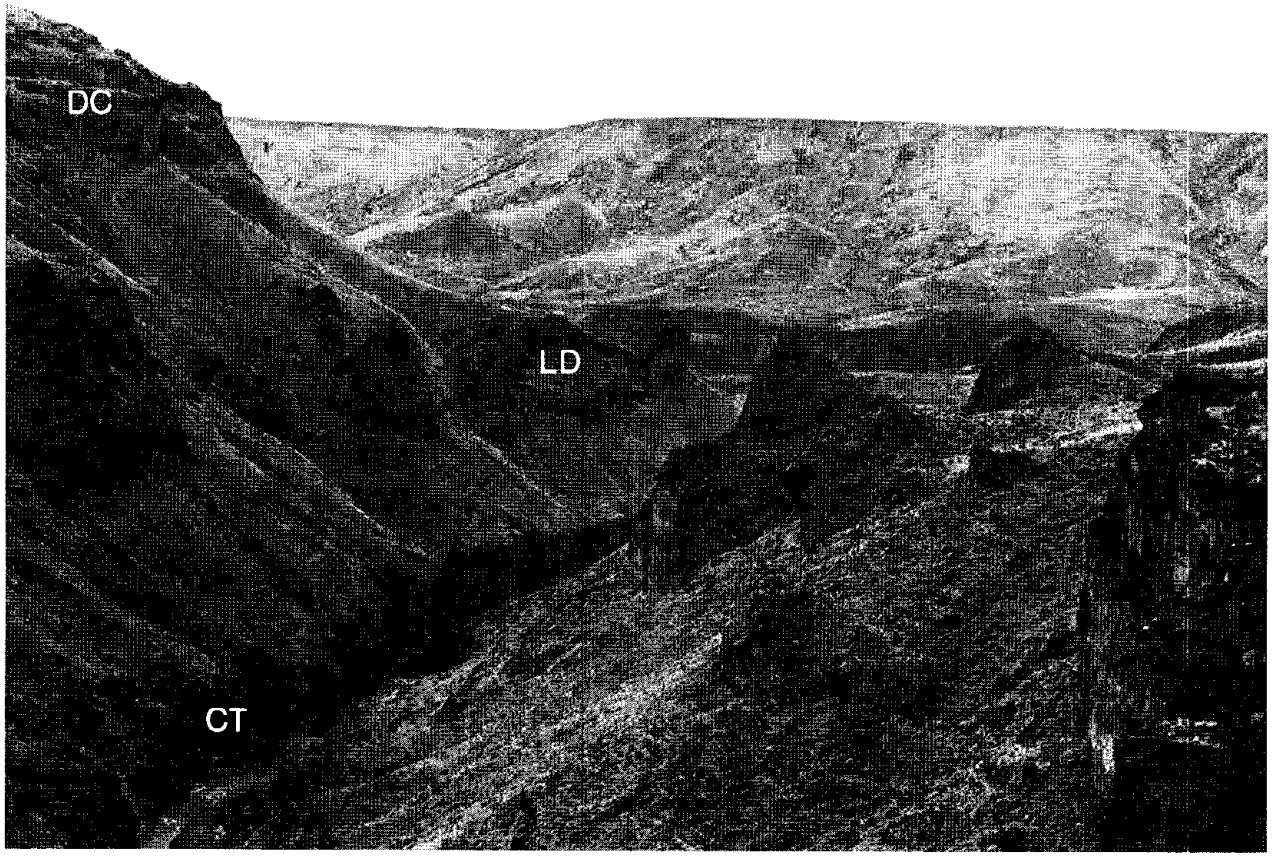

Figure 5. Looking southwestward in Bruneau Canyon from the northwestern part of sec. 18, T. 13 S., R. 7 E., at the Dorsey Creek rhyolite (DC) overlying the Long Draw rhyolite (LD), which overlies the Cedar Tree rhyolite (CT). Note the flow lobes in the Long Draw rhyolite.

kilometers in Bruneau Canyon from sec. 15, T. 12 S., R. 7 E., about 6 kilometers downstream from the mouth of the Jarbidge River, northward to a tributary of the Bruneau known as Miller Water in sec. 13, T. 9 S., R. 6 E. (see Figure 2, Bonnichsen, 1982b this volume, for locations). The southern limit of exposure in section 15 is the margin of the flow. The northern limit at Miller Water, however, is the result of downfaulting to the north so that the original margin is hidden. The Sheep Creek rhyolite is well exposed in the walls of Sheep Creek canyon from its mouth upstream for about 25 kilometers, to where its original margin is exposed near the mouth of Louse Creek in sec. 21, T. 12 S., R. 6 E. This flow appears to be 200 meters or more thick throughout much of its extent in Bruneau and Sheep Creek canyons (Figure 7).

At its southern limit in Bruneau Canyon the Sheep Creek rhyolite overlies the Bruneau Jasper rhyolite, and at its southern margin in Sheep Creek canyon it overlies the lower rhyolite at Louse Creek. Its stratigraphic position relative to the Dorsey Creek rhyolite has yet to be determined; based on their apparent end-to-end relationship north and south of the Indian Hot Springs area, both units appear to be about the same age (Figure 10, Bonnichsen, 1982b this volume). The potassium-argon ages recently reported by Hart and Aronson (in press) for the two units (see Table 3 in Bonnichsen, 1982b this volume) suggest that the Sheep Creek rhyolite is older than the Dorsey Creek rhyolite.

Five analyses show that the Sheep Creek rhyolite has the greatest abundance of iron of any of the rhyolite flows in the eruptive center and one of the lowest abundances of silica (Figure 1, symbol SC). The flow contains phenocrysts of plagioclase, augite, pigeonite, and opaque oxides. No sanidine has been found, but a few small quartz grains occur in two of the fourteen thin sections that were examined. The unit is characterized by normal magnetic polarity (Table 1, Bonnichsen, 1982b this volume).

The Sheep Creek rhyolite extends as far to the northwest as Big Jacks Creek where it is exposed in the northeast part of sec. 4, T. 10 S., R. 4 E., about

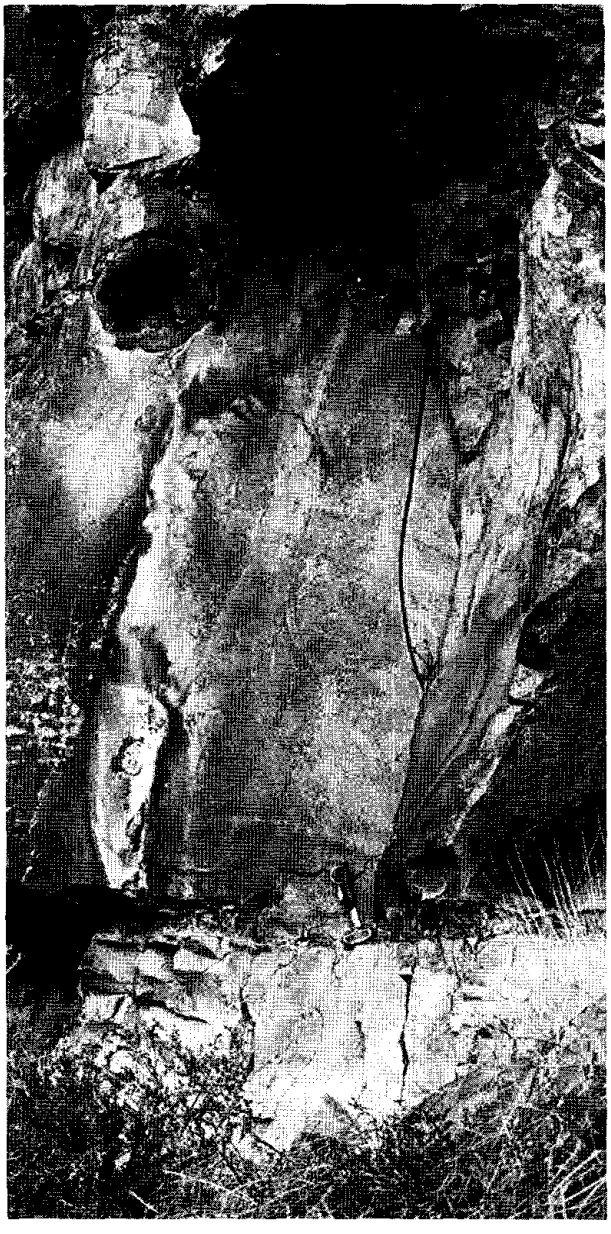

Figure 6. The basal vitrophyre of the Indian Batt rhyolite flow in the Bull Pens area of Bruneau Canyon. The flow lies directly on a baked buried soil horizon (below hammer). Note the large spherulites in the upper part of the view and the subhorizontal flow bands in the middle.

1.4 kilometers north-northeast of the mouth of Wickahoney Creek. At this location it lies above one of the thick rhyolite units included within the tuff of Little Jacks Creek by Ekren and others (1982 this volume). The flow below the Sheep Creek rhyolite at Big Jacks Creek is characterized by reverse magnetic polarity (Dan Kauffman, personal communication, 1982) and is in the middle part of the sequence of rhyolite units that constitute the tuff of Little Jacks Creek in that region.

Previously, the northwestern part of the Sheep Creek rhyolite was referred to as the rhyolite of the Big Hill area (Bonnichsen, 1981). However, sufficient chemical, petrographic, paleomagnetic, and field data have now been collected to establish that the large area involved is underlain by just one large flow. The name Sheep Creek rhyolite has been retained, and the name rhyolite of the Big Hill area has been dropped.

Altogether, the Sheep Creek rhyolite extends about 42 kilometers from southeast to northwest between Bruneau Canyon and Big Jacks Creek. With a known width of more than half its length, the flow has a minimum volume of about 200 cubic kilometers. As such, it appears to be the most voluminous of the rhyolite flows within the Bruneau-Jarbidge eruptive center.

LOWER RHYOLITE AT POISON CREEK

An unnamed rhyolite unit is exposed for about 4 kilometers beneath the Dorsey Creek rhyolite in the lower part of Jarbidge Canyon and in Poison Creek in T. 13 and 14 S., R. 8 E., 11 to 15 kilometers upstream from the mouth of the Jarbidge River (see Figure 2, Bonnichsen, 1982b this volume, for location). At its westernmost exposure, which appears to be the original margin of the unit, the lower rhyolite at Poison Creek overlies the Indian Springs basalt. At the southeastern limit of its exposure in Jarbidge Canyon, the lower rhyolite drops to an elevation lower than the bottom of the canyon, so that its southeastward extent is unknown.

The contact between the lower rhyolite and the overlying Dorsey Creek rhyolite is marked by only a few centimeters of ash and sediments and is characterized by paleo-topographic variation; locally it dips as steeply as 30 degrees. These observations, along with the rather vesicular nature of the upper part of the lower rhyolite, suggest that the Dorsey Creek rhyolite was extruded only a geologically short time after the lower rhyolite formed, and thus it preserved the initial irregularities in the upper surface of the lower rhyolite. The lower rhyolite at Poison Creek is about 100 meters thick in Jarbidge Canyon, 1 to 2 kilometers downstream from the mouth of Poison Creek (see Figure 6, Bonnichsen, 1981).

The lower rhyolite of Poison Creek is one of the least silicic and most iron-rich of the rhyolite lava flows in the eruptive center (Figure 1, symbol PC). Chemically, it is similar to the Sheep Creek rhyolite.

The unit contains phenocrysts of quartz, plagioclase, augite, pigeonite, and opaque oxides (three thin sections). Sanidine has not been observed and the quartz grains characteristically are sparse and in the form of euhedral dipyramids less than 0.3 millimeter across, very similar to those in the Dorsey Creek rhyolite, but not as abundant. Preliminary information (Table 1, Bonnichsen, 1982b this volume) suggests that the lower rhyolite at Poison Creek has normal magnetic polarity.

Because of its limited exposure, no meaningful estimate can be made of the volume of the lower rhyolite of Poison Creek. In view of its chemical composition, phenocryst assemblage, apparent magnetic polarity, and stratigraphic position, it is quite possible that the lower rhyolite of Poison Creek is part of the Sheep Creek rhyolite flow, or from the same magma system from which the Sheep Creek flow originated. The closest known exposures of these two units are about 13 kilometers apart, and the area between them is covered by basalt.

DORSEY CREEK RHYOLITE

The Dorsey Creek rhyolite is well exposed for about 40 kilometers in Jarbidge Canyon from its southeastern margin at Murphy Hot Springs to its northwestern margin near Indian Hot Springs where the Bruneau and Jarbidge Rivers join (see Figure 2, Bonnichsen, 1982b this volume, for location). It is exposed for about 12 kilometers in Bruneau Canyon upstream from Indian Hot Springs to the southwestern part of sec. 6, T. 14 S., R. 7 E. The unit is exposed between Jarbidge and Bruneau Canyons northward from Cowan Reservoir and is well exposed in the canyons of Cougar Creek and Dorsey Creek. The unit is named for this latter tributary to the Jarbidge River.

The Dorsey Creek rhyolite flow attains its greatest observed thickness in the central part of its exposure in Jarbidge Canyon, in T. 14 S., R. 8 E., where it exceeds 200 meters. Its maximum thickness cannot be determined because the base of the flow is below the canyon floor in that area. This thickest portion

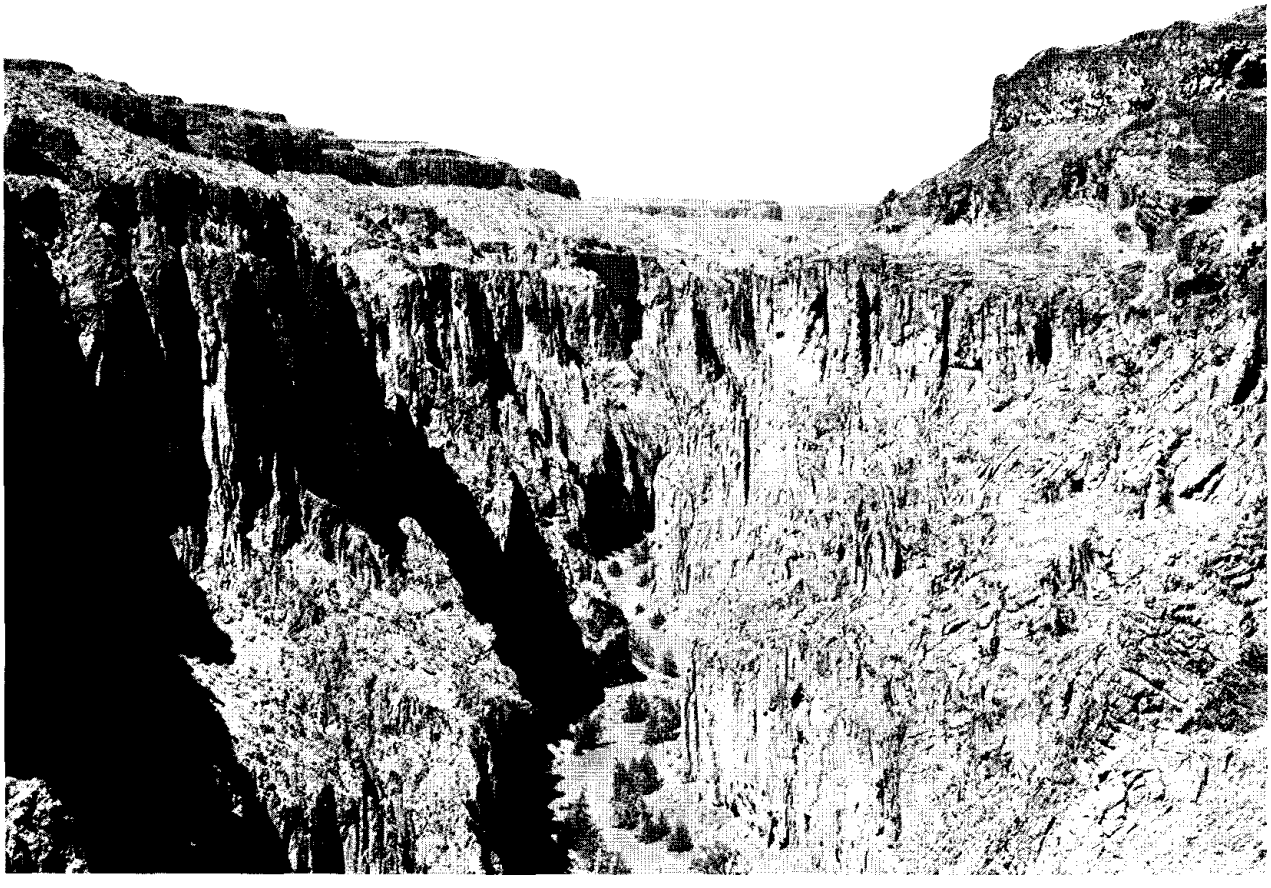

Figure 7. Looking northward at the Sheep Creek rhyolite near the mouth of Stiff Tree Draw in Bruneau Canyon. The central zone of the flow is exposed in the cliffs and the uper zone corresponds to the overlying slope. Banbury Basalt flows are exposed at the canyon rim. The central zone of the rhyolite flow is about 200 meters thick at this locality and the upper zone is 30 to 50 meters thick.

probably is near or over the zone from which part of the rhyolitic lava was erupted.

In the Indian Hot Springs area and to the southeast in Jarbidge Canyon, the Dorsey Creek rhyolite lies above the Indian Springs basalt (Figure 8). Southeast of this, 11 to 15 kilometers upstream from the mouth of the Jarbidge, it lies above the lower rhyolite of Poison Creek (Figure 6, Bonnichsen, 1981). Between the Murphy Hot Springs area and the mouth of Dorsey Creek in Jarbidge Canyon, the Dorsey Creek rhyolite lies above the Indian Springs basalt. In the Indian Batt Cabin area in Bruneau Canyon, the Dorsey Creek rhyolite overlies the Indian Batt rhyolite (Figure 7, Bonnichsen, 1981). These relationships reveal that the Dorsey Creek is the youngest rhyolite of all those exposed in Jarbidge Canyon and in Bruneau Canyon upstream from the Indian Hot Springs area (Figure 10, Bonnichsen, 1982b this volume).

The chemical compositions of two Dorsey Creek rhyolite samples (one in duplicate) are included in Table 1 (nos. 3-5). On the SiO_2-Fe_2O_3 plot (Figure 1) five Dorsey Creek rhyolite samples vary widely in composition in the middle part of the diagram. The two samples from the northern part of the unit (symbol DC-N) are substantially richer in silica and poorer in iron than the three from the southern part (symbol DC-S). The Dorsey Creek rhyolite contains phenocrysts of quartz, plagioclase, augite, pigeonite, and opaque oxides (eighteen thin sections). The quartz grains typically are euhedral to slightly rounded dipyramids less than about 0.5 millimeter in diameter. The quartz abundance ranges from only a few to nearly 50 grains per thin section. Where most abundant, mainly in samples from the northern part of the unit, the grains tend to be larger; quartz grains as much as a millimeter across have been observed. The Dorsey Creek rhyolite is characterized by normal magnetic polarity (Table 1, Bonnichsen, 1982b this volume).

The initial strontium isotope ratio for one Dorsey Creek rhyolite sample indicates the unit very likely

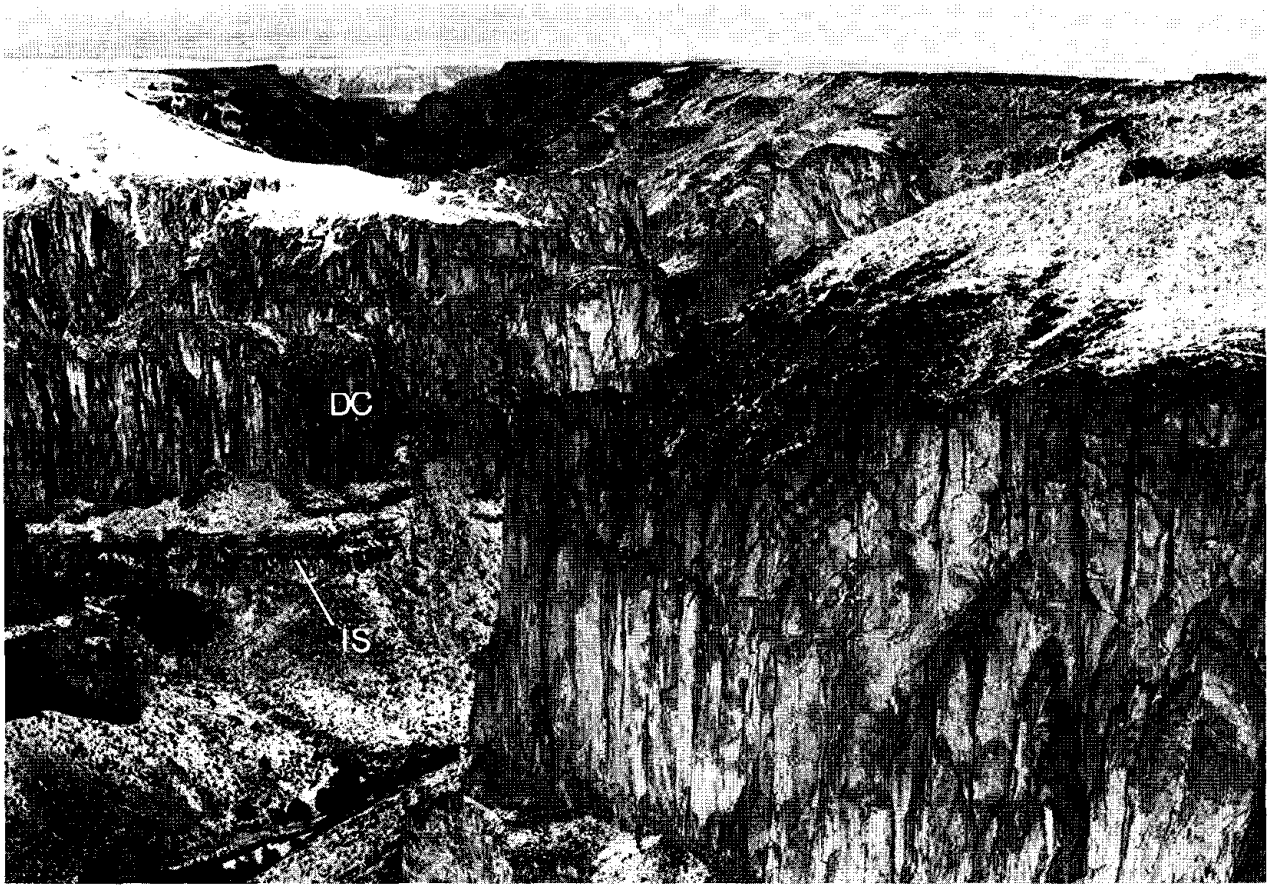

Figure 8. Looking northwestward in Jarbidge Canyon at the Dorsey Creek rhyolite (DC) overlying the Indian Springs basalt (IS). The cliff with the prominent vertical fractures corresponds to the central zone, and the overlying snow-covered slope is eroded in the upper zone of the rhyolite flow. The distant canyon rim is the Banbury Basalt. This view is from about 7 kilometers upstream from the mouth of the Jarbidge River.

was derived by the fusion of crustal materials (Table 2, Bonnichsen and Citron, 1982 this volume).

On the basis of its exposed area and thickness, the Dorsey Creek rhyolite is estimated to contain a minimum volume of about 75 cubic kilometers. The unit might be considerably larger, since it is entirely buried east of Jarbidge Canyon. The Three Creek rhyolite and the unnamed rhyolite in the Juniper-Clover area, which both occur to the east, are similar enough in stratigraphic position, chemical composition, phenocryst assemblage, and magnetic polarity to the Dorsey Creek rhyolite to permit either or both to be part of the Dorsey Creek unit. If this were so for either, then the unit would have a volume approximately equal to, or even larger than, that of the Sheep Creek rhyolite.

THREE CREEK RHYOLITE

In the southeastern part of the Bruneau-Jarbidge eruptive center a large area in T. 15 and 16 S., R. 10 and 11 E. is underlain by the Three Creek rhyolite lava flow, which is named for one of the streams in that area (see Figures 2 and 3, Bonnichsen, 1982b this volume, for location). The geologic map prepared by Citron (1976) shows this flow to be more than 17 kilometers from southwest to northeast and more than 7 kilometers from southeast to northwest. The Three Creek rhyolite lies above unit XIII of the Cougar Point Tuff. The stratigraphic relationship of this flow to all of the other rhyolite flows within the Bruneau-Jarbidge eruptive center is unknown, although its chemical, petrographic, and paleomagnetic characteristics suggest it possibly is either part of the nearby Dorsey Creek rhyolite or part of the rhyolite in the Juniper-Clover area.

The Three Creek rhyolite has more silica and less iron than many of the other flows (Figure 1, symbol TC). It contains phenocrysts of plagioclase, pigeonite, augite, and opaque oxides (six thin sections). At some localities a few small quartz grains occur, but they are absent in the thin sections from other areas. Even though it is relatively siliceous, the analyzed sample plotted on Figure 1 does not show quartz phenocrysts in its thin section. The unit is probably characterized by normal magnetic polarity (Table 1, Bonnichsen, 1982b this volume).

At the one location where the base of the Three Creek rhyolite is known to be well exposed (along the grade on the west side of Three Creek in the southwest part of sec. 34, T. 15 S., R. 11 E.), the flow is seen to overlie about 30 centimeters of friable, white, bedded volcanic ash of probable air-fall origin that in turn lies on a structureless tan silt layer (probably buried soil). This is quite a bit more basal fallout ash than has been observed at the base of the other rhyolite lava flows in the eruptive center, with the exception of the thick localized section of ash beneath the Triguero Homestead rhyolite. At its southern margin, the Three Creek rhyolite is quite vesicular and may be as thin as 20 meters. This is thinner than almost any other occurrence for a rhyolite lava flow in the eruptive center. These observations suggest that the lava for portions of this unit may have been somewhat more gassy than that for most of the other rhyolite lava flows in the eruptive center.

Based on its exposed area and assuming that the flow averages about 100 meters in thickness, which is the approximation for several other of the rhyolite flows in the eruptive center, the Three Creek rhyolite would have a minimum volume of about 10 cubic kilometers. It easily could be much larger, however, since its northwest side, which is toward the interior of the eruptive center, is buried.

RHYOLITE OF THE JUNIPER-CLOVER AREA

In the northeastern part of the Bruneau-Jarbidge eruptive center, between Bruneau Canyon and Clover Creek, a large area in T. 11 and 12 S., R. 8 and 9 E., and nearby, is underlain by rhyolite (see Figures 2 and 3, Bonnichsen, 1982b this volume, for location). None of the streams have eroded deeply enough to expose this rhyolite very well, so it is not clear if one or more flows are present in that region.

The silica and iron contents of four rhyolite samples from the Juniper-Clover area are plotted in Figure 1 (symbol J-C). These are relatively silica-rich and slightly iron-poor in comparison with other rhyolite flows in the eruptive center. The phenocrysts in the rhyolite of the Juniper-Clover area are quartz, plagioclase, augite, pigeonite, and opaque oxides (five thin sections). Insufficient magnetic polarity data are available to characterize the rhyolite of the Juniper-Clover area.

The fact that the chemical analyses and petrographic characteristics from all of the samples of the rhyolite in the Juniper-Clover area are quite similar to one another suggests that only one unit is present. If so, the flow would have a very large volume, like that of the Sheep Creek and Dorsey Creek flows. As noted previously, the chemistry, phenocryst assemblage, and stratigraphic position of the rhyolite of the Juniper-Clover area are enough like that of the nearby Dorsey Creek rhyolite to easily permit both to be part of the same unit.

MARYS CREEK RHYOLITE

The Marys Creek rhyolite is exposed in the western part of the Bruneau-Jarbidge eruptive center, and takes its name from a prominent stream in that region (Figure 2, Bonnichsen, 1982b this volume). The Marys Creek rhyolite is isolated from the other rhyolite lava flows in the eruptive center; thus, its relative stratigraphic position is not known. The Marys Creek rhyolite is exposed for about 25 kilometers along the Grasmere escarpment, from as far north as the China Creek area in sec. 15, T. 12 S., R. 4 E., to as far south as near Broken Wagon Draw in sec. 21, T. 14 S., R. 5 E. Whether it extends farther north or south of these localities has yet to be determined. To the east, it is covered by younger basalt flows and sedimentary deposits.

North of where Marys Creek crosses the Grasmere escarpment in sec. 29, T. 13 S., R. 5 E., the Marys Creek rhyolite is exposed along the base of the escarpment, with the flow's western margin lapping up against the older, but topographically higher, rhyolite of Grasmere escarpment; however, to the south of Marys Creek canyon, the Marys Creek rhyolite lies on top of the rhyolite of Grasmere escarpment. In this southern area, the Marys Creek rhyolite extends more than 5 kilometers west of the Grasmere escarpment, which is the western margin of the eruptive center. The east-west segment of Marys Creek canyon that crosses the escarpment approximately follows the north side of a generally east-west-oriented, pre-Marys Creek rhyolite, paleovalley (which probably was also a fault-bounded graben). The Marys Creek rhyolite evidently flowed from the Bruneau-Jarbidge eruptive center out into this wide and topographically lower area, whereas to the north the rhyolite was unable to flow west of the escarpment.

On the SiO_2-Fe_2O_3 plot (Figure 1), the Marys Creek rhyolite (symbol MC) has intermediate abundances of iron and silica in comparison with the other rhyolite lava flows. Phenocrysts found in the unit are quartz, sanidine, plagioclase, augite, pigeonite, and opaque oxides. The quartz grains are relatively abundant and large (grains are commonly more than a millimeter across) in comparison with the quartz crystals in other rhyolite units in the eruptive center, and some are moderately embayed. A few grains of sanidine were found in one of the two thin sections examined. Their irregular shape and broken habit suggest they might be xenocrysts. The Marys Creek rhyolite is characterized by normal magnetic polarity (Table 1, Bonnichsen, 1982b this volume).

The Marys Creek rhyolite may have been erupted from north-northwest trending fissures along the buried base of the Grasmere escarpment, or just to the east. An estimate of the minimum volume of the unit has not been made, since there is very little field control on its thickness or areal dimensions. It seems to be a relatively large unit, however, in view of its lengthy distribution along Grasmere escarpment.

RHYOLITE UNITS NORTHEAST OF THE ERUPTIVE CENTER

Northeast of the Bruneau-Jarbidge eruptive center, in an area that is about 50 kilometers long from northwest to southeast by about 30 kilometers wide, there are many exposures of rhyolite lava flows. A portion of this region is included within the area of Figures 2 and 3 in Bonnichsen (1982b this volume). The outlines of the general rhyolite areas in that region were mapped by Malde and others (1963), but the age of the rhyolite units there relative to those within the eruptive center is presently unknown.

Although stratigraphic relations and the distribution of individual flows in this northeastern area have yet to be worked out, it is clear that the rhyolite flows there are similar in their physical characteristics, large sizes, and most petrologic features to the flows within the eruptive center. Petrographic and chemical data are available for two groups of these flows.

One group of three samples collected from scattered localities (sec. 20, T. 10 S., R. 13 E.; sec. 11, T. 11 S., R. 11 E.; sec. 23, T. 12 S., R. 12 E.) have similar chemical and petrographic characteristics. The analysis for one (in duplicate) is included in Table 1 (nos. 6 and 7), and those for all three are given in Bonnichsen (1982a). In the SiO_2-Fe_2O_3 plot (Figure 1, symbol UF), the three are seen to be less silicic than any of the other units plotted and relatively enriched in iron. The phenocryst assemblage of these rocks includes plagioclase, augite, Ca-poor pyroxene, and opaque oxides. Two of the samples contain hypersthene in place of, or in addition to, pigeonite, as the Ca-poor pyroxene; but none contains quartz or potassium feldspar.

Three other samples, collected from the same, but unnamed, rhyolite lava flow in the Crows Nest area (sec. 14, T. 8 S., R. 10 E.; sec. 5, T. 9 S., R. 11 E.; sec. 33, T. 8 S., R. 11 E.) have almost identical compositions. In the SiO_2-Fe_2O_3 plot (Figure 1, symbol CN), they are seen to have silica and iron concentrations intermediate among the rhyolite flows in the Bruneau-Jarbidge eruptive center, but slightly to the side of the trend established by the flows within the eruptive center. The phenocryst assemblage of these three samples includes plagioclase, augite, hypersthene, and opaque oxides. In addition, pigeonite occurs in two of the samples, but no quartz or sanidine has been found.

Based on the above, somewhat limited, petrographic investigation, most of the rhyolite from the area northeast of the eruptive center differs from the rhyolite within the eruptive center by containing hypersthene in addition to, or instead of, pigeonite. For all of the rhyolite lava flows in the eruptive center, the only Ca-poor pyroxene that has been found is pigeonite; hypersthene seems to be nonexistent there. Other than these differences in pyroxenes, the phenocrysts in the flows from within and from outside the eruptive center are essentially the same.

PHYSICAL NATURE OF THE RHYOLITE LAVA FLOWS

The rhyolite lava flows vary in physical appearance depending on the observer's vertical position within a unit and whether one is near the margin or well within the flow interior. The interiors are fairly uniform. They consist of a thick zone of massive lithoidal rhyolite overlying a basal vitrophyre or breccia zone or both, and they are capped by an upper zone which commonly is structurally complex. Upper zones generally contain both glassy and lithoidal (crystallized or devitrified) portions, and consist of massive, sheeted, folded, flow-banded, and brecciated rhyolite. These zones contain gas cavities of widely varying dimensions and abundance. Flow margins typically consist of bulbous flow lobes of massive or sheeted rhyolite separated by rather chaotic appearing zones of steeply jointed or flow-banded rhyolite. The basal zone of a flow margin most commonly is a breccia. Figure 9 is a composite sketch illustrating the spatial relations among the zones and features of the rhyolite lava flows in the Bruneau-Jarbidge eruptive center.

The interior portions of the rhyolite lava flows typically are 50 meters or more thick and some are 250 meters or more thick. The flow margins tend to be thinner, although they seldom are less than about 25 meters. As noted in the previous section, several of the flows average about 100 meters thick, while the two very voluminous ones, the Dorsey Creek and Sheep Creek flows, are thicker.

Below, the larger parts of the rhyolite lava flows that are best viewed from some distance, these being the central zones in the flow interiors and the flow lobes at the flow margins, are discussed first. Then the thinner marginal portions of the flows which are best observed from close up, the upper zones and flow bases, are described. Finally, a variety of relatively small-scale structures and other features that occur in various parts of the flows are discussed. I have included photographs of examples of most types of large- and small-scale structures which typically are found in the rhyolite lava flows. The nomenclature followed in the text for depicting the relative positions of the various major parts of the flows is indicated in Figure 9. In that figure readers should also note the locations in the flows where many of the structural features are typically found.

CENTRAL ZONES OF THE FLOW INTERIORS

The rhyolite in the massive central zones of the flow interiors generally is characterized by its uniformity and dense, lithoidal condition, although gas cavities, folded flow banding, breccia zones, and even vitrophyre occur locally. The central zones contain well-developed vertical or locally inclined joints

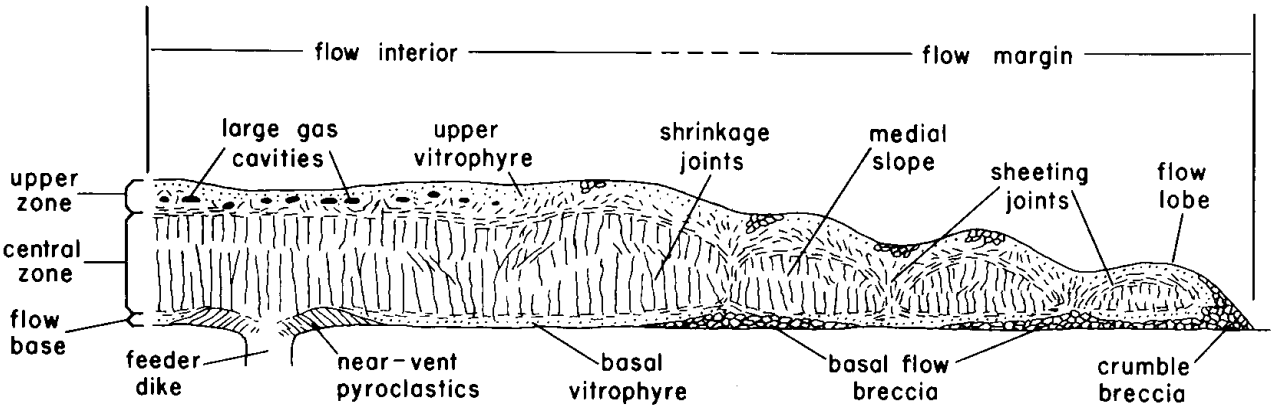

Figure 9. Schematic diagram illustrating the spatial relationships among the various zones and features typical of the rhyolite lava flows within the Bruneau-Jarbidge eruptive center. This composite section combines features occurring in many of the flows, but it deviates from some in certain details. The vertical scale and the size of some features have been exaggerated. See the text for typical dimensions of the features illustrated.

(shrinkage joints) that divide the flow into elongate masses that typically are a few to several meters across (Figures 3, 7, and 8). As illustrated in Figure 3, the shrinkage joints are a feature characteristic of lithoidal rhyolite and are distinct from the columnar jointing, locally seen in glassy portions of the rhyolite flows that resemble the columnar joints common in basalt flows. Also present in the central zones, and usually developed most conspicuously near the top and base of the zone, are closely spaced subhorizontal joints (sheeting joints) along which the rhyolite breaks into flaggy plates ranging from a few millimeters to several centimeters in thickness and from a few centimeters to a meter or more across.

In most of the rhyolite flows the central zones have eroded to an upper and a lower cliff separated by a medial interval of devitrified rhyolite with more abundant joints. The joints in this medial interval commonly are inclined at various angles and typically cause the medial sections to erode to a steep slope between the upper and lower cliffs (Figures 9 and 10, and also see Figures 2, 7, and 8). The double cliffs are most conspicuous in the thickest portions of the flows, but they also occur in thinner parts and even in some of the marginal flow lobes (Figure 11). The vertical shrinkage joints seen in the upper and lower cliffs generally do not continue through these medial intervals (Figures 7, 8, 9, and 10). The vertical joints in the upper and lower parts of the central zones most likely resulted from shrinkage after the lava had crystallized, and the sheeting joints had formed. The distribution of these shrinkage joints suggests that they propagated toward the flow interiors from both the upper and lower surfaces. This implies that, as might be expected, the medial slopes mark the positions of the most slowly cooled parts of the flows.

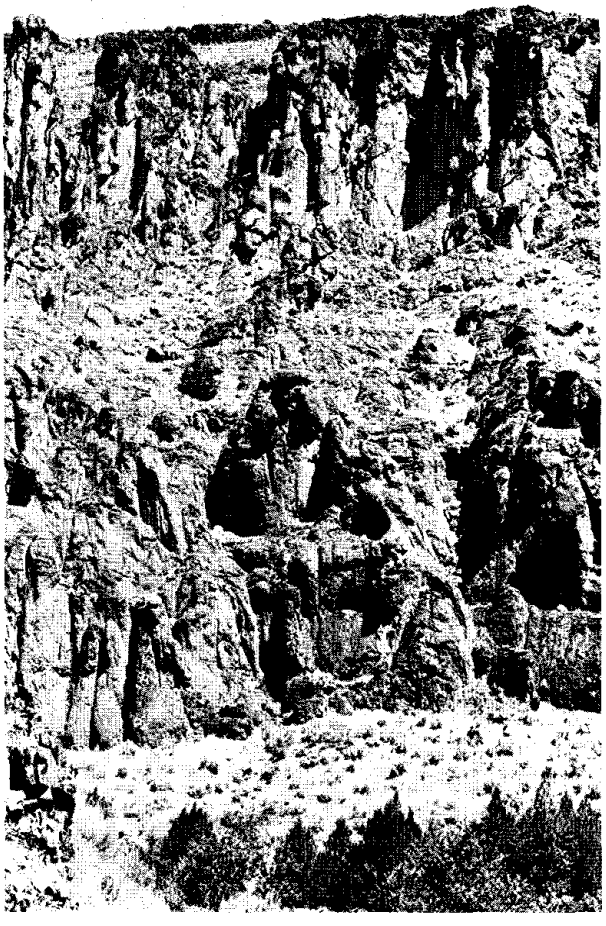

Figure 10. Well-developed double cliff in the central zone of the Dorsey Creek rhyolite at the mouth of Dorsey Creek. Note how the vertical shrinkage fractures in the upper and lower cliffs die out in the medial slope. The central zone of the unit is about 150 meters thick at this location.

FLOW LOBES

The flow margins commonly consist of a series of bulbous flow lobes of massive lithoidal rhyolite that are separated by zones of steeply sheeted, commonly folded and variably vesicular, lithoidal rhyolite and local vitrophyre (Figures 5, 9, 11, and 12; and Figure 8 in Bonnichsen, 1982b this volume). The juxtaposition of these diverse structural forms of rhyolite imparts a chaotic appearance to the marginal portions of the flows, and makes it difficult to easily recognize their lateral continuity (Figure 5). These marginal zones typically range from a few hundred meters to 2 kilometers in width and merge into the massive flow interiors by a decrease in the amount of nonmassive lithoidal rhyolite between adjacent lobes. Toward the interiors of the flows the lobes merge laterally into one another and become confined to the upper parts of the flows or are absent altogether (Figures 2, 7, 8, and 9). However, some flow lobes have been found well within the interiors of rhyolite flows (Figure 12). Such interior occurrences may record where one part of the lava became ponded against a previously emplaced portion.

The marginal zones of the rhyolite flows range generally from 50 to 100 meters in thickness, and it is uncommon for any to be thinner than about 25 meters. Some units, such as the Sheep Creek, Dorsey Creek, and Long Draw flows, are characterized by having numerous and prominent flow lobes. Other units, however, for example the Indian Batt and

Figure 11. A prominent flow lobe in the Dorsey Creek rhyolite near the mouth of Poison Creek. Note the double cliff, the vertical shrinkage fractures, and the sheeting joints wrapped around the upper right-hand part of the lobe. The poorly exposed unit below the flow lobe is the lower rhyolite at Poison Creek and the canyon-rim unit is Banbury Basalt.

Marys Creek flows, have fewer and less conspicuous marginal lobes and tend to be somewhat thinner near their margins than the flows with conspicuous lobes.

The flow bases in the marginal areas more commonly are breccias, rather than layers of massive vitrophyre. The upper zones in marginal parts of the flows show the same variety of structures which occur above the central zones in the flow interiors, and are continuous with the screens of structurally complex rhyolite between the flow lobes. Where the double cliffs of the central zone occur in flow lobes (Figure 11), the medial slopes commonly curve downwards near the edges of the lobes, somewhat mimicking the shape of the tops. Shrinkage joints at the edges of lobes commonly dip steeply or locally even shallowly, apparently from an inclination to form approximately perpendicular to the lobe margins (Figure 12).

Altogether, the flow lobes attest to the relatively viscous nature of the rhyolite lava as masses of it flowed across the surface. The lobes also suggest that the prevailing lateral-spreading mechanism was one in which internal inflation and extension of the lobes were caused by the horizontal injection of lava into the interior of a lobe from ponded lava closer to the source area. The breccias, which commonly occur at the bases of the lobes, mainly represent fragments that crumbled from the lobe fronts as they expanded and that became covered by the advancing lobes.

Figure 12. A flow lobe in the Dorsey Creek rhyolite in Jarbidge Canyon about 6 kilometers upstream from the mouth of the Jarbidge River. Note how the shrinkage fractures dip at various angles, all approximately perpendicular to the margin of the lobe. The lobe is about 150 meters high.

FLOW BASES

The basal zones of the rhyolite lava flows consist of either massive vitrophyre (Figure 6) or breccia (Figures 9, 13, and 14). The zones generally range from 2 to 5 meters in thickness but locally may exceed 10 meters. In the marginal portions of the flows, many of the basal zones are breccias. These basal breccias commonly consist of approximately equant blocks of vitrophyre in a matrix of finer fragments and ashy material (Figure 13). Many of the basal breccias are thought to have originated as crumble breccias at the steep fronts of slowly moving masses of rhyolitic lava where the fragments were overriden by the advancing lava (compare Figures 4 and 13). Much less commonly, the basal breccias consist of angular fragments of lithoidal rhyolite (Figure 14), suggesting that portions of the flow had crystallized

Figure 13. Breccia at the base of the Dorsey Creek rhyolite in Jarbidge Canyon, about 2 kilometers downstream from the mouth of Poison Creek. This breccia of vitrophyre blocks in an ashy matrix probably formed as the lava flowed over blocks that had crumbled from the flow margin.

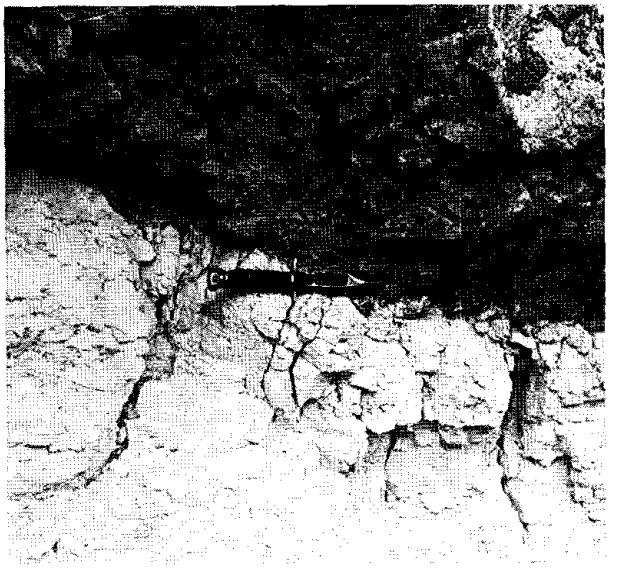

Figure 14. Breccia at the base of the Dorsey Creek rhyolite near the margin of the flow about a kilometer upstream from the mouth of Jarbidge Canyon. The rhyolite was devitrified before it was fragmented; note how angular the blocks are. The fine-grained sedimentary material beneath the flow probably was deposited in a shallow lake. The sediments probably were wet when the flow was emplaced and were slightly deformed by the overlying rhyolite.

prior to fragmentation and incorporation into the basal flow breccia.

In the interiors of the flows, the basal zones most commonly are uninterrupted layers of vitrophyre that contains local, tightly-folded flow bands (Figure 6, also see Figure 15) characteristically with subhorizontal axial planes, and sparse gas cavities that typically are greatly stretched. At some flow bases, as illustrated in Figure 15, such flow-banded rhyolite consists of intermixed glassy and lithoidal rhyolite.

Devitrification spherulites are common in the basal zones of the rhyolite flows. They are most abundant near the top of massive vitrophyre layers (Figure 6). Some are quite large; individuals as much as a meter across have been noted. Spherulites at the bases of the rhyolite lava flows generally tend to be larger than those in the basal vitrophyre zones of the Cougar Point Tuff units. Many, especially the larger ones, contain angular interior shrinkage cavities.

In parts of some rhyolite lava flows, layers of both massive vitrophyre and flow breccia occur together at the base. In such situations, the vitrophyre layer most commonly is above the breccia. In other areas lenses and irregular zones of breccia within otherwise massive vitrophyre (Figure 16) locally occur at some rhyolite flow bases. Note in Figure 16 how tightly the breccia fragments are packed in comparison to the much looser packing illustrated in Figure 13 for a typical overridden crumble-type of breccia. The tight fragment-packing and particle angularity illustrated in Figure 16 suggest that the fragments in this type of breccia have undergone little, if any, differential transport. The origin of these localized tightly packed breccia zones is obscure, but in-place brecciation due to a combination of movement in the overlying flow and to the concomitant forceful expansion of steam released from superheated water trapped in the basal part of the flow may have been involved. At flow bases, most commonly in the marginal parts of some flows, these tightly packed breccia zones locally grade into red-and-black breccias resembling those that are common in the upper zones of the flows and which are described in the next section.

The contacts between the basal vitrophyre layers and overlying lithoidal rhyolite of the central zones typically are sharp and have a subhorizontal attitude that can be followed for long distances (Figure 17). However, it is also common for these contacts to be somewhat to extremely irregular. Examples have been noted of glassy zones extending up into the overlying lithoidal material, of the interlayering of glassy and devitrified rhyolite (Figure 15), and of complex intermixing of vitrophyre and lithoidal rhyolite around spherulites and local breccia. Such occurrences impart a local gradational aspect to the boundary between the basal zone and the overlying central zone. In extreme examples, the contacts between vitrophyre and devitrified rhyolite assume bizarre forms (Figure 18) in which the devitrification

Figure 15. Flow banding and typical folds near the base of the Cedar Tree rhyolite flow, about a kilometer north of Indian Batt Cabin in Bruneau Canyon. The view consists of a mixture of glassy and lithoidal rhyolite in alternate bands. The axial planes of the folds nearly parallel the base of the flow, which dips toward the right.

followed fractures (which probably contained more water) down into the vitrophyre.

Columnar joints are locally, but conspicuously, developed at the bases of some of the rhyolite lava flows (Figure 3). They are most abundant in the Triguero Homestead and Cedar Tree flows in Bruneau Canyon. In some places, the columns are upright, but at many other places they are inclined, and locally even are horizontal or have fan-shaped arrangements, perhaps as a result of cooling next to local topographic irregularities. As is well illustrated by Figure 3, the columnar joints do not extend into the massive devitrified rhyolite of the overlying central zones, nor do they not connect with the vertical shrinkage fractures that divide the lithoidal rhyolite of the central zones into larger and more crudely shaped columns.

The basal vitrophyre and flow breccia layers most commonly rest on variably baked, generally structureless, tan, light gray, or reddish brown, silt-sized sedimentary material (Figure 6). Much of this material is thought to be old soil horizons, at least having partly originated as loess. The flows locally rest on other types of material, some of which is fine-grained, commonly white, clay-rich sediments that probably were deposited in very shallow lakes, and which may have been wet at the time of rhyolite flowage. In such circumstances, the upper meter or two of these materials have been deformed by the rhyolite flow (Figure 14), and baked mud locally constitutes the

Figure 16. Irregular lenses and tongues of breccia within the basal vitrophyre of the Long Draw rhyolite flow near the mouth of Long Draw in Bruneau Canyon. The breccia appears to have formed in place at the expense of the massive vitrophyre. The packing of the blocks and the configuration of the fragmental zones within the vitrophyre layer suggest that these are not breccia accumulations the magma flowed over, but that they may have resulted by some combination of yielding to local intense stresses at the flow base caused by resistance to flowage of the overlying material and by explosive steam release.

matrix to the breccia fragments in the lower few meters of some flows. Locally, clastic dikes of ashy material or sediment penetrate up into the basal vitrophyre of some of the rhyolite lava flows (Figure 19).

Very little volcanic ash occurs at the base of the rhyolite lava flows. Most exposures show none, and in the few where volcanic ash occurs the ash layer is only a few centimeters thick at the greatest. The only occurrence of a great amount of volcanic ash is at the base of the Triguero Homestead rhyolite, and as noted previously, it suggests proximity to the fissure through which that flow was erupted.

UPPER ZONES

The upper zones of the rhyolite flows range from a few meters to perhaps 50 meters in thickness and are

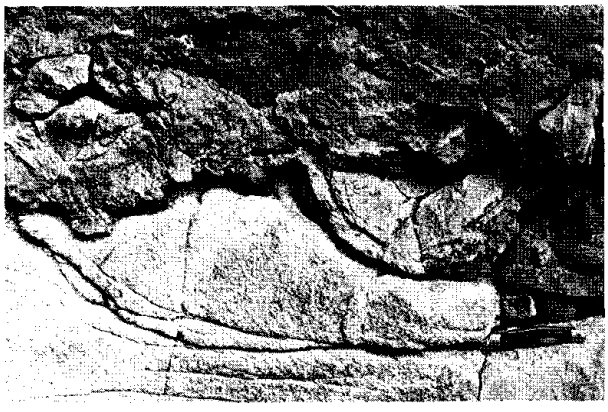

Figure 17. The sharp, but irregular, contact between the basal vitrophyre zone (below) and the bottom of the lithoidal central zone (above) of the Indian Batt rhyolite in Sheep Creek canyon. At the upper left, note the ghost of a spherulite and its irregular shrinkage cavity preserved in the lithoidal rhyolite.

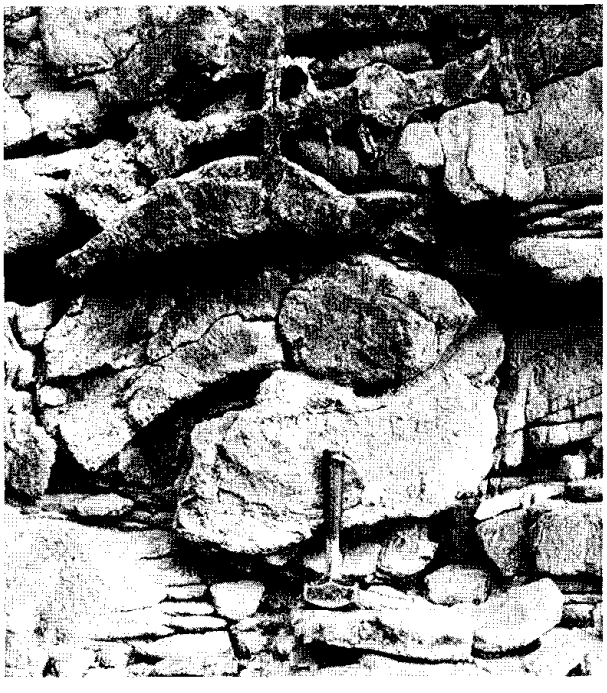

Figure 18. A rounded mass of lithoidal rhyolite enclosed within the basal vitrophyre of the Indian Batt rhyolite flow in Sheep Creek canyon. Note, at the top of the view, the thin vertical vein of lithoidal rhyolite with the medial fracture that extends from the top of the rounded lithoidal mass to connect with the bottom part of the lithoidal central zone of the flow and with the irregular horizontal layer of lithoidal rhyolite near the top of the basal vitrophyre. Devitrification was very selective here and evidently progressed much more rapidly along water-bearing fractures than it did through massive vitrophyre.

Figure 19. Fractures in the basal vitrophyre at the margin of the unnamed rhyolite lava flow between Cougar Point Tuff units XII and XIII at the north end of Black Rock escarpment. The fractures contain clastic dikes of light-colored volcanic ash that apparently moved upwards from beneath the flow margin.

structurally complex at many localities. These zones contain rhyolite in many forms including lithoidal and glassy types, dense to highly vesicular rock, folded, flow-banded, and variably jointed rock, several types of breccias, and local secondary silica deposits that probably formed as the flows cooled. In the marginal portions of the flows the upper zones merge into similarly complex zones between the flow lobes where steeply dipping sheeting joints are common. The upper zones are not as well exposed in the canyon walls as are the central zones of the flows (Figure 20).

Generally, the upper portion of the upper zones is vitrophyre which usually is black and rather massive (Figure 21), but which locally may be moderately vesicular and may be oxidized to red or brown.

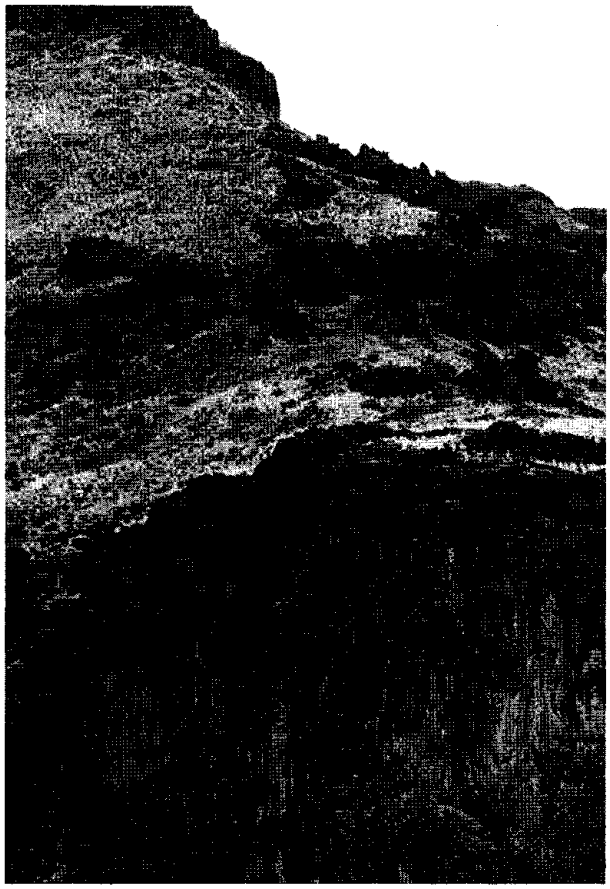

Figure 20. The boundary between the central zone (lower cliff) and the upper zone (scattered outcrops on slope) of the Sheep Creek rhyolite flow at the mouth of Stiff Tree Draw in Bruneau Canyon. Note the prominent subhorizontal sheeting at the top of the central zone and the subhorizontal layer of large gas cavities within the upper zone.

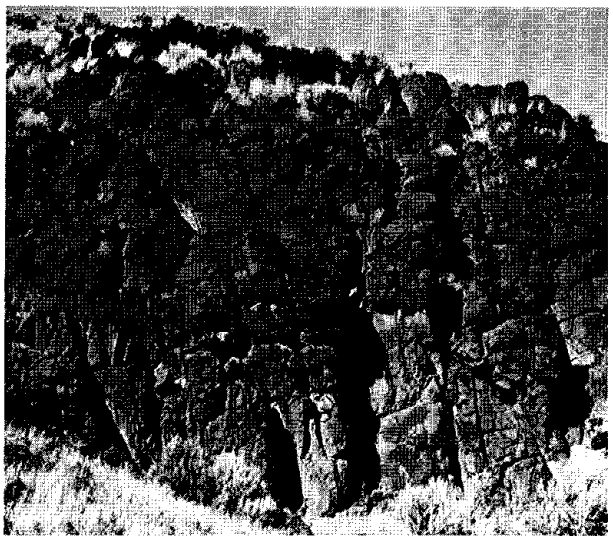

Figure 21. Thick vitrophyre layer at the top of the lower rhyolite at Louse Creek in Sheep Creek canyon. Note the blocky fracture pattern and the imperfectly developed columnar joints, but the complete lack of sheeting joints.

Crudely developed to well-developed columnar joints occur in the vitrophyre in the upper zones of some flows (Figure 21). Glassy rhyolite at the top of the upper zones commonly displays flow banding which is tightly folded and shows steeply dipping axial planes (Figure 22).

In the vitrophyre portions of the upper zones of some, and perhaps all, of the rhyolite flows, local areas of a type of red-and-black breccia occur, in which the fragments are equant cobble- to boulder-sized blocks of black vitrophyre, generally closely packed, set in a matrix of oxidized red vitrophyre (Figure 23). Flow-banding and folds are preserved in many of the clasts in this type of breccia. These breccias probably formed where relatively rapidly cooled glassy rhyolite was broken up and jostled about by movement within the underlying hotter and less viscous lava. The formation and oxidation of the matrix of this type of breccia probably resulted in part from the introduction of water into the top of the flow and its subsequent heating and re-release, perhaps in the form of explosive steam-venting. Locally this type of red-and-black breccia has been observed to grade downwards into lithoidal rhyolite in which both the blocks and matrix have been devitrified, so that only vestiges of its previous fragmental nature can be discerned. This establishes that devitrification of the breccia occurred after it had come to its final resting place. Local breccia areas have been found in the upper zones of some flows where the flowage had not yet entirely disrupted the previously formed flow bands and folds in glassy rhyolite (Figure 24). This also suggests that jostling about of the upper part of the flow, rather than extensive lateral transport, was responsible for a considerable amount of the upper zone fragmentation in the rhyolite lava flows.

An additional type of red-and-black breccia, also consisting of black glassy fragments in a red to orange glassy matrix, is common in the upper portions of all the flows. In this type of breccia the fragments are angular and isolated (Figure 25), and the matrix is seen to consist of fine-grained fragmented and oxidized glass particles that have been re-fused to a competent rock without being altered. Most likely this type of breccia is a product of explosive, very high-temperature, steam-release activity that occurred because water, which entered the flow tops, became superheated after following fractures down into hotter zones within the flows. Where they have been observed, the boundaries of the zones of this type of

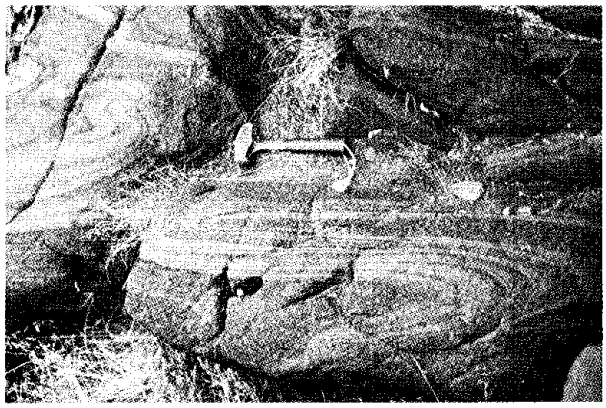

Figure 22. Folded flow bands in the upper vitrophyre of the Cedar Tree rhyolite, near the mouth of Long Draw in Bruneau Canyon. The flow bands and axial planes of the folds dip steeply; this attitude is typical near the top of a rhyolite flow.

red-and-black breccia generally have been found to grade into massive black vitrophyre by a change in proportion of angular blocks and matrix, until the only reddish matrix-type material occurs in veins that cut otherwise massive black vitrophyre.

Vitrophyre commonly predominates at the top of a flow, but downwards the proportion of devitrified rock increases. Within the upper zones the transition between glassy material and the underlying lithoidal rhyolite typically is complex; rarely is there a sharp subhorizontal contact that extends for more than a few meters. It is common for glassy and lithoidal rhyolite to be interlayered or intimately mixed together, and lithoidal spherulites and more irregular-shaped devitrification structures, some surrounding gas cavities, occur locally. The spherulites in upper zones are like those at the flow bases, including the presence of angular shrinkage cavities, but they typically are smaller and not as abundant.

Lithoidal rhyolite with abundant sheeting joints is common in the upper zones of the flows, and is especially common in the areas between lobes at the flow margin. In the upper zones, these closely spaced subparallel joints range widely in attitude, and commonly are contorted (Figure 26). It is common for the sheeting to dip very steeply in its upper occurrences and for the dip to diminish downwards to become subhorizontal near the boundary between the upper and central zones (Figure 20).

Dikelike, generally near-vertical, tabular masses of glassy rhyolite, ranging up to several meters wide and several tens of meters long, have been noted between walls of lithoidal rhyolite in the upper zones of some flows. These evidently are autointrusive, or rootless, dikes that formed when lava was squeezed up from the flow interior into fractures. Some of these autointrusive dikes have been devitrified and some are partially to completely brecciated. Less commonly, bulbous, domelike protrusions of rhyolite, also probably caused by late-stage lava squeeze-ups, occur in the upper zones. These are structurally gradational with the larger flow lobes that typify the flow margins.

Figure 23. A breccia of closely packed equant blocks of black vitrophyre set in a matrix of red, oxidized vitrophyre, from the upper part of the Dorsey Creek rhyolite near Jarbidge Canyon about 7 kilometers southeast of the mouth of the Jarbidge River. This type of red-and-black breccia probably results from movement in the rhyolite lava, which breaks up the upper zone, combined with the escape of high-temperature steam, which oxidizes the breccia matrix. Note the folded flow banding in some of the breccia blocks.

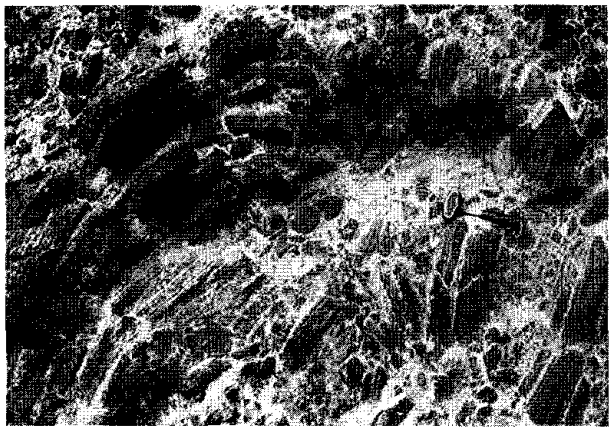

Figure 24. A breccia of flow-banded vitrophyre fragments set in a partially altered glassy matrix, in the upper part of the Cedar Tree rhyolite flow, from near the mouth of Long Draw in Bruneau Canyon. Note that not all of the fragments in the breccia have been moved from their original positions, so that part of a fold is preserved.

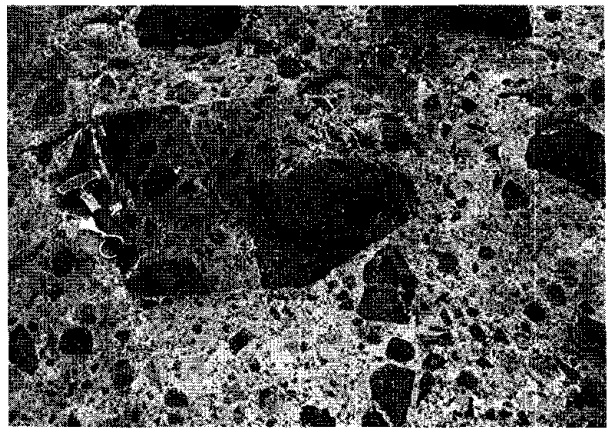

Figure 25. A typical red-and-black breccia from the upper part of the Cedar Tree rhyolite flow, at the mouth of Long Draw in Bruneau Canyon. In this type of breccia, separated angular fragments of black glassy rhyolite are set in a reddish matrix of comminuted and re-fused, oxidized but unaltered, glassy rhyolite. This type of red-and-black breccia is thought to result from the explosive escape of high-temperature steam at the tops of the rhyolite flows. Note the large angular block of refragmented breccia beside the hammer.

SHEETING JOINTS AND RELATED STRUCTURES

During and after the final stages of flowage and while the rhyolite lava flows cooled and crystallized, a variety of joint types and related structures, described in this section, formed within the flows. These include sheeting, pencil, and dimple joints, blocky breakage, tension gashes, elongate vesicles, and parallel streaks on joint surfaces. In the field many of these structures are conspicuous features of the rhyolite lava flows. This is especially true of the various jointing patterns because the rock fragments that have broken loose from the bedrock generally are bounded by preexisting joint planes.

Much of the lithoidal rhyolite in the flows contains closely spaced subparallel joints along which the rocks break into platy fragments (sheeting), typically ranging from a few millimeters to a few centimeters in thickness and from a few centimeters to a meter across (Figure 26). Throughout the central zones the sheeting generally is subhorizontal (Figure 20), but in the upper zones (Figure 26) and at the margins of the flow lobes and between, (Figures 9 and 11) it commonly is moderately to steeply inclined. Where the sheeting joints are very close together, as in the inner parts of the central zones, the rock surfaces are somewhat crumbly and difficult to sample, similar to the condition in the Cougar Point Tuff units.

Sheeting joints are essentially restricted to lithoidal rhyolite; they rarely occur in vitrophyre (Figures 3, 6, 16, 17, 19, 21, 22, and 23), and where they do occur they are very imperfect (Figures 18 and 24). Where sheeting in lithoidal rhyolite is followed into adjacent vitrophyre, the joints disappear over a distance of typically less than a meter (Figure 27). The relationship illustrated in Figure 27 has been observed at many localities and indicates that sheeting joints probably form at high temperature, concomitant with or immediately after, crystallization of the lava.

Figure 26. Typical steeply dipping and slightly folded sheeting joints developed in lithoidal rhyolite in the marginal part of the Marys Creek rhyolite flow, next to Marys Creek canyon about 5 kilometers west of the Grasmere escarpment.

Figure 27. The transition zone between sheeted lithoidal rhyolite on the left, and massive vitrophyre on the right, exhibited in the upper zone of the Indian Batt rhyolite flow in Sheep Creek canyon. The restriction of the sheeting joints to the lithoidal rhyolite suggests that they formed during or after devitrification.

The common parallelism of sheeting joints with flow bands suggests that the earlier flowage imparted a weakness parallel to alined crystallites and thin vesicle-rich layers in the bands. The fracturing which occurred during and after crystallization readily followed such a preexissting weakness direction. Such fracturing evidently accommodated both the shrinkage accompanying crystallization and the continued mass flowage of the lava. Anisotropic stresses which accompanied the flowage during and after devitrification evidently caused the sheeting joints to form. The preconditioning of the lava by the formation of flow bands most likely was convenient, but not required, for the sheeting joints to develop, inasmuch as many sets of intersecting sheeting joints have been noted (Figure 28), and only one set could follow preexisting flow bands.

Where the sheeting joints are widely spaced or absent, the rhyolite breaks into blocky rather than tabular fragments. This blocky type of breakage pattern is most common at the very base of the central zones, around the margins of flow lobes, and in portions of the upper zones. Blocky breakage is like the fracture pattern observed in glassy rhyolite (similar to that in Figures 21 and 27); many occurrences in lithoidal rhyolite probably indicate that the stresses necessary to form sheeting joints had dissipated prior to devitrification.

Where two or more closely spaced joint sets intersect (pencil jointing) elongate rock fragments

Figure 28. The development of pencil jointing in a zone where several, somewhat irregular, sets of sheeting joints intersect in lithoidal rhyolite, from the marginal part of the Sheep Creek rhyolite flow at Big Jacks Creek canyon.

(Figure 28) are formed. Pencil jointing is common at certain locations, such as at the margins of flow lobes, where bulk flowage evidently was continuing nearby even after the rhyolite had crystallized. Situations such as that shown in Figure 28, where several intersecting joint sets parallel one another in one direction, may have resulted from the rotation of local stresses (probably including the rotation of a shear couple) as the flow continued to advance even after it had crystallized.

An enigmatic type of structure that occurs locally in many flows are dimple joints (Figure 29). Dimple jointing has been observed principally in areas near zones of vitrophyre or adjacent to zones characterized by a blocky breakage pattern. Where dimple joints occur, the resulting fragments are partially bounded by curved fractures, and individual dimples may touch, as in Figure 29, or may be separated from one another. The dimples typically are between 5 and 40 centimeters across and occur as groups associated with simple sheeting joints or, as in Figure 29, in

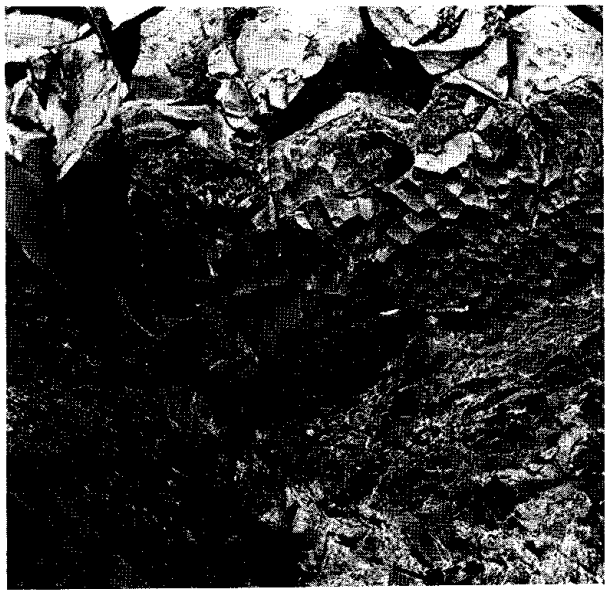

Figure 29. Dimple joints developed in lithoidal rhyolite at the boundary between a zone of closely spaced sheeting joints (below) and rather massive rhyolite with blocky joints (above), from the marginal part of the Sheep Creek rhyolite flow in Big Jacks Creek canyon.

complexly jointed lithoidal zones. Although the cause of this type of jointing is not fully understood, it seems noteworthy that dimple joints occur in most rhyolite lava flows but are extremely rare in the Cougar Point Tuff.

Open tension fissures a few centimeters apart (Figure 30) in folded lithoidal rhyolite occur locally in the basal and upper zones and marginal parts of several flows. Generally, as is the case for those in Figure 30, the fissures occur in certain flow bands but are sparse or lacking in adjacent bands. It is probable that such gashes formed after the rhyolite was partially to completely crystallized but still malleable, since the tension fissures do not normally accompany folds in glassy rhyolite (see, for example, Figures 15 and 22). Their preferential distribution suggests that marked local variation in viscosity existed and that flowage continued even after partial or complete crystallization had occurred. Tension gashes are commonly developed in proximity to late-stage, irregular-shaped gas cavities, such as the one in Figure 30.

Elongate vesicles and parallel streaks locally occur on sheeting joint surfaces (Figure 31) in the marginal and upper parts of some flows. These features are rare in comparison to the conspicuous streaks and abundant elongate vesicles in the Cougar Point Tuff, but the ones in the lava flows probably also originated from unidirectional flowage and the subsequent compaction of large elongate vesicles. The streaks in the

Figure 30. Open tension fissures a few centimeters apart within a layer of rhyolite from the upper zone of the Sheep Creek rhyolite flow at the mouth of Stiff Tree Draw in Bruneau Canyon. The gashes are developed on the wall of an open cavity at the nose of a tight fold.

lava flows most commonly appear on steeply dipping sheeting surfaces, like the nearly vertical surface pictured in Figure 31. They have not been observed to show a consistent orientation pattern, however, in contrast to their regional primary flow-direction pattern in the welded tuff units (Bonnichsen and Citron, 1982 this volume, Figure 20).

GAS CAVITIES

Gas cavities are abundant in the upper zones of the rhyolite flows and occur, but less commonly, in the central and basal zones. They range from ordinary small vesicles less than a millimeter across to giant cavities more than a meter across, and vary widely in shape. Some are spherical. Others have been greatly flattened or stretched; some have flat bottoms and domal tops, and many have irregular shapes. Commonly, gas cavities of a similar size and shape occur together in zones that may have the form of a horizontal layer, or a zone that is somewhat irregular in outline or extent. The abundance of gas cavities varies markedly from flow to flow. Some contain only sparse vesicles, even in their upper parts, whereas others contain local zones with enough cavities, especially small ones, to resemble scoriaceous basalt. The most vesicular rhyolite generally is found at flow tops and margins, and in some of the breccia fragments at the flow bases. The cavities in highly vesicular varieties of rhyolite commonly are elongated or flattened. The wide variation in their shapes largely reflects when gas cavities formed during the motion history of a flow; the highly stretched or flattened

Figure 31. The local occurrence of parallel flow marks, probably developed from the collapse of elongate vesicles, on near-vertical sheeting-joint surfaces in the marginal part of the Marys Creek rhyolite flow, from about 5 kilometers west of the Grasmere escarpment next to Marys Creek canyon.

ones evidently formed before those with equant and irregular shapes.

Giant gas cavities, some of which are considerably more than a meter across, occur in the upper zones of the flows; generally localized in their interior portions (Figure 9). Such large cavities are most abundant in the Dorsey Creek and Sheep Creek (Figure 20) flows. Their distribution suggests that only lava which did not flow far from the venting areas retained enough volatiles to permit such cavities to form and be preserved. Thus, their presence in only certain areas may indicate that those are the areas near the buried fissure systems through which the rhyolite was extruded.

JASPER AND OTHER SECONDARY DEPOSITS

Secondary silica has been deposited locally in fractures, gas cavities, spherulite shrinkage cavities, between breccia fragments, and in other openings in the rhyolite flows. Silica is most common in the upper zones. The silicious material may be opal, chalcedony, or jasper; red and brown jasper is the most common. These late-stage silica deposits evidently formed as the lava flows cooled and probably resulted from the leaching of silica by water, and its reprecipitation in cooler areas. The most notable occurrence is the Bruneau jasper deposit, which primarily is a manto of jasper-filled sperulite shrinkage cavities (Figure 32) and small fractures in the upper zone of the Bruneau Jasper rhyolite flow, in the Indian Hot Springs area (Figure 2, Bonnichsen, 1982b this volume). This

Figure 32. A jasper-filled cavity in the upper zone of the Bruneau Jasper rhyolite flow at the Bruneau jasper deposit near Indian Hot Springs in Bruneau Canyon. The irregular starlike shape of the jasper mass suggests that the cavity originated as a shrinkage fracture within a spherulite. The subsequent devitrification of the rhyolite and the jasper deposition have removed all traces of the spherulite except for the jasper-filled cavity.

deposit is at least a few hundred meters across and has been commercially exploited because the jasper is characterized by attractive colors and patterns and is available in fracture-free pieces up to several centimeters across. Similar deposits are common in the upper and marginal parts of other rhyolite flows, but the jasper at most other localities is too fractured to be easily worked.

In the upper zones and at the margins of some flows are local areas of hydrothermal alteration in which the rhyolite has been partially converted, mainly along fractures and other openings (Figure 24), to various unidentified hydrous minerals, perhaps including zeolites and clay minerals. All such alteration noted to date has been interpreted as the result of meteoric or shallow ground water interacting with the lava flow after it had been emplaced but was still cooling.

PETROGRAPHY

PHENOCRYST MINERALOGY

Plagioclase, augite, pigeonite, and opaque oxides are the principal phenocryst minerals in the rhyolite lava flows of the Bruneau-Jarbidge eruptive center. These minerals occur in all of the flows and are accompanied by quartz in more than half of the units

and by sanidine in a few (Figure 1). Magnetite is the principal opaque mineral and, in some rocks it is accompanied by ilmenite. Accessory minerals are zircon, monazite(?), and apatite. Notably absent are phenocrysts of hornblende, biotite, and fayalite. Hypersthene has not been found in any of the rhyolite flows within the eruptive center, but it does occur in some of the flows from adjacent areas. The phenocryst assemblages suggest that the rhyolitic magmas were relatively hot and dry when they were erupted.

Four different phenocryst assemblages have been noted in the rhyolite flows. All rocks contain plagioclase, augite, and opaque oxides, and most contain pigeonite as their Ca-poor pyroxene. Some contain quartz in addition, and a few of the quartz-bearing rocks contain sanidine as well. The fourth assemblage, so far noted only in quartz- and sanidine-free flows from outside of the eruptive center, contains hypersthene instead of pigeonite, or in addition to it. These different assemblages are noted in Figure 1 relative to the iron and silica contents of the various flows.

Different samples from a few of the flows (Sheep Creek, Marys Creek, and Three Creek) differ in that quartz and sanidine were not observed in all the thin sections from a given quartz- or sanidine-bearing unit. This probably is more the result of sampling than the complete lack of quartz or sanidine in portions of the units, since an individual thin section is of such a limited volume.

Plagioclase-pyroxene-opaque oxide cumulophyric aggregates, commonly with metamorphic or plutonic igneous textures, occur within all of the rhyolite flows. These vary in abundance from sample to sample and in general are more abundant than they are in the Cougar Point Tuff units (Bonnichsen and Citron, 1982 this volume). They are interpreted to be mainly fragments of protolithic material carried up from the magma source area, as they were in the Cougar Point Tuff. In addition, tiny chips of very fine-grained plagioclase, pyroxene, and opaque oxides in a granofelsic or poikiloblastic textural arrangement, occur in some thin sections. These chips are probably xenoliths from older volcanic rocks buried beneath the region.

Quartz occurs mainly as small, dipyramidal grains ranging up to a millimeter across in some flows, and in one, the Bruneau Jasper flow, to 3 millimeters across. The quartz varies from euhedral to rounded, and it may be embayed; the grains probably crystallized from the magma, and then locally were partially resorbed by it. The size and habit of the quartz is helpful in distinguishing some of the flows, as noted in the previous descriptions of the units and Table 2.

Sanidine occurs as independent grains, as a partial replacement of plagioclase phenocrysts, and locally as grains attached to plagioclase. The mineral has been found in only the Bruneau Jasper, Marys Creek, and Cedar Tree flows, and is abundant only in the Bruneau Jasper flow. Micrographic sanidine intergrowths with quartz, which occur in a few of the Cougar Point Tuff units (Bonnichsen and Citron, 1982 this volume), have not been found in any of the rhyolite lava flows.

Plagioclase is abundant, and several textural types commonly are seen together in individual thin sections. The plagioclase is mainly of intermediate composition (andesine and labradorite). Single plagioclase crystals are common, generally as subhedral tablets or laths. These crystals mainly are 0.5 to 2.0 millimeters long, but locally are as much as 5 millimeters long. Such grains may be phenocrysts which crystallized during magma ascent. Some of the plagioclase grains have combined albite-Carlsbad twinning and weakly to strongly developed normal or oscillatory zoning. Other grains have characteristics suggesting that they are refractory protolithic material which was not entirely melted during magma formation. These include anhedral grains and grain fragments, multigrain clots with annealed textures, grains with patchy, irregular, or negligible zoning, and grains with anhedral equant inclusions of pyroxene and opaque oxide minerals. The plagioclase grains in the cumulophyric aggregates typically have anhedral, internally complex forms. In most thin sections some of the plagioclase grains have been partially to extensively embayed, and some contain internal zones of brown glass inclusions. The most notable characteristic of the plagioclase (and the mineral is by far the most abundant phenocryst mineral in all of the rhyolite flows) is that grains with different histories typically occur together in almost every thin section that has been examined.

In all of the rhyolite flows from within the eruptive center the pyroxenes are a mixture of augite and pigeonite that occur mainly as rounded, equant to subhedral, prismatic single crystals, and as equant to irregular, anhedral crystals in the cumulophyric aggregates. Some pyroxene grains are wholly enclosed within plagioclase, and pyroxene grains locally enclose rounded opaque oxide grains in some aggregates. The individual crystals typically are 0.1 to 0.75 millimeter in size. In the rocks containing coexisting augite, pigeonite, and hypersthene from the area northeast of the eruptive center, the pigeonite grains commonly have thin, partial rims of augite, whereas the hypersthene grains do not show such reaction rims.

Opaque oxides occur in all of the rhyolite lava flows. Polished sections that have been examined from the Dorsey Creek, Cedar Tree, Bruneau Jasper, and Long Draw flows indicate that both magnetite and ilmenite are present, with magnetite being much more abundant than ilmenite. The magnetite grains

vary from euhedral octahedra to irregular grains and groups of grains. The magnetite grains generally contain exsolved lamellae of ilmenite, and these lamellae tend to be rather coarse in some grains. Within a given rock, the abundance and size of ilmenite lamellae in magnetite varies widely. Independent ilmenite grains have been noted in the above-named units, except for the Dorsey Creek rhyolite. Some of the independent ilmenite grains are characterized by fairly complex internal twinning. All of the independent ilmenite grains have anhedral, equant to slightly irregular shapes; no subhedral or euhedral platy grains were noted. Most of the opaque oxide grains are 0.5 millimeter or less across.

The accessory apatite, monazite(?), and zircon are most commonly associated with pyroxene and opaque oxide grains within the cumulophyric aggregates. Single crystals of the minerals have been noted, however, and some elongate grains of apatite occur enclosed within plagioclase.

THE GROUNDMASS

The groundmass varies from wholly glassy to crystallized in the rhyolite flows. Where glassy, it commonly is gray and contains abundant microlites, or it is brown with few, if any, microlites. The glass in embayments, and occurring as inclusions within plagioclase and other minerals, generally is free of crystallites and is brown. Most examples of vitrophyre that have been examined in thin section show flow banding. Generally, the bands consist of alternating brown glass and gray glass. The few samples which contain only brown glass have little or no banding, and the samples with only gray glass commonly have conspicuous banding. The flow bands typically are deformed around phenocrysts.

The flow bands in some rocks have been disrupted and broken by microfaults and microboudinage. Such instances indicate that although flowage of the glass was still continuing, the local viscosity had become so great that fracturing rather than plastic deformation became the strain mechanism. In some of these same rocks, the phenocrysts have been broken during flowage.

Rather than flow bands, a few vitrophyre samples, mainly from the upper interior parts of flows, have globule textures of two colors of glass, one generally enclosing the other. Although some of these textures show considerable compaction, they appear to record pyroclastic activity, perhaps whereby droplets of lava accumulated when the flows formed.

In the marginal parts of the flows, crystallized groundmass is commonly too fine grained to readily distinguish its mineralogy. In most samples from the interiors of flows, however, many of the grains in the groundmass are coarse enough to identify. In the interior of the thick units the cooling was prolonged enough so that groundmass quartz grew epitaxially from the surfaces of quartz phenocrysts to yield, in crossed polarizers, snowflake-like micrographic intergrowths with other groundmass constituents. Generally, the flow banding that is so evident in glassy rhyolite is absent, or only vaguely preserved, in rocks with crystallized groundmasses.

In samples that have been only partly crystallized, the devitrified parts generally consist of abundant microspherulites suspended in the glassy matrix. These commonly are accompanied by zones of devitrified groundmass attached to the surfaces of the plagioclase grains and sometimes the other phenocrysts.

Where the rhyolite has been devitrified, it is common for the mafic minerals to have been partially oxidized and to have imparted tan, brown, or red colors to most lithoidal rhyolite. Such oxidation has affected the rhyolite lava flows in varying amounts, but generally not as strongly as it has the Cougar Point Tuff (Bonnichsen and Citron, 1982 this volume). The general restriction of oxidation to lithoidal rhyolite and its rarity in the glassy parts of flows implies that it occurred during cooling, and is not an unrelated later feature.

The only glassy material noted to be strongly oxidized in the rhyolite lava flows is the red matrix portion of the red-and-black types of breccia. In these rocks the red matrix consists of fine-grained comminuted glass particles that have been oxidized to a red color, whereas the larger black fragments generally are brown, less oxidized glass.

The vesicles in the rhyolite lava flows most commonly do not have a filling mineral. Where a filling mineral occurs, it has been identified as tridymite. Such tridymite is considered to have been deposited during the cooling of the flows. Locally, calcite of probable secondary origin has been observed in a few vesicles.

CHEMISTRY

THE RHYOLITE FLOWS

The analyses for major oxides and some minor elements of a few typical rhyolite samples have been presented in Table 1, and Figure 1 is a plot of the iron and silica contents of the flows. Figure 1 illustrates very well the principal chemical variation among the flows in that some contain less and some more of the femic group of elements (Fe, Mg, Ca, Ti, Al, P, Mn),

and that this is opposite the variation in silica abundance. The SiO_2-Fe_2O_3 plot also shows that each unit, except for the Dorsey Creek rhyolite, has a relatively narrow compositional range.

The general correspondence of the types of phenocrysts in the flows with their compositions is also indicated in Figure 1. The sanidine-bearing samples are all relatively silica rich. Both the quartz-bearing and quartz-free samples span almost the entire range of compositions, but there is, as one might expect, a tendency for fewer of the low-silica samples to contain quartz than for those higher in silica. Hypersthene has been found only in samples with relatively low silica contents.

Overall, Figure 1 illustrates that the rhyolite lava flows, as a group, plot over a continuous compositional range. Further confirmation of this is given in Figure 33, in which the TiO_2 and CaO contents of the same samples shown in Figure 1 are plotted against their Fe_2O_3 contents. In Figure 33 only the field outlines are shown, but not the positions of the individual analyses. The information in Figure 33 shows the coherence among these three elements of the femic group, and illustrates again that although most of the flows are chemically somewhat distinct, as a group they form a continuous compositional field. Figure 33 also points out (as does Figure 1) that the samples from the area northeast of the eruptive center, where hypersthene is common, are on the fringe of the compositional field (symbols UF and CN in the figures). Perhaps the northeastern magmas were formed from a protolith of a slightly different

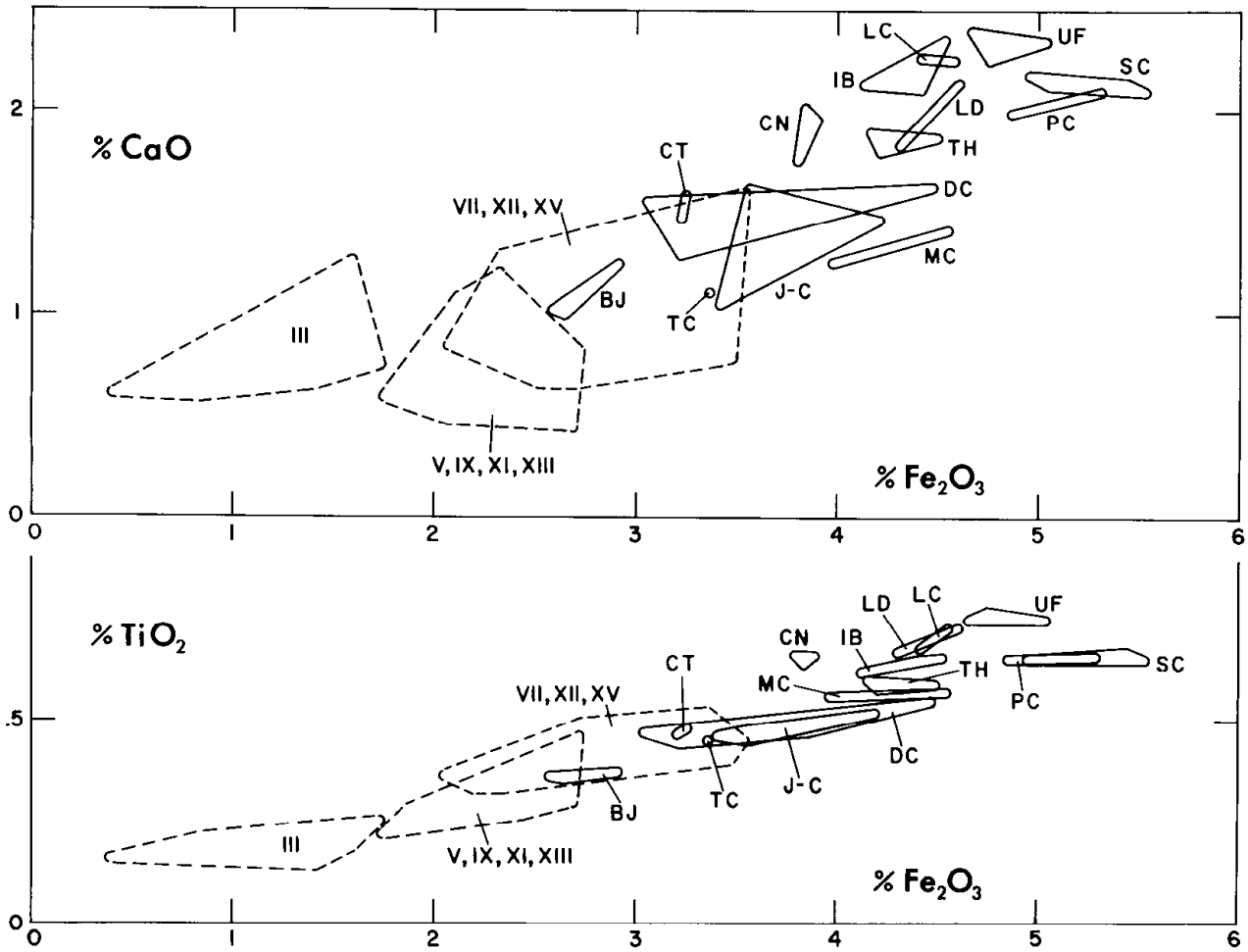

Figure 33. Plots of the weight percentages of CaO and of TiO_2 versus total iron expressed as Fe_2O_3 for the rhyolite flows (fields with solid outlines) in and northeast of the Bruneau-Jarbidge eruptive center, and for the Cougar Point Tuff (fields with dashed outlines). See Figure 1 for the symbols used to identify the various rhyolite lava flows. The same analyses of the lava flows were used for these plots as were used in Figure 1. The Cougar Point Tuff units (Bonnichsen and Citron, 1982 this volume) are divided into a more femic, cycle-top group (units VII, XII, and XV; 24 analyses), a less femic group (units V, IX, XI, and XIII; 21 analyses), and unit III, which is even less femic (5 analyses).

composition, or the magma genesis conditions there were slightly different from those for the rhyolite flows within the eruptive center.

COMPARISON WITH COUGAR POINT TUFF CHEMISTRY

The compositional ranges of the rhyolite lava flows in the Bruneau-Jarbidge eruptive center and of the Cougar Point Tuff overlap substantially. Together they form one large compositional field with no significant gaps. This is well illustrated by the TiO_2- and CaO-Fe_2O_3 plots (Figure 33). This figure also shows that the more femic cycle-top units (VII, XII, and XV) of the Cougar Point Tuff (Bonnichsen and Citron, 1982 this volume) are similar to the most silicic, and generally sanidine-bearing, rhyolite lava flows. Figure 33 also illustrates that the rhyolite lava flows are generally more femic as a group than the Cougar Point Tuff units (also see Figures 21 and 22 in Bonnichsen and Citron, 1982 this volume). Since the lava flows are younger than the Cougar Point Tuff, the general trend of the units becoming more femic with decreasing age continued from the ash-flow portion to the lava-flow portion of volcanic activity in the eruptive center.

The variations in proportions of several constituents are illustrated in triangular variation diagrams in Figures 34 and 35. These figures display the same analyses as Figures 21 and 22 of Bonnichsen and Citron (1982 this volume) and as reported in Bonnichsen (1982a). In both figures the rhyolite lava flows are portrayed by the small triangles, the more-femic Cougar Point Tuff units (VII, XII, and XV) by open circles, and the other, less-femic welded-tuff units, by filled circles.

Some of the principal variations among the major oxides are illustrated in Figure 34. Three of these plots (all except the CaO-P_2O_5-TiO_2 triangle at the lower right) illustrate again that the ash-flow units are less femic and richer in alkalis than the rhyolite lava flows, but that a continuous range of compositions with no apparent gaps exists among the units. Each group, however, has a discrete, fairly restricted compositional range, so that compositional overlap is limited.

The $(FeO+MgO)$-Na_2O-K_2O plot (upper left, Figure 34) illustrates that the K/Na ratio increases slightly when progressing from the rhyolite lava flows to the less femic ash-flow units. It is not known if this simply reflects more postemplacement alkali exchange (potassium enrichment or sodium depletion) in the basal vitrophyres of the most silicic ash-flow units, or if it is due to another cause. The K_2O-MgO-FeO plot (upper right, Figure 34) shows no significant variation in the Fe/Mg ratio over the entire range of compositions or flow types.

The CaO-$(FeO+MgO)$-(Na_2O+K_2O) plot (lower left, Figure 34) indicates a slight increase in the Ca/(Mg+Fe) ratio in progressing from the least to the most femic compositions. This probably reflects the greater abundance of plagioclase in the rhyolite lava flows than in most of the Cougar Point Tuff units.

The CaO-P_2O_5-TiO_2 plot (lower right, Figure 34) reveals very little variation in proportions of Ti and P over the entire range of compositions or flow types. This plot also shows that the rhyolite lava flows are enriched in CaO relative to P_2O_5 and TiO_2 compared with many of the ash-flow units. This probably also reflects the greater plagioclase abundance in the rhyolite flows.

The proportions of Zr, Rb, and Sr plotted in Figure 35 illustrate relationships very similar to those noted among the major oxides. Each unit is characterized by its own fairly narrow range, and except for the Sr- and Zr-impoverished sample from unit III, the group forms a continuous compositional field. The rhyolite lava flows and more femic ash-flow units have the greatest enrichment of Sr and Zr relative to Rb.

The proportions of normative quartz, albite, and orthoclase and of normative anorthite, albite, and orthoclase for the Cougar Point Tuff analyses reported in Table 1 of Bonnichsen and Citron (1982 this volume), along with those for the rhyolite lava flows from Table 1 of this paper, are plotted in Figure 36. In the Qz-Ab-Or plot, the Cougar Point Tuff units are shown to be richer in Or than either the rhyolite flows or the ternary minimum in the synthetic granite system (Tuttle and Bowen, 1958). The Cougar Point Tuff samples are clearly on the Or-rich side of the compositional field for granitic and rhyolitic rocks associated with petrogeny's residua system. The greater Or/Ab ratio for the Cougar Point Tuff than for the rhyolite lava flows probably reflects more plagioclase in the rhyolite flows. This greater Or/Ab ratio may also have resulted partially from an increase in the K/Na ratios in the basal vitrophyres of the ash-flow units, because of postemplacement alkali exchange.

In the An-Ab-Or plot in Figure 36, the Cougar Point Tuff units show higher Or and lower An contents than those in the rhyolite lava flows, and higher Or than that in most rhyolitic and granitic rocks (see Figure 67 in Tuttle and Bowen, 1958). Again, the greater abundance of plagioclase in the rhyolite flows than in the Cougar Point Tuff, and perhaps the effect of postemplacement alkali exchange in the ash-flow vitrophyres, may account for these variations in normative ratios, rather than any compositional differences among the silicate-melt portions of the magmas.

COMPARISON OF RHYOLITE FLOWS WITH THE COUGAR POINT TUFF

Many of the rhyolite flows in the eruptive center have been traced for many kilometers; such distances commonly are associated with welded ash-flow tuff units rather than rhyolite lava flows. The rhyolite flows have thick central zones of massive lithoidal rhyolite which lie above basal vitrophyre zones, and are capped by structurally complex upper zones, in a fashion similar to the Cougar Point Tuff units. With such characteristics, the rhyolite flows superficially resemble the Cougar Point Tuff units and perhaps other ash flows. This is especially true where poor exposures preclude a clear overall view of a unit whose mode of emplacement might be in question.

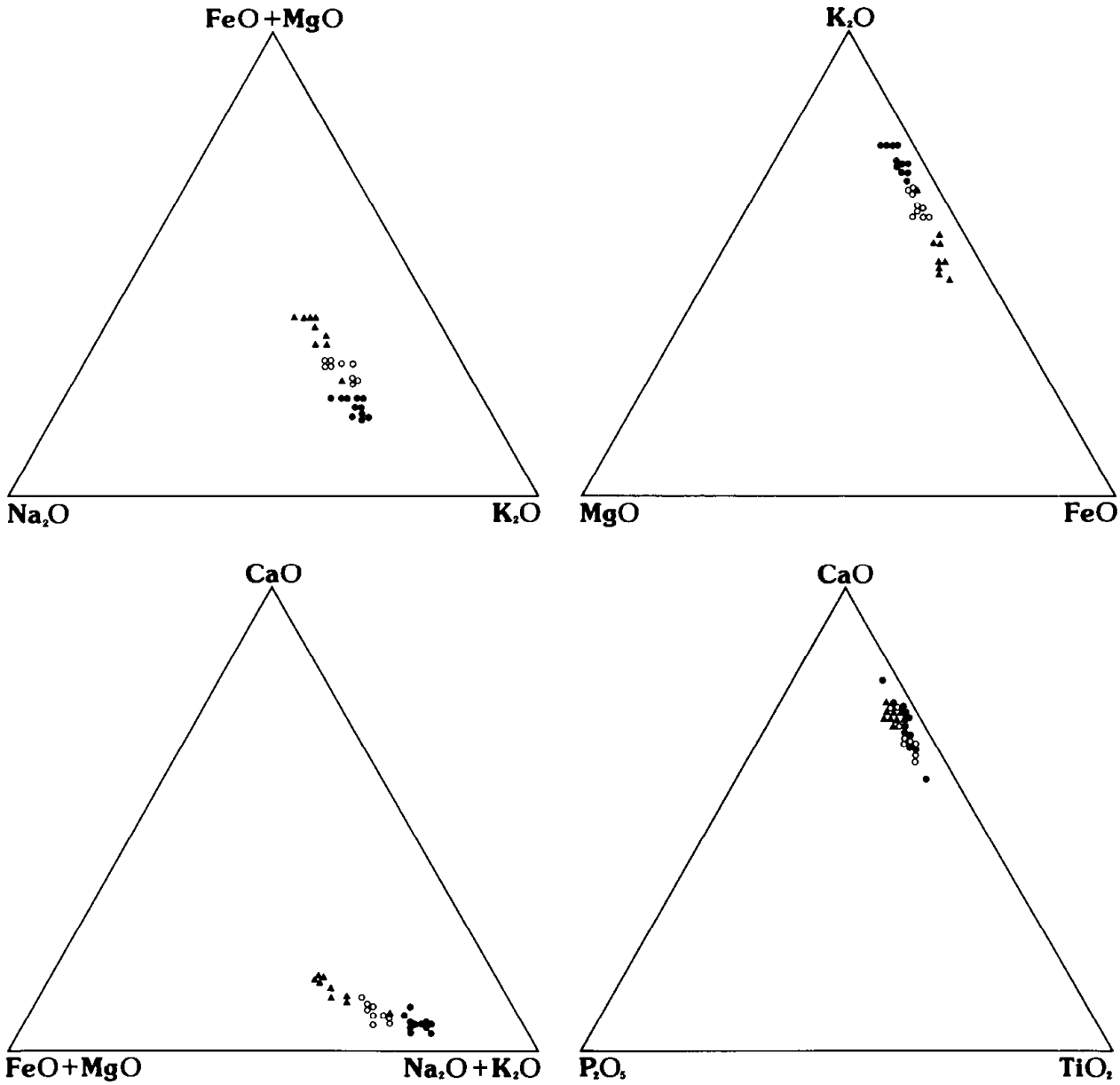

Figure 34. Variation diagrams showing the weight percentage proportions of various major oxides in the Cougar Point Tuff and in some of the rhyolite flows. Triangles are rhyolite flows; open circles are the more femic Cougar Point Tuff units (VII, XII, and XV); and the filled circles are the other Cougar Point Tuff units. The analytical data plotted here are reported in Tables 2 and 3 of Bonnichsen (1982a). The total iron content is expressed as FeO rather than Fe_2O_3.

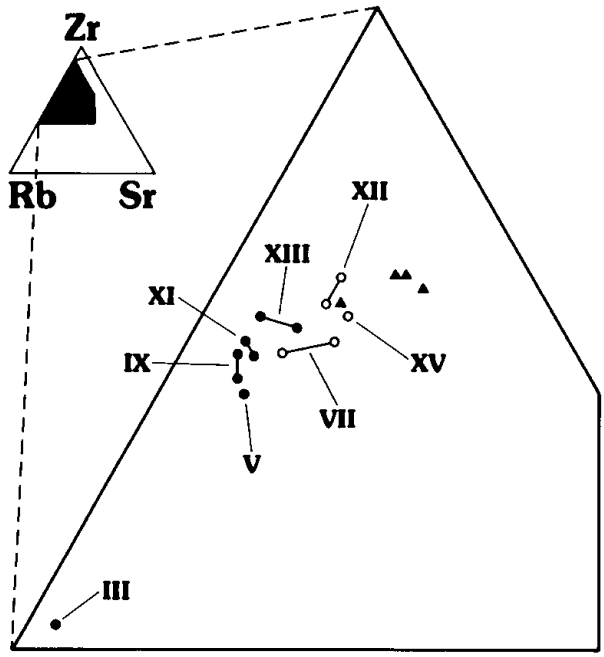

Figure 35. The proportions of Zr, Rb, and Sr in some of the rhyolite flows and in the Cougar Point Tuff units. Triangles are rhyolite flows; open circles are the more femic Cougar Point Tuff units (VII, XII, and XV); and the filled circles are the other Cougar Point Tuff units. The analyses for this plot are reported in Table 5 of Bonnichsen (1982a).

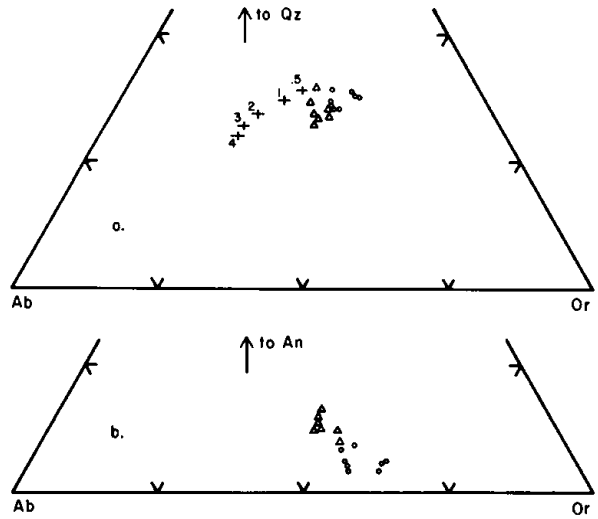

Figure 36. Plots of the rhyolite lava flow norms (triangles) from Table 1 compared with the Cougar Point Tuff norms (circles) from Table 1 of Bonnichsen and Citron (1982 this volume). Plot A is the lower part of the normative quartz-albite-orthoclase triangle, and plot B is the lower part of the normative anorthite-albite-orthoclase triangle. The crosses in plot A indicate the positions of the 0.5, 1, 2, and 3 kilobar minima on the ternary cotectic, and the 4 kilobar cross indicates the two feldspar-quartz eutectic in the synthetic granite system (from Tuttle and Bowen, 1958).

Specific features are noted below that might help determine the mode of emplacement of rhyolite units similar to those erupted from the Bruneau-Jarbidge eruptive center.

In canyon exposures, the central zones of the rhyolite lava flows typically erode to a double cliff (Figures 2, 7, 8, and 10); this is not true of the Cougar Point Tuff units. Conversely, many of the thicker welded tuff units are seen in good vertical exposures to be horizontally layered (Figures 2, 7, and 8, Bonnichsen and Citron, 1982 this volume).

None of the rhyolite lava flows has been observed to thin laterally to only a few meters in thickness, or to bifurcate to two or more separate cooling units in the same fashion as do the Cougar Point Tuff units. Instead, the rhyolite flows have relatively blunt ends and are characterized by marginal flow lobes and intervening zones of structurally complex, jointed and brecciated rhyolite.

The rhyolite lava flows most commonly lie on generally structureless, buried soil horizons or in some instances on clay-rich sedimentary materials that probably were in shallow lakes at the time of extrusion. Thin volcanic ash layers occur at the base of some lava flows, but do not generally exceed a few centimeters in thickness. The welded tuff units, on the other hand, typically lie on a meter or more of thinly layered air-fall tuff. Where exposures have cut deep enough, these air-fall layers can be seen to lie on older buried soil or on sedimentary horizons like those below the rhyolite lava flows (compare Figure 6 with Figure 12 in Bonnichsen and Citron, 1982 this volume).

The rhyolite lava flows commonly have breccias at their bases, expecially in their marginal zones, but such breccias have not been observed in any of the Cougar Point Tuff units. The lack of a basal breccia, however, is not evidence that a particular unit is a welded ash-flow tuff, since basal breccias are commonly absent in the interior parts of the rhyolite flows (Figure 9).

Other types of breccia (Figures 23, 24, and 25) occur in the upper zones of the rhyolite flows, but have not been observed in the Cougar Point Tuff units. Especially common in the upper zones of the rhyolite flows are the red-and-black types of breccias (Figures 23 and 25).

The basal vitrophyre layers in the lava flows commonly contain tightly folded flow-banding, generally with subhorizontal axial planes, whereas such banding and folding is unusual in the basal vitrophyre layers of the Cougar Point Tuff units. On the other hand, flattened pumice fragments occur, and locally are abundant, in the basal vitrophyres (and elsewhere) of the Cougar Point Tuff units, but have not been observed in any of the rhyolite flows.

In the basal vitrophyre zones of the rhyolite lava flows and ash-flow units, the upwards transition to devitrified rhyolite is similar and commonly involves variable amounts of spherulitic devitrification within the upper part of the basal vitrophyre. The sharp contact between glassy and lithoidal rhyolite at the top of the basal vitrophyre layers in the welded tuff units is generally more planar than it is in the rhyolite lava flows (compare Figures 15, 17, and 18 with Figures 12 and 13 in Bonnichsen and Citron, 1982 this volume). In the lava flows the vitrophyre-lithoidal rhyolite contacts locally are rather complex, with folded flow bands that are alternately glassy and lithoidal. The vitrophyre-lithoidal rhyolite contacts in the Cougar Point Tuff units, however, are in nearly all instances virtually subhorizontal planes. Swarms of closely spaced lithophysal cavities, commonly with devitrification coronas, locally occur in the basal vitrophyre zones of many of the Cougar Point Tuff units, but are not a feature observed in the basal zones of the rhyolite flows.

Upper vitrophyre zones are more common in the rhyolite flows, as are large gas cavities and autointrusive or rootless dikes. On the other hand, horizontal lenses and layers of abundant subequant lithophysal cavities, like those in the welded ash-flow tuffs, as shown in Figure 10 of Bonnichsen and Citron (1982 this volume), are not a feature of any of the rhyolite flows.

The sheeting joints in the rhyolite flows and in the Cougar Point Tuff units are quite similar. The pencil and dimple joints locally found in the lava flows, however, are not characteristic features of the Cougar Point Tuff. Conversely, the subhorizontal flow marks that are abundant in the Cougar Point Tuff are rare in the rhyolite flows, and where observed, the sheeting joints on which they are impressed have commonly been rotated to steep or vertical attitudes.

The lava flows and Cougar Point Tuff units are petrographically similar, especially where the groundmass is crystallized. If the groundmass is glassy, however, bubble-wall shards and small pumice fragments are common in the ash flows, although they may have been greatly flattened and deformed. Deformed bubble-wall shards and flattened pumice fragments are not a feature of the rhyolite flows. Microfaulting and microboudinage of flow banding in the lava flows, however, has locally resulted in fragmentation textures that resemble the deformed-particle textures of strongly compacted welded tuffs, so caution is advised in interpreting the volcanic glass textures.

In the ash-flow units a variable proportion of the plagioclase and sanidine phenocrysts are crystal fragments; evidently they were broken during the vesiculation and eruption or during the rapid flowage of the hot ash. Extensive crystal breakage, however, is uncommon in the rhyolite lava flows. There, it has mainly been noted in rocks that also show evidence of fracturing of the flow banding. In such rocks the crystal fragments commonly are still near one another, implying that the breakage occurred at the end of the flowage process, whereas it is very rare to find adjacent pieces broken from the same crystal in the Cougar Point Tuff.

ORIGIN AND EVOLUTION OF THE RHYOLITIC MAGMAS

The Cougar Point Tuff units and the rhyolite lava flows share several characteristics that suggest how the magmatic system associated with the Bruneau-Jarbidge eruptive center may have evolved. Some of these are summarized below.

The rhyolite flows and welded tuff units form a continuous compositional field (Figures 33, 34, 35, and 36). The principal variation is the antithetic behavior of silica and the femic constituents, with the most silicic rhyolites occurring only as ash-flow units, the least silicic only as lava flows, and with a large overlap between the two types. Nearly every batch of magma that erupted had a fairly restricted composition compared with the overall range, even though the units are large and the samples were collected many kilometers apart.

The Cougar Point Tuff has been divided into cycles in which successive units are less silicic than the preceding ones (see Figures 21 and 22 in Bonnichsen and Citron, 1982 this volume). In at least two of the cycles, the last magmas erupted as rhyolite lava flows. The rhyolite flows exposed on Black Rock escarpment between units XII (below) and XIII (above) of the Cougar Point Tuff form the last part of the underlying cycle. Cougar Point Tuff units XIII and XV, which form the uppermost cycle, are overlain by the Triguero Homestead and Indian Batt rhyolite flows. These two lava flows continue the compositional trend shown by the two Cougar Point Tuff units.

The lava flows and ash-flow units have plagioclase, Ca pyroxene, and opaque oxide phenocrysts, and nearly all contain pigeonite. Many units contain quartz; some contain sanidine, and a few of the ash-flow units carry fayalite. Amphiboles, biotite, and hypersthene are essentially absent. The plagioclase-pyroxene-opaque oxide cumulophyric aggregates in both the lava flows and ash-flow units, and other textural characteristics suggest that a portion of the plagioclase, pyroxene, and opaque oxide grains came from the protolithic rocks that were melted, rather than having been crystallized from the magmas that

carried them to the surface. Such protolithic material is more abundant in the lava flows. The ash-flow units and the lava flows contain plagioclase grains, and some carry other phenocrysts, that were embayed after the grains were in the magma. Quartz and sanidine in both types of units have shapes suggestive of growth from the magma and are not part of the cumulophyric aggregates. In some units, the quartz and sanidine grains are embayed; this may have occurred after the grains had crystallized from the magma.

ENVIRONMENT OF MAGMA FORMATION

The close association of basalt and rhyolite in the Bruneau-Jarbidge eruptive center, the apparent high temperatures and low water contents of the magmas and their initial Sr isotope ratios, and the other evidence cited for rhyolite genesis in the Snake River Plain volcanic province (see, for example, Christiansen, 1982 this volume; Ekren and others, 1982 this volume; and Leeman, 1982a and 1982b this volume) all suggest that the rhyolitic magmas were formed because large volumes of basalt magma rose from the mantle and melted portions of the crust. The relatively large size of the rhyolitic units suggests that the batches of basaltic magma were rather large. Perhaps some had volumes comparable with those of large flood basalt units such as the Pomona or Roza flows of the Columbia River basalt (Hooper, 1982), or with volumes similar to large differentiated mafic igneous complexes, such as the Stillwater Complex in Montana or some of the individual plutons within the Duluth Complex of Minnesota, or even with the individual basins of the Bushveld Complex of South Africa (Wager and Brown, 1967).

In considering the environment from which the rhyolitic magmas might have been erupted, it is worth examining some of the general aspects of large differentiated mafic plutons. Many are sill-like and were formed from the repeated injection of basaltic magma into the crust. Other large bodies of plutonic and hypabyssal mafic rocks typically occur subjacent to the complexes, also indicating repeated intrusion. Preexisting rocks in contact with, and residing as inclusions within, large mafic plutons commonly have lost substantial amounts of a granitic component to have become more refractory and dense. The upper parts of some differentiated mafic igneous complexes contain substantial quantities of granitic or granophyric rocks. Where roof rocks of such complexes are preserved, as is the case for portions of the Duluth Complex, rhyolitic hypabyssal and volcanic rocks are found to be intercalated with mafic volcanic rocks in a fashion suggesting both types were erupted from the same underlying large magma chamber (Bonnichsen, 1972, p. 371). Overall, the conditions during the injection of large amounts of basaltic magma into the continental crust and the subsequent evolution of the resulting differentiated mafic igneous complexes, are also conditions that are attractive for the formation of large volumes of rhyolitic magma.

With the idea that one or more large mafic plutons are probably buried beneath the Bruneau-Jarbidge eruptive center, the following discussion and speculations suggest how such a mafic magmatic system might have caused the rhyolite magmas to form and evolve in order to develop the features that the Cougar Point Tuff units and the subsequent rhyolite lava flows in the eruptive center possess.

A very large volume (for example 500-5,000 cubic kilometers) of basaltic magma would rise principally to a level in the crust above gabbroic or other rocks with a greater density, and then would tend to spread laterally beneath and into the zone of less dense upper crustal rocks containing substantial quantities of quartz and alkali feldspar. The regional geology north and south of the Snake River Plain (Bond, 1978; Stewart and Carlson, 1978) suggests that the upper crust beneath the Bruneau-Jarbidge eruptive center would have contained Precambrian quartzofeldspathic metamorphic rocks and granitic rocks similar to those in the Idaho batholith, perhaps accompanied by Paleozoic marine sediments and Eocene volcanic rocks and plutons.

A large amount of basaltic magma would yield much heat to the crustal rocks it invaded; part of this heat would raise their temperature, and part would melt quartz, alkali feldspar, and portions of the other minerals to form rhyolitic magmas. The amount of melting would depend on, among other things, the pre-injection temperature of the wall rocks and on how much water they contained. Both of these factors would be affected by how many magma batches had invaded the zone previously. If a mass of basaltic magma was injected into a quartz- and alkali feldspar-rich zone that had a high initial temperature, but which had undergone little previous melting, a relatively large volume of rhyolitic magma could be produced.

Horizontal and vertical crustal movements very likely would accompany the growth of the magma chamber during the injection of a large batch of basaltic magma. Regional crustal movements related to the tectonic processes responsible for the generation of the basaltic magma might occur concurrently. Such motion would generally be extensional, especially above the basalt magma as it rose and spread laterally. Such a situation could lead to substantial

fragmentation of the rocks being injected, so that much rock from which rhyolitic magma could be melted might rapidly come into intimate contact with invading basaltic magma. Rhyolitic magma formed in this fashion would initially be in close contact with the invading basaltic magmas; the rhyolitic magmas might even continue to increase in temperature as long as they remained in contact.

For at least part of the compositional ranges of basalts (Fe-rich) and rhyolites (K-rich), the two types of magmas are either immiscible (Roedder, 1951; Roedder and Weiblen, 1971) or show little disposition to mix when in intimate contact (Yoder, 1973). Consequently, much of the anatectic rhyolitic magma would have retained its compositional integrity, rather than mixing with the basaltic magma to form large amounts of magma with an intermediate composition. This incapacity to mix would have been enhanced by the generally water-poor conditions that apparently existed in the zone of melting. In addition, the portions of the basaltic magmas that lost their heat during the melting of wall rocks and inclusions would have crystallized and lost their ability to mix with the rhyolitic magmas.

Since rhyolitic magmas are less dense than basaltic magmas, they would rise to the upper parts of the magma chambers. This could occur rapidly for a large volume of magma if fragmentation was extensive in the melting zone. If large volumes of rhyolitic magma were rapidly formed in plagioclase-, pyroxene-, and opaque oxide-bearing rocks, clasts and individual grains of these minerals would probably become suspended in, and carried along with, the magma as it accumulated in the roof zone of the magma chamber. Plagioclase, pyroxenes, and opaque oxides would occur in most plausible protolithic rocks, whether metamorphic, plutonic, or volcanic.

Depending on the geometry and volumes involved, a series of local zones, or even a continuous horizontal layer of rhyolitic magma, might accumulate immediately above the basaltic magma pool. During and immediately after its accumulation, a layer of rhyolitic magma could be heated further until its temperature approached that of the underlying basaltic magma. This would further melt enclosed protolithic fragments and portions of the magma chamber roof. Amphiboles and micas that initially might have been in the protolithic rocks and in the roof zone would very likely have been dehydrated and converted to pyroxenes or other anhydrous minerals during the temperature rise. Volatiles released during the premelting metamorphism of the roof zone rocks would very likely be driven from the zone, probably upwards along fractures, rather than being incorporated into the magma pool below.

MAGMA ASCENT AND ERUPTION

A layer of rhyolitic magma would probably be less dense than the overlying rocks. This would be an unstable situation. The magma would exploit vertical weakness zones in the overlying material and start to rise. Its ascent rate would depend on the density contrast, its viscosity (which, in turn, is related to its temperature) and volume, and the distribution and nature of the fractures or other weaknesses in the overlying material and the stresses existing there. In all probability, the injection of basaltic magma into the crust, the consequent melting and rise of rhyolitic magma to the top of a developing basaltic magma chamber, and the further diapiric rise of rhyolitic magma toward the surface along fractures and other zones of weakness, would overlap in time.

If rhyolitic magma formed at great enough depth, the first part of its ascent might involve considerable plastic deformation of the surrounding materials. At higher levels, however, fractures would become important in determining its paths of ascent. The rise of magma at much lower levels, involving the deformation and pushing aside of the surrounding materials, would very likely proceed more slowly than magma ascent through fractured materials at higher levels. If a sufficient magma volume was available to supply an ever-lengthening column of magma, the ascent rate might increase upwards as the source layer migrated into and up a vertical weakness zone. For a long vertical fissure, the ascent rate at various locations along the fissure could vary markedly.

A relatively slow ascent rate, such as would probably prevail for smaller magma batches at lower temperatures and at greater depths, would probably permit significant upwards concentration of volatiles and selected elements to occur in a rising magma column. A slow ascent would allow substantial cooling of the magma and the crystallization of phenocrysts to occur. Conversely, a relatively fast ascent, which is more likely for larger magma batches at higher temperatures and shallower depths, would impede the selective upwards migration of volatiles and associated elements. Fast ascent would also result in greater heat retention and less crystallization of phenocrysts, or even their resorption, if the lowering of the fusion temperature for the phenocryst minerals was not offset by the loss of sufficient heat from the magma as the lithostatic pressure on it decreased. Such resorption would most likely occur in a magma with a very low water content because the crystallization temperatures of dry and nearly dry silicate melts increase with increasing pressure, rather than decreasing as they do under water saturated and

partially saturated conditions.

The resorption of plagioclase in most of the units, and of quartz and sanidine in some, suggests that the ascent was relatively rapid, especially for the magmas that erupted as rhyolite lava flows. In the case of the rhyolite lava flows, there appears to be ample evidence to suggest the magmas rose rapidly enough from their melting zones so that significant magmatic differentiation did not occur. For the ash-flow units, not enough evidence has been gathered to clearly establish how much differentiation might have occurred during magma ascent, but it would appear to be minimal.

The Cougar Point Tuff and rhyolite lava flow units ranged from violent pyroclastic eruptions to the relatively benign flow of magma from fissures across the surface. This variation must largely reflect the water contents of the different magma batches that rose, and especially of their upper portions, with the magmas that erupted as lava flows containing so little water that little or no disruptive vesiculation could occur (see Bonnichsen and Citron, 1982 this volume, for further comments on the eruption of the Cougar Point Tuff units).

COMPOSITIONAL VARIABILITY

The individual rhyolitic magma batches that erupted from the Bruneau-Jarbidge eruptive center evidently formed under fairly uniform conditions of temperature, water content, and protolithic composition, and they remained relatively homogeneous after being formed and aggregated into large masses. The relatively homogeneous chemical compositions and phenocryst assemblages of most of the rhyolite lava flows suggest that their magmas did not undergo extensive upwards volatile enrichment or other types of magmatic differentiation during ascent. Such overall compositional uniformity is harder to confirm in the ash-flow units than in the rhyolite lava flows, because the eruption and transport processes appear to have selectively separated the crystals from the distal portions of some of the ash flows, and post-emplacement alkali exchange may have changed the compositions of some of the basal vitrophyre samples which have been analyzed.

In contrast to the relative compositional uniformity within most of the individual rhyolite units, considerable variability is evident between the rhyolite units when they are treated as a group (Figures 1 and 33; and Figures 21 and 22 in Bonnichsen and Citron, 1982 this volume). The variations include an overall evolutionary trend in which the rhyolite lava flows generally are less silicic and more femic than the earlier ash-flow units of the Cougar Point Tuff (Figure 33) and the apparent compositional cycles that were noted by Bonnichsen and Citron (1982 this volume) within the succession of Cougar Point Tuff units.

I suggest that the general evolutionary trend, in which the later rhyolitic magma batches became more femic and contained less water than the earlier batches, reflects the progressive dehydration and the removal of the less refractory constituents from the entire crustal zone beneath the eruptive center, as batch after batch of basaltic magma was introduced.

The compositional cycles, in which successive rhyolite units become more femic, might have originated because of random preexisting inhomogeneities in the temperature, bulk composition, and water content of the protolithic rocks in different parts of the crust. Although such random variations may account for the cycles, their existence seems too convincing to entirely dismiss in this fashion, and similar trends have been noted in other volcanic systems. Furthermore, the compositional trends within the cycles are similar to the overall compositional evolution of the magmas from the eruptive center.

The explanation I prefer to account for these compositional trends, although certainly not proven, is that each succeeding batch of rhyolitic magma was obtained from the same general crustal zone as the preceding, because the zone was invaded by additional basaltic magma. Thus, the start of a new cycle simply indicates that the basaltic magmas were then being injected into a different, less depleted part of the crust. This generally seems consistent with the pattern of volcanism in the eruptive center and with the general properties of rhyolitic and basaltic magmas, but the collection of further data and the careful consideration of alternative hypotheses certainly is needed for all aspects of the volcanism which occurred in such a large and complex system.

ACKNOWLEDGMENTS

I take pleasure in thanking Dale Conover, Falma Moye, Carol Bonnichsen, Everett Bonnichsen, and James Bonnichsen for their assistance during the field work; Nancy Wotruba, Steve Devine, Ivan Herrick, and Peter Hooper for their assistance with the X-ray fluorescence analyses; and Fred Hutchison for performing the atomic absorption analyses. I am pleased to thank Bill Rehrig and Bob Wilson for making the arrangements with Conoco, Inc., to provide the minor element analyses; and finally, I would like to thank Margi Jenks, John Bernt, and Lisa McBroome for their helpful reviews of the manuscript.

REFERENCES

Bernt, John and Bill Bonnichsen, 1982, Pre-Cougar Point Tuff volcanic rocks near the Idaho-Nevada border, Owyhee County, Idaho, *in* Bill Bonnichsen and R. M. Breckenridge, editors, Cenozoic Geology of Idaho: Idaho Bureau of Mines and Geology Bulletin 26.

Bond, J. G., 1978, Geologic map of Idaho: Idaho Bureau of Mines and Geology, scale 1:500,000.

Bonnichsen, Bill, 1972, Southern part of Duluth Complex, *in* P. K. Sims and G. B. Morey, editors, Geology of Minnesota: A Centennial Volume: Minnesota Geological Survey, p. 361-387.

———, 1981, Stratigraphy and measurements of magnetic polarity for volcanic units in the Bruneau-Jarbidge eruptive center, Owyhee County, Idaho: Idaho Bureau of Mines and Geology Open-File Report 81-5, 75 p.

———, 1982a, Chemical composition of the Cougar Point Tuff and rhyolite lava flows from the Bruneau-Jarbidge eruptive center, Owyhee County, Idaho: Idaho Bureau of Mines and Geology Open-File Report 82-1, 22 p.

———, 1982b, The Bruneau-Jarbidge eruptive center, southwestern Idaho, *in* Bill Bonnichsen and R. M. Breckenridge, editors, Cenozoic Geology of Idaho: Idaho Bureau of Mines and Geology Bulletin 26.

Bonnichsen, Bill and G. P. Citron, 1982, The Cougar Point Tuff, southwestern Idaho and vicinity, *in* Bill Bonnichsen and R. M. Breckenridge, editors, Cenozoic Geology of Idaho: Idaho Bureau of Mines and Geology Bulletin 26.

Christiansen, R. L., 1982, Late Cenozoic volcanism of the Island Park area, eastern Idaho, *in* Bill Bonnichsen and R. M. Breckenridge, editors, Cenozoic Geology of Idaho: Idaho Bureau of Mines and Geology Bulletin 26.

Citron, G. P., 1976, Idavada ash-flows in the Three Creek area, southwestern Idaho, and their regional significance: Cornell University M.S. thesis, 83 p.

Ekren, E. B., D. H. McIntyre, E. H. Bennett, and R. F. Marvin, 1982, Cenozoic stratigraphy of western Owyhee County, Idaho, *in* Bill Bonnichsen and R. M. Breckenridge, editors, Cenozoic Geology of Idaho: Idaho Bureau of Mines and Geology Bulletin 26.

Hart, W. K. and J. L. Aronson, in press, K-Ar ages of rhyolite from the western Snake River Plain area, Oregon, Idaho, and Nevada: Isochron West no. 36, p. 17-19.

Hooper, P. R., 1982, The Columbia River basalts: Science, v. 215, p. 1463-1468.

Leeman, W. P., 1982a, Development of the Snake River Plain-Yellowstone Plateau province, Idaho and Wyoming: an overview and petrologic model, *in* Bill Bonnichsen and R. M. Breckenridge, editors, Cenozoic Geology of Idaho: Idaho Bureau of Mines and Geology Bulletin 26.

———, 1982b, Rhyolites of the Snake River Plain-Yellowstone Plateau province, Idaho and Wyoming: a summary of petrogenetic models, *in* Bill Bonnichsen and R. M. Breckenridge, editors, Cenozoic Geology of Idaho: Idaho Bureau of Mines and Geology Bulletin 26.

———, 1982c, Geology of the Magic Reservoir area, Snake River Plain, Idaho, *in* Bill Bonnichsen and R. M. Breckenridge, editors, Cenozoic Geology of Idaho: Idaho Bureau of Mines and Geology Bulletin 26.

Malde, H. E., H. A. Powers, and C. E. Marshall, 1963, Reconnaissance geologic map of west-central Snake River Plain, Idaho: U. S. Geological Survey Miscellaneous Geologic Investigations Map I-373, 1:125,000.

Roedder, E. W., 1951, Low temperature liquid immiscibility in the system K_2O-FeO-Al_2O_3-SiO_2: American Mineralogist, v. 36, p. 282-286.

Roedder, E. W. and P. W. Weiblen, 1971, Petrology of silicate melt inclusions, Apollo 11 and Apollo 12 and terrestrial equivalents: Proceedings of the Second Lunar Science Conference: Geochemica Cosmochimica Acta, Supplement 2, v. 1, p. 507-528.

Spear, D. B. and J. S. King, 1982, Geology of Big Southern Butte, Idaho, *in* Bill Bonnichsen and R. M. Breckenridge, editors, Cenozoic Geology of Idaho: Idaho Bureau of Mines and Geology Bulletin 26.

Stewart, J. H. and J. E. Carlson, 1978, Geologic map of Nevada: U. S. Geological Survey, scale 1:500,000.

Struhsacker, D. W., P. W. Jewell, J. Zeisloft, and S. H. Evans, Jr., 1982, The geology and geothermal setting of the Magic Reservoir area, Blaine and Camas Counties, Idaho, *in* Bill Bonnichsen and R. M. Breckenridge, editors, Cenozoic Geology of Idaho: Idaho Bureau of Mines and Geology Bulletin 26.

Tuttle, O. F. and N. L. Bowen, 1958, Origin of granite in the light of experimental studies in the system $NaAlSi_3O_8$-$KAlSi_3O_8$-SiO_2-H_2O: Geological Society of America Memoir 74, 153 p.

Wager, L. R. and G. M. Brown, 1967, Layered Igneous Rocks: W. H. Freeman and Company, San Francisco, 588 p.

Wilson, H. D. B., L. C. Kilburn, A. M. Graham, and Ken Ramlal, 1969, Geochemistry of some Canadian nickeliferous ultrabasic intrusions, *in* H. D. B. Wilson, editor, Magmatic Ore Deposits—

A Symposium: Economic Geology Monograph 4, p. 294-309.

Yoder, H. S., Jr., 1973, Contemporaneous basaltic and rhyolitic magmas: American Mineralogist, v. 58, p. 153-171.

Pre-Cougar Point Tuff Volcanic Rocks Near the Idaho-Nevada Border, Owyhee County, Idaho

by

John Bernt[1] and Bill Bonnichsen[2]

ABSTRACT

Along the Nevada border in south-central Owyhee County, Idaho, Eocene- and Miocene-age volcanic units in the upper Sheep Creek drainage are exposed beneath the areally extensive Cougar Point Tuff. The Eocene-age rocks, referred to as the Bieroth volcanics, consist of three units—the Alder Creek tuff, the Cedar Canyon tuff, and the volcanic neck of Browns Basin. The Bieroth volcanics are ferrolatitic to rhyodacitic in composition and contain abundant phenocrysts, including hornblende and biotite. The Bieroth volcanics are part of the Eocene province of calc-alkaline volcanism that extends southward, and generally becomes younger, from the Challis volcanic field in central Idaho into Nevada.

Six volcanic units of probable Miocene age have been identified as follows: the Rough Mountain rhyolite, the lapilli tuff of Sheep Creek, the Johnstons Camp rhyolite, the Browns Basin tuff, the Whiskey Draw rhyolite, and the Rattlesnake Draw tuff. All are rhyolitic in composition and all have chemical compositions and phenocryst assemblages indicating that the units belong to the Snake River Plain volcanic province. They contain fewer phenocrysts than the Eocene units and no hydrous phenocrysts, except for minor biotite in one unit.

Field evidence suggests that at least three of the Miocene units erupted from a local volcanic source, perhaps forming a small caldera, now buried, in the process. This postulated volcanic center is considered to be part of the southwest to northeast trend of major eruptive centers constituting the Snake River Plain volcanic province, and it predates the much larger Bruneau-Jarbidge eruptive center to the northeast, from which the overlying Cougar Point Tuff was erupted.

[1]Department of Geology, University of Idaho, Moscow, Idaho 83843.

[2]Idaho Bureau of Mines and Geology, Moscow, Idaho 83843.

INTRODUCTION

Several previously unreported Tertiary volcanic units are exposed along the Idaho-Nevada border in the Black Leg Creek and Indian Hay Meadows 7½-minute quadrangles in south-central Owyhee County, Idaho. These units, along with the overlying Cougar Point Tuff, were recently mapped by Bernt (1982) in the upper part of the Sheep Creek drainage. It is our purpose here to describe the stratigraphic relations, petrography, and chemical composition of these pre-Cougar Point Tuff volcanic units.

Two main groups of pre-Cougar Point Tuff volcanic rocks occur in the upper Sheep Creek drainage area (Figure 1). The older group, the Bieroth volcanics, consists of three units: the Alder Creek tuff, the Cedar Canyon tuff, and the volcanic neck of Browns Basin. These units are thought to be of Eocene age and are the approximate time equivalent of the undivided volcanic unit in northern Nevada which Bushnell (1967) called the "Bieroth Andesite." The younger group, thought to be Miocene in age, includes six units: the Rough Mountain rhyolite, the lapilli tuff of Sheep Creek, the Johnstons Camp rhyolite, the Browns Basin tuff, the Whiskey Draw rhyolite, and the Rattlesnake Draw tuff. The first three of these units apparently were erupted during the Miocene from a local center of volcanic activity. The Browns Basin and Whiskey Draw units, which at least partly overlie the first three units, may have been erupted locally or may have come from eruptions in another area. We lack good stratigraphic control for the Rattlesnake Draw tuff; thus, its assignment to the pre-Cougar Point Tuff Miocene-age group of volcanic units is only tentative.

In Idaho, the pre-Cougar Point Tuff volcanic units lie unconformably on Cretaceous-age biotite granodiorite of the Cottonwood Creek pluton (Coats and McKee, 1972; Bernt, 1982). The Cougar Point Tuff, which overlies the Bieroth volcanics and the earlier Miocene-age volcanic units, are welded ash-flow tuff units believed to have erupted from the Bruneau-Jarbidge eruptive center (Bonnichsen, 1982a this

Bernt, John and Bill Bonnichsen, 1982, Pre-Cougar Point Tuff volcanic rocks near the Idaho-Nevada border, Owyhee County, Idaho, *in* Bill Bonnichsen and R. M. Breckenridge, editors, Cenozoic Geology of Idaho: Idaho Bureau of Mines and Geology Bulletin 26, p. 321-330.

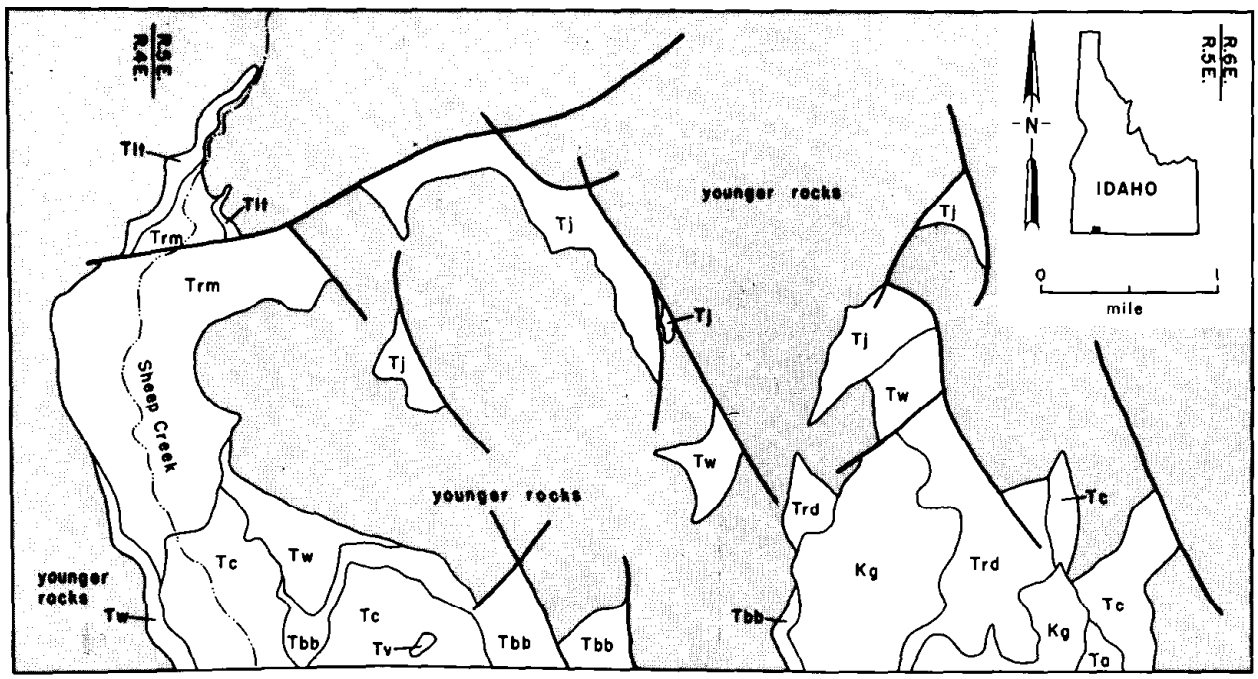

Volcanic units of Miocene age

Trd - Rattlesnake Draw tuff
Tw - Whiskey Draw rhyolite
Tbb - Browns Basin tuff
Tj - Johnstons Camp rhyolite
Tlt - lapilli tuff of Sheep Creek
Trm - Rough Mountain rhyolite

Bieroth volcanics of Eocene age

Tv - volcanic neck of Browns Basin
Tc - Cedar Canyon tuff
Ta - Alder Creek tuff

Kg - granodiorite of Cottonwood Creek pluton

Figure 1. Geologic map of the pre-Cougar Point Tuff volcanic units in the upper Sheep Creek drainage area, south-central Owyhee County, Idaho. Inset shows location of this area just north of the Idaho-Nevada border.

volume). The Cougar Point Tuff is described for the region by Bonnichsen and Citron (1982 this volume) and for the Sheep Creek drainage area by Bernt (1982). Overlying all of the intermediate and silicic volcanic units is the Banbury Basalt (Malde and Powers, 1962; Rember and Bennett, 1979) of late Miocene or Pliocene age, and various unconsolidated surficial deposits (Bernt, 1982).

These pre-Cougar Point Tuff volcanic rocks are exposed in a small area of relatively high elevation in the upper Sheep Creek drainage. The overall extent of these units to the south in Nevada is not known but is substantial. The stratigraphic position of each unit is not fully understood due to the general lack of outcrop in the area where they occur. The volcanic units typically have a very shallow northeast dip and are relatively undeformed structurally.

BIEROTH VOLCANICS OF EOCENE AGE

The units that constitute the Bieroth volcanics in the upper Sheep Creek drainage area have chemical compositions indicating they are better classified as rhyodacite or quartz latite, rather than andesite (Table 1). Consequently, we have dropped Bushnell's (1967) original name for the group. We agree with Bushnell, though, in assigning this group of rocks to the Eocene, based on their similarity in petrologic characteristics and stratigraphic position with nearby radiometrically dated units in the Jarbidge Mountains (Dead Horse Tuff of Coats, 1964; 40.9 million years, recalculated for new decay constants using the tables of Dalrymple, 1979), and in the Poison Creek area of

Table 1. Chemical analyses of samples of the Bieroth volcanics (1-5) and of the Miocene age volcanic rocks in the upper Sheep Creek drainage area (6-10).

Unit:	1 Alder Creek tuff	2 Cedar Canyon tuff	3 Cedar Canyon tuff	4 Cedar Canyon tuff	5 Volcanic neck of Browns Basin	6 Rough Mountain rhyolite	7 Lapilli tuff of Sheep Creek	8 Johnstons Camp rhyolite	9 Johnstons Camp rhyolite	10 Browns Basin tuff
					Major oxides in weight percent					
SiO_2	66.51	63.07	67.77	66.44	61.78	72.59	77.58	71.89	73.27	69.58
Al_2O_3	15.25	17.32	15.11	16.12	15.41	12.96	8.23	13.03	12.75	13.85
TiO_2	0.44	0.67	0.51	0.49	1.35	0.36	0.41	0.46	0.46	0.47
Fe_2O_3	3.36	5.00	3.61	3.57	8.23	2.07	2.25	3.16	3.34	4.14
MnO	0.02	0.06	0.05	0.04	0.07	0.02	0.05	0.02	0.01	0.03
CaO	1.38	4.35	3.12	3.74	3.91	0.80	1.57	1.04	0.69	1.27
MgO	0.49	0.94	1.41	2.03	0.98	0.15	0.46	0.45	0.33	0.26
K_2O	6.62	3.27	3.61	3.57	3.14	6.10	1.51	6.01	4.93	5.58
Na_2O	2.61	3.59	3.24	3.14	3.12	2.58	0.84	2.19	3.08	2.83
P_2O_5	0.09	0.19	0.16	0.14	0.48	0.04	0.06	0.06	0.07	0.07
Total	96.77	98.46	98.59	99.28	98.47	97.67	92.96	98.31	98.93	98.08
					Minor elements in parts per million					
Rb	166	96	92	130	81	210	73	264	153	178
Sr	243	645	511	481	492	122	294	162	155	151
Zr	362	320	268	337	397	386	392	529	539	558
Ba	1219	1110	991	1085	1447	835	2283	1653	1722	1519

Notes:
The samples were analyzed for major oxides by a combination of X-ray fluorescence and atomic absorption at Washington State University (XRF) and at the Idaho Bureau of Mines and Geology (AA), and for minor elements by X-ray fluorescence at Washington State University. Total iron is reported as Fe_2O_3.

1. Sample 372, devitrified rock from the Alder Creek tuff; NE¼NW¼ sec. 36, T. 16 S., R. 5 E., Owyhee County, Idaho.
2. Sample 361, glassy welded tuff from the Cedar Canyon tuff; NE¼SW¼ sec. 29, T. 16 S., R. 5 E., Owyhee County, Idaho.
3. Sample 371, glassy welded tuff from the Cedar Canyon tuff; SW¼SE¼ sec. 25, T. 16 S., R. 5 E., Owyhee County, Idaho.
4. Sample 395C, glassy welded tuff from the Cedar Canyon tuff; NE¼SE¼ sec. 17, T. 47 N., R. 56 E., Elko County, Nevada.
5. Sample 358A, volcanic breccia from the volcanic neck of Browns Basin; SW¼SE¼ sec. 29, T. 16 S., R. 5 E., Owyhee County, Idaho.
6. Sample 345A, vitrophyre from the Rough Mountain rhyolite; SE¼NW¼ sec. 30, T. 16 S., R. 5 E., Owyhee County, Idaho.
7. Sample 337, devitrified and altered rock from the lapilli tuff of Sheep Creek; NE¼NW¼ sec. 18, T. 16 S., R. 5 E., Owyhee County, Idaho.
8. Sample 264A, vitrophyre from the Johnstons Camp rhyolite; NW¼SE¼ sec. 14, T. 16 S., R. 5 E., Owyhee County, Idaho.
9. Sample 351, devitrified rock from the Johnstons Camp rhyolite; SE¼NW¼ sec. 20, T. 16 S., R. 5 E., Owyhee County, Idaho.
10. Sample 364A, basal vitrophyre of the Browns Basin tuff; NW¼NW¼ sec. 33, T. 16 S., R. 5 E., Owyhee County, Idaho.

northern Owyhee County (unnamed biotite rhyolite unit of the Challis Volcanics cited in Armstrong and others, 1980, p. 8, 44.7 million years).

ALDER CREEK TUFF

A light reddish purple tuff unit is exposed in a small area along Alder Creek near the Idaho-Nevada border (Figure 1). This unit was called the tuff of Alder Creek by Bernt (1982). Although field relations are somewhat obscure, the Alder Creek tuff appears to be overlain by the Cedar Canyon tuff and is therefore the oldest unit of the Bieroth volcanics in Idaho.

The Alder Creek tuff is moderately compacted and welded, and is extensively weathered and devitrified. The presence of flattened glass shards and pumice fragments shows that the unit is a welded ash-flow tuff. Subangular to subrounded lithic fragments, principally of basalt porphyry, are common. The relatively large size and abundance of the lithic and pumice fragments suggests a nearby source for the unit.

The tuff contains approximately 25 percent of phenocrysts of quartz, plagioclase (An_{45-50}), and sanidine, and accessory amounts of biotite, black opaques, apatite, and zircon. Tridymite(?) is present as a secondary mineral in pores.

An analysis of one sample of the Alder Creek tuff (Table 1, no. 1) has the composition of a rhyodacite, and is about as silicic as the most silicic of the three analyzed samples of the overlying Cedar Canyon tuff (Figure 2). The Alder Creek tuff analysis differs from the Cedar Canyon tuff, however, by being a little less femic and much richer in K_2O.

CEDAR CANYON TUFF

A rhyodacite welded tuff unit occurs widely in

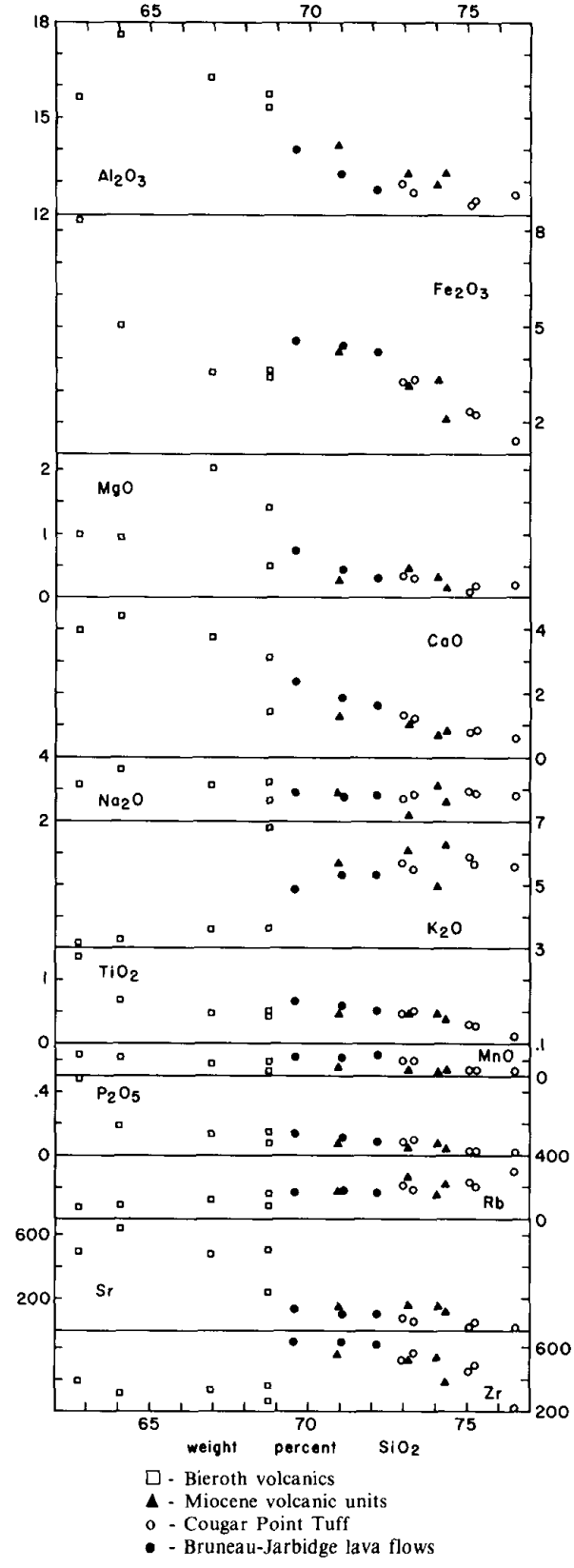

Figure 2. Silica variation diagram comparing the Bieroth volcanics and Miocene rocks in the upper Sheep Creek drainage area with the Cougar Point Tuff and rhyolite lava flows from the Bruneau-Jarbidge eruptive center. The Bieroth volcanics are analyses 1-5 in Table 1; the upper Sheep Creek Miocene volcanic units are analyses 6, 8, 9, and 10 in Table 1; the Cougar Point Tuff rocks are analyses 1-5 in Table 1 of Bonnichsen and Citron (1982 this volume); and the Bruneau-Jarbidge eruptive center rhyolite lava flows are analyses 1, 2, and 5 in Table 1 of Bonnichsen (1982b this volume). Weight percentages of the oxides were normalized to a sum of 100 percent for plotting.

both the eastern and western parts of the area shown in Figure 1. Nearly identical rhyodacite occurs near the confluence of McDonald Creek and the Bruneau River in northern Nevada, about 12 kilometers southeast of the area in Figure 1 (see Figure 2 in Bonnichsen, 1982a this volume, for this location). We have included all of these occurrences in the Cedar Canyon tuff unit, named for the side canyon which joins the Bruneau a short distance downstream from McDonald Creek. We recommend the Bruneau Canyon occurrence as a reference locality because of the good access and exposure there (Figure 3).

The Cedar Canyon tuff unit consists mainly of light to brownish gray, moderately to stongly compacted, vitric-crystal welded tuff. Three flows, each approximately 30 to 50 meters thick, are present along the Bruneau River. More than one flow unit probably occurs in the Sheep Creek area, but this was not confirmed because of poor exposures. The total thickness of the Cedar Canyon tuff is at least 90 meters. Flattened glass shards, angular crystal fragments, and pumice inclusions indicate that the unit consists of welded ash-flow tuff.

The Cedar Canyon tuff contains 30 to 50 percent of phenocrysts of quartz, plagioclase (An_{50-60}), and sanidine, and accessory amounts of hornblende, biotite, black opaques, apatite, zircon, hypersthene, and allanite(?). Secondary epidote, kaolinite, chlorite, and tridymite(?) occur locally. The matrix consists of glass and deformed glass shards with varying degrees of devitrification to microlites, but even where glassy the matrix is light colored. Minor amounts of accidental lithic fragments, which are apparently basalt, are present. The unit appears slightly altered along Sheep Creek, but elsewhere is relatively fresh.

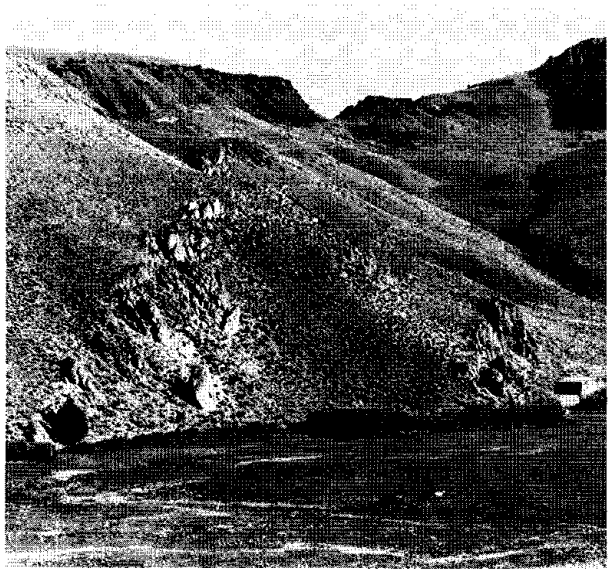

Figure 3. The two lower flow units in the Cedar Canyon tuff of the Bieroth volcanics (units dipping to left at lower part of slope) exposed beneath the Cougar Point Tuff (rocks high on slope with near horizontal attitude) in Bruneau Canyon near the mouth of McDonald Creek in northern Nevada.

Three analyses from the Cedar Canyon tuff are presented in Table 1 (no. 2, 3, and 4) and are plotted in Figure 2. The one from the Bruneau Canyon reference locality is intermediate in composition between the other two. Its petrography and chemistry reveal that the unit can be classified as a hornblende-biotite rhyodacite or biotite rhyodacite.

VOLCANIC NECK OF BROWNS BASIN

A volcanic neck is exposed in the central part of Browns Basin near the Idaho-Nevada border (Figure 1). The neck is roughly oval in outline with a maximum width of approximately 275 meters. It rises about 10 meters above the surrounding Cedar Canyon tuff which it intrudes (Figure 4). The rock of the neck consists of dusky red, scoriaceous to massive, brecciated ferrolatite which is moderately to strongly stained by iron oxides. No internal structures were found in the neck.

The rock contains scattered phenocrysts of plagioclase (An_{40-45}) and altered pyroxene. Secondary minerals include chlorite as an alteration of pyroxene and stilbite as druses in pores. The matrix is pervasively stained by limonite, but is predominantly glass with minor microlites.

An analysis of a sample (Table 1, no. 5) has a composition that could be classified as ferrolatite, or perhaps as iron-rich dacite. The composition of this sample is similar to the other Bieroth volcanic samples, except that it is significantly enriched in iron, titanium, and phosphorus and contains less silica and alumina (Figure 2). In this respect the volcanic neck is similar to some lavas in the nearby Snake River Plain volcanic province that Leeman (1982 this volume) suggests were produced by a combination of fractional crystallization and contamination of basaltic magmas. However, based on the spatial association of the volcanic neck with the Cedar Canyon tuff and its general chemical similarity to the other units of the Bieroth volcanics, we have included the volcanic neck as part of the Bieroth volcanics, and consider it to be Eocene in age. This must be considered as a tentative assignment, as field relations only indicate the volcanic neck to be younger than the Cedar Canyon tuff.

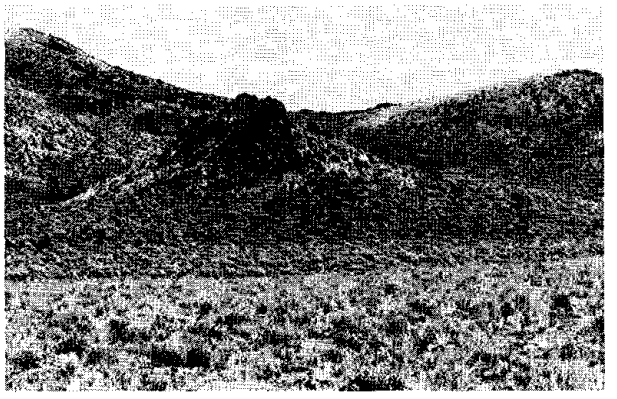

Figure 4. The volcanic neck of Browns Basin. The neck rises about 10 meters above the surrounding Cedar Canyon tuff of the Bieroth volcanics.

VOLCANIC UNITS OF MIOCENE AGE

ROUGH MOUNTAIN RHYOLITE

A thick rhyolitic welded-tuff unit, the Rough Mountain rhyolite, is exposed in the deep narrow canyon of Sheep Creek, 1.2-4.5 kilometers north of the Idaho-Nevada border (Figure 1). Previously (Bernt, 1982), this unit was called the rhyolite of Sheep Creek, but because that name would have been confused with that of the earlier-named Sheep Creek rhyolite, a large rhyolite lava flow in the Bruneau-Jarbidge eruptive center (Bonnichsen, 1981, 1982b this volume), the welded-tuff unit has been renamed for a prominent hill just west of Sheep Creek canyon. The Rough Mountain rhyolite is more than 170 meters thick and appears to be a single flow unit. The unit overlies the Bieroth volcanics and is overlain by the Whiskey Draw rhyolite, the lapilli tuff of Sheep Creek, the Johnstons Camp rhyolite, the Cougar Point Tuff, and the Banbury Basalt.

The Rough Mountain rhyolite is typically a reddish brown, massive, lithoidal welded tuff with abundant phenocrysts. No flow layering was observed in outcrop. A black vitrophyre is present along the southeast margin of the unit; along this margin the contact with the underlying Bieroth volcanics is nearly vertical, suggesting that the unit filled a paleo-depression in the older rocks. The vitrophyre contains features which resemble flattened pumice, and lithophysae with devitrification coronas occur near the base of the vitrophyre. Float at the base of the unit suggests that a pyroclastic base surge deposit occurs there.

A thin section of the vitrophyre contains phenocrysts of quartz (3 percent), sanidine (17 percent), plagioclase (An_{30-40}) (5 percent), and accessory amounts of hypersthene (3 percent), black opaques, and zircon (percentages are visual estimates). Sparse cumulophyric aggregates of feldspar and hypersthene are present. The matrix consists of dark glass with discontinuous, very elongate pieces of clear glass molded around the fragments of dark glass (Figure 5) and the phenocrysts. The clear glass may have been shards, which now are highly deformed.

A chemical analysis of a Rough Mountain rhyolite sample (Table 1, no. 6) reveals that the rock is a rhyolite very similar to several of the Cougar Point Tuff units, especially the more silicic ones (Figure 2; and compare with the analyses in Table 1 in Bonnichsen and Citron, 1982 this volume).

We interpret the Rough Mountain rhyolite unit to have been deposited as a single thick ash flow, because it lacks internal flowage structures and it contains deformed glass fragments and shards(?), flattened pumice fragments, and possible base surge deposits. The tuff has been greatly compacted, welded, and extensively devitrified; locally the sanidine has been pervasively altered to clay minerals. The relatively great thickness of this unit, its apparent confinement to a paleo-depression, and perhaps its somewhat altered condition suggest that it is an intracaldera facies of a more extensive ash-flow sheet.

LAPILLI TUFF OF SHEEP CREEK

A consolidated, but unwelded, tuff unit up to about 40 meters thick is exposed in Sheep Creek canyon north of the area underlain by the Rough

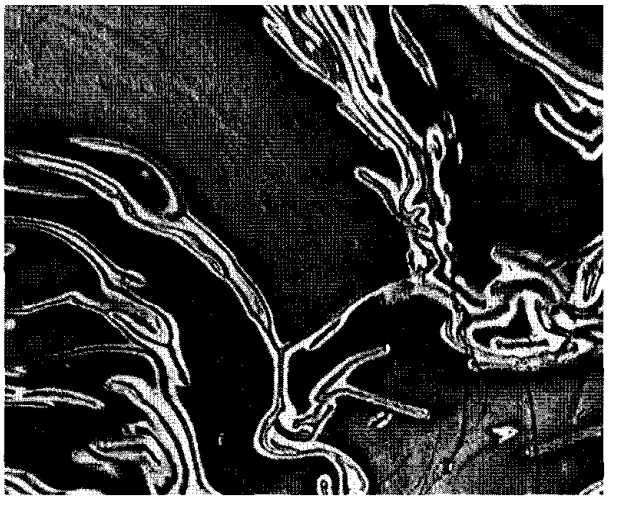

Figure 5. Photomicrograph of the basal vitrophyre of the Rough Mountain rhyolite. The thin irregular bands are clear glass that may be deformed shards, and the enclosed, relatively thick angular particles are fragments of dark-colored glass containing abundant mircolites. View is approximately 1 millimeter wide.

Mountain rhyolite (Figure 1). This unit is referred to as the lapilli tuff of Sheep Creek; it lies on the Rough Mountain rhyolite and is overlain by the Cougar Point Tuff. Its age relative to the Browns Basin tuff and to the Johnstons Camp rhyolite is not known, but it is thought to have formed at about the same time as those units, and during the same episode of volcanism.

The lapilli tuff of Sheep Creek is well bedded and moderately sorted, with some layers exhibiting bimodal grain sizes. The tuff is yellowish green and moderately dense with approximately 20 percent of irregular pore spaces. The unit is interpreted to be an air-fall pyroclastic deposit, and it is classified as a lapilli tuff on the basis of its particle size.

A thin section of the tuff contains approximately 15 percent of phenocrysts of sanidine and plagioclase (An_{45-50}), and accessory amounts of black opaques, and zircon. Tridymite is present as a secondary mineral in cavities. The matrix consists of undeformed glass shards, which are almost totally devitrified, and pervasive secondary silica. Pumice fragments and reddish lithic fragments up to a centimeter long are common. A green mineral, perhaps celadonite, coats the surfaces of some outcrops.

A chemical analysis of the lapilli tuff (Table 1, no. 7) shows that it has been strongly altered, with the partial loss of alkalis and alumina and a concomitant increase in silica (SiO_2 accounts for 83.5 weight percent of the cation oxides when the sum in Table 1 is normalized to 100 percent).

The considerable thickness and coarse particle size of the lapilli tuff of Sheep Creek suggests that it is a near-vent air-fall deposit. This unit's existence shows that volcanic activity occurred in the upper Sheep Creek drainage area before the Cougar Point Tuff was erupted.

JOHNSTONS CAMP RHYOLITE

A rhyolite lava flow with local domal forms is exposed at several places in the upper Sheep Creek drainage (Figure 1). Its name comes from exposures at Johnstons Camp in the Indian Hay Meadows quadrangle (Bernt, 1982). The Johnstons Camp rhyolite is overlain by the Whiskey Draw tuff and the Cougar Point Tuff, and is apparently above the Rough Mountain rhyolite, although this could not be proven in the field. The unit is locally at least 60 meters thick. It is poorly exposed and may consist of several individual volcanic domes, but we consider it more likely that it is a continuous lava flow with a limited areal extent and a local source.

The Johnstons Camp rhyolite consists of black vitrophyre and grayish red lithoidal rhyolite. The vitrophyre occurs at the top and along the margins of the flow, and the lithoidal rhyolite occurs in the flow interior. The base of the unit is not exposed and no internal flow layering was noted. The domal forms are thought to be preserved from the time of viscous flowage; similar bulbous forms are common in the marginal zones of most rhyolite lava flows in the Bruneau-Jarbidge eruptive center (Bonnichsen, 1982b this volume). Complex joint patterns characterize some parts of the unit (Figure 6); these joints probably were formed after bulk flowage in the unit had ceased, during the time of shrinkage and compaction that accompanied and followed devitrification and cooling.

Thin sections reveal that the rhyolite contains about 17 percent of phenocrysts of plagioclase (An_{40-50}), minor amounts of sodic sanidine, and accessory amounts of pigeonite, augite, black opaques, and zircon. The groundmass consists of microlites, and tridymite occurs as a secondary mineral in lithoidal rhyolite. No glass shards, pumice fragments, lithic fragments, or flowage structures were found. The rock is very dense and strongly compacted.

Two samples of the Johnstons Camp rhyolite were analyzed (Table 1, nos. 8 and 9; Figure 2); they are similar to one another and to the samples from the Rough Mountain rhyolite and the Browns Basin tuff. Figure 2 also shows that the Johnstons Camp rhyolite has a composition like that of the volcanic units associated with the Bruneau-Jarbidge eruptive center.

Our interpretation is that the Johnstons Camp

Figure 6. An exposure of lithoidal rhyolite in the Johnstons Camp rhyolite flow showing a complex sheeting-joint pattern that probably developed during cooling of the unit.

rhyolite is a lava flow of limited areal extent. By analogy with the situation in the Bruneau-Jarbidge eruptive center, we suggest that the Johnstons Camp unit is contained within a zone of subsidence which developed during the time or after the Rough Mountain rhyolite and perhaps other units had erupted.

BROWNS BASIN TUFF

A welded ash-flow tuff unit, varying up to about 60 meters thick, is exposed around the margins of Browns Basin, a small valley for which the unit was named (Bernt, 1982), located east of Sheep Creek canyon (Figure 1). The Browns Basin tuff unit lies above a thin layer of air-fall tuff, which, in turn, overlies the Cedar Canyon tuff unit of the Bieroth volcanics. Farther to the east (Figure 1), the Browns Basin tuff lies on the west flank of the Cottonwood Creek pluton. The Browns Basin tuff is overlain by the Whiskey Draw rhyolite and by the Cougar Point Tuff at various localities, but no field relationship has been observed to indicate its age relative to either the Johnstons Camp rhyolite or the lapilli tuff of Sheep Creek. The Browns Basin tuff extends southward into Nevada, where it is well exposed.

The Browns Basin tuff at most localities consists of a 2- to 3-meter-thick basal vitrophyre layer overlain by a pale red to grayish red lithoidal rhyolite layer. This layer commonly contains near its base a 3- to 6-meter-thick lithophysal zone with rounded to slightly elongate, 3- to 20-centimeter-long gas cavities. The unit is thoroughly compacted and densely welded throughout, and flattened pumice fragments occur locally.

A thin section from the basal vitrophyre contains approximately 35 percent of phenocrysts of sanidine (20 percent), plagioclase (An_{30-40}) (8 percent), quartz (3 percent), and accessory amounts of pigeonite (2 percent), augite (1 percent), black opaques, zircon, apatite, and monazite (percentages are visual estimates). The matrix consists of deformed glass shards and fine-grained, subangular to subrounded lithic fragments and fragments of glass. The rock can be classified as a vitric-crystal rhyolite tuff.

An analysis of a Browns Basin tuff sample (Table 1, no. 10) suggests that the unit is a little more femic than the Rough Mountain rhyolite, being more like the Johnstons Camp rhyolite in composition. Its composition is very similar to the more femic units of the Cougar Point Tuff (Figure 2; and compare with the analyses in Table 1, Bonnichsen and Citron, 1982 this volume).

Its more widespread distribution but thinner configuration in comparison with the Rough Mountain rhyolite suggest that the Browns Basin tuff may be an outflow-facies type of unit which flowed away from the area where it was erupted. A comparison of the assemblages and mutual abundances of phenocrysts in the Browns Basin tuff and the Rough Mountain rhyolite shows that the two are very similar. This suggests that they may be genetically related; perhaps both were erupted from different portions of the same magma chamber, with the Browns Basin tuff flowing away from the eruption site, whereas the Rough Mountain rhyolite filled a depression formed by surface collapse over the partially evacuated magma chamber. This suggestion must remain as speculation, however, until more is known about the distribution of the Browns Basin tuff in northern Nevada; the unit could also have flowed into Idaho from that region.

WHISKEY DRAW RHYOLITE

A rhyolite unit, named the Whiskey Draw rhyolite (Bernt, 1982) for its exposures in a small tributary to Black Leg Creek, occurs at several localities (Figure 1). The unit lies above the Rough Mountain rhyolite and the Browns Basin tuff, probably above the Johnstons Camp rhyolite, and below the Cougar Point Tuff. The unit has a maximum thickness of 90 meters.

The rhyolite is gray and typically hard, dense, and completely devitrified. Rounded to elliptical vesicles up to 3 centimeters across are abundant, and larger irregular gas cavities containing yellow to orange jasper locally occur near the top of the flow.

A thin section of the rhyolite contains about 7 percent of phenocrysts of sanidine, plagioclase (An_{35-40}), and quartz, and accessory amounts of black opaques and zircon. Tridymite(?) occurs in some of the vesicles, and secondary silica resulting from deuteric alteration is present. Poorly preserved shards were tentatively identified, suggesting the unit orginated as an ash flow.

A chemical analysis of a Whiskey Draw rhyolite sample (Bernt, 1982) reveals the unit to be similar to the rhyolites in the Bruneau-Jarbidge eruptive center and elsewhere in the Snake River Plain volcanic province; thus, we consider it to be Miocene in age. Like the Rattlesnake Draw tuff, the Whiskey Draw rhyolite is chemically very similar to the lowest Cougar Point Tuff unit (Bonnichsen and Citron, 1982 this volume). Its stratigraphic position suggests that the Whiskey Draw rhyolite might be the upper part of the Browns Basin tuff, but the differences in chemistry and phenocryst assemblages between the two units suggest that they probably are from separate eruptions and perhaps are from different areas. Currently we do not know if the Whiskey Draw rhyolite is from a local volcanic center, or if it might be an early unit from the Bruneau-Jarbidge eruptive center and should

be assigned to the Cougar Point Tuff.

RATTLESNAKE DRAW TUFF

A dense, generally altered welded tuff unit, the Rattlesnake Draw tuff, is exposed in the Cottonwood Creek and Rattlesnake Draw drainages in the southern part of the area in Figure 1. The unit overlies the Cedar Canyon tuff of the Bieroth volcanics and lies beneath the Cougar Point Tuff and perhaps beneath the Whiskey Draw rhyolite.

The tuff is very hard because of silicification and has undergone minor brecciation which has obscured its original character. The unit's occurrence northwest of the Cottonwood Creek pluton (Figure 1) is not as silicified as the localities to the east. All exposures of the unit are devitrified and vary from brown to grayish red in color. Phenocrysts of biotite, black opaques, and zircon are present, but those of feldspar and quartz were lacking or have been destroyed. Relict shards and flattened pumice(?) fragments occur locally, and small partially filled lithophysae are common. Veinlets and vug fillings of secondary silica are common throughout the unit.

The presence of biotite and the unit's field distribution suggest that the Rattlesnake Draw tuff could be part of the Eocene-age Bieroth volcanics. However, an analysis of a sample reported by Bernt (1982) reveals the rock to be chemically very similar to the Miocene-age rhyolite units in the Snake River Plain volcanic province. Its chemical composition is particularly similar to that of the lowest unit in the Cougar Point Tuff (Bonnichsen and Citron, 1982 this volume). At present insufficient data are available to determine if the Rattlesnake Draw tuff was erupted from a local volcanic center or if it is an early unit from the Bruneau-Jarbidge eruptive center and should be assigned to the Cougar Point Tuff.

SUMMARY AND DISCUSSION

We have shown by geologic mapping, chemical analyses, and petrography that two groups of Tertiary-age pre-Cougar Point Tuff volcanic rocks occur in Idaho in the upper Sheep Creek drainage area. The older group, the Bieroth volcanics, are thought to be Eocene in age and are part of a widespread province of calc-alkaline volcanism that extends southwards, and generally becomes younger (McIntyre and others, 1982 this volume; Leonard and Marvin, 1982 this volume; Stewart and Carlson, 1976), from the Challis volcanic field in central Idaho into Nevada.

The younger group, which in many respects is like other rhyolite units within the Snake River Plain volcanic province, is considered to be Miocene in age. Field relations suggest that at least three of the Miocene units—the Rough Mountain rhyolite, the lapilli tuff of Sheep Creek, and the Johnstons Camp rhyolite—were erupted from a local volcanic source prior to the development of the nearby, but much more extensive, Bruneau-Jarbidge eruptive center to the northeast. Not enough is yet known about the Browns Basin and Whiskey Draw units, which at least partially overlie the three locally erupted units, to indicate for sure if they came from the local volcanic center or from somewhere in northern Nevada, or if they might be the first units from the Bruneau-Jarbidge eruptive center, or perhaps have some other source. The remaining unit—the Rattlesnake Draw tuff—is tentatively assigned to the Miocene on the basis of its chemistry, but its field setting actually would not preclude it from belonging to the earlier group of Eocene-age units.

The Bieroth volcanics contain a relatively higher percentage of phenocrysts and typically carry biotite and hornblende, rather than pyroxenes, as their mafic minerals. These older volcanic units, as illustrated in Figure 2, clearly are not as silicic as are the Miocene-age group. The chemical analyses show that the Bieroth volcanics are calc-alkaline and include rocks of intermediate SiO_2 content. The Miocene-age volcanic units, on the other hand, are rhyolites and, as a group, are essentially indistinguishable chemically from other rhyolites associated with the Snake River Plain volcanic province, as is clearly shown in Figure 2.

The probable existence of a local volcanic center in the upper Sheep Creek drainage area is indicated by several lines of evidence. The considerable thickness but restricted areal distribution of the Rough Mountain rhyolite, which suggest it filled a paleo-depression, may signify that the unit has an intracaldera form. The existence of both the lapilli tuff of Sheep Creek and the Johnstons Camp rhyolite are strong evidence that volcanism occurred within the area. The lapilli tuff of Sheep Creek appears to be a near-vent air-fall pyroclastic unit, and the Johnstons Camp rhyolite is interpreted as a rhyolite lava flow covering the vent through which it was extruded. The Browns Basin tuff, which is thinner than but petrographically very similar to the Rough Mountain rhyolite on which it lies and extends away from (Figure 1), could easily be interpreted as an outflow sheet from the same eruption that formed the Rough Mountain rhyolite.

The mutual relationships among the units erupted from the local volcanic center, which we postulate to have existed in the upper Sheep Creek drainage area, imply that the center may have become a small

caldera during its evolution, so as to topographically confine the Rough Mountain rhyolite and the Johnstons Camp rhyolite. The southern margin of such a caldera would have been just north of the northern margin of the Bieroth volcanics and the Cottonwood Creek pluton exposures (Figure 1). The lapilli tuff of Sheep Creek might also be near the margin (northwestern?) of such a structure, but there is too much cover by younger rock units to readily tell. The remainder of such a structure is under the younger rocks, so we really cannot tell if a caldera developed as suggested; however, the idea is in reasonable accord with the rock units as they are exposed. Such a volcanic center would be part of the southwest to northeast trend of major volcanic centers constituting the Snake River Plain volcanic province.

REFERENCES

Armstrong, R. L., J. E. Harakal, and W. M. Neill, 1980, K-Ar dating of Snake River Plain (Idaho) volcanic rocks—new results: Isochron West, no. 27, p. 5-10.

Bernt, John, 1982, Geology of the southern J-P Desert, Owyhee County, Idaho: University of Idaho M.S. thesis, 73 p.

Bonnichsen, Bill, 1981, Stratigraphy and measurements of magnetic polarity for volcanic units in the Bruneau-Jarbidge eruptive center, Owyhee County, Idaho: Idaho Bureau of Mines and Geology Open-File Report 81-5, 75 p.

———, 1982a, The Bruneau-Jarbidge eruptive center, southwestern Idaho, *in* Bill Bonnichsen and R. M. Breckenridge, editors, Cenozoic Geology of Idaho: Idaho Bureau of Mines and Geology Bulletin 26.

———, 1982b, Rhyolite lava flows in the Bruneau-Jarbidge eruptive center, southwestern Idaho, *in* Bill Bonnichsen and R. M. Breckenridge, editors, Cenozoic Geology of Idaho: Idaho Bureau of Mines and Geology Bulletin 26.

Bonnichsen, Bill and G. P. Citron, 1982, The Cougar Point Tuff, southwestern Idaho and vicinity, *in* Bill Bonnichsen and R. M. Breckenridge, editors, Cenozoic Geology of Idaho: Idaho Bureau of Mines and Geology Bulletin 26.

Bushnell, Kent, 1967, Geology of the Rowland quadrangle, Elko County, Nevada: Nevada Bureau of Mines Bulletin 67, 38 p.

Coats, R. R., 1964, Geology of the Jarbidge quadrangle, Nevada-Idaho: U. S. Geological Survey Bulletin 1141-M, 24 p.

Coats, R. R. and E. H. McKee, 1972, Ages of plutons and types of mineralization, northwestern Elko County, Nevada, *in* Geological Survey Research 1972: U. S. Geological Survey Professional Paper 800-C, p. C165-C168.

Dalrymple, G. B., 1979, Critical tables for conversions of K-Ar ages from old to new constants: Geology, v. 7, p. 558-560.

Leeman, W. P., 1982, Evolved and hybrid lavas from the Snake River Plain, Idaho, *in* Bill Bonnichsen and R. M. Breckenridge, editors, Cenozoic Geology of Idaho: Idaho Bureau of Mines and Geology Bulletin 26.

Leonard, B. F. and R. F. Marvin, 1982, Temporal evolution of the Thunder Mountain caldera and related features, central Idaho, *in* Bill Bonnichsen and R. M. Breckenridge, editors, Cenozoic Geology of Idaho: Idaho Bureau of Mines and Geology Bulletin 26.

Malde, H. E. and H. A. Powers, 1962, Upper Cenozoic stratigraphy of the western Snake River Plain, Idaho: Geological Society of America Bulletin, v. 73, p. 1197-1210.

McIntyre, D. H., E. B. Ekren, and R. F. Hardyman, 1982, Stratigraphic and structural framework of the Challis Volcanics in the eastern half of the Challis 1° x 2° quadrangle, Idaho, *in* Bill Bonnichsen and R. M. Breckenridge, editors, Cenozoic Geology of Idaho: Idaho Bureau of Mines and Geology Bulletin 26.

Rember, W. C. and E. H. Bennett, 1979, Geologic map of the Twin Falls quadrangle, Idaho: Idaho Bureau of Mines and Geology Geologic Map Series, Twin Falls 2° quadrangle.

Stewart, J. H. and J. E. Carlson, 1976, Cenozoic rocks of Nevada: Nevada Bureau of Mines and Geology Map 52.

Chapter 6

Rhyolitic Volcanism Eastern Snake River Plain and Vicinity

Preliminary Stratigraphic Framework of the Pliocene and Miocene Rhyolite, Eastern Snake River Plain, Idaho

by

Glenn F. Embree[1], Lisa A. McBroome[2], and David J. Doherty[3]

ABSTRACT

Recent field studies along the margins of the eastern Snake River Plain, Idaho, have disclosed an extensive and complex stratigraphic succession of Pliocene and Miocene rhyolite pyroclastic deposits. Basalt forms a relatively thin veneer that conceals a thick sequence of rhyolite and related calderas. Rhyolite is more voluminous than basalt in the plain.

Five regionally extensive ash-flow tuff units occur along the southeastern margin of the eastern Snake River Plain, and three occur on the northern margin. In order from oldest to youngest, the tuff units on the southeastern margin are as follows: (1) the tuff of Arbon Valley extending from east of the Sublett Range to Blackfoot, Idaho; (2) the tuff of Spring Creek (6.5 million years) extending from Blackfoot to the eastern margin of the Rexburg caldera complex; (3) the Walcott Tuff which is present along the Snake River canyon and extends from the Sublett Range to the Bannock Range; (4) the tuff of Elkhorn Spring exposed in the southern part of the Rexburg caldera complex; and (5) the 4.3-million-year-old tuff of Heise, extending from Blackfoot to Teton National Park. The northern units from the oldest to youngest are as follows: (1) the tuff of Edie Ranch exposed in the southern Beaverhead and Centennial Mountains and the southern Lost River and Lemhi Ranges; (2) the tuff of Blue Creek exposed in the southern Lemhi Range and Beaverhead Mountains; and (3) the tuff of Kilgore, extending from at least the southern Lemhi Range to the southern foothills of the Centennial Mountains north of Kilgore, Idaho. Ages and total extent of all these units have yet to be determined.

The Rexburg caldera complex was the source of the tuff of Spring Creek. The tuff of Edie Ranch is similar to the tuff of Spring Creek petrographically and stratigraphically and is correlated with the tuff of Spring Creek. From geophysical and geological data, the tuffs of Blue Creek and Elkhorn Spring are interpreted as being equivalent units and having an eruptive center located south and east of the Lemhi Range and south of the Beaverhead Mountains. The tuff of Kilgore and the tuff of Heise are equivalent and have an eruptive center near Kilgore, Idaho.

INTRODUCTION

The Snake River Plain (Figure 1) is a structural graben which has been considered a Cenozoic basalt province (Stearns and others, 1939; Armstrong and others, 1975; Smith and Christiansen, 1980). However, subsurface drilling, geophysical studies, and recent mapping on the margins of the eastern Snake River Plain reveal that rhyolite is considerably more voluminous than basalt in this bimodal volcanic province (H. J. Prostka, G. F. Embree, D. J. Doherty, and L. A. McBroome, unpublished field data, 1972-1980). The basalt lava flows form a relatively thin veneer over a thick sequence of rhyolitic ash-flow tuff sheets and lava flows (Figures 2 and 3; Doherty, 1979a, 1979b; Doherty and others, 1979; Embree and others, 1979). More than 2,400 meters of rhyolite was found in a 3,160-meter-deep exploratory geothermal test well (INEL-1) beneath 745 meters of basalt and intercalated sediments (L. A. McBroome and D. J. Doherty, unpublished data, 1981).

This paper presents a brief and preliminary overview of the late Cenozoic rhyolite stratigraphy of the eastern Snake River Plain. Five regionally extensive ash-flow tuff sheets are the key units which form the framework of the rhyolite stratigraphy (Figure 4). We show the general distribution and relative ages of these units as well as the present interpretations on the locations of some of the source calderas for the ash-flow sheets.

The idea that rhyolite units and associated eruptive centers are concealed beneath the veneer of basalt lava flows of the eastern Snake River Plain is not

[1]Ricks College, Rexburg, Idaho 83440.
[2]U. S. Geological Survey, Federal Center, Denver, Colorado 80225.
[3]Arco Exploration Company, Dallas, Texas 75221.

Embree, G. F., L. A. McBroome, and D. J. Doherty, 1982, Preliminary stratigraphic framework of the Pliocene and Miocene rhyolite, eastern Snake River Plain, Idaho, *in* Bill Bonnichsen and R. M. Breckenridge, editors, Cenozoic Geology of Idaho: Idaho Bureau of Mines and Geology Bulletin 26, p. 333-343.

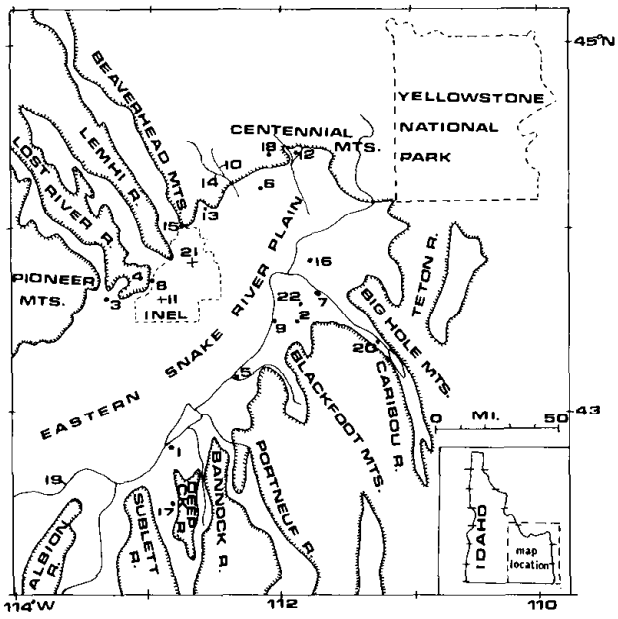

Figure 1. Index map of the eastern Snake River Plain, southeast Idaho. 1—American Falls, 2—Ammon, 3—Arco, 4—Arco Hills, 5—Blackfoot, 6—Dubois, 7—Heise, 8—Howe, 9—Idaho Falls, 10—Indian Creek, 11—INEL-1, 12—Kilgore, 13—Lidy Hot Springs, 14—Medicine Lodge Creek, 15—Reno Point, 16—Rexburg, 17—Rockland, 18—Signal Mountain, 19—Snake River, 20—Swan Valley, 21—Well 2-2A, 22—Willow Creek.

new. Mansfield and Ross (1935) commented on the general similarity in the appearance of the welded tuff sheets present on the northern and southern margins of the eastern Snake River Plain and suggested these rhyolite units were possibly buried beneath the basalts and sediments of the plain. Stearns and others (1939) suggested that the units had different sources and that the major sources were a chain of silicic volcanoes which extended from Boise toward the Yellowstone Plateau along the axis of the Snake River Plain. Kirkham (1931) proposed that the volcanic rocks became progressively younger toward the Yellowstone Plateau. These concepts are similar to current models for the evolution of the eastern Snake River Plain (for example, Smith and Christiansen, 1980; Leeman, 1982 this volume; Mabey, 1982 this volume).

GENERAL GEOLOGY

The eastern Snake River Plain is a 90-kilometer-wide, northeast-trending basin which extends from the vicinity of Twin Falls on the southwest to Yellowstone National Park on the northeast (Figure 1). The plain truncates generally northwest-trending basin and range structures on the northwest and southeast, with 1,200 to 1,400 meters of relief between the ranges and the relatively flat surface of the plain. The Island Park area, which contains partial rims of two rhyolite calderas that now are partially filled with Pleistocene basalt lava flows (Hamilton, 1965; Christiansen and Blank, 1972; Christiansen, 1982 this volume), marks the transition between the eastern Snake River Plain and the topographically higher, younger Yellowstone rhyolite plateau to the northeast.

The surface of the plain consists of numerous Pleistocene basalt shield volcanoes and northwest-trending rift zones (Kuntz and others, 1982 this volume). The basalt overlies rhyolite ash-flow tuff sheets and lava flows, fan gravels, and local basalt units of Tertiary age along the margins of the plain. The Tertiary units, in turn, lap onto the older rocks and form dip slopes on the surrounding mountain ranges. The surrounding ranges are structurally asymmetric horsts with eastward dips. Tertiary ash-flow tuffs extend for more than 55 kilometers from the margins of the plain and form part of the valley-fill in the marginal asymmetric grabens.

The caldera model for the origin of the eastern Snake River Plain (Smith and Christiansen, 1980) suggests that a succession of Yellowstone-like calderas have propagated northeastward along the axis of the plain. These eruptive centers subsequently have subsided and been buried beneath younger volcanic and sedimentary deposits. Subsurface data support the model of flooding by basalt lava flows and eventual total burial of the old caldera systems. The data suggest that the basalt cover progressively becomes thicker to the southwest (Doherty, 1979a, 1979b; Doherty and others, 1979; Embree and others, 1979). Armstrong and others (1975) suggested that three general facies (silicic volcanic rocks, basalt lava flows, and lacustrine and fluvial sediments) have shifted progressively from west to east at an approximate rate of 3.5 centimeters a year along the axis of the plain based on their potassium-argon radiometric studies. Age determinations show that volcanic activity began in the western Snake River Plain about 14.2 million years ago (Armstrong and others, 1980) and gradually propagated northeastward along the axis of the plain with the most recent activity occurring 0.6 million years ago in the Yellowstone Plateau (Christiansen and Blank, 1972; Christiansen, 1982 this volume).

The initial stage in caldera development is illustrated by the present-day Yellowstone rhyolite plateau where the eruption of several large-volume ash-flow tuff sheets was followed by caldera collapse.

The second stage in caldera development on the eastern Snake River Plain involves the cessation of major rhyolitic activity and gradual subsidence, ac-

companied by filling and eventual burial of the caldera by basalt lava flows. The 1.2 and 1.9-million-year-old caldera rims at Island Park, which are temporally and spatially transitional between the most recent rhyolite units (0.6 million years old) of the Yellowstone area (Christiansen and Blank, 1972; Christiansen, 1982 this volume) and the Pliocene and Miocene rhyolite units of the eastern Snake River Plain, represent an early part of this stage. The interior as well as the southern and western flanks of the Island Park basin has been completely inundated by Pleistocene basalt flows (Hamilton, 1965; Christiansen, 1982 this volume).

A more advanced stage of burial is represented by a 6.5-million-year-old caldera near Rexburg on the eastern margin of the plain about 50 kilometers south of the Island Park caldera (Figures 1 and 3; Prostka and Embree, 1978; Prostka, 1979; Prostka and others, 1979). The Rexburg caldera complex is 55 kilometers in diameter. Tertiary rocks of the caldera complex, along with small segments of the caldera fault system, are exposed around the margins of the caldera. Juniper Buttes (Kuntz, 1979) at the north edge of the Rexburg caldera north of St. Anthony, Idaho, consists of Pliocene rhyolite and basalt protruding through the Quaternary basalt cover. For the most part, however, the rocks associated with Juniper Buttes have been buried beneath the 4.3-million-year-old tuff of Heise (Armstrong and others, 1980) and the 1.9-million-year-old Huckleberry Ridge Tuff (Christiansen and Blank, 1972; Christiansen, 1982 this volume), Pleistocene basalt, and loess. Well data reveal that the Tertiary rhyolite of the central and western parts of the Rexburg caldera complex has been further buried beneath at least 134 meters of Quaternary Snake River Group basalt (Figure 2; Embree and others, 1979).

The full extent of the Rexburg caldera complex and the location of its western margin have been inferred in part from gravity data. These data disclose a large negative anomaly superimposed on the regional gravity high of the eastern Snake River Plain (Figure 5; Mabey and others, 1974; Mabey, 1978). The circular shape of the negative gravity anomaly, in contrast to the elongate anomalies related to the basin and range structures north and south of the

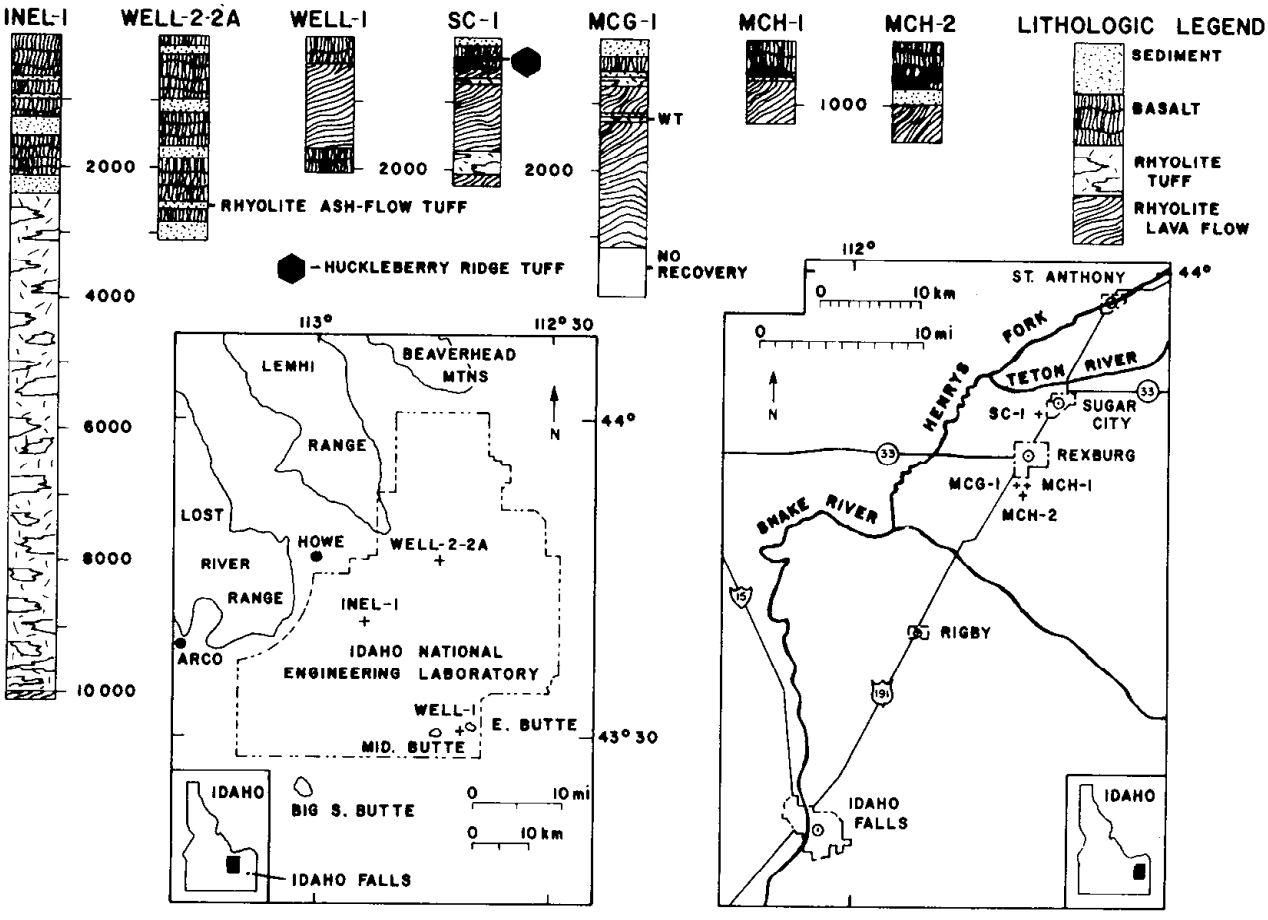

Figure 2. Lithologic logs from various exploratory boreholes on the eastern Snake River Plain (depths given in feet).

plain, suggests that the gravity low is related to a buried caldera. Mabey (1978) suggested that 1.0 to 2.5 kilometers of low-density caldera fill would account for an anomaly of this magnitude.

Geologic mapping, petrography, and regional gravity data suggest an area south and east of the Lemhi Range and south of the Beaverhead Mountains (Figure 5) as the site of a caldera that is buried even more deeply than the Rexburg caldera. The caldera is the source for the tuff of Blue Creek (McBroome, 1981).

The source caldera for the tuff of Blue Creek differs from the Rexburg caldera complex in that the Blue Creek caldera is centered on a positive gravity anomaly. Data obtained from the 3,160-meter-deep exploratory geothermal test well, INEL-1 (Figure 1), may provide an additional explanation. In the test well, 745 meters of basalt and intercalated tuffaceous sediments were found above 2,400 meters of intracauldron rhyolite (Doherty and others, 1979). Approximately 60 meters of dense latite (L. A. McBroome and D. J. Doherty, unpublished data, 1981) was found at the bottom of the test well; the denseness of the latite may be due to hydrothermal mineralization within a ring-fracture zone and may account for the positive gravity anomaly. No intrusive body is known to be associated with the Rexburg caldera complex. Gravity data as well as seismic refraction and borehole data suggest that the denser body is surrounded

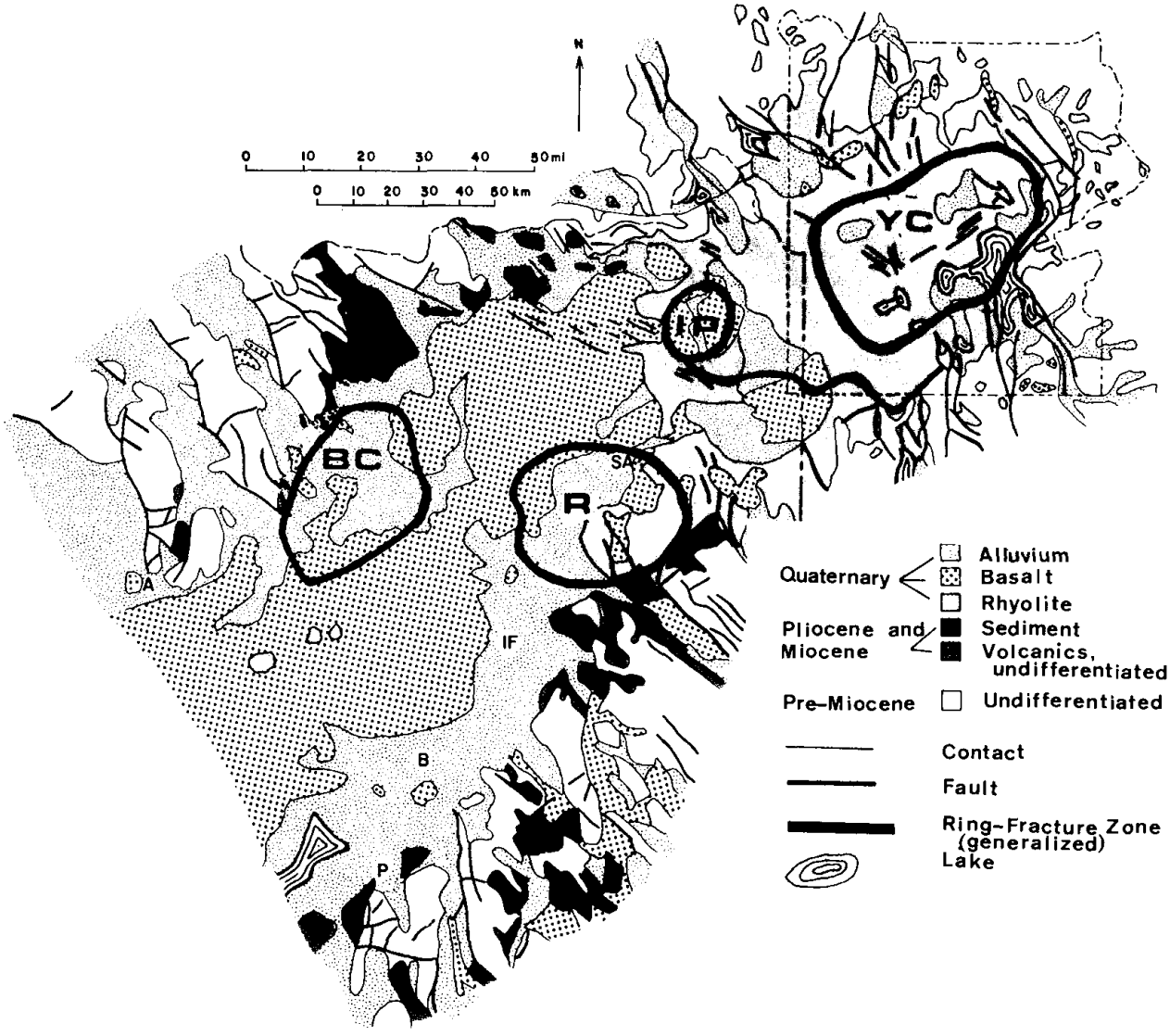

Figure 3. Generalized geologic map of the eastern Snake River Plain, Idaho, and Yellowstone National Park area modified from Bond (1978) and Smith and Christiansen (1980). A—Arco; B—Blackfoot; IF—Idaho Falls; SA—St. Anthony; P—Pocatello; BC—Blue Creek caldera; R—Rexburg caldera complex; IP—Island Park caldera; YC—Yellowstone caldera.

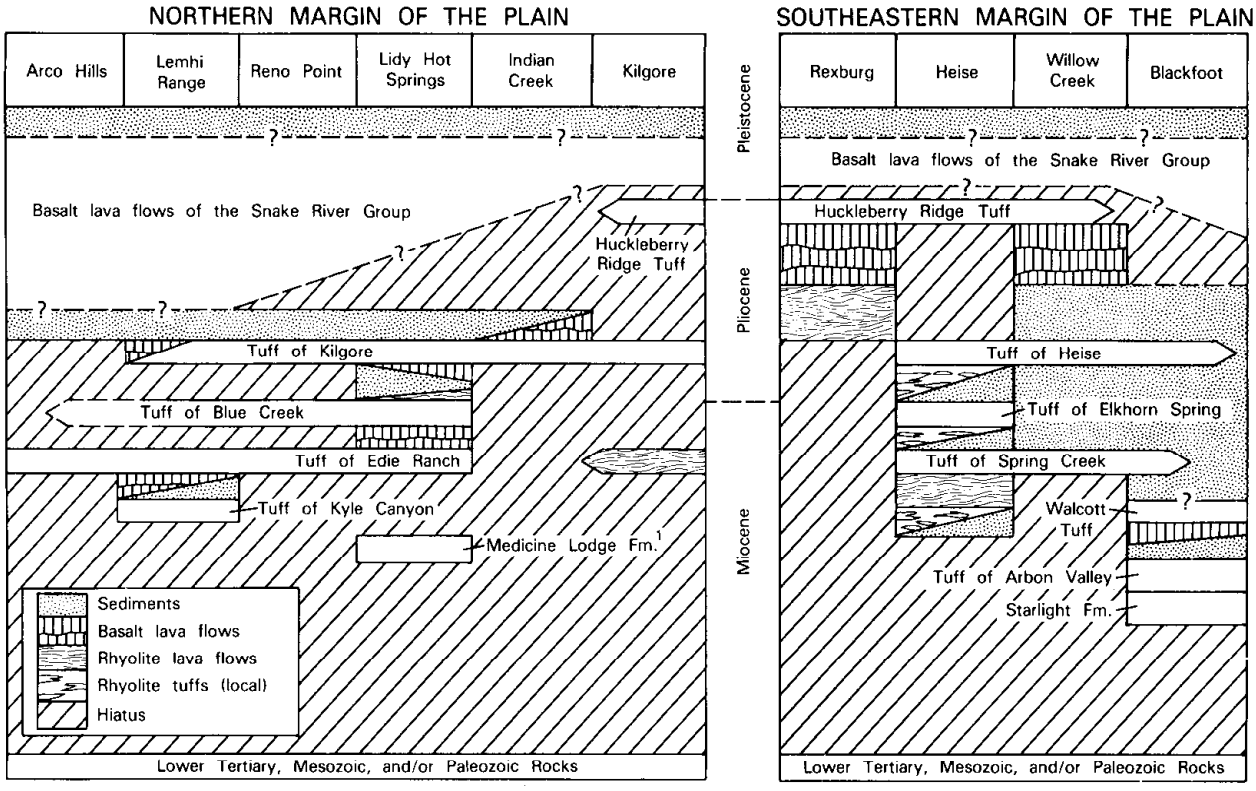

Figure 4. Correlation chart of stratigraphic units on both margins of the eastern Snake River Plain. (1) Scholten and others (1955).

by less dense rhyolitic pyroclastic deposits on the west and less dense tuffaceous lacustrine sediments on the east. The interpretation that less dense rhyolitic pyroclastic deposits are present west of the positive gravity anomaly is supported by seismic refraction data (Pankratz and Ackermann, 1981). Less dense tuffaceous sediment is interpreted to be present east of the positive gravity anomaly, as approximately 100 meters of tuffaceous sediment was recovered in the geothermal exploratory test well 2-2A (Figures 1 and 2; Doherty, 1979a) located in sec. 22, T. 2 N., R. 31 E. The positive gravity anomaly may have been enhanced by resurgence of the collapsed caldera or by a thicker accumulation of basalt lava flows within the caldera than in the adjacent region (McBroome, 1981).

The Island Park, Rexburg, and Blue Creek calderas, in connection with the borehole data obtained from the wells drilled near INEL and Rexburg (Figure 2) and major ash-flow sheets along the margins of the eastern Snake River Plain, suggest the existence of other large calderas concealed beneath the basalt elsewhere on the plain. The precise location of these calderas requires, among other things, a detailed examination of the structural and stratigraphic relations between the individual ash-flow tuff units produced by the major caldera-forming eruptions. The outflow facies of these ash-flow units, as exposed at the margins of the plain, are described below.

MAJOR ASH-FLOW TUFFS ALONG THE SOUTHEASTERN MARGIN, EASTERN SNAKE RIVER PLAIN

TUFF OF ARBON VALLEY

The tuff of Arbon Valley is the middle member of the Starlight Formation (Carr and Trimble, 1963; Trimble, 1976; Trimble and Carr, 1976). It is exposed along the southern margin of the eastern Snake River Plain from the Rockland area on the east side of the Sublett Range to just north of the Blackfoot River in the Caribou Range. The tuff of Arbon Valley is a compound cooling unit 60 meters thick where it is exposed 6 kilometers east of Blackfoot, Idaho. The unit is generally less than 30 meters thick.

The lower half of the tuff is poorly welded to nonwelded and contains about 10 percent of silky white pumice fragments up to 6 centimeters in diameter. The matrix is white and partly devitrified and contains 5 percent phenocrysts of sanidine, beta-

quartz, plagioclase, and biotite.

The middle part of the unit is densely welded, devitrified, eutaxitic with gray pumice 1 to 3 centimeters long set in a white to medium gray matrix. The phenocryst content is much higher in the middle and upper parts of the unit, increasing from 20 to 30 percent. Predominant phenocrysts are quartz, sanidine, and biotite. Although making up less than 1 percent of the total phenocryst content, biotite is significant because the tuff of Arbon Valley is the only major biotite-bearing ash-flow tuff in the area of this study.

The uppermost part of the tuff of Arbon Valley has generally been removed by erosion. Where preserved, it is white and poorly welded.

A potassium-argon age of 7.7 ± 0.1 million years has been determined for the tuff of Arbon Valley by Armstrong and others (1975).

WALCOTT TUFF

The Walcott Tuff was named by Stearns and Isotoff (1956) to describe a densely welded, obsidian-rich, crystal-poor, rhyolitic ash-flow tuff that is exposed along portions of the Snake River canyon near American Falls, Idaho. It varies up to 20 meters in thickness and consists of two members (Carr and Trimble, 1963). The lower member is a white to light gray, bedded, friable, vitroclastic tuff. Some beds contain accretionary lapilli up to 2 millimeters in diameter. The lower member ranges in thickness from 2 to 4 meters.

The upper member consists of a gray to black and pink, vitric, densely welded to nonwelded, crystal-poor, rhyolitic ash-flow tuff. In general, phenocrysts amount to less than 5 percent and consist of plagioclase, sanidine, hypersthene, augite, and minor mag-

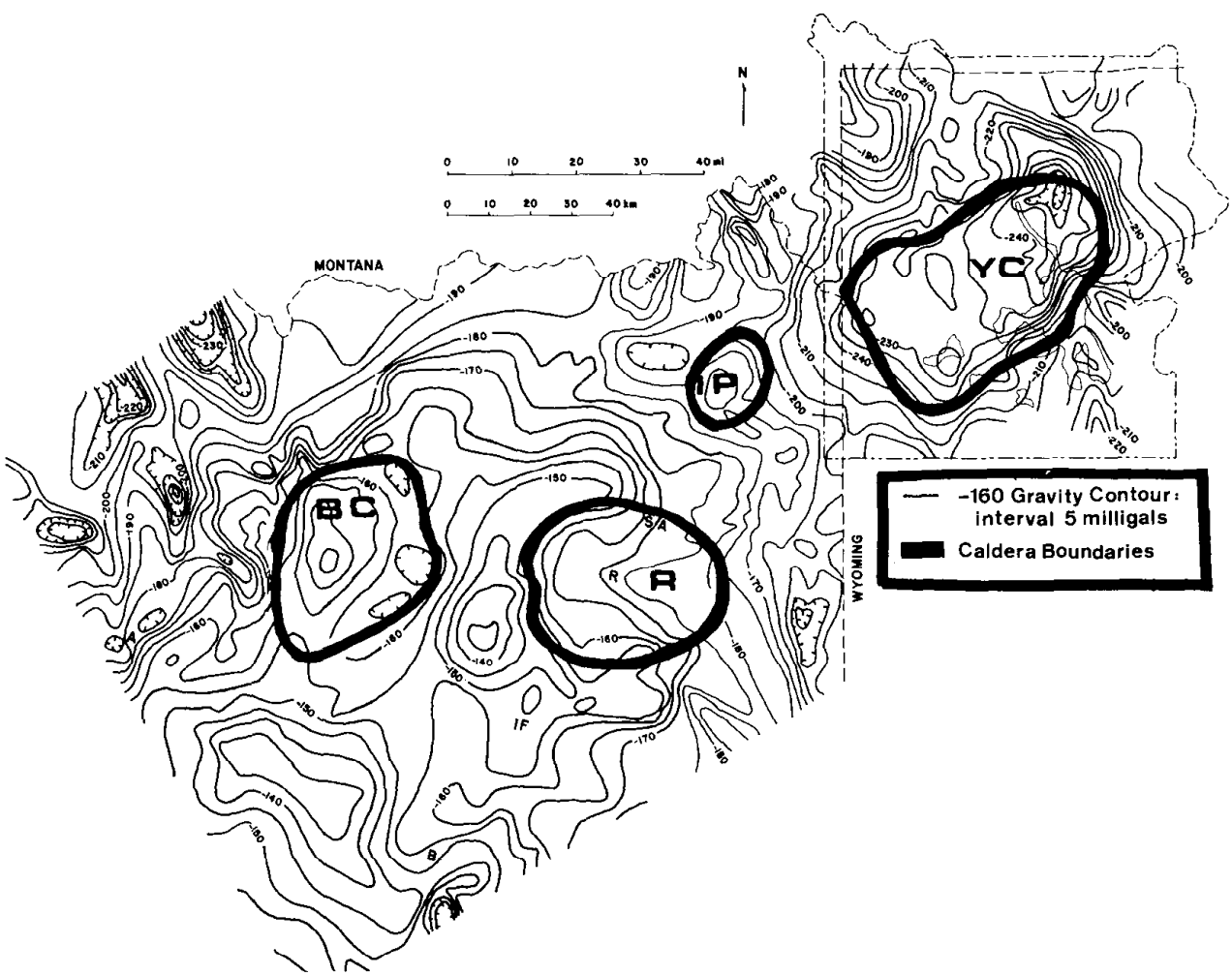

Figure 5. Gravity map of the eastern Snake River Plain, Idaho, and Yellowstone National Park area from Mabey and others (1974) and Smith and Christiansen (1980). The map shows the location of the Yellowstone (YC), Island Park (IP), Rexburg (R), and Blue Creek (BC) calderas. A—Arco; B—Blackfoot; IF—Idaho Falls; R—Rexburg; SA—St. Anthony.

netite. The thickness of the upper member ranges from 16 to 18 meters.

Carr and Trimble (1963) and Mansfield and Ross (1935, p. 310) suggest that the Walcott Tuff may correlate with a tuff unit near Ammon, Idaho, which Doherty (1981) described as the tuff of Heise, unit 2. The age of the Walcott Tuff, as determined by potassium-argon dating techniques, is 6.1 to 6.2 million years (Armstrong and others, 1975); the age of the tuff of Heise in the Ammon area is 4.3 ± 0.15 million years (Armstrong and others, 1980). Thus the tuff of Heise does not correlate with the Walcott Tuff.

TUFF OF SPRING CREEK

The type section for the tuff of Spring Creek has been described for exposures at Stinking Spring Creek (Prostka and Embree, 1978), located in sec. 10, T. 3 N., R. 41 E., Heise SE 7½-minute quadrangle; the tuff of Spring Creek originally was designated as the tuff of Heise A by Albee and others (1975).

The tuff of Spring Creek forms one of the most extensive Miocene ash-flow tuff sheets along the the southern margin of the eastern Snake River Plain. It is the oldest, large-volume, rhyolitic ash-flow tuff associated with the development of the Rexburg caldera complex which erupted 6.5 million years ago (Prostka and others, 1979). The tuff of Spring Creek is well exposed within and surrounding the southern and eastern segments of the complex; the tuff has been identified at least 50 kilometers south of the Rexburg caldera complex southeast of Blackfoot, Idaho. The exposed thickness of the tuff of Spring Creek ranges from 1 meter to at least 215 meters. Outside the caldera, the tuff of Spring Creek is well exposed in the western foothills of the Caribou Range where it occurs as an eroded and gently folded, discontinuous sheet that rests on Mesozoic sedimentary rocks.

The tuff of Spring Creek is typically densely welded, vitric to devitrified, eutaxitic, and in places, lithophysal. It is a gray to brown, crystal-rich tuff with phenocrysts of plagioclase, sanidine, quartz, augite, hypersthene, rare biotite, magnetite, and zircon. The tuff of Spring Creek is vertically zoned in phenocryst abundance and plagioclase composition. Phenocrysts constitute 15 to 20 percent of the rock near the base and gradually decrease to 3 to 5 percent near the top of the unit. Zoned plagioclase phenocrysts increase in anorthite content upward through the sheet from An_{27-37} at the base to An_{42-45} at the top. The lower part of the unit contains up to 2 percent green augite phenocrysts that are commonly corroded. Fluxgate magnetometer measurements show that the tuff of Spring Creek has normal magnetic polarity.

TUFF OF ELKHORN SPRING

The tuff of Elkhorn Spring has been described from its well-exposed type section near Elkhorn Spring, sec. 23, T. 4 N., R. 40 E., Heise 7½-minute quadrangle (Prostka and Embree, 1978). It was originally described as the tuff of Heise B by Albee and others (1975).

The tuff of Elkhorn Spring is a gray to purplish gray, devitrified, lithophysal to spherulitic, eutaxitic, densely welded, rhyolitic ash-flow tuff. Phenocrysts of plagioclase constitute less than 1 percent of the rock. The tuff ranges from 2 to approximately 70 meters in thickness. The tuff of Elkhorn Spring occurs above the 5.72-million-year-old (G. B. Dalrymple, personal communication, 1979) rhyolite of Kelly Canyon (Prostka and others, 1979) and below the 4.3-million-year-old tuff of Heise (Armstrong and others, 1980).

The tuff of Elkhorn Spring is restricted to the southeast edge of the Rexburg caldera complex near Heise, Idaho. In this area, the tuff of Elkhorn Spring forms steep cliffs marked by a prominent black, densely welded vitrophyre near the base. The outcrop pattern of the tuff of Elkhorn Spring is roughly arcuate in form and, in part, outlines the southeastern segment of the Rexburg caldera complex ring-fracture zone. The tuff of Elkhorn Spring may have been deposited in a local moat-type depression near Heise along the edge of the caldera.

The tuff of Elkhorn Spring is equivalent to the tuff of Blue Creek, based on petrographic and magnetic similarities as well as distribution characteristics of the volcanic facies (McBroome and others, 1981). Distribution patterns of these two tuff units suggest that their source is a buried caldera located south and east of the southern Lemhi Range and south of the Beaverhead Mountains.

TUFF OF HEISE

The tuff of Heise is a widely distributed and well-exposed Pliocene rhyolite ash-flow tuff sheet that crops out within the Rexburg caldera complex and surrounding mountains. It can be found in the vicinity of Teton National Park, Wyoming, and as far south as Blackfoot, Idaho. The tuff of Heise is the major Pliocene ash-flow sheet in the foothills of the Big Hole Mountains and the Snake River and Caribou Ranges. It is at least 40 meters thick in the Snake River graben near Swan Valley, Idaho. The tuff of Heise varies in thickness from 1 meter to 150 meters, reflecting emplacement onto irregular topography.

The type section has been described by Prostka and Embree (1978) and is exposed at the top of the

Heise cliffs in sec. 30, T. 4 N., R. 41 E., Heise 7½-minute quadrangle. Albee and others (1975) originally described this unit as the tuff of Heise C.

A potassium-argon age of 4.3 ± 0.15 million years has been determined for the tuff of Heise (Armstrong and others, 1980).

The tuff of Heise forms a compound cooling unit (Smith, 1960a, 1960b; Ross and Smith, 1960). In the area of the Rexburg caldera complex, the tuff of Heise consists of four individual partial cooling units. Of these four units, the bulk of the sheet is composed of the lower two units with a thin, capping veneer of the upper sheets. This relationship is best exposed near Heise, Idaho.

The tuff of Heise is compositionally zoned with the plagioclase becoming slightly more anorthitic upward through the sheet.

Petrographic, radiometric, and field studies reveal that the tuff of Heise is equivalent to the tuff of Kilgore, exposed on the northern margin of the eastern Snake River Plain (Troschinetz and Doherty, 1981). The distribution patterns of these tuff units suggest that their source caldera is near Kilgore, Idaho. The tuff of Heise represents the distal facies of the tuff of Kilgore where the tuff of Heise ponded in the Rexburg caldera complex.

MAJOR ASH-FLOW TUFFS ALONG THE NORTHERN MARGIN, EASTERN SNAKE RIVER PLAIN

Initially, the ash-flow tuffs on the northern margin of the eastern Snake River Plain were collectively described as the Edie School Rhyolite (Scholten and others, 1955). Since then, several stratigraphic units have been recognized.

TUFF OF EDIE RANCH

The tuff of Edie Ranch is an extensive ash-flow sheet exposed along the northern margin of the eastern Snake River Plain in the southern Lost River and Lemhi Ranges and southern Beaverhead and Centennial Mountains. The thickness averages 30 meters but ranges from 2 to 3 meters near Kilgore, Idaho, to 100 meters where the unit fills paleovalleys in the Beaverhead Mountains. The type section is in sec. 8, T. 12 N., R. 33 E., Edie Ranch 15-minute quadrangle (Skipp and others, 1979).

Phenocryst content decreases from 15 percent at the base to approximately 5 percent at the top of the unit. Phenocrysts include sodic plagioclase, sanidine, quartz, augite, and zircon; the relative amount of augite increases upward in the sheet. Magnetic remanence direction indicates normal polarity for the tuff of Edie Ranch (McBroome, 1981).

In the southern Lemhi and Lost River Ranges, the tuff of Edie Ranch is the outflow facies of an ash-flow sheet whose source (the Rexburg Caldera) is concealed partially beneath the basalt lava flows of the eastern Snake River Plain. The base of the unit generally consists of reversely graded air-fall ash and pumice. The overlying pyroclastic flow is a crystal-rich, densely welded, simple cooling unit (Smith, 1960a, 1960b; Ross and Smith, 1960). It is dark brown at the base, moderately to densely welded, and grades upward into a basal vitrophyre that is typically bluish black, crystal-rich, and slightly hydrated; a spherulitic zone overlies the vitrophyre. Above the spherulitic zone, the tuff of Edie Ranch is slightly less crystal-rich, has a well-developed lithophysal zone, and grades upward into densely welded, crystal-rich, devitrified tuff, which is capped locally by a thin vitric layer.

At various locations, the tuff of Edie Ranch overlies the tuff of Kyle Canyon (a local tuff of limited extent; Figure 4), alluvial fan gravels, and basalt flows. It is typically in contact with the overlying tuff of Blue Creek where both tuff units rest unconformably on top of Paleozoic sedimentary strata and form gentle, eastward-facing dip slopes.

Preliminary mapping and laboratory studies suggest that the tuff of Edie Ranch is equivalent to the tuff of Spring Creek. Their source is centered near Rexburg, Idaho, in the Rexburg caldera (Prostka and others, 1979).

TUFF OF BLUE CREEK

The tuff of Blue Creek is petrographically and magnetically distinct from the other ash-flow sheets on the northern margin of the plain. The tuff of Blue Creek rests conformably on the tuff of Edie Ranch. It is a crystal-poor, densely welded, glassy to devitrified, spherulitic and lithophysal ash-flow tuff that exhibits features typical of a simple cooling unit (Smith, 1960a, 1960b; Ross and Smith, 1960). It contains an average of 1 percent plagioclase phenocrysts and sparse amounts of pyroxene, magnetite, and zircon. Outflow facies of the tuff of Blue Creek occur in the southern Lemhi Range and the southern Beaverhead Mountains. The thickness varies up to 180 meters and averages 100 meters.

The original description of this unit was made by H. J. Prostka for the Blue Creek area in the southern Beaverhead Mountains (Skipp and others, 1979). A more accessible reference section, which is about 75 meters thick, is exposed in a roadcut on Idaho

Highway 33 at the southern tip of the Lemhi Range (sec. 35, T. 5 N., R. 31 E., Big Lost River 7½-minute quadrangle), where the entire thickness of the unit is exposed. The basal part of the tuff of Blue Creek consists of orange air-fall material overlain by a 1-meter-thick air-fall deposit; exposures of ground surge deposits are present and restricted to the extreme southern portions of the Lemhi Range and Beaverhead Mountains. A pumice-rich, eutaxitic, densely welded zone is characteristic of the lower portion of the tuff of Blue Creek and is easily identifiable by its stretched orange pumice fragments set in a matrix of black glass shards. The lower zone is in sharp contact with an overlying thin vitrophyre layer which, in turn, grades upward into a perlitic, spherulitic tuff zone. A sharp contact separates this spherulitic zone from an overlying devitrified zone which grades upward into a well-developed lithophysal zone at the top of the unit.

The source caldera of the tuff of Blue Creek is most likely located south and east of the Lemhi Range and Beaverhead Mountains (Figures 3 and 5). Evidence that this is the location of the source caldera includes (1) the distribution of near-source deposits; (2) the locations of related rhyolitic lava domes and flows; (3) the locations of caldera-related fault and deformation structures in the southern Lemhi Range and Beaverhead Mountains; (4) lithologic and petrographic data obtained from the exploratory geothermal well (INEL-1) (Figure 2; Doherty and others, 1979; L. A. McBroome and D. J. Doherty, unpublished data, 1981); (5) gravity and magnetic anomaly studies (Mabey and others, 1974); and (6) seismic and resistivity profiles (Pankratz and Ackerman, 1982; A. A. R. Zohdy, personal communication, 1980).

TUFF OF KILGORE

The tuff of Kilgore is exposed along the northern margin of the eastern Snake River Plain from the foothill area east of Howe Peak, in the southern Lost River Range, to the southern flank of the Centennial Mountains north of Kilgore (Figure 1). The tuff has been described as the tuff of Spencer (Skipp and others, 1979). The unit is thickest (100 meters) and apparently nearest to its source along the south side of the Centennial Mountains. It thins to the west, averaging 30 meters thick where it forms extensive dip slopes near Medicine Lodge Creek in the southern Beaverhead Mountains. In that area, the sheet laps onto the older volcanic units, including the tuffs of Blue Creek and Edie Ranch. Farther west the tuff of Kilgore is found in scattered patches in the foothills of the southern Lemhi Range and southern Beaverhead Mountains. It is generally less than 2 meters thick in most of these areas.

The tuff of Kilgore is a simple cooling unit. The basal vitrophyre is fairly thin (less than 1 meter) and is densely welded with a red and black matrix containing abundant black shards, sparse, black to light gray pumice, and 5 percent black and red grains of obsidian.

A lithophysal zone which constitutes about one-third of the thickness of the unit overlies the vitrophyre. Small (0.5 to 5 centimeters), white lithophysae make up about 50 percent of the rock, whereas the remainder is a medium gray, devitrified, densely welded tuff. Because the tuff is generally massive with little or no jointing, the lithophysal zone commonly forms a prominent cliff, whereas adjacent zones are eroded away or concealed by soil and colluvium.

The central part of the unit above the lithophysal zone is devitrified and slightly eutaxitic, has pronounced slabby parting, and generally displays a strong lineation on joint surfaces. Where the rock is nonlineated, it contains a few lithophysae which are larger than those in the lithophysal zone below. Lineations in the platy zone consist of white and maroon streaks up to 30 centimeters long, 1 to 3 centimeters wide, and only a millimeter or so thick. The streaks consist predominantly of vapor phase crystals. The near absence of large pumice fragments in other parts of the unit and at locations where the platy zone shows no lineation suggests that the lineated streaks may be stretched lithophysae produced by secondary flow.

The uppermost zone, where it has not been removed by erosion, is pink to red, vitric, and moderately welded. The vitric tuff contains light gray, silky pumice, red and black obsidian grains, and black shards like those in the basal vitrophyre.

In the more distal area to the west in the southern Lemhi Range, the tuff is dominantly vitric. Where the lithophysal and devitrified zones are missing, the sheet is only a meter or two thick.

The phenocryst content of the tuff of Kilgore ranges from 5 to 7 percent at the base of the unit to approximately 1 to 2 percent at the top. The predominant phenocryst mineral is plagioclase. In addition, sanidine, quartz, and very sparse, tiny, dark green augite crystals occur as rare phenocrysts.

SUMMARY

The preliminary stratigraphic framework of five major, large-volume ash-flow sheets exposed along the northern and southeastern margins of the eastern Snake River Plain includes descriptions of the tuff of Arbon Valley, the Walcott Tuff, and the tuffs of Edie

Ranch, Blue Creek, and Kilgore. The lithologic character and stratigraphic sequence of some of the ash-flow tuffs on the margins of the eastern Snake River Plain suggest the following correlations: (1) The tuff of Edie Ranch is equivalent to the tuff of Spring Creek and their eruptive source is the Rexburg caldera. (2) The tuff of Blue Creek and the tuff of Elkhorn Spring are equivalent; the tuff of Blue Creek represents the near-source, outflow facies, and the tuff of Elkhorn Spring represents the distal facies; the eruptive center for these units is on the northern margin of the eastern Snake River Plain south and east of the Lemhi Range and south of the Beaverhead Mountains. (3) The tuff of Kilgore is equivalent to the tuff of Heise; the tuff of Kilgore is the near-source facies whereas the tuff of Heise is the distal facies; the relationship of the facies suggests that the eruptive center for these units is located near Kilgore, Idaho.

ACKNOWLEDGMENTS

The preliminary stratigraphic framework and conceptual models for locating the Rexburg caldera complex as an eruptive source of some of the rhyolite units were established by H. J. Prostka during 1972-1977. Prostka's initial understanding of the volcanic stratigraphy and the application of his and R. L. Christiansen's conceptual models have made it possible for the authors of this paper to make rapid advances in the development and comprehension of the Pliocene and Miocene volcanic stratigraphy of the eastern Snake River Plain. We also acknowledge the work and helpful discussions with Paul L. Williams, Bart Ekren, and Dave McIntyre, all of the U. S. Geological Survey.

REFERENCES

Albee, H. F., H. J. Prostka, D. A. Jobin, and J. D. Love, 1975, Field trip guide to the Idaho-Wyoming thrust-fault zone: Geological Society of America, Rocky Mountain section, twenty-eighth annual meeting, Boise, Idaho, field trip 4.

Armstrong, R. L., W. P. Leeman, and H. E. Malde, 1975, K-Ar dating, Quaternary and Neogene volcanic rocks of the Snake River Plain, Idaho: American Journal of Science, v. 275, p. 225-251.

Armstrong, R. L., J. E. Harakel, and W. M. Neill, 1980, K-Ar dating of Snake River Plain (Idaho) volcanic rocks—new results: Isochron West, no. 27, p. 5-10.

Bond, J. G., 1978, Geologic map of Idaho: Idaho Bureau of Mines and Geology, scale 1:500,000.

Carr, W. J. and D. E. Trimble, 1963, Geology of the American Falls quadrangle, Idaho: U. S. Geological Survey Bulletin 1121-G, 44 p.

Christiansen, R. L., 1982, Late Cenozoic volcanism of the Island Park area, eastern Idaho, *in* Bill Bonnichsen and R. M. Breckenridge, editors, Cenozoic Geology of Idaho: Idaho Bureau of Mines and Geology Bulletin 26.

Christiansen, R. L. and H. J. Blank, Jr., 1972, Volcanic stratigraphy of the Quaternary rhyolite plateau in Yellowstone National Park: U. S. Geological Survey Professional Paper 729-B, 18 p.

Doherty, D. J., 1979a, Drilling data from exploration well 2-2A, NW¼, sec. 15, T. 5 N., R. 31 E., Idaho National Engineering Laboratory, Butte County, Idaho: U. S. Geological Survey Open-File Report 79-851, 1 p.

———, 1979b, Drilling data from exploration well 1, NE¼, sec. 22, T. 2 N., R. 32 E., Bingham County, Idaho: U. S. Geological Survey Open-File Report 79-1225, 1 p.

———, 1981, Volcanic geology of the southern portion of the Rexburg caldera complex: University of Nebraska Ph.D. dissertation.

Doherty, D. J., L. A. McBroome, and M. A. Kuntz, 1979, Preliminary geological interpretation and lithologic log of the exploratory geothermal test well (INEL-1), Idaho National Engineering Laboratory, eastern Snake River Plain, Idaho: U. S. Geological Survey Open-File Report 79-1248, 9 p.

Embree, G. F., M. D. Lovell, and D. J. Doherty, 1979, Drilling data from Sugar City exploration well, Madison County, Idaho: U. S. Geological Survey Open-File Report 79-1095, 1 p.

Hamilton, W. B., 1965, Geology and petrogenesis of the Island Park caldera of rhyolite and basalt, eastern Idaho: U. S. Geological Survey Professional Paper 504-C, 37 p.

Kirkham, V. R. D., 1931, Snake River downwarp: Journal of Geology, v. 39, p. 456-482.

Kuntz, M. A., 1979, Geologic map of the Juniper Buttes area, eastern Snake River Plain, Idaho: U. S. Geological Survey Miscellaneous Investigations Map I-1115.

Kuntz, M. A., D. E. Champion, E. C. Spiker, R. H. Lefebvre, and L. A. McBroome, 1982, The Great Rift and the evolution of the Craters of the Moon Lava Field, Idaho, *in* Bonnichsen and R. M. Breckenridge, editors, Cenozoic Geology of Idaho: Idaho Bureau of Mines and Geology Bulletin 26.

Leeman, W. P., 1982, Development of the Snake River Plain-Yellowstone Plateau province, Idaho and Wyoming: an overview and petrologic model, *in* Bill Bonnichsen and R. M. Breckenridge, edi-

tors, Cenozoic Geology of Idaho: Idaho Bureau of Mines and Geology Bulletin 26.

Mabey, D. R., 1978, Gravity and aeromagnetic anomalies in the Rexburg area of eastern Idaho: U. S. Geological Survey Open-File Report 78-382.

———, 1982, Geophysics and tectonics of the Snake River Plain, Idaho, *in* Bill Bonnichsen and R. M. Breckenridge, editors, Cenozoic Geology of Idaho: Idaho Bureau of Mines and Geology Bulletin 26.

Mabey, D. R., D. L. Peterson, and Carol Wilson, 1974, Preliminary gravity map of southern Idaho: U. S. Geological Survey Open-File Report 74-78, scale 1:500,000.

Mansfield, G. R. and C. S. Ross, 1935, Welded rhyolitic tuffs in southeastern Idaho: Transactions of the American Geophysical Union, p. 308-321.

McBroome, L. A., 1981, Stratigraphy and origin of Neogene ash-flow sheets on the north-central margin of the eastern Snake River Plain: University of Colorado M.S. thesis, 74 p.

McBroome, L. A., D. J. Doherty, and G. F. Embree, 1981, Correlation of major Pliocene and Miocene rhyolites, eastern Snake River Plain, Idaho: Montana Geological Society Field Conference and Symposium Guidebook to Southwest Montana, p. 323-330.

Pankratz, L. W. and H. D. Ackermann, 1982, Structure along the northwest edge of Snake River Plain interpreted from seismic refraction: Journal of Geophysical Research, in press.

Prostka, H. J., 1979, Buried calderas of the eastern Snake River Plain: EOS, American Geophysical Union, v. 60, no. 46, p. 945.

Prostka, H. J. and G. F. Embree, 1978, Geology and geothermal resources of the Rexburg area, Idaho: U. S. Geological Survey Open-File Report 78-1009.

Prostka, H. J., G. F. Embree, and D. J. Doherty, 1979, Pliocene Rexburg caldera complex, southeastern Idaho: Geological Society of America, Abstracts with Programs, 92nd Annual Meeting, v. 11, no. 7, p. 499.

Ross, C. S. and R. L. Smith, 1960, Ash flow tuffs, their origin, geologic relations, and identification: U. S. Geological Survey Professional Paper 366, 81 p.

Scholten, Robert, K. A. Keenmon, and W. O. Kupsch, 1955, Geology of the Lima region, southwestern Montana and adjacent Idaho: Geological Society of America Bulletin, v. 66, p. 345-404.

Sheridan, M. F., 1979, Emplacement of pyroclastic flows: a review: Geological Society of America Special Paper 180, p. 125-136.

Skipp, Betty, H. J. Prostka, and D. L. Schleicher, 1979, Preliminary geologic map of the Edie Ranch quadrangle, Clark County, Idaho, and Beaverhead County, Montana: U. S. Geological Survey Open-File Report 79-845, scale 1:62,500.

Smith, R. B. and R. L. Christiansen, 1980, Yellowstone Park as a window of the Earth's interior: Scientific American, v. 242, no. 2, p. 104-117.

Smith, R. L., 1960a, Ash flow tuffs: Geological Society of America Bulletin, v. 71, p. 795-842.

———, 1960b, Zones and zonal variations in welded ash flows: U. S. Geological Survey Professional Paper 354F, p. 148-159.

Sparks, R. S. J. and G. P. L. Walker, 1973, The ground surge deposit: a third type of pyroclastic rock: Nature, Physical Science, v. 241, p. 62-64.

Stearns, H. T., L. L. Bryan, and Lynn Crandall, 1939, Geology and water resources of the Mud Lake region, Idaho, including the Island Park area: U. S. Geological Survey Water-Supply Paper 818, 125 p.

Stearns, H. T. and Andrei Isotoff, 1956, Stratigraphic sequences in the Eagle Rock volcanic area near American Falls, Idaho: Geological Society of America Bulletin, v. 67, p. 19-34.

Trimble, D. E., 1976, Geology of the Michaud and Pocatello quadrangles, Bannock and Power Counties, Idaho: U. S. Geological Survey Bulletin 1400, 88 p.

Trimble, D. E. and W. J. Carr, 1976, Geology of the Rockland and Arbon quadrangles, Power County, Idaho: U. S. Geological Survey Bulletin 1399, 115 p.

Troschinetz, J. S. and D. J. Doherty, 1981, Stratigraphic relationships, chemical correlation, and possible source of the tuffs of Spencer and Heise of the eastern Snake River Plain, Idaho: Michigan Academy of Science and Arts and Letters, Newsletter, in press.

Late Cenozoic Volcanism of the Island Park Area, Eastern Idaho

by

Robert L. Christiansen[1]

ABSTRACT

Island Park is the westernmost part of the Yellowstone Plateau volcanic field and is geologically transitional between the eastern Snake River Plain and the active part of the volcanic field. The field comprises a bimodal volcanic association of rhyolitic and basaltic magmas. Although basaltic volcanism has been intermittently active around its margins throughout its history, most of the field has evolved in three cycles of rhyolitic volcanism, each of which climaxed with the eruption of a voluminous ash-flow sheet and the formation of a large caldera.

The topographic basin of Island Park is a compound feature of all three volcanic cycles, formed over a span of 2 million years, and should not be thought of as a single coherent caldera as some earlier studies have suggested. The southwestern part of the Island Park basin is partly enclosed by a rim segment of the 2.0-million-year-old first-cycle caldera, which extended eastward far beyond Island Park into the present area of the Yellowstone Plateau. The rim of the first-cycle caldera was intersected by the 1.3-million-year-old second-cycle caldera, and the northwestern part of the Island Park basin is enclosed by the highest part of the second-cycle caldera rim. The eastern side of the basin is enclosed by a constructional topography of rhyolitic lava flows of the third volcanic cycle that vented farther east; part of this east margin of Island Park is formed by a precaldera third-cycle lava flow and the rest by 150,000-year-old and younger postcaldera lava flows.

During the period of about a million years since the end of the second volcanic cycle, no rhyolitic activity has been centered at Island Park; the rhyolitic magma bodies of the first and second cycles beneath the area have solidified and partly cooled. As these plutonic bodies have cooled, the Island Park area has subsided and tectonic fracturing has broken them, allowing basaltic magmas to rise through them and to erupt and flood the floor of the basin with basaltic lavas.

Geophysical characteristics as well as the geologic history of the Island Park area indicate that its crust and upper mantle probably remain hotter than is typical for much of the surrounding region but are nevertheless cooler than the subsurface of the Yellowstone Plateau at comparable depths. It is uncertain whether a geothermal energy resource might be associated with the thermal anomaly of Island Park, but, if so, it should reflect a lower-temperature and more diffuse geothermal system than that of Yellowstone. If geothermal energy were ever to be produced from Island Park, special precautions would be necessary to assure that no adverse effects occurred in the surficial hydrothermal features of Yellowstone National Park.

INTRODUCTION

Island Park, situated at the northeastern end of the eastern Snake River Plain and the western foot of the Yellowstone Plateau (Figure 1), focuses attention on some important geologic relations between these two regions of voluminous late Cenozoic volcanism. An improved understanding of the unified volcanic and tectonic evolution of the two regions has become possible by recognizing their close genetic connections, and Island Park provides a crucial interpretational link.

Island Park forms a topograhic as well as a geologic transition between the plateau and the plain. The Yellowstone Plateau is an area of about 6,500 square kilometers at an average elevation of about 2,500 meters, surrounded on all sides but the southwest by mountainous terrain that rises to elevations of 3,000-4,000 meters. Southwestward, the plateau faces the Island Park area and nearby parts of the eastern Snake River Plain, which lie at elevations of about 1,600-1,900 meters.

Island Park is a nearly flat-floored basin, rimmed

[1]U. S. Geological Survey, Menlo Park, California 94025.

Christiansen, R. L., 1982, Late Cenozoic volcanism of the Island Park area, eastern Idaho, *in* Bill Bonnichsen and R. M. Breckenridge, editors, Cenozoic Geology of Idaho: Idaho Bureau of Mines and Geology Bulletin 26, p. 345-368.

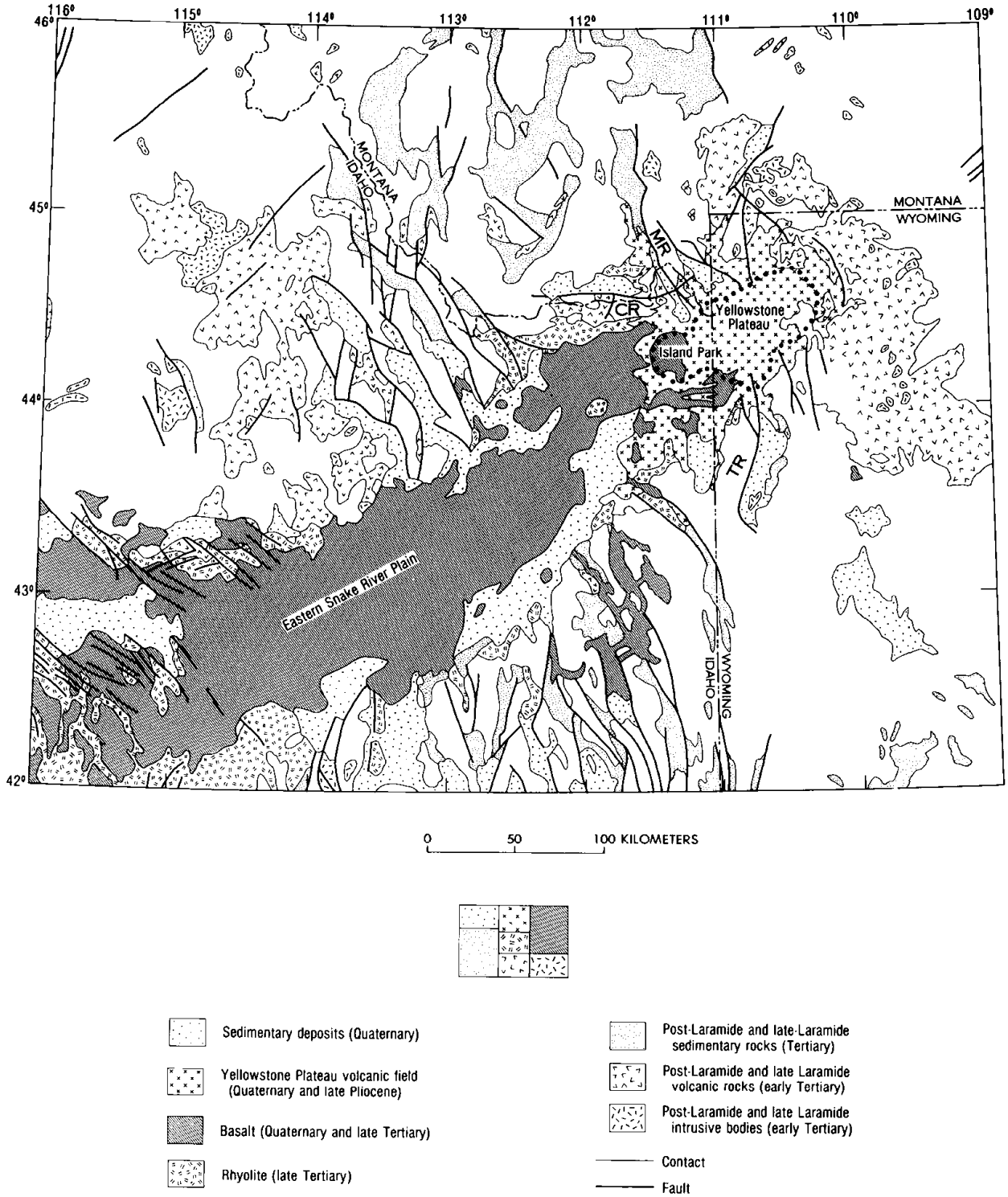

Figure 1. Location of Island Park, Idaho, in relation to surrounding post-Laramide and late-Laramide features. Dotted line encircles the Yellowstone-Island Park caldera complex. The eastern Snake River Plain shows as a major tectonic axis; parallel faults and basin sediments of both Tertiary and Quaternary age outline extensional tectonic elements of the basin-range region south of the plain and part of the northern Rocky Mountains north of the plain. CR, Centennial Range; MR, Madison Range; TR, Teton Range. Faults shown have displacements of middle Miocene and younger age.

on the southwest and west by Big Bend Ridge, on the northwest by Thurmon Ridge, and on the east by scarps at the west foot of the Madison Plateau and Moose Creek Butte—the westernmost portions of the Yellowstone Plateau (Figure 2). Henrys Fork of the Snake River rises in large springs at the base of the Madison Plateau just outside Island Park, flows into the basin at the east end of Thurmon Ridge, and exits near Snake River Butte at the east end of Big Bend Ridge. The Buffalo and Warm Rivers, tributaries of Henrys Fork, also rise in large springs at the base of the Madison Plateau within the Island Park basin.

The coherence of the Island Park basin as a volcanic structure was noted in early reconnaissance by Stearns and others (1938, 1939), who pointed out that the rocks of the basin consist almost entirely of young rhyolites and basalts. Hamilton (1965) also noted these features and further proposed that the basin is a caldera related to the eruption of voluminous rhyolitic ash flows. Hamilton thought that basalts and rhyolites are interlayered throughout Island Park and that both magma types were available for eruption within the basin throughout the caldera cycle. Although in detail both of Hamilton's major conclusions—the existence of a single large caldera and the long-term local availability of both rhyolitic and basaltic magmas—require revision on the basis of work reported here, the importance of the observational basis for his conclusions remains well grounded in major geologic features of the area.

ISLAND PARK AND THE YELLOWSTONE PLATEAU VOLCANIC FIELD

Geologic studies of the Yellowstone Plateau and the Island Park area since 1965 (for example, Christiansen and Blank, 1972; Christiansen, 1974, 1975, 1979) have shown clearly that Island Park is an integral part of the Yellowstone Plateau volcanic field. That field extends more than 100 kilometers from the west rim of Island Park past the east edge of the Yellowstone Plateau. The field has evolved during the past 2.2 million years through three cycles of rhyolitic volcanism. Each of the three cycles began with the eruption of relatively small volumes of both basalt and rhyolite, then continued for several hundred thousand years with the eruption of rhyolites from a growing system of arcuate fractures above a large and growing magma chamber. Each cycle then climaxed with the explosive eruption of a very large volume (hundreds to thousands of cubic kilometers) of fragmented rhyolitic magma in an extremely short time, probably no more than a few days. Partial emptying of the magma chamber in each of these catastrophic eruptions caused the chamber roof to collapse, forming a large caldera. Further eruptions of rhyolites from the residual magma chambers for several hundred thousand years partly filled each caldera by the close of the cycle. Since the cessation of rhyolitic volcanism, the melts within the magma chambers of at least the first two cycles have solidified. The rhyolitic source areas and the calderas of each of the three volcanic cycles covered different but overlapping areas. Basaltic magmas erupted intermittently in smaller volumes around the margins of the rhyolitic source area throughout each rhyolitic cycle; only when the rhyolitic magma had solidified and could sustain fractures, however, could basaltic magmas finally rise through fractures to the surface within the older parts of the caldera complex.

The stratigraphy and volcanic history of the Yellowstone Plateau volcanic field have been worked out mainly from the relations between major ash-flow sheets that erupted at the climax of each cycle. Collectively, these three ash-flow sheets are named the Yellowstone Group, and the individual sheets are named the Huckleberry Ridge Tuff (2.0 million years), Mesa Falls Tuff (1.3 million years), and Lava Creek Tuff (0.6 million years) (Christiansen and Blank, 1972).

PHYSIOGRAPHY AND STRUCTURE

The eastern Snake River Plain, a northeast-trending structural depression about 350 kilometers long that is perhaps a faulted downwarp (Kirkham, 1931), defines a major regional tectonic axis. The depression is flooded by basaltic lavas, but minor rhyolites crop out within the plain and abundant rhyolites, both as ash flows and as lavas, are associated with basalts along its margins in a compositionally bimodal assemblage. Recent drilling, as at the Idaho National Engineering Laboratory, reveals important volumes of rhyolite beneath the basalts of the plain (Doherty and others, 1979). Voluminous rhyolitic volcanism migrated from southwest to northeast along the eastern Snake River Plain during late Cenozoic time (Christiansen and Blank, 1969; Christiansen and Lipman, 1972; Armstrong and others, 1975; Christiansen and McKee, 1978). The trend of the eastern Snake River Plain is nearly normal to that of the basin-range fault blocks that form its northern and southern margins. Local structural relations (for example, Carr and Trimble, 1963) show that the Snake River Plain structure postdates major development of the basin-range normal faults, but all of these tectonic elements as well as the basaltic and bimodal

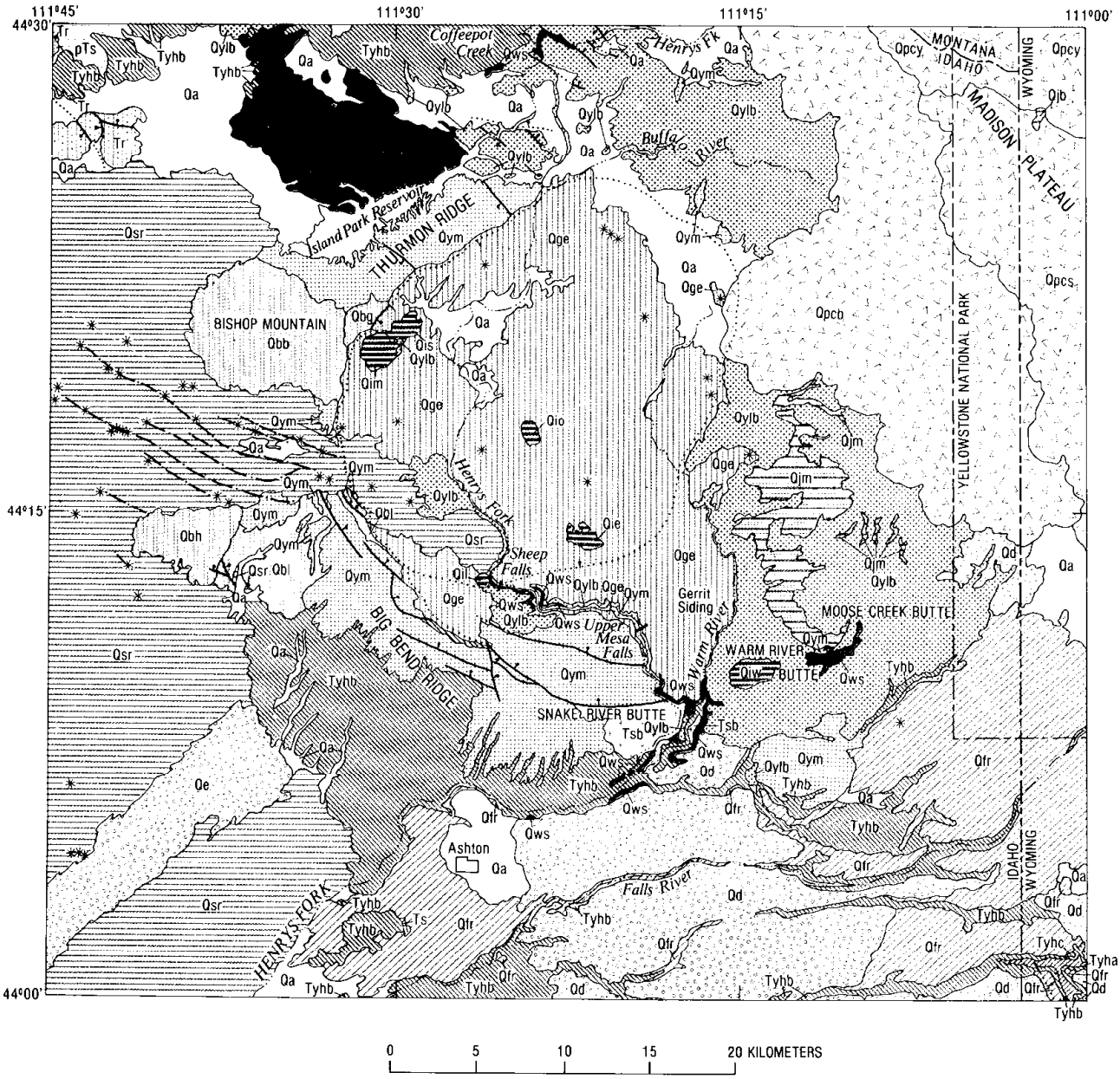

Figure 2. Geologic map of the Island Park area, Idaho and adjacent Wyoming and Montana. Mapping by R. L. Christiansen, 1968-1981.

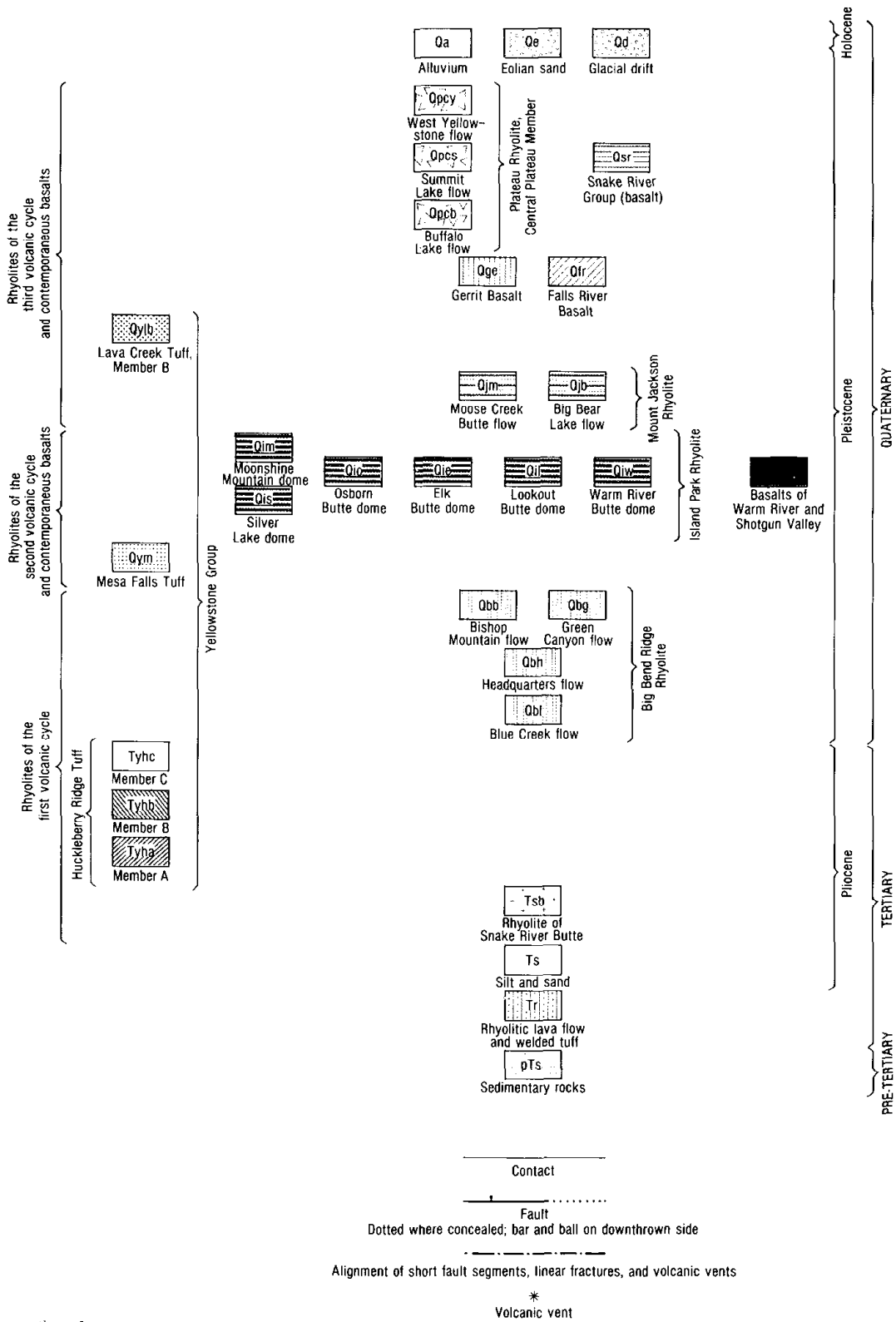

Figure 2. continued.

volcanism associated with them date only from middle Miocene and later time (Ruppel, 1964; Christiansen and Lipman, 1972; Armstrong and others, 1975).

The faults bounding the major structural blocks that border the eastern Snake River Plain are largely buried by upper Cenozoic volcanic and sedimentary rocks. Around both the plain and the Yellowstone Plateau, the relations of various dated ash-flow sheets and sedimentary deposits to the fault-block mountains and valleys show clearly that the main topographic elements of the region had been established before the ash-flow eruptions from nearby major volcanic centers. More recent displacements, however, have occurred locally along these marginal fault systems, and the continued growth of fault-block topography surrounding the Yellowstone Plateau volcanic field is recorded in the offlaps of successively younger volcanic units. The Centennial, Madison, Teton, and other ranges and their intervening valleys existed in essentially their present structural configurations some time before 4-10 million years ago, but with considerably lower relief.

The fault-block mountains and valleys controlled the form of the Yellowstone Plateau volcanic field and the distributions of its major ash-flow sheets. In their original form, the ash-flow sheets that contain most of the volume of the volcanic field extended around the flanks of the major mountain ranges, with extensions along structural valleys that led away from the central caldera complex. The only broad opening that bordered the field was toward the Snake River Plain; this opening allowed the oldest ash-flow sheet to spread far to the west and southwest. After the first major ash-flow eruptions and formation of the first-cycle caldera, however, the caldera basin partly blocked this direction to younger ash flows.

Growth of the basin-range faults along the margins of the eastern Snake River Plain and the Yellowstone Plateau is partly dated by the relations of various volcanic and sedimentary units to the faults. Volcanism similar to that which later occurred in the Yellowstone-Island Park region was active in the eastern part of the Snake River Plain in the few million years before the beginning of Yellowstone Plateau activity. A phenocryst-poor, generally lithophysal ash-flow sheet related to that volcanism, the 5.8-million-year-old Conant Creek Tuff (Christiansen and Love, 1978), partly buried the western border of the mountainous region east of the Snake River Plain. Along the margins of the eastern Snake River Plain extending about 100 kilometers farther west, at least four major ash flow sheets, ranging in age from about 4 to 10 million years, erupted from caldera sources that are now buried by basalts of the plain (McBroome, 1981; Embree and others, 1982 this volume). The distributions of these ash-flow sheets too were controlled by the preexisting ranges and basins that border the plain, but the ash-flow tuffs were subsequently uplifted on the lower flanks of the ranges.

East and southeast of the Yellowstone Plateau volcanic field the main late-Cenozoic tectonic trends are more or less north-south. North and west of the field, the fault trends change to northwesterly and westerly. Thus, the Hebgen Lake and Centennial fault scarps trend approximately east-west, virtually at right angles to the Teton fault trend (compare Figures 1 and 5). Internal structures in both the Centennial and Teton Ranges (Figure 1) tilt toward the axis of the Snake River Plain, and the flanks of the ranges are buried by young volcanic rocks near the margins of the plain, indicating the crustal downwarping along the plain. Discontinuous elements of this pattern continue southwestward along both margins of the plain. The Yellowstone Plateau volcanic field lies at the intersection of the tectonic axis of the eastern Snake River Plain with the change in trend of late-Cenozoic regional extensional elements and with the main belt of seismically active normal faults (see Figure 5) that bounds the eastern margin of the basin-range region of tectonic extension.

THE FIRST VOLCANIC CYCLE

Although the most coherent aspects of Island Park's structural pattern date from the second volcanic cycle, its structural and topographic framework was established in the first cycle. Big Bend Ridge (Figure 2), the largest topographic feature of the Island Park rim, dates from the first cycle.

EARLY RHYOLITIC AND BASALTIC VOLCANISM

Geologic mapping, stratigraphy, and potassium-argon dating show that the first and most voluminous volcanic cycle of the Yellowstone Plateau field began shortly before about 2.2 million years ago with small-volume eruptions, both rhyolitic and basaltic. One of those early rhyolitic flows forms Snake River Butte, north of Ashton, Idaho, and can be seen to underlie the Huckleberry Ridge Tuff along a railroad cut in the canyon of Warm River, about 400 meters east of the flank of the butte (Figure 2). The flow's vent, although not now exposed, must have lain near the margin of what was later to become the first-cycle caldera. The Snake River Butte flow has a potassium-argon age of 2.0 million years, and all the dated

precaldera rhyolites and basalts around the margins of the first-cycle volcanic field are between about 2.2 and 2.0 million years old (Christiansen and Blank, 1972; J. D. Obradovich, U. S. Geological Survey, written communication, 1982). The flow at Snake River Butte, as well as another near Broad Creek on the east margin of the first-cycle caldera, and possibly others now buried, may have vented along an incipient ring-fracture zone in the gently uplifted roof of an insurgent first-cycle rhyolitic magma body that extended more that 90 kilometers from Big Bend Ridge to near Broad Creek.

Precaldera basalts are present in the northern and western parts of the volcanic field. Because of cover by younger rocks, however, the extent of basaltic volcanism that occurred early in the first cycle is uncertain.

THE HUCKLEBERRY RIDGE TUFF

As so much of the main eruptive area of the first volcanic cycle is buried by younger rocks, most of our knowledge of the cycle is inferred from stratigraphic and petrologic relations in the Huckleberry Ridge Tuff, the extensive ash-flow sheet that erupted at its climax.

A basal deposit of fallout ash is present locally beneath the ash flows of the Huckleberry Ridge Tuff. The ash flows are divided into three members (Christiansen and Blank, 1972), designated A, B, and C (Christiansen, 1979). The principal phenocrysts in all three members are quartz, sanidine, plagioclase, magnetite, fayalite, and iron-rich clinopyroxene. Members A and B resemble one another closely, although A, the basal member, has fewer quartz and more plagioclase phenocrysts. Member C is lithologically distinctive and crops out only in the area between the southern margin of the Yellowstone Plateau and northern Jackson Hole. As it is not present in the Island Park area, it is not discussed further here. The Huckleberry Ridge covered an area of more than 15,000 square kilometers (Figure 3) and had a total erupted volume of more than 2,450 cubic kilometers, of which 1,340 cubic kilometers is within member B, which is closely associated with the formation of Island Park.

Member A occurs mainly around the margins of the Yellowstone Plateau but also as far as the northernmost exposures of Huckleberry Ridge Tuff, in the Madison and Gallatin Ranges and northern Yellowstone National Park (Figure 3). Member A is the thickest part of the Huckleberry Ridge in much of the area north of the plateau. There is a marked upward change in the percentage of phenocrysts in member A. Wherever it is observed, this change progresses upward from phenocryst-rich welded tuff at the base to quite phenocryst-poor rock at the top. Crystallized welded pumice is moderately abundant in the lower part of the member but, like the phenocrysts, becomes sparser upward. However, where rare pumice is found in these phenocryst-poor rocks, the pumice contains about the same percentage of phenocrysts as pumice in the more crystal-rich lower part of the member. This relation indicates that the vertical change in phenocrysts of member A is not a direct function of compositional zonation in its magma chamber, like that shown for many other ash-flow sheets (for example, Smith, 1979; Hildreth, 1981). Rather, the decrease probably relates to mechanical sorting during eruption and emplacement. As the eruption progressed, the magma must have been nearly completely disrupted to ash-sized material, many of the phenocrysts broken and comminuted, and the pumice fragments largely disaggregated. Lateral sorting during emplacement of the later ash flows must have concentrated the remaining phenocryst fragments near the eruptive source and allowed a marked relative increase in the amount of glassy shards and dust outward in the ash flows. Unfortunately, this hypothesis cannot be tested rigorously because the near-source parts of member A are completely buried by younger volcanic rocks in the area of the third-cycle Yellowstone caldera.

Members A and B are separated in most sections only by a parting at which the ash-flow tuff is less densely welded than just below or above, thus forming a compound cooling unit. Locally near their distal margins these subsheets grade laterally into separate cooling units, forming what Smith (1960) called a composite sheet. Only one significant zone of less dense welding occurs in most sections of members A and B, and it is demonstrably at a consistent stratigraphic horizon, as shown by the vertical phenocryst changes of both members A and B. Member B is relatively phenocryst-poor at its base, similar to the upper part of member A, but grades upward into progressively more phenocryst-rich rocks. The phenocryst-poor basal part of member B is thinner in most sections than the phenocryst-poor upper part of member A. By contrast to A, welded pumice inclusions in member B have phenocryst contents more or less in proportion to those of the whole rocks, indicating that in B the variation in proportion of phenocrysts probably does result from compositional zonation in the erupted magma. The phenocrysts in the relatively phenocryst-rich upper part of member B commonly are somewhat larger than those in member A, with large pinkish quartz phenocrysts being especially notable in places. The uppermost part of this phenocryst-rich part of member B contains cognate magmatic inclusions of two contrasting

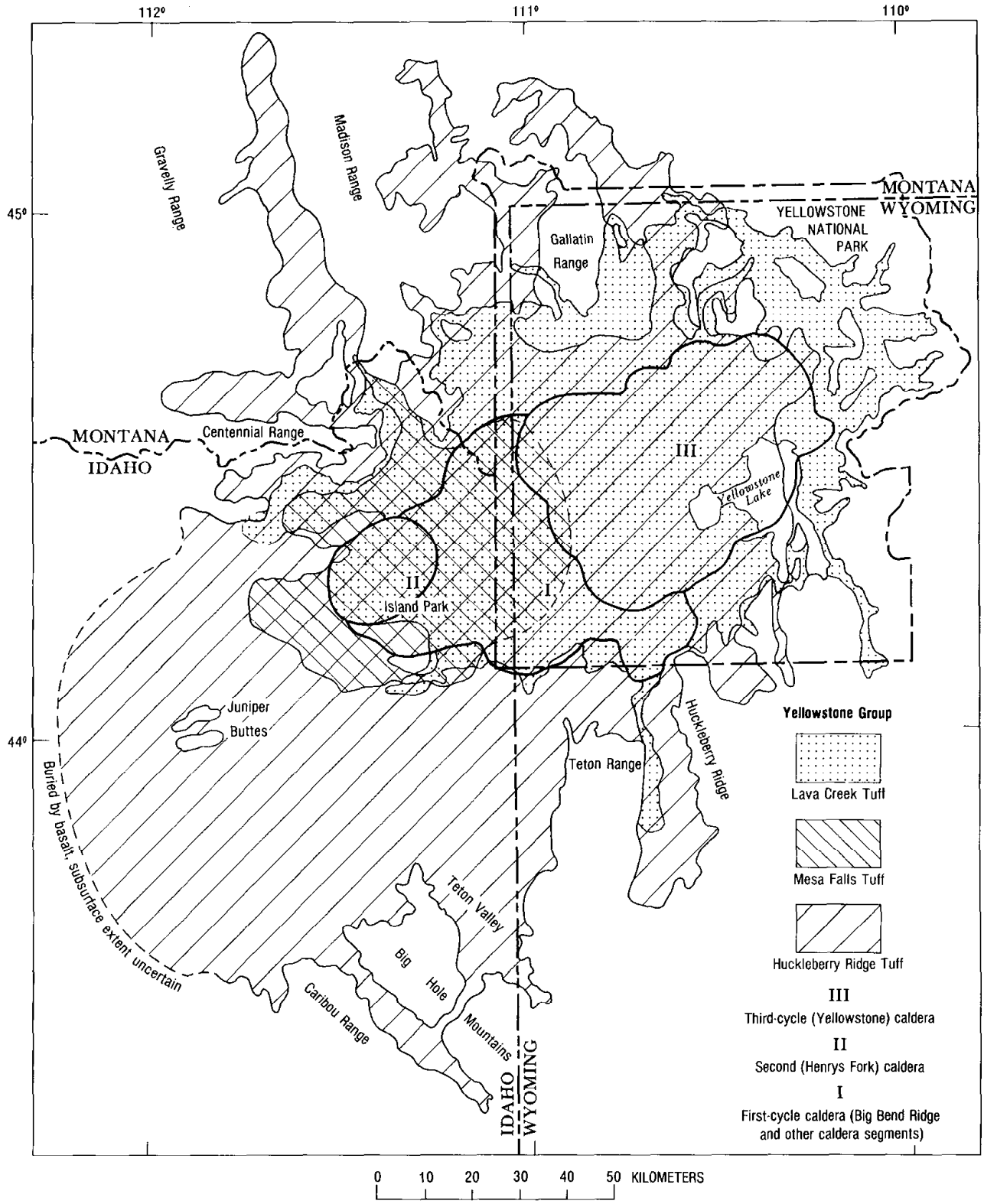

Figure 3. Map showing reconstructed original distributions of ash-flow sheets of the Yellowstone Group and interpreted configurations of calderas of the three cycles of the Yellowstone Plateau volcanic field.

compositions, both of which are generally welded and crystallized. The darker cognate inclusions in devitrified rocks are dark gray and weather brown, contrasting sharply with white inclusions in the same rocks. Vapor-phase minerals invariably occur in the dark crystallized inclusions and include a characteristic brownish acicular amphibole that has been noted in no other rhyolites of this field. Where glassy, the dark inclusions are black and scoriaceous rather than truly pumiceous. The light-colored pumice, where not densely welded, has a filamentous pumiceous structure; where it is welded densely but is still glassy, it forms obsidian or perlite. The upper part of member B is the only two-pumice zone known in any of the tuffs of the Yellowstone Group and thus forms an important lithologic marker for mapping.

Member B is present over most of the area of the Huckleberry Ridge Tuff. It is thickest—more than 150 meters—on Big Bend Ridge and in nearby areas to the southeast. The thickness remains about 100 to 150 meters north of Island Park, around the Madison Valley near West Yellowstone, and into drainages north of the Yellowstone Plateau. Member B thins eastward from there into northern Yellowstone National Park and also from the Island Park area eastward around the northern Tetons. In almost all exposures in the northern part of the area, member B lies directly on member A, only locally onlapping the higher parts of preexisting topography. On the high-standing slope south of Big Bend Ridge, however, member B is the only unit present in the Huckleberry Ridge Tuff.

As it thickens westward from the northern Teton Range toward Big Bend Ridge, member B gains a conspicuous lineation. The section of member B on Huckleberry Ridge, east of the northern Tetons, lacks lineation in outcrop, but in the area between the Tetons and the Yellowstone Plateau, a weak yet easily perceptible lineation of stretched pumice is apparent. Farther westward the lineation becomes progressively more pronounced, and wavy low-amplitude broad-wavelength folds of the welded-tuff foliation have axes parallel to the lineation. On the outer south flank of Island Park, where member B is very densely welded, the broad wavy folds are quite conspicuous. The deformed foliation and the lineation are so marked that some outcrops can be difficult to recognize as welded tuffs rather than rhyolitic lavas; an example is exposed beneath the Mesa Falls Tuff along the highway north of Ashton, Idaho. Around the outer flanks of Island Park, the lineation and the axes of the fold forms in the welded tuff are generally circumferential to the rim of the Island Park basin and verge away from the rim.

Lateral variations in mechanical composition and in crystallization zones of member B, as well as the thickness changes and lineations just noted, indicate the source area of the member to be in the area of Island Park. The member is present at the south rim, and the strong lineation and folding on the outer flank indicate that the unit was very hot there, being deformed to some degree as it was deposited and welded.

An unusual variety of lithologic features and internal structures suggest that part of the Huckleberry Ridge Tuff may have erupted into a lake that lay on the margin of the Snake River Plain at the edge of the slope of Big Bend Ridge. On the ridge, member B is very densely welded, strongly lineated, and entirely devitrified at exposed levels. At the south foot of the ridge, such as near Ashton Reservoir (Figure 2), the tuff is partly glassy and spherulitic. The welding generally remains dense, but small open spaces occur rather commonly in layers parallel to the foliation. In this area, foliation is intensely and irregularly deformed, locally taking any attitude. Certain layers parallel to foliation are devitrified, especially where foliation is nearly vertical, although other layers remain glassy. Lineation disappears as a conspicuous feature in the glassy rocks. In devitrified rocks of this area, the dark scoriaceous pumice characteristic of the member is clayey, greenish, and weathers easily. In the area as far as 20 kilometers south of Ashton, to the Teton River, the Huckleberry Ridge Tuff overlies fine-grained clastic sediments along an irregular but generally poorly exposed contact.

The Huckleberry Ridge Tuff remains predominantly vitrophyric to within ½ kilometer north of the Teton River. Just north of the river, the only devitrified or partially devitrified rocks are small pipelike masses that weather into knobs. The canyon of the Teton River is carved 150 meters into mainly devitrified welded tuff of members A and B, with a thick basal vitrophyre on the underlying sediments. Locally the sediments are highly contorted beneath the welded ash flows, rising in diapir-like masses into the ash-flow sheet; the contact of the ash flows with the sediments shows foldlike forms having amplitudes of tens of meters and locally steep attitudes in the walls of the canyon. Most of these, however, are not true folds. Internal stratigraphic horizons in the ash flows are deformed less than the amplitude of the distorted contact, and the vitrophyric zone that appears to define folds transgresses internal horizons in the ash-flow sheet. These relations demonstrate that the deformation occurred during welding and crystallization of the ash-flow sheet. In the areas where deformation is most intense, there are numerous millimeter- to meter-sized cavities in the devitrified welded ash flows, generally lined with lithophysal minerals (Prostka, 1977). Southward beyond the

Teton River, the degree of development of these deformational features decreases rather abruptly.

The features just described seem consistent with the hypothesis that the Huckleberry Ridge Tuff—erupted in part from the area bounded southward by Big Bend Ridge—flowed down a slope at the edge of the Snake River Plain, welding as it was emplaced, and entered a lake. The unit chilled quickly but deformed plastically in places where sediments on the lake floor slumped or compacted irregularly under the imposed load. The numerous cavities may have formed as trapped steam bubbles, generated by the hot ash flows in contact with lake water. The devitrified bands and pipes could have resulted from more prolonged cooling by the passage of steam along steeply inclined distorted layering or above pockets of vapor trapped below the welded tuff. Either the south shore of the lake was located just south of the present Teton River, or the ash flows had largely displaced the lake water by the time they reached that area.

The age of the Huckleberry Ridge Tuff has been determined by the potassium-argon method (J. D. Obradovich, written communication, 1982) on sanidines separated from each of the three ash-flow members of the formation; all give concordant ages of about 2.0 million years, thus falling near or just before the Pliocene-Pleistocene boundary (Berggren, 1972; Obradovich and others, 1982).

THE FIRST-CYCLE CALDERA

The members of the Huckleberry Ridge Tuff apparently had distinct source areas; however, all three members were erupted within an extremely short period of time, have no erosional breaks, and for the most part form a single compound cooling unit. Physical evidence for three separate segments to a first-cycle caldera (Figure 3) is incomplete, but available data are consistent with a concept, initially developed on better evidence for the third volcanic cycle (Christiansen, 1979), that the members represent eruptions from ring-fracture zones above separate culminations on a major high-level magma body, all connected at depth. With the approach of a critical state of saturation stability in the magma body as a whole, some process triggered vapor separation, the beginning of degassing, and voluminous eruption from one of the ring fracture zones, each such event then triggering eruption from the next ring-fracture zone.

Little is seen of the part of the collapse structure that formed with eruption of member A of the Huckleberry Ridge Tuff, since that caldera segment is now largely buried in the center of the Yellowstone Plateau. A depression partly filled by member C in the Red Mountains, at the south edge of the plateau in Yellowstone National Park, may be part of the member A caldera.

The source area of member B of the Huckleberry Ridge was in the vicinity of Island Park, and the eruption of member B caused collapse of the magma-chamber roof there to form a caldera, part of which is preserved at the southwest rim of Island Park, designated here as the Big Bend Ridge segment of the first-cycle caldera (Figures 2 and 3). Later collapse related to the Mesa Falls Tuff occurred in part of the same area, rejuvenating relatively minor displacements on the caldera faults along this southern rim. Most of the rest of the Big Bend Ridge caldera segment was subsequently disrupted or buried during the second and third volcanic cycles.

Figure 3 shows an interpretation of the first-cycle caldera of the Yellowstone Plateau volcanic field, based on the evidence just outlined, using the third-cycle caldera as a model.

POSTCOLLAPSE RHYOLITIC VOLCANISM

Four post-Huckleberry Ridge, pre-Mesa Falls rhyolitic lava flows, mapped as the Bishop Mountain, Green Canyon, Blue Creek, and Headquarters flows, are present on the rim and outer flank of Island Park between Big Bend and Thurmon Ridges (Figure 2). These flows are here formally designated together as the Big Bend Ridge Rhyolite.

As is typical of rhyolitic lavas, the thicknesses of the flows vary greatly; the exposed thickness on the caldera scarp at the base of Bishop Mountain, designated the type area for the Big Bend Ridge Rhyolite, is about 375 meters. The Headquarters flow overlies the Blue Creek flow, but the field stratigraphic relations among the others are unclear. All of these flows are shown by mapping (Figure 2) to overlie the Huckleberry Ridge Tuff and to underlie the Mesa Falls Tuff on the rim west of Island Park, although Hamilton (1965) regarded them as younger than all the ash flows of the Island Park rim. The Big Bend Ridge flows are roughly similar to one another in lithology and petrography. They all contain phenocrysts of quartz, sanidine, and plagioclase. Most of the flow surfaces are eroded so that little of their original glassy shells remain, but spherulitic zones are preserved widely. Mafic silicate minerals in the crystallized rocks commonly are altered to iron-oxide minerals; biotite occurs in the Bishop Mountain and Green Canyon flows and, as such, is notable because biotite is generally absent in rhyolites of the Yellowstone Plateau field.

The topographic high points of each flow are near the rim of the Big Bend Ridge caldera segment, but each flow was truncated by second-cycle collapse. Therefore, these high points do not represent the vent areas as Hamilton (1965) supposed in outlining his concept of an "Island Park caldera." The actual source vents for the flows are unknown but buried somewhere within the Island Park basin. They probably were in the ring-fracture zone of the first-cycle caldera.

It is difficult to state with certainty whether the Big Bend Ridge Rhyolite should be regarded as comprising postcollapse flows of the first volcanic cycle, precollapse flows of the second cycle, or both. Petrologic and geochemical studies, now underway but not discussed in detail in this paper, help to clarify their magmatic affinities and suggest a relationship of at least the Blue Creek and Headquarters flows to magmas of the first cycle. Also, although the flows of the Big Bend Ridge Rhyolite have not yet been dated directly, it is here considered to be earliest Pleistocene. Normal magnetic polarities of the Blue Creek and Headquarters flows suggest that they should be much closer in age to the 2.0-million-year-old Huckleberry Ridge Tuff than to the 1.3-million-year-old Mesa Falls Tuff (compare with the magnetostratigraphic chronology of Mankinen and Dalrymple, 1981). By contrast, the Bishop Mountain and Green Canyon flows have reverse magnetic polarity and probably are younger.

THE SECOND VOLCANIC CYCLE

The second volcanic cycle was the smallest of the three, but it nevertheless displays a sequence of events similar to the other two cycles. The second cycle was responsible for the formation of many of the present features of Island Park, and rhyolites of the second cycle are exposed only within the Island Park area. Volcanism of the second cycle was centered in an area nested within the first-cycle caldera in the northern part of Island Park. The climactic ash flows, forming the Mesa Falls Tuff, had a volume of more than 280 cubic kilometers.

POSSIBLE EARLY RHYOLITIC VOLCANISM

As noted earlier, at least part of the Big Bend Ridge Rhyolite probably represents a postcollapse first-cycle magma. With available data, it is possible that the Bishop Mountain and Green Canyon flows could be precaldera second-cycle lavas. Although other pre-Mesa Falls rhyolitic flows are not known, it is also possible that additional rhyolitic lavas of various ages could lie buried within the caldera complex.

THE MESA FALLS TUFF

The Mesa Falls Tuff, although having less volume and covering less area than either the Huckleberry Ridge or the Lava Creek Tuff, is a major ash-flow sheet. It is inferred to be present over more than 2,700 square kilometers in and near Island Park (Figure 3). The thickest exposed section occurs on Thurmon Ridge, the northern rim of Island Park, where it is about 150 meters thick. Elsewhere it commonly is about 50-70 meters thick. The mapped and inferred distribution of the Mesa Falls Tuff represents an initial volume of more than 280 cubic kilometers if its thickness within the first-cycle caldera is about the same as its average thickness outside. Probably, however, it is ponded more deeply there, could extend farther east beneath younger rocks, and thus could be correspondingly more voluminous. The Mesa Falls overlies the Huckleberry Ridge Tuff unconformably in many places, especially in the southern part of the Island Park area. The only intervening units on which the Mesa Falls Tuff is seen to lie locally are the Big Bend Ridge Rhyolite and a wedge of loess in roadcuts and quarries about 5 kilometers north of Ashton (compare with Hamilton, 1965, Figure 3). The Lava Creek Tuff overlies the Mesa Falls Tuff unconformably at many places, but elsewhere various basalts lie between them.

The Mesa Falls Tuff is lithologically the most distinctive of the three ash-flow sheets of the Yellowstone Group (except for certain subunits of the Huckleberry Ridge and Lava Creek Tuffs). The Mesa Falls Tuff generally forms large rounded boulderlike outcrops, commonly pinkish in color. It has abundant, very large phenocrysts, particularly the unbroken sanidines, which can be as large as 2-3 centimeters in pumice inclusions. Parts of the other two ash-flow sheets also have large sanidine crystals, but by comparison they generally are less than 1 centimeter and most of the phenocrysts in a given specimen are only a few millimeters across. Vertically throughout the Mesa Falls, the phenocrysts are large and conspicuous although they are volumetrically less abundant in the vapor-phase zone exposed locally high in the cooling unit. The principal phenocrysts include quartz, sanidine, plagioclase (about An_{15}), ferroaugite, magnetite, ilmenite, and fayalite. Large welded pumice inclusions, commonly up to 10 centimeters but locally more than 30 centimeters across, are abundant in the Mesa Falls Tuff. Lithic

inclusions are not abundant, but where present include welded tuff lithologies probably derived from the Huckleberry Ridge Tuff. These inclusions are sometimes useful in mapping because welded-tuff xenoliths are relatively uncommon in the Huckleberry Ridge, the unit most easily confused with the Mesa Falls.

A thick, bedded ash and pumice deposit is present at the base of the Mesa Falls Tuff and is well exposed in roadcuts and quarries along the southern outer flank of Island Park. This deposit generally is about 3-5 meters thick in these exposures and directly underlies the main Mesa Falls ash flows. The deposit is white, very well sorted, generally has good planar bedding, and contains abundant crystals of the same types present in the succeeding ash-flow tuff. The lower part of this bedded ash contains a marked concentration of crystals over glass. The upper, coarser part commonly consists predominantly of pumice lapilli, some of them up to 5 centimeters. Bedding in much of the unit is parallel to the underlying slope and mantles local irregularities of the buried surface with a nearly uniform thickness of ash and pumice, clearly representing a fallout origin for most of the deposit. However, near the top are some thin ash-flow tongues as well as channeled and cross-stratified units that may represent a phase of ground-surge deposition (Parsons and Doherty, 1974).

The Mesa Falls Tuff is exposed as a simple cooling unit. The source area of the Mesa Falls is in the Island Park area, as shown by its distribution, coherent thickness variations in its basal bedded deposit, and its presence at the top of the caldera scarp along Thurmon Ridge.

Sanidine from the Mesa Falls Tuff has been dated as about 1.3 million years old (J. D. Obradovich, written communication, 1982).

THE SECOND-CYCLE CALDERA

Eruption of the Mesa Falls Tuff from the Island Park area caused the roof of the magma chamber from which the eruptions occurred to collapse. This second-cycle caldera lies largely or entirely within the Big Bend Ridge segment of the first-cycle caldera (Figure 3). The second-cycle caldera, here named the Henrys Fork caldera (Figures 2 and 3), did not coincide exactly with the first-cycle caldera in the Island Park area. The north wall of the Henrys Fork caldera at Thurmon Ridge probably lay close to the old caldera wall. However, northward from the south rim of the Big Bend Ridge caldera segment, the Mesa Falls can be mapped almost halfway across the Island Park basin with fault displacements aggregating less than 100 meters, less than at the single scarp of the north caldera wall and much less than would account for a caldera volume proportional to the volume of the Mesa Falls Tuff. Thus, although the faults along the southern wall of the Big Bend Ridge caldera segment were rejuvenated during second-cycle collapse with individual displacements of a few meters or less, the main displacement was farther north. A circular positive gravity anomaly corresponds to the partly basalt-filled Henrys Fork caldera (Figure 4) and indicates that the main southern boundary of the caldera is now buried by younger rocks in the middle of the Island Park basin, defining a circular block nearly 20 kilometers across (Figures 2 and 3).

Because the Henrys Fork caldera was nested against the north side of the Big Bend Ridge caldera segment, ash flows of the Mesa Falls Tuff were virtually confined by the other preexisting caldera walls. On the southern outer flank of Big Bend Ridge, only airfall ash and pumice and a thin, slightly welded to nonwelded tuff of the Mesa Falls are present. By contrast, the high-standing northern wall of the second-cycle Henrys Fork caldera represents mainly second-cycle collapse and probably was adjacent to

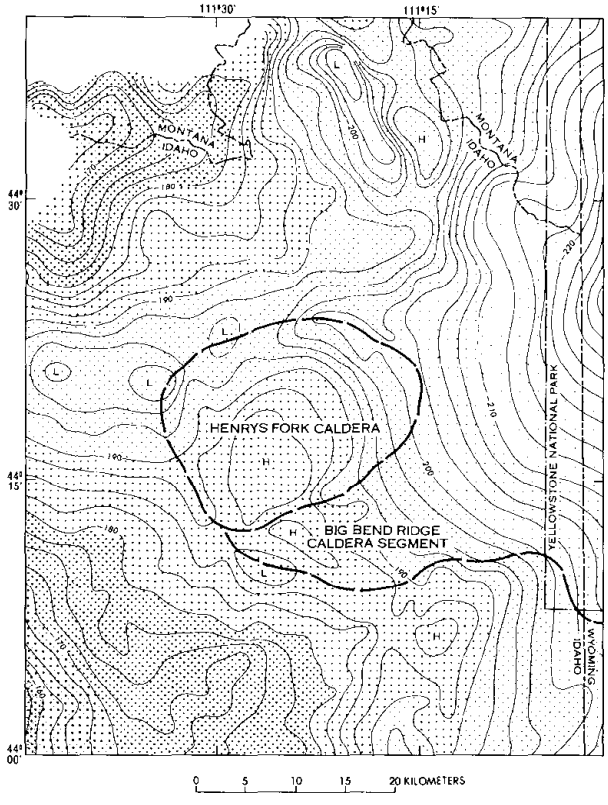

Figure 4. Complete Bouguer gravity map of the Island Park area. Contour interval 2.5 mGal, after Blank and Gettings (1974). Dashed lines, caldera boundaries. Closed contours: H, gravity high; L, gravity low.

the eruptive fissures; it has a thick, densely welded section of Mesa Falls ash-flow tuff.

POSTCOLLAPSE RHYOLITIC AND BASALTIC VOLCANISM

Six small rhyolite domes crop out within or adjacent to the Henrys Fork caldera; they are named formally together here as the Island Park Rhyolite. The exposed bodies that constitute the Island Park Rhyolite are the Moonshine Mountain, Silver Lake, Osborne Butte, Elk Butte, Lookout Butte, and Warm River Butte domes (Figure 2). Unfortunately, it is not possible to show unequivocal outcrop relations to the most important older and younger units at any of the six domes, because all are nearly buried by the younger Gerrit Basalt (Figure 2), named later in this paper. However, the relative ages can be established by other relations. Because the domes stand above the floor of the second-cycle Henrys Fork caldera, they must postdate the Mesa Falls Tuff and its penecontemporaneous caldera collapse. The Lava Creek Tuff that was later emplaced into the Henrys Fork caldera has normal paleomagnetic polarity, as do all younger units, but the domes of the Island Park Rhyolite all have reverse polarities. Thus, the Island Park Rhyolite must predate the Lava Creek Tuff. Because stratigraphic relations at no one place are diagnostic, the designation of a type area for the Island Park Rhyolite is somewhat artificial, but Lookout Butte is arbitrarily designated here as the type locality. The Mesa Falls and Lava Creek Tuffs are both present in the vicinity of Lookout Butte, and their topographic positions with respect to the butte are consistent with the correct stratigraphic relations, although exposures are too poor to show them clearly.

The Island Park Rhyolite is lithologically distinctive. It consists, in all six exposed bodies, of extremely phenocryst-rich rhyolite, the phenocrysts generally constituting more than half of the rock. The phenocrysts are very large, commonly one to several centimeters across. In this respect, their close petrographic relation to the Mesa Falls Tuff is apparent. The principal phenocrysts, as in most other rhyolites of the volcanic field, are quartz, sodic sanidine, sodic oligoclase, opaque oxides, ferroaugite, and fayalitic olivine.

The rhyolite bodies are typical, steep-sided, mainly endogenous domes with shell-like flow-structure patterns parallel to their sides and concentric around their vents. The domes occur in a linear belt about 30 kilometers long and less than 7 kilometers wide that trends northwestward across Island Park. Most of the domes are within the area of the Henrys Fork caldera, but Warm River Butte lies on the rim of the first-cycle Big Bend Ridge caldera segment. Hamilton (1965) mapped Warm River Butte with flows of his "Island Park caldera" rim. It is correlated here, however, with the Island Park Rhyolite, because it is lithologically similar to the other Island Park domes, has the same reverse paleomagnetic polarity, lies on the same linear trend, and does not appear to have been cut by faults during the second-cycle collapse as were other flows on the first-cycle rim. Other flows and domes of Island Park Rhyolite could lie buried within the Henrys Fork caldera, but the alignment of the exposed domes suggests a structural control. The vent zone is parallel to the structural domes in the two resurgent segments of the younger Yellowstone caldera, in Yellowstone National Park (see U. S. Geological Survey, 1972; Christiansen, 1979). Extrapolated southeastward, the vents of the Island Park Rhyolite trend toward Teton Valley, a similar-trending fault-bounded valley west of the Teton Range (Figure 3). Some of the active seismic zones in the Yellowstone Plateau region and its immediate surroundings also show this trend (Figure 5; see Pitt and others, 1979).

Known stratigraphic relations of the Island Park Rhyolite leave a rather large time span available for its eruption, but similar paleomagnetic directions of the Mesa Falls Tuff and the Island Park domes, as well as the petrographic similarity of the individual domes and their similarity to the Mesa Falls Tuff, suggest that they do not fill much of that time bracket. The only dated body, the Osborne Butte dome, is 1.3 million years old (J. D. Obradovich, written communication, 1982); all of the domes are probably only slightly younger than the Mesa Falls Tuff.

A number of basaltic lavas occur around and within part of the Island Park basin between the Mesa Falls and Lava Creek Tuffs. Southeast of Island Park, basalt flows of this stratigraphic position are mapped as the basalt of Warm River. One of these flows has been dated at 750,000 years (J. D. Obradovich, written communication, 1982), and the reverse paleomagnetic polarities of all the Warm River flows indicate that they are older than 730,000 years (Mankinen and Dalrymple, 1981). These flows commonly are 5-20 meters thick. Contacts with the underlying Mesa Falls Tuff and the overlying Lava Creek Tuff are exposed locally in the area between the settlement of Warm River and the south side of Moose Creek Butte. The basalt of Warm River is also present in Island Park near Sheep Falls. It is exposed more widely on both sides of Warm River in the 5-kilometer stretch above its mouth, but a thick mantle of upper Pleistocene loess covers much of the bedrock and all of the important contacts in natural exposures of that area. The eruptive vents of the basalt of Warm

River are unknown.

Other locally vented, post-Mesa Falls, pre-Lava Creek basalts are exposed north of Island Park, where they form the floor of Shotgun Valley and make rapids on Henrys Fork near Coffeepot Creek. Yet other basalts occupy this stratigraphic position southeast of the Island Park area, at Bitch Creek and near the Teton River.

The post-Mesa Falls basalts have sparse to moderately abundant phenocrysts of olivine and plagioclase; olivine and clinopyroxene are present together with plagioclase and opaque oxides in the fine-grained matrix. The rocks chemically are tholeiitic basalts, at least some of which have quite low contents of large-ion lithophile elements (see Doe and others, 1982).

THE THIRD VOLCANIC CYCLE

After the first two volcanic cycles had run their courses, the area of rhyolitic activity shifted entirely away from Island Park to the Yellowstone Plateau, and during the past one million years the rhyolitic magmas in chambers beneath Island Park have solidified. The Island Park area has subsided relative to the Yellowstone Plateau, probably by about 100-200 meters. In the past 200,000 years the solidified composite pluton beneath Island Park has been broken by tectonic fractures, and basalts have erupted through the fractured caldera floors.

Because the record of the third volcanic cycle is more complete than the records of the first two cycles, it provides a model for interpreting the older cycles. The third cycle began about 1.2 million years ago, shortly after the climax of the second cycle. For 600,000 years rhyolitic lavas erupted intermittently on the Yellowstone Plateau from a slowly forming set of arcuate fractures that eventually outlined the area that would later collapse as the third-cycle Yellowstone caldera. It is evident that a large magma chamber was forming at shallow crustal levels, doming and stretching its roof, and intermittently erupting lavas and sagging to form the arcuate fractures. One of the large precaldera flows forms Moose Creek Butte, the southeastern margin of the Island Park basin; the vent for the Moose Creek Butte flow is now buried beneath the Madison Plateau. By 630,000 years ago rhyolitic lavas had erupted through every major sector of the Yellowstone ring-fracture system. With the accumulation of a large shallow magma chamber and the generation of these ring fractures, conditions were set for the climactic eruption, which would vent through the ring fractures.

The climactic eruption of the third cycle emplaced more than 1,000 cubic kilometers of the Lava Creek Tuff; potassium-argon dating establishes its age as 630,000 years (J. D. Obradovich, written communication, 1982). Detailed stratigraphic studies show that the Lava Creek actually consists of two ash-flow sheets that erupted consecutively but so quickly that they welded and crystallized as a single cooling unit, much as was described earlier for the three members of the Huckleberry Ridge Tuff. Furthermore, the caldera that formed by collapse of the Lava Creek magma-chamber roof encompasses two adjacent and partly overlapping ring-fracture zones (see Figure 5). Thus, the ring-fracture system that formed during magmatic insurgence early in the third volcanic cycle, and through which the Lava Creek Tuff probably erupted, appears to reflect the formation of two intersecting annular zones, probably representing two broad culminations on the top of a single large underlying magma chamber.

During or immediately following the eruption of the Lava Creek Tuff, the roof of the magma chamber collapsed along the two ring fracture zones, forming the great Yellowstone caldera, which consists structurally of two segments bounded by the two previously formed ring-fracture zones (Christiansen, 1979). Post-collapse resurgence formed structural domes in each segment, and subsequent rhyolitic volcanism has largely filled the caldera.

On its western and southwestern margin, where the Yellowstone caldera intersected the older calderas of the volcanic field and where the rim was lowest, the intracaldera rhyolitic lavas spilled over the rim to the edge of the Island Park basin. The third-cycle intracaldera flows are exceptionally large and thick, the largest having maximum diameters of more than 30 kilometers and thicknesses of more than 300 meters. Although these very large flows have steep marginal scarps and lobate plans typical of rhyolitic lavas, they are so large that their gently convex profiles appear nearly flat, forming the Madison, Pitchstone, and Central Plateaus of Yellowstone National Park and vicinity. These lavas flowed from vents within the Yellowstone caldera, entirely outside the Island Park area. Hamilton (1965) regarded certain subsummits on the flows east of Island Park as marking vents, whose distributions he took to incidate a buried eastern ring-fracture boundary for an "Island Park caldera." However, surface flow structures show clearly that these flows all vented many kilometers farther east. The rhyolites that form these plateaus are between about 150,000 and 70,000 years old (J. D. Obradovich, written communication, 1982). Together with the precaldera third-cycle Moose Creek Butte flow, they form the eastern margin of Island Park.

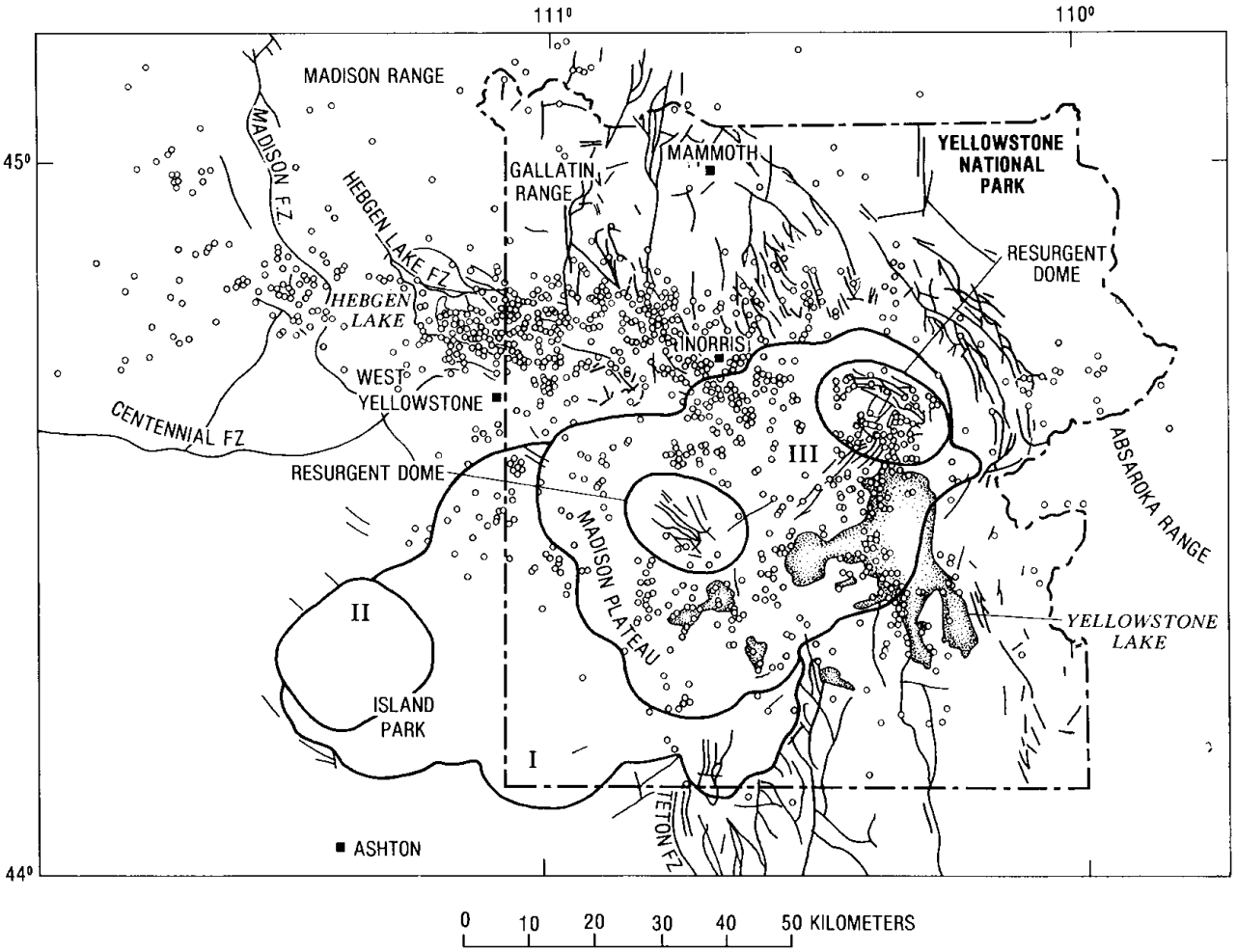

Figure 5. Earthquake-epicenter and fault map of the Yellowstone-Island Park region. Heavy lines labelled I, II, and III mark the first-, second-, and third-cycle calderas, respectively; heavy lines within Yellowstone caldera (III) outline two resurgent domes that delimit the inner edges of two ring-fracture zones. Named fault zones (FZ) as discussed in text. Epicenters (circles) shown for the period 1972 to 1978, after Pitt (1979) and Smith and Christiansen (1980).

The absence of basalt on the floor of the Yellowstone caldera, in contrast to its abundance in Island Park and older similar rhyolitic areas of the Snake River Plain farther west, suggests that an incompletely solidified magma body beneath the Yellowstone Plateau still prevents throughgoing fractures from penetrating the crust beneath the plateau to form conduits for basaltic magmas. Post-Lava Creek basalts are, however, common around the margins of the third-cycle Yellowstone caldera. Several of these have been defined, and some are discussed below. All of them are essentially similar in lithology, mineralogy, and chemistry; they are olivine tholeiites, and most have phenocrysts of labradorite and olivine. All have olivine and Ca-poor clinopyroxene as well as plagioclase and iron-titanium oxides in their groundmasses.

The Falls River Basalt, one of the basaltic units from vents marginal to the Yellowstone caldera, is generally conformable on the Lava Creek Tuff in the southwestern part of the Yellowstone Plateau and the northeast margin of the Snake River Plain, forming an apron that extends across the rhyolites south of Island Park.

With crystallization of the rhyolitic magma in the chambers beneath Island Park during the last million years, regional tectonic stresses have broken the solidified pluton to allow the intrusion of basaltic magmas and their eruption through vents on its floor, largely flooding the Island Park basin. The post-Lava Creek basalts on the floor of Island Park have not previously been given a formal designation. They were mapped by Hamilton (1965) as part of a sequence of interlayered rhyolite and basalt that he

thought was related to an "Island Park caldera." It is now evident, however, that most of the basalts and rhyolites from vents in the Island Park area are not interlayered; the exposed locally vented basalts are younger than all of the rhyolites. The widespread post-Lava Creek basalts that form the floor of Island Park are here formally designated together as the Gerrit Basalt, named after a railroad siding 5 kilometers east of Upper Mesa Falls (Figure 2). The type area for the Gerrit Basalt is here designated as the canyon of Henrys Fork of the Snake River, upstream for about 5 kilometers from Upper Mesa Falls. The basalt of the type area overlies an erosional surface cut on the Lava Creek and Mesa Falls Tuffs, both concordantly and discordantly. This basalt forms the canyon rim on the north and east sides of the river and also overlies a lower-level terrace cut on the Mesa Falls Tuff. The basalt in the type area is overlain only by upper Pleistocene loess and local fine-grained sand and silt deposited in small lakes and drainage courses. In only one place does a dated volcanic unit probably overlie the Gerrit Basalt; the Gerrit and the 150,000-year-old Buffalo Lake flow, a third-cycle postcaldera rhyolite that overflowed the Yellowstone caldera, are adjacent about 4½ kilometers east of Ripley Butte in the northern part of Island Park (Figure 2). A small vent for the basalt at that locality fed flows that extended short distances in all directions but appear not to have ponded at the rhyolite flow front. Furthermore, there are no inclusions of rhyolite in the basalt near the brecciated rhyolitic flow front, although it would have been easy for the basalt to pick up fragments if the rhyolite had been present there. The basalt, therefore, probably is older. The relation seems to be confirmed by a generally thicker and more continuous mantle of loess on the Gerrit Basalt than on flows of the Plateau Rhyolite adjacent to it. One of the youngest flows of the Gerrit Basalt yields a potassium-argon age of 200,000 years (J. D. Obradovich, written communication, 1982).

The Gerrit Basalt erupted from several separate small volcanoes in Island Park. Since the eruptions of the Gerrit Basalt, there have also been a few eruptions of basaltic cinder cones and flows from a linear vent zone that crosses the western wall of the Island Park basin (Figure 2). This zone is related structurally and chemically to basalts of the Snake River Group that underlie a large region to the west, called the Spencer-High Point rift zone by Kuntz (1977). Associated with this vent zone across the west rim of Island Park, in addition to typical Snake River basalts, are small amounts of alkalic ferrobasalt to ferrolatite (Hamilton, 1965), similar to certain highly evolved lavas associated with the Snake River Group farther southwest along the plain (Powers, 1960; Leeman and others, 1976; Leeman, 1982 this volume).

A MODEL FOR ISLAND PARK

IS THERE AN "ISLAND PARK CALDERA"?

The topographic basin of Island Park (Figure 2) is the product of events during each of the three cycles of the Yellowstone Plateau volcanic field. The first cycle climaxed about 2.0 million years ago, forming the largest of three calderas, at least 90 kilometers long and 30 kilometers across, and extending from the west side of Island Park to the Central Plateau of Yellowstone National Park. Big Bend Ridge, the western and southwestern rim of Island Park, dates from the first-cycle collapse. The second volcanic cycle climaxed about 1.3 million years ago to produce a somewhat smaller caldera, about 20 kilometers across, nested against the northwestern wall of the older one. Much of the rest of the older caldera was filled by erupted products of the second- and third-cycle volcanism. The eastern margin is formed by the flow-front scarps of younger rhyolitic lava flows of the third volcanic cycle that erupted from vents farther east. Thus, there is no "Island Park caldera" in the sense suggested by Hamilton (1965) but rather a complex basin formed by two separate caldera collapses with 700,000 years between them and by even younger, unrelated constructional volcanism (Figure 3). Island Park formed during three separate volcanic cycles over a span of about 2 million years; the term "Island Park caldera" is inappropriate for a feature of such complex and extended origin.

I have described separately the features of each of the three cycles in the Island Park area and have named them here separately where it seems appropriate. As defined by Williams (1941, p. 242), a caldera is a large craterlike topographic feature of volcanic origin; large calderas generally form by collapse of a magma-chamber roof. In that sense, one can identify in the Island Park area a first-cycle Big Bend Ridge caldera segment and a second-cycle Henrys Fork caldera; the topographic rim along the entire eastern sector of the Island Park basin is unrelated to any caldera faulting.

RELATIONS AMONG THE VOLCANIC CYCLES AT ISLAND PARK

It is worthwhile to consider relations among the three cycles of the Yellowstone Plateau volcanic field from the perspective of the history just presented. The volume of magma represented in the three ash-flow sheets of the Yellowstone Group is about 4,000 cubic kilometers, an enormous volume of erupted magma

accounting for two-thirds of the estimated magmatic volume of the entire volcanic field. These great volumes of material, erupted in three complex episodes of brief duration, played the key roles in the volcanic history of the field. The intrusive bodies that sustained the eruptive activity of each volcanic cycle, however, must have been many times larger (Smith and Shaw, 1975; Christiansen, 1979). Although all three cycles occurred within the same general region and overlapped to a considerable degree, each cycle was centered about a separate major area of eruptive activity. Part of the focus of the first cycle was in the Island Park area, and the second cycle was confined to Island Park.

Each cycle lasted about a million years. Each represents a complete sequence of volcanic events, following at least approximately the stages of the resurgent caldera cycle of Smith and Bailey (1968), except that resurgent doming itself cannot be documented in the Island Park area. It seems necessary to regard each of the volcanic cycles as related to (1) the emplacement of a large body of rhyolitic magma beneath the region of its major volcanic focus, (2) the rise of plutonic bodies to high crustal levels, (3) major degassing of these high-level magma bodies by surface volcanism, principally by the major pyroclastic eruptions but also continuingly for a considerable time by numerous smaller eruptions, and (4) eventual consolidation and cooling of the magma at depth. The time scale for this entire process during each cycle varied with the size and depth of the major intrusive bodies but seems to have been about a million years. Basaltic activity was intermittent around the flanks of each major focus of rhyolitic activity and is an important part of the volcanic field as a whole but was essentially independent of the individual rhyolitic cycles.

A possible exception to this picture of complete and virtually independent cycles of rhyolitic volcanism was the second cycle. Since it occurred entirely within the volcanic focus of the first cycle and appears to have been smaller and simpler than the others, the second cycle may in some respects represent a less truly independent magmatic cycle. There was, however, an elapsed time of about 700,000 years between the major ash flows of the first and second cycles, slightly longer than that between the second and third. The second-cycle volcanic focus did not merely reoccupy the older caldera but was nested within it and overprinted part of it. Also, the second cycle, though simpler, seems to have gone through at least most of the essential stages of activity represented by the other cycles. Thus, although the second cycle probably records the rise of a localized large magma body nearly to the surface, producing major eruptions, caldera collapse, and postcollapse intracaldera volcanism, it may represent renewed rise of a residual portion of the first-cycle magma body after most of it had crystallized (Christiansen, 1979). The absence of basalt in Island Park between the first two cycles, but its presence in the southern part of the basin between the last two cycles, is also consistent with this suggestion.

Hamilton (1963, 1965) based his concepts of the origins of the Yellowstone and Island Park regions on the idea that basalt and rhyolite were erupted simultaneously throughout the lifetimes of the volcanic systems, both magma types always being available for eruption from the regions of the principal volcanic foci. Further work confirms Hamilton's important observation that both rhyolite and basalt were erupted intermittently throughout the history of the volcanic field, although their roles in the magmatic evolution appear to have been somewhat different from those he envisioned. Some basalt probably was erupted before any of the rhyolite, but throughout each cycle, basalt erupted only around the margins of the rhyolitic focus. Hamilton (1965) based his inference that basalt and rhyolite are interlayered in the main Island Park basin upon relations on the east side of the canyon of the Henrys Fork at Upper Mesa Falls. The section there consists, however, of two directly superposed ash-flow sheets, the Mesa Falls and Lava Creek Tuffs, and the entirely younger Gerrit Basalt. The basalt occurs both concordantly on the Lava Creek at the rim of the canyon and unconformably on an erosional terrace that was carved through an erosionally nonresistant vapor-phase zone onto the more resistant densely welded zone of the Mesa Falls Tuff, about halfway down the present canyon wall. The basalt of Warm River does occur between the Mesa Falls and Lava Creek Tuffs within the first-cycle Big Bend Ridge caldera segment, but the location of its vent is unknown and the basalt is much younger than the first-cycle rhyolites related to that caldera segment.

TECTONIC AND GEOPHYSICAL CHARACTERISTICS

During the last 15-18 million years, much of western North America has undergone extensional tectonism and volcanism that is either predominantly basaltic, alkalic, or bimodally rhyolitic and basaltic (Christiansen and Lipman, 1972; Snyder and others, 1976; Christiansen and McKee, 1978). Regional tectonic extension has been accompanied by broad-scale uplift of the Great Basin region by about 1.5 kilometers. The Yellowstone Plateau volcanic field lies near the northeastern margin of this region of fundamentally basaltic volcanism, major tectonic

extension, and regional uplift. Normal-fault systems, including the Teton, Centennial, and several others in the Yellowstone Plateau region, have each had 2-4 kilometers of vertical displacement over a period of more than 10 million years.

Several studies have emphasized that, throughout the period of regional late Cenozoic tectonic extension, a series of bimodal magmatic systems characterized by voluminous caldera-forming rhyolitic ash-flow eruptions has propagated northeastward along the axis of the eastern Snake River Plain (Christiansen and Blank, 1969; Christiansen and Lipman, 1972; Armstrong and others, 1975; Christiansen and McKee, 1978). At any given time during the last 10-15 million years, there has been an active magmatic system that probably was topographically high and a focus of thermal and seismic activity and voluminous rhyolitic volcanism. The active locus of such systems has propagated northeastward at 2-4 centimeters per year along the 60-degree azimuth of the eastern Snake River Plain (Armstrong and others, 1975), and episodic basaltic volcanism continues in its wake. The region of former loci of rhyolitic volcanism has progressively subsided and been flooded by basalts to form the eastern Snake River Plain. The motion of the North American plate relative to the deep mantle, calculated by Smith and Sbar (1974) from the relative motions of the Pacific and North American plates and the motion of the Pacific plate relative to a presumed stationary Hawaiian melting anomaly, is 4.5 centimeters per year at an azimuth of 247 degrees. It thus appears that the Yellowstone system, like the Hawaiian system, is stationary relative to the deep mantle and that it propagates relative to the North American plate at the rate of and in the direction opposite to plate motion. This propagating system has been interpreted as a hot spot above a mantle convection plume (Morgan, 1971, 1972; Matthews and Anderson, 1973) or a geochemical anomaly (Hadley and others, 1976; Prostka and others, 1976), as a melting zone at the tip of a propagating fracture (Smith and others, 1974), and as a zone of localized shear melting at the base of the lithosphere (Christiansen and McKee, 1978). These three classes of hypotheses are not considered further here but they point out that the nature and origin of the Island Park-Yellowstone system must be considered in the light of regional tectonic and geophysical information.

As noted earlier, the Yellowstone Plateau volcanic field lies at an important tectonic intersection where the axis of the eastern Snake River Plain meets north-trending structural elements of the middle Rockies and eastern Great Basin region, which border it on the south, and northwest- and west-trending structural elements at the edge of the northern Rocky Mountains, which border the field on the north. Historical seismicity also defines these trends and intersections (Figure 5). Seismic activity occurs mainly in two belts, one trending north parallel to the eastern margin of the Basin and Range province through the Yellowstone Plateau and northwestward into Montana, and the other trending westward north of the Snake River Plain (Smith and Sbar, 1974). The Hebgen Lake earthquake of August 17, 1959, the largest historic earthquake in the region, was centered at the junction of the west- and northwest-trending zones just west of Yellowstone National Park (Ryall, 1962; Myers and Hamilton, 1964; Trimble and Smith, 1975). In some respects, the northern Rocky Mountains in late Cenozoic time have been allied geophysically and neotectonically more with the Basin and Range province than with the middle Rocky Mountains, into which they merge physiographically (Gilluly, 1963; Hamilton and Myers, 1966; Blackwell, 1969). The eastern Snake River Plain and Yellowstone Plateau volcanic field represent a transitional northern boundary of the tectonic extension of the Great Basin region; regional tectonic extension is dominant to the south but dies out gradually northward from this transitional zone (Christiansen and McKee, 1978; Eaton and others, 1978). The location of the volcanic field at such a major regional tectonic intersection and transition suggests a focus of lithospheric stresses that localize the formation and evolution of this major magmatic system.

The distribution and characteristics of seismic-swarm activity in the Yellowstone Plateau are related, at least in part, to its prominent high-temperature hydrothermal systems, which probably lie above an active magmatic heat source (Eaton and others, 1975; Smith and others, 1977; Pitt, 1979; Smith and Christiansen, 1980; Lehman and others, 1982). By comparison, the lack of conspicuous swarm seismicity in the Island Park area (Figure 5) suggests that no major hydrothermal convection system is circulating actively above a shallow heat source there.

Studies by Iyer and others (1981) define an area of anomalous teleseismic P-wave arrivals at Yellowstone, having delays of as much as 1.8 seconds relative to a standard station northeast of the Yellowstone caldera; these compare with delays of about ± 0.5 second measured in the surrounding region. Models of structures beneath the Yellowstone caldera indicate about a 15 percent reduction in P-wave velocities in the crust and a 5 percent reduction in the upper mantle to a depth of 250 kilometers. The zone of anomalous teleseismic arrivals extends through Island Park and down the eastern Snake River Plain (Evans, 1982), in contrast to its sharp cutoff in other directions. The P-wave delays at Island Park are not as large as those of the Yellowstone caldera but generally exceed those of the eastern Snake River

Plain. These results clearly show that a zone of anomalous crust and upper mantle, transitional from the active parts of the Yellowstone Plateau volcanic field, extends into the region beneath Island Park.

Seismic-refraction profiling of the crust and upper mantle of the Yellowstone Plateau region and eastern Snake River Plain reported by Smith and others (1982) similarly shows a transition in upper-crustal velocities in the Island Park area between those characteristic of the Yellowstone caldera and those of the eastern Snake River Plain. In particular, beneath a surficial volcanic and sedimentary layer, a laterally inhomogeneous upper-crustal layer about 5 kilometers thick beneath Island Park has P-wave velocities of about 5.7 kilometers per second. This layer is laterally equivalent to a layer 8-9 kilometers thick beneath Yellowstone that has velocities of 4.0-5.5 kilometers per second and a higher degree of seismic-wave attenuation. These layers in the Yellowstone Plateau volcanic field take the place of a relatively homogeneous regional upper-crustal layer about 15-20 kilometers thick that has a velocity of about 6.1 kilometers per second.

Gravity data for Island Park (Blank and Gettings, 1974), like the teleseismic data, indicate that a crustal anomaly that is quite pronounced beneath the Yellowstone caldera extends transitionally beneath Island Park. The gravity map for Island Park (Figure 4) defines a broad-wavelength negative anomaly. The principal gradient that bounds this gravity low lies beyond the caldera rims and thus cannot be due solely to a fill of low-density sediments and rhyolites in the overlapping calderas of the first and second cycles. Furthermore, the area of the second-cycle Henrys Fork caldera is marked by a positive gravity anomaly having relatively sharper gradients, within the larger negative anomaly. This relationship suggests, at least in part, that the basaltic fill in the Island Park basin is thickest within the Henrys Fork caldera. Thus, the larger negative anomaly probably is related to a subsurface intrusive mass of now solidified rhyolitic magma; the mass anomaly, however, is not as large as that beneath the Yellowstone caldera, which may outline a still partly molten magma body (Eaton and others, 1975; Smith and Christiansen, 1980; Smith and Braile, 1982).

A reconnaissance aeromagnetic survey (Zietz and others, 1978) shows a generally low magnetic-field intensity over Island Park, compared with that over the Snake River Plain but, again, not as low as that of the Yellowstone caldera area. A reasonable hypothesis for these observed large-scale magnetic features is that the average crustal temperature gradient at Island Park is intermediate between the high thermal gradients associated with the Yellowstone caldera (Morgan and others, 1977) and the lower, but still above average, eastern Snake River Plain gradients (Brott and Blackwell, 1979; Brott and others, 1981). Bhattacharyya and Leu (1975) interpreted the depth to the Curie temperature beneath the Yellowstone caldera to be about 6-10 kilometers; Curie depths in most other areas of the western United States are from 15 to 30 kilometers. Although no similar detailed analysis has been completed for Island Park, an intermediate depth of about 15 kilometers to the Curie isotherm might be reasonable and could fit the other geophysical data.

Audio-magnetotelluric and telluric surveys of the Island Park area (Hoover and Long, 1976) indicate high electrical resistivities (100-1,000 ohm-meters) within about 2 kilometers of the surface, with a band of the lowest resistivities along the western margin of the basin. The data suggest that the thickness of high-resistivity material is somewhat less under the Henrys Fork caldera than under the older Big Bend Ridge caldera segment. A magnetotelluric survey (Stanley and others, 1977) indicates that high resistivities (greater than 500 ohm-meters) persist to a depth of about 8 kilometers. Yellowstone, in contrast, has low resistivities—generally less than 50 ohm-meters above 5 kilometers depth and less than 5 ohm-meters below 5 kilometers. Although the significance of these resistivity interpretations is quite uncertain, the relatively higher resistivities at Island Park might indicate a lack of hydrothermal alteration at depth in the Island Park area or an impermeable deep zone in which electrically conductive thermal waters do not freely circulate.

Geophysical data, as well as topography and the history of volcanic evolution, thus imply an anomalous crustal and upper-mantle structure beneath the Yellowstone Plateau volcanic field. The geophysical properties of the crust beneath the older part of the volcanic field at Island Park are transitional between those of the Yellowstone Plateau and those of the eastern Snake River Plain. Low seismic velocities and high attenuations, low densities, high regional electrical conductivity, and a shallow depth to the Curie temperature all favor an upper-crustal body at high temperature beneath the Yellowstone caldera. Thermal bouyancy of a hot, plastically deformable, shallow subsurface mass sustains broad uplift of the Yellowstone region. The greater age of rhyolitic volcanism at Island Park than at Yellowstone and the eruption of basalts through the Island Park plutons indicate a considerably lower subsurface temperature in the crust beneath Island Park than beneath Yellowstone. Island Park appears to be a transitional, cooling and subsiding remnant of the Yellowstone Plateau magmatic system that must still be hotter at depth than its regional surroundings but that no longer contains rhyolitic magma and may not sustain

a high-temperature shallow hydrothermal system.

GEOTHERMAL RESOURCE POTENTIAL

The foregoing conclusions imply that Island Park is unlikely to hold a buried high-temperature geothermal system comparable with that of Yellowstone. Nevertheless the still-cooling crust beneath the area is likely to constitute a significant geothermal anomaly. As yet, no specific known geologic, geochemical, or geophysical evidence points to an exploitable geothermal resource beneath Island Park, but there has, nevertheless, been continuing commercial and research interest in the possibility of such a resource. Two basic factors account for that interest, the voluminous rhyolitic volcanism younger than about 2 million years and the proximity of the area to the well-known hydrothermal activity of Yellowstone National Park.

The most recent estimate of thermal energy in the Island Park igneous system, including its related plutonic component, is 16,850 x 10^{18} joules, using a model based upon consideration of the volumes and ages of the volcanic rocks (Smith and Shaw, 1979). According to this estimate, Island Park would have the second highest energy content of any igneous system in the United States, ranking only below Yellowstone itself and having over twice the energy estimated for the third-largest such system, the Valles caldera of New Mexico. It is important to note, however, that these are estimates of all thermal energy remaining in each of these igneous systems above an assumed ambient temperature of the earth at the depths of the magma chambers or plutons; they are not estimates of geothermal resources that might be recoverable in any specified manner. Brook and others (1979), comparing Island Park with other large volcanic systems, noted that if 1 percent of its thermal energy were in an undiscovered hydrothermal system, it would account for a very large estimated "undiscovered resource base" of 170 x 10^{18} joules.

Without data from deep drilling at Island Park, a high degree of uncertainty will remain about its geothermal potential. Beyond the geologic and geophysical evidence for a crustal thermal anomaly beneath the area, additional inferences can be based upon available hydrologic and chemical data for surface waters and shallow wells (Whitehead, 1978). Average precipitation is moderate at Island Park, but exceptionally high snowfall occurs on the Madison and Pitchstone Plateaus just to the east. The water table beneath Island Park is shallow, and much of its recharge is from infiltration on the plateaus to the east. The shallow hydrologic regimen of the drainage basin of Henrys Fork of the Snake River is dominated by a large flow of cold ground water. As in the massive Snake River Plain aquifer system (Brott and others, 1981), downward and lateral movement of the ground water maintains nearly constant temperatures in the shallow aquifer and could mask the surface thermal expression of any geothermal systems that may lie below it. Several minor thermal springs have been identified near Island Park, but the water in only one of them is warmer than 25° C (Ashton Hot Spring to the southwest, at 41° C); this is also the only spring for which geochemically indicated subsurface reservoir temperatures are greater than 90° C. Any chemical contributions of deep thermal waters to other springs are nearly overwhelmed by mixing with the voluminous shallow cold water.

Thus, if the possibility exists for a significant geothermal resource at some depth beneath Island Park, it is not likely to be a high-temperature system like Yellowstone's geyser basins. None of the available information indicates the definite presence of an exploitable geothermal energy resource. Although there may be other geophysical data that are not now publically available, the geothermal possibilities at Island Park will remain uncertain unless deep drilling is done.

The same data that suggest geothermal possibilities for Island Park must be examined as well for their bearing on possible adverse effects that eventual production of geothermal energy there could have on hydrothermal features of Yellowstone National Park. None of the available data specifically indicate a significant deep hydrologic connection between the two areas. Analysis of hydrogen-isotopic data for Yellowstone thermal waters (R. O. Rye and A. H. Truesdell, U. S. Geological Survey, oral communication, 1982) indicates that deep recharge to the Yellowstone hydrothermal system is from the northern part of the national park. No evidence is known to indicate a connection between the hydrologic basin of Henrys Fork and the hydrothermal basins that define the principal discharge of the Yellowstone system. Thus, detectable effects on most of Yellowstone's geothermal features are unlikely.

On the other hand, the histories of several areas document that natural hydrothermal discharge has been disturbed by nearby geothermal production, even where subsurface connections had not been previously recognized. The distances over which such effects have been noted are generally only a few kilometers or less, the greatest known distance being 1-4 kilometers between Wairakei and Tauhara in New Zealand (D. E. White, U. S. Geological Survey, written communication, 1979). No thermal areas of Yellowstone National Park would be closer than about 15 kilometers from the Henrys Fork caldera at

Island Park—probably the main target of commercial geothermal interest.

Because geothermal exploitation can utilize only the heat that could be transported by fluids, it would be possible to disturb Yellowstone's hydrothermal systems only by diverting fluids from Yellowstone to Island Park. Those fluids could move between the two areas through permeable zones only in response to gradients from higher to lower pressures. Thus, for such effects to occur, two conditions are necessary: (1) permeable interconnections must exist between the two areas and (2) exploitation must lower reservoir pressures at Island Park, thereby increasing the pressure gradient between the two areas and diverting deep water that otherwise would sustain hydrothermal features in Yellowstone National Park.

Of particular importance in this instance is the structural link that is formed between Yellowstone and Island Park by their overlapping calderas, especially the large caldera of the first volcanic cycle. Permeable sedimentary and volcanic fill in that caldera has been disrupted by faulting and is likely to have been annealed by hydrothermal alteration during volcanic activity of the second and third cycles. The importance of hydrothermal self-sealing in maintaining the pressure of locally discharing parts of the Yellowstone hydrothermal system was shown by research drilling at Yellowstone (White and others, 1975; Keith and others, 1978). Such self-sealing around separately upflowing or discharging parts of a hydrothermal system tends to maintain the pressure-independence of those parts. Thus, any present hydrologic connections between the deeper parts of the Island Park and Yellowstone systems would likely be through intersecting deep fractures, possibly old joints or faults related to the bridging calderas, that could be reopened episodically by seismic activity or by other deformations of the regionally stressed crust. However, seismicity at Island Park, or between it and the Madison Plateau, is notably weak (Figure 5).

In summary, Island Park probably represents a deep crustal geothermal anomaly. The existence of a geothermal energy resource related to that anomaly is possible but has not been demonstrated and cannot be determined without deep drilling. The likelihood that detectable effects on any of the hydrothermal features of Yellowstone National Park would occur as a result of geothermal production in Island Park is probably small but, nevertheless, must be considered carefully. Detailed pressure monitoring and the maintenance of reservoir pressure by the reinjection of any geothermal fluids produced at Island Park would be necessary precautions. Supplemental reinjection between any eventual geothermal production area and the hydrothermal features of Yellowstone National Park, equaling or even exceeding total withdrawals, might be required to assure that any pressure gradient toward Island Park would remain substantially unchanged.

ACKNOWLEDGMENTS

I am greatly indebted to many colleagues for their contributions to this study. My work at Island Park is only part of a comprehensive study of late Cenozoic volcanism of the Yellowstone Plateau volcanic field, in which I have been engaged since 1965. Much of the field work was done in collaboration with H. R. Blank, Jr., between 1965 and 1970. Petrologic and geochemical work, along with additional field studies, are still underway in collaboration with Wes Hildreth. Warren Hamilton generously shared his knowledge of the area at an early stage of the study and has remained helpful in many ways since. The manuscript benefited greatly from reviews by Patrick Muffler, Wes Hildreth, Mel Kuntz, and Bill Bonnichsen. Considerations of the geothermal potential of Island Park are dependent on the extensive research on the hydrothermal systems of Yellowstone National Park by Donald E. White, Robert O. Fournier, Alfred E. Truesdell, and L. J. Patrick Muffler, and were greatly aided by their comments on this paper.

REFERENCES

Armstrong, R. L., W. P. Leeman, and H. E. Malde, 1975, K-Ar dating, Quaternary and Neogene volcanic rocks of the Snake River Plain, Idaho: American Journal of Science, v. 275, p. 225-251.

Berggren, W. A., 1972, A Cenozoic time-scale—some implications for regional geology and paleobiogeography: Lethaia, v. 5, p. 195-215.

Bhattacharyya, B. K. and L. -K. Leu, 1975, Analysis of magnetic anomalies over Yellowstone National Park: mapping of Curie point isothermal surface for geothermal reconnaissance: Journal of Geophysical Research, v. 80, p. 4461-4465.

Blackwell, D. D., 1969, Heat-flow determinations in the northwestern United States: Journal of Geophysical Research, v. 74, p. 992-1007.

Blank, H. R., Jr., and M. E. Gettings, 1974, Complete Bouguer gravity map, Yellowstone-Island Park region, Idaho, Montana, Wyoming: U. S. Geological Survey Open-File Map 74-22, scale 1:125,000.

Brook, C. A., R. H. Mariner, D. R. Mabey, J. R. Swanson, Marianne Guffanti, and L. J. P. Muffler, 1979, Hydrothermal convection systems with reservoir temperatures ≥90°C, *in* L. J. P. Muffler, editor, Assessment of Geothermal Resources of the United States—1978: U. S. Geological Survey Circular 790, p. 18-85.

Brott, C. A. and D. D. Blackwell, 1979, Terrestrial heat-flow measurements in an underground river located in the eastern Snake River Plain, Idaho: Geothermal Resources Council Transactions, v. 3, p. 69-72.

Brott, C. A., D. D. Blackwell, and J. P. Ziagos, 1981, Thermal and tectonic implications of heat flow in the eastern Snake River Plain: Journal of Geophysical Research, v. 86, p. 11709-11734.

Carr, W. J. and D. E. Trimble, 1963, Geology of the American Falls quadrangle, Idaho: U. S. Geological Survey Bulletin 1121-G, 44 p.

Christiansen, R. L., 1974, Quaternary volcanism of the Yellowstone rhyolite plateau region, Wyoming-Idaho-Montana (abstract): American Geophysical Union Transactions (EOS), v. 56, p. 1189.

———, 1975, Origin and geothermal potential of Island Park, eastern Idaho: Geological Society of America, Abstracts with Programs, v. 7, p. 595-596.

———, 1979, Cooling units and composite sheets in relation to caldera structure, *in* C. E. Chapin and W. E. Elston, editors, Ash-Flow Tuffs: Geological Society of America Special Paper 180, p. 29-42.

Christiansen, R. L. and H. R. Blank, Jr., 1969, Volcanic evolution of the Yellowstone rhyolite plateau and eastern Snake River Plain, U.S.A., *in* Symposium on Volcanoes and Their Roots, Oxford, England, Volume of Abstracts: International Association of Volcanology and Chemistry of the Earth's Interior, p. 220-221.

———, 1972, Volcanic stratigraphy of the Quaternary rhyolite plateau in Yellowstone National Park: U. S. Geological Survey Professional Paper 729-B, 18 p.

Christiansen, R. L. and P. W. Lipman, 1972, Cenozoic volcanism and plate-tectonic evolution of the western United States: Part 2, late Cenozoic: Royal Society of London Philosophical Transactions, Series A, v. 271, p. 249-284.

Christiansen, R. L. and J. D. Love, 1978, The Pliocene Conant Creek Tuff in the northern part of the Teton Range and Jackson Hole, Wyoming: U. S. Geological Survey Bulletin 1435-C, 9 p.

Christiansen, R. L. and E. H. McKee, 1978, Late Cenozoic volcanic and tectonic evolution of the Great Basin and Columbia Intermontane regions, *in* R. B. Smith and G. P. Eaton, editors, Cenozoic Tectonics and Regional Geophysics of the Western Cordillera: Geological Society of America Memoir 152, p. 283-311.

Doe, B. R., W. P. Leeman, R. L. Christiansen, and C. E. Hedge, 1982, Lead and strontium isotopes and related trace elements as genetic tracers in the upper Cenozoic rhyolite-basalt association of the Yellowstone Plateau volcanic field: Journal of Geophysical Research, v. 87, p. 4785-4806.

Doherty, D. J., L. A. McBroome, and M. A. Kuntz, 1979, Preliminary geological interpretation and lithologic log of the exploratory geothermal test well (INEL-1), Idaho National Engineering Laboratory, eastern Snake River Plain, Idaho: U. S. Geological Survey Open-File Report 79-1248, 7 p.

Eaton, G. P., R. L. Christiansen, H. M. Iyer, D. R. Mabey, H. R. Blank, Jr., Isidore Zietz, and M. E. Gettings, 1975, Magma beneath Yellowstone National Park: Science, v. 188, p. 787-796.

Eaton, G. P., R. R. Wahl, H. J. Prostka, D. R. Mabey, and M. D. Kleinkopf, 1978, Regional gravity and tectonic patterns: their relations to late Cenozoic epeirogeny and lateral spreading in the western Cordillera, *in* R. B. Smith and G. P. Eaton, editors, Cenozoic Tectonics and Regional Geophysics of the Western Cordillera: Geological Society of America Memoir 152, p. 51-91.

Embree, G. F., L. A. McBroome, and D. J. Doherty, 1982, Preliminary stratigraphic framework of the Pliocene and Miocene rhyolites, eastern Snake River Plain, Idaho, *in* Bill Bonnichsen and R. M. Breckenridge, editors, Cenozoic Geology of Idaho: Idaho Bureau of Mines and Geology Bulletin 26.

Gilluly, James, 1963, The tectonic evolution of the western United States: Geological Society of London Quarterly Journal, v. 119, p. 133-174.

Hadley, D. M., G. S. Stewart, and J. E. Abel, 1976, Yellowstone: seismic evidence for a chemical mantle plume: Science, v. 193, p. 1237-1239.

Hamilton, Warren, 1963, Petrology of rhyolite and basalt, northwestern Yellowstone Plateau: Article 80 *in* U. S. Geological Survey Professional Paper 475-C, p. C78-C81.

———, 1965, Geology and petrogenesis of the Island Park caldera of rhyolite and basalt, eastern Idaho: U. S. Geological Survey Professional Paper 504-C, 37 p.

Hamilton, Warren and W. B. Myers, 1966, Cenozoic tectonics of the western United States: Reviews of Geophysics, v. 4, p. 509-550.

Hildreth, Wes, 1981, Gradients in silicic magma chambers: implications for lithospheric magmatism: Journal of Geophysical Research, v. 86, p. 10153-10192.

Hoover, D. B. and C. L. Long, 1976, Audio-magnetotelluric methods in reconnaissance geothermal exploration: Second United Nations Symposium on the Development and Use of Geothermal Resources, Proceedings, v. 2, p. 1059-1064.

Iyer, H. M., J. R. Evans, George Zandt, R. M. Stewart, J. M. Coakley, and J. N. Roloff, 1981, A deep low-velocity body under the Yellowstone caldera, Wyoming: delineation using teleseismic P-wave residuals and tectonic interpretation: Geological Society of America Bulletin, Pt. II, v. 92, p. 1471-1646.

Keith, T. E. C., D. E. White, and M. E. Beeson, 1978, Hydrothermal alteration and self-sealing in Y-7 and Y-8 drill holes in northern part of Upper Geyser Basin, Yellowstone National Park: U. S. Geological Survey Professional Paper 1054-A, 26 p.

Kirkham, V. R. D., 1931, Snake River downwarp: Journal of Geology, v. 39, p. 456-483.

Kuntz, M. A., 1977, Rift zones of the Snake River Plain, Idaho, as extensions of basin-range and older structures: Geological Society of America, Abstracts with Programs, v. 9, p. 1061-1062.

Leeman, W. P., 1982, Evolved and hybrid lavas from the Snake River Plain, Idaho, *in* Bill Bonnichsen and R. M. Breckenridge, editors, Cenozoic Geology of Idaho: Idaho Bureau of Mines and Geology Bulletin 26.

Leeman, W. P., C. J. Vitaliano, and Martin Prinz, 1976, Evolved lavas from the Snake River Plain: Craters of the Moon National Monument, Idaho: Contributions to Mineralogy and Petrology, v. 56, p. 35-60.

Lehman, J. A., R. B. Smith, M. M. Schilly, and L. W. Braile, 1982, Upper crustal structure of the Yellowstone caldera from seismic delay time analyses and gravity correlations: Journal of Geophysical Research, v. 87, p. 2713-2730.

Mankinen, E. A. and G. B. Dalrymple, 1981, Revised geomagnetic polarity time scale for the interval 0-5 m.y.B.P.: Journal of Geophysical Research, v. 84, p. 615-626.

Matthews, V. and C. E. Anderson, 1973, Yellowstone convection plume and break-up of the western United States: Nature, v. 243, p. 158-159.

McBroome, L. A., 1981, Stratigraphy and origin of Neogene ash-flow tuffs on the north-central margin of the eastern Snake River Plain, Idaho: University of Colorado M.S. thesis, 74 p.

Morgan, Paul, D. D. Blackwell, R. E. Spafford, and R. B. Smith, 1977, Heat flow measurements in Yellowstone Lake and the thermal structure of the Yellowstone caldera: Journal of Geophysical Research, v. 82, p. 3719-3732.

Morgan, W. J., 1971, Convection plumes in the lower mantle: Nature, v. 230, p. 42-43.

———, 1972, Plate motions and deep mantle convection: Geological Society of America Memoir 132, p. 7-22.

Myers, W. B. and Warren Hamilton, 1964, Deformation accompanying the Hebgen Lake earthquake of August 17, 1959: U. S. Geological Survey Professional Paper 435-I, p. 55-98.

Obradovich, J. D., C. W. Naeser, G. A. Izett, G. Pasini, and G. Bigazzi, 1982, Constraints upon the age of the proposed Pliocene-Pleistocene boundary stratotype in the Vrica section Italy: Nature (in press).

Parsons, W. H. and D. J. Doherty, 1974, Ground surge in Pliocene-Pleistocene ash and pumice deposits in eastern Idaho (abstract): Geological Society of America, Abstracts with Programs, v. 6, p. 465.

Pitt, A. M., 1979, Preliminary map of earthquake epicenters in Yellowstone National Park and vicinity, 1973-1978: U. S. Geological Survey Open-File Map 79-717, scale 1:250,000.

Pitt, A. M., C. S. Weaver, and William Spence, 1979, The Yellowstone Park earthquake of June 30, 1975: Seismological Society of America Bulletin, v. 69, p. 187-205.

Powers, H. A., 1960, Alkalic lava flow, with fluidity of basalt, in the Snake River Plain, Idaho: U. S. Geological Survey Professional Paper 400-B, p. B297.

Prostka, H. J., 1977, Joints, fissures, and voids in rhyolite welded ash-flow tuff at Teton damsite, Idaho: U. S. Geological Survey Open-File Report 77-211, 13 p.

Prostka, H. J., G. P. Eaton, and S. S. Oriel, 1976, Cordilleran thermotectonic anomaly: II. Interaction of an intraplate chemical plume mass and related mantle diapir: Geological Society of America, Abstracts with Programs, v. 8, p. 1054-1055.

Ruppel, E. T., 1964, Strike-slip faulting and broken basin-ranges in east-central Idaho and adjacent Montana, *in* Geological Survey Research, 1964: U. S. Geological Survey Professional Paper 501-C, C14-C18.

Ryall, Allan, 1962, The Hebgen Lake, Montana, earthquake of August 17, 1959, P-waves: Seismological Society of America Bulletin, v. 52, p. 235-271.

Smith, R. B. and L. W. Braile, 1982, Crustal structure and evolution of an explosive silicic volcanic system at Yellowstone, *in* Explosive Volcanism: National Academy of Sciences (in press).

Smith, R. B. and R. L. Christiansen, 1980, Yellowstone Park as a window on the earth's interior: Scientific American, v. 242, no. 2, p. 84-95.

Smith, R. B. and M. L. Sbar, 1974, Contemporary tectonics and seismicity of the western United States, with emphasis on the Intermountain Seismic Belt: Geological Society of America Bulletin, v. 85, p. 1205-1218.

Smith, R. B., M. M. Schilly, L. W. Braile, J. Ansorge, J. L. Lehman, M. R. Baker, C. Prodehl, J. H. Healy, S. Mueller, and R. W. Greensfelder, 1982, The 1978 Yellowstone-eastern Snake River Plain seismic profiling experiment: crustal structure of the Yellowstone region and experiment design: Journal of Geophysical Research, v. 87, p. 2583-2596.

Smith, R. B., R. T. Shuey, R. C. Friedline, R. M. Otis, and L. B. Alley, 1974, Yellowstone hot spot: new magnetic and seismic evidence: Geology, v. 2, p. 451-455.

Smith, R. B., R. T. Shuey, J. R. Pelton, and J. P. Bailey, 1977, Yellowstone hot spot: contemporary tectonics and crustal properties from earthquake and aeromagnetic data: Journal of Geophysical Research, v. 82, p. 3665-3676.

Smith, R. L., 1960, Zones and zonal variations in welded ash flows: U. S. Geological Survey Professional Paper 354-F, p. 149-159.

——— 1979, Ash-flow magmatism, *in* C. E. Chapin and W. E. Elston, editors, Ash-Flow Tuffs: Geological Society of America Special Paper 180, p. 5-27.

Smith, R. L. and R. A. Bailey, 1968, Resurgent cauldrons, *in* R. R. Coats, R. L. Hay, and C. A. Anderson, editors, Studies in Volcanology (Williams Volume): Geological Society of America Memoir 116, p. 613-662.

Smith, R. L. and H. R. Shaw, 1975, Igneous-related geothermal systems, *in* D. E. White and D. L. Williams, editors, Assessment of Geothermal Resources of the United States—1975: U. S. Geological Survey Circular 726, p. 58-83.

———, 1979, Igneous-related geothermal systems, *in* L. J. P. Muffler, editor, Assessment of Geothermal Resources of the United States—1978: U. S. Geological Survey Circular 790, p. 12-17.

Snyder, W. S., W. R. Dickinson, and M. L. Silberman, 1976, Tectonic implications of space-time patterns of Cenozoic magmatism in the western United States: Earth and Planetary Science Letters, v. 32, p. 91-106.

Stanley, W. D., J. E. Boehl, F. X. Bostick, and H. W. Smith, 1977, Geothermal significance of magnetotelluric sounding in the eastern Snake River Plain-Yellowstone region: Journal of Geophysical Research, v. 82, p. 2501-2514.

Stearns, H. T., L. L. Bryan, and Lynn Crandall, 1939, Geology and water resources of the Mud Lake region, Idaho, including the Island Park area: U. S. Geological Survey Water-Supply Paper 818, 124 p.

Stearns, H. T., Lynn Crandall, and W. G. Steward, 1938, Geology and groundwater resources of the Snake River Plain in southeastern Idaho: U. S. Geological Survey Water-Supply Paper 774, 268 p.

Trimble, A. B. and R. B. Smith, 1975, Seismicity and contemporary tectonics of the Hebgen Lake-Yellowstone Park region: Journal of Geophysical Research, v. 80, p. 733-741.

U. S. Geological Survey, 1972, Geologic map of Yellowstone National Park: U. S. Geological Survey Miscellaneous Geological Investigations Map I-711, scale 1:125,000.

White, D. E., R. O. Fournier, L. J. P. Muffler, and A. H. Truesdell, 1975, Physical results of research drilling in thermal areas of Yellowstone National Park, Wyoming: U. S. Geological Survey Professional Paper 892, 70 p.

Whitehead, R. L., 1978, Water resources of the upper Henrys Fork basin in eastern Idaho: Idaho Department of Water Resources Water Information Bulletin 46, 91 p.

Williams, Howel, 1941, Calderas and their origin: University of California Department of Geological Sciences Bulletin, v. 25, p. 239-346.

Zietz, Isidore, F. P. Gilbert, and J. R. Kirby, Jr., 1978, Aeromagnetic map of Idaho: color-coded intensities: U. S. Geological Survey Geophysical Investigations Map GP-920, scale 1:1,000,000.

Geology of the Magic Reservoir Area, Snake River Plain, Idaho

by

William P. Leeman[1]

ABSTRACT

The Magic Reservoir area occurs along the northern margin of the Snake River Plain, Idaho, in a structurally complex zone where the western and eastern limbs of the plain converge. Volcanic activity since middle Miocene time follows the general trend elsewhere in the Snake River Plain. Rhyolitic ash-flow and air-fall tuffs, subordinate basalt flows, and interbedded sediments were deposited intermittently between at least 10 million to about 5 million years ago; culminating eruptions of extensive rhyolite lavas filled a large depressed area which is inferred to be a buried caldera. Extensive mafic lavas of a hybrid or contaminated character were extruded over much of the inferred caldera, shortly following rhyolitic activity there, and were in turn followed by relatively minor pyroclastic eruptions and emplacement of domes of rhyolite as recently as 3 million years ago. Subsequent volcanic activity was basaltic, and vent loci apparently were controlled largely by older normal faults and caldera structures.

INTRODUCTION

Geologic mapping and geochronology of Tertiary rocks along margins of the Snake River Plain in Idaho can provide useful constraints on models for development of this province. The area near Magic Reservoir is of considerable interest in this respect because it lies in the zone where the northeast-trending eastern part of the plain and northwest-trending western part converge. Previous mapping in the area that includes the eastern Mount Bennett Hills and the Timmerman and Picabo Hills (Figure 1) provides a reasonably good view of the stratigraphic relations there (Schmidt, 1961; Malde and others, 1963; Smith, 1966; LaPoint, 1977; Struhsacker and others, 1982 this volume). In this paper a summary of geologic relations is presented, and evidence is cited for the presence of a partly buried caldera in the area of Magic Reservoir.

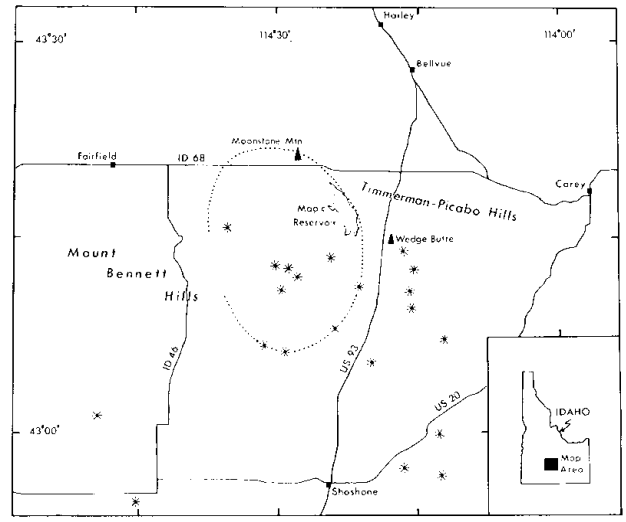

Figure 1. General location map for the Magic Reservoir area. Major highways and towns are shown. Two prominent rhyolite domes are identified (triangles) as are Quaternary basaltic vents (stars). Inferred caldera boundary is shown by dotted line (see Figure 2).

GEOLOGY OF THE MAGIC RESERVOIR AREA

Schmidt (1961) and Smith (1966) provide the most detailed descriptions of geologic units in the area. The regional geology is summarized on the Hailey 2° sheet (Rember and Bennett, 1979). A composite geologic map based on their work and on reconnaissance mapping by Malde and others (1963) and the author is shown in Figure 2. Stratigraphic relations are illustrated in Table 1. In the map area local outcrops of late Paleozoic sediments (MPs), Cretaceous granodioritic to quartz dioritic intrusive rocks (Kg) of the Idaho batholith, and erosional

[1]Department of Geology, Rice University, Houston, Texas 77001.

Leeman, W. P., 1982, Geology of the Magic Reservoir area, Snake River Plain, Idaho, *in* Bill Bonnichsen and R. M. Breckenridge, editors, Cenozoic Geology of Idaho: Idaho Bureau of Mines and Geology Bulletin 26, p. 369-376.

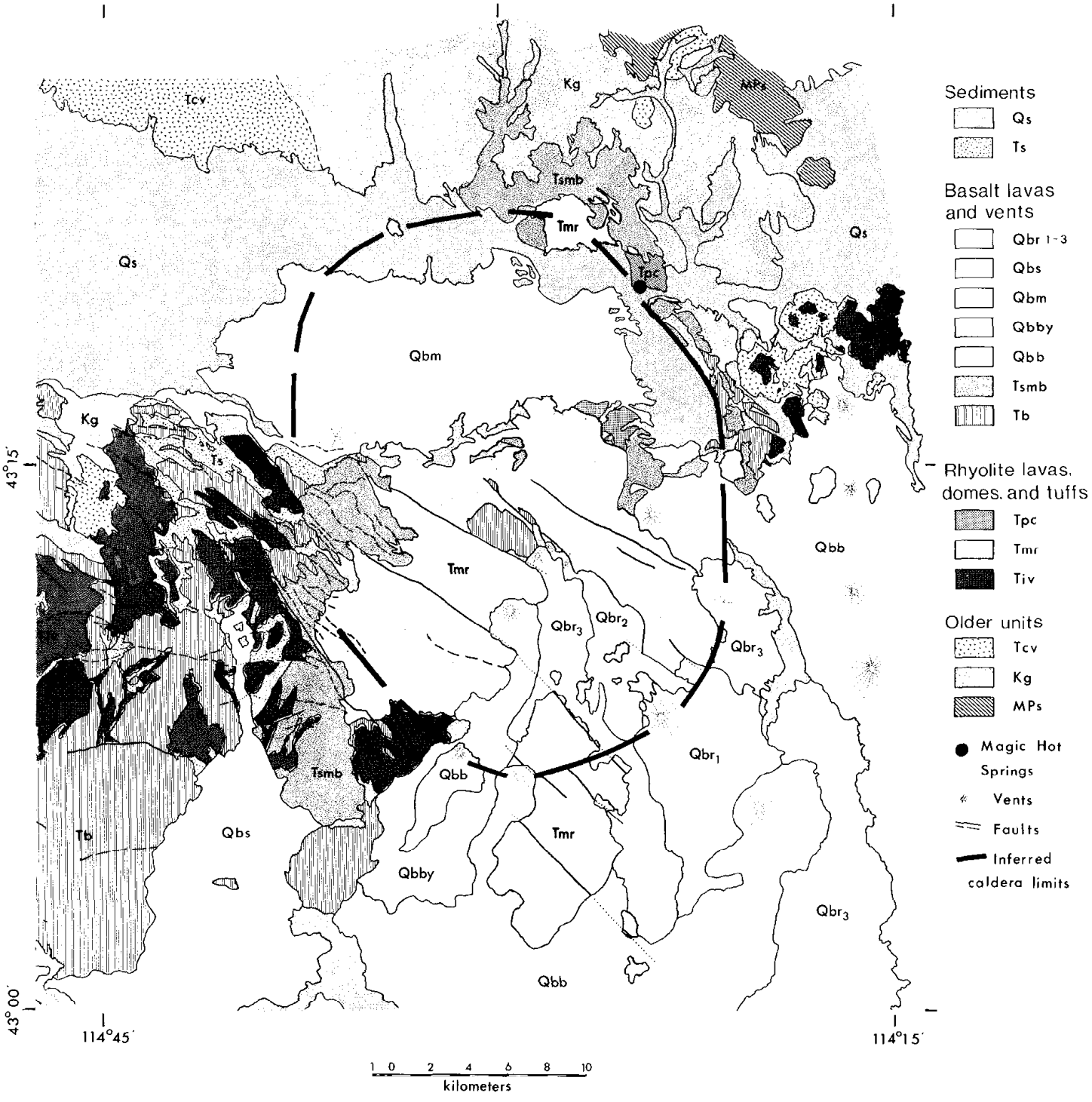

Figure 2. Geologic map for the Magic Reservoir area. Compiled mainly from Schmidt (1961), Malde and others (1963), and Smith (1966). Geologic units are as follows: undivided Quaternary and late Tertiary sediments (Qs and Ts); unnamed Recent basalts (Qbr_1, Qbr_2, Qbr_3, in increasing age sequence); Schooler Basalt (Qbs); Macon Basalt (Qbm); younger and older unnamed Bruneau basalts (Qbby and Qbb); Square Mountain Basalt (Tsmb); undivided Banbury basalts (Tb); Poison Creek Tuff (Tpc); undivided Moonstone Rhyolite (Tmr); undivided Idavada Volcanics rhyolitic volcanic rocks (Tiv); Challis Volcanics (Tcv); undivided granitoid rocks of the Idaho batholith (Kg); and undivided Mesozoic-Paleozoic sedimentary rocks (MPs). See text and Table 1 for further details.

remnants of andesitic to quartz latitic lavas and breccias and intercalated sediments of the Eocene Challis Volcanics (Tcv) form a basement to the younger rocks discussed in this paper.

STRATIGRAPHY AND VOLCANIC EVENTS

Late Miocene volcanic rocks and sediments lie unconformably on the basement rocks. The volcanic rocks consist mainly of rhyolitic ash-flow and air-fall tuffs and subordinate basaltic lavas. These rocks are interbedded with fluvial and lacustrine sediments (Ts) containing abundant volcaniclastic components. A sequence of rhyolite ash-flow tuffs and thick tuffaceous sediments (Picabo Tuff) has been mapped east of Magic Reservoir (Schmidt, 1961). This sequence has not been studied in detail, but two distinct ash-flow tuff members, each containing multiple cooling units, have been discerned. Schmidt notes that the ash-flow tuffs become more densely welded and appear to increase in thickness toward the west. Similar ash-flow tuff sequences have been

Table 1. Stratigraphic relations in the western Snake River Plain, Idaho.

Epochs[a]	Bellevue Area (Schmidt, 1961)	Eastern Mount Bennett Hills (Smith, 1966)	Western Snake River Plain (Malde and Powers, 1962)
Recent	Alluvial and glacial outwash sediments, local basalt flows (+)		Alluvial and glacial outwash sediments, numerous basalt flows (+) (<0.7 m.y.) of Snake River Group
Pleistocene	Bellevue Formation Priest Basalt (+)[b] Macon Basalt (+) Sonnars Basalt (+)	Bruneau Formation Macon Basalt (+) Schooler Basalt (+) Timber Gulch Basalt (+)	Black Mesa Gravel
	Myrtle Basalt (-) Upper Wind Ridge Basalt Lower Wind Ridge Basalt (-) Hay Basalt		Bruneau Formation—unconsolidated detritus, gravels; interbedded basalt flows (-) (0.7—1.5 m.y.)
(1.8 m.y.)	Alluvial gravels		Tuana Gravel
Pliocene	Clay Bank Basalt (including sediments) (+)		Glenns Ferry Formation—sediments, minor basalt flows and silicic ash (~3-4 m.y.)
(5.5 m.y.)	Poison Creek Tuff (+) (5-6 m.y.)		
	Square Mountain Basalt (+) Moonstone Rhyolite (+,-) (3-6 m.y.)	Square Mountain Basalt (+) Moonstone Rhyolite (+,-)	Chalk Hills Formation—sediments, silicic ash, and minor basalt flows (~6-9 m.y.)
Late Miocene	Picabo Tuff upper tuff (unit B) (-) lower tuff (unit A) (+)	Burnt Willow Basalt (including basal gravel) (-) City of Rocks Tuff (+) (6.5 m.y.) McHan Basalt (including basal gravel) (+) Fir Grove Tuff (+) Hash Spring Formation (gravel, sand, tuff) Gwin Spring Formation Upper Ignimbrite (+) Lower Ignimbrite (+) Older welded tuff (+) (9.8±0.3 m.y.)	Banbury Formation—basalt flows (4-10 m.y.) with interbedded fluvial-lacustrine sediments and ash
(10.5 m.y.) Middle Miocene		Pole Corral Gravel	Idavada Formation—rhyolite ash-flow and air-fall tuffs (~10-15 m.y.) interbedded sediments, and minor basalt flows
Late Eocene	Challis Volcanics	Challis Volcanics	Challis Volcanics
Late Cretaceous	Granodiorite of Idaho batholith	Granodiorite of Idaho batholith	Granodiorite of Idaho batholith

[a]Chronostratigraphic epochs after Berggren (1972). [b]Indicates magnetic polarity: normal (+), reverse (-).

mapped in the eastern Mount Bennett Hills (Smith, 1966). The latter rocks have been studied in greater detail, and four distinct periods of ash-flow tuff deposition can be inferred from intervening fluvial-lacustrine sediments and basalt flows (Table 1). Individual ash-flow tuff sequences comprise either multiple (Gwin Springs Formation and Fir Grove Tuff) or single cooling units (City of Rocks Tuff). The oldest tuff unit (older welded tuff, Table 1) is poorly exposed, and few details of its areal distribution or internal zonation are available. Armstrong and others (1980) report a potassium-argon age of about 10 million years for this unit. The City of Rocks Tuff thickens southward and may be correlative with the rhyolite exposed at Shoshone Falls, near Twin Falls (compare, Stearns and others, 1938; Stearns, 1955; Smith, 1966), which has been dated at 6.5 million years old (Armstrong and others, 1975). This highly tentative correlation is based only on the petrographic and lithologic similarities of the units. On the map (Figure 2) all ash-flow tuff units and some of the associated sediments are designated as Idavada Volcanics (Tiv) after Malde and Powers (1962). Cumulative thickness of these units is at least 800 meters and 400 meters, respectively, east and west of Magic Reservoir. Sources for these rhyolitic tuffs are uncertain; some of those in the Mount Bennett Hills apparently were derived from more southerly sources as they thicken in that direction.

Late Miocene basalts interbedded with tuff units in the Mount Bennett Hills were designated as Banbury Formation by Malde and others (1963) but were individually mapped by Smith (1966). These units consist of one or more flow units that originated from vents to the north and covered wide areas. Their aggregate thickness averages about 60 meters but is greater to the north. East of Magic Reservoir older basalts are locally exposed in the Clay Bank Hills; although they are demonstrably younger than Miocene basalts in the Mount Bennett Hills, all of these units are shown as undifferentiated Tertiary basalt (Tb) in Figure 2.

A major rhyolite unit, Moonstone Rhyolite (Tmr), covers more than 250 square kilometers in the central map area, mainly southwest of Magic Reservoir. This unit is a heterogeneous accumulation of rhyolite lava flows, possibly some welded ash-flow tuff in the central area, and numerous exogenous domes. The type area, Moonstone Mountain, is a large dome from which a small lava flow issued. Schmidt (1961) noted the problems involved in distributing viscous rhyolite lavas over such a wide area if Moonstone Mountain were considered as the main vent area. Thus, it is likely that numerous vents are within the area between Magic Reservoir and the Mount Bennett Hills. At least five domes of similar rhyolite occur south and southeast of Magic Reservoir, and extensive outcrops extend southward almost to the town of Shoshone. The thickness of this rhyolite is estimated as a minimum 150 meters in the central area. Available potassium-argon dates (Armstrong and others, 1975; Stanley Evans, personal communication, 1981) range widely from about 6 million years old for rhyolite near Magic Hot Springs to 3 million years old for the dome at Wedge Butte, southeast of Magic Reservoir.

Shortly following deposition of the Moonstone Rhyolite lavas, a distinctive basalt was extruded over much of the map area. This unit, the Square Mountain Basalt (Tsmb), consists of one or more flows with a maximum thickness of 200 meters immediately west of Moonstone Mountain. However, elsewhere this unit is considerably thinner (less than 10 meters). The great thickness of lava near Moonstone Mountain suggests its deposition in a local topographic or structural depression. This unit is notable because it contains abundant xenocrysts (embayed quartz, K-feldspar, anorthoclase) and xenoliths (Moonstone Rhyolite; granulitic and granitic gneiss, and rare gabbro all of which are partly fused). Xenoliths are exceedingly abundant in outcrops near Moonstone Mountain, and this area is considered to be a major vent area, although additional vents may have contributed to the wide distribution of the unit. It was postulated that this lava represents a hybrid mixture of basalt and rhyolite magma (Schmidt, 1961), but isotopic studies show that it has been heavily contaminated by Precambrian crustal rocks (Leeman, 1982a this volume). It is noteworthy that typical samples of Square Mountain Basalt contain about 59 percent SiO_2 and in most respects resemble ferrolatites from Craters of the Moon lava field (Leeman, 1982a this volume).

Additional rhyolite ash-flow and air-fall tuffs of the Poison Creek Tuff (Schmidt, 1961) were then deposited over restricted areas near Magic Reservoir. This unit consists of a local flow (or dome) and at least 150 meters of tuffs whose major vents are inferred to lie near Magic Hot Springs (Schmidt, 1961; Struhsacker and others, 1982 this volume). Xenoliths of older Moonstone Rhyolite and Square Mountain Basalt occur in some of the tuffs. Potassium-argon ages determined for two rhyolites of the Poison Creek Tuff range between 5 and 6 million years old (S. Evans, personal communication, 1981).

The Clay Bank Basalt, mentioned above with late Miocene basalts, is younger than the Poison Creek Tuff and consists of about 30 meters of olivine basalt flows. This unit outcrops only in the hills east of

Magic Reservoir where it forms prominent cliffs and landslide blocks. Its age is unknown but could be as young as late Pliocene.

Subsequent volcanic events included the extrusion of numerous Quaternary basalts as single or multiple flow units from widely dispersed vents in the map area. Most of these flow units can be distinguished readily (Schmidt, 1961; Smith, 1966; Malde and others, 1963; LaPoint, 1977) from outcrop patterns, geomorphology, and petrographic characteristics. They are complexly interbedded with Quaternary sediments of fluvial, lacustrine, or glacial origin. A detailed analysis of Pleistocene and Recent geomorphic and geologic development is given by Schmidt (1961) for the area northeast of Magic Reservoir. Pleistocene basalts in this area were assigned by Schmidt to the Bellevue Formation which was considered equivalent to the Bruneau Formation (Qbb) of Malde and Powers (1962). However, paleomagnetic data show that late Bellevue basalts (Sonnars, Macon-Qbm, and Priest Basalts) and those in the Mount Bennett Hills (Timber Gulch and Schooler-Qbs Basalts) are normally magnetized and thus may be equivalent to older Snake River Group lavas (Malde and Powers, 1962). The Timber Gulch Basalt is denoted as younger Bruneau Formation (Qbby) on the map. Extensive measurements of paleomagnetic orientations for dated (0.7 to 1.5 million years old) Bruneau basalts from the western Snake River Plain are reversely magnetized (Armstrong and others, 1975; Leeman, unpublished data).

Recent basalts (Qbr 1-3) erupted from several vents in an east-trending zone across the east-central map area. All of these flows are sparsely vegetated and are correlative with the Snake River Group.

Stratigraphic relations for all of the described units are summarized in Table 1 where they can be compared with a generalized stratigraphy for the western Snake River Plain (Malde and Powers, 1962; Malde and others, 1963; Malde, 1972). Results of the latter studies have been modified slightly by the available potassium-argon dating (Armstrong and others, 1975; 1980) and more recent stratigraphic studies (for example, Kimmel, 1979; Neville and others, 1979; Swirydczuk, 1980; summarized in Leeman, 1982b this volume). In Table 1 and in previous discussions the chronostratigraphic epochs referred to are those of Berggren (1972). Most notably, the easterly time-transgressive nature of many volcanic and sedimentary units is now recognized. The stratigraphic succession from a late Eocene to middle Miocene depositional hiatus is generally similar throughout the western Snake River Plain and in the Magic Reservoir area in that early volcanism is dominantly rhyolitic with minor intercalated basalt flows. With time basaltic volcanism became dominant. However, the continuation of rhyolitic volcanism to as recently as 3 million years ago in the Magic Reservoir area appears to be somewhat atypical for this part of the Snake River Plain. It is noteworthy that the composition of the 3-million-year-old Wedge Butte rhyolite is relatively "evolved" compared with most Snake River Plain rhyolites (Leeman, 1982c this volume), and it may represent highly differentiated magma erupted during the declining stages of activity of the Magic Reservoir volcanic center.

STRUCTURAL DEVELOPMENT

Structural development within the map area is partly known from the relations of geologic events, depositional history, and distribution of faults (Schmidt, 1961; Smith, 1966; Malde and others, 1963). In Miocene time, topographic highs apparently existed east of Magic Reservoir and in the eastern Mount Bennett Hills because alluvial gravels prograded northward from these areas and they influenced the distribution of sediments derived from the north. Early ash-flow tuffs were deposited on a dissected erosional surface of moderate relief. Later ash flows, apparently from southerly sources, thin to the north, which suggests that the depositional surface was tilted toward the south. In support of this inference in the Mount Bennett Hills, flow structures in some of these ash flows indicate that they partly drained downslope (southward) after deposition, and late Miocene basalts also flowed to the south. Smith (1966) documented a complex history of faulting, based on stratigraphic and depositional evidence, in which normal faults were activated intermittently and partly controlled the distribution of volcanic and sedimentary units. During Miocene and Pliocene time two dominant sets of normal faults were active: (1) an east-trending set which produced minor horst and graben structures and (2) a northwest-trending set which accommodated the greatest vertical displacements and horizontal extension. Major uplift of the Mount Bennett Hills apparently occurred after deposition of City of Rocks Tuff and prior to extrusion of Bruneau age basalts (Malde, 1959; Smith, 1966). Bruneau age and younger faulting was relatively minor and is represented by small displacements on east-trending faults. Tilting toward the south continued after deposition of the Clay Bank Basalt (late Pliocene ?) because these lavas dip southward about 5 to 10 degrees.

Smith (1966) interpreted fault patterns in the eastern Mount Bennett Hills as a conjugate system caused by dominantly right-lateral wrench faulting.

However, major extension normal to the northwest-trending fault set is also consistent with inferred southwest regional extension since middle Miocene time (Leeman, 1982c this volume). Analysis of these structures is not sufficiently detailed at present to evaluate adequately the causative stress field or temporal changes in it.

MAGIC RESERVOIR VOLCANIC CENTER—A BURIED CALDERA?

Several lines of evidence suggest the presence of a buried caldera near Magic Reservoir. A set of at least four domes of Moonstone Rhyolite define an arcuate trace along which Magic Hot Springs (Young and Mitchell, 1973) is located. This trace also includes inferred vent areas for Square Mountain Basalt and the Poison Creek Tuff and follows the prominent topographic scarp on the east side of Magic Reservoir. A set of four Quaternary basalt vents forms an arcuate extension of the trace to the south and west, and it is inferred that this trace continues northwestward into a zone of northwest-trending faults along which the northeastern block was downdropped (Smith, 1966) near the terminus of the Mount Bennett Hills (see inferred caldera limits, Figure 2). It is more difficult to estimate the trace in the northwest sector where young basalt and sediment cover is extensive. Within the inferred caldera structure, the oldest rocks exposed are Moonstone Rhyolite which forms an extensive lava plateau; this relationship is reminiscent of the Plateau Rhyolites within the Yellowstone caldera and intracaldera rhyolites of the Bruneau-Jarbidge eruptive center (Bonnichsen, 1982b this volume). The central area within the inferred caldera is topographically higher than its margins, not unlike a resurgent dome. Challis and Idaho batholith basement rocks and Idavada tuffs outcrop very close to the west, north, and east margins of the structure at higher elevations, yet they are not exposed within its limits. It is particularly difficult to explain the absence of Idavada rocks, which were extensively deposited along the north margin of the Snake River Plain, unless they subsided or were removed during a caldera-forming event. Further evidence supporting the presence of a caldera collapse structure is the great thickness (200 meters) of Square Mountain Basalt just south of the inferred caldera fault near Moonstone Mountain. North of this structure the Square Mountain Basalt lavas are considerably thinner where they were deposited on granodiorite basement.

Assuming that a caldera is buried in this area, it is of interest to review constraints on how and when it formed. Present data are too incomplete to assign this area as a source for any of the Idavada ash-flow tuffs. Many of those in the Mount Bennett Hills appear to thicken southward, suggesting that their source areas lie in that direction. Limited data for the Picabo Tuff (Schmidt, 1961) suggest that the lower member indeed thickens in the direction of Magic Reservoir. However, preliminary petrographic studies reveal that none of the Idavada tuffs is as porphyritic or contains phenocryst assemblages closely resembling Moonstone Rhyolite, which contains abundant phenocrysts of sanidine and quartz. More detailed chemical, mineralogical, and stratigraphic studies are required to firmly test a genetic relationship. The Poison Creek Tuff certainly originated from vents in the northeastern part of the inferred caldera, and these rocks are similar petrographically (though they are not as abundantly porphyritic) to certain Moonstone Rhyolite lithologies and contain xenoliths of Moonstone Rhyolite. The volume and areal extent of Poison Creek Tuff are not large, and this unit may only represent a late-stage eruptive episode from the inferred caldera. Based on limiting potassium-argon ages, dominant eruptive activity probably occurred between 5 to 10 million years ago, but emplacement of late-stage domes apparently continued to at least 3 million years ago.

Much detailed work remains before the geologic history and even the existence of a buried caldera are firmly established. The locations of buried calderas in other parts of the Snake River Plain, initially based on geological inferrences such as presented here (compare, Citron, 1976; Kuntz and Covington, 1979; Prostka, 1980; Embree and others, 1982 this volume; Bonnichsen, 1982a this volume), have been strongly confirmed by geophysical studies and deep drilling (for example, Prostka and Embree, 1978; Doherty and others, 1979). Such studies are desirable in the Magic Reservoir area and may be justifiable in terms of the geothermal potential of such a relatively young magma system.

ACKNOWLEDGMENTS

The basis of this paper is the high-quality field work by D. L. Schmidt and C. L. Smith. The present paper essentially updates and summarizes portions of their work and provides a unified map compilation with my own interpretations concerning the likely existence of a buried caldera. This work is supported by National Science Foundation Grant EAR80-18580. Manuscript preparation was immeas-

urably aided by A. Elsweiler and A. Walters on the keyboards and D. Hicken on map compilation.

REFERENCES

Armstrong, R. L., W. P. Leeman, and H. E. Malde, 1975, K-Ar dating, Quaternary and Neogene volcanic rocks of the Snake River Plain, Idaho: American Journal of Science, v. 275, p. 225-251.

Armstrong, R. L., J. E. Harakal, and W. M. Neill, 1980, K-Ar dating of Snake River Plain (Idaho) volcanic rocks—new results: Isochron West, no. 27, p. 5-10.

Berggren, W. A., 1972, A Cenozoic time-scale—some implications for regional geology and paleobiogeography: Lethaia, v. 5, p. 195-215.

Bonnichsen, Bill, 1982a, The Bruneau-Jarbidge eruptive center, southwesten Idaho, *in* Bill Bonnichsen and R. M. Breckenridge, editors, Cenozoic Geology of Idaho: Idaho Bureau of Mines and Geology Bulletin 26.

———, 1982b, Rhyolite lava flows in the Bruneau-Jarbidge eruptive center, southwestern Idaho, *in* Bill Bonnichsen and R. M. Breckenridge, editors, Cenozoic Geology of Idaho: Idaho Bureau of Mines and Geology Bulletin 26.

Citron, G. P., 1976, Idavada ash-flows in the Three Creek area, southwestern Idaho, and their regional significance: Cornell University M.S. thesis, 83 p.

Doherty, D. J., L. A. McBroome, and M. A. Kuntz, 1979, Preliminary geological interpretation and lithologic log of the geothermal exploration well (INEL-1), Idaho National Engineering Laboratory, eastern Snake River Plain, Idaho: U. S. Geological Survey Open-File Report 79-1248, 7 p.

Ekren, E. B., D. H. McIntyre, E. H. Bennett, and R. F. Marvin, 1982, Cenozoic stratigraphy of western Owyhee County, Idaho, *in* Bill Bonnichsen and R. M. Breckenridge, editors, Cenozoic Geology of Idaho: Idaho Bureau of Mines and Geology Bulletin 26.

Embree, G. F., L. A. McBroome, and D. J. Doherty, 1982, Preliminary stratigraphic framework of the Pliocene and Miocene rhyolites, eastern Snake River Plain, Idaho, *in* Bill Bonnichsen and R. M. Breckenridge, editors, Cenozoic Geology of Idaho: Idaho Bureau of Mines and Geology Bulletin 26.

Kimmel, P. G., 1979, Stratigraphy and paleoenvironments of the Miocene Chalk Hills Formation and Pliocene Glenns Ferry Formation in the western Snake River Plain, Idaho: University of Michigan Ph.D. thesis, 340 p.

Kuntz, M. A. and H. R. Covington, 1979, Do basalt structures and topographic features reflect buried calderas in the eastern Snake River Plain?: EOS, American Geophysical Union, v. 60, p. 945.

LaPoint, P. J. I., 1977, Preliminary photogeologic map of the eastern Snake River Plain, Idaho: U. S. Geological Survey Map MF-850.

Leeman, W. P., 1982a, Evolved and hybrid lavas from the Snake River Plain, Idaho, *in* Bill Bonnichsen and R. M. Breckenridge, editors, Cenozoic Geology of Idaho: Idaho Bureau of Mines and Geology Bulletin 26.

———, 1982b, Development of the Snake River Plain-Yellowstone Plateau province, Idaho and Wyoming: an overview and petrologic model, *in* Bill Bonnichsen and R.M. Breckenridge, editors, Cenozoic Geology of Idaho: Idaho Bureau of Mines and Geology Bulletin 26.

———, 1982c, Rhyolites of the Snake River Plain-Yellowstone Plateau province, Idaho and Wyoming, *in* Bill Bonnichsen and R. M. Breckenridge, editors, Cenozoic Geology of Idaho: Idaho Bureau of Mines and Geology Bulletin 26.

Malde, H. E., 1959, Fault zone along northern boundary of western Snake River Plain, Idaho: Science, v. 130, p. 272.

———, 1972, Stratigraphy of the Glenns Ferry Formation from Hammett to Hagerman, Idaho: U. S. Geological Survey Bulletin 1331-D, 19 p.

Malde, H. E. and H. A. Powers, 1962, Upper Cenozoic stratigraphy of western Snake River Plain, Idaho: Geological Society of America Bulletin, v. 73, p. 1197-1220.

Malde, H. E., H. A. Powers, and C. H. Marshall, 1963, Reconnaissance geologic map of the west-central Snake River Plain, Idaho: U. S. Geological Survey Miscellaneous Geologic Investigations Map I-373.

Neville, Colleen, N. D. Opdyke, E. H. Lindsay, and N.M. Johnson, 1979, Magnetic stratigraphy of Pliocene deposits of the Glenns Ferry Formation, Idaho, and its implications for North American mammalian biostratigraphy: American Journal of Science, v. 279, p. 503-526.

Prostka, H. J., 1980, Buried Pliocene calderas of the eastern Snake River Plain: EOS, American Geophysical Union, v. 60, p. 945.

Prostka, H. J. and G. F. Embree, 1978, Geology and geothermal resources of the Rexburg area, eastern Idaho: U. S. Geological Survey Open-File Report 78-1009, 15 p.

Rember, W. C. and E. H. Bennett, 1979, Geologic map of the Hailey quadrangle, Idaho: Idaho Bureau of Mines and Geology Geologic Map Series, scale 1:250,000.

Schmidt, D. L., 1961, Quaternary geology of the Bellevue area in Blaine and Camas Counties, Idaho: University of Washington Ph.D. thesis, 125 p.

Smith, C. L., 1966, Geology of eastern Mount Bennett Hills, Camas, Gooding, and Lincoln Counties, Idaho: University of Idaho Ph.D. thesis, 129 p.

Stearns, H. T., 1955, Pillar Falls mud flow and Shoshone Falls andesite near Twin Falls, Idaho: Geological Society of America Bulletin, v. 66, p. 463-464.

Stearns, H. T., Lynn Crandall, and W. G. Steward, 1938, Geology and ground-water resources of the Snake River Plain in southeastern Idaho: U. S. Geological Survey Water Supply Paper 774, 268 p.

Struhsacker, D. W., P. W. Jewell, Jon Zeisloft, and S. H. Evans, Jr., 1982, The geology and geothermal setting of the Magic Reservoir area, Blaine and Camas Counties, Idaho, *in* Bill Bonnichsen and R. M. Breckenridge, editors, Cenozoic Geology of Idaho: Idaho Bureau of Mines and Geology Bulletin 26.

Swirydczuk, Krystyna, 1980, Sedimentology of the Pliocene Glenns Ferry Oolite and its stratigraphic setting in the western Snake River Plain: University of Michigan Ph.D. thesis, 247 p.

Young, H. W. and J. C. Mitchell, 1973, Geothermal investigations in Idaho, Part 1, geochemistry and geologic setting of selected thermal waters: Idaho Department of Water Resources Water Information Bulletin 30, 43 p.

The Geology and Geothermal Setting of the Magic Reservoir Area, Blaine and Camas Counties, Idaho

by

Debra W. Struhsacker[1], Paul W. Jewell[2], Jon Zeisloft[3], and Stanley H. Evans, Jr.[2]

ABSTRACT

The Magic Reservoir area straddles the Blaine-Camas county line in south-central Idaho, along the northern boundary of the central Snake River Plain. The rocks exposed at Magic Reservoir include a 5.8-million-year-old rhyolite flow, the Pliocene Square Mountain Basalt, multiple cooling units of a 5.6-million-year-old rhyolite ash-flow tuff, a 4.7-million-year-old rhyolite dome, and Quaternary basalt flows and sediments. These newly reported ages for the rhyolites at Magic Reservoir reveal that they are the youngest, westernmost silicic volcanic rocks presently known in the Snake River Plain. They represent an anomalously young rhyolitic event that may include the Moonstone Mountain rhyolite dome to the northwest and the previously dated (Armstrong and others, 1975) 3-million-year-old Wedge Butte rhyolite dome to the southeast of Magic Reservoir.

The area is cut by numerous normal faults trending northwest, northeast, and west. The northwest-trending faults are the dominant structures. They form a horst block at Hot Springs Landing and parallel the regional structural grain.

The geothermal resource at Magic Reservoir occurs within the elevated heat flow province at the northern margin of the Snake River Plain. The system is probably controlled by the deep, convective circulation of fluids along faults at the intersection of the Hot Springs Landing horst with west- and northeast-trending fractures. Although the volcanic rocks in the Magic Reservoir area are young, they are too old to contribute any magmatic heat to the geothermal system.

[1]Chevron Resources Company, Golden, Colorado 80401.
[2]Department of Geology and Geophysics, University of Utah, Salt Lake City, Utah 84108.
[3]Earth Science Laboratory, University of Utah Research Institute, Salt Lake City, Utah 84108.

INTRODUCTION

The geology of the Magic Reservoir area in south-central Idaho (Figure 1) was studied to evaluate the Magic Reservoir geothermal system. The rocks in the Magic Reservoir area are primarily Pliocene to Quaternary rhyolites and basalts which are cut by numerous normal faults. The Magic Reservoir geothermal resource produces 57 liters per minute of 71°C (160°F) water from a 79-meter-deep well (Mitchell and others, 1980).

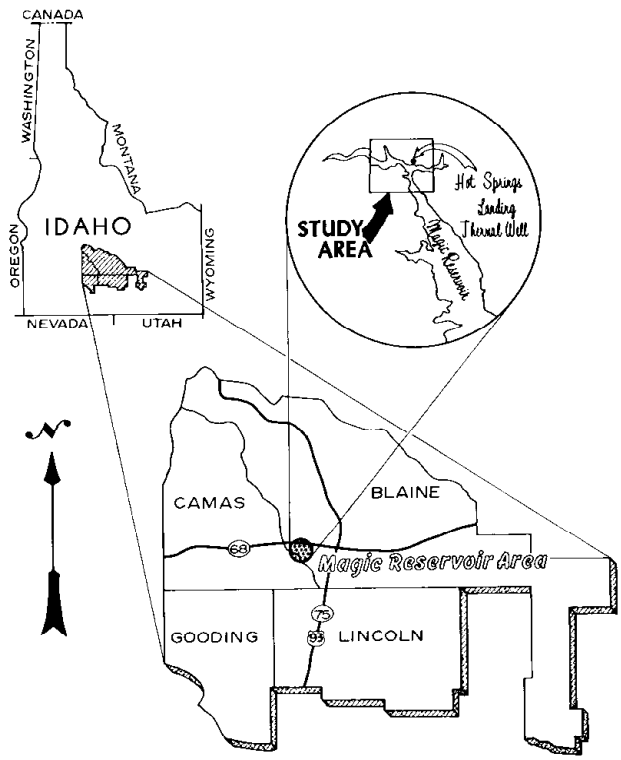

Figure 1. Index map of the Magic Reservoir area, Blaine and Camas Counties, Idaho.

Struhsacker, D. W., P. W. Jewell, Jon Zeisloft, and S. H. Evans, Jr., 1982, The geology and geothermal setting of the Magic Reservoir area, Blaine and Camas Counties, Idaho, *in* Bill Bonnichsen and R. M. Breckenridge, editors, Cenozoic Geology of Idaho: Idaho Bureau of Mines and Geology Bulletin 26, p. 377-393.

To understand the relationship between the Magic Reservoir geothermal system and the volcanic history of the region, the study area was examined in detail by geologic mapping on 1:20,000-scale aerial photographs, petrographic interpretation, whole-rock chemical analysis, and potassium-argon age dating. This paper attempts to place the Magic Reservoir volcanic rocks in the regional volcanic stratigraphic framework of the Snake River Plain. The mineralogy and composition of the Magic Reservoir rhyolitic rocks are compared with other nearby silicic volcanic rocks. Potassium-argon dates for the Magic Reservoir rhyolites contribute new data to the volcanic chronology of the central Snake River Plain. An analysis of the Magic Reservoir geothermal system both identifies the structures controlling geothermal fluid circulation and places this system within the context of the regional heat flow regime of the central Snake River Plain.

Previous geologic work in the Magic Reservoir area includes Schmidt's (1961) study of the Quaternary stratigraphy, Malde and others' (1963) reconnaissance-scale map of the west-central Snake River Plain, Smith's (1966) investigation of the Idavada Volcanics in the eastern Mount Bennett Hills, and Leeman's (1982a this volume) review. Ross (1971), Mitchell (1976), and Mitchell and others (1980) briefly discuss the geothermal system at Magic Reservoir.

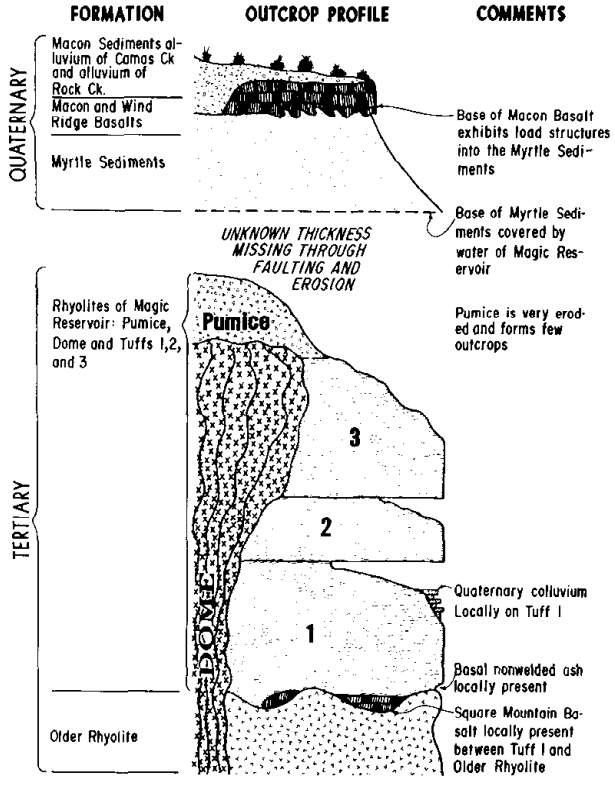

Figure 2. Diagrammatic stratigraphic column for the Magic Reservoir area, Blaine and Camas Counties, Idaho.

STRATIGRAPHY

Rocks exposed at Magic Reservoir (Figure 2) are mainly basalts and rhyolites, the bimodal volcanic assemblage characteristic of the Snake River Plain. The oldest rock exposed in the area is a coarsely porphyritic rhyolite lava flow, locally overlain by flows of Square Mountain Basalt. The next youngest rock at Magic Reservoir is a multiple cooling unit of rhyolite ash-flow tuff that is cut by the feeder system of a rhyolite dome. Quaternary basalt flows and sediments are the youngest rocks in the area.

OLDER RHYOLITE OF MAGIC RESERVOIR

The older rhyolite of Magic Reservoir is locally exposed in the northern and southeastern portions of the map area (Figure 3). It commonly forms rounded, hummocky outcrops. On the north side it is immediately overlain by the base of the ash-flow tuffs, a relationship best exposed 0.25 kilometer west-northwest of Hot Springs Landing (Figure 4) where a knob of the older rhyolite is overlain by the nonwelded, porous base of the ash-flow tuffs. On the southeastern side of the area, the older rhyolite is overlain by the Square Mountain Basalt except where irregular paleotopographic highs of the older rhyolite locally protruded above the basalt flows and were buried by the ash-flow tuffs.

The older rhyolite is coarsely porphyritic, with phenocrysts up to 15 millimeters in length. The phenocryst content ranges from 40 to 50 percent and is composed mainly of sanidine, quartz, and lesser amounts of plagioclase. The groundmass texture varies from glassy to completely devitrified. The glassy variety is generally restricted to the upper parts of the unit and is locally vesicular. Field relationships suggest that the older rhyolite is probably a blocky lava flow. A petrographic description of the older rhyolite is included in Table 1, and its chemical composition is shown in Table 2.

SQUARE MOUNTAIN BASALT

Porphyritic basalt occurs in the Clay Bank Hills (Figure 4), where a thickness of at least 100 meters is exposed in a prominent fault scarp overlooking

Magic Reservoir. The basalt becomes progressively thinner to the north, and exposures are absent near Hot Springs Landing. Additional outcrops of the basalt are mapped north of the landing by both Schmidt (1961) and Malde and others (1963). Malde and others (1963) map this unit as a part of the Banbury Basalt. Schmidt (1961) names it the Square Mountain Basalt after the type locality at Square Mountain, 10 kilometers northwest of Hot Springs Landing (Figure 4).

In the study area, the Square Mountain Basalt is massive with no clearly defined flows or columnar jointing. The rock is locally vesicular, although vesiculation does not define recognizable flow horizons. The basalt is dark gray to bluish black and contains distinctive subround feldspar phenocrysts, 5 to 10 millimeters long, which have cleavage faces with a dull luster. Smaller (1 millimeter long) plagioclase laths are observed locally. Quartz phenocrysts, 1 to 2 millimeters in diameter, are present in trace amounts and have a characteristic greenish brown tint. A petrographic description of this basalt is included in Table 1.

The thickening of the Square Mountain Basalt from north to south in the Clay Bank Hills and its absence around Hot Springs Landing could be due to the presence of an erosional paleo-topographic high of the older rhyolite prior to eruption of the Square Mountain Basalt, or localized erosion of the basalt prior to eruption of the overlying ash-flow tuffs. An alternative explanation is that the basalt north of Hot Springs Landing erupted from Square Mountain whereas the basalt in the Clay Bank Hills erupted from a presently unidentified vent area to the south of the landing. Armstrong and others (1975) comment on the extremely diverse ages and eruptive histories of Banbury-age basalts in this part of the Snake River Plain. More work on these rocks is needed before definite correlations can be made.

RHYOLITE ASH-FLOW TUFFS OF MAGIC RESERVOIR

The rhyolite ash-flow tuffs on the north side of Magic Reservoir are a multiple cooling unit composed of several simple cooling units of quartz-sanidine rhyolite ash-flow tuff. These rocks are exposed north, west, and southwest of Hot Springs Landing, where they form a section as thick as 110 meters. The section is much thinner southeast of the landing, measuring only 40 meters thick and consisting of only one ash-flow unit.

The ash-flow tuffs of Magic Reservoir, described briefly by Malde and others (1963) correspond to the Poison Creek Tuff mapped by Schmidt (1961). However, in order to avoid confusion with the Poison Creek time-stratigraphic unit used by Armstrong and others (1975) to describe upper Miocene silicic volcanic rocks near Bruneau, Idaho, in this study these rocks will be referred to as the rhyolitic ash-flow tuffs of Magic Reservoir.

Tuff 1

The base of the ash-flow sequence at Magic Reservoir, Tuff 1, is a 40-meter-thick simple cooling unit composed of a quartz-sanidine rhyolite ash-flow tuff exposed north, south, and west of Hot Springs Landing. The best exposure of the base of Tuff 1 occurs approximately 0.25 kilometer west-northwest of the landing, where it is draped unconformably upon a rounded knob of the older rhyolite. A 30-centimeter-thick, white, glassy, nonwelded porous zone forms the base of Tuff 1. Immediately overlying this nonwelded base is a densely welded black vitrophyre containing approximately 5 percent sanidine and quartz crystals. The basal vitrophyre grades into a densely welded, partially devitrified, red and black banded, granular tuff, locally containing fiamme of black glass. Pumice fragments in this section show extreme flattening and compaction. This partially devitrified zone grades upwards into a thoroughly devitrified zone characterized by a stony pink rather than a black, glassy appearance. The devitrified zone is overlain by a section of pink and orange, partially to slightly welded crystal lapilli tuff with porous pumice fragments showing decreasing amounts of compaction towards the top of the unit. Vapor-phase crystallization is common in these pumice fragments.

The top of Tuff 1 consists of a totally nonwelded grayish pink crystal tuff containing about 5 percent phenocrysts of quartz and sanidine and a trace of biotite. This zone is thoroughly devitrified with well-developed vapor-phase crystals of tridymite and alkali-feldspar in the pumice fragments. A petrographic description of Tuff 1 is included in Table 1, and its chemical composition is shown in Table 2.

On the southeastern side of the study area, Tuff 1 is about 40 meters thick and forms inconspicuous ridges along the northwest portion of the Clay Bank Hills. The nonwelded base of Tuff 1 is not seen; the black vitrophyre is only locally exposed. As on the northern side, Tuff 1 overlies the older rhyolite. However, on the southeastern side, Tuff 1 also locally overlies flows of Square Mountain Basalt where these basalts cover the older rhyolite. The partially welded and nonwelded portions of Tuff 1 are poorly exposed on the southeastern side and resemble the equivalent zones described to the north.

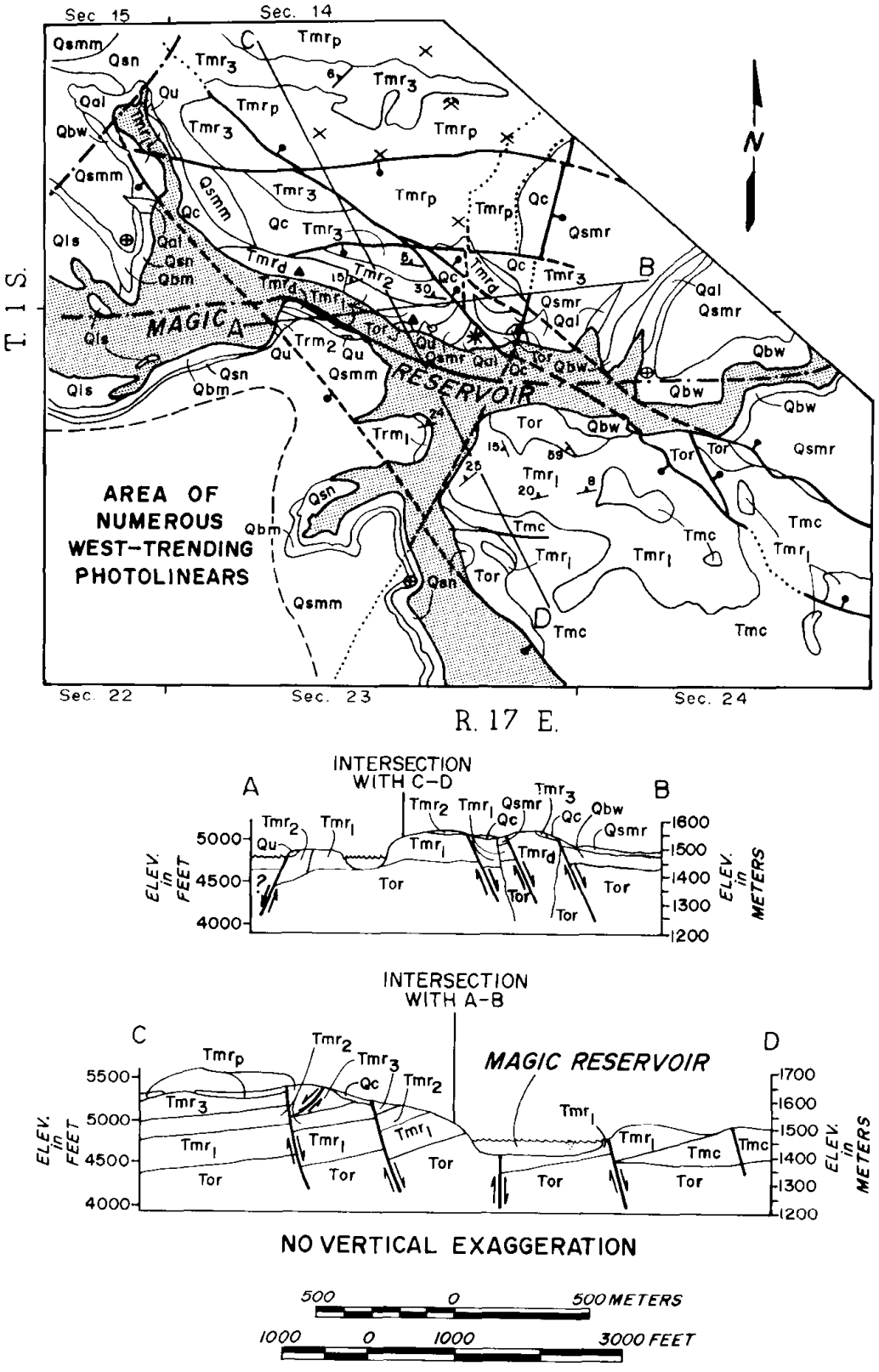

Figure 3. Geologic map and cross sections of the Magic Reservoir area, Blaine and Camas Counties, Idaho.

MAP UNITS

QUATERNARY

- Qls– Large-scale slump deposits
- Qc– Colluvium
- Qal– Alluvium
- Qu– Unnamed arkosic conglomerate
- Qsmm–Macon Sediments derived from Camas Creek
- Qsmr– Macon Sediments derived from Rock Creek
- Qbm– Macon Basalt
- Qbw– Wind Ridge Basalt
- Qsn– Myrtle Sediments

PLIOCENE

- Tmr_d – Rhyolite dome of Magic Reservoir (4.77±0.29m.y.)
- Tmr_p – Pumice of Magic Reservoir
- Tmr_3 – Tuff 3 of Magic Reservoir
- Tmr_2 – Tuff 2 of Magic Reservoir
- Tmr_1 – Tuff 1 of Magic Reservoir (5.64 ± 0.23m.y)
- Tmc– Square Mountain Basalt
- Tor– Older Rhyolite of Magic Reservoir (5.81 ±0.69m.y.)

EXPLANATION

- Contact
- Mapped fault–ball on downthrown side
- Inferred fault
- Photo interpreted extension of mapped fault
- Photo–linear
- Strike and dip of compaction foliation
- Horizontal bedding
- Prospect pit
- Quarry
- Age dating sample location
- Hot Springs Landing thermal well

Figure 3. continued.

Tuff 2

In the northern part of the study area, Tuff 1 is overlain by a 20-meter-thick ash-flow unit, Tuff 2. The exposed base of Tuff 2 is a densely welded, partially devitrified, crystal lapilli ash-flow tuff containing black fiamme in a pinkish gray groundmass. No underlying basal vitrophyre or porous nonwelded zones were observed. The middle zones of Tuff 2 become increasingly devitrified and less welded with increasing distance from the base. The top of the unit is a slightly welded lapilli crystal tuff with abundant tridymite and alkali-feldspar vapor-phase crystals in the porous pumice fragments. The pumice fragments are maroon and show very slight compaction; the groundmass is light pink. The phenocryst mineralogy is quite similar to Tuff 1, consisting of about 5 percent quartz and sanidine. Tuff 2 is absent from the southeastern portion of the map area.

Tuff 3

Tuff 3 is restricted to the northern part of the study area where it is approximately 50 meters thick. Like the base of Tuff 2, the nonwelded base of Tuff 3 was not observed. However, Tuff 3 does have a well-developed vitrophyre near its base. This vitrophyre is similar to the vitrophyre at the base of Tuff 1 and consists of about 5 percent of sanidine and quartz grains in a matrix of black glass with minor rust-colored glassy bands. This vitrophyre grades upwards into a gray to maroon, densely welded zone in which most megascopic pyroclastic features are obscured by devitrification. Spherulitic devitrification is common in Tuff 3 and is recognized in hand sample as well-developed lithophysae. Lithophysae are most abundant in the zone of partial welding where they measure up to 10 centimeters in diameter. This spherulitic devitrification is useful in distinguishing Tuff 3 from Tuffs 1 and 2. This zone has also undergone minor vapor-phase crystallization. The top of Tuff 3 is a slightly welded lapilli crystal tuff containing barely flattened pinkish red pumice fragments in a salmon-pink groundmass. Lithophysae are absent from this zone; vapor-phase crystals of tridymite and alkali-feldspar occur in the pumice fragments. The phenocryst mineralogy and groundmass characteristics of this unit are discussed in Table 1, and the chemical composition is listed in Table 2.

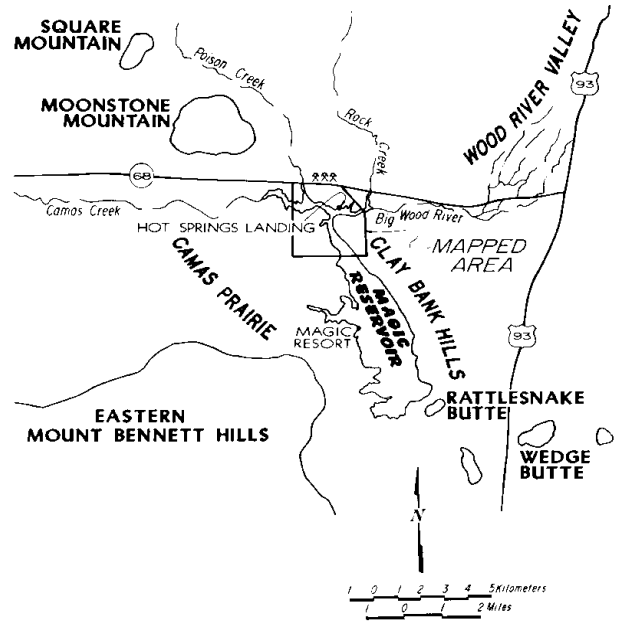

Figure 4. Physiographic map of the Magic Reservoir region, Blaine and Camas Counties, Idaho.

Table 1. Petrographic descriptions of the rhyolites and basalts at Magic Reservoir.

Rock Unit	Phenocryst Mineralogy	Groundmass Characteristics
The Older Rhyolite	This rock is comprised of 10 to 15% sanidine and anorthoclase laths, 10 to 15% subround quartz, 5% anhedral ferroaugite, lesser amounts of plagioclase, biotite, and opaque minerals, and accessory zircon and apatite. It also contains coarse-grained xenocrysts of microcline and plagioclase occurring as glomeroporphyritic clots associated with pyroxene and opaque minerals. The ferroaugite is altered in the devitrified portions of this unit to a fine-grained intergrowth of biotite, iron oxide, chlorite and serpentine.	The groundmass ranges from glassy to totally devitrified. The glassy portions are a hypocrystalline mixture of massive, nondevitrified glass, sparse patches of devitrified glass and tiny microlites. The devitrified variety consists mainly of patches of devitrified glass and microlites.
Square Mountain Basalt	This is a quartz-bearing basalt containing phenocrysts of plagioclase (An_{55}), glomeroporphyritic clots of 0.5 to 1.5 mm long plagioclase and minor pale-green augite and pigeonite, coarse-grained xenocrysts of plagioclase and microcline with a uniform "swiss-cheese texture," and sparse, 1 to 2 mm embayed quartz xenocrysts.	The groundmass consists of plagioclase, opaque minerals, dark brown interstitial glass and pyroxene microlites. This basalt has an intergranular texture.
Tuffs 1 and 2	These tuffs consist of a uniform phenocryst assemblage of 5 to 10% subhedral sanidine and anorthoclase, up to 1.0 mm in length, subround quartz ranging from 0.50 to 0.75 mm, minor plagioclase, biotite locally intergrown with chlorite and opaque minerals, and traces of apatite and zircon. These units also contain isolated grains and glomeroporphyritic clots of microcline, plagioclase associated with epidote and sericite, granophyric intergrowths of quartz and alkali feldspar, and moderately embayed quartz grains. The basal vitrophyre of Tuff 1 locally contains xenoliths of intergranular, augite-bearing basalt.	The basal vitrophyre of Tuff 1 is a nearly homogeneous black glass almost entirely lacking recognizable shard structures. All pumice fragments are completely collapsed and distorted, forming bands that resemble flow lines. Devitrification is minor; perlitic cracks are common. This vitrophyre resembles the zone of homogenization discussed by Smith (1960, p. 155) in which all pumice fragments, shards and glass dust are homogenized into a uniform glass. As welding decreases, the pumice fragments retain some of their original pore space. Vapor-phase crystallization becomes increasingly common in the porous pumice fragments in the partially welded to nonwelded portions of Tuff 1, and in small gas cavities within the groundmass. Devitrification is characterized by felty, radial, axiolitic and spherulitic intergrowths of alkali feldspar and cristobalite.
Tuff 3	Tuff 3 contains 5% phenocrysts of subround quartz, subhedral sanidine and anorthoclase, and minor plagioclase, hypersthene and opaque minerals. Hypersthene is altered to chlorite in the devitrified portions of this unit. The xenocryst content and mineralogy is similar to Tuff 1; no basaltic xenoliths were observed.	Except for the glassy, basal vitrophyre, this unit is characterized by abundant spherulitic devitrification. Spherulites consist of concentric bands of fine-grained intergrowth of cristobalite and alkali feldspar, exhibiting well-developed radial extinction. Vapor-phase crystallization is locally developed in gas cavities. Pumice fragments are recognizable throughout the unit. Glass shards, however, are difficult to identify due perhaps to their obliteration by extreme welding or devitrification.
The Rhyolite Dome	The flow-banded rhyolite contains 5 to 7% phenocrysts of fine-grained quartz, sanidine and anorthoclase, lesser amounts of plagioclase (An_{22-24}) and opaque minerals, minor biotite and orthopyroxene, and accessory zircon and apatite. The orthopyroxene commonly occurs in glomeroporphyritic clots with opaque minerals and biotite, and is altered to a fine-grained intergrowth of biotite, chlorite and iron-oxide pseudomorphs after pyroxene. The coarsely crystalline portions of the dome contain 15 to 20% phenocrysts with the same mineralogy as the flow-banded rhyolite. The phenocrysts are more altered than in the flow-banded rhyolite. The feldspar phenocrysts are partially altered to sericite and epidote, the mafic phenocryst clots are extremely corroded and altered.	The groundmass of the flow-banded rhyolite is largely devitrified, consisting mainly of spherulites exhibiting radial extinction. The flow-banding is faintly preserved in spite of the pervasive devitrification. Some of the flow bands remain glassy and reveal flowage around phenocrysts. The groundmass of the crystalline part of the dome is a cryptocrystalline intergrowth of quartz and feldspar.
Quaternary Basalts	The Quaternary basalts have an ophitic texture and consist of 1 mm augite grains enclosing 0.1 to 0.2 mm labradorite (An_{57-67}) laths, and glomeroporphyritic aggregates of labradorite, augite and minor olivine. The labradorite phenocrysts are acicular and radiate from a common point. Altered olivine and fresh augite microphenocrysts occupy the interstices of the radiating feldspars.	The groundmass consists of plagioclase and pyroxene microlites, abundant disseminated opaque minerals and interstitial glass.

Pumice of Magic Reservoir

The pumice of Magic Reservoir overlies Tuff 3 in the northern part of Tuff 1 in the southeastern part of the map area. It is well exposed in prospect pits and outcrops north of Hot Springs Landing and in a quarry on the north side of Idaho Highway 68, about 1.2 kilometers north-northwest of the landing (Figure 4). On the southeastern side of the study area, the pumice occurs only as float and is not mapped as a separate unit. The relationship between the pumice and Tuff 3 is unclear. The pumice probably represents a separate event from Tuff 3. However, it could also be the nonwelded top of Tuff 3.

This unit is a distinctive pale orange, poorly sorted pumice flow. Textural variations include pumiceous crystal tuff, pumiceous crystal lapilli tuff, and agglomerate. The pumice contains about 1 percent crystals of quartz and sanidine with minor biotite and obsidian. The fragments range in size from 30 millimeters to 1 meter and are identical in appearance to the surrounding tuff matrix. The pumice has a silky, vitreous luster and a filamentous texture. Exposed within the pumice unit in the quarry is a thin unit of air-fall tuff consisting of well-sorted, subround pumiceous lapilli identical to those described above.

Source Area for the Magic Reservoir Rhyolite Ash-Flow Tuffs

The source area for the Magic Reservoir ash-flow tuffs is unknown. The presently known areal distribution of these rocks is limited to the vicinity of Magic Reservoir (Rember and Bennett, 1979), suggesting a local source. The pumiceous agglomerate and air-fall tuff exposed in the quarry are characteristic of near-vent pyroclastic deposits. However, these rocks could be significantly younger than the Magic Reservoir ash-flow tuffs.

The extreme degree of welding in the Magic Reservoir ash-flow tuffs may also imply a nearby source. Dense welding is characteristic of either thick cooling units or high temperatures of emplacement (Smith, 1960; Ross and Smith, 1961). Because the individual cooling units at Magic Reservoir have a maximum thickness of only 50 meters, the observed

Table 2. Chemical composition of Magic Reservoir and other Snake River Plain rhyolites.*

	Tuff 1		Tuff 3	Dome		Older Rhyolite**		Other Snake River Plain Rhyolites		
	ID/BE-10C	ID/BE-6	ID/BE-12A	ID/BE-106	ID/BE-21A	ID/MR-6	ID/BE-115	Idavada Composite††	Moonstone Mountain§§	Wedge Butte§§
SiO_2	73.54	75.03	74.59	76.77	76.22	74.93	70.54	74.55	74.31	74.67
TiO_2	0.24	0.22	0.22	0.24	0.21	0.31	0.64	0.39	0.23	0.10
Al_2O_3	11.34	11.64	11.44	11.73	11.58	12.46	12.47	12.80	12.61	12.57
#Fe_2O_3	2.11	2.00	2.03	2.18	1.93	2.34	4.92	1.63	2.20	1.53
FeO	--	--	--	--	--	--	--	0.82	0.44	0.26
MnO	0.03	0.02	0.03	0.03	0.01	0.01	0.05	0.04	0.049	0.034
MgO	0.25	0.16	0.17	0.22	0.11	0.17	0.42	0.22	0.09	0.02
CaO	0.83	0.66	0.62	0.61	0.51	0.75	1.81	1.03	0.83	0.70
Na_2O	2.42	2.98	2.96	2.85	2.79	3.14	2.93	3.06	3.34	3.94
K_2O	5.86	5.41	5.47	5.69	5.60	5.60	5.33	5.42	5.17	4.91
P_2O_5	0.03	0.04	0.04	0.05	0.30	0.04	0.20	0.05	0.04	0.14
LOI	2.88	0.83	0.72	1.11	0.95	1.37	1.83	--	--	--
Oxide Total	99.53	98.99	98.29	101.48	100.21	101.12	101.14	100.01	99.31	98.87
Ba(ppm)	689	689	710	728	625	1,177	2,078	--	--	--
Zr(ppm)	272	276	274	274	267	388	697	--	--	--
†Sr(ppm)	58	50	50	51	49	106	188	--	--	--
†Be(ppm)	6.1	6.4	6.2	5.8	6.4	4.3	3.6	--	--	--
§Li(ppm)	32	42	43	19	42	28	20	--	--	--

*All analyses determined by lithium metaborate fusion ICP spectrographic techniques by R. Kroneman at the Earth Science Laboratory, University of Utah Research Institute, unless otherwise noted.
†Analysis determined by acid digestion ICP spectrographic technique.
§Lithium analyses determined by atomic absorption.
#Total Fe calculated as Fe_2O_3 for Magic Reservoir rhyolites.
**The variability in these two analyses is probably due to alteration. ID/MR-6 is somewhat altered; ID/BE-115 is glassy and fresh.
††Leeman and Manton, 1971.
§§W. P. Leeman, 1982a this volume.

dense welding is probably due in large part to high eruptive temperature. Since the hottest portion of an ash flow is likely to be close to the vent area, the inferred hot nature of the Magic Reservoir ash-flow tuffs may suggest a nearby source.

Schmidt (1961) speculates that Moonstone Mountain (Figure 4) is an eruptive center and the source of the Moonstone Rhyolite. The chemical composition of the Moonstone Rhyolite and the Magic Reservoir ash-flow tuffs is similar (Table 2). In addition, the potassium-argon age relationships discussed below suggest that the Moonstone Rhyolite and the Magic Reservoir ash-flow tuffs are contemporaneous. Additional field work, age-dating, and petrochemical study are needed to ascertain whether the Magic Reservoir ash-flow tuffs can be correlated with the Moonstone Rhyolite.

RHYOLITE DOME

The rhyolite dome of Magic Reservoir crops out 200 meters due north of the landing and along the waterfront west-northwest of the landing. This unit is best exposed in the massive cliffs 500 meters west-northwest of the landing where it attains a maximum thickness of 60 meters.

There are two textural varieties of this rhyolite. The most abundant type is a massive, vertically flow-banded rock. Large-scale vertical and concentric joints are developed parallel to the flow banding. Erosion along these joints produces ravines, crags, and spires. Flow banding is continuous for several meters but is locally folded and contorted. The rock is light gray and contains approximately 5 percent fine-grained phenocrysts of quartz and sanidine. Much of the flow banding retains a slightly glassy luster and is darker gray than the surrounding rock. This unit locally contains gas cavities and spherulites; minor vesiculation is common in the upper portions.

The second textural variety of this rhyolite, exposed near the waterline 0.75 kilometer west of the landing, is more coarsely crystalline and contains up to 15 percent phenocrysts of quartz, sanidine, biotite, and magnetite. The phenocrysts in this phase are more altered than those in the fine-grained, banded portion. Iron-oxide staining fringes the mafic and opaque phenocrysts; the feldspars are partially altered. This portion of the unit occurs at the base and in the interior of the dome. More detailed descriptions of the rhyolite dome are included in Table 1, and the chemical composition is listed in Table 2.

The contact between the dome and the ash-flow tuffs is very sharp. The feeder zone of the dome cross-cuts the ash-flow tuffs at a high angle. The contact is well exposed 500 meters west of Hot Springs Landing, a short distance above the water line. Locally the contact is a marginal friction-breccia (Williams and McBirney, 1979, p. 193) of angular ash-flow tuff fragments incorporated in the sides of the dome.

The steep concentric joints, flow banding, and rugged, spiney form of this rhyolite is characteristic of many silicic domes (Williams and McBirney, 1979, p. 188-190). The glassy, flow-banded rhyolite occurs in the upper and exterior parts of the dome; the more coarsely crystalline variety is from the more slowly cooled base and interior. The breccia of ash-flow tuff fragments locally developed along the contact of the rhyolite dome with the ash-flow tuffs clearly demonstrates that the dome is younger than the ash flows. Potassium-argon age relationships presented below verify this chronology. The breccia also suggests that this is a vent area which has been filled by the feeder zone of the rhyolite dome.

QUATERNARY SEDIMENTS, SEDIMENTARY ROCKS, AND BASALTS

Quaternary rocks are exposed throughout the study area and include three units of sediment, one sedimentary rock unit, and two basalts. These will be discussed in chronological order.

Myrtle Sediments

The oldest sedimentary unit in the area, the Myrtle sediments (Schmidt, 1961), is a sequence of fluvial and lacustrine arkosic sediments best exposed in prominent bluffs along the west side of Magic Reservoir from Magic Resort to Hot Springs Landing (Figure 4). This unit is also seen a short distance up Camas and Rock Creeks and in one small area 900 meters due south of Hot Springs Landing where it lapped onto a horst.

The Myrtle sediments form a 17-meter-thick outcrop at the west side of Poison Creek inlet. It may be much thicker since a driller's log of a water well at Hot Springs Landing indicates the presence of 79 meters of sand, gravel, and shale. The base is not exposed, even when the reservoir is near its lowest level. The upper contact is a conformable, although irregular, surface with the Quaternary Macon Basalt. The load-deformed top of the sediments 800 meters south-southwest of the landing displays 0.5 to 1-meter-thick interpenetrations with the base of the basalt.

This oldest sedimentary unit is so poorly lithified that sedimentary structures are not generally discernable. Where such structures are seen, the thinly

laminated to thinly cross-laminated strata, together with the presence of oscillation ripple marks, suggest lacustrine sedimentation. This unit is composed of both a subarkose and a subordinate amount of light gray-green shaley siltstone. The subarkose is medium to very coarse grained with scattered granitic and gneissic pebbles. It is poorly sorted with subangular to subrounded clasts, indicating rapid transportation and sedimentation from a nearby source area. The gray-green siltstone is best exposed along the west side of Poison Creek inlet where approximately 2 meters of beds are exposed when the reservoir is at low water level.

Quaternary Basalts

Two flat-lying Quaternary basalt flows are mapped near Hot Springs Landing. Malde and others (1963) assign these flows to the Bruneau Formation. Armstrong and others (1975) report a potassium-argon date of 0.8 million years for a Bruneau basalt flow 10.5 kilometers southeast of Hot Springs Landing. Schmidt (1961) assigns these basalts to the Bellevue Formation.

The two basalt flows are separated by a northwest-trending horst at Hot Springs Landing (Figure 3). Schmidt (1961) named the basalts southwest of the landing the Macon Member and the flows east of the landing the Wind Ridge Member. The basalts are distal tongues of flows which erupted from two widely spaced eruptive centers (Schmidt, 1961).

In the study area, the Macon Basalt has only one recognizable flow, whereas the Wind Ridge Basalt has at least three flows, each 4 to 8 meters thick. Otherwise, the two basalts are similar. The tops and bottoms of the flows are rubbly and vesicular. The interior portions display well-developed columnar jointing. On fresh surfaces, the basalt is medium to dark gray and has vesicles which are commonly filled with calcium carbonate. The rock is very fine grained with local aggregates of feldspar, pyroxene, and altered, bronze olivine. A petrographic description of the Quaternary basalts is included in Table 1.

Macon Sediments

The second sedimentary unit, the Macon sediments of Schmidt (1961), occurs at lower elevations throughout the study area and is up to 5 meters thick. The unit is totally unlithified and forms no outcrops. It is present only as a veneer of loose sand, gravel, and scattered cobbles. The base of the Macon sediments is not prominently exposed but appears to be conformable where it overlies the Macon Basalt and the Myrtle sediments. Otherwise, it is nonconformable with the older igneous units. The coarser clasts are dominantly gray orthoquartzite; the sand is arkosic. The Macon sediments were largely derived from Camas Creek, west of the Hot Springs Landing horst, and Rock Creek to the east.

Unnamed Quaternary Conglomerate

Unnamed Quaternary arkosic, silica-cemented conglomerates were recognized at four places in the study area. Along the east side of Poison Creek inlet (Figure 3) they form approximately 5-meter-thick resistant ledges, unconformable with the underlying Tuff 1. This conglomerate contains clasts of Magic Reservoir tuffs up to 30 centimeters long with smaller fragments of metasedimentary and granitic rocks. The conglomerate exhibits only the vaguest indications of bedding and was probably formed by a mixing of colluvium and Macon sediments transported to the site by Poison Creek.

A variant of this conglomerate occurs 200 meters N. 75° W. of the landing and 500 meters and 750 meters west of the landing on the south side of Camas Creek. Although similar to the conglomerate at Poison Creek, these three occurrences differ in having a greater proportion of locally derived tuff fragments, by having ferruginous and siliceous cement, and by exhibiting much smaller average clast size (10 centimeters maximum length). This ferruginous conglomerate is in close proximity to the major west-trending fault mapped along Camas Creek. The westernmost of these three outcrops is along the western horst-bounding fault. The ferruginous and siliceous nature of this conglomerate and its proximity to major faults in the area suggest that the silica and iron cements may be from fluids of possible thermal origin.

Quaternary Alluvium

The youngest sediment present in the area is Quaternary alluvium. No detailed study was done on these sediments, but where seen they are obvious mixtures of the lithologies from their respective drainages.

STRUCTURE

The structure of the Magic Reservoir area (Figure 3) is dominated by extensional tectonics. High-angle normal faults displace all pre-Quaternary rock units and give the area a block-faulted configuration. Major faults trend west, northwest, and northeast. A west-trending series of linear features extending from the southwestern portion of the mapped area to the Camas Prairie to the west (Figure 4) is also observed.

A major west-trending fault parallels the east-west segment of the Wood River east of Hot Springs Landing and Camas Creek west of the landing (Figure 4). This fault is mapped on the basis of stratigraphic offset and inferred from the presence of a prominent linear feature observed on aerial photographs. The south side of the fault has dropped relative to the north side. The amount of displacement is speculative because of the lack of a definitive marker horizon across the fault. Since the exposed thickness of Tuff 1 both north and south of the fault is the same, the base of Tuff 1 may represent a level, pre-ash-flow depositional surface, and therefore would be a relatively good marker horizon. If so, then the south side has dropped 200 meters relative to the north side.

Three minor west-trending faults are mapped in the area. Two are immediately north of Hot Springs Landing. The other is mapped in the Clay Bank Hills to the south. The displacement along these minor west-trending faults appears to be minimal, suggesting that they are nearly vertical, tensional fractures. Where observed, the relative movement of these faults is south side down. These smaller faults are probably step faults which formed in response to displacement of the larger fault. The persistent northerly dips of the ash-flow tuffs throughout the study area might be explained in terms of a slight rotation along the west-trending faults that formed a tilted, step-fault block pattern. A similar mechanism is postulated for the structures observed in fault blocks of the Basin and Range province (Stewart, 1971).

In addition to the west-trending faults, high-angle northwest- and northeast-trending normal faults also cut the silicic volcanic rocks and the Square Mountain Basalt. The two fault sets bound a horst, which will be referred to as the Hot Springs Landing horst. Because of the relatively continuous fault traces of these two sets of faults, they are believed to postdate the west-trending faults.

The northwest-trending faults are better exposed than the northeast-trending faults. As shown in Figure 3, a northwest-striking fault forms the prominent scarp along the west side of the Clay Bank Hills, isolates a small peninsula of ash-flow tuffs southwest of Hot Springs Landing, and forms the northwest-trending inlet of Poison Creek. Displacement is difficult to determine, but it is at least 150 meters, the height of the Clay Bank Hills fault scarp. Roughly paralleling this to the northeast is a less conspicuous fault which is mapped on the basis of a 14 meter offset in the ash-flow stratigraphy north of Hot Springs Landing.

A northeast-trending fault marks the boundary between the Magic Reservoir rhyolites and the Quaternary rocks east of Hot Springs Landing. Its southward extension is marked by a short linear scarp at the tip of the Clay Bank Hills. Continuation of the fault to the south beneath younger basalts and sediments is drawn on the basis of photo-linear interpretation. Topographic evidence suggests an offset in excess of 95 meters.

The overall pattern produced by the northwest- and northeast-trending faults is a scissors-type arrangement in which the Clay Bank Hills and the ridge north of Hot Springs Landing are separate V-shaped horsts. It is likely that this block faulting was established before the emplacement of the Quaternary basalts and sediments which are flat lying, largely unfaulted, and limited in areal distribution by the horsts.

The west- and northwest-trending features in the Magic Reservoir area conform to the regional structural patterns in this part of the Snake River Plain. The west-trending faults and linear features near Magic Reservoir parallel the east-west structural grain defined by the physiography in Camas Prairie to the west and the Mount Bennett Hills to the southwest (Figure 4). Both are prominent east-west-trending features in the north-central portion of the Snake River Plain, although their structural development and age relative to other features of the plain are unknown (Mitchell, 1976).

The northwest-striking faults coincide with the dominant regional structural grain mapped in the Mount Bennett Hills-Magic Reservoir area by Malde and others (1963), Smith (1966), and Mitchell (1976). A strong northwest-trending gravity anomaly just east of Hot Springs Landing (Mabey and others, 1974) parallels this northwest-trending fracture pattern. The high-angle, northwest-striking faults are believed to be the result of a tensional stress field that has existed for the last 5 million years in the north-central portion of the Snake River Plain (Furlong, 1979).

COMPARISON OF THE MAGIC RESERVOIR RHYOLITES WITH OTHER NEARBY SILICIC VOLCANIC ROCKS

The rhyolites of Magic Reservoir differ mineralogically and chemically from the Idavada Volcanics in the nearby eastern Mount Bennett Hills (Figure 4). The eastern Mount Bennett Hills Idavada sequence is composed of a series of silicic ash-flow tuffs and minor intercalated basalts with an aggregate thickness of 457 meters (Smith, 1966). These ash-flow tuffs are apparently less silica-rich than the units at Magic Reservoir. The SiO_2 content of the eastern Mount

Bennett Hills Idavada Volcanics ranges from 67 to 71 percent, as determined by Smith (1966) from measurements of refractive indices of fused glass samples from the welded portions of the tuffs (complete chemical analyses for these rocks are not available). The SiO_2 content of the Magic Reservoir rocks ranges from 70.54 to 76.77 percent as determined by inductively coupled argon plasma (ICP) spectroscopy (Table 2). In contrast to the sanidine-rich Magic Reservoir rhyolites, the feldspar phenocryst assemblage of the eastern Mount Bennett Hills Idavada Volcanics is composed mainly of plagioclase with minor sanidine (Smith, 1966). The chemistry of a composite sample of Idavada Volcanics is shown in Table 2. Additional work on the petrochemistry of silicic volcanic rocks in the Snake River Plain is needed to ascertain whether there is significant chemical variation between the Magic Reservoir rhyolites and other Snake River Plain rhyolites.

The Moonstone Rhyolite exposed in the extreme eastern portion of the Mount Bennett Hills (Smith, 1966; Schmidt, 1961) and at Moonstone Mountain (Schmidt, 1961) is mineralogically and chemically similar to the older rhyolite of Magic Reservoir. Moonstone Mountain is an endogenous rhyolite dome containing abundant phenocrysts of fresh sanidine, rounded resorbed quartz, altered plagioclase, pigeonite, oxyhornblende, and accessory magnetite, zircon, apatite, and allanite (Schmidt, 1961). Schmidt (1961) states that a rhyolitic composition has been determined for the rocks of Moonstone Mountain, although a chemical analysis is not provided. The base of the dome is described by Schmidt (1961) as dark brown, dense, glassy, and highly porphyritic. Reconnaissance field examination of the lobate flow extending southeast from the base of Moonstone Mountain reveals striking textural and mineralogical similarity between this unit and the older rhyolite of Magic Reservoir. As shown in Table 2, the older rhyolite of Magic Reservoir and Moonstone Rhyolite are chemically similar. In addition, the Moonstone Rhyolite is locally overlain by the Square Mountain Basalt and thus occupies the same stratigraphic position as the older Magic Reservoir rhyolite in the southeastern part of the study area. On the basis of their stratigraphic position, and mineralogical and chemical similarity, these two units are tentatively correlated with each other. Additional work is needed to verify this correlation.

Four silicic domelike features, Rattlesnake Butte, Wedge Butte, and two unnamed buttes, occur southeast of Magic Reservoir (Figure 4). Reconnaissance field examination suggests that these are circular, funnel-shaped structures with well-developed flow layering and steep concentric jointing. Petrographic examination of the silicic lavas from Rattlesnake Butte reveals many similarities to the more coarsely crystalline interior portions of the rhyolite dome at Magic Reservoir. A chemical analysis of the rhyolite at Wedge Butte is included in Table 2.

REGIONAL VOLCANIC STRATIGRAPHY AND AGE RELATIONSHIPS OF THE MAGIC RESERVOIR RHYOLITES

Three rhyolites from the Magic Reservoir study area were selected for potassium-argon dating (Table 3). These newly reported ages suggest that silicic volcanism in the Magic Reservoir area spans the period between 5.81 ± 0.69 million years and 3.06 ± 0.04 million years. The 3.06 million-year date was obtained by Armstrong and others (1975) from feldspars in the rhyolite of Wedge Butte. On the basis

Table 3. Potassium-argon dates and analytical data for the Magic Reservoir rhyolites.

Sample No.	Unit	Material Dated	Weight (gm)	%K	$^{40}Ar_{rad}$(x10^{11}) (Moles/gm)	$\%^{40}Ar_{atm}$	Age (m.y.)
ID/BE-21A	Dome (Tmrd)	Sanidine	0.20200	6.19	5.123	75	4.77 ± 0.29
ID/BE-10C	Tuff 1 (Tmr_1)	Anorthoclase	0.21614	7.86	7.699	53	5.64 ± 0.23
ID/BE-115	Older Rhyolite (Tor)	Anorthoclase	0.21061	4.58	4.626	88	5.81 ± 0.69

Constants Used:

$\lambda_\beta = 4.962 \times 10^{-10}$/yr.

$\lambda_\epsilon = 0.581 \times 10^{-10}$/yr.

$^{40}K/K_{Tot.} = 1.167 \times 10^{-4}$ Atom/Atom

Potassium-argon dating performed by S. H. Evans, Jr., at the University of Utah.
Potassium analyses done by lithium metaborate fusion technique of Suhr and Ingamells (1966).
Argon analyses used standard isotope dilution techniques slightly modified from those of Dalrymple and Lanphere (1969).
Error limits to one standard deviation.

of these dates, there appears to be two periods of silicic magmatism in the Magic Reservoir area. The earliest event, the Magic Reservoir event, occurred around 5.81 million years ago. This period includes both the older rhyolite and the ash-flow tuffs at Magic Reservoir. (Since the age dates for these rocks are statistically indistinguishable, they are considered the same event.) The Magic Reservoir period is also inferred to include the Moonstone Rhyolite on the basis of the tentative correlation between the Magic Reservoir older rhyolite and the Moonstone Rhyolite. This inferred age relationship lends support to the contention that Moonstone Mountain may be the source of the Magic Reservoir ash-flow tuffs.

The second period of silicic magmatism in the Magic Reservoir area is the 3.06-million-year-old Wedge Butte event. The available information presently limits this stage to Wedge Butte, since the ages of the three other nearby domes are unknown. The 4.77-million-year-old Magic Reservoir dome might be an earlier phase of this volcanism. However, the nearly identical ages and chemistry of the Magic Reservoir dome and ash-flow tuffs suggest that the dome probably represents the waning stages of the Magic Reservoir event. In contrast to the explosive nature of the Magic Reservoir volcanism, no pyroclastic rocks have yet been identified with the Wedge Butte period.

REGIONAL SIGNIFICANCE OF THE MAGIC RESERVOIR RHYOLITES

Regional age-dating studies of silicic and basaltic volcanic rocks in the Snake River Plain (Armstrong and others, 1975, 1980) demonstrate that volcanism in the Snake River Plain migrates with time from west to east. The Idavada silicic volcanic sequence began about 15 million years ago in the western Snake River Plain and about 5 million years ago in the eastern Snake River Plain. Although few caldera structures are known in the western Snake River Plain due to burial by younger basalts, the Idavada Volcanics probably erupted from a series of nested or coalescing calderas. Subsidence along the axes of these coalescing calderas may, in part, form the axial downwarp of the Snake River Plain (Christiansen and Lipman, 1972; Suppe and others, 1975; Prostka, 1975; Bonnichsen, 1982 this volume; Ekren and others, 1982 this volume; Embree and others, 1982 this volume; and Leeman, 1982b this volume).

This phase of silicic volcanism is followed by dominantly basaltic volcanism which has filled and buried most of the caldera structures. Like the silicic volcanic event, basaltic volcanism is also time-transgressive, occurring about 10 million years ago in the western Snake River Plain and shifting eastward with time to its present position in the eastern Snake River Plain (Armstrong and others, 1975).

The rhyolites of the Magic Reservoir area do not fit well into this described pattern of eastward-transgressive silicic volcanism. The potassium-argon dates for the Magic Reservoir rhyolites and for Wedge Butte are anomalously young when compared with the ages of nearby Idavada volcanic rocks. For example, in the eastern Mount Bennett Hills, the base of the Idavada Volcanics is 10.0 million years old. In the northern Mount Bennett Hills an 11.0-million-year date is reported for an unidentified horizon in the Idavada sequence (Armstrong and others, 1980). Other silicic volcanic rocks in this portion of the Snake River Plain range in age from 6.25 million years at Shoshone Falls, east-northeast of Twin Falls, to 9.2 million years in the Malta Range, east-southeast of Twin Falls (Armstrong and others, 1975; Williams and others, 1982 this volume). These dates are shown in the time-space profile of Figure 5. On the basis of these age dates it is clear that the flows and pyroclastic rocks of Magic Reservoir should not be grouped with the rhyolites from the eastern Mount Bennett Hills or other rhyolites in the central Snake River Plain. The Magic Reservoir rhyolites are comparatively young and represent a local renewal of silicic volcanism. They are the youngest silicic volcanic rocks presently known this far west in the Snake River Plain.

The young age of the Magic Reservoir rhyolites can perhaps be best understood when placed within the regional framework of time-transgressive volcanism in the Snake River Plain. Although the initiation of silicic and basaltic volcanism in the western Snake River Plain predates the initiation in the eastern Snake River Plain (Figure 5), there are abundant examples of contemporaneous Pleistocene basalts throughout the Snake River Plain. The presence of Pleistocene basalts in the western Snake River Plain suggests that it is the inception of volcanism and not the termination of volcanism that migrates with time. Once volcanism has commenced in an area, it may persist. The Magic Reservoir rhyolites represent a unique example of persistent silicic volcanism in the central Snake River Plain. Possible analogs of persistent, anomalously young silicic volcanism in and near the eastern Snake River Plain might include the 0.08-million-year-old China Hat rhyolite dome east of Pocatello or the 0.3-million-year-old rhyolites (Armstrong and others, 1975) at Big Southern Butte west-southwest of Idaho Falls (Figure 5).

The wide range of ages of silicic volcanic rocks in this portion of the Snake River Plain could also be due to the stratigraphic complexity of the Idavada

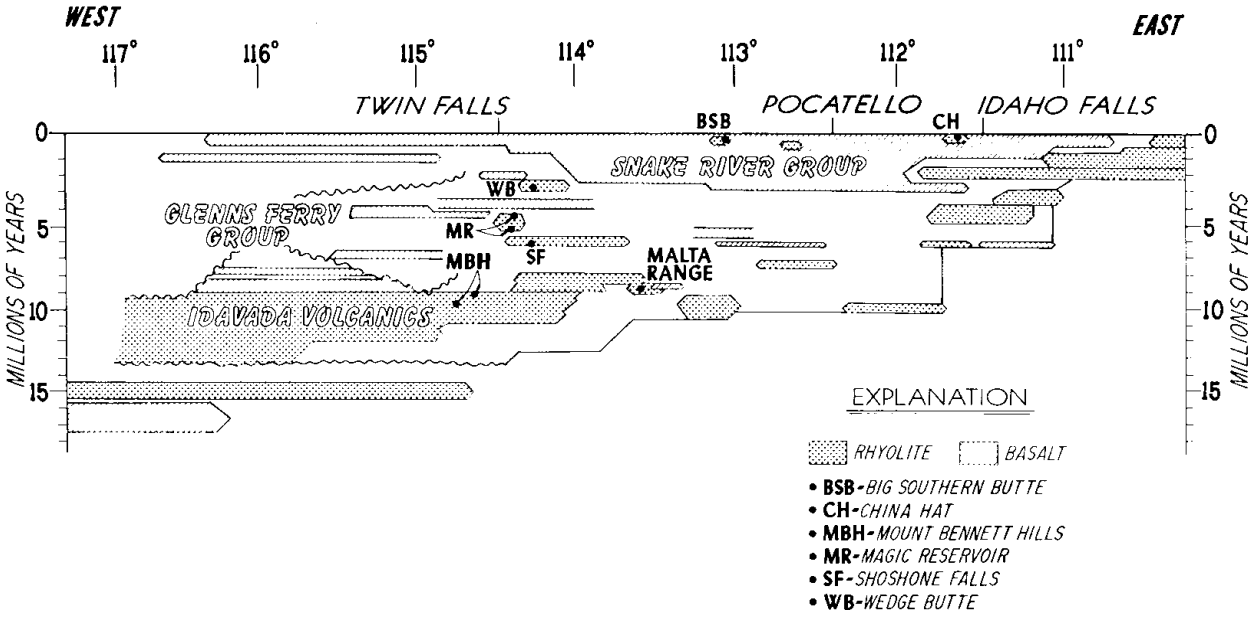

Figure 5. Space-time profile of volcanic rocks along the Snake River Plain, Idaho (modified after Armstrong and others, 1980).

Volcanics. The space-time profile of Figure 5 is probably overly simplified (W. P. Leeman, 1981, verbal communication), since the stratigraphy of the Idavada Volcanics is largely unknown. It is thus unclear whether the dates for Idavada rocks from one location can be meaningfully compared with dates from another location. Divergent dates could represent, in part, different stratigraphic positions within the Idavada volcanic sequence. With this in mind, it would be useful to obtain a date from the top of the Idavada volcanic rocks in the eastern Mount Bennett Hills for comparison with the age of the Magic Reservoir event.

GEOTHERMAL GEOLOGY OF THE MAGIC RESERVOIR AREA

The developed geothermal resource at Hot Springs Landing presently consists of a 79-meter-deep well that produces 57 liters per minute of 71° C (160° F) water (Mitchell and others, 1980). This well was drilled at the former site of Magic Reservoir Hot Springs. The hot springs, which dried up following drilling of the well, had a reported temperature of 36° C (100° F) and a flow rate of 492 liters per minute (Ross, 1971). The ferruginous, silica-cemented sediments west and northwest of the landing may be an additional manifestation of the geothermal system. Fluid samples from the geothermal well yield a mean geothermometer estimate of reservoir temperature at depth of 149° C (300° F) (Muffler, 1979).

Like many of the geothermal resources in the Snake River Plain, the Magic Reservoir system is associated with normal faults. The system probably derives its heat from deep circulation of fluids along fractures. Fluids, which become heated at depth by conduction of heat from the rocks, may rise due to thermal expansion and become part of a hydrothermal convective cell as shown in Figure 6. Where favorable permeable structures like fault zones intersect this convective cell, the geothermal fluids may rise to the surface, forming hot springs. The area immediately surrounding the zone of upward-flowing water will have an elevated geothermal gradient due to the local convection of hot water. This convective gradient and associated heat flow anomaly are commonly limited in areal extent and should not be extrapolated to depth or to areas removed from the immediate hot spring vicinity. Isothermal zones may occur along the fault in systems with rapid upward convective flow (Figure 6).

Numerous faults near Magic Reservoir might serve as suitable geothermal fluid conduits. The intersection of the southeastern corner of the Magic Reservoir horst with the fractures trending north-northeast and west is immediately east-southeast of the landing. Fault intersections commonly play a role in localizing geothermal systems due to the enhancement of fracture-induced permeability. As suggested by Mitchell (1976), the hot springs present before the drilling of the well at Hot Springs Landing may have been controlled by the intersection of these fracture zones. Since northwest-trending structures are domi-

nant on both a local and regional scale, the northwest-trending fractures may play the most important role in controlling the circulation of geothermal fluids.

Geothermometers (Fournier and others, 1974) are commonly used indicators of equilibrium temperature at depth. When coupled with nearby conductive geothermal gradient data, the minimum depth of circulation necessary to attain a geothermometer-predicted temperature can be estimated. The flowing geothermal well reflects a convective geothermal gradient and is not representative of the background conductive gradient (Figure 6). Unfortunately, no geothermal gradient data are available from the immediate vicinity of Magic Reservoir. The nearest available conductive geothermal gradient is 60° C per kilometer measured in a 52-meter-deep well at sec. 21, T. 2 S., R. 20 E., about 28 kilometers east-southeast of Hot Springs Landing (Brott and others, 1976). Extrapolating this conductive gradient to the Magic Reservoir area and assuming a yearly average shallow ground-water temperature of 15° C implies that the Magic Reservoir fluids must circulate to a minimum depth of 2.2 kilometers to attain a temperature of 149° C, the mean geothermometer estimate of reservoir temperature. Mitchell (1976) predicts a similar depth to the geothermal reservoir. Due to the slow and inefficient transfer of heat from rocks to water, fluids must probably circulate much deeper to reach this temperature. In zones of upward flow of geothermal fluids, 149° C water might be found at significantly shallower depths due to the upward-bowing of isotherms along zones of enhanced permeability and rapid convective flow, as shown in Figure 6. Such a zone of anomalous fluid temperature and fluid flow would be the target of a geothermal exploration program in the Magic Reservoir area.

The presence of young silicic volcanic rocks in the area does not suggest a molten or partially molten magma body at depth acting as a heat source for the Magic Reservoir system. As Figure 7 indicates, Smith and Shaw (1975, 1979) show that magma bodies with volumes between 1 and 10 cubic kilometers lose a significant amount of their magmatic heat and reach ambient temperatures at the depth of emplacement within 100,000 years after eruption. The age of the silicic volcanic rocks in the Magic Reservoir area implies that the system would have to be on the order

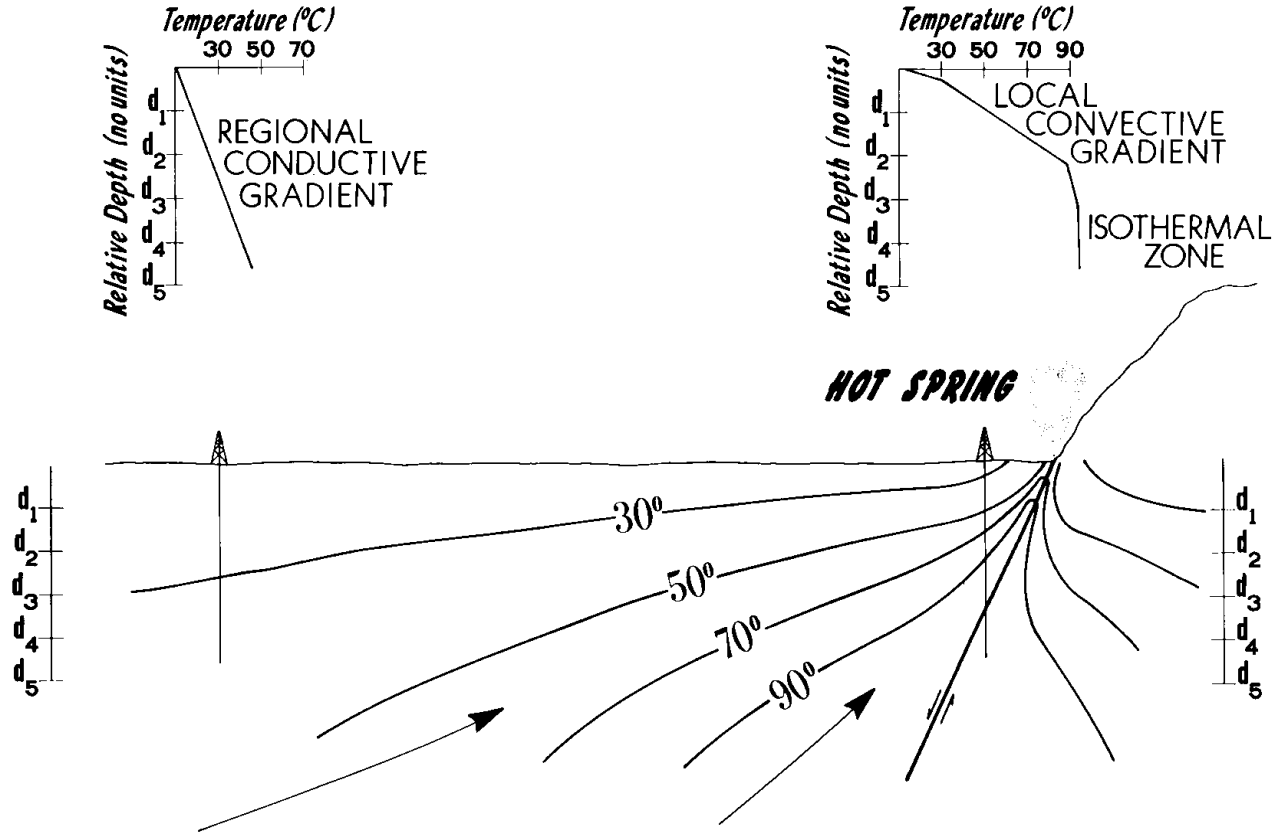

Figure 6. Idealized cross section and temperature-depth profiles of a geothermal convection system (isotherms modified after Wilson and Chapman, 1980).

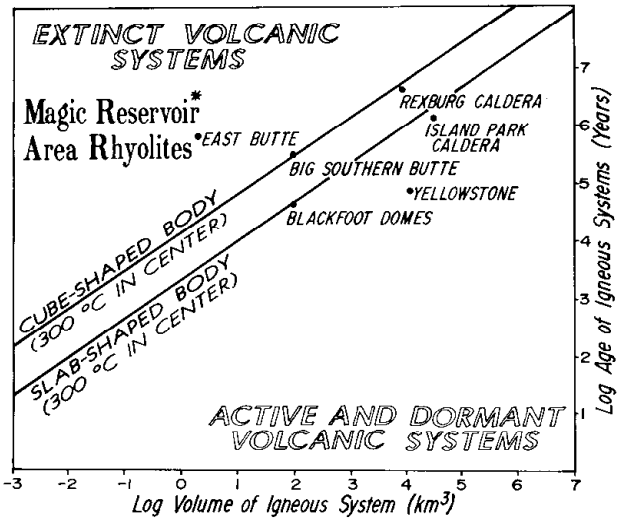

Figure 7. The relationship of theoretical conductive cooling models to age, size, and shape of selected young igneous systems in Idaho and Wyoming (modified after Smith and Shaw, 1979).

of 1,000 cubic kilometers to retain any magmatic heat. No evidence is available to suggest that the volcanic system is this large. Assuming an approximate volume of 3 cubic kilometers for the Magic Reservoir system based upon the presently known areal distribution of about 20 square kilometers and an average thickness of 150 meters, and assuming that the erupted volume corresponds to the volume of the remaining magma chamber (Smith and Shaw, 1979), the inferred 3 cubic kilometer Magic Reservoir magma body would cool to 300°C in the center within 10,000 to 100,000 years after eruption (Figure 7). A more accurate estimate of the volume of the Magic Reservoir system cannot be made since the source area for these rocks is unknown. However, even if the distribution of the Magic Reservoir volcanic rocks is broadened to include the Wedge Butte event, the other undated domes southeast of Hot Springs Landing, and the southwestern extension of the Moonstone Rhyolite (Schmidt, 1961; Smith, 1966), the system is still too small to be molten. It is thus apparent that the heat flow observed at Magic Reservoir is due to the regional conductive heat flow and is not augmented by any latent magmatic heat.

The 0.8-million-year-old Bruneau basalt 10.5 kilometers southeast of Hot Springs Landing (Armstrong and others, 1975) and the younger but undated Shoshone basalts south of the landing (Malde and others, 1963) are examples of the widespread recent basaltic volcanism common throughout much of the Snake River Plain, suggesting that the area is still an active basaltic magmatic province. However, like the silicic volcanic rocks, these basalts probably have insufficient volume to act as sources of magmatic heat. The conditions that may give rise to basalt formation, such as partial melting in the mantle due to elevated mantle temperatures, may enhance the regional conductive geothermal gradient and heat flow.

Despite the absence of a magmatic heat source, this part of Idaho has high heat flow. The average heat flow for the western Snake River Plain ranges from 1.7 HFU (heat flow unit) in the center and up to 3.0 HFU along the margins, compared with the average continental crustal heat flow of 1.5 HFU for the stable interior of the North American Plate (Brott and others, 1976; Mabey, 1982 this volume). Recent gravity modeling of the western Snake River Plain (Mabey, 1976) reveals that this area has an anomalously thin upper crust which may provide less insulation than crust of normal thickness to heat flux from the mantle below, resulting in the observed elevated thermal regime. Areas of high heat flow are commonly associated with zones of thin crust (Condie, 1976, p. 60).

The position of the Magic Reservoir system along the northern border of the Snake River Plain, adjacent to the Idaho batholith, may also contribute to the elevated heat flow of the area. The southern and northern margins of the western Snake River Plain are areas of anomalously high heat flow compared with the interior of the western Snake River Plain. Brott and others (1978) attribute this enhanced heat flow to refraction of heat from high-conductivity granitic rocks of the Idaho batholith in contact with the lower-conductivity sedimentary and volcanic rocks of the Snake River Plain.

SUMMARY AND SUGGESTIONS FOR ADDITIONAL WORK

Additional geologic mapping, petrochemical study, and radiometric dating of the silicic volcanic rocks in the Magic Reservoir-Mount Bennett Hills area could help unravel the eruptive history of this part of the Snake River Plain. The regional stratigraphic and age relationships of the Magic Reservoir rhyolites to other nearby silicic volcanic rocks should be determined. In particular, the correlation proposed in this study between the Magic Reservoir rhyolites and the Moonstone Rhyolite should be tested. The top of the Idavada Volcanics in the eastern Mount Bennett Hills should be dated for comparison with the Moonstone Rhyolite and Magic Reservoir rhyolites. The age of the pumice at Magic Reservoir should be obtained in order to date the youngest, local pyroclastic event. The three undated domes southeast of the landing should be studied to see whether they correlate with

Wedge Butte or are closer in age to the dome at Magic Reservoir. Additional study of the distribution, age relationships, and petrochemical affinity of these rocks may identify their eruptive source or sources and refine our understanding of the volcanic history of the western Snake River Plain.

The geothermal system at Magic Reservoir is controlled by deep circulation of fluids along fractures. The system probably does not derive any heat from the silicic volcanic rocks in the area since they are apparently too old to be associated with a molten or partially molten magma body. Thermal gradient drilling and testing are needed to evaluate further the geothermal potential of the area.

ACKNOWLEDGMENTS

This study was performed under the User Assistance Program at the Earth Science Laboratory/University of Utah Research Institute. Funding was provided by the U. S. Department of Energy, Division of Geothermal Energy, under contract number DE-AC07-80ID12079. The authors wish to thank D. Foley, J. Moore, D. Nielson, J. Stringfellow, and E. Struhsacker for reviewing this paper, K. Wallwork and G. Mitoff for typing the manuscript, K. Thompson and D. Cullen for drafting the figures, and R. Kroneman for performing the chemical analyses.

REFERENCES

Armstrong, R. L., W. P. Leeman, and H. E. Malde, 1975, K-Ar dating, Quaternary and Neogene volcanic rocks of the Snake River Plain, Idaho: American Journal of Science, v. 275, p. 225-251.

Armstrong, R. L., J. E. Harakal, and W. M. Neill, 1980, K-Ar dating of Snake River Plain (Idaho) volcanic rocks—new results: Isochron West, no. 27, p. 5-10.

Bonnichsen, Bill, 1982, The Bruneau-Jarbidge eruptive center, southwestern Idaho, *in* Bill Bonnichsen and R. M. Breckenridge, editors, Cenozoic Geology of Idaho: Idaho Bureau of Mines and Geology Bulletin 26.

Brott, C. A., D. D. Blackwell, and J. C. Mitchell, 1976, Geothermal investigations in Idaho, Part 8, heat flow study of the Snake River Plain, Idaho: Idaho Department of Water Resources Water Information Bulletin 30, 195 p.

———, 1978, Tectonic implications of the heat flow of the western Snake River Plain: Geological Society of America Bulletin, v. 89, p. 1697-1705.

Christiansen, R. L. and P. W. Lipman, 1972, Cenozoic volcanism and plate-tectonic evolution of the western United States—Part II, Late Cenozoic: Royal Society of London Philosophical Transactions, series A, v. 271, p. 249-284.

Condie, K. C., 1976, Plate tectonics and crustal evolution: Pergamon Press, Inc., New York, 288 p.

Dalrymple, G. B. and M. A. Lanphere, 1969, Potassium-argon dating: W. H. Freeman and Company, San Francisco, 250 p.

Ekren, E. B., D. H. McIntyre, E. H. Bennett, and R. F. Marvin, 1982, Cenozoic stratigraphy of western Owyhee County, Idaho, *in* Bill Bonnichsen and R. M. Breckenridge, editors, Cenozoic Geology of Idaho: Idaho Bureau of Mines and Geology Bulletin 26.

Embree, G. F., L. A. McBroome, and D. J. Doherty, 1982, Preliminary stratigraphic framework of the Pliocene and Miocene rhyolites, eastern Snake River Plain, Idaho, *in* Bill Bonnichsen and R. M. Breckenridge, editors, Cenozoic Geology of Idaho: Idaho Bureau of Mines and Geology Bulletin 26.

Fournier, R. O., D. E. White, and A. H. Truesdell, 1974, Geochemical indicators of subsurface temperature—Part 1, basic assumptions: U. S. Geological Survey Journal of Research, v. 2, no. 3, p. 259-262.

Furlong, K. P., 1979, An analytic stress model applied to the Snake River Plain (northern Basin and Range province, U.S.A.): Tectonophysics, v. 58, p. 11-15.

Leeman, W. P., 1982a, Geology of the Magic Reservoir area, Snake River Plain, Idaho, *in* Bill Bonnichsen and R. M. Breckenridge, editors, Cenozoic Geology of Idaho: Idaho Bureau of Mines and Geology Bulletin 26.

———, 1982b, Development of the Snake River Plain-Yellowstone Plateau province, Idaho and Wyoming: an overview and petrologic model, *in* Bill Bonnichsen and R. M. Breckenridge, editors, Cenozoic Geology of Idaho: Idaho Bureau of Mines and Geology Bulletin 26.

Leeman, W. P. and W. I. Manton, 1971, Strontium isotopic composition of basaltic lavas from the Snake River Plain, southern Idaho: Earth and Planetary Science Letters, v. 11, p. 420-434.

Mabey, D. R., 1976, Interpretation of a gravity profile across the western Snake River Plain, Idaho: Geology, v. 4, p. 53-55.

———, 1982, Geophysics and tectonics of the Snake River Plain, Idaho, *in* Bill Bonnichsen and R. M. Breckenridge, editors, Cenozoic Geology of Idaho: Idaho Bureau of Mines and Geology Bulletin 26.

Mabey, D. R., D. L. Peterson, and L. W. Wilson, 1974, Preliminary gravity map of southern Idaho:

U. S. Geological Survey Open-File Report 74-78, 1 sheet, scale 1:500,000.

Malde, H. E., H. A. Powers, and C. H. Marshall, 1963, Reconnaissance geologic map of west-central Snake River Plain, Idaho: U. S. Geological Survey Miscellaneous Geologic Investigations Map I-373, scale 1:125,000.

Mitchell, J. C., 1976, Geothermal investigations in Idaho, Part 7, geochemistry and geologic setting of the thermal waters of the Camas Prairie area, Blaine and Camas counties, Idaho: Idaho Department of Water Resources Water Information Bulletin 30, 44 p.

Mitchell, J. C., L. L. Johnson, and J. E. Anderson, 1980, Geothermal investigations in Idaho, Part 9, potential for direct heat application of geothermal resources: Idaho Department of Water Resources Water Information Bulletin 30, 396 p.

Muffler, L. J. P., editor, 1979, Assessment of geothermal resources of the United States—1978: U. S. Geological Survey Circular 790, 163 p.

Prostka, H. J., 1975, Structure and origin of the eastern Snake River Plain, Idaho (abstract): Geological Society of America, Abstracts with Programs, v. 7, no. 5, p. 637.

Rember, W. C. and E. H. Bennett, 1979, Geologic map of the Hailey quadrangle, Idaho: Idaho Bureau of Mines and Geology, Geologic Map Series, Hailey 2° quadrangle, scale 1:250,000.

Ross, C. S. and R. L. Smith, 1961, Ash-flow tuffs: their origin, geologic relations and identification: U. S. Geological Survey Professional Paper 366, 81 p.

Ross, S. H., 1971, Geothermal potential of Idaho: Idaho Bureau of Mines and Geology Pamphlet 150, 72 p.

Schmidt, D. L., 1961, Quaternary geology of the Bellevue area in Blaine and Camas Counties, Idaho: University of Washington Ph.D. thesis, 135 p.

Smith, C. L., 1966, Geology of eastern Mount Bennett Hills, Camas, Gooding and Lincoln Counties, Idaho: University of Idaho Ph.D. thesis, 170 p.

Smith, R. L., 1960, Zones and zonal variations in welded ash-flows: U. S. Geological Survey Professional Paper 354-F, p. F149-F159.

Smith, R. L. and H. R. Shaw, 1975, Igneous-related geothermal systems, *in* D. E. White and D. L. Williams, editors, Assessment of Geothermal resources of the United States—1975: U. S. Geological Survey Circular 726, p. 58-83.

———, 1979, Igneous-related geothermal systems, *in* L. J. P. Muffler, editor, Assessment of Geothermal Resources of the United States—1978: U. S. Geological Survey Circular 790, p. 12-17.

Stewart, J. H., 1971, Basin and range structure: a system of horsts and grabens produced by deep-seated extension: Geological Society of America Bulletin, v. 82, p. 1019-1044.

Suhr, N. H. and C. O. Ingamells, 1966, Solution technique for analysis of silicates: Analytical Chemistry, v. 38, p. 730-734.

Suppe, John, Christine Powell, and Robert Berry, 1975, Regional topography, seismicity, Quaternary volcanism, and the present day tectonics of the western United States: American Journal of Science, v. 275-A, p. 397-436.

Williams, Howel and A. R. McBirney, 1979, Volcanology: Freeman, Cooper, & Company, San Francisco, 397 p.

Williams, P. L., H. R. Covington, and K. L. Pierce, 1982, Cenozoic stratigraphy and tectonic evolution of the Raft River basin, Idaho, *in* Bill Bonnichsen and R. M. Breckenridge, editors, Cenozoic Geology of Idaho: Idaho Bureau of Mines and Geology Bulletin 26.

Wilson, W. R. and D. S. Chapman, 1980, Three topical reports: I. thermal studies at Roosevelt Hot Springs, Utah; II. heat flow above an arbitrary dipping plane of heat sources; III. a datum correction for heat flow measurements made on an arbitrary surface: University of Utah Report, DOE/ID/12079-19, 144 p.

The Geology of Big Southern Butte, Idaho

by

Dallas B. Spear[1] and John S. King[2]

ABSTRACT

Big Southern Butte is the largest of three prominent buttes which rise above the relatively flat accumulations of Quaternary basalt flows between Arco and the Idaho Falls-Blackfoot area on the eastern Snake River Plain in Idaho. It stands 760 meters above the plain and has a diameter of 6.5 kilometers at its base. It is a 300,000 year old rhyolitic dome complex that consists of two coalesced cumulo domes and an elevated section of older basalt flows approximately 350 meters thick. The basalt section covers most of the northern slope of the butte.

Big Southern Butte began its development as a laccolithic intrusion but due to its shallow emplacement broke through to the surface and continued its evolution by endogenous growth. The emplacement of the rhyolite was controlled by two intersecting structural trends: one, northeast-southwest, paralleling the long axis of the plain and the other, northwest-southeast, reflecting the extension of basin and range faulting onto the plain. The northeast-southwest trend is defined by the concentration of large eruptive centers and may be due to a high thermal input concentrated along the axis of the Snake River Plain at depth.

INTRODUCTION AND SETTING

Three buttes rise prominently above the relatively flat accumulations of Quaternary basalt flows between Arco and the Idaho Falls-Blackfoot area on the eastern Snake River Plain in Idaho. These unique features are aligned on a northeast trend and from southwest to northeast are known as Big Southern Butte, Middle Butte, and East Butte (Figure 1). Big Southern Butte and East Butte are rhyolite domes, and Middle Butte is an elevated block of basalt flows, dipping about 10 degrees to the south. Although no rhyolite crops out at Middle Butte, magnetic and gravity data suggest that a silicic intrusion underlies the basalt cap rock (Schoen, 1974).

Big Southern Butte is by far the most prominent topographic feature of this entire area. It is about 6½ kilometers across at its base and stands 760 meters above the surrounding terrain (Figure 2). The slopes of Big Southern Butte are steep—commonly in excess of 30 degrees—and are dissected by ravines and canyons which contribute debris to the broad apron of talus surrounding the butte. On the northwest side a deep canyon merges at the lower end with a broad alluvial fan. The slope up this fan and canyon allows

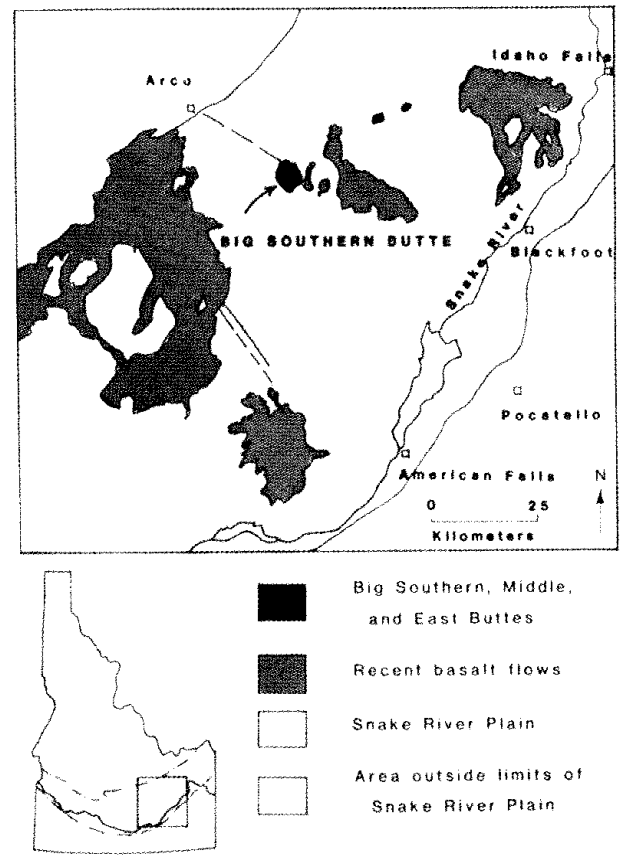

Figure 1. Eastern Snake River Plain, Idaho, showing location of Big Southern Butte.

[1]Arco Exploration Company, Houston, Texas 75221.
[2]State University of New York at Buffalo, Amherst, New York 14226.

Spear, D. B. and J. S. King, 1982, The geology of Big Southern Butte, Idaho, *in* Bill Bonnichsen and R. M. Breckenridge, editors, Cenozoic Geology of Idaho: Idaho Bureau of Mines and Geology Bulletin 26, p. 395-403.

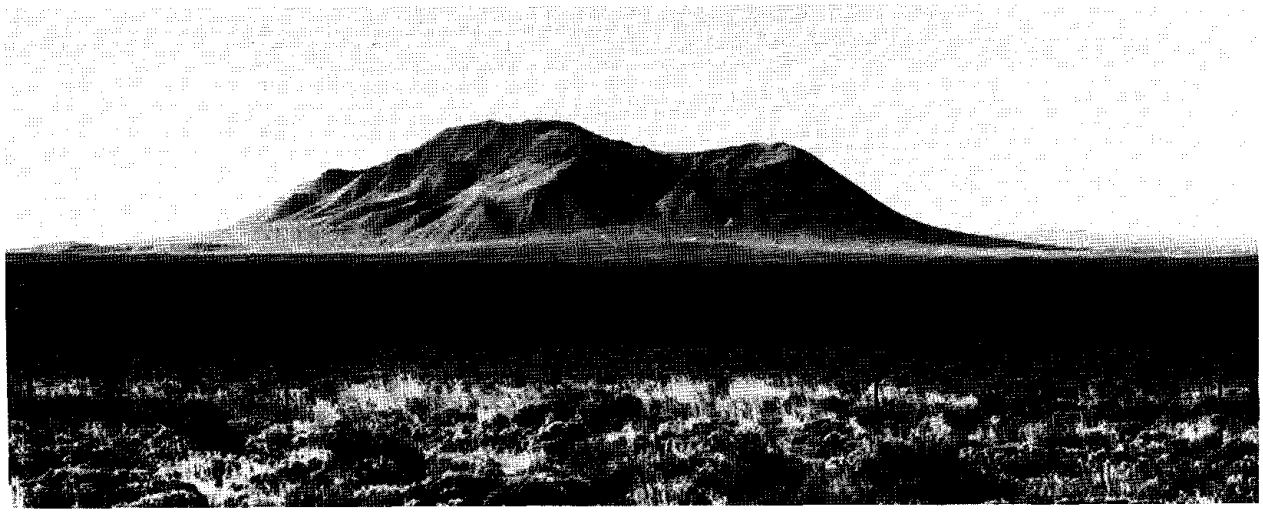

Figure 2. Big Southern Butte rises 760 meters above the eastern Snake River Plain between Arco and the Idaho Falls-Blackfoot area in southern Idaho.

access up the butte by way of a Bureau of Land Management service road which runs to the top.

Mapping of Big Southern Butte at a scale of 1:12,000 (Spear, 1979) revealed that it consists of two coalesced cumulo domes and a 350-meter-thick section of older basalt flows which dominates the northern slope (Figure 3, note scale is reduced). The basalt block was uplifted and tilted as a contiguous unit by the developing domes. The flow sequence of the block dips about 45 degrees to the northeast and has resulted in a large, prominent, flat area on the northern side of the butte (N½ sec. 23, SE¼ sec. 15, NE¼ sec. 22).

The contact between the two cumulo domes is not obvious. Rather, the division is based on overall morphology in combination with minor, but nonetheless characteristic, lithologic differences. The two domes which make up Big Southern Butte are aligned along a trend of N. 45° W., resulting in a slight northwest-southeast elongation of the butte. Radioisotope dates (Armstrong and others, 1975; Dalrymple, 1978) suggest that Big Southern Butte developed about 300,000 years ago. East Butte is dated at 600,000 years and Middle Butte remains undated inasmuch as the intrusive dome, which is inferred to have uplifted the basalt block, is not exposed at the surface.

GEOLOGY OF BIG SOUTHERN BUTTE

Big Southern Butte is made up of two coalesced domes, which are here identified as the northwestern and the southeastern dome, and a fault block of older basalt flows.

SOUTHEASTERN DOME

The southeastern dome was the first of the two domes to develop. It is characterized by lavender gray, aphyric rhyolite containing abundant devitrification spherulites. Flow-layering is also common, on the order of a few centimeters or less; attitudes of the layering are generally tangential to the flanks of the dome. The flow-layered rhyolite locally grades upward through a transition zone of a few meters into a white sugary-textured rhyolite. The transition can be seen clearly in the deep canyons on Big Southern Butte's southern slope.

The sugary rhyolite is interpreted to be the early upper crust of the gradually expanding dome. Although it appears to be more susceptible to erosion than the flow-layered variety, and undoubtedly much has been removed in that manner, it does not seem to have been present over the entire dome. Supporting evidence for this interpretation comes from the locations of numerous autoclastic breccias that occur above, but not below, the upper limits of the sugary rhyolite. Based on the criteria of Fisher (1966) autoclastic breccias form as a dome expands and grows, and they result from localized ruptures of the solidified dome surface. They are typified by nonsorted, nonbedded angular clasts set in a fine-grained matrix. The lithology of the clasts at Big Southern Butte is predominantly flow-layered rhyolite, although obsidian and white rhyolite are also found. The sizes of the clasts range from less than 1 centimeter to over 1 meter, and average about 10 centimeters. We suspect that during latter periods of dome development accelerated growth produced two primary results: the formation of autoclastic breccias from

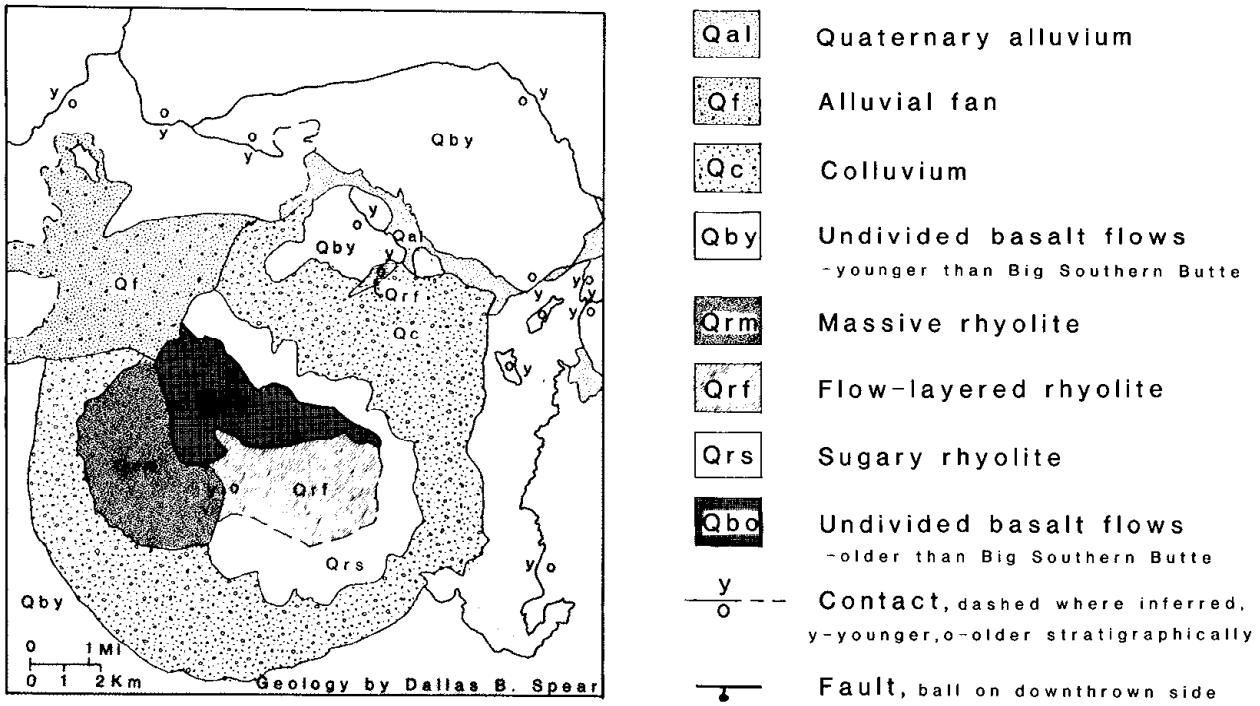

Figure 3. Generalized geologic map of Big Southern Butte, Idaho.

localized ruptures of the surface and the development of flow-layered rhyolite rather than sugary rhyolite on the surface.

Two other types of breccias also occur on the southeastern dome. Crumble breccia covers much of the lower two-thirds of the slopes. These blocky breccias are unconsolidated and have resulted from the destruction of early surfaces during dome growth. The other breccia is a graded sequence of explosion breccia which is exposed in a road cut near the top of the dome near the center of Big Southern Butte (Figure 4). It is at least 35 meters thick. The base is made up of a chaotic, heterolithologic assemblage of angular to subrounded blocks up to 1 meter in size. Much of the basal material has undergone some alteration and is distinguished by an earthy red and yellow color. The average clast size decreases upward and grades to well-sorted, bedded lapilli. Two prominent ash layers occur between the lower blocky section and the bedded lapilli.

This graded breccia is interpreted to have resulted from explosive venting through the surface of the flow-layered dome. It is not believed to mark the location of a primary vent or conduit at Big Southern Butte but simply preserves a local event or events in the on-going development of the dome. Explosive blowouts are common during the development of domes, and several eye witness accounts describe them (Williams, 1932). Washington (1926) described explosions he witnessed on the upper part of the Santorini dome. These explosions occurred at many different points and often simultaneously at several points but never from any one point. Solid blocks were thrown out by the explosions and many of these fell back on the dome. It is this origin that is hypothesized for the Big Southern Butte roadcut breccia.

In addition to the various breccias, banded spherulitic obsidian, light gray pumice, and honey-brown welded pumice are present on the flow-layered southeastern dome. Small outcrops of obsidian are common on the upper parts of the dome and are interpreted to be rapidly cooled localized extrusions or, in some places, the rapidly cooled upper surface of the dome. The gray and the honey-brown welded pumices are minor rock types of limited extent, but their presence documents some short-lived vent activity or perhaps minor explosive outbreaks on the surface of the dome. Some fumarolic activity is indicated in at least two localities on this dome by sulfur encrustation and a tufa-like deposit.

In summary, the development of the flow-layered southeastern dome was predominantly by endogenous growth; that is, internal expansion. However, particularly during the later stages of its evolution, localized ruptures at the surface produced autoclastic breccias. Minor extrusions of viscous lava also contributed to the resulting dome morphology. The attitude of the

flow-layering, which is generally tangential to the slopes of the dome, and the distribution of the breccias support the hypothesis of a gradually expanding dome.

NORTHWESTERN DOME

The younger northwestern dome of Big Southern Butte is generally homogeneous and dominantly a massive aphyric white rhyolite distinct in its lack of abundant spherulites. Locally the rhyolite grades to a sugary variety similar to that observed on the southeastern dome, but this is not common. Flow layering was observed in only one outcrop on the northeast side of this younger dome (SW¼NE¼ sec. 22). Significantly, the only autoclastic breccia found on the entire northwestern dome occurs near this flow-layered outcrop. This association coupled with the observed relationship between flow layering and autoclastic breccia on the southeastern dome strongly suggests that the breccias are by-products of the flow-layering process. The flow layering is believed to result from local surges in the emplacement of a viscous magma.

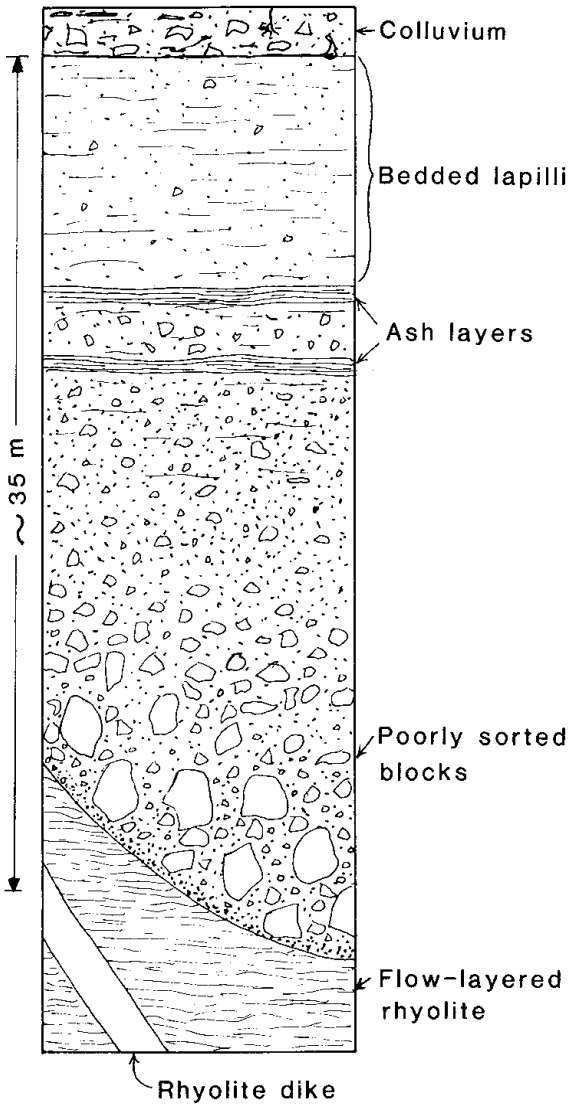

Figure 4. Generalized stratigraphic section of explosion breccia exposed in a roadcut near the top of Big Southern Butte.

Whereas the flow-layered southeastern dome has a varied topography with rugged slopes, the massive northwestern dome has relatively smooth, unbroken slopes. It has an arcuate outline, and apparently it developed symmetrically around an intrusive center. A shallow, circular basinlike depression approximately 800 meters in diameter occurs in the center of the top of the northwestern dome (center of sec. 22). This is believed to have formed as a result of deflation following withdrawal of magma down the conduit. Other factors which may have played a minor role in the development of this depression include both thermal contraction and the release of internal pressure through the escape of gasses from the magma. Daly (1925) proposed such an origin for a basined dome on Ascension Island.

BASALT FAULT BLOCK

A large block of older basalt flows at least 350 meters thick covers much of the northern slope of Big Southern Butte but does not extend all the way to the base (Figure 5). The basalt block has a steep slope, and a distinct break in slope marks the contact of this block with rhyolite near the base of Big Southern Butte. This basalt block was formerly part of the continuous flow surface of the Snake River Plain but was uplifted and tilted to its present orientation during the emplacement of the rhyolite domes. The contact between the basalt block and rhyolite is exposed only locally. Where exposed, it is demarcated by a narrow zone of basalt fragments in a rhyolitic matrix.

The basalt block is made up of fifteen to twenty individual flows or flow units which dip approximately 45 degrees to the northeast (Figure 6). The lower part of the block is exposed in a canyon on the northwest side of Big Southern Butte (NE¼ sec. 22). The oldest flows of the block have been extensively altered, probably from the action of hydrothermal fluids which accompanied the rhyolitic intrusion. This interpretation is supported by the occurrence of similarly altered basalt near another basalt-rhyolite contact higher in the section. Away from the contact this same flow is relatively unaltered.

A sequence of evolved tholeiite lavas is found near

Figure 5. View of the northern slope of Big Southern Butte from 8 kilometers. The flat area on the left (east) side of the canyon is part of the block of older basalt lavas uplifted and tilted during the emplacement of the rhyolite.

the base of the Big Southern Butte basalt block where it is interlayered between typical Snake River Plain olivine tholeiite flows. Evolved tholeiites form differentiated sequences and are distinctive for their high iron enrichment and high alkali content (see Leeman, 1982 this volume). Experimental work by Tilley and Thompson (1970) demonstrated that this is due to the fractionation of apatite, magnetite, olivine, plagioclase, and in the late stages, clinopyroxene. They further suggest that evolved tholeiite magmas developed through fractionation at the base of the crust from a parental Snake River Plain olivine tholeiite magma. These evolved tholeiite lavas are not common among the volcanic rocks of the Snake River Plain, and it is tempting to relate the Big Southern Butte sequence to Cedar Butte, a large shield volcano located about 7 kilometers east of Big Southern Butte which is composed of a differentiated suite of evolved tholeiite lavas. However, a ferrolatite flow known to be from Cedar Butte caps the entire basalt section on Big Southern Butte, and at least ten olivine tholeiite flows separate this cap from the evolved sequence near the base of the basalt block. Furthermore, some features associated with the evolved sequence of the Big Southern Butte basalt block, including both welded spatter and a single glassy layer, suggest that the source for this evolved flow was local.

Hamilton (1965) states that the upper 100 meters of the basalt section at Big Southern Butte is made up of interlayered basalt and rhyolite. No such interlayering was observed in this study, although a small conspicuous rhyolite dike was noted near the top of the basalt section.

Three large mounds, each 500 to 750 meters across at the base, occur in sections 11 and 12 near the northern base of Big Southern Butte (Figure 3). The mounds are covered with basalt rubble and, based on morphology alone, could be collectively identified as a small shield volcano. However, flow-layered rhyolite occurs in outcrop near the base of the east side of the mounds and, on close examination, the rubble which covers the surface is found to be composed of many basalt lithologies. This rules out a single local source for this material. The mounds are interpreted to be small domal intrusions of rhyolite.

PETROLOGY

The rhyolite of Big Southern Butte is mineralogically and chemically homogeneous. The macroscopic characteristics, such as color variations and flow layering, which were used for the purposes of mapping, are not related to any significant compositional variations.

PETROGRAPHY

In thin sections, the rhyolite appears as fine-grained intergrowths of microcrystalline quartz and alkali feldspar. Fine-grained anhedral phenocrysts of quartz are rare. Mafic minerals are very rare and include microphenocrysts of variably altered fayalite and dark green, pleochroic clinopyroxene. Magnetite is present as small equant grains.

The flow-layered rhyolite has abundant devitrification spherulites, and the massive rhyolite is holocrystalline with a "snowflake" texture due to the slightly larger anhedral crystals of quartz distributed throughout the microcrystalline groundmass.

CHEMISTRY

Major element data and CIPW norms for seven

Figure 6. Northern slope of Big Southern Butte; view to the northwest. Note the steeply dipping (45° NE) layers of basalt.

samples of rhyolite representative of Big Southern Butte are presented in Table 1. The analyses document the relative homogeneity throughout the dome complex. Chemically, the rhyolite is mildly peralkaline (molecular excess of $Na_2O + K_2O$ over Al_2O_3) and is classified as comendite based on the criteria of Nicholls and Carmichael (1969).

EMPLACEMENT HISTORY OF BIG SOUTHERN BUTTE

The large tilted block of older lavas on the north side of Big Southern Butte attests to the fact that Big Southern Butte began its development as a laccolithic intrusion. However, both intrusion and extrusion of silicic magma interacted to form Big Southern Butte.

Initially silicic magma ascended along a fracture and intruded beneath the basalt sequence of the Snake River Plain to form an elliptical sill-like intrusion. This early phase underwent a period of lateral growth that was followed by a laccolithic stage during which the intrusion began to dome the overlying basalt flows. Doming continued until the yield strength of the overburden was exceeded. When this occurred, it marked the transition in development of Big Southern Butte from intrusive to extrusive.

During the early stages of extrusive growth, the dome was mantled by blocky debris (crumble breccia) and a massive crust of white rhyolite. As the dome continued to increase in size by endogenous growth, the early crust was fractured, autoclastic breccias formed, and minor extrusions quickly chilled at the surface to form localized areas of obsidian. An explosion formed the breccia and lapilli tuffs now exposed near the top of Big Southern Butte.

Following these events, the intrusive center shifted to the northwest, and a second endogenous dome began to grow (the northwestern dome). Cessation of the supply of magma caused the top of the dome to sag slightly, producing the basined depression seen there today. These events essentially ended the volcanic development of Big Southern Butte. Figure 7 summarizes the sequence of events.

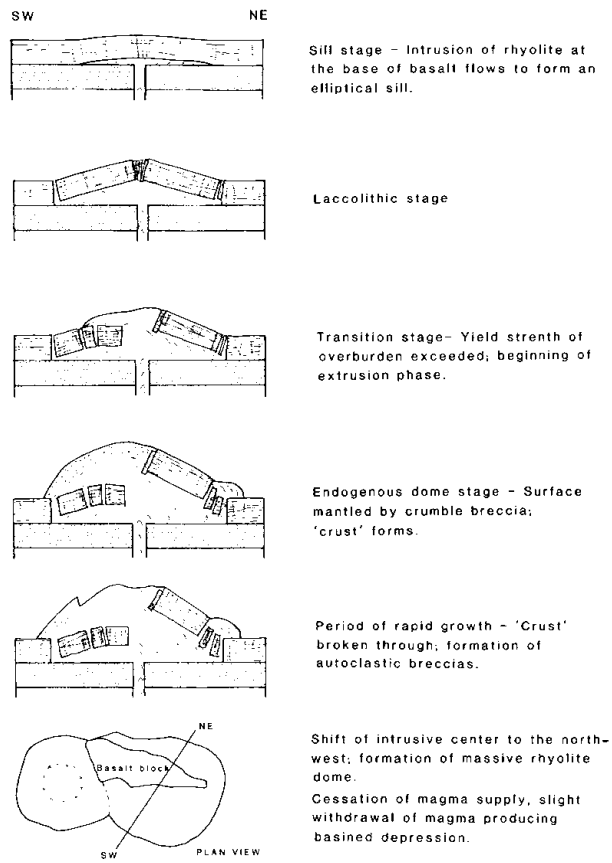

Figure 7. Summary of emplacement history of Big Southern Butte.

STRUCTURAL CONTROL OF VOLCANISM

One of the intriguing questions concerning Big Southern Butte is its location. With Middle Butte and East Butte, it is situated along a topographic high which coincides with the logitudinal axis of the eastern Snake River Plain.

Doherty and others (1979) suggest that Big Southern Butte, Middle Butte, East Butte, and two other volcanic centers, Cedar Butte and an unnamed rhyolite dome, lie along the ring fractures of a buried caldera complex. In addition to the location of the buttes, their interpretation is based on a thick sequence of rhyolitic rocks (which they interpret as caldera fill) found in an exploratory geothermal test well (INEL-1), on the absence of numerous basaltic vents within the inferred rim, and on recent faulting on the north side of the plain.

It is generally accepted that caldera development has played an important role in the overall volcanic evolution of the eastern Snake River Plain. Probably the rhyolite of Big Southern Butte is genetically related to some late-stage caldera development. However, we do not believe that structural control for the emplacement of rhyolite at Big Southern Butte is directly related to ring fractures of a buried caldera complex as suggested by Doherty and others (1979).

Close inspection of the area shows two dominant, linear structural trends. One is northeast-southwest and parallels the longitudinal axis of the eastern Snake River Plain; the other is northwest-southeast, more or less perpendicular to the axis (Figure 8). The surface expression of these two trends differs considerably. The northeast-southwest trend is defined

Table 1. Major element analyses (weight percent) and CIPW norms for Big Southern Butte samples.

	BS-1[1]	BS-2	BS-3	BS-4	BS-5	BS-6	BS-7[1]
SiO_2	76.22	75.32	75.84	76.02	75.99	76.08	75.82
TiO_2	.09	.10	.10	.10	.10	.10	.09
Al_2O_3	12.22	12.18	12.12	12.28	12.22	12.14	12.09
Fe_2O_3	1.17	1.66	1.31	1.94	1.70	1.76	1.76
FeO	.72	.13	.44	.03	.10	.04	.06
MnO	.04	.05	.05	.03	.03	.03	.04
MgO	.00	.02	.03	.03	.03	.03	.01
CaO	.47	.44	.48	.40	.45	.48	1.03
Na_2O	4.40	4.32	4.27	4.24	4.31	4.35	4.32
K_2O	4.76	4.76	4.66	4.69	4.68	4.72	4.67
P_2O_5	.01	.03	.02	.02	.03	.03	.02
H_2O+	.30	.32	.27	--	--	--	.26
CO_2	.01	.04	.03	.08	.05	.05	.44
Loss on ignition	--	--	--	--	--	--	--
TOTALS	100.36	99.56	99.55	99.73	99.59	99.71	100.51
Q	31.22	31.41	32.15	32.34	32.04	31.79	31.56
Or	28.03	28.25	27.66	27.79	27.77	27.97	27.46
Ab	36.23	36.31	36.30	35.98	36.62	36.27	36.00
An	--	--	.14	.63	.18	--	--
Ne	--	--	--	--	--	--	--
Ac	.77	.36	--	--	--	.57	.32
Di Wo	.92	.73	.81	.30	.65	.78	.91
Di En	--	.03	.05	.02	.04	.04	.01
Di Fs	1.04	.79	.86	.32	.69	.84	1.02
Hy En	--	.02	.03	.06	.04	.04	.01
Hy Fs	.72	.73	.57	1.19	.73	.75	.50
Ol Fo	--	--	--	--	--	--	--
Ol Fa	--	--	--	--	--	--	--
Mt	.57	.69	.87	.96	.87	.59	.72
Il	.17	.19	.19	.19	.19	.19	.19
Ap	.02	.07	.05	.05	.07	.07	.05

[1]Dave Borden, analyst; all others by D. B. Spear.

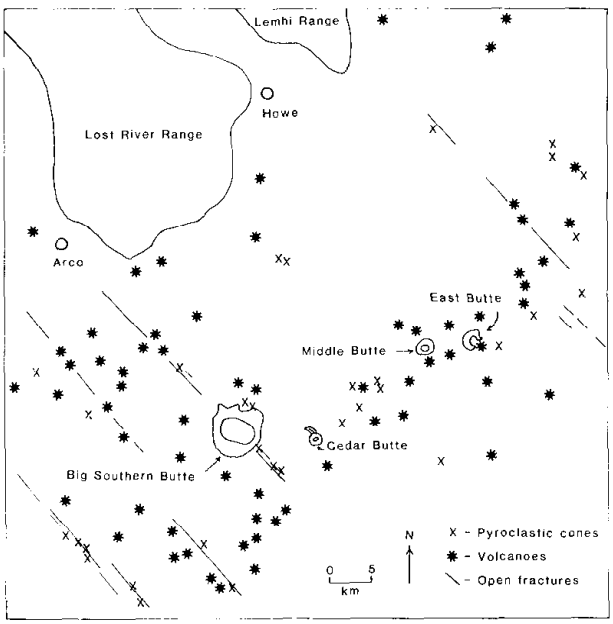

Figure 8. Localization of volcanism in part of the eastern Snake River Plain in the vicinity of Big Southern Butte. Two dominant structural trends, northeast-southwest and northwest-southeast, are defined by the concentration of volcanoes and northwest-southeast trending fractures.

by the concentration of large basaltic eruptive centers, Cedar Butte, a differentiated sequence of evolved tholeiite lavas, and Big Southern, Middle, and East Buttes. These constructs contribute to make the longitudinal axis topographically high. The northeast-southwest trend may also, in part, be due to a broad, gentle arching of the Snake River Plain related to a high thermal input concentrated along the axis at depth.

The northwest-southeast trend is marked by numerous open fractures, elongated craters, alignment of vents, and sites of recent small-scale fissure eruptions. Although not obvious in Figure 8, most of the volcanic vents not concentrated along the northeast-trending axis of the plain lie along fractures with a definite northwest-southeast trend. This trend probably owes its existence to the same stress field which produced the basin and and range-type mountain front faults north of the plain. Extension of these faults onto the plain can be inferred from the aeromagnetic map of Zietz and others (1978).

We believe that the location of Big Southern Butte is best explained in the light of two intersecting linear trends rather than a more or less circular pattern as might be expected from a buried caldera. The rectilinear distribution of volcanic vents and the strong orthogonal pattern of the aeromagnetic data as interpreted by Zietz and others (1978) offer support for this hypothesis. These dominant structural trends, coupled with a probable high thermal concentration along the longitudinal axis of the eastern Snake River Plain at depth, are the controlling factors responsible for the location of Big Southern Butte.

SUMMARY AND CONCLUSIONS

Big Southern Butte is a volcanic dome complex that formed approximately 300,000 years ago. It is composed of two coalesced rhyolite domes and an elevated block of older basalt flows covering most of its northern side. Big Southern Butte began its development as a laccolithic intrusion but due to its shallow emplacement broke through to the surface and continued its evolution by endogenous growth. Subsequent to its formation olivine tholeiite basalt flows, erupted from nearby vents, have surrounded it.

The rhyolite of Big Southern Butte is distinctive in outcrop for mapping purposes but mineralogically and chemically homogeneous. It occurs in thin section primarily as fine-grained intergrowths of microcrystalline quartz and alkali feldspar. Devitrification spherulites are characteristic in the flow-layered variety which occurs on the southeastern dome. Chemically the rhyolite is mildly peralkaline and is classified as comendite.

The emplacement of the rhyolite at Big Southern Butte was controlled by two intersecting linear trends: one northeast-southwest and the other northwest-southeast. These dominant structural trends coupled with high thermal concentration along the axis of the Snake River Plain at depth are responsible for the localization of Big Southern Butte.

ACKNOWLEDGMENTS

We wish to thank John C. Fountain, Dave Borden, and Charlie C. Clemancy, State University of New York at Buffalo and Steven S. Oriel, Mel A. Kuntz, and Jack Barraclough of the U. S. Geological Survey for their help and suggestions during the course of this investigation. Naturally they are not to be held accountable for our interpretations. Financial support for most of this project was covered by NASA Planetology Grant NGR 33-014-108 awarded to John S. King.

REFERENCES

Armstrong, R. L., W. P. Leeman, and H. E. Malde, 1975, K-Ar dating and Neogene volcanic rocks of

the Snake River Plain, Idaho: American Journal of Science, v. 275, p. 225-251.

Dalrymple, G. B., 1978, *in* M. A. Kuntz, Geologic map of the Arco-Big Southern Butte area, Butte, Blaine, and Bingham Counties, Idaho: U. S. Geological Survey Open-File Report 78-302.

Daly, R. A., 1925, The geology of Ascension Island: Proceedings, American Academy of Arts and Science, v. 60, no. 1, p. 1-80.

Doherty, D. J., L. A. McBroome, and M. A. Kuntz, 1979, Preliminary geologic interpretation and lithologic log of the exploratory geothermal test well (INEL-1), Idaho National Engineering Laboratory, eastern Snake River Plain, Idaho: U. S. Geological Survey Open-File Report 79-1248, 9 p.

Fisher, R. V., 1966, Rocks composed of volcanic fragments and their classification: Earth-Science Reviews, v. 1, p. 287-298.

Hamilton, W. C., 1965, Geology and petrogenesis of the Island Park caldera of rhyolite and basalt, eastern Idaho: U. S. Geological Survey Professional Paper 504-C, 37 p.

Leeman, W. P., 1982, Evolved and hybrid lavas from the Snake River Plain, Idaho, *in* Bill Bonnichsen and R. M. Breckenridge, editors, Cenozoic Geology of Idaho: Idaho Bureau of Mines and Geology Bulletin 26.

Nicholls, J. and I. S. E. Carmichael, 1969, Peralkaline acid liquids—a petrologic study: Contributions to Mineralogy and Petrology, v. 20, p. 268-294.

Schoen, R., 1974, III. Geology, *in* J. B. Robertson, R. Schoen, and J. Barraclough, Influence of liquid waste disposal on the geochemistry of water at the National Reactor Testing Station, Idaho: U. S. Geological Survey Open-File Report, IDO 22053, 231 p.

Spear, D. B., 1979, The geology and volcanic history of the Big Southern Butte-East Butte area, eastern Snake River Plain, Idaho: State University of New York at Buffalo Ph.D. dissertation, 136 p.

Tilley, C. E. and R. N. Thompson, 1970, Melting and recrystallization relations of the Snake River basalts of southern Idaho, USA: Earth and Planetary Science Letters, v. 8, no. 1, p. 79-92.

Washington, H. S., 1926, Santorini eruption of 1925: Geological Society of America Bulletin, v. 37, p. 349-384.

Williams, Howel, 1932, The history and character of volcanic domes: University of California Department of Geological Science Bulletin, no. 21, p. 51-146.

Zietz, Isidore, F. P. Gilbert, and J. R. Kirby, Jr., 1978, Aeromagnetic map of Idaho: color coded intensities: U. S. Geological Survey Geophysical Investigations Map GP-920.

Chapter 7

Basaltic Volcanism Eastern Snake River Plain and Vicinity

The Style of Basaltic Volcanism in the Eastern Snake River Plain, Idaho

by

Ronald Greeley[1]

ABSTRACT

The Pleistocene and Holocene basaltic rocks in the eastern Snake River Plain are composed of lava flows erupted and emplaced primarily in one of three forms: (1) low shield volcanoes, which are central-vent features having flank slopes averaging less than 1 degree, (2) fissure flows, and (3) tube-fed flows emplaced through major systems of lava tubes. The interplay of these forms results in a relatively flat basaltic plain which represents a style of volcanism that is gradational between flood basalt volcanism (fissures, rift zones, flat surface) and Hawaiian volcanism (central vents, lava tube flows).

INTRODUCTION

The Pleistocene and Holocene basaltic rocks in the eastern Snake River Plain (Figure 1) represent a style of volcanism that is gradational between flood basalt volcanism and Hawaiian volcanism. The expression "basaltic plains" has been proposed (Greeley, 1976, 1982) to describe basaltic regions represented by the eastern Snake River Plain. In this article, major basaltic terrains and types of lava flows are reviewed briefly and related to the eastern Snake River Plain; then the volcanic morphology of the plain is described and discussed in terms of styles of eruption and modes of flow emplacement.

BASALTIC TERRAINS

The eruption of basaltic magmas can produce a wide variety of landforms, as listed in Table 1. Of these, three forms constitute major terrains (Figure 2): flood basalt plateaus, major shield volcanoes, and basaltic plains. Flood basalt plateaus are characterized by flows or flow units commonly exceeding 10 meters in thickness. The flows were erupted at high rates of effusion from linear vent systems. The Roza Member of the Yakima Basalt in the Columbia Plateau can be considered a type example for a flood basalt. Most of its 1,500 cubic kilometer volume was erupted from a vent system more than 130 kilometers long at a rate estimated to be 1 cubic kilometer per day (Swanson and others, 1975). In contrast, the formation of major shield volcanoes (typified by the Hawaiian and large Icelandic shields) involved eruptions from central vents at rates of effusion that were several orders of magnitude lower than flood eruptions. The shields are built of relatively thin flows and flow units about 3 to 5 meters thick. Basaltic plains volcanism combines elements of both shields and flood basalt plateaus; the plains involve multiple, thin flow units erupted from central vents commonly aligned along fissures.

LAVA FLOWS

Walker (1972) proposed the terms "compound lava flows" and "simple lava flows" to distinguish differences in the internal structure of lava flows and to infer rates of effusion and modes of emplacement. Walker builds on the recognition by Nichols (1936) that many lava flows can be separated into flow units that represent individual "gushes" of lava, but which are all part of the same eruptive sequence. Compound lava flows consist of multiple flow units that range in thickness from 5 centimeters to more than 10 meters, although most are 50 centimeters to 5 meters thick. Although the interval between emplacement of flow units can be very short, lava crusts typically develop that are sufficiently thick to preserve the individuality of the unit. Thus, compound lava flows are made up of a sequence of thin units which, to some degree, behave as individual cooling units.

In contrast to compound lava flows, simple lava flows consist of single, often thicker, flow units that are essentially single cooling bodies. Walker (1972)

[1]Department of Geology and Center for Meteorite Studies, Arizona State University, Tempe, Arizona 85281.

Greeley, Ronald, 1982, The style of basaltic volcanism in the eastern Snake River Plain, Idaho, *in* Bill Bonnichsen and R. M. Breckenridge, editors, Cenozoic Geology of Idaho: Idaho Bureau of Mines and Geology Bulletin 26, p. 407-421.

Table 1. Landforms resulting from the eruption of basaltic magmas (after Greeley, 1977).

Landform	Eruptive style	Typical features	Example
1. Flood basalt plateau	Fissure eruption, high volume-highly fluid; probably short duration	Pahoehoe flows; massive, dense low vesicularity; vertical jointing; few flow features	Columbia River Plateau
2. Basalt "plains"	Fissure and central vent, moderately high volume and rate; fluid lavas; lava tubes and channels	Pahoehoe, tube and toe-fed; aa flows; variable textures, from massive to vesicular; vertical joints and horizontal platy units	Eastern Snake River Plain
3. Shield volcanoes	Central vent with associated fissures; high rate, moderate volume, long duration; fluid lavas, lava tubes and channels	Pahoehoe, tube and toe-fed, vesicular, platy jointing	Mauna Loa, Hawaii
4. Composite cones	Central vent, explosive alternating with flows; tubes and channels infrequent	Pyroclastics and vesicular to dense flows; pahoehoe and aa	Cascades
5. Cinder cones	Explosive, infrequent flows	Pyroclastics	Many
6. Domes	Central vent, low volume, low rate, viscous lavas	Block flows	Few

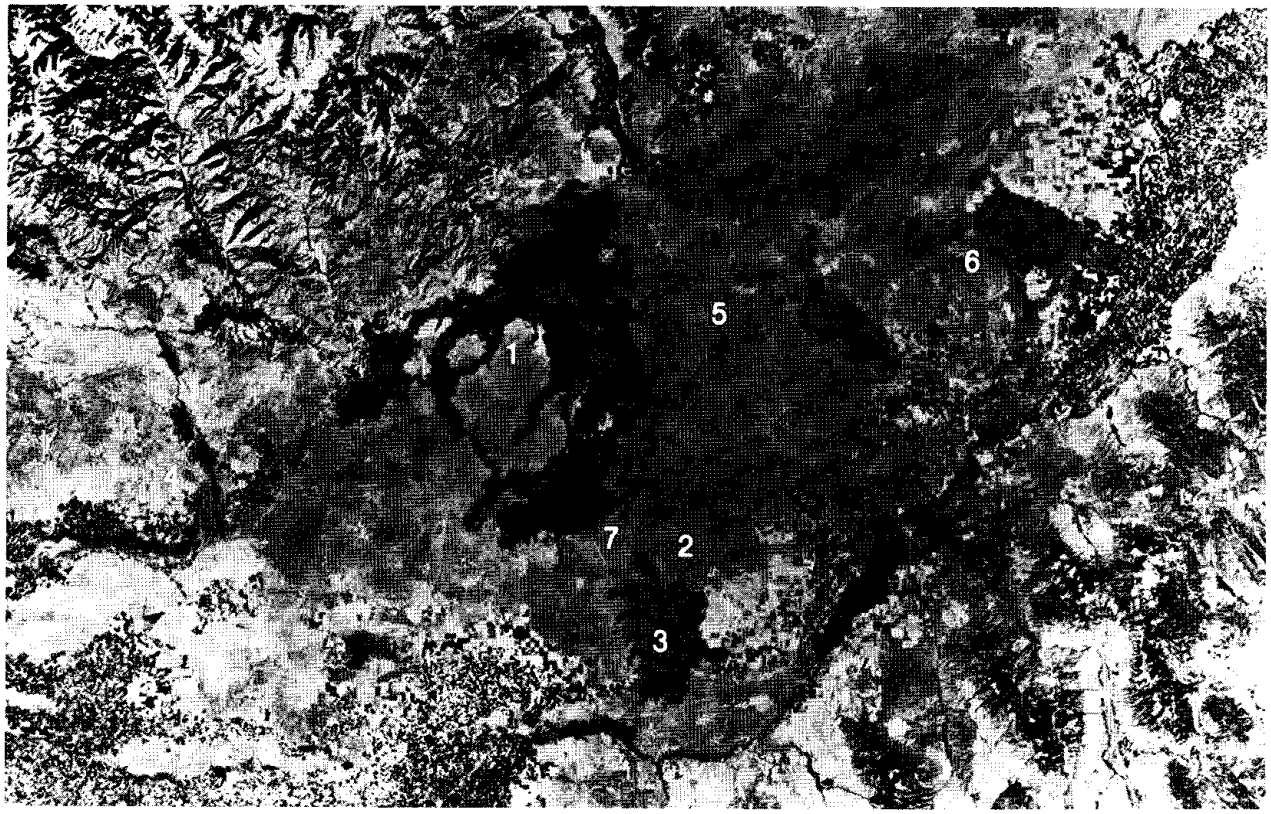

Figure 1. LANDSAT images of the eastern Snake River Plain: (1) Craters of the Moon, (2) Kings Bowl lava field, (3) Wapi lava field, (4) Shoshone Ice Cave, (5) Big Southern Butte, (6) Hells Half Acre lava field, and (7) Bear Trap lava tube.

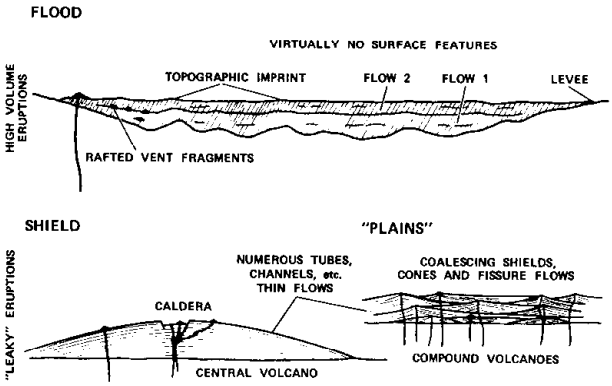

Figure 2. Diagrams illustrating three major types of basaltic terrain (from Greeley, 1976).

attributes the difference primarily to the rate of effusion: a low rate leads to the development of compound flows, whereas a high rate, typical of flood eruptions, produces simple flows. Thus, the identification of the predominant flow type in any one region would provide insight into the prevailing rate (high versus low) of effusion that was involved in the eruption of the lavas.

Most basalt flows in the eastern Snake River Plain appear to be pahoehoe basalts that were emplaced as compound lava flows. Cross sectional exposures of lava flows, however, are rather limited in the eastern Snake River Plain because of the lack of erosion. Although some flows are exposed in the walls of summit craters, they are probably not typical for the main bodies of the flows that make up the plains away from the vents. The Kings Bowl rift (Figure 1) provides an opportunity to observe a cross section of several flows and flow units which are probably typical of those making up the eastern Snake River Plain. Nearly 30 meters of vertical section are exposed, with only the upper few meters being composed of flows erupted from fissures associated with the Kings Bowl rift. Most of the flows in the section (Figure 3) originated from vents several kilometers or more distant, as determined by geological mapping currently in progress. As seen in Figure 3, flows are of the compound type, with individual flow units ranging in thickness from 1 to 5 meters.

Fresh surfaces of the pahoehoe flows in the eastern Snake River Plain are typically rather hummocky, with local relief as much as 10 meters. Collapse depressions, pressure plateaus, pressure ridges, and flow ridges are common (Figure 4). These features are typical of many lava flows and apparently result from the manner in which the flows advance through a series of budding toes, described by Wentworth and Macdonald (1953) and others. The weathering of the flow-surface features and the accumulation of wind-blown sediments in low-lying areas result in a smoothing of the surface relief to the degree that in older flows only remnants of the prominent features, such as some ridges, are visible. Although not as extensive as pahoehoe flows, aa flows are also present in the eastern Snake River Plain, predominantly in Craters of the Moon National Monument (Figure 1).

BASALT MORPHOLOGY OF THE SNAKE RIVER PLAIN

The regional geology of the Snake River Plain is described in several reports, including Russell (1902) and Stearns and others (1938). Aspects of the plain pertinent to this discussion are described by Stearns (1928), Murtaugh (1961), Trimble and Carr (1961), Prinz (1970), Greeley and King (1975a, 1975b), LaPoint (1975, 1977), King (1982 this volume), Kuntz and others (1982 this volume), and Womer and others (1982 this volume). The eastern Snake River Plain is formed by the accumulation of lavas in three types (Greeley, 1982): (1) flows forming low shields, (2) fissure flows, and (3) major tube flows, plus various miscellaneous flows. The relationships of these accumulations are shown diagrammatically in Figures 5 and 6. Although flood-type flows may also be present in the plain, none are exposed or documented.

LOW SHIELDS

Most of the basalt flows in the eastern Snake River Plain are associated with low-profile shield volcanoes. Noe-Nygaard (1968) described a subcategory of shield volcanoes in the Faroe Islands which he termed "shield volcano of scutulum type" (from the Latin scutulum, the diminutive of scutum, meaning shield). Noe-Nygaard described the structures as very flat shield volcanoes having slope angles of about 0.5 degree. The shields described are about 15 kilometers across and are estimated to consist of less than 7 cubic kilometers of lava. Similar shields occur in many areas, including Iceland, Hawaii, and in the western United States. Mauna Iki in Hawaii has similar morphology and comparable dimensions, and Macdonald (1972) used the term "lava cone" to describe it and similar low-profile shields. It is primarily the small size and low profile of these shields that led Noe-Nygaard and Macdonald to separate the scutulum or lava cone type shields from the larger Hawaiian and major Icelandic shield volcanoes. To prevent confusion with composite cones and to avoid the awkward phrase "shield

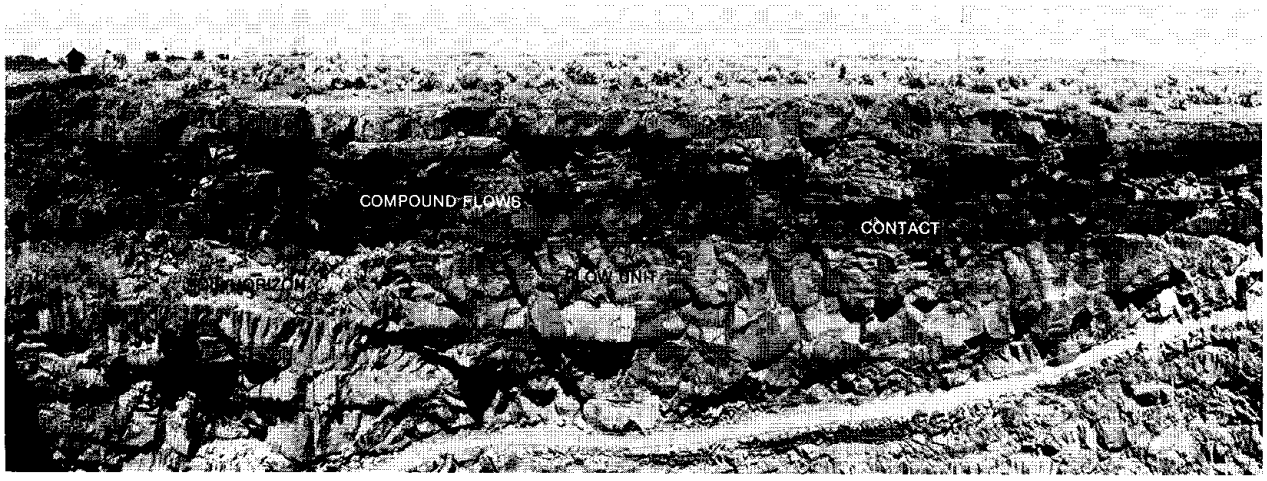

Figure 3. Panoramic view of the east wall of Kings Bowl, showing lava flows typical of the Snake River Plain: compound lava flows consisting of multiple, typically thin flow units.

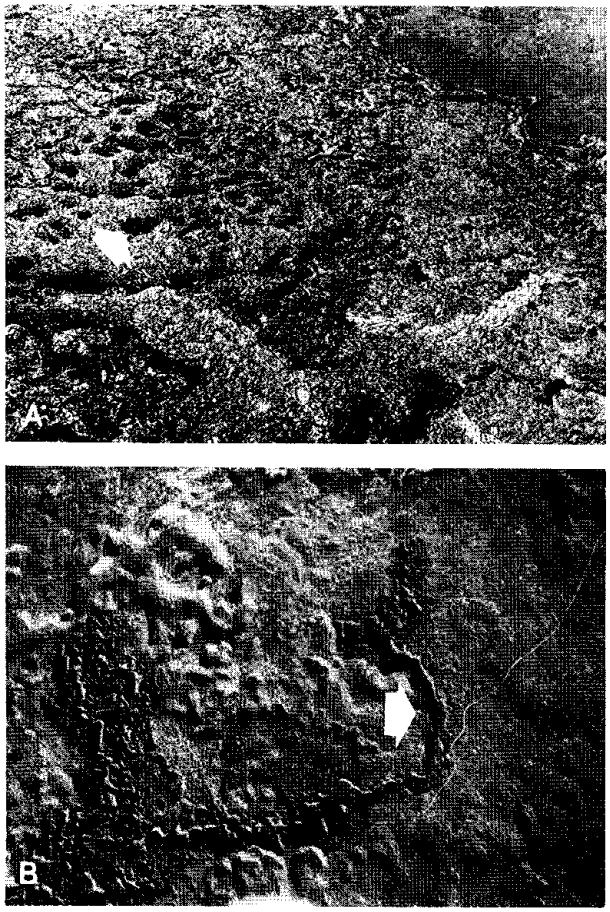

Figure 4. Surface features typical of pahoehoe basalt flows on the plain: (A) Oblique aerial view of the Wapi lava field showing elevated pressure plateaus and collapse depressions (arrow); also seen is a ridge parallel to the flow margin (upper right); collapse depressions are about 10 meters across and indicate scale. (B) Near-vertical view of the Wapi lava field showing flow ridge (arrow); white line is jeep trail and indicates scale.

volcano of scutulum type," the term "low shield" was proposed (Greeley, 1982) to describe this category of volcano.

Low shield volcanoes are typical of the Snake River Plain, and regardless of the term applied, they appear to represent a distinctive form of volcanism. The Wapi lava field is a typical low shield in the eastern Snake River Plain (Figure 1). It covers more than 300 square kilometers and is composed of compound lava flows consisting of pahoehoe lavas of the degassed variety described by Swanson (1973), plus small-volume aa flows in the vent region. Lava toes, collapse depressions, flow ridges, and pressure ridges are common, but no lava tubes have been found on the main part of the field (Champion, 1973). The areal extent of the Wapi lava field, one of the larger young fields on the plain (dated by carbon-14 methods at 2,270 ± 50 years, Greeley, 1982), is considerably less than the 40,000-square-kilometer Roza Member of the Yakima Basalt (Swanson and others, 1975), a representative flood basalt.

The Wapi low shield displays two prominent slopes; the main part of the shield has slopes less than 0.5 degree, whereas the summit region steepens to about 5 degrees. The same type of profile is seen at Hells Half Acre and older low shields on the plain. As older shields were encroached by subsequent flows from other sources, the steeper and topographically higher vent areas commonly remain unburied.

The steeper summit for low shields can be explained partly by the nature of the flows that make up the summit region. Pillar Butte, the summit region for the Wapi low shield, has a high proportion of short, low-volume aa flows that elevated the vent. In comparison with the pahoehoe flows of the main field, the aa flows were more viscous and may

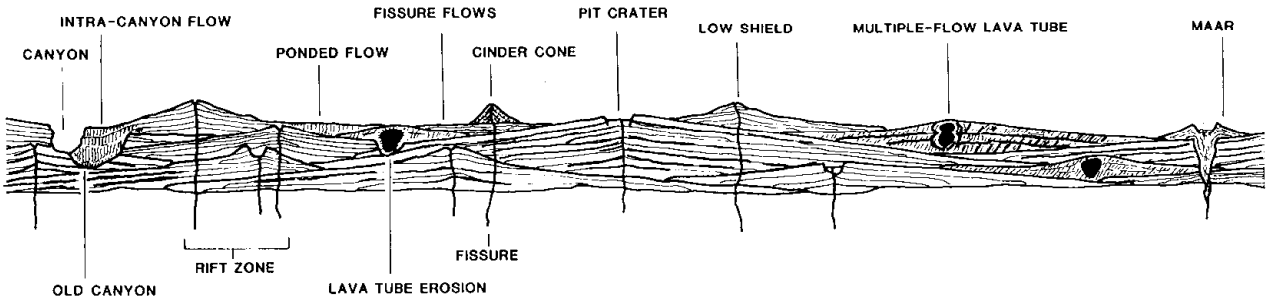

Figure 5. Schematic cross section to show the salient features of a "plains" basalt region, typified by the Snake River Plain. The vertical scale surface relief and small features (for example, lava tubes) are greatly exaggerated in order to show detail that would otherwise be lost. The predominant lava is pahoehoe basalt in the form of flow units that seldom exceed 10 meters in thickness. The primary features are: (1) Low shields, many of which have summit pit craters; the summits of most low shields are marked by steeper profiles than the rest of the construct, resulting partly from last-stage, low volume eruptions of aa lava. (2) Flows fed by large lava tubes that wind between coalescing low shields; multiple eruptions often use the same lava tube as the conduit to feed advancing flow fronts and to add "second stories" above previous flows and tubes; in some instances lava tubes may entrench into older flows by erosion. (3) Fissures produce thin flows with relatively low surface gradients; the flows may be pahoehoe or aa, some of which are emplaced by networks of small tubes and channels; "point source" eruptions along fissures can result in infrequent cinder-and-spatter cones. (4) Flows more than 10 meters thick are occasionally found in "plains" type regions; these may represent flood-type eruptions, but more frequently, they are the result of lava ponding in low-lying regions and as intracanyon flows (left side of diagram); regardless of origin, thick flows are infrequent and appear to contribute comparatively little to the total volume of the "plains" region. (5) Maar craters that result from ground water and magma interactions (after Greeley, 1982).

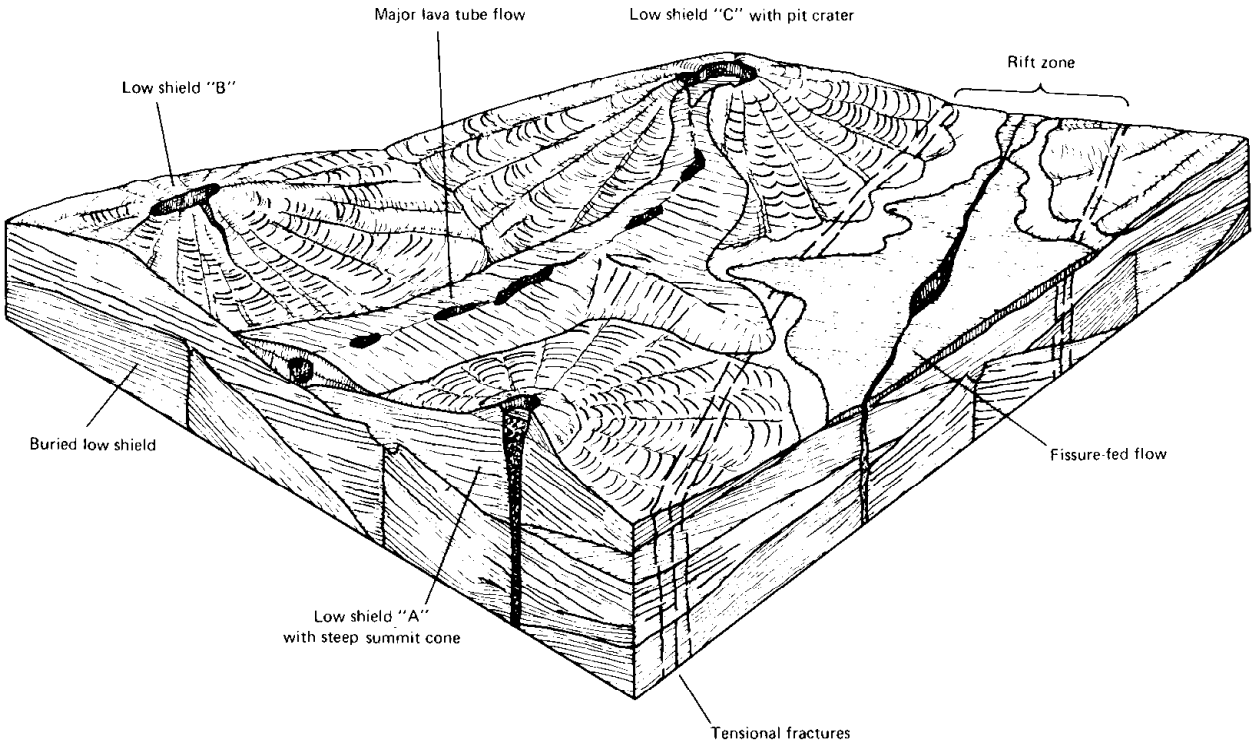

Figure 6. Block diagram showing the relationship of low shields, major lava tube flows, and fissure flows (after Greeley, 1981).

represent the final stages of eruption. However, the complex sequence of development from steep cone to low shield to spatter rampart, observed during the short history of Mauna Ulu (Swanson and others, 1979), would caution against assuming that earlier, steeper summit regions might not be buried at Pillar Butte.

The profiles of the low shields in the eastern Snake River Plain typically show an asymmetry toward the north side of the low shield. This is accounted for by the regional topographic slope to the south (Figure 7). Erupted lavas tended to flow south, rather than north, resulting in the offset of the vent and summit region with respect to the shield in plan view.

The summits of many of the low shields are marked by one or more irregular craters, commonly pit craters. Many craters show evidence of multiple collapse (Figure 8) and were source vents for large lava tubes or channels (Figure 9). Rarely, spatter ramparts, built of pasty agglutinate, occur at the summit (Figure 10).

Many low shields appear to be aligned in distinctive rift zones (Figure 11), with shields along each zone roughly contemporaneous in age. An example is the Inferno Chasm rift zone (Greeley and King, 1975b). The aligned shields may represent a style of fissure eruption in which effusion was localized at various points along the fissure. Individual shields, however, are built of flow units a few meters thick, akin to Hawaiian activity. Once the low shields on the plain appear to have reached a maximum size, the eruption vent shut off.

Figure 8. Vertical aerial photograph of Wildhorse Corral (illumination from the left side of the photograph). The vent is about 52 meters deep and 1 kilometer long, its length being oriented north-south on the Inferno Chasm rift zone. Wildhorse Corral appears to have a complex eruptive history, indicated by terraces within the crater walls and multiple flow units, some of which were tube-fed (from Greeley and King, 1975a; NASA-Ames photograph 951, 8-15, 17; May, 1969).

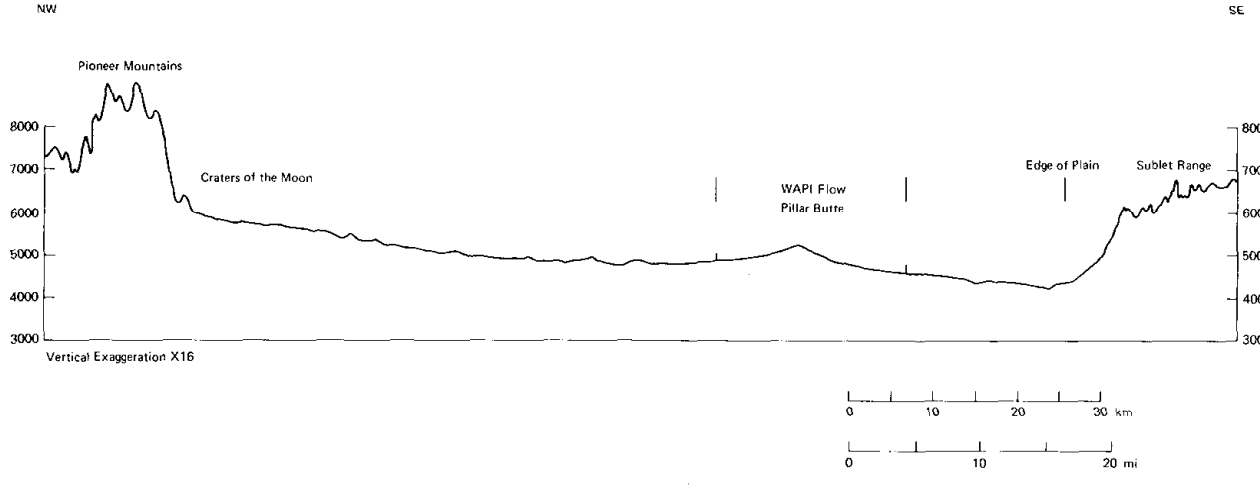

Figure 7. Topographic profile across the eastern Snake River Plain showing regional slope to the southeast and the slight offset of the Pillar Butte vent region from the center of the Wapi lava field.

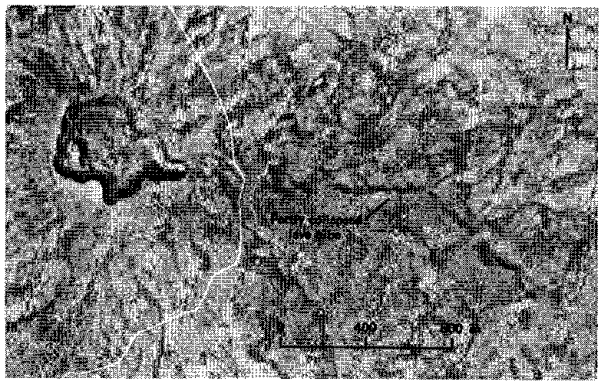

Figure 9. Vertical aerial photograph of an unnamed pit crater (left) side of photograph), about 2.5 kilometers north of Mosby Well, Idaho, that was the source for a major lava tube flow; lava tube can be traced eastward (out of view on photograph) more than 5 kilometers by a series of collapses that show as dark areas. U. S. Geological Survey photograph GS SWEZ 6-205; September, 1971.

Figure 10. Low-altitude oblique view northward to the Pillar Butte area, the summit vent region for the Wapi low shield. The knob on the horizon is Pillar Butte, a spatter rampart associated with the summit vents. Dark patches are aa flows; a large pressure ridge is visible at the bottom of the photograph. NASA-Ames photograph by Mike Lovas, 1969.

FISSURE FLOWS

Most fissure vents are associated with rift zones. The youngest fissure flows on the plain are found at Kings Bowl and in the Craters of the Moon National Monument. Craters of the Moon flows consist of aa and pahoehoe flows erupted from fissures and cones along the Great Rift (Figure 1) and cover more than 1,500 square kilometers (see Kuntz and others, 1982 this volume). Among these are the largest fissure flows identified on the plain, but their volumes are much less than those of flood basalt flows. For example, the Roza Member in the Columbia Plateau originally covered at least 40,000 square kilometers (Swanson and others, 1975).

The Kings Bowl lava field covers only about 3 square kilometers and consists of several flow units (Greeley and King, 1975a), some of which were ponded as small lava lakes. The thickness of individual flows is less than about 1.5 meters, although some of the lava lakes may have been more than 4 meters deep in places. The Kings Bowl flows were erupted from a prominent fissure (Figure 12); in some places, possible feeder dikes are exposed (Figure 13).

Although the main characteristic of fissure flows is the nearly continuous effusion of lava along several kilometers or more of the fissure, an eruption at point-sources along the fissure may occur either independently or contemporaneously with lava effusion along the fissure. Point-source eruptions produce small spatter cones, or in a few places, substantial cinder cones, as in Craters of the Moon (Figure 14). Phreatic eruption may also occur along fissures, as at Kings Bowl (Figure 15). Such point-source structures are rare on the plain and contribute little to the total accumulation of volcanic materials.

MAJOR LAVA TUBE FLOWS

It is only recently that the role of lava tubes and channels in the emplacement of some basalt flows has been appreciated. A study of Mauna Loa (Greeley and others, 1976) shows that more than 80 percent of the flows exposed on the surface at least partly involved flow through lava tubes and channels during their emplacement. Lava tubes and to a lesser extent channels efficiently transport lavas great distances from their vents. Lava tube systems longer than 20 kilometers are common in many basalt areas, including the eastern Snake River Plain.

Lava tubes and channels develop in Hawaiian-type eruptions in which the rate of effusion is moderately high (for example, 10 to 100 cubic meters per second) but not as high as in flood eruption. Tube formation also seems enhanced by sporadic eruption, involving multiple flow units with intervening periods of quiescence. This kind of activity was typical for the approximately 6-year history of Mauna Ulu, Hawaii, a low shield having complex networks of lava tubes (Greeley, 1971, 1972; Peterson and Swanson, 1974).

Lava tubes also played an important role in the emplacement of some of the flows in the eastern Snake River Plain. Although they are not as common as in Hawaiian flows, some of the tubes in the plain appear to be larger than those in Hawaii. A preliminary survey of part of the eastern plain (east of U. S. Highway 93 and west of U. S. Highway 26) suggests that more than a fifth of the flows contain lava tubes

Figure 11. Oblique aerial view northeastward across the Inferno Chasm rift zone (Inferno Chasm is out of view to the right).

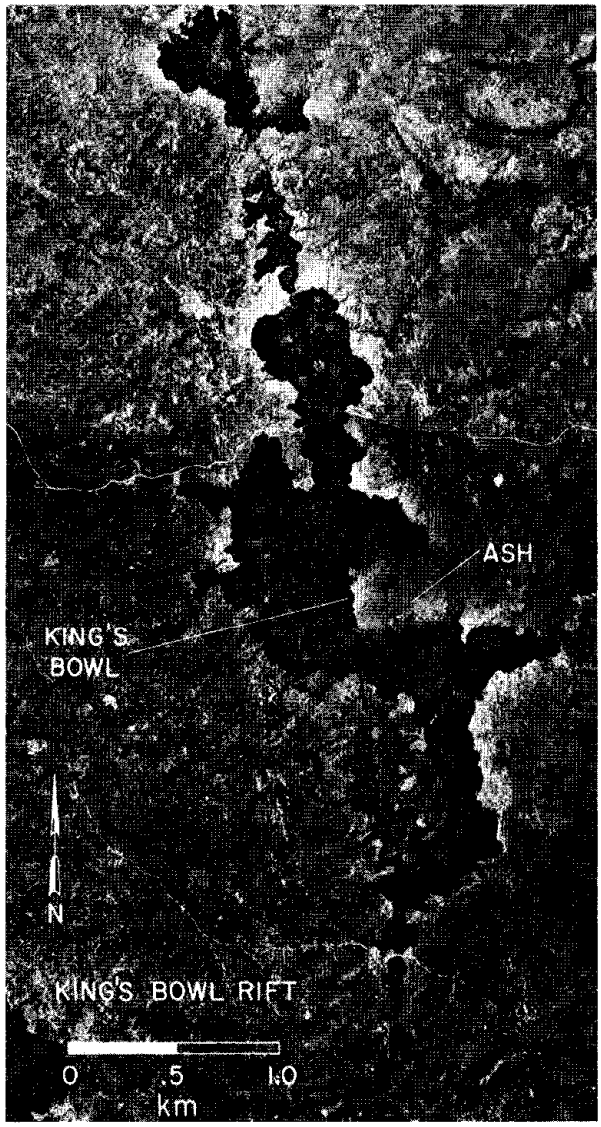

Figure 12. Vertical aerial photograph of the Kings Bowl rift and the Kings Bowl lava field, a compound lava flow fed by the main fissure. A phreatic eruption and subsequent collapse created Kings Bowl, the elongate crater on the fissure; prevailing winds from the west (left) at the time of the eruptions carried ash and other fine particles eastward from the fissure. U. S. Department of Agriculture photograph.

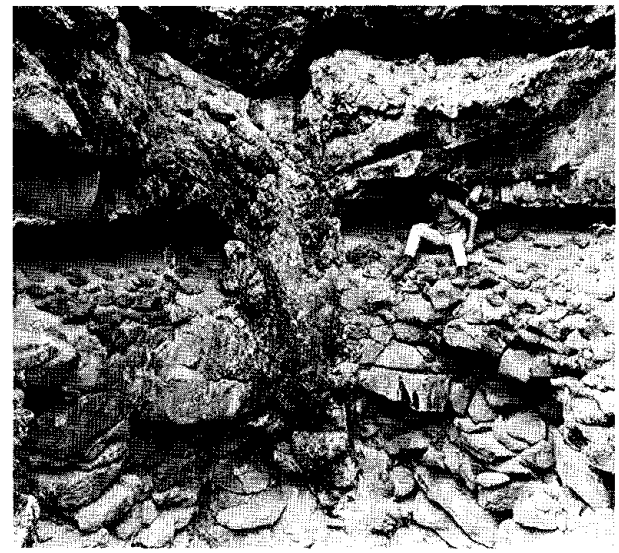

Figure 13. View of a possible feeding dike along the main fissure at Kings Bowl lava field. Photograph by James Papadakis, from Greeley and King, 1975a.

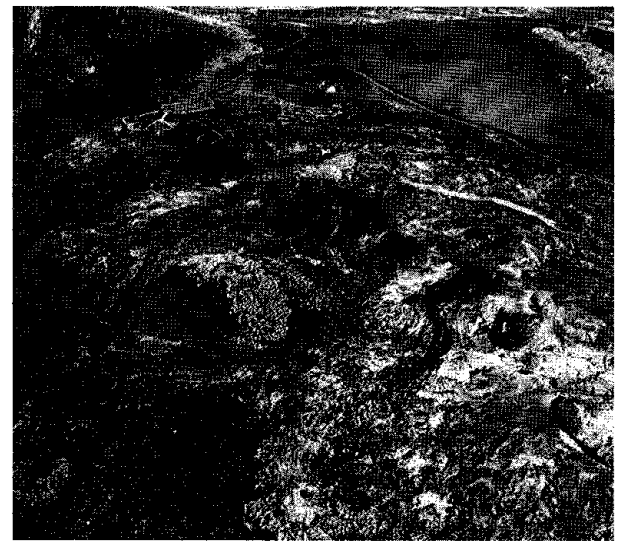

Figure 14. Low oblique aerial view of cinder-and-spatter cones aligned on a fissure in Craters of the Moon National Monument.

and channels (Greeley, 1977). Lava tubes 0.5 meter to 5 meters across are abundant in many of the low shield and fissure flows. Major lava tube-fed flows, however, are emplaced by tubes typically larger than 10 meters across.The resulting flow is long, narrow, and somewhat sinuous, in many places demonstrating the control exerted by preflow topography. Although the sources for the tubes are not always obvious, low shields, pit craters, and possible fissures were often sources for major lava tube-fed flows.

Flows associated with Bear Trap lava tube northwest of Kings Bowl and Shoshone Ice Cave lava tube are examples of this class of flow on the plain. The Shoshone Ice Cave flow (Figure 16) is one of the youngest and least altered flows on the plain. Shoshone Ice Cave is one segment of the lava tube that has been developed as a tourist attraction; it is part of a complex lava tube-lava channel system, which during active flow involved both roofed and unroofed segments. Many of the formerly roofed parts col-

Figure 15. Low altitude, oblique aerial photograph of Kings Bowl lava field, showing ash from phreatic explosions (arrows) and series of perched lava ponds (1, 2, and 3).

Figure 16. Vertical aerial photograph of the main vent region (upper right) for the Shoshone Ice Cave lava flow, a compound lava flow consisting of pahoehoe and aa flow units, many of which were fed through lava tubes. Parts of the collapsed lava tube are visible as dark spots. Side road and parking area adjacent to the main highway (U. S. Highway 93) mark Shoshone Ice Cave, a segment of the lava tube open to the public. U. S. Department of Agriculture photograph CVR-1KK-157, 158.

lapsed, leaving open trenches. The compound flows associated with the Shoshone lava tube system cover about 210 square kilometers and consist of both aa and pahoehoe flow units. Numerous small distributary lava tubes and channels were important in carrying lava away from the main tube and contributed to the development of a subtle topographic arch along the axis of the main tube, typical of many lava tubes.

Bear Trap lava tube and the flows associated with it (Figure 17) make up one of several tube-flow systems that apparently originated from Wild Horse Corral, northeast of the Kings Bowl rift. The tube can be traced by a series of collapsed segments for more than 21 kilometers westward where it becomes buried by Holocene basalt flows from Craters of the Moon (Greeley and King, 1975a). The axial trace of the tube is defined by a broad topographic swell which, to some degree, has controlled the emplacement of subsequent lava flows. The Bear Trap lava tube flows were also controlled by the topography generated by an older lava tube system to the south (Figure 18). Most of the Bear Trap lava tube system is collapsed, but two uncollapsed segments close to the Arco-Minidoka road are readily accessible. Although the total extent of the flows associated with Bear Trap lava tube cannot be determined because the flanks of the tube-arch and the distal end of the flows are buried, the exposed part of the flow is estimated to be about 60 square kilometers.

Lava tube-fed flows contribute substantially to maintaining the flatness of the plain in that they fill in the low-lying region between adjacent, coalescing low shield volcanoes (Figure 6).

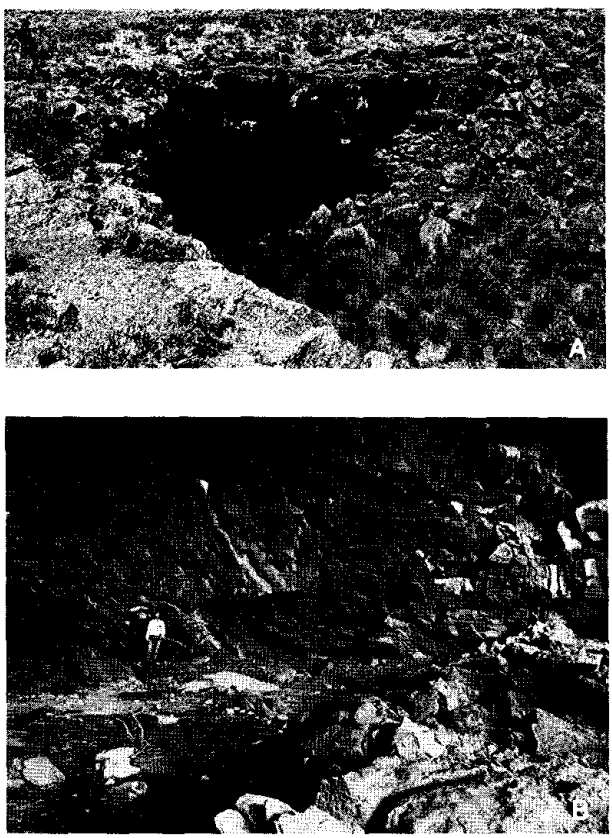

Figure 17. View of Bear Trap lava tube, part of a lava tube system more than 13 kilometers long that fed a major compound lava flow: (A) view of entrance to tube; (B) view of the interior showing massive "lining" of tube.

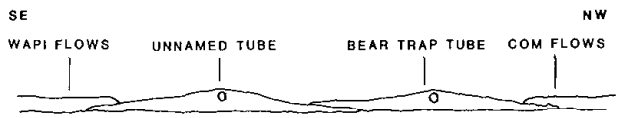

Figure 18. Stylized cross section through flows associated with Bear Trap lava tube and an unnamed lava tube. As shown here, the axes of lava tubes frequently mark the topographically highest parts of tube-fed flows which can exert some control on the emplacement of subsequent flows. (Not to scale, but corresponds approximately to position marked "7" on Figure 1).

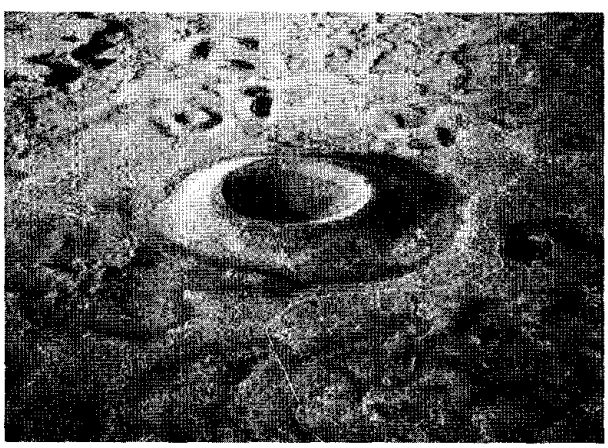

Figure 19. Oblique aerial view southwestward across China Cap, a small scoria cone about 385 meters across that is 14 kilometers southwest of Big Southern Butte. This nearly perfectly circular cone contains a crater 30 meters deep. The rim is composed mostly of scoria with some blocks and bombs and at least one layer of agglutinate. Like Split Butte and Sand Butte, the flanks of China Cap have been partly buried by younger lava flows, creating a distinctive moatlike ring around the cone where the flow front solidified. Photograph by Ronald Greeley, 1970.

MISCELLANEOUS VENT STRUCTURES AND FLOWS

Relatively minor accumulations of lava flows and other volcanic products occur on the plain and on the margins of the plain. These features include tuff-and-cinder cones, such as China Cap (Figure 19) and maar craters such as Sand Crater (Figure 20; see Womer and others, 1982 this volume) and Split Butte (Figure 21). Cinder and spatter cones are rare and appear to be associated with fissures, as discussed above. Some elongate vents and flows are aligned over fissures and may be transitional between fissure flows and low shields associated with rift zones.

Some flows from tubes, central vents, or fissures formed natural levees and developed into lava lakes. The lakes may have been centered over the vent, as at Kings Bowl and Split Butte, or they may have formed perched lava ponds (Figures 11, 15; Holcomb and others, 1974).

Several rivers cut the Snake River Plain into canyons (Figure 22). Throughout the history of the plain, older canyons probably existed, and lava flows may have spilled into the canyons, forming intracanyon flows. Sources for intracanyon flows may have been low shields, fissures, or major lava tubes. Intracanyon flows occur mainly in the western parts of the Snake River Plain, becoming progressively more limited toward the east. Thus, their significance in the accumulation of lavas in the eastern Snake River Plain cannot be assessed fully. Intracanyon flows, however, are probably of relatively limited areal extent and may not be very representative for the eastern plain.

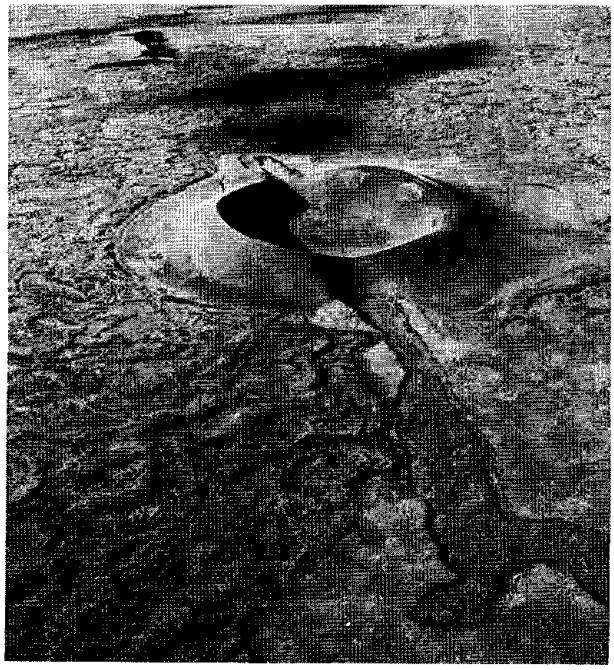

Figure 20. Oblique aerial view northeastward across Sand Butte, a tephra cone 1.2 kilometers in diameter that contains a 650 meter crater. Although most of the inner and outer slopes are covered with vegetation, several outcrops show the outward-dipping tephra layers that make up the cone. Sand Butte is astride a north-south fissure along which flow has occurred, and which has given rise to other vents, such as the series of low spatter ramparts in the upper left part of the photograph. The lower flanks of the cone have been covered by pahoehoe flows, identified here by the hummocky surface and pressure ridges. Photograph from Greeley and King, 1975a.

Figure 21. Oblique aerial view of Split Butte, a maar crater that contained an inner lava lake.

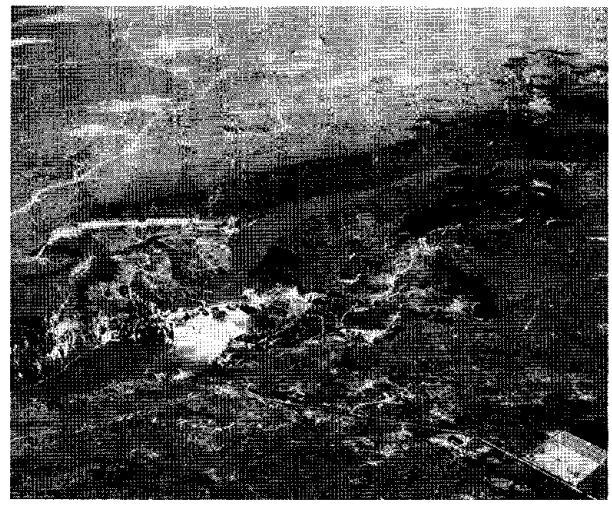

Figure 22. Low oblique aerial view northeastward across the Snake River at Shoshone Falls near Kimberly, Idaho, showing typical canyon cut through basalt flows into older rhyolite flows. Such canyons have been the site for intracanyon flows which in many places are relatively thick flow units, but are limited in lateral extent.

SUMMARY

The Snake River Plain represents a style of volcanism, termed "plains volcanism" (Greeley, 1976, 1982). It is gradational in character between eruptions of flood lava flows and of flows which form shield volcanoes. Distinctions of style are based on thickness, extent, and other properties of the flows for each type of eruption and on gross geomorphology of the three types of basaltic terrains.

As used here, the term "flood eruption" is restricted to the production of flows that exceed 20 to 30 meters in thickness and that are erupted at very high rates of effusion; flood eruptions produce flows that are predominantly single-body cooling units, typified by the Roza Member of the Yakima Basalt in the Columbia Plateau (Swanson and others, 1975). These flows apparently lack well-defined surface flow features such as lava tubes and lava channels. Vent systems are long, narrow fissures that are seldom active for more than one eruption. Vent structures, such as cinder and spatter cones, typically are not preserved on the surface.

Large shield volcanoes of the Hawaiian and Iceland type are formed by relatively quiet lava outpourings, erupted more slowly than in flood eruptions. The flows typically are of the compound type and are emplaced through tubes. Flows are erupted predominantly from central vents—hence the formation of the shield—but can also emanate from fissures.

In contrast, basaltic plains regions, typified by the Snake River Plain, combine aspects of both flood eruptions and shield-forming eruptions. The basaltic lavas in the eastern Snake River Plain accumulated in three main types: flows which formed low shields (small, low profile, central vent volcanoes), flows emplaced by major lava tubes, and flows erupted from fissures, all of which coalesce and interweave in space and time. Based on these criteria, "plains volcanism" is also recognized in the Modoc Plateau of northern California and parts of Iceland. Although low shields are the predominant structure, eruptions appear to have been limited inasmuch as the shields never reached the enormous proportion of the shield volcanoes in Hawaii, the Galapagos, and elsewhere.

REFERENCES

Champion, D. E., 1973, The relationship of large scale surface morphology to lava flow direction, Wapi lava field, southeastern Idaho: State University of New York at Buffalo M.A. thesis, 44 p.

Greeley, Ronald, 1971, Observations of actively forming lava tubes and associated structures, Hawaii: Modern Geology, v. 2, p. 207-233.

———, 1972, Additional observations on actively forming lava tubes and associated structures, Hawaii: Modern Geology, v. 3, p. 157-160.

———, 1976, Modes of emplacement of basaltic terrains and an analysis of mare volcanism in the Orientale Basin: Proceedings of the 7th Lunar Science Conference, p. 2747-2759.

———, 1977, Basaltic "Plains" volcanism, *in* Volcanism of the Eastern Snake River Plain, Idaho: A Comparative Planetary Geology Guidebook, National Aeronautics and Space Administration CR-154621, p. 23-44.

———, 1982, The Snake River Plain, Idaho: Representative of a new category of volcanism: Journal of Geophysical Research, v. 87, p. 2705-2712.

Greeley, Ronald and J. S. King, 1975a, Geologic field guide to the Quaternary volcanics of the south-central Snake River Plain, Idaho: Idaho Bureau of Mines and Geology Pamphlet 160, 49 p.

———, 1975b, Rift zones in the south-central Snake River Plain, Idaho: Geological Society of America, Abstracts with Programs, v. 7, p. 610-611.

Greeley, Ronald, Donna Storm, and Curtis Wilbur, 1976, Frequency distribution of lava tubes and channels on Mauna Loa Volcano, Hawaii: Geological Society of America, Abstracts with Programs, v. 8, p. 892.

Holcomb, R. T., D. W. Peterson, and R. I. Tilling, 1974, Recent land forms at Kilauea Volcano: a selected photographic compilation, *in* Ronald Greeley, editor, Geologic Guide to the Island of Hawaii, National Aeronautics and Space Administration CR-152416, p. 49-86.

LaPoint, P. J. I., 1975, Photogeologic study of volcanic and structural features of the eastern Snake River Plain, Idaho: Geological Society of America, Abstracts with Programs, v. 7, no. 5, p. 620.

———, 1977, Preliminary photogeologic map of the eastern Snake River Plain, Idaho: U. S. Geological Survey, MF-850.

Macdonald, G. A., 1972, Volcanoes: Prentice-Hall, Englewood Cliffs, New Jersey, 510 p.

Murtaugh, J. G., 1961, Geology of Craters of the Moon National Monument: University of Idaho M.S. thesis, 99 p.

Nichols, R. L., 1936, Flow units in basalt: Journal of Geology, v. 44, p. 617-630.

Noe-Nygaard, Arne, 1968, On extrusion forms in plateau basalts: Visindafelag Islendinga, anniversary volume, Reykjavik, p. 10-13.

Peterson, D. W. and D. A. Swanson, 1974, Observed formation of lava tubes during 1970-71 at Kilauea Volcano, Hawaii: Studies on Speleology, v. 2, pt. 6, p. 209-224.

Prinz, Martin, 1970, Idaho rift system, Snake River Plain, Idaho: Geological Society of America Bulletin 81, p. 941-947.

Russell, I. C., 1902, Geology and water resources of the Snake River Plains of Idaho: U. S. Geological Survey Bulletin 199, 192 p.

Stearns, H. T., 1928, Craters of the Moon National Monument, Idaho: Idaho Bureau of Mines and Geology Bulletin 13, 57 p.

Stearns, H. T., Lynn Crandall, and W. G. Steward, 1938, Geology and groundwater resources of the Snake River Plain in southeastern Idaho: U. S. Geological Survey Water Supply Paper 774, 268 p.

Swanson, D. A., 1973, Pahoehoe flows from the 1969-1971 Mauna Ulu eruption, Kilauea Volcano, Hawaii: Geological Society of America Bulletin 84, p. 615-626.

Swanson, D. A., W. A. Duffield, D. B. Jackson, and D. W. Peterson, 1979, Chronological narrative of the 1969-71 Mauna Ulu eruption of Kilauea Volcano, Hawaii: U. S. Geological Survey Professional Paper 1056, 55 p.

Swanson, D. A., T. L. Wright, and R. T. Heltz, 1975, Linear vent systems and estimated rates of magma production and eruption for the Yakima Basalt on the Columbia Plateau: American Journal of Science, v. 275, p. 877-905.

Trimble, D. E. and W. J. Carr, 1961, Late Quaternary history of the Snake River Plain in the American Falls region, Idaho: Geological Society of America Bulletin 72, no. 12, p. 1739-1748.

Walker, G. P. L., 1972, Compound and simple lava flows and flood basalts: Bulletin Volcanologique, v. 36, p. 579-590.

Wentworth, C. K. and G. A. Macdonald, 1953, Structures and forms of basaltic rocks in Hawaii: U. S. Geological Survey Bulletin 994, 98 p.

The Great Rift and the Evolution of the Craters of the Moon Lava Field, Idaho

by

Mel A. Kuntz[1], Duane E. Champion[2], Elliott C. Spiker[3], Richard H. Lefebvre[1,4], and Lisa A. McBroome[5]

ABSTRACT

The Snake River Plain of southern Idaho is a region of late Cenozoic and Quaternary basalt volcanism and many volcanic rift zones. The most spectacular volcanic rift zone on the plain is the Great Rift, an 85-kilometer-long and 2- to 8-kilometer-wide belt of cinder cones, shield volcanoes, eruptive fissures, and open cracks. The Holocene and latest Pleistocene Craters of the Moon lava field is alined along a 45-kilometer segment of the northern part of the Great Rift. The lava field is a composite of more than forty lava flows that have erupted from more than twenty-five vents. It covers an area of about 1,650 square kilometers, contains about 30 cubic kilometers of lava, and is the largest dominantly Holocene basalt lava field in the conterminous United States. Radiocarbon and paleomagnetic data reveal that lava flows of the Craters of the Moon lava field were emplaced in at least eight eruptive periods that began about 15,000 years ago and ended about 2,000 years ago. The lava flows of the Craters of the Moon field were erupted from cinder cones and fissures, most of which are in the Craters of the Moon National Monument. Two other Holocene lava fields on the Great Rift, the Kings Bowl and Wapi fields, represent a small-volume (about 0.005 cubic kilometer) fissure eruption and a large-volume (about 6 cubic kilometers) shield eruption, respectively.

INTRODUCTION

The Snake River Plain of southern Idaho is a region of geologically young basalt volcanism. As many as eight lava fields in the area are known or believed to be younger than 20,000 years old: they include the Craters of the Moon, Kings Bowl, Wapi, Hells Half Acre, Cerro Grande, North Robbers, South Robbers, and Shoshone lava fields (Figure 1).

The Craters of the Moon, Wapi, and Kings Bowl lava fields lie along the Great Rift, an 85-kilometer-long and 2- to 8-kilometer-wide belt of shield volcanoes, cinder cones, eruptive fissures, associated lava flows, and noneruptive fissures. In this report, we describe the largest of these lava fields—the Craters of the Moon field. This lava field, the largest accumulation of dominantly Holocene lava in the conterminous United States, covers an area of 1,650 square kilometers and contains approximately 30 cubic kilometers of lava. The Wapi and Kings Bowl lava fields to the southeast have been described and mapped by Kuntz and others (1980, 1981), King (1977), Covington (1977), Champion (1973), and Champion and Greeley (1977); they are described in only minor detail in this report.

REGIONAL SETTING

The Snake River Plain is an arcuate topographic depression, 50 to 100 kilometers wide, that extends from near Payette, Idaho, on the west for about 250 kilometers southeastward to Twin Falls and then for about 300 kilometers northeastward to near Ashton, Idaho (Figure 1). It is bounded on the north by Mesozoic and early Tertiary granitic rocks of the Idaho batholith and by Tertiary and Quaternary basin-range, block-faulted mountains. The southeast side of the plain is also bounded by basin-range, block-faulted mountains. The southwest side of the plain is bounded by Tertiary rhyolitic and basaltic rocks of the Owyhee Plateau. Upper Tertiary and Quaternary rhyolitic and basaltic rocks of the Yellowstone Plateau occur at the northeast end of the plain. Geologists and geophysicists have traditionally divided the Snake River Plain into eastern, central, and western parts based on different geological histories

[1]U. S. Geological Survey, Denver, Colorado 80225.
[2]U. S. Geological Survey, Menlo Park, California 94025.
[3]U. S. Geological Survey, Reston, Virginia 22092.
[4]Department of Geology, Grand Valley State Colleges, Allendale, Michigan 49401.
[5]Department of Geology and Geophysics, University of Hawaii, Honolulu, Hawaii 96822.

Kuntz, M. A., D. E. Champion, E. C. Spiker, R. H. Lefebvre, and L. A. McBroome, 1982, The Great Rift and the evolution of the Craters of the Moon lava field, Idaho, *in* Bill Bonnichsen and R. M. Breckenridge, editors, Cenozoic Geology of Idaho: Idaho Bureau of Mines and Geology Bulletin 26, p. 423-437.

and geophysical features in each part (Mabey, 1976, 1978, and 1982 this volume).

GENERAL FEATURES OF THE CENTRAL AND EASTERN SNAKE RIVER PLAIN

The central and eastern Snake River Plain is a broad, flat lava plain consisting, at the surface, of basalt lava flows and thin, discontinuous, interbedded loess, eolian sand, and alluvial fan deposits that together have a total thickness of about 1 to 2 kilometers near the area described in this report (Zohdy and Stanley, 1973; Stanley and others, 1977; Doherty and others, 1979). Lava flows of the central and eastern Snake River Plain were erupted from low volcanic vents that are generally alined with and parallel to volcanic rift zones that trend mainly at right angles to the long axis of the eastern Snake River Plain. We define a volcanic rift zone as a narrow belt of faults, grabens, noneruptive fissures, eruptive fissures, spatter cones, spatter ramparts, cinder cones, lava cones, pit craters, and shield volcanoes. Most eruptive vents in volcanic rift zones are elongated and are believed to overlie eruptive fissures (Wentworth and Macdonald, 1953; Kuntz, 1977a, 1977b). Well-defined volcanic rift zones of the Snake River Plain are as much as 10 kilometers wide and 120 kilometers long. The Great Rift is the best example of a volcanic rift zone in the Snake River Plain.

In the central and eastern Snake River Plain, the basaltic volcanism represents the latest phase of a complex and poorly understood tectonic and volcanic history that also includes an earlier phase of rhyolitic volcanism. Available geological, geophysical, radiometric, and drilling data suggest that the rhyolitic

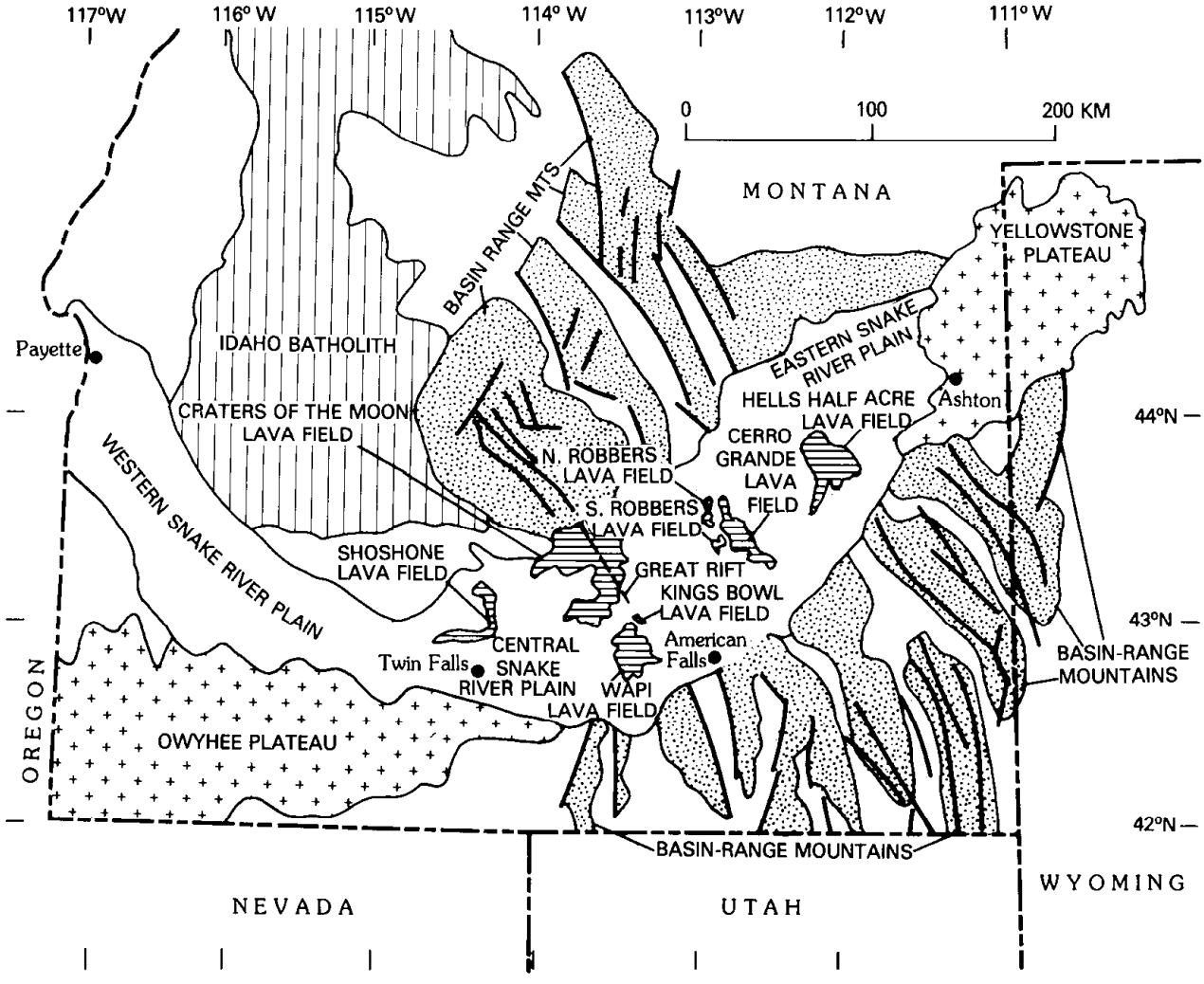

Figure 1. Generalized map of southern Idaho showing major geologic and physiographic features and locations referred to in the text.

rocks were erupted from rhyolitic calderas alined in a northeast-trending belt. The earliest calderas are believed to have formed originally about 12 to 15 million years ago near Twin Falls and to have become progressively younger northeastward to Yellowstone National Park. Models describing the formation of the belt of calderas are discussed by Armstrong and others (1975), Eaton and others (1975), Christiansen and McKee (1978), Mabey and others (1978), and Leeman (1982 this volume).

BASALTIC VOLCANISM IN THE CENTRAL AND EASTERN SNAKE RIVER PLAIN

Basaltic volcanism has occurred as fissure eruptions within volcanic rift zones in many parts of the world, including Hawaii (Macdonald and Abbott, 1970), Iceland (Macdonald, 1972), and the eastern Snake River Plain (Kuntz, 1977a, 1977b), especially along the Great Rift. Based on well-documented Hawaiian eruptions, we believe that typical eruptions along the Great Rift consisted of distinct, though gradational, stages. The stages described below represent a generalized gradational sequence during a prolonged basaltic eruption cycle; individual eruptions along the Great Rift may have included only some of the phases described. Distinctive volcanic landforms representative of each phase of such an eruptive cycle are found along the Great Rift.

Eruptions generally began with a long line of lava fountains that extended for hundreds of meters and locally for a few kilometers along a single fissure or a series of en echelon fissures. Voluminous outwelling of fluid lava along nearly the entire fissure accompanied fountaining. The basaltic lava in the early eruptive stages was extremely fluid and heavily charged with dissolved gases. The early stages of such eruptions led to the development of spatter ramparts and downwind blankets of fine-grained tephra.

After several hours or days, the eruption generally diminished and lava fountains became localized along short segments of fissures. Spatter ramparts were succeeded by spatter or cinder cones which built up around the lava fountains.

After several hours, days, or weeks, a decrease in magma pressure and in the amount of dissolved gas in the magma produced a corresponding decrease in the height of lava fountains and thus to a change in the types of volcanic processes and landforms. During historic, long-lived Hawaiian activity and, by inference, during prehistoric volcanic activity along the Great Rift, fountaining diminished and was followed by quiet but voluminous outpourings of lava over or through the existing spatter or cinder cones. A prolonged period of overflow of lava in most places produced a lava cone composed largely of sheets of pahoehoe lava that mantled the older cone structure. Lava-cone summits are typically indented by an elongated crater. The elongation of the crater is generally parallel to the underlying fissure or rift, which served as the channelway for magma to the vent. Large craters were formed by collapse of the crater walls, accompanied by repeated crater filling and draining.

Where eruption of fluid basaltic lava extended over periods of months and possibly years at a single vent, large lava cones or shield volcanoes were produced. These broad, low, rounded, shield-shaped landforms grew by the continued buildup of thin, far-spreading pahoehoe and, to a lesser extent, áa lava flows. Little explosive activity was involved in the shield-building stage.

PREVIOUS WORK AND METHODS OF THE PRESENT STUDY

This report summarizes various field and laboratory studies that we have carried out over the last ten years. Our studies of the Craters of the Moon lava field were prompted by the U. S. Geological Survey's regional study of the basalt volcanism of the eastern Snake River Plain and by the Survey's study and evaluation of the geology and mineral resources potential of the Great Rift Wilderness Area, a proposed U. S. Bureau of Land Management wilderness area that includes most of the Craters of the Moon and Wapi lava fields (Kuntz and others, 1980, 1981).

The Craters of the Moon lava field has been studied in more detail than any other lava field in the Snake River Plain. Reports by Russell (1902), Stearns (1928), Murtaugh (1961), and Prinz (1970) outlined the basic geologic framework of the lava field. Lefebvre (1975) identified four major groups of lava flows or eruptive pulses in the evolution of the Craters of the Moon lava field by analyzing Landsat images. Champion and Greeley (1977) conducted preliminary studies on the paleomagnetic properties of the Craters of the Moon lava flows and found that paleomagnetic methods could be used for relative dating of individual flows and for correlation of flows that are separated from one another but are believed to be coeval on the bases of field characteristics and stratigraphic relations. Our combined field studies in the summers of 1978 and 1979 made use of Lefebvre's gross stratigraphic relations for major eruptive units, Champion's paleomagnetic data, and preliminary photogeologic maps of the Craters of the Moon lava field compiled at a scale of 1:24,000. We mapped the

entire lava field and collected samples for radiocarbon, paleomagnetic, and petrographic studies and for chemical analyses. Maps of the Craters of the Moon, Wapi, and Kings Bowl lava fields and of structures along the Great Rift, all at a scale of 1:125,000, were published by Kuntz and others (1980, 1981).

The suspected youthfulness of the lava flows erupted along the Great Rift was confirmed by the first published radiocarbon ages of charcoal obtained from beneath lava flows of the Kings Bowl lava field and from tree molds in some of the youngest lava flows in the Craters of the Moon lava field. Prinz (1970) reported an age of 2,130 ± 60 years b.p. for the Kings Bowl lava field, and Bullard and Rylander (1970) and Valastro and others (1972) reported ages of about 2,100 years b.p. for some of the youngest flows in the Craters of the Moon lava field.

We have determined thirty-five additional radiocarbon ages for flows in the Craters of the Moon lava field from organic soil and charcoal samples. The soil and some of the charcoal samples were obtained by excavating beneath the lava flows with a backhoe. The radiocarbon dating study has yielded ages of variable accuracy that require further analysis and interpretation, but the relative ages of major groups of flows for the Craters of the Moon lava field were determined with reasonable accuracy (Table 1). The informal names and the stratigraphic order of the lava flows in each group of flows and approximate ages of the groups of flows are also given in Table 1.

Paleomagnetic measurements on samples from the lava flows of the Craters of the Moon lava field have been used to correlate lava flows, to obtain rough age designations for individual flows and groups of flows, and thereby to decipher the volcanic history of the lava field (D. E. Champion, unpublished data). Each lava flow in the lava field has preserved a record of the local geomagnetic field at the time of its cooling. With the knowledge that secular variation of the geomagnetic field occurs at a geologically rapid rate (4 degrees per century, Champion and Shoemaker, 1977), comparisons of paleomagnetic directions have permitted assignment of lava flows to groups of similar paleomagnetic direction. Conversely, dissimilar paleomagnetic directions are strong evidence that two lava flows do not belong to the same group.

THE GREAT RIFT AND ASSOCIATED VOLCANIC DEPOSITS

The Great Rift (Stearns, 1928; Prinz, 1970) consists of volcanic vents, eruptive fissures, and noneruptive fissures that extend approximately 85 kilometers from the southern Pioneer Mountains southeastward through Craters of the Moon National Monument to Pillar Butte in the Wapi lava field, located about 30 kilometers northwest of American Falls (see Figures 1, 2, and 3A). Three Holocene and latest Pleistocene lava fields—the Craters of the Moon, Wapi, and Kings Bowl—are alined along the trend of the Great Rift. The Kings Bowl lava field is made up of lava flows that originated during a single volcanic episode from fissures on the southern part of the Great Rift. The Wapi lava field is a broad shield volcano with a main vent complex at Pillar Butte on the southern part of the Great Rift. Paleomagnetic (Champion and Greeley, 1977) and radiocarbon studies show that the lava flows of the Wapi lava field and the Kings Bowl lava field were erupted simultaneously about 2,250 years ago over a period of a few tens of years and possibly as short as several weeks or months.

Cinder cones and eruptive fissures occur along the 45-kilometer-long, N. 35° W.-trending Craters of the Moon segment of the northern part of the Great Rift, but they are especially abundant within the Craters of the Moon National Monument. At the southeastern limit of the Craters of the Moon lava field, the Great Rift emerges from beneath lava flows as four sets of open cracks that trend N. 27° W. to N. 43° W., and from which no lava has erupted. Farther south, the Kings Bowl lava field formed along an 11-kilometer-long, N. 15° W.-trending segment of open cracks and eruptive fissures in the Great Rift. The lava flows of the Wapi lava field were erupted from at least five craters that form the vent complex at Pillar Butte. The elongated vents at Pillar Butte are alined in a N. 20° W. direction and suggest that a segment of the Great Rift is buried beneath the Wapi lava field.

Many volcanic rift zones in the central and eastern Snake River Plain appear to be extensions onto the plain of northwest-trending range-front faults that bound basin-range block-fault mountains along the margins of the plain (Kuntz, 1977a, 1977b). In contrast, the Great Rift does not lie on an extension of a range-front fault, but it may be a southeastward extension of a basement structure in older rocks that extends northwest from the margin of the plain. A magnetic high and gravity low centered in the area of Craters of the Moon National Monument probably reflects a deep-seated intrusive body (Kuntz and others, 1980). The magnetic anomaly extends northwestward and is continuous with a northwest-trending magnetic high over a zone of Tertiary intrusive rocks that extends for about 90 kilometers northwest of the plain. The Great Rift and the zone of Tertiary intrusive bodies probably are the expression in the upper crust of a northwest-trending basement structure that extends across nearly the entire width of the

Table 1. Eruptive periods, approximate age of eruptive periods, informal names of lava flows of the upper part of the Snake River Group, and source vents for lava flows in the Craters of the Moon, Wapi, and Kings Bowl lava fields.

Eruptive period and approximate age	Informal name and lava type of major flows* (in order of ascending stratigraphic position)	Source vents (queried where uncertain)
A 2,100 to 2,300 years b.p.	Broken Top (p)	Broken Top, east and south sides
	Blue Dragon (p)	Eruptive fissures south of Big Craters cinder cone
	Trench Mortar Flat (p)	Eruptive fissures between Big Cinder Butte and The Watchman cinder cone
	North Crater (p)	North Crater cinder cone
	Big Craters (Green Dragon) (p)	Eruptive fissure at north end of Big Craters cinder cone
	Kings Bowl (p)	Fissure vents north and south of Kings Bowl
	Wapi (p)	Vents at Pillar Butte
	Serrate (a-b)	North Crater(?)
	Devils Orchard (a-b)	North Crater cinder cone(?)
	Highway (a-b)	North Crater cinder cone(?) or tholoid vent
B 3,500 to 4,500 years b.p.	Vermillion Chasm (p)	Eruptive fissures at Vermillion Chasm
	Deadhorse (p)	Eruptive fissures north and south of Black Top Butte cinder cone
	Devils Cauldron (p)	Devils Cauldron
	Minidoka (p)	Obscure vents located about 5 kilometers northeast of New Butte cinder cone
	Larkspur Park (p)	
	Rangefire (p)	Black Top Butte cinder cone(?)
C 5,800 to 6,200 years b.p.	Indian Wells north (a)	Big Cinder Butte cinder cone(?)
	Indian Wells south (a)	Big Cinder Butte cinder cone(?)
	Sawtooth (a)	Big Cinder Butte cinder cone
	South Echo (p)	Eruptive fissures south of Echo Butte cinder cone
	Sheep Trail Butte (p-a)	Sheep Trail Butte cinder cone
	Fissure Butte (p-a)	Fissure Butte cinder cone
	Sentinel west (p)	The Sentinel cinder cone
	Sentinel south (p)	The Sentinel cinder cone
D About 6,600 years b.p.	Silent Cone (a)	Silent Cone cinder cone
	Carey Kipuka (a)	Silent Cone cinder cone(?)
	Little Park (a)	Silent Cone cinder cone(?)
	Little Laidlaw Park (a)	Silent Cone cinder cone(?)
E 7,300 to 7,800 years b.p.	Grassy Cone (p)	Grassy Cone cinder cone
	Laidlaw Lake (p)	Grassy Cone cinder cone
	Lava Point (a)	Great Rift northwest of Echo Crater
F 10,000 to 11,000 years b.p.	Pronghorn (p)	Great Rift near Sheep Trail Butte
	Bottleneck Lake (p)	Great Rift near Sheep Trail Butte
	Heifer Reservoir (p)	Great Rift near Crescent Butte
G 12,000 to 12,900 years b.p.	Sunset (p)	Sunset Cone cinder cone
	Carey (p)	Sunset Cone cinder cone
	Lava Creek (p-a)	Vents near Lava Creek
H About 15,000 years b.p.	Kimama (p)	unknown
	Bear Den Lake (p)	unknown
	Baseline (p)	unknown
	Little Prairie (p)	unknown Echo Crater and (or) Crescent Butte(?)
	Lost Kipuka (p)	unknown
	No Name (p)	unknown
	Brown flow (p)	unknown

*(p) chiefly pahoehoe flows
(a) chiefly áa flows
(a-b) áa and block flows
(p-a) pahoehoe and áa flows

central and eastern Snake River Plain and into the region to the northwest.

CRATERS OF THE MOON LAVA FIELD

The Craters of the Moon lava field is a composite of more than forty lava flows erupted from more than twenty-five cinder cones and eruptive fissures, most of which are in Craters of the Moon National Monument (Figure 2). The lava field formed during at least eight periods of eruptive activity, each of which was about 1,000 years or less duration and separated by intervals of quiescence lasting from a few hundred years to more than two thousand years. The sequential development of the Craters of the Moon lava field during its eight periods of eruptive activity is shown in Figure 3.

LAVA FLOWS

Most flows of the lava field are pahoehoe; they have hummocky, billowy, ropy, and wrinkled surfaces that reflect the fluid nature of the lava. The upper centimeter of many fresh, unweathered flows consists of vesicular to dense glass that has a striking blue to green irridescence. The pahoehoe flows were typically fed through lava tubes and tube systems. Localized collapse of the roofs of the lava tubes in the Broken Top and Blue Dragon flows (Figure 3A) formed "skylights" and entrances to lava tunnels that are popular attractions to visitors in Craters of the Moon National Monument. Pressure ridges and pressure plateaus are common large-scale features of the surfaces of the pahoehoe flows.

Some flows are of áa lava that has a rough, jagged, clinkery surface. Large areas of the surface of áa flows consist of irregular blocks of broken lava, some of which are broken slabs of pahoehoe. The inner parts of the áa flows are typically massive. Many surfaces of áa flows in the Craters of the Moon lava field are littered with blocks and monoliths of well-bedded cinder and spatter material as much as hundreds of meters across, which were broken from cinder cones at the source vent; notable examples are the Serrate, Sawtooth, and Silent Cone áa flows (Figures 2 and 3A). A few flows such as the Highway flow (Figures 2 and 3A) consist of block lava that is characterized by irregular blocks of dense, glassy lava with smooth surfaces. The lava flows (informal units in the upper part of the Snake River Group), cinder cones, and eruptive fissures of the Craters of the Moon, Wapi, and Kings Bowl lava fields lie on older lava flows of the Snake River Group. The younger lava flows (Holocene and latest Pleistocene informal units of the Snake River Group) in the Craters of the Moon lava field have fresh, nearly unweathered, glassy (typically blue) crusts, and they are not covered by eolian deposits. The older (Pleistocene) lavas are generally covered by a variable thickness of eolian deposits, and exposed parts of the flows are light colored, less dense, weathered, and weakly to strongly oxidized.

ERUPTIVE FISSURES

Eruptive fissures are strikingly displayed in the Craters of the Moon National Monument, particularly in the Trench Mortar Flat area between Big Cinder Butte and The Watchman cinder cones (Figure 2). During early parts of eruptions along these fissures, fountains of lava, commonly called "curtains of fire," erupted on fissure segments as long as several kilometers. The fountains built spatter ramparts and low walls of agglutinated spatter along the margins of the fissures. Copious volumes of lava flowed away from the fissures to form extensive flows. After the curtain-of-fire phase of a fissure eruption, lava typically erupted from one or two places along the fissures and formed low spatter and cinder cones.

CINDER CONES

Cinder cones are widely scattered throughout the eastern Snake River Plain but they are best developed in size, shape, and number along the Great Rift, mainly within the Craters of the Moon National Monument (Figure 2). More than twenty-five cones occur in a zone about 28 kilometers long and as much as 2.5 kilometers wide. The cinder cones are composed of agglutinated and nonagglutinated tephra layers interbedded with thin lava flows. In the Monument area, prevailing winds from the west and southwest caused greater downwind accumulation of tephra on the east or northeast sides of many cinder cones. Particularly good examples of asymmetric cinder cones are Paisley Cone and Inferno Cone (Figure 2). Composite cinder cones such as Sunset Cone and Big Craters (Figure 2) formed by overlapping accumulations of ejecta from several contemporaneous or nearly contemporaneous lava fountains. The composite cones contain many pits and have elongate crater walls alined along the eruptive fissure. Many of the cinder cones are breached on the northwest or southeast flanks or both. The breaches probably formed by a number of mechanisms: (1) by the burrowing of lava flows erupted along a feeder fissure

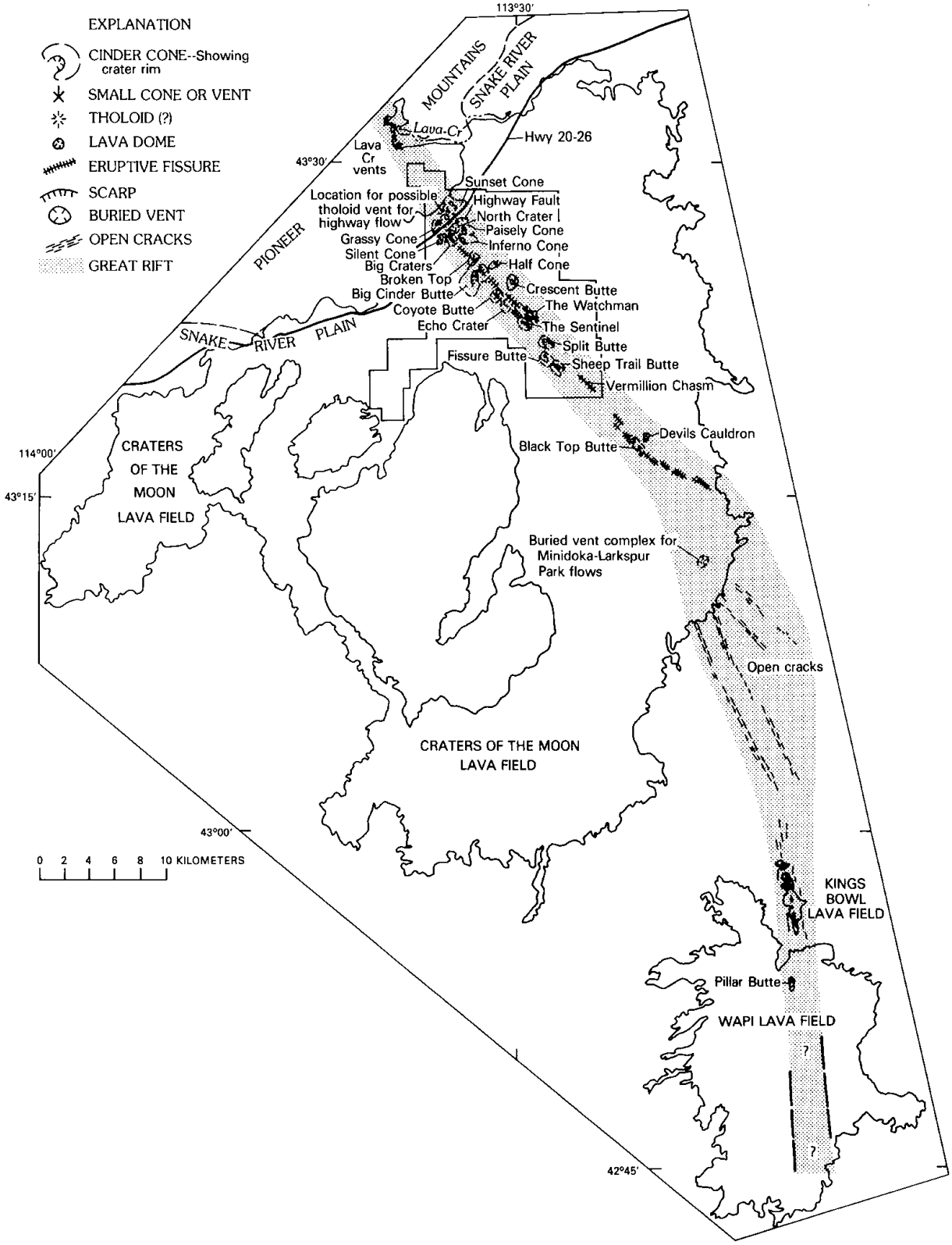

Figure 2. Map of the Great Rift showing geographic, volcanic, and structural features.

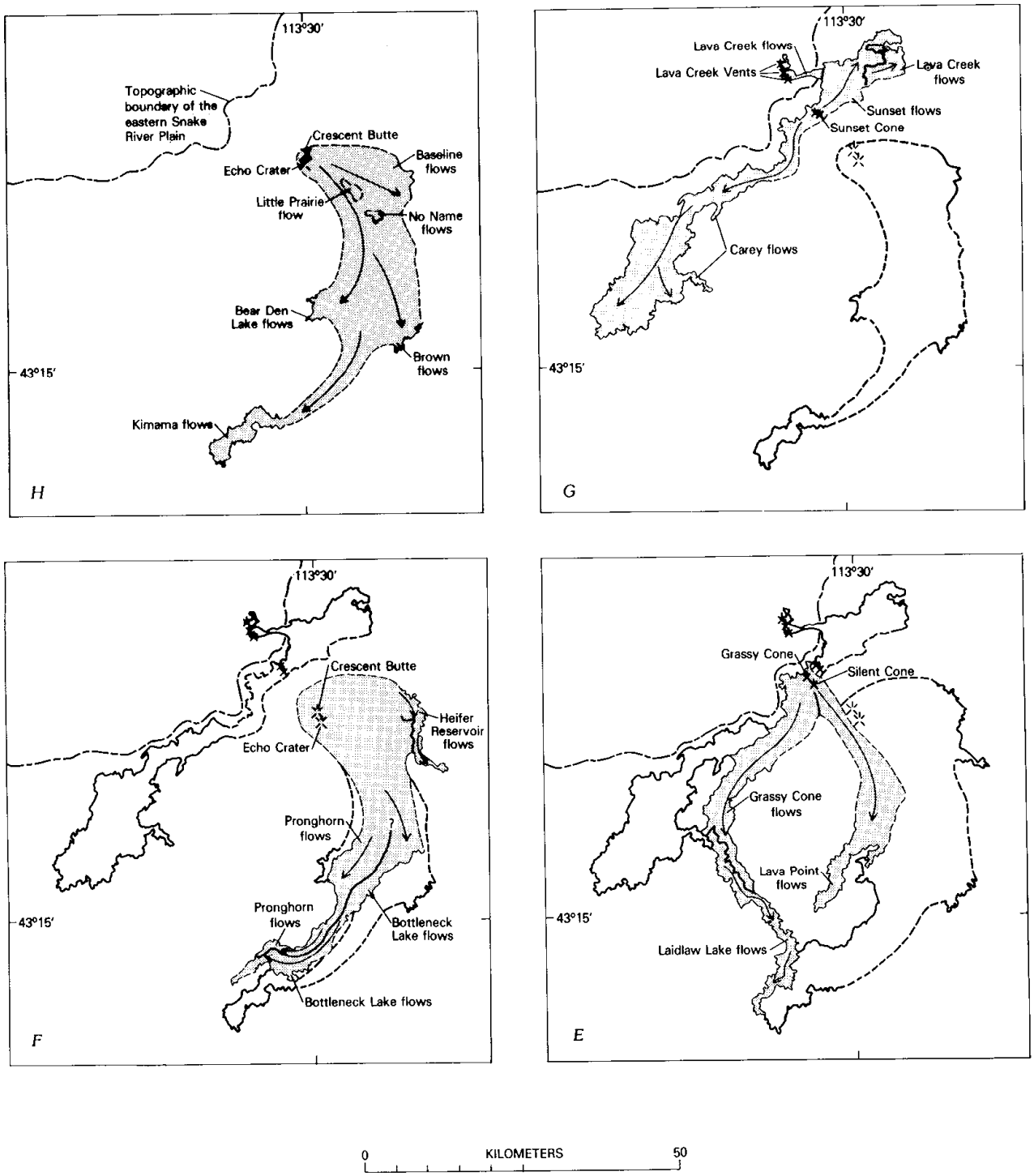

Figure 3. Diagram showing the sequential development of the Craters of the Moon lava field from the oldest eruptive period (H) to the youngest eruptive period (A).

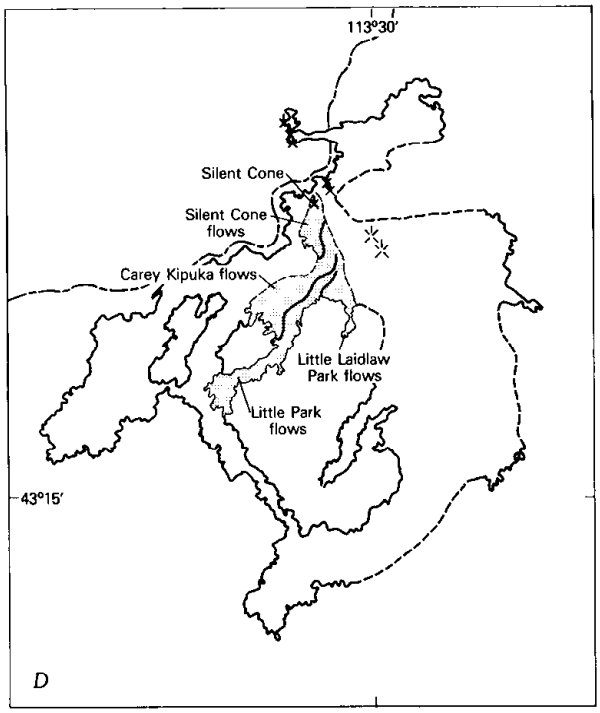

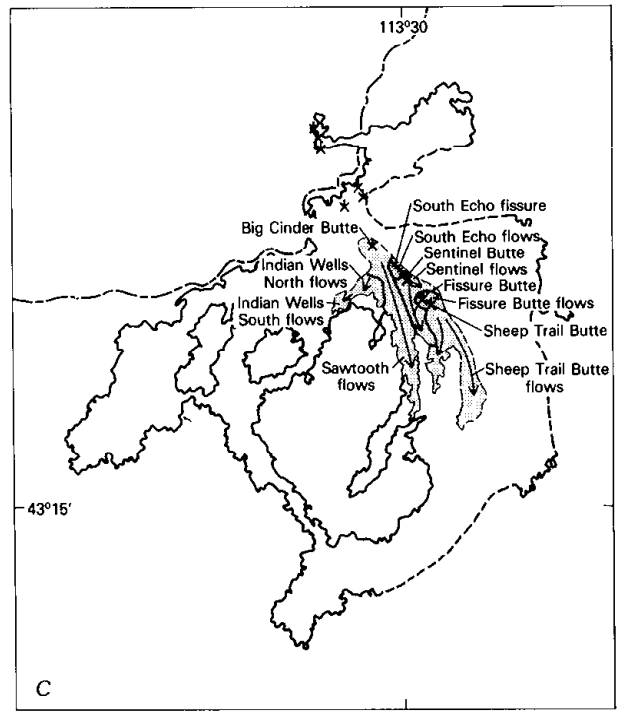

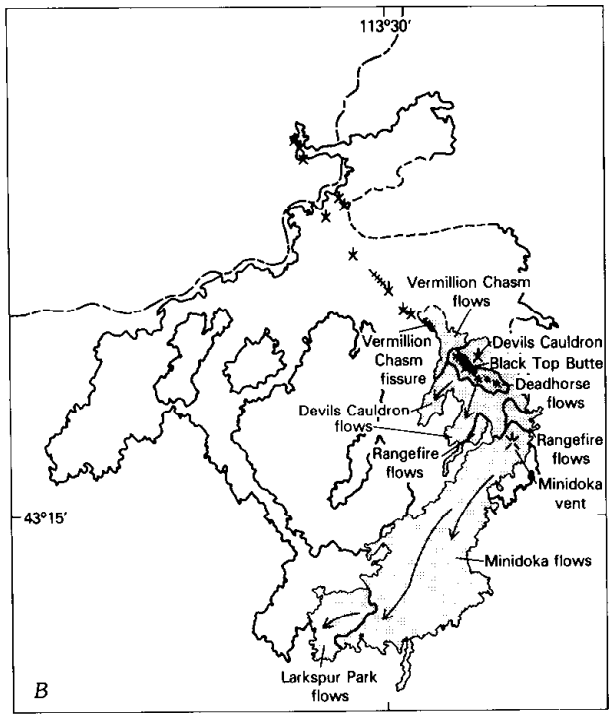

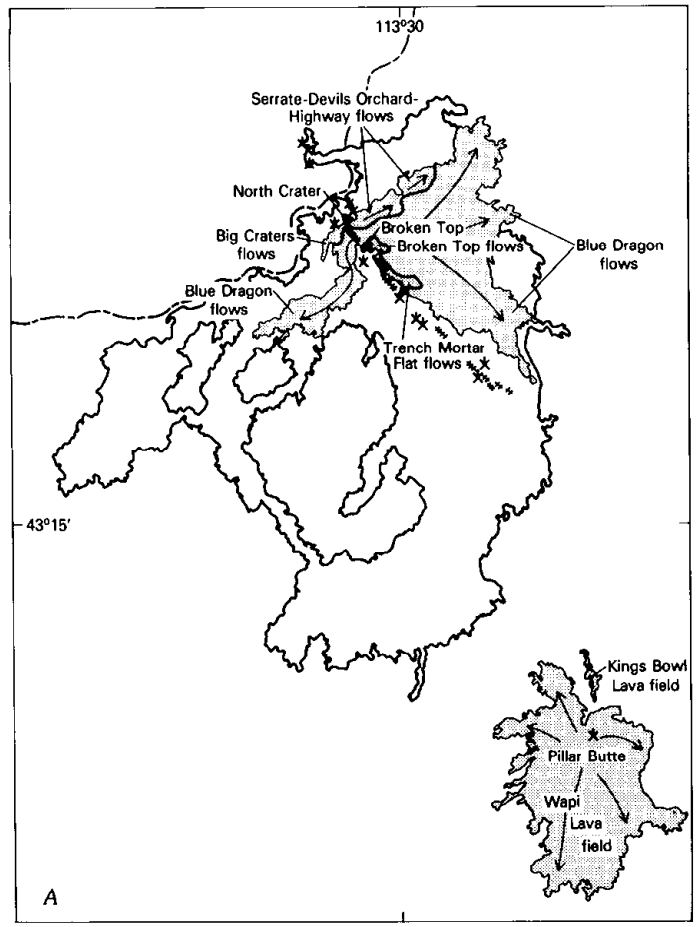

Figure 3. continued.

beneath the cones after they formed, (2) by the burrowing of lava flows through, and erosion of, the walls of the cinder cone, (3) or by the removal of ejecta by a lava stream that flowed from the feeder fissure during formation of the cones. Some cinder cones appear to have had a multistage history. Younger lava erupted from vents in North Crater, The Watchman, and Sheep Trail Butte cinder cones (Figure 2) as volcanic activity in and near them was rejuvenated.

VOLCANIC HISTORY

Lava flows and groups of flows that are believed to have similar ages, based on field, radiometric, and paleomagnetic data, can be grouped into what we term "eruptive periods." Eight eruptive periods (A through H) are presently recognized in the Craters of the Moon lava field. Because we have sampled only some of the flows from each eruptive period and because our radiocarbon studies have yielded only minimum ages, the ages of the beginning and end, and thus the durations of each eruptive period are uncertain. Paleomagnetic studies show, however, that the durations of most of the younger eruptive periods were probably less than a few hundred years. The intervals between eruptive periods may have been times of volcanic quiescence or sporadic volcanic activity, and the times within eruptive periods may have been periods of nearly constant or irregular eruptive activity; we cannot be more specific because many lava flows have not been dated or they cannot be dated.

The oldest lava flows that we assign to the Craters of the Moon lava field flowed away from the general location of the Great Rift. This relationship suggests that the Great Rift was a locus of source vents for even the earliest flows of the Craters of the Moon lava field, and that these early flows are covered by younger flows. Thus, we recognize that our studies may treat only the later part of the history of the Craters of the Moon lava field rather than its complete history.

Figure 3 is a generalized set of diagrams prepared from more detailed geologic maps of the Craters of the Moon lava field (Kuntz and others, 1980, 1981). The figure shows the sequential development of the Craters of the Moon lava field from the oldest recognizable eruptive period (H) through the youngest eruptive period (A). Generalized contacts between individual flows and names of source vents for the flows are shown on diagrams for each individual eruptive period, but they are not repeated on diagrams for succeeding eruptive periods.

Eruptive Period H

The earliest recognized eruptive period (H) in the formation of the Craters of the Moon lava field produced pahoehoe lava flows about 15,000 years ago. These flows are now exposed near the margins of the Craters of the Moon lava field and along the Great Rift south of Crescent Butte (Figure 3H). Source vents have not been identified for these flows, but their distribution and flow directions indicate a source on the Great Rift, possibly at Echo Crater or Crescent Butte.

The flows of eruptive period H have surfaces that are more weathered than younger flows of the Craters of the Moon lava field, but the flows of eruptive period H have little or no cover of eolian sand or loess; thus we distinguish the flows of period H from still older, loess- and sand-covered, more deeply weathered flows that are probably not part of the Craters of the Moon lava field. Because the flows of eruptive period H occur as widely scattered exposures and because we have few radiocarbon ages for flows of the group, the stratigraphic order of the flows (Table 1) and their absolute age are largely speculative.

Eruptive Period G

About 12,500 years ago, eruptions took place from at least four vents along an extension of the Great Rift in the southern Pioneer Mountains, about 2 to 5 kilometers northwest of the northern boundary of Craters of the Moon National Monument near the headwaters of Lava Creek (Figures 2 and 3G). The flows from the Lava Creek vents traveled as much as 19 kilometers to the east onto the Snake River Plain. They are some of the least evolved lavas (that is, about 44 SiO_2; see Leeman and others, 1976) of any erupted along the Great Rift; thus they probably acquired their áa character because they descended steep slopes from their source vents to the plain. The complex Sunset Cone cinder cone and its associated flows were also formed during this eruptive period. Voluminous pahoehoe lava of the Sunset flows traveled as much as 20 kilometers to the northeast over the Lava Creek flows, and pahoehoe lava of the Carey flows traveled as much as 53 kilometers to the southwest. We correlate the Sunset and Carey flows with the same source vent at Sunset Cone based on similar paleomagnetic directions for the two flows.

Eruptive Period F

The Pronghorn and Bottleneck Lake pahoehoe flows along the southwestern margin of the Craters of

the Moon lava field (Figure 3F) were erupted about 10,000 to 11,000 years ago. The distribution and flow directions of the Pronghorn and Bottleneck Lake flows suggest a source vent on the Great Rift south of the present site of Sheep Trail Butte. The Heifer Reservoir pahoehoe flows at the east margin of the Craters of the Moon lava field (Figure 3F) have a radiocarbon age of about 10,700 years; thus we group them with the Pronghorn and Bottleneck Lake flows. Flow directions for the Heifer Reservoir flows suggest a source vent on the Great Rift near Crescent Butte and Echo Crater.

Eruptive Period E

We believe that eruptive period E began about 7,800 years ago with the eruption of the Lava Point áa flows. The Lava Point flows are contiguous with other áa flows located near the southern boundary of Craters of the Moon National Monument, suggesting a similar age for all the áa flows. However, we believe the Lava Point áa flows are considerably older than the other áa flows, and we assign them to eruptive period E based upon a radiocarbon age of about 7,800 years. The proximal parts of the Lava Point flows are covered by younger flows, but flow directions on exposed distal parts suggest a source vent on the Great Rift northwest of Echo Crater (Figures 2 and 3E).

Grassy Cone, a complex cinder cone on the Great Rift in the northern part of the Craters of the Moon National Monument (Figure 2), formed after the eruption of the Lava Point áa flows. Pahoehoe flows from Grassy Cone traveled as much as 52 kilometers to the south and formed the Grassy Cone and Laidlaw Lake flows which, together, created the long, narrow, composite flow along the western and southwestern margins of the Craters of the Moon lava field (Figure 3E). The stratigraphic and radiocarbon data show that the Laidlaw Lake flows are slightly older than the Grassy Cone flows, that both flows formed after the Lava Point flows, and that both flows were erupted within a short time about 7,400 years ago.

Eruptive Period D

Eruptive period D is characterized by bulbous, monolith-strewn áa flows. All of the áa flows are covered by younger flows in their proximal parts, but their flow directions and paleomagnetic data suggest that all or most of them were erupted from Silent Cone (Figure 3D). Slumped walls and cone wall remnants suggest that eruptions of áa-forming lavas destroyed the north side of Silent Cone.

Eruptive Period C

Eruptions from fissures and cinder cones along a 9-kilometer-long segment of the Great Rift between Sheep Trail Butte and Echo Crater produced the Sentinel, Fissure Butte, Sheep Trail, and South Echo lava flows (Figure 3C). Paleomagnetic evidence shows that the eruption of the Sentinel flows preceded the other flows of eruptive period C by several decades or perhaps by as much as a century. These flows consist of pahoehoe near their source vents, but several flows become áa several kilometers away from their vents. Eruptive period C ended with the formation of áa flows and Big Cinder Butte, the largest cinder cone along the Great Rift (Figures 2 and 3C). The bulbous, monolith-strewn Sawtooth, Indian Wells South, and Indian Wells North áa flows were probably all erupted from the slumped and broken southern part of Big Cinder Butte.

We have been able to obtain a radiocarbon age only for the Sawtooth flows of eruptive period C, so we cannot place limits on the beginning or the end of the period. We suspect that most of the earlier group of pahoehoe-áa flows (Sentinel, Fissure Butte, Sheep Trail, and South Echo) were erupted within a short time, probably less than 100 years. The subsequent eruptions of period C about 6,000 years ago centered at Big Cinder Butte, the source vent for the Sawtooth and probably for the Indian Wells North and the Indian Wells South áa flows. The time between the eruption of the pahoehoe-áa group of flows and the áa group of flows is unknown, but we estimate it to be several hundred years or less.

Eruptive Period B

Radiocarbon data suggest that eruptive period B began about 4,500 years ago and lasted for about 1,000 years. Black Top Butte (also called Blacktail Butte), the southeasternmost cinder cone along the Great Rift in the Craters of the Moon lava field (Figure 2), formed early in eruptive period B and is probably the source vent for the Rangefire flows (Figure 3B). Fluid pahoehoe from obscure vents along the Great Rift about 10 kilometers southeast of Black Top Butte cinder cone formed the voluminous Larkspur Park and Minidoka flows (Figure 3B) about 3,600 years ago. A small driblet spire and a few small depressions now mark the site of a formerly larger vent complex for the Larkspur Park-Minidoka flows. The vent complex was inundated by lava flows; thus its size and shape are unknown.

A broad lava cone at Devils Cauldron (Figure 3B) is indented by two steep-sided vents that formerly contained lava lakes. The lava cone is the source area

for the Devils Cauldron pahoehoe flows (Figure 3B) that are stratigraphically younger than the Minidoka flows. Eruptive fissures paralleled by spatter ramparts and thin blankets of tephra extend as much as 9 kilometers northwest and southeast of Black Top Butte cinder cone (Figure 3B). The fissures are the source vents for the Deadhorse and Vermillion Chasm shelly pahoehoe flows (Figure 3B). These flows appear dusty brown, altered, and anomalously old due to weathering of their thin, highly vesicular crusts.

Eruptive Period A

We do not have radiocarbon ages on critical flows that formed during eruptive period A, such as the Highway, Devils Orchard, Serrate, Big Craters, and North Craters flows, but the stratigraphic order for flows of eruptive period A (Table 1) is reasonably well known from field relations. The absolute age of the Highway-Devils Orchard-Serrate group of áa and block lava flows is unknown, but we assume that the group formed no more than a few hundred years before the next youngest flows (Big Craters) erupted from the northern part of the Great Rift. We therefore include the Highway-Devils Orchard-Serrate group of flows as part of eruptive period A. Paleomagnetic intensity measurements suggest that the Highway flow was erupted during a peak of geomagnetic field intensity about 2,300 years ago. We cannot, however, discount the possibility that the áa-block lava group of flows is considerably older, possibly as much as several hundred or several thousand years, and represents a separate eruptive period unrelated to the eruption of the younger group of dominantly pahoehoe flows.

The sequence of events that led to the eruption of the Highway-Devils Orchard-Serrate flows is extremely difficult to decipher in the field. At present, we still disagree among ourselves about the sequence of events even after many days of careful field work. We present here two possible sequences of events for the formation of the Highway-Devils Orchard-Serrate group of flows. Additional field studies may help us to choose among and refine some of the ideas presented here.

In the first sequence of events, we suggest that eruptive period A began about 2,300 years ago with eruptions in North Crater (Figure 2) that produced a large, viscous, block lava flow (Highway) which flowed northward down the flanks of North Crater into the valley between Sunset Cone and Grassy Cone cinder cones (Figures 2 and 3A). The eruptions destroyed a large part of the north flank of North Crater and possibly other cinder cones that may have been located to the north and northeast of North Crater. The eruption of the block lava of the Highway flow was accompanied by a collapse of the north side of North Crater, during which the "highway fault" (Figure 2) formed. The "highway fault" is an arcuate, steep scarp, 1 to 10 meters high, that appears to be a segment of a ring fracture that may record the collapse of the north flank of North Crater during the eruption of the Highway flow. The Highway flow reversed its direction of flow back toward North Crater after the "highway fault" formed and after the north flank of North Crater was destroyed. Continuation of the eruption produced additional áa and block lavas that formed the Devils Orchard and Serrate flows that moved to the north and east of North Crater (Figure 3A). The Devils Orchard and Serrate flows are strewn with monoliths that were carried away from the slumped and broken northern flank of North Crater. The Highway, Devils Orchard, and Serrate flows are not in mutual contact and their proximal parts are covered by younger flows (Figure 3A), thus it is not possible to determine the age relations among them or even to determine their source vent or vents unequivocally. However, we feel that (1) the three flows may represent the eruption of successively less evolved lavas, (2) that the eruption of the highly evolved Highway flow (about 63 percent SiO_2) was so violent that it destroyed much of North Crater, and (3) that the subsequent Devils Orchard (about 61 percent SiO_2) and Serrate (about 58 percent SiO_2) lavas were viscous enough to transport large blocks of broken crater walls of North Crater for distances of several kilometers.

In the second sequence of events, we suggest that the Highway flow formed as a steep-sided tholoid in the area between Grassy Cone and Sunset Cone cinder cones (Figures 2 and 3A). Evidence for a vent beneath the northern part of the Highway flow is weak, but the viscous lava of the Highway flow may well have built up over the vent and obscured it. The southern edge of the tholoid overtopped a low ridge, and part of the viscous lava flowed to the south toward the site of North Crater. The eruption then moved southward along a fissure system and centered at North Crater (Figure 2). Viscous lava erupted from North Crater and began to destroy its northern flank and formed the Devils Orchard flow. Continued eruption of viscous lava and concomitant collapse of the north flank of North Crater formed the monolith-strewn Serrate flows (Figure 3A).

After the eruption of the Highway, Devils Orchard, and Serrate flows, about 2,250 years ago, basaltic lava erupted from two fissure systems on the southern part of the Great Rift and formed the Kings Bowl and Wapi lava fields (Figure 3A). The youngest eruptions

in the Craters of the Moon lava field occurred about 2,100 years ago. These eruptions were mainly from fissures and cinder cones at Big Craters in the northern part of the Great Rift in the area between Inferno Cone and North Crater (Figures 2 and 3A). The lava from the Big Craters vents is of the pahoehoe type and has a characteristic greenish brown glassy crust. Eruptive fissures in the Trench Mortar Flat area between Big Cinder Butte and The Watchman cinder cones (Figures 2 and 3A) formed flanking spatter ramparts and thin flows of gas-charged shelly pahoehoe. Voluminous eruptions of pahoehoe lava with iridescent blue glassy crusts (Blue Dragon flows) then occurred from fissures and lava domes located south of Big Craters (Figures 2 and 3A). Most of the lava erupted from this locality flowed to the east through a series of large lava tubes. Much of the lava in the distal parts of the Blue Dragon flows was erupted from rootless vents along the lava tubes. The youngest eruptions in the Craters of the Moon lava field occurred from obscure vents on the east side of Broken Top cinder cone (Figures 2 and 3A).

SUMMARY

This paper is a general summary of our investigations of the late Pleistocene-Holocene history of the Great Rift area of the Snake River Plain. Our paleomagnetic, radiocarbon, petrographic, and geochemical studies are still in progress and will be left for later reports.

Our regional studies show that the Great Rift area is unique in the Snake River Plain. We know of only one other area, the Spencer-High Point volcanic rift zone in the northeastern part of the plain, where lava flows have been erupted repeatedly on a short segment of a fissure system in a relatively short time. In contrast, the eruptions of lava that formed the Kings Bowl and Wapi lava fields represent simple eruptive bursts of short duration that appear to be typical of most eruptions on the Snake River Plain. Why one volcanic rift zone has experienced a more complex, short-term volcanic history and why other volcanic rift zones appear to have experienced a more simple, yet prolonged volcanic history are problems that have no obvious answers at present. Factors such as regional stress buildup and release, mechanisms of magma formation and migration to the surface, and regional tectonic models that relate to volcanism are yet to be formulated into a comprehensive model for the central and eastern Snake River Plain.

ACKNOWLEDGMENTS

We are grateful to Cy Hentges and David Clark of Craters of the Moon National Monument for their advice and guidance in planning our field work. Boyd Robertson of Darlington, Idaho, operated a backhoe with a surgeon's skill and was able to provide us with radiocarbon samples from localities that appeared, in many cases, to be inaccessible. Sam Buckley of Mountain States Helicopters Inc., Rigby, Idaho, provided us with excellent helicopter service.

REFERENCES

Armstrong, R. L., W. P. Leeman, and H. E. Malde, 1975, K-Ar dating of Quaternary and Neogene volcanic rocks of the Snake River Plain, Idaho: American Journal of Science, v. 275, no. 2, p. 225-251.

Bullard, F. M. and D. L. Rylander, 1970, Holocene volcanism in the Craters of the Moon National Monument and adjacent areas, south-central Idaho: Geological Society of America, Abstracts with Programs, v. 2, no. 4, p. 273-274.

Champion, D. E., 1973, The relationship of large-scale surface morphology to lava flow direction, Wapi lava field, southeast Idaho: State University of New York at Buffalo M.A. thesis, 44 p.

Champion, D. E. and Ronald Greeley, 1977, Geology of the Wapi lava field, Snake River Plain, Idaho, *in* Ronald Greeley and J. S. King, editors, Volcanism of the Eastern Snake River Plain, Idaho; A Comparative Planetology Guidebook: Washington, D.C., National Aeronautics and Space Administration, p. 133-152.

Champion, D. E. and E. M. Shoemaker, 1977, Paleomagnetic evidence for episodic volcanism on the Snake River Plain, Abstracts for the Planetary Geology Field Conference on the Snake River Plain, Idaho: National Aeronautics and Space Administration Technical Memorandum TM-78,436, p. 7-9.

Christiansen, R. L. and E. H. McKee, 1978, Late Cenozoic volcanic and tectonic evolution of the Great Basin and Columbia intermontane regions, *in* R. B. Smith and G. P. Eaton, editors, Cenozoic Tectonics and Regional Geophysics of the Western Cordillera: Geological Society of America Memoir 152, p. 283-312.

Covington, H. R., 1977, Preliminary geologic map of the Pillar Butte, Pillar Butte NE, Pillar Butte SE, and Rattlesnake Butte quadrangles, Bingham, Blaine, and Power Counties, Idaho: U. S. Geological Survey Open-File Report 77-779, scale 1:48,000.

Doherty, D. J., L. A. McBroome, and M. A. Kuntz, 1979, Preliminary geological interpretation and lithologic log of the exploratory geothermal test well (INEL-1), Idaho National Engineering Laboratory, eastern Snake River Plain, Idaho: U. S. Geological Survey Open-File Report 79-1248, 10 p.

Eaton, G. P., R. L. Christiansen, H. M. Iyer, A. M. Pitt, D. R. Mabey, H. R. Blank, Isidore Zietz, and M. E. Gettings, 1975, Magma beneath Yellowstone National Park: Science, v. 188, no. 4190, p. 787-796.

King, J. S., 1977, Crystal Ice Cave and King's Bowl Crater, eastern Snake River Plain, Idaho, *in* Ronald Greeley and J. S. King, editors, Volcanism of the Eastern Snake River Plain, Idaho; A Comparative Planetology Guidebook: Washington, D.C., National Aeronautics and Space Administration, p. 133-152.

Kuntz, M. A., 1977a, Extensional faulting and volcanism along the Arco rift zone, eastern Snake River Plain, Idaho: Geological Society of America, Abstracts with Programs, v. 9, no. 6, p. 740-741.

———, 1977b, Rift zones of the Snake River Plain, Idaho, as extensions of Basin-Range and older structures: Geological Society of America, Abstracts with Programs, v. 9, no. 7, p. 1061-1062.

Kuntz, M. A., R. H. Lefebvre, D. E. Champion, L. A. McBroome, D. R. Mabey, W. D. Stanley, and H. R. Covington, 1983, Geological and geophysical investigations of the proposed Great Rift Wilderness Area, Idaho: U. S. Geological Survey MF-report (in press).

Kuntz, M. A., R. H. Lefebvre, D. E. Champion, L. A. McBroome, D. R. Mabey, W. D. Stanley, H. R. Covington, James Ridenour, and R. B. Stotelmeyer, 1980, Geological and geophysical investigations and mineral resources potential of the proposed Great Rift Wilderness Area, Idaho: U. S. Geological Survey Open-File Report 80-475, 48 p.

LaPoint, P. J. I., 1977, Preliminary photogeologic map of the eastern Snake River Plain, Idaho: U. S. Geological Survey MF-map 850.

Leeman, W. P., 1982, Development of the Snake River Plain-Yellowstone Plateau province, Idaho and Wyoming: an overview and petrologic model, *in* Bill Bonnichsen and R. M. Breckenridge, editors, Cenozoic Geology of Idaho: Idaho Bureau of Mines and Geology Bulletin 26.

Leeman, W. P., C. J. Vitaliano, and Martin Prinz, 1976, Evolved lavas from the Snake River Plain; Craters of the Moon National Monument, Idaho: Contributions to Mineralogy and Petrology, v. 56, p. 35-60.

Lefebvre, R. H., 1975, Mapping in the Craters of the Moon volcanic field, Idaho, with LANDSAT (ERTS) imagery: International Symposium on Remote Sensing of the Environment, 10th, Proceedings, v. 2, no. 10, University of Michigan, Ann Arbor, p. 951-957.

Mabey, D. R., 1976, Interpretation of a gravity profile across the western Snake River Plain, Idaho: Geology, v. 4, p. 53-55.

———, 1978, Regional gravity and magnetic anomalies in the eastern Snake River Plain, Idaho: U. S. Geological Survey Journal of Research, v. 6, no. 5, p. 553-562.

———, 1982, Geophysics and tectonics of the Snake River Plain, Idaho, *in* Bill Bonnichsen and R. M. Breckenridge, editors, Cenozoic Geology of Idaho: Idaho Bureau of Mines and Geology Bulletin 26.

Mabey, D. R., Isidore Zietz, G. P. Eaton, and M. D. Kleinkopf, 1978, Regional magnetic patterns in part of the Cordillera in the western United States, *in* R. B. Smith and G. P. Eaton, editors, Cenozoic Tectonics and Regional Geophysics of the Western Cordillera: Geological Society of America Memoir 152, p. 93-106.

Macdonald, G. A., 1972, Volcanoes: Englewood Cliffs, N. J., Prentice-Hall Inc., 510 p.

Macdonald, G. A. and A. T. Abbott, 1970, Volcanoes in the Sea: Honolulu,University Press of Hawaii, 441 p.

Murtaugh, J. G., 1961, Geology of Craters of the Moon National Monument, Idaho: University of Idaho M.S. thesis, 99 p.

Prinz, Martin, 1970, Idaho rift system, Snake River Plain, Idaho: Geological Society of America Bulletin, v. 81, no. 3, p. 941-947.

Russell, I. C., 1902, Geology and water resources of the Snake River Plains of Idaho: U. S. Geological Survey Bulletin 199, 192 p.

Stanley, W. D., J. E. Boehl, F. X. Bostick, and H. W. Smith, 1977, Geothermal significance of magnetotelluric soundings in the eastern Snake River Plain-Yellowstone region: Journal of Geophysical Research, v. 82, p. 2501-2514.

Stearns, H. T., 1928, Craters of the Moon National Monument, Idaho: Idaho Bureau of Mines and Geology Bulletin 13, 57 p.

Valastro, S., Jr., E. M. Davis, and A. G. Zarela, 1972, University of Texas radiocarbon ages: Radiocarbon, v. 14, p. 468-470.

Wentworth, C. K. and G. A. Macdonald, 1953, Structures and forms of volcanic rocks in Hawaii: U. S. Geological Survey Bulletin 994, 98 p.

Zohdy, A. A. R. and W. D. Stanley, 1973, Preliminary interpretation of electrical sounding curves obtained across the Snake River Plain from Blackfoot to Arco, Idaho: U. S. Geological Survey Open-File Report 73-370, 5 p.

Selected Volcanic Features of the South-Central Snake River Plain, Idaho

by

John S. King[1]

ABSTRACT

Several volcanic constructs and craters localized on the south-central Snake River Plain including Wildhorse Corral, Horse Butte, Cottrells Blowout, Mosby Butte, Split Butte, and Kings Bowl were studied to learn more about the volcanic styles of that setting. All of these features are associated with Snake River Group Pleistocene and Holocene lava flows. In each study, field observations were coupled with petrographic and chemical data to aid in the reconstruction of a sequence of events in the evolution of the feature and, where possible, to establish the age or structural relationship of a specific feature to other nearby features. A synopsis of these studies is presented.

INTRODUCTION AND PURPOSE

Over the past decade, graduate students and staff of the Department of Geological Sciences at the State University of New York at Buffalo have undertaken studies of a variety of volcanic features located largely to the north and east of the Wapi lava flow (Figure 1), one of the youngest and most prominent lava flows of the south-central Snake River Plain in Idaho. Although one study was carried out on the Wapi flow itself (Champion, 1973), most of the other studies have involved features associated with older lava flows. The exact ages of these flows are unknown, but they are all assigned to the Snake River Group of Pleistocene and Holocene age and are all older than the Wapi flow dated at 2,270 ± 50 years (Ronald Greeley, personal communication, 1980). Despite their relative youth, outcrops of the lava features have been subdued somewhat by erosion, and windblown deposits of varying thicknesses now largely cover the flows. Interest in this region was initially attracted by the rift systems that transect the Snake River Plain at this location (Prinz, 1970; Greeley and King, 1975a, 1975b) but was soon expanded to include the more prominent craters and volcanic constructs.

The purpose of these studies was to better understand volcanic features of the Snake River Plain and the characteristics of volcanism in that province. This has been accomplished by an analysis of the morphologies of selected features, noting their relative distribution and their relationship to surrounding features and flows. In each study, detailed field information has been reinforced with petrographic, mineralogical, and chemical data to gain insight into the volcanic processes responsible for these features.

The basalts of the central and eastern Snake River Plain are dominantly olivine tholeiites which have strong mineralogical and chemical similarities (Leeman, 1974, 1982 this volume). Nevertheless, many of the flows detailed in these studies can be characterized and identified by subtle but nonetheless unique petrologic and fabric differences. Thus the size, shape, or grouping habit of plagioclase phenocrysts coupled with their abundance and/or the abundance or scarcity and habit of olivine phenocrysts commonly allows field identification of a particular flow. These observations together with other characteristics such as topography and degree of weathering aid in identifying the distribution of individual flows.

Each of these studies has been developed independently with the immediate objective of understanding the origin and development of the selected feature or features. Comparisons may subsequently be made to other features of similar morphology, physical proximity, or common structural control.

WILDHORSE CORRAL, COTTRELLS BLOWOUT, AND HORSE BUTTE

Wildhorse Corral, Cottrells Blowout, and Horse Butte are volcanic constructs located northeast of

[1]Department of Geological Sciences, State University of New York at Buffalo, Amherst, New York 14226.

King, J. S., 1982, Selected volcanic features of the south-central Snake River Plain, Idaho, *in* Bill Bonnichsen and R. M. Breckenridge, editors, Cenozoic Geology of Idaho: Idaho Bureau of Mines and Geology Bulletin 26, p. 439-451.

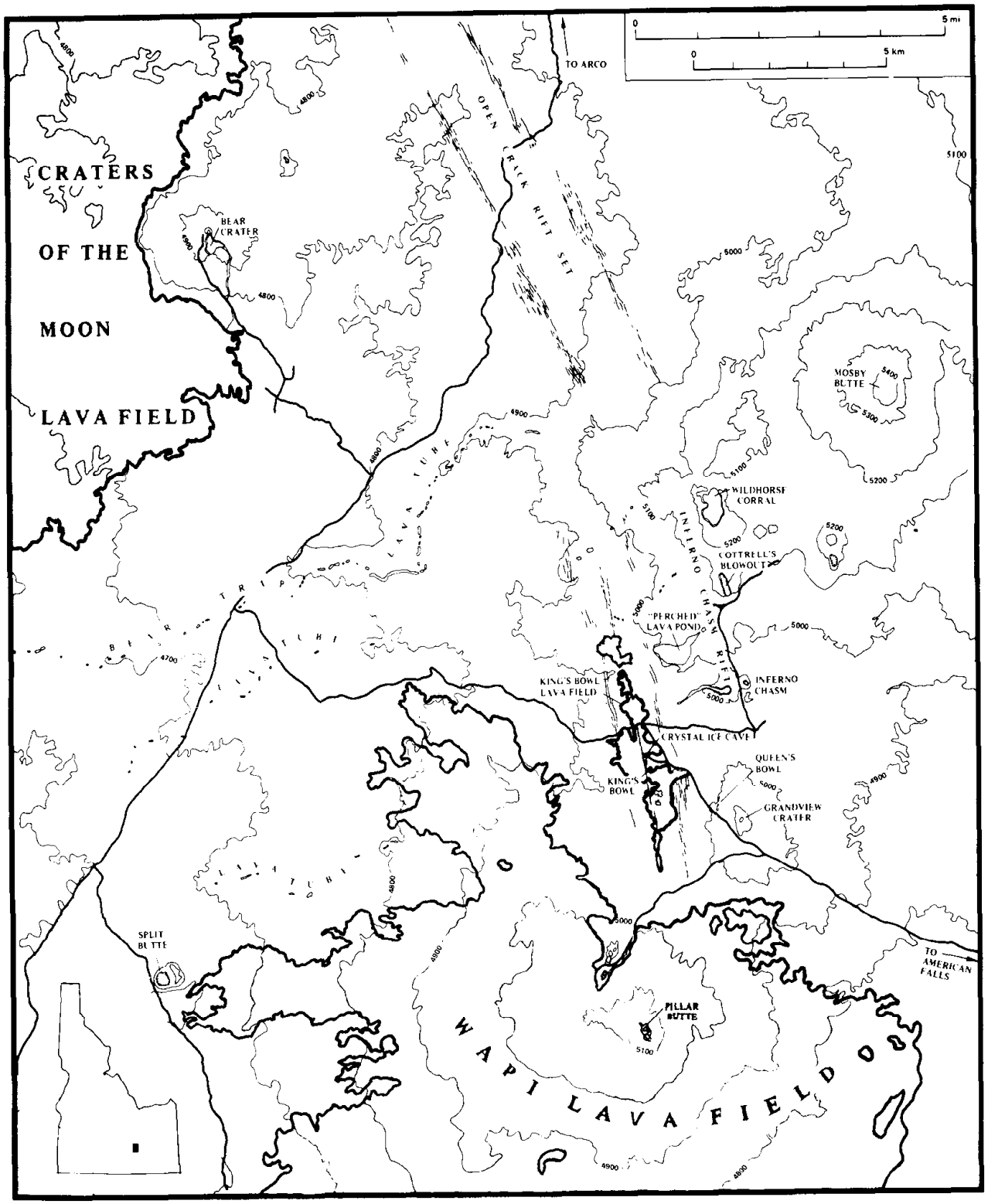

Figure 1. Topographic sketch map of the south-central Snake River Plain showing the location of features discussed in this paper (modified from Greeley and King, 1975b).

Kings Bowl (Figures 1 and 2). Mercer (1979) mapped the flows related to each of the vents and identified two vent morphologies. One morphology shared by Wildhorse Corral and Cottrells Blowout is characterized by broad summit profiles with slopes of 4 to 5 degrees and large ovoid vent craters as much as 45 meters deep with nearly vertical walls. These craters are the result of extensive collapse following magma withdrawal in late stages of vent activity. The second morphology, shown by Horse Butte, has a steeper profile of about 15 degrees and two shallow, irregular summit depressions not believed to be the result of collapse.

All three of these features are on the Inferno Chasm rift set (Figure 1), a set proposed by Greeley and King (1975a) as one of two supplements to the four component sets of the Idaho rift originally identified by Prinz (1970). Although no fractures are visible, the Inferno Chasm rift set is indicated by a trend subparallel to the Kings Bowl rift set marked by the alignment of several prominent volcanic features of about the same age: Grandview Crater, Inferno Chasm, Cottrells Blowout, and Wildhorse Corral. Greeley and King (1975b) suggested that the Inferno Chasm rift set might also include the vent which fed the Papadakis perched lava pond.

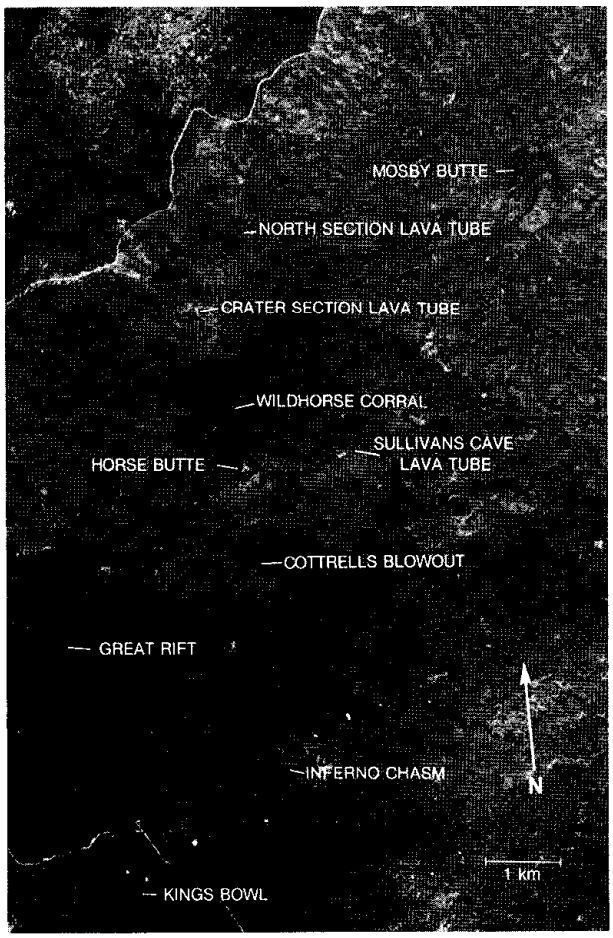

Figure 2. Index aerial photograph showing the location of features discussed in this paper.

At the time the Inferno Chasm rift set was defined, Horse Butte was not recognized as a separate vent with its own flow but was believed to be a part of the Wildhorse Corral complex. This lack of identity was due at least in part to disruption of the symmetry of the Horse Butte shield by encroachment of its north flank by the Wildhorse Corral crater. Mercer's study (1979) demonstrated through overlap relations and differences in degree of weathering between these flows that Horse Butte was indeed a separate vent older than both Cottrells Blowout and Wildhorse Corral. The Horse Butte shield formed a barrier to lavas erupted from Cottrells Blowout, forcing channel-fed outflow from the Cottrells' vent to the south.

The time separation between these three features is unknown. Mercer (1979) has proposed a sequential tapping of the same magma chamber for both the Wildhorse Corral and the Cottrells Blowout flows. He believes that the initial eruption for these two vents was at Cottrells Blowout. Ultimately this vent closed and activity at Cottrells Blowout ceased. This was accompanied by withdrawal of magma followed by a relatively short period of quiescence during which the magma continued to differentiate. With renewed eruptive activity, new vents opened at the Wildhorse Corral site with the eruption of slightly cooler lava. This interpretation (Mercer, 1979) is based on a comparison of phenocryst size and the ratio of olivine to plagioclase in lavas from the vents of the two structures. The relative age of the three constructs is thus Horse Butte followed by Cottrells Blowout and finally Wildhorse Corral. The flows from all three of these vents are pahoehoe basalts with gently undulating, locally ropy surfaces. Many flows have lava tubes associated with them.

HORSE BUTTE

Horse Butte (Figure 3) is a small shield volcano with a slightly ovoid summit cone about 1,250 meters in diameter marked by two depressions at the vent each about 5 meters deep. The Horse Butte lava covers an area of about 18 square kilometers. Mercer (1979) hypothesized that activity at Horse Butte was fracture controlled and began as a fissure eruption. The eruption gradually concentrated along a short length of the fissure with transition to a more central-type eruption which, through successive outpourings of lava, ultimately resulted in the low shield cone.

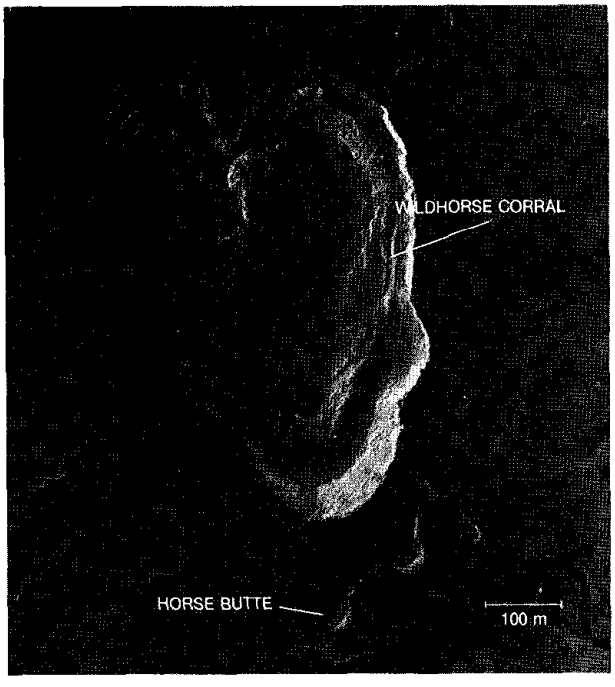

Figure 3. Low altitude aerial photograph of Wildhorse Corral and Horse Butte. The Wildhorse Corral terrace is about 23 meters below the rim. Horse Butte is marked by two shallow summit depressions. Note how the Wildhorse Corral crater is superimposed on the Horse Butte shield.

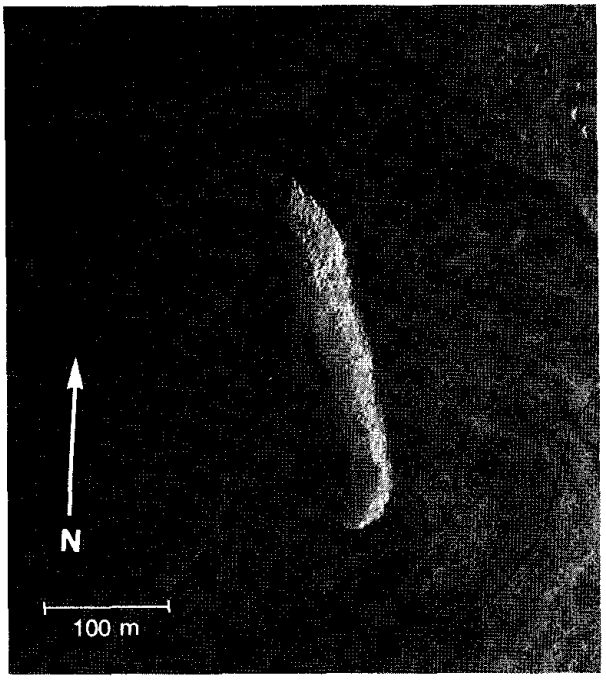

Figure 4. Low altitude aerial photograph of Cottrells Blowout. The elongation of this crater parallels the Inferno Chasm rift set. A small back flow is located at the north end.

Horse Butte stands about 52 meters above the local surface of the surrounding plain.

Sullivans Cave lava tube (Figure 2) is associated with the Horse Butte lava flow and is believed by Mercer (1979) to have been active at the time of the centralized eruptions. The Sullivans Cave lava tube is about 500 meters long and extends east from the Horse Butte vent. Greeley and King (1979b) suggest that the Sullivans Cave tube developed from a lava channel which became roofed over. Evidence supporting this includes the steep gradient, thick roof, and lack of layered lava exposed in the walls of the tunnel.

COTTRELLS BLOWOUT

Cottrells Blowout is believed to have begun its eruptive history from a fissure vent along a segment of the Inferno Chasm rift set somewhat shorter than the length of the present crater (Mercer, 1979). Cottrells Blowout (Figure 4) is about 595 meters long and 160 meters wide. Its maximum depth is about 43 meters. The rims at both ends of the crater are low and attain maximum height midway along the sides. As pointed out by Mercer (1979), the flows from this vent are limited in extent and cover only about 4.5 square kilometers.

Early activity at the vent is marked in the stratigraphic sequence by thin (about 10 centimeters), areally restricted, gas-charged flows. The early thin flows are overlain by what Mercer (1979) has termed the main massive unit which represents a fissure eruption. This main massive unit flowed southward as a result of the Horse Butte shield already in place to the north.

A remnant of a raised lava channel in the main massive unit extends about 1.8 kilometers from the southwest edge of Cottrells Blowout. As described by Mercer (1979), the channel has a flat bottom and averages 13 meters in width. Lava levees about 1.5 meters high mark the edges of this channel. Both channel width and levee height decrease away from the source. This lava channel, when coupled with the small volume and simple characteristics of the massive flow, suggests that the effusion rate for this flow was high over a relatively short time.

Following eruption of the main massive flow, the Cottrells fissure vent is believed to have decreased to a point source from which numerous thin (10-25 centimeters), gas-charged, amoeboid-shaped flows were discharged. Their thin character allowed relatively rapid cooling which trapped gas in the lava and caused the present vesicular character of the flows. The concentration of these flows around the smaller vent accounts for the build up of the summit region of

Cottrells Blowout according to Mercer (1979).

Collapse marked the final stage of development at the Cottrells Blowout vent. Mercer (1979) believes that collapse directly followed a final minor eruptive stage which is marked by a small back-flow channel at the north end of the present crater. Collapse, resulting in the present elongate Cottrells Blowout crater, is believed to have been caused by withdrawal of magma down the vent.

WILDHORSE CORRAL

Wildhorse Corral is by far the largest and most prominent of these three Inferno Chasm rift set features. It is an irregular-shaped depression with its longest axis subparallel to the rift set (Figures 1 and 3). Wildhorse Corral is 935 meters long, 565 meters wide, and 41 meters deep. A terrace which averages 53 meters in width outlines most of the crater about 23 meters below the rim. At the northern end of Wildhorse Corral, the terrace is disrupted and broken into large outward-dipping slabs up to 30 meters long and 6 meters thick. The floor of Wildhorse Corral below the terrace level is nearly flat. Wildhorse Corral is a complex feature with a more complicated eruptive history than the other two vents already described.

Mercer (1979) believes that the Wildhorse complex commenced with eruptions at two points along the Inferno Chasm rift set. These two sources expanded during the early eruptive phase and eventually coalesced into a single large fissure-type vent which predetermined the present elongate shape of the crater. Three massive flow units, each up to 3 meters thick and representing a period of high effusion, are identified as the basal units erupted from this vent. With a plentiful magma source, such flows can cover very large areas.

The Bear Trap lava tube and its associated flow is located west of Wildhorse Corral. The course of the Bear Trap lava tube is quite apparent on topographic maps, and it appears to head about 4.5 kilometers west-northwest of the Wildhorse vent. Mercer (1979) believes that the Bear Trap lava flow originated from the Wildhorse Corral vent. His conclusion is based in part on the massive Wildhorse Corral flows which suggest sufficiently large volumes of lava from this vent. He supports his hypothesis by noting a similarity in texture, phenocryst composition, and inferred crystallization sequence between the Wildhorse Corral and the Bear Trap flows. He further points out the probable presence of a lava tube between Wildhorse Corral and the apparent head of the Bear Trap lava tube based on both the topography of the intervening ground and the elevation difference between the two points.

The early high effusive stage at the Wildhorse Corral vent was followed by a period of minor eruptions characterized by a thin zone (1 meter) made up of extremely thin vesicular layers of limited areal extent. The main Wildhorse Corral flow overlies the thin vesicular flows and was identified by Mercer (1979) as consisting of six relatively massive flow units. A prominent lava tube system occurs in the main massive unit and extends north-northwest from the Wildhorse Corral crater. Mercer (1979) divided this lava tube system into two sections (Figure 2). That section which extends about 1.6 kilometers north from Wildhorse Corral is designated the crater section, and an L-shaped branch which trends east and then north from the crater section is called the north section.

Greeley (1971) observed that most actively developing lava tubes form along the axis of highest velocity within a flow and will follow a course marked by stream beds, rifts, grabens, or fracture zones. It is apparent from the continuity of the crater section lava tube with the Inferno Chasm rift set features that the trend of the lava tube was predetermined by the rift. Mercer (1979) suggests that the crater section developed along the fracture zone as a fairly linear channel which roofed over in some sections and not in others. He believes that close to the vent the crater section channel did not roof over but existed as open lava ponds which themselves acted as sources for short-lived distributary channels.

A remarkably hemispherical basalt dome about 20 meters in diameter and 4.5 meters high protrudes from the crusted pond near the head of the crater section lava tube. Mercer (1979) favors the hypothesis that this dome formed due to hydrostatic pressure within the lava tube where flow velocity was greatest. An alternative explanation is that drainage through the tube was temporarily blocked and, with continued feeding from the source, a pressure build up caused the dome.

The north section of the Wildhorse Corral lava tube system consists of lower gradient segments with more regularly layered lava exposed in the walls and roofs. Based on Ollier and Brown (1965), Mercer (1979) believes that the formation of this section of the tube resulted from lower velocity laminar-type flow of the lava.

The Wildhorse Corral crater is believed to have enlarged somewhat during the eruption sequence, and Mercer (1979) proposes that a lava lake filled the vent crater to the rim for a time. A small overflow from this lava lake has been identified on the southwest edge of the present crater. Ultimately the lake probably drained to the northwest, possibly when a previously formed lava tube reopened to act

as a conduit. Following the draining of the lava lake, the summit region of the vent collapsed, causing the present irregular-shaped crater. The collapse occurred along fractures which both paralleled and intersected the Inferno Chasm rift set at high angles of up to 90 degrees. These fracture lines are evident in linear segments of the southern half of the Wildhorse Corral crater and are related by Mercer (1979) to an earlier period of dilation of the summit region of the volcano.

A second lava lake occupied the crater following the first collapse and is partially preserved in the 50-meter-wide terrace of Wildhorse Corral. On the basis of thickness of this lava lake "unit" and the cooling rates measured in Hawaiian lakes, Mercer (1979) estimates a minimum time of existence for this lake of 300 days.

MOSBY BUTTE

Mosby Butte is a prominent shield volcano about 4 kilometers northeast of Wildhorse Corral (Figures 1 and 2). The Mosby Butte flows cover about 36 square kilometers and show a profile of about 12 degrees near the vent which shallows to about 2 degrees away from the vent toward the more distal parts. One of the early objectives in the study of Mosby Butte was to determine whether chemical or petrographic differences occurred between rocks of the vent area and those of the distal parts of the flow which could be related to the slope differences. Another objective was simply to identify the Mosby Butte flow limits and determine the relationship to surrounding flows.

No significant chemical or petrographic difference was determined between the distal and vent portions of the Mosby Butte flow. The slope difference was explained by Foster (1978) to be the result of increased accumulation of cooler, more viscous lava late in the eruptive sequence. An alternative explanation is that the slope difference resulted from lower effusion rates late in the eruptive sequence which restricted outflow and lead to accumulation in the immediate vent area. Eight flows including the Wildhorse Corral flow were identified by Foster (1978) surrounding the Mosby Butte flow. Nine such flows are now recognized inasmuch as the Wildhorse flow was subsequently subdivided by Mercer (1979) who recognized and separated the Horse Butte vent and its associated flow.

Based on Walker's graph (1973) relating average rate of effusion with length of a flow, Foster (1978) calculated an average rate of effusion for the Mosby Butte vent at about 5.7 cubic meters per second. Coupling this value with assumptions covering both areal size and thickness of the flow, he calculated a minimum duration of 2 years for the eruptive period of Mosby Butte. In spite of the many assumptions in this determination, the result nonetheless provides a realistic approximation for a minimum time span necessary for the Mosby Butte construct to develop. It also provides a useful value for approximating the development times of other major constructs in the area.

SPLIT BUTTE

Split Butte is about 10 kilometers southwest of the Kings Bowl (Figure 1). It has been identified as a maar crater (Womer, 1977; Womer and others, 1980; 1982 this volume) and is distinctly different from the other Snake River Group features discussed in this summary. Split Butte is a vent from which lava issued but with which no major flow is associated, although an outflow point from a contained lava lake has been suggested by Greeley and King (1975b). The limits of this suggested outflow have never been defined however; it remains an obscure entity indicated by a single low point in the Split Butte rim.

Split Butte is named after a prominent gap or discontinuity which exists in the upper layers of the tephra sequence found on the east side of the structure (Figure 5). The tephra ring is asymmetric and higher on the east side than on the west. This asymmetry is attributed to prevailing west winds at the time of eruption which caused a greater accumulation of ejecta on the downwind side of the vent. Inasmuch as the "split" is also on the east side, it too has most likely been caused by prevailing west winds during and subsequent to eruption. Although other hypotheses could be advanced to explain this split, no field evidence has ever been found to support any cause other than wind erosion.

Split Butte crater is unique among the constructs of this discussion owing to its tephra ring which indicates a pyroclastic phase of the eruption. The eruptive sequence has been described by Greeley and King (1975) and detailed by Womer (1977) and Womer and others (1980; 1982 this volume). Briefly summarizing, when the vent at Split Butte first erupted, lava came into direct contact with ground water. The interaction of the hot lava with cool ground water caused the formation of a glassy ash which was erupted early in the sequence as base surge but later was dominantly air fall (Womer, 1977). A rampart of tephra layers developed around the vent with opposing dips to the layers on the outside and inside of the ring. Intermittent explosive intervals occurred and carried larger blocks of material out of

Figure 5. Oblique aerial view of Split Butte viewed to the southwest (east is toward the left hand side of the picture). The "split" is a gap or discontinuity in the tephra rampart and is visible on the left. The split is oriented with its long axis nearly due east. The low point in the tephra ring is visible in the upper right portion of the construct and is marked by the trail. The tephra ring of Split Butte contained a lava lake which crusted and collapsed leaving the present inner terrace. Photograph by Ronald Greeley.

the vent and into the ash-dominated tephra rampart.

In time the water-lava contact within the Split Butte conduit was sealed causing a change in eruptive style. Material was no longer forcibly ejected from the vent but rose to the surface where it was confined by the earlier-formed tephra ring as a lava lake. The rise of lava in the conduit was insufficient to overtop the tephra rampart with the possible exception of the limited overflow mentioned above. Thus the contained lava cooled and the lake crusted over. The solidified upper portion of the conduit remained stable only as long as lava was being forced toward the surface. Ultimately, withdrawal of liquid material in the subsurface allowed the central portion of the lava lake to subside. The result is the present structure of Split Butte which appears in aerial photographs as a group of nested craters made up of the outer tephra ring, a relatively flat inner terrace, and the down-dropped central portion. The inner terrace marks the level of the lava lake when it crusted.

Split Butte exemplifies a type of eruption that is unusual but not unique on the Snake River Plain. Among other examples of pyroclastic eruptions on the eastern plain are Sand Butte and Menan Buttes. Each of these features has a distinct history reflecting the sequence of lava-water interaction during the eruption. The vent at Split Butte predates the nearby Wapi flow inasmuch as a tongue of Wapi lava reaches to and covers the lower part of the Split Butte structure on the east side (Womer, 1977; Womer and others, 1982 this volume).

KINGS BOWL AND RELATED FEATURES

Kings Bowl is a prominent, ovoid crater about 85 meters long, 30 meters across at the widest point, and 30 meters deep situated on the main fracture of the Great Rift. This crater marks the vent for the Kings Bowl lava flow (Figures 1 and 2), which has been dated at 2,130 ± 130 years (Prinz, 1970).

On an aerial view (Figure 6), the Kings Bowl flow can be readily distinguished by its low albedo and by flow pattern directed away from the Kings Bowl crater. Other features visible by aerial photograph inspection are a light-colored ash field east of the rift near Kings Bowl and a discontinuous ring of basalt mounds (Figure 6). When connected, these basalt

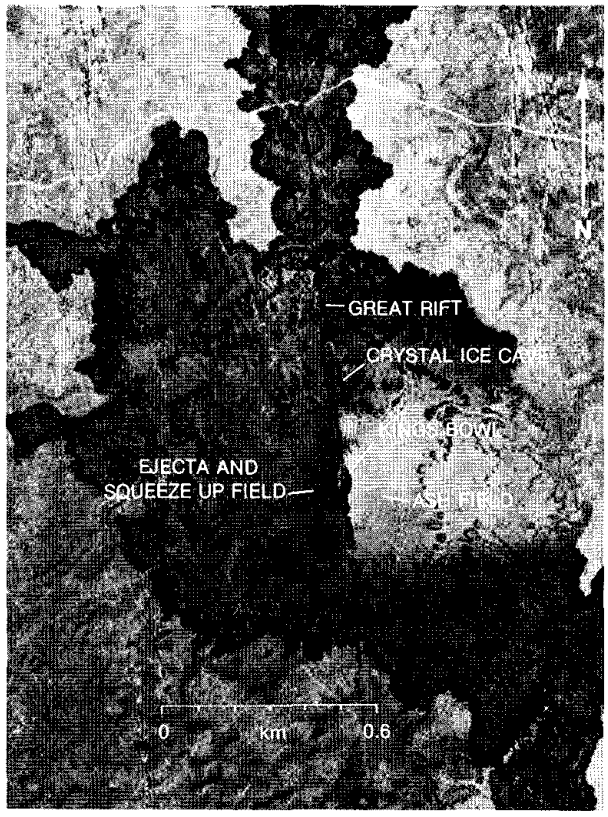

Figure 6. Vertical aerial view of the Kings Bowl flow showing the location of the various features discussed in the text. Note the irregular outline of basalt mounds distributed around the Kings Bowl vent. USGS photograph CYN-7B-103.

mounds appear to mark temporary but nonetheless definite locations where movement of lava outward from the vent was arrested for a time.

Field examination of the Kings Bowl flow reveals two phenomena west of the Kings Bowl which are not visible on aerial photos. One is an ejecta field, and the other is an area of squeeze-up locations where very viscous lava oozed up through fractures in the solid crust.

The ejecta field (Figures 7 and 8) extends about 245 meters west from the Kings Bowl crater. The largest blocks in the field are found adjacent to the crater, and the ejecta fragments become progressively smaller away from the crater. The squeeze-ups (Figures 9, 10, and 13) are located within the ejecta field. Many of the squeeze-ups have been struck by solid ejecta from Kings Bowl suggesting a brief and violent event at or near the end of the eruptive sequence. Many of the impacted squeeze-ups have irregular open holes in their surfaces from which fractures radiate (Figure 11). In some, the block which caused the hole and the fractures still remains wedged in the hole, while in others these blocks may be found on a floor inside the convex shell of the squeeze-up. These relationships show that some of the squeeze-ups had developed a sufficiently thick crust at the time of impact of the blocks to behave as brittle material. The relationships also show that the central part of some of the squeeze-ups had drained after they crusted leaving them as hollow structures. In other of the squeeze-ups, however, the oozing lava of the squeeze-up is found wrapped around fragments which are obviously blocks ejected from the Kings Bowl vent. This suggests that solid blocks from the vent may have been responsible for some of the fractures where squeeze-ups developed.

Collectively, all of the features found on the flow (basalt mounds, ash field, ejecta field, and the squeeze-ups) support reconstruction of a sequence of events in the Kings Bowl eruption. The original vent in the Kings Bowl eruption is believed to have been a short fissure, perhaps even a point source located somewhere in the area of the present Kings Bowl crater. At the time of the initial eruption it is believed that the rift was not present as such but defined as a zone of weakness which controlled the positioning of the vent. Lava extruded at the surface and cooled as it flowed away from the vent. A confining levee was built and a shallow lava lake developed (Figure 12). Subsequently outflow may have become restricted or reduced by changes in the vent, and a build up of pressure caused tumescence around the vent which in

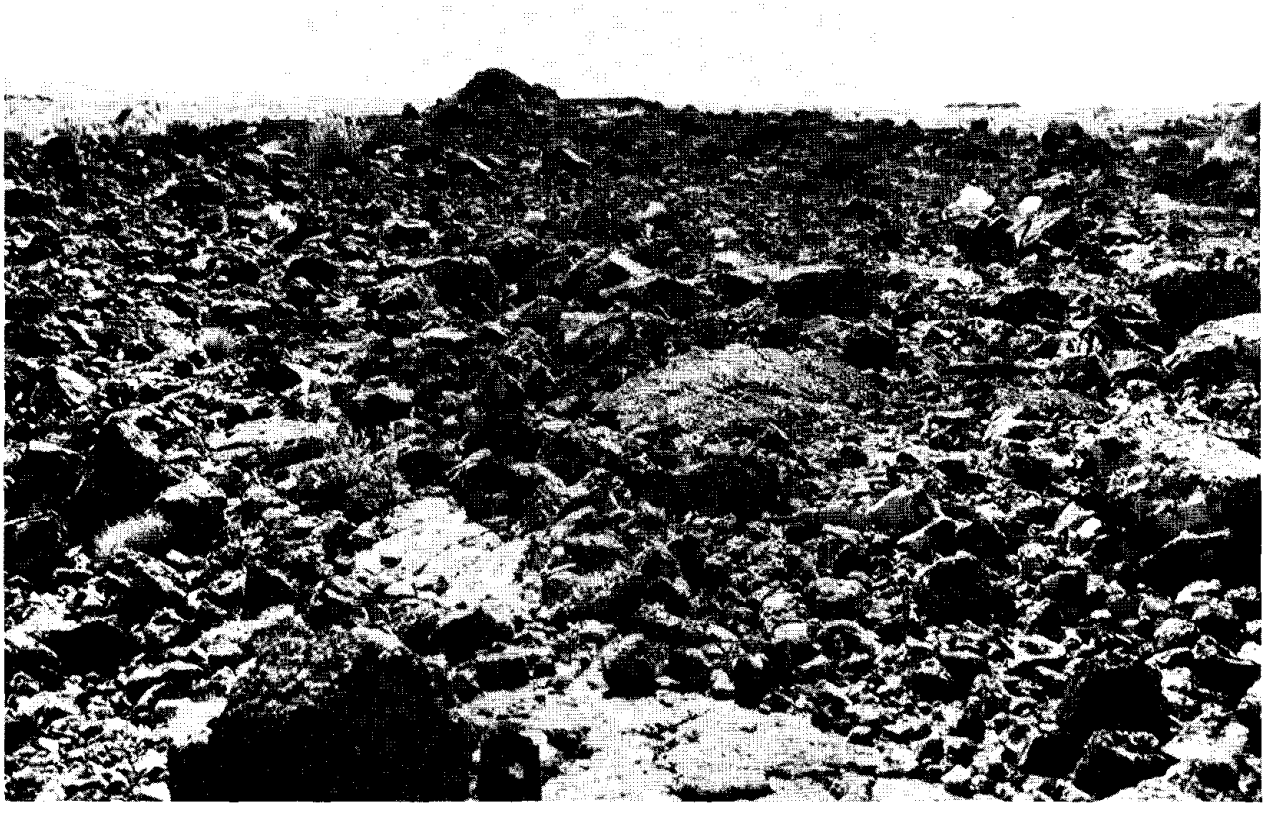

Figure 7. A view to the southeast of the ejecta field close to the vent and on the west side of Kings Bowl.

turn weakened or even fractured the lake-confining levee. When outflow at the vent resumed, these weak zones in the levee developed into channelways for molten lava and are believed to have enlarged as the lava continued to flow through. Portions of the levee were thus removed resulting in the present discontinuous ring of basalt mounds (Figures 12 and 13). Depending on how the present mounds are connected, this hypothesized sequence could have occurred once or twice during the early eruption. It appears that there are two concentric rings of basalt mounds, but particularly on the west side, large gaps exist in this pattern and the distribution of the mounds could be interpreted as a single more complex ring. Outflow patterns between these mounds can be seen both on the aerial photographs and at locations in the field (Figure 14).

It is believed that a once continuous levee or levees thus confined a lava lake (or lakes) and that near the end of the Kings Bowl eruptive sequence the lake crusted over with a layer of cooled lava several centimeters thick. Because lava was still coming into the lake, the system remained dynamic; the lake crust fractured, and individual plates or slabs of crust were the result.

The eruptive climax apparently occurred when upwelling lava in the conduit came in contact with ground water. This stage is indicated by both the ash and the ejecta field. Solid ejecta is found dominantly on the west side of Kings Bowl suggesting that the water-lava contact was asymmetric in relation to the conduit. Thus the trajectory of solid fragments was directed toward the west at a relatively low angle. The eruption was analogous to pressure relief from a boiler. Enough force was generated to carry large fragments (up to 1.5 meters in diameter) out of the conduit to locations close to the vent while smaller blocks were carried farther from the vent with the smallest being deposited about 245 meters west of the crater. Simultaneously, ash-sized lithic ejecta was carried up by the same force but was winnowed out of the erupting cloud by strong prevailing winds from the west. This was the prevailing wind direction at the time Split Butte was active as well.

It should not be forgotten that a lava lake existed at the time of the eruptive climax. Perhaps some lava had already developed squeeze-ups at plate intersections, most probably at points where several crustal plates came together. Some of these early-formed squeeze-ups were sufficiently cooled so that their crust was able to behave as brittle material when struck by solid ejecta. This accounts for the squeeze-ups with impact holes or fracture patterns on them. At the same time but elsewhere, ejected solid blocks

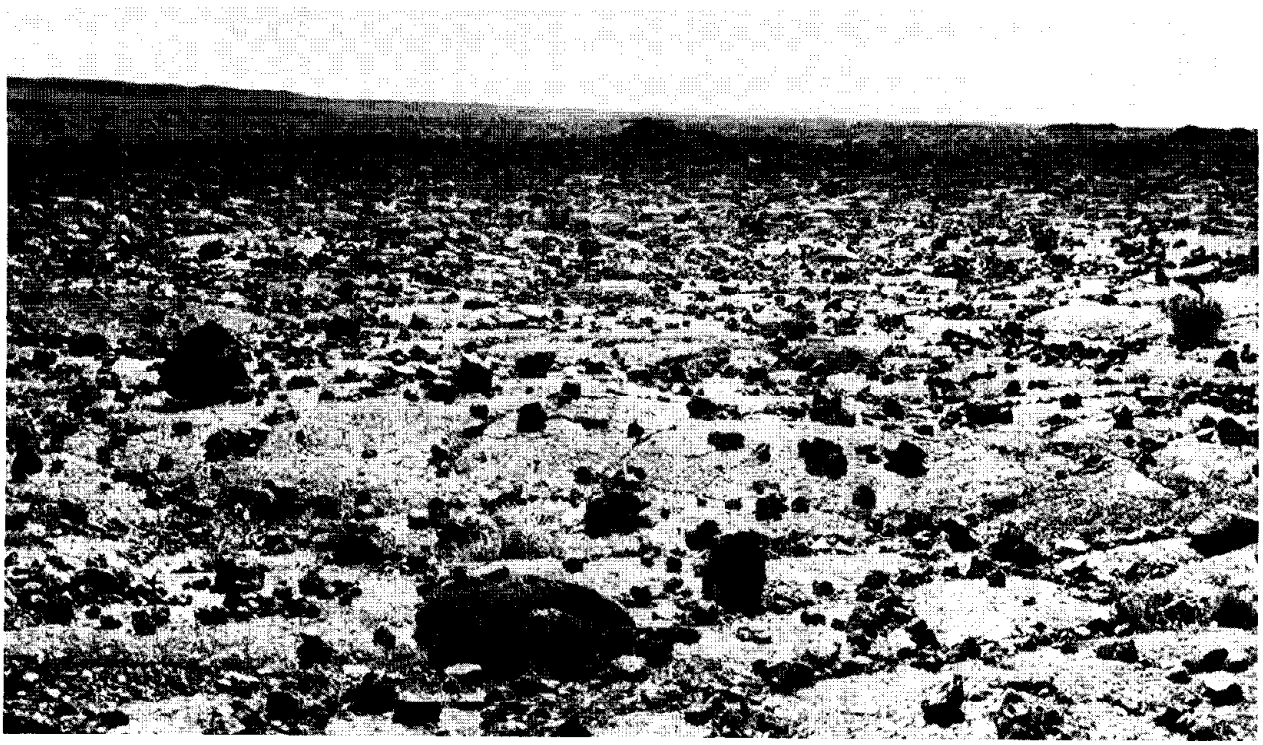

Figure 8. A view to the southeast of the Kings Bowl ejecta field farther from the vent than view in Figure 7. The trace of the Great Rift is obvious in the upper portion of the photograph. The hemispherical mound in the center foreground is a squeeze-up.

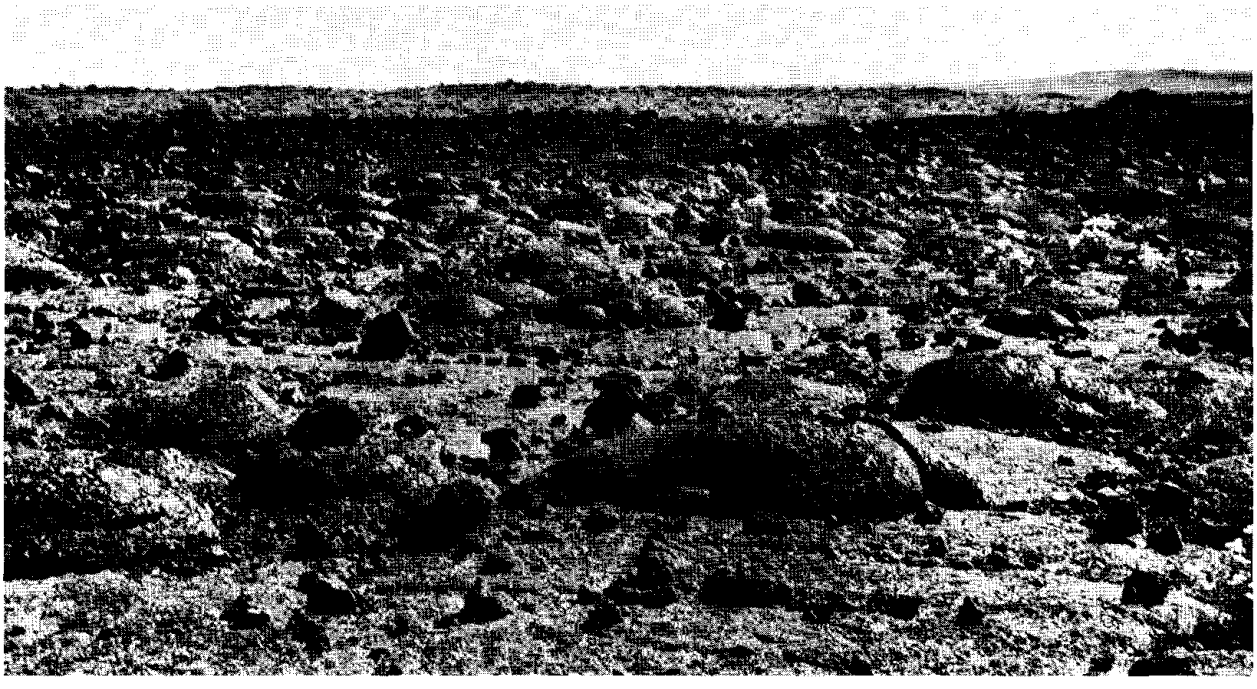

Figure 9. A view to the east of an area of the ejecta field densely covered with squeeze-ups. The Great Rift trends left-right through the picture at the edge of the vegetated region.

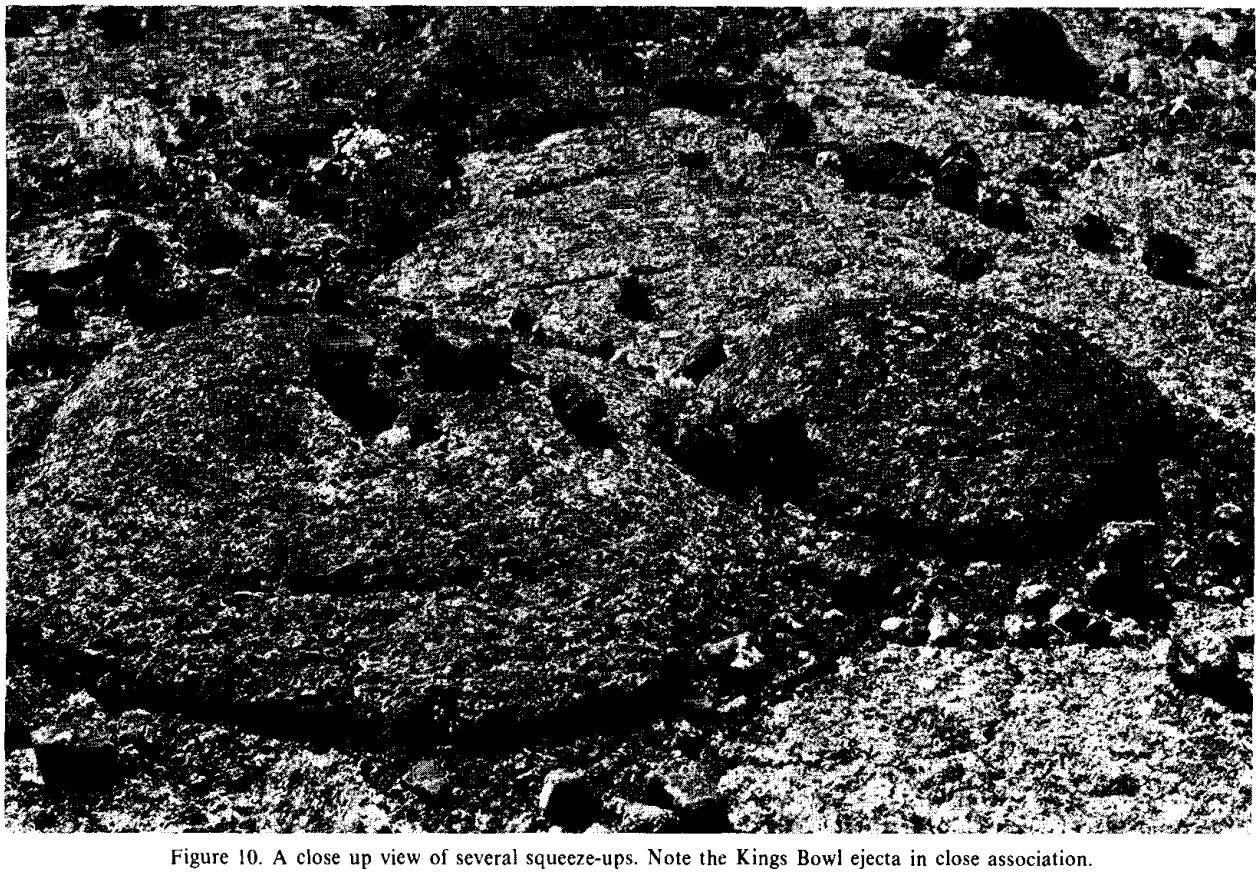

Figure 10. A close up view of several squeeze-ups. Note the Kings Bowl ejecta in close association.

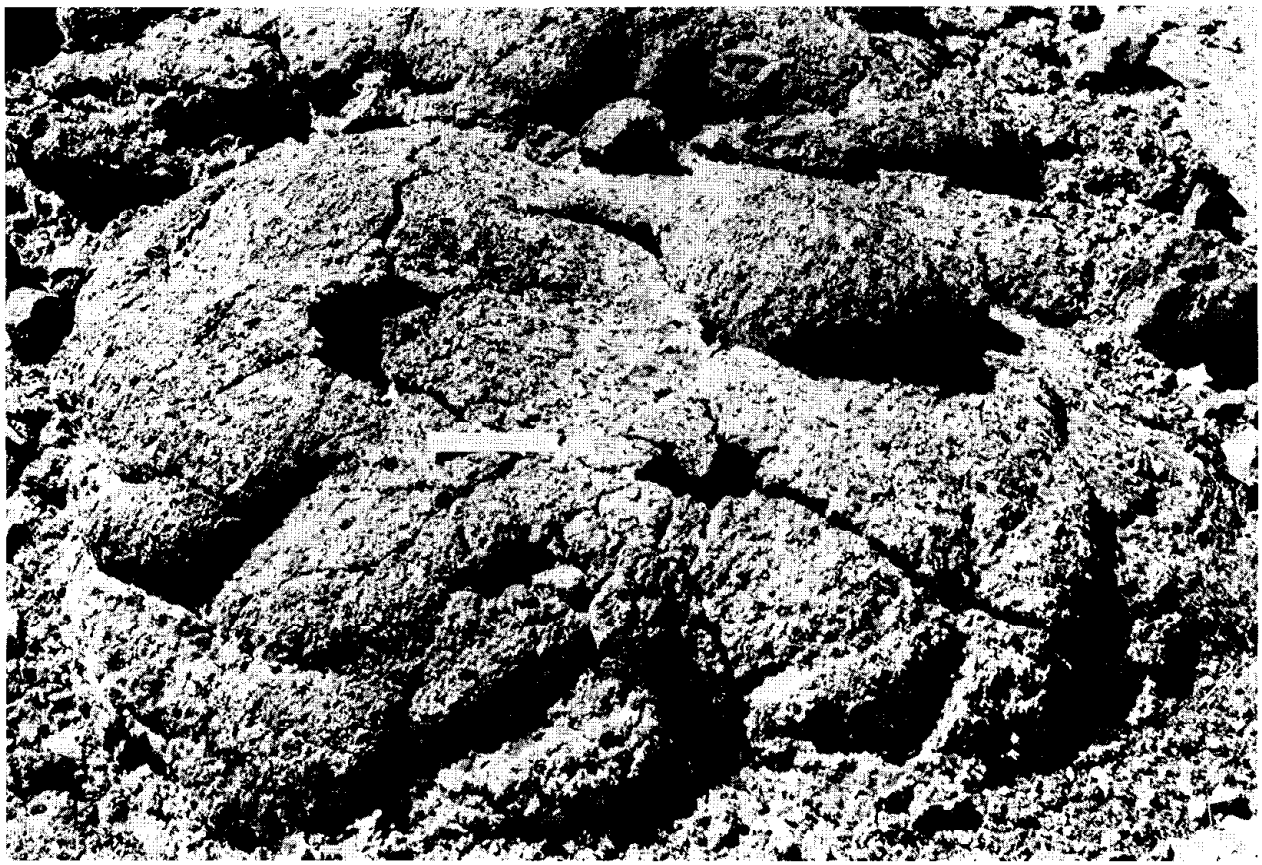

Figure 11. Impact holes in the squeeze-ups caused by blocks thrown from the Kings Bowl vent. The scale is 6 inches long.

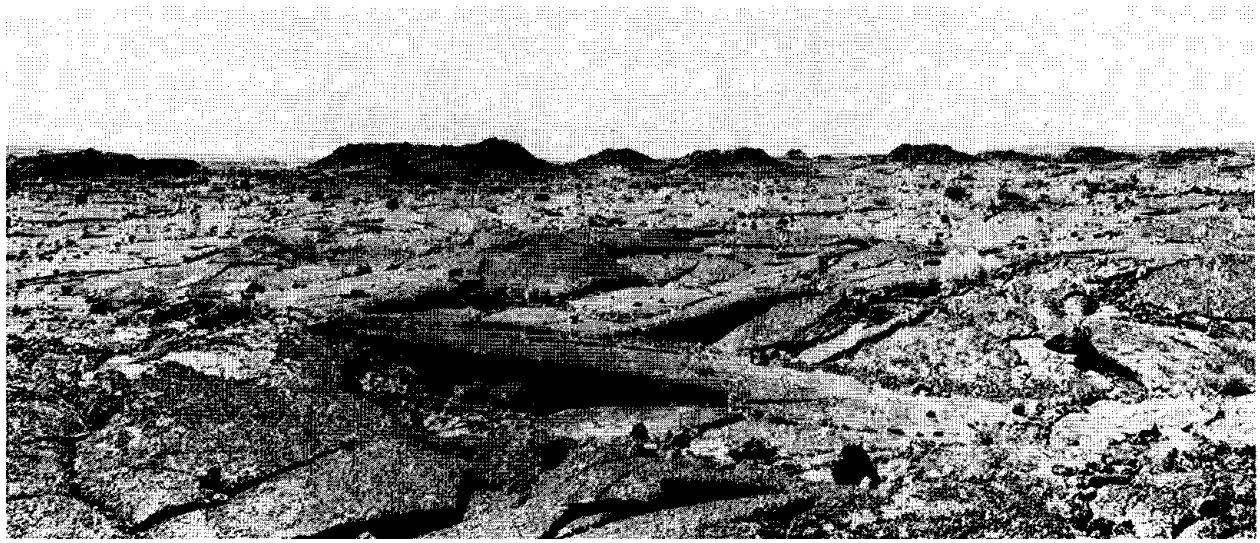

Figure 12. The surface of the Kings Bowl lava lake viewed to the southeast. Ejected blocks from Kings Bowl are visible and part of the ring of basalt mounds are evident in the background.

Figure 13. View of the squeeze-up field with some of the basalt mounds visible in the background. Photograph by J. Papadakis.

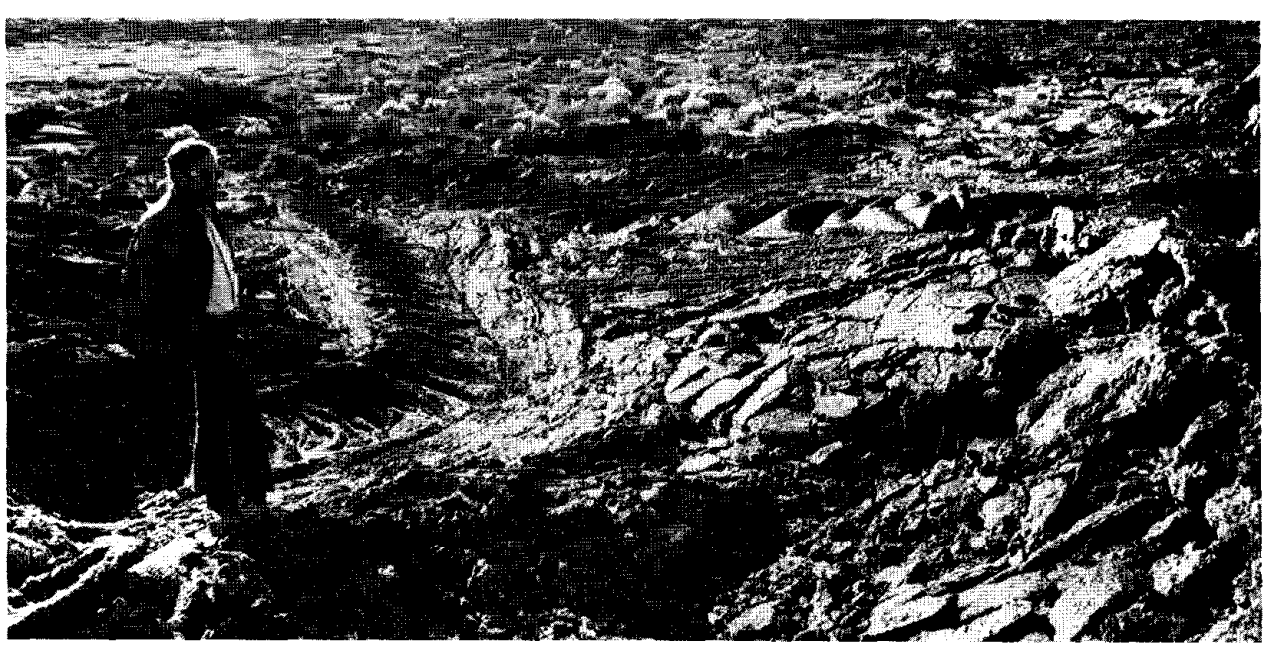

Figure 14. Part of an outflow channel between two of the basalt mounds. This is located at the northwest end of the Kings Bowl lava lake.

from the vent broke through parts of the lava lake crust allowing still-molten lava beneath the crust to ooze up and flow around the impacting blocks.

If the entire area of the present ejecta field of the Kings Bowl vent were imagined to be covered by a layer of the largest-size ejected fragments, the resulting volume would be insufficient to refill the present Kings Bowl crater. Thus the final phase at the Kings Bowl site was collapse, probably related to the withdrawal of magma back down the conduit.

CONCLUSION

Each eruptive complex studied is unique in one sense but in another shares some characteristics with surrounding flows and features. The result of lava-water interaction is quite marked, reflecting the continuing presence of abundant ground water in the basalt flows of the Snake River Plain. An easily overlooked stage associated with many if not most of the vents is a collapse stage, usually late in the evolution of the feature. This is particularly significant in the development of the elongate vents associated with the rift sets. However, it is also important in understanding the evolution of features such as the nested craters at Split Butte.

Even in settings of such apparent similarity as the Recent basalt flows of the Snake River Plain, it is often possible to reconstruct an eruptive sequence. Studies such as the ones summarized here provide insight into the volcanic styles of the eastern Snake River Plain. In many instances the knowledge gained in such studies is applicable as well to similar-appearing volcanic features on other planets and to a better understanding of the volcanic regimes associated with them.

ACKNOWLEDGMENTS

These studies have been supported through National Aeronautics and Space Administration grant NGR 330-151-08.

REFERENCES

Champion, D. E., 1973, The relationship of large scale surface morphology to lava flow direction, Wapi lava field, southeastern Idaho: State University of New York at Buffalo M.A. thesis, 44 p.

Foster, P. W., 1978, The study of Mosby Butte, a volcanic construct of the south-central Snake River Plain, Idaho: State University of New York at Buffalo M.A. thesis, 48 p.

Greeley, Ronald, 1971, Observations of actively forming lava tubes and associated structures, Hawaii: Modern Geology, v. 2, p. 207-223.

Greeley, Ronald and J. S. King, 1975a, Rift zones in the south central Snake River Plain, Idaho: Geological Society of America, Abstracts with Programs, v. 7, no. 5, p. 610-611.

_____, 1975b, Geologic field guide to the Quaternary volcanics of the south-central Snake River Plain, Idaho: Idaho Bureau of Mines and Geology Pamphlet 160, 49 p.

Leeman, W. P., 1974, Part 1, Petrology of basaltic lavas from the Snake River Plain, Idaho: University of Oregon Ph.D. dissertation, 337 p.

_____, 1982, Olivine and tholeiitic basalts of the Snake River Plain, Idaho, *in* Bill Bonnichsen and R. M. Breckenridge, editors, Cenozoic Geology of Idaho: Idaho Bureau of Mines and Geology Bulletin 26.

Mercer, M. F., 1979, The origins of three volcanic constructs on the south central Snake River Plain, Idaho: State University of New York at Buffalo M.A. thesis, 94 p.

Ollier, C. D. and M. C. Brown, 1965, Lava caves of Victoria: Bulletin Volcanologique, v. 28, p. 215-229.

Prinz, Martin, 1970, Idaho rift system, Snake River Plain, Idaho: Geological Society of America Bulletin, v. 81, p. 941-947.

Walker, G. P. L., 1973, Lengths of lava flow: Philosophical Transactions of the Royal Society of London, A, 274, p. 107-118.

Womer, M. B., 1977, A study of the ash rings of Split Butte; a maar crater of the south-central Snake River Plain, Idaho: State University of New York at Buffalo M.A. thesis, 53 p.

Womer, M. B., Ronald Greeley, and J. S. King, 1980, The geology of Split Butte, a maar of the south-central Snake River Plain, Idaho: Bulletin Volcanologique, v. 43, p. 453-471.

_____, 1982, Phreatic eruptions of the eastern Snake River Plain of Idaho, *in* Bill Bonnichsen and R. M. Breckenridge, editors, Cenozoic Geology of Idaho: Idaho Bureau of Mines and Geology Bulletin 26.

Phreatic Eruptions of the Eastern Snake River Plain of Idaho

by

Michael B. Womer[1], Ronald Greeley[2], and John S. King[3]

ABSTRACT

Split Butte and Sand Butte are tuff cones representing phreatomagmatic eruptions. Both buttes are nested, subcircular structures consisting of a tephra ring and an inner lava lake modified by a pit crater. Split Butte lies west of the Wapi lava flow, about 40 kilometers west-northwest of American Falls, and consists of vitric ash that forms a ring 600 meters across. Sand Butte is 30 kilometers southwest of Craters of the Moon National Monument and consists of palagonitized vitric ash and abundant lithic fragments which form a cone 1.2 kilometers across; a deeper level of magma-water interaction at Sand Butte than at Split Butte is suggested by a greater fraction of lithic ejecta and less vesiculation of the juvenile fraction.

INTRODUCTION

Pleistocene volcanism in the Snake River Plain, Idaho, is dominated by basaltic lava flows that were erupted during relatively quiet activity. In some areas, notably in Craters of the Moon National Monument, more explosive activity produced cinder cones. Although rare in the Snake River Plain, even more violent eruptions occurred in several locations where maars were formed.

In this report the geology of two phreatomagmatic structures of the Snake River Plain is discussed in terms of their formational processes. Split Butte is an asymmetric tuff ring that has been deeply eroded. Sand Butte is a symmetrical tuff cone lying astride a north-south tensional fissure. Both buttes were described in Greeley and King (1975); Womer (1977) and Womer and others (1980) discuss grain size analyses of Split Butte tephra.

[1]Amoco International Oil Co., Houston, Texas 77210.
[2]Department of Geology and Center for Meteorite Studies, Arizona State University, Tempe, Arizona 85281.
[3]Department of Geological Sciences, State University of New York at Buffalo, Amherst, New York 14226.

SPLIT BUTTE

Split Butte is in the south-central Snake River Plain (Figure 1). It overlies basalt flows of the Snake River Group (undifferentiated) and was encroached from the southeast by a lobe of the Wapi lava flow, which has been dated at 2,270 ± 50 years (Greeley, 1982 this volume) to place a lower boundary on the age of Split Butte. The butte consists of vitric ash that forms a ring 600 meters across (Figures 2 and 3). The ring is assymmetrical, having a greater accumulation on the east, the result of prevailing winds from the west during the eruption. The tephra ring is also slightly elliptical, with its long axis oriented approximately N. 60° E. It is unknown whether ring ellipticity resulted from vent geometry or prevailing winds. Although the eroded ring stands 50 meters above the surrounding plain, an original ash thickness of 80 meters on the east is estimated from the dip of the

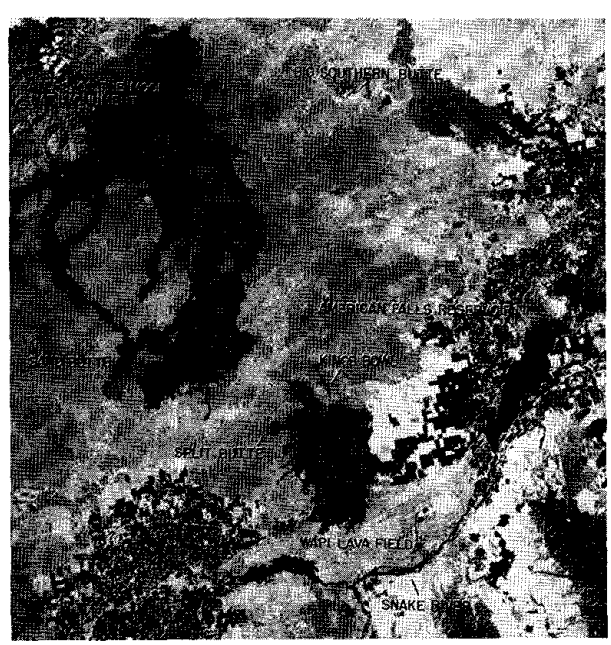

Figure 1. LANDSAT image of the central Snake River Plain, Idaho, showing the location of Sand Butte and Split Butte.

Womer, M. B., Ronald Greeley, and J. S. King, 1982, Phreatic eruptions of the eastern Snake River Plain of Idaho, *in* Bill Bonnichsen and R. M. Breckenridge, editors, Cenozoic Geology of Idaho: Idaho Bureau of Mines and Geology Bulletin 26, p. 453-464.

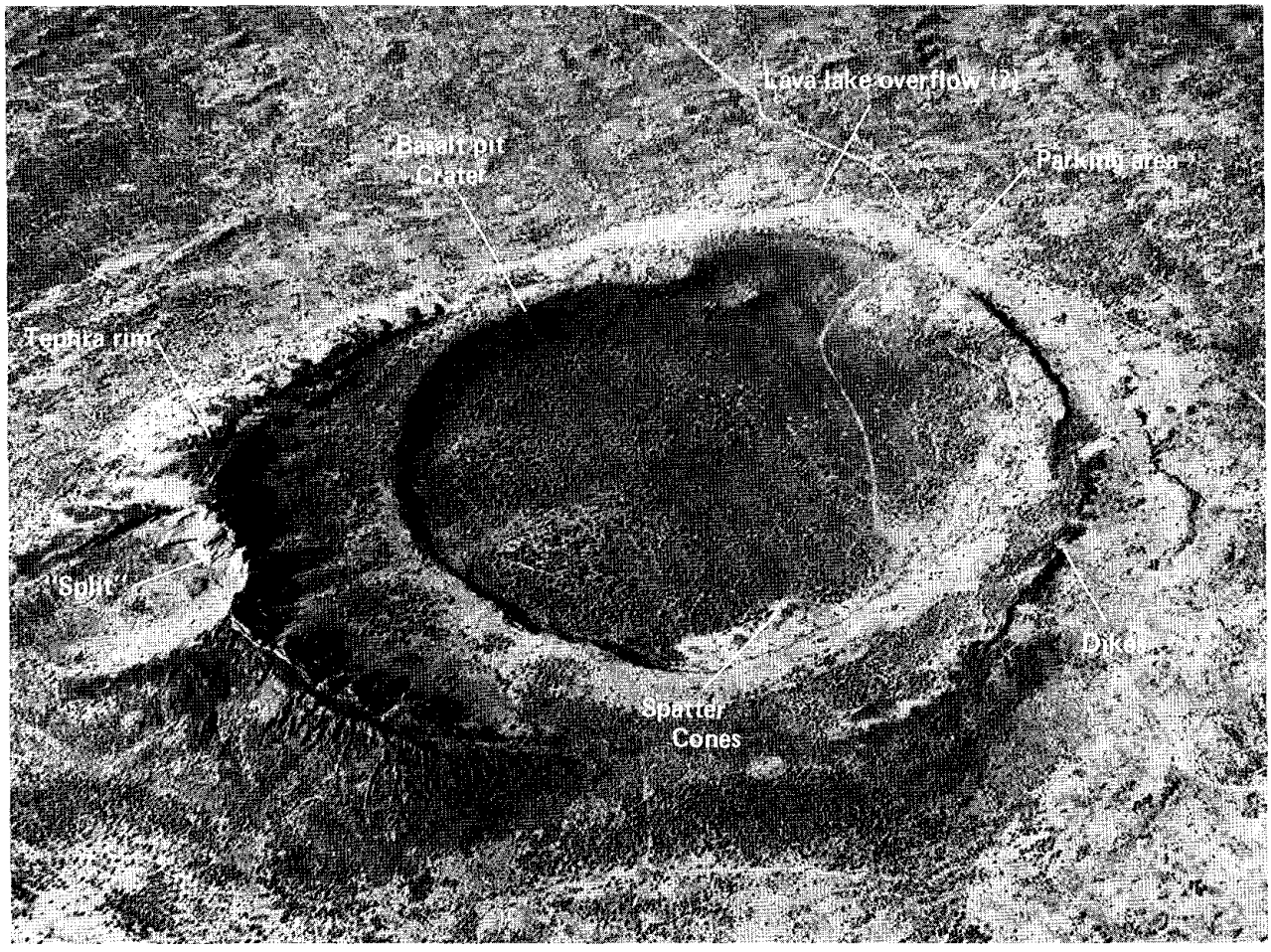

Figure 2. Oblique aerial view toward the southwest of Split Butte. Photograph by Ronald Greeley.

beds and the ring diameter. A topographic notch or erosional "split" approximately 150 meters wide occurs in the thick eastern ash accumulation (Figure 2).

The tephra ranges in color from reddish brown to olive green to black. Basal layers tend to be massive, fine grained, poorly sorted, and extensively palagonitized. Above the basal zone lie thin planar beds of coarser and better sorted ash. Palagonitization and oxidation are less prevalent in these upper layers, which constitute the bulk of the deposits. Beds range in thickness from 2 to 10 centimeters in the upper zone and from a few tens of centimeters to over a meter in the lower zone. Accidental basaltic fragments are abundant and range in size from granules to 1.25 meter-sized blocks. In many places blocks are visible in outcrop with bedding sags in the ash layers below (Figure 4). The layers thin plastically below the blocks and thicken beside them; fracturing of layers is not evident. Lithic fragments are most abundant in the basal tephra layers. The tephra is composed of dense clasts and scoriaceous grains of partially palagonitized sideromelane and a matrix of very finely divided volcanic ash. Scoria grains are found in only a few places in the basal tephra but are the dominant component of the upper, well-bedded layers. The tephra also contains from 3 to 5 percent volume primary plagioclase and olivine crystals, and secondary calcite is locally abundant in palagonitized samples.

A central lava lake was retained by the tephra ring and is in disconformable contact with the tephra (Figure 5; Greeley and King, 1975). Minor lake overflow occurred on the low southwest section of the ring. The lava lake margin is preserved as a narrow circular shelf of basalt, but the central portion has subsided to form a pit crater 20 meters deep and 420 meters across. Two low mounds of spatter occur along the pit crater scarp. The spatter consists of highly oxidized scoria and may represent a degassing outlet for postsubsidence liquids.

Four en echelon basalt dikes intruded the tephra on the northwest section of the ring (Figures 2 and 3).

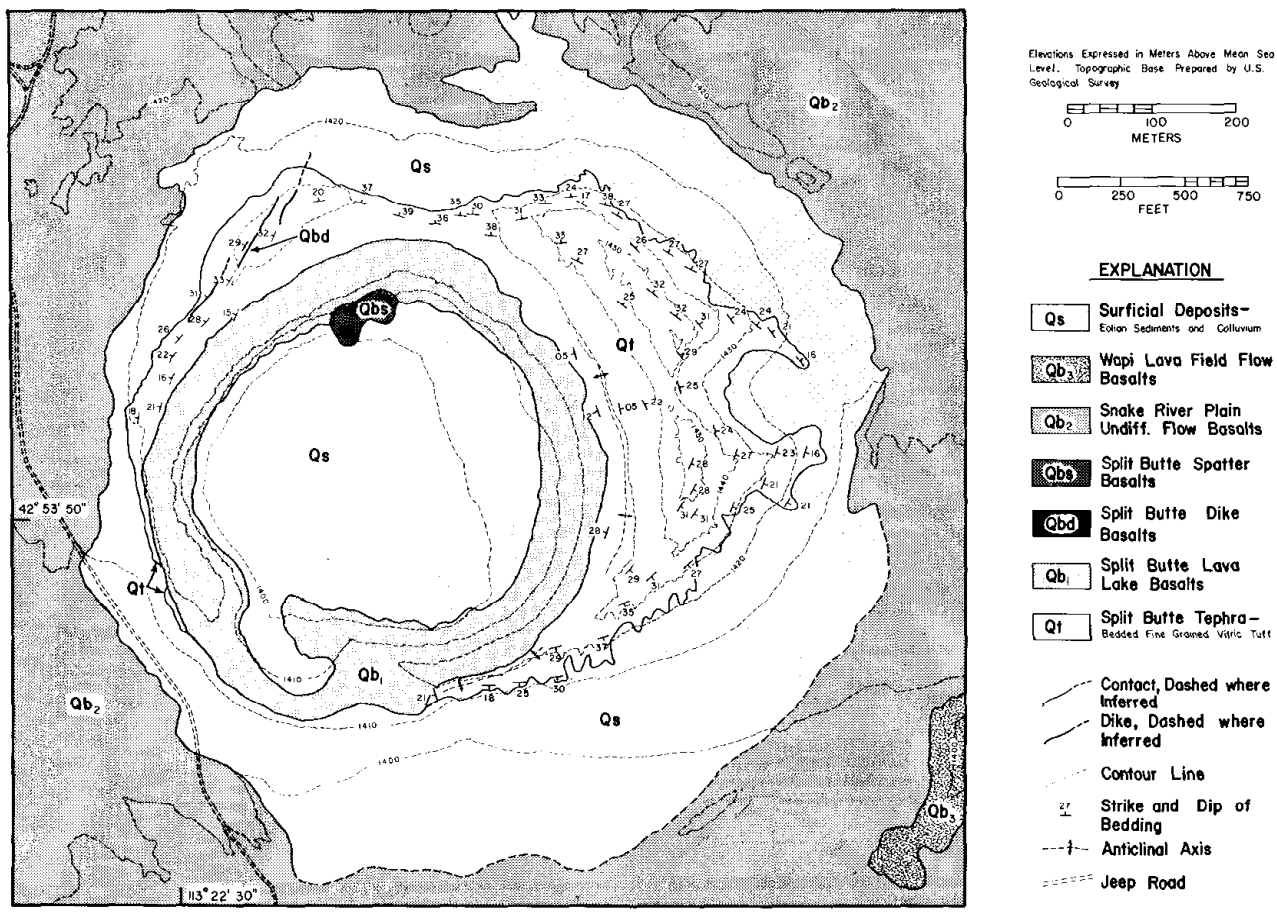

Figure 3. Geologic sketch map of Split Butte.

The nearly vertical dikes are 20 to 30 centimeters thick and have baked tephra along the contacts. They trend tangentially to the ring and can be traced for over 250 meters before disappearing below colluvium.

GENESIS OF SPLIT BUTTE

From field observations and laboratory studies of the ash, we consider Split Butte to be a tuff ring or maar resulting from the interaction of basaltic magma and ground water, followed by an effusive phase of eruption (Figure 6). The ash consists primarily of clear, light brown sideromelane clasts that are locally palagonitized, indicating rapid quenching in a water-rich environment (Fisher and Waters, 1970; Heiken, 1971; Walker and Croasdale, 1971; Macdonald, 1972). The clasts typically are blocky and angular and have few vesicles (Figure 7a), which are small (less than 0.5 millimeter) and spherical. Both the clast shape (Walker and Croasdale, 1971) and arrested vesicle growth (Heiken, 1971) are evidence of quenching by water. Accretionary lapilli are abundant in the tephra and typically consist of a glassy or lithic nucleus coated with an irregular or incomplete layer of fine ash (Figure 7b). Though accretionary lapilli may form by other means, their presence generally indicates the presence of a moist ash cloud during their deposition (Stearns, 1925; Moore and Peck, 1962).

Other evidence for a phreatomagmatic origin are (1) the plastic deformation of ash layers under ejecta blocks (Heiken, 1971; Figure 4); (2) the presence of abundant secondary minerals, calcite, and zeolite in the ash; and (3) the general lack of cinder cone pyroclastics, in particular glass shards as described by Macdonald (1972) and Walker and Croasdale (1971).

Grain size analyses of the tephra also indicate a phreatic origin for the tuff ring. Plots of median diameter versus sorting reveal that phreatomagmatic (Surtseyan) and cinder cone (Strombolian) pyroclastics fall in different fields (Figure 8). Split Butte samples fall mostly within the Surtseyan field, with some extension into the Strombolian field. Separation

Figure 4. Plastic bedding sag in tephra layers under ejecta block approximately 10 centimeters in diameter. Outcrop face is approximately tangential to tephra ring.

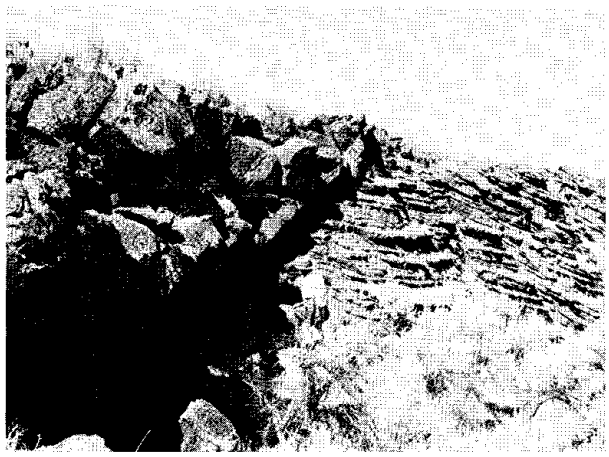

Figure 5. Disconformable contact between massive basalts of the lava lake on the left and uniformly dipping planar beds of tephra on the right.

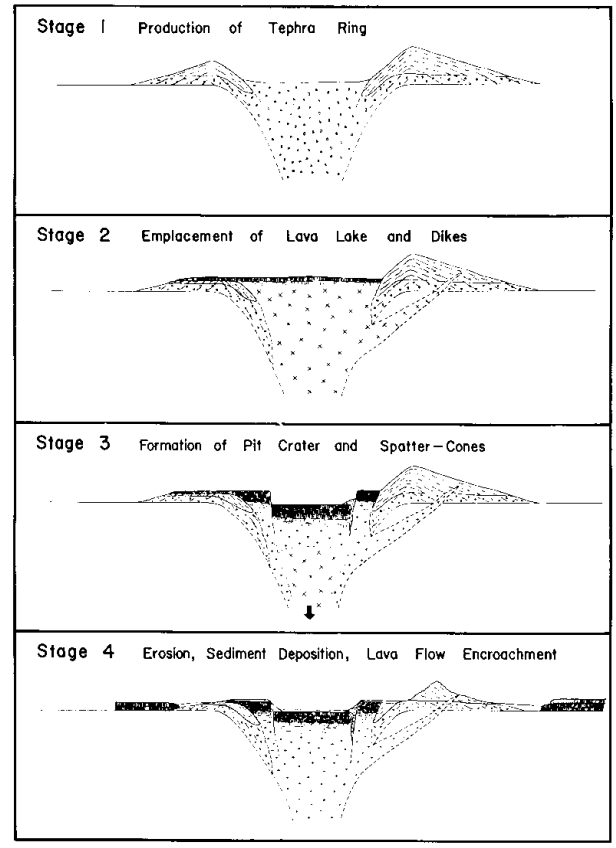

Figure 6. Sequence of events that formed Split Butte (modified from Greeley and King, 1975).

of the samples into massive and bedded deposits shows that massive beds plot within the phreatic field and that the bedded deposits fall in both fields (Figure 9). This and the observations discussed above suggest that the basal tephra resulted from the interaction of magma and abundant ground water. This early phase was followed by a transitional period represented by the sequence of interlayered tephras, during which the degree of magma-water interaction varied sporadically. Finally, interaction stabilized at a decreased level and the planar beds of locally scoria-rich ash were produced.

A change in eruption from explosive to effusive activity led to the emplacement of the central lava lake. This shift in activity is a common feature of tuff rings (Lorenz and others, 1971) and results from a cessation of magma-water interaction. Cessation of the interaction may have resulted from the consumption of ground-water supplies, the removal of access of water to the vent, or an increased eruption rate of magma. Although the lava lake was relatively quiet, as evidenced by the lack of spatter, motion within the lake was sufficient to erode most of the inward-dipping tephra. The slumping of ash into the lava lake caused the disconformable contact visible between the lake basalts and thick tephra deposits in the east. Conformable contacts are prevalent along the low tephra deposits in the west.

Subsequent to partial solidification of the lava lake, the removal of support formed the central pit crater. Though the floor of the crater is largely sediment covered, its horizontal and undisrupted nature argue against a catastrophic collapse. Two mounds of spatter on the ring fracture appear to represent the last volcanic activity at Split Butte.

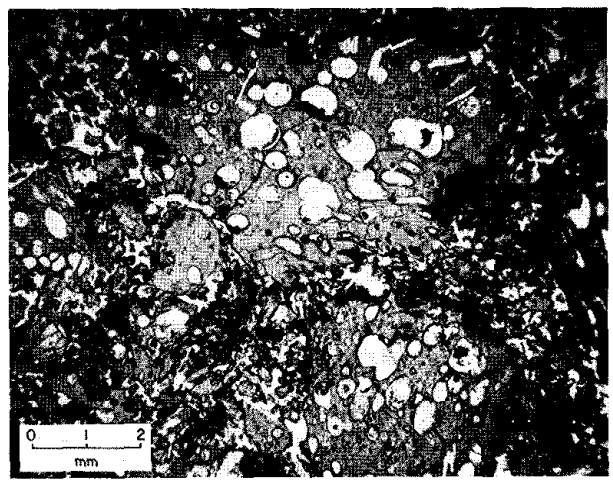

Figure 7a. Photomicrograph of Split Butte tephra under plane-polarized light. Two large vesicular sideromelane grains lie in a matrix of blocky dense clasts, irregular shards, and finely comminuted volcanic dust.

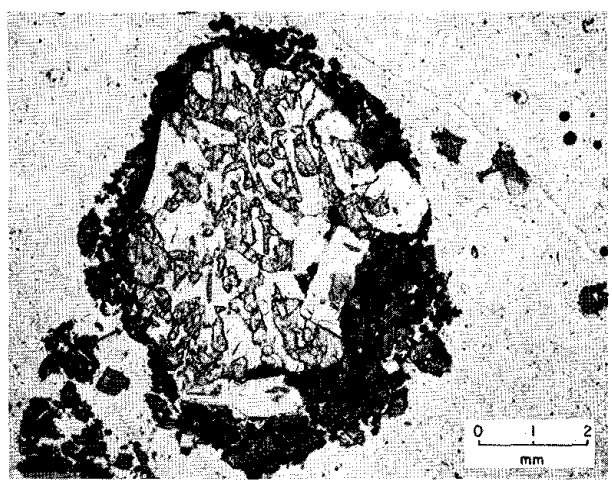

Figure 7b. Photomicrograph of accretionary lapillus in Split Butte tephra under plane-polarized light. Lapillus consists of a lithic clast nucleus approximately 4 millimeters in diameter with a discontinuous and irregular shell of small glass clasts and dust.

SAND BUTTE

Sand Butte lies about 38 kilometers southwest of Craters of the Moon National Monument (Figure 1). It consists of a tuff cone containing a lava lake and is astride a north-south fissure 5 kilometers long (Figure 10). The fissure is a depression 5 to 8 meters deep and 60 to 125 meters wide (Figure 11). Flow units from the fissure typically are 5 to 10 centimeters thick and dip away from the fissure about 5 degrees; dip decreases to 1 to 2 degrees about 100 meters from the vent area. Activity was concentrated locally along the fissure, as indicated by accumulations of spatter. A well-developed lava tube near the southern end of the fissure represents an area of particularly active outflow. The tube is 2 meters wide by 1.4 meters high at the fissure and more than 60 meters long.

The tuff cone is 1.2 kilometers across and 80 meters high and consists of palagonitized vitric ash and abundant lithic fragments. The tephra ranges in color from buff to deep brownish maroon and is typically poorly bedded. Beds range in thickness from 2 to 3 centimeters for a few planar beds to over 2 meters for massive layers. Beds are defined by changes in the grain size, color, and composition of constituent materials; contacts range from gradational to sharp; thin stringers of coarser lithic and juvenile material are seen in many places within beds. Poorly developed cross-bedding of thin laminae is locally present. The beds are typically planar and continuous for tens of meters; dune forms are not visible. The

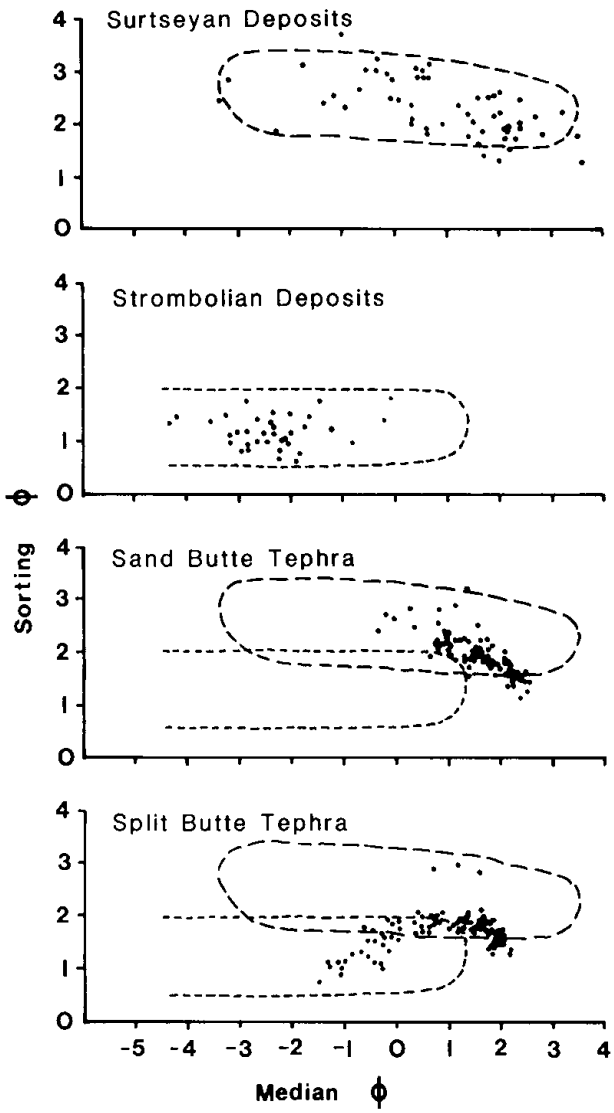

Figure 8. Plots of median diameter versus sorting in ϕ units (ϕ = -log$_2$ particle diameter) for grain size analyses of Strombolian and Surtseyan near vent deposits of Walker and Croasdale (1971) and Sand Butte and Split Butte tephras. The median diameter represents the ϕ value at which the cumulative frequency curve crosses the 50 percent point. The deviation $\sigma\,\phi$ is defined as $\phi 84 - \phi 16/2$ where $\phi 84$ is the ϕ value at which the cumulative frequency curve crosses the 84 percent point and $\phi 16$ is the value at the 16 percent point. Field outlined by short dashes is the Strombolian Field of Walker and Croasdale (1971), and the field outlined by long dashes is the Surtseyan Field.

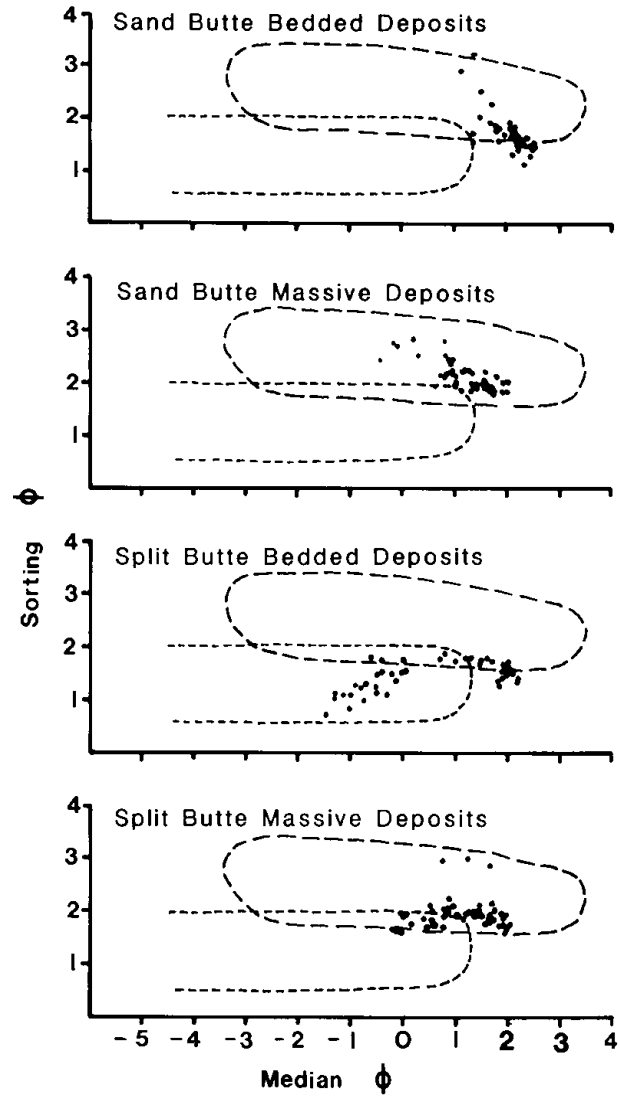

Figure 9. Plots of median diameter versus sorting in ϕ units for massive and bedded deposits of Sand Butte and Split Butte. Dashed outlines are explained in Figure 8.

tephra dips radially outward from 10 to 30 degrees; inward dipping layers are not visible. Lithic ejecta blocks are very abundant throughout the tephra sequence but are slightly more common in the massive ash layers. They consist entirely of basalt and range in size from small granules to 1 meter-sized blocks. Most are angular, although many of the larger blocks (over 40 centimeters) were apparently rounded before emplacement. These larger blocks caused many plastic impact sags in the ash layers below (Figure 12). Slightly coarser fill occurs in front of and behind blocks, and thinning of ash layers over blocks is visible.

The tephra consists of moderately to heavily palagonitized sideromelane clasts and vesicular grains, olivine and plagioclase crystal fragments, and lithic inclusions in a matrix of very fine ash (Figure 13a, b). The clasts are the dominant component and have angular shapes. They tend to be dense, with relatively few vesicles that are small and spherical where present. Vesicular grains are ovoid to irregular and scoriaceous, with numerous stretched and deformed vesicles (Figure 13a); they are locally concentrated in thin (less than 2 millimeters) layers but are subordinate to the smaller clasts. Samples of bedded tephra consistently contain a greater proportion of vesicular grains than do massive layers. Secondary calcite and zeolite are locally abundant in the heavily palagonitized samples.

Sand Butte displays only minor assymmetry, with slightly more voluminous deposits on the eastern flank, evidently the result of prevailing winds. The ring is slightly elongate in a north-south direction, due to vent geometry. Two notches occur in the tephra ring where it intersects the trace of the underlying fissure. The southern notch lowers the rim by some 15 meters, whereas the cone is completely breached on the north. Both notches resulted from the erosion of tephra by effusive activity along the fissure, though activity was more vigorous in the north. This is indicated by the depth of the north gap and the presence of spatter high in the walls of the notch, derived from a north-south striking dike exposed in the west wall of the notch, 15 meters below the tephra rim.

The cone retained a central lava lake that subsequently subsided to form a shallow pit crater. The original lava level is preserved as a discontinuous scarp of massive basalt in contact with the inner tephra walls (Figure 14). Colluvium discontinuously mantles the lava lake surface, which exhibits the swirling pattern of pahoehoe ropes typical of some Hawaiian lava lake activity. The lava lake and fissure basalts are very similar compositionally but display wide variation in texture. Olivine is the only phenocryst phase present in the fissure flows; plagioclase is present as unoriented groundmass laths that are typically 0.5 millimeter long. Lava lake basalts are coarsely crystalline with both plagioclase and olivine phenocrysts present. At the contact of lake basalts with tephra, however, phenocrysts of embayed olivine lie in a fine-grained matrix of flow-oriented plagioclase microlites and subophitic clinopyroxene crystals.

A moatlike depression approximately 5 meters deep encircling Sand Butte was formed by the encroachment onto the Butte of a lava flow of the Snake River Group (Figure 11). This lava flow also entered the south channel, which it partly filled, and the north channel where only a minor lobe of the flow is visible.

GENESIS OF SAND BUTTE

Sand Butte is a tuff cone formed by the phreatomagmatic interaction of ground water and basaltic magma. Evidence for this conclusion is the same as that presented for Split Butte. The tephra is dominantly palagonitized sideromelane that shows textural evidence of rapid chilling (Figure 13). Accretionary lapilli, occasionally without nucleii, are abundant in the tephra. Field evidence for phreatomagmatic activity includes the plastic deformation in impact sags, the abundance of ejecta blocks, and the paucity of scoria in the tuff beds.

Pyroclastic flow was apparently the dominant depositional mechanism at Sand Butte, based on several lines of evidence. First, the large-wavelength undulatory nature of the rim is characteristic of tuff rings where flow has been active (K. Wohletz, personal communication). Although radial exposures of the tuff are poorly developed, some cross-bedding in the ash is locally visible. Tephra layers overlying basalt ejecta blocks thin visibly over the blocks, and air-fall "drapes" are not evident. In addition, ash fill behind impact blocks is coarser than in surrounding beds. Bedding sags under ejecta blocks, however, indicate the presence of some air-fall activity.

We conclude that Sand Butte tephra is mostly phreatic and that pyroclastic flow was the dominant depositional mechanism, forming most of the poorly bedded to massive layers. Air-fall activity was minor, and these deposits are limited to the thinly bedded layers. Although tephra production and effusion of fissure lavas may have overlapped, we consider the phreatic phase of the eruption to have ended essentially before most of the basalt was erupted. The relationship between fissure activity and tephra is clearly evident in the west wall of the north gap, where tongues of spatter disconformably overlie the tephra. These spatter deposits have run down the tephra slope and originated from a possible basalt

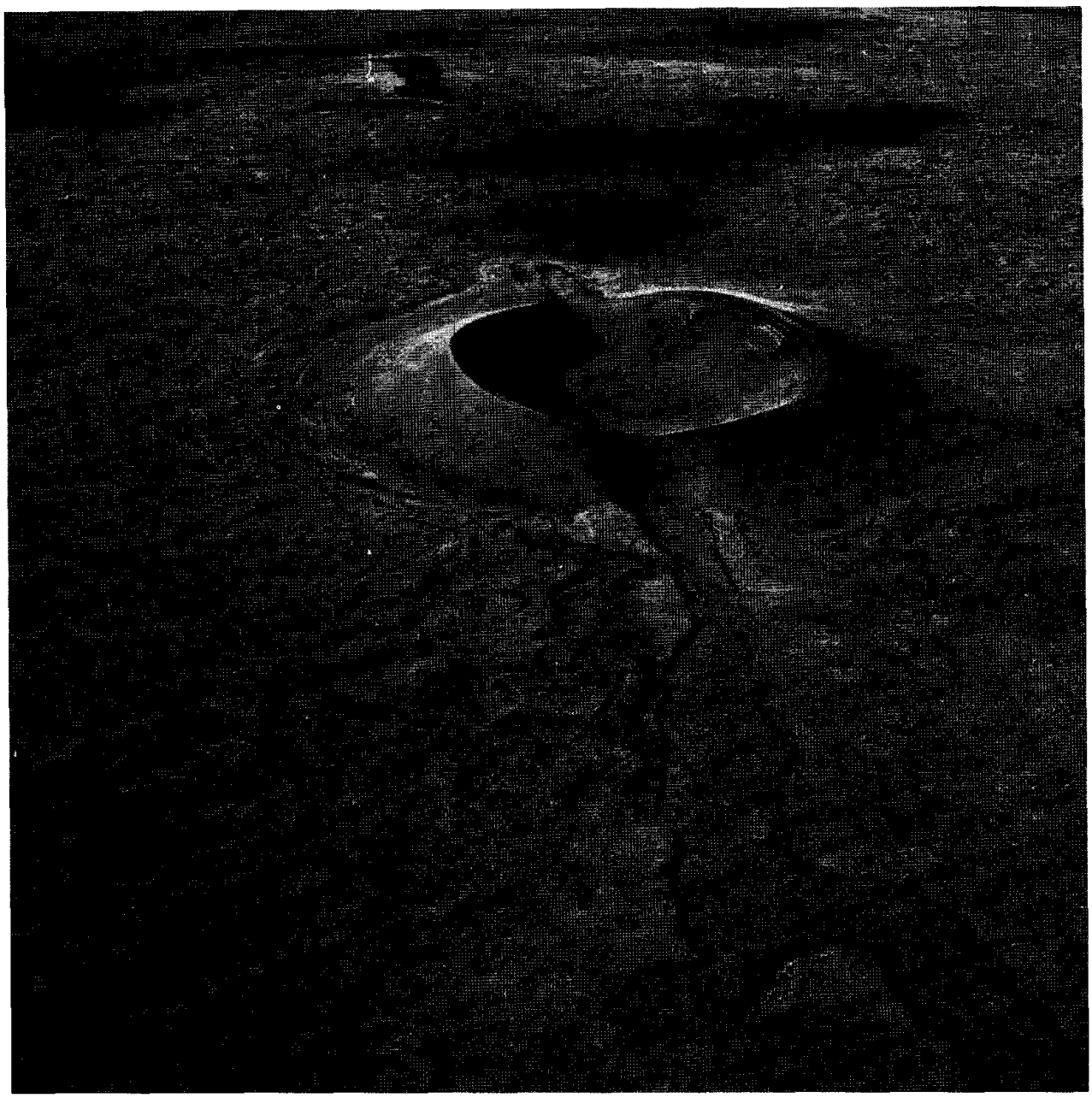

Figure 10. Oblique aerial view of Sand Butte. Photograph by Ronald Greeley.

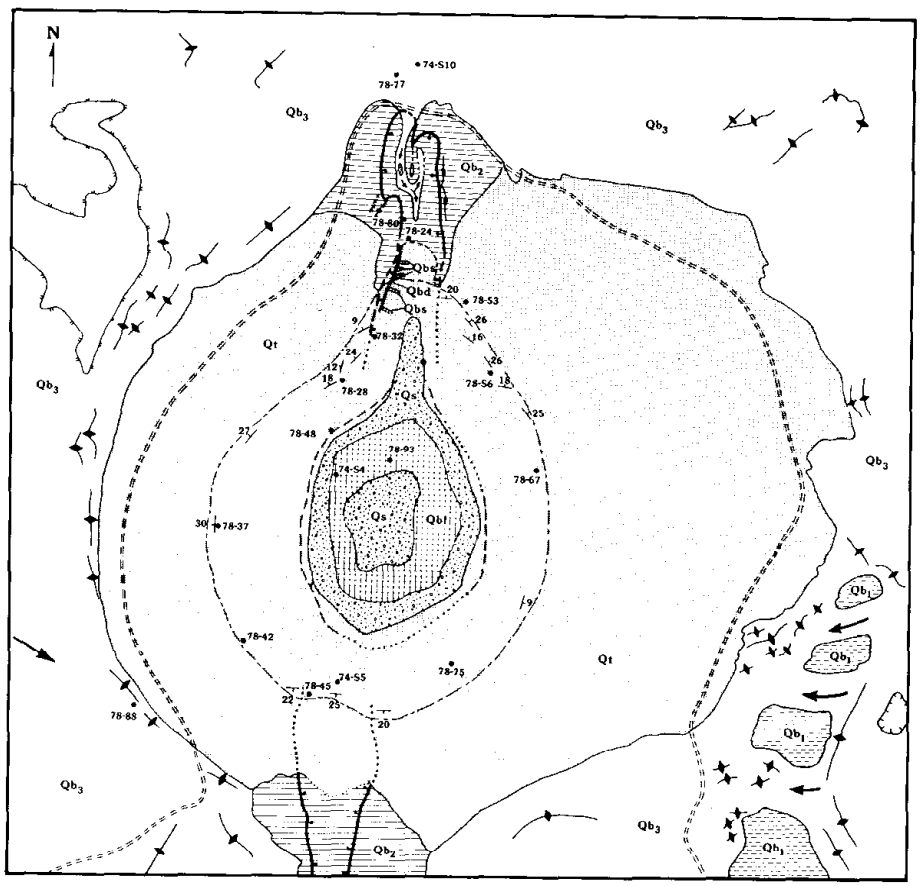

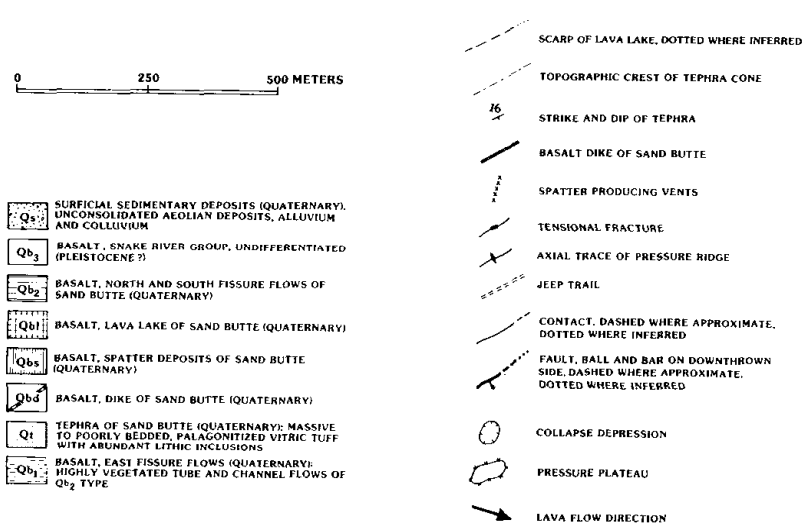

Figure 11. Geologic sketch map of Sand Butte.

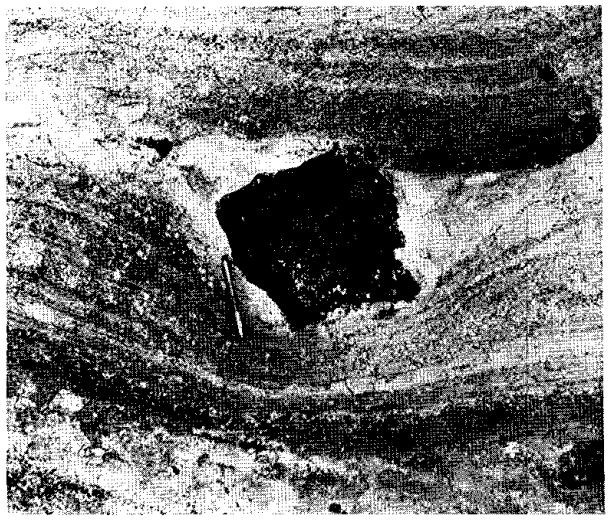

Figure 12. Impact block approximately 23 centimeters across with characteristic asymmetric sag in tephra layers below. Center of crater is to left. Note shadow zones on front of and behind block.

dike (Figure 11). The possible dike consists of a curviplanar sheet of lava, striking north-south and dipping 60 to 70 degrees east, that crops out high in the gap wall. The emplacement of the lava lake postdated the formation of the north gap, as indicated by the lake scarp following the topographic contours of the north gap area (Figure 11). The lake apparently never rose high enough to flow through the north gap area.

COMPARISON OF SPLIT AND SAND BUTTES

Both features consist of subcircular tephra deposits with a central crater 500 to 600 meters in diameter. Both involved an early phase of phreatomagmatic activity, followed by an effusive phase that resulted in the emplacement of a lava lake; both lakes subsided to form shallow pit craters. There are differences, however, in eruptive and depositional processes that are reflected in their morphology and in the tephra. Sand Butte is nearly symmetrical, whereas Split Butte is strongly asymmetrical, with much thicker ash deposits on the downwind side of the vent. We consider this evidence that Split Butte formed while strong westerly winds were active and that Sand Butte formed during a relatively calm period. Split Butte may be best described as a tuff ring, whereas the more voluminous deposits of Sand Butte form a tuff cone. Although the height-width ratio at Split Butte may be as great as 1:12 for the thickest ash deposits, the average height-width ratio is much lower, probably in the range of 1:25 to 1:30. The height-width ratio of Sand Butte is a relatively uniform 1:15. Heiken (1971) has suggested that the differences in height-width ratios of cinder cones and tuff rings and cones are partly dependent upon the depth of water-magma interaction, with deeper interaction resulting in higher constructs. The ash layers of Split Butte display a transition from massive and poorly bedded to planar beds in the upper sequence. Tephra at Sand Butte displays no such transition; beds are poorly bedded to massive throughout the sequence with only few planar beds visible. These planar beds have grain size distributions indicative of air-fall deposition and represent the lower energy regime of a base surge explosion.

The tephra displays compositional differences as

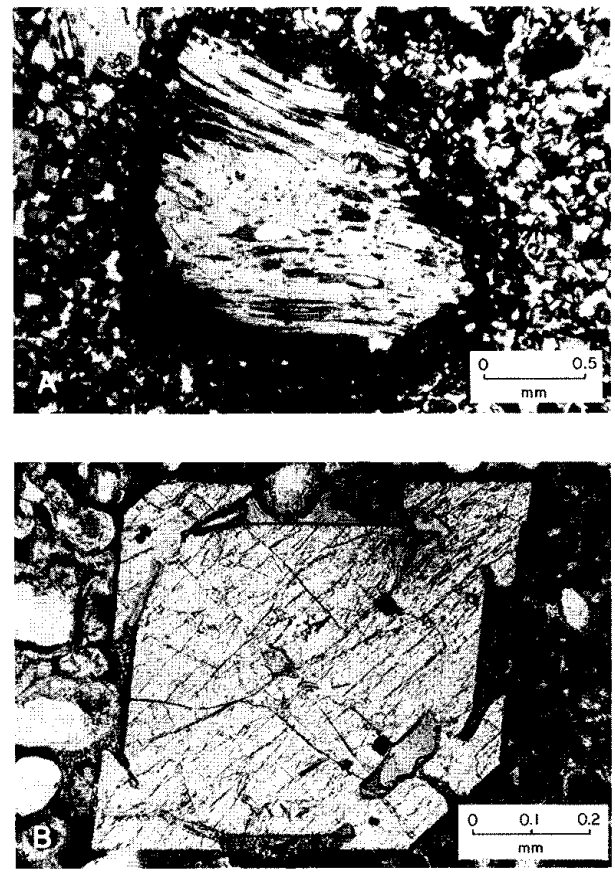

Figure 13. Photomicrographs of Sand Butte tephra under plane-polarized light: (A) a large accretionary lapillus in a matrix of blocky to irregular clasts and fine dust. The core of the lapillus consists of a grain of vesicular and plastically deformed sideromelane. (B) a phenocryst of olivine that was embayed along a probable magnesium-rich zone by magmatic liquid that was quenched to form sideromelane.

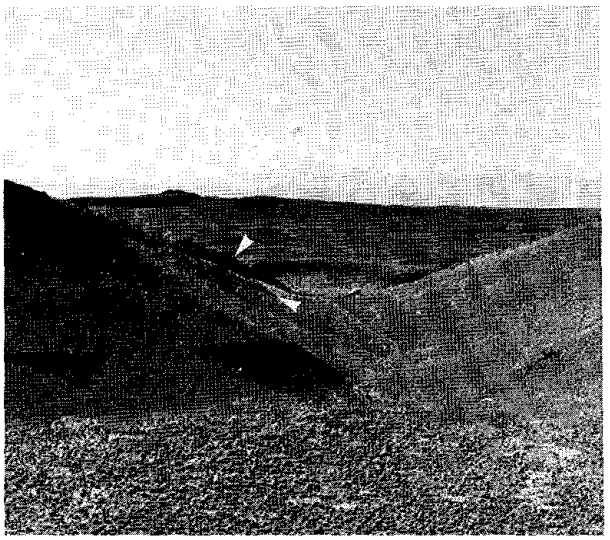

Figure 14. View facing north across the interior of the Sand Butte crater showing the lava lake in foreground and north gap and fissure in photo center. Fissure flows and spatter overlying tephra marked with arrows. Prominant horizontal scarp on right near base of tephra represents high level of the lava lake.

well. The Sand Butte ash is finer grained and rich in palagonite and secondary minerals, and it contains a higher fraction of lithic fragments than Split Butte tephra. Whereas Split Butte tephra has a large component of vesicular grains in the millimeter-size range, the tephra of Sand Butte displays relatively minor quantities of these grains. The highly vesicular glass grains of Split Butte indicate exsolution of juvenile gas at shallow level (Lorenz and others, 1971). As they are present primarily in the upper ash layers, an upward migration of magma-water interaction is implied. These compositional and structural differences are reflected in grain size analyses. Figure 8 illustrates the presence of a single, poorly sorted population of tephra at Sand Butte and of the bimodal population of tephras at Split Butte. This bimodality is the result of Surtseyan pyroclastics in the massive layers and a mixture of Surtseyan and Strombolian pyroclastics in the bedded layers (Figure 9).

SUMMARY AND CONCLUSIONS

We conclude that both buttes are largely phreatic in origin but that there are essential differences in energy, depth, and degree of magma-water interaction. A deeper level of magma-water interaction at Sand Butte is suggested by a greater fraction of lithic ejecta and the less vesicular nature of the juvenile fraction. The decrease in eruptive energy at Split Butte is also responsible for the change to thin planar beds that are largely air fall. At Sand Butte, however, a larger fraction of lithic blocks and the lack of planar beds show that a higher eruptive energy and dominance of pyroclastic flow deposition were maintained with the greater depth of interaction.

Both buttes appear as nested, subcircular structures, consisting of a tephra ring or cone and an inner lava lake modified by a pit crater. Both are several hundreds of meters across and 50 to 80 meters high. Differences in morphology and structure between the two were caused by variation in external conditions and eruptive processes. A strong wind caused Split Butte tephras to form asymmetrical deposits, whereas Sand Butte deposits are nearly symmetrical.

ACKNOWLEDGMENTS

We appreciate the helpful discussions with K. Wohletz and M. Sheridan regarding tephra deposits and explosive volcanism. The field assistance of E. Theilig is gratefully acknowledged. M. E. Hahn assisted with the laboratory analysis. All aspects of the study were supported by grants from the NASA Office of Planetary Geology.

REFERENCES

Fisher, R. V. and A. C. Waters, 1970, Base surge bed forms in maar volcanoes: American Journal of Science, v. 268, p. 157-180.

Greeley, Ronald, 1982, The style of basaltic volcanism in the eastern Snake River Plain, Idaho, *in* Bill Bonnichsen and R. M. Breckenridge, editors, Cenozoic Geology of Idaho: Idaho Bureau of Mines and Geology Bulletin 26.

Greeley, Ronald and J. S. King, 1975, Geologic field guide to the Quaternary volcanics of the south-central Snake River Plain, Idaho: Idaho Bureau of Mines and Geology Pamphlet 160, 49 p.

Heiken, G. H., 1971, Tuff rings: examples from the Fort Rock-Christmas Lake Valley basin, south-central Oregon: Journal of Geophysical Research, v. 76, p. 5616-5626.

Lorenz, V., A. R. McBirney, and Howel Williams, 1971, An investigation of volcanic depressions, part III—Maars, tuff rings, tuff cones and diatremes: National Aeronautics and Space Administration Progress Report.

Macdonald, G. A., 1972, Volcanoes: Prentice-Hall Publishing Company, 510 p.

Moore, J. G. and D. L. Peck, 1962, Accretionary lapilli in the volcanic rocks of the western continental United States: Journal of Geology, v. 70, p. 182-193.

Stearns, H. T., 1925, The explosive phase of Kilauea volcano, Hawaii, in 1924: Bulletin Volcanologique, v. 5-6, p. 193-208.

Walker, G. P. L. and R. Croasdale, 1971, Characteristics of some basaltic pyroclastics: Bulletin Volcanologique, v. 35, p. 303-317.

Womer, M. B., 1977, The origin of Split Butte, a maar crater of the south-central Snake River Plain, Idaho, Chapter 12, *in* Volcanism of the Eastern Snake River Plain, Idaho: A Comparative Planetary Geology Guidebook, National Aeronautics and Space Administration CR-154621, p. 190-202.

Womer, M. B., Ronald Greeley, and J. S. King, 1980, The geology of Split Butte, a maar of the south-central Snake River Plain, Idaho: Bulletin Volcanologique, v. 43, p. 453-471.

Mineralogy and Petrology of Tertiary-Quaternary Volcanic Rocks in Caribou County, Idaho

by

Donald W. Fiesinger[1], William D. Perkins[2], and Barbara J. Puchy[3]

ABSTRACT

Basaltic lavas of Caribou County, Idaho, comprise the extensive interconnected Blackfoot, Willow Creek, and Gem Valley lava fields with small valley flows occurring within Enoch, Upper, Wooley, and Slug Creek Valleys. These lavas consist primarily of olivine tholeiite, with minor tholeiite and tholeiitic trachybasalt. The olivine tholeiite is similar to that of the Snake River Plain, as it is olivine and hypersthene normative, does not contain calcium-poor pyroxene, and shows an affinity with alkali olivine basalt on the alkali-silica diagram. The tholeiite and tholeiitic trachybasalt are hypersthene and quartz normative with silica contents ranging from 48 to 53 percent. The trachybasalt is higher in total alkalies, P_2O_5, and Fe/(Fe + Mg) than the tholeiite and has alkali feldspar as a groundmass phase.

Flows of plagioclase basalt porphyry occur at Cinder Island within the Blackfoot Reservoir and at Nelson and King Canyons within the Bear River Range east of Gem Valley. This porphyry consists of approximately 30 percent plagioclase phenocrysts, 5 to 20 millimeters in length, set in an aphanitic to opaque groundmass.

A potassium-rich alkali trachyte occurs at the southern end of Slug Creek Valley. It consists of olivine and diopsidic augite phenocrysts in a groundmass of alkali feldspar, olivine, and augite, with minor plagioclase, exsolved iron-titanium oxides, and traces of amphibole and biotite.

Olivine tholeiite is considered to be the parental magma from which other basaltic lavas have originated. Fractionation of 40 to 60 percent crystals from olivine tholeiite will yield a liquid with the composition of tholeiite or trachybasalt. As removal of groundmass phases is required, filter pressing during late-stage crystallization is the proposed mechanism. In contrast to this, plagioclase basalt porphyry can be derived by the removal of olivine and the accumulation of plagioclase, both common phenocryst phases.

Although olivine tholeiite may be derived with 10 percent partial melting of pyrolite, equilibrium between the derived olivine tholeiite and the residuum from partial melting cannot be demonstrated. Using mica peridotite to represent a more potassic mantle composition, alkali trachyte may be derived with 30 percent partial melting. These contrasting magmas are considered to be indirect evidence for mantle inhomogeneity or perhaps different mantle structures beneath the Basin and Range province and the Middle Rocky Mountain province in southeastern Idaho.

INTRODUCTION

Tertiary-Quaternary basaltic lavas in Caribou County, Idaho, comprise the extensive interconnected Blackfoot, Willow Creek, and Gem Valley lava fields near Soda Springs and the small valley flows to the east within Enoch, Upper, Wooley, and Slug Valleys. Rhyolite also occurs in the region, forming three conspicuous domes at the south end of Blackfoot Reservoir and two islands within the reservoir.

This paper represents the synthesis of three projects: (1) a study of the mineralogy and petrology of the lavas in the vicinity of Gem Valley (Perkins, 1979), (2) a study of the mineralogy and petrology of the lavas in the Overthrust Belt (Puchy, 1981), and (3) a study of basaltic volcanism in the Blackfoot Reservoir region as part of a geothermal evaluation made in cooperation with the Department of Geology and Geophysics at the University of Utah for the U. S. Geological Survey.

The objectives of this paper are (a) to present the chemistry and mineralogy of volcanic rocks representing the various lava fields and valley flows in the region, (b) to compare the basaltic lavas of Caribou County with those of the eastern Snake River Plain,

[1]Department of Geology, Utah State University, Logan, Utah 94322.
[2]Andover Oil, Tulsa, Oklahoma 74172.
[3]Terra Resources, Inc., Englewood, Colorado 80111.

Fiesinger, D. W., W. D. Perkins, and B. J. Puchy, 1982, Mineralogy and petrology of Tertiary-Quaternary volcanic rocks in Caribou County, Idaho, *in* Bill Bonnichsen and R. M. Breckenridge, editors, Cenozoic Geology of Idaho: Idaho Bureau of Mines and Geology Bulletin 26, p. 465-488.

and (c) to present a petrogenetic model for the origin of these volcanic rocks.

PREVIOUS WORK

A comprehensive study of the geology of southeastern Idaho was undertaken by Mansfield (1927). As part of this study, he classified the lavas in this region as olivine basalt, because they contain olivine and feldspar phenocrysts in a groundmass of augite, feldspar, olivine, and magnetite, with minor apatite and hematite. In a later investigation, Mansfield (1929) also described the lavas in Portneuf Valley, the northern end of the Gem Valley lava field, as olivine basalt, with mineralogy similar to that mentioned above.

In an investigation of late Pleistocene stratigraphy in the Gem Valley area, the lavas of the Gem Valley lava field have been described as porphyritic olivine basalt, having phenocrysts of plagioclase, olivine, and augite in a groundmass of plagioclase, olivine, augite, magnetite, and glass (Bright, 1963, 1967). Potassium-argon dates by Armstrong and others (1975) give an age of 0.1 ± 0.03 million years for these basalts. Bright (1963, 1967) estimated an age of 33,500-27,000 years for one flow in Gem Valley on the basis of stratigraphic relationships with Lake Thatcher sediments dated by carbon-14 methods.

A series of geophysical investigations have dealt with the origin, structure, and prebasalt topography of the Blackfoot and Gem Valley lava fields (Mabey and Armstrong, 1962; Mitchell and others, 1965; Oriel and others, 1965; Mabey and Oriel, 1970; Mabey, 1971). The geologic map of the Soda Springs quadrangle (Armstrong, 1969) and the preliminary geologic map of the Bancroft quadrangle (Oriel, 1968) delineate the extent of the basalt flows and the locations of numerous eruptive centers.

The small valley flows to the east of the Blackfoot and Willow Creek lava fields have been reported by Mansfield (1927). The vesicular lava in Slug Valley has been briefly described by Cressman (1964) as olivine basalt no younger than Pliocene in age. The distribution of lavas in Caribou County is shown on the generalized composite geologic maps of Mabey and Oriel (1970) and Oriel and Platt (1980). These maps incorporate the work of Mansfield (1927, 1929), Armstrong (1969), Oriel (1968), and Cressman (1964).

GEOLOGIC SETTING

Caribou County lies in both the northeastern part of the Basin and Range province and the western part of the Middle Rocky Mountain province (Figure 1).

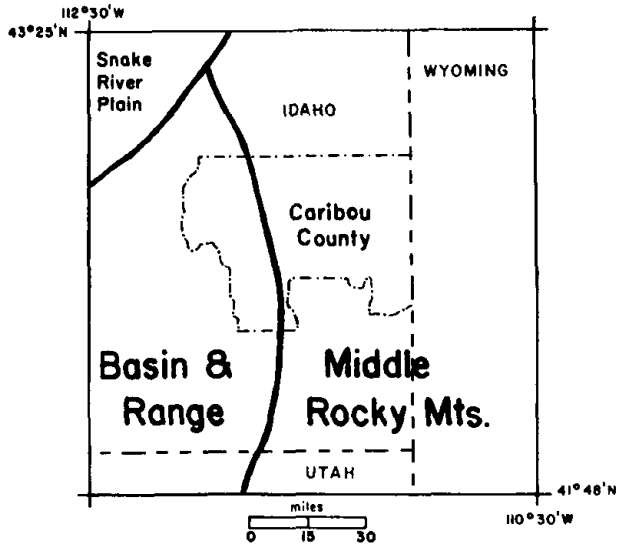

Figure 1. Index map of southeastern Idaho, showing Caribou County, Idaho, the Snake River Plain, and the Basin and Range and Middle Rocky Mountains physiographic provinces.

In general, the western portion of the county is dominated by fault block mountains composed of Paleozoic sedimentary rocks locally overlain by Tertiary sediments. The eastern portion of the county is part of the Overthrust Belt dominated by upper Paleozoic and Mesozoic sedimentary rocks involved in a westward-dipping imbricate thrust zone (Armstrong and Cressman, 1963). The distribution of lavas within Caribou County is shown in Figure 2. In parts of the Blackfoot, Willow Creek, and Gem Valley lava fields, the flows are well-exposed along the extensive northwest-southeast scarp system which runs through the area. The scarp trends indicated by Armstrong (1969) for the Soda Springs area have been observed to continue more than 10 miles to the north, beyond the Blackfoot Reservoir. Individual scarps may be traced visibly for many miles, and where covered by loess, their presence can be inferred from topography and alignment of sink holes. The scarp system is best exposed and most continuous immediately adjacent to and south of the Blackfoot Reservoir.

A study of aerial photographs and ground checks undertaken as part of the present study indicates only minor deviation in the lateral extent of the basaltic lavas from that reported by Mansfield (1927, 1929), Oriel (1968), and Armstrong (1969). The occurrence of basaltic cinder and cinder cones, however, is more widespread than revealed in earlier studies. In the area south of Henry and southeast of the Blackfoot Reservoir, numerous cinder pits have been dug and at least six conspicuous topographic depressions in this area are probably cinder cones masked by loess. Throughout the entire region, loess overlies most

flows and cinder cones.

The western part of the Blackfoot lava field near Tenmile Pass has a thick covering of loess with few cinder cones and few scarps visible. The alignment of sinks through the loess suggests the presence of scarps at depth, which parallel the northwest-southeast trend observable to the east. Similarly, in the eastern part of the Blackfoot lava field, south of Henry and east of the Blackfoot River, volcanic features are subdued. This area lies approximately 300 feet higher in elevation than the remainder of the Blackfoot lava field and has a thick covering of loess. Scarps are not well-exposed, show little relief, and are discontinuous. This area corresponds with negative magnetic anomalies interpreted by Mabey and Oriel (1970) to represent reversely magnetized basalt that is older than the flows to the southwest.

Mabey and Oriel (1970) also observed negative magnetic anomalies in Lower, Wooley, and Upper Valleys and at the southern end of Enoch Valley, which were interpreted to result from reversely magnetized basalt. Positive anomalies attributed to normally magnetized basalt were reported for the northern end of Enoch Valley and the western side of the Willow Creek lava field. Since there have been twenty or more reversals in the Earth's magnetic field since Eocene time (Doell and Cox, 1962), specific ages of these lavas cannot be determined from magnetic polarity, but the presence of both normal and reverse magnetization shows that the flows are not all equivalent in age. The reversely magnetized flows would have to have an age greater than 0.7 million years (Mabey and Oriel, 1970).

The dominant northwest-southeast scarp system is somewhat coincident with block fault patterns recognized within adjacent mountain ranges. This fault pattern probably originated in the Tertiary, and this style of faulting has continued to the present (Armstrong and Oriel, 1965). The occurrence of isolated eruptive centers in the Bear River Range, Soda Springs Hills, Reservoir Mountain, and Pelican Ridge and the alignment of cinder cones in Gem Valley also indicate an association between volcanism and faulting (Mansfield, 1927; Armstrong, 1969).

Field evidence indicates continued faulting throughout the period of volcanic activity in the region. Age relationships between volcanism and scarp formation are generally not clear and can be established only locally. Cinder cones are commonly located on scarps, with no recognizable offset, indicating eruption along older, inactive scarps. Similarly, scarps project through (under?) the rhyolite domes south of Blackfoot Reservoir, but only the southwestern portion of China Hat shows evidence of possible offset by faulting. Other cinder cones have been truncated by scarps indicating post-eruption displacement. Examples include the cinder cones south and southwest of China Hat, the cinder cone on the eastern side of Reservoir Mountain, and cinder cones east of the Blackfoot Reservoir.

Field evidence reveals that basaltic volcanism took longer than the emplacement of the rhyolite domes. Three small lobes of basalt occur on the lower slopes of Middle Cone, on the northwestern and southeastern sides. Associated with the basaltic lobe to the southeast is flow-banded, pumiceous rhyolite containing blebs of basalt (3 to 5 centimeters in diameter) and larger xenoliths of basalt and white quartzite up to 20 centimeters in length. Three basaltic xenoliths were examined petrographically. Mineralogies and textures are somewhat typical of fine-grained basaltic lavas from the region. Unusual features include the presence of amphibole and alkali feldspar(?) as groundmass phases in one, and the presence of quartz and plagioclase xenocrysts and rounded inclusions of vesicular brown glass with trichites in the others.

Armstrong and others (1975) have dated the rhyolites of China Hat and Middle Cone at 0.1 million years, whereas Leeman and Gettings (1977) obtained dates of about 0.05 million years. The rhyolite of Sheep Island, within Blackfoot Reservoir, has been dated at 1.4 million years (S. H. Evans, University of Utah, personal communication).

SAMPLING AND ANALYTICAL PROCEDURES

Samples were taken from basaltic flow units and eruptive centers representing the various lava fields and valley flows within the region. After a preliminary petrographic study of more than sixty-five specimens, twenty-six samples were selected for further study. Samples selected are relatively free of oxidation, alteration, and vesiculation and represent diversity as suggested by their textures, mineralogies, and occurrences. Sample locations are shown in Figure 2; brief descriptions are presented in Table 1.

Whole rock chemical analyses were obtained using volumetric, gravimetric, and colorimetric methods described by Carmichael and others (1968). Mineral analyses were obtained using the ARL EMX electron probe micro-analyzer at the University of Utah, following standard procedures for silicate and oxide analysis. Phenocryst phases were analyzed systematically from core to rim, with an average of five spot analyses obtained from each of ten randomly selected phenocrysts or microphenocrysts. Groundmass phases were analyzed by taking two to three spot analyses from each of twenty to twenty-five randomly selected mineral grains. Correction procedures used on microprobe data follow the methods of Bence and Albee

(1968) and Albee and Ray (1970) and were made using the computer program of Nicholls and others (1977). In all samples where iron was analyzed by microprobe, total iron is reported as FeO. Modal analysis consisted of mineral determination at approximately 1,600 points covering 2 to 3 square centimeters using a spot interval of 0.1 millimeter.

PETROGRAPHY

Colors and textures of lavas within the region are variable and range from gray to black for the denser lavas and gray to black to dark red for the more vesicular lavas. Samples collected from cinder cones tend to have distinctive flow banding and are commonly heterogeneous in mineral distribution, grain size, and grain orientation, whereas samples collected from scarps and thick flow units tend to be homogeneous in texture.

Modal analyses of the twenty-six analyzed lavas are presented in Table 2. Undifferentiated groundmass consists of birefringent material too small for more exact identification. Most lavas tend to be nonporphyritic to microporphyritic with typical basaltic mineralogy and textures. The nonporphyritic lavas generally have less than 5 percent phenocrysts; the microporphyritic lavas generally have more than 10 percent phenocrysts. Phenocryst assemblages consist of plagioclase and olivine, commonly clustered in a glomeroporphyritic texture. The olivine phenocrysts are euhedral to subhedral, average 0.6 to 1.0 millimeter in diameter, and commonly have euhedral crystals of magnetite attached. Skeletal olivine crystals are found in some lavas. The plagioclase phenocrysts average 1.5 millimeters in length, and are commonly twinned according to the albite, Carlsbad, and Carlsbad-albite twin laws. Plagioclase and olivine commonly exhibit a continuous size gradation between phenocrysts and groundmass in most lavas.

A variety of groundmass textures have been observed in the basaltic lavas including ophitic, subophitic, intergranular, and hyaloophitic. Flow-banded lavas show subparallel alignment of plagioclase phenocrysts or groundmass laths in a pilotaxitic texture. The groundmass assemblage consists of plagioclase, olivine, augite, iron-titanium oxides, and apatite.

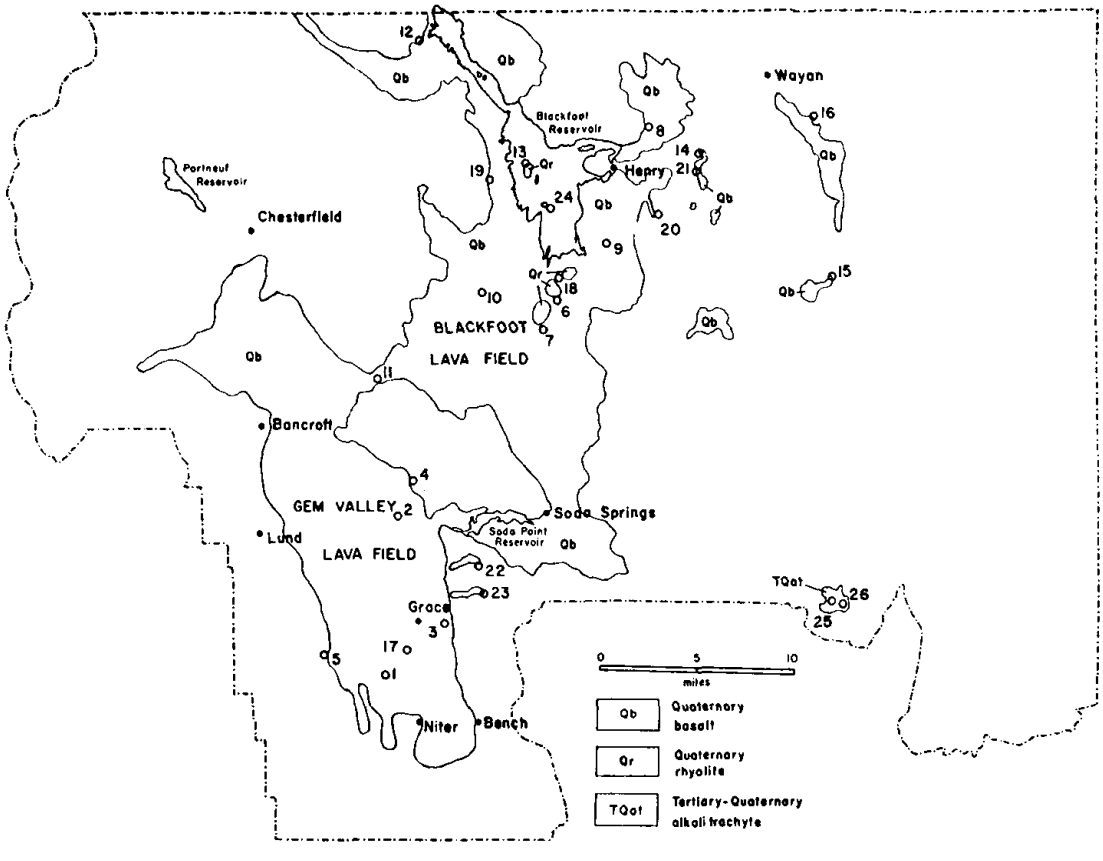

Figure 2. Map of Caribou County, Idaho, showing the general distribution of volcanic rock. The Willow Creek lava field lies north of Henry; Enoch Valley and Wooley Valley lie east of Henry. Upper Valley lies south of Wayan. Sample locations are indicated by open circles.

Plagioclase commonly dominates the groundmass, with laths being 0.1 to 0.2 millimeter in length, and albite twinning being ubiquitous. Groundmass olivine occurs as equant anhedral grains, ranging from 0.1 to 0.5 millimeter in diameter. Augite is commonly in an ophitic to subophitic relationship with plagioclase. Single, optically continuous augite crystals greater than 2 millimeters in length have been recognized. The iron-titanium oxides generally average less than 0.3 millimeter in maximum dimension. Magnetite grains are characteristically equant, commonly occurring as euhedral cubic crystals, whereas the ilmenite grains are typically elongate or needlelike. In addition to these groundmass constituents, two samples (6 and 12) contain diffuse laths of alkali feldspar and have been classified as trachybasalt.

Interstitial glass, containing abundant microlites, is present in many lavas. Glass is the major constituent within the pillow lavas of Gem Valley (sample 5). The outer margins of these pillow structures are similar to those described by Moore (1970) for Hawaiian submarine eruptions. They contain an outer pale-brown layer of sideromelane that becomes progressively opaque with an increase in microlites going inward from the rim.

In contrast to these lavas, a distinctive basalt porphyry forms Cinder Island, within the Blackfoot Reservoir (sample 24), and the flows in Nelson and King Canyons within the Bear River Range, east of Gem Valley (samples 22 and 23). This porphyry consists of approximately 30 percent plagioclase phenocrysts, 5 to 20 millimeters in length, in an aphanitic to opaque groundmass. These phenocrysts are commonly fractured or fragmented, suggesting

Table 1. Locations of analyzed samples from lavas of Caribou County, Idaho.

Sample Number	Collection Number	Location
1	GV76-4	Basalt, cinder cone near Cedar Hollow, Gem Valley. SE¼SW¼ sec. 22, T. 10 S., R. 40 E.
2	GV76-6	Basalt, Alexander Crater, Gem Valley. NW¼SE¼ sec. 11, T. 9 S., R. 40 E.
3	GV77-6	Basalt, scarp east of Grace, Gem Valley. SE¼SE¼ sec. 6, T. 10 S., R. 41 E.
4	GV77-7	Basalt, cinder cone, Soda Springs Hills. SW¼SW¼ sec. 36, T. 8 S., R. 40 E.
5	GV78-1	Pillow basalt, road cut at China Hill, Gem Valley. NW¼SE¼ sec. 18, T. 10 S., R. 40 E.
6	SSV78-1	Basalt, southeast flank of Middle Cone. SE¼NE¼ sec. 18, T. 7 S., R. 42 E.
7	SSV78-7	Basalt, cone cut by scarp, south of China Hat. NE¼NE¼ sec. 25, T. 7 S., R. 41 E.
8	SSV78-16	Basalt, Willow Creek lava field, scarp paralleling Idaho Highway 34. NE¼SW¼ sec. 26, T. 5 S., R. 42 E.
9	SSV78-20	Basalt, scarp paralleling Idaho Highway 34. NE¼SW¼ sec. 33, T. 6 S., R. 42 E.
10	SSV78-22	Basalt, south of Broken Crater. SW¼NE¼ sec. 16, T. 7 S., R. 41 E.
11	SSV78-25	Basalt flow extending through Tenmile Pass. SE¼SW¼ sec. 3, T. 8 S., R. 40 E.
12	SSV78-29	Basalt, road cut on north side of Blackfoot River. SE¼NE¼ sec. 11, T. 5 S., R. 41 E.
13	SSV78-31	Basalt, northwest part of Sheep Island, Blackfoot Reservoir. SW¼SE¼ sec. 11, T. 6 S., R. 41 E.
14	BPV78-5	Basalt, Henry cutoff, Enoch Valley. NE¼NW¼ sec. 8, T. 6 S., R. 43 E.
15	BPV78-7	Basalt, Upper Valley. SW¼NE¼ sec. 9, T. 7 S., R. 44 E.
16	BPV78-8	Basalt, east of Lanes Creek road, Upper Valley. NE¼NE¼ sec. 31, T. 5 S., R. 44 E.
17	GV77-13	Basalt, cinder cone southwest of Grace, Gem Valley. NW¼SW¼ sec. 13, T. 10 S., R. 40 E.
18	SSV78-8	Basalt, north wall of explosion pit, east of Middle Cone. NE¼SE¼ sec. 7, T. 7 S., R. 42 E.
19	SSV78-12	Basalt, northern rim of crater above cinder pit, east flank of Reservoir Mountain. NE¼SE¼ sec. 16, T. 6 S., R. 41 E.
20	SSV78-14	Basalt, columnar jointed flow, east side of Long Valley. SW¼SW¼ sec. 24, T. 6 S., R. 42 E.
21	BPV78-10	Basalt, Enoch Valley. NE¼SW¼ sec. 8, T. 6 S., R. 43 E.
22	GV77-10	Basalt porphyry, Nelson Canyon, Bear River Range. NW¼NW¼ sec. 29, T. 9 S., R. 41 E.
23	GV77-14	Basalt porphyry, King Canyon, Bear River Range. NW¼SW¼ sec. 32, T. 9 S., R. 41 E.
24	SSV78-33	Basalt porphyry, southeast part of Cinder Island, Blackfoot Reservoir. NE¼SW¼ sec. 24, T. 6 S., R. 41 E.
25	BPV78-S1	Alkali trachyte, Slug Creek Valley. NW¼NE¼ sec. 4, T. 10 S., R. 44 E.
26	BPV78-2D	Alkali trachyte, west of Horseshoe Springs, Slug Creek Valley. SE¼SW¼ sec. 34, T. 9 S., R. 44 E.

that they were broken during emplacement. Twinning is similar to that described above for microphenocrysts, and extinction patterns indicate normal concentric zoning. There is no evidence of resorption.

The lava at the southern end of Slug Valley (samples 25 and 26) has been previously described as olivine basalt (Mansfield, 1927; Cressman, 1964), and it does have the appearance of basalt in hand specimen. In thin section, this lava is found to contain olivine and augite phenocrysts, up to 2 millimeters in diameter, in a groundmass of alkali feldspar, olivine, and augite, with minor plagioclase, exsolved iron-titanium oxides, and traces of amphibole and biotite. Petrographically, this lava is similar to a fine-grained shonkinite (Williams and others, 1954) and has tentatively been classified as alkali trachyte (Streckeisen, 1979).

Xenocrysts of sodic plagioclase and quartz occur in many of the lavas and are commonly found throughout the Blackfoot lava field. The largest

Table 2. Modal analyses of lavas from Caribou County, Idaho (volume percent).

Sample Number	Phenocrysts		Groundmass					Other
	Plagioclase	Olivine	Plagioclase	Olivine	Augite	Opaques	Undifferentiated	
Nonporphyritic Basalt								
1	2.5	0.6	25.5	10.9	--	30.3	30.2	
2	2.2	2.0	37.6	6.9	23.7	17.4	10.2	
3	3.7	3.0	51.6	7.4	23.8	6.0	4.5	
4	3.7	1.0	29.1	3.9	2.0	20.1	40.2	
5	2.7	5.7	24.3	2.8	--	--	--	glass 64.5
6	--	--	13.2	5.2	14.2	13.0	14.4	plagioclase xenocrysts 0.3; alkali feldspar 39.7
7	--	1.2	27.9	8.4	30.4	17.0	15.1	
8	0.6	3.2	33.9	9.2	11.5	12.6	25.4	plagioclase xenocrysts 3.6; quartz xenocrysts trace
9	--	2.5	38.5	7.0	27.3	13.4	11.3	
10	1.2	2.9	33.6	13.6	23.9	12.3	12.5	
11	0.8	1.9	35.6	13.9	14.7	15.1	18.0	
12	--	--	30.8	19.2	3.4	11.6	35.0	
13	0.5	2.2	50.7	19.7	19.1	7.9	--	
14	1.4	2.9	45.5	4.3	1.6	23.9	20.4	
15	2.3	2.7	41.5	6.6	6.3	23.7	17.6	
16	0.9	2.2	37.8	3.2	5.7	23.1	27.1	
Microporphyritic Basalt								
17	8.3	1.8	38.2	8.0	13.8	16.4	13.5	
18	8.9	4.0	32.2	4.6	8.8	12.9	28.1	plagioclase xenocrysts 0.3; quartz xenocrysts 0.2
19	15.2	5.9	6.5	--	--	--	71.2	plagioclase xenocrysts 0.7; opaque phenocrysts 0.5
20	10.7	7.1	33.5	8.9	15.0	13.3	11.5	
21	10.1	3.8	36.3	1.7	19.3	15.9	12.9	
Plagioclase Basalt Porphyry								
22	31.1	1.4	15.2	6.6	--	21.4	24.3	
23	32.4	2.0	7.5	4.7	--	14.0	39.4	
24	29.6	7.2	31.3	7.5	13.3	11.1	--	
Alkali Trachyte								
25	--	10.9	1.3	0.4	4.6	16.8	20.7	augite phenocrysts 6.6; sanidine 38.8
26	--	10.5	2.2	1.2	4.8	9.7	28.2	augite phenocrysts 2.4; sanidine 39.7; biotite 1.3

plagioclase xenocryst, measuring 1 by 2 by 4 centimeters, was found in the lavas of Sheep Island in the Blackfoot Reservoir. Xenocrysts are more commonly less than 5 millimeters in maximum dimension. Quartz xenocrysts tend to be rounded and have fine-grained reaction rims of augite. Plagioclase xenocrysts show resorption features such as embayments, honey-combed interiors, complex zoning, rounded to irregular outlines, and replacement by iron-titanium oxides. Xenocrysts of hypersthene, up to 3 millimeters in diameter and with compositions of En_{60} to En_{70}, have been found in lavas from Gem Valley and Upper Valley. Xenoliths of silt are present in the lavas of Gem Valley and are probably derived from the sediments of Lake Thatcher (Bright, 1963).

MINERALOGY

FELDSPARS

Plagioclase is the only feldspar within most samples of nonporphyritic and microporphyritic basalt, pillow basalt, and basalt porphyry. It coexists with alkali feldspar as groundmass in trachybasalt, and it is subordinate to alkali feldspar as groundmass in alkali trachyte. In general, zoning in plagioclase phenocrysts tends to be normal, from calcic cores to sodic rims. Groundmass plagioclase is less calcic than coexisting phenocrysts and is zoned to more sodic compositions. Representative partial analyses of plagioclase phenocrysts and groundmass are presented in Table 3; zoning trends are shown in Figure 3.

Compositions of plagioclase phenocrysts and groundmass in basaltic lavas lie between An_{80} and An_{35} with the average compositions of both within the labradorite field, An_{70} to An_{50}. Pillow basalt (sample 5) has the most calcic plagioclase phenocrysts, with core compositions near An_{80} (Figure 3b). Plagioclase is generally more calcic in nonporphyritic basalt than in microporphyritic basalt. The most extensive zoning is found in a basalt with diabasic texture from Gem Valley (Figure 3a). The large phenocrysts in the plagioclase basalt porphyry (samples 22, 23, and 24) show limited normal zoning from An_{70} to An_{60}.

Sample 8 contains numerous plagioclase xenocrysts of more sodic composition than that of the coexisting phenocrysts (Figure 3c). The phenocryst zoning trend for this sample is more sodic than that of the coexisting groundmass suggesting that the phenocryst trend may include some xenocrysts approaching equilibration with the magma. Sample 18 is unusual in that the zoning trends of the coexisting phenocrysts and groundmass do not overlap, suggesting that the phenocrysts are out of equilibrium with the magma (Figure 3i).

Samples of trachybasalt (samples 6 and 12) have average plagioclase compositions that are more sodic than those of other basaltic lavas. The plagioclase is more extensively zoned in sample 6 than in sample 12.

OLIVINE

Olivine is present as both phenocrysts and groundmass in most samples of basaltic lava and alkali trachyte. It is restricted to the groundmass in trachybasalt (samples 6 and 12). The extent of zoning in both phenocrysts and groundmass is illustrated in Figure 4; average compositions are presented in Table 4. In general, zoning in olivine is normal, from forsteritic cores to fayalitic rims. In the basaltic lavas, phenocryst zoning generally overlaps that of the groundmass, with groundmass compositions being more iron-rich. Compositions of phenocrysts range from Fo_{80} to Fo_{40}; coexisting olivines in the groundmass range in composition from Fo_{75} to Fo_{25}. Some lavas show limited compositional variation, such as the pillow lava (sample 5), reflecting rapid extrusion and cooling. In four lavas, samples 2, 9, 17, and 19, phenocryst and groundmass compositions do not overlap, suggesting that the phenocrysts were out of equilibrium with the magma. Groundmass olivine in trachybasalt is more iron-rich than that in other basaltic lavas, with compositions ranging from Fo_{48} to Fo_{30}. The olivine phenocrysts in alkali trachyte are more magnesium-rich than those of most basaltic lavas, with compositions ranging from Fo_{85} to Fo_{72}.

AUGITE

Compositions and zoning trends are illustrated in Figure 5; representative analyses are presented in Table 5. Augite is present in the groundmass of all basaltic lavas except the pillow basalt (sample 5). Zoning is more extensive and compositions more iron-rich in the microporphyritic lavas (Figure 5g) than in the nonporphyritic ones (Figure 5a-d). Compositions tend to be more calcic than the tholeiitic Skaergaard trend (Brown and Vincent, 1963), consistent with the lack of a coexisting calcium-poor pyroxene. Augite occurs as both phenocrysts and groundmass in the samples of alkali trachyte (samples 25 and 26) where it is noticeably diopsidic and zoned toward hedenbergite (Figure 5e, f). The two samples (6 and 12) of trachybasalt show distinct augite composition fields suggesting differentiation (Figure 5c).

Sample 3 is diabasic, has cooled at a relatively slow rate, and shows a strong trend toward hedenbergite (Figure 5a). Sample 16 is aphanitic and

hypocrystalline, has cooled rapidly, and shows a calcium-enrichment trend (Figure 5d). This unusual zoning of sample 16 is similar to that observed by Leeman and Vitaliano (1976) in some augites of the McKinney Basalt and by Smith and Lindsley (1971) in a flow from the Picture Gorge Basalt. Smith and Lindsley (1971) proposed that this "quench trend" of calcium-iron substitution reflects a metastable crystal-liquid partitioning during rapid crystallization.

IRON-TITANIUM OXIDES

Coexisting magnetite and ilmenite occur as groundmass phases in all lavas studied. Representative analyses are presented in Tables 6 and 7. Analyses were not made where these oxide phases were found to be exsolved, oxidized, or extremely small and disseminated. Two generations of oxides are present in sample 19. The magnetite microphenocrysts (P) are noticeably enriched in Cr_2O_3, Al_2O_3, and MgO and depleted in CaO relative to the magnetite groundmass (G). The major difference in the coexisting ilmenites is the higher MgO content and lower CaO content of the microphenocrysts. These trends are consistent with those reported by Carmichael and others (1974) for fractionating tholeiitic magmas. Magnetite within the basalt porphyry (sample 24) is noticeably enriched in Al_2O_3 and MgO, containing 3.55 percent Al_2O_3 and 2.64 percent MgO compared with a range of 1.8 to 2.4 percent Al_2O_3 and a range of 0.5 to 2.4 percent MgO in magnetites of the other basaltic lavas studied. These values of Al_2O_3 and MgO tend to straddle the typical values reported for titanomagnetites of basic

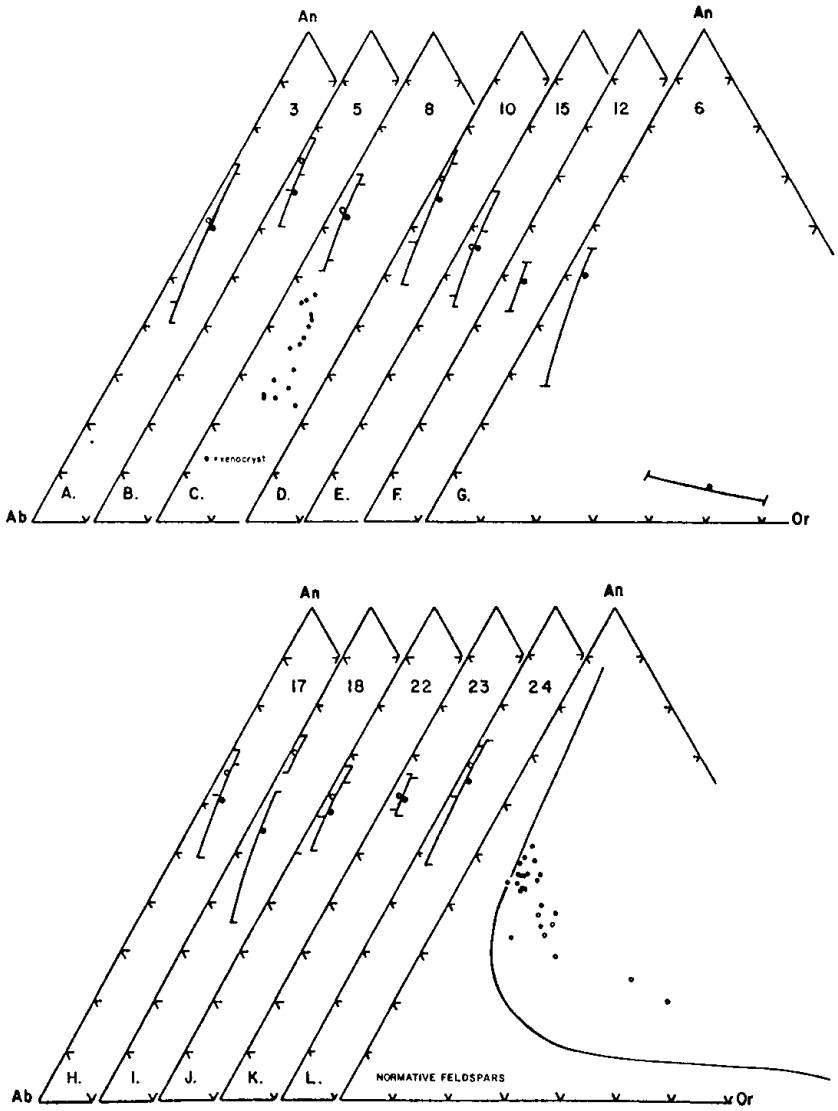

Figure 3. Zoning trends of feldspars in lavas of Caribou County, Idaho (molecular percent An, Ab, Or). Open circles indicate average phenocryst compositions; filled circles indicate average groundmass compositions. For normative feldspars, filled circles indicate olivine tholeiites; open circles indicate tholeiite, trachybasalt, and alkali trachyte. A-G = nonporphyritic basalt; H and I = microporphyritic basalt; and J-L = plagioclase basalt porphyry.

lavas with low silica activity, and tholeiitic lavas (Carmichael and others, 1974). Compositions of the magnetite-ulvospinel solid solution range from 30 to 54 molecular percent magnetite whereas compositions of the coexisting hematite-ilmenite solid solution range from 88 to 96 molecular percent ilmenite.

PETROLOGY

CHEMISTRY AND CLASSIFICATION

Chemical analyses and CIPW norms of lavas analyzed for this study are presented in Table 8. The silica contents range from 45 to 53 percent for basaltic lavas and from 53 to 56 percent for alkali trachyte. Using the normative classification of Yoder and Tilley (1962), the basaltic lavas are saturated to oversaturated with silica; they contain normative hypersthene with olivine or quartz and are classified as olivine tholeiite and tholeiite respectively. It should be noted that no calcium-poor pyroxene is present in the groundmass of any of these lavas, nor is there any evidence of olivine reaction to form a calcium-poor pyroxene.

The occurrence of normative quartz in samples 4, 22, and 24, and the low amount of normative olivine in sample 17 (less than 1.0 percent) is attributed to oxidation of iron. These four samples have $FeO/(FeO + Fe_2O_3)$ ratios ranging from 0.36 to 0.60 compared with a range of 0.73 to 0.87 for all other basaltic lavas. The high silica content and normative quartz content of sample 18 is attributed to the assimilation of pumiceous rhyolite from Middle Cone or crustal rock. Trachybasalt (samples 6 and 12) and basalt of Upper Valley (samples 15 and 16) contain normative hypersthene and quartz and are classified as tholeiitic.

The designation of most basaltic lavas as olivine

Table 3. Representative average microprobe analyses of feldspars in lavas from Caribou County, Idaho.

Sample Number	Weight Percent Oxides			Weight Percent End Members				Molecular Percent End Members		
	CaO	Na_2O	K_2O	An	Ab	Or	Total	An	Ab	Or
Nonporphyritic Basalt										
3(P)	12.98	4.02	0.34	64.4	34.0	2.0	100.4	62.9	35.2	1.9
3(G)	12.65	4.21	0.36	62.7	34.9	2.1	99.7	61.1	36.8	2.1
5(P)	15.08	2.76	0.24	74.8	23.4	1.4	99.6	74.0	24.6	1.4
5(G)	13.85	3.43	0.38	68.7	29.0	2.2	99.9	67.5	30.3	2.2
6(G-PL)	10.60	5.31	0.64	52.6	44.9	3.8	101.3	50.6	45.8	3.6
6(G-AF)	1.30	5.26	8.13	6.4	44.9	48.0	99.3	6.3	46.6	47.1
10(P)	14.18	3.29	0.20	70.3	27.8	1.2	99.3	69.6	29.2	1.2
10(G)	13.28	3.72	0.31	65.9	31.5	1.8	99.2	65.2	33.0	1.8
12(G)	12.84	3.94	0.38	63.7	33.3	2.3	99.3	49.1	47.4	3.4
15(P)	11.71	4.82	0.50	58.1	39.7	2.9	100.7	56.3	40.9	2.8
15(G)	11.65	4.67	0.60	57.8	38.8	3.5	100.1	55.9	40.7	3.4
Microporphyritic Basalt										
17(P)	13.84	3.58	0.28	68.5	30.2	1.6	100.3	67.0	31.4	1.6
17(G)	12.79	4.04	0.42	63.4	34.2	2.5	100.1	62.1	35.5	2.4
18(P)	14.35	3.19	0.22	71.2	27.0	1.3	99.5	70.4	28.3	1.3
18(G)	11.21	4.86	0.52	55.6	41.2	3.1	99.9	54.3	42.7	3.0
Plagioclase Basalt Porphyry										
22(P)	12.89	4.02	0.38	63.9	34.1	2.3	100.3	62.5	35.3	2.2
22(G)	12.39	4.26	0.37	61.5	36.1	2.2	99.8	60.3	37.6	2.1
23(P)	12.82	4.02	0.40	63.5	34.0	2.4	99.9	62.3	35.4	2.3
23(G)	12.71	4.13	0.37	63.0	34.9	2.2	100.1	61.6	36.2	2.2
24(P)	13.93	3.48	0.27	69.1	29.4	1.6	100.1	67.3	31.0	1.7
24(G)	12.35	4.42	0.37	61.3	37.4	2.2	100.9	64.5	33.7	1.8

(P) = phenocrysts
(G) = groundmass
(PL) = plagioclase
(AF) = alkali feldspar

tholeiite, using normative rather than mineralogical criteria, is consistent with other studies of lavas from the Snake River Plain, such as Tilley and Thompson (1970), Thompson (1975), Leeman and Manton (1971), and Leeman and Vitaliano (1976). Characteristics of the Snake River Plain olivine tholeiite include MgO between 6.4 and 11.2 percent and phenocryst of olivine ± plagioclase set in a groundmass of olivine, plagioclase, augite, and iron-titanium oxides (Thompson, 1975).

The association between the various volcanic rocks, and the change in normative constituents as a function of ferrous-ferric ratio, are illustrated on the normative olivine-diopside-quartz (Ol-Di-Qtz) diagram (Figure 6). The indicator ratio (I.R.) of Coombs (1963) may be calculated from normative constituents [(Hy + 2Qz)/Hy + 2(Qz + Di)] or determined from this diagram by projecting a line from the 01 apex, through the sample data point, to the Di-Qtz join. There is an apparent clustering of samples of nonporphyritic olivine tholeiite (filled circles) with I.R.'s between 0.0 and 0.3, in the field of mildly alkaline and transitional basalt. This is comparable with the I.R.'s reported for Snake River Plain basaltic lavas (Stout and Nicholls, 1977).

The differentiation index (D.I.) of Thorton and Tuttle (1960), defined as the sum of normative quartz, orthoclase, albite, nepheline, leucite, and kaliophilite, ranges from 26 to 31 for samples of nonporphyritic olivine tholeiite (Table 8). This range is also comparable with that of Snake River Plain basaltic lavas (Stout and Nicholls, 1977). Samples designated as tholeiitic have D.I.'s ranging from 36 to 44, whereas alkali trachyte samples have D.I.'s greater than 48.

The alkali-silica variation diagram has been used by Macdonald and Katsura (1964) in their study of Hawaiian lavas to distinguish alkali-olivine basalt from tholeiitic basalt. Figure 7 shows that most lavas have an alkali-olivine basalt affinity, with only three samples in or near the tholeiite field. These three samples have been discussed previously, with samples 15 and 16 being classified as tholeiitic and sample 18 containing xenocrysts of alkali feldspar and quartz.

The AFM diagram (Figure 8) indicates the relationships between the lavas of Caribou County, the Snake River Plain olivine tholeiites, and the lavas from Craters of the Moon. In general, the samples of nonporphyritic olivine tholeiite from Caribou County (filled circles) lie within or near the field of Snake River Plain olivine tholeiites. The three samples of plagioclase basalt porphyry (22, 23, and 24; open circles with horizontal bars) and two samples of tholeiite (15 and 16; filled circles with vertical bars) are more alkali-rich than the other olivine tholeiites. The alkali and iron enrichment of trachybasalt (samples 6 and 12; filled circles with horizontal bars) is also apparent, as these two samples plot close to the Craters of the Moon field.

Characteristics of the Craters of the Moon-type lavas include high TiO_2, FeO, P_2O_5, and total alkalies (Leeman and others, 1976). Samples 6 and 12 are noticeably higher in P_2O_5, total alkalies, and Fe/(Fe + Mg) than the other analyzed samples, but they contain alkali feldspar in the groundmass which has not been reported previously for basaltic lavas of the Snake River Plain, and they contain normative quartz. In addition, the groundmass of these lavas is hypocrystalline rather than glassy to opaque as reported

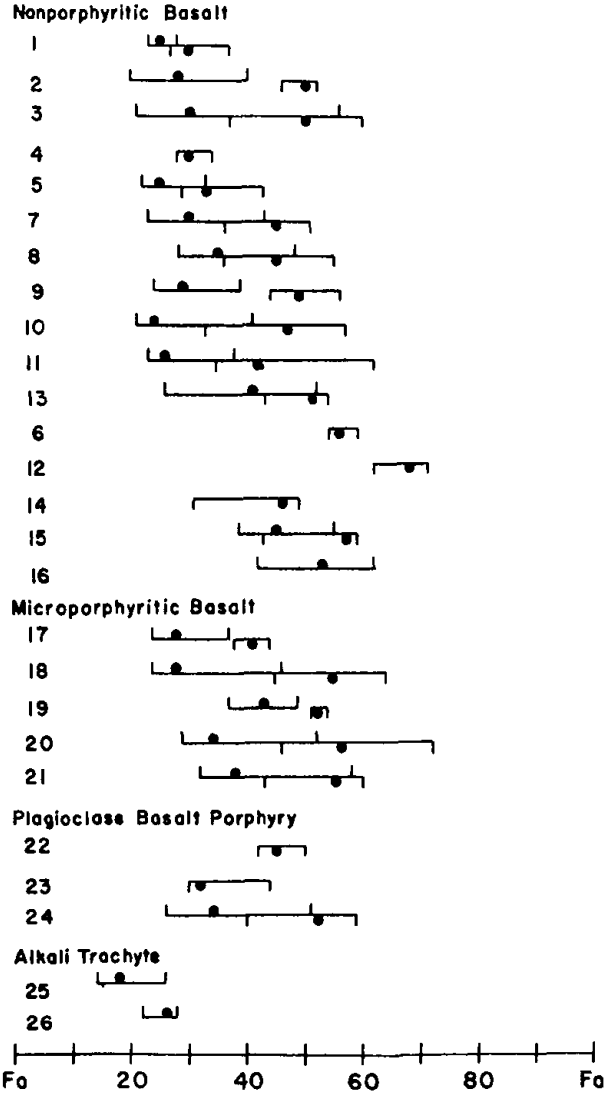

Figure 4. Zoning trends of olivines in lavas of Caribou County, Idaho (molecular percent Fo, Fa). Filled circles above horizontal bars indicate average phenocryst compositions; filled circles below horizontal bars indicate average groundmass compositions.

for the ferrobasalt of Leeman and others (1976), and the high-iron lavas of Stout and Nicholls (1977).

The two samples of alkali trachyte (25 and 26; open diamonds) lie completely away from the basaltic lavas indicating the lack of a petrogenetic relationship. The scatter of the remaining samples (18, 19, and 8; open circles) is attributed to the occurrence of quartz and alkali feldspar xenocrysts.

Similar relationships are also indicated on the iron enrichment diagram (Figure 9). There is a cluster of data points for nonporphyritic olivine tholeiite (filled circles), and a distinct separation of tholeiite (filled circles with vertical bars), trachybasalt (filled circles with horizontal bars), plagioclase basalt porphyry (open circles with horizontal bars), and alkali trachyte (open diamonds). The microporphyritic lavas (open circles) which contain xenocrysts of quartz and alkali feldspar show considerable scatter. The uniqueness of alkali trachyte is indicated as it lies well away from any iron enrichment trend of the basaltic lavas.

GEOTHERMOMETRY

Coexisting magnetite-ulvospinel and ilmenite-hematite solid solutions in sixteen samples representing tholeiitic lavas have been analyzed permitting the application of the geothermometer of Buddington and Lindsley (1964). Microprobe analyses were recalculated using the method of Carmichael (1967a), and the temperatures and fugacities were calculated using the equations derived by Powell and Powell (1977). Results of these calculations are presented in Table 9 and Figure 10. The temperatures of equilibration and corresponding oxygen fugacities plot close to the fayalite-magnetite-quartz buffer curve, indicating internal buffering of oxygen by the crystal-liquid assemblage (Carmichael and Nicholls, 1967). Temperatures range from a high of 1101° C to a low of 805° C with a corresponding range in oxygen fugacity (-log fO_2) of 8.6 to 15.0. Sample 19, containing both microphenocryst and groundmass oxides, shows a

Table 4. Representative average microprobe analyses of olivines in lavas from Caribou County, Idaho.

Sample Number	Weight Percent Oxides FeO	MgO	CaO	Weight Percent End Members Fa	Fo	La	Total	Molecular Percent End Members Fa	Fo	La
Nonporphyritic Basalt										
3(P)	27.1	35.0	0.39	38.4	61.1	0.6	100.1	30.3	69.1	0.6
3(G)	41.6	23.0	0.49	58.9	40.2	0.8	99.9	50.0	49.2	0.8
5(P)	22.3	38.6	0.42	31.6	67.4	0.7	99.7	24.3	75.1	0.6
5(G)	27.7	34.0	0.55	39.3	59.4	0.8	99.5	31.2	68.0	0.8
6(G)	45.8	19.7	0.69	65.0	34.3	1.1	100.4	56.0	42.9	1.1
10(P)	22.5	38.6	0.73	31.9	67.4	1.1	100.4	24.5	74.5	1.0
10(G)	39.0	24.7	0.87	55.3	43.1	1.3	99.7	46.4	52.3	1.3
12(G)	52.2	14.7	0.66	65.9	33.1	1.1	100.1	66.0	33.0	1.1
15(P)	37.4	26.7	0.71	53.0	46.7	1.1	100.8	43.6	55.4	1.0
15(G)	44.7	20.9	0.69	63.4	36.4	1.1	100.9	54.1	44.8	1.1
Microporphyritic Basalt										
17(P)	25.0	36.5	0.38	35.4	63.8	0.6	99.8	27.6	71.8	0.5
17(G)	36.1	27.8	0.50	51.2	48.5	0.8	100.5	41.8	57.4	0.8
18(P)	25.4	36.5	0.67	36.0	63.8	1.0	100.8	27.9	71.1	0.9
18(G)	44.8	20.1	0.71	63.6	35.0	1.1	99.7	55.0	43.9	1.1
Plagioclase Basalt Porphyry										
22(G)	39.1	25.8	0.26	55.4	45.0	0.4	100.8	45.8	53.8	0.4
23(G)	28.7	33.6	0.39	40.7	58.6	0.6	99.9	32.2	67.2	0.6
24(P)	30.4	31.8	0.78	43.1	55.5	1.2	99.8	34.5	64.4	1.1
24(G)	42.8	21.9	0.71	60.6	38.2	1.1	99.9	51.7	47.2	1.1
Alkali Trachyte										
25(P)	17.5	42.8	0.50	24.9	74.7	0.8	100.4	18.6	80.7	0.7
26(P)	22.6	38.3	0.45	32.0	66.8	0.7	99.5	24.7	74.7	0.6

(P) = phenocryst
(G) = groundmass

decrease in temperature and oxygen fugacity going from microphenocrysts to groundmass as is expected. Reported iron-titanium oxide equilibration temperatures for Snake River Plain olivine tholeiites and Craters of the Moon high-iron lavas range from 1095° C to 915° C, and corresponding oxygen fugacities (-log fO_2) range from 9.6 to 12.8 (Stout and Nicholls, 1977).

The presence of groundmass olivine and augite permits the application of a second geothermometer, that of Powell and Powell (1974). Calculated temperatures, using average olivine and augite groundmass compositions and an assumed pressure of one bar, range from 1013° C to 993° C (Table 9). The apparent poor correlation between the olivine-clinopyroxene geothermometer and the iron-titanium oxide geothermometer reflects the uncertainty of both methods (± 30°) and the use of average compositions for zoned groundmass phases. In addition, the uncertainty of the olivine-clinopyroxene geothermometer increases with increasing pressure, 5° ± 5° per kilobar (Powell and Powell, 1974).

PETROGENESIS

As previously indicated in the discussion of chemistry and classification, the analyzed lavas from Caribou County do not comprise a coherent population. To evaluate the presence of a liquid line of descent, lavas to be considered should be fine grained and nonporphyritic. An assumption is made that these lavas represent samples from an evolving magmatic system. Because of the chemical similarity in the samples of nonporphyritic olivine tholeiite collected from diverse parts of Caribou County, their low silica content, and high MgO content, these lavas most likely approximate a parental magma (Figure 11). Processes of assimilation and low-pressure fractionation can then be evaluated using whole-rock chemical analyses from Table 8, mineral analyses from Tables 3, 4, 5, 6, and 7, and the interactive computer program and procedures outlined by Stormer and Nicholls (1978). The quality of fit for each test is expressed as the sum of squares of residuals, where the residual of each component oxide is obtained by subtracting the

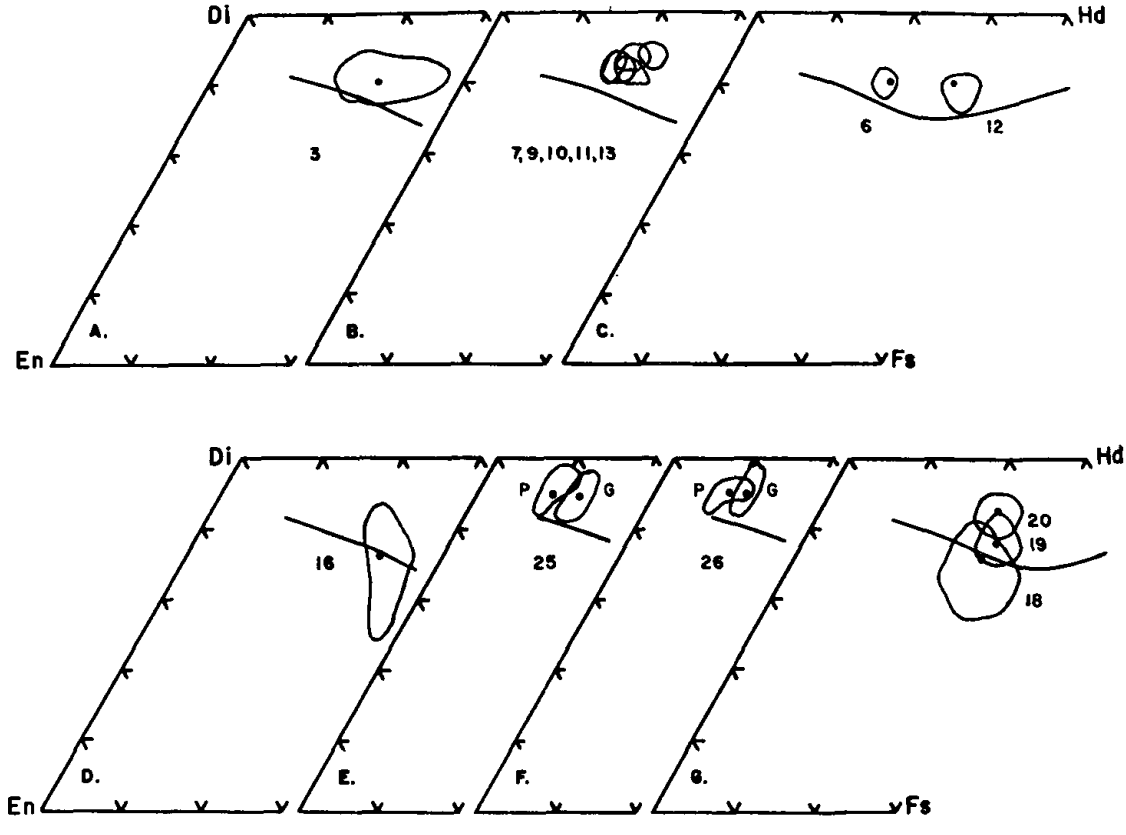

Figure 5. Zoning trends of augites in lavas of Caribou County, Idaho (molecular percent Wo, En, Fs). Irregular oval fields indicate extent of zoning within individual lavas; small filled circles indicate average compositions. Curve is zoning trend of augites from the Skaergaard intrusion (Brown and Vincent, 1963). A-D = nonporphyritic basalt; G = microporphyritic basalt; and E and F = alkali trachyte.

calculated difference between parent and daughter from the observed difference between parent and daughter. The smaller the value of the sum of squares term, the better the fit; tests with values less than one are given further consideration. Acceptability as a petrologic model depends on consistency between the calculated amounts of fractionated/assimilated phases and petrographic observations. Representative fractionation schemes are presented in Table 10.

Tholeiite and Trachybasalt

Models tested to determine the relationship between parental olivine tholeiite and daughter products, tholeiite and trachybasalt, consisted of the fractionation of olivine, plagioclase, augite, and iron-titanium oxides and the assimilation of rhyolite (unpublished analyses from W. P. Nash, University of Utah). As shown in Table 10, tholeiite, represented by sample 16, and trachybasalt, represented by sample 6, can be derived from olivine tholeiite (sample 10) by fractionating olivine, plagioclase, augite, and iron-titanium oxides. The transition from tholeiite sample 15 to tholeiite sample 16 can also be accounted for by fractionation of these same phases. The transition from trachybasalt sample 6 to trachybasalt sample 12 requires the fractionation of feldspar, olivine, augite, and ilmenite and the addition of a small amount of magnetite. Similar testing with rhyolite included as an additional phase made no significant difference in residuals or in the amounts of other phases, showing that assimilation was not a significant factor in the formation of these lavas.

Most fractionation models require the removal of all analyzed phases found within these basaltic lavas, rather than just the early formed microphenocrysts,

Table 5. Representative average microprobe analyses (weight percent) of augites in lavas from Caribou County, Idaho.

	Nonporphyritic Basalt Samples					Microporphyritic Basalt Samples		Plagioclase Basalt Porphyry Samples	Alkali Trachyte Samples			
	3	6	10	12	15	17	18	24	25(P)	25(G)	26(P)	26(G)
SiO_2	49.61	51.05	47.75	49.79	50.22	48.79	50.00	49.65	51.53	50.09	52.42	50.18
TiO_2	1.73	1.44	3.06	1.62	1.48	1.51	1.71	2.00	0.90	1.12	0.82	1.47
Al_2O_3	2.70	2.44	4.21	2.22	2.64	2.88	3.34	3.18	3.36	3.74	2.74	4.27
FeO	12.58	12.94	11.85	16.90	13.76	11.29	14.04	11.92	6.12	7.95	5.95	7.16
MnO	0.27	0.45	0.28	0.56	0.38	0.30	0.37	0.32	0.16	0.19	0.14	0.17
MgO	13.67	13.37	12.41	10.41	13.90	14.03	14.61	13.12	16.88	15.04	16.76	15.73
CaO	20.03	19.36	20.43	18.81	17.59	20.16	17.57	20.28	22.19	21.14	22.37	21.65
Na_2O	0.39	0.39	0.47	0.34	0.36	0.40	0.33	0.41	0.28	0.41	0.27	0.33
Total	100.98	101.44	100.46	100.65	100.34	99.36	101.97	100.88	100.42	99.68	101.47	100.96
Number of ions on the basis of 6 oxygens												
Si_{IV}	1.865	1.904	1.807	1.908	1.893	1.858	1.858	1.864	1.875	1.871	1.902	1.845
Al_{IV}	0.120	0.096	0.188	0.092	0.107	0.130	0.142	0.136	0.125	0.129	0.098	0.155
Ti_{VI}	0.015	--	0.005	--	--	0.012	--	--	--	--	--	--
Al_{VI}	--	0.012	--	0.009	0.011	--	0.004	0.004	0.019	0.036	0.020	0.030
Ti	0.034	0.040	0.082	0.047	0.042	0.031	0.048	0.056	0.025	0.129	0.022	0.041
Fe^{+2}	0.396	0.404	0.375	0.542	0.435	0.360	0.436	0.374	0.186	0.248	0.181	0.220
Mn	0.009	0.014	0.009	0.018	0.012	0.010	0.012	0.010	0.005	0.006	0.004	0.005
Mg	0.766	0.743	0.700	0.595	0.781	0.796	0.809	0.734	0.917	0.835	0.909	0.860
Ca	0.807	0.774	0.828	0.772	0.711	0.823	0.700	0.816	0.866	0.844	0.871	0.854
Na	0.028	0.028	0.035	0.025	0.026	0.030	0.024	0.030	0.020	0.030	0.019	0.024
Molecular Percent												
Fe	20.1	21.2	19.7	28.6	22.0	17.6	22.8	19.2	9.5	12.8	9.2	11.3
Mg	38.7	38.3	36.3	30.9	39.5	42.1	41.9	37.3	46.0	42.8	46.1	44.1
Ca	41.2	40.5	44.0	40.5	38.5	40.3	35.3	43.1	44.5	44.4	44.7	44.6

(P) = phenocryst
(G) = groundmass

Table 6. Representative average microprobe analyses (weight percent) of magnetites in lavas from Caribou County, Idaho.

	Nonporphyritic Basalt Samples								Microporphyritic Basalt Samples			
	1	2	6	7	10	13	15	16	18	19(P)	19(G)	21
SiO_2	0.51	0.37	1.02	1.01	0.75	1.18	1.42	1.63	1.44	1.41	1.46	1.35
TiO_2	23.28	18.50	18.41	22.26	21.81	15.31	22.63	22.58	19.68	17.08	16.72	23.99
Al_2O_3	2.19	1.92	1.89	1.94	1.97	2.48	1.78	2.09	2.01	2.40	1.68	2.30
V_2O_3	0.78	1.18	0.59	0.87	1.00	1.34	1.06	0.74	0.98	1.07	1.09	1.25
Cr_2O_3	0.29	0.25	--	0.69	0.44	0.55	0.37	0.23	0.16	2.56	0.08	0.30
FeO	68.28	72.82	73.62	67.29	68.58	73.99	66.34	66.79	72.62	71.39	73.05	67.42
MnO	0.59	0.42	0.58	0.49	0.50	0.39	0.65	0.63	0.45	0.44	0.32	0.64
NiO	--	--	--	<0.03	--	<0.02	0.13	0.12	--	<0.03	--	0.08
MgO	1.75	1.61	1.23	2.38	2.17	1.48	1.80	1.70	0.43	1.68	0.81	1.55
CaO	0.41	0.23	0.38	0.53	0.34	0.49	0.30	0.34	0.48	0.36	0.55	0.40
ZnO	<0.02	<0.03	0.12	0.13	<0.03	0.16	1.11	1.08	0.17	0.15	0.16	1.10
Sum	98.09	97.36	97.85	97.62	97.61	97.41	97.58	97.92	98.40	98.57	95.91	100.38
Fe_2O_3	20.30	29.81	29.51	20.96	22.47	33.19	19.01	18.91	25.07	28.11	29.90	17.53
FeO	50.02	45.99	47.07	48.43	48.36	44.12	49.23	49.78	50.09	46.09	46.15	51.65
Total	100.13	100.32	100.80	99.72	99.85	100.72	99.49	99.82	100.96	101.39	98.92	102.14
Molecular fractions												
Mt	0.342	0.475	0.456	0.352	0.373	0.537	0.322	0.319	0.405	0.485	0.475	0.306
Usp	0.658	0.525	0.544	0.648	0.627	0.463	0.678	0.681	0.595	0.515	0.525	0.694

(P) = phenocryst
(G) = groundmass

Table 7. Representative average microprobe analyses (weight percent) of ilmenites in lavas from Caribou County, Idaho.

	Nonporphyritic Basalt Samples								Microporphyritic Basalt Samples			
	1	2	6	7	10	13	15	16	18	19(P)	19(G)	21
SiO_2	1.30	0.37	1.03	0.99	1.08	1.15	1.49	1.66	1.48	1.27	1.55	1.32
TiO_2	45.30	48.60	49.33	48.70	48.63	49.79	48.67	47.94	48.10	49.26	49.24	49.11
Al_2O_3	1.49	0.31	0.42	0.42	0.36	0.40	0.49	0.66	0.43	0.36	0.41	0.49
V_2O_3	0.13	0.33	0.13	0.32	0.22	0.25	0.60	0.44	0.41	0.15	0.25	0.55
Cr_2O_3	<0.02	0.11	--	<0.03	--	<0.05	0.11	0.10	--	0.30	--	0.10
FeO	47.31	46.30	47.04	45.22	45.62	46.67	45.02	45.29	48.35	45.44	45.42	46.42
MnO	0.65	0.54	0.70	0.52	0.58	0.52	0.66	0.67	0.55	0.47	0.52	0.68
NiO	--	--	--	--	--	<0.02	<0.04	<0.05	--	--	--	<0.05
MgO	1.36	2.83	2.01	2.80	2.42	2.51	1.94	1.61	0.72	2.77	1.56	1.64
CaO	0.63	0.35	0.38	0.70	0.56	0.61	0.40	0.50	0.57	0.33	0.65	0.66
ZnO	0.35	0.27	--	0.06	0.09	<0.05	0.86	0.90	0.09	0.10	0.06	0.92
Sum	98.55	100.00	101.05	99.76	99.57	102.02	100.28	99.83	100.71	100.47	99.66	101.95
Fe_2O_3	10.24	9.36	6.92	7.47	7.01	7.07	5.45	5.81	6.64	6.17	3.87	6.66
FeO	38.09	37.88	40.81	38.50	39.32	40.30	40.11	40.06	42.37	39.89	41.94	40.42
Total	99.57	100.94	101.73	100.52	100.27	102.73	100.83	100.40	101.37	101.07	100.05	102.61
Molecular fractions												
Ilm	0.881	0.905	0.929	0.922	0.928	0.927	0.935	0.931	0.928	0.934	0.955	0.926
Hm	0.119	0.095	0.071	0.078	0.072	0.073	0.065	0.069	0.072	0.066	0.045	0.074

(P) = phenocryst
(G) = groundmass

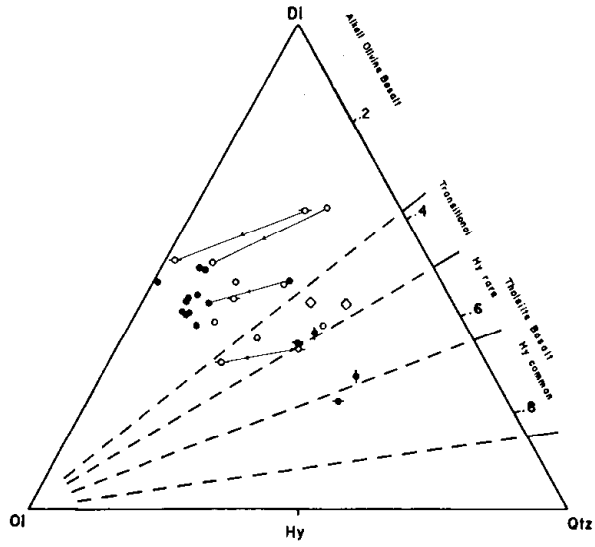

Figure 6. Normative olivine-diopside-quartz (Ol-Di-Qtz) diagram for lavas of Caribou County, Idaho. Symbols used: filled circles—nonporphyritic basalt; open circles—microporphyritic basalt; open circles with horizontal bars—plagioclase basalt porphyry; filled circles with vertical bars—tholeiite; filled circles with horizontal bars—trachybasalt; open diamonds—alkali trachyte; lines with arrows indicate changes in normative constituents with increase in ferrous-ferric ratio. Indicator ratio of Coombs (1963) is shown on the Di-Qtz join.

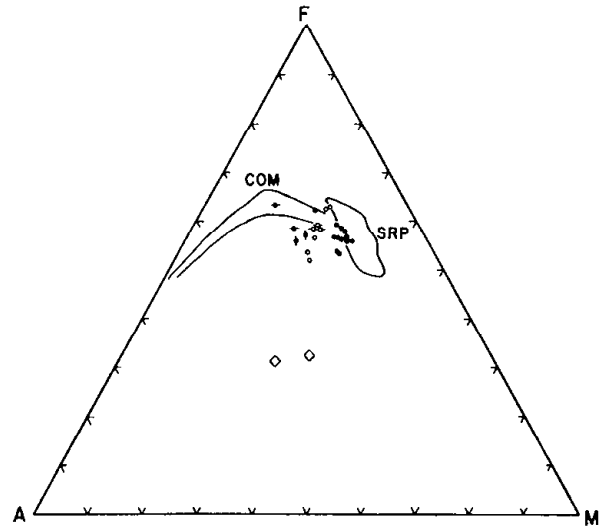

Figure 8. AFM diagram for lavas of Caribou County, Idaho. A = weight percent $K_2O + Na_2O$; F = weight percent $FeO + Fe_2O_3$; M = weight percent MgO. Symbols used: filled circles—nonporphyritic basalt; open circles—microporphyritic basalt; filled circles with vertical bars—tholeiite; filled circles with horizontal bars—trachybasalt; open circles with horizontal bars—plagioclase basalt porphyry; open diamonds—alkali trachyte. SRP indicates distribution of Snake River Plain olivine tholeiites and COM indicates distribution of Craters of the Moon lavas (Leeman and others, 1976).

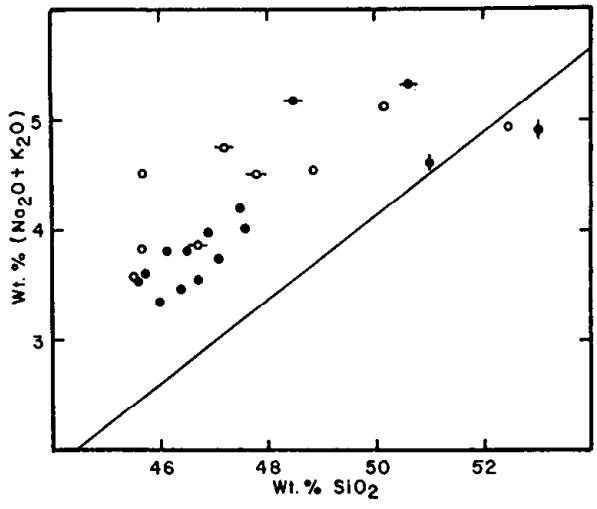

Figure 7. Alkali-silica diagram for lavas of Caribou County, Idaho. Symbols used: filled circles—nonporphyritic basalt: open circles—microporphyritic basalt; filled circles with vertical bars—tholeiite; filled circles with horizontal bars—trachybasalt; open circles with horizontal bars—plagioclase basalt porphyry. Diagonal line is alkali olivine basalt-tholeiite boundary of Macdonald and Katsura (1964).

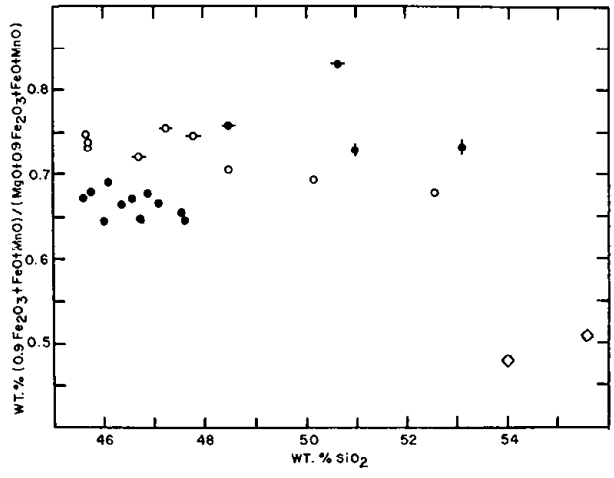

Figure 9. Iron enrichment diagram for lavas of Caribou County, Idaho. Symbols used: filled circles—nonporphyritic basalt; open circles—microporphyritic basalt; filled circles with vertical bars—tholeiite; filled circles with horizontal bars—trachybasalt; open circles with horizontal bars—plagioclase basalt porphyry; open diamonds—alkali trachyte.

olivine with magnetite, and plagioclase, as observed in thin section. As mentioned previously, augite does not occur as distinctive phenocrysts, but rather as an ophitic to subophitic groundmass phase. This suggests that a process such as filter pressing may have been in operation, rather than gravity settling or flowage differentiation. This process would drive off interstitial liquid, leaving a crystal mush of microphenocrysts and groundmass crystallization products.

When deriving the tholeiite and trachybasalt, estimated amounts of fractionated crystals range from 40 to 60 percent; that is, 40 to 60 percent of the parent magma would have crystallized at the time of separation of the daughter lavas. This is not unlike the 65 to 70 percent crystallization required to derive the iron-rich Craters of the Moon lavas of Stout and Nicholls (1977).

The fractionation of olivine and plagioclase, the microphenocrysts commonly found in olivine tholeiite, has been proposed by Leeman and Vitaliano

Table 8. Whole-rock chemical analyses (weight percent) and CIPW norms of lavas from Caribou County, Idaho.

	Nonporphyritic Basalt Samples															
	1	2	3	4	5	6	7	8	9	10	11	12	13	14	15	16
SiO_2	46.87	47.53	47.08	45.63	47.60	48.47	46.72	50.15	45.75	46.01	46.55	50.62	45.59	46.35	50.96	53.07
TiO_2	3.07	2.47	2.83	3.97	2.35	3.20	2.80	2.34	3.23	2.82	2.85	2.52	3.16	2.68	2.56	2.23
Al_2O_3	14.85	15.43	14.80	13.15	15.62	14.71	15.08	16.08	14.42	14.78	15.26	13.55	14.34	14.86	14.58	14.53
Fe_2O_3	2.34	1.68	2.65	10.38	1.52	2.94	1.74	2.24	2.98	2.56	1.91	2.75	2.56	2.48	2.20	2.43
FeO	11.56	11.03	10.74	5.76	10.56	10.11	11.48	9.37	11.87	10.90	11.50	11.26	11.91	10.93	10.14	8.43
MnO	0.22	0.22	0.19	0.24	0.18	0.21	0.19	0.19	0.22	0.21	0.21	0.24	0.23	0.15	0.25	0.15
MgO	6.58	6.69	6.65	5.22	6.60	4.14	7.18	5.13	6.96	7.38	6.54	2.85	7.03	6.71	4.62	4.13
CaO	9.29	9.78	9.95	8.93	9.68	7.96	9.67	8.10	9.77	10.15	9.62	7.10	9.57	10.35	8.12	7.22
Na_2O	2.89	2.92	2.93	3.12	2.62	3.11	2.48	2.96	2.68	2.51	2.72	2.93	2.66	2.62	2.87	2.82
K_2O	1.09	1.25	0.80	1.37	1.38	2.08	1.06	2.18	0.93	0.84	1.08	2.41	0.87	0.83	1.72	2.08
P_2O_5	0.79	0.57	0.56	1.17	0.52	1.32	0.69	0.60	0.81	0.65	0.72	1.67	0.81	0.53	0.64	0.69
H_2O+	0.46	0.26	0.70	0.62	0.64	0.51	0.56	0.43	0.14	0.32	0.34	0.96	0.19	0.78	0.94	0.55
H_2O-	0.09	0.04	0.00	0.11	0.05	0.29	0.18	0.11	0.13	0.19	0.14	0.28	0.11	0.18	0.34	0.49
Total	100.10	99.87	99.80	99.67	99.32	99.05	99.83	99.88	99.89	99.32	99.44	99.14	99.03	99.45	99.94	99.32
Q	--	--	--	2.69	--	0.13	--	--	--	--	--	4.56	--	--	2.35	6.28
or	6.44	7.39	4.73	8.10	8.15	12.29	6.26	12.88	5.50	4.96	6.38	14.24	5.14	4.90	10.16	12.29
pl	48.78	50.01	49.66	44.23	48.96	46.35	47.87	49.20	47.25	47.82	49.26	41.50	47.13	48.51	46.11	44.71
(ab)	24.45	24.71	24.79	26.40	22.17	26.32	20.98	25.05	22.68	21.24	23.02	24.79	22.51	22.17	24.28	23.86
(an)	24.33	25.30	24.87	17.83	26.79	20.04	26.89	24.15	24.57	26.58	26.24	16.70	24.62	26.34	21.82	20.85
di	13.68	16.08	17.09	14.64	14.70	8.99	13.65	10.00	15.30	16.00	13.85	6.45	14.46	17.72	11.87	8.68
(wo)	6.93	8.14	8.69	7.86	7.45	4.52	6.92	5.06	7.77	8.15	7.01	3.18	7.33	9.00	5.96	4.37
(en)	3.57	4.15	4.67	6.79	3.84	2.14	3.62	2.56	4.11	4.50	3.54	1.07	3.84	4.77	2.77	2.08
(fs)	3.18	3.79	3.73	--	3.41	2.33	3.11	2.38	3.42	3.34	3.31	2.21	3.28	3.96	3.14	2.22
hy	6.64	0.26	5.69	6.21	5.60	17.09	9.02	14.01	5.59	6.63	5.60	18.51	6.81	5.30	18.64	16.96
(en)	3.51	0.14	3.16	6.21	2.96	8.17	4.85	7.27	3.05	3.80	2.89	6.03	3.67	2.90	8.74	8.20
(fs)	3.13	0.12	2.53	--	2.63	8.91	4.17	6.74	2.54	2.82	2.70	12.48	3.14	2.41	9.90	8.76
ol	12.95	17.39	11.50	--	13.35	--	12.85	4.17	13.66	12.83	14.02	--	13.60	12.14	--	--
(fo)	6.52	8.67	6.12	--	6.75	--	6.60	2.06	7.13	7.06	6.91	--	7.00	6.34	--	--
(fa)	6.42	8.72	5.38	--	6.60	--	6.25	2.11	6.53	5.77	7.11	--	6.60	5.80	--	--
mt	3.39	2.44	3.83	7.87	2.20	4.26	2.52	3.25	4.32	3.71	2.77	3.99	3.71	3.60	3.19	3.52
il	5.83	4.69	5.37	7.53	4.46	6.08	5.32	4.44	6.13	5.36	5.41	4.79	6.00	5.09	4.86	4.24
ap	1.87	1.35	1.34	2.78	1.23	3.13	1.63	1.42	1.92	1.54	1.71	3.96	1.92	1.26	1.52	1.63
Total	99.59	99.60	99.21	99.00*	98.66	98.32	99.12	99.37	99.66	98.84	99.00	97.99	98.77	98.52	98.69	98.31
Salic	55.22	57.40	54.39	55.02	57.11	58.78	54.13	62.08	52.74	52.78	55.64	60.29	52.27	53.41	58.62	63.28
Femic	44.37	42.20	44.82	43.98	41.55	39.54	44.99	37.29	46.92	46.06	43.36	37.69	46.50	45.11	40.08	35.03
D.I.	30.90	32.09	29.52	37.19	30.32	38.74	27.25	37.93	28.17	26.20	29.40	43.59	27.65	27.07	36.80	42.43

*Total includes 4.95 percent normative hematite

(1976) to account for the variation in composition of the McKinney Basalt, and also by Tilley and Thompson (1970) to account for the variation in their suite of Snake River Plain lavas. Similarly, olivine and plagioclase fractionation can account for the variation within the samples of olivine tholeiite from Caribou County. But there is still the possibility that the slight scatter of data for olivine tholeiite may result from the presence of more than one liquid line of descent or the presence of more than one parental magma. Age relationships have not been sufficiently established to conclude that all samples of olivine tholeiite in Caribou County are contemporaneous, and magnetic data discussed previously certainly indicates otherwise.

Contaminated Lavas

The presence of numerous xenocrysts of quartz and feldspar, possibly derived from the incorporation of rhyolite, together with differentiation, may account for the compositional variation among lava samples

Table 8. continued.

	Microporphyritic Basalt Samples					Plagioclase Basalt Porphyry Samples			Alkali Trachyte Samples	
	17	18	19	20	21	22	23	24	25	26
SiO_2	46.09	52.53	48.86	45.68	45.69	47.21	47.77	46.69	53.99	55.56
TiO_2	3.12	2.23	2.53	3.64	3.42	2.87	2.78	2.64	1.26	1.19
Al_2O_3	14.49	14.64	15.17	14.71	14.28	17.67	17.89	18.08	14.60	14.61
Fe_2O_3	6.18	2.24	3.37	2.73	2.81	6.01	3.15	4.90	3.08	3.49
FeO	8.57	8.49	9.25	12.82	12.14	6.00	8.72	7.52	3.48	2.55
MnO	0.23	0.16	0.19	0.20	0.31	0.20	0.19	0.18	0.19	0.10
MgO	6.41	5.07	5.24	5.53	5.46	3.77	4.00	4.71	7.01	5.57
CaO	9.53	7.82	9.12	9.04	10.06	9.79	9.56	10.07	7.20	6.41
Na_2O	2.79	3.00	2.84	2.55	2.57	3.37	3.32	2.83	2.48	2.26
K_2O	0.98	1.92	1.70	1.29	0.99	1.38	1.17	1.06	4.35	5.54
P_2O_5	0.91	0.46	0.71	0.75	0.96	0.92	0.79	1.14	0.71	0.84
H_2O+	0.42	0.24	0.32	0.26	0.92	0.36	0.27	0.10	0.93	0.85
H_2O-	0.03	0.13	0.08	0.15	0.25	0.06	0.15	0.19	0.18	0.32
Total	99.75	98.93	99.38	99.35	99.86	99.61	99.76	100.11	99.46	99.29
Q	–	3.23	–	–	–	0.48	–	0.12	1.36	4.09
or	5.79	11.35	10.05	7.62	6.10	8.15	6.91	6.26	25.71	33.38
pl	47.73	46.20	47.66	46.46	49.54	57.53	58.55	57.45	36.84	34.33
(ab)	23.61	25.38	24.03	21.58	24.05	28.52	28.09	23.95	20.98	20.70
(an)	24.12	20.81	23.63	24.88	25.54	29.01	30.46	33.50	15.86	13.63
di	13.83	12.31	13.94	12.52	15.95	10.73	9.74	7.29	11.99	10.57
(wo)	7.19	6.25	7.09	6.29	7.98	5.66	4.93	3.76	6.36	5.29
(en)	4.85	3.33	3.82	2.92	4.35	4.30	2.51	2.37	5.03	5.28
(fs)	1.79	2.73	3.04	3.31	3.63	0.77	2.31	1.16	0.61	0.01
hy	14.26	16.92	14.42	9.94	10.45	6.00	7.27	13.94	13.94	10.42
(en)	10.41	9.30	8.03	4.65	5.70	5.09	3.79	9.36	12.43	10.41
(fs)	3.85	7.63	6.39	5.29	4.75	0.91	3.49	4.58	1.51	0.01
ol	0.70	–	1.58	9.79	7.79	–	5.18	–	–	–
(fo)	0.50	–	0.84	4.35	3.44	–	2.57	–	–	–
(fa)	0.20	–	0.74	5.44	4.15	–	2.61	–	–	–
mt	8.96	3.25	4.89	3.96	4.07	8.71	4.57	7.10	4.47	5.06
il	5.93	4.24	4.81	6.91	6.50	5.45	5.28	5.01	2.39	2.26
ap	2.16	1.09	1.68	1.78	2.27	2.18	1.87	2.70	1.68	1.99
Total	99.35	98.58	99.02	98.98	98.74	99.24	99.38	99.88	98.39	98.16
Salic	53.52	60.77	57.70	54.08	52.10	66.16	65.46	63.83	63.91	69.55
Femic	45.83	37.81	41.31	44.90	46.64	33.07	33.92	36.05	34.47	28.61
D.I.	29.40	39.96	34.08	29.20	27.60	37.15	35.01	30.33	48.05	56.19

18, 19, and 8. Sample 18, for example, can be accounted for by adding approximately 25 percent rhyolite to parental olivine tholeiite (sample 7). Sample 19 can be derived by fractionating a small amount of olivine and magnetite from olivine tholeiite (sample 9) and adding approximately 9 percent rhyolite (Table 10). Sample 8, in turn, can be derived by fractionating olivine, augite, plagioclase, and iron-titanium oxides and adding less than 5 percent rhyolite (Table 10).

Sample 18, however, is the only lava close to rhyolite, but the assimilation of 25 percent rhyolite in the near-surface environment leaving less than 1 percent xenocrysts is probably unrealistic. Alternatively, the incorporation of quartzofeldspathic crustal rocks at depth would have to be considered for all three samples, but this process cannot be evaluated at this time.

Plagioclase Basalt Porphyry

The texture of plagioclase basalt porphyry, represented by samples 22, 23, and 24, indicates the accumulation of plagioclase phenocrysts. Using olivine tholeiite (sample 9) as the parent, plagioclase basalt porphyry (sample 24) can be derived by fractionating olivine, augite, and less than 1 percent iron-titanium oxides and adding 15 percent plagioclase (Table 10). The accumulation of plagioclase in the plagioclase basalt porphyry may result from processes such as flowage differentiation, bubble transport, or the buoyancy of plagioclase in a more dense magma. Both olivine and plagioclase occur as dominant phenocrysts in microporphyritic lavas in the region, but only plagioclase is selectively concentrated in these rocks suggesting that bubble transport or density contrast may be significant. Densities of olivine tholeiite were calculated over a range of temperature from 1000° C to 1200° C using the procedure of Bottinga and Weill (1970). Densities of plagioclase over this same temperature interval were determined for compositions An_{60} and An_{70} using data presented in Campbell and others (1978). This range in composition encompasses that of the average plagioclase in the three analyzed samples of plagioclase basalt porphyry. Calculations for anhydrous conditions yield liquid densities consistently greater than that of plagioclase. For calculations with water contents greater than 1 molecular percent, the density contrast is reversed, with the density of the magma being less than that of plagioclase (Table 11). For density contrast to have been effective in producing the plagioclase basalt porphyry, a low water content must be assumed for the differentiating magma. This is consistent with the lack of resorption features within the plagioclase phenocrysts.

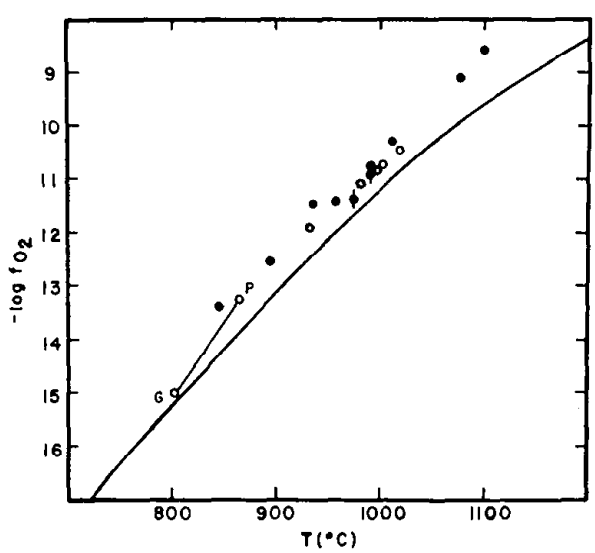

Figure 10. Temperatures of iron-titanium oxide equilibration for lavas of Caribou County, Idaho. Symbols used: filled circles—nonporphyritic basalt; open circles—microporphyritic basalt; filled circles with vertical bars—tholeiite; P—phenocryst; G—groundmass. Curve indicates fayalite-magnetite-quartz buffer.

Table 9. Temperatures of equilibration for lavas from Caribou County, Idaho.

Sample Number	Magnetite-Ilmenite -log fO_2	Magnetite-Ilmenite Temperature (°C)	Olivine-Clinopyroxene Temperature (°C)
Nonporphyritic Basalt			
1	8.56	1101	--
2	11.38	936	1002
6	12.57	894	993
7	10.76	992	1008
8	10.81	999	1006
9	11.12	981	1001
10	11.42	959	1008
11	9.09	1076	1013
13	13.40	846	999
14	10.24	1009	1001
15	11.27	977	996
16	10.91	994	1003
Microporphyritic Basalt			
18	11.88	932	998
19(P)	13.25	863	--
19(G)	15.02	805	1004
20	10.77	1004	1000
21	10.37	1021	1001

(P) = phenocryst
(G) = groundmass

Table 10. Representative fractionation schemes for derivation of lavas from Caribou County, Idaho.

Parent	Daughter	Phases (+ = percentage added to parent; - = percentage subtracted from parent)			Sum of Squares
Olivine Tholeiite Sample 10	Tholeiite Sample 16	-24.8 $An_{70}Ab_{29}Or_1$ -6.5 $Mt_{37}Usp_{63}$	-8.6 $Fo_{75}Fa_{25}$ -0.1 $Il_{93}Hm_7$	-17.8 $Wo_{44}En_{36}Fs_{20}$	0.4256
Olivine Tholeiite Sample 10	Trachybasalt Sample 6	-18.7 $An_{70}Ab_{29}Or_1$ -3.6 $Mt_{37}Usp_{63}$	-7.9 $Fo_{75}Fa_{25}$ -0.3 $Il_{93}Hm_7$	-15.3 $Wo_{44}En_{36}Fs_{20}$	0.1667
Olivine Tholeiite Sample 10	Olivine Tholeiite Sample 9	-7.5 $An_{70}Ab_{29}Or_1$	-2.5 $Fo_{75}Fa_{25}$		0.9224
Olivine Tholeiite Sample 9	Contaminated Lavas Sample 19	+8.9 rhyolite	-4.1 $Fo_{71}Fa_{29}$	-1.2 Mt_{33} Usp_{67}	0.4847
Sample 9	Sample 8	-7.5 $An_{69}Ab_{30}Or_1$ -5.3 $Mt_{33}Usp_{67}$	-3.5 $Fo_{71}Fa_{29}$ +0.1 $Il_{93}Hm_7$	-12.9 $Wo_{43}En_{39}Fs_{18}$ +4.9 rhyolite	0.5082
Olivine Tholeiite Sample 9	Plagioclase Basalt Porphyry Sample 24	+15.7 $An_{59}Ab_{30}Or_1$ -0.4 $Mt_{33}Usp_{67}$	-3.0 $Fo_{71}Fa_{29}$ -0.3 $Il_{93}Hm_7$	-6.6 $Wo_{43}En_{39}Fs_{18}$	0.2621

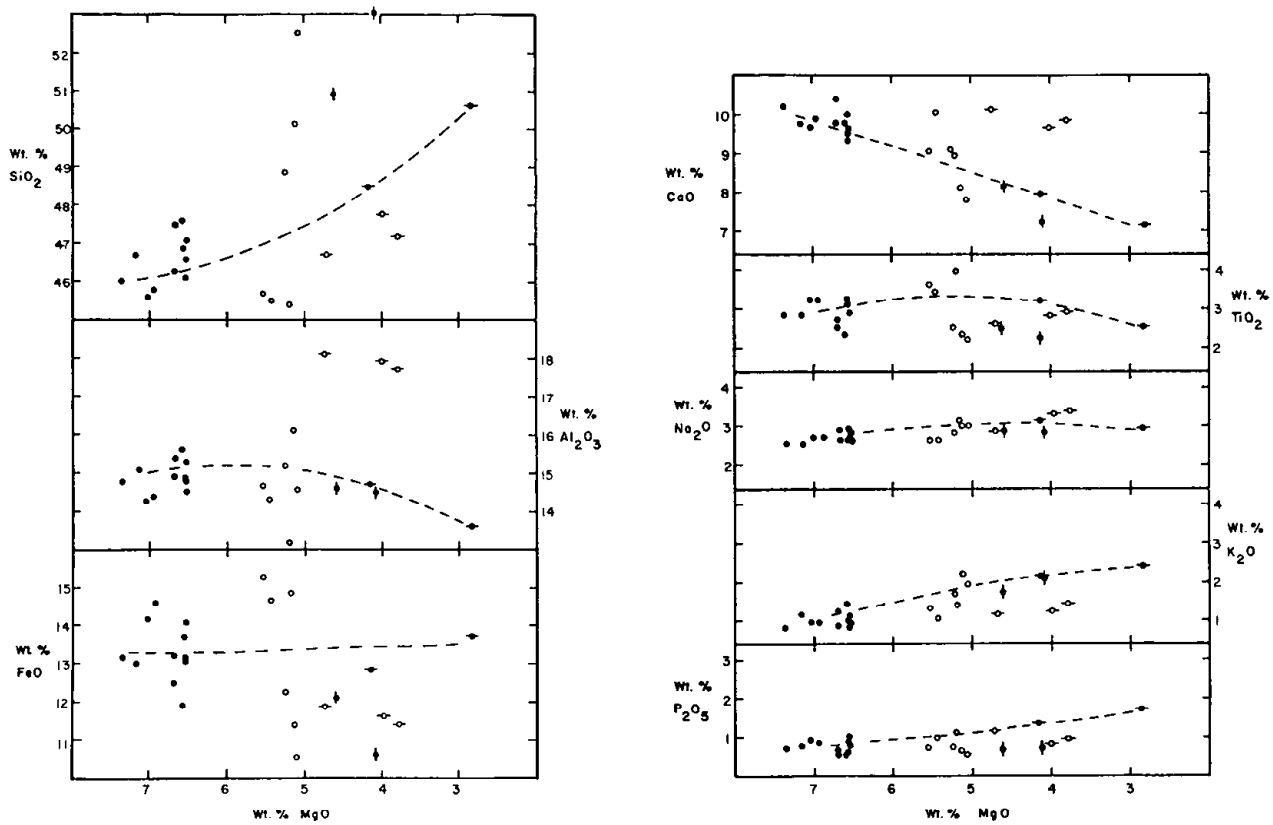

Figure 11. MgO variation diagram for lavas of Caribou County, Idaho. Symbols used: filled circles—nonporphyritic basalt; open circles—microporphyritic basalt; filled circles with vertical bars—tholeiite; filled circles with horizontal bars—trachybasalt; open circles with horizontal bars—plagioclase basalt porphyry.

Table 11. Densities (gm/cc) of olivine tholeiite and coexisting plagioclase.

Temperature (°C)	Wet*	Range for An_{60} to An_{70}	Dry
1000	2.66	2.68 - 2.70	2.76
1100	2.62	2.66 - 2.69	2.73
1200	2.59	2.65 - 2.69	2.70

* >1.5 molecular percent H_2O

Alkali Trachyte

The high MgO, silica, and alkali content, and low total iron content of the samples (25 and 26) of alkali trachyte from Slug Valley preclude the derivation of this lava from olivine tholeiite. Comparing these samples with other potassium-rich alkaline rocks, they are most similar to orenditic rocks, saturated rocks with K_2O in excess over Na_2O (Sahama, 1974). The lavas from Slug Valley are quartz normative with a K_2O:Na_2O ratio of approximately 2:1; but they are noticeably less potassic than the "average" orendites of Sahama (1974), and they contain magnetite which is uncommon in rocks of orenditic affinity (Carmichael, 1967b). Orenditic rocks are rare and occur in a few restricted areas, such as the Leucite Hills in Wyoming, the Fitzroy Basin of Western Australia, and southeastern Spain, where they are confined to volcanic or subvolcanic environments and lack plutonic counterparts (Sahama, 1974).

Carmichael (1967b) considered the orenditic lavas to be of mantle origin, and Prider (1960) proposed the derivation of the Fitzroy Basin rocks to be from a mica peridotite magma. In a recent review of hypotheses for the origin of highly potassic magmas, Gupta and Yagi (1980) concluded that the origin is related to partial melting of a phlogopite peridotite-bearing upper mantle.

If a similar origin is to be assumed for the Slug Valley lavas, the amount of partial melting can be determined using an addition-subtraction diagram (Bowen, 1928). To represent the mantle composition, mica peridotite analyses from Best and others (1968) were used. These peridotites are part of an association of highly potassic, silica-poor igneous rocks located east of Salt Lake City, Utah, at the western end of the east-west trending Uinta Arch. The related volcanic rocks are reported to be similar to those of the Leucite Hills (150 miles northeast of the Utah locality) and range in age from upper Eocene to lower Pliocene (Best and others, 1968). Partial melting on the order of 30 to 35 percent is required to derive the Slug Valley lavas from this mica peridotite.

Olivine Tholeiite

The origin of olivine tholeiite, considered to be the parental magma from which tholeiite, trachybasalt, and plagioclase basalt porphyry have been derived, must now be evaluated. Considering the studies of Snake River Plain olivine tholeiite, Stout and Nicholls (1977) proposed partial melting of a pyrolite mantle; Leeman and Vitaliano (1976) and Leeman (1976) proposed partial melting of a spinel-peridotite mantle, or derivation from a deeper source and equilibration with a spinel-peridotite mantle; and Thompson (1975) proposed partial melting of a relatively iron-rich spinel-lherzolite upper mantle. Thus, the percentages of partial melting were calculated, using the pyrolite of Green and Ringwood (1967) and a spinel lherzolite analysis from Bacon and Carmichael (1973) as hypothetical mantle compositions (Table 12). For a pyrolite mantle, approximately 10 percent partial melting is required, whereas for a spinel lherzolite mantle, less than 2 percent melting is required. The amount of partial melting required before liquid will separate from the mantle depends on such variables as water content in the mantle and conduit geometry. As the percentages of partial melting for the pyrolite mantle are greater than that for a lherzolite mantle, the segregation of a larger volume of melt should occur more readily. As demonstrated by Stout and Nicholls (1977), the residual material derived from partial melting of pyrolite has a composition similar to spinel lherzolite. Thus, if the mantle is similar to pyrolite, spinel lherzolite represents depleted mantle. Regardless of the interpretation, spinel lherzolite nodules are not associated with tholeiitic magmas, nor have they been found in lavas of the Snake River Plain or in those of the present study.

To pursue the issue further, the residual material was recast as a mineral assemblage of olivine, clinopyroxene, orthopyroxene, and spinel, that is, a spinel lherzolite using the method of Nicholls (1977b). The temperature of equilibration was assumed to be 1200° C and the pressure of equilibration was taken to be 12 kilobars (12 x 10^5 kPa) based on a crustal thickness of approximately 40 kilometers for this area (Smith, 1978). The resulting calculated mineral com-

Table 12. Percentage of partial melting required to derive selected olivine tholeiites from hypothetical mantles of pyrolite and lherzolite composition.

Olivine tholeiite	Pyrolite	Lherzolite
Sample 3	10.6	1.2
Sample 5	9.3	0.7
Sample 10	9.1	1.2
Sample 14	11.1	1.2

positions and modal amounts of these minerals are relatively insensitive to moderate changes in pressure and temperature. The next step is to estimate pressure and temperature conditions of equilibration between the parental magma and the calculated residual assemblage. The procedure used was that of Nicholls (1977a), based on the thermodynamics of heterogeneous equilibria using activity-composition relationships in silicate melts and solid phases (see also Carmichael and others, 1977; Evans and Nash, 1979). In this procedure, pressure-temperature curves are calculated representing equilibration between the activities of components in the solid residuum and activities of those same components in the magma. Theoretically, the intersection of these curves would then indicate the pressure and temperature of equilibration. As many as five pressure-temperature curves were calculated for a given magma-residuum pair. Equilibrium, based on curve intersections, was not indicated at any reasonable pressures and temperatures. It is thus concluded that pyrolite is not a realistic source composition for the olivine tholeiite.

CONCLUSIONS

The volcanic rocks of Caribou County, Idaho, consist primarily of olivine tholeiite, sharing many characteristics with the olivine tholeiite of the Snake River Plain. Petrographic similarities include the presence of olivine and plagioclase phenocrysts, the lack of calcium-poor pyroxene, the presence of olivine in the groundmass, and the occurrence of ophitic to subophitic groundmass augite. Chemically, the similarity is apparent when analyses are plotted on AFM and the alkali-silica diagram, and on a comparison of the differentiation index and Coomb's indicator ratio.

Minor occurrences of tholeiite and tholeiitic trachybasalt may be genetically related to parental olivine tholeiite by fractionation of olivine, plagioclase, augite, and iron-titanium oxides, leaving 40 to 60 percent residual liquid. As this requires removal of all crystalline phases rather than just microphenocrysts, filter pressing within a compressed near-surface magma chamber is proposed for the mechanism of formation.

Plagioclase basalt porphyry, containing 30 percent plagioclase phenocrysts, occurs at Cinder Island in the Blackfoot Reservoir and at Nelson and King Canyons in the Bear River Range east of Gem Valley. Its derivation from parental olivine tholeiite may be accomplished by fractionating 5 percent olivine and accumulating 15 percent plagioclase. Density calculations indicate an appropriate density contrast between liquid and plagioclase under anhydrous conditions, for plagioclase crystals to rise through the magma. The lack of resorption features and limited zoning suggest that water pressure was probably very low during emplacement.

Alkali trachyte, which is high in MgO, silica, and alkalies, occurs at the southern end of Slug Creek Valley and is unrelated to other lavas in the area. It is chemically similar to orendites and may be related to the Leucite Hills in Wyoming (130 miles to the southeast).

The origin of olivine tholeiite and alkali trachyte has been evaluated with the partial melting of various hypothetical mantle compositions. The derivation of olivine tholeiite would require less than 2 percent melting of spinel lherzolite or approximately 10 percent melting of pyrolite. The migration of magma would be facilitated with larger amounts of melt, favoring a pyrolite model. Equilibration studies between melts and residuum from pyrolite, recast as spinel lherzolite representing depleted mantle, show that pyrolite, however, is not a reasonable source composition. The origin of the alkali trachyte, with its high K_2O content, necessitates a potassic source, such as mica peridotite. Mica peridotite is associated with potassic lavas at the western end of the Uintas (130 miles to the south) and was used as the hypothetical mantle composition. The derivation of alkali trachyte requires 30 percent partial melting of such mica peridotite. The occurrence of these two different magmas, both of which are assumed to be mantle derived, indicates contrasting source regions or in homogeneities in the mantle. This may be indirect evidence for differences in the mantle, either in composition or structure, between the Basin and Range province and the Middle Rocky Mountain province.

ACKNOWLEDGMENTS

Financial support for this work was provided in part by U. S. Geological Survey Grant No. 14-08-0001-G-545; a summer Fellowship, Utah State University (to Perkins); Research Assistantships, Utah State University (to Perkins and Puchy); and the College of Science, Utah State University (computer costs). We thank William P. Nash and Stan Evans, University of Utah, for use of the electron microprobe, unpublished analyses of rhyolite, and age dates.

REFERENCES

Albee, A. L. and Lily Ray, 1970, Correction factors for electron probe microanalysis of silicates, carbonates, phosphates and sulphates: Analytical Chemistry, v. 42, p. 1408-1414.

Armstrong, F. C., 1969, Geologic map of the Soda Springs quadrangle, southeastern Idaho: U. S. Geological Survey Miscellaneous Geological Investigations Map I-557.

Armstrong, F. C. and E. R. Cressman, 1963, The Bannock thrust zone, southeastern Idaho: U. S. Geological Survey Professional Paper 374-J, 22 p.

Armstrong, F. C. and S. S. Oriel, 1965, Tectonic development of the Idaho-Wyoming thrust belt: American Association of Petroleum Geologists Bulletin, v. 49, no. 11, p. 1847-1866.

Armstrong, R. L., W. P. Leeman, and H. E. Malde, 1975, K-Ar dating, Quaternary and Neogene volcanic rocks of the Snake River Plain, Idaho: American Journal of Science, v. 275, p. 225-251.

Bacon, C. R. and I. S. E. Carmichael, 1973, Stages in the P-T path of ascending basalt magma: an example from San Quintin, Baja California: Contributions to Mineralogy and Petrology, v. 41, p. 1-22.

Bence, A. E. and A. L. Albee, 1968, Empirical correction factors for the electron microanalysis of silicates and oxides: Journal of Geology, v. 76, p. 382-403.

Best, M. G., L. F. Henage, and J. A. S. Adams, 1968, Mica peridotite, wyomingite, and associated potassic igneous rocks in northeastern Utah: American Mineralogist, v. 53, p. 1041-1048.

Bottinga, Yan and D. F. Weill, 1970, Densities of liquid silicate systems calculated from partial molar volumes of oxide components: American Journal of Science, v. 269, p. 169-182.

Bowen, N. L., 1928, The evolution of the igneous rocks: Princeton, Princeton University Press, 332 p.

Bright, R. C., 1963, Pleistocene lakes Thatcher and Bonneville, southeastern Idaho: University of Minnesota Ph.D. dissertation, 292 p.

———, 1967, Late Pleistocene stratigraphy in Thatcher Basin, southeastern Idaho: Tebiwa, v. 10, no. 1, p. 1-7.

Brown, G. M. and E. A. Vincent, 1963, Pyroxenes from the late stages of fractionation of the Skaergaard Intrusion, east Greenland: Journal of Petrology, v. 4, p. 175-197.

Buddington, A. F. and D. H. Lindsley, 1964, Iron-titanium oxide minerals and synthetic equivalents: Journal of Petrology, v. 5, p. 310-357.

Campbell, I. H., P. L. Roeder, and J. M. Dixon, 1978, Plagioclase buoyancy in basaltic liquids as determined with a centrifuge furnace: Contributions to Mineralogy and Petrology, v. 67, p. 369-377.

Carmichael, I. S. E., 1967a, The iron-titanium oxides of salic volcanic rocks and their associated ferromagnesian silicates: Contributions to Mineralogy and Petrology, v. 14, p. 36-64.

———, 1967b, The mineralogy and petrology of the volcanic rocks from the Leucite Hills, Wyoming: Contributions to Mineralogy and Petrology, v. 15, p. 24-66.

Carmichael, I. S. E., J. Hampel, and R. N. Jack, 1968, Analytical data on the USGS standard rocks: Chemical Geology, v. 3, p. 59-64.

Carmichael, I. S. E. and Jim Nicholls, 1967, Iron-titanium oxides and oxygen fugacities in volcanic rocks: Journal of Geophysical Research, v. 72, p. 4665-4687.

Carmichael, I. S. E., Jim Nicholls, F. J. Spera, B. J. Wood, and S. A. Nelson, 1977, High-temperature properties of silicate liquids: applications to the equilibration and ascent of basic magma: Philosophical Transactions of the Royal Society of London, Series A, v. 286, p. 373-431.

Carmichael, I. S. E., F. J. Turner, and John Verhoogen, 1974, Igneous Petrology: McGraw-Hill, 739 p.

Coombs, D. S., 1963, Trends and affinities of basaltic magmas and pyroxenes as illustrated on the diopside-olivine-silica diagram: Mineralogical Society of America, Special Paper 1, p. 227-250.

Cressman, E. R., 1964, Geology of the Georgetown Canyon-Snowdrift Mountain area, southeastern Idaho: U. S. Geological Survey Bulletin 1153, 105 p.

Doell, R. R. and Allan Cox, 1962, Determination of the magnetic polarity of rock samples in the field: U. S. Geological Survey Professional Paper 450-D, p. 105-108.

Evans, S. H. and W. P. Nash, 1979, Petrogenesis of xenolith-bearing basalts from southeastern Arizona: American Mineralogist, v. 64, p. 249-267.

Green, D. H. and A. E. Ringwood, 1967, The genesis of basaltic magmas: Contributions to Mineralogy and Petrology, v. 15, p. 103-190.

Gupta, A. K. and Kenzo Yagi, 1980, Petrology and genesis of leucite-bearing rocks: Springer-Verlag, 252 p.

Leeman, W. P., 1976, Petrogenesis of McKinney (Snake River) olivine tholeiite in light of rare-earth element and Cr/Ni distribution: Geological Society of America Bulletin, v. 87, p. 1582-1586.

Leeman, W. P. and M. E. Gettings, 1977, Holocene rhyolite in southeast Idaho and geothermal poten-

tial: Transactions of the American Geophysical Union, v. 58, no. 12, p. 1249.

Leeman, W. P. and W. I. Manton, 1971, Strontium isotopic composition of basaltic lavas from the Snake River Plain, southern Idaho: Earth and Planetary Science Letters, v. 11, p. 420-434.

Leeman, W. P. and C. J. Vitaliano, 1976, Petrology of McKinney Basalt, Snake River Plain, Idaho: Geological Society of America Bulletin, v. 87, p. 1777-1792.

Leeman, W. P., C. J. Vitaliano, and Martin Prinz, 1976, Evolved lavas from the Snake River Plain: Craters of the Moon National Monument, Idaho: Contributions to Mineralogy and Petrology, v. 56, p. 35-60.

Mabey, D. R., 1971, Geophysical data relating to a possible Pleistocene overflow of Lake Bonneville at Gem Valley, southeastern Idaho: U. S. Geological Survey Professional Paper 750-B, p. 122-127.

Mabey, D. R. and F. C. Armstrong, 1962, Gravity and magnetic anomalies in Gem Valley, Caribou County, Idaho: U. S. Geological Survey Professional Paper 450-D, p. 73-75.

Mabey, D. R. and S. S. Oriel, 1970, Gravity and magnetic anomalies in the Soda Springs region, southeastern Idaho: U. S. Geological Survey Professional Paper 646-E, 15 p.

Macdonald, G. A. and Takashi Katsura, 1964, Chemical composition of Hawaiian lavas: Journal of Petrology, v. 5, p. 82-133.

Mansfield, G. R., 1927, Geography, geology, and mineral resources of part of southeastern Idaho: U. S. Geological Survey Professional Paper 152, 448 p.

———, 1929, Geography, geology, and natural resources of the Portneuf quadrangle, Idaho: U. S. Geological Survey Bulletin 803, 110 p.

Mitchell, C. M., F. F. Knowles, and F. A. Petrafeso, 1965, Aeromagnetic map of the Pocatello-Soda Springs region, southeastern Idaho: U. S. Geological Survey Geophysical Investigations Map GP-521.

Moore, J. G., 1970, Pillow lava in a historic lava flow from Hualalai volcano, Hawaii: Journal of Geology, v. 78, p. 239-243.

Nicholls, Jim, 1977a, The activities of components in natural silicate liquids, *in* D. G. Fraser, editor, Thermodynamics in Geology: D. Reidel Publishing Co., p. 327-348.

———, 1977b, The calculation of mineral compositions and modes of olivine-two pyroxene-spinel assemblages: Contributions to Mineralogy and Petrology, v. 60, p. 119-142.

Nicholls, Jim, D. W. Fiesinger, and V. G. Ethier, 1977, Fortran IV programs for processing routine electron microprobe data: Computers and Geosciences, v. 3, p. 49-83.

Oriel, S. S., 1968, Preliminary geologic map of the Bancroft quadrangle, Caribou and Bannock Counties, Idaho: U. S. Geological Survey open-file map.

Oriel, S. S., D. R. Mabey, and F. C. Armstrong, 1965, Stratigraphic data bearing on the inferred pull-apart origin of Gem Valley, Idaho: U. S. Geological Survey Professional Paper 525-C, p. 1-4.

Oriel, S. S. and L. B. Platt, 1980, Geologic map of the Preston 1° x 2° quadrangle, southeastern Idaho and western Wyoming: U. S. Geological Survey Miscellaneous Investigations Series Map I-1127, scale 1:250,000.

Perkins, W. D., 1979, Petrology and mineralogy of Quaternary basalts, Gem Valley and adjacent Bear River Range, southeastern Idaho: Utah State University M.S. thesis, 91 p.

Powell, Marjorie and Roger Powell, 1974, An olivine-clinopyroxene geothermometer: Contributions to Mineralogy and Petrology, v. 48, p. 249-263.

Powell, Roger and Margorie Powell, 1977, Geothermometry and oxygen barometry using coexisting iron-titanium oxides: a reappraisal: Mineralogical Magazine, v. 41, p. 257-263.

Prider, P. T., 1960, The leucite lamproites of the Fitzroy Basin, Western Australia: Journal of the Geological Society of Australia, v. 6, p. 71-118.

Puchy, B. J., 1981, Mineralogy and petrology of lava flows (Tertiary-Quaternary) in southeastern Idaho and at Black Mountain, Rich County, Utah: Utah State University M.S. thesis, 73 p.

Sahama, T. G., 1974, Potassium-rich alkaline rocks, *in* H. Sorensen, editor, The Alkaline Rocks: J. Wiley and Sons, p. 96-109.

Smith, Douglas and D. H. Lindsley, 1971, Stable and metastable augite crystallization trends in a single basalt flow: American Mineralogist, v. 56, p. 225-233.

Smith, R. B., 1978, Seismicity, crustal structure, and intraplate tectonics of the interior of the western Cordillera, *in* R. B. Smith and G. P. Eaton, editors, Cenozoic tectonics and regional geophysics of the western Cordillera: Geological Society of America Memoir 152, p. 111-144.

Stormer, J. C. and Jim Nicholls, 1978, XLFRAC: a program for the interactive testing of magmatic differentiation models: Computers and Geosciences, v. 4, p. 143-159.

Stout, M. Z. and Jim Nicholls, 1977, Mineralogy and petrology of Quaternary lavas from the Snake River Plain, Idaho: Canadian Journal of Earth Sciences, v. 14, p. 2140-2156.

Streckeisen, Albert, 1979, Classification and nomenclature of volcanic rocks, lamprophyres, carbonatites, and melilitic rocks: recommendations and suggestions of the I. U. G. S. Subcommission on the Systematics of Igneous Rocks: Geology, v. 7, p. 331-335.

Thompson, R. N., 1975, Primary basalt and magma genesis, II: Snake River Plain, Idaho, U.S.A.: Contributions to Mineralogy and Petrology, v. 52, p. 213-232.

Thornton, C. P. and O. F. Tuttle, 1960, Chemistry of igneous rocks: part I, differentiation index: American Journal of Science, v. 258, p. 664-684.

Tilley, C. E. and R. N. Thompson, 1970, Melting and crystallization relations of the Snake River basalts of southern Idaho, U.S.A.: Earth and Planetary Science Letters, v. 8, p. 79-92.

Williams, Howel, F. J. Turner, and C. M. Gilbert, 1954, Petrography, an Introduction to the Study of Rocks in Thin Section: W. H. Freeman and Co., 406 p.

Yoder, H. S. and C. E. Tilley, 1962, Origin of basaltic magmas: an experimental study of natural and synthetic rock systems: Journal of Petrology, v. 3, p. 342-532.

Chapter 8

Stratigraphy and Structural Relationships Southeastern Idaho

Cenozoic Stratigraphy and Tectonic Evolution of the Raft River Basin, Idaho

by

Paul L. Williams[1], Harry R. Covington[2], and Kenneth L. Pierce[2]

ABSTRACT

The Raft River basin, a north-trending structure in the Basin and Range province south of the Snake River Plain, Idaho, is filled with upper Cenozoic sediments to a depth of about 1,700 meters. The basin fill is mainly the Salt Lake Formation of Miocene to Pliocene age, which consists of four members: (1) a lower tuffaceous member of shale, siltstone, and sandstone; (2) a wedge of calc-alkalic rhyolite flows with associated volcanic domes here named the Jim Sage Volcanic Member; (3) an upper tuffaceous and conglomeratic member; and (4) olivine basalt flows in the northern Cotterel Mountains. Isotope dating of volcanic rocks and paleomagnetic data reveal that the age of the Salt Lake Formation here ranges from more than 11 to about 2-3 million years, with nearly continuous deposition in the center of the basin. In Quaternary time, basalts erupted from vents in the northern part of the basin, and main stream alluvial deposits, alluvial fans, and successive loess blankets indicate changes in Pleistocene climate. Subsurface and geophysical studies show that the basin fill is considerably faulted, yet it rests on a low-relief surface of lower Paleozoic(?) and Precambrian metamorphic rocks. The Cenozoic structure of the basin is primarily the result of mid-Tertiary uplift of gneiss domes in the Albion Mountains west of the basin. Uplift gave rise to low-angle detachment faults involving transport of large masses of upper Paleozoic rocks eastward across the low-relief surface. Numerous listric faults, their lower parts merging with the detachment surface, and subsidiary fractures formed in the basin fill, and these became the conduits for the southern Raft River Valley geothermal system, although they are of insufficient depth to account for the high water temperatures observed.

[1]U. S. Geological Survey, APO New York, New York 09697.
[2]U. S. Geological Survey, Denver Federal Center, Denver, Colorado 80225.

INTRODUCTION

The purpose of this report is to summarize the Cenozoic stratigraphy and structure of the Raft River basin, as it is now understood in the light of new data, and to present some of the reinterpretations of geologic history and basin geometry that form the basis for reports now in progress. We conclude that deposition in the basin was nearly continuous from early Miocene time and that gravity faulting related to uplift of mid-Tertiary metamorphic core complexes (gneiss domes) is the dominant tectonic mode.

The Raft River Valley occupies a north-trending intermontane tectonic basin about 60 kilometers long and 20 to 24 kilometers wide, with an average valley floor elevation of about 1,400 meters (Figure 1). The valley opens northward onto the broad Snake River Plain. On the west, south, and east sides, the basin is flanked by mountain ranges of varied heights. On the west flank, the Cotterel and Jim Sage Mountains, making up the Malta Range, rise to maximum elevations of about 2,500 meters. Directly west of the Cotterel and Jim Sage Mountains, and separated from them by a narrow valley, lie the Albion Mountains (3,000 meters). South of the basin are the Raft River Mountains (3,000 meters), one of the few east-trending mountain ranges in the North American Cordillera. On the east side of the basin are the Sublett and Black Pine Ranges (2,000 meters and 2,900 meters).

The geology of the basin and surrounding ranges was first mapped by Anderson (1931), who described rocks ranging in age from Precambrian to Quaternary. The U. S. Geological Survey has carried out several ground-water studies of the Snake River Plain region (Russel, 1902; Stearns and others, 1938) and of the Raft River basin (Nace and others, 1961; Mundorff and Sisco, 1963; Walker and others, 1970).

Designation in 1971 of the Raft River KGRA (Known Geothermal Resource Area) (Godwin and others, 1971) and the discovery in 1975 of a major intermediate temperature, liquid-dominated geothermal

Williams, P. L., H. R. Covington, and K. L. Pierce, 1982, Cenozoic stratigraphy and tectonic evolution of the Raft River basin, Idaho, *in* Bill Bonnichsen and R. M. Breckenridge, editors, Cenozoic Geology of Idaho: Idaho Bureau of Mines and Geology Bulletin 26, p. 491-504.

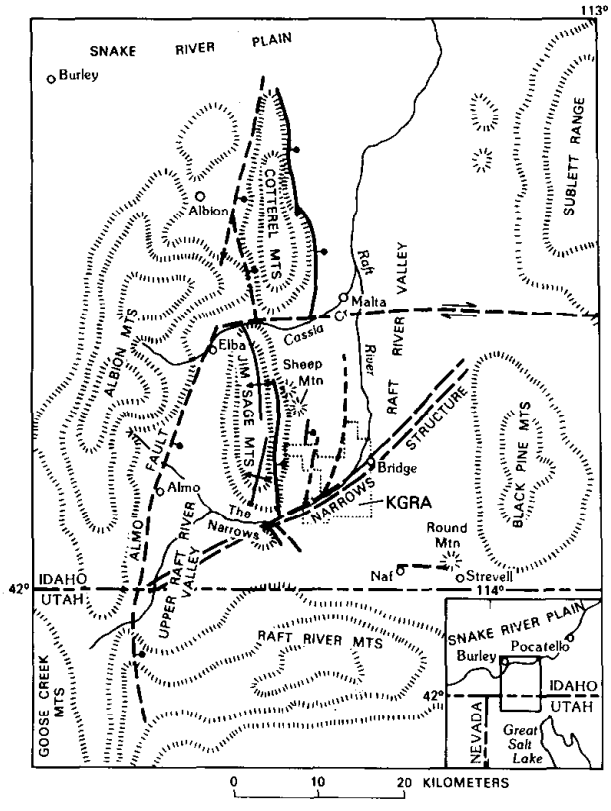

Figure 1. Index map of Raft River region showing Narrows structure (NE-trending dashed lines), structures affecting alluvium (short-dashed lines), transcurrent fault (east-west dashed line), and normal faults (lines with bar and ball showing downthrown side).

resource led to the multidisciplinary investigations in the area, including geologic mapping (Williams and others, 1974; Pierce and others, in press) and exploration with various geophysical techniques. Results of these studies were summarized early by Williams and others (1976) and later by Mabey and others (1978a). Subsurface studies incorporating results from both intermediate (about 300 meters) and deep (about 1,800 meters) boreholes are described by Crosthwaite (1976), Covington (1977a, 1977b, 1977c, 1977d, 1978, 1979a, 1979b), and Oriel and others (1978).

GEOLOGIC SETTING

The Raft River basin lies in the northeast part of the Basin and Range province just south of the Snake River Plain and about 100 kilometers west of the Overthrust Belt of the northern Rocky Mountains. It is within the Cordilleran thermotectonic anomaly (CTTA) (Eaton and others, 1976, 1978), which is roughly coextensive with the Basin and Range province and which is interpreted as the product of large-scale crustal extension resulting in high heat flow, much volcanism throughout middle and late Cenozoic time, and basin-range block faulting (Stewart, 1978). In the Raft River region, the base of the magnetized crust (locus of the Curie isotherm for magnetite, about 580°C) is 12 kilometers below sea level, a relatively shallow depth compared with other parts of the Snake River Plain region (Bhattacharyya and Mabey, 1980; Mabey, in press).

The depositional, tectonic, and thermal history of the Raft River region is long and complex, and it has been the subject of considerable study (Armstrong, 1968, 1970, 1976, unpublished data; Compton, 1972, 1975; Compton and others, 1977; Miller and others, 1980; Smith, 1982). In brief, a late Precambrian to Triassic miogeoclinal succession about 12,000 meters thick was deposited on a 2.5 billion-year-old Archean basement of adamellite and subordinate schist, gneiss, and amphibolite. These younger rocks are grouped as the Raft River assemblage (R. L. Armstrong, unpublished data). High-pressure load metamorphism during Jurassic time was followed by thrusting of the Sevier orogeny in Cretaceous time, during which a late Precambrian-Paleozoic allochthon (quartzite assemblage of R. L. Armstrong, unpublished data) was thrust eastward over an autochthon and parautochthon consisting of the Raft River assemblage. Great allochthons of upper Paleozoic rocks were subsequently thrust eastward over older rocks. An early to middle Tertiary rise in thermal activity produced plutons at depth, gneiss domes in the Albion and Raft River Mountains, and considerable attenuation of the sedimentary cover on the domes. Late Tertiary events, largely the result of crustal extension, include folding and faulting to form the present mountains and sediment-filled basins and local rhyolitic volcanism. Eruption of the Jim Sage Volcanic Member coincided with the northeastward passage of the thermal pulse now under Yellowstone National Park (Christiansen and Lipman, 1972). During the Quaternary, extensional tectonics probably continued, and flood basalts of the Snake River Group were erupted from centers at the north end of the Raft River Valley. Alluvial deposits of main and tributary streams, alluvial fan gravels on piedmont slopes, and successive loess blankets record cyclic climatic changes during Pleistocene time.

CENOZOIC STRATIGRAPHY

The Raft River basin is filled with Cenozoic rocks

to a maximum known depth, based on deep drilling, of about 1,700 meters. Because of structural complications, however, this thickness only approximates the actual depositional thickness, and rocks penetrated successively in drilling are not necessarily a stratigraphic succession (Covington, 1977a, 1977b, 1977c, 1977d, 1978, 1979a, 1979b, 1980; Pierce and others, in press). Accordingly, the stratigraphic sequence as presently known is fragmentary and is deduced from exposed sections and from well records from which only the existence, but not the magnitude, of folding and faulting can be confidently inferred.

SALT LAKE FORMATION

The Salt Lake Formation (Hayden, 1869; Mansfield, 1920; Walker and others, 1970) rests on Precambrian rocks in the area of the KGRA and at least as far north as Malta; in the southeastern part of the basin, near Strevell, it rests on Paleozoic rocks. In the KGRA and probably elsewhere,the Tertiary-Precambrian contact is a detachment surface related to growth faulting along listric fault surfaces (Covington, 1980; Pierce and others, in press).

In the Raft River basin, the Salt Lake Formation consists of four principal members: lower and upper tuffaceous members; an intervening wedge of rhyolite flows (Jim Sage Volcanic Member) in the western part of the basin; and the basalt of the northern Cotterel Mountains (Figure 3).

Lower Tuffaceous Member

The lower tuffaceous member is exposed in the southern half of the Jim Sage Mountains, mainly in the upper valleys of Chokecherry and Cottonwood Creeks and in the bluffs both north and south of the Raft River Narrows. A measured section at the top of the member near Dry Canyon in the southern Jim Sage Mountains consists of 130 meters of gray, poorly consolidated, massive to thin-bedded, tuffaceous sandstone and tuff, and sandy tuffaceous shale and siltstone. Alternating units of sandstone and shale-siltstone are about 10 to 20 meters thick. Thin beds of grit and fine conglomerate are locally present. The lower part of the member, as deduced from well cuttings, consists largely of light brown siltstone alternating with light green tuff and tuffaceous sandstone in units 10 to 30 meters thick (Covington, 1977a, 1977b, 1977c, 1977d, 1978, 1979a, 1979b). Both green and brown rocks are commonly calcareous. Total thickness of the lower tuffaceous member is about 500 meters in the Raft River basin, but it is probably 1,000 meters or more in the upper Raft River basin southwest of the Narrows.

Jim Sage Volcanic Member

The Jim Sage Volcanic Member is formally proposed herein for a thick wedge of rhyolite flows with subordinate bedded tuff and ash-flow tuff that were deposited on the lower tuffaceous member along the western margin of the Raft River basin. The type locality is in the southern Jim Sage Mountains, approximately 42°05′-42°08′ lat, 113°28′-113°32′ long. This member forms most of the Jim Sage and Cotterel Mountains and consists of three parts: the lower and upper successions of rhyolite flows and a middle unit of varied lithology. Maximum thickness is about 1,200 meters.

The lower and upper rhyolite flows are similar and consist mostly of dark gray to black, glassy porphyritic rhyolite that weathers dark reddish brown. Individual flows range in thickness from 20 to 200 meters; thicker flows commonly have a light gray devitrified zone in the middle part, enclosed in an envelope of glass. The rock is commonly flow banded, and columnar joints, square in cross section, are well developed. In the field, the lower flows can be distinguished by their reversed magnetic polarity from the upper flows, which have normal polarity.

The middle unit is 30 to 100 meters thick and consists mostly of a distinctive vitrophyre breccia made up of nonsorted particles of angular to subrounded, gray, glassy rhyolite ranging in size from coarse sand to 1-meter blocks set in a matrix of either yellow to orange palagonitic hydrated glass or white to gray tuff. Thin rhyolite flows are locally present. Fine-grained, probably in part lacustrine, sediments above and below the breccia suggest that it formed as an explosion breccia produced by rhyolite flowing into a body of water. In the southern Cotterel Mountains, the breccia is overlain by two thin, vitric rhyolite ash-flow tuffs that were erupted from sources to the east. The tuffs are overlain by a few meters of white to gray tuffaceous sandstone and siltstone.

Volcanic domes that consist of rhyolite similar to the lower and upper rhyolite flows occur in three areas in the Raft River basin (Td, Figure 2): in the southernmost Cotterel Range, just north of Cassia Creek; at Sheep Mountain, east of the central Jim Sage Mountains; and along the southern margin of the basin north of the Raft River Mountains and west of the Black Pine Range. The most prominent of the domes is Sheep Mountain, a roughly conical steep-sided hill about 1 kilometer in diameter that rises 170 meters above the alluvial-fan surface east of the Jim Sage Mountains. The dome consists of an outer shell 10 to 20 meters thick of brown devitrified rhyolite that is generally brecciated and seamed with chalcedony veinlets; the shell encloses a core of gray glassy porphyritic rhyolite. The rhyolite clearly in-

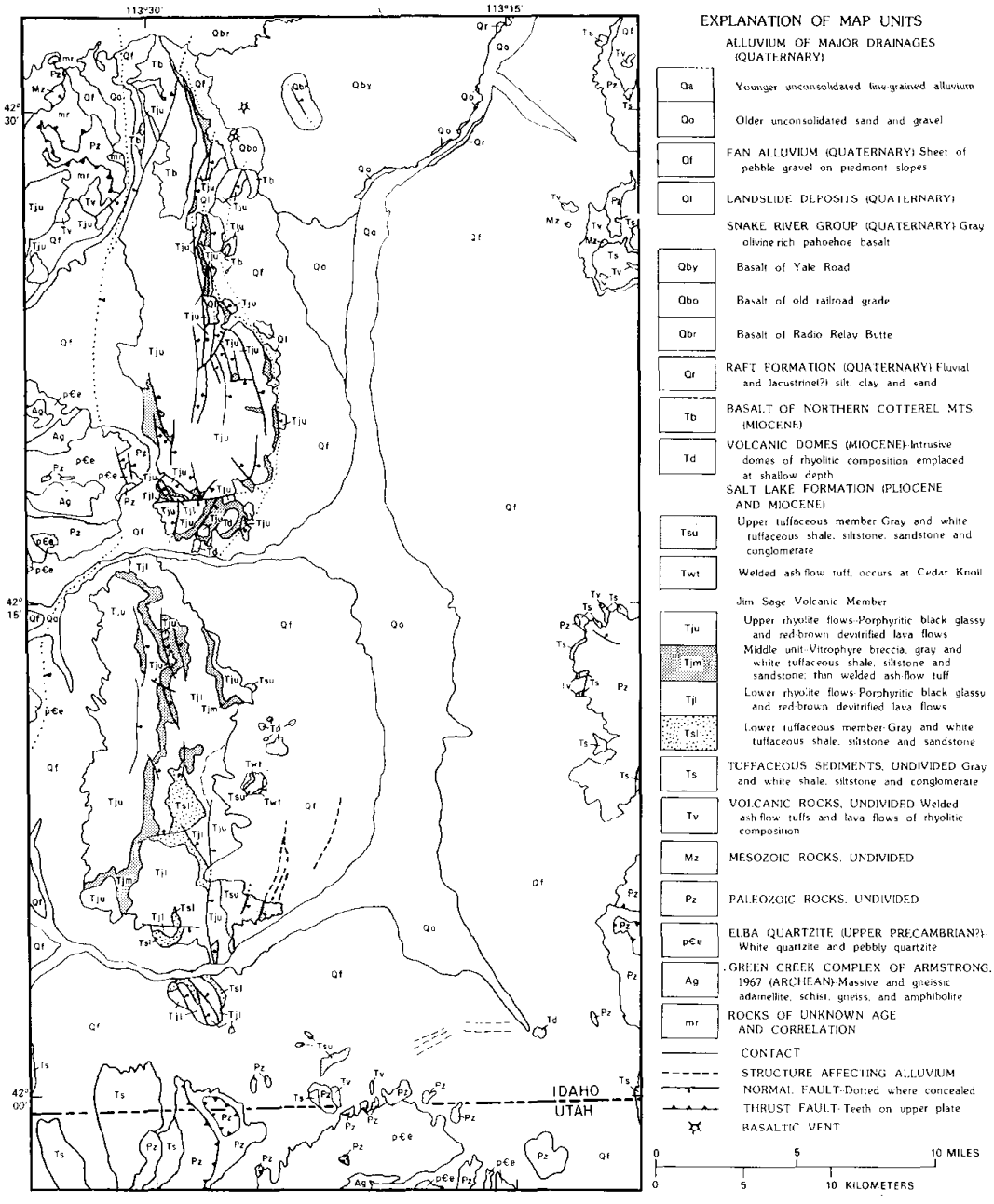

Figure 2. Geologic map of the Raft River basin, Cassia County, Idaho (after Armstrong and others, 1978; Compton, 1972, 1975; Williams and others, 1974; Pierce and others, in press).

trudes the upper tuffaceous member of the Salt Lake Formation; a thin dikelike extension of the shell surrounded by altered tuff is exposed at the east end of Sheep Mountain. At the southern end of the Raft River basin, several small exposures of rhyolite occur along an east-northeast-trending line that appears to be fault controlled.

The rhyolites and volcanic domes of the Jim Sage Member are similar petrographically. Phenocryst content ranges from 6 to 23 percent and averages 15 percent. The phenocrysts are mostly plagioclase (An_{29-33}), with 1 to 2 percent augite and pigeonite (hypersthene occurs in the uppermost thick flow), 0.5 percent opaque minerals, 0.5 percent quartz, and rare sanidine. Microscopically, glassy rocks commonly have a well-developed perlitic crack pattern and radial spherulites that indicate incipient devitrification; the groundmass of gray devitrified rock is a

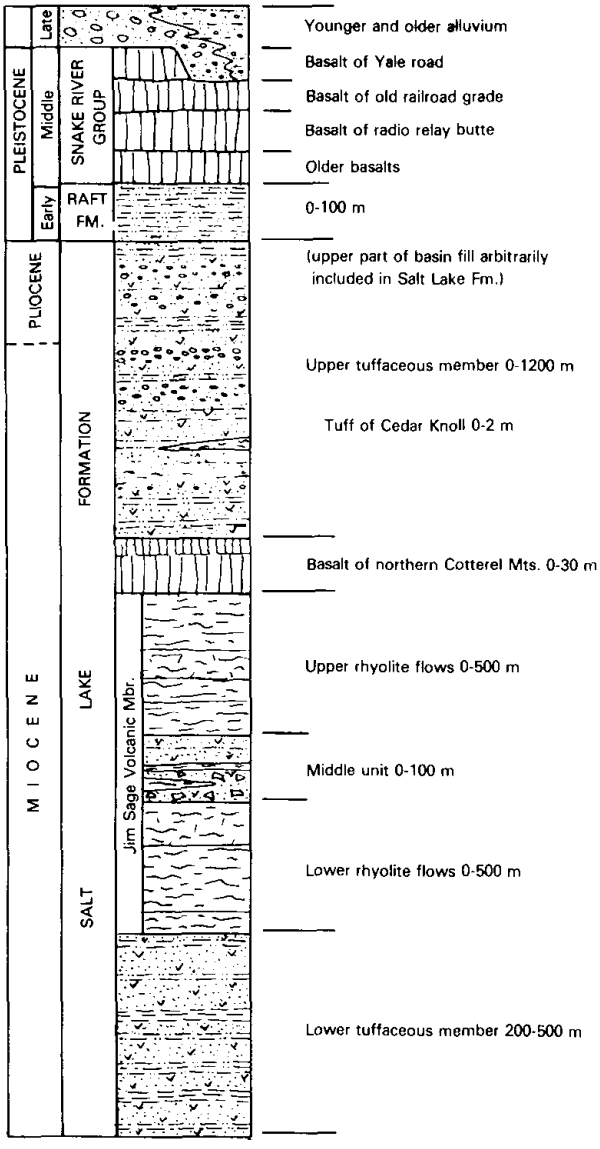

Figure 3. Composite stratigraphic column for Cenozoic rocks, Raft River basin, Idaho.

mosaic of quartz and feldspar. Lithophysal cavities lined with tridymite and feldspar were found only in the thick, uppermost flow of the Jim Sage Volcanic Member and indicate minor vapor-phase activity.

The rhyolites are similar chemically as well as petrographically. Analyses from upper and lower flows and the volcanic dome have the average composition shown in Table 1; deviation from the average is slight. This composition is close to that of the average calc-alkalic rhyolites of Nockolds (1954), but the Jim Sage Volcanic Member contains more total Fe, MgO, CaO, and TiO_2, and less of the alkalis and silica.

The basalt of the northern Cotterel Mountains (Figure 3) is the oldest basalt in the Raft River region and consists of two flows that cap the north end of the west-dipping cuesta that forms the range. A single flow is exposed in fault blocks along the northeast and northwest flanks of the range. The rock is gray to light gray with a reddish oxidation tint and contains glomeroporphyritic clots of olivine and plagioclase in a dense groundmass of fine-grained plagioclase, olivine, pyroxene, opaque minerals, and glass (Pierce and others, in press). Radiometric ages (Figure 4) are in agreement with its conformable position overlying the upper flows of the Jim Sage Volcanic Member.

Upper Tuffaceous Member

The upper tuffaceous member of the Salt Lake Formation is poorly exposed in the Raft River basin and is known mostly from the subsurface. The lower 600 meters or so consists of gray tuffaceous sandstone and tuff and of white, gray, and light green thin-bedded to papery shale and tuffaceous siltstone. Thin rhyolite flows of the upper part of the Jim Sage Volcanic Member are intercalated with the basal beds of the member. East of the central Jim Sage Mountains the tuff of Cedar Knoll, a thin vitric ash-flow tuff, is intercalated with the bedded tuff. A similar but thicker intercalated crystal-poor ash-flow tuff, the tuff of upper Raft River Valley (R. L. Armstrong, unpublished data) forms a low cuesta about 8 kilometers west of the Narrows. The succeeding 500 meters or so of the member is similar in lithology but conglomeratic; most of the pebbles and sand grains were derived from the Jim Sage Volcanic Member. Carbonaceous material is sparsely present in the uppermost part of the member.

In a recent petrographic study, Devine and Bonnichsen (1980) noted that the principal lithologies in the tuffaceous members of the Salt Lake Formation are shale, siltstone, sandstone, and tuff. The sandstones are feldspathic graywackes and lithic wackes (Pettijohn and others, 1972) in which quartz, feldspar, rock fragments, and mica are the principal detrital components. The composition of the texturally immature sediments reflects the mixed provenance from the varied rock types in the mountain ranges surrounding the basin. Devine and Bonnichsen found the volcanic provenance dominant in the upper part of the basin fill, indicated by a high ratio of non-undulatory (volcanic) quartz to undulatory (metamorphic) quartz and by a high ratio of volcanic to metamorphic rock fragments; both ratios strongly decrease downward in the Salt Lake Formation. The downward decrease in average grain size of the basin fill, suggested by the absence of conglomerate in the lower part, is further indicated by a downward decrease in detrital quartz and feldspar and a corres-

ponding increase in nondetrital carbonate (Devine and Bonnichsen, 1980, p. 35).

Age and Correlation

The Salt Lake Formation is dated as late Miocene, at least in part, by a clustering of radiometric ages between about 7 and 11 million years for the Jim Sage Volcanic Member, by the basalt of the northern Cotterel Mountains, and by the tuff of Cedar Knoll (Figure 4 and Table 2). The oldest dates, from the upper rhyolite flows of the Jim Sage Volcanic Member, indicate an age of 9 to 11 million years; the conformable basalt of the northern Cotterel Mountains is about the same age. The volcanic domes are about 7 to 9 million years old. The ash-flow tuffs in the middle unit of the Jim Sage in the southern Cotterel Mountains were not dated but appear to be the same as tuffs in the Sublett Range, dated by Armstrong at between 8 and 11 million years. A similar date, 8.8 million years, obtained for the tuff of upper Raft River Valley (G. B. Dalrymple, written communication, 1980) suggests that the tuffs in the three areas are the same unit; they are lithologically very similar and preliminary petrographic data confirm the correlation. The youngest radiometric date for the Salt Lake Formation is that of 7 million years for the tuff of Cedar Knoll, although a large analytical uncertainty permits a range of 5 to 9 million years. The tuff of Cedar Knoll is lithologically similar to the Walcott Tuff (Carr and Trimble, 1963; Trimble and Carr, 1976) which has potassium-argon ages of about 6 million years (Marvin and others, 1970; Armstrong and others, 1975).

Preliminary findings from recent paleomagnetic studies by S. L. Bressler (written communication, 1979) permit estimates of the rate of sedimentation in the basin. The magnetic polarity of a suite of samples from intermediate-depth core-hole no. 3, total depth 408 meters (Crosthwaite, 1976), probably indicates a good correlation with the standard late Cenozoic polarity scale and apparently uniform sedimentation rates for the interval represented. Rocks from the bottom of the well apparently date from the top of the Gauss normal epoch, about 2.6 million years, which would indicate an average sedimentation rate of about 160 meters per million years. If sedimentation rates did not vary greatly, the basal sediments in the basin could thus be about 10 to 11 million years old. However, the finer grained rocks in the lower part of the Salt Lake Formation probably accumulated more slowly than the coarser clastics of the upper tuffaceous member, implying a somewhat greater age for the basin, perhaps extending to early Miocene or late Oligocene time.

Although a detailed regional correlation of units is not within the scope of this report, it is worth noting that recently published radiometric dates of volcanic rocks (Marvin and others, 1970; Armstrong and others, 1975, 1980; Williams and others, 1976) have been extremely useful in clarifying the regional stratigraphy. Thus, the Starlight Formation, the Walcott Tuff, and perhaps the Little Creek Formation (Carr and Trimble, 1963; Trimble and Carr, 1976) are probably equivalent to the upper tuffaceous member of the Salt Lake Formation of the Raft River basin. In the Cassia Mountains west of the Albion Mountains, a thick succession of rhyolite ash-flow sheets 8.5 to 11.0 million years old (Armstrong and others, 1975, 1980) overlies the Beaverdam Formation of Axelrod (1964), which contains the Trapper Creek flora of middle Miocene age. The Beaverdam Formation is probably at least partly equivalent to the lower tuffaceous member of the Salt Lake Formation of the Raft River basin.

Table 1. Average chemical composition of the Jim Sage Volcanic Member. (Average of ten rapid-rock analyses by P. Elmore, U. S. Geological Survey, Denver, Colorado.)

	Weight Percent
SiO_2	72.1
Al_2O_3	13.5
Fe_2O_3	2.0
FeO	1.8
MgO	0.6
CaO	2.0
Na_2O	2.7
K_2O	4.4
TiO_2	0.6
P_2O_5	0.1

YOUNGER CENOZOIC ROCKS

In the northern part of the Raft River Valley, adjacent to the Snake River Plain, basaltic volcanism occurred intermittently from late Miocene to middle Pleistocene time. Quaternary basalts form broad, low shields and thin, tabular flows that blocked and diverted the Raft River eastward. The basalts and surficial deposits, some of which formed as the result of basalt dams, are described by Pierce and others (in press).

Raft Formation

The Raft Formation (Carr and Trimble, 1963; Walker and others, 1970), originally the "Raft lake beds" (Stearns and others, 1938), consists of fine-grained lacustrine and fluvial deposits, principally

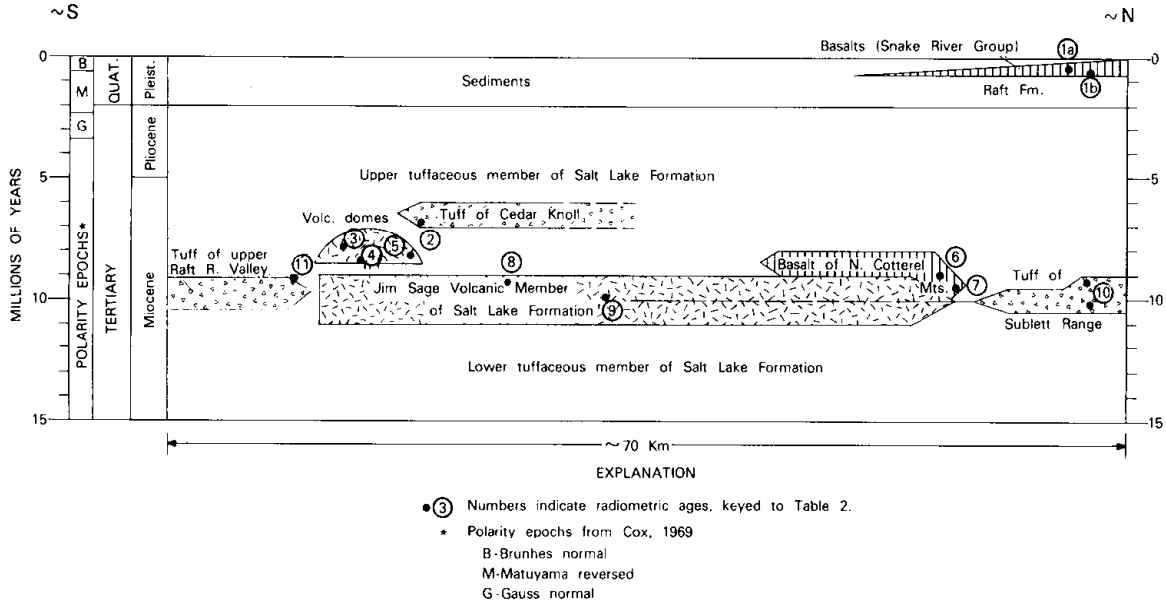

Figure 4. Chronostratigraphic diagram for Cenozoic rocks in the Raft River basin, Idaho.

clay, silt, and sand, that were deposited on the Salt Lake Formation in the Raft River basin. Deposition was probably in response to an elevation of base level by the emplacement of basalt flows of the Snake River Group some distance downstream from the mouth of the Raft River. The formation is not exposed in the southern part of the basin but is believed by Walker and others (1970, p. 24) to be up to 300 meters thick in drill holes. We did not recognize the Raft Formation either in outcrop or in subsurface in the southern part of the basin. In the northern part, the Raft Formation is poorly exposed along the Raft River, but it is well exposed in bluffs 40 meters high along the Snake River a few kilometers east of the mouth of the Raft River. Molluscs collected from localities in that area indicate a Pleistocene age for the Raft Formation (Trimble and Carr, 1976).

Basalt

Basalt flows mapped by Pierce and others (in press) as "older basalt" of probable early Pleistocene age occur as kipukas surrounded by younger lava just north of the Cotterel Mountains. The basalt occurs as pahochoc lava and near-vent pyroclastic deposits and

Table 2. Sources of radiometric age dates (see Figure 4).

No.	Unit	Age, million years	Method	By	Reference
1a	Basalt of Radio Relay Butte	0.446 ± 0.220	K-Ar whole rock	G. B. Dalrymple	Pierce and others, in press
1b	----do----	0.709 ± 0.210	----do----	----do----	Do.
2	Tuff of Cedar Knoll	7.0 ± 2.0	Fission track, zircon	C. W. Naeser	Williams and others, 1976
3	Sheep Mountain volcanic dome	7.8 ± 1.1	----do----	----do----	Do.
4	----do----	8.42 ± 0.2	K-Ar Plagioclase	J. D. Obradovich	Do.
5	Round Mountain volcanic dome	8.3 ± 1.7	Fission track, zircon	C. W. Naeser	Do.
6	Basalt of North Cotterel Mountains	9.2 ± 1.5	K-Ar, whole rock	R. L. Armstrong	Armstrong and others, 1975
7	----do----	9.81 ± 1.02	----do----	G. B. Dalrymple	Pierce and others, in press
8	Upper ryholite, Jim Sage Volcanic Member	9.2 ± 0.5	----do----	R. L. Armstrong	Armstrong and others, 1975
9	----do----	9.4 ± 1.6	Fission track, zircon	C. W. Naeser	Williams and others, 1976
10a	Tuff of Sublett Range	10.4 ± 0.14	K-Ar whole rock	R. L. Armstrong	Armstrong and others, 1975
10b	----do----	8.2 ± 0.2	----do----	----do----	Do.
10c	----do----	10.8 ± 0.2	K-Ar, biotite	----do----	Do.
10d	----do----	9.4 ± 0.14	K-Ar, feldspar	----do----	Do.
11	Tuff of upper Raft River Valley	8.8 ± 0.188	K-Ar, plagioclase	G. B. Dalrymple	Written communication, 1980

consists of gray to reddish banded rock with 1 to 2 percent phenocrysts of olivine and plagioclase.

The basalt of Radio Relay Butte (Pierce and others, in press) forms an extensive series of loess-mantled flows across the north end of the basin and makes up Horse Butte, a prominent kipuka (but not a basalt vent) east of the Cotterel Mountains. The basalt is gray, dense, and fine grained, with 1 to 3 percent small phenocrysts of olivine and plagioclase. Two potassium-argon ages (Table 2) of 0.709 ± 0.210 and 0.446 ± 0.220 million years indicate a middle Pleistocene age. Normal magnetic polarity coupled with the potassium-argon dates indicates an age of less than 0.73 million years (Pierce and others, in press).

The basalt of the old railroad grade (Pierce and others, in press) forms pahoehoe flows of limited extent that were erupted from a small vent 3 kilometers southwest of Horse Butte. The basalt is gray, porous, and finely porphyritic, with 2 to 3 percent phenocrysts of olivine 0.2 to 1.0 millimeter in diameter and plagioclase 0.5 to 1.0 millimeter long.

The youngest basalt in the area is the basalt of Yale Road, which was erupted from a vent marked by a fresh-looking crater 2 kilometers west of Horse Butte. Thin but extensive lava flows spread eastward and diverted the course of the Raft River northeastward to its present position. The basalt is light gray, porous, and, like the other basalts, porphyritic with 1.5 to 3.0 percent phenocrysts of olivine, 0.3 to 1.0 millimeter in diameter, and plagioclase laths 0.5 to 1.0 millimeter long. The groundmass consists on the average of about 35 percent plagioclase laths, 15 percent olivine, 25 percent augite, 12 percent opaque minerals, and 12 percent glassy matrix. Groundmass textures range from ophitic to hyalo-ophitic and hyalopilitic.

Both the basalt of the old railroad grade and the basalt of Yale Road have normal magnetic polarity, as measured in the field by a fluxgate magnetometer. They are assigned a middle Pleistocene age (Pierce and others, in press).

UNCONSOLIDATED SURFICIAL DEPOSITS

Unconsolidated surficial deposits that consist of fan gravels, main stream gravels thickly mantled by fine sediments, and loess cover most of the area shown in Figure 2. Except for the fine sediment along the flood plains of the main drainages, nearly all these surficial materials are Pleistocene in age, deposited under climatic conditions different from the present (Pierce and Scott, 1982 this volume).

Fan Gravels

Gravelly alluvial fans occur at the base of the ranges bordering the Raft River basin. The clasts in these fans are mostly rhyolite on the west side of the basin, mostly carbonate rocks on the east side, and a mixture of granitic, quartzitic, and carbonate rock on the south side. The fan gravels typically display stone-on-stone fabric, with spaces between stones being either open or filled with a matrix of relatively coarse sand. They are remarkably well washed, containing only 3 to 5 percent silt and clay (Pierce and Scott, 1982 this volume; Pierce and others, in press). Most beds are 0.2 to 0.5 meter thick and more than 5 meters in horizontal extent. Fewer beds are lens shaped, representing channel fills a few meters across and half a meter deep.

Different ages of fan gravels are readily apparent from sequence relations evident on aerial photographs; the age relations between adjacent fan deposits can generally be determined from the drainage pattern on the fans and the relative degree of dissection. For an alluvial-fan sequence deposited by a given stream, as many as eight subdivisions based on age can locally be mapped (Williams and others, 1974; note caret symbols). Age grouping of similar-age fan segments throughout the Raft River basin presents problems because different relative-age criteria need to be used in different parts of the basin. Where thick loess has accumulated on the southern and eastern sides of the valley, the number of loess units on a fan deposit indicates increasing age; on fans where the mantling loess contains one buried soil more strongly developed than the surface soil, the underlying gravels are probably at least 130,000 years old. On the west side of the valley, where loess is thin, ages of fan segments are based on relative-age criteria such as soil development, thickness of carbonate coatings on stones, and degree of fan dissection by drainages that head on the fan (Pierce and others, in press).

Along each drainage that heads well back in a range, a relatively young pie-shaped segment of fan gravel can be identified by (1) little dissection by small drainages on the fan, (2) almost perfect conical form as shown by contours on topographic maps, (3) loess mantle only about 10 to 30 centimeters thick, and (4) weak soil development generally without an argillic B horizon and without any carbonate cementation. The largest such young fan in the Raft River basin is the Meadow Creek-Warm Creek fan which covers about 130 square kilometers north of the Black Pine Range. Based on soil development and relation to Holocene deposits, the gravels forming these relatively young fan segments are estimated to be between 25,000 and 10,000 years old, or late

Wisconsin in age.

Fan deposits of Holocene age are much more limited in extent and were deposited by streams with much less competence than the Pleistocene streams. Fans of poorly bedded silt occur along the margin of Raft River bottoms; they consist mostly of reworked loess. Holocene gravelly deposits occur at the heads of the fans or within the ranges. These deposits are commonly either silty gravel or lobate pods of gravel without a matrix.

Main Stream Deposits

Deposits of fine-grained Holocene alluvium floor the bottom lands along the perennial streams that cross the basin. This alluvium ranges in thickness from 3 to 5 meters along the Raft River to about 1 meter along Cassia Creek. It is mostly silt, with interbeds of sand, clayey silt, and poorly sorted gravel. Dark gray humic layers are common. Two carbon-14 ages of 8,370 ± 250 and 7,720 ± 250 years were obtained from the lower part of this unit in the southern Raft River basin (Pierce and others, in press). A volcanic ash bed about 2 centimeters thick from about 1.7 meters below the surface of this unit near Bridge has properties similar to the Mazama ash, which is about 6,600 years old (R. E. Wilcox, written communication, 1974). Based on these ages and the stratigraphic relations to upper Pleistocene gravel deposits, this fine-grained alluvium is Holocene in age.

Beneath the fine-grained Holocene alluvium is a well-sorted gravel, which is commonly found in water wells. Exposures of this gravel are scarce, but an excavation 4 meters deep near Bridge did expose 3 meters of fine-grained alluvium overlying well-rounded gravel in an abundant matrix of sand. This gravel represents the main stream equivalent of the younger fan gravel and dates from a time when conditions permitted the entire drainage system to transport gravel. Although the streams transported gravel in late Pleistocene time, in Holocene time they were not competent to carry the entire load of silt through the drainage system, resulting in aggradation of muds along the major drainages (Pierce and Scott, 1982 this volume).

Older deposits of main stream gravel occur in the northern Raft River Valley beneath, adjacent to, and south of the basalt of Yale Road (Figure 2). These gravels are moderately well washed, with only 2 percent silt and clay. Compared with the fan gravels, this main stream gravel generally does not display openwork textures and has about twice as much medium and fine sand (Pierce and others, in press).

The basalt of Yale Road dammed the Raft River and diverted it northeastward to its present course around the edge of the flow. By studying water-well records the old channel and its gravels can be traced beneath the basalt of Yale Road for about 25 kilometers (Pierce and others, unpublished data). The Raft River aggraded, forming the large, nearly horizontal plain east of Idahome after emplacement of the flow across its path.

Loess Deposits

Loess consists of wind-blown silt, with smaller amounts of clay and sand. The geologic record in the Snake River Plain region reveals that there has been little wind erosion or loess deposition during Holocene time. However, as a result of disruption of the plant cover by man, modern dust storms erode and redeposit loess at rates that would be geologically quite significant if continued. The surface soil on the upper loess unit is similar in development to soils on Bonneville Flood deposits and younger fan gravels, which suggests both that the upper loess unit has been stable during Holocene time and that the last period of loess deposition occurred in late Pleistocene time. In the Raft River Valley, stratigraphic sequences with multiple loess units, separated from each other by buried soils, show that this two-fold sequence (loess deposition followed by soil development) has been repeated at least four times in about the last half-million years (Pierce and others, in press). Beneath the upper loess unit, a buried soil developed in loess occurs on the basalt of Yale Road, the basalt of the old railroad grade, and the older gravels of the Raft River. This next older loess unit is considered to be about 150,000 years old, for reasons explained in Pierce and others (1982 this volume, Figure 2, column 10).

Loess thickness varies drastically in the Raft River basin and can be related to the following inferred late Pleistocene conditions: (1) westerly winds, (2) large topographic features upwind, (3) local and regional loess sources that at least, in part, were floodplains of Pleistocene rivers, and (4) age of the underlying deposits.

Loess is generally more than 1 to 2 meters thick on most alluvial fans on the eastern side and less than half a meter thick on the western side of the Raft River basin. On the alluvial fans from the Raft River Mountains at the south end of the basin, loess is generally more than 1 meter thick.

An exception to the pattern of thin loess on the west side of the basin occurs along the traces of structures just west of the KGRA. There the loess is commonly more than 1 meter thick and locally as much as 3 meters thick. The lush vegetation associated with springs and shallow ground water along these structures was apparently also present during

loess deposition and aided in trapping loess and preventing it from being eroded.

For the northern Raft River basin, Pierce and others (in press, Figures 1, 2, and 3) show details of the loess distribution as controlled by large- and small-scale topographic features and the prevailing late Pleistocene wind directions. There, at the margin of the Snake River Plain in the lee of the Cotterel Range, a loess drift accumulated in the Horse Butte area. This drift is mostly the upper loess unit and covers about 100 square kilometers to thicknesses of 12 meters.

STRUCTURAL EVOLUTION OF THE BASIN

The geomorphic setting of the Raft River basin is that of a broad, flat-floored alluvial valley flanked by locally steep-fronted, north-trending mountain ranges. This setting evokes the traditional block-fault structural model for late Cenozoic tectonic activity in the Basin and Range province, long recognized as a region dominated by extensional tectonics. North-trending normal faults are numerous and conspicuous in the Cotterel and Jim Sage Mountains, implying block faulting; but detailed mapping of the area and deep borehole data now require reinterpretation of the structure, with important implications for the geothermal system and regional Cenozoic tectonics.

Mapping has not confirmed the existence of major normal faults along the range fronts (Figure 2). Faults are present on the east flank of the Cotterel Mountains, but offset on any fault is generally less than 200 meters (Pierce and others, in press). Mapping by R. L. Armstrong (unpublished data) in the Sublett Range and by Smith (1982) in the Black Pine Range confirm the absence of range-front faults on the east side of the basin, as first noted by Anderson (1931). Also, frontal faults have not been recognized along the south margin of the basin adjacent to the Raft River Mountains (Compton, 1972, 1975). Normal faults occur at the eastern flank of the southern Jim Sage Mountains and east of the range, but these faults have small displacement; the range is fundamentally a faulted anticline (Figure 2), the east flank of which dips 15 to 35 degrees toward the basin. Steep faults and numerous steep fractures cut the Salt Lake Formation in the KGRA, as observed in core-holes and limited outcrops.

Structures about 3 kilometers east of the Jim Sage Range look like fault scarps (Figure 6), but trenching across these features shows they are not. No offsets with the east side down were observed. The contact between a unit of unfaulted bouldery alluvium and the underlying indurated greenish tuffaceous sand of the Salt Lake Formation dips 4 degrees for 50 meters across the structurally disturbed zone, whereas the gradient of the alluvial fan surface is about 1.5 degrees. This suggests that tilting across this zone accounts for about two-thirds the relief across it. The bottom of the trench exposed three vertical filled fissures about 10-30 centimeters wide cutting partially indurated sand of the Salt Lake Formation. Vertical offsets of about 10 centimeters occur across two of these fissures, each with the west, or mountain, side down. These filled fissures are locally associated with emergence of ground water in the trench bottom and appear aligned with the zones of higher, lusher vegetation (Figure 6). The loess mantling the fan gravels thickens several times in the vicinity of the vertical fractures, apparently as a result of its being trapped by lusher vegetation localized along this disturbed zone during times of loess deposition. This thickening of the loess accounts for the remainder of the relief, and for the several escarpments in the structurally disturbed zone (Figure 6). The age of these structures is middle Quaternary or older as indicated both by unaffected units in the upper part of the trench and along strike to the north. These trench exposures favor interpretation of this disturbed zone as formed by extension above a subhorizontal fault rather than a high-angle fault, although a genetic relationship between the zones and the numerous high-angle faults in the basin fill cannot be ruled out.

A steep, northeast-trending tectonic feature, the "Narrows structure" or "Narrows zone" (Figure 1), was postulated from indirect geologic and geophysical evidence (Williams and others, 1976; Mabey and others, 1978a). The nature of this feature is somewhat enigmatic; it lies along a regional northeast-trending magnetic zone interpreted to be a basement feature (Mabey and others, 1978b), and it forms the southern limit of gravity and magnetic highs in the western part of the basin (Mabey and others, 1978a). Yet seismic refraction studies (Ackerman, 1979) and deep seismic reflection profiles do not show this feature (Ackerman, written communication, 1980); its significance in the Cenozoic history is unknown.

Subsurface studies based on deep drilling in the KGRA showed that the basin fill, which is made up of tilted and faulted beds of the Salt Lake Formation, rests on a relatively flat, unbroken surface of early Paleozoic(?) and Precambrian rocks (Covington, 1977a, 1977b, 1977c, 1977d, 1978, 1979a, 1979b). No intervening upper Paleozoic rocks are present even though thick successions of these rocks occur in the surrounding ranges. Subsurface data also indicate many faults and fractures in the fill and the presence

of a tectonic breccia at the Tertiary-Precambrian contact. Mabey and others (1978a) postulated low-angle gravity faulting from the Jim Sage Mountains toward the Raft River basin, with the principal glide plane being the Salt Lake Formation-Precambrian boundary and with displacements of up to 3 kilometers. Seismic reflection profiles across the southern part of the basin in the area of the KGRA confirm the structural complexity of the basin fill, the absence of offset of the basement surface, and the presence of low-angle normal, listric faults. Major low-angle faulting of late Tertiary age is also known to have occurred within the Salt Lake Formation east of the Grouse Creek Mountains (Todd, 1975; Compton and others, 1977; Miller and others, 1980).

Our concept of the late Cenozoic structural history of the Raft River basin that has evolved from surface mapping and geophysical and subsurface studies is one of gravity-induced movement along low-angle glide surfaces (Covington, 1980; Pierce and others, in press). About 20 to 40 million years ago, greatly increased crustal heat flow accompanied emplacement of gneiss domes in a stress field of strong regional extension, culminating in marked uplift of the mountains relative to the surrounding basins. A detachment surface (perhaps the plane of an earlier thrust fault) developed between masses of lower and upper Paleozoic rocks on the domes. The upper Paleozoic rock masses moved eastward on the detachment surface away from the rising gneiss domes, eventually forming the present Sublett and Black Pine Ranges. The ever-widening trough between the gneiss domes and the eastward-moving allochthonous block was filled with tuffaceous sediments; listric glide faults and low-angle faults developed in the fill. Figure 5 is a generalized, partly diagrammatic structure section extending from the Jim Sage Mountains to the east side of the basin. Two sets of listric faults are portrayed; east-dipping faults are shown as generally younger than west-dipping ones, a relationship suggested by the seismic profiles. These faults and subsidiary fractures, some of which have moved in the Pleistocene and possess the potential for future movement, and the detachment surface at the bottom of the basin fill make up the complex plumbing of the geothermal system. It is unlikely, however, that the faults of this system are the primary conduits that introduce hot water from depth; none extends to depths that, with the ambient geothermal gradient, would supply water at temperatures as high as those observed (Williams and others, 1976).

The Jim Sage Volcanic Member, which forms the Cotterel and Jim Sage Mountains, was erupted only 9 to 10 million years ago into a long, narrow moat east of the Albion Mountains; it was subsequently displaced no more than a kilometer or so eastward along the detachment surface. The relations shown on the geologic map (Figure 2) suggest right-lateral offset, along inferred east-west-trending transcurrent faults, between the Cotterel and Jim Sage Mountains and between the hills of rhyolite north and south of the Raft River Narrows. Possibly the east-west structures mark steep boundaries between major units of the eastward-moving allochthonous mass. A similar suggestion of right-lateral offset between the Sublett and Black Pine Ranges is evident in Figure 1.

Our understanding of the Cenozoic tectonic history is still far from complete and is the subject of our continuing study. Current interpretations differ considerably from earlier concepts of late Cenozoic Basin-Range tectonics, but they are compatible with the structure schemes now evolving from studies in other

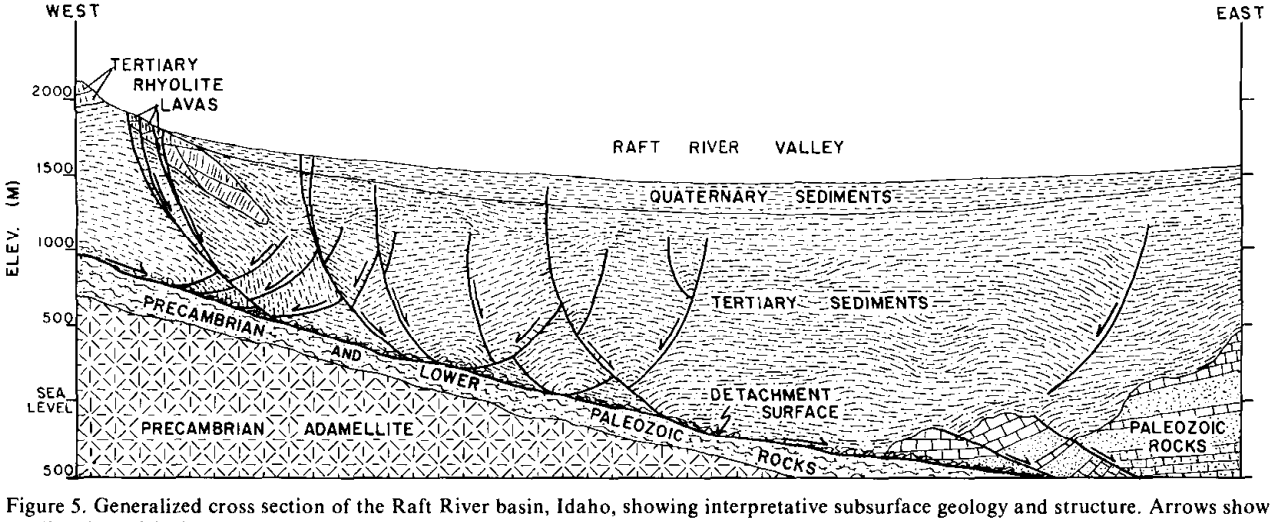

Figure 5. Generalized cross section of the Raft River basin, Idaho, showing interpretative subsurface geology and structure. Arrows show direction of fault movement.

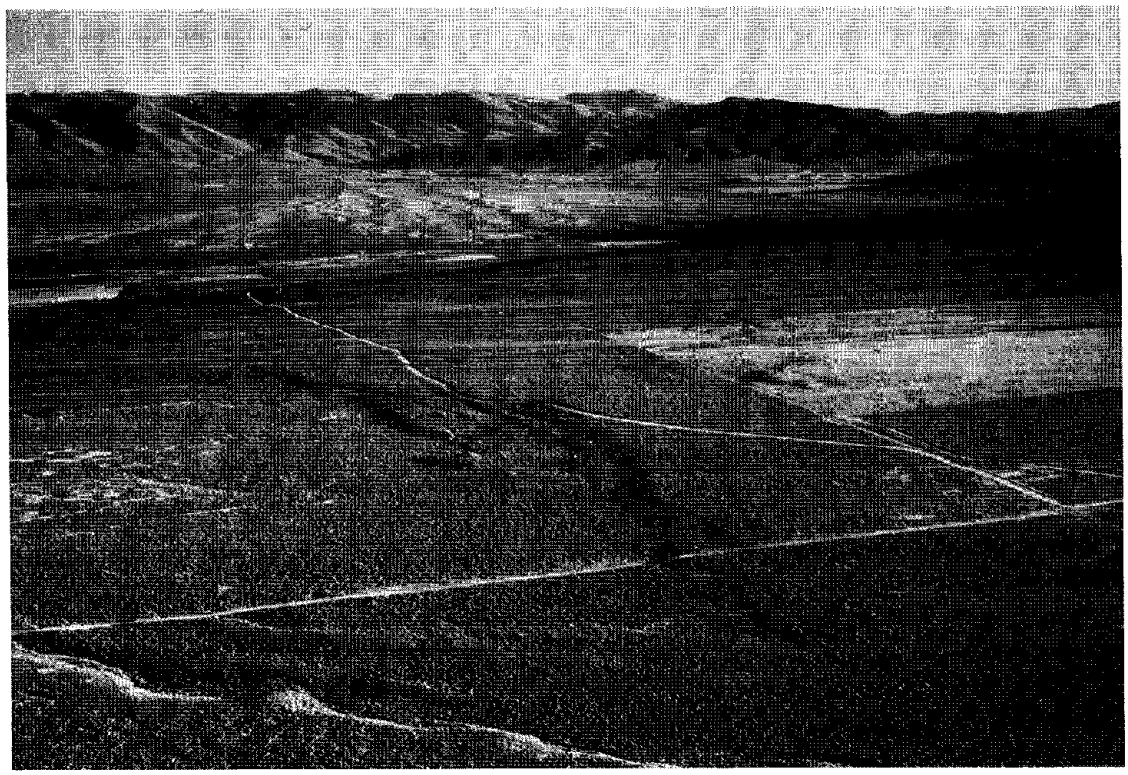

Figure 6. Oblique aerial photograph, looking south, of "Horse well" structurally disturbed zone about 3 kilometers east of the range front of the Jim Sage Mountains. See text for results of trenching studies across this feature. Alluvial-fan gravels on the trend of this structure (lower right) postdate the structural disturbance affecting the alluvium in middle of the photograph.

parts of the Basin and Range province (Davis and Coney, 1979; Crittenden and others, 1978; Howard, 1971; Wright and others, 1974).

REFERENCES

Ackermann, H. D., 1979, Seismic refraction study of the Raft River geothermal area, Idaho: Geophysics, v. 44, p. 216-255.

Anderson, A. L., 1931, Geology and mineral resources of eastern Cassia County, Idaho: Idaho Bureau of Mines and Geology Bulletin 14, 149 p.

Armstrong, R. L., 1968, Mantled gneiss domes in the Albion Mountains, southern Idaho: Geological Society of America Bulletin, v. 79, p. 1295-1314.

_____, 1970, Mantled gneiss domes in the Albion Range, southern Idaho: a revision: Geological Society of America Bulletin, v. 81, p. 909-910.

_____, 1976, The geochronometry of Idaho: Isochron West, no. 15, p. 1-33.

Armstrong, R. L., J. E. Harakal, and W. M. Neill, 1980, K-Ar dating of Snake River Plain (Idaho) volcanic rocks—new results: Isochron West, no. 27, p. 5-10.

Armstrong, R. L., W. P. Leeman, and H. E. Malde, 1975, K-Ar dating, Quaternary and Neogene volcanic rocks of the Snake River Plain, Idaho: American Journal of Science, v. 275, p. 225-251.

Armstrong, R. L., J. F. Smith, H. R. Covington, and P. L. Williams, 1978, Preliminary geologic map of the west half of the Pocatello 1° x 2° quadrangle, Idaho: U. S. Geological Survey Open-File Report 78-533.

Axelrod, D. I., 1964, The Miocene Trapper Creek flora of southern Idaho: University of California Publications in Geological Sciences, v. 51, 180 p.

Bhattacharyya, B. K. and D. R. Mabey, 1980, Interpretation of magnetic anomalies over southern Idaho using generalized multibody models: U. S. Geological Survey Open-File Report 80-457, 49 p.

Carr, W. J. and D. E. Trimble, 1963, Geology of the American Falls quadrangle, Idaho: U. S. Geological Survey Bulletin 1121-G, 44 p.

Christiansen, R. L. and P. W. Lipman, 1972, Cenozoic volcanism and plate tectonic evolution of the western United States II: Late Cenozoic: Royal

Society of London Philosophical Transactions, Series A, v. 271, p. 249-284.

Compton, R. R., 1972, Geologic map of the Yost quadrangle, Box Elder County, Utah, and Cassia County, Idaho: U. S. Geological Survey Miscellaneous Geologic Investigations Map I-672.

———, 1975, Geologic map of the Park Valley quadrangle, Box Elder County, Utah, and Cassia County, Idaho: U. S. Geological Survey Miscellaneous Geologic Investigations Map I-873.

Compton, R. R., V. R. Todd, R. E. Zartman, and C. W. Naeser, 1977, Oligocene and Miocene metamorphism, folding, and low-angle faulting in northwestern Utah: Geological Society of America Bulletin, v. 88, p. 1237-1250.

Covington, H. R., 1977a, Deep drilling data, Raft River geothermal area, Idaho: Raft River geothermal exploration well no. 1: U. S. Geological Survey Open-File Report 77-226, 1 sheet.

———, 1977b, Deep drilling data, Raft River geothermal area, Idaho: Raft River geothermal exploration well no. 2: U. S. Geological Survey Open-File Report 77-243, 1 sheet.

———, 1977c, Deep drilling data, Raft River geothermal area, Idaho: Raft River geothermal exploration well no. 3: U. S. Geological Survey Open-File Report 77-616, 1 sheet.

———, 1977d, Deep drilling data, Raft River geothermal area, Idaho: Raft River geothermal exploration well no. 3, sidetrack C: U. S. Geological Survey Open-File Report 77-883, 1 sheet.

———, 1978, Deep drilling data, Raft River geothermal area, Idaho: Raft River geothermal exploration well no. 4: U. S. Geological Survey Open-File Report 78-91, 1 sheet.

———, 1979a, Deep drilling data, Raft River geothermal area, Idaho, Raft River geothermal production well no. 5: U. S. Geological Survey Open-File Report 79-382, 1 sheet.

———, 1979b, Deep drilling data, Raft River geothermal area, Idaho: Raft River geothermal production well no. 4: U. S. Geological Survey Open-File Report 79-662, 1 sheet.

———, 1980, Subsurface geology of the Raft River geothermal area, Idaho: Geothermal Resources Council Transactions, v. 4, p. 113-115.

Cox, Allan, 1969, Geomagnetic reversals: Science, v. 63, p. 237-245.

Crittenden, M. D., Jr., P. J. Coney, and G. H. Davis, 1978, Penrose Conference report: tectonic significance of metamorphic core complexes in the North American Cordillera: Geology, v. 6, p. 79-80.

Crosthwaite, E. G., 1976, Basic data from five core holes in the Raft River geothermal area, Cassia County, Idaho: U. S. Geological Survey Open-File Report 76-665, 12 p.

Davis, G. H. and P. J. Coney, 1979, Geologic development of the Cordilleran metamorphic core complexes: Geology, v. 7, p. 120-124.

Devine, S. C. and Bill Bonnichsen, 1980, Petrography of drill cores from the Raft River geothermal area, southern Idaho: Idaho Bureau of Mines and Geology Open-File Report 80-10, 81 p.

Eaton, G. P., H. J. Prostka, S. S. Oriel, and K. L. Pierce, 1976, Cordilleran thermotectonic anomaly: I. geophysical and geological evidence of coherent late Cenozoic intraplate magmatism and deformation: Geological Society of America, Abstracts with Programs, v. 8, no. 6, p. 850.

Eaton, G. P., R. R. Wahl, H. J. Prostka, D. R. Mabey, and M. D. Kleinkopf, 1978, Regional gravity and tectonic patterns: their relation to late Cenozoic epeirogeny and lateral spreading in the western Cordillera, *in* R. B. Smith and G. P. Eaton, editors, Cenozoic Tectonics and Regional Geophysics in the Western Cordillera: Geological Society of America Memoir 152, p. 51-92.

Godwin, L. H., L. B. Haigler, R. L. Rioux, D. E. White, L. J. P. Muffler, and R. G. Wayland, 1971, Classification of public lands valuable for geothermal steam and associated geothermal resources: U. S. Geological Survey Circular 647, 17 p.

Hayden, F. V., 1869, U. S. Geological and Geographical Survey Territory Report on Colorado and New Mexico, 3rd Annual Report: U. S. Government Printing Office, Washington, D. C., p. 92.

Howard, K. W., 1971, Paleozoic metasediments in the northern Ruby Mountains, Nevada: Geological Society of America Bulletin, v. 82, p. 259-264.

Mabey, D. R., in press, Geothermal resources of southern Idaho: U. S. Geological Survey Circular.

Mabey, D. R., D. B. Hoover, J. E. O'Donnell, and C. W. Wilson, 1978a, Reconnaissance geophysical studies of the geothermal system in southern Raft River Valley, Idaho: Geophysics, v. 43, no. 7, p. 1470-1484.

Mabey, D. R., Isidore Zietz, G. P. Eaton, and M. D. Kleinkopf, 1978b, Regional magnetic patterns in part of the Cordillera in the western United States, *in* R. B. Smith and G. P. Eaton, editors, Cenozoic Tectonics and Regional Geophysics in the Western Cordillera: Geological Society of America Memoir 152, p. 93-106.

Mansfield, G. R., 1920, Geography, geology, and mineral resources of the Fort Hall Indian Reservation, Idaho: U. S. Geological Survey Bulletin 713, 152 p.

Marvin, R. F., H. H. Mehnert, and D. C. Noble, 1970, Use of Ar^{36} to evaluate the incorporation of air by ash flows: Geological Society of America Bulletin, v. 81, p. 3385-3392.

Miller, D. M., V. R. Todd, R. L. Armstrong, and R. R. Compton, 1980, Geology of the Albion-Raft River-Grouse Creek Mountains area, northwestern Utah and southern Idaho: Geological Society of America, Rocky Mountain Section, 33rd Annual Meeting, Guidebook for field trip.

Mundorff, M. J. and H. G. Sisco, 1963, Ground water in the Raft River basin, Idaho, with special reference to irrigation use, 1956-60: U. S. Geological Survey Water-Supply Paper 1619-CC, 23 p.

Nace, R. L. and others, 1961, Water resources of the Raft River basin, Idaho-Utah: U. S. Geological Survey Water-Supply Paper 1587, 138 p.

Nockolds, S. R., 1954, Average chemical compositions of some igneous rocks: Geological Society of America Bulletin, v. 65, no. 10, p. 1007-1032.

Oriel, S. S., P. L. Williams, H. R. Covington, W. S. Keys, and K. C. Shaver, 1978, Deep drilling data, Raft River geothermal area, Idaho: Standard American Oil Company Malta, Naf and Strevell petroleum test boreholes: U. S. Geological Survey Open-File Report 78-361, 2 sheets.

Pettijohn, F. J., P. E. Potter, and Raymond Siever, 1972, Sand and Sandstone: Springer-Verlag, New York, 618 p.

Pierce, K. L., H. R. Covington, P. L. Williams, and D. H. McIntyre, in press, Geologic map of the Cotterel Mountains and northern Raft River Valley, Idaho: U. S. Geological Survey Miscellaneous Geologic Investigations Map I-1450.

Pierce, K. L., M. A. Fosberg, W. E. Scott, G. C. Lewis, and S. M. Colman, 1982, Loess deposits of southeastern Idaho: age and correlation of the upper two loess units, *in* Bill Bonnichsen and R. M. Breckenridge, editors, Cenozoic Geology of Idaho: Idaho Bureau of Mines and Geology Bulletin 26.

Pierce, K. L. and W. E. Scott, 1982, Pleistocene episodes of alluvial-gravel deposition, southeastern Idaho, *in* Bill Bonnichsen and R. M. Breckenridge, editors, Cenozoic Geology of Idaho: Idaho Bureau of Mines and Geology Bulletin 26.

Russell, I. C., 1902, Geology and water resources of the Snake River Plains of Idaho: U. S. Geological Survey Bulletin 199, 192 p.

Smith, J. F., Jr., 1982, Geologic map of the Strevell 15-minute quadrangle, Cassia County, Idaho: U. S. Geological Survey Miscellaneous Investigations Map I-1403.

Stearns, H. T., Lynn Crandall, and W. G. Steward, 1938, Geology and ground-water resources of the Snake River Plain in southeastern Idaho: U. S. Geological Survey Water-Supply Paper 774, 268 p.

Stewart, J. H., 1978, Basin-range structure in western North America: a review, *in* R. B. Smith and G. P. Eaton, editors, Cenozoic Tectonics and Regional Geophysics in the Western Cordillera: Geological Society of America Memoir 152, p. 1-31.

Todd, V. R., 1975, Late Tertiary low-angle faulting and folding in the Matlin Mountains, northwestern Utah: Geological Society of America, Abstracts with Programs, v. 7, p. 381-382.

Trimble, D. E. and W. J. Carr, 1976, Geology of the Rockland and Arbon quadrangles, Power County, Idaho: U. S. Geological Survey Bulletin 1399, 115 p.

Walker, E. H., L. C. Dutcher, S. O. Decker, and K. L. Dyer, 1970, The Raft River basin, Idaho-Utah as of 1966: a reappraisal of the water resources and effects of ground-water development: Idaho Department of Water Administration Water Information Bulletin 19, 95 p.

Williams, P. L., D. R. Mabey, A. A. R. Zohdy, Hans Ackermann, D. B. Hoover, K. L. Pierce, and S. S. Oriel, 1976, Geology and geophysics of the southern Raft River Valley geothermal area, Idaho, U.S.A., *in* United Nations Symposium on the Development and Use of Geothermal Resources, 2nd, San Francisco, California, May 20-29, 1975, Proceedings, v. 2, p. 1273-1282.

Williams, P. L., K. L. Pierce, D. H. McIntyre, and P. W. Schmidt, 1974, Preliminary geologic map of the southern Raft River Valley, Cassia County, Idaho: U. S. Geological Survey Open-File Report.

Wright, L. A., J. K. Otton, and B. W. Troxel, 1974, Turtleback surfaces of Death Valley viewed as phenomena of extensional tectonics: Geology, v. 2, p. 53-54.

Sequence of Late Cenozoic Deformation in the Blackfoot Mountains, Southeastern Idaho

by

Richard W. Allmendinger[1]

ABSTRACT

The Blackfoot Mountains, located 25 kilometers south-southeast of Idaho Falls, Idaho, are ideally suited for contrasting the styles and ages of Basin and Range and Snake River Plain deformation. An extensive suite of ash-flow tuffs, rhyolite and basalt lava flows, and syntectonic conglomerates record the deformation and uplift of the mountains. Four sets of late Cenozoic high-angle faults have been mapped. The two earlier sets, trending north (older) and east (younger), are best developed on the west side of the range. Most of the Basin and Range style uplift and tilting occurred along the oldest (north-trending) set shortly after the oldest ash flow (dated at 5.86 million years) was deposited on an erosional surface, only remnants of which now remain at the mountain tops between 2,210 and 2,255 meters. Faults of this oldest set do not cut the youngest ash flow (dated at 4.7 million years), which probably lapped around a preexisting mountain range. On the east side of the range, the younger two high-angle fault sets trend northeast (older) and northwest (younger). The older parallels the Snake River Plain and is interpreted as deformation related to flexing and downwarping of the crust adjacent to the plain. The younger fault set is parallel to the Swan Valley graben and the youngest structures on and north of the plain.

Thus, Basin and Range uplift of the Blackfoot Mountains (at a rate of 0.08 centimeter a year) postdates the initiation of late Cenozoic magmatism in the region, but it may predate structures related to downwarping of the Snake River Plain. The youngest, northwest-trending faults and related linear grabens to the east are interpreted as effects of the youngest Basin and Range extension in crust that was not previously thinned during the Proterozoic rifting of western North America. Sparse evidence from the northern part of the Basin and Range province suggests that the eastern boundary of Basin and Range extension may have migrated eastward at rates between 3.5 and 6.5 centimeters a year, but that rate slowed markedly (to 1.7 centimeters a year) at the Wasatch Line separating crust that was thinned during the Proterozoic on the west from nonthinned crust on the east.

[1]Department of Geological Sciences, Cornell University, Ithaca, New York 14853.

INTRODUCTION

The Basin and Range province and Snake River Plain are prominent Cenozoic tectonic provinces in the western United States that intersect in southeastern Idaho. The two provinces contain structures and deposits of roughly the same age, and their detailed interaction is not well understood. Their interaction, however, has important implications because the style and history of Cenozoic deformation and volcanism in the western United States changes from south to north across the Snake River Plain.

Late Cenozoic structures in the Blackfoot Mountains, along the intersection of the two provinces 25 kilometers south of Idaho Falls, Idaho (Figure 1), may reflect Snake River Plain and Basin and Range interaction. Sufficient structures and rocks are present to document the tectonic and morphological development of the area. The history that emerges may have regional implications.

Before the Pliocene the region around the present Blackfoot Mountains had a small amount of local relief. Silicic ash-flow tuffs, probably erupted from the advancing front of the Snake River Plain then located northeast of the area, were deposited on that erosional surface. Rapid uplift along normal faults bounding the west side of the range produced most of the relief observable today within about 1 million years. Snake River Plain volcanics changed composition from silicic to mixed and then to primarily basic rock suites. Northeast-trending faults paralleling the plain may indicate subsequent downwarping of the plain, possibly due to loading of the crust with a thick pile of volcanic rocks. The final event was the

Allmendinger, R. W., 1982, Sequence of late Cenozoic deformation in the Blackfoot Mountains, southeastern Idaho, *in* Bill Bonnichsen and R. M. Breckenridge, editors, Cenozoic Geology of Idaho: Idaho Bureau of Mines and Geology Bulletin 26, p. 505-516.

development of a north-northwest-trending fault set that may be related to the development of the Swan Valley grabens farther to the east. These latest structures did not produce significant uplift or modification of relief in the Blackfoot Mountains.

The Blackfoot Mountains were first mapped and described by Mansfield (1952), who provided an excellent background for later studies but misinterpreted many key relations regarding Cenozoic structures and deposits (see Armstrong and Cressman, 1963, for a discussion of similar problems). The present paper is based on new mapping of the northern Blackfoot Mountains (Allmendinger, 1980) covering the southern half of the Ammon 15-minute quadrangle (Bone and Wolverine 7½-minute quadrangles). Pre-Cenozoic structural geometry and related deformation are discussed elsewhere (Allmendinger, 1981, in press).

REGIONAL GEOLOGIC SETTING

The Basin and Range province, as used here, refers to the system of discrete linear mountain ranges and broad sedimentary basins that developed as a result of normal faulting and regional extension, beginning 17 million years ago in central Nevada (Stewart, 1971; Zoback and Thompson, 1978). This definition is as much morphological as it is structural and is specifically intended to exclude mid-Tertiary extensional tectonics recently documented in many parts of the Great Basin (for example, Davis and Coney, 1979). The Wasatch Front forms the impressive eastern morphological boundary of much of the Basin and Range province, even though geophysical characteristics of the province extend farther east (Smith, 1978). In southeastern Idaho, however, there is no distinct morphological boundary. Instead, the isolated mountain blocks and "jackstraw" arrangement of normal faults that are typical of most of the province give way eastward to a system of long, linear grabens separated by broader mountain ranges. These features resemble structures on the western margin of the Colorado Plateau (Best and Hamblin, 1978), except that the faults in Idaho may be controlled by older thrust belt structures (for example, Royse and others, 1975). The Intermountain seismic belt (Smith and Sbar, 1974; Smith, 1978) generally corresponds to this zone of linear grabens. The grabens may represent structures developed during the eastward propagation of the Basin and Range, or perhaps a change in style of extensional tectonism during the Quaternary.

The area described here lies on the southeast side of the eastern Snake River Plain between Twin Falls,

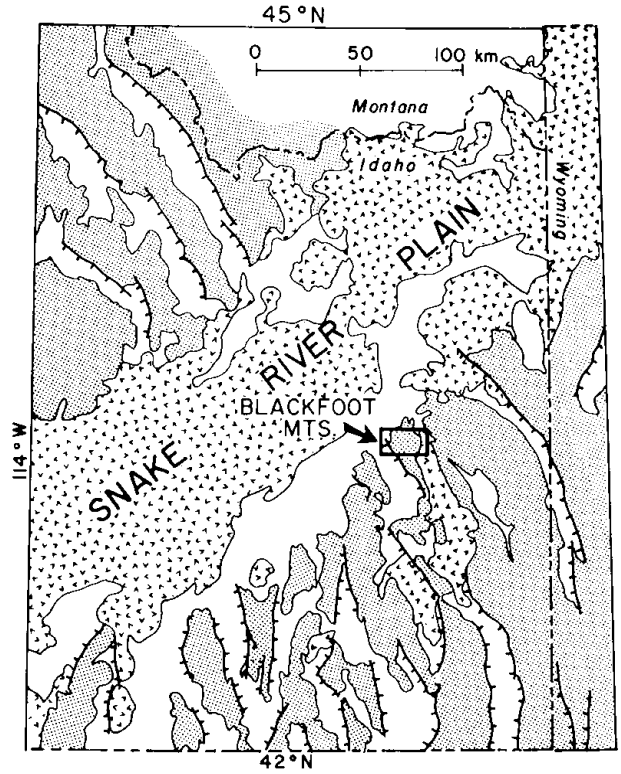

Figure 1. Generalized tectonic index map of southeastern Idaho and vicinity, showing the location of the Snake River Plain and the Blackfoot Mountains. Only selected normal faults are shown. Note the narrow belt of linear grabens near Idaho-Wyoming border. Open pattern—late Cenozoic basin fill and alluvium, vee pattern—late Cenozoic volcanic rocks of the Snake River Plain, stippled pattern—pre-Cenozoic sedimentary and metamorphic rocks.

Idaho, and Yellowstone National Park. This area first became active about 10 million years ago in south-central Idaho and can be traced, becoming younger to the northeast, by a series of silicic and basic volcanic assemblages (Armstrong and others, 1975; Leeman, 1982a this volume). Initial deposits of these assemblages are voluminous silicic ash-flow tuffs, which grade upward into tuffs that interfinger with basalts and clastic sediments. The final deposits are dominantly basalt lavas with interbedded clastics (Armstrong and others, 1975).

The Snake River Plain is a product of magmatism and volcanism. Geophysically, the plain is characterized by a gravity high, suggesting crustal thinning, and excluding Yellowstone, normal to below normal heat flow (less than 1.5 heat flow units) (Mabey and others, 1975; Kuntz and Holcomb, 1979; Blackwell, 1978; Eaton and others, 1978; Mabey, 1982 this volume). The northwest alignment of basalt vents, tilting, and northwest-trending fractures and faults all suggest that the youngest deformation on the eastern

part of the plain is extension in a northeast-southwest direction (Kuntz and Holcomb, 1979).

CENOZOIC GEOLOGY OF THE NORTHERN BLACKFOOT MOUNTAINS

Interpretation of late Cenozoic tectonics requires an understanding of the morphological development of the region. The wide variety and distribution of Cenozoic rocks in the northern Blackfoot Mountains record much of the history of uplift and erosion.

STRATIGRAPHY

Late Cenozoic units, derived mainly from local source areas, are continental and were deposited on an irregular topographic surface. As a result, the Cenozoic section is quite heterogeneous, and any one unit has a limited distribution which is more dependent on the morphology at the time of its deposition than on later erosion. Each unit is described briefly in the following paragraphs, starting with the oldest, and is depicted in Figure 2, which also contains the summary of the structural and tectonic evolution of the Blackfoot Mountains. Figure 3 shows the distribution of late Cenozoic rocks and faults in the southern half of the Ammon 15-minute quadrangle.

Oldest Ash-Flow Tuff

The oldest Cenozoic volcanic unit preserved in the Blackfoot Mountains is rich in phenocrysts which, in addition to feldspar and quartz, include a relatively high proportion of small mafic grains. The mafic grains increase in abundance higher in the flow, probably indicating a zoned magma chamber. Pumice fragments are sparce or absent, but this may only be due to the extreme degree of welding and devitrification. No inclusions of country rock have been observed. The ash-flow tuff is purple-brown and stained yellow on weathered surfaces. Most float commonly is platy. The basal part of the tuff is a thin, black vitrophyre with well-developed perlitic cracking. The unit has normal magnetic polarity based on five field determinations with a hand-held fluxgate magnetometer. Large, zoned plagioclases (An_{18-22}) are the most abundant phenocrysts. Subhedral sanidine is next most common, followed by small, anhedral, partially resorbed quartz. The mafic mineral is not possible to identify due to alteration and plucking during thin section grinding; however, eight-sided cross-sections suggest pyroxene. Very small, euhedral zircons are scarce accessories.

The oldest ash flow is limited in distribution to the tops of several of the highest hills within the range at or above 2,225 meters (Figure 3). These high points are remnants of the oldest erosional surface in the mountain range. The ash-flow tuff, therefore, was originally deposited on a surface with a gentle relief prior to uplift of the Blackfoot Mountains. Originally named the Gannett peneplain (Mansfield, 1952), this terminology is not used here because it implies unsubstantiated correlations with other erosional surfaces in southeastern Idaho. In the northern half of the Ammon quadrangle, the ash flow has been noted at the bottom of Henrys Creek Canyon at an elevation of 1,600 meters (T. 1 N., R. 39 E., sec. 29 SE¼). Since its deposition, the Blackfoot Mountains have been uplifted at least 625 meters relative to Henrys Creek owing to later tectonic activity. Wherever found, the oldest ash-flow tuff directly overlies pre-Cenozoic sediments and is overlapped by younger Cenozoic deposits. Thus, the tuff is probably the oldest Cenozoic unit preserved in the Blackfoot Mountains. Potassium-argon dating of sanidine separates from the tuff, collected in the interior of the range suggests an age of 5.86 ± 0.18 million years (B. Dalrymple, personal communication, 1979). The age and lithology indicate a possible correlation with part of unit "A" of the Tuff of Heise (Prostka and Embree, 1978; Embree and others, 1982 this volume) in the Heise, Idaho, area northeast of the Blackfoot Mountains.

Middle Ash-Flow Tuff

The middle ash flow resembles the oldest lithologically, but is thinner, somewhat less crystal rich, and largely glassy. This ash flow is also grayer, though both have the same platy weathered aspect. Where both are present, there are no intervening sediments, and field magnetic data do not distinguish them. The middle tuff is now exposed only on the east flank of the Blackfoot Mountains where it dips gently east.The spatial relations and lithologies of the two oldest ash flows suggest a close genetic relation; they may be cooling units of the same flow or flow complex. However, the more limited distribution of the middle ash flow might indicate that some uplift of the Blackfoot Mountains had occurred.The radiometric age of the middle ash flow is not known.

Sediments of the Salt Lake Formation

The name "Salt Lake Formation" is applied throughout southeastern Idaho and northern Utah to a poorly defined group of Neogene conglomerates, diamictites, sandstones, and tuffs generally assumed

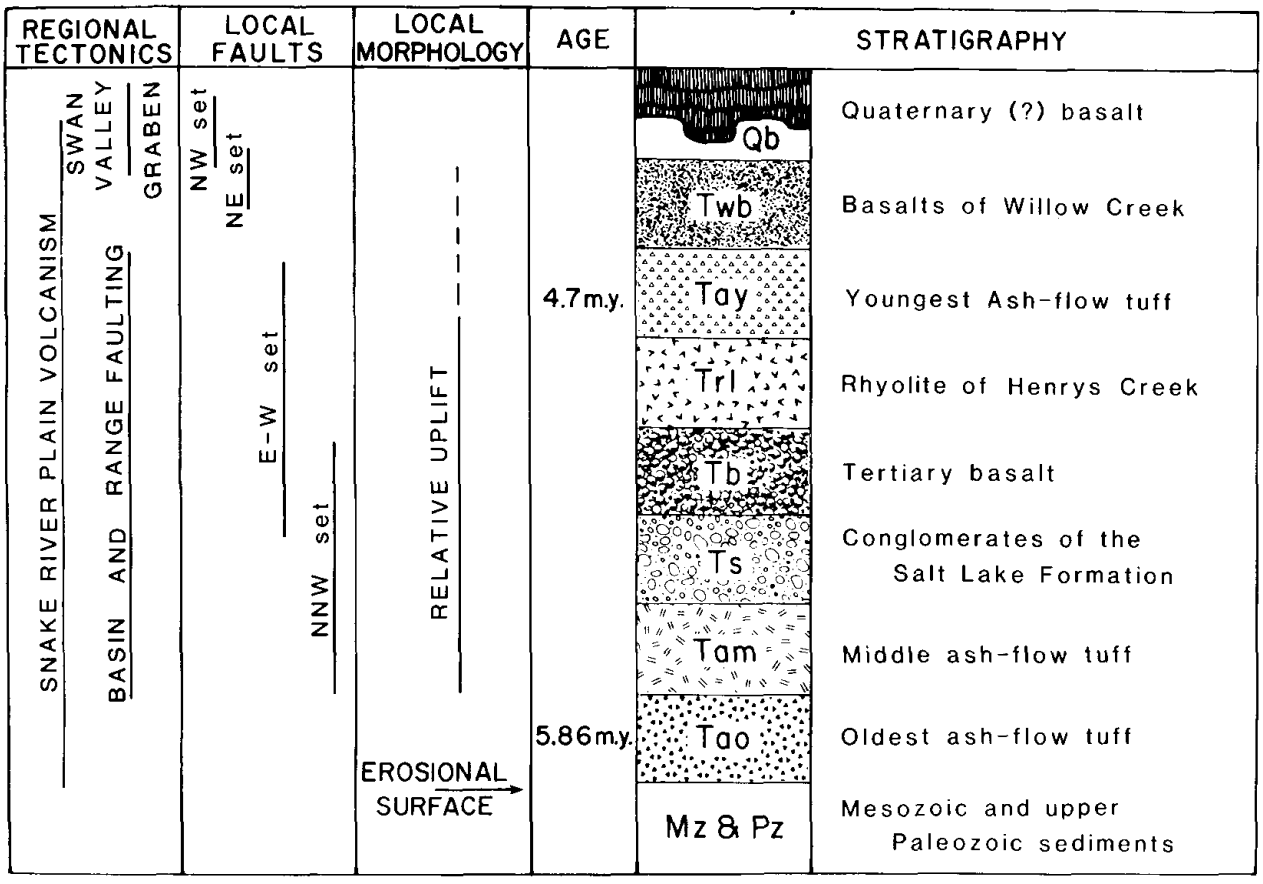

Figure 2. Composite late Cenozoic stratigraphic section and summary of tectonic and morphological evolution of the Blackfoot Mountains. Section does not show relative thicknesses of units and is not linear in age.

to be related to Basin and Range tectonics (Mansfield, 1927; Williams, 1964). Trimble (1976; Trimble and Carr, 1976) has abandoned the name in favor of the Starlight Tuff, which includes as the middle member, the tuff of Arbon Valley (9.6 million years; Armstrong and others, 1975). This usage has been followed by other workers near the Snake River Plain (Armstrong and others, 1975). The Salt Lake nomenclature is used here without great conviction for the conglomerate and finer grained clastic rocks, while the tuff units are described and mapped separately.

Most of the Salt Lake Formation here is conglomerate with well-rounded, locally derived clasts. Most of the clasts are cobble size, but boulders up to 0.7 meter in diameter are not unusual. Sand, silt, and volcanic ash make up the matrix. The Salt Lake also includes beds of sandstone and siltstone, and outside the southern half of the Ammon quadrangle, thick air-fall tuffs are interbedded with other lithologies (Mansfield, 1952).

The main occurrence of conglomeratic Salt Lake Formation in the Blackfoot Mountains is in the southwest corner of the Ammon quadrangle (Figure 3). There, the unit underlies younger Tertiary basalts and the youngest ash-flow tuff. Locally derived lithologies and a crude reduction in clast size moving away from major north-northwest- and east-west-trending late Cenozoic fault sets suggest that sediments of the Salt Lake Formation were derived in part from uplift along those faults. Conglomerate is also exposed on the northeast flank of the Blackfoot Mountains (Figure 3) where, in addition to clasts from Cretaceous and older rocks, it contains rounded cobbles and boulders of the oldest and middle ash flows. The youngest ash-flow tuff overlies the Salt Lake Formation.

On the basis of these relations, the conglomerates on both sides of the Blackfoot Mountains probably represent a single episode of rapid uplift and erosion that took place after the deposition of the two oldest ash-flow tuffs but before the eruption of the Tertiary basalt or the youngest tuff. The much greater amount of conglomerate on the west side of the range is probably due to the presence of the north-northwest-

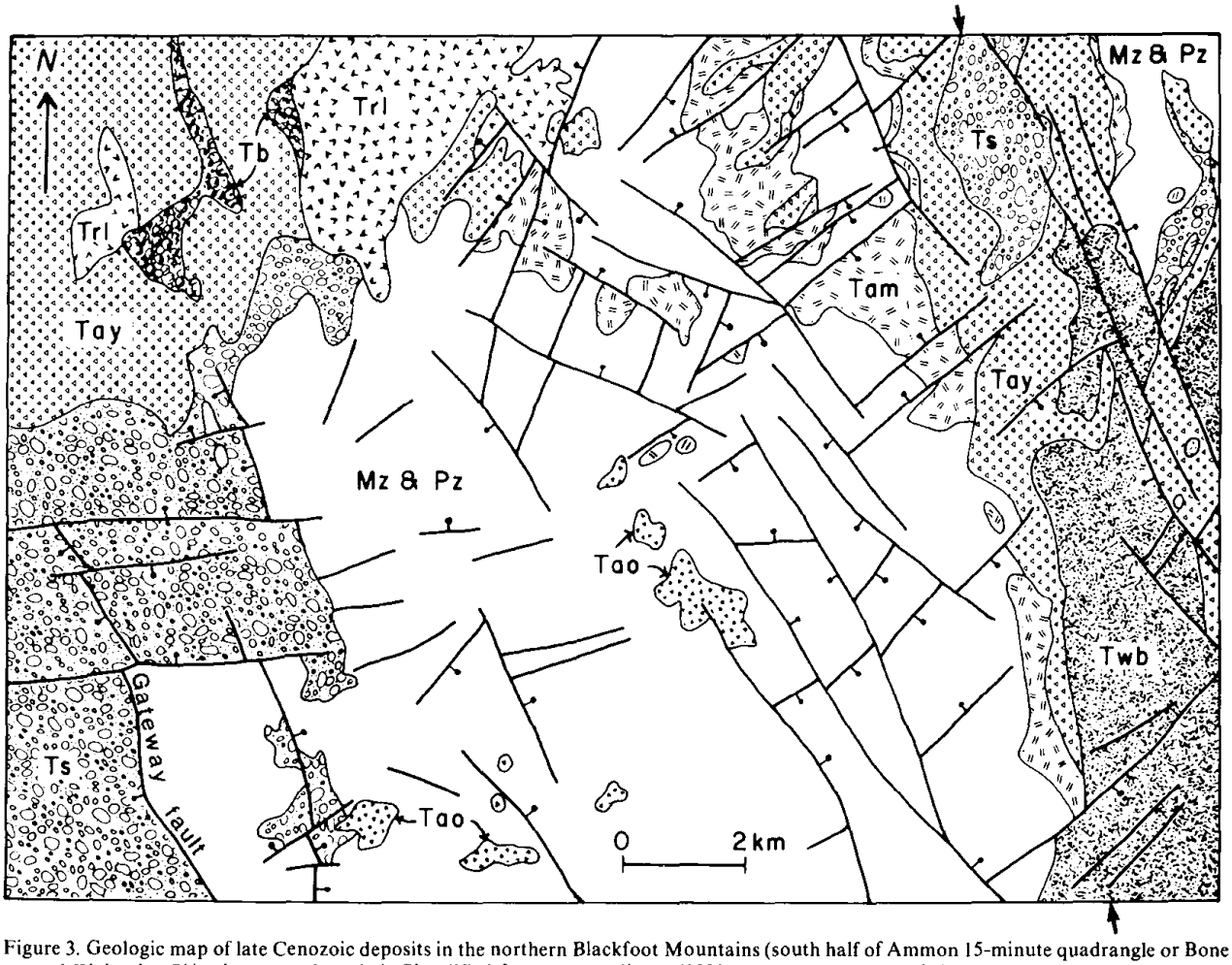

Figure 3. Geologic map of late Cenozoic deposits in the northern Blackfoot Mountains (south half of Ammon 15-minute quadrangle or Bone and Wolverine 7½-minute quadrangles). Simplified from Allmendinger (1980); contacts have been inferred beneath Quaternary cover (not shown). The white area (upper Paleozoic and Mesozoic sediments) generally corresponds to higher elevations in the interior of the mountains. See Figure 2 for key to units. Normal faults with ball and bar on downthrown side. Arrows on north and south edges on east side of map show location of hinge line for tilting.

and east-west-trending faults and the development of the greatest relief on that side. Since the Salt Lake conglomerate described here is younger than 5.86 million years, it cannot be temporally correlative with the Starlight Tuff of Trimble (1976).

Tertiary Basalt

At scattered localities on the northwest side of the mountains, a dense, fine-grained basalt flow rests on Salt Lake conglomerate (Figure 3). In hand specimen, small phenocrysts of altered olivine are most apparent. Thin section examination of the rock shows an ophitic texture and primary composition of augite and plagioclase (An_{60-70}) with smaller groundmass olivine (in addition to the olivine phenocrysts). This mineral assemblage suggests an olivine tholeiite similar to those discussed by Leeman (1982b this volume) and by Fiesinger and others (1982 this volume). Four outcrops of the basalt have reversed magnetic polarity.

The distribution of the Tertiary basalt shows that it was erupted after relative uplift began but before the present morphology of the Blackfoot Mountains was fully established. The source area is unknown but may have been located to the west or northwest.

Rhyolite of Henrys Creek

The rhyolite of Henrys Creek is a pinkish gray rhyodacite lava flow which is exposed over a large area in the northwest part of the Blackfoot Mountains (Figure 3) near Henrys Creek. Outcrops of the rhyolite are commonly flow banded, and autobreccia

is locally well developed. A thick vitrophyre is present at the base. The lava flow has normal magnetic polarity. The rhyolite is easily distinguished from the silicic ash-flow tuffs, but where it lacks flow banding, it resembles the two oldest ash flows and has similar phenocryst compositions. The source of the lava was apparently at the northern edge of the Bone 7½-minute quadrangle (southeast quarter of the Ammon 15-minute quadrangle). This may also have been the source for the oldest and middle ash-flow tuffs. Scattered outcrops of the rhyolite are present in the northwest corner of the southern half of the Ammon 15-minute quadrangle and farther west in the Goshen quadrangle (J. Karlo, personal communication, 1978).

Youngest Ash-Flow Tuff

The youngest ash-flow tuff is the most widespread of any late Cenozoic deposits (Figure 3). The ash flow is rhyolitic in composition, with sparse to abundant phenocrysts of sanidine, quartz, and subsidiary plagioclase. Brown and brick-red pumice fragments are typical of parts of the flow, as is microporosity. The unit commonly has abundant, large lithophysae. Welding ranges from very slight to moderate, but few localities are as strongly welded as the older ash flows. The youngest ash flow forms the cap rock on hogbacks on the flanks of the mountains and was never deposited in the interior of the range. The youngest ash flow is probably a series of closely related flows or cooling units (not differentiated in this study) that correlate with unit C of Prostka and Embree (1978). Air-fall tuff is interlayered with the ash flow, and conglomerates of the Salt Lake Formation underlie it.

The youngest ash-flow tuff clearly had a source area to the northeast (H. Prostka, personal communication, 1977; Prostka and Embree, 1978). A sample of the unit from the northern half of the Ammon quadrangle was dated at 4.7 ± 0.10 million years (Armstrong and others, 1975). By the time this flow was deposited, the Blackfoot Mountains were fully uplifted.

Basalts of Willow Creek

Three basalt flows have been mapped in the Willow Creek valley on the east side of the Ammon quadrangle (Figure 3). The oldest and youngest are very limited in exposure compared with the middle flow. The oldest crops out only at one small locality in the canyon of Willow Creek (T. 2 S., R. 40 E., sec. 10). This flow has a fine-grained granular texture and lacks phenocrysts. Fresh surfaces have an olive-green tint. Weathered surfaces are dark chocolate brown. Outcrops are agglomeratic and flow banded, with large vesicles increasing in abundance toward the top of the unit. Columnar jointing is absent.

The middle Willow Creek basalt flow occurs throughout the eastern third of the southern half of the Ammon quadrangle. The rock has abundant equigranular plagioclase phenocrysts set in a dark matrix. Also apparent is well-developed microporosity due to finely disseminated vesicles. The mineralogy, texture, and grain size give the rock a salt-and-pepper appearance on both fresh and weathered surfaces; that is its most characteristic feature. At numerous localities, the middle basalt flow directly overlies the youngest ash flow. Where Willow Creek has cut through the flow, numerous large blocks have slid into the river valley posing a significant landslide hazard. In thin section, the basalt has a subophitic texture with abundant plagioclase and subordinate augite grains. There are sparse anhedral olivine crystals in the groundmass as well.

The youngest basalt of the Willow Creek group is present only in the northeastern corner of the map area (T. 1 S., R. 40 E., sec. 4; T. 1 N., R. 40 E., sec. 32). It has a dense, very fine-grained matrix and large (up to 1 centimeter), sparsely distributed plagioclase phenocrysts. Vesicles, though not abundant, are quite large. This upper basalt was an intracanyon flow, filling part of a deep, narrow canyon of the ancestral Willow Creek. Willow Creek has since exhumed most of this old valley and has cut 30 to 40 meters deeper. Small intracanyon basalt flows are also present on the northwest side of the mountains, but their relation to the youngest basalt of Willow Creek is unknown.

None of the Willow Creek basalt flows has been dated radiometrically, and their magnetic polarity has not been determined. They have not been significantly tilted but are cut by some of the younger faults in the region. The basalt flows directly overlie one another where the contacts are exposed. The morphology and drainage system of the Blackfoot Mountains was well established by the time of the basaltic volcanism.

SUMMARY: DEVELOPMENT OF THE LATE CENOZOIC MORPHOLOGY OF THE BLACKFOOT MOUNTAINS

The distributions and ages of the late Cenozoic rocks in the study area provide an excellent basis for interpreting the morphological evolution of the present-day Blackfoot Mountains. Parts of this evolution are dated by the potassium-argon ages of the oldest and youngest ash-flow tuffs. Dating of other units in the sequence should provide added resolution to the timing of these events and rates of uplift.

During the Neogene, before the deposition of the

oldest ash-flow tuff 5.86 million years ago, the morphology of the area was that of a gently rolling erosional surface underlain by deformed pre-Cenozoic sediments. Relative uplift commenced during or shortly after the middle ash flow was deposited, and the uplift was probably most rapid during the deposition of the Salt Lake conglomerate. The greatest relief during this phase was on the west side of the range where the greatest thickness of conglomerates are presently found. By the time the Tertiary basalt was deposited, the interior of the Blackfoot area constituted a significant positive element. The Blackfoot Mountains had attained their present form by the time the youngest ash-flow tuff was deposited 4.7 million years ago. Since then, relative uplift slowed considerably.

STRUCTURE

The late Cenozoic structure of the northern Blackfoot Mountains is dominated by high-angle faults and, locally, tilting and broad, gentle warping. All of these features postdate the oldest ash-flow tuff and are related to the evolution of the Basin and Range province and Snake River Plain.

High-angle faults in the Blackfoot area are shown in Figure 3. In the interior of the mountains where Tertiary deposits are missing, it is difficult to distinguish some steep faults of different orogenic affinities, since Mesozoic tear faults have the same trend as one of the late Cenozoic sets. The steep Cenozoic faults can be divided into four classes based on their orientation: (1) north-northwest-trending, west-dipping set, (2) east-west-trending set, (3) northeast-trending set, and (4) northwest-trending set. The relative ages have been established by cross-cutting relations, stratigraphic relations, and distribution. The four sets are described below from oldest to youngest.

Fault Set 1 (North-Northwest Trending)

The oldest Tertiary faults in the northern Blackfoot Mountains are restricted in occurrence to the western margin of the range where they comprise the prominent, range front-bounding fault system (Figure 3). This system of faults is responsible for the first and largest amount of uplift. The youngest sediments demonstrably offset are conglomerates of the Salt Lake Formation. One of the best and most typical examples of set 1 faults can be seen in the field at the Gateway to Wolverine Creek Narrows (T. 2 S., R. 38 E., secs. 2 W½, 3 E½, 11 W½). Referred to below as the Gateway fault, it has a strike of N. 20° W. The minimum stratigraphic throw, based on the presence of the upper Wells Formation on the downthrown side of the fault, is 775 meters, but the actual dip slip may be closer to 1,000 meters. Beds of the Salt Lake Formation dip 20-25 degrees east into the fault plane. Thus, they were not draped unconformably over this surface but were actually cut and deformed by faulting.

Data bearing on the dip of the Gateway fault are contradictory. Using the standard three-point construction method on the fault trace (mapped as the contact between Tertiary conglomerate and Mississippian limestone), the fault surface was determined to dip 20 degrees west. However, to the northwest across a younger east-west fault (Figure 3), the Gateway fault has a steeper dip and at this locality is actually a package of several parallel, closely spaced high-angle faults. A further indication that the Gateway fault has a moderate dip is provided by a seismic reflection survey across it, about 10 kilometers and a few intervening east-west faults to the south in the Paradise Valley quadrangle. The seismic profile shows a normal fault with a dip of about 45 degrees west that cuts all older thrust faults (R. Standaert, oral communication, 1978).

With these data, it is not known whether the Gateway fault is a moderately dipping, relatively straight fault, or a listric normal fault that merges into an older thrust surface, as suggested by Royse and others (1975) for other normal faults farther east. The fault probably has not been rotated to a shallow west dip by younger faulting farther east. Such faults are not known in the interior of the range, and more importantly none of the late Cenozoic sediments or volcanic rocks in the interior of the range are tilted more than 5 degrees east.

Because the Gateway fault represents the only major mountain front fault system and the structural relief is greatest on the west side of the range (Allmendinger, 1980), the Blackfoot Mountains must be a large tilted block. The hinge line for tilting can be approximately located where the regional eastward dip of the middle and upper ash-flow tuffs ceases and changes to smaller fault blocks with a variety of dips. This location can be determined to within a kilometer in an east-west direction, and the hinge line parallels the Bone Road on the east side of the mountains, 13 kilometers east of the Gateway fault. Given the location of the hinge line and the angle of tilting during the late Cenozoic (4 degrees eastward, based on the regional dip of the middle ash flow), the amount of relative uplift can be determined. The simple geometric construction shown in Figure 4 is based on the assumption that the area of the Blackfoot Mountains was a relatively flat erosional surface prior to movement on the Gateway fault and that there are no other major fault sets responsible for the

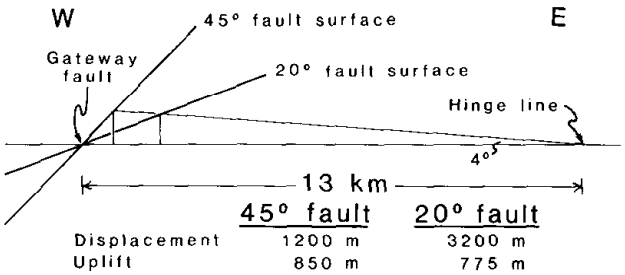

Figure 4. Geometric construction to determine amount of Late Cenozoic uplift of the Blackfoot Mountains based on the observed regional tilts and hinge lines in the oldest ash-flow tuffs. Table at bottom shows cases for a 45 degree fault and a 20 degree fault.

principal uplift of the mountains. Two cases are shown with displacements and uplifts given for the 45 degree fault and the 20 degree fault. Although the displacements for the two cases vary by nearly a factor of three, the relative uplifts are very similar, ranging between 775 and 850 meters. These figures are close to the minimum stratigraphic throw, suggesting that the assumptions are valid. If the uplift occurred in about 1 million years (the difference in age between the youngest and oldest ash-flow tuffs), the relative rate of uplift was approximately 0.08 centimeter a year.

Fault Set 2 (East-West Trending)

The north-northwest faults are cut by a second set that trends due east or east-northeast. Set 2 is also developed only on the west side of the mountains. The faults dip steeply northward (at least 55 degrees) and are downthrown on the north. Many of this set have a scissors or hinge fault geometry (Dennis, 1967), with a pivot point near the Cenozoic and pre-Cenozoic contacts, and an increasing displacement toward the Snake River Plain. Though most of the conglomerate of the Salt Lake Formation was derived during earlier north-northwest faulting, some of it was probably also deposited during movement along the east-west faults. These faults do not offset units younger than the youngest ash-flow tuff (Figures 2 and 3).

Fault Set 3 (Northeast Trending)

Northeast-trending, high-angle faults are most conspicuous on the north and east sides of the Blackfoot Mountains, whereas on the northwest side they may be obscured by ubiquitous loess. The faults commonly have a consistent strike of N. 40°-50° E., though a few trend more to the north-northeast. The dominant trend is almost exactly parallel to the Snake River Plain at this locality. Faults of this set have steep dips, mainly small offsets, and are downthrown either to the north or south (Figure 3). They cut all late Cenozoic units at least up to the intracanyon basalt in Willow Creek.

Since these faults parallel the nearby Snake River Plain but do not appear to be formed until after the deposition of all of the silicic ash-flow tuffs in the Blackfoot Mountains (that is, at least 1 million years after the start of Snake River Plain volcanism in the immediate vicinity), they may best be interpreted as a structural response to mechanical loading of the crust with the thick pile of volcanics on the plain to the northwest. Thus these structures do not appear to be evidence of premagmatism rifting, nor do they indicate any significant strike-slip faulting parallel to the southeast margin of the plain.

Fault Set 4 (Northwest Trending)

Faults of the third set are offset by the youngest faults in the Blackfoot Mountains, which strike to the northwest (N. 35°-60° W.) and have steep dips. Displacements on this set are generally less than 75 meters, with a negligible amount of tilting. These faults cut the youngest intracanyon basalt flows in the range, but there is no conclusive evidence that any Quaternary deposits are cut by this youngest set.

The youngest fault set is oriented parallel to the alignments of the youngest basalt vents and fractures on the Snake River Plain and also to the Grand Valley fault and Swan Valley graben (for example, Staatz and Albee, 1966). The Swan Valley graben and other long, linear grabens along the eastern margin of the Basin and Range province lie within the Intermountain seismic belt (Smith and Sbar, 1974; Smith, 1978). These northwest-trending structures are indicative of young and on-going extension and represent the initial structures formed at the eastern margin of the Basin and Range province. Their structural morphology differs from that in more maturely developed parts of the Basin and Range province, and in the Blackfoot Mountains this probably represents a renewed or much-slowed episode of Cenozoic extension.

Warping

Since dips are relatively gentle in all late Cenozoic deposits, it is commonly not possible to determine whether the inclinations are due to initial depositional processes or later deformation. Ash-flow tuffs may have gentle primary dips resulting from cooling and compaction over buried topography. On the northwest side of the Blackfoot Mountains, loess has obscured at least 90 percent of the bedrock. Scattered exposures are abundant enough, however, to make a

structural contour map on the top of the youngest ash flow (Figure 5). The contours define two broad anticlinal warps with northwest-trending axes. Because the orientations are the same, these warps may well be related to the youngest fault set. Limited exposures obscure whether the ash flow is cut by the faults or the warps represent fault-drape folds.

CONCLUSIONS: LATE CENOZOIC EVOLUTION OF THE NORTHERN BLACKFOOT MOUNTAINS

The late Cenozoic tectonic history of the northern Blackfoot Mountains and general vicinity is summarized below, starting with the oldest events:

(1) Before the Pliocene an erosional surface was developed in the region of the future Blackfoot Mountains. Any topographic relief related to pre-Pliocene structures had largely been removed before the development of Basin and Range and Snake River Plain tectonism (as defined in the introduction).

(2) The oldest ash-flow tuff was deposited on the undeformed erosional surface 5.86 million years ago. This initial evidence of the Snake River Plain silicic assemblages predates any structures responsible for the relative uplift of the present Blackfoot Mountains.

(3) Deposition of conglomerates of the Salt Lake Formation signals rapid uplift along north-northwest- and east-trending faults on the west side of the Blackfoot Mountains, forming a gently (4 degree) east-tilted block. Most of the present relief of the Blackfoot Range was created during this single phase of relative uplift between 4.7 and 5.86 million years ago. This deformation can be characterized as typical Basin and Range based on the morphological definition used here.

(4) The character of Snake River Plain volcanism in the area changed from silicic to mixed silicic-basic assemblages sometime during the latter phases of uplift that typifies the Basin and Range province.

(5) Since 4.7 million years ago, volcanism in the immediate vicinity of the Blackfoot Mountains has been entirely basaltic. Following the initiation of the basalt phase, northeast-trending faults that parallel the regional trend of the Snake River Plain were formed. These faults are interpreted as resulting from loading and flexure of the crust by Snake River Plain volcanics.

(6) The youngest structures in the region are northwest-trending faults that are probably related to the formation of the Swan Valley graben and similar linear grabens to the south and east. In the Blackfoot Mountains, however, significant uplift had ceased prior to activity on the final fault set. The uplift

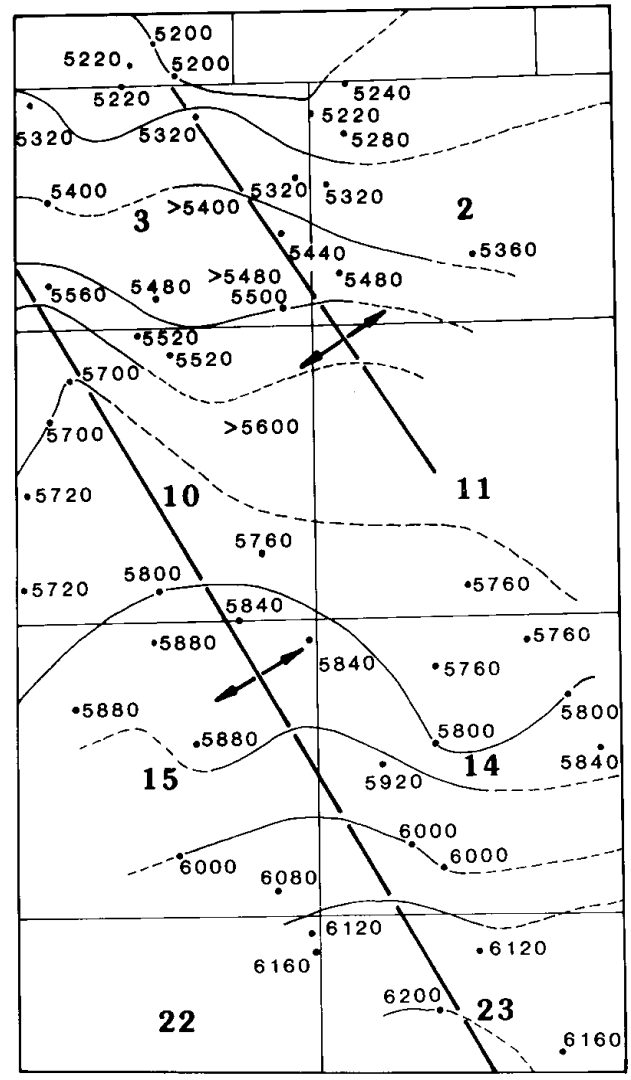

Figure 5. Structural contour map (elevations in feet) on the top of the youngest ash-flow tuff on the northwest side of the Blackfoot Mountains. Sections shown are in T. 1 S., R. 38 E. Anticlinal axes shown with dashed lines. Loess covers most of the area.

history and the location of the Intermountain seismic belt east of the area suggest that large earthquakes might not be expected today in the Blackfoot Mountains; however, landslides in Willow Creek Valley are a significant hazard.

One of the most interesting results of this study is that no normal faults paralleling the Snake River Plain appear to have formed prior to or synchronous with the earliest phase of local magmatic activity. There is little evidence that major northeast-trending rifting preceded magmatism. On this basis, the eastern arm of the plain is probably not a typical intracontinental rift, and is perhaps best considered dominantly

a magmatic feature rather than a simple structural feature.

IMPLICATIONS FOR BASIN AND RANGE TECTONICS

The age data presented here support the idea that the eastern edge of Basin and Range deformation has migrated eastward from its origin in north-central Nevada 17 million years ago (Stewart, 1971; Zoback and Thompson, 1978) to its present locus of activity in the Intermountain seismic belt. From the dates on initial Basin and Range uplift in north-central Nevada, the Raft River Mountains of northwest Utah (Compton and others, 1977), and the Blackfoot Mountains, a crude estimate of the rate of migration of the eastern boundary can be determined (Figure 6). The boundary moved eastward at rates of 6.5 centimeters a year in eastern Nevada during the middle and late Miocene, of 3.5 centimeters a year across northwest Utah and southeastern Idaho in the late Miocene, and of 1.7 centimeters a year across the present zone of linear grabens east of the Blackfoot Mountains from Pliocene to Recent. Clearly such calculations, based on only four data points in this complex region, involve numerous assumptions, many of which cannot be substantiated with presently available data. However, it is interesting to speculate on the reasons for the apparent steady decrease in the rate of migration.

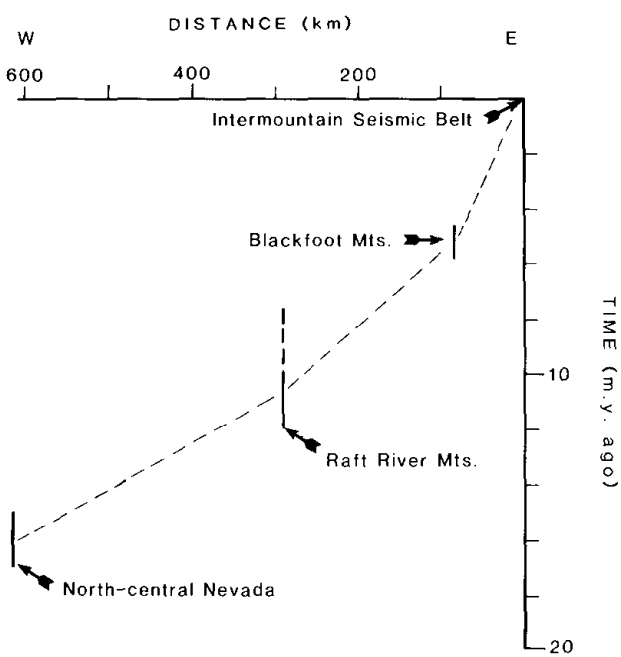

Figure 6. Graph showing possible rate of eastward migration of the eastern boundary of the Basin and Range province, based on initial uplifts of present mountain ranges plotted against distance from eastern edge of province. Data from Stewart (1971), Zoback and Thompson (1978), Compton and others (1977), and this report. The present edge of the Basin and Range is taken as the eastern edge of the Intermountain seismic belt (Smith and Sbar, 1974).

The position where the rate slowed from 3.5 centimeters to 1.7 centimeters a year is roughly correlative with the hinge at the transition from shelf facies to miogeoclinal facies of late Proterozoic and Paleozoic sediments (Armstrong and Oriel, 1965; Stokes, 1976), based on palispastic reconstructions after Royse and others (1975). This regional hinge line may be interpreted as the eastern limit of significant crustal thinning during the Proterozoic rifting of western North America. Although Precambrian crystalline basement is inferred to extend to central Nevada, the crust there was probably significantly thinned as a consequence of that Proterozoic rifting event. A hypothesis worth further testing is that Basin and Range extension was easiest in the thinnest continental crust (that is, in central Nevada), but eastward propagation became increasingly difficult as thicker and thicker continental crust was found to the east. The rate of migration may have slowed most markedly when Cenozoic extensional tectonism encountered continental crust, which was relatively undeformed either in the Proterozoic rifting or during Mesozoic thrust faulting.

ACKNOWLEDGMENTS

The mapping on which this paper is based was part of the U. S. Geological Survey's Snake River Plain project under the direction of S. S. Oriel. I am grateful to H. Prostka, M. Kuntz, and R. Holcomb for discussions of late Cenozoic tectonics of southern Idaho. B. Dalrymple kindly dated the oldest ash-flow tuff for me. B. Bonnichsen and S. S.Oriel provided excellent reviews of the manuscript, though they may not agree with all the conclusions. Special thanks must go to Steven S. Oriel who first introduced me to the geology of this fascinating region.

REFERENCES

Allmendinger, R. W., 1980, Geologic map of the south half of the Ammon quadrangle, Bingham and Bonneville Counties, Idaho: U. S. Geological Survey Miscellaneous Field Studies Map, MF-1259.

———, 1981, Structural geometry of the Meade plate in the northern Blackfoot Mountains, south-

eastern Idaho: American Association of Petroleum Geologists Bulletin, v. 65, p. 509-525.

_____, in press, Analysis of microstructures in the Meade plate of the Idaho-Wyoming foreland thrust belt, U.S.A.: Tectonophysics.

Armstrong, F. C. and E. R. Cressman, 1963, The Bannock thrust zone, southeastern Idaho: U. S. Geological Survey Professional Paper 374-J, 22 p.

Armstrong, F. C. and S. S. Oriel, 1965, Tectonic development of Idaho-Wyoming thrust belt: American Association of Petroleum Geologists Bulletin, v. 49, p. 1847-1866.

Armstrong, R. L., W. P. Leeman, and H. E. Malde, 1975, K-Ar dating, Quaternary and Neogene volcanic rocks of the Snake River Plain, Idaho: American Journal of Science, v. 275, p. 225-251.

Best, M. G. and W. K. Hamblin, 1978, Origin of the northern Basin and Range province: implications from the geology of its eastern boundary, *in* R. B. Smith and G. P. Eaton, editors, Cenozoic Tectonics and Regional Geophysics of the Western Cordillera: Geological Society of America Memoir 152, p. 313-340.

Blackwell, D. D., 1978, Heat flow and energy loss in the western United States, *in* R. B. Smith and G. P. Eaton, editors, Cenozoic Tectonics and Regional Geophysics of the Western Cordillera: Geological Society of America Memoir 152, p. 175-208.

Compton, R. R., V. R. Todd, R. E. Zartman, and C. W. Naeser, 1977, Oligocene and Miocene metamorphism, folding, and low-angle faulting in northwestern Utah: Geological Society of America Bulletin, v. 88, p. 1237-1250.

Davis, G. H. and P. J. Coney, 1979, Geologic development of Cordilleran metamorphic core complexes: Geology, v. 7, p. 120-124.

Dennis, J. G., editor, 1967, International tectonic dictionary: American Association of Petroleum Geologists Memoir 7, p. 49.

Eaton, G. P., R. R. Waho, H. J. Prostka, D. R. Mabey, and M. D. Kleinkopf, 1978, Regional gravity and tectonic patterns: their relation to late Cenozoic epeirogeny and lateral spreading in the western Cordillera, *in* R. B. Smith and G. P. Eaton, editors, Cenozoic Tectonics and Regional Geophysics of the Western Cordillera: Geological Society of America Memoir 152, p. 51-92.

Embree, G. F., L. A. McBroome, and D. J. Doherty, 1982, Preliminary stratigraphic framework of the Pliocene and Miocene rhyolites, eastern Snake River Plain, Idaho, *in* Bill Bonnichsen and R. M. Breckenridge, editors, Cenozoic Geology of Idaho: Idaho Bureau of Mines and Geology Bulletin 26.

Fiesinger, D. W., D. W. Perkins, and B. J. Puchy, 1982, Mineralogy and petrology of Tertiary-Quaternary volcanic rocks in Caribou County, Idaho, *in* Bill Bonnichsen and R. M. Breckenridge, editors, Cenozoic Geology of Idaho: Idaho Bureau of Mines and Geology Bulletin 26.

Kuntz, M. A. and R. T. Holcomb, 1979, Structural and volcanic characteristics of the Snake River Plain, Idaho: Geological Society of America, Abstracts with Programs, v. 11, p. 88.

Leeman, W. P., 1982a, Development of the Snake River Plain-Yellowstone Plateau province, Idaho and Wyoming: an overview and petrologic model, *in* Bill Bonnichsen and R. M. Breckenridge, editors, Cenozoic Geology of Idaho: Idaho Bureau of Mines and Geology Bulletin 26.

_____, 1982b, Olivine tholeiitic basalts of the Snake River Plain, Idaho, *in* Bill Bonnichsen and R. M. Breckenridge, editors, Cenozoic Geology of Idaho: Idaho Bureau of Mines and Geology Bulletin 26.

Mabey, D. R., 1982, Geophysics and tectonics of the Snake River Plain, Idaho, *in* Bill Bonnichsen and R. M. Breckenridge, editors, Cenozoic Geology of Idaho: Idaho Bureau of Mines and Geology Bulletin 26.

Mabey, D. R., D. L. Peterson, and C. W. Wilson, 1975, Regional gravity and magnetic studies of the Snake River Plain: Geological Society of America, Abstracts with Programs, v. 7, p. 624-625.

Mansfield, G. R., 1927, Geography, geology, and mineral resources of part of southeastern Idaho: U. S. Geological Survey Professional Paper 152, 409 p.

_____, 1952, Geography, geology, and mineral resources of the Ammon and Paradise Valley quadrangles, Idaho: U. S. Geological Survey Professional Paper 238, 92 p.

Proffett, J. M., 1977, Cenozoic geology of the Yerington district, Nevada, and implications for the nature and origin of Basin and Range faulting: Geological Society of America Bulletin, v. 88, p. 247-266.

Prostka, H. J. and G. F. Embree, 1978, Geology and geothermal resources of the Rexburg area, eastern Idaho: U. S. Geological Survey Open-File Report 78-1009, 15 p.

Royse, F., M. A. Warner, and D. L. Reese, 1975, Thrust belt structural geometry and related stratigraphic problems, Wyoming-Idaho-northern Utah: Rocky Mountain Association of Geologists Symposium, p. 41-54.

Smith, R. B., 1978, Seismicity, crustal structure and intraplate tectonics of the interior of the western Cordillera, *in* R. B. Smith and G. P. Eaton, editors, Cenozoic Tectonics and Regional Geophysics of the Western Cordillera: Geological Society of America Memoir 152, p. 111-144.

Smith, R. B. and M. L. Sbar, 1974, Contemporary tectonics and seismicity of the western United States with emphasis on the Intermountain seismic belt: Geological Society of America Bulletin, v. 85, p. 1205-1218.

Staatz, M. H. and H. F. Albee, 1966, Geology of the Garns Mountain quadrangle, Bonneville, Madison, and Teton Counties, Idaho: U. S. Geological Survey Bulletin 1205, 122 p.

Stewart, J. H., 1971, Basin and Range structure: a system of horsts and grabens produced by deep-seated extension: Geological Society of America Bulletin, v. 82, p. 1019-1043.

———, 1972, Initial deposits in the Cordilleran geosyncline: evidence of a Late Precambrian (850 m.y.) continental separation: Geological Society of America Bulletin, v. 83, p. 1345-1360.

Stokes, W. L., 1976, What is the Wasatch Line?: Rocky Mountain Association of Geologists Symposium, p. 11-25.

Trimble, D. E., 1976, Geology of the Michaud and Pocatello quadrangles, Bannock and Power Counties, Idaho: U. S. Geological Survey Bulletin 1400, 88 p.

Trimble, D. E. and W. J. Carr, 1976, Geology of the Rockland and Arbon quadrangles, Power County, Idaho: U. S. Geological Survey Bulletin 1399, 115 p.

Williams, J. S., 1964, The age of the Salt Lake Group in Cache Valley, Utah-Idaho: Utah Academy of Science, Arts, and Letters Proceedings, v. 41, pt. 2, p. 269-277.

Zoback, M. L. and G. A. Thompson, 1978, Basin and Range rifting in northern Nevada: clues from a mid-Miocene rift and its subsequent offsets: Geology, v. 6, p. 111-116.

Chapter 9

Stratigraphy of Lacustrine Sediments Western Snake River Plain

Fish Biostratigraphy of Late Miocene to Pleistocene Sediments of the Western Snake River Plain, Idaho

by

Gerald R. Smith[1], Krystyna Swirydczuk[2], Peter G. Kimmel[3], and Bruce H. Wilkinson[1]

ABSTRACT

The Chalk Hills and Glenns Ferry Formations represent a large lacustrine system with peripheral and capping fluvial and floodplain facies. Both formations are bounded by unconformities. They are separated by at least 1 million years at exposures along the south flank of the Snake River Plain, but were possibly continuous some place in the basin.

The Chalk Hills Formation is late Miocene (about 8.5 to 5.5 million years). Fish fossils define three biostratigraphic zones: (1) An upper zone immediately above and below the lower Horse Hill ash layer is characterized by the presence of *Mylocheilus inflexus* and *M. copei* (two large minnows with molar teeth) and *Hucho larsoni* (a large troutlike fish). (2) A middle zone, well below the lower Horse Hill ash layer and above the Hot Spring limestone, is characterized by the presence of *Mylopharodon doliolus* (a primitive minnow) and *Orthodon onkognathus* (a herbivorous minnow), as well as the three species in the upper zone. (3) A lower zone, presently known only from Brown Creek in Owyhee County, is characterized by the salmonlike fish, *Smilodonichthys*, as well as the five species in the upper and middle zones.

The Pliocene Glenns Ferry Formation lacks the six species listed above; it is characterized by the presence of *Prosopium prolixus* (a whitefish), *Mylocheilus robustus* (a minnow with molar teeth), and *Kerocottus divaricatus* (an endemic sculpin). Middle and upper zones within the Glenns Ferry Formation are defined by a reduction in the tooth formula of *Mylocheilus robustus* and the addition of four species of sculpins. The upper zone, defined by the presence of *Kerocottus pontifex* and *hypoceras* (spiny sculpins) and *Myoxocephalus antiquus* and *idahoensis* (northern sculpins), possessed the richest fish fauna (24 species) known in ancient or Holocene western North America.

Most lake beds studied are transgressive, beach-shoreface sands and offshore silts of the Glenns Ferry Formation. They are capped by a regressive sequence exposed at about 3,400 feet along the southern basin margin and at about 2,900 feet near the center of the basin. Floodplain silts with a distinct Pliocene fish assemblage are exposed from 2,900 feet to 3,300 feet at the Hagerman Cliffs. Pleistocene floodplain deposits are exposed at about 2,700 feet in the center of the basin. Following drainage of the lake, possibly through the Pleistocene capture at Hells Canyon, about half of the fish species became extinct.

INTRODUCTION

> *...the entire basin, from the Rocky Mountains to the Blue Mountains of Oregon, was a freshwater lake, on whose bottom was deposited a curious succession of sand and clay beds.... At the exposures of these rocks in the cañon-walls of the present drainage system are found ample evidences of the kind of life which flourished in the lake itself and lived upon its borders. Savage fishes, of the garpike type [trouts], and vast numbers of cyprinoids, together with mollusks, are among the prominent water-fossils.... From being a wide and beautiful expanse of water, edged by winding mountain shores, with forest-clad slopes containing a fauna whose remains are now charming those light-minded fellows, the paleontologists, the scene has entirely changed, and a monotonous, blank desert now spreads itself as far as the eye can reach.*
>
> Clarence King (1903, p. 229)
> on the Snake River Plain

Clarence King (1878) recognized that the late Cenozoic history of the western United States was domi-

[1]Museum of Paleontology and Department of Geological Sciences, University of Michigan, Ann Arbor, Michigan 48109.
[2]Exploration Research Division, Conoco, Inc., Ponca City, Oklahoma 74601.
[3]Department of Chemistry, George Mason University, Fairfax, Virginia 22030.

Smith, G. R., Krystyna Swirydczuk, P. G. Kimmel, and B. H. Wilkinson, 1982, Fish biostratigraphy of late Miocene to Pleistocene sediments of the western Snake River Plain, Idaho, *in* Bill Bonnichsen and R. M. Breckenridge, editors, Cenozoic Geology of Idaho: Idaho Bureau of Mines and Geology Bulletin 26, p. 519-541.

nated by a vast lacustrine system with climate, life, and geological processes markedly different from those of today. E. D. Cope (1870, 1883a, 1883b) distinguished separate, smaller lakes and assigned Pliocene and Pleistocene ages to some of them, primarily on the basis of fossil fishes collected by J. C. Schenk of King's Survey of the 40th Parallel and by Cope's collectors, Charles Sternberg and J. L. Wortman. The question that attracted King and Cope is still of interest: What were the environments and processes responsible for the late Cenozoic freshwater deposits of the Snake River Plain? After 100 years of research the answers are still interconnected with the evolutionary history of the associated fishes.

In this paper we describe several sedimentary units in the western Snake River Plain and discuss their stratigraphy and environments of deposition as illuminated by fossil fishes. Our purpose is to describe the distribution and variation of fishes that occupied the western Snake River Plain during the late Miocene, Pliocene, and early Pleistocene. Fishes are the most common macroscopic fossils in these lake beds, and they provide a stratigraphic biozonation as well as new information about environment and climate.

Malde and Powers (1962) provided the most complete description of the stratigraphy of the Snake River Plain. They classified sedimentary and volcanic rocks of Miocene to Pleistocene series into seven formations of the Idaho Group, and they documented the history of stratigraphic understanding from Cope's "Lake Idaho" to their conception, which is used here.

We are especially interested in the four major units containing lake deposits exposed south of the Snake River from southeastern Oregon to Hagerman, Idaho. These are, from oldest to youngest: (1) the Poison Creek Formation of late Miocene age—mostly fluvial deposits generally south and west of Murphy, Owyhee County, Idaho, unconformably deposited on the Miocene Idavada Volcanics; (2) the Chalk Hills Formation—lacustrine and fluvial deposits of late Miocene age unconformably deposited on Idavada rocks south of Grand View and Bruneau in Owyhee County; (3) the Glenns Ferry Formation—lacustrine, fluvial, and floodplain sediments of Pliocene age, unconformably deposited on the Chalk Hills Formation or on basalts over the whole length of the western Snake River Plain; and (4) the Bruneau Formation—middle Pleistocene lake beds and basalts resting on the Glenns Ferry Formation from Hagerman to Murphy, Idaho. All four formations dip toward the axis of the basin. The lake beds of the Bruneau Formation and the fluvial deposits of the Poison Creek Formation contain a few fish fossils, and we have little to add to the account of Malde and Powers. The sediments of the Chalk Hills and Glenns Ferry Formations, especially the lacustrine silts and fine, shoreface sands south of Grand View and Bruneau, are superficially similar. They contain distinctive ash beds and fossil fishes and are bounded by unconformities that allow some clarification, but their stratigraphic relations are complicated in many places.

We focus on the Chalk Hills and Glenns Ferry Formations because the two lakes in which they were deposited were the site of evolution of the most diverse fish fauna in late Cenozoic western North America (Smith, 1981). The fishes permit biostratigraphic zonation consistent with the recognized rock stratigraphy. The resulting correlations are comparable with those based on volcanic ashes (Swirydczuk and others, 1982 this volume) and suggest extensions of stratigraphy to surrounding areas.

PALEONTOLOGICAL BACKGROUND

Paleontological contributions to stratigraphy of the Idaho Group are based primarily on mammalian and molluscan remains, summarized by Malde and Powers (1962), Taylor (1966), Zakrzewski (1969), Shotwell (1970), Bjork (1970), and Neville and others (1979). The major difficulty with paleontological evidence has been the inability to distinguish between temporal and environmental changes in faunal composition.

The Poison Creek Formation, best exposed in Reynolds Creek, has produced few fossils. It consists of fine-grained terrigenous clastics and siliceous volcanic ash deposits. The fauna, including horse teeth (*Hipparion*) identified by Buwalda (1924) and Shotwell (in Malde and Powers, 1962) and an otter, in the absence of the horse *Pliohippus*, is correlated with the Clarendonian Juntura and Deer Butte Formations of southeast Oregon (Shotwell, 1963, p. 28). The overlying Banbury Basalt is in turn overlain by Chalk Hills Formation, which contains a basalt dated by Armstrong and others (1975) as at least 8.4 million years old. The Chalk Hills Formation contains fluvial sands and lacustrine sands and silts that yielded beaver (*Dipoides*), rhinoceros, camel, horse (*Hipparion*), sloth (*Megalonyx*), and a molluscan fauna that indicate a Hemphillian age (Malde and Powers, 1962; Armstrong and others, 1975). Fission-track dates on volcanic ashes indicate sedimentation until about 5 or 6 million years ago (Kimmel, 1982 this volume).

The Glenns Ferry Formation has produced molluscs and at least two large Blancan mammalian faunas of broad stratigraphic significance. The late Pliocene age of these fossils was clearly indicated by molluscan evidence (Taylor *in* Malde and Powers,

1962; Taylor, 1966). Unfortunately, several sources of confusion led to a Pleistocene interpretation of the mammalian evidence, prior to clarification through potassium-argon dates of 3.5, 3.3, and 3.2 million years on the Deer Gulch lava flow and two ashes at Hagerman (Evernden and others, 1964), a fission-track date of 3.75 ± .36 million years on zircon from the Peters Gulch Ash Bed (Izett, 1981), and thorough mammalian paleontology by Zakrzewski (1969) and Bjork (1970), working with Claude W. Hibbard.

The lack of laterally continuous beds has prevented an understanding of the relationship of the Hagerman sequence (over 100 fossil localities) to localities at Sand Point (across the Snake River from Hammett), Jackass Butte (west of Grand View), and the lake beds south of Grand View and Bruneau. Hibbard and Zakrzewski (1967) presented evidence, in the form of variation in dental characters of mice referred to *Ophiomys*, that the Sand Point fauna is younger than the Hagerman and that the Grand View local fauna is still younger. Although Shotwell (1970) argued that these faunas could be the same age because differences among them might have been environmental, Zakrzewski (1969) and Bjork (1970) showed that the Hagerman local fauna was early Blancan and Pliocene and that the Grand View local fauna was latest Blancan and early Pleistocene. Correlation of mammalian and magnetic stratigraphy by Neville and others (1979) verified this, placing the Hagerman fauna correlative to the Gilbert reversed and Gauss normal epochs, and the Sand Point and Grand View faunas correlative to the Matuyama reversed epoch. Bjork (1970, p. 13) placed the Sand Point fauna nearer the Hagerman fauna. The Blancan chronology by Neville and others (1979) is in accord with that usually accepted, differing from that of Armstrong and others (1975), in suggesting younger dates for the Glenns Ferry Formation and the Blancan.

Interpretation of the above relationships was advanced by Malde's (1972) measured sections and facies interpretations. Malde recorded extensive fluvial deposits in addition to the floodplain and lacustrine sediments. However, we interpret some of the fluvial sands as nearshore lacustrine sands, partly on the basis of fish paleontological evidence.

The major sedimentary units referred to in the following are (1) transgressive shoreface sands and offshore silts of the Chalk Hills Formation, and (2) transgressive shoreface sands and offshore silts overlain by regressive sands and floodplain silts of the Glenns Ferry Formation. The floodplain deposits at Hagerman probably span much of the time represented by the Glenns Ferry Formation. Upper Glenns Ferry floodplain deposits extend westward in local outcrops across the entire study area. The transgressive beach deposits, however, including major phosphatic, oolitic, and conglomeratic systems, seem to progress eastward and southward, marking the expansion of the Glenns Ferry lake. Regressive sands, overlain by poorly sorted silts, are found capping lake deposits from Shoofly Creek to Castle Creek. The Chalk Hills and Glenns Ferry sands that we interpret as shoreface sand deposits have produced the most abundant and diverse fish collections; the Glenns Ferry floodplain deposits produce a mixture of fishes and other vertebrates.

FISH PALEONTOLOGY

Fishes have been collected from 190 localities in the Chalk Hills and Glenns Ferry Formations between Hagerman, Idaho, and Adrian, Oregon (Figure 1). Of 35,000 specimens, mostly bone fragments picked from the ground surface, 14,000 have been classified. Thirty-nine kinds of fishes are recognized. Some have limited range, defining stratigraphic zones; others indicate lacustrine or fluvial habitat preference. Our method of analysis has been to compare vertical distributions of kinds of fishes from section to section, testing potential zone limits with lateral correlation based on ashes and other sedimentological markers. Comparisons of fish occurrences with sediment characteristics and the presence or absence of mammalian fossils led to hypotheses about environments of deposition. These hypotheses are tested by their internal consistency relative to the general sedimentological model and evolutionary patterns here described.

The fishes are members of six families common to the late Cenozoic of North America (Smith, 1981). These include whitefish, trouts, and salmon (family Salmonidae) in the genera *Prosopium*, *Rhabdofario*, *Hucho*, *Oncorhynchus*, *Smilodonichthys*, and perhaps *Salmo*. The most abundant remains are from the suckers (family Catostomidae), strictly freshwater fishes represented by *Chasmistes*, of zoogeographic importance (Taylor, 1960; Miller and Smith, 1981) and *Catostomus*, which has at least five species in the system. The most diverse family is the Cyprinidae (minnows), a strictly freshwater group which gained access to North America from northeast Asia probably in the Oligocene and which shows its earliest and most extreme western American diversification in the Miocene and Pliocene lakes described here. The genera are *Acrocheilus* and *Orthodon*, large herbivores; *Ptychocheilus*, a large carnivore; *Mylocheilus*, a group of molluscivores; *Idadon*, a small herbivore; *Mylopharodon*, a medium-sized molluscivore (?) that preferred fluvial habitats; and *Gila* and *Richardsonius*, medium- and small-sized generalists. The fourth

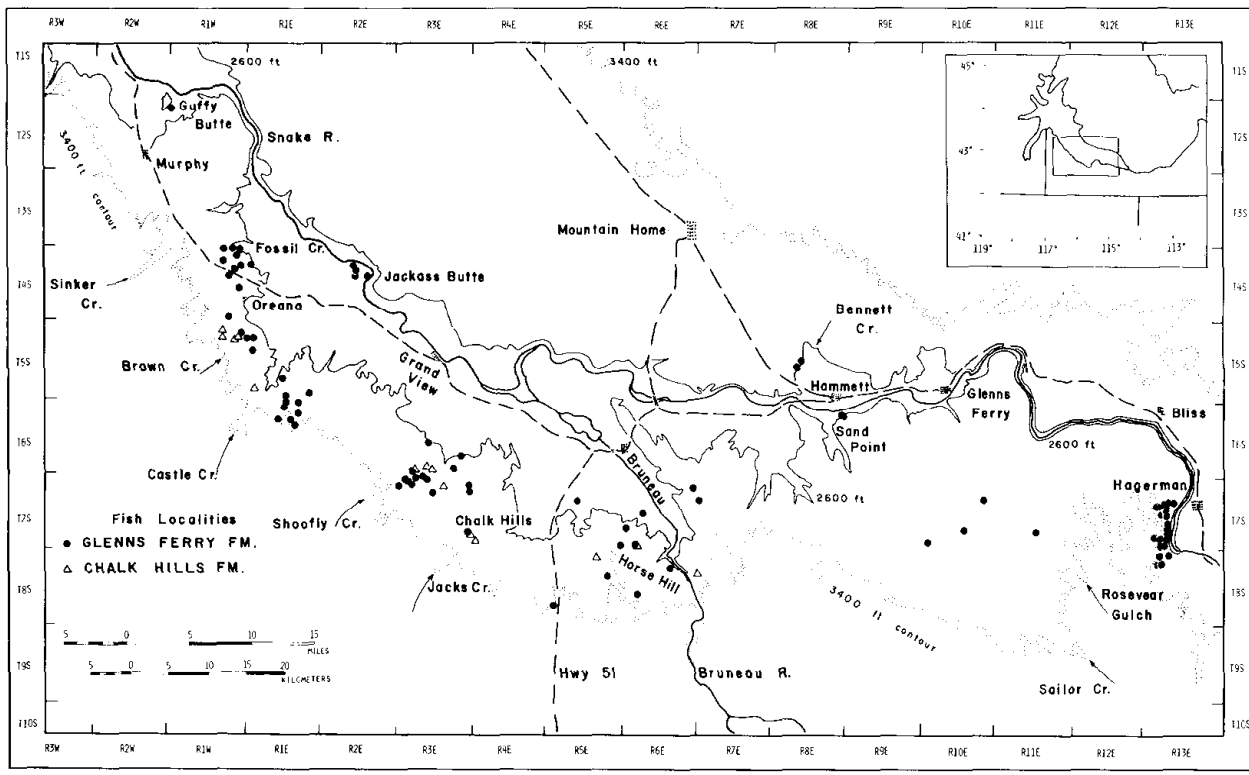

Figure 1. The western Snake River Plain. ● Glenns Ferry fish localities; Δ Chalk Hills fish localities.

diverse group in the fauna includes small benthic sculpins of the family Cottidae. These are represented by the arctic and subarctic relict genus *Myoxocephalus*, the endemic lacustrine genus *Kerocottus*, and the widespread genus *Cottus*. The fauna also contains abundant catfish (*Ictalurus*, Ictaluridae) and sunfish (*Archoplites*, Centrarchidae), common to lakes and streams. In the accounts below we stress forms with stratigraphic or environmental significance. Additional descriptions, illustrations, and taxonomic analyses were presented by Smith (1975) and Kimmel (1975).

Fish localities are listed in Table 1, which also gives the recorded occurrences of each species.

FAMILY SALMONIDAE, TROUTS

Subfamily Coregoninae, Whitefishes

Prosopium prolixus Smith (Figure 3A, B, C). This large whitefish is a reliable indicator of the Glenns Ferry Formation. It has not been found below the unconformity at the base of the formation. *Prosopium* is uncommon in the Hagerman floodplain silts and absent from the Grand View local fauna. A Holocene species, *Prosopium williamsoni*, inhabits the Snake River, but continuity is not implied. The two species are different in the relative lengths of the facial bones—*prolixus* being a unique, large-mouthed species and *williamsoni* being small-mouthed and more typical of *Prosopium*.

The genus is northern or high-elevation in North America and Siberia, being restricted to relatively cold waters. Its appearance, simultaneously with the distributionally similar Cottidae, indicates immigration from the north facilitated by a cooling climate between Chalk Hills and Glenns Ferry time. The long, simple, toothless jaws are easily identified stratigraphic indicators.

Subfamily Salmoninae, Trouts

Smilodonichthys Cavender and Miller (Figure 2A, B). This genus is based on a large salmonlike fish from the Miocene (Barstovian-Hemphillian) of Oregon and California. On the Snake River Plain it is known only from the lowest levels of the Chalk Hills Formation, as exposed in Brown Creek. The presence of this form and the distinct *Mylopharodon* from the same level indicates that these beds are older than other Chalk Hills sediments. The enlarged conical teeth, at the end of otherwise nearly toothless jaws, are unique and unmistakable indicators.

Oncorhynchus salax Smith. This species was attributed to the Glenns Ferry Formation by Smith (1975, p. 11), but reevaluation of the type locality at Shoofly Creek shows that the fine-grained concretion in which it is found is from Chalk Hills lake beds. *Oncorhynchus* has been found at a number of localities in the Chalk Hills and Glenns Ferry Formations, and no stratigraphic value has been discovered.

Rhabdofario carinatum Kimmel (Figure 2F, G, H). This species was described from what we now recognize as Chalk Hills sediments southwest of the Snake River in Malheur County, Oregon (Kimmel, 1975, p. 73). It has since been collected from numerous localities in the Chalk Hills Formation of Idaho. Compared with its Glenns Ferry counterpart, *R. lacustris*, the maxilla is somewhat salmonlike, with a low-angled premaxillary process that is broadly connected to the tooth-bearing part of the bone. The maxillary teeth are evenly graded in size. The dentaries develop less expanded exostosis near the symphysis.

Rhabdofario lacustris Cope (Figure 2C, D, E). This species is restricted to the Glenns Ferry Formation. Compared with *R. carinatum*, the premaxillary process of *Rhabdofario lacustris* is spatulate with a longitudinal groove under the anteromesial edge. It is proximally restricted and normally projects at a greater angle. The maxillary teeth are abruptly smaller on the posterior half of the bone. Many large specimens show bony expansion near the dentary symphysis.

Relationships of this genus are uncertain. It is found in Pliocene sediments at Honey Lake, Lassen County, California (Taylor and Smith, 1981), and a similar form is known from Pliocene sediments in the Chappala Formation, north of Lake Chappala, Mexico. Near the top of the Glenns Ferry lake beds, at Fossil Creek and Bennett Creek, it becomes uncommon, being partially replaced by smaller trout much more like *Salmo*. Whether they are part of the same lineage is not known.

Hucho larsoni (Kimmel) (Figure 2I, J, K). This species was described in the genus *Paleolox* from Chalk Hills sediments southwest of the Snake River in Oregon. It shares several characteristics with *Hucho perryi* of Asia, including a transverse row of teeth at the anterior end of the prevomer, the strong retroarticular notch in the angular, and an elevated premaxillary process of the maxilla. Some features are similar to *Salvelinus*; the premaxilla is identical to that of *Salvelinus confluentus* Cavender. Except for several specimens, one with several associated parts, reported from Horse Hill by Smith (1975, p. 18), this species is restricted to the Chalk Hills Formation. Some of the Horse Hill specimens collected first could have been from below the unconformity before it was recognized; some are weathered and are possibly from reworked concretions. Otherwise, the species seems to be a useful Chalk Hills indicator. It is especially abundant in lower Chalk Hills sediments. Maxillae and angulars are common and easily identified (Figure 2I, J).

Unidentified salmonids. Several additional kinds of salmonids are present in the Glenns Ferry Formation, but specimens are fragmentary or of uncertain taxonomic allocation (see account of *Rhabdofario lacustris* above). The most distinctive form, possibly *Salmo*, is represented by flat maxillae with minute teeth, from the Horse Hill beach deposits (Smith, 1975, Figure 4D).

FAMILY CATOSTOMIDAE, SUCKERS

Chasmistes spatulifer Miller and Smith (Figure 3D, E). This species is an abundant and useful indicator of the Glenns Ferry Formation and possibly the Bruneau Formation. A similar form has been collected in four older samples (see below). The elongate jaw bones are diagnostic, and their abundance in Glenns Ferry shoreface sands is often helpful to biostratigraphy in the field. The genus is also found in Pliocene to Holocene lakes in the Great Basin (Miller and Smith, 1981).

Chasmistes sp. (Miller and Smith, Figure 11D, J). Specimens related to the previous species but with shorter, less attenuate jaw bones are found in four Chalk Hills(?) samples and in many Glenns Ferry samples. The specimens from the Bruneau Formation are tentatively referred to this category. The oldest known *Chasmistes* is from Sand Hollow, 6 miles west of Vale, Oregon, sec. 33, T. 19 S., R. 44 E. Except for the *Chasmistes* the specimens appear to be a Chalk Hills equivalent, with *Mylocheilus inflexus*. The other fishes present are *Acrocheilus latus*, *Ptychocheilus arciferus*, *Orthodon onkognathus*, *Idadon*, *Catostomus* sp., *Ictalurus peregrinus*, and *Archoplites taylori*. Specimens of *Chasmistes* sp. have also been collected from the Chalk Hills Formation at Parker Ranch and from two localities 2 miles southwest of Horse Hill. The last three occurrences are possibly lag contaminants from the overlying Glenns Ferry beds, but they are too numerous and too similar to dismiss. Related forms were native to the upper Snake River drainage and Fossil Lake, Oregon (Miller and Smith, 1981).

Catostomus (*Deltistes*) *owyhee* (Miller and Smith). This distinctive, highly specialized species is present at nearly all Glenns Ferry sites except the Grand View local fauna and equivalents. It is rare in floodplain sediments, but abundant in what we interpret as lake beds. A more generalized form of what is clearly the same lineage is common in Chalk Hills samples, but the differences are slight. Maxillae, dentaries, and skulls are described and figured by Miller and Smith

Table 1. Locality information for the samples that form this report, with presence of fish species indicated by X.

	NUMBER OF SAMPLES	TOWNSHIP	RANGE	SECTION	ELEVATION (feet)	*Smilodonichthys sp.	*Hucho lassoni	Rhabdofario cornatum	Istiaturus peregrinus	*Orthodon onkognathus	*Mylopharodon doliotus	*Mylochelius reflexus	*Mylochelius copei	*Mylochelius robustus (early)	*Mylochelius robustus (late)	Chasmistes sp.	*Chasmistes spatulifer	*Prosopium prolixus	*Cottus bairdi	*Kerocottus divaricatus	*Kerocottus hypoceras	*Kerocottus pontifex	*Myoxocephalus idahoensis	*Catostomus macrochellus	*Catostomus crissatus	Catostomus shoshonensis	Catostomus oxykee	Catostomus arenatus	Orthodon hadrognathus	Idaodon condonianus	Idaodon hibbardi	Mylopharodon hagermanensis	Gila miller	Richardsonius durranti	Ptychocheilus arcifertus	Acrocheilus lanus	Ictiabrus vesperinus	Archoplites taylori	Archoplites sp.	Myoxocephalus antiquus	Cottus calkatus	Rhabdofario lacustris	Oncorhynchus spp.	Salmonidae unidentified
PLEISTOCENE																																												
Bruneau Formation	2	(T3S, R1E, S21 & T7S, R5E, S36)														X																		X		X									
Grand View local fauna	7	4S	2E	9,15,16	2525-2600											X			X					X				X				X	X		X	X	X								
Guffy Butte	1	2S	2W	NE12	2700																											X	X		X	X	X	X							
PLIOCENE																																												
UPPER GLENNS FERRY FORMATION																																												
Bennett Creek	2	5S	8E	SW16	2730										X	X		X		X	X	X	X	X			X	X	X	X		X	X	X	X	X	X	X	X	?			X		X
Sand Point	3	6S	8E	SW1	2600-2690										X		X	X		X		X	X	?	X		X	X	X	X		X	X	X		X	X	X	X	X			X	X	
Shoofly regressive beach	2	7S	3E	5,6	3317										X		X	X		X	X	X	X		X		X	X		X		X				X	X	X	X				X		
Birch Creek regressive beach	1	6S	1E	NW2	3244										X	X	X	X		X	X	X	X		X		X	X		X		X	X			X	X	X	X				X		
Castle Creek regressive beach	1	6S	1E	NW3	3322										X		X	X		X		X	X		X		X	X				X				X	X		X						
Crayfish Hill (Fossil Creek)	7	4S	1W	SW1	2825-2875										X	X	X	X		X	X	X	X		X		X	X	X	X	X	X	X	X		X	X	X	X	X			X	X	
GLENNS FERRY FINE SANDS																																												
Henderson Creek	2	4S	1E	7	2875										X		X	X		X	X	X	X		X		X	X	X	X		X		X	X	X	X	X	X	X			X		X
Lower Fossil Creek	2	4S	1W	11,12	2940,2875										X		X	X		X	X	X	X				X	X		X	X	X				X	X	X					X		X
Fossil Creek roadcut	7	4S	1W	11,14	3010										X		X	X		X		X	X	?	X		X	X		X	X	X		X		X	X	X	X	X	X	X	X	X	X
Picket Creek	1	4S	1W	24	2970										X		X	X		X	X	X	X				X	X		X	X	X	X			X	X		X				X		X
Rosevear Gulch	1	7S	10E	SW12	2975										X		X			X								X			X			X		X	X	X	X						
Twenty-mile Gulch	1	6S	3E	SW32	3130										X		X			X					X		X	X			X	X				X	X		X				X		
6 miles E Horse Hill	1	7S	6E	NW25	3210										X		X	X				X			X			X		X						X	X	X	X				X		
HORSE HILL BEACH																																												
6 miles E Horse Hill	1	7S	6E	NW25	3200										X		X	X		X		X			X			X			X					X	X		X				X		
3 miles NE Horse Hill	1	7S	6E	17,20	2720										X	X																				X		X	X						
4 miles NE Horse Hill	1	7S	6E	NW21	2825										X	X									X			X								X	X	X							
4 miles E Horse Hill	1	7S	6E	SW33	3010										X	X		X		X					X		X	X	X		X					X	X	X	X				X		
North side Horse Hill	6	7S	5E	35,36	3025		r					r			X		X	X		X		X			X		X	X		X	X	X		X		X	X	X	X	X		X	X	X	X
5 miles NW Horse Hill	1	7S	5E	SW9	2800										X		X	X									X	X								X		X	X							X
3 miles S Horse Hill	1	8S	3E	11,14	3225										X		X	X		X					X		X	X			X	X				X	X	X	X						
5 miles SE Horse Hill	1	8S	6E	NW20	3250										X		X	X		X					X		X	X				X		X		X	X	X	X				X		
7 miles SE Horse Hill	1	8S	6E	29	3320										X		X	X		X					X			X		X		X				X	X	X	X				X		
Highway 51 roadcut	2	8S	5E	30	3400										X			X		X							X	X			X	X				X	X	X	X			X	X		X
Dove Spring	1	7S	10E	NE31	3100										X		X	X		X					X		X					X	X			X	X	X	X						
SANDS ABOVE OOLITE																																												
Shoofly	3	7S	3E	5,6	3150										X		X	X		X					X		X	X		X		X				X	X	X	X						
Castle Creek	1	5S	1E	SW34	3200										X		X	X		X					X		X	X				X				X	X		X						
Brown Creek	1	5S	1E	NW7	2975										X			X		X							X	X								X	X								
Hart Creek	1	4S	1W	33	3400										X		X	X		X					X		X	X		X		X				X	X		X						
Blackjack Butte, Oregon	1	22S	46E	8,18	3200,3320										?		X	X		X					X		X	X		X	X					X	X	X	X				X		
Shoofly between limonites	3	6S	3E	35	2975										?		X	X		X					X			X			X	X				X		X	X				X		
Birch Creek between oolites	4	6S	1E	NE15	3475										?		X	X		X					X		X	X			X	X				X	X	X	X				X	X	
Castle Creek between oolites	3	6S	1E	SE9	3500										?		X	X		X					X		X	X				X				X	X	X	X				X		

Table 1. continued

	NUMBER OF SAMPLES	TOWNSHIP	RANGE	SECTION	ELEVATION (feet)	*Smilodonichthys sp.	*Hucho larsoni	Rhabdofario carinatum	Ictalurus peregrinus	*Orthodon onkognathus	*Mylopharodon dolatus	*Mylocheilus inflexus	*Mylocheilus copei	*Mylocheilus robustus (early)	*Mylocheilus robustus (late)	Chasmistes sp.	*Chasmistes spatulifer	*Prosopium prolixus	*Cottus bairdi	*Kerocottus divaricatus	*Kerocottus hypoceras	*Kerocottus pontifex	*Myoxocephalus idahoensis	*Catostomus macrocheilus	*Catostomus cristatus	Catostomus shoshonensis	Catostomus owyhee	Catostomus arenatus	Orthodon hadrognathus	Idaldon condonianus	Idaldon hibbardi	Mylopharodon hagermanensis	Gila miller	Richardsonius durantii	Ptychocheilus arcifferus	Acrocheilus latus	Ictaburus vesperinus	Archoplites taylori	Archoplites sp.	Myoxocephalus antiquus	Cottus calcatus	Rhabdofario lacustris	Oncorhynchus spp.	Salmonidae unidentified
GLENNS FERRY BASAL SANDS																																												
Ag Lime Butte (Shoofly Creek)	2	7S	3E	NE9	3150									X				X								X	X			X				X	X		X				X		
Shoofly	4	7S	3E	4-6	3025-3250							r		X			X	X							X	X	X		X	X	X	X			X	X	X	X				X	X	
Birch Creek	2	6S	1E	10,11	3310-3400									X												X	X									X	X								
Castle Creek	2	5,6S	1E	3,28	3000-3175									X												X	X									X		X							
Brown Creek	4	5S	1E	(12),	2850-3150							r		X		X		X		X			X		X	X	X	X	X	X	X	X				X	X	X	X				X	X	
			1W	(12,18)																																								
Parker Ranch (Jacks Creek)	2	7S	3E	NE36	3125									X			X	X		X					X	X	X				X				X	X	X	X			X	X		
NE Shoofly	1	6S	3E	35	2975									X			X			X					X		X				X				X							X		
Davis Ranch (Shoofly Creek)	2	6S	3E	SW25	2840									X			X	X		X					X	X	X			X	X				X	X	X	X				X	X	X
Sand Pits (Shoofly Creek)	4	6S	3E	21	2800									X			X	X		X		X				X	X	X	X	X	X	X				X	X	X	X				X		
Hagerman cliffs,	96	7S	13E	16,17,20,21,28,29,32										X			X	X						?		X	X	X	X		?	X	X		X	X	X	X				?		X
2,900-3,500 feet		8S	13E	4,5,8																																								
CHALK HILLS FORMATION (MIOCENE)																																												
2 miles E Horse Hill	1	7S	6E	NE31	3025		X		X			X	X												?		?	?		X		?	?			X	X		X					X	
2 miles SW Horse Hill	1	8S	5E	NW11	3150		X	X	X			X	X			?												?								X			X			?			
2 miles SW Horse Hill	1	8S	5E	SW3	3060		X	X	X			X				X										?						?	?			X	X		X						
Parker Ranch (Jacks Creek)	2	7S	3E	25,36	3080,3105			?	X			X				X									?		?	?	?				?	?		X	X		X					X	
Twenty-mile Gulch	1	6S	3E	32	3060			?	X			X	X												?		?	?			X		?			X	X		X						
Shoofly	2	6S	3E	33	2990				X			X	X												?		?	?		X	?		?			X	X		X					X	X
NE Shoofly	1	6S	3E	35	2935				X			X															?									X			X						
Ag Lime Butte (Shoofly Creek)	1	7S	3E	3	3050			?	X			X	X														?						?			X	X		X					X	X
East of Bruneau River	1	8S	7E	SW7	3120				X			X													?		?						?			X			X						X
OREGON, MALHEUR COUNTY, NEAR ADRIAN																																												
Schenk Ranch	2	22S	46E	36	2750			X	X			X	X																	X	X					X	X		X						
Tunnel Road	4	22S	46E	15,16	2500-2600		X	X	X	X		X	X												?		?			X	X					X	X		X						X
Tunnel Mountain	3	22S	46E	22	2640-2720		X	X	X	X		X	X												?		?	?		X	?					X	X		X		?	X			X
Redrock	3	22S	46E	SE21	2540-2700			X	X			X	X												?						X					X	X		X						X
MIDDLE CHALK HILLS FORMATION, IDAHO																																												
Upper Castle Creek	1	5S	1E	NE31	3290				X			X													?							?	?				X		X						X
2 miles E Horse Hill	3	7S	6E	NE31	3005			?	X	X	X	X	?							c					?		?				X					X	X		X					X	
LOWER CHALK HILLS FORMATION, IDAHO																																												
Brown Creek	3	5S	1W	2	3040		X	X	X	X		X	X	X											?		?									X	X		X						

*=zone-defining form; X=present; r=reworked; c=contamination from above; ?=precise identification uncertain. Horse Hill localities are measured from the bench mark at the northwest corner of section 36, at the north side of Horse Hill.

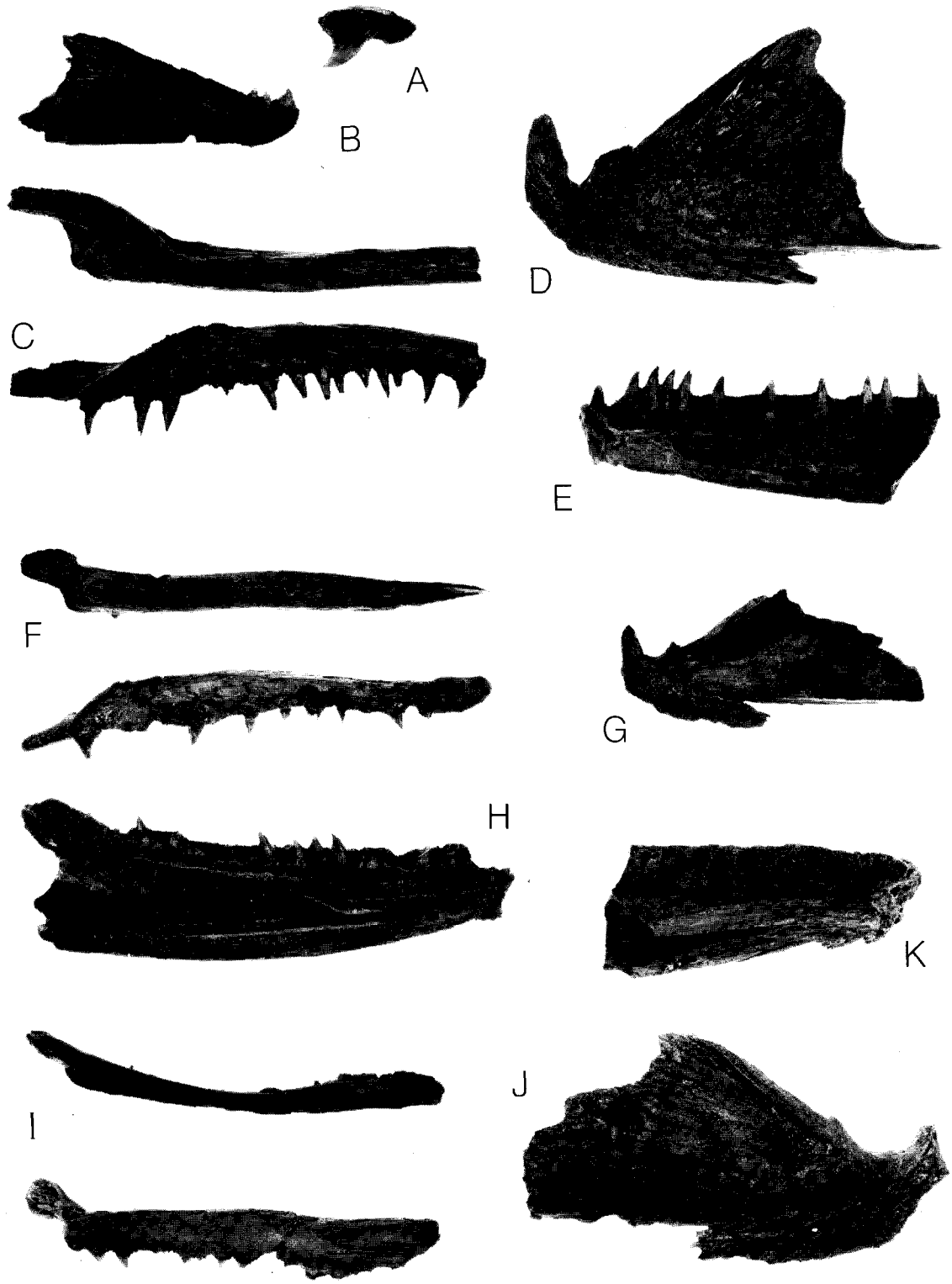

Figure 2. Diagnostic trout. (A,B) Premaxilla and dentary of *Smilodonichthys* sp., zone indicator for the lower Chalk Hills Formation, X¾ (C,D,E) Maxilla, angular, and dentary of *Rhabdofario lacustris* of the Glenns Ferry Formation, X1 (F,G,H) Maxilla, angular, and dentary of *Rhabdofario carinatum* of the Chalk Hills Formation, X¾ (I,J,K) Maxilla, angular, and dentary of *Hucho larsoni* of the Chalk Hills Formation.

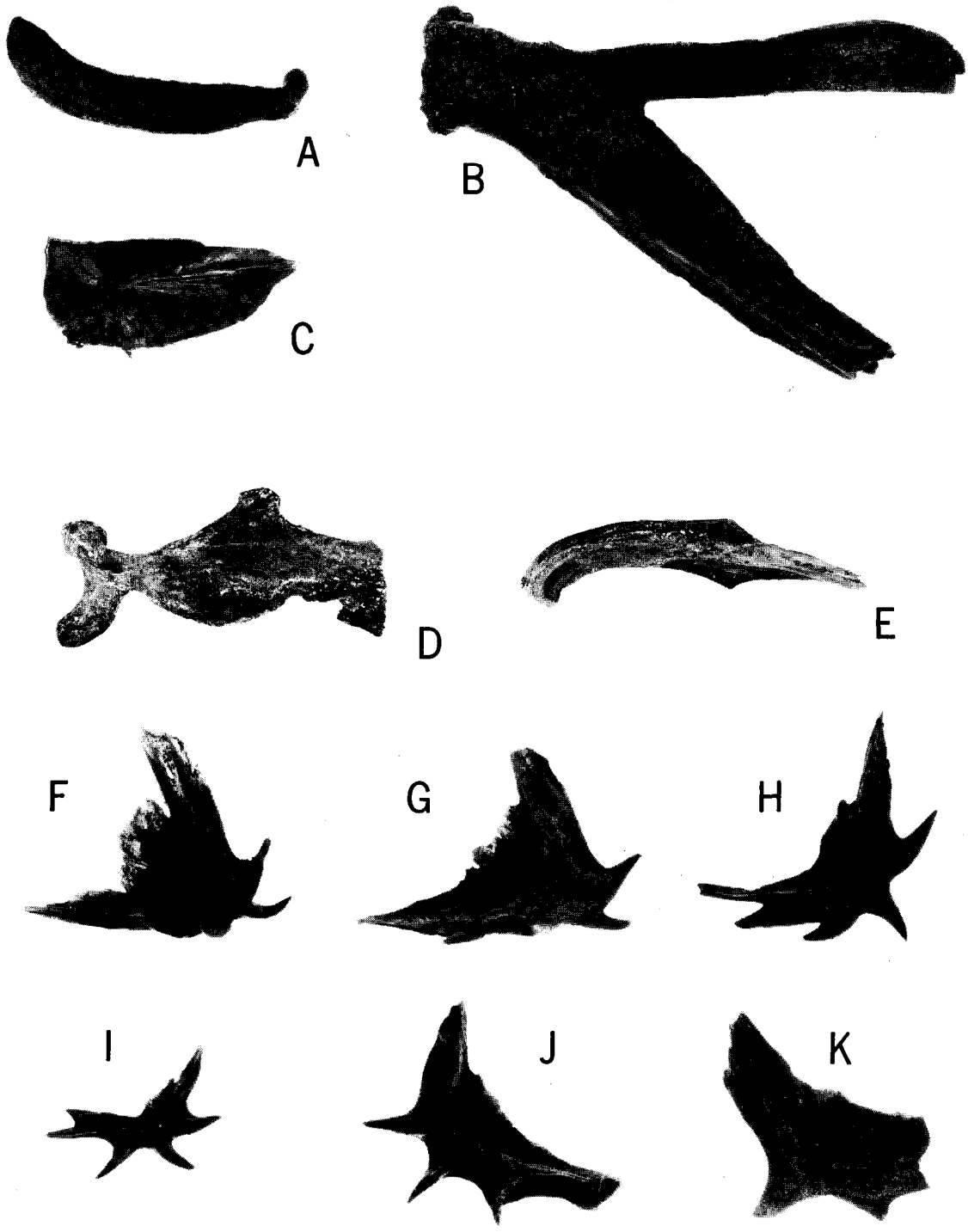

Figure 3. (A,B,C) Maxilla, dentary, and frontal of *Prosopium prolixus,* zone indicator for the Pliocene part of the Glenns Ferry Formation, X½. Chasmistes spatulifer, (D) Maxilla, (E) dentary, X½. Preopercles of sculpins, Cottidae, of the Glenns Ferry Formation, X2. (F) *Kerocottus divaricatus*, (G) *Kerocottus pontifex*, (H) *Kerocottus hypoceras*, (I) *Myoxocephalus antiquus*, (J) *Myoxocephalus idahoensis*, (K) *Cottus calcatus*.

(1967, Figures 3, 4A), and Smith (1975, Figures 10E, 11B-G, 12B, F, K).

Catostomus (*Deltistes*) *shoshonensis* Cope. This name is based on a skull, but records listed here are based on maxillae of the "*ellipticus*" form (Miller and Smith, 1967, Figure 4C; Smith, 1975, Figure 12A). Dentaries attributed to *cristatus* by Smith (1975, Figure 12C) might actually belong with *shoshonensis* maxillae. Dentaries thought to be associated with this species by Smith (1975, Figure 12D, E, J) might be *owyhee*. In the Glenns Ferry Formation, this species is distinct, at least on the basis of maxillae; in the Chalk Hills Formation, the differences between this and the following form are difficult to demonstrate. The species is absent from Grand View sediments.

Catostomus (*Catostomus*) *cristatus* Cope. This name is based on a skull, but records listed here are based on maxillae (Smith, 1975, Figure 12G, and probably I). The species is distinct in the Glenns Ferry Formation, except that maxillae and dentaries grade into forms similar to *Catostomus macrocheilus*, especially near the top of the formation. In the Chalk Hills samples, maxillae of this species are most abundant, but difficult to separate from *shoshonensis*. In floodplain sediments this is the most abundant sucker.

Catostomus (*Pantosteus*) *arenatus* Miller and Smith (1967, Figure 5B, C). This species is rare in the study area, especially in lake beds, and of no known significance as a stratigraphic indicator.

FAMILY CYPRINIDAE, MINNOWS

The most abundant fossils of the family Cyprinidae are pharyngeal arches—the only tooth-bearing bones they possess. The teeth show differentiation in size, shape, number, and arrangement. In the genus *Mylocheilus* evolutionary changes in teeth permit stratigraphic zonation.

Mylocheilus inflexus (Cope) (Figure 4A). This species is based on specimens collected by J. L. Wortman near Sinker Creek, but the type locality has not been relocated. *Mylocheilus inflexus* has been taken at all Chalk Hills fish localities. It is the most reliable indicator of the Chalk Hills Formation, except that abraded specimens are occasionally found reworked in the basal one meter of the Glenns Ferry Formation. Because of its distinctive shape and exceptional durability, it is a useful zone marker in the field. The arches are asymmetrical, most having five teeth on the left arch and four (occasionally three or five) on the right. Tooth sockets for missing teeth are easily recognized. Teeth of the left and right arches worked side-by-side in the fish, grinding upward against the basioccipital process of the skull. These details are stratigraphically helpful, because they are the basis for distinguishing between *Mylocheilus inflexus* and its sister species described below.

Mylocheilus copei Smith and Kimmel new species (Figure 4B, C). A second species of *Mylocheilus* is found with *inflexus* in the Chalk Hills Formation. It is restricted to the Chalk Hills Formation as far as is known, and is therefore reliable as a zone indicator, but not so easy to use because of its similarity to the Glenns Ferry species, *Mylocheilus robustus*. *Mylocheilus copei* is described here to make the name available, but will be redescribed in more detail in a later report.

Description. The holotype, UMMP 62681 (Figure 4B), is a left pharyngeal arch with two associated cleithra, one opercle, and the basioccipital collected by Peter Kimmel from the Chalk Hills Formation in Malheur County, Oregon, sec. 22, T. 22 S., R. 46 E., elevation 2,640 feet. The arch has a maximum length of 32 millimeters. The tooth row is 18 millimeters long, with five teeth in the major row, the first being only slightly smaller than the second, and two relatively large teeth in the minor row. Orientation of the major row enabled the teeth of the two arches to grind in opposition, rather than against the basioccipital as in most minnows. The anterior limb is 12 millimeters long and deflected into a face that articulates with the opposite arch; the posterodorsal limb is 16 millimeters long. The teeth range from subconical (minor row and tooth 5 of major row) to molariform (teeth 1, 2, 3, and 4). Tooth counts of several large samples from the type locality and elsewhere in the Chalk Hills Formation show that the major rows of the left and right arches have five teeth with few exceptions; minor rows almost invariably have two teeth (Table 2; Figure 5). There is no ontogenetic loss of teeth.

Diagnosis. A cyprinid fish with smooth molariform pharyngeal teeth. There are five teeth in the major row; two in the minor. The species differs from *Mylopharodon* in having more flattened molariform teeth and a shorter posterodorsal limb on the arch. Pharyngeal arches of *copei* differ from *Mylocheilus inflexus* in having a minor row of teeth, modally five teeth on the right, and a short posterodorsal limb. *M. copei* differs from *robustus* in the maintenance of the tooth formula throughout life (Figure 5) and in the large molariform first tooth of the major row and stronger teeth in the minor row. *Mylocheilus caurinus* has the first tooth of the major row larger than the second and normally has a single tooth in the minor row.

Etymology. For Edward Drinker Cope.

Mylocheilus robustus (Leidy) (Figure 5). This species is limited to the Glenns Ferry Formation below the level of the Grand View local fauna on the Snake River Plain. What appears to be the same

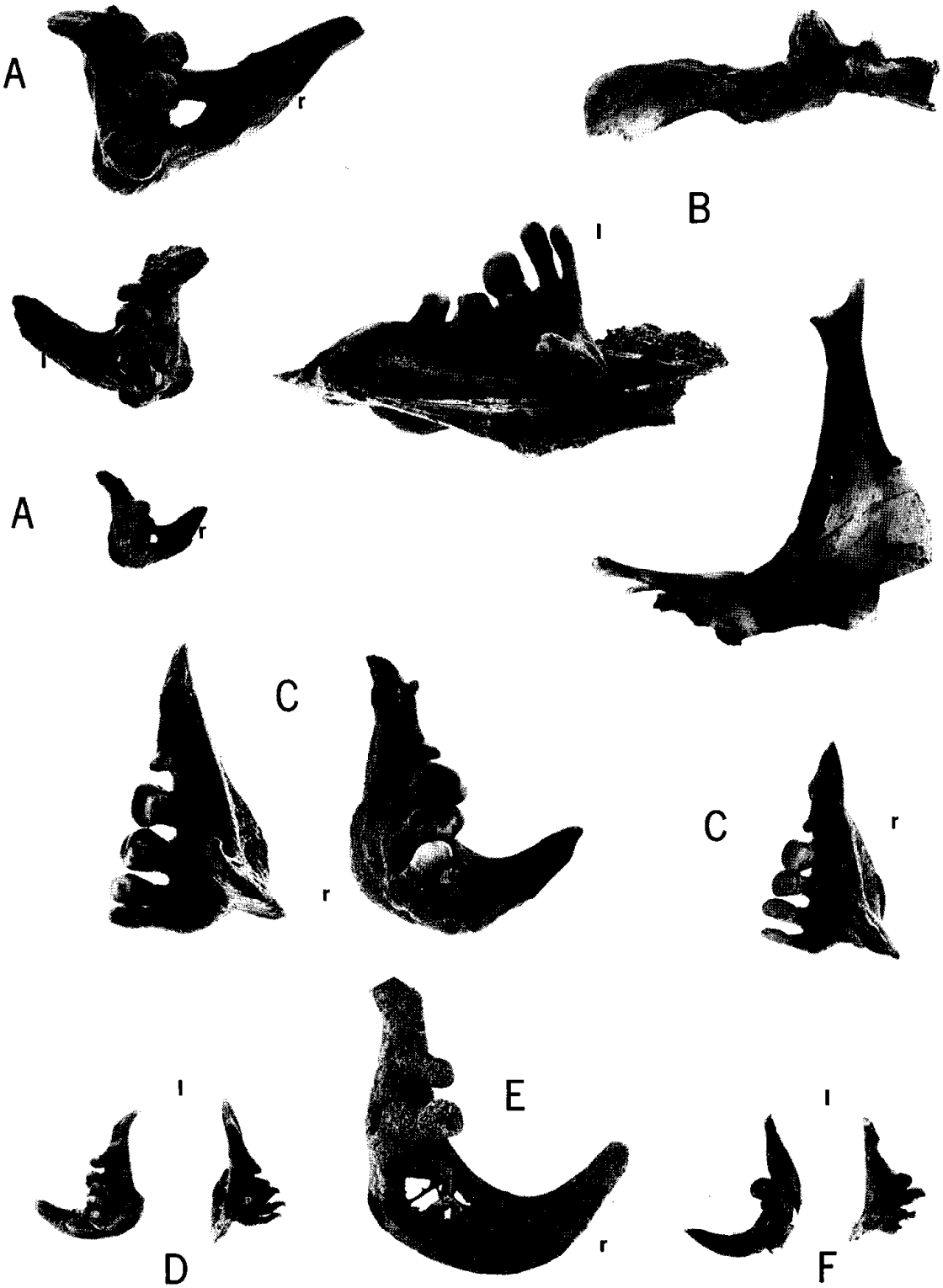

Figure 4. (A) Graded size series of pharyngeal arches of *Mylocheilus inflexus* of the Chalk Hills Formation, showing change in shape. L (left), R (right). (B) Holotype of *Mylocheilus copei* of the Chalk Hills Formation (UMMP 62681), left pharyngeal arch, basioccipital, cleithrum (associated). (C) Pharyngeal arches of *Mylocheilus copei*. (D) *Mylopharodon hagermanensis*. (E) Holotype of *Mylopharodon doliolus* Smith and Kimmel, new species, from the lower Chalk Hills Formation at Horse Hill (UMMP 74197). (F) *Mylocheilus doliolus* from the lower Chalk Hills Formation at Brown Creek. All bones X½.

species has been collected from Idaho Group sediments (coarse sands) near Idaho City in the Boise River drainage (UMMP 31901, washed out of a mining claim 200 feet below the surface). *Mylocheilus inflexus* and *robustus* are reported from the Cache Valley Formation in northern Utah by McClellan (1977). The group will prove to have broader stratigraphic significance when its range is better known.

On the Snake River Plain variation in *robustus* permits stratigraphic zonation. The morphological change through the Glenns Ferry Formation is expressed as a reduction in teeth. The first sign of reduction is loss of the anterior tooth on the right arch of large individuals. Evidently selective pressure for fewer, larger teeth led to increasingly early tooth replacement and reduction (seen as increased frequency of arches with four rather than five major teeth in progressively smaller individuals as we go higher in the section). Reduction in teeth in the minor row follows a similar pattern. In basal Glenns Ferry sands, small fish have a tooth formula of 2,5-5,2 (2 left minor, 5 left major, 5 right major, 2 right minor). Small fish are defined as having no teeth larger than 4 millimeters in diameter; the largest tooth in the middle-sized fish is between 4 and 8 millimeters in diameter. Middle-sized *robustus* in the basal sands usually have 2,5-[4 or 5],2; large fish usually have 2,5-4,2 (Table 2; Figures 5A-C, 6).In the latest lake beds, for example at the old railroad grade at Bennett Creek in Elmore County, small fish usually have 1,5-4,1; middle-sized fish usually have 1,[4 or 5]-4, [0 or 1]; the larger fish have 1,4-4,1 with some variation

Table 2. Variation in numbers of pharyngeal teeth in the major $_{(M)}$ and minor $_{(m)}$ rows in *Mylocheilus copei* and *robustus*, as a function of size. (N) sample size.

Locality		$Left_m$	N	$Left_M$	N	$Right_M$	N	$Right_m$	N
M. robustus (late phenotypes)									
Bennett Creek	large	-	-	-	-	4	1	1	1
	medium	.9	25	4.4	25	4	11	.6	14
	small	1	4	5	8	4	4	1	5
Fossil Creek roadcut	large	1	3	4	4	4.1	9	.2	9
	medium	.9	7	4.8	9	4.3	4	2	2
	small	1.4	5	5	7	4	3	1	4
Fossil Creek (lower)	large	1	18	4.5	14	4	15	.6	11
	medium	1	6	4.8	5	4.7	5	1.3	4
	small	1.7	5	5	3	-	-	-	-
Crayfish Hill	large	0	4	4.1	7	4	4	-	-
	medium	1	4	4.6	8	4	11	1	9
	small	1.3	3	4.8	5	4.7	3	1	2
Horse Hill	large	1.2	16	4.3	15	4.1	19	1.1	19
	medium	1.6	33	4.8	34	4.2	43	1.4	41
	small	2	1	5	2	4.3	3	1.5	4
Deerwater Spring	large	1	3	5	1	4	1	-	-
	medium	1	1	5	1	4	1	1.5	2
	small	1	1	5	2	-	-	2	1
Hot Creek (2 miles SE of Horse Hill)	large	2	1	4	1	4.5	2	2	3
	medium	1.7	4	4.5	4	4	9	1.5	10
	small	-	-	-	-	4	1	1	1
Rosevear Gulch	large	-	-	4	1	4.5	4	1.7	4
	medium	1	1	4	1	4	1	0	1
Dove Spring	large	2	3	4	4	4	4	1.5	4
	medium	2	3	5	1	4	1	1.3	3
Highway 51 roadcut	large	2	1	4	4	-	-	-	-
	medium	1	1	4	1	-	-	-	-
Shoofly (over oolite)	large	-	-	-	-	4	1	1.5	2
	medium	-	-	-	-	4	2	1.5	2
Castle Creek (between oolites)	large	1.3	3	4.3	3	4	2	1	2
	medium	2	1	5	2	4	3	.7	3
Birch Creek (between oolites)	large	.8	5	4.2	5	4	11	1.1	7
	medium	-	-	4	1	4	2	2	1
	small	-	-	-	-	5	2	2	2

(Table 2; Figures 5F, H, 6). Table 2 shows that the evolutionary change through time is a shift toward fewer teeth—the lower number being expressed at an earlier growth stage in later Glenns Ferry time. It can also be seen that the evolutionary change is asymmetrical—tooth reduction in the right arch is developmentally and evolutionarily earlier. The asymmetry and growth-dependence of the evolutionary change

Table 2. continued.

Locality		$Left_m$	N	$Left_M$	N	$Right_M$	N	$Right_m$	N
M. robustus (early phenotypes)									
Blackjack Butte	large	1	2	4	2	-	-	-	-
(Oregon)	medium	1	2	5	1	-	-	-	-
	small	-	-	5	1	-	-	-	-
Davis Ranch	large	1.7	7	4.9	7	4	9	1.6	7
	medium	1.6	24	4.7	20	4.1	26	1.6	28
	small	1.9	11	4.9	12	4.3	10	1.6	12
Parker Ranch	large	1	4	5	2	4	1	1.5	2
	medium	1.5	2	5	3	4	3	2	3
	small	2	3	5	5	4.3	9	2	8
Castle Creek (below	large	1	2	4	2	4	1	2	1
oolite)	medium	2	1	5	1	4	1	2	1
	small	2	1	5	4	5	1	1	1
Sand Pits	large	1.8	11	4.5	10	4	14	1.5	14
	medium	1.9	18	5	21	4.5	15	1.7	12
	small	1.8	9	5	12	4.5	8	2	5
Shoofly	large	1.8	6	4.5	4	4	3	1.7	3
	medium	1.9	27	4.8	28	4.3	24	1.8	33
	small	1.9	33	5	28	4.96	26	1.9	23
Shoofly	large	2	2	4.8	5	4.2	6	.7	3
(at Ag Lime Butte)	medium	2	3	5	3	5	2	2	2
	small	1	1	5	1	-	-	-	-
Shoofly	large	2	1	4	2	4	2	2	1
(at Poison Creek)	medium	1.8	4	5	3	4.7	3	1.5	2
Brown Creek	large	1.3	7	4.3	7	4	4	1.7	3
(below oolite)	medium	2	3	5	5	4.3	6	1.7	4
	small	2	3	5	4	5	1	-	-
M. copei									
Shoofly sec. 32,	large	1.7	3	5	4	4.6	5	1.7	3
3,060 feet	medium	2	4	5	7	5	4	1.8	6
	small	2	1	5	1	5	1	-	-
Shoofly sec. 33,	large	2	10	5	2	5	13	2	7
2,990 feet	medium	2	20	5	28	5	27	2	37
	small	1.9	9	5	5	5	9	1.9	14
Shoofly sec. 3	large	2	1	5	1	5	1	2	1
	medium	2	2	5	2	5	5	2	5
	small	2	4	5	4	5	2	2	2
Parker Ranch	large	-	-	-	-	-	-	-	-
	medium	2	3	5	3	5	6	2	6
	small	2	1	5	1	5	1	2	2
Schenk Ranch	large	2	2	5	3	4.6	5	2	5
	medium	2	2	5	2	5	5	2	2
	small	2	1	5	1	-	-	-	-
Tunnel Mountain	large	2	6	4.6	8	5	4	2	4
	medium	2	15	5	15	5	13	1.9	14
	small	1.9	14	5	14	5	14	2	13

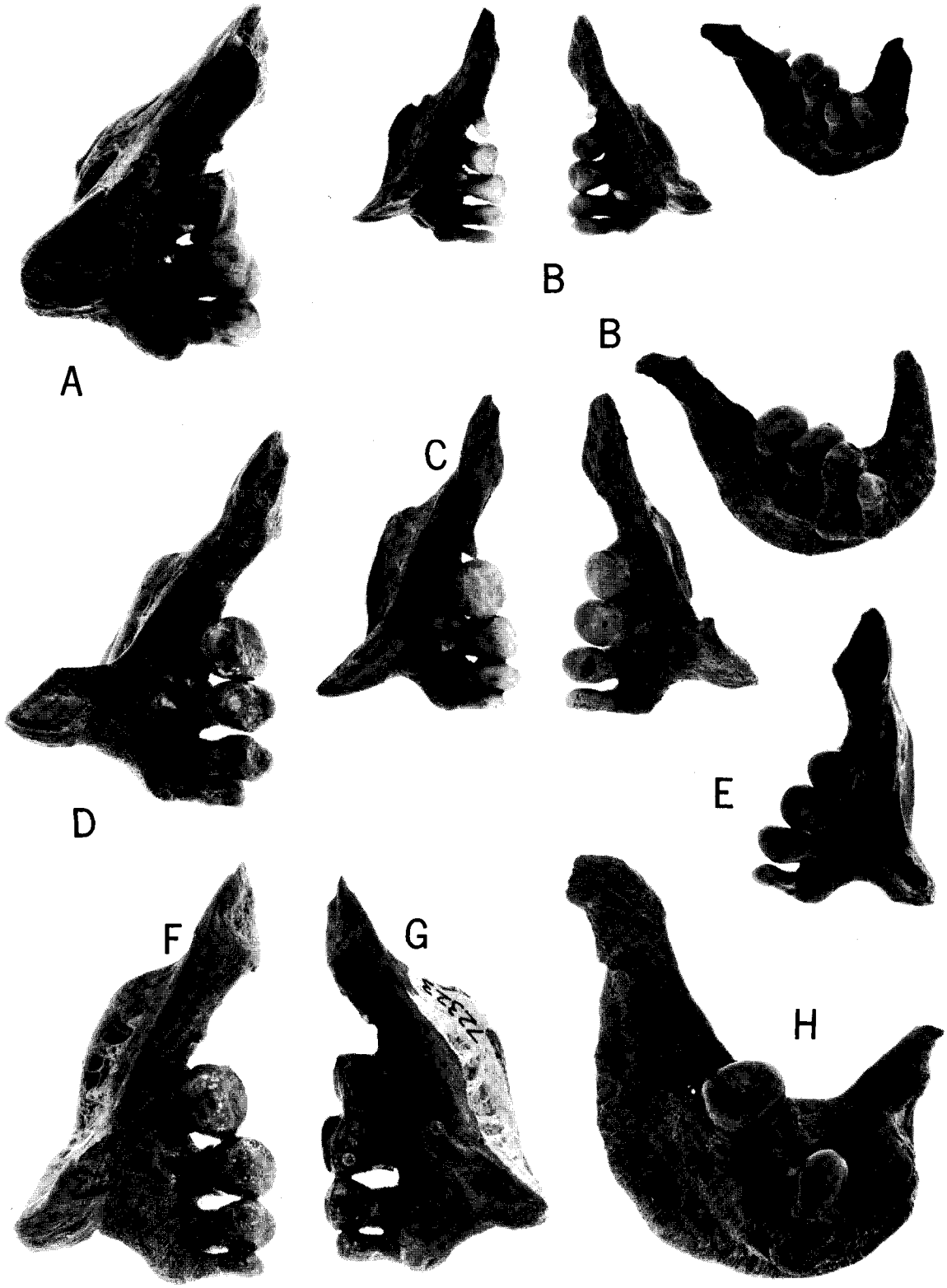

Figure 5. Pharyngeal arches of *Mylocheilus robustus* of the lower (A-C) and middle (D-H) Glenns Ferry Formation, X½. Right arches are on the right side of the page. (A) UMMP 67785, Davis Ranch; (B) 74211, Parker Ranch; (C) 67785, Parker Ranch; (D) 58121, Horse Hill; (E) 59119, Horse Hill; (F) 58137, Fossil Creek; (G) 72323, Rosevear Gulch; (H) 58139, Fossil Creek. Advanced forms show reduction in the first tooth (anterior, toward top of page) of the major row, and of the minor row, especially in right arches.

renders this system a little complicated for field-stratigraphic use, yet the abundance of these fossils makes them useful. Basically, if there are modally (but not uniformly) two teeth in the minor row (counting empty sockets) in a large sample, the stratigraphic level is lower Glenns Ferry Formation; if one tooth is the mode, the stratigraphic level is middle or upper Glenns Ferry. Similarly, the larger the proportion of small and medium right arches with four teeth, the later is the sample. Counting major teeth on left arches is surprisingly unhelpful, so left and right arches must be distinguished.

Mylocheilus robustus is rare or absent from floodplain sediments. The single countable arch from Hagerman (high in the sequence—3,280-3,300 feet in N½NE¼NW¼ sec. 5, T. 8 S., R. 13 E., in fine gray sands) is a large right arch with 4,0 teeth. If it is representative (and assuming that the base of the section is lower Glenns Ferry), it shows that the floodplain sequence in the Hagerman cliffs spans much of the time represented by the lake beds to the west.

Mylopharodon hagermanensis Uyeno (Figure 4D). This is the most abundant species of fish at Hagerman, Grand View, and Guffy Butte. It is common at Sand Point and the Bennett Creek railroad grade and uncommon in the coarse sands at the top of the Crayfish Hill section in Fossil Creek. Other specimens are isolated occurrences that show the species was in existence in the drainage but in a different habitat. This distribution reveals that it was a river, creek, and perhaps marsh dweller whose habitat was more extensive at the east part of the Glenns Ferry depositional system until the end of the lacustrine

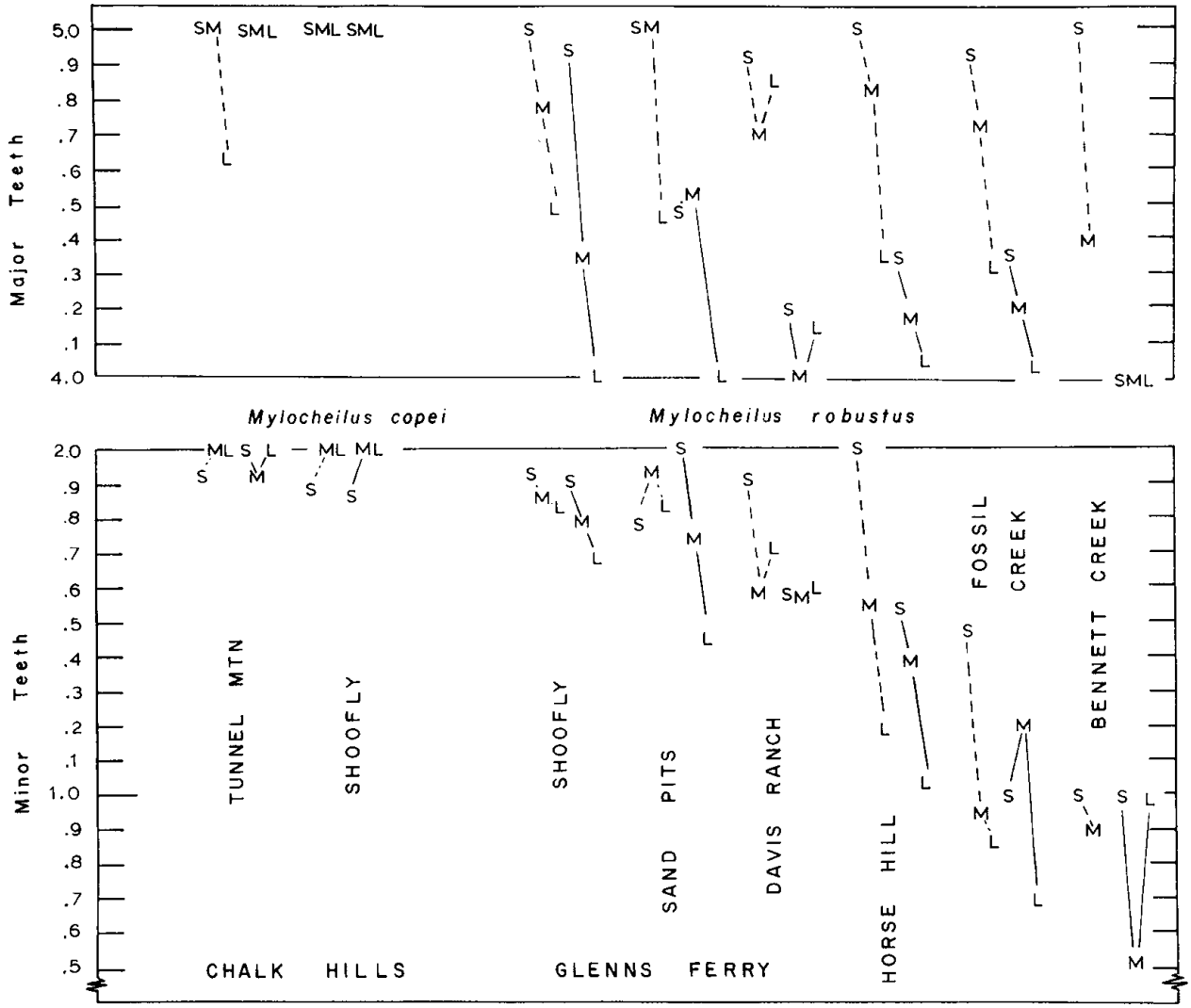

Figure 6. Trends in tooth counts of *Mylocheilus copei* and *robustus*. S (small), M (medium), L (large) specimens.

cycle, when, with its habitat, it spread west at least as far as Murphy.

The upper Chalk Hills *Mylopharodon* is morphologically intermediate between *hagermanensis* and the species described below. A similar form was collected by J. A. Shotwell and D. E. Russell from the Hemphillian Black Butte local fauna of the Juntura Formation in Malheur County, Oregon. In lowest Chalk Hills beds in Idaho, a distinct *Mylopharodon* is present.

Mylopharodon doliolus Smith and Kimmel new species (Figure 4E, F). Large pharyngeals of a *Mylopharodon* with barrel-shaped teeth have been collected from lower Chalk Hills sediments 2 miles east of Horse Hill above the Hot Spring algal limestone (Jones and others, 1978), 2 miles southwest of Horse Hill, near Adrian, Oregon, and at Brown Creek with *Smilodonichthys* (Table 1). A similar pharyngeal was collected by Steve Moore of the U. S. Geological Survey from the Esmeralda Formation of Esmeralda County, Nevada. It may be one of the most primitive North American minnows.

Holotype. A right pharyngeal arch (UMMP 74197) that was 35 millimeters in maximum length (about 2 millimeters broken from anterior limb) bearing a major tooth row 19 millimeters long with four teeth. There is one tooth socket in the minor row, opposite the position of the fourth major tooth. The anterior limb is deflected and was 12 millimeters long; the posterior limb is 16 millimeters long. The arch is 11 millimeters wide at its maximum, under the third tooth, and 7 millimeters wide under the second tooth. The rounded first tooth is 4.5 millimeters high and 3 millimeters in diameter; the second tooth is flattened terminally, 6.8 millimeters long, and 3.9 millimeters in diameter. The teeth are oval in cross section. The specimen is one of two collected from fine-grained sands at 3,010 feet in the Chalk Hills Formation (measured section in Figure 8, Swirydczuk and others, 1982 this volume).

Description. A cyprinid with stout, peglike, slightly molariform teeth (smoothly rounded unless worn flat) in the first and second positions of the major row, slightly hooked teeth in positions three to five of the major row and in the two teeth of the minor row. The tooth formula is apparently 2,5-4,2, with a tendency to lose one of the minor teeth. The arch lacks an alar expansion and a high tooth platform. The anterior limb is short but longer than in *hagermanensis*; under the second tooth the arch is enlarged and round in cross section. The postdorsal limb is elongate, but shorter, and with a less abrupt bend than in *hagermanensis*. Large individuals have widely spaced teeth. Smaller arches in the same sample have the same shape and number of teeth, but are more hooked and closely spaced.

Diagnosis. *Mylopharodon doliolus* differs from *hagermanensis* and *conocephalus* (from the Sacramento system, California) in lacking preformed grinding surfaces on the dorsal faces (opposing the basioccipital) of the anterior two or three teeth. In *doliolus* the second teeth are flattened at the tip by wear, and oppose each other. In *hagermanensis* and *conocephalus* each tooth has a characteristically constricted neck below the dentine cap. The arch has an expanded alar margin opposite the second tooth, and a sharp angle to the posterodorsal process. *Mylopharodon doliolus* differs from *Mylocheilus* in lacking preformed, flat molariform surfaces on the ends of the anterior teeth; any flatness is due to wear.

Etymology. From *doliolum* L. (little barrel) referring to shape of the anterior teeth.

Ptychocheilus arciferus (Cope). This long-jawed, long-toothed carnivore is found throughout the Chalk Hills and Glenns Ferry Formations in all facies. A similar form was collected by J. A. Shotwell and D. E. Russell from the Black Butte local fauna of the Juntura Formation in Malheur County, Oregon. *Ptychocheilus oregonesis* is found in rivers and reservoirs on the western Snake River Plain today. *Ptychocheilus* from the Bruneau Formation are not complete enough to identify to species. No stratigraphic change has been found among fossils of this abundant and widespread species.

Acrocheilus latus (Cope). This large herbivore is found throughout Chalk Hills and Glenns Ferry sediments. It and a species of *Orthodon* are abundant in the Hagerman section, and a smaller form is found in the Juntura Formation, collected by J. A. Shotwell and D. E. Russell at Black Butte. It is represented by the smaller, generalized *Acrocheilus alutaceus* in the lower Snake River and Columbia River drainage today. No useful stratigraphic variation has been found among the fossils.

Orthodon hadrognathus Smith (1975, Figure 19D) and *Orthodon onkognathus* Kimmel (1975, Figures 4G, 6A). These species are known from dentaries of the Chalk Hills and Glenns Ferry Formations. They are part of a formerly diverse group in western North America (Casteel and Hutchison, 1973; Hopkirk, 1973; Casteel and Rymer, 1975; Casteel and Adams, 1977, Figure 3D-I). The pharyngeal teeth are similar to those of *Acrocheilus* but slenderer, with a less robust arch. *Orthodon onkognathus* is limited to Chalk Hills beds in the Idaho Group; it is also found with *Chasmistes* at the Sand Hollow locality 6 miles west of Vale.

Idadon condonianus (Cope) and *Idadon hibbardi* Smith (1975, Figures 16B, 19B, 21C, D, 23; Kimmel, 1975, Figure 6B). These species are separable by development of molariform teeth in *I. condonianus*. The diagnostic rugosity on the grinding surface of the

teeth of *Idadon* is present in juvenile *Lavinia* (of the Sacramento drainage) and in a cyprinid from the Miocene or Pliocene Cache Valley Formation in northern Utah. Future study might show all of these forms to be *Lavinia*. Ted Cavender and R. R. Miller (in McClellan, 1977) saw evidence that the Cache Valley form was related to *Lavinia*, and Smith and Miller (in press) have noticed features of *Lavinia* in the small cyprinid from the Bidahochi Formation of Miocene or Pliocene age in northern Arizona. Despite the potential for regional correlations, these fishes do not appear to show stratigraphically useful variation within the Idaho Group, except that they are rare or absent from the lowest Chalk Hills beds in Brown Creek, Owyhee County, and *condonianus* is not present in the upper Glenns Ferry Formation.

Gila milleri Smith (1975, Figures 15B, 18F, 21A). Variation in this species is not stratigraphically significant, but its distribution and abundance indicate a preference for fluvial habitats; it is rare in lacustrine beds. *Gila milleri* is possibly present in the Chalk Hills Formation at Parker Ranch. It is abundant in the Hagerman beds and common in upper Glenns Ferry localities. H. E. Malde collected material of *Gila* from the Bruneau Formation at Wildhorse Butte.

Richardsonius durranti Smith (1975, Figure 17C). This small fish is not yet well enough known to be stratigraphically useful. It has been found only in very fine sands in the upper Glenns Ferry Formation.

FAMILY ICTALURIDAE, CATFISH

Ictalurus peregrinus Lundberg (1975, Figures 5A-E, Plate VIIC, D, Plate VIIIA; Kimmel, 1975, Figures 5F, 6C, D). This species was described from the Juntura Formation in Oregon. Kimmel (1975) commented on the gradation between the characteristics of *peregrinus* and *vespertinus* and the failure of the original diagnosis to separate the species. Nevertheless, Miocene forms of the lineage have, on the average, a shorter postventral spine on the cleithrum, with a shorter rugose patch which has tubercles randomly spaced. The boss over the socket for the pectoral spine is more bulbous in *peregrinus*. On the pectoral spine of this species the proximal posterior denticulations are usually on a central ridge (compare below). Kimmel (1975) noted a high proportion of abnormal variants in several populations of this species in southwest Oregon.

Ictalurus vespertinus Miller and Smith (1967, Figures 6, 7; Lundberg, 1975, Figure 5, Plates VII-IX; Smith, 1975, Figure 24). If large, well-preserved specimens are available, this species is usually distinguishable from *I. peregrinus*. *Ictalurus vespertinus* has a longer cleithral spine with a large patch of generally aligned tubercles. The convexity over the socket for the pectoral spine is not as elevated as in *peregrinus*. The proximal posterior dentations of the pectoral spines are usually aligned in a groove ventral to the posterior ridge. The species is common throughout the Glenns Ferry Formation. It forms a larger proportion of the fish fauna from fluvial deposits than from lacustrine deposits.

FAMILY CENTRARCHIDAE, SUNFISH

Archoplites taylori Miller and Smith (1967, Figures 8, 9; Smith, 1975, Figure 25; Kimmel, 1975, Figure 6E). This group was widespread in the Miocene of western North America from southern Nevada to Alaska (Smith and Miller, in press). Its morphology is surprisingly uniform in the Idaho Group except for slight variation in dentaries and nonstratigraphic variation in the striation of the opercles. Dentaries from the Chalk Hills Formation (especially lower) tend to have a wider tooth patch than Glenns Ferry specimens.

The most common condition of the opercle is strongly striate externally (Smith, 1975, Figure 25A). This is the condition from throughout Hagerman cliffs and at Rosevear Gulch. Nonstriate opercles have been collected at Crayfish Hill in Fossil Creek, Horse Hill, upper Henderson Creek, and in the regressive beach deposits at the top of the Shoofly section. At Sand Point, the type locality of *A. taylori*, both types of opercles are present. At the Bennett Creek railroad grade a large, intermediate specimen was collected. The significance of this variation is not yet understood, but it seems to be correlated with habitat, not time.

Archoplites drops out of the fauna before the time of the Grand View local fauna. The only surviving representative of this genus (*A. interruptus*) lives in the Sacramento system.

FAMILY COTTIDAE, SCULPINS

Cottus calcatus Kimmel (1975, Figure 3K). This strange species is occasionally present as rare weathered specimens at all levels except the Pleistocene. Its relationship to other sculpins in the system seems remote.

Cottus bairdi Girard. This small, Holocene species has not been collected from any of the Pliocene or earlier samples from the Idaho Group. It is known only from the Grand View local fauna, where it is the only sculpin present.

Kerocottus divaricatus, *pontifex*, and *hypoceras* Cope (Linder, 1970, Figure 1; Smith, 1975, Figures

26, 27A, B, C, 28; Kimmel, 1975, Figure 6G; Figure 3F, G, H). This group of species is known only from the Glenns Ferry Formation, for which it is a reliable indicator. Co-occurrence with Miocene *Mylocheilus inflexus* was recorded by Kimmel (1979) from the stream bed in Brown Creek, but contamination is probable. The genus is absent from Hagerman, indicating avoidance of the floodplain, but is well represented at Sand Point and Bennett Creek, apparently indicating lacustrine environments at or near those localities.

Kerocottus divaricatus (Figure 3F) is characterized by small sensory canal pores on the preopercle. It is the first species of *Kerocottus* to appear in the sequence, in the basal sands of the Glenns Ferry Formation, and it is present in almost all large samples above that level. *Kerocottus pontifex* (Figure 3G) is characterized by large sensory canal pores. It is represented by a single specimen in the basal sands, and is otherwise absent until rather high in the section. It is abundant in the fine sands at Fossil Creek and near Oreana, and in the regressive beach sands at the top of the Glenns Ferry lacustrine deposits from Shoofly to Castle Creek. *Kerocottus hypoceras* (Figure 3E) is characterized by the absence of sensory canal pores on the preopercle. It is present at the localities where pontifex is abundant, but not below. All three species are present at the Bennett Creek railroad grade, but not above that level.

Myoxocephalus antiquus Smith (1975, Figures 26I, 27D; Figure 3I). This is a sculpin of uncertain affinities, characterized by preopercles with straight spines in one plane and medium-sized sensory canal pores. It is known only from Fossil Creek and is therefore of limited stratigraphic use. A small fragmentary dentary with medium-sized pores was collected from the Tunnel Mountain locality of the Chalk Hills Formation in Malheur County, Oregon (Kimmel, 1975, Figure 6K).

Myoxocephalus idahoensis Smith (1975, Figures 27E, 28; Figure 3G). This species is known from numerous skull bones. It is characterized by large sensory canal pores similar to those of *Myoxocephalus thompsoni* of arctic North America and deep waters of the Great Lakes. It is restricted to latest Pliocene fine-grained lacustrine sands of the Glenns Ferry Formation: at Fossil Creek, nearby Henderson Creek, and Picket Creek, at regressive beach sands from Shoofly to Castle Creek, at Sand Point, and at the Bennett Creek railroad grade. It would appear to be a good stratigraphic indicator, based on the abruptness of its first and last occurrence. Its environmental significance lies in its lacustrine habitat and its occurrence at the Sand Point and Bennett Creek localities.

STRATIGRAPHIC SUMMARY

Distribution patterns of the fishes described above and in Table 1 allow clear separation of the Chalk Hills and Glenns Ferry Formations. The Chalk Hills Formation can be subdivided into three zones. The Glenns Ferry Formation includes a diverse and subdivided Pliocene assemblage and a strikingly reduced, modern-looking Pleistocene fish fauna. The Pliocene portion of the Glenns Ferry Formation can be further classified into facies and time stages.

CHALK HILLS FORMATION

The unconformity at the upper limit of the Chalk Hills Formation marks the end of a faunal zone characterized by *Hucho larsoni*, *Mylocheilus inflexus*, and *Mylocheilus copei*. *Rhabdofario carinatum* and *Ictalurus peregrinus* are associated with the Chalk Hills Formation by definition; they are transitional to their Glenns Ferry counterparts. The Chalk Hills beds are also characterized by the absence of *Prosopium*, *Kerocottus*, *Myoxocephalus*, and usually *Chasmistes*.

In Brown Creek there are older beds characterized by the Chalk Hills species listed above and *Smilodonichthys*, *Mylopharodon doliolus*, and *Orthodon onkognathus*. Deposits of the *Smilodonichthys* zone consist of interbedded, coarse-grained sands and silts suggesting fluvial deposition; the fossils are primarily fish and wood, suggesting a beach environment. No discontinuity has been discovered between these beds and overlying Chalk Hills sediments. Basalts within the lower Chalk Hills Formation at Hot Creek, south of Horse Hill, have been dated at 8.4 and 8.2 million years by Armstrong and others (1975). The Brown Creek Tuff underlying the Chalk Hills Formation in Brown Creek has been dated at 10.7 and 11.1 million years by Neill (in Ekren and others, 1978).

Above the *Smilodonichthys* zone but well below the lower Horse Hill ash layer are sands with *Mylopharodon doliolus* and *Orthodon onkognathus* and the other Chalk Hills species. Two miles east of Horse Hill this zone overlies the Hot Spring limestone, an algal carbonate of 30 square miles found in the shallow-water transgressive lacustrine sequence formerly thought to be basal Glenns Ferry (Jones and others, 1978). A similar "middle Chalk Hills" fauna occurs in sands near Adrian, Oregon, below the ash correlated with the lower Horse Hill ash layer (Swirydczuk and others, 1982 this volume; measured section, Figure 3A).

Above and below the lower Horse Hill ash layer, which is at an elevation of 3,025 feet, 2 miles east of

Horse Hill (Swirydczuk and others, 1982 this volume; measured section, Figure 8; Table 1), is a characteristic upper Chalk Hills fauna (as defined above, but lacking *Orthodon onkognathus* and with intermediate *Mylopharodon*). The same fauna is found 2 miles southwest of Horse Hill, at Parker Ranch, Twentymile Gulch, the Shoofly area, and east of the Bruneau River (Table 1). Fission-track dates by Kimmel (1982 this volume) suggest that ashes low in this general zone (in the Shoofly area) are about 8 million years old. Kimmel shows that the uppermost Chalk Hills sediments dated are 5 to 6 million years old. At least 1 million years are missing in the erosional interval separating the Chalk Hills and Glenns Ferry Formations. This is not to say that lacustrine habitat disappeared from the basin—Table 1 shows that most of the lake species were still present, though slightly modified, when the Glenns Ferry lake transgressed the southern slopes of the former Chalk Hills basin.

GLENNS FERRY FORMATION

The oldest fission-track date on glass in the Glenns Ferry lacustrine beds is 3.2 million years from basal sands above the unconformity in Brown Creek, near Oreana in Owyhee County. Other Glenns Ferry dates from that area are around 2 to 2.5 million years (see Kimmel, 1982 this volume, for discussion). Glass shards in the Peters Gulch ash, near the base of the Hagerman cliffs, gave an anomalously old fission-track date (Kimmel, 1979), but Izett (1981) dated zircons from this ash at 3.75 ± 0.36 million years. Ashes near the middle of the Hagerman section and the Deer Gulch lava yield potassium-argon dates of 3.3, 3.2, and 3.5 million years (Everndon and others, 1964; Bjork, 1970). This correlation suggests that the lower part of the Hagerman section is older than Glenns Ferry beds in Owyhee County and that part of the upper section at Hagerman is time-equivalent to lacustrine beds in Owyhee County. This is consistent with the summary by Malde and Powers (1962, p. 1207):

> *The lower 400 feet of floodplain facies at Hagerman grades westward into a lacustrine facies at Deer Gulch 8 miles southeast of Glenns Ferry and into arkosic deposits between Clover Creek and Glenns Ferry. These arkosic deposits are overlain by 650 feet of lacustrine deposits at Glenns Ferry. A floodplain facies in the upper part of the northern canyon wall at Glenns Ferry grades southwestward into the fluvial facies at Hammett. A floodplain facies at Castle Creek merges northwestward with yellow silt of a lacustrine facies near the mouth of Sinker Creek, 8 miles distant.*

The lacustrine beds referred to by Malde and Powers are generally structureless, bioturbated silts near the axis of the basin. They contain few fish fossils and few ash beds; they are clearly a deep-water lacustrine facies.

We interpret part of the fluvial facies of Malde and Powers (1962, p. 1206), at least as exposed at Bennett Creek, at Horse Hill near the head of Bruneau Valley 8 miles south of Bruneau, and at Fossil Creek along the paved road 17 miles northwest of Grand View (but not at Sand Point), as shoreface deposits. They are well-sorted fine sands with some cross bedding but no channels or point bars. They have abundant fossil fishes, locally common mollusks, birds such as cormorants and grebes, but few mammalian remains. The fish fauna is strikingly different from that of the Hagerman and Grand View floodplain deposits, containing more diversity, an abundance of exceptionally large individuals, and forms expected to be restricted to lakes. We propose the following list of lacustrine species, interpreted as being good indicators of lake deposits and unlikely in fluvial deposits: *Kerocottus divaricatus*, *pontifex*, and *hypoceras*; *Myoxocephalus idahoensis*; and *Mylocheilus robustus*. If these fish occurred in the Hagerman Cliffs (for example near channel deposits), our hypothesis would be rejected, but they are not represented among the thousands of fish fragments from the floodplain deposits, except for one pharyngeal arch and several isolated teeth of *Mylocheilus robustus* at Hagerman. *Prosopium prolixus*, *Idadon*, *Catostomus owyhee*, and *C. shoshonensis* are abundant in lacustrine but uncommon in floodplain sediments. On the other hand, *Mylopharodon hagermanensis* is abundant in floodplain sediments and uncommon elsewhere, except at Sand Point and Bennett Creek, which also have mammalian remains. *Ictalurus* and *Catostomus cristatus* are more abundant in floodplain than in lacustrine environments.

By these criteria, the beds at Sand Point and Bennett Creek have faunas intermediate between floodplain and lacustrine aspect. In the Laurentian Great Lakes such a faunal mixture would be found near the mouths of rivers or in the lower few miles of large rivers.

At Sand Point, lacustrine fishes are present but not abundant; *Mylopharodon hagermanensis* and mammals are common. The mammals include muskrat, horse, proboscidian, pocket gophers, rabbits, and voles. Distinct mollusks are present (Hibbard, 1959; Malde and Powers, 1962). The sedimentary units are laterally restricted or variable, and vertically variegated. A fluvial environment near the lake is indicated.

At the Bennett Creek railroad grade lacustrine fishes are abundant, and *Mylopharodon* less common. Mammals are rare, but this is the type locality of *Prodipodomys idahoensis*, a kangaroo rat that

might have been living in sand dunes. The proximity and similarity of this lacustrine assemblage to the fluvial assemblage at Sand Point suggests that the Bennett Creek sediments are lacustrine, but near the mouth of a major tributary.

To the west, particularly south of Bruneau and Grand View, most fish-bearing beds of the Glenns Ferry Formation are basal transgressive beach deposits and overlying shoreface fine sands. The beach deposits generally lie between 2,800 and 3,400 feet, 6 to 12 miles southwest of the Snake River, and dip about 3 degrees northeast. The overlying shoreface sands (fluvial sands of Malde and Powers, 1962) are best seen between 2,850 and 3,100 feet. They are generally missing from the higher flanks of the basin, having been eroded prior to deposition of Pleistocene alluvium. Exceptions are found at 3,400 feet southwest of Horse Hill and in upper Hart Creek (Table 1). The shoreface sands grade into the deeper lacustrine silts in the axis of the basin. The relationship of these facies must be taken into account in attempts to correlate time-equivalent units through the basin. The three main nearshore deposits discussed here are the base of the Shoofly oolite, the Horse Hill beach of quartzite cobbles, and the upper Shoofly (regressive) beach.

The Shoofly oolite (Swirydczuk, 1980; Swirydczuk and others, 1979, 1980a, 1980b, 1981, 1982 this volume) crops out in a northwest-southeast belt 30 miles long, from southwest of Murphy to south of Grand View, attaining a thickness of more than 100 feet. Most of the oolite is underlain by well-sorted, coarse, fossiliferous sands which in turn lie unconformably on fine offshore lacustrine deposits of the Chalk Hills Formation. Based on the lack of mammals and the abundance of mollusks, disarticulated fish bones (including occasional reworked Chalk Hills species), wood, and clasts of underlying Chalk Hills silt, the basal sands are interpreted as beach deposits. The oolite makes up a series of nearshore progradational deposits conformably overlain by lacustrine silts and ashes deposited in deeper water. The overall sequence is thus transgressive.

Fossil fishes in the basal sands include the early form of *Mylocheilus robustus* (modally five teeth in the major row and two teeth in the minor row of the right arch, except in large specimens). With one peculiar exception (*K. pontifex* at the Sand Pits), *Kerocottus divaricatus* is the only sculpin present. Lateral variance in fossils along the oolite and associated sands is not significant and provides no evidence of time transgression. Occasional specimens of *M. robustus* within the oolite indicate little advancement from the primitive form, except at Parker Ranch (Table 2). The sample from Davis Ranch is unusual and may represent a slightly advanced form. Sampling variation and probable evolutionary fluctuation prevent fine-scale stratigraphic use of subspecific variation by itself. Sands directly above the oolite have not produced large enough samples of fossils to be decisive.

The next younger unit is the Horse Hill beach deposits (Figure 6, Table 2), according to the more advanced state of *Mylocheilus robustus* and the definite presence of *Kerocottus pontifex*. Malde and Powers (1962, p. 1207) refer to a lag concentration of quartzite cobbles south of Bruneau as being possibly correlated with a conglomerate 15 miles south of Glenns Ferry. The origin of the cobble unit is not obvious. The cobbles were probably transported by the ancestral Bruneau River from Paleozoic deposits in the Jarbidge Mountains, 70 miles to the south. They occur in a single layer a few feet above the Chalk Hills Formation. The entire unit covers about 50 square miles, dipping north from about 3,300 feet south of Horse Hill to about 2,900 feet between Horse Hill and Bruneau. The cobbles are largest (over 1 foot long) at the north end of Horse Hill, and diminish in size toward the edges of the unit. They armour Horse Hill from erosion by Sugar Creek. Abundant fish fossils and mollusks (*Sphaerium*) are cemented among the cobbles in a coarse, limonitic, and occasionally phosphatic matrix that fines upward to offshore sands within a few feet. Glenns Ferry lacustrine silts and ashes continue upward several hundred feet. The presence of lake fishes and clams, along with cormorants and grebes, but no mammals in the cobble unit, constitutes the basis for referring to it as a beach. The fining-upward sequence is interpreted as transgressive. The composition of the fish fauna suggests that the Horse Hill beach might be a slightly later southeastward extension of the beach deposits found under the Shoofly oolite.

Lacustrine silts directly over the beach deposits do not have demonstrably younger faunas. Closer to the center of the basin, however, in the Fossil Creek area between 2,850 and 3,020 feet, the fauna is decidedly advanced. These fine, micaceous (sometimes coated) sands have all four species of *Kerocottus*, two kinds of *Myoxocephalus*, and advanced *Mylocheilus robustus*. They are rich in ostracods (Jones and Anderson, 1965). In the lower Fossil Creek area (Crayfish Hill, Table 1), the shoreface sands coarsen upward to a fine gravel with channels (2,875 feet) and *Mylopharodon hagermanensis*, and are interpreted as deposits laid down by the regressive phase of the Glenns Ferry system.

Other possible examples of the regressive beach are preserved in Shoofly, Birch, and Castle Creeks. A poorly sorted, thin (4-inch thick) brown sand unit is traceable over 15 miles at an elevation of 2,740 to 3,300 feet, dipping to the northeast. The fauna

is distinctly advanced, with all three species of *Kerocottus*, as well as *Myoxocephalus idahoensis*, advanced *Mylocheilus robustus*, and some *Mylopharodon hagermanensis*. Pleistocene alluvial gravels or poorly sorted sands appear a few feet above this horizon. At Shoofly Creek it is capped by an extensive section of upper Glenns Ferry Formation floodplain and marsh deposits.

Stratigraphically near the lake beds are Sand Point fluvial deposits and Bennett Creek shoreface sands already discussed. Their species are the most advanced we have seen (Table 1), and represent the last occurrence of a diversity of minnows, suckers, sculpins, catfish, and sunfish.

If the above inferences about the regressive beaches and environments are correct, they imply that lake levels dropped about 400 feet in a short period. The timing of this event was probably early Pleistocene (Kimmel, 1982 this volume). Its cause was probably the capture of the upper Snake River through Hells Canyon (Wheeler and Cook, 1954).

Following drainage of the lake, floodplain deposition advanced westward along the axis of the basin. These beds are seen at Jackass Butte (Grand View), Wildhorse Butte (Shotwell, 1970), and in our collection at Guffy Butte. These early Pleistocene deposits have a depauperate fish fauna (Table 1) of small, essentially modern fishes. In contrast to the interval between the Chalk Hills and Glenns Ferry lakes, during which lake fishes found a refuge, the elimination of lake habitat at the close of deposition of the Glenns Ferry Formation must have been complete. The middle Pleistocene Bruneau lake beds also have only the sparse modern fauna.

ACKNOWLEDGMENTS

We thank H. E. Malde for assisting our work on this project. We are grateful to our families, especially Beverly Smith, and many University of Michigan students for field work. R. L. Elder helped with the field work, sorted and cataloged the fossils, and read the manuscript. Linda Krakker typed the manuscript.

REFERENCES

Armstrong, R. L., W. P. Leeman, and H. E. Malde, 1975, K-Ar dating, Quaternary and Neogene volcanic rocks of the Snake River Plain, Idaho: American Journal of Science, v. 275, p. 225-251.

Bjork, P. R., 1970, The Carnivora of the Hagerman local fauna (late Pliocene) of southwestern Idaho: Transactions of the American Philosophical Society, v. 60, pt. 7, p. 3-54.

Buwalda, J. P., 1924, The age of the Payette formation and the old erosion surface in Idaho: Science, 60(1564), p. 572-573.

Casteel, R. W. and D. P. Adams, 1977, Pleistocene fishes from Alameda County, Calfornia: U. S. Geological Survey Journal of Research, v. 5, no. 2, p. 209-215.

Casteel, R. W. and J. H. Hutchison, 1973, *Orthodon* (Actinopterygii, Cyprinidae) from the Pliocene and Pleistocene of California: Copeia, no. 2, p. 358-361.

Casteel, R. W. and M. J. Rymer, 1975, Fossil fishes from the Pliocene or Pleistocene Cache Formation, Lake County, California: U. S. Geological Survey Journal of Research, v. 3, no. 5, p. 619-622.

Cavender, Ted and R. R. Miller, 1972, *Smilodonichthys rastrosus*, a new Pliocene salmonid fish from western United States: Bulletin, Museum of Natural History, University of Oregon, v. 13, p. 1-44.

Cope, E. D., 1870, On the fishes of a fresh-water Tertiary in Idaho, discovered by Capt. Clarence King: Proceedings of the American Philosophical Society, v. 11, p. 538-547.

———, 1878, Descriptions of new vertebrata from the upper Tertiary formations of the West: Proceedings of the American Philosophical Society, v. 18, p. 219-231.

———, 1883a, On the fishes of the Recent and Pliocene lakes of the western part of the Great Basin, and of the Idaho Pliocene lake: Proceedings of the Academy of Natural Science, Philadelphia, p. 134-166.

———, 1883b, A new Pliocene formation in the Snake River valley: American Naturalist, v. 17, p. 867-868.

Ekren, E. B., D. H. McIntyre, and E. H. Bennett, 1978, Preliminary geologic map of the west half of Owyhee County, Idaho: U. S. Geological Survey Open-File Report 78-341, 14 p.

Evernden, J. F., D. E. Savage, G. H. Curtis, and G. T. James, 1964, Potassium-argon dates and the Cenozoic mammalian chronology of North America: American Journal of Science, v. 262, p. 145-198.

Hibbard, C. W., 1959, Late Cenozoic microtine rodents from Wyoming and Idaho: Papers of the Michigan Academy of Science, Arts, and Letters, (1958), v. 44, p. 3-40.

Hibbard, C. W. and R. J. Zakrzewski, 1967, Phyletic trends in the late Cenozoic microtine *Ophiomys* gen. nov., from Idaho: Contributions of University of Michigan Museum of Paleontology, v. 21, no. 12, p. 255-271.

Hopkirk, J. D., 1973, Endemism of fishes of the Clear Lake region of central California: University of California Publications in Zoology, v. 96, p. 1-135.

Izett, G. A., 1981, Volcanic ash beds—recorders of Upper Cenozoic silicic pyroclastic volcanism in the western United States: Journal of Geophysical Research, v. 86, no. B11, p. 10200-10222.

Jones, D. J. and N. R. Anderson, 1965, A faunule of unusual nonmarine ostracoda from the Pliocene of Idaho: Journal of Paleontology, v. 30, no. 4, p. 1010.

Jones, F. G., B. H. Wilkinson, and G. R. Smith, 1978, Tertiary algal carbonate reefs from Snake River Plain Idaho: American Association of Petroleum Geologists-Society of Economic Paleontologists and Mineralogists Annual Convention Abstracts 1978, p. 78.

Kimmel, P. G., 1975, Fishes of the Miocene-Pliocene Deer Butte Formation, southeast Oregon: Papers on Paleontology, University of Michigan Museum of Paleontology, v. 14, p. 69-87.

———, 1979, Stratigraphy and Paleoenvironments of the Miocene Chalk Hills Formation and Pliocene Glenns Ferry Formation in the western Snake River Plain, Idaho: University of Michigan Ph.D. thesis, 331 p.

———, 1982, Miocene-Pliocene lacustrine sediments of the western Snake River Plain: their stratigraphy, age, and tectonic setting, *in* Bill Bonnichsen and R. M. Breckenridge, editors, Cenozoic Geology of Idaho: Idaho Bureau of Mines and Geology Bulletin 26.

King, Clarence, 1878, Systematic Geology: U. S. Geological Exploration of the 40th Parallel, v. I, Washington, D. C., 803 p.

———, 1903, Mountaineering in the Sierra Nevada: Charles Scribner's Sons, New York, 378 p.

Linder, A. D., 1970, Fossil sculpins (Cottidae) from Idaho: Copeia, 1970, v. 4, p. 755-756.

Lundberg, J. G., 1975, The fossil catfishes of North America: Papers on Paleontology, University of Michigan Museum of Paleontology, v. 11, p. 1-51.

Malde, H. E., 1972, Stratigraphy of the Glenns Ferry Formation from Hammett to Hagerman, Idaho: U. S. Geological Survey Bulletin 1331-D, p. 1-19.

Malde, H. E. and H. A. Powers, 1962, Upper Cenozoic stratigraphy of western Snake River Plain, Idaho: Geological Society of America Bulletin 73, p. 1197-1220.

McClellan, P. H., 1977, Paleontology and paleoecology of Neogene freshwater fishes from the Salt Lake Beds, northern Utah: University of California, Berkeley, M.S. thesis, 243 p.

Miller, R. R. and G. R. Smith, 1967, New fossil fishes from Plio-Pleistocene Lake Idaho: Occasional Papers, University of Michigan Museum of Zoology, v. 654, p. 1-24.

———, 1981, Distribution and evolution of *Chasmistes* (Pisces:Catostomidae) in western North America: Occasional Papers, University of Michigan Museum of Zoology, v. 696, p. 1-46.

Neville, Colleen, N. D. Opdyke, E. H. Lindsay, and N. M. Johnson, 1979, Magnetic stratigraphy of Pliocene deposits of the Glenns Ferry Formation, Idaho, and its implications for North American mammalian biostratigraphy: American Journal of Science, v. 279, p. 503-526.

Shotwell, J. A., 1963, The Juntura Basin: studies in earth history and paleoecology: Transactions of the American Philosophical Society, v. 53, no. 1, p. 1-77.

———, 1970, Pliocene mammals of southeast Oregon and adjacent Idaho: University of Oregon Museum of Natural History Bulletin 17, p. 1-103.

Smith, G. R., 1975, Fishes of the Pliocene Glenns Ferry Formation, southwest Idaho: Papers on Paleontology, University of Michigan Museum of Paleontology, v. 14, p. 1-68.

———, 1981, Late Cenozoic freshwater fishes of North America: Annual Review of Ecology and Systematics, v. 12, p. 163-193.

Smith, G. R. and R. R. Miller, (in press), Taxonomy of fishes from Miocene Clarkia Lake Beds, Idaho, *in* Alan Leviton and C. J. Smiley, editors, Western Division, American Association for the Advancement of Science.

Swirydczuk, Krystyna, 1980, Sedimentology of the Pliocene Glenns Ferry Oolite and its stratigraphic setting in the western Snake River Plain: University of Michigan Ph.D. thesis, 247 p.

Swirydczuk, Krystyna, G. P. Larson, and G. R. Smith, 1982, Volcanic ash stratigraphy of the Glenns Ferry and Chalk Hills Formations, western Snake River Plain, Idaho, *in* Bill Bonnichsen and R. M. Breckenridge, editors, Cenozoic Geology of Idaho: Idaho Bureau of Mines and Geology Bulletin 26.

Swirydczuk, Krystyna, B. H. Wilkinson, and G. R. Smith, 1979, The Pliocene Shoofly Oolite: lake-margin aragonite deposition in the southwestern Snake River Plain: Journal of Sedimentary Petrology, v. 49, no. 3, p. 995-1004.

———, 1980a, The Pliocene Glenns Ferry Oolite II: sedimentology of oolitic lacustrine terrace deposits: Journal of Sedimentary Petrology, v. 50, no. 4, p. 1237-1248.

———, 1980b, The Pliocene Glenns Ferry Oolite: lake-margin carbonate deposition in the southwestern Snake River Plain—reply: Journal of Sedimentary Petrology, v. 50, p. 999-1001.

———, 1981, Synsedimentary lacustrine phosphorites from the Pliocene Glenns Ferry Formation of

southwestern Idaho: Journal of Sedimentary Petrology, v. 51, no. 4, p. 1205-1214.

Taylor, D. W., 1960, Distribution of the freshwater clam *Pisidium ultramontanum*: a zoogeographic inquiry: American Journal of Science, v. 258a, p. 325-334.

———, 1966, Summary of North American Blancan nonmarine mollusks: Malacologia, v. 4, no. 1, p. 1-172.

Taylor, D. W. and G. R. Smith, 1981, Pliocene molluscs and fishes from northeastern California and northwestern Nevada: Papers on Paleontology, University of Michigan Museum of Paleontology, v. 25, no. 18, p. 339-418.

Uyeno, Teruya, 1961, Late Cenozoic cyprinid fishes from Idaho with notes on other fossil minnows in North America: Papers of the Michigan Academy of Science, Arts, and Letters, v. 46, p. 329-344.

Wheeler, H. E. and E. F. Cook, 1954, Structural and stratigraphic significance of the Snake River capture, Idaho-Oregon: Journal of Geology, v. 62, no. 6, p. 525-536.

Zakrzewski, R. J., 1969, The rodents from the Hagerman local fauna, upper Pliocene of Idaho: Contributions of University of Michigan Museum of Paleontology 23, p. 1-36.

Volcanic Ash Beds as Stratigraphic Markers in the Glenns Ferry and Chalk Hills Formations from Adrian, Oregon, to Bruneau, Idaho

by

Krystyna Swirydczuk[1], Gerald P. Larson[2], and Gerald R. Smith[3]

ABSTRACT

Volcanic ash beds were sampled from Miocene and Pliocene sedimentary rocks of the western Snake River Plain in Idaho and correlated using concentrations of major and trace elements. Neutron activation analysis of cleaned bulk samples and electron microprobe analysis of glass shards provided twenty-three elemental abundances used for characterizing each of the beds. Principal component and cluster analysis provided a classification of the samples based on their chemical similarities and differences. One mafic group and several silica-rich groups were distinguished; each of the silica-rich groups is believed to represent volcanic ash from an individual source. Correlation of contemporaneous beds by chemical analyses and field studies has established two time-stratigraphic horizons in the Chalk Hills Formation and seven in the Glenns Ferry Formation. The algal limestone, previously thought to be equivalent to the oolite at the base of the Glenns Ferry Formation, is now correlated to the type Chalk Hills sediments. Sediments in the vicinity of Adrian, Oregon, were laid down in both the Chalk Hills and Glenns Ferry depositional systems, but were separate from the Deer Butte system.

INTRODUCTION

The late Cenozoic sedimentary sequence west of Glenns Ferry, Idaho, has not been previously described in detail, and no stratigraphic framework exists for this area. The rocks are entirely continental and consist of lacustrine silts and sands interbedded with volcanic rock in an area of faulting and downwarping. The tectonic activity apparently controlled deposition in the Miocene and Pliocene (Malde and Powers, 1962; Mabey, 1976).

Interpreting this structurally controlled sedimentation depends on establishing a stratigraphic framework. Volcanic ash layers provide the necessary marker beds. Each ash unit is initially assumed to be a wind-deposited and water-laid collection of a single fall transported from a single drainage area and concentrated in a depositional basin. Chemical and statistical analyses were designed to distinguish the ash layers. Chemical analyses used are neutron activation analysis of the cleaned bulk ash samples for trace elements and major elements, and electron microprobe analysis of glass shards for six major elements. A multivariate statistical analysis of the elemental concentrations together with petrologic observations and stratigraphic position is used to distinguish ashes. The similarity within groups of samples is assumed to be due to their origin from a common source. These correlations provide a stratigraphic framework for this region by allowing a series of sections to be linked.

GEOLOGIC SETTING

The Snake River Plain is an arcuate depression of low topographic relief extending more than 300 miles across southern Idaho and can be distinguished from areas to the north and south by gravity and magnetic anomalies, seismic profiles, pattern of volcanism, and type of sediments. In the west the northern side of the Snake River Plain is grabenlike; but at least part of the southwestern margin is downwarped rather than faulted (McIntyre, 1972; Kirkham, 1931). Abundant faults trend northwest-southeast, with downfaulting towards the center of the basin (Malde and others, 1963). The time of faulting has been established by

[1]Exploration Research Division, Conoco, Inc., P.O. Box 1267, Ponca City, Oklahoma 74601.
[2]Deceased.
[3]Museum of Paleontology, The University of Michigan, Ann Arbor, Michigan 48109.

Swirydczuk, Krystyna, G. P. Larson, and G. R. Smith, 1982, Volcanic ash beds as stratigraphic markers in the Glenns Ferry and Chalk Hills Formations from Adrian, Oregon, to Bruneau, Idaho, *in* Bill Bonnichsen and R. M. Breckenridge, editors, Cenozoic Geology of Idaho: Idaho Bureau of Mines and Geology Bulletin 26, p. 543-558.

geologic mapping as early to middle Pliocene (Malde, 1959; Axelrod, 1968); at least 5,000 feet of vertical displacement along a zone of northwest-trending, high-angle faults has placed the western Snake River Plain downward in relation to the highlands in the north during this time, and 4,000 feet of subsidence has taken place since that time. Mabey (1976) suggested that the faulting and downwarping of the area began as early as the Miocene and continued throughout post-Miocene time. Rocks of early Pliocene and younger age appear to be displaced downward toward the center of the basin in progressively diminishing amounts. Proposed tectonic and geophysical models for evolution of the Snake River Plain imply considerable structural control of the accumulation of sediments since the Miocene.

West of Twin Falls, Idaho, a thick section of upper Cenozoic clastic and volcanic rocks, the Idaho Group, crops out over a region of several thousand square miles (Figure 1). The earliest geologic maps of the region were published by Lindgren (1900) and Russell (1902). Littleton and Crosthwaite (1957) studied the ground-water geology and provided a map and description of the Bruneau-Grand View area. Malde and Powers (1972) mapped the Glenns Ferry-Hagerman area of the west-central Snake River Plain, and Malde and others (1963) produced a reconnaissance geologic map of the same area. Their studies provided the foundations for the modern view of the overall stratigraphy of the upper Cenozoic

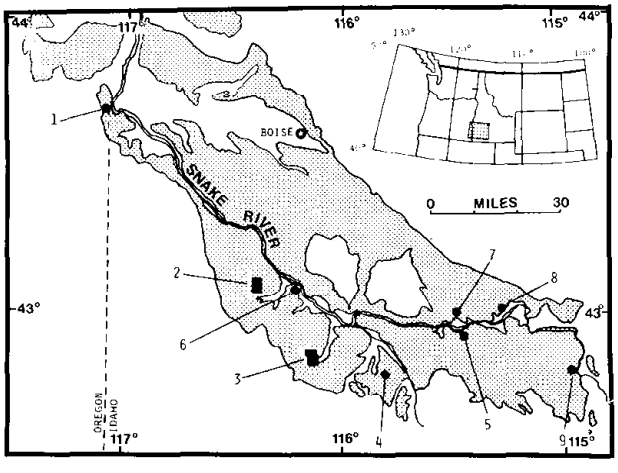

Figure 1. Western Snake River Plain showing the distribution of sedimentary rocks of the Idaho Group (modified from Malde and Powers, 1962) and localities of ash beds reported here. Oregon, Malheur County: (1). Idaho, Owyhee County: (2) Crayfish Hill, Fossil Creek, and Picket Creek localities; (3) Shoofly Creek, Poison Creek, and Twentymile Gulch localities; (4) Horse Hill locality; (5) Sand Point locality; and (6) Jackass Butte locality. Idaho, Elmore County: (7) Bennett Creek locality; and (8) Glenns Ferry locality. Idaho, Twin Falls County: (9) Peters Gulch locality.

deposits in the western Snake River Plain and especially the detailed stratigraphy of the Glenns Ferry Formation of late Pliocene age in the region from Hammett to Hagerman. Powers and Malde (1961) proposed two volcanic ash beds as stratigraphic markers in the Hagerman-Glenns Ferry deposits on the basis of unique chemistry. They made correlations over a distance of 20 miles on the Peters Gulch ash horizon and 7 miles on the Narrows ash horizon. In later work in the same area Malde (1972) made use of numerous lava flows, basaltic pyroclastic layers, and silicic volcanic ash layers as marker beds, and he was able to establish a stratigraphic framework for the intertonguing sedimentary facies of the Glenns Ferry Formation.

The rocks reviewed by Malde and Powers (1962) were divided into four units: an unnamed sequence of Miocene age, the Idavada Volcanics, the Idaho Group, and the Snake River Group (Figure 2). The Miocene rocks include sedimentary deposits and gold-bearing rhyolite and basalt in the Owyhee Mountains (McIntyre, 1972; Ekren and others, 1981). The Idavada Volcanics consist of nonmineralized silicic latite and rhyolite. The Idaho Group includes younger sedimentary deposits and some interbedded basalts. The Snake River Group consists principally of the Snake River Basalt and a small amount of sedimentary deposits. Ekren and others (1981) have recently mapped both the volcanic and sedimentary rocks west of longitude 116°.

Cope (1884, p. 135) originated the term "Idaho Formation" for the sedimentary deposits at Castle Creek in Owyhee County. He determined that the fish collected there by J. L. Wortmann indicated a Pliocene age (Malde and Powers, 1962). Other workers (Lindgren, 1900; Russell, 1902; Merriam, 1918; Buwalda, 1923, 1924; Kirkham, 1931; Stearns, 1936; Stearns and others, 1938) referred to related deposits as far upstream as Hagerman and west into Oregon. Malde and Powers (1962) divided these deposits, which unconformably overlie the Idavada Volcanics, into seven overlapping formations. The choice of formations was governed as much by structural relationships and geographical extent as by lithology and fossils. A composite section of these deposits would measure almost 5,000 feet and consist of clastic beds and some intercalated basalt flows. The clastic beds are weakly consolidated but not lithified. According to Malde and Powers (1962) the seven formations in ascending order are the Poison Creek Formation of mostly siliceous volcanic ash and fine-grained tuffaceous detrital material; the Banbury Basalt (Armstrong and others, 1975; Kimmel, 1979); the Chalk Hills Formation of large amounts of siliceous volcanic ash interbedded with abundant sand and silt; the Glenns Ferry Formation of lacustrine,

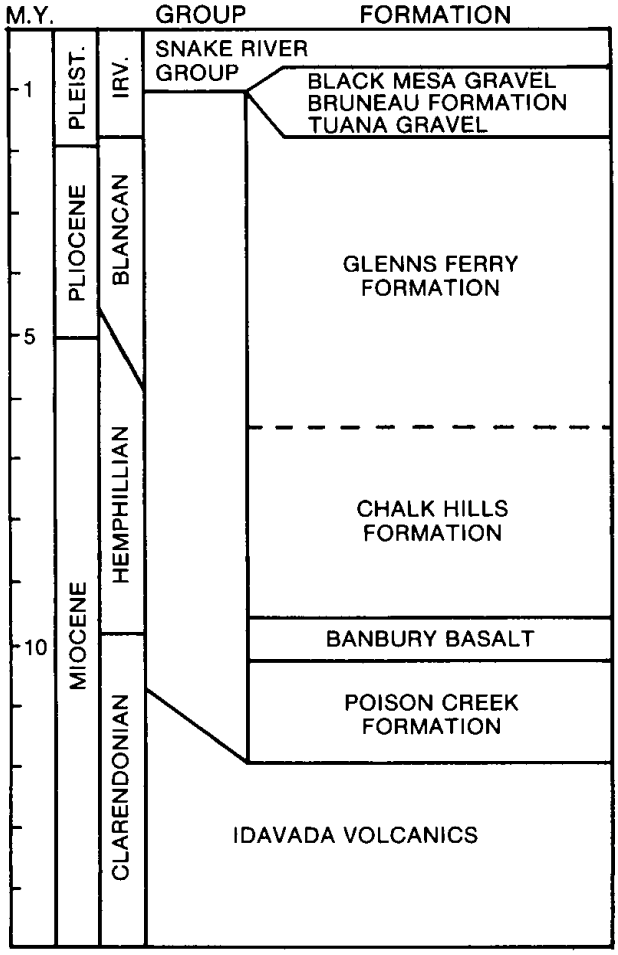

Figure 2. Sequence of upper Cenozoic rocks in the western Snake River Plain, Owyhee County, Idaho (modified from Armstrong and others, 1975; Malde and Powers, 1962).

fluvial, and floodplain facies; the Tuana Gravel; the Bruneau Formation of lacustrine deposits and lava flows; and finally the Black Mesa Gravel (Figure 2).

The Glenns Ferry Formation takes its name from the type area of characteristic clastic deposits exposed both north and south on both sides of the Snake River and for some miles upstream and downstream from Glenns Ferry. The formation is exposed as far east as the canyon wall west of Hagerman and as far west as Oregon (Kimmel, 1975). Thus, the Glenns Ferry Formation and stratigraphically equivalent units are believed to embrace several thousand square miles. The exposed thickness of the formation in the type area is about 2,000 feet. The Glenns Ferry Formation makes up a significant part of the Idaho Group both in volume and areal extent.

Three principal facies exist in the Glenns Ferry Formation: lacustrine, fluvial, and floodplain (Malde, 1972, Figure 2). The lacustrine facies is distinguished by massive layers of tan silt and is the greatest of the three facies in both volume and area. The fluvial facies is characterized by thick beds of brownish gray sands, some of which are cross bedded and ripple marked. The fluvial facies merges into the floodplain facies which consists mainly of thin beds of calcareous, pale olive silt and dark clay.

METHODS

Previous studies (Carmichael and McDonald, 1961; Cann and Renfrew, 1964; Jack and Carmichael, 1969; Borchardt and others, 1971; Bowles and others, 1973; Howorth and Rankin, 1975; Richardson and Ninkovich, 1976; Edsall, 1976; Sarna-Wojcicka, 1976; Izett, 1981) have demonstrated that trace element and minor element assemblages are diagnostic of silicic volcanic materials. Smith and Westgate (1969) developed the use of a rapid electron microprobe technique for characterizing pyroclastic deposits by the composition of their glass. Most previous analyses have been carried out on the glassy separates of the pyroclastics, because density sorting of phenocrysts during wind transportation changes the bulk chemistry of the resulting deposits laterally.

In this study, samples are analyzed by neutron activation and electron microprobe methods to obtain abundances of trace, rare earth, and major elements. These abundances are used to characterize and identify ash horizons. Cleaned bulk samples were irradiated for neutron activation analysis. Standards were USGS rock standard BCR-1 and a synthetic liquid standard. Replicates of USGS rock standard GSP-1 and RGM-1 were included in the analysis to evaluate the accuracy and precision of the analytical method. Twenty-seven elemental abundances were obtained from measuring their radioactive decay after long irradiation; nine elemental abundances were measured after short irradiation (see Swirydczuk and others, 1981, Table 2, for element abundances).

A comparison of observed and known values for RGM-1 gave consistent results for all but four of the elements. Fourteen elements, aluminum (Al), calcium (Ca), cerium (Ce), europium (Eu), iron (Fe), hafnium (Hf), lanthanum (La), manganese (Mn), sodium (Na), antimony (Sb), scandium (Sc), samarium (Sm), thorium (Th), and ytterbium (Yb), were used to characterize the samples; many other elements were below the detectable limit or were imprecise and were not used. Descriptions of the cleaning method and the neutron activation analysis procedure are summarized in Swirydczuk (1977).

Glass shards were analyzed for aluminum (Al), calcium (Ca), iron (Fe), potassium (K), magnesium

(Mg), and silicon (Si) by electron microprobe analysis. Analysis was carried out at voltages of 10 KeV and with a beam current of 0.005 μa to avoid volatilization of the alkali metals (see Swirydczuk and others, 1981, Table 2, for elemental abundances).

Elemental abundances of the different samples were compared by multivariate statistical techniques (principal component analysis, Morrison, 1967) and by cluster analysis. The former method ordinates groups of similar ash samples based on correlation among the samples; the latter forms clusters using the summed differences among samples. Both statistical techniques were carried out on standardized data, first on data from neutron activation analysis (bulk chemistry) and then on the combined data from neutron activation analysis and electron microprobe analysis. Significant differences between the results of the two approaches would be due to the effect of any microphenocrysts in the samples and would demonstrate that density sorting was a significant factor affecting the bulk chemistry. No significant differences were detected between analyses.

Cluster analysis gives an independent classification, which was compared with that by principal component analysis. The first two principal components were also used for cluster analysis as advocated by Howorth and Rankin (1975). All analyses are summarized in Swirydczuk (1977).

DESCRIPTION OF LOCALITIES

Fifty-one volcanic ash samples were collected from the Glenns Ferry Formation and the upper part of the Chalk Hills Formation in southwestern Idaho and the Deer Butte Formation in southeastern Oregon (Figure 1). Stratigraphic sections were measured and graphic profiles were drawn in the field.

OREGON, MALHEUR COUNTY

Samples M1, M2, M51-53, and M72 were collected from five separate localities in the Deer Butte Formation in Malheur County, Oregon, by Peter Kimmel (1975), who reported on associated fossil fishes.

Shenk Ranch

Shenk Ranch locality is in sec. 21, T. 22 S., R. 46 E., Adrian quadrangle, Malheur County, Oregon.

Sample M51, a white ash, was collected from a sandstone sequence at an elevation of 2,500 feet.

Tunnel Mountain

Tunnel Mountain locality is in SW¼ sec. 22, T. 22 S., R. 46 E., Adrian quadrangle, Malheur County, Oregon.

Sample M52 was collected from a white ash bed located within a sandstone and conglomerate sequence at an elevation of 2,640 feet (Figure 3B).

Rimrock

Rimrock locality is in SE¼SW¼ sec. 28, T. 21 S., R. 46 E., Adrian quadrangle, Malheur County, Oregon.

Sample M53 was collected from an ash bed at an elevation of 2,800 feet.

Tunnel Road

Tunnel Road locality is in SE¼SE¼ sec. 16, T. 22 S., R. 46 E., Adrian quadrangle, Malheur County, Oregon, 1 mile south on South Canal Road.

Samples M1 and M2 were collected from two ash beds 20 feet apart, sample M1 being the lower at an elevation of 2,600 feet. These ashes are part of a sandstone and conglomerate sequence (Figure 3A).

U. S. Highway 95

U. S. Highway 95 locality is in NW¼SE¼ sec. 19,

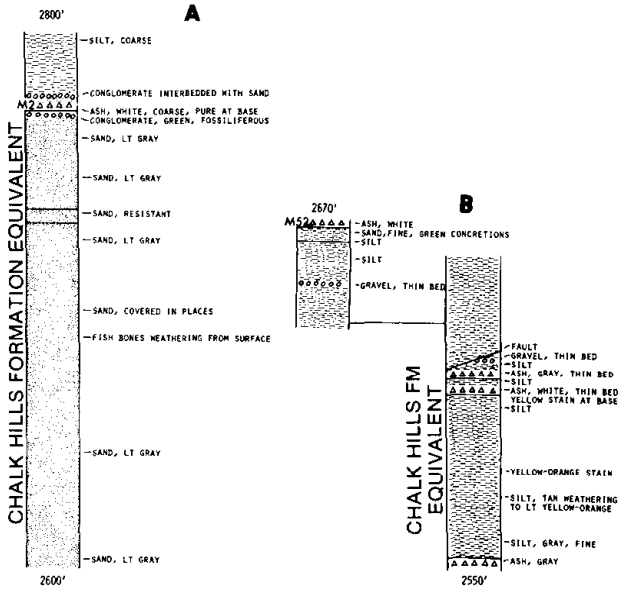

Figure 3. Stratigraphic sections from: (A) Tunnel Road locality, SE¼SE¼, sec. 16, T. 22 S., R. 46 E., and (B) Tunnel Mountain locality, SW¼, sec. 22, T. 22 S., R. 46 E., Malheur County, Oregon. M2 correlates to the lower Horse Hill ash.

T. 31 S., R. 42 E., Adrian quadrangle, Malheur County, Oregon.

Sample M72 was collected from an uncontaminated white ash bed 3 feet thick at an elevation of 3,650 feet, 50 feet below the top of the grade on U. S. Highway 95.

IDAHO, OWYHEE COUNTY, SHOOFLY CREEK-POISON CREEK AREA

Poison Creek

Poison Creek locality (Figures 4A, 4B) is at the south side of the butte, northwest of the stage station, NW¼SW¼ sec. 5, T. 7 S., R. 3 E., Chalk Hills quadrangle, Owyhee County, Idaho. Fossil fishes from these beds were reported by Smith (1975). Two hundred fifty-five feet of section is exposed in a traverse from this location to a point 0.8 mile west-northwest of the stage station in sec. 5, T. 7 S., R. 3 E., 1,600 feet north, 850 feet east of the southwest corner of sec. 5. The section is divided by an oolitic unit. The base of this section is established at an elevation of 3,065 feet from its location 61 feet below the oolite bed. This oolitic carbonate has been defined as the base of the Glenns Ferry Formation by Malde and Powers (1962) but as the top of the Chalk Hills Formation by Warner (1976). The lower section consists almost entirely of silts with numerous ash units that represent the Chalk Hills Formation. The Glenns Ferry Formation overlies these units.

Sample P1: ash, dark gray, medium grained; sampled from a bed 18 inches thick at an elevation of 3,080 feet.

The upper part of this section represents the Glenns Ferry Formation (Figure 4B) and consists of oolitic carbonate, 30 to 40 feet thick, at the base of the section, overlain by over 80 feet of silts with occasional fine-grained sands and ash units. The lacustrine deposits grade into 65 feet of coarse fluvial sands and silts. Two ash units, P2 and P3, are sampled from the lacustrine deposits.

Sample P2: ash, thin light gray, medium grained; elevation 3,202 feet.

Sample P3: ash, gray, fine grained; elevation 3,218 feet.

South of Poison Creek

Sample P40: ash, dark gray, medium grained; elevation 3,075 feet. South of stage station, east side of NE¼NW¼ sec. 9, T. 7 S., R. 3 E., Chalk Hills quadrangle, Owyhee County, Idaho; 800 feet south, 2,600 feet east of the northwest corner of sec. 9.

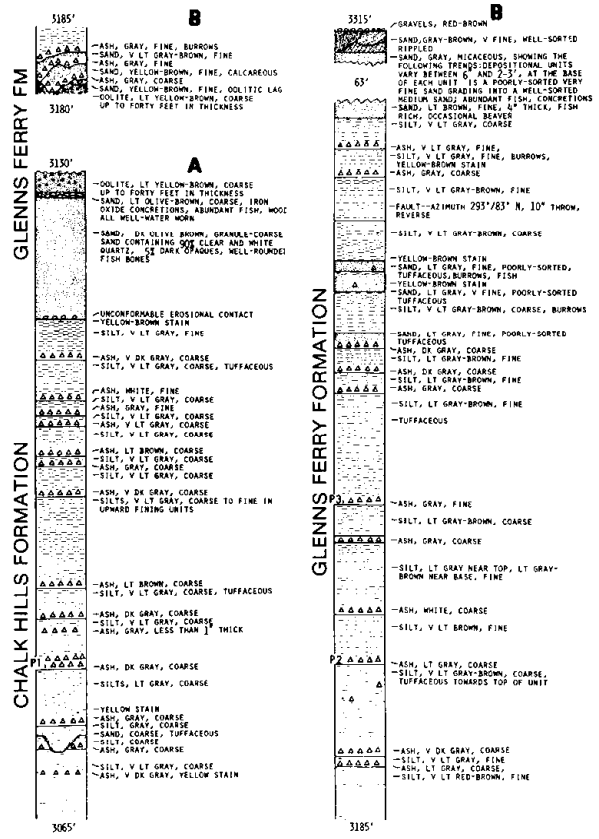

Figure 4. Stratigraphic sections from: (A) the lower part of the Poison Creek locality, NW¼SW¼ sec. 5, T. 7 S., R. 3 E., Owyhee County, Idaho, and (B) the upper part of the Poison Creek locality NW¼SW¼ sec. 5, T. 7 S., R. 3 E., Owyhee County, Idaho. P2 correlates to the basal Crayfish Hill ash; P3 correlates to the upper Horse Hill ash.

Sample P38: ash, dark gray, pumaceous; elevation 3,025 feet, 150 feet below the oolite bed. South of stage station, SW corner of NE¼NW¼ sec. 9, T. 7 S., R. 3 E., Chalk Hills quadrangle, Owyhee County, Idaho, north of butte, south of stage station; 1,100 feet south, 1,500 feet east of the northwest corner of sec. 9.

Shoofly Creek

Shoofly Creek locality (Figure 5A) is in the northwest corner of SW¼NE¼ sec. 4, T. 7 S., R. 3 E., Chalk Hills quadrangle, Owyhee County, Idaho; 2,700 feet east, 1,300 feet south of the northwest corner of sec. 4. Seventy feet of section is exposed with a base elevation of 2,950 feet; the section is composed of fine silt through medium-grained sand beds, which make up approximately 80 percent of the section, and numerous thin ash units and a few thicker ashes, which together make up almost 20

percent of the section. The beds show no structure, occasionally are calcareous, and contain fish (Smith, 1975) and molluscs; they are poorly sorted and stained.

Sample S1: ash, gray, medium grained, about 1 foot thick at an elevation of 2,996 feet.

Sample S2: overlying the horizon from which sample S1 was collected and separated from it by another thin ash and a fine-grained sand unit, a thick (1-2 feet), pink, fine-grained ash was collected at an elevation of 2,998 feet.

Sample S3: separated from the bed of sample S2 by 12 inches of coarse silt, a gray medium-grained ash lies at an elevation of 3,000 feet; it is finer at its base and top, coarsest in the center.

Sample S4: immediately overlying the bed from which sample S3 was collected lies a coarse-grained gray ash from which a sample was taken at an elevation of 3,002 feet.

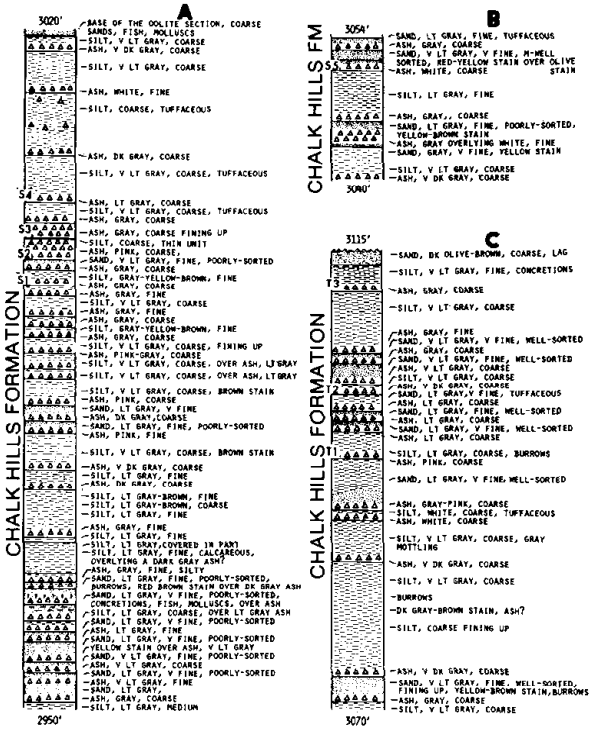

Figure 5. Stratigraphic sections from: (A) the Shoofly Creek locality northwest corner of the SW¼NW¼ sec. 4, T. 7 S., R. 1 W.; (B) the upper Shoofly Creek locality, center of NW¼ sec. 4, T. 7 S., R. 3 E. (this stratigraphic section (B) can be linked to the Shoofly Creek section (A) by tracing the ash from elevation 3,200 feet in A to elevation 3,040 feet in B); and (C) the Twentymile Gulch locality, SW¼ sec. 32, T. 6 S., R. 3 E., Owyhee County, Idaho. S1 and T3 correlate and make up the lower Shoofly ash; beds S3 and S4 correlate to the lower Horse Hill ash.

Upper Shoofly Creek

Upper Shoofly Creek locality (Figure 5B) is in the center of NW¼ sec. 4, T. 7 S., R. 3 E., Chalk Hills quadrangle, Owyhee County, Idaho. On the south-facing slope of an eastward promontory a 13-foot section is exposed with a base at an elevation of 3,040 feet. It is located 1,500 feet east, 1,600 feet south of the northwest corner of sec. 4. The section consists of massive silts interbedded with ash units and, near the top, with very fine sands. The base of this section can be directly correlated by tracing the beds from the top of the Shoofly Creek section.

Sample S5: thin ash, white, very fine grained; collected from an elevation of 3,050 feet. This ash is 29 feet above a horizon which can be traced laterally to where sample S4 was collected. The ash unit from which sample S2 was collected can be traced laterally to the west where it lies directly below the coarse sands and oolitic carbonate unit. This places the Shoofly Creek section in the Chalk Hills Formation.

Twentymile Gulch

Twentymile Gulch locality (Figure 5C) is in the SW¼ sec. 32, T. 6 S., R. 3 E., Perjue Canyon quadrangle, Owyhee County, Idaho. Ninety feet of section is exposed with a base at an elevation of 3,070 feet, 2,500 feet west, 1,400 feet north of the southeast corner of sec. 32. The section consists of interbedded massive silts, fine- to medium-grained sands, and thin ash beds. The sands are structureless, occasionally cemented by carbonates, and contain occasional concretions. The ash layers constitute less than 10 percent of the section. Fish and molluscs are found near the top of the section.

Sample T1: thin ash, pink, medium grained; elevation 3,096 feet.

Sample T2: thin ash, very light gray, medium grained; elevation 3,102 feet.

Sample T3: thin ash, gray, medium grained, exhibiting ball and pillow structure; collected at an elevation of 3,113 feet.

Sample T128: pink, medium-grained ash from a section on the same side of the valley as the section from which samples T1-T3 were collected; SE¼SW¼ sec. 32 at an approximate elevation of 3,096 feet.

IDAHO, OWYHEE COUNTY, FOSSIL CREEK AREA

Crayfish Hill 1

Crayfish Hill 1 locality (Figure 6A) is in the southeast corner NW¼ sec. 1, T. 4 S., R. 1 W.,

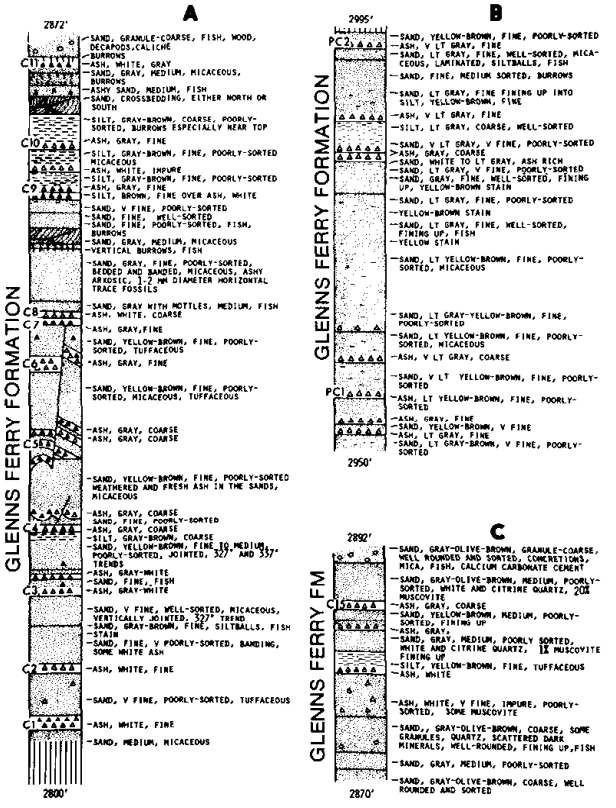

Figure 6. Stratigraphic sections from: (A) the Crayfish Hill locality, southeast corner of the NW¼ sec. 1, T. 4 S., R. 1 W.; (B) the Picket Creek locality, NE¼SW¼ sec. 24, T. 4 S., R. 1 W.; and (C) northwest of the Crayfish Hill locality, SE¼NW¼ sec. 1, T. 4 S., R. 1 W., Owyhee County, Idaho. C1 is the basal Crayfish Hill ash; C2 correlates to the Fossil Creek Ash; C3 correlates to the middle Horse Hill ash; C4 correlates to the upper Horse Hill ash; C6 and PC1 correlate and make up the lower Picket Creek ash; and PC2 is the upper Picket Creek ash.

Oreana quadrangle, Owyhee County, Idaho. Seventy-two feet of section is exposed at 1,900 feet east, 2,100 feet north of the southwest corner of sec. 1, with a base at an elevation of 2,800 feet; the section is composed of fine- to very fine-grained sands and silts interbedded with numerous volcanic ashes varying in thickness and in purity. The top of the section is at 1,600 feet east, 2,250 feet north of the southwest corner of sec. 1. Ash units make up almost 15 percent of the total section exposed; the remaining 85 percent is made up of variably sorted, structureless, generally noncalcareous fine clastic material. All units within the section are interpreted as lacustrine. Some units contain abundant fish (Smith, 1975) and small amounts of ash. Samples C1 through C11 were collected from this section.

Sample C1: ash, white, very fine grained, 18 inches thick; elevation 2,806 feet.

Sample C2: ash, white, very fine grained, less than 1 foot thick; elevation 2,812 feet.

Sample C3: ash, gray-white, less than 1 foot thick; elevation 2,818 feet.

Sample C4: ash, gray, fine grained, approximately 6 inches thick; elevation 2,825 feet.

Sample C5: ash, gray, fine grained, elevation 2,834 feet. This is the middle of three gray ash units that are separated by fine sand and total 4 feet in thickness.

Sample C6: ash, gray, fine grained, 18 inches thick; elevation 2,842 feet.

Sample C7: thin ash, gray, very fine grained; elevation 2,846 feet.

Sample C8: ash, white, fine grained, about 8 inches thick immediately overlying and in contact with the bed from which sample C7 was taken; elevation 2,847 feet.

Sample C9: thin ash, gray; elevation 2,858 feet.

Sample C10: thin ash, gray; elevation 2,863 feet.

Sample C11: thin ash, gray; elevation 2,869 feet.

Crayfish Hill 2

Crayfish Hill 2 locality (Figure 6C) is in coarse sands, SE¼NW¼ sec. 1, T. 4 S., R. 1 W., Oreana quadrangle, Owyhee County, Idaho, 1,000 feet east, 2,500 feet north of the southwest corner of sec. 1. Twenty-two feet of section is exposed with a base at an elevation of 2,870 feet; this section contains two ash beds in an otherwise coarse clastic sequence consisting of medium- to coarse-grained sands which are generally poorly sorted. This section is noncalcareous except for a concretion zone. At the top of the section the Glenns Ferry sands (Oreana sands of Anderson, 1965) are exposed; here they are coarse grained (granule) and rich in fish bone.

Sample C15: ash, gray, fine grained, the higher of the two ashes; elevation 2,886 feet.

Crayfish Hill 3

Crayfish Hill 3 locality (Figure 7C) is in sands and oolites, NW¼NW¼ sec. 1, T. 4 S., R. 1 W., Oreana quadrangle, Owyhee County, Idaho, 700 feet east, 1,100 feet south of the northwest corner of sec. 1. Fifteen feet of section is exposed with a base at an elevation of 1,860 feet; this section consists of the characteristic gray olive-brown sands of the Glenns Ferry Formation (Oreana sands, Anderson, 1965). Interbedded in this sequence is a unit consisting of 50 percent ooids. Near the top of the section silts are similar to those seen in the Crayfish Hill section but contain more mica. These coarser sediments are interpreted as nearshore lacustrine sediments. Fossil

fish and wood are abundant. Only one ash bed is found here. Units high in the section may be aeolian.

Sample C16: thin ash, white, fine grained; elevation 2,866 feet.

Crayfish Hill 4

Crayfish Hill 4 locality is in faulted fine-grained sands, SE¼NW¼ sec. 1, T. 4 S., R. 1 W., Oreana quadrangle, Owyhee County, Idaho, 1,400 feet east 2,300 feet north of the southwest corner of sec. 1. This is an exposure of the "Oreana Formation," including the "Gravel member," of Anderson (1965) that is lithologically and texturally identical to the Crayfish Hill section. The "Gravel member" of Anderson is mapped as Bruneau Formation by Malde in Ekren and others (1981). Underlying the contact with the "Gravel member," an ash bed is interbedded with 25 feet of poorly sorted fine-grained folded sands.

Sample C17: ash, light gray; elevation 2,880 feet.

Crayfish Hill 5

Crayfish Hill 5 locality is in the "Montini Formation" of Anderson (1965), SW¼NW¼ sec. 7, T. 4 S., R. 1 E., Oreana quadrangle, Owyhee County, Idaho. It has also been mapped as sediments of Bruneau Formation by Ekren and others (1981).

Sample C18: a moderately indurated black basaltic tuff was sampled from the upper member of the "Montini Formation" (Anderson, 1965) at an elevation of 2,925 feet.

Fossil Creek

Fossil Creek locality (Figure 7A) is in NW¼ sec. 12, T. 4 S., R. 1 W., Oreana quadrangle, Owyhee County, Idaho; 1,100 feet east, 1,500 feet south of the northwest corner of sec. 12. Sixty-eight feet of section is exposed with a base elevation of 2,850 feet; the section is composed of medium oolitic sands at the base and grades into medium to fine-grained sands and coarse silts interbedded with numerous thin ash units. These are interpreted as nearshore lacustrine deposits. Ash units make up around 15 percent of the total section; the rest of the section is made up of alternating, well-sorted and poorly sorted sand and silt beds, many fining upwards. Bedding is poor or nonexistent. Fish fossils are abundant. Concretions are common in the lower part of the section, and burrowing occurs throughout the section.

Sample F1: ash, white, fine grained, less than 8 inches thick; elevation 2,857 feet.

Sample F2: ash, very light gray, medium grained; elevation 2,875 feet.

Sample F3: a thick (almost 2 feet) ash, light gray, fine grained; elevation 2,914 feet.

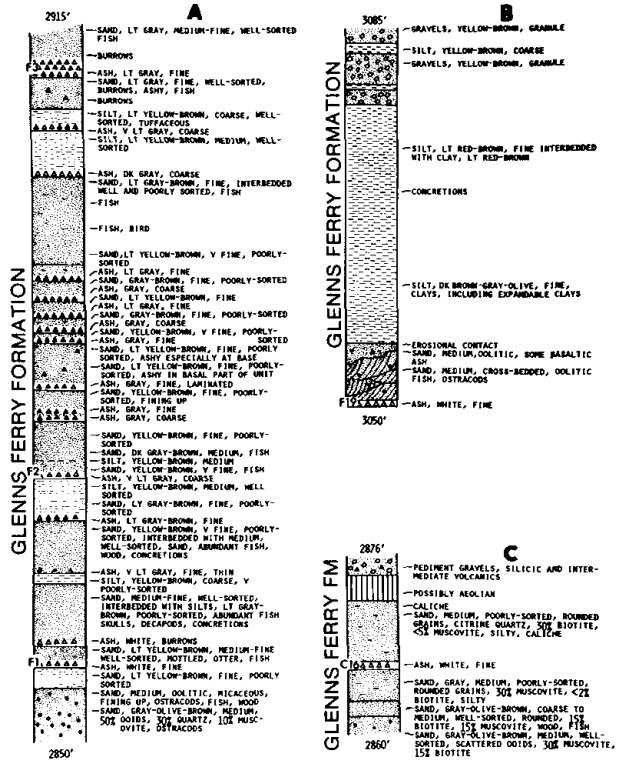

Figure 7. Stratigraphic sections from: (A) the Fossil Creek locality, NW¼ sec. 12, T. 4 S., R. 1 W.; (B) south of the U. S. Highway 78 roadcut of Smith (1975), SE¼NW¼ sec. 14, T. 4 S., R. 1 W., and (C) northwest of Crayfish Hill locality, NW¼NW¼ sec. 1, T. 4 S., R. 1 W., Owyhee County, Idaho. F1 and C16 correlate and make up the Fossil Creek ash. F3 correlates to the upper Picket Creek ash.

U. S. Highway 78

U. S. Highway 78 locality (Figure 7B) is in SE¼NW¼ sec. 14, T. 4 S., R. 1 W., Oreana quadrangle, Owyhee County, Idaho, 0.3 mile south-southeast of High Roadcut locality of Smith (1975); 1,900 feet east and 2,300 feet south of the northwest corner of sec. 14. An exposed 35-foot section can be traced to the above locality from which the sample was taken. The section has a base elevation at 3,050 feet and consists of basal units of medium, cross-bedded oolitic sands, fining upward into 22 feet of silt units, which in turn are overlain by interbedded coarse silts and granule gravels. These are believed to be part of the upper Glenns Ferry Formation (Oreana sands of Anderson, 1965).

Sample F19: ash, white, at an elevation of 3,050 feet lying 6 feet below the contact with the Oreana sands of the 35-foot section.

Picket Creek

Picket Creek locality (Figure 6B) is in NE¼SW¼ sec. 24, T. 4 S., R. 1 W., Oreana quadrangle, Owyhee County, Idaho; 2,900 feet south, 2,100 feet east of the northwest corner of sec. 24. Forty-five feet of section is exposed with a base elevation at 2,950 feet; this section consists of monotonous fine-grained sands interbedded with numerous thin ash units. The sands are poorly sorted, noncalcareous, and in some places silty. No bedding or sedimentary structures are seen.

Sample PC1: thin ash, light gray, fine grained; elevation 2,955 feet.

Sample PC2: ash, very light gray, very fine grained; elevation 2,994 feet.

IDAHO, OWYHEE COUNTY, OTHER LOCALITIES

Horse Hill

Horse Hill locality (Figures 1 and 8) is in NW¼SW¼ sec. 32, T. 7 S., R. 6 E., Sugar Valley quadrangle, Owyhee County, Idaho. The base of the exposed section was measured from the algal limestone in the northeast corner of NW¼SW¼ sec. 32 toward the saddle between the two buttes to the west. Elevation at the base is 2,950 feet. The algal limestone at the base of the section was believed to be time equivalent to the oolitic carbonate rocks exposed to the west in the Shoofly Creek and Poison Creek sections (Malde and Powers, 1962). Swirydczuk (1977) showed this algal limestone to be older and in the Chalk Hills Formation. Overlying the limestone and a covered section of 48 feet, a medium-grained, cross-bedded sand unit and overlying fine structureless sands and interbedded ash horizons extend 45 feet, ending in fluvial sands. At an elevation of 3,045 feet is an erosional contact overlain by a monolayer of large quartzite cobbles and a thin fining-upward unit rich in molluscs, fish, and wood debris. These sands and the quartzite cobble layer are believed to be the base of the Glenns Ferry Formation in this area. The upper 90 feet consists of silts, fine sands, and interbedded ashes, generally becoming coarser toward the top.

Sample H1: SE¼NE¼SE¼NE¼ sec. 31, a gray ash bed many feet in thickness is exposed with its base at 3,025 feet; the ash is coarse grained, without silt, and lies immediately above a fish fauna containing *Mylocheilus inflexus*.

Sample H2: NE¼SE¼SW¼NE¼ sec. 31, a thin ash, gray, fine grained; elevation 3,065 feet. The ash is pure and interbedded with massive silty clay beds.

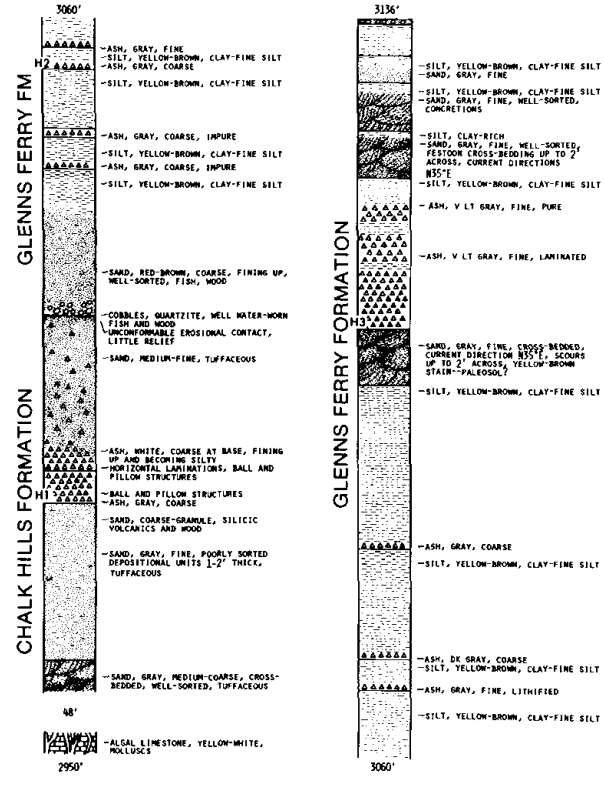

Figure 8. Stratigraphic section from the Horse Hill locality, NW¼SW¼ sec. 32, T. 5 S., R. 6 E., Owyhee County, Idaho. H1 is the lower Horse Hill ash; H2 is the middle Horse Hill ash; H3 is the upper Horse Hill ash.

Sample H3: NW¼SE¼SW¼NE¼ sec. 31, pure ash, very light gray, fine grained; elevation 3,110 feet. The ash unit totals 12 feet in thickness with silt laminae 6 feet and 10 feet above its base.

Sand Point

Sand Point locality (Figure 1) is in SE¼SW¼ sec. 1, T. 6 S., R. 8 E., Hammett quadrangle, Owyhee County, Idaho.

Sample SP43: ash, medium gray, collected from ash-rich bed at an elevation of 2,700 feet. Fossils from this locality are described by Hibbard (1959), Hibbard and Zakrzewski (1967), Miller and Smith (1967), and Smith (1975).

Jackass Butte

Jackass Butte locality (Figure 1) is in NE¼SE¼ sec. 9, T. 4 S., R. 2 E., Jackass Butte quadrangle, Owyhee County, Idaho.

Sample J41: ash, white, phenocryst-rich; elevation 2,465 feet.

IDAHO, ELMORE COUNTY

Bennett Creek

Bennett Creek locality (Figure 1) is in SW¼NE¼NW¼SE¼ sec. 16, T. 5 S., R. 8 E., Indian Cove quadrangle, Elmore County, Idaho (near old railroad grade).

Sample B42: collected at an elevation of 2,680 feet from 12 feet of dark gray-brown, cross-bedded ash.

Glenns Ferry

Glenns Ferry locality (Figure 1) is in SW¼NE¼ sec. 21, T. 5 S., R. 10 E., Glenns Ferry quadrangle, Elmore County, Idaho. Roadcut east of Glenns Ferry on U. S. Highway 30.

Sample GF46: a thin black, basaltic ash was collected at an elevation of 2,575 feet from the Glenns Ferry Formation. This is Bed P of Malde (1972).

IDAHO, TWIN FALLS COUNTY

Peters Gulch

Peters Gulch locality (Figure 1) is in SE¼SE¼NE¼ sec. 32, T. 7 S., R. 13 E., Hagerman quadrangle, Twin Falls County, Idaho.

Sample PG44: ash, white, collected from the Peters Gulch Ash Layer of Powers and Malde (1961) at an elevation of 2,970 feet.

East of Peters Gulch

Locality east of Peters Gulch is in SW¼NW¼ sec. 33, T. 7 S., R. 13 E., Hagerman quadrangle, Twin Falls County, Idaho.

Sample PG45: a black, basaltic ash; elevation 3,050 feet. This is Bed F of Malde (1972).

CHEMICAL COMPOSITION AND CLASSIFICATION OF SAMPLES

Prior to statistical analysis of elemental abundances of the ash samples, the mafic ash samples were separated from the rhyolitic and rhyodacitic ash samples. Principal component analysis of the neutron activation data (without microprobe data) shows that several groups of chemically similar silicic ashes can be distinguished (Figure 9). Cluster analysis of the same data categorized the samples into similar groups. The lines joining the samples in Figure 9 represent linkages obtained from cluster analysis.

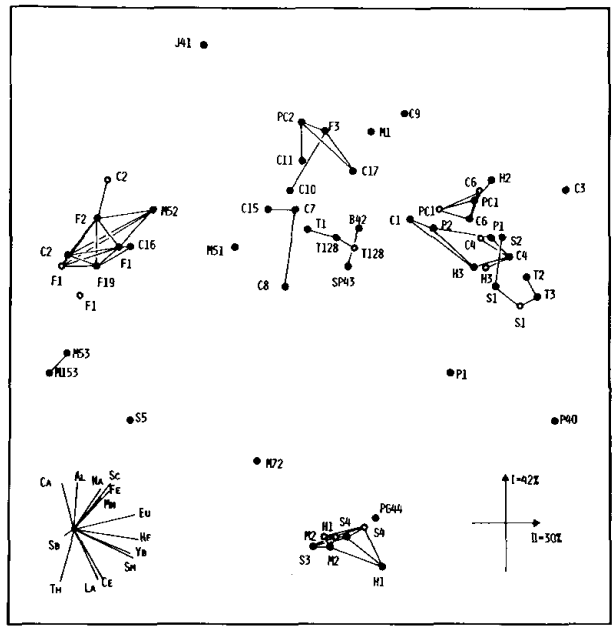

Figure 9. Scatter diagram of the principal component scores of fifty-eight samples based on the data obtained from neutron activation analysis. Axes are components I and II. Closed circles represent 63-125 σm fraction; open circles represent the coarser fractions. Lines joining samples are taken from the original distance matrix which was based on neutron activation analysis data. The star diagram in the lower left illustrates the correlations between individual elemental abundances and the components.

Each group of ash samples defined here represents a single volcanic source. Elements which appear to best distinguish the different groups of ash samples are cerium, lanthanum, potassium, and to a lesser extent hafnium. A simplified representation of the variability of the groups using concentrations of europium and the ratio of potassium to silicon is shown in Figure 10. Definition of the groups is less obvious than in the analysis based on fourteen or more elements.

CONCLUSIONS

Most of the volcanic ash samples in this study may be classified in seven groups. These groups of chemically similar ash horizons are generally interpreted as contemporaneous units. However, repetition of an ash sample in the same stratigraphic section suggests either reworking and redeposition or chemically similar ashes being erupted over a period of time. A tentative stratigraphic framework connecting the various localities and measured sections must therefore be based on the following criteria:

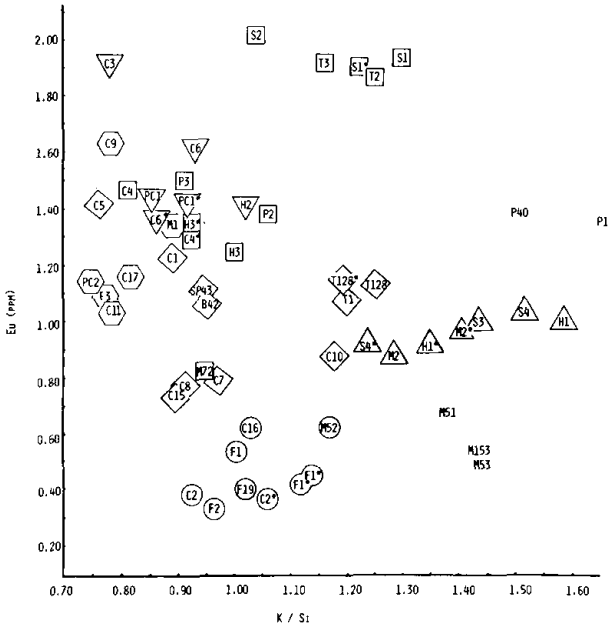

Figure 10. Graph of europium content versus potassium/silicon ratio for fifty-eight samples. Asterisk denotes coarser fraction. Different symbols correspond to the clusters in Figure 9.

(1) The variation within a correlated group of samples was always less than or equal to the variation within the measures of replicates of the standard RGM-1, or less than or equal to the variation due to the analysis of different size fractions of the same sample.

(2) The similarity of refractive indices of the glass, the shape of the glass shards, and the phenocryst assemblage of the samples were noted.

(3) Correlations were made so as to be consistent with the principle of superposition (except in cases of reworked ashes in the same section).

The inferences made from the chemical and optical analyses and field observations of stratigraphic sections and field study of the ash samples are summarized in Figure 11. Nine marker horizons have resulted from this study (Table 1) and are discussed below. Several ash samples have not been included in the discussions as they are chemically distinct from all other samples in this study. These include the Peters Gulch ash (PG44) and an ash from Sand Point (SP43), Bennett Creek (B42), and Jackass Butte (J41). Both the Peters Gulch and Jackass Butte samples were from pure ash beds. The Peters Gulch ash was most similar to an ash here called the lower Horse Hill ash, but its lower thorium and barium and higher iron and chromium distinguished it from that ash layer (see Swirydczuk and others, 1981, Table 2). The Jackass Butte ash was phenocryst rich, and so without separation of the glass fraction, a comparison of its chemical signature with almost pure glass samples could not be made. Both Sand Point and Bennett Creek samples were collected from cross-bedded sands and silts and were contaminated with terrigenous detrital material. The three mafic samples in this study (the "Montini" tuff C18, the Glenns Ferry ash GF46, and the basaltic ash east of Peters Gulch (PG45) are each chemically distinct. Their elemental abundances are listed in Table 2 of Swirydczuk and others (1981).

CHALK HILLS FORMATION AND EQUIVALENT UNITS

Two distinct ash units, the lower Shoofly ash layer and the lower Horse Hill ash layer, both in the Chalk Hills Formation silts of the Shoofly Creek section (Figure 5A), link this section to stratigraphic sections in Twentymile Gulch and Horse Hill and to localities at Tunnel Road in southeastern Oregon. The lower Shoofly ash layer comprises T3 and S1 and represents one eruption. This correlation is only of local significance, because it links sections in adjacent valleys. The lower Horse Hill ash layer, including H1, S3, S4, and M2, is significant both stratigraphically and geographically. It establishes a correlation between the Chalk Hills Formation and part of the sequence called the Chalk Butte Formation in southeastern Oregon (Corcoran and others, 1962); Kimmel (1975) erroneously referred to this as the Deer Butte Formation. This correlation is supported by the occurrence, in both formations, of *Mylocheilus inflexus*, a cyprinid fish of limited temporal range. Smith (1975) erroneously referred all fish localities at Shoofly Creek to the Glenns Ferry Formation, and not the Chalk Hills Formation.

The correlation of ashes below the oolite in the Shoofly Creek section with ashes above the algal limestone in the basal part of the Horse Hill section negates the possibility of the limestones being time equivalent. Ash units S3 and S4 in Chalk Hills sedimentary units lie stratigraphically below the oolitic carbonate, and are equivalent to ash bed H1, which lies some 70 feet above the algal limestone. Therefore, the algal limestone must be placed in the Chalk Hills Formation. We suggested (Swirydczuk and others, 1981) that the break between the Chalk Hills and Glenns Ferry Formations be placed at an unconformable erosional contact seen some 25 feet above the H1 ash at the quartzite cobble bed and associated sands at the Horse Hill section (Figure 8). This interpretation of an older age for the algal limestone is in accordance with the occurrence of *Mylocheilus inflexus* with a few feet of H1. The base of the Glenns Ferry is still considered to be at the base

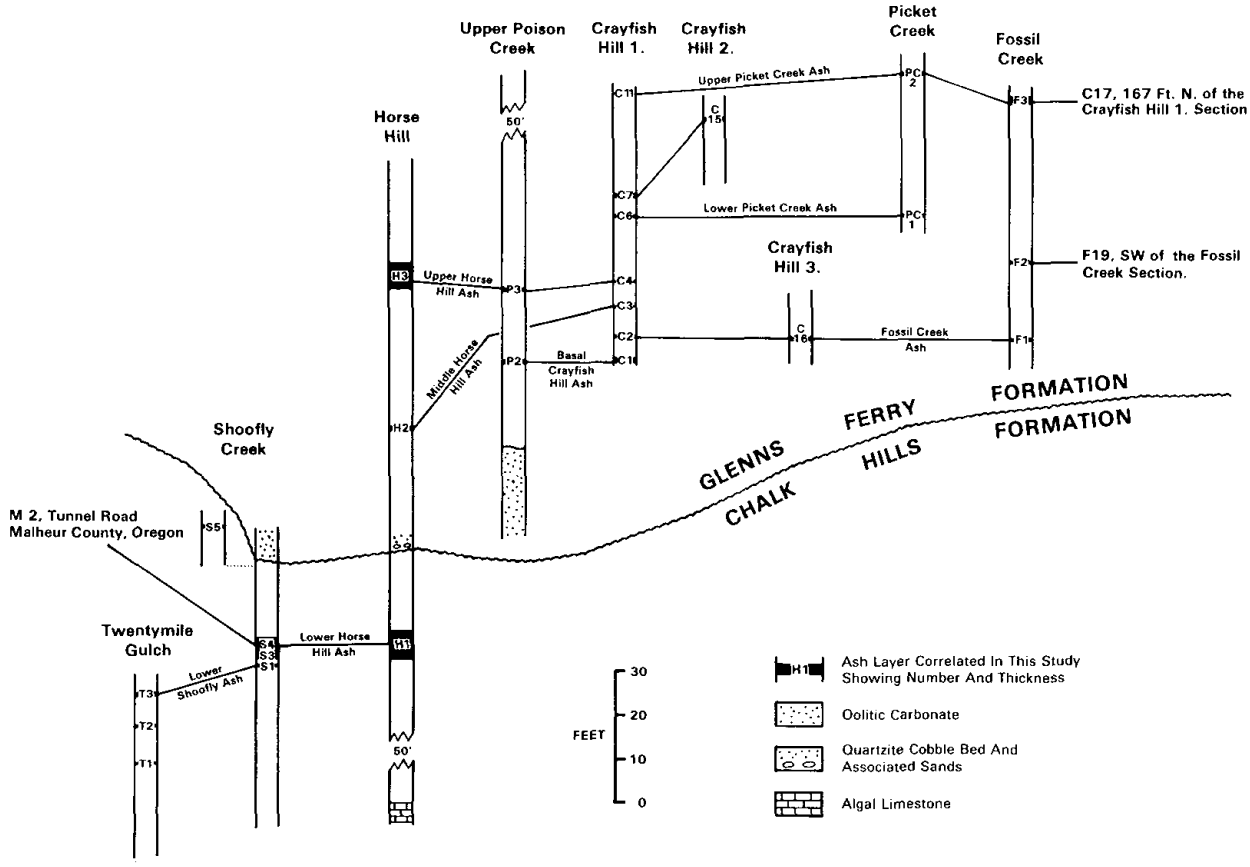

Figure 11. Correlation of stratigraphic sections. Volcanic ashes shown in black. The Twentymile Gulch, Shoofly Creek, and Horse Hill sections up to the unconformity, are in the Chalk Hills Formation. Other sections are in the Glenns Ferry Formation.

of the sand and oolite section in the vicinity of Shoofly Creek. Warner (1976) suggested that the oolitic carbonate was deposited in a terminal evaporitic lake stage and, as such, is part of the upper unit of the Chalk Hills Formation. Because a major unconformity below the oolite cuts out tens of feet of section in some areas and represents more than one million years (Kimmel, 1979), we interpret the oolite as a progradational sequence within a transgressive episode beginning a new lake stage and place it at the base of the Glenns Ferry Formation (Swirydczuk and others, 1979, 1980).

GLENNS FERRY FORMATION

Seven stratigraphic horizons have been established in the Glenns Ferry Formation and shall be discussed in ascending stratigraphic order.

The Fossil Creek ash layer, as it is called here, refers to samples from five ash units, C2, C16, F1, F2, and F19, which cannot be isochronous, because two of them (F1 and F2) lie within one stratigraphic section and are separated by 20 feet of silt and sands (Figure 7A). It is possible that F2 and F19 may represent an eruption from the same source as C2, C16, and F1, but at a later time. We have made a tentative correlation between the two stratigraphic sections in the Fossil Creek localities based on the chemical similarity of F19 and F2. Similarly, samples C2, F1, and C16 are tentatively linked as one time-equivalent unit.

Samples C3 and H2 are chemically and optically similar (Table 1) and possibly represent an ash unit, here called the middle Horse Hill ash layer. H2 lies some 22 feet above the quartzite cobble layer which marks the base of the Glenns Ferry Formation. This correlation links sections from the Crayfish Hill locality and the Horse Hill locality and is stratigraphically important, because it shows that the upper part of the Horse Hill section is Glenns Ferry in age. This correlation is substantiated by the similarity of fossil fish (see Smith and others, 1982 this volume).

Samples C1, C4, H3, P2, and P3 join stratigraphic sections from Crayfish Hill locality, Horse Hill local-

ity, and Poison Creek locality (Table 1). Two eruptions may be involved: the ash beds C1 at an elevation of 2,806 feet (Crayfish Hill) and P2 at 3,202 feet (Poison Creek) constitute part of the basal Crayfish Hill ash layer. Ash beds C4 at 2,825 feet (Crayfish Hill), H3 at 3,110 feet (Horse Hill), and P3 at 3,218 feet (Poison Creek) constitute the Upper Horse Hill ash layer. H3 is 67 feet above the quartzite cobble layer at the base of the Glenns Ferry Formation.

Samples C6 and PC1, making up the lower Picket Creek ash layer, contain identical elemental abundances of major and trace elements and are identical in their refractive index of glass and assemblage of microphenocrysts (Table 1). Stratigraphic sections from the Crayfish Hill and Picket Creek localities are linked by these beds. Similar large fossil fish faunas occur at these localities.

Samples C7, C8, C10, and C15 are proposed to have originated from the same source because of their distinctive and similar chemistry and their microphenocryst assemblages (Table 1). Samples C7 and C8 are in contact and could be the same eruption, but sample C10 is 16 feet higher in the section. This marker horizon links two stratigraphic sections in the Crayfish Hill area.

Three samples, C17, F3, and PC2, probably repre-

Table 1. Summary of chemical characteristics of ashes used as stratigraphic markers. INAA—instrumental neutron activation analysis of cleaned bulk samples; EMPA—electron microprobe analysis of glass shards. All abundances are given in parts per million, except those marked with an asterisk which are given in percent.

		Lower Shoofly Creek Ash	Lower Horse Hill Ash	Basal Crayfish Hill Ash	Fossil Creek Ash	Middle Horse Hill Ash	Upper Horse Hill Ash	Lower Picket Creek Ash	Middle Crayfish Hill Ash	Upper Picket Creek Ash
Samples		T3, S1	H1, M2, S3, S4	C1, P2	C2, C16, F1	C3, H2	C4, H3, P3	C6, PC1	C7, C8, C15	C17, F3, PC2
Refractive Index		1.506	1.496	1.508	1.494	1.510	1.508	1.512	1.504	1.512
Characteristic Chemistry										
INAA:	Al	7.8	6.8	8.5	7.7	7.7	7.7	8.4	7.5	8.9
	Ba*	0.11	0.09	0.11	0.13	0.08	–	0.08	0.09	0.10
	Ca*	0.48	0.34	1.1	1.2	1.45	0.9	1.62	1.0	1.9
	Ce	76	132	60	35	65	67	70	40	43
	Co	0.4	0.7	1.9	3.5	3.7	2.3	4.2	1.9	4.7
	Cr	–	2.7	5.1	10.2	12.3	7.2	4.3	8.6	15.2
	Cs	2.1	4.0	3.1	4.07	2.6	3.0	3.2	2.9	2.6
	Eu	1.91	0.96	1.30	0.49	1.45	1.37	1.46	0.80	1.14
	Fe*	1.55	0.89	2.01	1.10	2.75	2.20	3.04	1.72	2.55
	Hf	9.4	7.4	8.4	3.2	8.5	9.3	8.7	6.5	6.6
	La	38	71	31	18	30	32	36	21	22
	Lu	1.1	0.9	0.9	0.3	0.7	0.9	0.6	0.7	0.6
	Mn*	0.08	0.03	0.06	0.06	0.09	0.09	0.08	0.05	0.06
	Na*	2.35	1.80	3.09	2.10	3.29	2.89	2.83	3.26	3.06
	Rb	67	156	70	90	50	60	67	42	57
	Sb	0.9	0.3	0.6	0.7	0.6	0.5	0.7	0.8	1.1
	Sc	9.1	1.8	8.1	4.1	11.9	9.0	8.8	6.3	8.9
	Sm	9	9	8	2	8	8	7	4	5
	Th	6	26	5	10	4	6	8	6	5
	U	3	10	7	6	–	4	4	6	6
	Yb	6	6	5	2	5	6	4	4	2
EMPA:	Si*	30.68	33.16	31.32	33.87	31.22	30.55	29.89	31.26	30.37
	Fe*	1.82	1.03	2.12	0.66	2.85	2.16	3.24	1.68	2.90
	Mg*	0.40	0.16	0.25	0.24	0.35	0.35	0.74	0.19	0.50
	K*	3.75	4.67	3.04	3.52	2.82	2.87	2.65	2.89	2.36
	Ca*	0.59	0.35	0.60	0.50	0.93	0.73	1.34	0.59	1.20
	Al*	7.26	6.28	7.05	6.40	7.63	7.35	7.59	7.29	7.46

sent one eruption, here named the upper Picket Creek ash layer. There is no indication of any reworking of the samples; therefore, ashes are assumed to represent a time-stratigraphic horizon. Sample C11 is identical to the three samples except for its lower lanthanum content (13 ppm compared with approximately 22 ppm). These beds link stratigraphic sections from the following localities: Crayfish Hill, Fossil Creek, and Picket Creek. Similar fossil fish faunas at the three localities support this interpretation (Smith and others, 1982 this volume).

SUMMARY

The correlation of ash horizons by chemical and optical similarity combined with field study, provides a stratigraphic cross-section for the Glenns Ferry Formation and upper part of the underlying Chalk Hills Formation. Twentymile Gulch, Shoofly Creek, Tunnel Road, and the basal part of the Horse Hill are the oldest sections. The Shoofly Creek section makes up the top part of the Chalk Hills Formation exposed in this area and is unconformably overlain by a sand and oolite sequence, which is considered to be the base of the Glenns Ferry Formation. The Twentymile Gulch section and the base of the Horse Hill section below the quartzite cobble bed (elevation 3,040 feet in the measured section) are placed in the Chalk Hills Formation. The Chalk Hills Formation, therefore, includes the algal limestone and some 90 feet of overlying clastic and volcaniclastic units previously assigned to the Glenns Ferry Formation.

Near Adrian, Oregon, part of the Chalk Butte Formation of Corcoran and others (1962) is laterally equivalent to the Chalk Hills Formation; beds higher in the "Chalk Butte Formation" at Blackjack Butte have a Glenns Ferry fish fauna (Kimmel, 1975). This evidence shows that sediments at our localities in the area of Adrian, Oregon, were laid down in the Chalk Hills and Glenns Ferry depositional systems, which were separate from the Deer Butte system.

The Glenns Ferry Formation is represented in beds at Crayfish Hill, Fossil Creek, Picket Creek, Poison Creek (overlying the oolite), and the upper part of the Horse Hill section (above the quartzite cobble bed). The Horse Hill section and the combined Shoofly Creek-Poison Creek sections span most of the time involved in this study and include lithologically similar Chalk Hills and Glenns Ferry beds which are separated by an unconformity seen in two sections.

Rhyolitic glasses predominate in the ash layers in the older rocks; dacitic glass characterizes the ash layers correlating younger rocks, but the distinction does not coincide with the formation boundary. The source of these ash beds is not known. The Lower Horse Hill Ash Layer decreases both in thickness and average grain size to the west, which argues against a western source for that eruption.

ACKNOWLEDGMENTS

This is part of a study begun in 1973 by Gerald P. Larson of the Department of Geological Sciences, the University of Michigan, who collected samples and measured sections before losing his life in a field accident on June 25, 1974. Peter G. Kimmel, Bruce H. Wilkinson, and Beverly Smith participated in field work. The laboratory work was carried out with special help from John Beollstorff, Eric J. Essene, Tom Meyers, Peter Kimmel, Bruce H. Wilkinson, and Paul L. Cloke. Chemical analysis was done at the Phoenix Memorial Laboratory with the help of John D. Jones, Ward Riggot, Tom Meyers, and other staff members and at the Electron Microprobe Laboratory, Department of Engineering, the University of Michigan. Computations were done at the Computing Center; programs and assistance were provided by the Statistical Research Laboratory, the University of Michigan. The Scott Turner Committee provided financial assistance.

REFERENCES

Anderson, N. R., 1965, Upper Cenozoic stratigraphy of the Oreana, Idaho, 15′ quadrangle: University of Utah Ph.D. dissertation, 212 p.

Armstrong, R. L., W. P. Leeman, and H. E. Malde, 1975, K-Ar dating, Quaternary and Neogene volcanic rocks of the Snake River Plain, Idaho: American Journal of Science, v. 275, p. 225-251.

Axelrod, D. I., 1968, Tertiary floras and topographic history of the Snake River basin, Idaho: Geological Society of America Bulletin, v. 79, p. 713-734.

Borchardt, G. A., M. E. Harward, and R. A. Schmitt, 1971, Correlation of volcanic ash deposits by activation analysis of glass separates: Quaternary Research, v. 1, p. 247-260.

Bowles, F. A., R. N. Jack, and I. S. E. Carmichael, 1973, Investigation of deep-sea volcanic ash layers from equatorial Pacific cores: Geological Society of America Bulletin, v. 84, p. 2371-2388.

Buwalda, J. P., 1923, A preliminary reconnaissance of the oil and gas possibilities of southwestern and south-central Idaho: Idaho Bureau of Mines and Geology Pamphlet 5, 10 p.

———, 1924, The age of the Payette Formation and the old erosion surface in Idaho: Science, v. 60, p. 572-573.

Cann, R. J. and C. Renfrew, 1964, The characterization of obsidian and its application to the Mediterranean region: Proceedings, Prehistorical Society, v. 30, p. 111-131.

Carmichael, I. S. E. and A. McDonald, 1961, The geochemistry of some natural acid glasses from the Northern Atlantic Tertiary Volcanic Province: Geochimica et Cosmochimica Acta, v. 25, p. 189-222.

Cope, E. D., 1884, On the fishes of the Recent and Pliocene lakes of the western part of the Great Basin, and the Idaho Pliocene lake: Philadelphia Academy of Natural Science Proceedings, 1883, v. 35, p. 134-166.

Corcoran, R. E., R. A. Doak, P. W. Porter, F. I. Pritchett, and M. C. Privrasky, 1962, Geology of the Mitchell Butte quadrangle, Oregon: Oregon Department of Geology and Mineral Industries Map GMS2.

Edsall, D. W., 1976, Trace elements in tephra as indicators of magmatic composition in the Aleutian Arc: Geological Society of America Bulletin, v. 87, p. 1269-1272.

Ekren, E. B., D. H. McIntyre, E. H. Bennett, and H. E. Malde, 1981, Geologic map of Owyhee County, Idaho, west of longitude 116° W.: U. S. Geological Survey Miscellaneous Geologic Investigations Map I-1256.

Hibbard, C. W., 1959, Late Cenozoic microtine rodents from Wyoming and Idaho: Papers of the Michigan Academy of Sciences, Arts, and Letters, v. 44, p. 3-40.

Hibbard, C. W. and R. J. Zakrzewski, 1967, Phyletic trends in the late Cenozoic microtine *Ophiomys* gen. nov. from Idaho: Contributions to Museum of Paleontology, University of Michigan, v. XXI, no. 12, p. 255-271.

Howorth, R. and P. C. Rankin, 1975, Multi-element characterization of glass shards from stratigraphically correlated rhyolitic tephra units: Chemical Geology, v. 15, p. 239-250.

Izett, G. A., 1981, Volcanic ash beds: recorders of upper Cenozoic silicic pyroclastic volcanism in the western United States: Journal of Geophysical Research, v. 86, B11, p. 10200-10222.

Jack, R. N. and I. S. E. Carmichael, 1969, The chemical "fingerprinting" of acid volcanic rocks: California Division of Mines and Geology Special Report 100, p. 17-32.

Kimmel, P. G., 1975, Fishes of the Miocene-Pliocene Deer Butte Formation, southeast Oregon: University of Michigan, Museum of Paleontology, Papers in Paleontology, v. 14, p. 69-87.

———, 1979, Stratigraphy and paleoenvironments of the Miocene Chalk Hills Formation and Pliocene Glenns Ferry Formation in the western Snake River Plain, Idaho: University of Michigan Ph.D. dissertation, 331 p.

Kirkham, V. R. D., 1931, Revision of the Payette and Idaho Formations: Journal of Geology, v. 39, p. 193-239.

Kittleman, L. R., A. R. Green, G. H. Haddock, A. R. Hagood, A. M. Johnson, J. M. McMurray, R. G. Russel, and D. A. Weeden, 1967, Geologic map of the Owyhee region, Malheur County, Oregon, scale 1:125,000: University of Oregon Museum of Natural History Bulletin 8.

Lindgren, Waldemar, 1900, The gold and silver veins of Silver City, DeLamar, and other mining districts in Idaho: U. S. Geological Survey 20th Annual Report, pt. 3, p. 65-256.

Littleton, R. T. and E. G. Crosthwaite, 1957, Groundwater geology of the Bruneau-Grand View area, Owyhee County, Idaho: U. S. Geological Survey Water-Supply Paper 1460-D, p. 147-198.

Mabey, D. R., 1976, Interpretation of a gravity profile across the Snake River Plain, Idaho: Geology, v. 4, p. 53-55.

Malde, H. E., 1959, Fault zone along the northern boundary of the western Snake River Plain, Idaho: Science, v. 131, p. 272.

———, 1972, Stratigraphy of the Glenns Ferry Formation from Hammett to Hagerman, Idaho: U. S. Geological Survey Bulletin 1331-D, 19 p.

Malde, H. E. and H. A. Powers, 1962, Upper Cenozoic stratigraphy of the western Snake River Plain, Idaho: Geological Society of America Bulletin, v. 73, p. 1197-1220.

———, 1972, Geologic map of the Glenns Ferry-Hagerman area, west-central Snake River Plain, Idaho: U. S. Geological Survey Miscellaneous Geologic Investigations Map I-696.

Malde, H. E., H. A. Powers, and C. H. Marshall, 1963, Reconnaissance geologic map of west-central Snake River Plain, Idaho: U. S. Geological Survey Miscellaneous Geologic Investigations Map I-373, scale 1:125,000.

McIntyre, D. H., 1972, Cenozoic geology of the Reynolds Creek experimental watershed, Owyhee County, Idaho: Idaho Bureau of Mines and Geology Pamphlet 151, 115 p.

Merriam, J. C., 1918, New mammalia from the Idaho Formation: California University Publications in Geological Sciences, v. 10, p. 523-530.

Miller, R. R. and G. R. Smith, 1967, New fossil fishes from Plio-Pleistocene Lake Idaho: University of Michigan, Occasional Papers in Museum of Zoology 654, p. 1-24.

Morrison, D. F., 1967, Multivariate Statistical Methods: McGraw Hill, Inc., 338 p.

Powers, H. A. and H. E. Malde, 1961, Volcanic ash beds as stratigraphic markers in basin deposits near Hagerman and Glenns Ferry, Idaho: U. S. Geological Survey Professional Paper 424-B, Paper No. 70, p. B167-170.

Richardson, Darlene and Dragoslav Ninkovich, 1976, Use of K_2O, Rb, Zr and Y versus SiO_2 in volcanic ash layers of the eastern Mediterranean to trace their source: Geological Society of America Bulletin, v. 87, p. 110-116.

Russell, I. C., 1902, Geology and water resources of the Snake River plains of Idaho: U. S. Geological Survey Bulletin 199, 192 p.

Sarna-Wojcicka, A. M., 1976, Correlation of late Cenozoic tuffs in the central Coast Range of California by use of trace and minor element chemistry: U. S. Geological Survey Professional Paper 972.

Smith, D. G. W. and J. S. Westgate, 1969, Electron microprobe techniques for characterizing pyroclastic deposits: Earth and Planetary Science Letters, v. 5, p. 313-319.

Smith, G. R., 1975, Fishes of the Pliocene Glenns Ferry Formation, southwest Idaho: University of Michigan, Museum of Paleontology, Papers in Paleontology, v. 14, p. 1-68.

Smith, G. R., Krystyna Swirydczuk, P. G. Kimmel, and B. H. Wilkinson, 1982, Fish biostratigraphy of late Miocene to Pleistocene sediments of the western Snake River Plain, Idaho, *in* Bill Bonnichsen and R. M. Breckenridge, editors, Cenozoic Geology of Idaho: Idaho Bureau of Mines and Geology Bulletin 26.

Stearns, H. T., 1936, Origin of the large springs and their alcoves along the Snake River in southern Idaho: Journal of Geology, v. 44, p. 429-450.

Stearns, H. T., Lynn Crandall, and W. G. Steward, 1938, Geology and ground-water resources of the Snake River Plain in southwestern Idaho: U. S. Geological Survey Water-Supply Paper 774, 268 p.

Swirydczuk, Krystyna, 1977, Tephra stratigraphy of sedimentary rocks associated with the Glenns Ferry Formation, western Snake River Plain: University of Michigan M.S. thesis, 150 p.

Swirydczuk, Krystyna, G. P. Larsen, and G. R. Smith, 1981, Volcanic ash stratigraphy of the Glenns Ferry and Chalk Hills Formations, western Snake River Plain: Idaho Bureau of Mines and Geology Open-File Report 81-1, 60 p.

Swirydczuk, Krystyna, B. H. Wilkinson, and G. R. Smith, 1979, The Pliocene Glenns Ferry oolite; lake margin carbonate deposition in the southwestern Snake River Plain: Journal of Sedimentary Petrology, v. 49, p. 995-1004.

———, 1980, The Pliocene Glenns Ferry oolite: sedimentology of oolitic lacustrine terrace deposits: Journal of Sedimentary Petrology, v. 50, p. 1237-1248.

Warner, M. M., 1976, Special aspects of Cenozoic history of southern Idaho and their geothermal implications: Proceedings, 2nd United Nations Symposium on the Development and Use of Geothermal Resources, v. 1, p. 653-663.

Stratigraphy, Age, and Tectonic Setting of the Miocene-Pliocene Lacustrine Sediments of the Western Snake River Plain, Oregon and Idaho

by

Peter G. Kimmel[1]

ABSTRACT

Correlations of lacustrine sediments based on comparisons of fossil fish faunas, volcanic ash chemistries, and lithologies show that sediments of the late Miocene Chalk Hills and Pliocene Glenns Ferry Formations in the western Snake River Plain were deposited by two successive, large lakes. Fission track dates of volcanic ashes show that several million years elapsed between episodes of lacustrine deposition. The extent of Miocene and Pliocene fish localities from the Oregon-Idaho border eastward to Glenns Ferry, Idaho, along the southwest edge of the plain suggests that these lakes occupied approximately the same basin.

The Grassy Mountain and Blackjack basalts, deposited in eastern Oregon just before late Miocene and early Pliocene lacustrine deposition, may have blocked drainage outlets from the western Snake River Plain. Other basalts at about the same stratigraphic levels, deposited as far east as Hagerman, Idaho, suggest widespread volcanism at these two times. The two separate episodes of widespread volcanism and subsequent lacustrine deposition suggest the formation of the western Snake River Plain by episodic rifting.

Subsidence at the drainage outlet of the plain may have ended lacustrine deposition in the Miocene. Nearshore sediments of the Chalk Hills Formation closest to the outlet are over 60 meters lower than time-equivalent lacustrine sediments to the southeast. Nearshore sediments of the Glenns Ferry Formation in the same area are not lower than lacustrine sediments to the southeast, suggesting that subsidence ended before deposition of the Glenns Ferry Formation. Lacustrine deposition of the Glenns Ferry Formation probably ended with the erosion of a new, lower outlet to the Columbia River drainage system.

[1]Department of Geology, George Mason University, Fairfax, Virginia 22030.

INTRODUCTION

An understanding of the nature and timing of sedimentation in the western Snake River Plain is essential in interpreting the tectonic history of the basin. This paper will outline the history of lacustrine deposition on the western plain during the Miocene and Pliocene (as defined by Van Couvering, 1978) and will discuss the implications for tectonic activity along the plain.

Lacustrine sediments were recognized in the western Snake River Plain by the first geological surveys in the area. King (1878) hypothesized that the sediments were deposited in an enormous lake covering parts of southern Idaho, Utah, and eastern Oregon. Later, other geologists suggested that the lakes were more restricted and that some sediments were deposited by streams and rivers. More recently, Malde (1972, p. D13) interpreted Pliocene sediments near Glenns Ferry, Idaho, and eastward (Figure 1) as deposits of a river flowing in "a wide valley marked by temporary lakes and by broad stretches that were seasonally flooded." Fossils and sediments in the western plain have also been interpreted as evidence for a large, permanent lake occupying most of the basin (Smith, 1975; Kimmel, 1975; Smith and others, 1982 this volume) during the late Miocene and most of the Pliocene. The lacustrine sediments discussed in this paper are characterized by light tan siltstones, abundant and pure volcanic ash beds, and occasional fossiliferous sandstones and conglomerates.

Part of the problem in determining the nature of sedimentation in this basin stems from difficulties in correlating and dating the lacustrine sediments. The scarcity of mammal fossils, abrupt facies changes, and faulting often prevent correlations among lacustrine sediments. Lacustrine sediments of different ages usually have similar lithologic properties. Basalt flows within the sediments are not common, are often altered, and have yielded contradictory potassium-argon dates (Armstrong and others, 1975). Several

Kimmel, P. G., 1982, Stratigraphy, age, and tectonic setting of the Miocene-Pliocene lacustrine sediments of the western Snake River Plain, Oregon and Idaho, *in* Bill Bonnichsen and R. M. Breckenridge, editors, Cenozoic Geology of Idaho: Idaho Bureau of Mines and Geology Bulletin 26, p. 559-578.

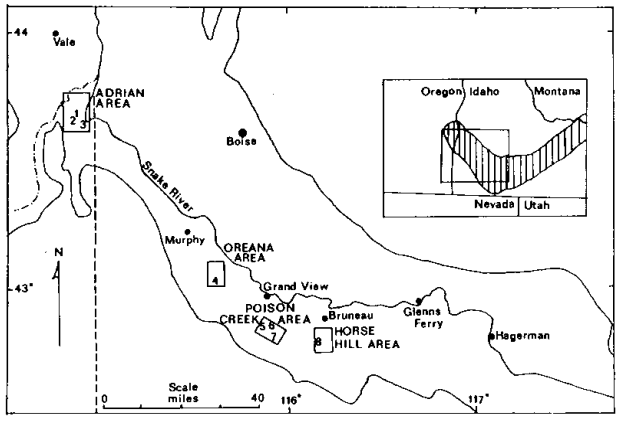

Figure 1. Locations of measured sections and ash sampling localities. Solid line is 4,000-foot contour. Vertical lines in the inset show the Snake River Plain.

additional methods of correlating and dating lacustrine sediments have recently been applied successfully to this basin. The correlations used in this paper are based on fossil fish faunas (see Smith and others, 1982 this volume), volcanic ash chemistry (see Swirydczuk and others, 1982 this volume), and depositional sequences of volcanic ashes. Fission track dates of volcanic ashes provide absolute ages for some of the important ash horizons. These methods provide data for a reevaluation of depositional models and their relation to the tectonic history of the western Snake River Plain during the late Miocene and Pliocene.

STRATIGRAPHY

STRATIGRAPHIC SETTING

Most lacustrine sediments in the western Snake River Plain can be placed in the late Miocene Chalk Hills Formation and the Pliocene Glenns Ferry Formation (Figure 2). Before 1962 these sediments were included in the Idaho Formation of Cope (1883). Malde and Powers (1962) revised the upper Cenozoic stratigraphy of the western Snake River Plain and elevated the Idaho Formation to group status by dividing it into seven separate formations ranging in age from middle Miocene to middle Pleistocene (Figure 2). The sediments of the Idaho Group are confined to the western Snake River Plain and are underlain by the Idavada Volcanics, thought to have been deposited before or during the formation of the western plain (Malde and Powers, 1962). Formations older than the Idavada Volcanics such as the Deer Butte Formation, the Owyhee Basalt, and the Sucker Creek Formation are not exposed within the Snake River Plain and do not show evidence that the plain existed during their deposition. These older formations were deposited in north-trending basins and are now exposed mainly to the south and west of the plain in Oregon (Kittleman and others, 1965; Corcoran and others, 1962).

The Chalk Hills and Glenns Ferry Formations are bounded by unconformities.The Chalk Hills Formation unconformably overlies the Idavada Volcanics as well as unnamed basalts within the Idaho Group (Armstrong and others, 1975). The Glenns Ferry Formation unconformably overlies the Banbury Basalt near Hagerman and the Chalk Hills Formation along most of the rest of the southwestern edge of the plain. Malde and Powers (1962) report a moderate angular unconformity at the base of the Glenns Ferry Formation. From Grand View to Murphy, Idaho, the basal sediments are oolitic limestones. Swirydczuk and others (1979, 1980) show that this oolite was a transgressive lacustrine deposit. Although Malde and Powers (1962) correlated these oolitic limestones with an algal limestone south of Bruneau, Idaho, additional work (Swirydczuk and others, 1982 this volume) shows that the algal limestone is actually in the Chalk Hills Formation and that the basal Glenns Ferry Formation in this area is represented by a quartzite conglomerate. The Glenns Ferry Formation is unconformably overlain by the early Pleistocene Tuana Gravel, the middle Pleistocene Bruneau Formation, and other younger formations.

Age in m.y.	Series	Idaho Formations		Oregon Formations
		Snake River Group		
1	Pleistocene	Black Mesa Gravel Bruneau Formation Tuana Gravel	IDAHO GROUP	
2				
3	Pliocene	Glenns Ferry Formation		Glenns Ferry Formation
4				
5		Banbury Basalt		Blackjack Basalt
6				
7		Chalk Hills Formation		Chalk Butte Formation
8	Miocene			
9		unnamed basalts		Grassy Mountain Formation
10				
11		Poison Creek Formation		Kern Basin Formation

Figure 2. Stratigraphy of the western Snake River Plain. Idaho formations are modified from Malde and Powers (1962) and Armstrong and others (1975). Oregon formations are modified from Corcoran and others (1962) and Bryan (1929).

Extent of the Chalk Hills Formation

As originally described, the Chalk Hills Formation included sediments from the Bruneau area to the Oreana area, Idaho, along the southwestern edge of the western Snake River Plain (Figure 1). More recent correlations suggest that sediments in the Adrian area, Oregon, should also be included in this formation. When first mapped these sediments were placed in the Chalk Butte Formation, a partial equivalent of the Chalk Hills Formation (Corcoran and others, 1962). Later they were assigned to the middle-Miocene Deer Butte Formation on the basis of supposed lithologic similarities (Kittleman and others, 1965). Recent correlations based on fish fossils (Smith and others, 1982 this volume), volcanic ash chemistry (Swirydczuk and others, 1982 this volume), and fission track dates confirm the presence of late Miocene lacustrine sediments in this part of Oregon. The name Chalk Hills Formation is preferred instead of Chalk Butte Formation for these sediments because the Chalk Butte Formation includes sediments of widely differing ages (Shotwell, 1970), including some now correlated with the Pliocene Glenns Ferry Formation (Smith and others, 1982 this volume; Kimmel, 1979). The sediments also appear to have been deposited in the same basin as those of the Chalk Hills Formation.

Extent of the Glenns Ferry Formation

Malde and Powers (1962) recognized intermittent exposures of the Glenns Ferry Formation along the southwestern edge of the western Snake River Plain from Hagerman to Homedale, Idaho, on the basis of geologic mapping and fossil collections. Fossil evidence suggests that equivalent sediments are also present from Boise, Idaho, to Ontario, Oregon, along the northeastern edge of the plain (Taylor, in Malde and Powers, 1962). Fossil fish evidence (Kimmel, 1975) shows that Glenns Ferry sediments are also present in Oregon along the southwestern edge of the plain near Adrian, Oregon.

STRATIGRAPHIC METHODS

Fossil fish faunas are useful in distinguishing between sediments of the Chalk Hills Formation and those of the Glenns Ferry Formation. Chalk Hills faunas are characterized by the presence of a minnow, *Mylocheilus inflexus*, and a salmon, *Paleolox larsoni*, both of which are absent from all but the lowest Glenns Ferry sediments. Many fossils in the basal Glenns Ferry Formation are worn and may be reworked from older sediments. *Mylocheilus robustus*, a minnow, and *Prosopium prolixus*, a whitefish, are common in the Glenns Ferry Formation. *Mylocheilus robustus* is also increasingly abundant in stratigraphically higher faunas of the Chalk Hills Formation. A third minnow, *Mylopharodon hagermanensis*, is found primarily in nonlacustrine sediments of the Glenns Ferry Formation. *Mylocheilus robustus* fossils are rare in these sediments. Fossils of at least one of these minnows are found in almost every sizable fish collection. Additional differences between the fish faunas of these two formations are discussed in a later paper (Smith and others, 1982 this volume). A fossil fish collection can almost always be used to assign lacustrine sediments to the Chalk Hills or Glenns Ferry Formation.

Volcanic ash beds are useful in correlating among outcrops of lacustrine sediments. Ash chemistry can be used to "fingerprint" individual ashes for correlations over long distances. Correlations among measured sections in the Horse Hill, Poison Creek, Oreana, and Adrian areas used in this paper were proposed by Swirydczuk and others (1982 this volume) based on comparisons of ash chemistry.

Over shorter distances ash beds may not change appreciably in color, relative thickness, or relative spacing, and these properties may be used to correlate outcrops. Figure 3 illustrates the variations in color, thickness, and spacing of several ash beds traced over three quarters of a mile along a single outcrop. In Figure 4, a comparison of longer measured sections containing more ashes suggests that correlations can be made over a distance of 20 miles. Correlations can be made only between areas which had similar rates of deposition over long periods of time and which show excellent preservation and exposure of ash beds. Nearshore lacustrine environments appear to fit these criteria.

The reliability of correlations which use lithologic properites of several ashes in sequence can be tested by comparing such correlations with those established using ash chemistry. Because not all correlations based on the lithology of ashes in sequence include ashes that have been chemically analyzed (Swirydczuk and others, 1982 this volume), only six correlations between measured sections of the Glenns Ferry Formation can be compared. Five of these correlations match with those based on ash chemistry (Figure 4). The exception, where two different ashes are correlated with a third using the different methods, is also consistant with ash chemistry data since all three of the ashes involved have nearly identical chemistries. Swirydczuk and others (1982 this volume) speculate that these ash layers represent multiple eruptions from the same source or redeposition of one ashfall from separate drainage systems. Thus correlations of localities using only the chemistry of

single ash layers may be ambiguous.

An additional correlation by ash chemistry illustrates the limits of correlation using lithologies of several ashes in sequence. Two ashes from the Glenns Ferry Formation near Horse Hill were chemically correlated with ashes in other sections using ash chemistry (Swirydczuk and others, 1982 this volume). One of the ashes (H3 at Horse Hill) is 10 feet thick, but it correlates with an ash at Crayfish Hill only 1 foot thick. The Horse Hill area appears to have had much higher rates of deposition than other areas studied (Swirydczuk and others, 1982 this volume). Only three of the ten ashes in this measured section resembled those in other sections using ash lithology. Thus correlations between areas with different depositional characteristics are not possible using this method.

Simple lithologic correlations are also possible among sediments of the Chalk Hills and Glenns Ferry Formations, based on the transition from nonlacustrine to lacustrine sedimentation. Measured sections are shown in Figures 5 through 10. Fossiliferous beach sands and conglomerates, oolitic limestones, and algal limestones all indicate the beginning of lacustrine deposition. The angular unconformity between Chalk Hills and Glenns Ferry sediments and the transgressive nature demonstrated for most of these layers shows that the layers are not necessarily time-equivalent and were probably deposited while the basin was filling with water.

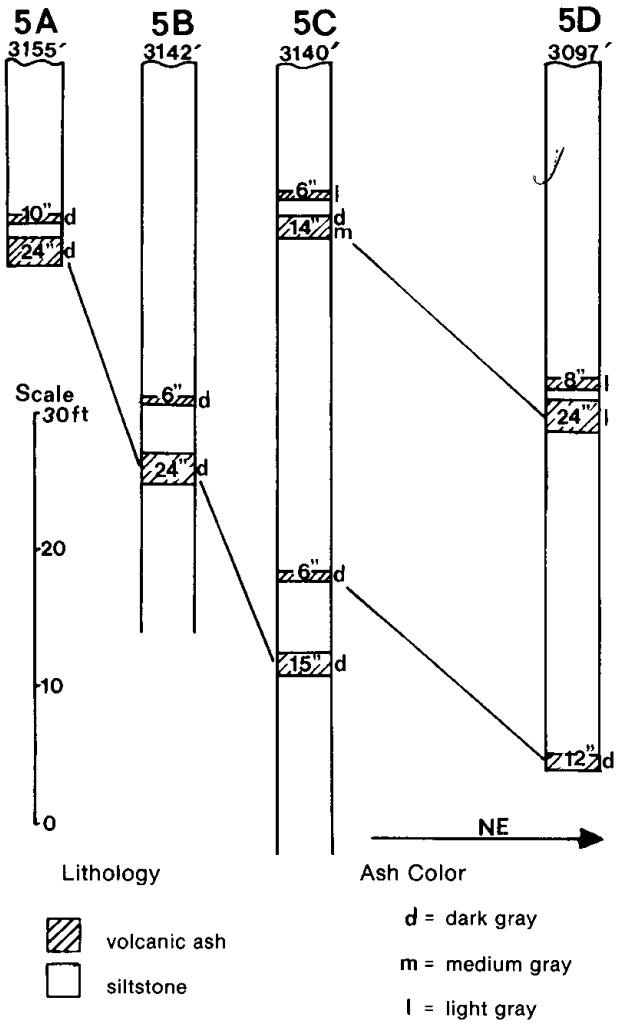

Figure 3. Lateral variations in ashes of the Chalk Hills Formation over a distance of ¾ mile in the Poison Creek area (Figure 1, location 5). Only ashes 6 inches or more in thickness are shown. Locations of measured sections: 5A—NW¼SW¼ sec. 5, T. 7 S., R. 3 E., Owyhee County, Idaho; 5B and 5C—SW¼ sec. 5, T. 7 S., R. 3 E., Owyhee County, Idaho; 5D—NE¼SE¼ sec. 5, T. 7 S., R. 3 E. Elevations given are for the top of each measured section.

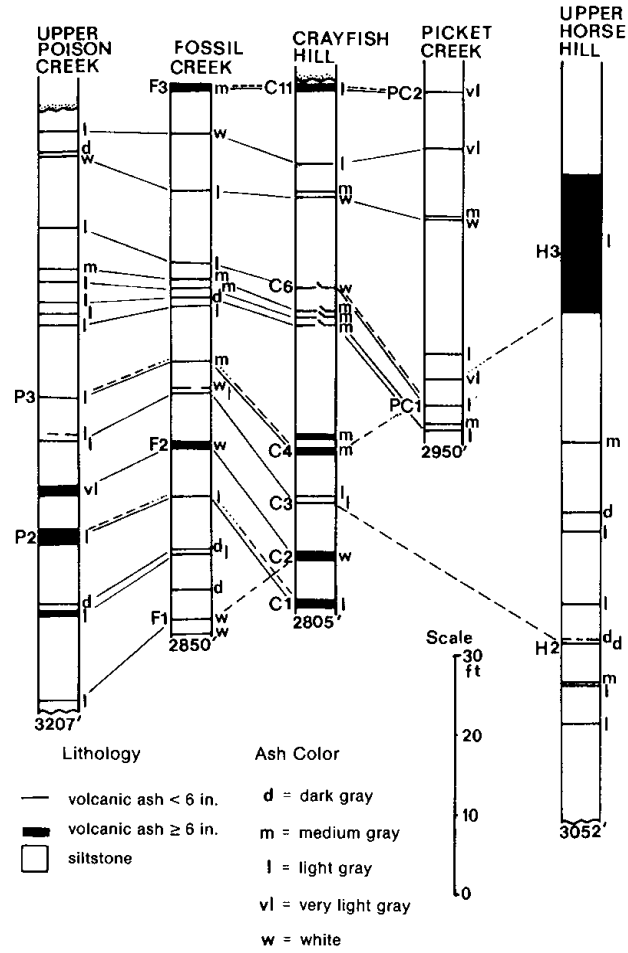

Figure 4. Ash correlations within lacustrine siltstones of the Glenns Ferry Formation. Correlations based on ash chemistry are shown by dashed lines (dotted where an ash within a section was not analyzed). Correlations based on ash thickness, color, and spacing are shown by solid lines. Modified from Swirydczuk and others (1982 this volume).

STRATIGRAPHIC RESULTS

Lithostratigraphic and biostratigraphic correlations and the fossil fish faunas suggest that lacustrine sediments of the Chalk Hills and Glenns Ferry Formations were deposited in a large, permanent lake. Such a depositional model would not require substantial local subsidence during deposition, but would imply a large and relatively stable basin. This depositional model fits well with regional tectonic models for the formation of the western Snake River Plain.

A second model for deposition of the Glenns Ferry Formation has been proposed by Malde (1972) based on sediments studied between Hammett and Hagerman, Idaho. Malde recognized three major facies: fluvial sands, lacustrine silts, and floodplain silts and clays. Malde interprets the pattern of sedimentary facies in this area as a wide valley with a river, temporary lakes, and broad stretches that were seasonally flooded. This model conflicts with the hypothesis that the lacustrine sediments were deposited in a large lake in a relatively stable basin. There are two ways of reconciling Malde's data with a large lake model. Either Malde's fluvial sands can be reinterpreted as near shoreface sands (Smith and others, 1982 this volume), or the time-equivalence of lacustrine and fluvial sediments can be questioned.

The facies relationships between floodplain and lacustrine facies is consistent with a large lake in the basin. Malde (1972) shows that eastern floodplain sediments near Hagerman pass westward into lacustrine sediments, whereas floodplain sediments to the west rest on lacustrine silts. This pattern of facies suggests that floodplain environments coexisted with a lacustrine environment near the margins of the basin, replacing lacustrine environments near Glenns Ferry as the lake drained or was filled with sediments.

The time-equivalence of lacustrine and fluvial sediments near the axis of the basin does not fit the large lake model for deposition of lacustrine sediments. Malde's correlation of lacustrine and fluvial facies is not direct but depends on correlations with sections in the floodplain facies. One important correlation depends on the chemical and physical similarities of two ash samples. Since chemically

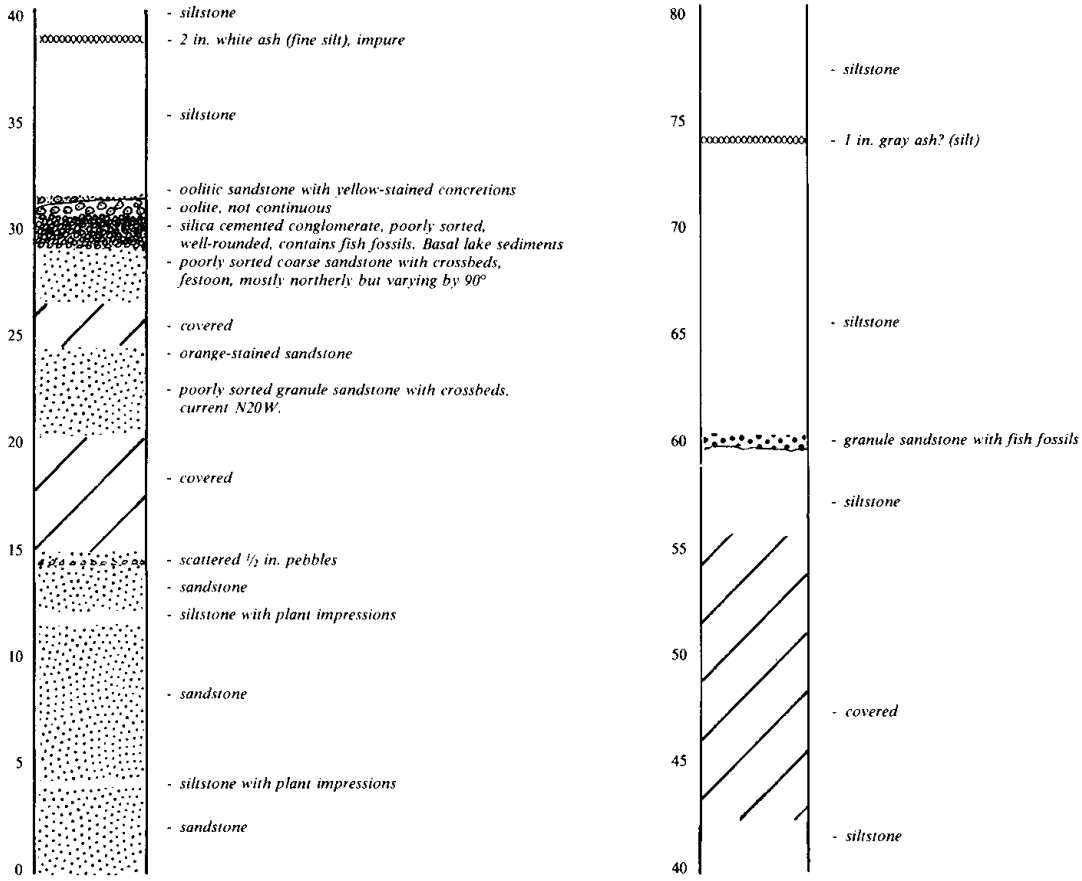

Figure 5. Measured section at location PK1. Located in the NW¼NW¼ sec. 8, T. 22 S., R. 46 E., Malheur County, Oregon. Base elevation is 3,380 feet.

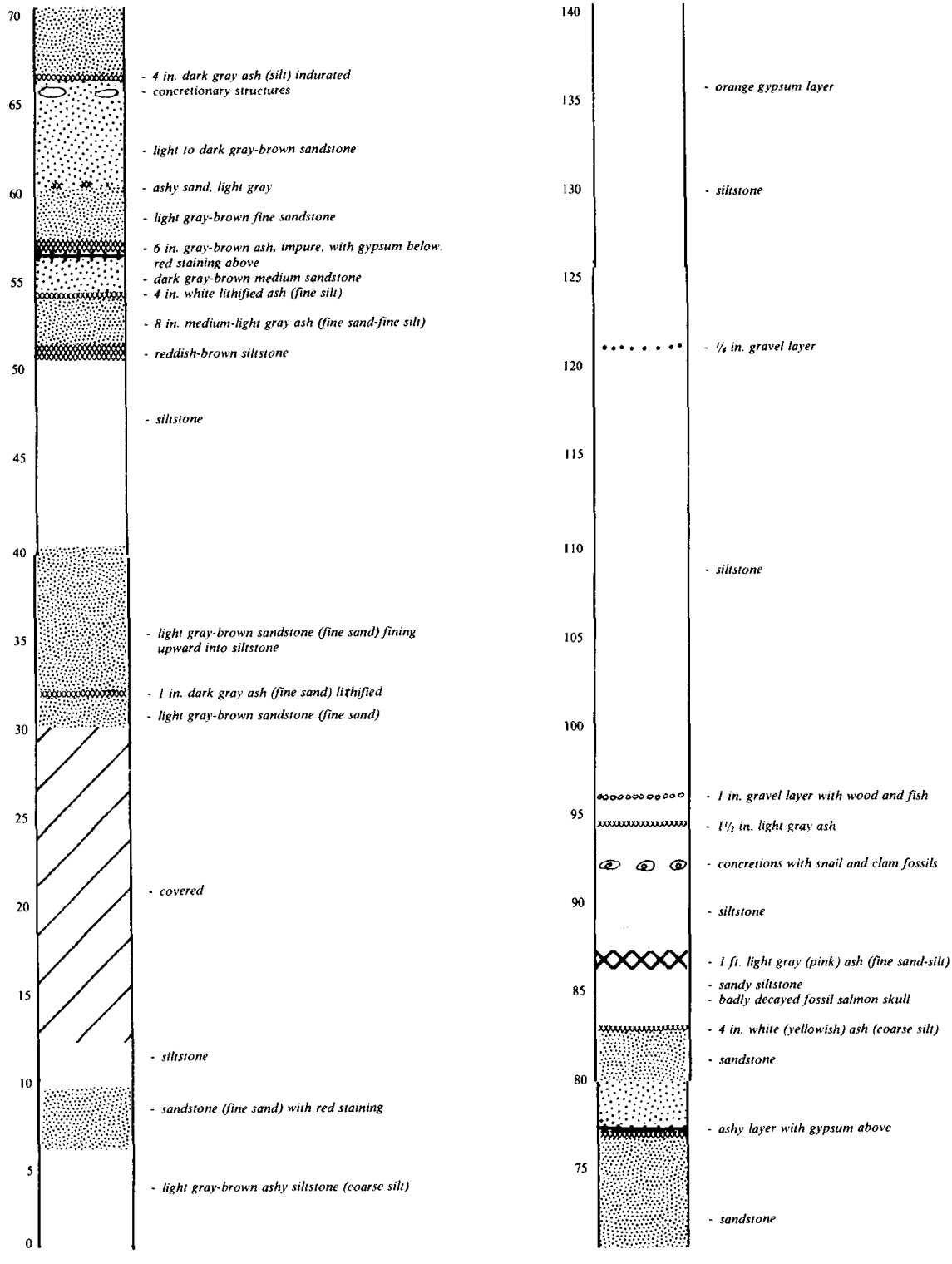

Figure 6. Measured section at location PK3A. Located in the SW¼SW¼ sec. 22, T. 22 S. R. 46 E., Malheur County, Oregon. Base elevation is 2,560 feet.

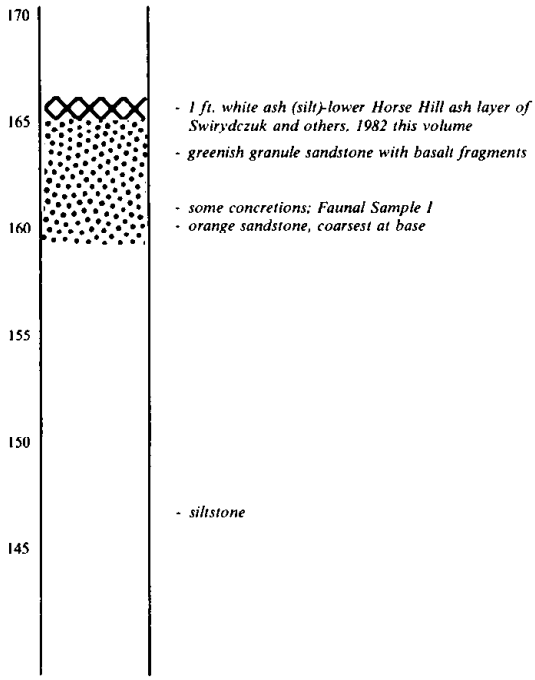

Figure 6. continued.

indistinguishable ashes can occur at different horizons within the same measured section (Swirydczuk and others, 1982 this volume), this correlation and the time-equivalence of fluvial and lacustrine sediments need to be reevaluated.

If the lacustrine and the fluvial facies are not time-equivalent, the distribution of these facies can be explained as a result of the draining of the Glenns Ferry lake. Lacustrine deposition over the whole basin is followed by fluvial deposition along the axis of the plain, precisely where Malde maps the fluvial facies. Malde also reports that in some measured sections lacustrine sediments are overlain by flood-plain sediments. This could have occurred as the lake drained or as it filled in some areas with sediments. Lacustrine deposition may have ceased when drainage capture by a tributary of the Columbia River created a new, lower outlet from the western Snake River Plain (Wheeler and Cook, 1954).

Smith (1975) argued on the basis of the diversity of the fossil fish and mollusk fauna, the size of individual fossil specimens, and the nature of specializations in the fossil fish that some sediments of the Glenns Ferry Formation must have been deposited in a large lake. Kimmel (1975) reported on a similar fauna from the Chalk Hills Formation (which he incorrectly referred to as the Deer Butte Formation) and reached a similar conclusion. The known distribution of fossil fish localities in the Chalk Hills and Glenns Ferry Formations supports the large-lake depositional model. Figure 11 shows collecting localities for fossil fish recorded by University of Michigan field parties. All of the localities west of Glenns Ferry, Idaho, contain lacustrine species and are found in lacustrine sediments. In addition to the University of Michigan localities shown on Figure 11, Cope (1883) reported fish species known elsewhere only from Glenns Ferry lacustrine sediments in a locality along "Willow Creek, Oregon," north of Vale, Oregon. This distribution of fossil fish faunas suggests that the Chalk Hills lake covered at least 80 miles and the Glenns Ferry lake at least 110 miles of the southwestern edge of the western Snake River Plain. Other areas of the plain have not been examined by the author for fish localities.

The extent of some volcanic ash beds also supports the presence of large lakes during the late Miocene and Pliocene. Correlations using ash chemistry (Swirydczuk and others, 1982 this volume) and the lithology of ash beds show that the lower Horse Hill ash layer of Swirydczuk and others (1982 this volume) in the Chalk Hills Formation is present in all the study areas. Similar comparisons of ashes from the Glenns Ferry Formation show that ash beds can be correlated from localities near Bruneau, Idaho, to Oreana, Idaho. Comparisons of ash thickness, spacing, and color show that these ashes were deposited in nearly identical environments (Figure 4). This similarity of environments of deposition over wide stretches (up to 40 miles in length) suggests that deposition occurred in a large lake rather than in several small lakes.

Lithologic correlations, strengthened by fossil fish correlations, support the large-lake model. Oolitic limestones are found in the Poison Creek, Oreana, and Adrian areas (Figure 1), just above the base of the Glenns Ferry Formation. These widely separated oolites suggest either synchronous changes in lake chemistry for several lakes, or one change in lake chemistry in a large lake.

Lithologic correlations also suggest that lake levels were affected simultaneously in widely separated areas. In the upper part of the Glenns Ferry Formation measured sections at Poison Creek and Crayfish Hill show a coarse-grained fossiliferous layer at about the same stratigraphic position (Figure 4). Overlying sediments do not show evidence of lacustrine deposition such as fish fossils or interbedded volcanic ash beds and siltstones. Similar fossiliferous sandstones containing wood, fish, bird, and mammal fossils are found near the top of the Chalk Hills Formation in the Horse Hill and Adrian areas (Figures 6 and 10). These sands are immediately overlain by the lower Horse Hill ash layer, but no other lacustrine deposition is present above the sands. These fossiliferous sands may represent beach deposits laid down as lake

levels dropped. The presence of regressional beach sands laid down simultaneously in widely separated areas supports the large-lake depositional model. Intermediate measured sections (Figures 8 and 9) do not show beach deposits at the same level, and lacustrine siltstones and volcanic ash beds are found above the lower Horse Hill ash layer of Swirydczuk and others (1982 this volume). These intermediate sections suggest that lacustrine deposition continued at lower elevations and that lake levels dropped slowly and may have fluctuated.

GEOCHRONOLOGY

SETTING

Early workers in the Snake River Plain based age determinations of sediments on fossil faunas. Cope (1883) on the basis of fish fossils suggested a Pliocene age for the sediments now placed in the Glenns Ferry Formation. Malde and Powers (1962) relied on fossil mammal faunas in dating the Chalk Hills as late Hemphillian and the Glenns Ferry Formation as Blancan. Early potassium-argon dates (Evernden and others, 1965) provided absolute ages for these mammal faunas and a date of 3.5 million years for the Glenns Ferry Formation. Later potassium-argon dates revealed a more complicated situation. Armstrong and others' (1972) potassium-argon dates of 8.5 million years for a basalt below the Chalk Hills Formation agree with accepted biostratigraphy. However Armstrong and others' dates for basalts within the Glenns Ferry Formation range from 4.4 to 6.2 million years, older by 2.1 million years than radiometric dates associated with other Blancan mammal faunas. Armstrong and others note that the two Glenns Ferry dates older than 4.5 million years are from basalts with unusually large atmospheric argon corrections.

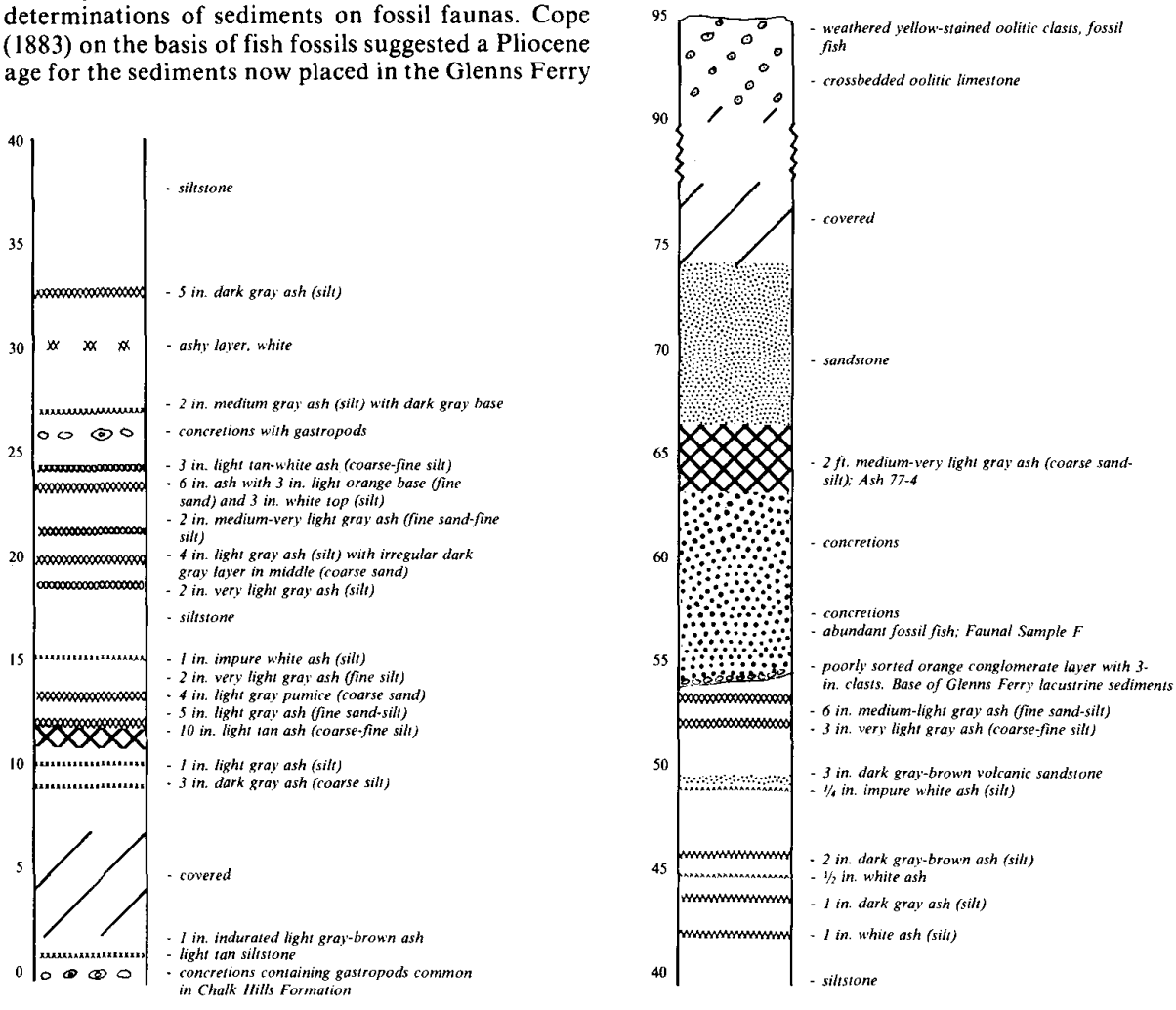

Figure 7. Measured section at location PK4. Located in the SE¼NE¼ sec. 12, T. 5 S., R. 1 W., Owyhee County, Idaho. Base elevation is 2,900 feet.

The older potassium-argon dates could be caused by fractionation of atmospheric argon during its removal by a bake-out procedure, although Armstrong and others feel this effect is minor. If the basalts which they sampled flowed into a very deep lake, the rapid cooling and high pressures could also lead to a potassium-argon date older than the true age (Dalrymple and Lanphere, 1969).

In the Hagerman area, Armstrong and others (1972) dated the Banbury Basalt, formerly thought to be older than the Chalk Hills Formation, at 4.4 to 4.9 million years. These dates also cast doubt on dates of 4.4 to 6.2 million years for the Glenns Ferry basalts since the Banbury Basalt underlies the Glenns Ferry Formation. Armstrong and others felt these dates for the Banbury Basalt may be too young because of pervasive weathering, but the dates are consistent with all their evidence except their Glenns Ferry basalt dates.

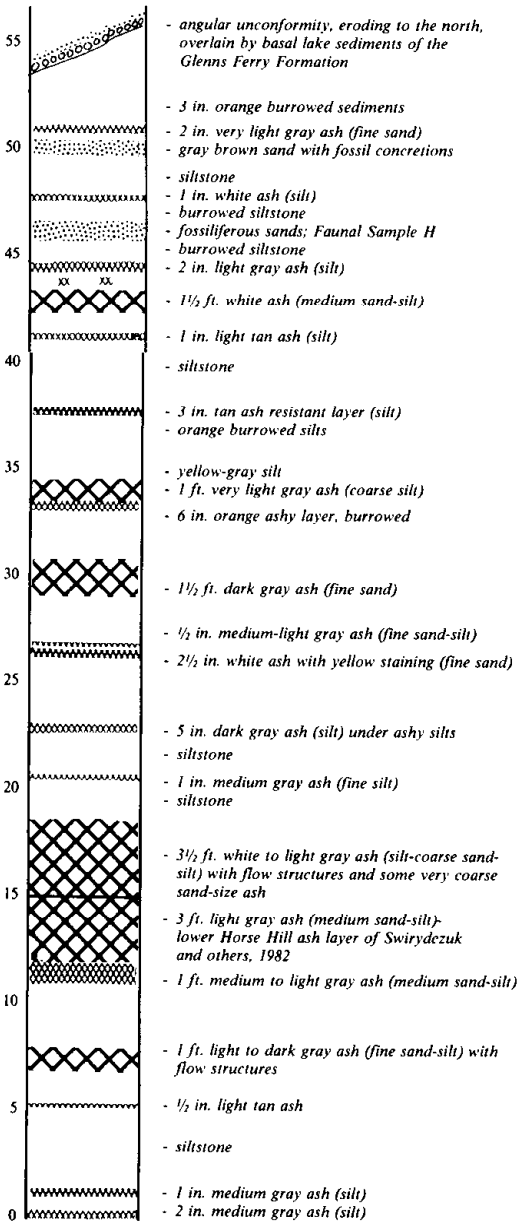

Figure 8. Measured section at location PK3A. Located in the SW¼SW¼ sec. 22, T. 22 S., R. 46 E., Malheur County, Oregon. Base elevation is 2,560 feet.

The potassium-argon dates and the stratigraphic position of the Banbury Basalt suggest a period of volcanism between the deposition of the Chalk Hills and Glenns Ferry Formations. Other basalts are found in the western Snake River Plain in a similar stratigraphic position. In the Oreana area the Glenns Ferry Formation directly overlies a basalt that may itself overlie the Chalk Hills Formation (Anderson, 1965). In the Adrian area Glenns Ferry sediments, as determined by fish fossils, are underlain by the Blackjack Basalt. This basalt was named by Bryan (1929) and later mistakenly synonomized with the Owyhee Basalt. Although no correlations using fish fossils or volcanic ashes have been made with sediments directly below the Blackjack Basalt, fossil molluscan faunas and general stratigraphic relationships suggest that the sediments are part of the upper Chalk Hills Formation and that the basalt is roughly equivalent in age to the Banbury Basalt.

FISSION TRACK METHODS

Fission track dating can give the age of an unaltered, coarse-grained volcanic ash. The eleven ash samples dated in this study were collected from six ash layers in the Chalk Hills and Glenns Ferry Formations. Although one ash layer was sampled at five widely separated localities, the abundance of ash beds within measured sections and the lack of precision of the ash dates did not allow correlation among ash samples using fission track dating. Instead, correlation among ash layers is based on comparisons of ash chemistry and lithology. The fission track dates provide the time of deposition for these ash layers.

These ashes were dated using methods outlined by Boellstorff and Steineck (1975). Glass shards appropriate for fission track dating were separated from bulk samples by sieving, ultrasonic cleaning, and, where necessary, heavy liquid separation. These techniques were necessary to produce samples of large, clean, glass shards. Two aliquots of the treated ash were taken. One was irradiated with a thermal neutron dose of about 10^{15} neutrons/cm^2, along with a standard of known age and uranium content. The two aliquots were then etched under identical conditions in 24 percent reagent grade hydrofluoric acid for up to 2 minutes to enlarge fission tracks into etch

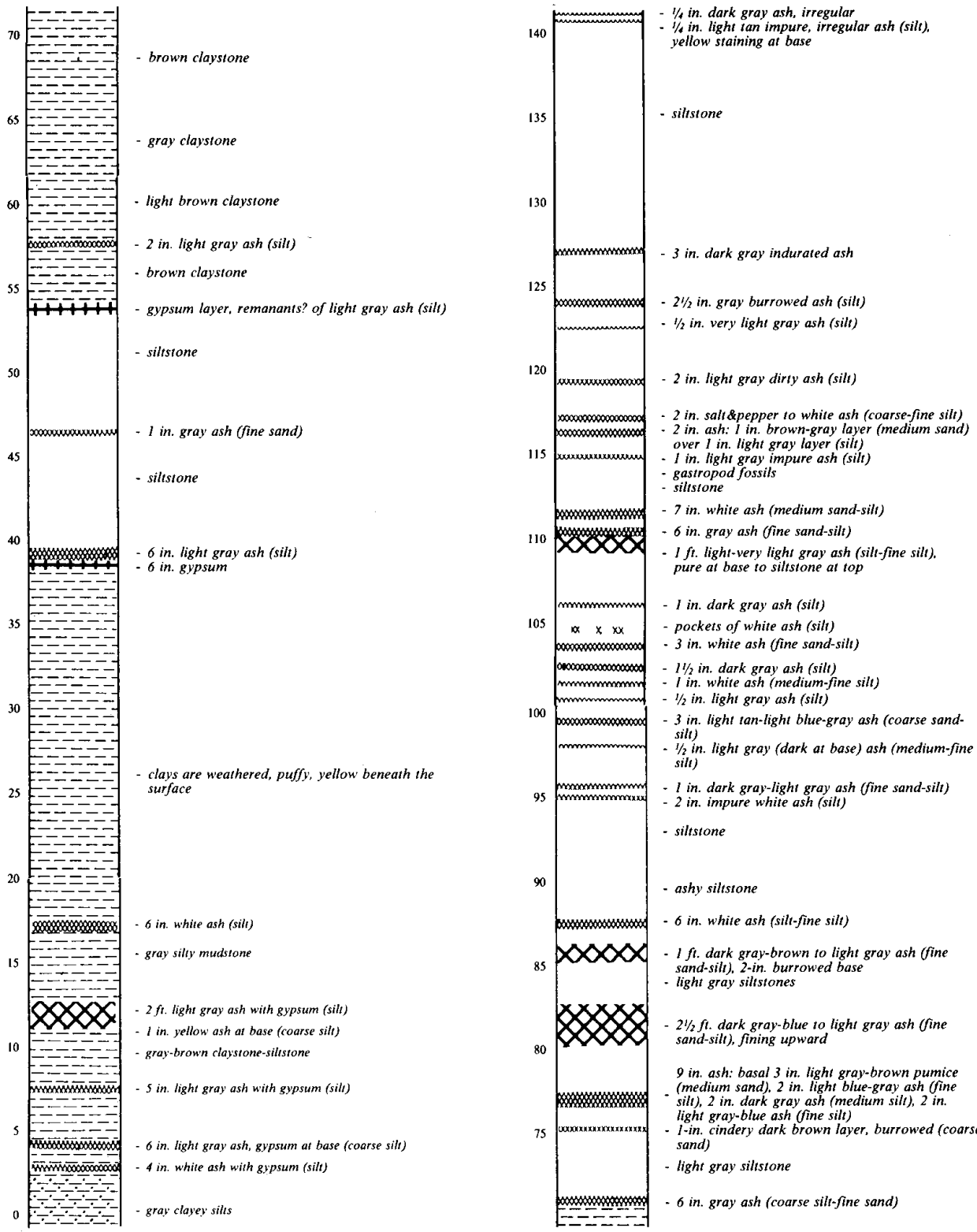

Figure 9. Measured section at location PK7. This is the reference section for correlations involving the comparison of sequences of ash beds. Located in the NW¼SW¼ sec. 19, T. 7 S., R. 4 E., Owyhee County, Idaho. Base elevation is 2,930 feet.

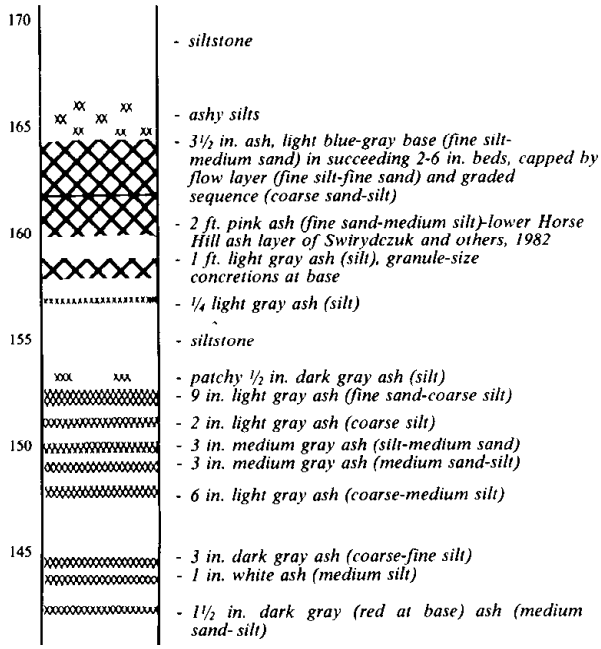

Figure 9. continued.

pits visible at 560 magnification under an optical microscope. Etch pit densities for the irradiated and original aliquots were determined by placing flat, platey shards in the field of view with a point-count stage and using a counting grid to outline an area of the shard. All fission tracks within this area were counted. The track densities determined from the aliquot that was not irradiated are a measure of ρ_s, the density of spontaneous fission tracks, while track densities in the irradiated sample give $\rho_s + \rho_i$, the combined density of spontaneous and irradiated tracks. The exact neutron dose is measured using the fission track densities of a standard. The age is calculated using the following formula (Boellstorff and Steineck, 1975):

$$\text{Age} = 1.49 \times 10^{10} \left[\log_{10} \left(1 + \phi \times \frac{\rho_s}{\rho_i} \times 9.5 \times 10^{-18}\right)\right]$$

The value of 9.5×10^{-18} represents $\frac{\lambda_d \sigma I}{\lambda_f}$, where λ_d = the total decay constant for uranium ($1.54\ 10^{-10}$ years), λ_f = the decay constant for U^{238} (6.85×10^{-17} years^{-1}), σ = the cross-sectional value for U^{235} for thermal neutrons (5.8×10^{-24} cm^2), and I = the natural isotopic ratio of U^{235} to U^{238} (7.25×10^{-3}).

The precision of each date is expressed as a 95 percent confidence interval and is based on the calculation of the standard deviation using four or more separate age determinations. Because the separate age determinations are not based on uniform sample sizes, these confidence intervals are only an approximate measure of the true precision of the dates. Only four determinations were available for some ashes, thus a T-table was used to determine the 95 percent confidence interval. A normal distribution for the ages of ashes in this study was assumed. Samples used in the fission track dating were collected by G. P. Larson, field parties from the University of Michigan in 1975 and 1976, and the author. Localities and measured sections for most of the samples are given in Swirydczuk and others (1982 this volume). Additional localities and measured sections are given in Table 1.

The accuracy of these fission track dates may be affected by three factors. If the ash was heated after the time of deposition, the fission tracks in the glass shards may have been erased or annealed. The apparent age of the ash represents the time when the ash cooled enough for new fission tracks to form. Preliminary dates of 3.5-4.0 million years for some ashes in the Chalk Hills Formation near Oreana, Idaho, suggest that these ashes have been annealed, presumably by hydrothermal action. Partial annealing is suspected in an ash sample from Horse Hill (H1), which gives a date significantly younger than other ash samples in the same ash layer. Hydrothermal activity, which can cause annealing, is still present at Indian Bathtub hot springs, several miles to the south. Since other ashes dated in this study may also have been partially annealed, their ages must be regarded as minimum dates.

Contamination of one ash by shards from another ash could also affect the apparent fission track age of the ash, especially if the differences in ages of the two ashes were great. Shards which are more resistant to the etching process would have an even greater effect as contaminants. Contamination during or after deposition is unlikely for the samples used in the study which were from clean ash beds deposited in lacustrine siltstones.

A third factor may affect the accuracy of the fission track dates. Neutron doses were measured during irradiation using an interlaboratory standard, the Borchers Ash. This is a local name for the Huckleberry Ridge Ash (formerly Pearlette "B") of Izett (1981). The term Borchers Ash is retained here as a laboratory standard because it pertains only to ash from a specific locality rather than the entire Huckleberry Ridge Ash. Seward (1979, 1980) suggested that samples of this standard are partially annealed. She finds that fission track ages measured on glass shards are younger than fission track ages measured using zircon crystals (which are less easily annealed) when neutron doses are measured using National Bureau of Standards (NBS) copper-calibrated glass standards NBS 962 and NBS 963. Seward believes that earlier fission track ages using glass matched those using zircons because an inaccurate standard was used to determine the neutron dose for

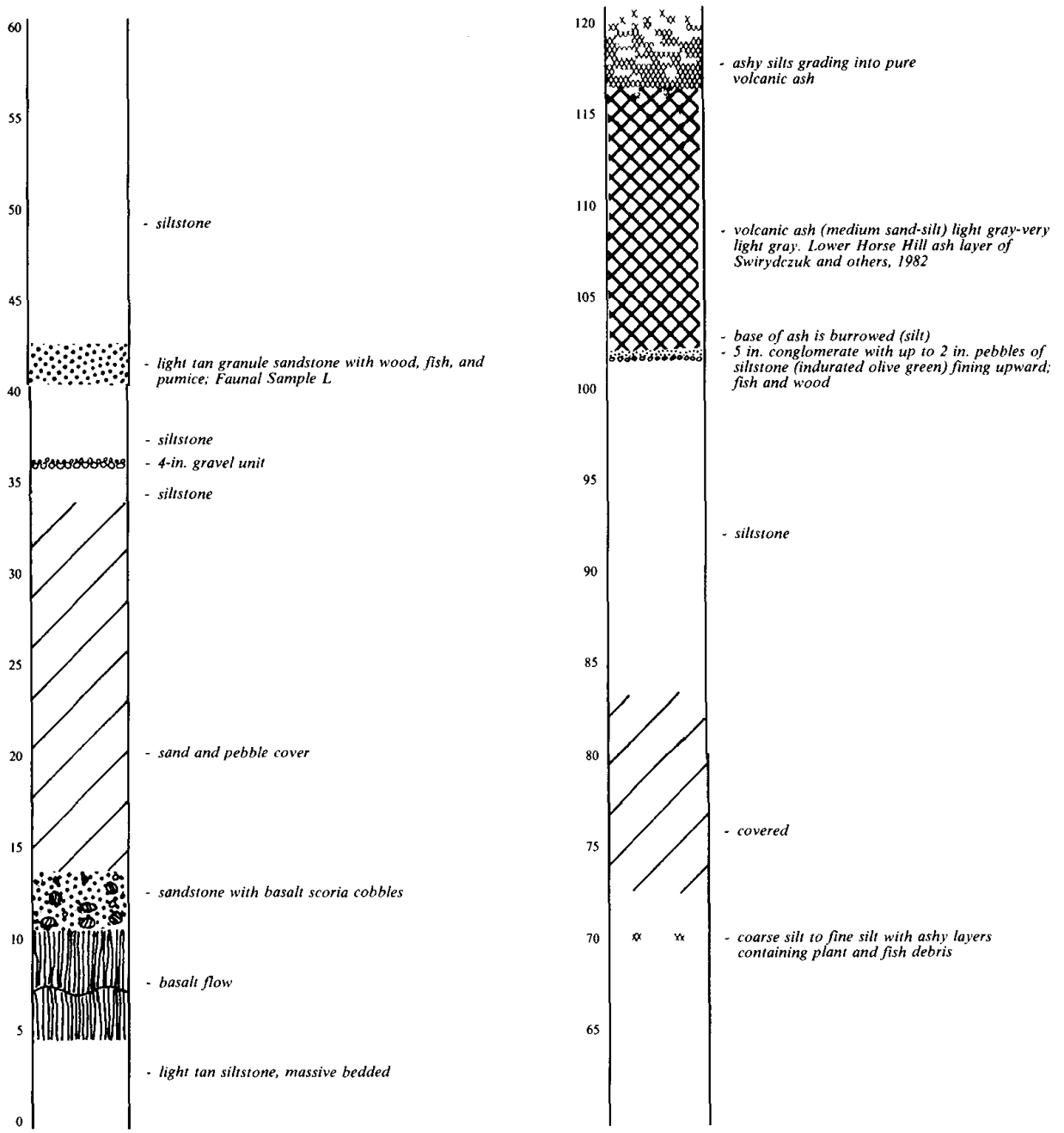

Figure 10. Measured section at location PK8. Located in SE¼ sec. 3, T. 8 S., R. 5 E., Owyhee County, Idaho. Base elevation is 3,025 feet.

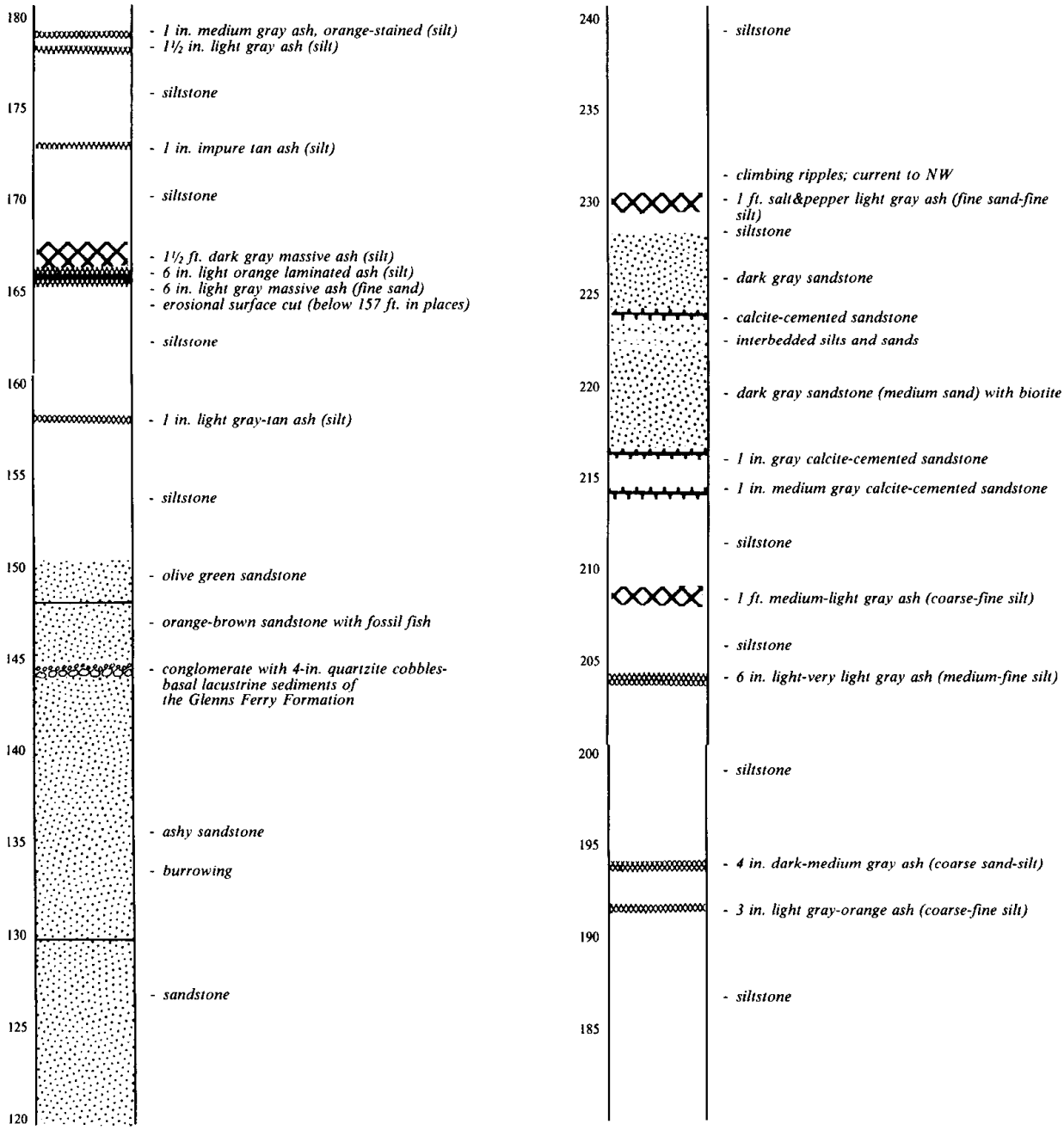

Figure 10. continued.

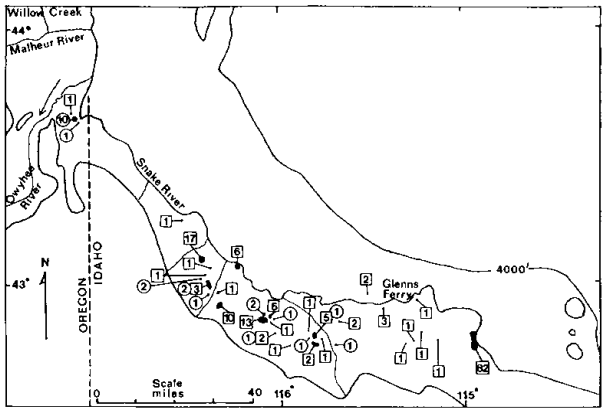

Figure 11. Collecting localities for fossil fish recorded by University of Michigan field parties. Symbols indicate Glenns Ferry fish faunas (squares) and Chalk Hills fish faunas (circles). The number within each symbol represents the number of different collections in each area. The arrow near the Oregon border shows the proposed outlet for the western Snake River Plain drainage in the late Miocene and Pliocene. Solid line is the 4,000-foot contour line.

the glass age determinations. Boellstorff, who suggested the Borchers Ash as an interlaboratory standard, believes that calibration of the newer NBS standards may be at fault (Boellstorff and Alexander, 1980). If Seward is correct and the Borchers Ash has been annealed, dates determined using the Borchers Ash as a standard are too old. A comparison of ages calculated for the interlaboratory standard using the older NBS standard and the new NBS standards (Seward, 1979) reveals that dates using the Borchers Ash standard and assuming no annealing are 29 percent older than those dates calculated by assuming that annealing did take place. This correction factor can be used only if all samples of the Borchers Ash have been uniformly annealed, a likely assumption since workers have consistently reported similar fission track ages (Seward, 1979; Boellstorff and Steineck, 1975). Table 1 gives ages based on the Borchers Ash standard as well as ages corrected using Seward's data for the Borchers Ash to approximate use of the new NBS standard. The discussion below uses dates based on the Borchers Ash standard.

FISSION TRACK RESULTS

Two ash samples (F-2 and 19-A-02) from stratigraphic levels about 25 feet apart in the Glenns Ferry Formation give statistically identical dates (at .05 level) of 2.4 ± .2 and 2.5 ± 1.0 million years. Ash beds from the Poison Creek and Oreana areas were correlated by ash chemistry and lithology. Both ashes contain very thin glass shards which almost completely dissolve during 1 minute of etching in hydrofluoric acid. This lowered the number of fission tracks that could be counted for these samples, resulting in a large standard deviation for one of these dates.

Table 1. Fission track dates for volcanic ashes. Localities for all ash samples except 19-A-02 and 77-4 are given in Swirydczuk and others (1982 this volume). Ash sample 19-A-02 is from an ash layer at Poison Creek, equivalent to the ash at 3,183 feet in Figure 4B of Swirydczuk and others. Ash 77-4 was collected from the Oreana area (Figure 1, location 4) at 2,965 feet (see Figure 7). Each ash date is an average of four or more determinations. The error represents a 95 percent confidence interval based on the standard deviation of the determinations. It does not include a possible 15 percent error in the neutron dose. The Borchers Ash, a local name for the Huckleberry Ridge Ash, (age = 1.96 million years) was used as a standard for these dates. If the Borchers Ash is annealed, the second column of dates, based on Seward's (1979) dates for the Borchers Ash using an NBS standard are more nearly correct. Ash H1 is not included in the average of the lower Horse Hill ash layer because it is near an area of hydrothermal activity and is significantly younger than other samples from this ash layer.

Ash Sample	Number of Spontaneous Tracks Counted	Ash Dates (million years) Using Borchers Ash Standard	Ash Dates (million years) Based on NBS Standard
	Glenns Ferry Formation		
F2	262	2.4 ± 0.2	1.8
19-A-02	144	2.5 ± 1.0	1.9
77-4	402	3.3± 0.4	2.4
	Chalk Hills Formation		
M2	410	6.6 ± 1.0	4.8
S4	256	7.6 ± 0.5	5.5
S3	412	7.1 ± 0.6	5.1
T2	223	6.9 ± 1.2	5.0
H1	420	5.9	4.2
Lower Horse Hill Ash Layer		7.0 ± 0.5	5.0
P1	245	7.9 ± 0.7	5.6
P40	404	9.1 ± 0.9	6.5
P38	1133	8.5 ± 1.2	6.1

A third ash (77-4) was sampled from sands just above the unconformity separating the Chalk Hills and Glenns Ferry Formations. This ash from the Oreana area gives a date of 3.23 ± .4 million years. Because this ash is found in transgressive beach sands at the base of the Glenns Ferry Formation, it may have been reworked from older annealed ashes in the Chalk Hills Formation. Reworking is unlikely, however, since the ash bed is very pure. Preliminary fission track dates of 3.8 and 4.3 million years for ashes nearby suggest that some annealing has occurred in this area and that the ash age must be considered a minimum age.

An ash layer in the upper Chalk Hills Formation

was sampled in three of the four study areas from five separate sampling sites. Four of the dates are not statistically different (.05 level) from each other, giving an average age of 7.0 million years. The remaining ash, from the Horse Hill area near Hot Creek, gives a date of 5.9 million years and may be partially annealed. It is within 10 miles of a present-day hot spring and near another sampling site in the lower Chalk Hills Formation which has given a preliminary date of 3.3 million years.

Ash dates from the lower Chalk Hills Formation show greater standard deviations and less consistency than other ash dates. Three ash samples give dates of 7.9 ± .5, 8.5 ± 1.2, and 9.1 ± .7 million years based on the Borchers Ash standard. The oldest and youngest dates are from the same ash layer as correlated by ash chemistry (Swirydczuk, personal communication, 1981) and by ash lithologies between localities 1.5 miles apart. These fission track dates suggest that the lower Chalk Hills Formation is about 8.5 million years old. The large standard deviations for the dates may have been caused by variations in preparation and counting techniques or by altered distribution of uranium in the ashes. Annealing seems unlikely for three reasons: there is no evidence of hydrothermal activity, additional ashes (S3, S4) from the same area are not annealed, and the ashes showing different dates are found in close proximity to each other.

TECTONIC SETTING

Two generally accepted tectonic models have been proposed for the formation of the western Snake River Plain. One calls on rifting to create the western plain, the other calls on cooling and contraction of rocks in the wake of the Yellowstone Hotspot to form both the western and eastern Snake River Plain. Zoback and Thompson (1978) proposed that the formation of the western Snake River Plain was part of a larger pattern of extensional movement that also formed the northern Nevada aeromagnetic anomaly and influenced the northwest-southeast alignment of feeder dikes for the Columbia River basalts. Smith and Sbar (1974), Morgan (1971), Matthews and Anderson (1973), Eaton and others (1975), and Armstrong and others (1975) did not separate the formation of the eastern and western parts of the Snake River Plain, hypothesizing that all of the plain was formed by the passage of a hot spot now centered under Yellowstone Park.

The eastern Snake River Plain was probably formed by subsidence following the passage of the Yellowstone Hotspot. The magnetic and gravitational anomaly patterns suggest a series of volcanic centers cooling and sinking with time (Mabey, 1978). Armstrong and others (1975) show that the oldest silicic volcanic rocks increase in age away from Yellowstone Park along the eastern Snake River Plain. Seismic evidence suggests that the eastern plain is still active, particularly in the vicinity of Yellowstone. The western plain shows no evidence of seismicity or microseismicity, indicating either no tectonic movement or very fluid conditions below the plain (Pennington and others, 1974).

Several lines of evidence suggest that the eastern and western plains were not formed by the same process. Gravitational and magnetic anomalies for the western Snake River Plain show a comparatively simple pattern, indicating a thick, dense layer of magnetic rock (Mabey, 1976), rather than the more complex pattern of local highs and lows of the eastern plain which indicate varying thicknesses of Cenozoic rocks (Mabey, 1978). The dense layer, up to 5 kilometers thick, may include basalts of the Columbia River Group (Mabey, 1976).

The structural geology of the eastern part of the Snake River Plain is also different from the western part. The eastern plain lacks bounding faults (Kirkham, 1931; Armstrong and others, 1975) and seems to have formed entirely by downwarping, while the western plain shows evidence for faulting as well as downwarping along its boundaries (Malde, 1959; Kirkham, 1931). The trend of the western plain is almost 90 degrees from that of the eastern plain. If both were formed by the same hotspot, they indicate either a drastic change in the direction of movement of the North American plate or a change in the direction of movement of the Yellowstone Hotspot. Regional tectonic evidence does not suggest that the North American plate changed direction in the last 15 million years. Smith and Sbar (1974) show that the Yellowstone Hotspot has been fixed with respect to two other hotspots, the Hawaiian and Raton hotspots, for at least the last 10 million years. It is possible that the Yellowstone Hotspot was moving independently before 10 million years and then began moving in concert with the other two hotspots, but the difference between the eastern and western parts of the plain makes this hypothesis unlikely.

Other hypotheses for the formation of the western Snake River Plain are less likely. Hamilton and Meyers (1966) proposed that batholiths in the western United States serve as subplates. They postulated that the movement of the Idaho batholith to the northwest led to the rifting of the eastern Snake River Plain. Their theory does not explain the formation of the western Snake River Plain unless the batholith was heading to the northeast in the late Miocene. Their hypothesis predicts that the western Snake River

Plain should now be a left-lateral, strike-slip fault. The absence of earthquakes in the western Snake River Plain and along most of the eastern plain (Suppe and others, 1975; Pennington and others, 1974) argues against this hypothesis. In addition, Taubeneck (1971) has shown that structural and lithologic trends in the Idaho batholith continue across the western plain in granitic rocks on the southwest side, indicating that the Idaho batholith was cut by the rift, rather than causing the rift by its movement.

DISCUSSION

The two most likely tectonic models for the origin of the western Snake River Plain predict different patterns of sedimentation. If rifting formed the western Snake River Plain, one would expect to find the oldest lacustrine sediments near the location of the initial rifting. As rifting continued further along the axis of the western plain, the size of the basin would increase and younger lacustrine sediments would therefore be deposited over a wider area. Episodic rifting might have caused periodic draining and filling of the basin as faulting and volcanic activity modified the elevation of the drainage outlet from the plain.

If subsidence following the passage of a hotspot formed the western Snake River Plain, one would expect to find the oldest lacustrine sediments in the west. Younger lacustrine sediments would be deposited further to the east as crustal cooling behind the hotspot created a depression. Large permanent lakes would not be expected with such a model unless some additional tectonic activity raised the drainage outlet from the plain. Although not enough sedimentologic or stratigraphic data exist to reject either model, our data favor the rifting model.

As presently known, the minimum extent of younger lacustrine sediments in the western Snake River Plain is intermediate between distributions predicted by the two models. Only the eastern limits of lacustrine deposition are known. Additional delineation of the lacustrine/nonlacustrine boundary in the Glenns Ferry Formation may eliminate one of these tectonic models.

The presence of an unconformity between the Chalk Hills and Glenns Ferry Formations demonstrates that lake levels fell near the end of the Miocene, lowering or completely draining the lake. This period was ended by deposition of transgressive lacustrine sediments of the Glenns Ferry Formation. This drop in lake level may have been caused by climatic changes, tectonic activity, or erosion of the outlet of the basin.

The sediments and fish faunas of the Chalk Hills and Glenns Ferry Formations show little evidence of climatic control of lake levels. Evaporite deposits have not been reported from lacustrine facies of the western Snake River Plain. The gypsum that is abundant in some areas may be an alteration product from volcanic ash. It is found in many places as a layer within ash beds. The basal oolite of the Glenns Ferry Formation, which might otherwise indicate increasing salinities during evaporitic conditions, was deposited as a progradational unit in an overall transgressive event (Swirydczuk and others, 1980). In addition diverse fossil faunas just below and just above the boundary between the two formations contain families and genera of fish now found in cool or northern waters (Kimmel, 1979). Included are genera of minnows, salmon, and sculpins (Smith, 1975; Kimmel, 1975). These faunas suggest cooler climates rather than the warmer climates expected with a climatically caused fall in lake levels. The diversity of these faunas is much higher than expected for a lake with fluctuating salinities. Thus, climatically caused changes in lake levels seem unlikely.

The filling of the lake basin during the late Miocene and again in the Pliocene may be due to volcanic activity blocking the outlet of the plain. Volcanism occurred in the same area before and possibly during deposition of the Chalk Butte Formation, which is equivalent to the Chalk Hills Formation in Idaho. The Grassy Mountain Formation, which underlies the Chalk Butte Formation, consists of more than 1,000 feet of basalts interbedded with sediments. Thus it may have filled a previous western outlet from the western Snake River Plain, creating the lake which deposited the Chalk Hills lacustrine sediments. The Blackjack Basalt, overlain by Glenns Ferry lacustrine sediments, demonstrates that volcanic activity also occurred in the area of the outlet just before Pliocene lacustrine deposition. Volcanism was also occurring at about the same time in other areas of the western Snake River Plain. This widespread episodic volcanism can be explained by episodic rifting. It is not explained by the hotspot-passage theory.

Uplift or subsidence along the edge of the western Snake River Plain could create apparent changes in lake levels without additional climatic change. Subsidence and uplift at the outlet of the plain could also have caused the changes in lake levels. Examination of patterns of tectonic activity along the edge of the western Snake River Plain makes it possible to evaluate these two tectonic hypotheses.

Correlation of nearshore lacustrine sediments and ashes among different areas along the edge of the western Snake River Plain should make it possible

to determine whether significant subsidence has occurred. The elevation of each ash or sediment layer at the time of deposition varies with the shape of the lake basin. Figure 12 (and Tables 2 and 3) shows that the elevations of Chalk Hills ash layers in most areas decrease toward the axis of the western Snake River Plain. If the lake basin retained the same configuration between deposition of the Chalk Hills and Glenns Ferry Formations, the beds in both formations in the same area should show similar slopes toward the axis of the basin. Subsidence of the Chalk Hills sediments in the center of the basin or filling of the basin with sediments would result in Chalk Hills strata showing a steeper slope toward the axis of the plain than the Glenns Ferry strata. Uplift of the center of the basin or increased erosion there between deposition of the Chalk Hills and Glenns Ferry Formations would result in Glenns Ferry strata showing a steeper slope toward the center of the basin. As Figure 12 demonstrates, both Chalk Hills ashes and the basal Glenns Ferry lacustrine sediments from measured sections in the Horse Hill and Poison Creek areas decrease in elevation toward the axis of the basin. The Chalk Hills ashes show a slightly greater slope, suggesting minor subsidence or continued deposition along the axis during the late Miocene. The ashes of the Chalk Hills Formation in the Poison Creek area show a much steeper slope toward the axis than ashes from other areas, possibly because of variations in the paleoslope of the Chalk Hills lake or because of greater subsidence in that area.

Considering only ash layers and sediments deposited in nearshore lacustrine environments provides a relatively small range of elevations, assuming that the sediments were deposited in one large lake. Several important ash correlations presented earlier use ashes associated with beach deposits. This combination of time indicators and shoreline indicators allows direct comparison of paleoelevations for some

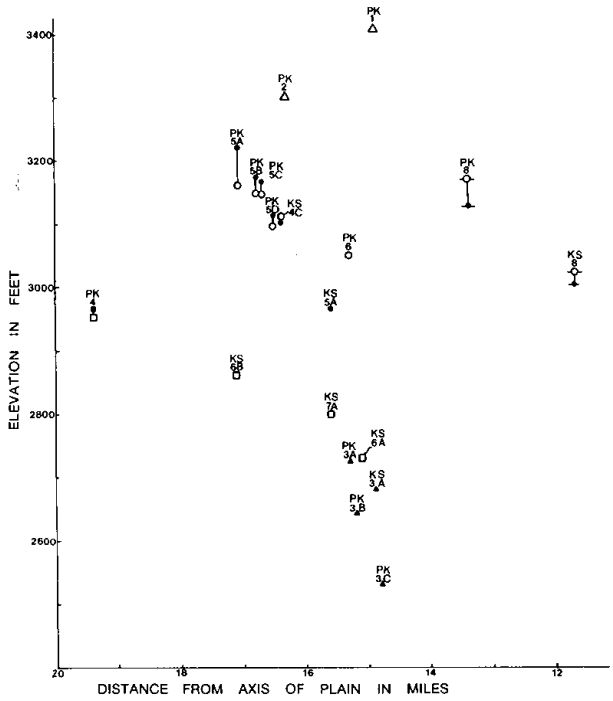

Figure 12. Comparison of elevations of ash layers within the Chalk Hills Formation and elevation of the lowest lacustrine siltstones of the Glenns Ferry Formation versus distance from the axis of the western plain. Elevations of Chalk Hills strata are shown by solid symbols, and those of the Glenns Ferry strata by open symbols. Solid lines link strata from the same measured section. The basis for each correlation is given in Table 2. Squares are from the Oreana area, circles from the Poison Creek area, triangles from the Adrian area, and barred circles from the Horse Hill area. Table 2 gives sources for precise locality data. Table 3 gives additional locations.

Table 2. Methods of correlation among and between localities used in Figure 6. Locations prefixed by PK are described in Table 3 and Figures 3, 5, 6, 7, 8, 9, and 10. Locations labeled KS are described in Swirydczuk and others (1982 this volume). The location number corresponds with the figure number for the measured sections in Swirydczuk and others.

Methods	Locations Correlated
Physical tracing of ash beds between localities	PK5A-PK5C-PK5D PK3C-KS3A PK3A-PK3B
Matching ash chemistries between localities	KS4B-KS6A-KS6B-KS7A KS3A-KS5A-KS8
Comparing sequences of ash layers with a reference section at location PK7	KS5A-KS5C-PK4-PK5C
Matching of fossil faunas and lithologic changes (that is, first appearance of lacustrine sediments)	PK1-PK2 PK4-PK5C PK3A-KS3A PK8-KS5A

Table 3. Additional data for points in Figure 12.

Point	Elevation in Feet	Location	Lithologic Unit and Remarks
PK2	3,300	SW¼NW¼ sec. 18	Fine-grained oolitic limestone correlated with an oolitic limestone at 3,410 feet elevation in Figure 5. This unit is overlain by a Glenns Ferry fish fauna.
PK3B	2,640	Center, SW¼ sec. 22	Ash bed correlated with an ash at 2,725 feet elevation in Figure 6.
PK3C	2,532	SW¼SW¼ sec. 15	Ash bed correlated with Ash M2 (Figure 3A of Swirydczuk and others, 1982 this volume).

beds. In only one area along the edge of the plain do we find evidence for major subsidence between deposition of the Chalk Hills and Glenns Ferry Formations. In the Adrian area localities less than 3 miles apart show Chalk Hills sediments more than 800 feet below Glenns Ferry sediments at about the same distance from the axis of the plain. This difference in elevation is probably due to a combination of initial differences in paleoelevations of the two localities, subsidence of the Chalk Hills sediments, and uplift of the Glenns Ferry sediments.

At least some of this difference must be due to subsidence after deposition of the Chalk Hills Formation since ashes and shoreline indicators are within inches of each other in the Adrian area, even though they are hundreds of feet lower than time-equivalent nearshore and beach sediments in the Horse Hill and Poison Creek areas. The Glenns Ferry sediments in the Adrian area are among the highest along the southwest edge of the plain and could have been deposited during the high-water stage of the Glenns Ferry lake. Only two thin ash beds are present in the sediments, and less than 50 feet of unquestionably lacustrine sediments are present, suggesting that the sediments were deposited over a short time during a high stand of the Glenns Ferry lake. The range of elevations present among the localities in this area, all at about the same distance from the axis of the plain, may be a result of an eastward-dipping paleoslope rather than one perpendicular to the axis of the plain.

Faulting could account for the difference between the elevation of the Glenns Ferry lacustrine sediments and those of the Chalk Hills Formation in the Adrian area and may have occurred at any time after the deposition of the Chalk Hills Formation. Although faults have been mapped in the Adrian area, no major faults have been mapped between the localities for the Chalk Hills and Glenns Ferry Formations (Bryan, 1929; Corcoran and others, 1962; Kittleman and others, 1967). If faulting is not responsible for the high elevation of the Glenns Ferry sediments, then the subsidence of the Chalk Hills sediments must have occurred in the late Miocene or early Pliocene, before deposition of the Glenns Ferry sediments.

Evidence for subsidence in the Adrian area is significant because it is near the Owyhee River, the proposed outlet for the Snake River Plain during the late Miocene and Pliocene (Wheeler and Cook, 1954). Comparisons of fossil fish and molluscan faunas from the Snake River Plain with faunas from northern and central California support Wheeler and Cook's proposed drainage route from eastern Oregon south to central California (Smith, 1975; Taylor, 1966).

The draining of the Glenns Ferry lake may not be related to the tectonic activity. Wheeler and Cook (1954) suggest that drainage from the western Snake River Plain was diverted to the Columbia River by stream (lake) capture or by rising lake waters and that subsequent erosion at this new outlet drained the Glenns Ferry lake.

CONCLUSIONS

Glenns Ferry and Chalk Hills lacustrine sediments were deposited in the late Miocene and Pliocene by large lakes occupying much of the western Snake River Plain. Lacustrine deposition was preceded by volcanic activity in eastern Oregon near the Owyhee River, an area that may have been the outlet for the plain in the late Miocene and Pliocene. This volcanism may have created the lakes by blocking the outlet in the Miocene and again in the early Pliocene. Other basaltic activity of approximately the same ages suggests that the volcanism and the resulting lacustrine deposition are related to episodic rifting along the Snake River Plain rather than to subsidence following the passage of the Yellowstone Hotspot. Comparisons of present elevations of upper Chalk Hills nearshore sediments of the same age suggest that the area nearest the outlet underwent subsidence in the late Miocene. This may have caused the draining of the Chalk Hills lake. Diversion of the drainage of the Snake River Plain into the Columbia River drainage system and the subsequent erosion of a new, lower outlet from the plain may have caused the draining of the Glenns Ferry lake.

ACKNOWLEDGMENTS

Financial assistance for this investigation was provided by Phoenix Memorial Laboratory, the Scott Turner Committee, and the Sigma Xi Chapter, all at the University of Michigan. The Museum of Paleontology and the Department of Geological Sciences at the University of Michigan provided field support and equipment. G. P. Larson and field crews from the University of Michigan collected many ash and fossil fish samples. Discussions and field conferences with G. R. Smith, K. Swirydczuk, B. H. Wilkinson, and D. W. Taylor were particularly helpful. J. D. Boellstorff provided instruction and advice on fission track dating. R. Burns helped set up irradiation procedures for the fission track dating.

REFERENCES

Anderson, N. R., 1965, Upper Cenozoic stratigraphy of the Oreana, Idaho, 15-minute quadrangle: University of Utah Ph.D. dissertation, 212 p.

Armstrong, R. L., W. P. Leeman, and H. E. Malde, 1975, K-Ar dating, Quaternary and Neogene volcanic rocks of the Snake River Plain, Idaho: American Journal of Science, v. 275, p. 225-251.

Boellstorff, J. D. and D. R. Alexander, 1980, Comment on "Comparison of zircon and glass fission-track ages from tephra horizons": Geology, v. 8, p. 468-469.

Boellstorff, J. D. and P. L. Steineck, 1975, The stratigraphic significance of fission-track ages on volcanic ashes in the marine late Cenozoic of southern California: Earth and Planetary Science Letters, v. 27, p. 143-154.

Bryan, Kirk, 1929, Geology and dam sites with a report on the Owyhee Irrigation Project, Oregon: U. S. Geological Survey Water-Supply Paper 5-A, 89 p.

Cope, E. D., 1883, On the fishes of the Recent and Pliocene lakes of the western part of the Great Basin; and of the Idaho Pliocene lake: Philadelphia Academy of Natural Science Proceedings, v. 35, p. 134-167.

Corcoran, R. E., R. A. Doak, P. W. Porter, F. I. Pritchett, and N. C. Privrasky, 1962, Geology of the Mitchell Butte quadrangle, Oregon: Oregon Department of Geology and Mineral Industry Map GMS2.

Dalrymple, G. B. and M. A. Lanphere, 1969, Potassium-Argon Dating: Freeman and Company, San Francisco, 258 p.

Eaton, G. P., R. L. Christiansen, H. M. Iyer, A. M. Pitt, D. R. Mabey, H. R. Bank, Jr., Isidore Zeitz, and M. W. Gettings, 1975, Magma beneath Yellowstone National Park: Science, v. 188, p. 787-796.

Evernden, J. F., D. E. Savage, G. H. Curtis, and G. T. James, 1964, Potassium-argon dates and the Cenozoic mammalian chronology of North America: American Journal of Science, v. 262, p. 145-198.

Hamilton, Warren and W. B. Meyers, 1966, Cenozoic tectonics of the western United States: Reviews of Geophysics, v. 4, p. 509-549.

Izett, G. A., 1981, Volcanic ash beds: recorders of upper Cenozoic silicic pyroclastic volcanism in the western United States: Journal of Geophysics Research, v. 86, p. 10200-10222.

Kimmel, P. G., 1975, Fishes of the Miocene-Pliocene Deer Butte Formation, southeast Oregon: University of Michigan Museum of Paleontology Papers in Paleontology, v. 14, p. 69-87.

———, 1979, Stratigraphy and paleoenvironments of the Miocene Chalk Hills Formation and Pliocene Glenns Ferry Formation in the western Snake River Plain, Idaho: University of Michigan Ph.D. dissertation, 331 p.

King, Clarence, 1878, Systematic Geology: U. S. Geologic Exploration of 40th Parallel (King), v. 1, 803 p.

Kirkham, V. R. D., 1931, The Snake River Downwarp: Journal of Geology, v. 39, p. 456-482.

Kittleman, L. R., Jr., A. R. Green, A. R. Hagood, A. M. Johnson, J. M. McMurray, R. G. Russel, and D. A. Weeden, 1965, Cenozoic stratigraphy of the Owyhee region, southeastern Oregon: University of Oregon Museum of Natural History Bulletin 1, 45 p.

Mabey, D. R., 1976, Interpretation of a gravity profile across the western Snake River Plain, Idaho: Geology, v. 4, p. 53-55.

———, 1978, Regional gravity and magnetic anomalies in the eastern Snake River Plain, Idaho: U. S. Geological Survey, Journal of Research, v. 6, p. 553-562.

Malde, H. E., 1959, Fault zone along northern boundary of western Snake River Plain, Idaho: Science, v. 130, p. 272.

———, 1972, Stratigraphy of the Glenns Ferry Formation from Hammett to Hagerman, Idaho: U. S. Geological Survey Bulletin 1331-D, p. 1-19.

Malde, H. E. and H. A. Powers, 1962, Upper Cenozoic stratigraphy of the western Snake River Plain, Idaho: Geological Society of America Bulletin, v. 73, p. 1197-1220.

Matthews, Vincent, III, and C. E. Anderson, 1973, Yellowstone convection plume and break-up of the western United States: Nature, v. 243, p. 158-159.

Morgan, W. J., 1971, Convection plumes in the lower mantle: Nature, v. 230, p. 42-43.

Pennington, W. D., R. B. Smith, and A. B. Trimble, 1974, A microearthquake survey of parts of the Snake River Plain and central Idaho: Seismological Society of America, v. 64, p. 307-312.

Seward, Diane, 1979, Comparison of zircon and glass fission-track ages from tephra horizons: Geology, v. 7, p. 479-482.

———, 1980, Reply on "Comparison of zircon and glass fission-track ages from tephra horizons": Geology, v. 8, p. 469-470.

Shotwell, J. A., 1970, Pliocene mammals of southeast Oregon and adjacent Idaho: University of Oregon Museum of Natural History Bulletin 17, 103 p.

Smith, G. R., 1975, Fishes of the Pliocene Glenns Ferry Formation, southwest Idaho: University of Michigan Museum of Paleontology Papers in Paleontology, v. 14, p. 1-68.

Smith, G. R., Krystyna Swirydczuk, P. G. Kimmel, and B. H. Wilkinson, 1982, Fish biostratigraphy of late Miocene to Pleistocene sediments of the western Snake River Plain, Idaho, *in* Bill Bonnichsen and R. M. Breckenridge, editors, Cenozoic Geology of Idaho: Idaho Bureau of Mines and Geology Bulletin 26.

Smith, R. L. and M. L. Sbar, 1974, Contemporary tectonics and seismicity of the western United States with emphasis on the Intermountain seismic belt: Geological Society of America Bulletin, v. 85, p. 1205-1218.

Suppe, John, Christine Powell, and Robert Berry, 1975, Regional topography, seismicity, Quaternary volcanism, and the present-day tectonics of the western United States: American Journal of Science, v. 275-A, p. 397-436.

Swirydczuk, Krystyna, B. H. Wilkinson, and G. R. Smith, 1979, The Pliocene Glenns Ferry oolite: lake-margin carbonate deposition in the southwestern Snake River Plain: Journal of Sedimentary Petrology, v. 49, p. 995-1004.

———, 1980, The Pliocene Glenns Ferry oolite: sedimentology of oolitic lacustrine terrace deposits: Journal of Sedimentary Petrology, v. 50, p. 1237-1248.

Swirydczuk, Krystyna, G. P. Larson, and G. R. Smith, 1982, Volcanic ash beds as stratigraphic markers in the Glenns Ferry and Chalk Hills Formations from Adrian, Oregon, to Bruneau, Idaho, *in* Bill Bonnichsen and R. M. Breckenridge, editors, Cenozoic Geology of Idaho: Idaho Bureau of Mines and Geology Bulletin 26.

Taubeneck, W. H., 1971, Idaho batholith and its southern extension: Geological Society of America Bulletin, v. 82, p. 1899-1928.

Taylor, D. W., 1966, Summary of North American Blancan non-marine mollusks: Malocologia, v. 4, p. 1-172.

Van Couvering, J. A., 1978, Status of late Cenozoic boundaries: Geology, v. 6, p. 169.

Wheeler, H. E. and E. F. Cook, 1954, Structural and stratigraphic significance of the Snake River capture, Idaho-Oregon: Journal of Geology, v. 62, p. 525-536.

Zoback, M. L. and G. A. Thompson, 1978, Basin and Range rifting in northern Nevada: clues from a mid-Miocene rift and its subsequent offsets: Geology, v. 6, p. 111-116.

Chapter 10

Stratigraphy and Paleontology American Falls Area

Revised Quaternary Stratigraphy and Chronology In the American Falls Area, Southeastern Idaho

by

William E. Scott[1], Kenneth L. Pierce[1],
J. Platt Bradbury[1], and Richard M. Forester[1]

ABSTRACT

New information about the stratigraphy, paleoecology, and geochronology of the American Falls area in southeastern Idaho adds to and modifies previously published interpretations of the late Quaternary geologic history.

Based on evidence from the Bonneville basin, the Bonneville Flood occurred about 14,000-15,000 years ago, rather than 30,000 years ago as suggested by previous researchers in the American Falls basin. This revised age for the flood is in accord with geologic evidence from the American Falls basin as estimated from stratigraphic relationships with loess deposits and alluvial gravels of late Pleistocene age. Radiocarbon dates from the flood deposits are all too old, probably because the dated materials were reworked from older deposits by the flood. The basalt of Portneuf Valley, which was dated previously by radiocarbon as 30,000 to 35,000 years old and therefore was presumed to be only slightly older than the flood, has a potassium-argon age of 0.583 ± 0.104 million years, which is also supported by the stratigraphy of loess and buried soils that overlie portions of the flow. The flood exhumed the flow from a valley fill and scoured its surface.

The flood caused the draining of American Falls Lake, which was formed by the blocking of the Snake River by a lava flow from Cedar Butte about 72,000 ± 14,000 years ago. Paleoenvironmental interpretations based on the microfossil assemblages in deposits in the American Falls area support the conclusion of Ridenour (1969) that the lower part of the American Falls Lake Beds of Trimble and Carr (1961b) is of alluvial origin. This fine-grained alluvium was probably deposited not long before 72,000 years ago. The alluvial gravel that underlies the fine-grained alluvium of the upper part of the American Falls Lake Beds and contains the remains of *Bison latifrons* and other vertebrates may therefore also be not much older than 72,000 ± 14,000 years, although its age may exceed 100,000 years.

[1]U. S. Geological Survey, Federal Center, Denver, Colorado 80225.

INTRODUCTION

The American Falls area (Figures 1 and 2) has been recognized as a significant locality for studies of Quaternary geology ever since an important vertebrate fauna, that includes the giant bison, *Bison latifrons*, was discovered there (Hopkins, 1951). In addition, key evidence and dates for the catastrophic Bonneville Flood have come from this area (Malde, 1960; Trimble and Carr, 1961a, 1961b). The sediments in the American Falls basin also provide an analogue for comparison with older, similar sequences of sediments in lava-dammed basins along the Snake River, such as the Burley Lake Beds and sediments of the Bruneau Formation. Our interest here began during our studies of the surficial geology of the eastern Snake River Plain. It soon became apparent that investigations in the American Falls area would probably provide critical stratigraphic and chronologic information regarding regionally extensive alluvial and eolian deposits. Rather than attempt a comprehensive study of the Quaternary geology of the area, we concentrated on several important topics in Quaternary stratigraphy, geochronology, and paleoecology. The purpose of this report is to present new information obtained from these studies and to propose a revision of aspects of the published late Quaternary history in light of our findings.

In an early reconnaissance study, Stearns and others (1938, p. 69-72) recognized that the Snake River had been dammed by upper Pleistocene lava flows from Cedar Butte, a basaltic shield volcano 15 kilometers southwest of American Falls, thus forming a lake that extended about 65 kilometers

Scott, W. E., K. L. Pierce, J. P., Bradbury, and R. M. Forester, 1982, Revised Quaternary stratigraphy and chronology in the American Falls area, southeastern Idaho, *in* Bill Bonnichsen and R. M. Breckenridge, editors, Cenozoic Geology of Idaho: Idaho Bureau of Mines and Geology Bulletin 26, p. 581-595.

upstream, almost to the present site of Blackfoot (Figures 1 and 2). Sediments in the American Falls basin thought to have been deposited in the lake were named the American Falls Lake Beds by Trimble and Carr (1961b). Detailed study of the sedimentary characteristics of the American Falls Lake Beds by Ridenour (1969) showed that the lower part of this unit is alluvial and that only the upper part is lacustrine. Evidence of catastrophic flooding down the Portneuf and Snake Rivers during the rapid outflow of water from Lake Bonneville through Red Rock Pass, Idaho (Gilbert, 1890), 80 kilometers southeast of American Falls, was found by detailed geologic mapping and stratigraphic studies (Malde, 1960; Trimble and Carr, 1961a, 1961b). The floodwaters cut the present canyon of the Snake River into the Cedar Butte Basalt and underlying rocks, and American Falls Lake was drained. Radiocarbon ages of 25,000 to 35,000 years for the flood-scoured basalt of Portneuf Valley (Bright, 1963; Ives and others, 1964; Malde, 1968, p. 10) and an age of 30,000 years on mollusk shells from deposits of the Bonneville Flood in the American Falls area (Trimble and Carr, 1961b) were used to support an age of about 30,000 years for the flood (Malde, 1968, p. 10-11).

In other studies, abundant vertebrate remains were described from gravelly alluvium that underlies the deposits of American Falls Lake (Hopkins, 1951, 1955; Hopkins and others, 1969), as well as from deposits of the Bonneville Flood (McDonald and Anderson, 1975).

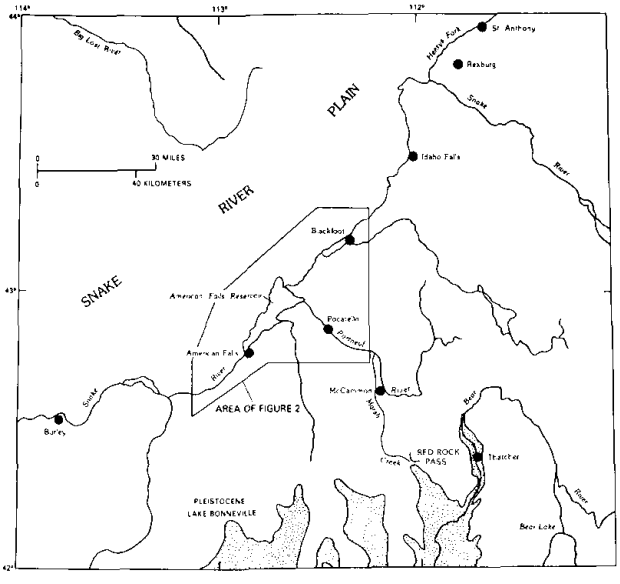

Figure 1. Location of the American Falls area, southeastern Idaho. Stippled area represents the maximum northern extent of Lake Bonneville in late Wisconsin time.

In general, this sequence of events is confirmed in this report; the main contribution is to better define the age of these events and to present information obtained from paleoecologic studies of the sequence of alluvial and lacustrine deposits in the American Falls basin. We conclude that the late Pleistocene American Falls Lake was dammed in early Wisconsin time, 72,000 ± 14,000 years ago, that the catastrophic overflow of Lake Bonneville occurred about 14,000 to 15,000, rather than 30,000, years ago, and that the flood-scoured basalt flow in the Portneuf Valley is much older than previously thought and was exhumed from a Quaternary fill by the flood, rather than being closely related in time to the flood. New information on key geologic events will be presented first, followed by our proposed revision of the late Quaternary geologic history and the implications of our results to related Quaternary studies in southeastern Idaho.

NEW INFORMATION ON KEY GEOLOGIC EVENTS

Recent stratigraphic studies in the Bonneville basin and American Falls area and two potassium-argon dates provide new information on the ages of (1) the Bonneville Flood, (2) the basalt of Portneuf Valley, and (3) the Cedar Butte Basalt. In addition, we present the results of investigations of the stratigraphy and paleoecology of alluvial and lacustrine deposits in the American Falls area.

AGE OF BONNEVILLE FLOOD

Geologists studying deposits of the Bonneville Flood in the American Falls and downstream areas have suggested that the flood occurred about 30,000 years ago, partly on the basis of radiocarbon dating in the American Falls area and partly on an inferred relation between the diversion of Bear River into the Bonneville basin (Bright, 1963, 1967) and the overflow of Lake Bonneville (Trimble and Carr, 1961a, 1961b, 1976; Carr and Trimble, 1963; Malde, 1968; Trimble, 1976). However, studies of Lake Bonneville history (Bright, 1963; Morrison, 1965, 1966; Currey, 1980; Scott and others, 1980, 1982) have placed the age of the overflow between 12,000 and 15,000 years ago, during the last lake cycle, which is well dated by radiocarbon as 26,000 to 11,000 years ago or late Wisconsin in age. The following discussion concludes that strong evidence exists in the Bonneville basin for the overflow occurring sometime between 14,000 and 15,000 years

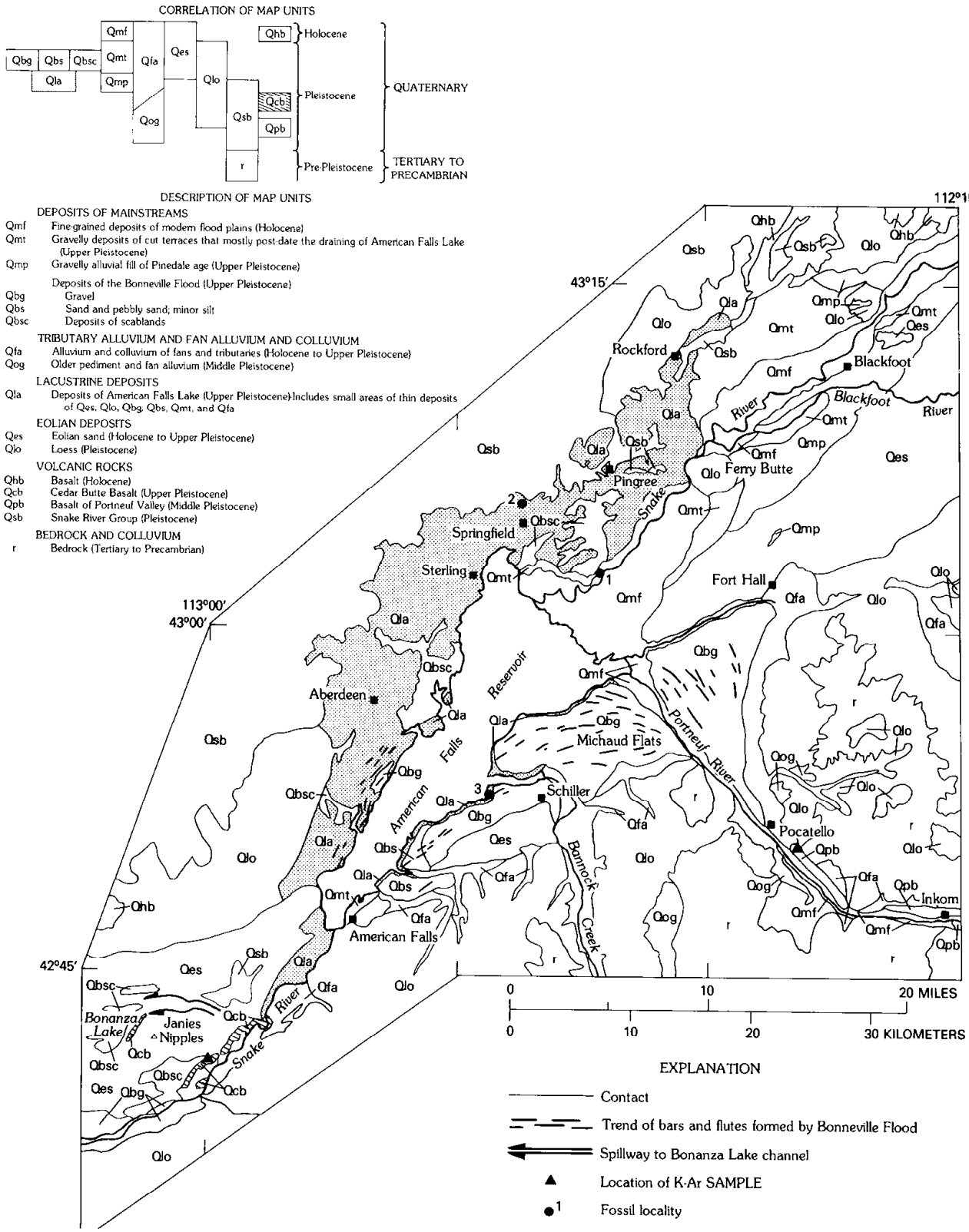

Figure 2. Generalized surficial geologic map of the American Falls area, Idaho. Modified from Scott (in press).

ago, but that none of the evidence for a 30,000-year-old flood is compelling. A late Wisconsin age for the flood is also compatible with geologic evidence from the American Falls area.

Recent work on the chronology of Lake Bonneville (Currey, 1980; Scott and others, 1980, 1982) confirms the conclusions of previous investigators that the lake dropped rapidly from the Bonneville shoreline to, or close to, the Provo shoreline (Gilbert, 1890, p. 175), a vertical distance at Red Rock Pass of about 100 meters. The most convincing evidence for the rapid drop includes the lack of regressive deposits between the two shorelines, even though abundant such deposits exist below the Provo shoreline. The deposits of the numerous shorelines between the Bonneville and Provo levels all relate to the transgressive phase of the last lake cycle or to older lake cycles, as shown by radiocarbon dating and by stratigraphic relations.

The rapid fall of the lake from the Bonneville shoreline to the Provo shoreline has not been dated directly; however, its age is bracketed by several radiocarbon dates. By about 16,800 years ago, during the transgressive phase of the last lake cycle, the lake stood about 15 meters below the Bonneville shoreline (Scott and others, 1982). Several dates ranging from 12,800 to 13,900 years (W-899, Bright, 1963; W-200, Marsters and others, 1969; W-943, Morrison, 1965) on shells collected from shallow-water or shoreline sediments deposited below the Provo shoreline provide minimum ages for the rapid fall of the lake. Allowing for the remaining transgression to the Bonneville shoreline after 16,800 years ago, for a period of stabilization at the Bonneville shoreline, and for an occupation of the Provo shoreline, an age of 14,000 to 15,000 years for the rapid fall of the lake appears likely (Currey, 1980; Scott and others, 1980, 1982).

Many researchers infer that the Bonneville Flood occurred during this rapid fall of lake level (Gilbert, 1890, p. 175; Currey, 1980; Scott and others, 1980, 1982). Another view, which is summarized by Malde (1968, p. 10-11), is based on evidence of a lake level at least 10 meters higher than the Bonneville shoreline (Bright and Rubin, 1965). In this interpretation, the flood was caused by rapid erosion of the outlet from a level not more than 35 meters above the Bonneville shoreline to the Bonneville shoreline (Malde, 1968, p. 12); erosion of the outlet from Bonneville to Provo levels occurred at a much slower rate. The evidence for a lake level higher than the Bonneville shoreline has not been described fully; however, nowhere else in the Bonneville basin has any convincing evidence of a lake level higher than the Bonneville shoreline been found (Gilbert, 1890, p. 96-98; Currey, 1980).

In addition, for the flood to have occurred 30,000 years ago, a deep lake must have occupied the Bonneville basin; however, there is no evidence to suggest a deep lake existed at this time (Morrison, 1966, p. 94; Scott and others, 1980, 1982). Two lines of evidence suggest that from 22,000 to about 125,000 years ago, there were no deep lakes in the basin (Scott and others, 1980, 1982). First, the degree of development of the soil or soil complex that is developed in deposits of the penultimate lake cycle and that is buried by deposits of the last lake cycle indicates a time interval between these two lake cycles of about 100,000 years. Second, amino-acid evidence suggests that the penultimate lake cycle may be as much as ten times older than the last lake cycle, which culminated about 15,000 years ago.

Six radiocarbon dates on materials from deposits of the Bonneville Flood (Michaud Gravel) in the American Falls area are all older than our estimated age of the flood, and range in age from 21,500 to greater than 38,000 years (Table 1). A date of 29,700 years on shells from deposits thought to postdate—or, more likely, to represent the waning phase of the flood (Trimble and Carr, 1961b)—has been used to support a minimum age of 30,000 years for the flood (Trimble and Carr, 1961b; Malde, 1968; Trimble, 1976). Malde collected shells from the Michaud Gravel near Schiller that yielded ages of greater than 29,000 and greater than 33,000 years (Kelley and others, 1978). Two dates on bone from the Michaud Gravel are 21,500 and 31,300 years (McDonald and Anderson, 1975). A transported peat chunk yielded an age of greater than 38,000 years (Ives and others, 1964). We infer two reasons why none of these dates come close to our estimated age of 14,000 to 15,000 years: (1) the ages are apparently too old due to contamination or some geochemical cause; and (2) the dated materials were reworked from older deposits by the flood.

For the dated materials to have been living shortly before or during the flood and to give radiocarbon ages significantly greater than the age of the flood, they must either have been contaminated with old carbon since deposition or have lived in an environment from which they acquired a very low initial $^{14}C/^{12}C$ ratio. Both of these possibilities appear unrealistic. First, a 15,000-year-old sample would require contamination with dead carbon equal to about seven times its weight of carbon or replacement of almost 90 percent of its carbon with dead carbon to give an apparent age of 30,000 years. The dated specimens probably would not survive intact after an addition or replacement of this magnitude. Second, the dated materials probably could not acquire a low enough initial $^{14}C/^{12}C$ ratio from the water of streams and ponds in the area to

give an apparent age 15,000 years too old. Broecker and Walton (1959, p. 33) estimate an uncertainty of 500 years for dates on organisms that lived in closed Great Basin lakes, although the age uncertainty could be as high as 2,000 years. Rubin and others (1963) estimate a maximum error in snail dates of 1,000 years owing to the uptake of ^{14}C-free inorganic carbon. These values are much less than the 15,000-year difference in age between the flood and the dated materials from the flood deposits. Although these factors may be partly responsible for this age difference, they cannot explain a discrepancy of this magnitude.

A more likely cause for these too old and widely scattered ages is that the dated materials were reworked by the flood from older deposits. The vertebrate fauna in the Michaud Gravel represents a variety of habitats including aquatic, grassland, and forest or scrub. Bone is scattered throughout the deposit, and, except for microfauna, no large concentrations of bone are found. Significantly, no articulated specimens are found, and some of the

Table 1. Potassium-argon and radiocarbon ages from the American Falls area, Idaho.

Lab number	Age	Material dated	Reference	Remarks
Potassium-argon ages on basalt				
	0.1 ± .2 m.y.	Cedar Butte Basalt	1	Normal magnetic polarity.
76G031	0.072 ± .014 m.y.	Cedar Butte Basalt	2	From top of cliff, center sec. 31, T. 8 S., R. 30 E.
	0.14 ± .03 m.y.	Lowest basalt flow at Inkom	1	Normal magnetic polarity.
76G032	0.583 ± .104 m.y.	Basalt of Portneuf Valley	2	From SW¼ sec. 6., T. 7 S., R. 35 E.
Radiocarbon ages from deposits of Bonneville Flood				
W-2512	>29,000	Clam shells	3	Shells probably reworked from older deposits.
W-2514	>33,000	Snail shells	3	Shells probably reworked from older deposits.
WSU-1423	21,500 ± 700	Bone	4	Bone probably reworked from older deposits.
WSU-1424	31,300 ± 2,300	Bone	4	Bone probably reworked from older deposits.
W-932	>38,000	Peat	5	Peat probably reworked from older deposits.
W-731	29,700 ± 1,000	Shells	6	From Aberdeen terrace deposits of Trimble and Carr (1961b). Shells probably reworked from older deposits.
Radiocarbon ages from deposits of American Falls Lake				
W-929	>42,000	Peat	7	Thought by Trimble (1976) to be from near the top of the deposits of American Falls Lake; however, Hopkins and others (1969) think that it is from the base.
Grn-6022	>51,900	Peat	8	The same peat layer as W-929. Lies 1.5 meters from base of lake deposits, which have a total thickness of 4.5 meters.
Radiocarbon ages from alluvial deposits that underlie deposits of American Falls Lake				
M-939	>30,000	Charcoal	9	Associated with skull of *Bison latifrons*.
W-358	>32,000	Charcoal	10	Associated with skull of *Bison latifrons*.
Radiocarbon ages related to basalt of Portneuf Valley				
W-1121	33,000 ± 1,600	Soil organic matter below flow	5	Overlying basalt has K-Ar age of about 600,000 years. Finite ages reflect contamination by young organic matter; living roots extend below base of flow.
W-1177	35,000 ± 3,000		5	
W-1329	30,000 ± 2,000		11	
W-1334	25,000 ± 2,000		11	
W-1221	32,500 ± 1,500	Mollusk shells from deposits of flow-dammed lake	7	This interpretation is different from that of Bright given in (5). If shells are related to flow, they are contaminated with young carbon.

References

1. Armstrong and others (1975); 2. G. B. Dalrymple (written communication, 1979); 3. Kelley and others (1978); 4. McDonald and Anderson (1975); 5. Ives and others (1964); 6. Trimble and Carr (1961b); 7. Trimble (1976); 8. Bright (1982 this volume); 9. Crane and Griffin (1961); 10. Rubin and Alexander (1958); 11. Bright *in* Malde (1968).

large bones are broken and waterworn (McDonald and Anderson, 1975). These observations imply reworking of bones from deposits of various environments and perhaps from deposits of various ages. The dated mollusk shells were almost surely transported by the flood, because the short duration, high turbidity, and turbulence of the flood flow cannot be expected to have provided an hospitable environment for development of an indigenous molluscan fauna. The radiocarbon samples may have contained mollusks living along the flood path immediately prior to the flood and mollusk shells eroded from older sediments in the valleys of Portneuf River and Marsh Creek, which include stream, marsh, and lake deposits of middle and early Pleistocene age that contain mollusk shells and other fossils (Steele, 1980). The scarp-bounded inner valley along Marsh Creek and the lower Portneuf River was probably largely excavated in these deposits by the flood, and the eroded sediments, including any fossils, are a likely source of the Michaud Gravel and thin sheets of sand and gravel in the American Falls basin. The shell sample with the 30,000-year age (W-731) could have contained as much as 12 percent of 15,000-year-old shells (organisms living at the time of the flood) if the remainder of the sample had been composed of old shells containing no ^{14}C. Alternatively, the sample could have been composed entirely of old shells that were contaminated with a few percent young carbon and therefore yielded a 30,000-year age.

The 14,000- to 15,000-year age for the Bonneville Flood is also in accord with other geologic evidence in the American Falls area. The thin blanket of loess that has accumulated on the flood-scoured basalt of Portneuf Valley and deposits of the Bonneville Flood suggests that the flood predates the cessation of loess deposition, but that the flood is appreciably younger than the beginning of deposition of the upper loess blanket of the region, which is estimated roughly to be in the beginning of Wisconsin time (Pierce and others, 1982 this volume). Deposits of the Bonneville Flood along Marsh Creek, Portneuf River, and Snake River have been little buried or reworked by streams since the flood. As widespread deposition of gravel alluvium on fans and along main streams was a result of glacial climates in southeastern Idaho (Scott, in press; Pierce and Scott, 1982 this volume), the flood deposits probably do not long predate the streams' change to their less active Holocene regimens. In addition, tributary streams along the flood path have built only small alluvial fans since the flood. In contrast, if the flood occurred 30,000 years ago, which is before late Wisconsin glacial time, we would expect to find more reworking of the flood deposits and thicker loess mantles and greater volumes of alluvial-fan gravel on the flood deposits and flood-scoured surfaces.

AGE OF BASALT OF PORTNEUF VALLEY

The Bonneville Flood scoured the basalt of Portneuf Valley, and radiocarbon dates of 25,000 to 35,000 years on organic material from below this basalt and a date of 32,500 years on shells from lake sediments thought to relate to the flow were considered to be in accord with a 30,000-year age for the flood (Table 1; Malde, 1968, p. 10; Trimble, 1976, p. 56-58). The basalt, which presumably erupted in Gem Valley, flowed down Portneuf Valley as far as Pocatello. Bright (1963, p. 98) considers the basalt to be related in time and general location to other flows that dammed ancient Lake Thatcher in Gem and Gentile Valleys. Lake Thatcher overflowed southward about 27,000 years ago (Bright, 1963, 1967), or 30,000 years ago if a few radiocarbon dates are rejected as anomalous (Trimble and Carr, 1961b; Malde, 1968, p. 10), thereby diverting Bear River into the Bonneville basin. Consequently, the basalt of Portneuf Valley was thought to provide a maximum limiting age for the flood, and perhaps a closely limiting age if the flow were closely related in time to the diversion of Bear River and if this diversion led to the Bonneville Flood (Malde, 1968, p. 10-11; Trimble, 1976, p. 57). However, one radiocarbon date of greater than 38,000 years on shells from near the top of the Thatcher sequence (W-1126, Bright, 1963) suggests that Lake Thatcher may be older than the finite radiocarbon dates indicate.

Two types of evidence show that the basalt of Portneuf Valley is much older than 25,000 to 35,000 years. First, G. B. Dalrymple (U. S. Geological Survey, written communication, 1979) obtained a whole-rock, potassium-argon date of 0.583 ± 0.104 million years on a sample of the basalt of Portneuf Valley collected near Pocatello (Figure 2; Tables 1 and 2), and Armstrong and others (1975) report an age of 0.14 ± 0.03 million years for a sample of the basalt collected at Inkom (Table 1). Second, east of McCammon, a sequence of several loess blankets that are separated by buried soils overlies the basalt of Portneuf Valley in a sidestream area not scoured by the flood (Figures 3 and 4). The buried soils are each more strongly developed than the soil formed in the upper loess blanket. Pierce and others (1982 this volume) demonstrate that the upper loess blanket is of Wisconsin age. The loess sequence shown in Figures 3 and 4 probably represents several

hundred thousand years, which supports the older potassium-argon age. Apparently, the basalt of Portneuf Valley flowed down Portneuf Valley during middle Pleistocene time and was then buried by valley-fill deposits that are preserved adjacent to and in scarps that extend above the flow, and by loess that is locally preserved on the flow. The Bonneville Flood first exhumed and then scoured and trenched the basalt flow about 14,000 to 15,000 years ago.

The finite radiocarbon dates on organic material from below the flow must therefore reflect contamination by younger organic carbon. Rootlets from modern vegetation were noted in this material and were avoided as much as possible during sampling (Ives and others, 1964, p. 54). However, older, decayed roots may have contributed carbon to the sampled horizon after exhumation of the flow by the Bonneville Flood. Such roots and possible additional contamination by humic and fulvic acids probably provided the small amount of young carbon (contamination equivalent to about 1 percent modern carbon) necessary to yield the reported finite ages. The 32,500-year age on shells from lake sediments presumably related to the flow (Table 1) also probably reflects contamination with young carbon, a common problem with thin-walled mollusk shells (Mangerud, 1972, p. 156). Morrison (1965) discusses several instances of mollusk shells from Lake Bonneville deposits yielding radiocarbon ages of about 30,000 years, even though their true ages are much older.

AGE OF CEDAR BUTTE BASALT

Two whole-rock potassium-argon analyses of a sample of Cedar Butte Basalt yielded a weighted mean age of 72,000 ± 14,000 years (Tables 1 and 2; G. B. Dalrymple, written communication, 1979). This age improves the precision of a previous age of 0.1 ± 0.2 million years (Armstrong and others, 1975), and is also consistent with the late Pleistocene age of the American Falls Lake Beds based on vertebrate and molluscan faunas (Carr and Trimble, 1963).

Bright's (1982 this volume) reconstruction of environmental conditions at the time of the damming of American Falls Lake lends additional information for interpreting the potassium-argon age of 72,000 ± 14,000 years. Bright infers that the climate at the time of the formation of the lake was similar to today, that is, interglacial. This interpretation is also in agreement with the climatic conditions inferred from the ostracode assemblage in the fine-grained alluvium and pond deposits that underlie the deposits of American Falls Lake (Table 3). According to the marine oxygen-isotope record of Shackelton and Opdyke (1973), the last interglacial ended about 75,000 years ago at the boundary between isotope stages 5 and 4. This suggests that if the damming of American Falls Lake occurred during an interglacial, then the Cedar Butte Basalt was probably erupted prior to 75,000 years ago. However, if conditions were also like today during the early part of isotope stage 3, then the lake may not have been dammed until about 60,000 years ago, an age within the error limits of the potassium-argon date.

The stratigraphy of the loess mantle on the flow is in accord with an age of about 72,000 years or early Wisconsin. Several backhoe pits (dug in cooperative studies with M. A. Fosberg, University of Idaho) exposed only the upper loess blanket of the region, which is of Wisconsin age (Pierce and others, 1982 this volume). As there appeared to be little weathering of the basalt below the loess, we infer that the flow cannot be appreciably older than the beginning of Wisconsin time—about 75,000 years ago. The 2-meter thickness of loess on the flow, which is about the thickness of the upper loess unit on physiographically similar surfaces of pre-Wisconsin age nearby, suggests that the flow has been present for most of Wisconsin time and probably is not much younger than early Wisconsin.

Table 2. Whole-rock analytical data and potassium-argon ages of basalts in the American Falls area, Idaho (G. B. Dalrymple, written communication, 1979). Ages were calculated using the constants of Steiger and Jager (1977) for the radioactive decay and abundance of ^{40}Ar. Sample localities are shown in Figure 2 and described in Table 1.

UNIT	NUMBER	NO. ANALYSES	K_2O MEAN ± 1 S.D. (%)	^{40}Ar(%)	AGE (m.y.)	WEIGHTED MEAN AGE (m.y.)
Cedar Butte Basalt	76G031	4	1.104 ± .006	4.9	0.086 ± .017	
				2.3	0.046 ± .023	0.072 ± .014
Basalt of Portneuf Valley	76G032	4	0.628 ± .005	2.2	0.622 ± .156	
				2.5	0.553 ± .138	0.538 ± .104

Figure 3. Sequence of loess and buried soils mantling basalt of Portneuf Valley in areas above the level of intense scour by the Bonneville Flood. Exposure along irrigation canal south of U. S. Highway 30, 6 kilometers southeast of McCammon (NW¼NE¼, sec. 21, T. 9 S., R. 37 E.). Walls along flowing canal are so steep that exposure was not examined in detail. Two or three strongly developed buried soils in loess overlie basalt; the upper loess unit and surface soil are largely removed. Maximum thickness of loess and buried soil sequence is about 2 meters.

STRATIGRAPHY AND PALEOECOLOGY OF UPPER PLEISTOCENE DEPOSITS IN THE AMERICAN FALLS BASIN

Our observations and those of Ridenour (1969) support revisions and additions to the previously proposed stratigraphic framework for deposits of late Pleistocene age in the American Falls basin (Trimble and Carr, 1961b; Carr and Trimble, 1963; Trimble, 1976). The elements of this preestablished framework important to this discussion include, from oldest to youngest, (1) American Falls Lake Beds, including a basal, alluvial gravel, (2) Grandview terrace deposits, which probably are marginal deposits of American Falls Lake, (3) Michaud Gravel, which was deposited by the Bonneville Flood, (4) Aberdeen terrace deposits, which were cut into and deposited on the Michaud Gravel while the flood was abating, and (5) Sterling terrace deposits.

Carr and Trimble (1963, p. G28-G29) included a thin, basal, alluvial gravel and 12 meters of finer grained deposits in the American Falls Lake Beds. The alluvial gravel was deposited by the Snake River and its major tributaries (Trimble and Carr, 1961b; Ridenour, 1969) and contains a rich vertebrate fauna, including *Bison latifrons* (Hopkins, 1951, 1955; Hopkins and others, 1969).

The finer grained part of the American Falls Lake Beds that lies above the alluvial gravel was interpreted as lacustrine by Trimble and Carr (1961b), Carr and Trimble (1963), and Trimble, (1976). In contrast, Ridenour (1969) and Hopkins and others (1969) concluded that two different environments are represented in these deposits. The upper part consists of 2 to 6 meters of lacustrine diatomaceous clay, clay, and silt that form a prominent, blocky-weathering layer (Figure 5; unit C on Figure 6) in the cliffs surrounding the reservoir. The lower part (units D and E on Figure 6) consists of crossbedded sand in stream-channel deposits, silt with minor sand and clay in channel and flood-plain deposits, and clayey silt in flood-plain deposits. Ridenour (1969) inferred that fine-grained alluvium of the lower part was deposited in response to an increase in base level related to an initial lava flow from Cedar Butte. The resulting decrease in gradient limited the river and its tributaries to transport and deposit only sand and finer grained sediments in the American Falls basin. Then, the upper part was deposited in a large lake dammed by a second lava flow from Cedar Butte. In support of this hypothesis, a lava flow from Cedar Butte overlies a basalt of similar lithology in

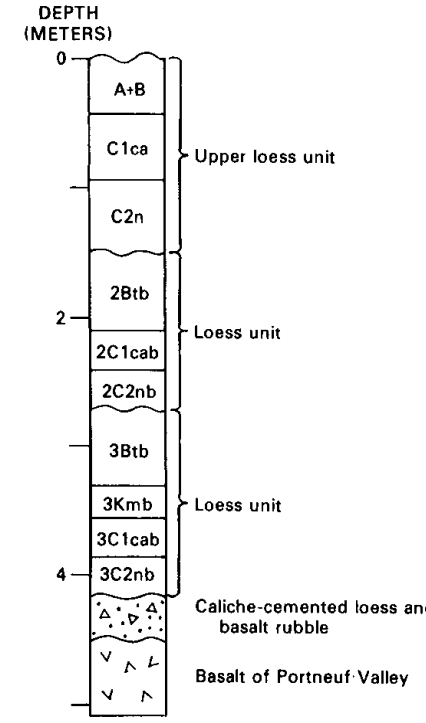

Figure 4. Stratigraphic section from largely vegetated roadcuts on south side of Price Road, immediately west of Union Pacific underpass, 2.5 kilometers southeast of McCammon (center sec. 19, T. 9 S., R. 37 E.). Upper loess unit was disturbed during road and railroad construction and horizon thicknesses are estimated. The two buried soils are each more strongly developed than the surface soil. The caliche-cemented rubble on the flow may represent the remnants of another buried soil.

Table 3. Microfossils in samples of deposits of American Falls Lake and underlying fine-grained alluvium. Localities are shown on Figure 2 and stratigraphic sections and positions of samples are shown in Figure 7. Locality 1 lies near the head of former American Falls Lake. The exposures are on a cut bank on the north side of the Snake River about 1 kilometer north of Springfield in roadcuts on the south side of the valley of Danielson Creek (north-central part of sec. 11, T. 4 S., R. 32 E.). Locality 3 is near the center of the former lake at Rainbow Beach on American Falls Lake (E½SE¼, sec. 21, T. 6 S., R. 32 E.).

MICROFOSSILS	LOCALITY	1						2	3	
	SAMPLE(S)	1	2	3	4	5	6	1-3	1	2-3
DIATOMS										
Smphora sp.				X						
Amphora proteus				X						
Anomoeoneis costata				X						
Campylodiscus clypeus				X						
Cocconeis placentula			X							
Cyclotella bodamica					X					X
Cymatopleura solea								X		
Cymbella cistula								X		
Cymbella mexicana		X	X							
Cymbella minuta		X						X		
Cymbella muelleri		X								
Denticula elegans								X		
Epithemia adnata			X							
Epithemia argus								X		
Epithemia argus var. *protracta*				X						
Epithemia turgida		X	X							
Fragilaria brevistriata		X*	X*					X		
Fragilaria construens		X	X		X					
Fragilaria construens var. *venter*		X								
Fragilaria vaucheriae								X		
Gomphonema truncatum		X								
Hantzschia amphioxys		X								
Melosira ambigua						X				
Melosira italica		X								
Melosira granulata					X					X
Navicula halophila				X						
Navicula oblonga		X								
Navicula radiosa								X		
Nitzschia denticula					X					
Rhopalodia gibba								X		
Rhopalodia gibberula				X						
Scoliopleura peisonis				X						
Stephanodiscus niagarae					X*	X*	X			X
Surirella peisonis				X						
Snyedra sp.								X		
OSTRACODES										
Candona caudata				X	X	X	X			X
Candona rawsoni		X		X						
Candona cf. *C. surbana*				X						
Candona sp. indet.			X			X				
Candona sp. indet. juveniles								X	X	
Cyclocypris ampha				X						
Cyclocypris serena		X								
Cyprinotus glaucus		X								
Limnocythere itasca				X						
Limnocythere sappaensis		X		X						
Limnocythere staplini		X		X						
Physocypria sp. indet.				X		X				
OTHER FOSSILS										
Conchostraca, genus and sp. indet.									X	
Fish bones		X		X					X	
Fish teeth		X								
Gastropods		X		X					X	
Mollusk shell fragments			X			X		X		
Plant fragments									X	

*dominant diatom species, where determined

roadcuts on the east side of the canyon below Bonanza Lake (H. R. Covington, U. S. Geological Survey, personal communication, 1981). A thin bed of cinders separates the two flows. Trimble and Carr (1961b) also noted that two flows are present locally. Alternative hypotheses are that the aggradation of the fine-grained alluvium was caused by basalt from another source or by circumstances of river regimen unrelated to lava flows.

The lake beds and the underlying, fine-grained alluvium have yielded well-preserved diatoms and ostracodes and, locally, impressions of conchostracans and vascular plants. Paleoenvironmental interpretations based on these fossils are in accord with the inferred origin of these deposits. Two localities (localities 1 and 3, Figure 2), where both units are exposed, were examined in detail. The diatoms and ostracodes of both sections (Figure 7) indicate a sequence of marshes and shallow ponds of variable salinity followed by a large, freshwater lake of moderate depth.

The marshes and ponds were apparently limited in extent, probably being related to poorly drained flood plains or to shallow basins impounded by lava flows. The ostracode assemblage present in the sequence of fine-grained alluvium (locality 1, samples 1-3, Table 3) today inhabits small lakes and ponds on the prairies and parklands of the northern United States and Canada. In these ponds, the water is often fresh, less than 1 ppt TDS (parts per thousand of total dissolved solids) in the spring, but increases in salinity during the summer to 5-7 ppt. The salinity may go higher in late summer or early fall, but this usually happens after the ostracode life cycle is complete. This assemblage indicates a semiarid (prairie) climate with dominant precipitation in the form of winter and spring snowfall or rains and a cold temperate, temperature regime. The diatoms in some of the samples of the lower unit (locality 1, samples 1 and 2) are all epiphytic and benthic species that indicate shallow water with abundant aquatic vegetation. Sample 3 (locality 1) includes species that suggest a shallow, somewhat turbid, saline pond of high alkalinity.

At locality 3, a bed a few millimeters thick between the lower alluvial deposits and the overlying lake sediments contains conchostracan remains and impressions of emergent aquatic plants, which together suggest a shallow and possibly a saline and very turbid environment. This bed probably represents the vestiges of shallow marshes and flood plains that were flooded by rising lake waters following emplacement of the upper flow of Cedar Butte Basalt.

In contrast, the microfossils in the lake beds (Table 3) indicate a large and comparatively deep lake. A maximum depth of 30 meters is estimated from the difference in altitude between the lowest lake beds and the shoreline. The diatom flora (locality 1, samples 4, 5, and 6; locality 3, samples 2 and 3), consisting of dominantly open-lake, planktic diatoms, primarily *Stephanodiscus niagarae*, characterizes fresh (generally less than 1 ppt TDS), moderately eutrophic waters. The ostracode, *Candona caudata*, occupies a broad range of habitats, but often when alone it signifies a low-oxygen (eutrophic) environment, such as those of stratified or highly turbid lakes in which most of the oxygen is used in

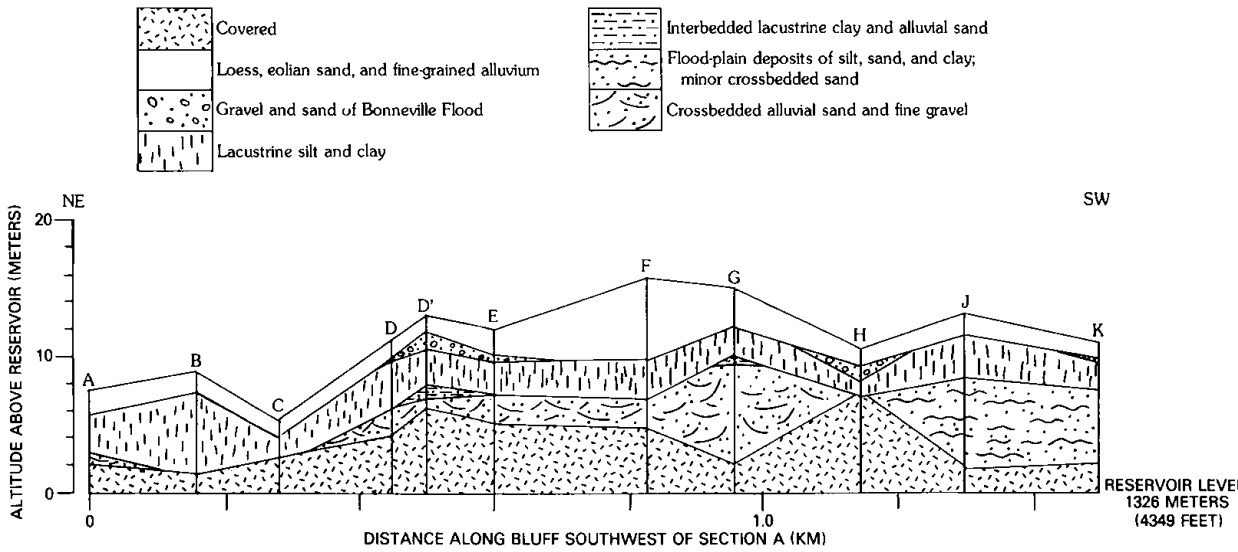

Figure 5. Stratigraphic section of bluffs along southeastern shore of American Falls Reservoir in sec. 2, T. 7 S., R. 31 E., northeast of Seagull Bay. Section A is 200 meters south of the north line of section 2. Vertical exaggeration = 20.

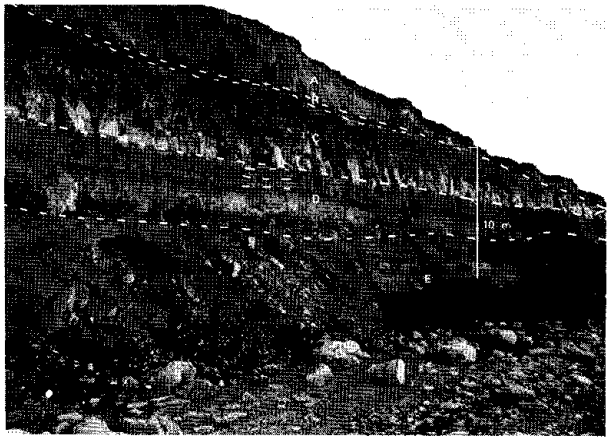

Figure 6. Exposure in bluff on southeast shore of American Falls Reservoir, section K of Figure 5 (SE¼SW¼, sec. 2, T. 7 S., R. 31 E.). Units: A = loess and fine-grained alluvium; B = discontinuous sand and gravel of Bonneville Flood; C = deposits of American Falls Lake, diatomaceous silt and clay grading upward to clay and silty clay; D = flood-plain deposits of massive silty clay to sandy silt, short dashed lines are drawn at tops of weakly developed soils (Entisols) having 10-to-30-centimeter-thick A horizons with root tubes, disseminated charcoal, and scattered fragments of plant stems; E = flood-plain, levee, and point-bar deposits of silty clay, silt, silty sand, and fine to medium sand.

oxidizing organic material.

A relatively high concentration of diatoms in the lower deposits of American Falls Lake indicates a low rate of influx of clastic material, which suggests that the lake was deep. By comparison, samples from the upper lake beds at locality 1 contain a large amount of clay and relatively few diatoms, thus implying lower lake levels or the presence of an advancing delta at the head of the lake. A similar increase in clay is seen in the upper beds at locality 3, perhaps due to an influx of sediment from Bannock Creek.

The shoreline deposits of American Falls Lake are little exposed, but interbedded sand and silt just north of Springfield (locality 2, Figure 2; Figure 7) at an altitude of about 1,353 meters (4,440 feet) were probably deposited in a nearshore zone. The beds contain mollusk shells but only rare and broken diatoms (Table 3). The diatoms are benthic forms that probably were transported to the shore zone from nearby marshes. The high-energy environment at the margin of the lake is reflected in the scarcity and fragmentation of the diatoms. Shoreline deposits are also exposed in a few excavations north and west of Aberdeen, but they provide little information on lake history. Carr and Trimble (1963, p. G31) mapped these beds as Grandview terrace deposits and noted their probable origin as marginal deposits of American Falls Lake.

Alluvial sand, silt, and clay, which was presumably deposited as topset beds on the delta at the head of American Falls Lake, is poorly exposed up to an altitude of about 1,356 meters (4,450 feet) near Rockford and Moreland. These deposits grade southwestward to lacustrine clay and silt that overlie basalt between Rockford and the head of American Falls Reservoir. On Figure 2, the deltaic deposits are not differentiated from those of lacustrine origin because exposures in this area are poor.

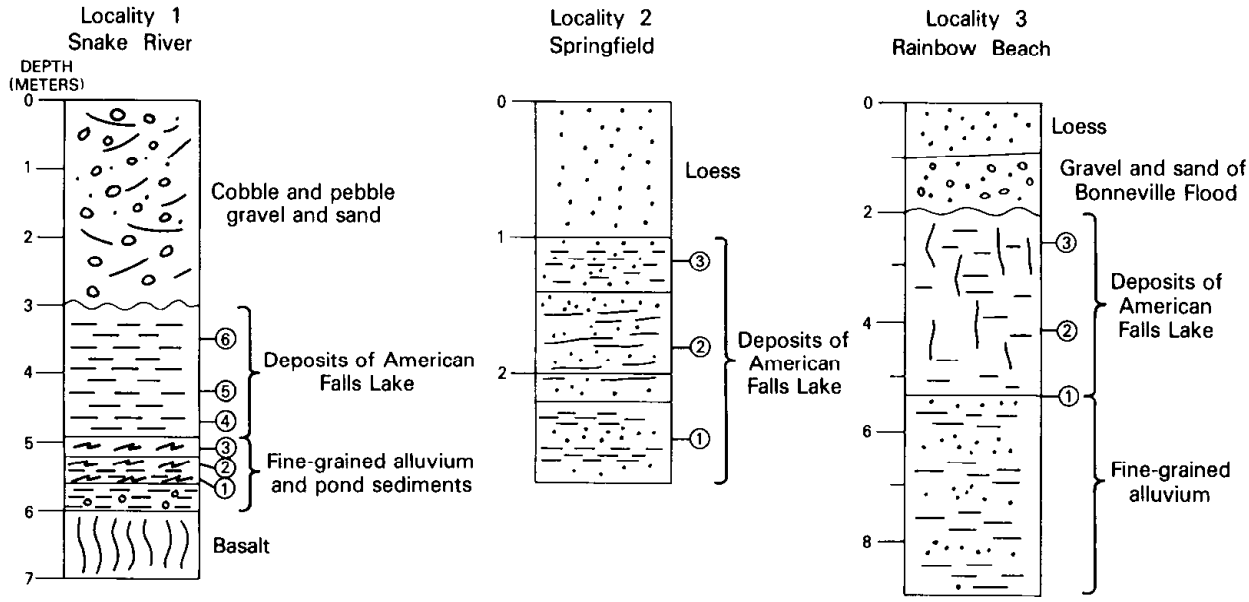

Figure 7. Stratigraphic sections at localities 1, 2, and 3 (see Table 3 for geographic locations) from which samples listed in Table 3 were analyzed for microfossils.

During the time that American Falls Lake was at or near its maximum level, the Snake River aggraded its course upstream from the lake in response to two conditions: (1) the increase of base level caused by American Falls Lake and (2) the abundant sediment supply accompanying Pinedale glacial climate (Pierce and Scott, 1982 this volume). As a result, as much as several tens of meters of gravelly alluvium was deposited in the reach upstream from American Falls Lake (Figure 1).

Sometime before the Bonneville Flood, American Falls Lake may have fallen to a level of about 1,345 meters (4,410-4,415 feet) rather than standing at its maximum level of 1,355 meters (4,440-4,450 feet). Support for this interpretation comes from differences in the thickness of loess west and southwest of Aberdeen. Augering shows that the loess is from 4 meters to more than 5 meters thick between 1,345 and 1,355 meters in altitude, but the loess is generally less than 2 meters thick below 1,345 meters. Because no buried soils or disconformities were found, we regard the loess as the upper loess blanket, which accumulated throughout Wisconsin time. This difference in loess thickness may be due to one or both of the following factors: (1) The lake fell to about 1,345 meters, and the exposed lake floor was thereby able to accumulate loess for a longer period of time than the area that remained covered by the lake. (2) Any loess below 1,345 meters may have been more intensely stripped by the flood than the loess at higher altitudes. In addition, the stratigraphic evidence from the bluffs surrounding American Falls Reservoir suggests that the lake stood at a level of at least 1,338 meters (4,390 feet) at the time of the flood. Nowhere in these exposures, which reach as high as 1,338 meters, has evidence been found of lake recession below this level prior to the flood. Consistently in these exposures, thin deposits of the flood and post-flood loess lie disconformably on lacustrine sediments (Figure 5). However, removal of such evidence by the flood cannot be dismissed as a possibility.

The 1,345-meter level is approximately the altitude of the toe of the scarp at the back of the Aberdeen terrace, which Carr and Trimble (1963, p. G34-G35) interpret as having been cut during the Bonneville Flood by the waves of a lake whose level was maintained by the spillway at the head of the Bonanza Lake channel. The change in loess thickness that occurs at about 1,345 meters suggests that the lake level may have been controlled at about this altitude by the spillway at the head of the Bonanza Lake channel prior to the Bonneville Flood.

The Sterling terrace, which lies below the Aberdeen terrace, was interpreted as a fluvial terrace that was cut during a later phase of the flood (Trimble and Carr, 1961b) or later in Pinedale time (Trimble, 1976, p. 76). The lack of gradient of this surface and the thinness of the alluvium underlying it suggest that this landform is unlike a typical fluvial terrace. The thin (less than 1 meter) alluvium of gravel and sand overlies lake beds or basalt and is similar in texture and lithology to the Bonneville Flood deposits that are present in the western part of the basin. We interpret the Sterling terrace as a flood-scoured portion of the floor of American Falls Lake, rather than a surface related to base-level-controlled fluvial dissection.

DISCUSSION

Figure 8 shows our interpretation of the age of key geologic events in the late Quaternary history of the American Falls area as contrasted with previous interpretations. We agree that American Falls Lake was dammed in late Pleistocene time. The major revisions we propose are (1) that the Bonneville Flood occurred about 14,000 to 15,000 years ago rather than 30,000 years ago and (2) that the basalt of Portneuf Valley is about 600,000 years old rather than 30,000 to 35,000 years old.

The age of the upper flow of Cedar Butte Basalt, 72,000 ± 14,000 years, confirms the findings of previous investigators that the damming of the Snake River, which formed American Falls Lake, occurred in late Pleistocene time. A radiocarbon date of greater than 42,000 years on a sample of peat from deposits thought to be in the upper part of the American Falls Lake Beds (Trimble, 1976, p. 55-56) is also consistent with this interpretation. Bright (1982 this volume) reports an age of greater than 51,900 years (Grn-6022) for this same peat, but he interprets the peat as lying in the lower one-third of the deposits of American Falls Lake. The Bonneville Flood eroded the present canyon of the Snake River into the Cedar Butte Basalt and older rocks and caused the draining of American Falls Lake about 14,000 to 15,000 years ago. Thus, the deposits of American Falls Lake offer a potential record of environmental change that spans much of Wisconsin time. Unfortunately, the Bonneville Flood scoured at least the upper part of the lake sequence, and at present there is no reliable way of estimating the age of the uppermost exposed sediments. However, the possibility for obtaining valuable paleoclimatic and other information (Bright, 1982 this volume) should spur interest in further investigations.

The 72,000 ± 14,000-year age for the Cedar Butte Basalt provides a minimum age for the vertebrate

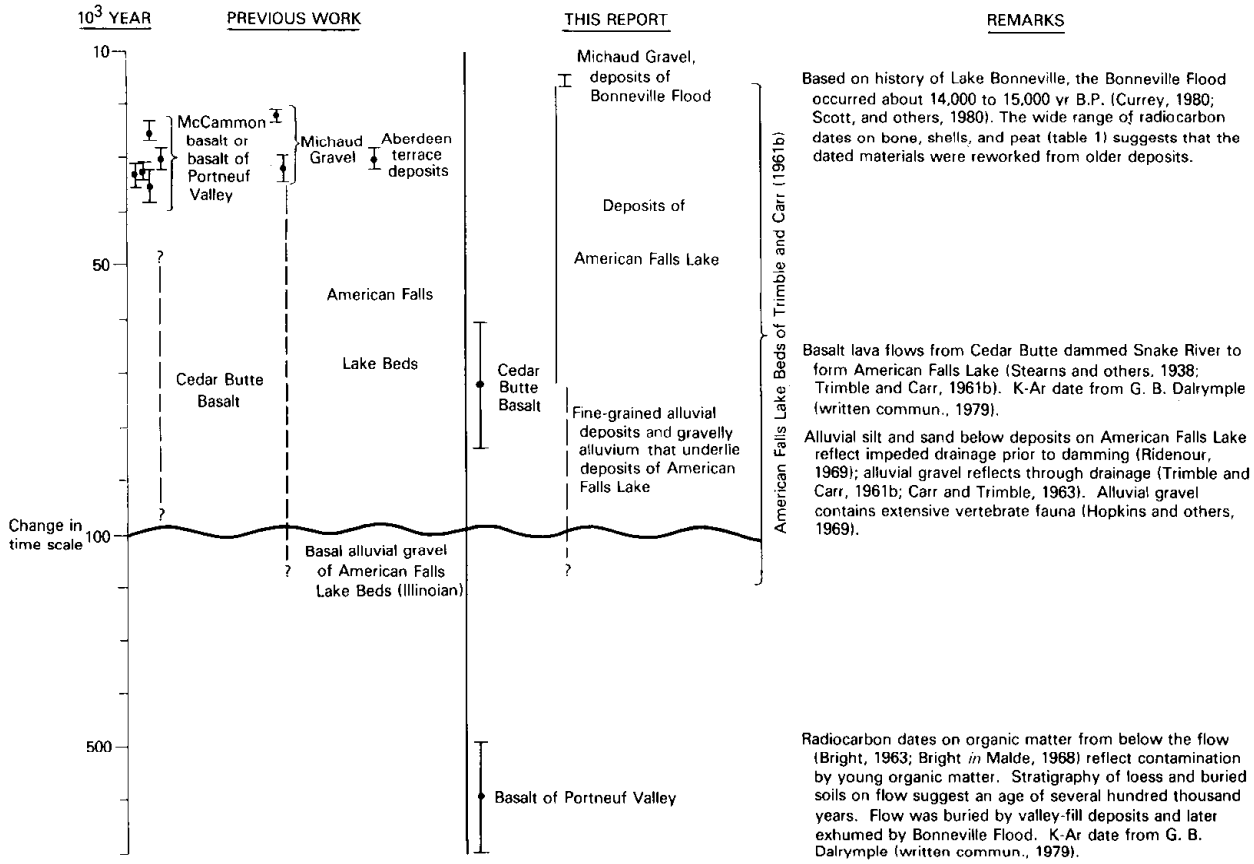

Figure 8. Comparison of revised chronology of key geologic events and deposits in the American Falls area with previous interpretations. Data and interpretations of previous work are from Trimble and Carr (1961b, 1976), Bright (1963), Carr and Trimble (1963), Malde (1968), McDonald and Anderson (1975), Trimble (1976), and Kelley and others (1978). Solid vertical lines represent age ranges of dated deposits; dashed vertical lines represent estimated age ranges.

fauna, including *Bison latifrons*, which was collected from alluvial gravel that underlies the fine-grained alluvium that, in turn, underlies the deposits of American Falls Lake (Hopkins and others, 1969). Remains that possibly may be *B. latifrons* have also been collected from a clay unit thought to be close to the base of the deposits of American Falls Lake (Hopkins and others, 1969). The correct identification of these remains is critical because their age is probably close to that of the Cedar Butte Basalt. The age of the alluvial gravel is more difficult to estimate. If the fine-grained alluvium did accumulate as a result of an older lava flow from Cedar Butte, it may not be greatly older than 72,000 years, because in Bonanza Lake channel the flows are separated only by a thin bed of cinders; no other subaerial deposits or signs of weathering are found (H. R. Covington, personal communication, 1981). In addition, Kuntz and others (1982 this volume) find that multiple lava flows from single vents are closely spaced in time. Therefore, because the alluvial gravel lies conformably below the fine-grained alluvium, the gravel may also be not much older than 72,000 ± 14,000 years. In contrast, Carr and Trimble (1963, p. G29) estimated an Illinoian age for the gravel, which in today's understanding of Pleistocene chronology is older than 125,000 years. If the gravel is this old, the time of deposition of the sequence of fine-grained alluvium and the time represented by the weak buried soils within the sequence and any other hiatuses must represent a time interval of about 50,000 years, which seems unlikely to us. Better constraints on the age of the upper range of *Bison latifrons* must await further investigations.

Caution is necessary in any paleontologic interpretations of the fossils present in the flood deposits because of the possibility of reworking. The Bonneville Flood occurred about 14,000 to 15,000 years ago; however, the dates on a variety of materials from flood and related deposits in the American Falls area are all older than this age and range from about 20,000 years to greater than 38,000 years (Figure 8; Table 1). The most likely cause of this discrepancy is the reworking of the dated materials

from older sediments by the flood. Therefore, such suggestions as extending the stratigraphic and chronologic range of *Bison latifrons* based on its presence in deposits of the Bonneville Flood (McDonald and Anderson, 1975) appear illfounded.

The middle Pleistocene age of the basalt of Portneuf Valley has several implications to geologic studies in southeastern Idaho. First, the basalt is much older than the Bonneville Flood and was exhumed from a valley fill by the flood. Its youthful appearance results from having been scoured by the flood and from presently occupying a position close to the level of the modern streams. Second, if the basalt did erupt from vents in Gem Valley, which seems likely (Bright, 1963, 1967; Mabey, 1971), then the volcanic rocks in Gem Valley, in part, date from much earlier times of the Pleistocene than previously inferred.

ACKNOWLEDGMENTS

We thank G. B. Dalrymple, U. S. Geological Survey, for providing the potassium-argon ages. We also thank R. C. Bright for helpful discussions on aspects of the Quaternary history of southeastern Idaho. The manuscript benefited greatly from constructive reviews by H. E. Malde and P. E. Carrara.

REFERENCES

Armstrong, R. L., W. P. Leeman, and H. E. Malde, 1975, K-Ar dating, Quaternary and Neogene volcanic rocks of the Snake River Plain, Idaho: American Journal of Science, v. 275, no. 3, p. 225-251.

Bright, R. C., 1963, Pleistocene Lakes Thatcher and Bonneville, southeastern Idaho: University of Minnesota Ph.D. dissertation, 292 p.

———, 1967, Late-Pleistocene stratigraphy in Thatcher Basin, southeastern Idaho: Tebiwa, v. 10, no. 1, p. 1-7.

———, 1982, Paleontology of the lacustrine member of the American Falls Lake Beds, southeastern Idaho, *in* Bill Bonnichsen and R. M. Breckenridge, editors, Cenozoic Geology of Idaho: Idaho Bureau of Mines and Geology Bulletin 26.

Bright, R. C. and Meyer Rubin, 1965, Red Rock Pass, *in* G. M. Richmond, Roald Fryxell, John Montagne, and D. E. Trimble, editors, Guidebook for Field Conference E, Northern and Middle Rocky Mountains: International Association for Quaternary Research, 7th Congress, Lincoln, Nebraska, Nebraska Academy of Sciences, p. 105-106.

Broecker, W. S. and A. Walton, 1959, The geochemistry of C^{14} in fresh-water systems: Geochimica et Cosmochimica Acta, v. 16, p. 15-38.

Carr, W. J. and D. E. Trimble, 1963, Geology of the American Falls quadrangle, Idaho: U. S. Geological Survey Bulletin 1121-G, p. G1-G44.

Crane, H. R. and J. B. Griffin, 1961, University of Michigan radiocarbon dates VI: Radiocarbon, v. 3, p. 105-125.

Currey, D. R., 1980, Coastal geomorphology of Great Salt Lake and vicinity, *in* J. W. Gwynn, editor, Great Salt Lake: A scientific, historical, and economic overview: Utah Geological and Mineral Survey Bulletin 116, p. 69-82.

Gilbert, G. K., 1890, Lake Bonneville: U. S. Geological Survey Monograph 1, 438 p.

Hopkins, M. L., 1951, *Bison* [*Gigantobison*] *latifrons* and *Bison* [*Simbobison*] *alleni* in southeastern Idaho: Journal of Mammalogy, v. 32, no. 2, p. 192-197.

———, 1955, Skull of fossil camelid from the American Falls Lake Bed area of Idaho: Journal of Mammalogy, v. 36, no. 2, p. 278-282.

Hopkins, M. L., Robson Bonnichsen, and David Fortsch, 1969, The stratigraphic position and faunal associates of *Bison* [*Gigantobison*] *latifrons* in southeastern Idaho—a progress report: Tebiwa, v. 12, no. 1, p. 1-8.

Ives, P. C., Betsy Levin, R. D. Robinson, and Meyer Rubin, 1964, U. S. Geological Survey radiocarbon dates VII: Radiocarbon, v. 6, p. 37-76.

Kelley, Lea, Elliott Spiker, and Meyer Rubin, 1978, U. S. Geological Survey radiocarbon dates XIV: Radiocarbon, v. 20, no. 2, p. 283-312.

Kuntz, M. A., D. E. Champion, E. C. Spiker, R. H. Lefebvre, and L. A. McBroome, 1982, The Great Rift and the evolution of the Craters of the Moon lava field, Idaho, *in* Bill Bonnichsen and R. M. Breckenridge, editors, Cenozoic Geology of Idaho: Idaho Bureau of Mines and Geology Bulletin 26.

Mabey, D. R., 1971, Geophysical data relating to a possible Pleistocene overflow of Lake Bonneville at Gem Valley, southeastern Idaho: U. S. Geological Survey Professional Paper 750-B, p. B122-B127.

Malde, H. E., 1960, Evidence in the Snake River Plain, Idaho, of a catastrophic flood from Pleistocene Lake Bonneville: U. S. Geological Survey Professional Paper 400-B, p. B295-B297.

———, 1968, The catastrophic late Pleistocene Bonneville Flood in the Snake River Plain, Idaho: U. S. Geological Survey Professional Paper 596, 52 p.

Mangerud, Jan, 1972, Radiocarbon dating of marine shells, including a discussion of apparent age of recent shells from Norway: Boreas, v. 1, p. 143-172.

Marsters, Beverly, Elliott Spiker, and Meyer Rubin, 1969, U. S. Geological Survey radiocarbon dates X: Radiocarbon, v. 11, no. 1, p. 210-227.

McDonald, H. G. and Elaine Anderson, 1975, A late Pleistocene vertebrate fauna from southeastern Idaho: Tebiwa, v. 18, no. 1, p. 19-37.

Morrison, R. B., 1965, New evidence on Lake Bonneville stratigraphy and history from southern Promontory Point, Utah: U. S. Geological Survey Professional Paper 525-C, p. C110-C119.

———, 1966, Predecessors of present Great Salt Lake: Utah Geological Society, Guidebook to the Geology of Utah, no. 20, p. 77-104.

Pierce, K. L., M. A. Fosberg, W. E. Scott, G. C. Lewis, and S. M. Colman, 1982, Loess deposits of southeastern Idaho: age and correlation of the upper two loess units, *in* Bill Bonnichsen and R. M. Breckenridge, editors, Cenozoic Geology of Idaho: Idaho Bureau of Mines and Geology Bulletin 26.

Pierce, K. L. and W. E. Scott, 1982, Pleistocene episodes of alluvial-gravel deposition, southeastern Idaho, *in* Bill Bonnichsen and R. M. Breckenridge, editors, Cenozoic Geology of Idaho: Idaho Bureau of Mines and Geology Bulletin 26.

Ridenour, James, 1969, Depositional environments of the late Pleistocene American Falls Formation, southeastern Idaho: Idaho State University M.S. thesis, 82 p.

Rubin, Meyer and Corrine Alexander, 1958, U. S. Geological Survey radiocarbon dates IV: Science, v. 127, no. 3313, p. 1476-1487.

Rubin, Meyer, R. C. Likins, and E. G. Berry, 1963, On the validity of radiocarbon dates from snail shells: Journal of Geology, v. 71, no. 1, p. 84-89.

Scott, W. E., in press, Surficial geologic map of the eastern Snake River Plain and adjacent areas, 111° to 115° W., Idaho and Wyoming: U. S. Geological Survey Miscellaneous Investigations Map I-1373, scale 1:250,000.

Scott, W. E., W. D. McCoy, R. R. Shroba, and R. D. Miller, 1980, New interpretations of the late Pleistocene, Rocky Mountain cell, field trip to Little Valley and Jordan Valley, Utah: U. S. Geological Survey Open-File Report 82-845, 58 p.

Scott, W. E., W. D. McCoy, R. R. Shroba, and R. D. Miller, 1980, New interpretations of the late Quaternary history of Lake Bonneville, western United States: American Quaternary Association, Abstracts with Programs, sixth biennial meeting, p. 168-169.

Shackelton, N. J. and N. D. Opdyke, 1973, Oxygen isotope and paleomagnetic stratigraphy of equatorial Pacific core V28-238: Oxygen isotope temperatures and ice volumes on a 10^5 year and 10^6 year scale: Quaternary Research, v. 3, p. 39-55.

Stearns, H. T., Lynn Crandall, and W. C. Steward, 1938, Geology and ground-water resources of the Snake River Plain in southeastern Idaho: U. S. Geological Survey Water-Supply Paper 774, 268 p.

Steele, E. A., 1980, Depositional environments of Marsh Valley, Idaho: Geological Society of America, Abstracts with Programs, v. 12, no. 6, p. 305-306.

Steiger, R. H. and E. Jager, 1977, Subcommission of geochronology—Convention on the use of decay constants in geo- and cosmochronology: Earth and Planetary Science Letters, v. 36, p. 359-362.

Trimble, D. E., 1976, Geology of the Michaud and Pocatello quadrangles, Bannock and Power Counties, Idaho: U. S. Geological Survey Bulletin 1400, 88 p.

Trimble, D. E. and W. J. Carr, 1961a, The Michaud delta and Bonneville River near Pocatello, Idaho: U. S. Geological Survey Professional Paper 424-B, p. B164-B166.

———, 1961b, Late Quaternary history of the Snake River in the American Falls region, Idaho: Geological Society of America Bulletin, v. 72, p. 1739-1748.

———, 1976, Geology of the Rockland and Arbon quadrangles, Power County, Idaho: U. S. Geological Survey Bulletin 1399, 115 p.

Paleontology of the Lacustrine Member of the American Falls Lake Beds, Southeastern Idaho

by

Robert C. Bright[1]

ABSTRACT

A wide variety of fossils from one exposure of the lacustrine member of the American Falls Lake Beds provides new information about the nature of the lake as well as the local climate and vegetation during part of its existence.

Pollen and spores from the basal 1.5 meters of the section indicate a climate and vegetation very similar to the present, less than 72,000 ± 14,000 years and greater than 51,900 years ago. Sagebrush and chenopod steppe existed in the area around the lake during that time, and there were coniferous forests in the mountains. The climate was certainly warm and semiarid but might have been slightly cooler or moister than now, at least locally. Based on the climatic interpretation, the lowermost 1.5 meters of sediment were probably deposited during a period of nonglaciation, that is, either late Sangamon or a Wisconsinan interstadial.

The lake was large, freshwater, mesotrophic, and very productive. Rooted aquatic and semiaquatic plants were dense in many nearshore areas and supported populations of diatoms and a variety of invertebrates.

INTRODUCTION

The purpose of this study was to determine the nature of American Falls Lake and the local climate during its existence by interpreting the fossils of the lacustrine member of the American Falls Lake Beds, and also to date the sediments more accurately, if possible.

The geology of the American Falls area is reviewed by Scott and others (1982 this volume). Of significance to this report is Ridenour's (1969) demonstration that the sediments in about the lower three-fourths of the American Falls Lake Beds are of fluvial origin and that only the upper 2-6 meters are truly lacustrine. He also showed that the boundary between the two units is marked by an organic-rich clay in the southern part of the basin. That organic-rich clay lies at the base of the section studied (see stratigraphic column in Figure 2). Ridenour's (1969) upper lacustrine member is informally referred to herein as the "lacustrine member," the base of which is now dated as 72,000 ± 14,000 years old (Scott and others, 1982 this volume).

The site chosen for the study is a large irrigation ditch excavated on the Blackfoot Indian Reservation, about 5 miles northwest of Pocatello (Figure 1), in NE¼NW¼, sec. 1, T. 6 S., R. 33 E., at the mouth of the Portneuf River, and on the south side of Pleistocene American Falls Lake. Here the lacustrine member is well exposed and is about 4.5 meters thick.

POLLEN AND SPORES

Although the entire lacustrine section at the site was sampled for pollen and spores, only the lowermost 1.5 meters contained enough well-preserved material to be able to construct a satisfactory pollen diagram (Figure 2), which is divisible into three pollen assemblage-zones.

ZONE AF3

The basal sediments of Zone AF3 are rich in plant debris (Figure 2), mostly unidentifiable. This material represents surface debris incorporated into clay and silt as American Falls Lake began to fill 72,000 ± 14,000 years ago (Scott and others, 1982 this volume) and is thus interpreted here as a transgressive deposit. The sediments of the upper 8 centimeters of the zone are thin-bedded to laminated silty clays, are clearly lacustrine, and were deposited in deeper water than the basal sediments.

[1]Bell Museum of Natural History, University of Minnesota, Minneapolis, Minnesota 55455.

Bright, R. C., 1982, Paleontology of the lacustrine member of the American Falls Lake Beds, southeastern Idaho, *in* Bill Bonnichsen and R. M. Breckenridge, editors, Cenozoic Geology of Idaho: Idaho Bureau of Mines and Geology Bulletin 26, p. 597-614.

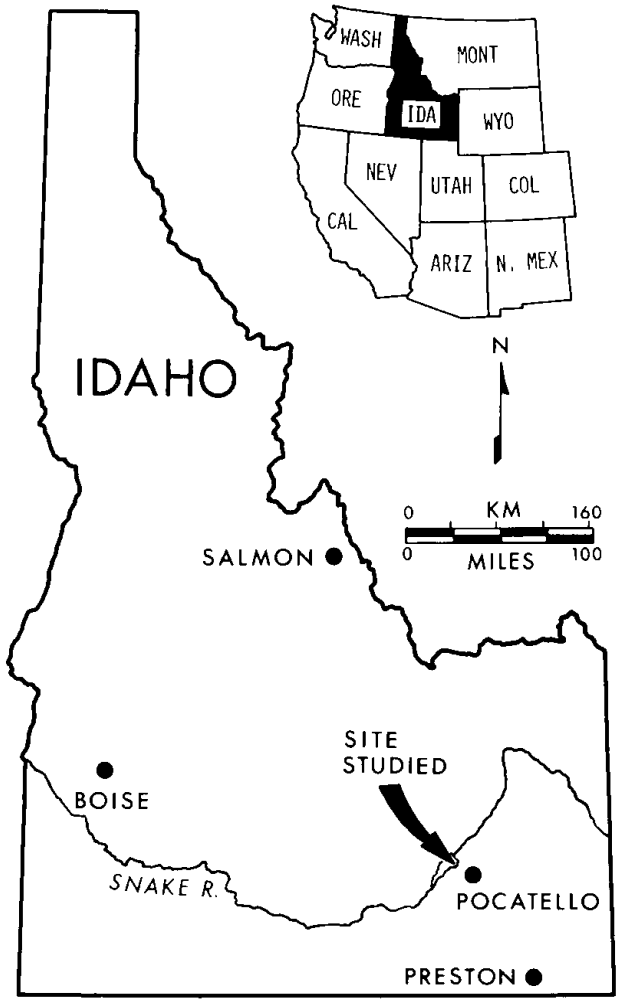

Figure 1. Map of Idaho showing location of the site studied.

The top of the zone is defined by a marked increase of *Cystopteris fragilis* spores and a decreased proportion of Cyperaceae pollen. Grass and Compositae pollen are a few percent higher than in Zone AF2 above. *Lycopodium* spores were found only at the base of the zone, and *Myriophyllum*, *Sagittaria*, and Urticaceae pollen are almost all confined to Zone AF3. Proportions of major regional pollen types such as *Artemisia*, *Sarcobatus*, Cheno-Ams, *Ambrosia*, and *Pinus* are little different than in the overlying Zone AF2. Thus it appears that only the pollen of plants growing in the nearshore parts of the lake (*Sagittaria*, *Myriophyllum*) or those expected to be growing along the shore either decreased in abundance (grass, sedge, *Ambrosia*, Urticaceae) or were nearly eliminated at or near the top of Zone AF3. This suggests a rapidly rising lake level, transgression of the shoreline to the south, and drowning of tributary streams.

There are but two pollen diagrams with which these data can be compared, as they are the only ones from nearby sites at about the same elevation and in the same vegetation zones. The pollen spectra of Zone AF3 closely match the middle Holocene (6,000 years ago, Zone S3) and the post-1,700 year spectra (Zone S1) of Swan Lake (Bright, 1966) with two exceptions. *Sarcobatus* percentages are four times higher than at Swan Lake and no *Cystopteris* was found there. However, the *Sarcobatus* percentages of Zone AF3 are consistent with surface samples from the central part of the Snake River Plain (Cassia County), where O. K. Davis (personal communication) has found as much as 35 percent in areas where it is fairly abundant. Davis' diagram from Rattlesnake Cave (Bright and Davis, in press) shows spectra with 20 to 30 percent Cheno-Ams that are about 7,000 years old, which are quite comparable to those of Zone AF3 in the American Falls Lake Beds. His surface sample data (Bright and Davis, in press) from chenopod steppe and the base of the *Artemisia* steppe on the north side of the Snake River Plain also closely match the data of Zone AF3. The spectra of Zone AF3, then, most closely resemble middle to late Holocene and modern ones representing chenopod and *Artemisia* steppe. Thus it appears that the dominant vegetation types around the lake were *Artemisia* and chenopod steppe (*Sarcobatus* being more common than today), with riparian types on the edge of the lake and in stream valleys (birch, willow, composites, sedges, etc.). There were junipers in the foothills and a coniferous forest at higher altitudes in the nearby mountains. In summary, the vegetation represented by Zone AF3 was very similar to that found in the area today.

An exception to this conclusion is the presence of many spores and a few sporangia (Table 1) of *Cystopteris fragilis*. No modern analog with the pollen assemblage shown in Figure 2 is known that contains more than an occasional spore of that fern. According to Cronquist and others (1972), Hitchcock and others (1969), Davis (1952), and Porter (1962), *C. fragilis* occurs in moist (humid) to moderately dry places, in crevices of cliffs, among rocks, or on moist soil under rocks and roots, and it ranges from the foothills to over 10,000 feet in the mountains. Only two localities are published from Idaho in the sagebrush steppe—one "east of Bruneau" (Owyhee County), probably in Bruneau Canyon, and another at Montpelier (Bear Lake County) (Blaisdell, 1963). *Cystopteris fragilis* also occurs "one-third up the north slope of Big Butte in an open dry area" (Arco desert, Butte County, Idaho) and on the north side of the eastern Snake River Plain "in cracks in basalt, five miles east of Kilgore at an elevation of 6,000 feet" (Karl Holte, personal communication). Percentages

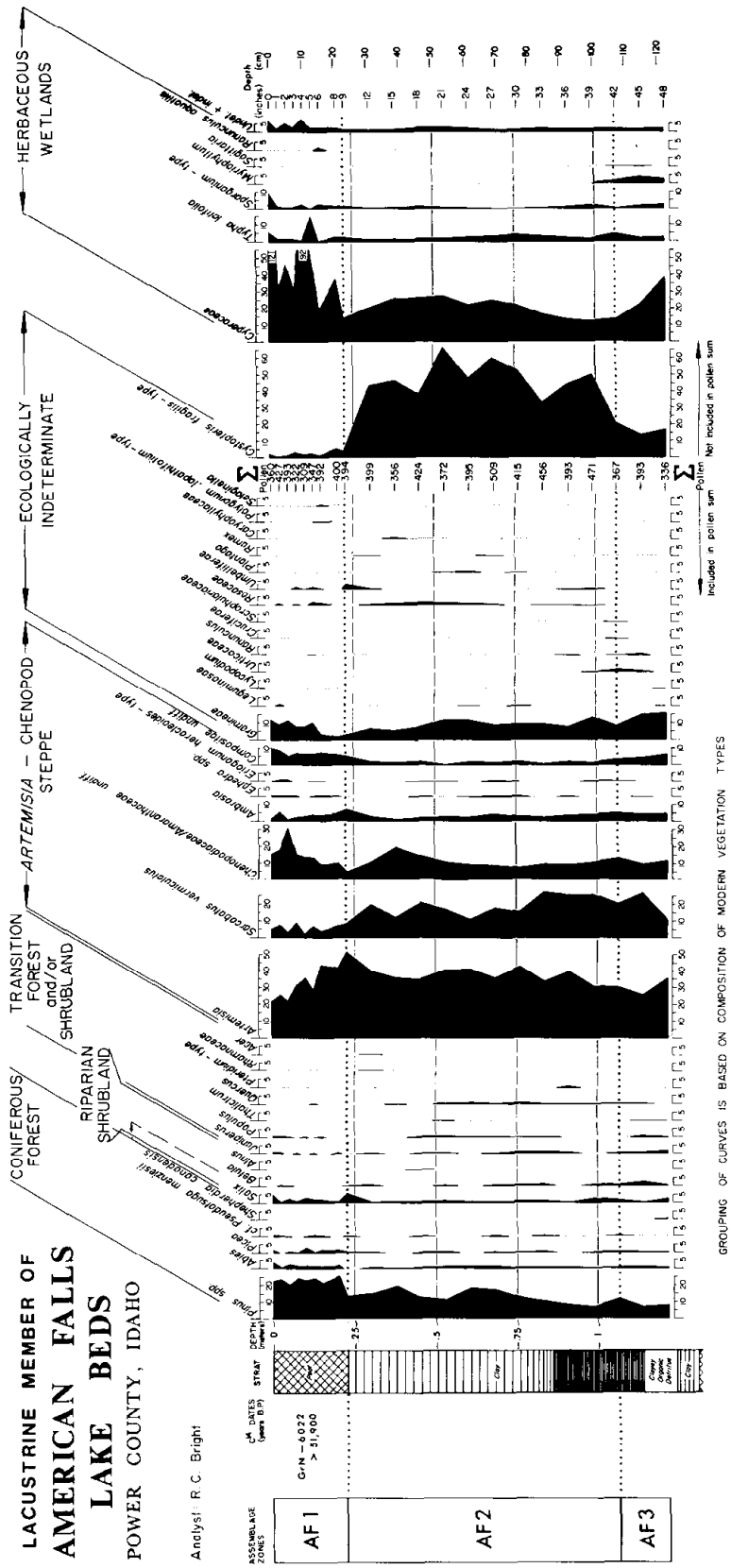

Figure 2. Pollen diagram of the lower part of the lacustrine member of the American Falls Lake Beds.

of *C. fragilis* spores range from 15 to 20 in Zone AF1, which suggests that the fern was common, at least locally, and this conclusion is supported by the presence of sporangia. Whether *C. fragilis* grew in a special habitat along tributary stream valleys, along the lakeshore, or was actually a part of the semiarid steppe vegetation cannot be determined from this pollen diagram.

The vegetation deduced from the fossils indicates a climate very similar to now, and the presence of *Cystopteris* suggests slightly cooler or moister summers or maybe slightly cooler mean annual temperatures. On the other hand, a local effect, such as lower summer temperature, might have been caused by the lake itself, thereby permitting the growth of *Cystopteris* locally.

ZONE AF2

The sediments of Zone AF2 are thin-bedded to laminated silty clay and represent lacustrine conditions.

The only major difference between the curves of Zones AF3 and AF2 is the remarkable increase

Table 1. Occurrence of plant macrofossils in the lacustrine member of American Falls Lake Beds.

Name	Zone AF3	Zone AF2	Zone AF1	Above Zone AF1
Carex cf. *fesicaria* (perigynia & seeds)			C	
Carex indet. (perigynia)			U	
Carex indet. (seed)	R			
Chara sp. (oospores)	U	R	C	U
Chenopodium album-type (seed)			C	
Chenopodium cf. *rubrum* (seed)	U	R	C	R
Chenopodium sp. (seed)			R	R
Compositae indet. (achene)			R	
Compositae indet. (achene)			R	
Cystopteris fragilis (sporangia)	C	A		
Eleocharis macrostachya (seed)	U		C	
Lycopus sp. (seed)			R	
Mentha arvensis (seed)		R	R	
Myriophyllum spicatum (=*exalbescens*) (seed)			R	
Najas flexilis (seed)			R	
Potamogeton foliosus (seed)			U	
Potamogeton gramineus (seed)			U	
Potamogeton pectinatus (seed)	U	R	C	
Potentilla sp. (seed)			U	
Rumex maritimus var. *Fueginus* (Perianths)			U	
Rumex sp. (seed)			R	
Scirpus acutus-validus (seed)	C	U	A	R
Sparganium eurycarpum (fruit)			R	
Triglochin cf. *maritima* (seed)			R	
Typha latifolia (seed)			R	
Umbelliferae indet. (seed)			R	
Urtica sp. (seed)			R	
Verbena hastata (nutlet)			R	
Zannichellia palustris (achene)			U	
Unknown 1 (seed)			R	
Unknown 2 (seed)			R	
Unknown 3 (seed)			R	
Moss fragments			A	

A = abundant
C = common
U = uncommon
R = rare

in *Cystopteris* spores to 40-60 percent. *Cystopteris* sporangia are also very abundant in this zone (Table 1). These data indicate *C. fragilis* was even more abundant, at least locally, than during the time represented by Zone AF3. The vegetation around the lake represented by the polen in this zone is the same as in Zone AF3, *Artemisia*-chenopod steppe.

ZONE AF1

The sediments of this zone consist of medium- to very coarse-grained detrital peat, with common wood fragments and some logs up to 20 centimeters in diameter and 1 meter long. The peat thickens eastward to about 25 centimeters at the Portneuf River. Apparently this unit of the lacustrine member is confined to the area around the mouth of the Portneuf River, as it has not been found elsewhere. This suggests that debris from the Portneuf River was trapped near its mouth in some sort of basin, perhaps a quiet lagoon behind a bar or a marsh in a floodplain or delta. Such sediments normally collect in quiet water less than about 2 meters deep, commonly with abundant rooted aquatic and semiaquatic vegetation. Most of the debris is unidentifiable, but one wood fragment was from a conifer, a few fragments were determined to be monocot stems, and the abundant seeds are identified in Table 1.

A radiocarbon date on a log from this horizon is greater than 51,900 years (sample Grn-6022). This is the same peat dated by Trimble and Carr (1976, p. 68) as greater than 42,000 years old. Thus the entire pollen sequence reported here is older than 51,900 years and younger than 72,000 ± 14,000 years.

The major difference between this pollen zone and the preceding one (AF2) is the marked decrease of *Cystopteris* spores. Whatever circumstance was responsible for the abundance of that fern near the site during the time represented by Zone AF2 was certainly not in effect during the time represented by this zone.

Other differences in the pollen distinguish this zone from the preceding one. Pine is increased to about 25 percent, the proportions of fir and spruce are a bit higher, and *Salix*, Cyperaceae, and Compositae proportions are markedly higher. *Artemisia* and *Sarcobatus* percentages are lower than in Zone AF2.

The marked increase in the proportion of Cyperaceae pollen (most likely *Scirpus*, *Carex*, and *Eleocharis*, based on the seeds; see Table 1) indicates very shallow water, the same conclusion derived from the sediment type. Slight increases in *Sparganium*-type percentages and peaks of *Typha* pollen also indicate shallow water. These are common marsh plants found in the region today.

The decrease in *Sarcobatus* could represent lowered lake level, hence lowered water table, because that species is very sensitive to the height of the water table and its abundance decreases as the water table drops (Fautin, 1946).

The small increases in the proportions of pine, spruce, and fir probably represent pollen reworked from lacustrine sediments exposed by lower water levels. This might also account for the slightly increased *Ambrosia* percentages. The rise in Compositae pollen, however, is deemed significant and probably represents invasion of such plants as *Iva*, *Solidago*, *Antennaria*, *Helianthus*, *Helenium*, and *Cirsium*, all of which are common along lake shores and edges of marshes and reservoirs in southeastern Idaho today.

Pollen evidence from Zone AF1 indicates a vegetation very similar to the present, semiarid *Artemisia* and chenopod steppe around the lake.

PLANT MACROFOSSILS

The remains of thirty-one types of aquatic, semiaquatic, wet-ground, and upland plants were found in the lacustrine member of the American Falls Lake Beds (Table 1); most are illustrated on Plates 1, 2, and 3. By far the best-preserved material was found in the upper peat (Zone AF1), which also contained the richest flora. With the exception of *Cystopteris fragilis* all types represent plants common in wetlands of the region today.

All but two of the taxa found in Zone AF3 sediments are shallow-water aquatics and semiaquatics derived from nearshore plants as the lake transgressed. The *Chenopodium* cf. *rubrum* plants were probably growing on the lake shore, and their seeds became incorporated into the sediments as the water rose. The abundance of *Cystopteris* sporangia suggests that fern was growing close to the shore of the lake. Many of the sporangia were full of spores (Plate 1, figure 5) and probably did not disperse far.

The seeds incorporated into the lacustrine silts and clays of Zone AF2 also represent nearshore, shallow-water forms. Their rarity suggests they were transported some distance. *Cystopteris* sporangia are abundant in this zone. If the shoreline was to the south of the site (deep water indicated by the sediment), then chances are good that the sporangia were washed in from some distance and that the fern was indeed more abundant than earlier.

The macrofossil flora of Zone AF1 is what one might find in marshes or a shallow, quiet bay of a lake in southeastern Idaho today, with Compositae, *Chenopodium*, *Potentilla*, *Sparganium*, and *Triglo-*

PLATE 1

Figures 1 and 2. *Cystopteris fragilis* spores, with echinate perispore having attenuate spines with acute apices; equatorial view, untreated. X1000

3. *Cystopteris fragilis* spore with perispore; surface view showing distribution of spines; untreated. X1000

4. *Cystopteris fragilis* spore without perispore; surface view, acetolysed. X750

5. Leptosporangium of *Cystopteris fragilis* with some spores extruded. This specimen is the source of the spores in figures 1-3. X100

6, 7, 9, and 10. Leptosporangia of *Cystopteris fragilis* showing the vertical annulus, nature of the stomium, and distal three-celled tier of the stalk (figures 9 and 10); note the abundant pyrite cubes in figure 10. X250

8. Portion of coenobium of *Pediastrum boryanum*, a planktonic green alga. X1000

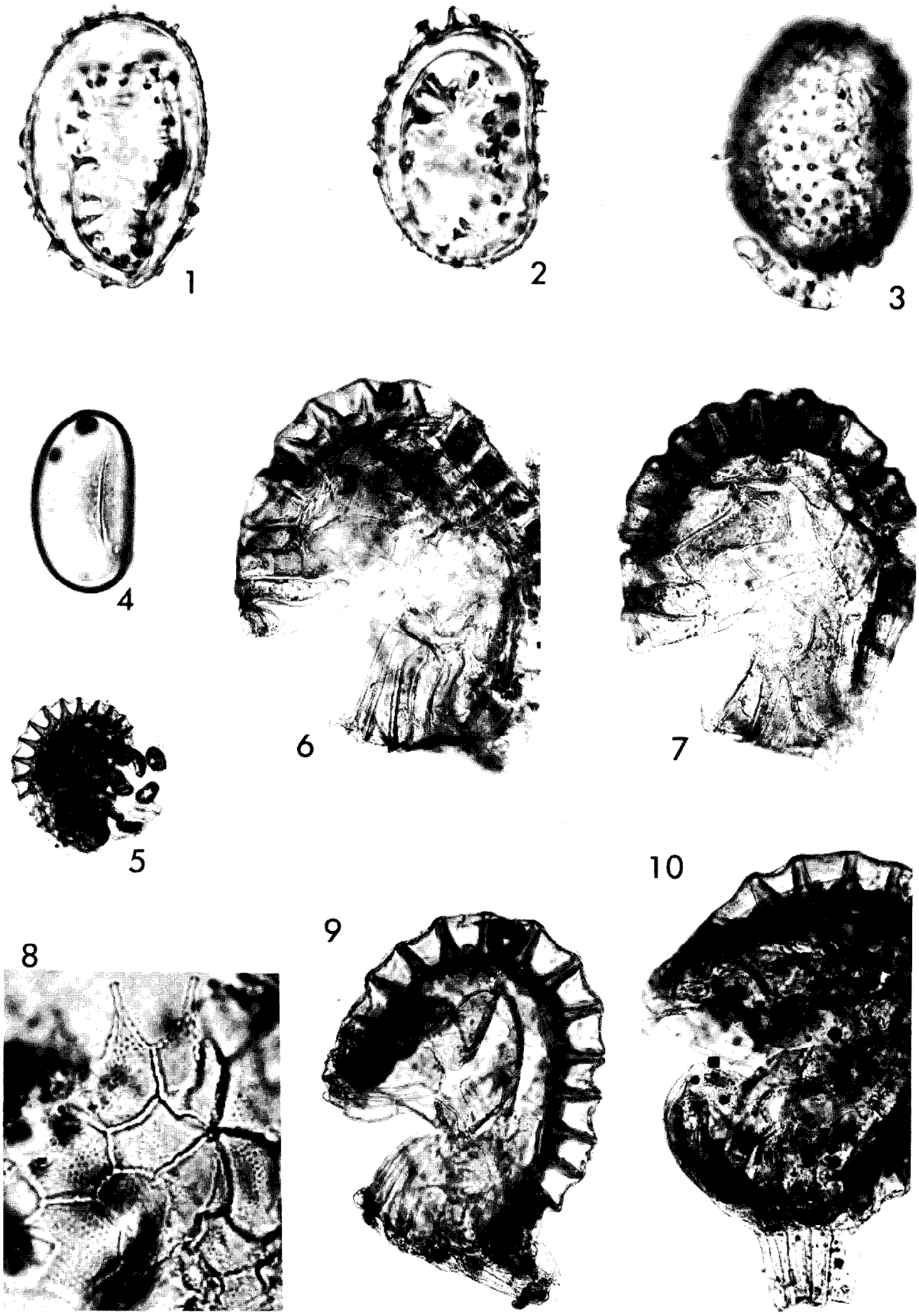

Plate 1

PLATE 2

Figure 1. *Sparganium eurycarpum* fruit. X15

2. *Lycopus* sp. nutlet, adaxial view, the marginal flange missing. X25

3. *Rumex maritimus* var. *fueginus* achene, removed from a perianth. X25

4. *Scirpus acutus-validus* achene, with three remaining bristles. X25

5. *Myriophyllum spicatum* (=*exalbescens*) nutlet, badly worn, adaxial view. X25

6. *Verbena hastata* nutlet, badly worn, abaxial view. X25

7 and 8. *Potamogeton* fruitstone. Figure 8 shows a section of the same specimen as shown in figure 7, note the nearly horizontal upper seam. X15

9. Flattened *Carex* sp. perigynium. X15

10. *Carex* cf. *vesicaria* achene. X25

11. *Rumex maritimus* var. *fueginus* perianth. X25

Plate 2

PLATE 3

Figure 1. Undetermined Compositae achene (transmitted light). X25

2. *Urtica* achene (transmitted light). X25

3. Flattened *Najas flexilis* nutlet (transmitted light). X25

4. Flattened *Triglochin* cf. *maritima*, carpel and enclosed seed (transmitted light). X25

5. *Zannichellia palustris* achene (transmitted light). X25

6. Incomplete carapace of the cladoceran *Chydorus sphaericus* (transmitted light). X100

7. *Typha* sp., ovary with style (transmitted light). X25

8, 12, and 13. Statoblasts of the bryozoan *Cristatella mucedo*; details of a spine and terminal hook (figure 8) (transmitted light) X400, a clear specimem without spines (figure 12) (transmitted light) X25, and a partly pyritized specimen with spines (figure 13) (transmitted light) X25.

9. Unusually complete carapace of an oribatid water mite, *Hydrozetes* sp. (transmitted light) X100

10 and 11. Cells of the planktonic green alga *Tetraedron minimum* (transmitted light) X1000

14. *Chenopodium* sp. seed. X15

15. *Potentilla* sp. achene. X25

16. *Mentha arvensis* nutlet. X25

17. *Eleocharis macrostachya* achene, distal tubercle missing. X25

1

2

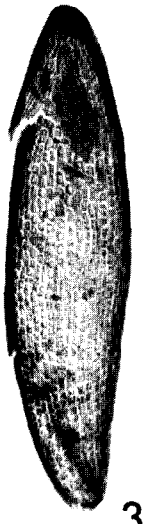
3

4

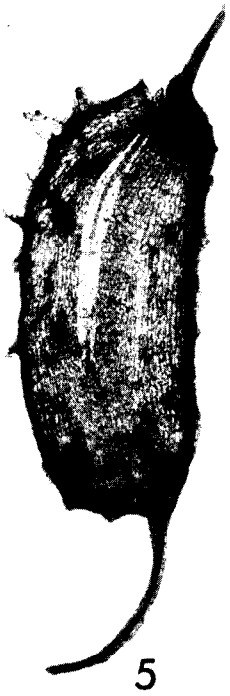
5

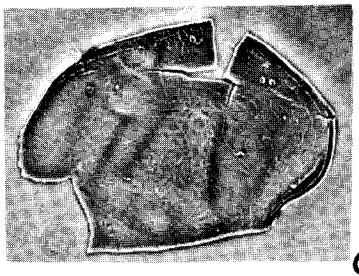
6

7

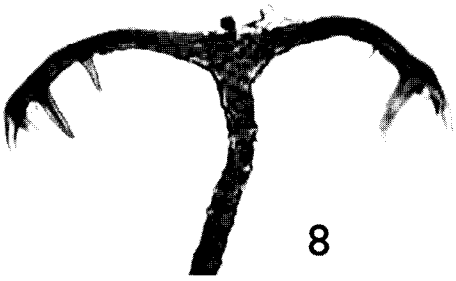
8

9

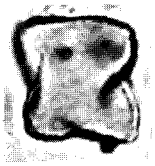
10

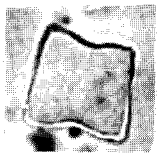
11

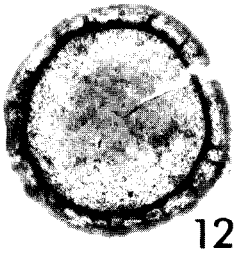
12

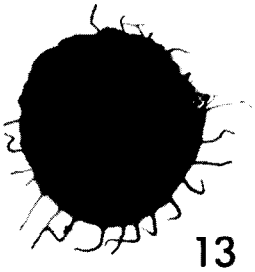
13

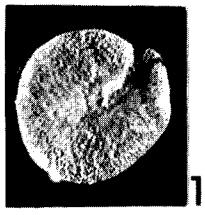
14

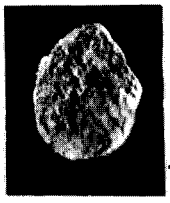
15

16

17

Plate 3

chin growing around the wet margins. This suite represents water less than a meter deep and reinforces the interpretation of shallow-water sediment.

MOLLUSKS

This entire section of the lacustrine member was sampled for mollusks. The shells were scattered throughout the member but several lenses were found with large concentrations. As no clear stratigraphic trends were noted, the data from all levels are summarized by species (Table 2).

The aquatic fauna indicates perennial water that was well oxygenated, clear, and less than about 3 meters deep. There were areas in which the rooted aquatic vegetation was thick and open areas in which the substratum was firm and sandy.

Some of the species live in marshy situations today where the water is less than 0.5 meter deep and where there is abundant aquatic vegetation. Thus there is a possibility that two habitats are represented by the fossil fauna.

Only two of the land snails could be identified. "In the Rocky Mountains *Pupilla muscorum* is found in higher, forested parts of the range. It occurs in places with some moisture, under logs, bark, stones, or other cover" (Hibbard and Taylor, 1960, p. 132). The presence of this species suggests a slightly cooler and moister climate than now, which might also explain the abundance of the fern *Cystopteris fragilis* less than 72,000 ± 14,000 and greater than 51,900 years ago.

Table 2. Mollusca of the lacustrine member of American Falls Lake Beds.

Freshwater clams
Sphaerium striatinum
Pisidium casertanum
Pisidium compressum

Freshwater snails
Valvata humeralis
Valvata utahensis
Stagnicola caperata
Stagnicola palustris
Stagnicola sp.
Gyraulus parvus
Carinifex newberryi
Helisoma anceps
Armiger crista
Promenetus exacuous
Physa gyrina

Land snails
Pupilla muscorum
Vallonia cyclophorella
cf. *Succinea*
Discus sp.
Oreohelix sp.

According to Hibbard and Taylor (1960, p. 137) "*Vallonia cyclophorella* generally occurs in the higher, forested parts of the western United States, in either coniferous or deciduous forest. It is to be found under logs, bark, stones, or other cover in places with some moisture." It is also known to occur in the sagebrush steppe near Montpelier, at St. Charles, near McCammon, and at Franklin in southeastern Idaho, and at Lake Point near Tooele, Utah (Pilsbry, 1948, p. 1036). Moreover, dead specimens were found in grass tufts on the Snake River Plain in the sagebrush steppe about 48 kilometers north of American Falls Reservoir (Bright and others, 1978, p. 214). Thus, this species may not necessarily indicate a cooler and moister climate as suggested by Hibbard and Taylor and it is not used as such an indicator in this study.

DIATOMS

The lacustrine member of the American Falls Lake Beds is extremely diatomaceous at the study site, with 127 taxa being recovered (Table 3). Diversity is low in the transgressive basal beds (Zone AF3), increases rapidly upwards (Zone AF2), reaches a maximum in the upper detrital peat (Zone AF1), and then abruptly decreases in the uppermost deposits.

ZONE AF3

The diatoms in Zone AF3 are mostly benthic and epiphytic forms, but the plankter *Stephanodiscus* niagarae is also present, reflecting open water offshore. This zone is dominated by littoral *Epithemia* spp. that are characteristic of alkaline water somewhat enriched in nutrients.

ZONE AF2

In Zone AF2 diatom frustules constitute from 15 to 50 percent of the sediment, and the sediments of this zone probably correlate with the diatomaceous blocky layer near the center of the basin. Plankters and tychoplankters, such as species of *Melosira*, *Cyclotella*, *Nitzschia*, *Synedra*, and *Stephanodiscus*, range from 20 to 60 percent of the flora. Benthic, epiphytic, and littoral forms make up the remainder.

Stephanodiscus niagarae is the dominant plankter, a species that now "has a restricted geographical distribution" and "is characteristic of the larger North American lakes, especially the Canadian ones" (Lund, 1962, p. 1504). This species occurs in lakes that range from oligotrophic to mesotrophic and that are large and cool. It is tempting to conclude that the presence

of *S. niagarae* in the lacustrine member of the American Falls Lake Beds indicates a cooler climate, but its distribution in the western United States is so poorly known that such a conclusion would be premature.

Overall, the diatom flora of this zone indicates a large, cool, open oligotrophic to mesotrophic lake with abundant rooted aquatic and semiaquatic vegetation around the shores and a pH of 7 to 8.

ZONE AF1

Epiphytic diatoms dominate the flora of Zone AF1, suggesting shallower water than that represented by Zone AF2.

The presence of *Denticula elegens* was a surprise because it is a characteristic inhabitant of hot springs or hot water. The only hot springs in the area today are upstream on the Portneuf River.

Several species of diatoms found at the site seem to prefer brackish water with a fairly high mineral content, such as *Epithemia adnata* var. *porcellus*, *Epithemia sorex*, *Mastogloia smithii* var. *amphicephala*, *Gomphonema sphaerophorum*, *Navicula oblonga*, *Navicula pupula*, *Navicula heufleri*, and *Rhoicosphenia curvata*. Moreover, *Navicula pupula*, *Rhoicosphenia curvata*, and *Rhopalodia parallela* are halophils and require some salt. These species were most likely derived from brackish marshes or ponds along the periphery of the lake and were washed into the lake by storms.

ABOVE ZONE AF1

The diatoms of this zone represent deeper water, as they are dominated by plankters and tychoplankters. *Stephanodiscus niagarae* is the most abundant. The habitat was about the same as represented by Zone AF2.

MAMMALS

Marie Hopkins (personal communication) investigated this same site for mammal remains. She found *Mammuthus* sp., *Equus* (*Equus*) sp., and *Bison* sp., all associated with the upper peat. Until the specific identity of those specimens is known, they add little information concerning the age of the sediments or the terrestrial environment at the time of deposition of the upper peat.

SPONGES

Although sponge spicules and gemmules occurred sparsely throughout the section, they were especially abundant in the upper peat (Zone AF1) and these were studied carefully.

Gemmules and gemmule spicules of *Heteromyenia tubispermis*, *Ephydatia fluviatilis*, and *Ephydatia mulleri* were found, as were skeleton spicules. Also, skeleton spicules that could be *Spongilla lacustris* or *Eunapius fragilis* were observed. All these are illustrated on Plate 4.

From Harrison's (1974) summary of the ecology of freshwater sponges, the following conditions of American Falls Lake are indicated for the time of deposition of the upper peat (Zone AF1).

Alkalinity (methyl orange)	110-230 ppm
Chloride	5-20 ppm
Conductivity (micromhos/cm)	350-500
Dissolved oxygen	about 5 ppm
Hardness ($CaCO_3$)	140-250 ppm
pH	6-8
Temperature	12-34°C
Water depth	less than 1.5 meters

All the species found are known to occur in lakes and ponds, but *Heteromyenia tubispermis* prefers smooth to rapidly flowing streams suggesting input from the Portneuf River. Although Harrison (1974, p. 41) suggested that *Ephydatia fluviatilis* "may be limited to waters of high conductivity as in Louisiana waters high in carbonates or sodium chloride," this species is not uncommon in modern freshwater ponds and lakes with very low chloride in southeastern Idaho and western Wyoming.

OTHER FOSSILS

Siliceous chrysophyte cysts were common throughout the entire lacustrine member but were concentrated in the upper peat (Zone AF1). The same distribution was noted for synuran scales and phytoliths (most of which appeared to be grass types). The upper peat was rich in moss remains, but no attempt was made to identify them. Cells of the planktonic green alga *Tetraedron minimum* (Plate 3, figures 10 and 11) were common in the pollen preparations, the highest concentration being in the upper peat. A few coenobia of *Pediastrum boryanum* (Plate 1, figure 8), another planktonic green alga, were found occasionally throughout the section. Statoblasts of the freshwater bryozoan *Cristatella mucedo* (Plate 3, figures 8, 12, and 13) were mostly concentrated in the upper peat, where they were common. They suggest water

PLATE 4

Figures 1 and 2. *Heteromyenia tubispermus*, birotulate spicules removed from a gemmule. X1000

3. cf. *Ephydatia fluviatilis* or *Spongilla lacustris*, smooth skeleton spicule. X250

4. cf. *Heteromyenia tubispermus*, moderately microspined skeleton spicule. X250

5. *Ephydatia fluviatilis*, very sparsely microspined skeleton spicule. X250

6 and 7. *Ephydatia fluviatilis*, birotulate spicules removed from a gemmule; note the fragment of a very sparsely microspined skeleton spicule in figure 6. X400

8 and 9. cf. *Spongilla lacustris* or *Eunapius fragilis*, gemmule spicules. X400

10, 13, and 14. *Heteromyenia tubispermus*, details of a gemmule and its foraminal tube and tendrils. X250, X100, X400

11. *Ephydatia mulleri*, end view of a birotulate gemmule spicule. X1000

12. *Heteromyenia tubispermus*, end view of a birotulate gemmule spicule. X1000

15. *Ephydatia mulleri* (left) densely microspined skeleton spicule and *Ephydatia fluviatilis* (right) skeleton spicule. The large diatom is *Epithemia*. X400

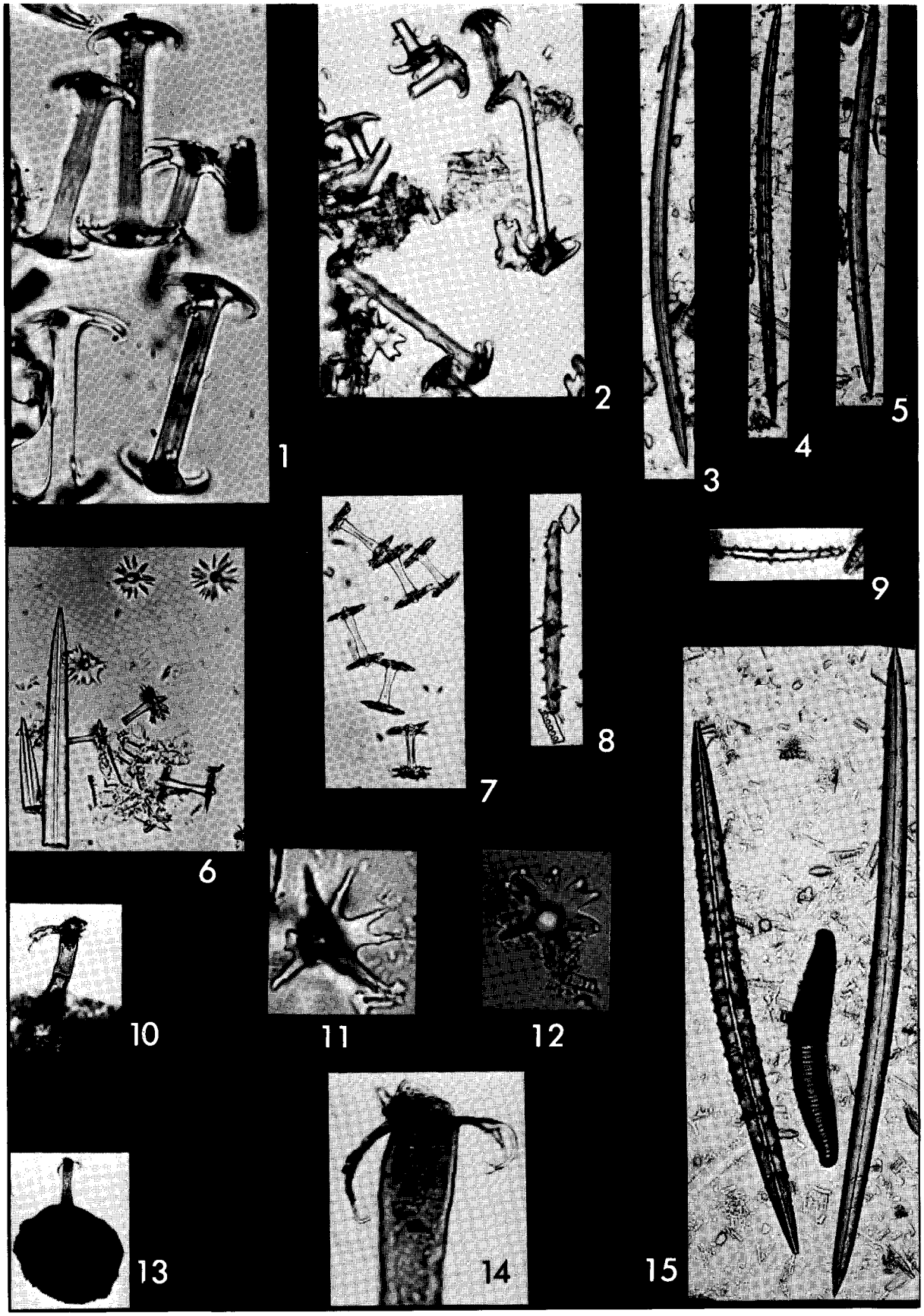

Plate 4

Table 3. Diatoms of the lacustrine member of American Falls Lake Beds.

Name	Zone AF3	Zone AF2	Zone AF1	Above Zone AF1
Acnanthes conspicua			X	
Acnanthes lanceolata			X	
Amphora ovalis var. *affinis*		X	X	X
Amphora ovalis var. *pediculus*			X	
Anomoeoneis sphaerophora			X	
Caloneis sp.		X	X	
Caloneis bacillum			X	
Caloneis lewisii			X	
Caloneis ventricosa var. *truncatula*			X	
Cocconeis sp.		X		
Cocconeis limosa			X	
Cocconeis placentula var. *euglypta*		X	X	X
Cocconeis placentula var. *lineata*			X	
Cocconeis thumensis			X	
Cyclotella sp.		X		X
Cyclotella antiqua			X	
Cyclotella compta		X	X	X
Cyclotella meneghiniana	X		X	X
Cyclotella stelligera			X	
Cymatopleura elliptica			X	
Cymatopleura solea			X	
Cymbella sp.	X	X		
Cymbella amphicephala			X	
Cymbella angustata		X	X	X
Cymbella aspera			X	
Cymbella cistula		X	X	X
Cymbella cuspidata			X	
Cymbella cymbiformis		X	X	X
Cymbella diluviana			X	
Cymbella inequalis			X	
Cymbella mexicana		X	X	X
Cymbella minuta		X	X	X
Cymbella norvegica			X	
Cymbella triangulum			X	
Cymbella turgida		X	X	X
Denticula sp.			X	
Denticula elegans			X	
Diatoma sp.		X	X	
Diatoma hiemale			X	
Diploneis elliptica			X	
Diploneis oblongella			X	
Epithemia sp.	X	X	X	X
Epithemia adnata	X	X	X	X
Epithemia adnata var. *porcellus*			X	
Epithemia adnata var. *saxonica*			X	
Epithemia argus		X	X	X
Epithemia sorex	X	X	X	X
Epithemia sorex var. *lapponica*		X		
Epithemia turgida	X	X	X	X
Eunotia sp.			X	
Eunotia valida			X	
Fragilaria brevistriata	X	X	X	X
Fragilaria brevistriata var. *capitata*	X	X	X	X
Fragilaria construens		X	X	X
Fragilaria construens var. *binodis*		X	X	
Fragilaria construens var. *pumila*		X	X	X
Fragilaria construens var. *venter*		X	X	X
Fragilaria lapponica		X	X	
Fragilaria leptostauron	X	X	X	X
Fragilaria pinnata	X	X	X	X
Fragilaria pinnata var. *lancettula*			X	
Fragilaria vaucheriae			X	
Fragilaria virescens		X	X	X
Gomphonema sp.		X		X
Gomphonema angustatum var. *sarcophagus*			X	
Gomphonema dichotomum		X	X	X
Gomphonema dichotomum var. *vibrio*		X	X	X
Gomphonema intricatum			X	
Gomphonema sphaerophorum			X	
Gomphonema subtile		X		X
Gomphonema truncatum			X	
Gomphonema truncatum var. *capitatum*			X	
Gyrosigma sp.		X	X	
Gyrosigma attenuatum			X	
Hantzschia sp.		X	X	
Hantzschia amphioxys		X	X	X
Mastogloia smithii var. *amphicephala*			X.	
Mastogloia smithii var. *lacustrix*	X	X	X	X
Melosira distans var. *lirata*			X	
Melosira islandica ssp. *helvetica*			X	X
Melosira italica			X	
Melosira granulata		X	X	X
Meridion circulare			X	
Navicula sp.		X	X	X
Navicula amphibola			X	
Navicula balfouriana			X	
Navicula capitata			X	
Navicula cuspidata			X	
Navicula cuspidata var. *ambigua*	X	X		X
Navicula elginensis			X	
Navicula globosa			X	
Navicula heufleri			X	
Navicula maior			X	
Navicula mutica			X	
Navicula oblonga	X	X	X	
Navicula pupula			X	
Navicula pupula var. *rectangularis*			X	
Navicula radiosa		X	X	X
Navicula tuscula			X	
Navicula wittrockii			X	
Neidium iridis			X	
Neidium iridis var. *amphigomphus*			X	
Nitzschia amphibia		X	X	X
Pinnularia sp.	X	X	X	X
Pinnularia acuminata var. *bielawskii*			X	
Pinnularia brebissonii			X	
Pinnularia brevicostata			X	
Pinnularia viridis var. *commutata*			X	
Rhoicosphenia curvata			X	
Rhopalodia sp.	X	X	X	X
Rhopalodia gibba			X	
Rhopalodia gibberula		X	X	X
Rhopalodia parallela			X	
Stauroneis anceps f. *gracilis*			X	
Stauroneis phoenocenteron		X	X	X
Stephanodiscus sp.		X		
Stephanodiscus astraea var. *minutula*			X	
Stephanodiscus niagarae	X	X	X	X
Surirella sp.			X	
Surirella biseriata var. *bifrons*			X	
Surirella ovata			X	
Synedra sp.	X	X		X
Synedra acus		X	X	X
Synedra capitata		X	X	
Synedra delicatissima			X	X
Synedra rumpens			X	
Synedra ulna		X		

of low turbidity. Carapaces of an oribatid water mite, *Hydrozetes* sp. (Plate 3, figure 9) were found throughout the section but were particularly common in the upper peat. Ostracod shells were common throughout the entire lacustrine member, but they were not studied.

Fragments of cladocera carapaces were found throughout the section, but were especially common in the upper peat. Only one carapace was complete enough for identification and that was of the cosmopolitan species *Chydorus sphaericus* (Plate 3, figure 6).

SUMMARY

A study of the numerous and varied fossils at a site near the south shore of ancient American Falls Lake has provided new insight concerning the lake and its history, the upland vegetation, and the climate of the area less than 72,000 ± 14,000 years and greater than 51,900 years ago.

Pollen, spores, and seeds from the lower part of the lacustrine member of the American Falls Lake Beds indicate that the vegetation was similar to the present: coniferous forest in the mountains, junipers in the foothills, *Artemesia*-chenopod steppe on the nearby Snake River Plain, and riparian vegetation (for example, birch, willow, sedges) along the shores and up tributary stream valleys. The aquatic and semiaquatic flora was the same as in southeastern Idaho today. The fern *Cystopteris fragilis* was abundant near the site, a situation for which there is no modern analog.

Based on the vegetation reconstruction, the climate less than 72,000 ± 14,000 years and greater than 51,900 years ago must have been very similar to the present. The occurrence of the land snail *Pupilla muscorum* suggests a slightly cooler and moister climate then, as the abundance of *Cystopteris fragilis* might also suggest. It might be argued that the ancient vegetation was more like that found today at a slightly higher elevation on the *Artemisia* steppe, but it would then be difficult to explain the abundance of chenopod pollen (Figure 2). In either case, Zones AF3-AF1 represent a time of warmth and semiaridity and therefore a time of nonglaciation. Until we are accurately able to distinguish interglacial periods from interstadial ones on the basis of fossils in the northern Great Basin and until the age of the beginning of the Wisconsinan is resolved, it cannot be reliably determined if Zones AF1-AF3 represent late Sangoman or a Wisconsinan interglacial.

Study of the sediments and the fossils indicates a transgressive phase of American Falls Lake at the site, a deeper lacustrine phase, a shallow phase (water less than 1.5 meters deep), followed by another deeper lacustrine phase of unknown duration. The shallow phase may or may not be related to climatic change, a problem that requires further investigation.

The lake was certainly freshwater, large, not very turbid, mesotrophic, and very productive, with a pH of 7 to 8, moderate alkalinity, moderate chloride content, and moderate hardness. Rooted aquatic and semiaquatic plants were dense in many nearshore areas, but there were open places with a firm sandy bottom. There were marshy places along shore where *Scirpus*, *Typha*, *Eleocharis*, and *Carex* were abundant.

Further investigation of these interesting sediments is needed, especially the micro-fauna, the phytoliths, and the pollen in the younger beds of the lacustrine member.

ACKNOWLEDGMENTS

I wish to extend my appreciation to the following people for helping in various ways during this study: Marie Hopkins, Dave Fortsch, Mary Strawn, Claudia Wang, H. E. Wright, Owen Davis, H. B. Tordoff, and Roger Woo, who took the photographs. The Shoshone-Bannock Tribe, Inc., and the Bureau of Indian Affairs freely gave permission to work at the site, and the staff at the Portneuf Pumping Station provided assistance in the field. Special thanks is due Dr. W. G. Mook, Groningen University, Netherlands, for the radiocarbon date.

REFERENCES

Blaisdell, R. F., 1963, A monographic study of the fern genus *Cystopteris:* Memoir Torrey Botanical Club, v. 21, no. 4, 102 p.

Bright, R. C., 1966, Pollen and seed stratigraphy of Swan Lake, southeastern Idaho: Its relation to regional vegetation history and to Lake Bonneville history: Tebiwa, Journal Idaho State Museum, v. 9, no. 2, 47 p.

Bright, R. C. and O. K. Davis, in press, Quaternary paleoecology of the Idaho National Engineering Laboratory, Snake River Plain, Idaho: American Midland Naturalist.

Bright, R. C., O. K. Davis, and B. K. Eikum, 1978, Paleontology of the Idaho National Engineering Laboratory Site, *in* O. D. Markham, editor, Ecological Studies on the Idaho National Engineering Laboratory Site, 1978 Progress Report: U. S. Department of Energy IDO-12087, p. 209-218.

Cronquist, Arthur, A. H. Holmgren, N. H. Holmgren, and James Reveal, 1972, Intermountain flora: New York Botanical Garden, v. 1, p. 217.

Davis, R. J.,1952, Flora of Idaho: W. C. Brown Co., Dubuque, Iowa, p. 37-38.

Fautin, R. W., 1946, Biotic communities of the northern desert shrub biome in western Utah: Ecological Monographs, v. 16, p. 251-310.

Harrison, F. W., 1974, Sponges (Porifera: Spongillidae), *in* C. W. Hart and S. L. H. Fuller, editors, Pollution Ecology of Freshwater Invertebrates: Academic Press, Inc., New York, p. 29-66.

Hibbard, C. W. and D. W. Taylor, 1960, Two late Pleistocene faunas from southwestern Kansas: Contributions of the Museum of Paleontology, University of Michigan, v. 16, no. 1, 223 p.

Hitchcock, C. L., Arthur Cronquist, Marion Ownbey, and J. W. Thompson, 1969, Vascular plants of the Pacific Northwest: University of Washington Press, pt. 1, p. 71.

Lund, J. W. G., 1962, Phytoplankton from some lakes in northern Saskatchewan and from Great Slave Lake: Canadian Journal of Botany, v. 40, p. 1499-1514.

Pilsbry, H. A., 1948, Land mollusca of North America: Academy of Natural Sciences of Philadelphia Monograph 3, v. 2, pt. 2, p. 1036.

Porter, C. L., 1962, A flora of Wyoming: University of Wyoming Agricultural Experiment Station Bulletin 402, pt. 1, p. 27.

Ridenour, James, 1969, Depositional environments of the late Pleistocene American Falls Formation, southeastern Idaho: Idaho State University M.S. thesis, 82 p.

Scott, W. E., K. L. Pierce, J. P. Bradbury, and R. M. Forester, 1982, Revised Quaternary stratigraphy and chronology in the American Falls area, southeastern Idaho, *in* Bill Bonnichsen and R. M. Breckenridge, editors, Cenozoic Geology of Idaho: Idaho Bureau of Mines and Geology Bulletin 26.

Trimble, D. E. and W. J. Carr, 1976, Geology of the Rockland and Arbon quadrangles, Power County, Idaho: U. S. Geological Survey Bulletin 1399, p. 68.

Chapter 11

Pleistocene Lava Dams and Canyon History

The Yahoo Clay, a Lacustrine Unit Impounded by the McKinney Basalt in the Snake River Canyon Near Bliss, Idaho

by

Harold E. Malde[1]

ABSTRACT

Damming of the ancestral Snake River by the late Pleistocene McKinney Basalt formed a temporary, but long lasting, lake as much as 600 feet deep, which is here called McKinney Lake. The lake extended upstream from the town of Bliss along a canyon much like the present canyon through Hagerman Valley and the Thousand Springs area to Melon Valley. Pillow lava of the McKinney Basalt partly filled the lower reach of McKinney Lake, and lacustrine clay then filled the remainder of the lake. The clay—here named the Yahoo Clay of the Snake River Group for deposits found near the mouth of Yahoo Creek southwest of Hagerman—is misidentified on published geologic maps as being part of the Bruneau Formation, an older unit which is now considered to be limited to the area west of Bliss. Accordingly, evidence for relatively cool and moist conditions, which is provided by fossil mollusks and pollen from lake clay upstream from Bliss, pertains to the Yahoo Clay, not to the Bruneau Formation. The relations of the Yahoo Clay to McKinney pillow lava and to older deposits are described here from features found at numerous outcrops, and certain puzzling relations of the lake clay that can be found on the published maps are explained in light of this new stratigraphic knowledge. Curiously, McKinney Lake did not overflow until the Yahoo Clay had accumulated nearly to the height of the McKinney lava dam. This finding suggests that the buildup of thick lacustrine deposits behind other lava dams in the region may have been aided by a controlled process of leakage, which inhibited overflow and downcutting. Finally, the age of the Crowsnest Gravel at Hagerman is now considered to be younger than the McKinney Basalt because of its position on the Yahoo Clay. Gravel downstream from Bliss that appears to have been deeply incised before eruption of the McKinney Basalt probably has been wrongly correlated with the Crowsnest Gravel at Hagerman.

[1]U. S. Geological Survey, Denver, Colorado 80225.

INTRODUCTION

The interplay of late Pleistocene lava flows and the ancestral Snake River in southern Idaho has produced many complex, sometimes bewildering, stratigraphic and physiographic features. No features found thus far are as puzzling as those associated with the McKinney Basalt, which erupted from McKinney Butte 9 miles northeast of the town of Bliss, Idaho (Figure 1).

The role of the McKinney Basalt in damming a former course of the Snake River was explained in an earlier paper (Malde, 1971), thereby accounting for the accumulation of thick deposits of McKinney pillow lava in the resulting temporary lake. The present paper is concerned with evidence that lacus-

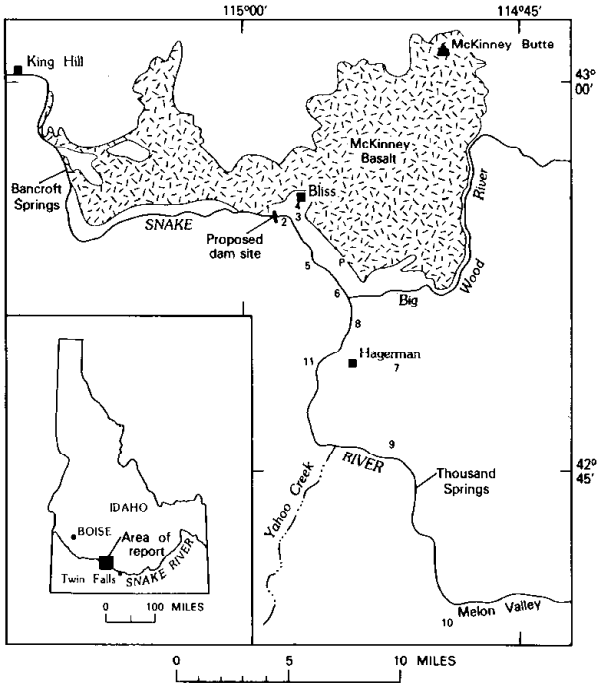

Figure 1. Index map showing numbered localities of Yahoo Clay described in the text. The letter P marks an outcrop of pillow lava shown in Figure 8.

Malde, H. E., 1982, The Yahoo Clay, a lacustrine unit impounded by the McKinney basalt in the Snake River Canyon near Bliss, Idaho, *in* Bill Bonnichsen and R. M. Breckenridge, editors, Cenozoic Geology of Idaho: Idaho Bureau of Mines and Geology Bulletin 26, p. 617-628.

trine clay in the canyon upstream from the lava dam, which was previously assigned to an older lacustrine unit (the Bruneau Formation), was also deposited in the same lake. The significance of the lake clay for understanding the physiographic history of the Snake River canyon is then briefly mentioned. Finally, the age of river gravel that overlies the lake clay (the Crowsnest Gravel) is also redefined. The former and present classifications of the local stratigraphy are shown in Figure 2.

AGE	FORMER CLASSIFICATION AND SEQUENCE		PRESENT CLASSIFICATION AND SEQUENCE	
Late Pleistocene	Snake River Group	Melon Gravel McKinney Basalt Wendell Grade Basalt Sand Springs Basalt Crowsnest Gravel Thousand Springs Basalt Madson Basalt	Snake River Group	Melon Gravel Crowsnest Gravel Yahoo Clay McKinney Basalt Wendell Grade Basalt Sand Springs Basalt Thousand Springs Basalt Madson Basalt
Older rocks		Bruneau Formation Tuana Gravel Glenns Ferry Formation Banbury Basalt Idavada Volcanics		Tuana Gravel Glenns Ferry Formation Banbury Basalt Idavada Volcanics

Figure 2. Listing of former and present classifications of the stratigraphy in the area extending upstream from Bliss to Melon Valley, Idaho.

GEOLOGIC SETTING

The McKinney Basalt is the youngest and most westerly volcanic unit in an area distinguished by the overlap of late Pleistocene basaltic lava flows on thick, older formations of basalt and poorly consolidated stream and lake deposits (Malde, 1965). The boundary between these two major geologic divisions is steep and is broadly traced by the canyon of the Snake River, with the older deposits forming a dissected canyon wall 700 feet high to the left of the river, and the younger lava flows forming cliffs that reach more than 500 feet above the river on the right. (Left and right are to be understood in the sense of looking downstream.) The canyon floor is variously composed of both the older and younger geologic units, depending on vagaries of past deposition and erosion (Figure 3).

When the geologic units are subdivided and mapped in greater detail, the Snake River is seen to have become entrenched in its present canyon at Bliss by downcutting that was impeded from time to time by the eruption and spread of the late Pleistocene lava flows. As the river cut downward, it was forced progressively farther south and west along the margins of successive canyon-filling lava flows (Malde, 1971, Figure 11). With respect to the present canyon, the most significant geologic event was the eruption of the canyon-filling McKinney Basalt. The basalt dammed the ancestral Snake River at a place still concealed from 2 to 3 miles west of Bliss, thus forming a temporary lake more than 600 feet deep that extended many miles upstream along the canyon of that time. In this paper, the body of water impounded by the lava dam of McKinney Basalt is informally named McKinney Lake. The McKinney Basalt was deposited in two facies: upland lava flows at the level of the canyon rim and pillow lava that formed within the ancestral canyon near Bliss where basalt spilled into the canyon (Figure 4).

From evidence described later in this paper, lacustrine clay began to accumulate in McKinney Lake immediately after deposition of the pillow lava and ultimately reached a height nearly equal to the level of the McKinney lava dam. Eventually, the lake overflowed, and the lava dam was breached along its southern margin by downcutting in poorly consolidated silt and clay of the Glenns Ferry Formation. The Snake River thus began to cut its present canyon west of Bliss, and McKinney Lake was correspondingly lowered and drained. When downcutting had reached a level about 300 feet above the present Snake River in Hagerman Valley, about 8 miles upstream from Bliss, terrace deposits called the Crowsnest Gravel were formed, mostly on the lacustrine clay of McKinney Lake. After the Snake River canyon had nearly achieved its present width and depth, flood debris from catastrophic overflow of Pleistocene Lake Bonneville was deposited in large bars along the canyon floor, in places reaching heights more than 200 feet above the modern river (Malde, 1968). Erosion during entrenchment of the canyon and the havoc produced by the Bonneville Flood have limited the exposures of the McKinney pillow lava to discontinuous outcrops, and the lacustrine clay is correspondingly preserved in widely scattered remnants.

RELATION OF THE LACUSTRINE CLAY AND THE McKINNEY BASALT

The knowledge that McKinney pillow lava is overlain by lacustrine clay came initially from stratigraphic information in a proposal by the Idaho Power Company, dated August 26, 1980, to build a dam on the Snake River near Bliss. Core drilling in

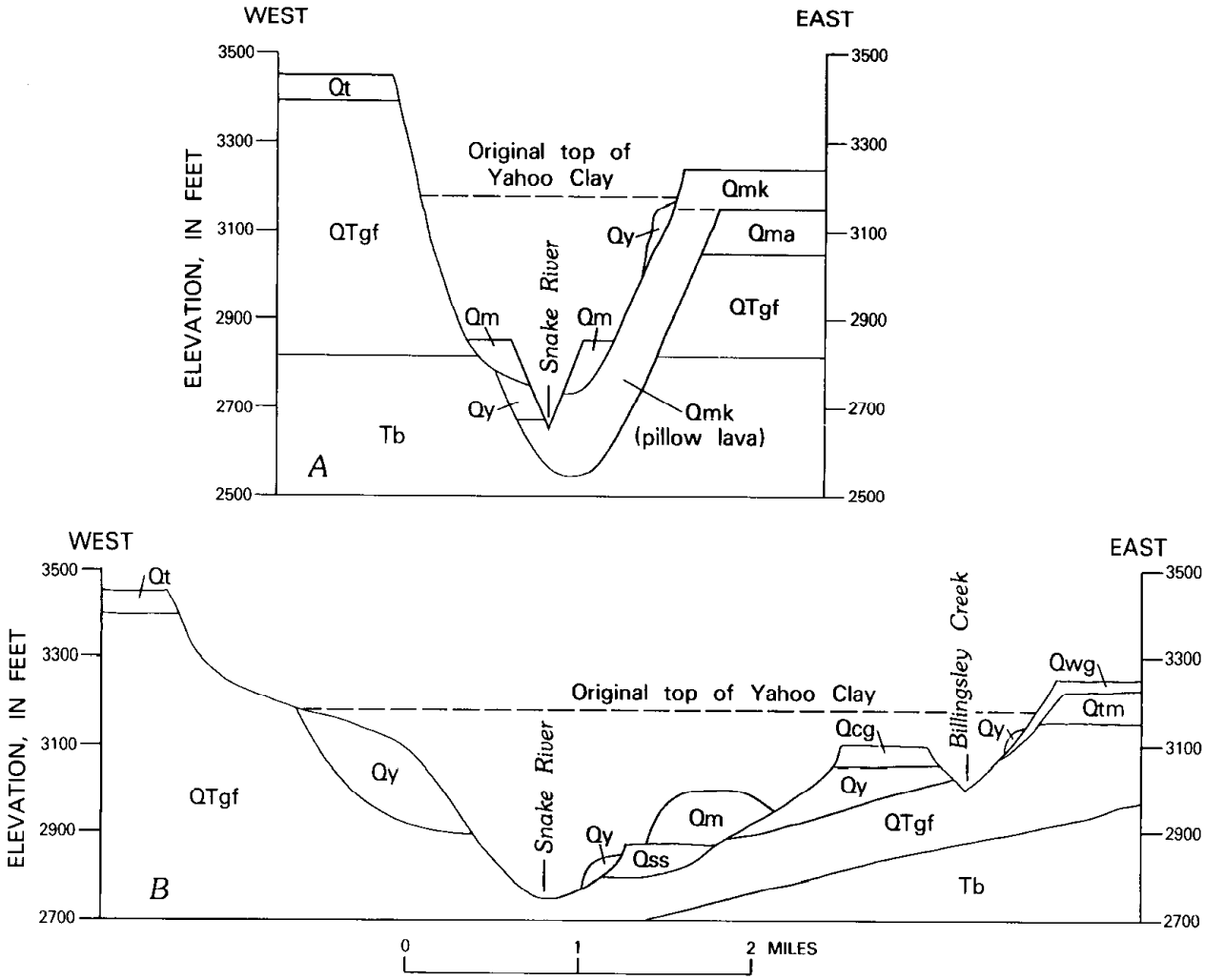

Figure 3. Diagrammatic cross sections of the Snake River canyon near Bliss (*A*) and at Hagerman, Idaho (*B*). The geologic units are identified as follows: Qm, Melon Gravel; Qcg, Crowsnest Gravel; Qy, Yahoo Clay; Qmk, McKinney Basalt; Qwg, Wendell Grade Basalt; Qss, Sand Springs Basalt; Qtm, Malad Member of Thousand Springs Basalt; Qma, Madson Basalt; Qt, Tuana Gravel, all of Quaternary age; QTgf, Glenns Ferry Formation of Quaternary(?) and Tertiary age; and Tb, Banbury Basalt of Tertiary age.

the north abutment at the proposed site had penetrated as much as 90 feet of thinly laminated clay resting on a southward-dipping surface of McKinney pillow lava (Figure 5).

This finding prompted me in September and October, 1980, to review the geology extending upstream from the proposed dam site. Several new exposures were found, showing lacustrine clay on McKinney pillow lava, and the new stratigraphic knowledge caused me to reinterpret previously ambiguous field relations. My understanding in the 1960s, because I had not then seen the lacustrine clay on McKinney Basalt, was that the clay is correlative with clay of the Bruneau Formation and, hence, is older than the McKinney Basalt. To my chagrin, but to my satisfaction, the investigations by the Idaho Power Company, together with my own recent observations, now show that the Bruneau Formation does not exist at the proposed dam site or in the present canyon area above Bliss. Rather, the Bruneau Formation is found only farther downstream, where it occupies a broad older canyon. Its base where intercepted by the Snake River canyon some 11 miles west of Bliss is at an altitude of 2,675 feet—an elevation considerably too high to account for lacustrine clay at the same altitude near river level at the dam site. In short, all the clay previously mapped as Bruneau lake beds upstream from the proposed dam (that is, unit Qbs on Sheet 1 of the map by Malde and Powers, 1972) is incorrectly identified. The lacustrine clay is a unique geologic unit that accumulated behind the lava dam formed by the McKinney Basalt, and the clay occupies

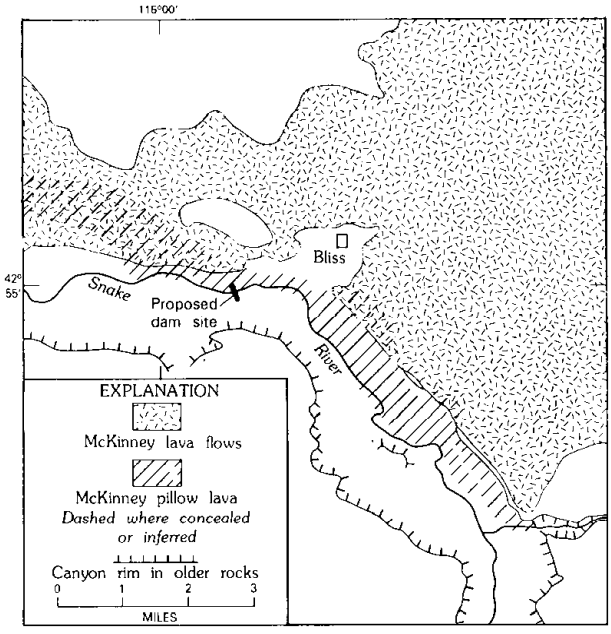

Figure 4. Sketch map showing the distribution of McKinney Basalt near Bliss, Idaho. This geologic unit consists of pillow lava that occupies a former canyon of the Snake River and lava flows that rest on the pillow lava as well as on the surrounding upland of older rocks. Edges of the lava flows are exposed as rimrock by erosion along the right side of the present canyon.

an ancestral canyon of the Snake River that is much younger than the canyon occupied by the Bruneau Formation.

The contact of the clay on McKinney pillow lava is not widely exposed, but certain outcrops that are described below show that the clay was deposited directly on the pillow lava. In one particularly instructive outcrop, layers of glassy basaltic fragments that were produced during formation of the pillow lava grade upward into laminated clay (locality 2 described below). This relationship suggests that the clay began to accumulate immediately after the pillow lava was deposited, at least in the initial deposits of clay at low altitudes in the canyon of that time. Other outcrops show that the lacustrine clay accumulated from an altitude of 2,650 feet at present river level near Bliss to an altitude of 3,180 feet, thus deeply filling the canyon upstream from the McKinney lava dam. The distribution of the clay suggests that the ancestral canyon was physiographically much like the present canyon in its width, depth, and location.

STRATIGRAPHY AND DISTRIBUTION OF THE LACUSTRINE CLAY

In retrospect, H. A. Powers recognized many aspects of the stratigraphy of the lacustrine clay during his field work in 1954 and 1955, although he obviously did not know its relation to the McKinney Basalt. Powers found that the most continuous and best exposed deposits of the lacustrine clay are in a dissected area near the mouth of Yahoo Creek, which joins the Snake River about 4 miles south-southwest of Hagerman.

NAME AND TYPE LOCALITY

Accordingly, although the physical relations of the clay to McKinney Basalt can be determined only at other outcrops, the lacustrine clay associated with the McKinney Basalt is here named the Yahoo Clay from remnants of the clay in the area of the lower reach of Yahoo Creek. The clay at its type locality rests on an inclined surface cut on the Glenns Ferry Formation (part of the left wall of a former canyon of the Snake River) in sections 3, 4, and 5, T. 8 S., R. 13 E., and in

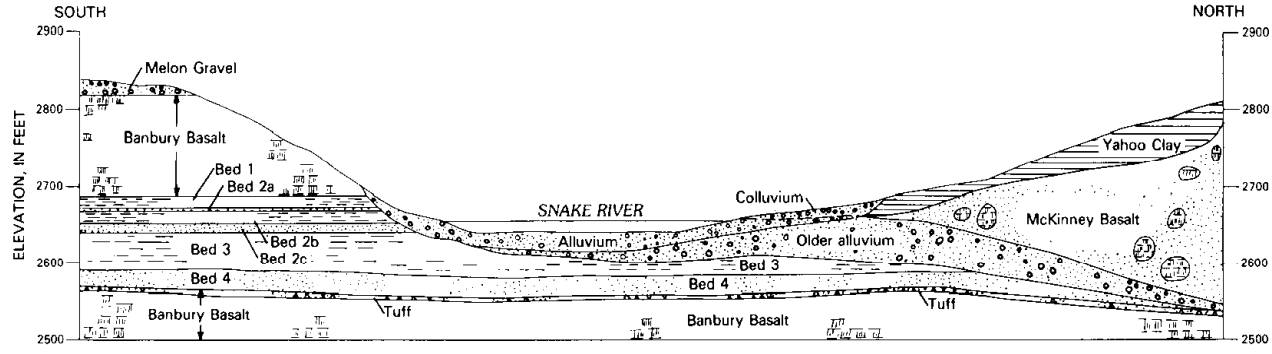

Figure 5. Cross section between the left and right abutments of a proposed dam on the Snake River about a mile downstream from Bliss, Idaho (at mile 565 near the center of sec. 12, T. 6 S., R. 12 E., Bliss quadrangle). The unit labeled "Older alluvium" is a local body of mixed debris at the base of the pillow lava facies of the McKinney Basalt. Beds 1-4 are local sedimentary layers interbedded in the Banbury Basalt. (Adapted from a drawing submitted by the Idaho Power Company to the Federal Energy Regulatory Commission, August 26, 1980.)

the adjacent parts of sections 8, 9, and 10 to the south, as shown on the map by Malde and Powers (1972). The abrupt contact on the Glenns Ferry is well exposed where crossed by the Crowsnest Road (3,400 feet N., 2,000 feet E., SW cor., sec. 10, T. 8 S., R. 13 E., Yahoo Creek quadrangle).

The Yahoo Clay in this area rises continuously from its base at an altitude of 2,900 feet near the mouth of Yahoo Creek to an altitude of 3,180 feet in sections 4, 5, 8, and 9. (Because of mistakes made when compiling the published map, the clay is erroneously shown as locally reaching altitudes higher than 3,180 feet in this area.) Throughout this area, the Yahoo Clay is monotonously uniform in its lithology, consisting of laminated clay and sparse amounts of silty clay, commonly in laminae about ¼ inch thick. The color, when freshly exposed, ranges from pinkish white (7.5YR 8/2) to light yellowish brown (10YR 6/4), based on terminology used on the *Munsell Soil Color Charts* (1954 edition). The clay is compact and hard when dry, breaking with a conchoidal fracture, but readily slakes in water. The eroded surface weathers to form a loose, "popcorn" surficial layer a foot or more thick, possibly because of the presence of clays that swell when wet.

At the top of the Yahoo Clay in this area, as well as at other places described later in the cliffs to the west of Hagerman, the clay is weathered to form a soil profile about 6 feet thick. On the soil is as much as 15 feet of surficial sand and silt that have been mapped as some of the deposits of an erosion surface related to the Crowsnest Gravel (Malde and Powers, 1972). In 1955, I noted that the upper part of the soil on the Yahoo Clay has weathered to dark brown (10YR 4/3) and that the lower part of the soil is mottled with nodules of secondary calcium carbonate.

REFERENCE LOCALITIES

In addition to the type locality of the Yahoo Clay at Yahoo Creek, several other localities provide further information about the stratigraphy and distribution of the clay. These places, which are indicated by numbers on Figure 1, are described below as reference localities.

Locality 1. The farthest downstream remnant of Yahoo Clay is preserved in the right abutment of the proposed dam at altitudes between 2,675 and 2,800 feet, resting on a southward-dipping surface of McKinney pillow lava (Figure 5). Contiguous outcrops of the clay extend half a mile upstream and rise to an altitude of 2,900 feet.

Locality 2. At the south end of the Shoestring Road Bridge (2,150 feet N., 800 feet E., SW cor., sec. 7, T. 6 S., R. 13 E., Bliss quadrangle) and at an altitude of 2,675 feet, a recent excavation for the road shows that Yahoo Clay overlies rubble composed of unsorted angular blocks of Madson Basalt mingled with McKinney pillow lava. The rubble grades upward to as much as 5 feet of bedded fragments of glassy basalt and then to lacustrine clay (Figure 6). The transition to Yahoo Clay is within an interval 8 inches thick marked by alternating laminae of clay, silt, and basaltic fragmental material. The relations suggest an uninterrupted transition from deposition of the McKinney pillow lava to deposition of the Yahoo Clay. In short, the pillow lava and the clay appear to be nearly contemporaneous.

Locality 3. Above and below old U. S. Highway 30, 1 mile south of Bliss along an east-west nose in the canyon wall, the Yahoo Clay rests on a steep, westward-plunging slope of McKinney pillow lava, which drops from an altitude of about 3,050 feet to 2,925 feet (the contact on the highway is exposed at 1,750 feet N., 500 feet W., SE cor., sec. 7, T. 6 S., R. 13 E., Bliss quadrangle).

Locality 4. Yahoo Clay makes up much of the exposed material of a large landslide immediately south of Bliss. The highest exposure of clay (1,600 feet S., 200 feet E., NW cor., sec. 8, T. 6 S., R. 13 E., Bliss quadrangle) is at an altitude between 3,150 and 3,175 feet, adjacent to a cliff of Madson Basalt at the head of the landslide. The exposure is contiguous to an outcrop of the Glenns Ferry Formation at the same altitude.

Locality 5. A recent excavation made for the King Hill Canal (1,250 feet N., 2,500 feet E., SW cor., sec. 20, T. 6 S., R. 13 E., Bliss quadrangle) exposes Yahoo Clay on as much as 6 feet of steeply dipping colluvium, which in turn rests on the eroded Glenns Ferry Formation. The colluvium contains abundant angular blocks from the Madson Basalt (which is preserved as a remnant ¼ mile southeast and 125 feet higher) as well as rounded pieces of older basalt and pebbles similar to those found in Tuana Gravel higher in the canyon wall. Good exposures in this area make the Yahoo Clay continuously recognizable from river level to an altitude of 3,175 feet in the canyon wall to the west.

Locality 6. Landsliding and gully erosion in Yahoo Clay at the west end of the former siphon for the King Hill Canal (750 feet N., 150 feet E., SW cor., sec. 27, T. 6 S., R. 13 E., Hagerman quadrangle) has exposed the base of the clay at an altitude of about 2,800 feet. The clay rests on rubble that has some of the characteristics of rubble at the Shoestring Road Bridge (locality 2 described above). The rubble contains substantial amounts of fragmental glassy McKinney lava as well as scattered McKinney pillows. The rubble may have originated as colluvium (such as a former talus deposit), but it locally contains sorted

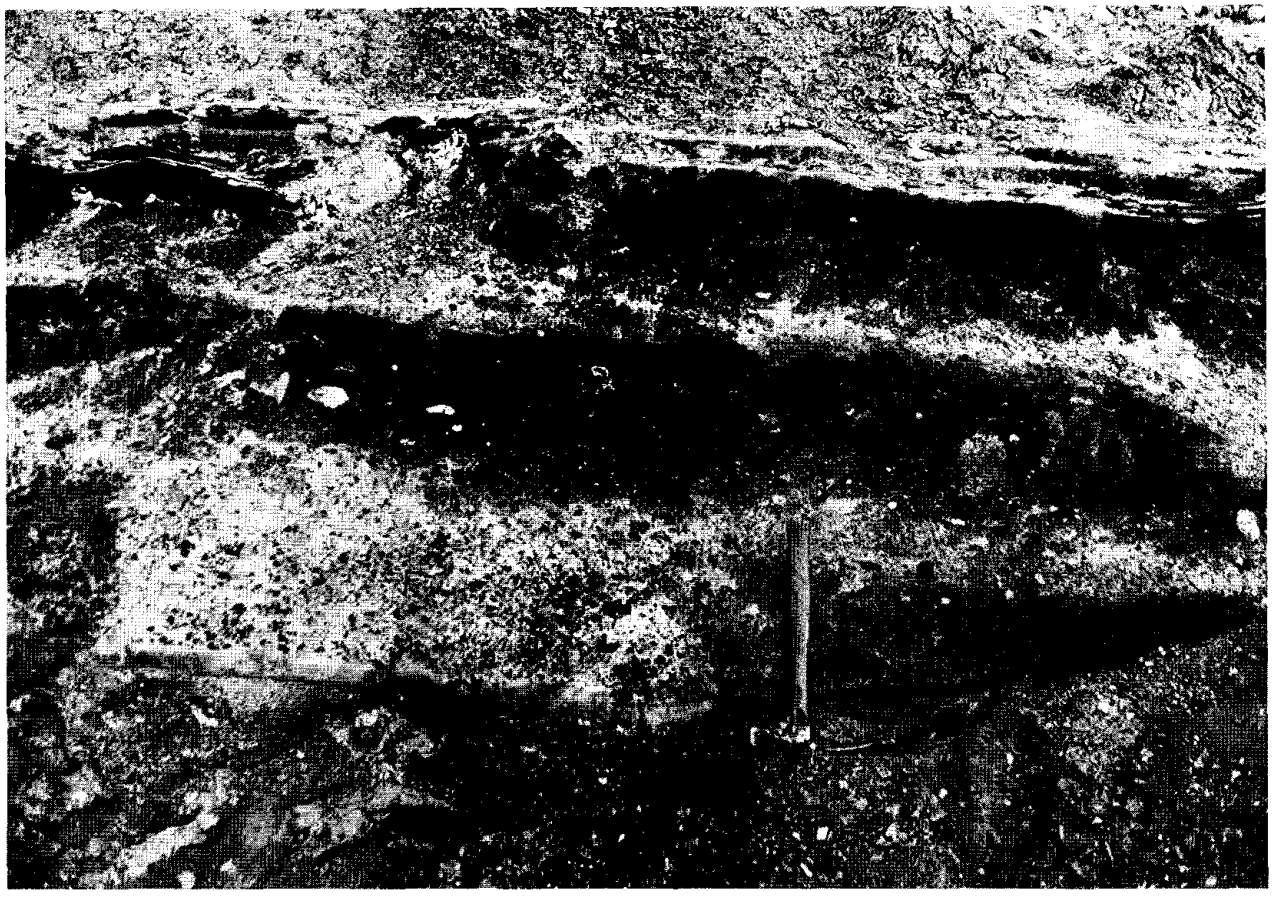

Figure 6. Outcrop at the south end of the Shoestring Road bridge (locality 2 on Figure 1) showing layers composed dominantly of glassy fragments typical of the McKinney pillow lava overlain by laminated Yahoo Clay. The upward change from fragmental basalt to clay takes place in an interval about 8 inches thick, which is characterized by alternating laminae of these contrasting materials.

layers in the upper part. Irregularities on the upper surface of the rubble, which dips steeply toward the river, are filled by laminae of the overlying Yahoo Clay (Figure 7). Like locality 2 at the Shoestring Road Bridge, these features suggest the lack of a hiatus between deposition of the McKinney pillow lava and the Yahoo Clay.

Locality 7. Along a road known as the Tupper Grade, on the east side of Billingsley Creek, which here forms the eastern edge of the Snake River canyon, a new road cut shows that Yahoo Clay overlies Wendell Grade Basalt at an altitude of 3,090 feet (800 feet S., 1,400 feet E., NW cor., sec. 19, T. 7 S., R. 14 E., Tuttle quadrangle). The clay is continuously exposed at least as high as 3,120 feet. The Wendell Grade Basalt here forms a small cascade that spilled from the canyon rim onto talus and landslide debris along the ancestral canyon wall. Much of this old debris is still in place and is now exposed, having been exhumed by erosion of the Yahoo Clay. Remnants of Yahoo Clay are also found in an alcove in the eastern wall of Billingsley Creek ¾ mile to the south (SW¼SW¼ sec. 19). The alcove is evidently inherited from an embayment in the canyon wall that existed when the clay was being deposited.

Locality 8. Excavation of a new ditch to collect spring water from the base of Sand Springs Basalt half a mile downstream from Lower Salmon Falls and about 30 feet above the Snake River (550 feet S., 2,050 feet E., NW cor., sec. 2, T. 7 S., R. 13 E., Hagerman quadrangle) has exposed Yahoo Clay lying against a cliff formed by the basalt and on talus derived from the basalt. The basalt has previously been mapped as part of the Glenns Ferry Formation (Malde and Powers, 1972), but the new exposure shows that all the basalt here is the Sand Springs.

Locality 9. At an altitude of 3,050 feet along the Brailsford Ditch southeast of Hagerman, the terminus of the Thousand Springs Basalt is overlain by Yahoo Clay (the outcrop extends half a mile southeast from 700 feet S., 1,500 feet E., NW cor., sec. 6, T. 8 S., R. 14 E., Tuttle quadrangle). The clay is capped at an altitude of 3,100 feet by a terrace deposit of Crowsnest Gravel. The Thousand Springs Basalt at this locality

Figure 7. Outcrop at the west end of the former siphon for the King Hill Canal (locality 6 on Figure 1) showing laminae of Yahoo Clay that fill irregularities at the upper boundary of blocky rubble. The rubble contains substantial amounts of glassy fragments typical of the McKinney pillow lava. The glassy fragments are visible in the photograph as darker areas of granules and small pebbles, which occur as interstitial material and as larger masses surrounded by the blocks.

has been erroneously mapped as a detached remnant, resting against the lacustrine clay (Malde and Powers, 1972). Instead, the basalt appears to be connected with the main body of the Snake Plain aquifer—hence, with the main body of the Thousand Springs Basalt—as shown by newly exposed springs that discharge from pillow lava at its base. The Thousand Springs Basalt in this outcrop probably rests on the Banbury Basalt, as it does elsewhere.

Locality 10. The canyon stretching upstream from Thousand Springs to Melon Valley, which is cut in Banbury Basalt along the margin of the Thousand Springs Basalt, has many scattered remnants of Yahoo Clay. The highest outcrops of the clay reach an altitude of 3,180 feet, where the clay provides the base level for an upland erosion surface related to the Crowsnest Gravel, now considerably dissected. In places, some of the clay is close to river level. Identifying the clay as Yahoo is consistent with the post-Thousand Springs age of the canyon, but correlating the clay with the Bruneau Formation—a stratigraphic unit much older than the Thousand Springs Basalt—requires highly improbable geologic circumstances.

Locality 11. The canyon wall west and southwest of Hagerman, besides the extensive deposits of Yahoo Clay near Yahoo Creek, has many scattered remnants of the clay, which rest on the dissected Glenns Ferry Formation. The highest remnants reach an altitude of 3,180 feet and are overlain by surficial sand and silt that are considered to be part of the Crowsnest erosion surface.

RELATION TO THE ANCESTRAL CANYON

The reference localities described above show that the Yahoo Clay was deposited in the ancestral canyon of the Snake River as it existed at the time of the eruption of the McKinney Basalt. Near Hagerman, the canyon was limited on the east by the canyon wall of Billingsley Creek, covered in at least one place by a

cascade of Wendell Grade Basalt. On the west the canyon was defined by a wall eroded in the Glenns Ferry Formation. These limits still exist today, having been exhumed by erosion of the clay. The depth was also much like the present, as shown by Yahoo Clay on eroded Sand Springs Basalt near river level at Lower Salmon Falls. Upstream from Hagerman, where the canyon is outlined on the east by a rim of Thousand Springs Basalt, remnants of the clay similarly suggest that the present canyon is simply the exhumed equivalent of the former canyon. As explained elsewhere (Malde, 1971), this reach of the canyon was not cut until after eruption of the Sand Springs Basalt.

FOSSILS

In 1955, D. W. Taylor collected molluscan fossils from the Yahoo Clay west of Hagerman, as well as sediment samples that have yielded identifiable pollen.

From sandy colluvium at the base of the Yahoo (USGS Washington Cenozoic catalog number 19225; center SW¼ sec. 16, T. 7 S., R. 13 E., altitude 2,875 to 2,940 feet, Hagerman quadrangle), Taylor reported the following mollusks (manuscript report, May 23, 1967): *Fossaria dalli* (F. C. Baker), *Lymnaea caperata* Say, *Gyraulus circumstriatus* (Tryon), *Pupilla muscorum* (Linnaeus), *Vertigo ovata* Say, *Vallonia gracilicosta* Reinhardt, *Succinea*?, and *Discus cronkhitei* (Newcomb). In addition, Taylor reported *Lymnaea caperata* from three nearby localities of the brown soil at the top of the Yahoo Clay—all at an altitude of 3,180 feet, and all buried by surficial deposits related to the Crowsnest Gravel—as follows: USGS 19219 (500 feet N., 250 feet E., to 700 feet N., 350 feet E., SW cor., sec. 16, T. 7 S., R. 13 E., Hagerman quadrangle); USGS 19222 (1,525 feet N., 150 feet W., to 1,625 feet N., 50 feet W., SE cor., sec. 17, T. 7 S., R. 13 E.); and USGS 20410 (1,750 feet S., 175 feet W., NE cor., sec. 17, to 1,950 feet S., 350 feet E., NW cor., sec. 16, T. 7 S., R. 13 E.). Although the fauna is modern, Taylor pointed out that some of the mollusks no longer live in the immediate vicinity. *Gyraulus circumstriatus* is characteristic of seasonal ponds, a habitat lacking in southwest Idaho, and its nearest occurrences are at higher elevations in southeast Idaho and northern Nevada. *Vertigo ovata* and *Vallonia gracilicosta* are land snails that might be expected in mountains of southwest Idaho, but their nearest known occurrences are also in the southeast part of the state. Thus, he explains, the fossil mollusks provide some evidence that the summers were less hot and dry than at present, at least during the onset of Yahoo time.

According to E. B. Leopold (written communication, January 24, 1957), a pollen sample collected by Taylor from the brown soil at the site of USGS 20410, which is identified as Pollen Locality D1120, yielded the following counts of pollen grains: *Picea* (16 grains), *Pinus* (2), *Populus* (1), *Abies* (1), Cyperaceae (2), Gramineae (1), Compositae (5), pollen type $P_{20}R$-1 (1), pollen type C_3R-1 (1), unidentified dicots (11), and spores (3). Taylor's sample of Yahoo Clay 3.5 feet below the soil (Pollen Locality D1121) yielded single grains identified as cf. *Lycopodium* and as Gramineae. Colluvium at the base of the Yahoo where Taylor collected USGS 19225 yielded 2 grains of *Pinus* and one of Chenopodiaceae (Pollen Locality D1117). Leopold comments that the abundant spruce pollen in the brown soil (D1120), together with the pollen of pine, poplar, and fir, indicates the presence of trees now found several thousand feet higher in central Idaho. Hence, she suggests that the buried soil formed during a time that was wetter and cooler than the present.

RELATION OF YAHOO CLAY TO PILLOW LAVA OF McKINNEY BASALT

In addition to the outcrops already mentioned, the distribution of Yahoo Clay with respect to the McKinney pillow lava upstream from Bliss supports the conclusion that the clay began to accumulate in McKinney Lake immediately after the pillow lava was deposited. In particular, the Yahoo Clay in the area of the McKinney Basalt is largely limited to the left side of the canyon, in places reaching the canyon floor. McKinney pillow lava, on the other hand, is virtually confined to the right side of the canyon. This distribution of the clay and the pillow lava takes on added significance when it is realized that the existing canyon in this reach closely matches the course of the ancestral canyon when the pillow lava was deposited. It appears that the contact between the pillow lava and the clay was steep and that the pillow lava was deposited first on the right side of the ancestral canyon, leaving the remainder of the canyon to be filled with Yahoo Clay.

Some signs of the steepness of the contact are preserved in the right abutment of the proposed dam and in contiguous outcrops that climb 100 feet higher a short distance upstream (locality 1 described above). A steep contact of clay on pillow lava is also expressed by the field relations a mile south of Bliss (locality 3 described above).

The existence of discrete depositional areas for the pillow lava and the clay, and the evidence of a steep

Figure 8. Deltaic foreset beds of McKinney pillow lava plunging to the left (southwest) over Madson Basalt, seen here at the lower right, which formed the rim of the ancestral Snake River canyon (locality P on Figure 1). The pillow lava terminates upward, more or less abruptly, at an altitude of 3,175 feet and is overlain by a subaerial lava flow of McKinney Basalt, which forms the present canyon rim. The outcrop is a roadcut on U. S. Highway 30 (2,000 feet N., 1,100 feet W., SE cor., sec. 21, T. 6 S., R. 13 E., Bliss quadrangle).

contact between them, are understandable from the origin and mode of deposition of the McKinney Basalt. McKinney lava spilled southward and westward into McKinney Lake, building steeply inclined beds of subaqueous pillow lava that advanced into the canyon until the supply of lava ceased. Meanwhile, lava flows at the level of the upland advanced over the subaqueous pillow lava much like the advance of topset beds over the foreset beds of a delta. The result was a rim of lava flows along the right side of the canyon from which a face of pillow lava plunged steeply to the bottom of the lake (Figure 8). Because the lava flows of the canyon rim are subaerial, their contact on the pillow lava marks the level of McKinney Lake when these lavas were deposited. On this basis, lake level was at times as high as about 3,175 feet, virtually the same as the altitude of the highest deposits of Yahoo Clay. The floor of the lake was in places at least as low as an altitude of 2,550 feet, or 100 feet below present river level, as shown by the base of the McKinney pillow lava under the right abutment of the proposed dam (Idaho Power Company drill hole DH-69, 2,550 feet S., 1,950 feet E., NW cor., sec. 12, T. 6 S., R. 12 E., Bliss quadrangle).

DRAINAGE OF McKINNEY LAKE

The geologic record of McKinney Lake suggests that its lava dam was more or less tight but also that the dam was surprisingly leaky. On the one hand, the lava dam was capable of holding water deep enough to account for deposits of pillow lava that reach the canyon rim, and to account for deposits of lacustrine clay that reach virtually the same height. On the other hand, the geologic record shows that McKinney Lake must have leaked voluminously throughout its lifetime, and that it leaked enough to prevent overflow of the lava dam. The path of leakage could only have

been via the canyon fill of McKinney pillow lava and thence through the lava dam of McKinney Basalt farther downstream. The evidence of a lava dam that was surprisingly leaky, yet effective in obstructing the ancestral Snake River, is the subject of the remarks that follow. Besides the significance of this discussion for understanding the local late Pleistocene history, the example of Lake McKinney may be of interest when considering the geomorphic consequences of other lava dams on the Snake River.

The argument that McKinney Lake leaked voluminously is based on the inference that the lake could not have overflowed for any substantial period of time while the Yahoo Clay was being deposited. Overflow, if it had occurred, would have brought running water in contact with clays and silts of the Glenns Ferry Formation at the southern margin of the lava dam, and rapid erosion of these poorly consolidated sediments would have lowered the lake level, thus preventing buildup of the clay to its observed height. The clay, in fact, as explained above, accumulated throughout the area of McKinney Lake to an altitude of 3,180 feet, a height only slightly below the highest McKinney lava flow in the area of the lava dam. Clearly, the lake surface was virtually at the level of the lava dam when the last of the clay was being deposited. Eventually, of course, McKinney Lake did overflow, downcutting in the Glenns Ferry Formation was thereby initiated, and the lake was progressively lowered. The process of downcutting ultimately formed the present canyon of the Snake River west of Bliss.

The conclusion is inescapable that water was discharged from McKinney Lake not by overflow but by leakage through the canyon-filling McKinney Basalt. Evaporation from McKinney Lake probably was not greater than the present annual evaporation of 37 inches (Meyers, 1962, plate 3) and obviously would have been insufficient to prevent overflow, given the large discharge of the Snake River. (The discharge is discussed below.) Further, the geologic evidence suggests that the lake leaked at a more or less controlled rate, thus maintaining a high stand of lake water, not only when the last of the Yahoo Clay was accumulating, but also when the McKinney pillow lava was being deposited. A condition of equilibrium is implied. The water level was probably achieved and maintained by a relationship between the hydrostatic pressure, the rate of leakage, and the cross-sectional area of the canyon-filling McKinney Basalt at a given depth of lake water. As mentioned below, the accumulation of Yahoo Clay must also have influenced the rate of leakage.

The volume of water lost from McKinney Lake by leakage through the McKinney lava dam must have been substantial, and this loss must have been maintained continuously while the Yahoo Clay was being deposited. The present discharge of the Snake River at this place averages 10,720 cubic feet per second and amounts to about 8 million acre-feet annually (U. S. Geological Survey, 1974, streamflow data for Snake River at King Hill). To this amount must be added the water depleted for irrigation, which is typically 2.5 million acre-feet annually (Simons, 1953). Thus the present annual discharge is about 10.5 million acre-feet. Probably the late Pleistocene discharge of the Snake River was even greater.

The conclusion that McKinney Lake lost water by seepage must be considered in light of the evidence for present-day leakage through the McKinney Basalt. The concealed lava dam formed by the basalt, given the low hydrostatic head produced by the present Snake River, now leaks only a small amount, although the river flows on permeable canyon-filling deposits of McKinney pillow lava that are obviously connected with the lava dam. The leakage is thought to be represented by a discharge of somewhat more than 200 cubic feet per second that rises in the bed of the Snake River at Bancroft Springs, 9 miles downstream, where the canyon-filling McKinney Basalt is intercepted by the present canyon (data credited to Carl Tappan, in an unpublished Idaho Power Company report, "A J Wiley Hydro Electric Development," June 5, 1953). The above-river flow from Bancroft Springs is only 17 cubic feet per second (Decker and others, 1970). Probably, the explanation for the small amount of leakage under existing conditions lies in the characteristics of the concealed canyon-filling deposits between Bliss and Bancroft Springs, which are still to be investigated by drilling. The hydrologic properties of McKinney Basalt above present river level, within the vertical range of the Yahoo Clay, are also uncertain.

A final matter worthy of consideration is the means by which the water in McKinney Lake was channeled to the leaky lava dam. Conclusions about the path of leakage are necessarily speculative, but geologic relations suggest that the lake leaked primarily by underflow through the McKinney pillow lava. Most significantly, like the clay used to seal man-made reservoirs, the deposition of the Yahoo Clay almost surely impeded direct leakage from McKinney Lake. Also, leakage from the upper few feet of the lake when it became nearly filled with clay cannot be assumed to have been sufficient to discharge the full flow of the Snake River—although some leakage at this level presumably took place until it was reduced by further buildup of the clay. In short, substantial flow through pillow lava under the Yahoo Clay is indicated.

REVISED AGE OF CROWSNEST GRAVEL

The fluvial deposits in Hagerman Valley that are known as the Crowsnest Gravel were previously thought to represent an episode of aggradation during canyon cutting associated with the late Pleistocene lava flows of the area. In particular, the gravel was thought to be older than the Sand Springs Basalt, which terminates 300 feet lower on the canyon floor, and hence was considered to be older than the McKinney Basalt (Malde, 1971). It is now clear, however, that the Crowsnest Gravel rests on a surface that was formed during dissection of the Yahoo Clay, and that the gravel is younger than the McKinney Basalt. Accordingly, the Crowsnest Gravel of the Hagerman area is here assigned to a stratigraphic position above the Yahoo Clay.

Downstream from Hagerman, deposits identified as Crowsnest Gravel are not found until the area around King Hill. These deposits form a terrace that appears to have been deeply incised by canyon cutting before eruption of the McKinney Basalt. Thus, although the field relations have not yet been examined from the perspective of the findings discussed here, it is probable that the deposits called Crowsnest Gravel downstream from Hagerman are older than the McKinney Basalt and, hence, have been wrongly correlated with the typical deposits at Hagerman.

DISCUSSION

The stratigraphic relations described here, besides resolving several inconsistencies in my previous understanding of the local geology, provide a new perspective on the Pleistocene history of the western Snake River Plain. On the one hand, the discovery that the McKinney Basalt is associated with a thick body of lake deposits—the Yahoo Clay—explains puzzling and contradictory relations of lake clay to the Thousand Springs Basalt, the Sand Springs Basalt, and the McKinney Basalt itself, as represented on published geologic maps. Furthermore, placing the Yahoo Clay in its proper stratigraphic position makes its presence in a canyon of late Pleistocene age fully comprehensible, whereas the prior assignment of the lake clay to the Bruneau Formation was physiographically improbable. The Bruneau Formation, on the other hand, is now found to be limited to the area west of Bliss, at least in its exposed deposits. Consequently, the evidence that mollusks and pollen from lake clay upstream from Bliss indicate relatively cool and moist conditions applies to the Yahoo, not to the Bruneau.

The conclusion that the McKinney lava dam maintained the height of its impounded water through a controlled process of leakage suggests a mechanism that may explain comparatively thick sections of lacustrine deposits behind other lava dams in the region, such as those of the Bruneau Formation farther west (Malde, 1965). Overflow of such lava dams, unless entirely across basaltic rocks, probably would have caused rapid downcutting and would have prevented the buildup of lake deposits. In other words, the presence of a substantial thickness of lake deposits behind a lava dam appears to be related to the leakiness of the dam and to the resulting delay in initiating a new canyon by overflow.

The revised age of the Crowsnest Gravel is of interest for comprehending the late Pleistocene history, to the degree that the gravel may reflect climatic conditions that influenced the regimen of the ancestral Snake River. It has been suggested that deposition of the Crowsnest may have coincided with mountain glaciation (Malde and Powers, 1962, p. 1215). If so, the glacial episode was younger than the McKinney Basalt. By the same token, the older gravel downstream from Bliss, which I have mistakenly correlated with Crowsnest Gravel in previous reports, may represent glaciation older than the McKinney Basalt.

ACKNOWLEDGMENTS

I thank Peter Leitzke of the Federal Energy Regulatory Commission for arranging a field conference on October 20-21, 1980, to review the geology of the McKinney Basalt and the Yahoo Clay. Douglas E. Sprenger and Donald E. Westcott, representing the Idaho Power Company, participated in the field conference and freely provided stratigraphic and other geological information from their investigations of the proposed dam site at Bliss. Some of the geologic features described here were also reviewed in the field with Harry R. Covington, Robert L. Schuster, and Richard L. Whitehead, all of the U. S. Geological Survey, and I am grateful to them for their advice and counsel.

REFERENCES

Decker, S. O., R. E. Hammond, L. C. Kjelstrom, and others, 1970, Miscellaneous streamflow measurements in Idaho, 1894-1967: U. S. Geological Survey, Boise, Idaho, Basic-Data Release, 310 p.

Malde, H. E., 1965, Snake River Plain, *in* H. E. Wright, Jr., and D. G. Frey, editors, The Quaternary of the United States, A Review Volume for the VII Congress of the International Association for Quaternary Research: Princeton, New Jersey, Princeton University Press, p. 225-263.

———, 1968, The catastrophic late Pleistocene Bonneville Flood in the Snake River Plain, Idaho: U. S. Geological Survey Professional Paper 596, 52 p.

———, 1971, History of Snake River canyon indicated by revised stratigraphy of Snake River Group near Hagerman and King Hill, Idaho, with a section on paleomagnetism by Allan Cox: U. S. Geological Survey Professional Paper 644-F, 21 p.

Malde, H. E. and H. A. Powers, 1962, Upper Cenozoic stratigraphy of the western Snake River Plain, Idaho: Geological Society of America Bulletin, v. 73, p. 1197-1220.

———, 1972, Geologic map of the Glenns Ferry-Hagerman area, west-central Snake River Plain, Idaho: U. S. Geological Survey Miscellaneous Geologic Investigations Map I-696.

Meyers, J. S., 1962, Evaporation from the 17 western States: U. S. Geological Survey Professional Paper 272-D, p. 71-100.

Simons, W. D., 1953, Irrigation and streamflow depletion in Columbia River basin above The Dalles, Oregon: U. S. Geological Survey Water-Supply Paper 1220, 126 p.

U. S. Geological Survey, 1974, Surface water supply of the United States, 1966-70, Part 13, Snake River basin: U. S. Geological Survey Water-Supply Paper 2134, 821 p.

Canyon-Filling Lavas and Lava Dams on the Boise River, Idaho, and Their Significance for Evaluating Downcutting During the Last Two Million Years

by

K. A. Howard[1], J. W. Shervais[2], and E. H. McKee[1]

ABSTRACT

Basalts that periodically dammed the Boise River and its South Fork over the last 2 million years reveal the canyon history and illustrate how lava interacted with impounded river water. Intracanyon basalt flows record a granite canyon successively filled by lava and then recut at least five times in the last 2 million years. The most voluminous flow, Steamboat Rock Basalt, reached 60 kilometers downstream and spread out on the Snake River Plain just east of Boise. Lavas that reached the river were erupted from vents bordering the main canyon and adjacent tributaries. The river canyon was periodically flooded by basalt from these eruptions, reentrenched to a new lower level, then flooded again. This succession resulted in terraces of older flows high above the river and of younger flows lower on the canyon walls. The canyon-filling flows dammed the river and created deltas of pillow basalt and hyaloclastite overlain by massive subaerial basalt. Foreset beds in the hyaloclastite deposits and inclined pillows indicate flow into reservoirs behind the lava dams. A well-documented example of a lava dam is the one formed by the Smith Prairie Basalt, which is about 0.2 million years old. Potassium-argon ages calibrate a canyon history in which the river was lowered at a rate between 0.005 and 0.01 centimeter a year over the last 2 million years. The lava dams interrupted this lowering but were each rapidly incised in about a quarter of a million years at rates averaging 0.03 to 0.07 centimeter a year.

INTRODUCTION

Basalt terraces along the granite canyons of the Boise River show that successive lava dams up to 60 kilometers long alternated with downcutting. The dam and the deltas of foreset pillow basalt formed by the Smith Prairie Basalt are particularly well displayed. We examine here the building and incision of the lava dams and the canyon history over the last 2 million years, based on detailed mapping of the Smith Prairie area (Howard and Shervais, 1973) and reconnaissance elsewhere along the Boise River (Shervais and Howard, 1975). Three manmade reservoirs obscure some of the geologic relationships along the Boise River canyon, but we have reconnoitered the basalt terraces exposed during low water in Arrowrock Reservoir and have made use of unpublished engineering reports on the dam sites and topographic maps of the reservoir areas prepared by the Bureau of Reclamation and the Corps of Engineers. Rates of downcutting are calculated from potassium-argon ages of the basalts.

SETTING

The Boise River and its South Fork drain highlands of the Idaho batholith just north of the Snake River Plain (Figure 1). The river flows through canyons several hundred meters deep, largely in granitic bedrock. Lindgren (1898, 1900) and Russell (1902) observed that basalt terraces follow the canyon for 80 kilometers (Figure 2). The lava flows erupted onto the granitic highlands near the river, forming outliers related to the basalts of the Snake River Plain. The river canyon was periodically flooded by basalt from these eruptions, reentrenched to a new level deeper than before, and then flooded again. This history has resulted in terraces of older intracanyon flows high above the river and rimrock benches of younger flows lower on the canyon walls (Crosby, 1911). These relations are illustrated in cross sections and a longitudinal profile

[1]U. S. Geological Survey, Menlo Park, California 94025.
[2]Department of Geological Sciences, University of California, Santa Barbara, California 93106.

Howard, K. A., J. W. Shervais, and E. H. McKee, 1982, Canyon-filling lavas and lava dams on the Boise River, Idaho, and their significance for evaluating downcutting during the last two million years, *in* Bill Bonnichsen and R. M. Breckenridge, editors, Cenozoic Geology of Idaho: Idaho Bureau of Mines and Geology Bulletin 26, p. 629-641.

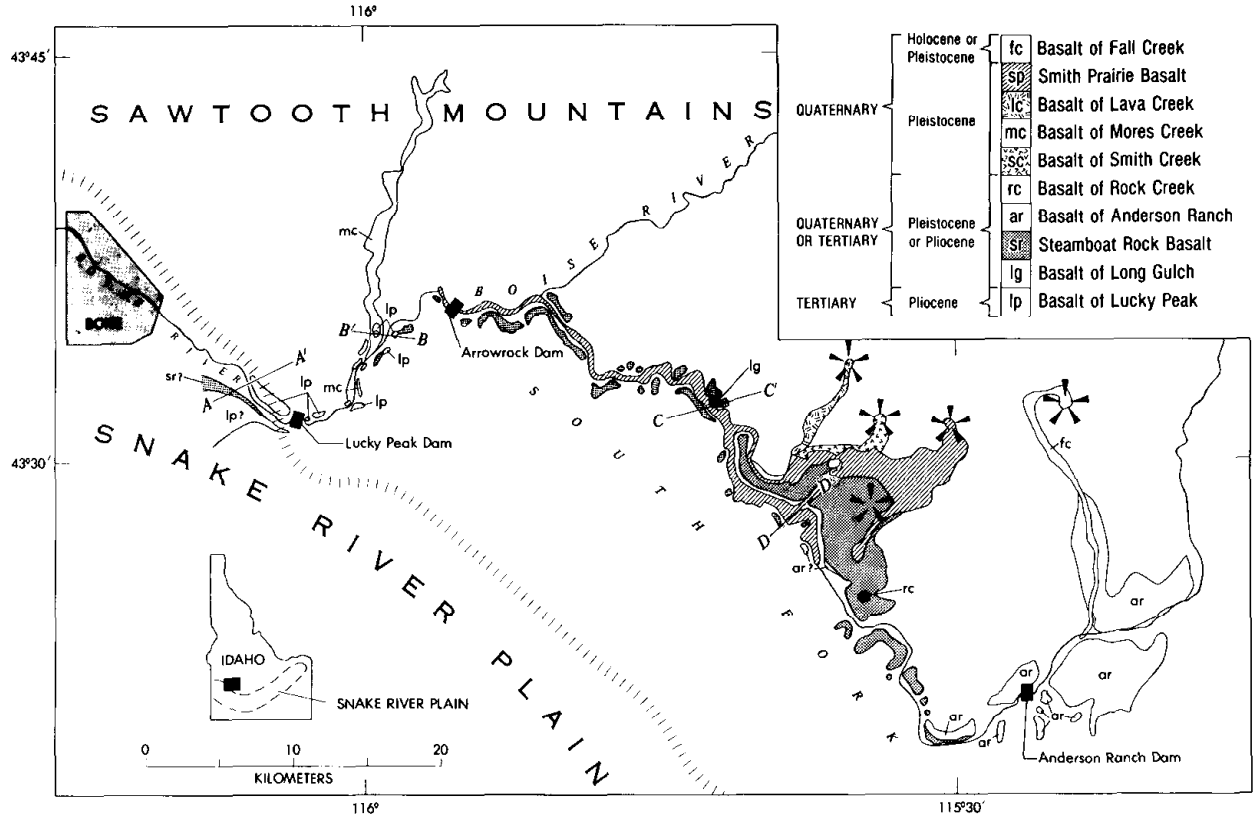

Figure 1. Generalized map of intracanyon basalt flows along the Boise River, Idaho. Star symbols indicate vents. Cross sections shown in Figure 3.

along the canyon showing the elevations of flow tops (Figure 3).

BASALT FLOWS

A correlation chart (Figure 4) shows ten recognized basalt units. Older basalt flows probably once were present, as suggested by a variety of basalt cobbles in old gravels beneath the Steamboat Rock Basalt at Long Gulch. Vent locations are known for five of the basalts (Figure 1). Detailed descriptions of the basalt of Long Gulch, basalt of Rock Creek, basalt of Smith Creek, Steamboat Rock Basalt, and Smith Prairie Basalt are given by Howard and Shervais (1973). The Steamboat Rock and Smith Prairie Basalts form the most extensive terraces.

Basalt of Lucky Peak is exposed in cliffs as a single thick flow unit overlying gravel and forming terraces downstream from Lucky Peak Dam (Figure 3, section A-A′). We correlate this basalt with a single hackly jointed basalt flow 40 meters thick that rims Lucky Peak Reservoir at the mouth of Mores Creek, against which the younger Steamboat Rock Basalt is juxtaposed (Figure 3, section B-B′).

Basalt of Long Gulch is known only from one exposure at Long Gulch, where two flows of this unit, separated by gravel, lie below another gravel bed, that in turn is covered by the Steamboat Rock Basalt. The stratigraphy indicates that each of these flows formed the canyon floor before the canyon was filled by the Steamboat Rock Basalt.

Steamboat Rock Basalt occurs in numerous pahoehoe flow units 2 to 20 meters thick, forming a rimrock high above the Boise River South Fork from Smith Prairie to Lucky Peak Reservoir (Figure 2a). Its shield-volcano source is a broad tableland known as Smith Prairie. The basalt fills an ancestral canyon broader and shallower than the present one and is as much as 150 to 180 meters thick. Downstream beyond Lucky Peak Dam, a ledge of basalt that probably correlates with the Steamboat Rock Basalt occurs at an elevation lower than the basalt of Lucky Peak and continues out onto the Snake River Plain as a layer 25 meters thick near Boise. The Steamboat Rock Basalt thus flowed at least 60 kilometers downstream from its source to the Snake River Plain and had an original volume of

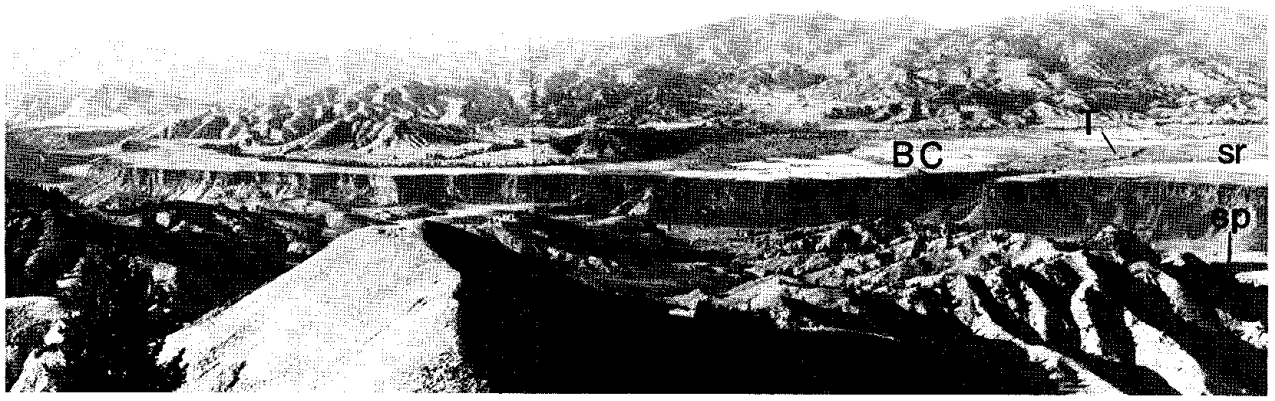

Figure 2a. View northward of high terrace of Steamboat Rock Basalt (sr) and a lower terrace formed by the younger Smith Prairie Basalt (sp) above the Boise River South Fork. The Smith Prairie Basalt reached the river canyon from the high plateau of Smith Prairie (*right*) via a lava tube (T) and spillover at Black Canyon (BC).

several cubic kilometers. It has since been deeply incised.

Basalt of Anderson Ranch, which occurs upstream on the South Fork around Anderson Ranch Reservoir, forms rimrock composed of many flow units high above the river bed. More than one basalt flow may be present. Malde and others (1963) correlated this rock with the Pleistocene Bruneau Formation, part of the Idaho Group in the Snake River Plain. The elevation difference between the top and lowest exposure of the basalt (C. J. Okeson, U. S. Bureau of Reclamation, written communication, 1969) gives a minimum thickness of about 180 meters near Anderson Ranch Dam. Two outcrops downstream that possibly represent remnants of this basalt form a terrace 30 meters lower and probably younger than the Steamboat Rock Basalt. One outcrop is on the southwest flank of Smith Prairie (sec. 10, T. 1 N., R. 7 E.), and the other is nearby Steamboat Rock itself. These were originally assigned to the Steamboat Rock Basalt by Howard and Shervais (1973).

Basalt of Rock Creek is exposed over a small area, where it rests on the Steamboat Rock Basalt; it is at most 10 meters thick.

Basalt of Smith Creek forms a flow 8 kilometers long in Smith Prairie, mostly along the margin of the older and underlying Steamboat Rock Basalt (Figure 5A). The flow, which does not reach the river canyon, was erupted from a now-dissected cinder cone on Smith Creek. The basalt of Smith Creek is distinctive in that it contains numerous granitic xenoliths. Rare granitic xenoliths are also known from the basalts of Lava Creek and Fall Creek.

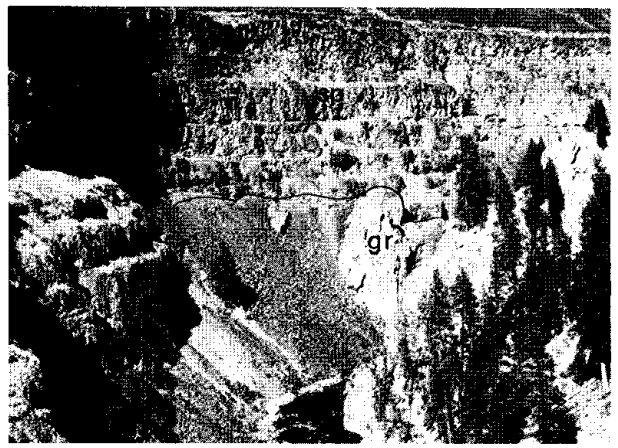

Figure 2b. Terrace (t) underlain by Smith Prairie Basalt showing numerous flow units in an ancestral canyon that is incised in light-colored granodiorite (gr).

Basalt of Mores Creek forms terraces along the canyon of Mores Creek, a tributary to the Boise River at Lucky Peak Reservoir. The basalt ledges continue downstream along the river in the reservoir at a lower elevation than the older basalt of Lucky Peak and the Steamboat Rock Basalt. Ledges at elevations appropriate for the basalt of Mores Creek occur within the western part of the reservoir, according to a detailed topographic map of the reservoir basin (Corps of Engineers, 1958). A flow not far above the river bed at Lucky Peak Dam (Corps of Engineers, 1949, 1951-1955), now excavated, probably was a continuation of the basalt of Mores Creek.

Basalt of Lava Creek forms an aa flow 10 kilometers long from a slightly eroded cinder cone

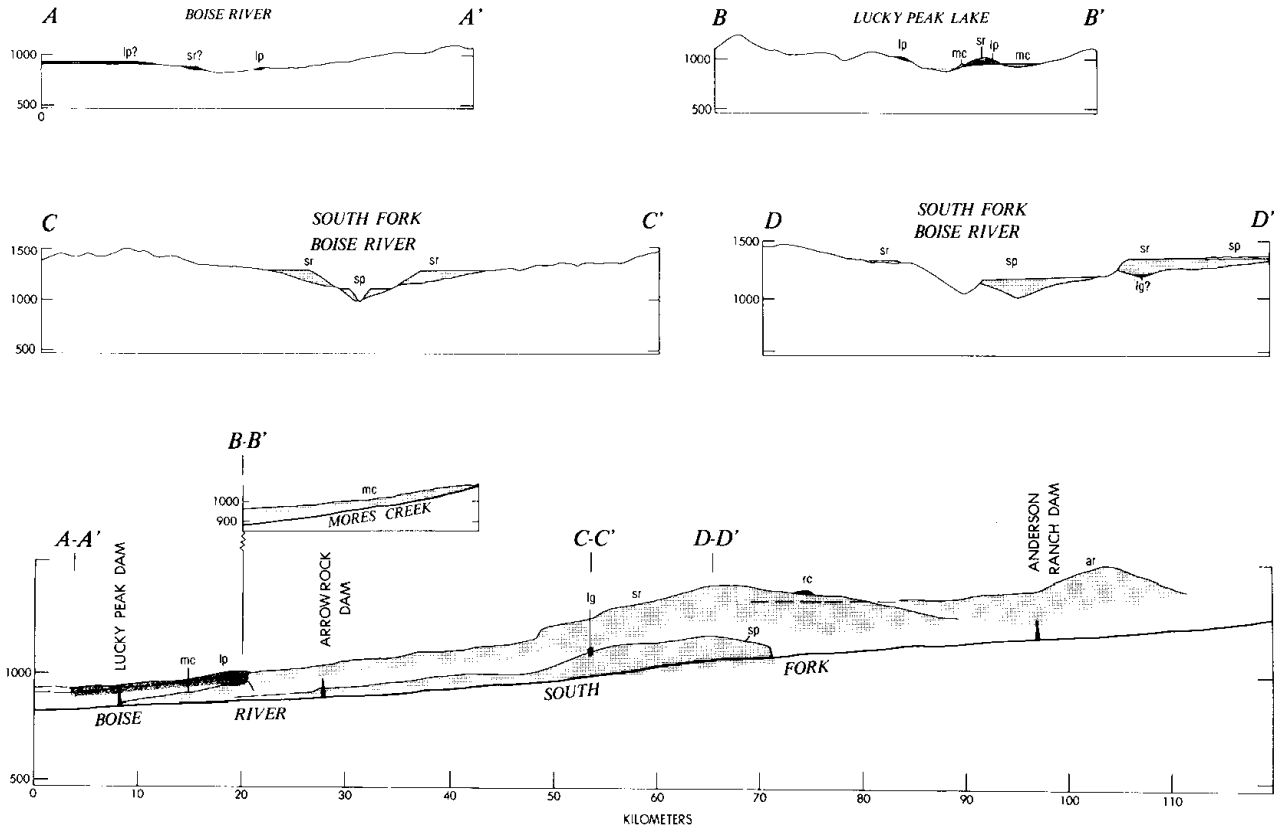

Figure 3. *Top.* Cross sections of river canyon at true scale at places A-A′, B-B′, C-C′, and D-D′ indicated in Figure 1 and bottom of Figure 3. Elevations in meters. *Bottom.* Longitudinal profile, constructed along the present Boise River and its South Fork, showing elevations (in meters) of tops and (poorly constrained) lowest exposed bottoms of basalt flows. Inset shows tributary Mores Creek. Vertical scale exaggerated 20X. Basalt units as follows: sp, Smith Prairie Basalt; mc, basalt of Mores Creek; rc, basalt of Rock Creek; ar, basalt of Anderson Ranch; sr, Steamboat Rock Basalt; lg, basalt of Long Gulch; lp, basalt of Lucky Peak.

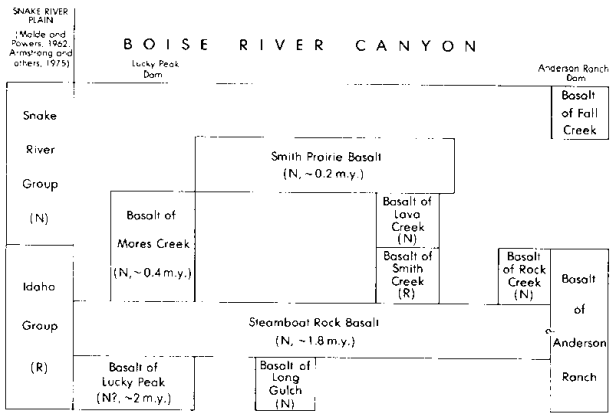

Figure 4. Correlation chart of intracanyon flows along Boise River from northwest (*left*), downstream to southeast (*right*), upstream. Potassium-argon ages reported in this paper and reconnaissance field measurements of magnetic polarity (N, normal; or R, reversed) are indicated. Correlation with Idaho and Snake River Groups (Malde and Powers, 1962; Correlation with Idaho and Snake River Groups (Malde and Powers, 1962; Armstrong and others, 1975) is based on surface preservation (Howard and Shervais, 1973), polarity, and potassium-argon ages.

near Smith Prairie. The flow lapped over the Steamboat Rock Basalt and basalt of Smith Creek but did not extend to the river canyon (Figure 5A).

Smith Prairie Basalt is the best known lava flow of the area (Howard and Shervais, 1973) and illustrates well the processes of canyon filling and building of a lava dam. The basalt overlies the Steamboat Rock Basalt and the basalts of Smith Creek and Lava Creek. It erupted after the South Fork of the Boise River had cut through the Steamboat Rock Basalt and an additional 150 meters of granodiorite. Two of three tongues of the Smith Prairie Basalt spill through notches over a high rimrock of eroded Steamboat Rock Basalt (Figure 2a) and join a fill of basalt up to 150 meters thick in the river canyon (Figure 2b). Remnants of this lava fill occur 35 kilometers downstream in Lucky Peak Reservoir; one remnant forms part of the foundation for Arrowrock Dam. The lava surface and vents of the Smith Prairie Basalt are fresh and little eroded except in the river canyon, where downcutting has exposed nearly the complete

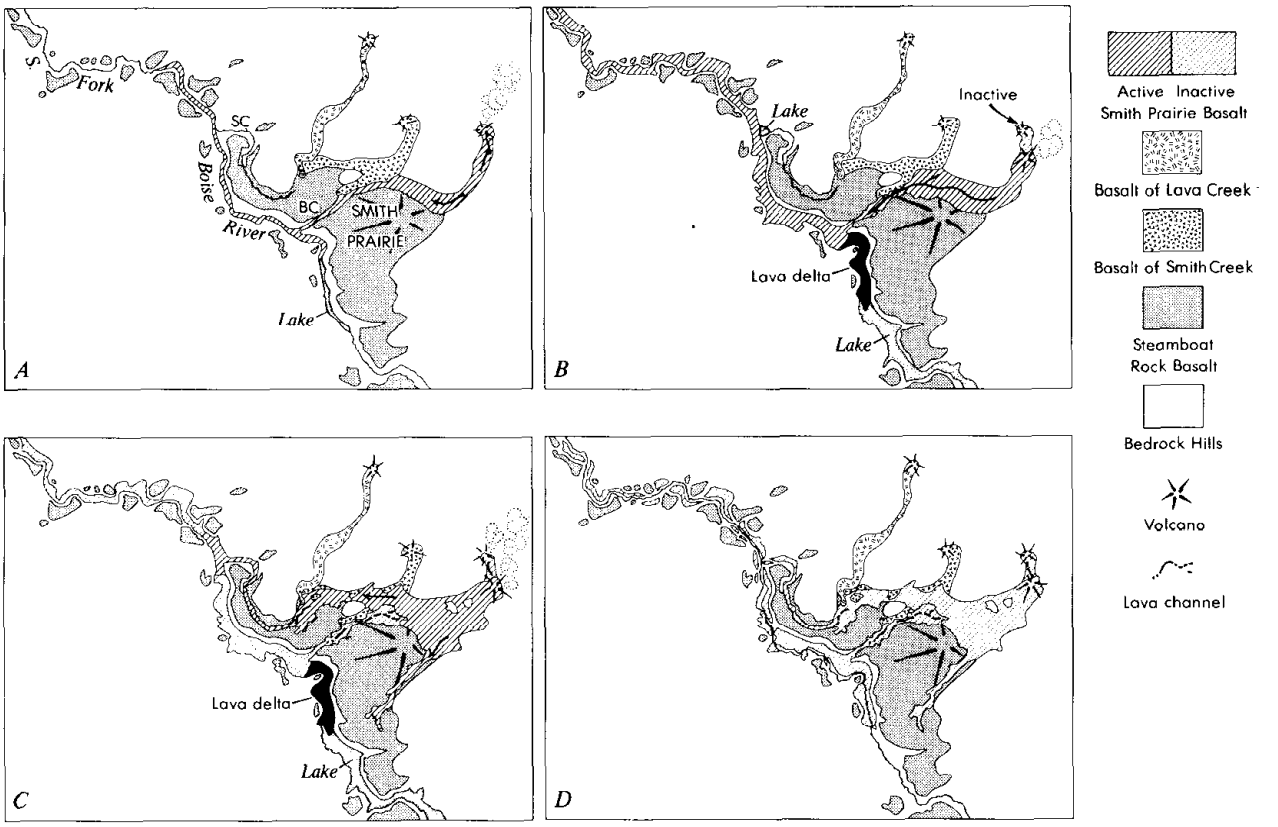

Figure 5. Maps of Smith Prairie area showing sequential development of Smith Prairie Basalt (Howard and Shervais, 1973). Vents for each flow are indicated by radial symbol. Heavy line indicates lava tubes. SC, Smith Creek; BC, Black Canyon. Panel D shows the Smith Prairie Basalt after erosion.

150 meter thickness of the canyon fill. Pillow basalt in a lava delta associated with the intracanyon flow will be described in a later section. The eruptive history can be summarized as follows (Figure 5A-C).

The initial eruption of porphyritic Smith Prairie Basalt built a cone of cinder and agglutinate 90 meters high near Smith Prairie (Figure 5A). A thin lava stream from this vent flowed 10 kilometers through Smith Prairie, around a broad shield of the Steamboat Rock Basalt and along a creek bed to the rimrock edge of Smith Prairie, where it cascaded 340 meters in elevation through Black Canyon (BC in Figure 2a) across rimrock of the Steamboat Rock Basalt to the floor of the ancestral South Fork. Two flow units of this early porphyritic basalt, with a combined thickness of 15-25 meters, crop out 8 to 10 kilometers downstream in the thalweg of the lava fill in the river canyon; the modern Boise River South Fork has not yet cut through to the base. The uppermost of these flow units has an aa clinker top, in contrast to the pahoehoe nature of the rest of the Smith Prairie Basalt.

Eruption of microporphyritic basalt from a new shield vent 1.5 kilometers south of the cinder cone followed the same path and filled the river canyon to a depth of 120 meters with ten or more flow units (Figure 5B) having a total volume of approximately 0.5 cubic kilometer. This huge fill, more than 35 kilometers long, was fed by a lava tube only 10 meters wide (T in Figure 2a) that developed just upstream from Black Canyon. Stearns and others (1938) described an analogous lava tube that drained the Sand Springs Basalt into the Snake River canyon. Insulated flow in lava tubes allows for long distance transport of pahoehoe in Hawaii (Peterson and Swanson, 1974). Surprisingly, we found no evidence for tubes in the long canyon fill of Smith Prairie Basalt or in any of the other basalt canyon fills.

Eventually, another tongue of lava made its way off Smith Prairie by following the narrow gully of Smith Creek to the river canyon (Figure 5C). A lava tube also developed just upstream from this gully. The tongue deposited a single flow unit of relatively viscous, pressure-ridged basalt up to 30 meters thick on the thick basalt fill already in the river canyon. Pahoehoe festoons in the underlying basalt fill show that it had reached the river via Black Canyon and

flowed up Smith Creek from the river canyon.

The final basalt to erupt from the shield vent was more viscous than earlier flows, as suggested by numerous pressure ridges and by increased phenocryst content nearer the vent; it sent off a third tongue of lava 6 kilometers long on Smith Prairie (Figure 5C).

Basalt of Fall Creek originates at a fresh cinder cone named Red Mountain. The lava forms a narrow rough-surfaced tongue down the canyon of Fall Creek. Observations made before Anderson Ranch Dam was built show the basalt extending onto the present floor of the reservoir (C. J. Okeson, U. S. Bureau of Reclamation, written communication, 1969). This position on the reservoir floor suggests that the basalt of Fall Creek is younger than the Smith Prairie Basalt downstream, which is now deeply dissected by the Boise River South Fork (Figure 2b).

FLOW OF LAVA INTO WATER

Many lava flows in the Pacific Northwest have blocked stream drainages, often resulting in deltas of pillow lava and fragmented basaltic glass, and lake beds deposited on the upstream side of the lava dam (Russell, 1902; Wright, 1906; Fuller, 1931; Stearns, 1931; Stearns and others, 1938; Peterson and Groh, 1970; Malde, 1965, 1971, 1982 this volume; Waters, 1960; Brown, 1969). The dam formed by the Smith Prairie Basalt provides an unusually well-displayed example of pillow-lava deltas. The Steamboat Rock Basalt also exposes part of its delta.

Pillow basalt alternates with subaerial pahoehoe in the upstream part of the canyon fill of the Smith Prairie Basalt, showing that the lava repeatedly built deltas into a reservoir of river water dammed behind it (Figures 6, 7). The basalt pillows (Figures 8 and 9) have glassy margins, are between 0.1 and 1 meter across, and are elongate and interconnecting like those described by Jones (1968), Moore (1970), and Moore and others (1971, 1973). The elongate pillows plunge upstream, in the direction of lava flow, at angles up to 90 degrees but averaging about 30 degrees. A small amount of hyaloclastic debris fills the interstices between pillows. The external mold of a horizontal log 0.3 meter across was found in the pillows.

The upper, approximately horizontal contact of each layer of pillow basalt of the Smith Prairie Basalt is gradational with overlying massive subaerial basalt. Elongate pillow fingers connect with and extend down from massive columnar basalt at the contact (Figure 9a). This contact, termed the passage

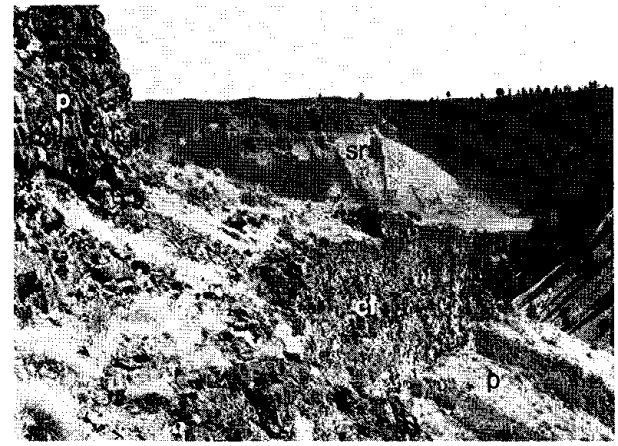

Figure 6. Foreground shows interlayered pillow basalt (p, typically covered by talus) and subaerial basalt in dam of Smith Prairie Basalt upstream from Black Canyon. Cliff-forming subaerial basalt of Cougar Flat flow unit (cf) grades down through a passage zone into underlying pillow basalt and is overlain by pillow basalt of a younger flow unit. High rimrock beyond is Steamboat Rock Basalt (sr).

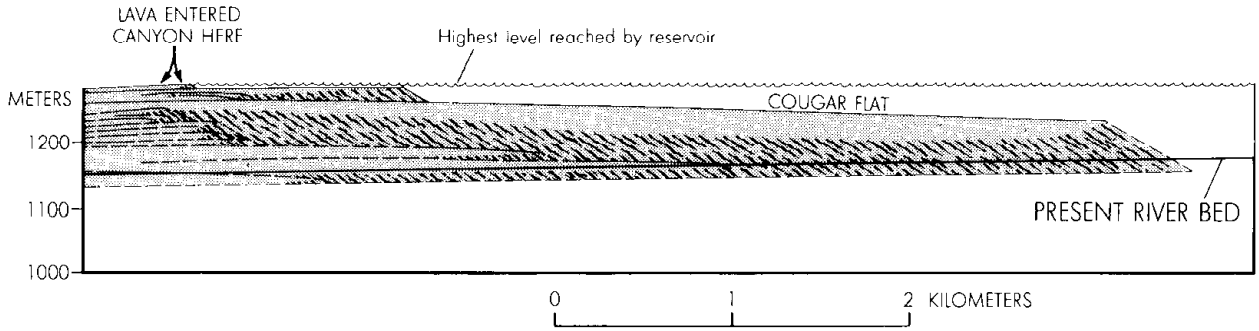

Figure 7. Reconstructed longitudinal section of the lava delta on the upstream face of (shaded) dam formed by the Smith Prairie Basalt. Several flow units of massive basalt grade downward into pillow basalt (wavy lines). Dashed where inferred. Much of the pillow basalt is concealed under talus slopes. The delta is 0.4 kilometer wide and 6 kilometers long. The reservoir backed behind the dam was upriver to the right.

Figure 8. Pillows in Smith Prairie Basalt, here nearly free of fragmental hyaloclastic material.

zone by Jones and Nelson (1970), indicates the water level at the time of emplacement of a flow unit that built its own delta of pillow "foresets" topped by subaerial pahoehoe "topsets." A section through the lava dam, as reconstructed in Figure 7, shows that wedges of pillow foresets thicken upstream in the river canyon from the crest of the lava dam and that subaerial basalts thin upstream. It can be concluded from this relationship that successive layers of the lava dam each built deltas out into the reservoir backed behind the dam, and that the water level rose and overtopped the lava between the delta-building episodes (Figure 10).

Changes in the elevation of the passage zone are interpreted to record fluctuations in water level (Jones and Nelson, 1970; Furnes and Fridleifsson, 1974). The passage zone in the largest exposed delta (Cougar Flat flow unit of Smith Prairie Basalt, Figure 7) drops 40 meters as the delta is traced upstream, then rises 40 meters as the subaerial part of the flow unit thins out. This suggests that the lake lost water, perhaps by evaporation or leakage, during the initial building of this delta, then the lava supply slowed as the lake rose and overtopped the subaerial lava.

The lake held about 0.4 to 0.5 cubic kilometer of water when full, a volume approximately equal to the basalt volume in the dam. The lake may have overflowed from time to time and was full when the last lava was emplaced, as indicated by pillow basalt nearly at the crest of the lava dam. The average supply of water therefore exceeded the average supply of lava. At the modern average discharge of the river (about 30 cubic meters per second as extrapolated from gauging records in U. S. Geological Survey, 1968), the lake would have filled, if leakage is discounted, in about six months. Pillow lavas at the mouths of Smith and Trail Creeks show that water backed up these tributaries while the dam was still building. If the average supply rate of lava to the dam through its lava tube were comparable to the tube discharge at the 1969-1971 eruption of Kilauea Volcano (Swanson, 1973; Swanson and others, 1971), the dam could have been built in 4-6 years. The copious 1783 eruption at Lakagicar in Iceland built a dam 100 kilometers long and as much as 180 meters thick in only a month (Stearns, 1931; Thorarinsson, 1969).

The Steamboat Rock Basalt also formed deltas where it flowed into water dammed behind it. An exposure on the south side of Smith Prairie (Howard and Shervais, 1973) displays subaerial basalt passing downward across a horizontal passage zone into foreset-bedded fragmental basaltic glass, containing lenses of pahoehoe, pillows, and pillow fragments, which together dip 30 degrees upriver (Figure 11). The subaqueous interval is more than 50 meters thick measured vertically. This exposure strikingly resembles a lava delta formed by the flow of lava into the sea from Kilauea Volcano in 1971 (Moore and others, 1973, Figure 4). Deltaic lava that is transitional between bedded breccia and pillow basalt is represented by an exposure of pillows in hyaloclastite matrix 2.3 kilometers to the south (Figure 12). The pillows and breccia underlie claystone lake beds and unconformably overlie arkosic colluvium. The claystone appears to underlie higher flow units of Steamboat Rock Basalt. These relationships record a complex sequence of canyon cutting, colluviation, erosion of arkosic talus, damming of the river by the Steamboat Rock Basalt, advance of a lava delta into the reservoir backed behind the dam, deposition of lake beds, and ultimate eruption of final parts of the Steamboat Rock Basalt. Material for the delta of Steamboat Rock Basalt probably was supplied across a broad front, in contrast to the simple point at which the Smith Prairie Basalt was supplied to its delta owing to the confined path of the lava.

Lava dams are common in the western United States, as along the Snake River, Idaho (Malde, 1965, 1971, 1982 this volume), Deschutes and Crooked Rivers, Oregon (Stearns, 1931; Peterson and Groh, 1970), Tieton and Naches Valleys, Washington (Smith, 1903), and Grand Canyon, Arizona (McKee and others, 1968; Hamblin, 1969; Hamblin and Best, 1970). Historic eruptions have dammed rivers in Iceland (Stearns, 1931; Thorarinsson, 1969) and in British Columbia (Brown, 1969; Symons, 1975; Wright, 1906). The building of the deltas formed by the Smith Prairie Basalt may model many of those lava dams.

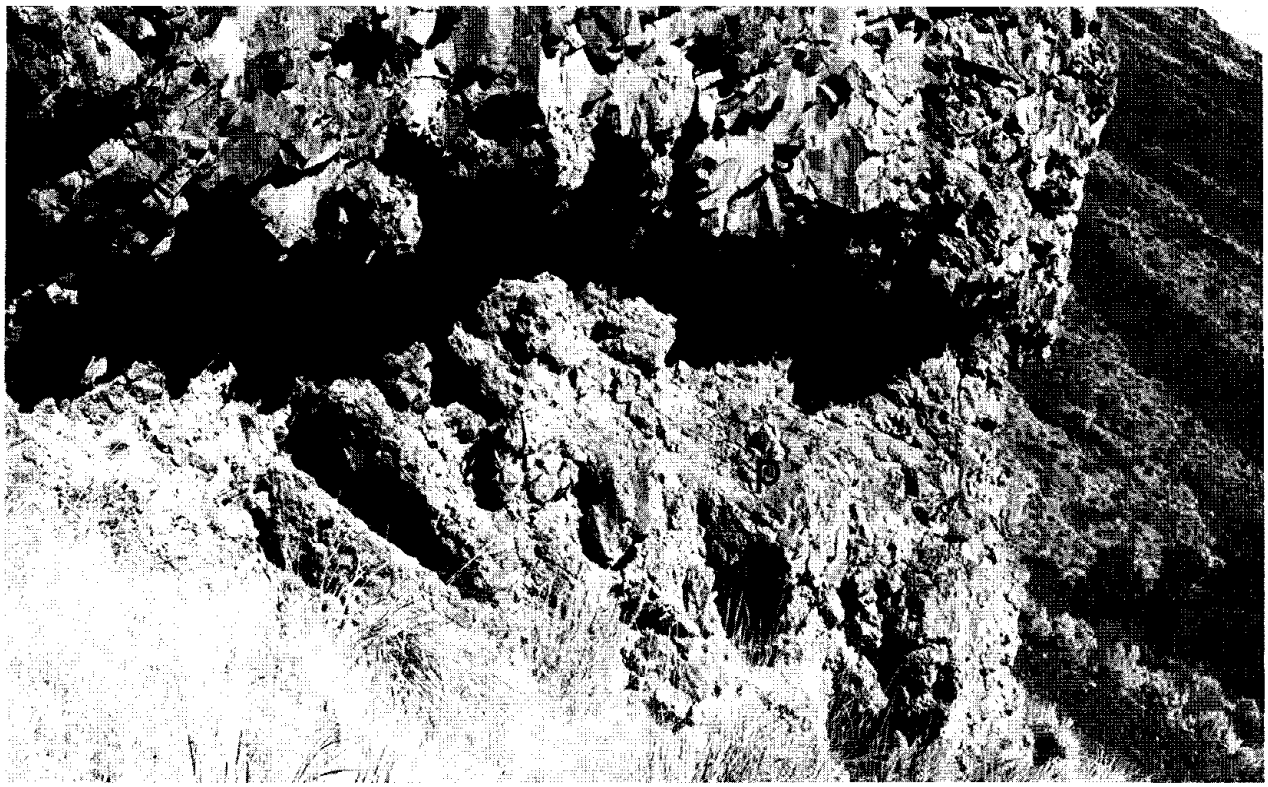

Figure 9a. Passage zone (overhang) from subaerial basalt (s) above pillow basalt (p) in the Cougar Flat flow unit of the Smith Prairie Basalt.

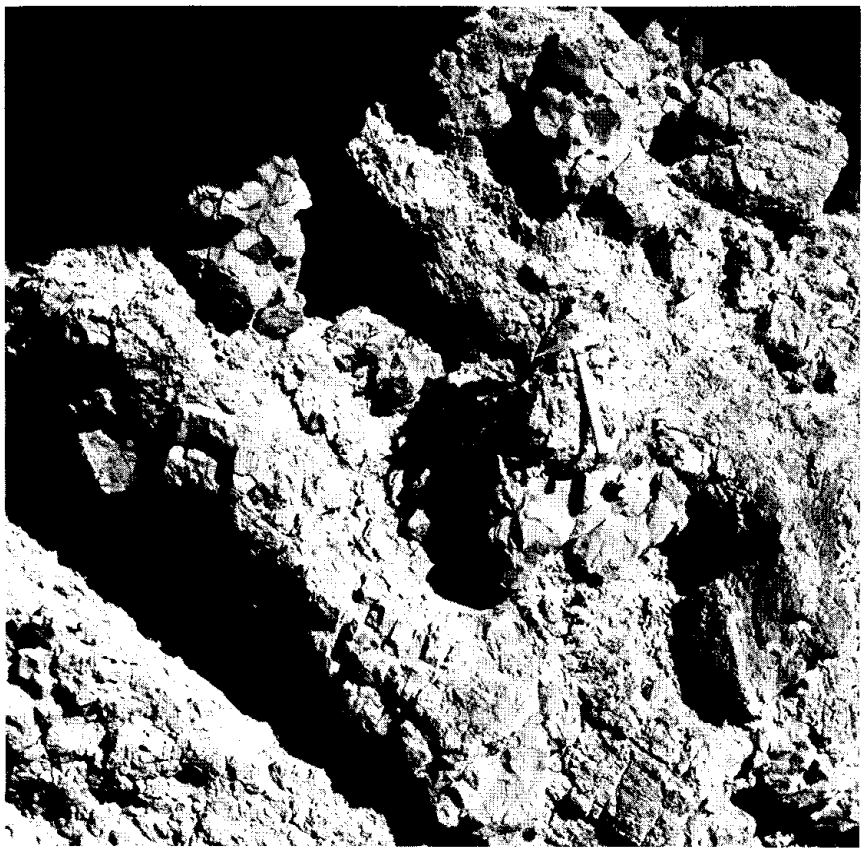

Figure 9b. Close-up of the upper part of the pillow lava showing elongate tubelike pillows plunging down to the right. Interstices all filled with fragmental basaltic glass.

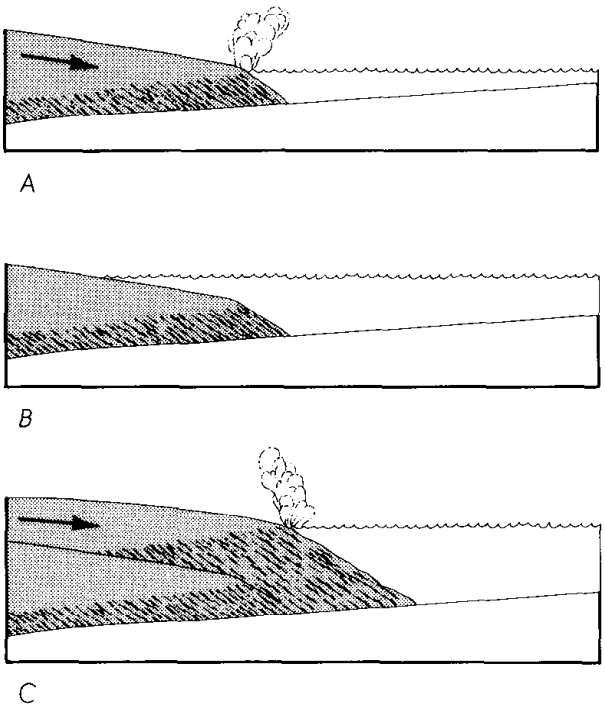

Figure 10. Schematic section to illustrate how successive lava deltas form wedges of dipping pillow lavas (foresets) between massive subaerial lavas (topsets) as the water level rises. Passage zones record the water level changes.

Figure 11. Delta deposits of Steamboat Rock Basalt. Foreset-bedded hyaloclastite dips upriver to left below ledges of subaerially deposited part of Steamboat Rock Basalt. Exposed combined thickness of both is 150 meters. View north across Rock Creek at Smith Prairie tableland.

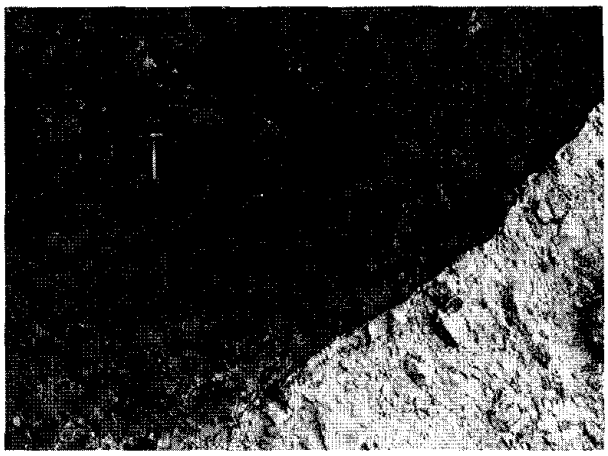

Figure 12. Pillows of Steamboat Rock Basalt in breccia matrix, unconformably over a west-dipping erosion surface in east-dipping arkosic colluvial breccia. Hammer for scale. Sec. 22, T. 1 N., R. 7 E.

POTASSIUM-ARGON AGES

Potassium-argon age determinations were made on samples of basalt from seven flows in the Boise River canyon (Table 1). Four of the flows were dated twice to evaluate the accuracy of the age determinations. Sample preparation and argon and potassium analyses were carrried out in the U. S. Geological Survey laboratories at Menlo Park, California. The basalts were crushed, sieved to 60 to 100 mesh size, washed and treated for 1 minute in 5 percent HF and 30 minutes in 14 percent HNO_3 solution, then loaded into a high-vacuum gas-extraction system. This treatment has proved advantageous in eliminating atmospheric argon from whole-rock basalt samples (Keeling and Naughton, 1974). Potassium analyses were performed by a lithium metaborate flux fusion-flame photometry technique, the lithium serving as an internal standard (Ingamells, 1970). Argon analyses were performed by standard isotope-dilution procedures, using a 60 degrees sector, 15.2-centimeter-radius, Neir-type mass spectrometer, operated in the static mode for mass analysis. The error limit shown in Table 1 as a ± value in millions of years is a weighted value combining the analytical precision at one standard deviation with an estimate of the similarity in analyzed amounts of K_2O and Ar from splits of the same sample. In general the ratios of radiogenic ^{40}Ar from the sample to total ^{40}Ar is an index of the ± figure. Samples reported here range from 9.9 to 2.5 percent radiogenic ^{40}Ar and have a weighted ± value of between about 20 to 50 percent of the age. Six determinations yielded less than 2 percent radiogenic ^{40}Ar and are not listed here because their ± value is so great that the age is considered meaningless. Similar difficulties in dating young basalts of the Snake River Plain were found by Armstrong and others (1975) and Kuntz and Dalrymple (1979).

Table 1. Potassium-argon ages of basalts in Boise River area.

Field number	Rock unit	Longitude	Latitude	K_2O%	$^{40}Ar^{rad}$mole/g	$^{40}Ar^{rad}/^{40}Ar$	Age (m.y.)
HSP-181	Smith Prairie Basalt[1]	115°41.4′	43°31.1′	1.315 1.310	3.8336×10^{-13}	2.5%	0.20±0.15
HSP-186	Smith Prairie Basalt[1]	115°42.2′	43°32.1′	2.047 2.047	7.7602×10^{-13}	7.5%	0.26±0.16
H79 BOISE-4	Basalt of Mores Creek	115°58.3′	43°40.7′	1.561	9.9120×10^{-13}	4.0%	0.44±0.20
HSP-13	Steamboat Rock Basalt[1]	115°37.5′	43°28.5′	0.597 0.606	1.5276×10^{-12}	9.9%	1.8 ±0.3
H79 BOISE-1	Basalt of Long Gulch[1]	115°42.3′	43°32.4′	1.013	9.9714×10^{-13}	3.9%	0.68±0.25[2]
H79 BOISE-3	Basalt of Lucky Peak	116°05.4′	43°32.6′	0.545	1.6373×10^{-12}	7.7%	2.1 ±0.5

[1]HSP-181 and HSP-186 are from the early porphyritic part of the Smith Prairie Basalt. HSP-13 is from the middle of the Steamboat Rock Basalt. H79 BOISE-1 is the upper flow of basalt of Long Gulch.

[2]Age considered too young based on stratigraphic relationships with other dated flows.

$\lambda_\beta + \lambda_{\epsilon'} = 0.581 \times 10^{-10} yr^{-1}$; $\lambda_\beta + 4.962 \times 10^{-10} yr^{-1}$; $^{40}K/K = 1.167 \times 10^{-4}$ mole/mole

The ages in Table 1 suggest the following chronology consistent with stratigraphic position, magnetic polarity (Figure 4), geomorphic position, and degree of lava preservation. Basalt of Lucky Peak is roughly 2 million years old. The Steamboat Rock Basalt is roughly 1.8 million years old. Basalt of Mores Creek is about 0.4 million years old. The Smith Prairie Basalt is about 0.2 million years old. Basalt of Lava Creek is older than the Smith Prairie Basalt and has normal magnetic polarity, so it is younger than 0.7 million years, the beginning of the Brunhes normal polarity epoch. Basalt of Smith Creek is younger than the Steamboat Rock Basalt and has reverse magnetic polarity, so it is older than 0.7 million years.

CANYON HISTORY AND INCISION

The Boise River drainage was established more than 2 million years ago before eruption of the basalt of Lucky Peak. The successive lava dams punctuate a record of progressive deepening accompanied by steepening of the canyon walls. A chronology of incision (Figure 13) demonstrates a long-term rate of lowering, averaging 0.005 to 0.01 centimeter a year over the last 2 million years. Upstream reaches have deepened faster than downstream reaches. Each dam of basalt interrupted this lowering but was rapidly cut through. In the last 0.2 million years since the Smith Prairie Basalt partly filled the canyon, the South Fork has cut down nearly to its former level before eruption of the Smith Prairie, incising at an average rate of 0.07 centimeter a year (C-C′ and D-D′, Figure 13). This compares with the modern rate of 0.05 centimeter a year estimated for the Dearborn River in Montana, decreased from an average rate of 0.20-0.25 centimeter a year over the last 25,000 years (Foley, 1980). At Mores Creek (B-B′, Figure 13) the Boise River cut each of its basalt dams at rates averaging 0.03 centimeter a year for about a quarter of a million years.

The erosional history of the Smith Prairie Basalt illustrates how its dam was cut. River-laid cobbles and boulders on the crest of the dam suggest that sediments filled its reservoir and overtopped the dam before significant erosion. Sands in the reservoir basin are exposed near Danskin bridge. As the river coursed over the dam, it commonly followed its margins as described by Crosby (1911):

> The lateral contact of the lava terrace and the granite slope against which it was formed is usually marked by a depression, which must be regarded as an original feature, the surface of the lava, after the manner of lava streams, being lower along the margins than in the middle of the valley. The River would naturally follow one or the other of these lateral depressions, and we thus find a ready explanation of the fact that lava terraces of corresponding elevation rarely occur coincidently on opposite sides of the river.

Smaller streams also typically followed flow margins as documented by modern and abandoned stream courses on Smith Prairie (Howard and Shervais, 1973).

Over time the river entrenched itself partly in the Smith Prairie Basalt and partly in less resistant granodiorite at the margins of the basalt fill (Figure 2b). The grade of the river is steepest where incision of resistant lava is incomplete (Figure 3, bottom). The river presumably incises by abrasion during floods when its thick bed of gravel (see caption, Figure 13) is in motion. On tributary Smith Creek, erosion instead

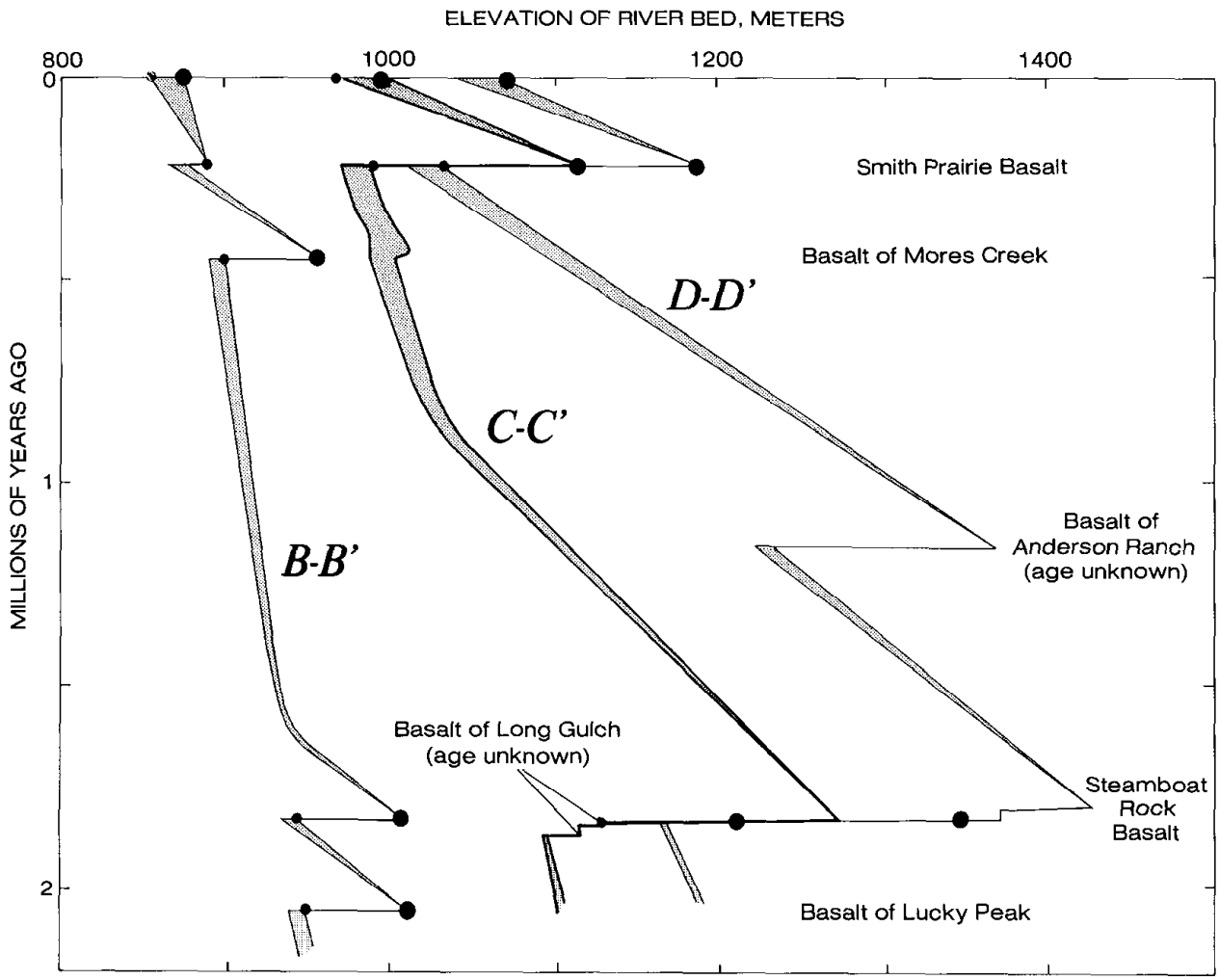

Figure 13. Incision history inferred for the Boise River and its South Fork at locations B-B', C-C', and D-D' (Figures 1 and 3) based on basalt potassium-argon ages and top and bottom elevations of the lava dams. Large dots are better data points; small dots are less well-constrained data points. Gravel fill (shaded) below streambed is estimated from its modern thickness before construction at Lucky Peak Dam (23 meters, Corps of Engineers, 1949, 1951-55), at Arrowrock Dam (20-27 meters, Crosby, 1911) and at a site 5 kilometers upstream from Arrowrock Dam (25 meters, Crosby, 1911). Gravel 1 meter thick underlies probable basalt of Mores Creek at Lucky Peak Dam (Corps of Engineers, 1949, 1951-55), and gravel 3 meters thick underlies the Steamboat Rock Basalt at Long Gulch (C-C'). Bed thickness beneath the other paleocanyons is unknown.

proceeds by headward retreat of 30-meter-high Smith Creek Falls where resistant basalt is underlain by less resistant pillow basalt.

Whether downcutting is fastest when the river begins to cut a basalt dam, or after incision is more nearly complete, is not clear, for a basalt dam offers higher gradients but increased resistance to erosion. After incision of a basalt dam is complete, downcutting slows to a long-term lowering probably brought about in part by relative lowering of the base level downstream.

The intracanyon basalts contain no obvious evidence of tectonic lowering of the Snake River Plain relative to the Idaho batholith to account for the lowered Boise River. No fault offsets of any of the lava terraces have been found. Nor are older flows demonstrably tilted, for their gradients (Figure 3) show little downstream convergence toward younger flows, if dome-shaped profiles near each lava source are discounted. The domes resemble shield volcanoes and may result from the decreased number of flow units and increased viscosity away from the source. Excluding the domes, lava gradients upriver from Arrowrock Dam, subparallel to the margin of the Snake River Plain, compare favorably with those downriver and along Mores Creek that are more or less perpendicular to the plain. Downtilting toward the plain would have been expected to result in higher gradients of lava canyon fills perpendicular rather than parallel to the plain.

REFERENCES

Armstrong, R. L., W. P. Leeman, and H. E. Malde, 1975, K-Ar dating, Quaternary and Neogene volcanic rocks of the Snake River Plain, Idaho: American Journal of Science, v. 275, no. 3, p. 225-251.

Brown, A. S., 1969, Aiyansh lava flow, British Columbia: Canadian Journal of Earth Sciences, v. 6, no. 6, p. 1460-1468.

Crosby, W. O., 1911, Geological report on the proposed main storage dam of the Boise River, Idaho, irrigation project: U. S. Reclamation Service unpublished report, April 25, 1911, 41 p.

Foley, M. G., 1980, Quaternary diversion and incision, Dearborn River, Montana: summary: Geological Society of America Bulletin, pt. I, v. 91, p. 576-577.

Fuller, R. E., 1931, The aqueous chilling of basaltic lava on the Columbia River Plateau: American Journal of Science, v. 221, p. 281-300.

Furnes, Harald and I. B. Fridleifsson, 1974, Tidal effects on the formation of pillow lava/hyaloclastite deltas: Geology, v. 2, no. 8, p. 381-384.

Hamblin, W. K., 1969, Late Cenozoic lava flows in the Grand Canyon of the Colorado River, Arizona: Four Corners Geological Society Guidebook, p. 41-60.

Hamblin, W. K. and M. G. Best, 1970, The western Grand Canyon district: Utah Geological Society Guidebook 23, 154 p.

Howard, K. A. and J. W. Shervais, 1973, Geologic map of Smith Prairie, Elmore County, Idaho: U. S. Geological Survey Map I-818.

Ingamells, C. O., 1970, Lithium metaborate flux in silicate analysis: Analytica Chimica Acta, v. 52, p. 323-334.

Jones, J. G., 1968, Pillow lava and pahoehoe: Journal of Geology, v. 76, no. 4, p. 485-488.

Jones, J. G. and P. H. H. Nelson, 1970, The flow of basalt lava from air into water—its structural expression and stratigraphic significance: Geological Magazine, v. 107, no. 1, p. 13-19.

Keeling, D. L. and J. J. Naughton, 1974, K-Ar dating: addition of atmospheric argon on rock surface from crushing: Geophysical Research Letters, v. 1, p. 43-46.

Kuntz, M. A. and G. B. Dalrymple, 1979, Geology, geochronology and potential volcanic hazards in the Lava Ridge—Hells Half Acre area, eastern Snake River Plain, Idaho: U. S. Geological Survey Open-File Report 79-1657, 66 p.

Lindgren, Waldemar, 1898, The mining districts of the Idaho Basin and the Boise Ridge, Idaho: U. S. Geological Survey 18th Annual Report, p. 617-720.

———, 1900, The gold and silver veins of Silver City, DeLamar, and other mining districts in Idaho: U. S. Geological Survey 20th Annual Report, pt. III, p. 65-256.

Malde, H. E., 1965, Snake River Plain, *in* H. E. Wright and D. G. Frey, editors, The Quaternary of the United States: Princeton University Press, Princeton, New Jersey, p. 255-263.

———, 1971, History of Snake River Canyon indicated by revised stratigraphy of Snake River Group near Hagerman and King Hill, Idaho: U. S. Geological Survey Professional Paper 644-F, 21 p.

———, 1982, The Yahoo Clay, a lacustrine unit impounded by the McKinney Basalt in the Snake River canyon near Bliss, Idaho, *in* Bill Bonnichsen and R. M. Breckenridge, editors, Cenozoic Geology of Idaho: Idaho Bureau of Mines and Geology Bulletin 26.

Malde, H. E. and H. A. Powers, 1962, Upper Cenozoic stratigraphy of western Snake River Plain, Idaho: Geological Society of America Bulletin, v. 73, no. 10, p. 1197-1220.

Malde, H. E., H. A. Powers, and C. H. Marshall, 1963, Reconnaissance geologic map of western Snake River Plain, Idaho: U. S. Geological Survey Map I-373.

McKee, E. D., W. K. Hamblin, and P. E. Damon, 1968, K-Ar age of lava dam in Grand Canyon: Geological Society of America Bulletin, v. 79, no. 1, p. 133-141.

Moore, J. G., 1970, Pillow lavas in a historic lava flow from Hualalai Volcano, Hawaii: Journal of Geology, v. 78, no. 2, p. 239-243.

Moore, J. G., Renato Cristofolimi, and Antonio Lo Giudice, 1971, Development of pillows on the submarine extension of recent lava flows, Mt. Etna, Sicily, *in* Geological Survey Research 1971: U. S. Geological Survey Professional Paper 750-C, p. C89-C97.

Moore, J. G., R. L. Phillips, R. W. Grigg, D. W. Peterson, and D. A. Swanson, 1973, Flow of lava into the sea, 1969-1971, Kilauea Volcano, Hawaii: Geological Society of America Bulletin, v. 84, no. 2, p. 537-546.

Peterson, D. W. and D. A. Swanson, 1974, Observed formation of lava tubes during 1970-71 at Kilauea Volcano, Hawaii: Studies in Speleology, v. 2, pt. 6, p. 209-223.

Peterson, N. V. and E. A. Groh, 1970, Geologic tour of Cove Palisades State Park near Madras, Oregon: The Ore Bin, v. 32, no. 8, p. 141-168.

Russell, I. C., 1902, Geology and water resources of the Snake River plains of Idaho: U. S. Geological Survey Bulletin 199, 192 p.

Shervais, J. W. and K. A. Howard, 1975, Intracanyon basalts of the Boise River, central Idaho: Geological Society of America, Abstracts with Programs, v. 7, no. 5, p. 640-641.

Smith, G. O., 1903, Ellensburg folio: U. S. Geological Survey Atlas, folio no. 86.

Stearns, H. T., 1931, Geology and water supply resources of the middle Deschutes River basin, Oregon: U. S. Geological Survey Water Supply Paper 637, p. 125-212.

Stearns, H. T., Lynn Crandall, and W. G. Steward, 1938, Geology and ground-water resources of the Snake River Plain in southeastern Idaho: U. S. Geological Survey Water Supply Paper 774, 268 p.

Swanson, D. A., 1973, Pahoehoe flows from the 1969-1971 Mauna Ulu eruption, Kilauea Volcano, Hawaii: Geological Society of America Bulletin, v. 84, no. 2, p. 615-626.

Swanson, D. A., D. B. Jackson, W. A. Duffield, and D. W. Peterson, 1971, Mauna Ulu eruption, Kilauea Volcano: Geotimes, v. 16, no. 5, p. 12-16.

Symons, D. T. A., 1975, Age and flow direction from magnetic measurements on the historic Aiyansh flow, British Columbia: Journal of Geophysical Research, v. 80, no. 17, p. 2622-2626.

Thorarinsson, Sigurdur, 1969, The Lakagicar eruption of 1783: Bulletin Volcanologique, v. 33, p. 910-929.

U. S. Army Corps of Engineers, 1949, Basis of design, definite project report on Lucky Peak Dam, Boise River, Idaho: Walla Walla District, U. S. Army Corps of Engineers, v. 1, appendix B, Geology, 11 p.

———, 1951-55, Lucky Peak foundation report, Chapters I-V, Lucky Peak Dam, Boise River, Idaho: Office of the District Engineer, Walla Walla, Washington, U. S. Army Corps of Engineers.

———, 1958, Topographic map of Lucky Peak Dam reservoir area: Walla Walla District, U. S. Army Corps of Engineers, 1:4,800 scale, 5 sheets (unpublished).

U. S. Geological Survey, 1969, Water resources data for Idaho.

Waters, A. C., 1960, Determining direction of flow in basalts: American Journal of Science, v. 258-A, Bradley Volume, p. 350-366.

Wright, F. E., 1906, Unuk River mining region: British Columbia Ministry of Mines, Annual Report, p. 68-74.

Chapter 12
Mountain Glaciation

Glacial Reconnaissance of the Selway-Bitterroot Wilderness Area, Idaho

by

Craig M. Dingler[1] and Roy M. Breckenridge[2]

ABSTRACT

Photogeologic mapping and reconnaissance field investigations of the glacial geology in the Selway-Bitterroot Wilderness Area of Idaho and western Montana have revealed that multiple glaciations occurred in the region during the late Quaternary and that they were more extensive than previously believed. Two major glaciations are recognized, with a late episode of cirque glaciation.

The Grave Peak glaciation, the oldest and most extensive glaciation in the area, was characterized by ice caps and large valley glaciers. The later Canteen Creek glaciation was typified by alpine-type valley glaciers. The Legend Lake glaciation, the latest period of ice accumulation, was characterized by cirque glaciers. Periglacial processes were active during the late Wisconsinan and Holocene.

The formation of a detailed Quaternary stratigraphy and chronology for this region is hampered by the paucity of terminal moraines and other relative age-dating variables. A correlation with the established glacial sequences of other Rocky Mountain regions is not possible at this time.

INTRODUCTION

Although the glaciation of the mountains of Wyoming, Montana, and the Cascade Range in western Washington has been the subject of many investigations, the alpine glaciation of Idaho has been largely overlooked by geologists more interested in bedrock geology and mineral deposits.

The Selway-Bitterroot Wilderness Area and associated rugged, mountainous terrain in Idaho and conterminous western Montana (Figure 1) have been topographically modified by Pleistocene alpine glaciation. The objective of this paper is to describe the extent of multiple glaciations in the Selway-Bitterroot Wilderness Area and to compare the geomorphology with alpine glaciation in other mountains of northern Idaho. Photogeology and field mapping of the surficial geology reveal multiple glaciations in this region greater in extent than previously reported in the literature. The existence of a variety of glacier types, ranging from a mountain ice cap to cirques, is indicated by the geomorphology.

The wilderness area is drained by three major rivers, the Bitterroot on the east side of the continental divide and the Lochsa and Selway on the west side. It incorporates two major mountain masses, the Bitterroot Range and the Clearwater Mountains. The undulating plateau formed by the nearly accordant crests of the Clearwater Mountains (the "Idaho Peneplain" of Fenneman, 1931, and the Clearwater Plateau of later researchers) has an elevation of about 7,000 feet (2,135 meters), with several peaks in excess of 8,000 feet (2,440 meters). Peaks in the Bitterroot Range increase in elevation from north to south, with the highest elevation in the area at Trapper Peak (10,157 feet; 3,098 meters).

Climate in the wilderness region is related to the east-west elevation gradients across the area and the effect of maritime polar air masses that influence the annual precipitation originating from the west. Mean annual precipitation, mostly concentrated in the winter and spring, ranges from about 40 inches (102 centimeters) in the west to over 60 inches (152 centimeters) in the higher elevations of the Bitterroot Range. High elevations in the Bitterroot Range have a July temperature average of 60°F (16°C) and a January average of 18°F (-8°C) (Habeck, 1976).

Most of the study area is underlain by the Bitterroot lobe of the Idaho batholith (Armstrong, 1975; Hyndman and Williams, 1977). Metasedimentary rocks, correlated with the Precambrian Belt Supergroup, occur primarily along the eastern and western edges of the wilderness (Ross, 1950; Reid and others, 1970; Greenwood and Morrison, 1973). Meta-igneous rocks, varying in composition from ultramafic to

[1]Geology Department, University of Idaho, Moscow, Idaho 83843.
[2]Idaho Bureau of Mines and Geology, Moscow, Idaho 83843.

Dingler, C. M. and R. M. Breckenridge, 1982, Glacial reconnaissance of the Selway-Bitterroot Wilderness Area, Idaho, *in* Bill Bonnichsen and R. M. Breckenridge, editors, Cenozoic Geology of Idaho: Idaho Bureau of Mines and Geology Bulletin 26, p. 645-652.

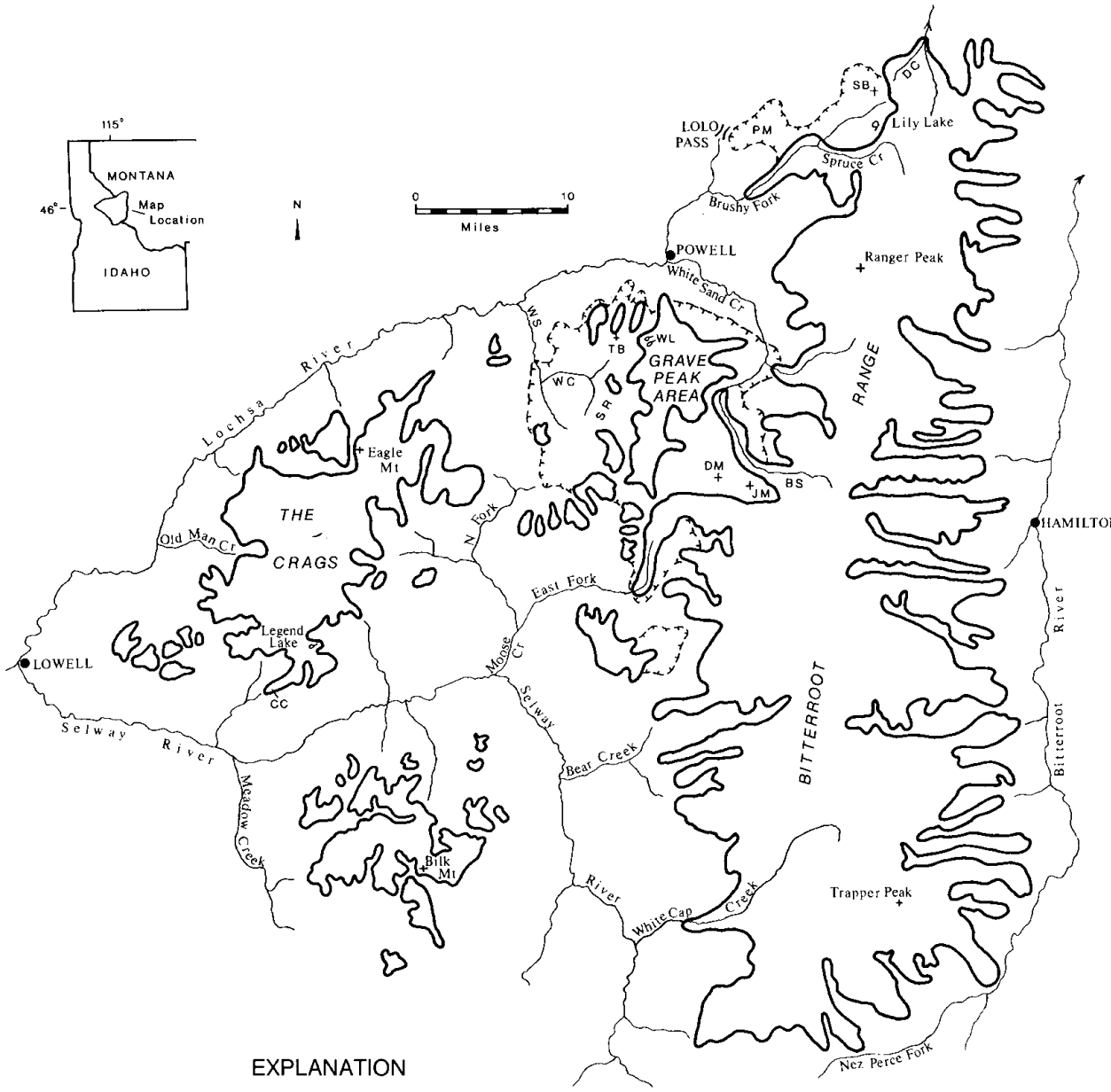

EXPLANATION

BS	Big Sand Creek
CC	Canteen Creek
DC	Dick Creek
DM	Diablo Mountain
JM	Jeannette Mountain
PM	Packer Meadows
SB	Skookum Butte
SR	Saturday Ridge
TB	Tom Beal Peak
WC	Wind Lakes Creek
WL	Walton Lakes
WS	Warm Springs Creek

Extent of ice during Canteen Creek glaciation—late Pleistocene glacial maxiumum

Extent of Grave Peak glaciation—ice cap phase

Figure 1. Generalized map of glaciation in the Selway-Bitterroot Wilderness Area.

granitic masses and ranging in age from Precambrian to Mesozoic, intrude the metasediments in several areas (Greenwood and Morrison, 1973). Migmatites represent the contact zone between the late Mesozoic igneous rocks of the Idaho batholith and the metasedimentary and meta-igneous rocks of earlier time.

The structural geology of this area is complex and related to the emplacement of the batholith and secondary plutons. The most interesting structural feature is the eastern boundary of the Bitterroot Range. Many researchers have discussed the tectonic origin of the abrupt and straight mountain front (Lindgren, 1904; Greenwood and Morrison, 1973). The wilderness area has probably experienced uplift throughout late Cenozoic time.

PREVIOUS INVESTIGATIONS

Much of the previous geomorphology done in this region focused on Montana, the moraines of the southwestern Bitterroot Valley and features of Glacial Lake Missoula (Pardee, 1910, 1942). Lindgren (1904) studied galcial features in this area and speculated on the glaciation of some other areas in Idaho. Stone (1900) noted the existence of glaciated terrain in this part of Idaho from reconnaissance work and recognized the lack of well-developed moraines and the possibility of piedmont glaciers. Alden (1953) described glacial geology of the Bitterroot Valley in detail. Weber (1972) tried to correlate the moraine sequences in the major southwestern Bitterroot Range canyons with the fluctuations in Glacial Lake Missoula. Weis and others (1972) noted glaciation in the Salmon River Breaks Primitive Area (now known as the River of No Return Wilderness).

GLACIAL GEOLOGY

The complex glacial geology of the Selway-Bitterroot Wilderness Area is outlined broadly in this paper. Evidence for two major glaciations in most drainages can usually be recognized, followed by a period of cirque glaciation and periglacial activity.

The terms Pinedale, Bull Lake, and pre-Bull Lake Glaciations (Blackwelder, 1915; Richmond, 1965; Mears, 1974) have been avoided here because no definite ages can be assigned to deposits and because the correlation of surficial stratigraphic units from the Wind River Mountains of Wyoming with those of Idaho cannot be traced by continuous mapping or by lithologic characteristics from their type area (Pierce, 1979; Birkeland and others; 1979; Evenson and others, 1982 this volume).

Terminal moraines are common only in the valleys on the east front of the Bitterroot Range. The lack of terminal moraines or persistent till deposits throughout the Selway-Bitterroot area makes it difficult to correlate surficial stratigraphic units between drainages, and hampers the establishment of a comprehensive Quaternary stratigraphic sequence and chronology for this region. However, a similar sequence of advances can be recognized for the area, and a system for its recognition is valuable. Therefore, a local nomenclature based on observable criteria and relationships was established. Correlation of this nomenclature with other regions of the Rocky Mountains is not possible at this time.

The three glacial periods in the Selway-Bitterroot Wilderness Area have been informally named (Dingler, 1981) as the Grave Peak, Canteen Creek, and Legend Lake glaciations. The Grave Peak glaciation is the earliest recognizable episode. It was the most extensive and had at least four advances. The Canteen Creek glaciation was, in most places, less extensive and had at least two advances. The Legend Lake glaciation was a period of cirque glaciation. A recognizable period of periglacial activity occurred peripheral to glacial areas during the Legend Lake glaciation, or during a later time (Neoglaciation?).

The existence of a variety of glaciers is indicated by the geomorphology, including (1) a mountain ice cap in the Grave Peak area with its associated (2) piedmont lobe in the Big Sand Creek drainage and (3) associated outlet glaciers; (4) transection glaciers; (5) alpine-type valley glaciers in most drainages that originate from catchment areas having an elevation of 6,000 feet (1,830 meters) or greater; and (6) cirque glaciers.

GRAVE PEAK GLACIATION

The Grave Peak glaciation is the oldest and most extensive ice accumulation recognized in the wilderness area. The geomorphology of the Grave Peak area, located in Idaho along the arcuate highland between The Crags and the northern Bitterroot Range, shows evidence of massive ice accumulations such as the Grave Peak ice cap, the associated Big Sand Creek piedmont lobe, and the extensive valley glaciers of Brushy Fork and East Fork of Moose Creek.

The ridge extending north and south of Grave Peak (NE¼ sec. 8, T. 35 N., R. 14 E.) was the central accumulation area of a mountain ice cap. Evidence for this ice cap is both morphological and depositional. The western side of this ridge is very smooth, and grades into a number of north-south trending

glacial troughs with no sharp breaks in slope. The topography is equally well-rounded northwest of the ridge, as shown by the smooth crest and southern slopes of Tom Beal Peak (sec. 24, T. 36 N., R. 13 E.). Erratics give depositional evidence of the ice cap. Large erratics occupy the crest of the glacial headwall above Walton Lakes and the slope southeast of Tom Beal Park (Figure 2).

The maximum extent of this ice cap is difficult to determine due to subsequent valley glaciation. To the west, ice flowed into and accumulated in the Saturday Creek valley as indicated by the smooth hills in the interior of the basin and the rounded Saturday Ridge. Outlet valley glaciers extended down Wind Lake and Warm Springs Creeks to a stream elevation of 4,600 feet (1,403 meters). To the east, Lindgren (1904) envisioned a neve field extending from Grave Peak to Diablo Mountain (sec. 8, T. 34 N., R. 15 E.). Morphology shows that the ice cap was larger than this and that it extended and joined the Big Sand Creek valley glacier and flowed through the valleys of Jeanette and Dolph Creeks, and joined the East Fork of Moose Creek valley glacier. After joining the glacier in Big Sand Creek, ice flowed into White Sand Creek valley, forming a large piedmont lobe that extended to an elevation near 4,200 feet (1,281 meters). The East Fork of Moose Creek valley glacier extended to a stream elevation of 3,200 feet (976 meters) at this time, the lowest glaciation recognized in the area.

The Grave Peak ice cap and its outlet valley glaciers apparently covered an area of approximately 200 square miles (520 square kilometers). No evidence was found in the wilderness for other ice caps.

In the northern Bitterroot Range, a large valley glacier existed in the Brushy Fork drainage with tributary glaciers descending from the upper Brushy Fork valley and the Spruce Creek drainage (Figure 1). The glacier in the valleys of Spruce Creek and its North Fork overtopped the north wall in the Lily Lake area (sec. 13, T. 38 N., R. 16 E.) and coalesced with the west-flowing Brushy Fork valley glacier to form a large body of ice.

Portions of this valley glacier overflowed northward into the Dick Creek drainage, and other portions flowed around (and possibly over) Skookum Butte into the East Fork of Lolo Creek drainage. Most of the valley glacier flowed west in the Brushy Fork drainage, but some ice formed a piedmont lobe in the Packer Meadows area, directly east of Lolo Pass. An end(?) moraine in Packer Meadows is cut by Forest Service Road No. 373 approximately 0.25 mile (0.4 kilometer) east of the U. S. Highway 12 turnoff at Lolo Pass (SE¼ sec. 15, T. 38 N., R. 15 E.).

Thick ice accumulations are associated with the existence of the Brushy Fork valley glacier during the Grave Peak glaciation. Ice thicknesses in the North Fork of Spruce Creek had to exceed 1,200 feet (366 meters) in order to overtop the drainage divide in the Lily Lake area. In the Skookum Butte area, an ice thickness of over 1,200 feet (366 meters) polished the wall northwest of Granite Lake and overrode the

Figure 2. Granitic erratics on the slope southeast of Tom Beal Peak deposited during the Grave Peak glaciation.

whaleback forms at the head of the Dick Creek valley (sec. 6 and W½ sec. 5, T. 38 N., R. 17 E.).

At least four advances during the Grave Peak glaciation are indicated by nested lateral moraines in the Warm Springs Creek valley (secs. 4, 5, 8, and 9, T. 35 N., R. 13 E.; Table 1).

The degree of soil development, useful as a relative age-dating method, shows that till deposits of the Grave Peak glaciation have a depth of weathering up to 20 inches (51 centimeters). This is deeper than any soils recognized on deposits of younger glaciations, although not all deposits show a uniform degree of development due to the effects of alpine climate, varying topography, and the influence of younger horizons of volcanic ash.

CANTEEN CREEK GLACIATION

Areas affected by the Grave Peak glaciation have been topographically modified by a later, less extensive period of alpine-type valley glaciation informally named the Canteen Creek glaciation. Geomorphic evidence for this latest major glaciation includes the enormous area of glacially carved, youthful alpine topography and a number of drainages with lateral moraines upvalley from the terminal areas of earlier glaciations. Major drainages with catchment areas above 6,000 feet (1,830 meters) have been affected by this glacial episode.

The Canteen Creek glaciation was less extensive than the Grave Peak glaciation in both the volume and the length of valley glaciers. No evidence was found for the presence of ice caps of other large ice masses in the wilderness area related to this later glacial episode.

A minimum of two advances during the Canteen Creek glaciation are indicated by nested lateral moraines in the valleys of Canteen Creek (Figure 3; secs. 8, 9, 16, and 17, T. 32 N., R. 10 E.) and Walton Creek (sec. 11, T. 36 N., R. 14 E.), and by terminal(?) moraines in the Warm Springs Creek valley (NE¼ sec. 21 and NE¼ sec. 27, T. 35 N., R. 13 E.).

Soils that have developed on till deposits from the Canteen Creek glaciation generally have a thinner B horizon and a thinner cover of loess and volcanic ash than those formed on Grave Peak glacial deposits. Although the reconnaissance soil investigation of this study reveals variations in different age soils, it could not be determined whether the Canteen Creek glaciation followed a significant soil-forming episode or whether it represents a readvance following a waning of the large ice masses and other glaciers of the Grave Peak glaciation.

LEGEND LAKE GLACIATION

The latest glaciation in the Selway-Bitterroot Wilderness Area was a period of cirque glaciation, as

Table 1. Characteristics of moraines exemplifying the three glaciations in the Selway-Bitterroot Wilderness Area of north-central Idaho and western Montana.

Typical Areas	Location	Moraine Elevations (feet)	Soil Development	Surface Morphology	Orientation
Grave Peak glaciation (ice cap and extensive valley glaciation)					
Tom Beal Creek	Grave Peak Area	8,300-6,400	mature	erratics, ground moraine	N-SW
Warm Springs Creek	Grave Peak Area	5,900-4,600	mature(?)	four broad-crested, nested laterals	N (all)
Walton Creek	Grave Peak Area	4,300-3,900	mature(?)	broad-crested lateral	N
Canteen Creek glaciation (extensive valley glaciation)					
Canteen Creek	The Crags	5,700-4,200	immature	two narrow-crested laterals	WSW
Warm Springs Creek	Grave Peak Area	5,450-5,150	immature(?)	two small, knobby terminals	WNW
Legend Lake glaciation (cirque glaciation)					
Legend Lake	The Crags	6,750	immature	bouldery, narrow-crested	NNE
Crystal Lake	The Crags	6,150	immature	bouldery, narrow-crested	N
Spruce Lake (Paradise Creek)	southwestern Bitterroot Range	6,700	immature	bouldery, narrow-crested	ESE

Figure 3. View to the north of nested lateral moraines and the glaciated lower valley of Canteen Creek.

indicated by the ubiquitous cirque lakes dammed by moraines (Table 1, Figure 4). This glacial episode is informally named the Legend Lake glaciation after a moraine-dammed lake (sec. 35, T. 33 N., R. 10 E.).

Moraines that formed during the Legend Lake glaciation occur on cirque lips or a short distance downvalley and are typical Neoglacial positions. Soils on these deposits, although poorly developed, are able to support vegetation. The capacity of these soils to support vegetation may be an effect of the regional climate, or may indicate that the deposits are older than Neoglacial because Neoglacial deposits in the Rocky Mountains usually do not support substantial vegetation. The later hypothesis may be substantiated in a study by Mehringer and others (1977) which showed that sedimentation began approximately 12,000 years ago in a cirque of the Bitterroot Mountains south of this study area. In either case, the age of the Legend Lake glaciation is in doubt until more detailed studies are undertaken.

PERIGLACIAL FEATURES

Periglacial processes were active in the study area, either peripheral to glaciers during the late Wisconsinan or during Neoglaciation. Sorted stone circles in outwash deposits and debris islands are found on till in The Crags, and a number of rock glaciers are located in cirques along the eastern Bitterroot Range.

SUMMARY

Multiple glaciations in the Selway-Bitterroot Wilderness Area of Idaho and western Montana were greater in extent than has been described in the literature. Two major glaciations are recognized, followed by an episode of cirque glaciation. Respectively, these have been informally named the Grave Peak, Canteen Creek, and Legend Lake glaciations. Periglacial processes were active in the study area, either peripheral to glaciers during the late Wisconsinan or forming during Neoglaciation, or both.

The Grave Peak glaciation was the most extensive and had at least four pulses. The geomorphology of the study area was influenced by numerous glaciers of various morphologies during this episode, including a mountain ice cap in the Grave Peak region and its associated piedmont lobe in Big Sand Creek, transection glaciers, and alpine-type valley glaciers in numerous drainages such as the large ones in the Brushy Fork and East Fork of Moose Creek.

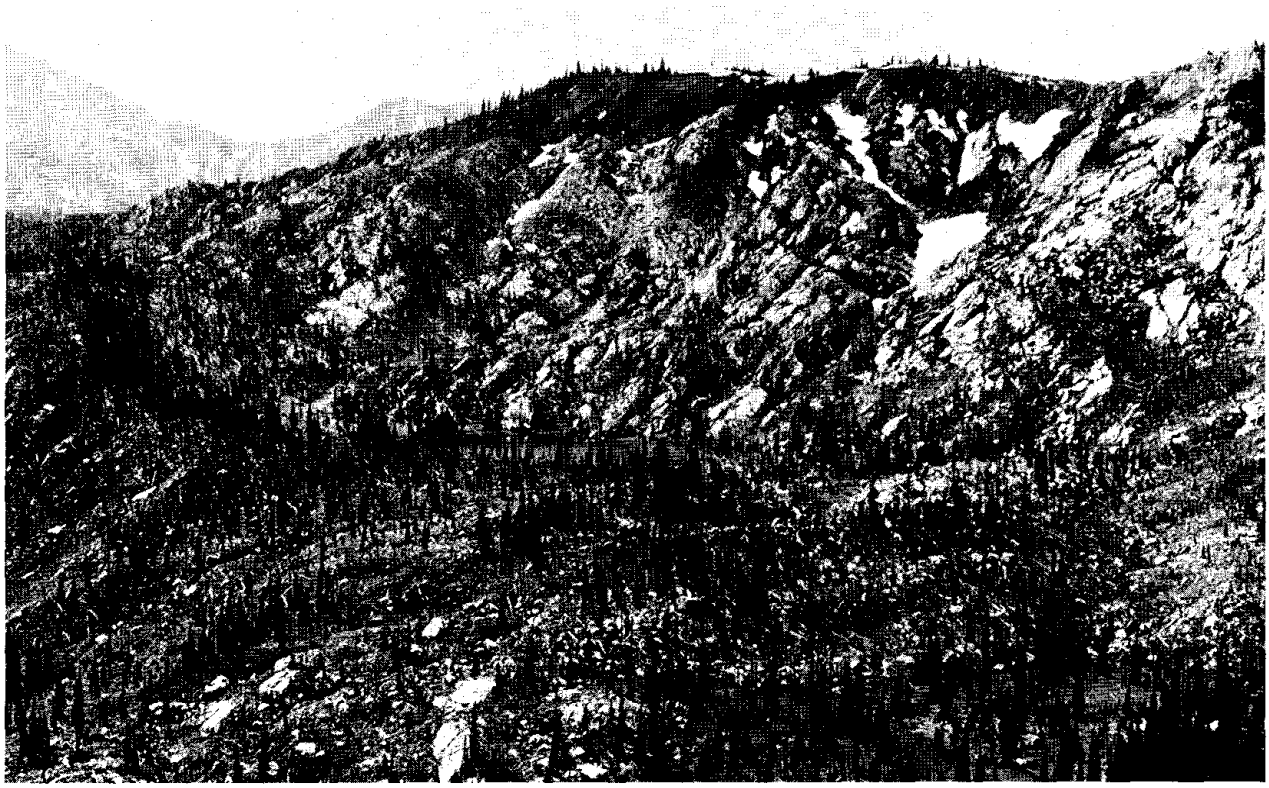

Figure 4. View to the south of cirque moraines damming Crystal Lake at the head of the Rhoda Creek valley in The Crags.

The Canteen Creek glaciation was less extensive and had at least two advances. Alpine-type valley glaciers were prevalent during this ice advance. The Legend Lake glaciation was characterized by cirque glaciers.

The paucity of terminal moraines and other deposits for relative age-dating limited our ability to correlate surficial stratigraphic units between drainages, and hampers the establishment of a comprehensive Quaternary stratigraphic sequence and chronology for this region. The glacial record of this region cannot be correlated to the glacial sequences of other Rocky Mountain regions at this time.

REFERENCES

Alden, W. C., 1953, Physiography and glacial geology of western Montana and adjacent areas: U. S. Geological Survey Professional Paper 231, 200 p.

Armstrong, R. L., 1975, The geochronometry of Idaho: Isochron West, no. 14, p. 1-50.

Birkeland, P. W., S. W. Colman, R. M. Burke, R. R. Shroba, and T. C. Meierding, 1979, Nomenclature of alpine glacial deposits, or, What's in a name?: Geology, v. 7, p. 532-536.

Blackwelder, Eliot, 1915, Post-Cretaceous history of the mountains in central western Wyoming: Journal of Geology, v. 23, p. 97-117, 193-217, 307-340.

Dingler, C. M., 1981, Reconnaissance glacial geology of the Selway-Bitterroot Wilderness and surrounding lower elevations, Idaho and Montana: University of Idaho M.S. thesis, 184 p.

———, in press, Reconnaissance glacial geologic map of the Selway-Bitterroot Wilderness and surrounding lower elevations, Idaho and Montana: Idaho Bureau of Mines and Geology Open-File Report, scale 1:125,000, 1 plate.

Evenson, E. B., J. F. P. Cotter, and J. M. Cinch, 1982, Glaciation of the Pioneer Mountains: a proposed model for Idaho, *in* Bill Bonnichsen and R. M. Breckenridge, editors, Cenozoic Geology of Idaho: Idaho Bureau of Mines and Geology Bulletin 26.

Fenneman, N. M., 1931, Physiography of the western United States: McGraw-Hill, New York, 534 p.

Greenwood, W. R. and D. A. Morrison, 1973, Reconnaissance geology of the Selway-Bitterroot Wilderness Area: Idaho Bureau of Mines and Geology Pamphlet 154, 30 p.

Habeck, J. R., 1976, Forests, fuels and fire in the Selway-Bitterroot Wilderness, Idaho: Proceedings of the Montana Tall Timbers Fire Ecology Conference and Fire and Land Management Sympo-

sium No. 14 (1974), Tall Timbers Research Station, Tallahasse, Florida, p. 305-352.

Hyndman, D. W. and L. D. Williams, 1977, The Bitterroot lobe of the Idaho batholith: Northwest Geology, v. 6, p. 1-16.

Lindgren, Waldemar, 1904, A geological reconnaissance across the Bitterroot Range and Clearwater Mountains in Montana and Idaho: U. S. Geological Survey Professional Paper 27, 123 p.

Mears, Brainerd, Jr., 1974, Evolution of the Rocky Mountain glacial model, *in* D. R. Coates, editor, Glacial Geomorphology: State University of New York at Binghampton Publications in Geomorphology, p. 345-368.

Mehringer, P. J., Jr., S. F. Arno, and K. L. Peterson, 1977, Postglacial history of Lost Trail Pass Bog, Bitterroot Mountains, Montana: Arctic and Alpine Research, v. 9, p. 345-368.

Pardee, J. T., 1910, The Glacial Lake Missoula: Journal of Geology, v. 18, p. 376, 386.

———, 1942, Unusual currents in Glacial Lake Missoula, Montana: Bulletin of the Geological Society of America, v. 53, p. 1569-1600.

Pierce, K. L., 1980, History and dynamics of glaciation in the northern Yellowstone region: U. S. Geological Survey Professional Paper 780-D, 90 p.

Reid, R. R., W. R. Greenwood, and D. A. Morrison, 1970, Precambrian metamorphism of the Belt Supergroup in Idaho: Geological Society of America Bulletin, v. 81, p. 915-917.

Richmond, G. M., 1965, Glaciation of the Rocky Mountains, *in* H. E. Wright, Jr., and D. G. Frey, editors, The Quaternary of the United States: Princeton University Press, p. 217-230.

Ross, C. P., 1950, The eastern front of the Bitterroot Range, Montana: U. S. Geological Survey Bulletin 974-E, p. 135-175.

Weber, W. M., 1972, Correlation of Pleistocene glaciation in the Bitterroot Range, Montana, with fluctuations of Glacial Lake Missoula: Montana Bureau of Mines and Geology Memoir 42, 42 p.

Weis, P. L., L. J. Schmitt, Jr., and E. T. Tuchek, 1972, Mineral resources of the Salmon River Breaks Primitive Area, Idaho: U. S. Geological Survey Bulletin 1353-C, 91 p.

Glaciation of the Pioneer Mountains: A Proposed Model for Idaho

by

Edward B. Evenson[1], James F. P. Cotter[1], and J. Michael Clinch[1]

ABSTRACT

The glacial deposits of three basins in the Pioneer Mountains, central Idaho, have been mapped, and the glacial stratigraphy and history have been determined from those deposits. These three basins, locally known as the Copper Basin, Wildhorse Canyon, and the North Fork drainage, constitute the headwaters of the Big Lost River. Within each basin, two major episodes of glacial advance can be differentiated by relative-dating (RD) criteria, including soil properties and moraine morphology. Second-order events within each glacial advance are subdivided on the basis of moraine position, geometry, and terrace relationships.

To avoid unwarranted long-range correlations with the established Rocky Mountain chronology (Pinedale-Bull Lake) and also to avoid conflicts with the American Commission on Stratigraphic Nomenclature, an informal chronology has been established for each basin, where each RD-separable package of deposits is assigned to an "advance" with local informal names, and where second-order "events" within each "advance" are designated by Roman numerals. To facilitate communication, these "advances" are then correlated to regional "glaciations." At this time, two major, well-documented glaciations are recognized and informally named in the Pioneer Mountains: the Potholes glaciation (younger) and the Copper Basin glaciation (older). Elevated gravels of assumed glacial origin provide evidence for a third, yet older, glaciation herein named the "Pioneer glaciation." Additional areas in central Idaho have been tentatively correlated to this glacial model.

Reconstruction of ice deployment shows that glaciation was extensive during the Copper Basin glaciation, when major lobes (herein named the "Copper Basin Lobe," the "Wildhorse Canyon Lobe," and the "North Fork Lobe") developed in each drainage basin. Ice-dammed lakes developed in the Copper Basin Flats and in the canyon of the East Fork of the Big Lost River (herein named "Glacial Lake East Fork"). Catastrophic drainage of Glacial Lake East Fork is documented by the presence of flood-transported boulders well downcanyon from the ice dam.

Ice deployment during the Potholes glaciation was similar but less extensive than during the Copper Basin glaciation. The Copper Basin and Wildhorse Canyon Lobes re-formed, but the three valley glaciers in the North Fork drainage did not coalesce to reconstitute the North Fork Lobe. Glacial Lake East Fork was dammed again, and again drained catastrophically. Deglaciation during the Potholes glaciation featured the progressive retreat of the ice lobes, the breakup into individual valley glaciers, and the readvance of individual glaciers. No moraines younger than the Potholes glaciation have been mapped.

INTRODUCTION

This paper reviews the results of seven years of research on the glacial history and deposits of the Pioneer Mountains of central Idaho (Figure 1).

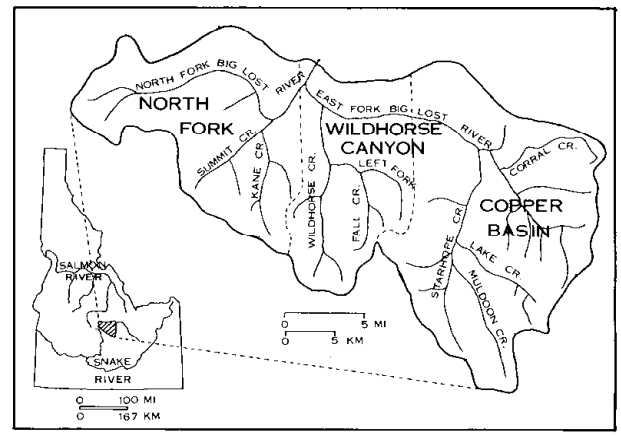

Figure 1. Location map and Lost River drainage, showing Copper Basin, Wildhorse Canyon, and North Fork area and principal streams.

[1]Department of Geological Sciences, Lehigh University, Bethlehem, Pennsylvania 18015.

Evenson, E. B., J. F. P. Cotter, and J. M. Clinch, 1982, Glaciation of the Pioneer Mountains: a proposed model for Idaho, *in* Bill Bonnichsen and R. M. Breckenridge, editors, Cenozoic Geology of Idaho: Idaho Bureau of Mines and Geology Bulletin 26, p. 653-665.

Detailed mapping, relative age dating, pedologic investigations, provenance analysis, and theoretical glacial reconstructions have been employed to develop a local stratigraphy based on relative-dating (RD) techniques (Birkeland and others, 1979). A stratigraphic model, herein called the "Idaho Glacial Model," is proposed. This model further extends the "Rocky Mountain Glacial Model" of Mears (1974) yet remains independent and dynamic by means of a separate, informal, stratigraphic nomenclature. As the areal extent of detailed investigation grows, the model can be extended, expanded, and correlated with those generated in adjacent areas of the Rocky Mountains.

LOCATION AND BEDROCK GEOLOGY

The Pioneer Mountains and their northeastern extension, the Boulder Mountains, are located in central Idaho, north of the Snake River Plain and east of the town of Mackay. The study area includes about 400 square kilometers on the northern side of the Pioneer Mountain divide in the glaciated headwaters of the Big Lost River. For logistic purposes, three separate but adjacent areas were mapped individually (Figure 1). These areas are known locally as the Copper Basin, Wildhorse Canyon, and the North Fork drainage.

The geomorphologic setting of the area, as evidenced by the high relief, has been greatly influenced by Quaternary glacial and fluvial activity. Most streams in glaciated valleys are underfit, and uplands display classic Alpine-type glaciated features including cols, aretes, horns, and cirques. Hyndman Peak, altitude 3,681 meters, is the highest point in the study area.

The Pioneer Mountains consist structurally of two north-trending elongated domes. These domes are cored by autochthonous Precambrian metamorphic units surrounded by a number of allochthonous, upper Paleozoic clastic units which were emplaced by thrust faulting (Dover, 1966, 1969). During the formation of the Idaho batholith (Cretaceous), small "satellite" intrusive bodies were emplaced in the western Pioneer Mountains. Stratigraphically overlying all of these units are the Challis Volcanics of Tertiary age. These volcanic rocks, consisting of interbedded lava and tuffaceous units, probably blanketed the entire region at one time, but uplift and erosion has resulted in the exposure of underlying units. Tertiary through Quaternary age block faulting is believed to be the cause of this uplift and the present relief (Umpleby and others, 1930; Dover, 1966, 1969).

PREVIOUS WORK

Umpleby and others (1930) and Nelson and Ross (1969) were the first researchers to map and subdivide glacial deposits in the Pioneer Mountains. More recently, Dover (1966, 1969) and Dover and others (1976) mapped and described the surficial deposits as part of a detailed investigation of the stratigraphy and structure of the area.

Mapping by students from Lehigh University has resulted in seven master's theses. These include mapping and provenance analysis in the Copper Basin (Wigley, 1976; Pasquini, 1976), Wildhorse Canyon (Stewart, 1977; Brugger, in preparation), North Fork drainage (Cotter, 1980; Repsher, 1980), and provenance analysis of glaciofluvial terraces (Pankos, in preparation).

In each of the three glacial basins of the northern Pioneer Mountains, glacial and glaciofluvial deposits were mapped and differentiated by employing relative-dating techniques that have been used previously in the Rocky Mountains (Birkeland and others, 1979). In addition, models of ice deployment were developed and reported by Evenson and others (1979), Repsher and others (1980), and Brugger (in preparation).

RELATIVE-DATING (RD) TECHNIQUES

The lack of organic matter suitable for radiocarbon dating and of datable tephras within the glacial deposits has forced us to resort to the application of semiquantitative relative-dating (RD) techniques to subdivide the glacial deposits of the area. Relative dating is based on the premise that weathering parameters are time dependent and therefore can be used to distinguish episodes of deposition (Burke and Birkeland, 1979). As succinctly demonstrated by Burke and Birkeland (1979), a multiparameter approach to relative dating increases the reliability of local till subdivisions and increases the chances of obtaining criteria useful for regional correlation. The parameters utilized for relative dating in the Pioneer Mountains include moraine morphology (number and freshness of ice-disintegration hollows, preservation of original morainic form, and degree of secondary dissection), extent of glaciation downvalley (older moraines are

downvalley or "outside" younger deposits), spatial relationships of moraines and glaciofluvial terraces (terraces are graded to a moraine of the same age and dissect older moraines and terraces), and soil properties (color, structure, texture, carbonate concentrations, clay mineralogy, and soil chemistry).

Relative-dating techniques have been used throughout the Rocky Mountains by numerous researchers (for example, Richmond, 1948, 1965, 1976; Moss, 1949, 1951a, 1951b; Holmes and Moss, 1955; Birkeland, 1964, 1973; Crandell, 1967; Carroll, 1974; Mahaney, 1974; Pierce and others, 1976; Evenson and others, 1979) and have proven extremely useful, on a local level, for the subdivision of glacial deposits. There are, however, problems associated with the formal naming of glacial deposits on the basis of physical features resulting from postdepositional modification (relative dating). As pointed out by Birkeland and others (1979), the problem arises because the "Code of Stratigraphic Nomenclature" currently makes no provision for defining glacial units on the basis of multiple, relative-dating parameters.

The American Commission on Stratigraphic Nomenclature (1970) has approved a variety of classifications (that is, time-, rock-, and soil-stratigraphic units) for the distinction and correlation of Quaternary deposits, but none of them embraces the multiple parameters used in relative-age dating. In each of the code-approved classifications an individually defined parameter must be used to delimit a stratigraphic unit, whereas relative dating relies on the application of multiple parameters which are utilized in other stratigraphic systems. Our use of multiple, relative-dating techniques (for example, both soil and morphologic features) must therefore result in a mixed or "hybrid" stratigraphic classification (Birkeland and others, 1979) not formally recognized by the Stratigraphic Code. However, because RD data does not generate a code-approved stratigraphic classification does not mean that RD-based units cannot be named on an informal or even formal basis (see Burke and Birkeland, 1979). It is important, however, that care be taken to avoid the proliferation of even informal stratigraphic nomenclature. As discussed by Birkeland and others (1979) and Burke and Birkeland (1979), only first-order events (Porter, 1971) are worthy of even informal names.

Following the suggestion of Birkeland and others (1979), we now advocate the use of RD-based units for the glacial deposits of the Pioneer Mountains. Multiple relative-dating techniques have been used in each of the three basins (Copper Basin, Wildhorse Canyon, and North Fork) in the Pioneer Mountains, and in each area different techniques have been shown to be of varying effectiveness in the differentiation of glacial deposits. The RD units developed within separate drainages were then assigned their own informal stratigraphic names. We feel this facilitates communication, avoids conflict with the Stratigraphic Code, and allows correlation between individual basins; however this does not imply age equivalence (as is the case when the same term is extended from basin to basin) where it is not warranted or intended.

STRATIGRAPHIC NOMENCLATURE

The problems associated with stratigraphic nomenclature of glacial deposits in the Rocky Mountains have existed since Blackwelder (1915) used the same terms in a morpho-, time-, and climato-stratigraphic sense (for example, Pinedale moraine or drift, Pinedale epoch, and Pinedale Glacial stage). Since then, researchers in the Rocky Mountains have generally taken two approaches when naming glacial deposits: either the same stratigraphic names (that is, Pinedale) are used over a large area, or new formal names for stratigraphic units are designated for every drainage basin. As Birkeland and others (1979) have stated, the problem with the first approach is that the use of the same name implies (however inadvertently) correlations which are often not substantiated. On the other hand, the use of new formal terms results in both an exorbitant number of terms and confusion for those who are not familiar with the area.

To avoid this problem, Birkeland and others (1979) have suggested using letter designations to differentiate stades or glacial events ("first-order events," for example, Crandell, 1967). We do not feel that letter or number designations are adequate for the delineation of first-order events with obvious morphological and other RD differences as those found throughout the Pioneer Mountains. For example, neither communication nor convenience is served by referring to "Advance A of Wildhorse Canyon" or "Advance B of the Copper Basin." The use of letters is clumsy and stratigraphically invalid, and it implies some correlation. We do agree, however, with this method for identifying second-order depositional episodes (events) within first-order events (advances) and have used a variant of this method (that is, North Fork I, North Fork II, and so on) in the Pioneer Mountains (Wigley and others, 1978; Cotter, 1980). At the same time, we do not favor the continued use and extension of the terms "Pinedale" and "Bull Lake" as this implies

correlation with the type areas of these deposits in the Wind River Range and with other deposits to which these names have been applied.

As our work in the Pioneer Mountains continues it is becoming apparent that an independent, simple, rational classification of relative-dating (RD) defined deposits is required for local and regional correlation. In each of the drainages we have studied, detailed mapping of glacial and glacial-fluvial deposits resulted in the differentiation of two first-order glacial events (and probable evidence of a third) based on the clear separation of deposits through the relative-dating techniques previously discussed. In the past, we (Wigley and others, 1978; Evenson and others, 1979) and others (Nelson and Ross, 1969) have referred to deposits of these first-order events as Pinedale (younger) and Bull Lake (older). Older deposits of assumed glacial origin were also recognized and simply called "Pre-Bull Lake" to indicate antiquity. This system, however, is unacceptable for the reasons already discussed. The nomenclature system we currently favor is the establishment of a set of informal stratigraphic terms for each of the RD differentiable deposits (mapped as moraines and terraces) within a given (local) drainage. The terms till and gravel are avoided because these are rock stratigraphic terms. Mapping of these deposits delimits the first-order glacial events which we call "advances" (that is, Wildhorse Canyon advance, Devil's Bedstead advance, North Fork advance, and the like). Second-order episodes (which we call "events") within these advances are designated by Roman numerals appended to the advance name (that is, North Fork I, North Fork II, and so on) after the suggestion of Birkeland and others (1979). This system yields independent, informal stratigraphic units which can then be correlated with local and regional stratigraphic units. The advantage of this system is that RD-based units can be correlated without the undesirable extension of a stratigraphic term over large areas. If errors in correlation are later detected, the correlation and not the stratigraphic name can be simply and easily changed. This system of naming units and subsequent correlation is an accepted geologic practice which allows the concomitant development of stratigraphic units and unambiguous correlation. The system is flexible and can evolve as new information becomes available.

Admittedly, this system results in a proliferation of stratigraphic terms confusing to persons not thoroughly familiar with the literature of the area. To solve this problem and to aid in communication on a regional basis (within central Idaho), we propose the establishment of regional terms (glaciations) to which local informal units can be tentatively correlated. These regional terms will provide a system, to which local stratigraphies within central Idaho can be correlated, facilitating communication yet avoiding the possible overextension of the terms utilized in the Rocky Mountain Glacial Model. The terms which we propose for this purpose are Potholes glaciation (younger), Copper Basin glaciation, and Pioneer glaciation (oldest). Using this system it is possible to name advances, subdivide events, and correlate units locally defined by RD criteria and simultaneously have a regional set of terms to which all advances may be correlated (glaciations). Glaciations, advances, and events in turn may then be correlated with other chronologies, such as those used in the Cascade Range, the Central Rocky Mountains, and the midcontinent.

IDAHO GLACIAL MODEL

Table 1 summarizes the nomenclature we now use for the three drainages we have studied in detail in central Idaho. In addition, it presents our correlation of local units with each other and with the Idaho Glacial Model. The terminology for the North Fork drainage follows that proposed by Cotter (1980). The nomenclature for Wildhorse Canyon and the Copper Basin is new, as is that proposed for regional use within central Idaho.

As shown on Table 1, the Idaho Glacial Model recognizes and names three periods (glaciations) of glacial activity. They are called "Potholes glaciation" (youngest), Copper Basin glaciation, and Pioneer glaciation (oldest). The nomenclature for the Idaho Glacial Model is based on deposits in the Copper

Table 1. Nomenclature used in the Idaho Glacial Model and correlation with local stratigraphies developed for individual basins.

IDAHO GLACIAL MODEL	NORTH FORK DRAINAGE (COTTER, 1980)	WILDHORSE CANYON (STEWART, 1977)	COPPER BASIN (WIGLEY, 1976)
POTHOLES GLACIATION	NORTH FORK ADVANCE IV III II I	WILDHORSE CANYON ADVANCE IV III II I	ROAD CREEK ADVANCE IV III II I
COPPER BASIN GLACIATION	KANE ADVANCE	DEVIL'S BEDSTEAD ADVANCE II I	RAMEY CREEK ADVANCE II I
PIONEER GLACIATION	NOT RECOGNIZED	POLE CREEK ADVANCE	BELLAS CANYON ADVANCE

Basin where the characteristics of each of the deposits are well displayed. We will begin our discussion of the model by defining the physical characteristics of the deposits of each glaciation, beginning with the youngest.

POTHOLES GLACIATION

Moraines assigned to the Potholes glaciation are easily recognized by their fresh surface morphology. They are sharp crested and kettled and preserve ice-disintegration features that often contain water (Figure 2). Surface-boulder frequencies are very high, and boulders occasionally show ice-scour features. Soils developed on deposits of the Potholes glaciation are weakly developed (Wigley, 1976; Stewart, 1977; and Cotter, 1980) and lack appreciable calcium carbonate (Cca) buildup. The deposits correlated with the Potholes glaciation include those assigned to the North Fork advance by Cotter (1980) in the North Fork drainage and those assigned to the Pinedale glaciation by Stewart (1977) in Wildhorse Canyon and by Wigley (1976) in the Copper Basin. The deposits called "Pinedale" by Stewart (1977) and Wigley (1976) are herein informally renamed "Wildhorse Canyon advance" and "Road Creek advance," respectively (Table 1). An informal type locality for the deposits of the Potholes glaciation is here designated as the moraine mapped as "Pt-1" by Wigley (1976) on the west side of the Copper Basin in the area of Road Creek (Figure 2).

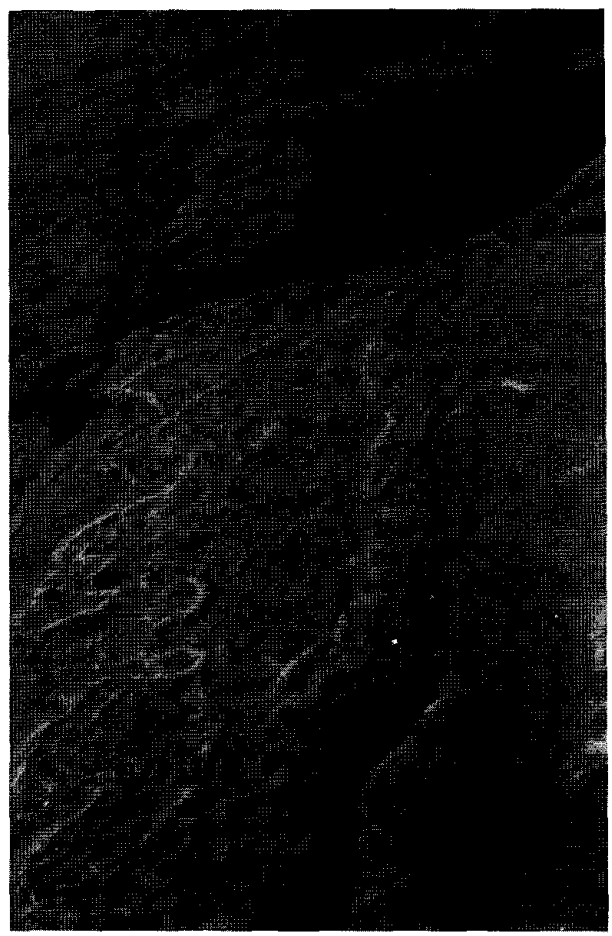

Figure 2. Photo of moraines in Copper Basin. Road Creek moraines (Potholes glaciation) on left of photograph have a fresh, irregular morphology. Ramey Creek moraines (Copper Basin glaciation) on right side of photograph have a subdued morphology.

COPPER BASIN GLACIATION

Moraines assigned to the Copper Basin glaciation are the oldest well-preserved glacial deposits in the study area. Generally, moraines of the Copper Basin glaciation extend 0.5 to 1.0 kilometer further down valley than those of the Potholes glaciation. Moraines of the Copper Basin glaciation are subdued, bulky, and well dissected by tributary streams. Moraine surfaces are irregular but mature in appearance, having filled or breached surface depressions (Figure 2). Surface-boulder frequencies are low to moderate, characterized by scattered, fractured large boulders. Boulder surfaces are well pitted, removing all evidence of ice-scour features. Soils developed on tills of the Copper Basin glaciation are weakly developed, but commonly have a well-developed calcium carbonate buildup (Cca-horizon) at depth (Wigley, 1976; Stewart, 1977; Wigley and others, 1978; Cotter, 1980).

The deposits assigned to the Copper Basin glaciation include those assigned to the Kane advance by Cotter (1980) in the North Fork drainage and those assigned to the Bull Lake glaciation by Stewart (1977) in the Wildhorse Canyon and by Wigley (1976) in the Copper Basin. The deposits called "Bull Lake" by Stewart (1977) and Wigley (1976) are herein informally renamed "Devil's Bedstead advance" and "Ramey Creek advance" in Wildhorse Canyon and Copper Basin, respectively (Table 1). An informal type locality for the deposits of the Copper Basin glaciation is here designated as the moraine mapped as "BT" by Wigley (1976) on the west side of the Copper Basin in the area of Ramey Creek (Figure 2).

PIONEER GLACIATION

The term "Pioneer glaciation" is here used to

include all deposits of assumed glacial origin older than the deposits of the Copper Basin glaciation. Because the origin, age, and correlation of numerous, isolated deposits within the Pioneer Range and elsewhere in central Idaho are difficult to document, we show these terms with question marks on Table 1. The Pioneer glaciation provides an all-inclusive regional term for this small, but important, group of deposits. In addition, the inclusion of the poorly documented Pioneer glaciation in the Idaho Glacial Model insures that the model has the capacity to accommodate additional glacial deposits older than the Copper Basin glaciation.

Deposits of the Pioneer glaciation are characterized by their elevated position, degree of dissection, and extensive weathering, all of which indicate their antiquity. Because of the isolated distribution, limited extent, and unknown origin of the deposits of the Pioneer glaciation, no detailed description or type area is given for these deposits. In this paper we simply wish to give informal local names to the two deposits, previously mapped as Pre-Bull Lake by Wigley (1976) and Stewart (1977). Herein, we propose the informal names Bellas Canyon advance and Pole Creek advance for the deposits mapped as Pre-Bull Lake by Wigley (1976) and Stewart (1977) in the Copper Basin and Wildhorse Canyon, respectively (Table 1). Deposits of the Pioneer glaciation were not recognized in the North Fork drainage, and subdivision (into events) of the Bellas Canyon and Pole Creek advances is not possible.

GLACIAL HISTORY OF THE CENTRAL PIONEER MOUNTAINS

The moraines and glaciofluvial terraces of the Pioneer Mountains have, on a local basis, been differentiated using relative age criteria, assigned to first-order advances, and subdivided into second-order events. Advances have been correlated with each other and with Idaho Glacial Model (Figure 1).

On the basis of relative-dating based correlations, detailed mapping, and numerical modeling we have reconstructed the geometry of ice deployment at specific times in our relative-age time scale. Evenson and others (1979) previously presented an ice deployment model for this region at the Potholes glaciation maximum (then called "Pinedale maximum"), and we now present a more complete review of the glacial history and ice deployment.

PIONEER GLACIATION

Gravels assigned to the Pioneer glaciation are present as isolated remnants in the Copper Basin (Bellas Canyon advance) and in the East Fork Canyon between the Copper Basin and Wildhorse Canyon (Pole Creek advance). These deposits are so scattered that no reconstruction of the ice deployment or glacial history is possible.

COPPER BASIN GLACIATION

Deposits of the Copper Basin glaciation are the oldest well-preserved deposits in the area. These deposits consist of both terraces and moraines. As described previously, moraines of the Copper Basin glaciation are morphologically subdued and quite weathered. Based on morphology alone, moraines within this glaciation cannot be differentiated from one another; however, two distinct glaciofluvial terrace levels provide evidence of at least two separate advances during the Copper Basin glaciation.

Moraine geometry suggests that ice deployment was similar during both the Potholes and Copper Basin glaciations, but the extent of ice advance was greater during the Copper Basin glaciation.

Three distinct sources of ice were present in the Copper Basin during the Ramey Creek advance (correlated to the Copper Basin glaciation). An intermontane piedmont complex (the Copper Basin Lobe, Figure 3) was fed from Lake, Muldoon, and Starhope Canyons to the south of the basin and from several small canyons to the west of the basin. The steep topography on the west side of the basin and the constricted valley of the East Fork of the Big Lost River to the northwest caused the ice to expand eastward onto the area locally known as Copper Basin Flats and upcanyon into the lower reaches of Corral Creek.

A second area of ice accumulation in the Copper Basin was located east of the piedmont complex, in Anderson, Smelter, Steve, Charcoal, and Coal Canyons. The glacial history of these drainages consists wholly of isolated valley glaciers.

The third area of ice accumulation and outflow was in Corral Creek (the Corral Creek Lobe), a southwest-oriented valley. Ice advance was restricted by the unfavorable orientation of the valley, but during the Ramey Creek advance, ice from the Copper Basin Lobe and from the Corral Creek Lobe met, as documented by provenance data (Evenson and others, 1979). This confluence of ice dammed a large ice marginal lake (Figure 3) in the Copper Basin Flats as shown by thick lake clay underlying the flats.

In Wildhorse Canyon and the North Fork drainage, the geometry of Devil's Bedstead and Kane advance moraines indicates more extensive glaciation

than during the ensuing Wildhorse Canyon and North Fork advances, but at no time did the glaciers expand beyond the confines of the valley walls. Glaciers in these drainages are much narrower due to the confining topography.

In the drainage of Wildhorse Creek, the three principal trunk glaciers from Wildhorse, Fall, and Left Fork Canyons coalesced to form the Wildhorse Canyon Lobe that flowed northward into the East Fork Canyon to deposit moraines of the Devil's Bedstead advance (Figure 3). The occupation of this portion of East Fork Canyon occurred numerous times during the Pleistocene, and each time it resulted in the damming of westward flowing drainage from the Copper Basin and in the forming of a lake (Evenson and others, 1979; Stewart, 1977). This lake is herein named "Glacial Lake East Fork" (Figure 3). Although individual lake levels cannot be distinguished, ice-rafted boulders and deltaic gravels well above the present canyon floor indicate lake depths of up to 120 meters. Because this lake was dammed by an active ice margin, minor retreats of the terminus of the Wildhorse Canyon Lobe resulted in rapid or catastrophic drainage of the lake waters. Large erratic boulders located well beyond the extent of glaciation, which caused early researchers some confusion (Umpleby and others, 1930, Figure 4), are presently believed to have been deposited by jokulhlaup activity. Lakes were dammed in the East Fork Canyon not only during the Devil's Bedstead advance (Copper Basin glaciation correlative) but also during the Wildhorse Canyon advance (Potholes glaciation correlative).

In the North Fork drainage only scattered remnants of Kane advance moraines (Copper Basin glaciation) are preserved. Provenance data (Cotter, 1980; Repsher, 1980) suggest that the three principal trunk glaciers originating in North Fork, Summit, and Kane Canyons coalesced and flowed northwest as a complex valley glacier. The geometry of the younger North Fork advance moraines shows that this coalescence (to form the North Fork Lobe) occurred only during the Copper Basin glaciation (Figure 3).

POTHOLES GLACIATION

Moraines of the Potholes glaciation are morphologically fresh and little weathered. Although no absolute proof can be offered in the Pioneer Mountains, the Potholes glaciation correlatives (Road Creek advance, Wildhorse Canyon advance, and North Fork advance) are assumed to represent a major climatically controlled, widespread glacial event that was temporally distinct from the Copper Basin glaciation correlatives. This belief is based on the marked contrast in relative-dating parameters exhibited by deposits assigned to the Copper Basin and Potholes glaciations.

Moraines assigned to the Potholes glaciation are numerous, and all are located upcanyon from moraines of the Copper Basin glaciation, documenting that glaciation was less extensive during the Potholes glaciation. Well-developed moraines and paired terraces document four distinct depositional events during the Potholes glaciation throughout the Pioneer Mountains (Table 1). Moraines of this glaciation, although indistinguishable from each other on the basis of morphological or weathering characteristics, can be differentiated on the basis of downvalley position and their relationship to terrace levels. Several moraines were deposited by readvances, as shown by provenance data, cross-cutting relationships, and moraine geometry (Evenson and others, 1979; Brugger, in preparation, but it is unknown whether most moraines represent a single, continuous deglaciation or a series of retreat and advance events to successive upvalley ice-margin positions.

Moss (1974) has discussed the relationship between glaciofluvial terraces and moraines in Wyoming. He found a genetic relationship between moraine positions and terrace levels graded to them, and he has implied synchroneity of glaciofluvial terrace deposition and associated moraine construction. In the Pioneer Mountains, the terrace gravels are assumed to be glaciofluvial in origin and formed during periods of glacial advance or stillstand. Conversely, downcutting and the attainment of a new terrace level is assumed to be associated with deglaciation and interglacial conditions. Terrace levels were therefore extremely useful in differentiating moraines of the Potholes glaciation and in correlating events from basin to basin.

Four separate moraine complexes of the Potholes glaciation are correlated throughout the Pioneer Mountains. Moraines of the Road Creek I, Wildhorse Canyon I, and North Fork I events (considered as terminal moraines of the Potholes glaciation) are located furthest downvalley but are associated with outwash gravels only in the Copper Basin Flats. No terraces of this advance are preserved in the constricted valleys of Wildhorse Canyon or the North Fork drainage, which served as the only drainage path for meltwater. The existence of Glacial Lake East Fork, between Wildhorse Canyon and the Copper Basin (Figure 4), precluded the formation of a terrace graded to the Road Creek I moraines of the Copper Basin. Downstream from the Wildhorse Canyon I and North Fork I moraines, the Big Lost River Canyon is narrow; consequently

later terrace-forming events and jokulhlaups from the lake dammed in the East Fork could easily remove or bury all traces of the earlier terraces.

The highest continuous terrace in the Pioneer Mountains cuts through the outermost (oldest) moraines (Road Creek I, Wildhorse Canyon I, and North Fork I) correlated with the Potholes glaciation and grades to moraines farther upvalley. The moraines that grade into this upper terrace are assigned to the Road Creek II, Wildhorse Canyon II, and North Fork II events, and as these moraines all grade to the same terrace level, they can be conclusively correlated. In the same manner, moraines further upvalley that grade to a lower terrace which developed in all three drainage basins are assigned to the Road Creek III, Wildhorse Canyon III, and North Fork III events and are also explicitly correlated.

All moraines upvalley from those graded to the lower continuous terrace are arbitrarily assigned to the Road Creek IV, Wildhorse Canyon IV, and North Fork IV events. These moraines are restricted to the individual source canyons and are associated with limited terraces that cannot be traced continuously between adjacent canyons. No exact correlation of these deposits is possible. It is likely that some moraines were formed after ice had disappeared from lower cirques.

In the Pioneer Mountains, ice deployment in the advances correlated with the Potholes glaciation was similar to ice deployment during the Copper Basin glaciation, but less extensive. In the North Fork drainage, North Fork I ice margins of the three principal valley glaciers (Figure 4) were located about 1 kilometer upvalley from the inferred Kane advance terminus (Figure 3). The three trunk glaciers did not coalesce, but they were in contact with each other, as shown by moraine geometry (Cotter, 1980) and provenance data (Repsher, 1980).

In the Wildhorse Canyon area (Figure 4), ice again expanded into the canyon of the East Fork of the Big Lost River during the Wildhorse Canyon I event, again impounding Glacial Lake East Fork by damming drainage from the Copper Basin. The depth and extent of the lake which formed during this time was probably similar to the lake which existed during the Devil's Bedstead advance; however, the lack of well-developed strandlines prevents an accurate reconstruction of the varying lake stands. The frequency of jokulhlaup activity probably reached its peak during the Wildhorse Canyon I advance, as only minor fluctuations in ice margin position would be required to initiate impoundment and release of the waters of Glacial Lake East Fork.

In the Copper Basin, a large intermontane piedmont lobe—the Copper Basin Lobe—fed by catchment areas to the south and west again formed during the Road Creek I event (Figure 4). The geometry of Road Creek I moraines shows that ice did not extend very far northwestward into the East Fork Canyon, nor did the piedmont lobe spread eastward onto the Copper Basin Flats. It was during the Road Creek I that the moraine locally known as "the Potholes" was deposited. This moraine (Figure 2) succinctly illustrates the morphologic characteristics of the moraines of the Potholes glaciation.

Local glaciers developed in Coal, Charcoal, Steve, Smelter, and Anderson Canyons to the east of the piedmont lobe. The glacial history of these canyons during the Road Creek advance (Potholes glaciation) is similar to the history during the Ramey Creek advance (Copper Basin glaciation) and consists solely of isolated valley glaciation. The record of deposits in most of the canyons is incomplete, but it is well displayed in Anderson Canyon. An isolated glacier also existed in Corral Creek, but it did not meet ice moving upvalley from the piedmont lobe as it did during the Ramey Creek advance.

Moraines assigned to the North Fork II, Wildhorse Canyon II, and Road Creek II events can be correlated on the basis of their association with the upper continuous terrace, as discussed earlier. During this advance, ice margins were located farther upvalley than during earlier advances, but the pattern of ice deployment was similar (Figure 5). In the North Fork drainage, none of the three trunk glaciers were in contact. In Wildhorse Canyon, ice did extend to the East Fork Canyon, but there is little evidence that drainage from the Copper Basin was dammed. In the Copper Basin, the Copper Basin Lobe still existed, but it was not as large in areal extent or in volume as it had been during previous advances.

Ice continued to retreat and then may have readvanced during the North Fork III, Wildhorse Canyon III, and Road Creek III events. Ice deployment was relatively unchanged in the North Fork drainage but radically different in the other two basins (Figure 6). The glacier occupying Wildhorse Canyon had split into at least two separate glaciers, leaving Wildhorse Canyon III moraines at the junction of Wildhorse Creek and Fall Creek and at the mouth of Left Fork Creek. Provenance data and moraine geometry (Brugger, in preparation) reveal that ice from the upper reaches of Wildhorse Creek expanded into lower Fall Creek Canyon, suggesting that the Wildhorse Canyon III event may have been a readvance.

The piedmont lobe in the Copper Basin had split into six individual glaciers by the time the Road Creek III moraines had been formed. Moraine cross-cutting relationships and provenance data suggest

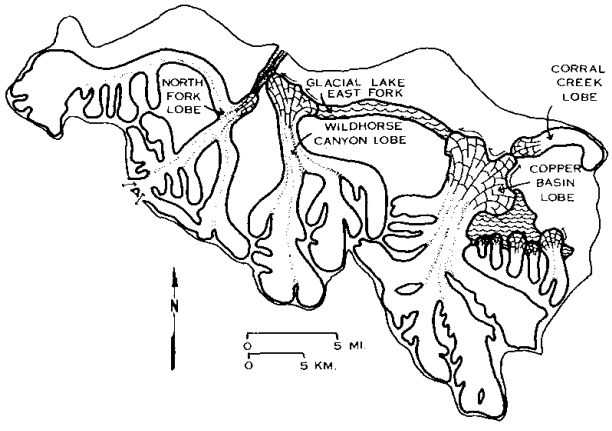

Figure 3. Reconstruction of ice margins, fluvial, and lacustrine systems at maximum of Copper Basin glaciation (Kane advance; Devil's Bedstead I and Ramey Creek I events).

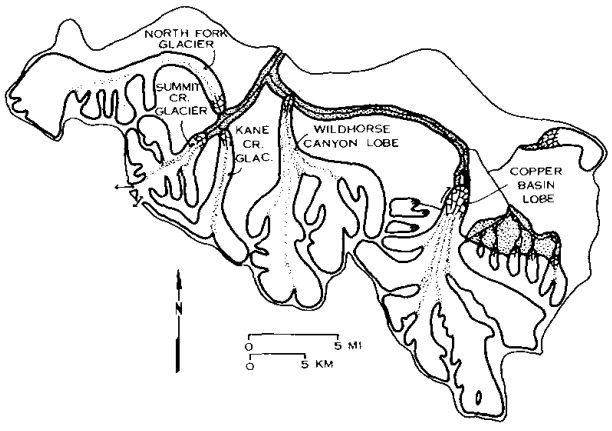

Figure 5. Reconstruction of ice margins and fluvial systems at North Fork II, Wildhorse Canyon II, and Road Creek II event maxima (Potholes glaciation).

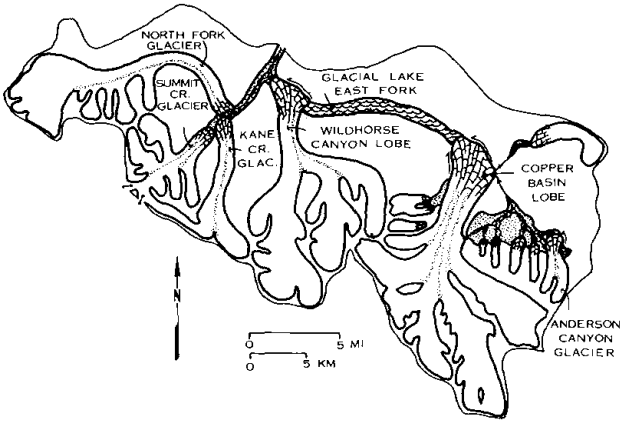

Figure 4. Reconstruction of ice margins, fluvial and lacustrine systems at maximum of Potholes glaciation (North Fork I, Wildhorse Canyon I, and Road Creek I events).

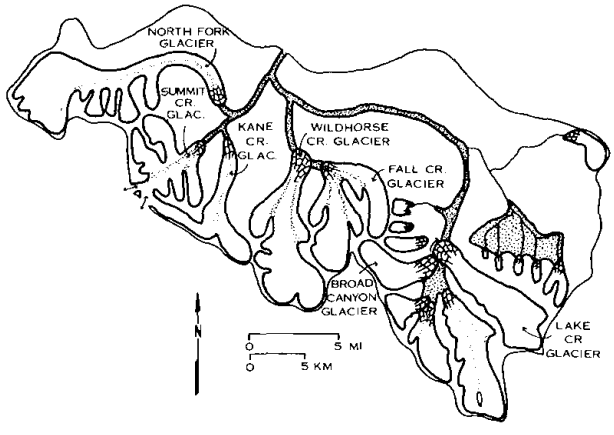

Figure 6. Reconstruction of ice margins and fluvial systems at North Fork III, Wildhorse Canyon III, and Road Creek III event maxima (Potholes glaciation).

that ice from Lake Creek and perhaps Broad Canyon readvanced and crossed the main drainage channel (Pasquini, 1976; Evenson and others, 1979). There is no evidence whether the remaining glaciers readvanced or simply melted back to their Road Creek III positions.

Moraines assigned to the North Fork IV, Wildhorse Canyon IV, and Road Creek IV events are restricted to the source canyons and cannot be reliably correlated. The record of glaciation during these advances is probably incomplete, as no moraines are preserved in some major canyons, while abundant moraines are preserved in adjacent canyons. It is believed that the duration and timing of the deposition of these late moraines may have varied from valley to valley. Therefore, the correlation of these moraines must be considered tenuous at best.

YOUNGER DEPOSITION EVENTS

Deposits younger than the Potholes glaciation in the Pioneer Mountains appear to consist entirely of alluvium, alluvial fan, rock slide, talus, and rock-glacier deposits. We currently recognize no moraines younger than the Potholes glaciation. At this time, insufficient evidence exists to subdivide the depositional events younger than the Potholes glaciation; therefore, we make no attempt to do so.

CORRELATION OF OTHER STUDY AREAS WITH THE IDAHO GLACIAL MODEL

Glacial deposits have been mapped in detail in

only a small portion of central Idaho. Early researchers focused primarily on bedrock geology and economic deposits; consequently, surficial geology was mapped only when necessary. Descriptions of moraine morphology are brief, and when correlations were made, they were to the Midwest chronology, such as Wisconsinan or Nebraskan. Several researchers, however, have completed projects in central Idaho during the past thirty years using the nomenclature of the Rocky Mountain Glacial Model (Mears, 1974) with some modification. These chronologies are here reviewed and tentatively correlated with the Idaho Glacial Model (Table 2). We recognize that these correlations are tentative at best and that they will require a great deal of detailed work to substantiate them.

Williams (1961) mapped deposits in the southern part of the Stanley Basin and adjacent highlands. He describes deposits of four separate ages: Pre-Bull Lake till found in isolated patches on ridge crests east and north of the basin, Bull Lake and Pinedale moraines on the floor of the basin, and Neoglacial rock glaciers in the cirques of the Sawtooth Mountains. On the basis of Williams' description of the units and reconnaissance investigations during two field seasons, we suggest a correlation of Williams' Pinedale and Bull Lake glaciations with the Potholes glaciation and Copper Basin glaciation, respectively, of the Idaho Glacial Model (Table 2).

In a similar study, Schmidt and Mackin (1970) also mapped Pinedale and Bull Lake moraines in Bear Valley and the surrounding area. Published descriptions and reconnaissance investigations also suggest correlations between Pinedale and our Potholes glaciation and between Bull Lake and our Copper Basin glaciation (Table 2).

Knoll (1977) made a detailed study of deposits in four small canyons in the Lemhi Mountains, north of our study area. He correlated his deposits with the Rocky Mountain Glacial Model. He also attempted to subdivide second-order events (stadials) and correlate these with the stades in the Rocky Mountain Glacial Model. Knoll found one to three stadials in one stade of Sacagawea Ridge, two to three stadials in two to three stades of Bull Lake, nine stadials in three stades of Pinedale, and five stadials in three stades of Neoglacial events. From published descriptions we suggest a correlation between the Pinedale of Knoll and our Potholes glaciation and between his Bull Lake and our Copper Basin glaciation. No correlation can be made between his second-order events and the second-order events of the Pioneer Mountains (for example, Wildhorse Canyon II), because the number of events may vary depending on the definition each researcher uses and also on the number of events actually preserved in each canyon. Knoll's Sacagawea Ridge has no exact match in the Pioneer Mountains, as no moraines older than those correlated to the Copper Basin glaciation have been found. At this time, the moraines Knoll mapped as Sacagawea Ridge and the Pre-Bull Lake till that Williams (1961) describes are correlated with our Pioneer glaciation.

Table 2. Correlation of time stratigraphic chronologies used in Idaho with the Idaho Glacial Model.

IDAHO GLACIAL MODEL	STANLEY BASIN (WILLIAMS, 1961)	BEAR VALLEY (SCHMIDT AND MACKIN, 1970)	LEMHI MOUNTAINS (KNOLL, 1977)	LONG VALLEY (SCHMIDT & MACKIN, 1970; COLMAN & PIERCE, 1981)
	NEOGLACIAL		NEOGLACIAL: GANNETT PEAK, AUDOBON, TEMPLE LAKE	NEOGLACIAL
POTHOLES GLACIATION	PINEDALE	PINEDALE	PINEDALE: LATE, MIDDLE, EARLY	PINEDALE 20,000 YRS; INTERMEDIATE 60,000 YRS
COPPER BASIN GLACIATION	BULL LAKE: LATE, EARLY	BULL LAKE	BULL LAKE: III, LATE, EARLY	BULL LAKE 140,000 YRS
PIONEER GLACIATION	PRE-BULL LAKE		SACAGAWEA RIDGE	PRE-BULL LAKE

The remaining area in central Idaho that has been studied in detail is the area near McCall at the north end of Long Valley. The original mapping was done by Schmidt and Mackin (1970). They found evidence for four distinct ages of deposits: a Pre-Bull Lake moraine, Bull Lake and Pinedale moraines, and a Neoglacial rock glacier. They did not divide each group of deposits into second-order events, although reconnaissance data suggest that this is possible. Their stratigraphy has been modified by Colman and Pierce (1981), who defined an additional advance between the Pinedale and Bull Lake moraines on the basis of the thickness of basalt weathering rinds. By making a correlation between the Bull Lake of the McCall area and the Bull Lake moraines of the West Yellowstone Basin, which are dated by obsidian hydration (Pierce and others, 1976), to calibrate their basalt-weathering curve, Colman and Pierce obtained approximate dates of 20,000 years for the Pinedale moraines, 60,000 years for the intermediate moraines, and 140,000 years for the Bull Lake moraines. The oldest moraine could not be dated by this method. They estimated a 10 to 20 percent error in their ages due to error limits on the weathering-rind-thickness data.

Based on the published descriptions of the Long Valley units and also on reconnaissance mapping, we would correlate the Pinedale moraines with our Potholes glaciation, and the Bull Lake moraines

with our Copper Basin glaciation. No known analog of the intermediate moraines exists in the Pioneer Mountains, and no correlation can be made. On the basis of surface morphology, the intermediate moraine is similar to the Bull Lake moraines and may thus be correlated with the Copper Basin glaciation. Alternatively, the intermediate moraine may represent a separate glaciation not as extensive as the Potholes glaciation and thus not preserved in the Pioneer Mountains. Further study will be needed to resolve the status of the intermediate moraine.

CONCLUSIONS

The drainages of the northern Pioneer Mountains have been modified by at least two and perhaps three episodes of glaciation. The two younger, well-documented glaciations are represented by multiple moraine complexes. These moraines have been differentiated by relative-age dating techniques (moraine morphology, pedogenic characteristics, extent of glaciation, and terrace associations) and have been grouped into two informal units: the Potholes glaciation (younger) and the Copper Basin glaciation (older). Isolated high gravels of assumed glacial origin are assigned to the Pioneer glaciation (oldest). Accurate correlation between basins, combined with provenance and moraine geometry, has allowed reconstruction of modes of ice-deployment of two principal glacial episodes (Potholes and Copper Basin glaciation) and also resulted in the development of a detailed deglaciation chronology of the Potholes glaciation within the Pioneer Mountains.

The relative-age stratigraphic nomenclature developed for this study provides a regional standard (the Idaho Glacial Model) to which local stratigraphies may be compared and correlated. As the Idaho Glacial Model continues to be extended it can be correlated to other regional stratigraphies. The Rocky Mountain Glacial Model (Mears, 1974) may then be expanded to include these intra-correlated regional stratigraphies without over-extending the terms Pinedale and Bull Lake. It is not possible, at this time, to correlate deposits in this study area with the stratigraphic units of the Rocky Mountain Glacial Model at their type localities in the Wind River Range, Wyoming. However, deposits of the two advances mapped in the Pioneer Mountains (Potholes and Copper Basin glaciations) have been accurately correlated from basin to basin in the Pioneer Mountains and have been tentatively correlated with other regions of Idaho.

ACKNOWLEDGMENTS

We thank T. O. Vorren, Keith Brugger, Jim Zigmont, and Jim Bloomfield and two anonymous reviewers for helpful comments on the development of the Idaho Glacial Model. We are grateful to Vic Johnson and his family for field support and Beth Peters and Laurie Cambiotti for preparation of the manuscript. This study was supported in part by grants from Sigma Xi and Lehigh University.

REFERENCES

American Commission of Stratigraphic Nomenclature, 1970, Code of Stratigraphic Nomenclature, 2nd edition: American Association of Petroleum Geologists, 21 p.

Birkeland, P. W., 1964, Pleistocene glaciation of the northern Sierra Nevada, north of Lake Tahoe, California: Journal of Geology, v. 72, p. 810-825.

———, 1973, Use of relative age dating methods in a stratigraphic study of rock glacier deposits, Mt. Sopris, Colorado: Arctic and Alpine Research, v. 5, p. 401-416.

Birkeland, P. W., S. M. Colman, B. M. Burke, R. R. Shroba, and T. C. Meirding, 1979, Nomenclature of alpine glacial deposits, or, What's in a name?: Geology, v. 7, p. 532-536.

Blackwelder, Elliot, 1915, Post-Cretaceous history of the mountains of central western Wyoming, Part III: Journal of Geology, v. 23, p. 307-340.

Brugger, K. A., in preparation, Provenance studies and ice reconstruction of the Wildhorse Canyon Glacier, Custer County, Idaho: Lehigh University M.S. thesis.

Burke, R. M. and P. W. Birkeland, 1979, Reevaluation of multiparameter relative dating techniques and their application to the glacial sequence along the eastern escarpment of the Sierra Nevada, California: Quaternary Research, v. 11, p. 21-52

Carroll, Tom, 1974, Relative age dating techniques and a late Quaternary chronology, Arikaree Cirque, Colorado: Geology, v. 2, p. 321-325.

Clinch, J. M., in preparation, A remote sensing interpretation of surficial geology, central Idaho: Lehigh University M.S. thesis.

Crandell, D. R., 1967, Glaciation at Wallowa Lake, Oregon: U. S. Geological Survey Professional Paper 575-C, p. C145-C153.

Colman, S. M. and K. L. Pierce, 1981, Weathering rinds on andesitic and basaltic stones as a Quaternary age indicator, western United States: U. S. Geological Survey Professional Paper 1210, 56 p.

Cotter, J. F. P., 1980, The glacial geology of the North Fork of the Big Lost River, Custer County, Idaho: Lehigh University M.S. thesis, 102 p.

Dover, J. H., 1966, Bedrock geology of the Pioneer Mountains, Blaine and Custer Counties, Idaho: University of Washington Ph.D. thesis, 138 p.

———, 1969, Bedrock geology of the Pioneer Mountains, Blaine and Custer Counties, central Idaho: Idaho Bureau of Mines and Geology Pamphlet 142, 66 p.

Dover, J. H., W. E. Hall, S. W. Hobbs, C. M. Tschanz, J. M. Batchelder, and F. S. Simons, 1976, Geologic map of the Pioneer Mountains region, Blaine and Custer Counties, Idaho: U. S. Geological Survey Open-File Report 76-75.

Evenson, E. B., T. A. Pasquini, R. A. Stewart, and George Stephens, 1979, Systematic provenance investigations in areas of alpine glaciation: applications to glacial geology and mineral exploration, *in* Christian Schluchter, editor, Moraines and Varves: A. A. Balkema, Rotterdam, p. 25-42.

Holmes, G. W. and J. H. Moss, 1955, Pleistocene geology of the southwestern Wind River Mountains, Wyoming: Geological Society of America Bulletin, v. 66, p. 629-654.

Knoll, K. M., 1977, Chronology of alpine glacier stillstands, east-central Lemhi Range, Idaho: Idaho State Museum of Natural History, Pocatello, Idaho, 230 p.

Mahaney, W. C., 1974, Soil stratigraphy and genesis of Neoglacial deposits in the Arapaho and Henderson Cirques, central Colorado Front Range, *in* W. C. Mahaney, editor, Quaternary Environments—Proceedings of a Symposium: York University-Atkinson College (Toronto) Geographical Monograph No. 5, p. 197-240.

Mears, Brainerd, Jr., 1974, The evolution of the Rocky Mountain Glacial Model, *in* D. R. Coates, editor, Glacial Geomorphology: New York State University Press, New York, p. 11-40.

Moss, J. H., 1949, Possible new glacial substage in the Middle Rocky Mountains: Geological Society of America Bulletin, v. 60, p. 19-72.

———, 1951a, Early man in the Eden Valley: University of Pennsylvania Museum Monograph, 124 p.

———, 1951b, Late glacial advance in the southern Wind River Mountains, Wyoming: American Journal of Science, v. 249, p. 865-883.

———, 1974, The relation of river terrace formation to glaciation in the Shoshone River Basin, western Wyoming, *in* D. R. Coates, editor, Glacial Geomorphology: Publications in Geomorphology, Binghamton, New York, p. 293-315.

Nelson, W. H. and C. P. Ross, 1969, Geology of the Mackay 30-minute quadrangle, Idaho: U. S. Geological Survey Open-File Report, 161 p.

Pankos, Maria, in preparation, Provenance investigations of outwash terraces, Big Lost River drainage, Custer County, Idaho: Lehigh University M.S. thesis.

Pasquini, T. P., 1976, Provenance investigation of the glacial geology of the Copper Basin, Idaho: Lehigh University M.S. thesis, 136 p.

Pierce, K. L., J. D. Obradovich, and Irving Friedman, 1976, Obsidian hydration dating and correlation of Bull Lake and Pinedale glaciations near West Yellowstone, Montana: Geological Society of America Bulletin, v. 87, p. 703-710.

Porter, S. C., 1971, Fluctuations of late Pleistocene alpine glaciers in western North America, *in* K. K. Turekian, editor, The Late Cenozoic Glacial Ages: Yale University Press, p. 307-329.

Repsher, A. A., 1980, Provenance of glacial deposits in the Pioneer Mountains, Blaine and Custer Counties: Lehigh University M.S. thesis.

Repsher, A. A., J. F. P. Cotter, and E. B. Evenson, 1980, Glacial history, provenance and mineral exploration in an area of alpine glaciation, Custer and Blaine Counties, Idaho: Geological Society of America, Abstracts with Programs, v. 12, no. 6, p. 301.

Richmond, G. M., 1948, Modification of Blackwelder's sequence of Pleistocene glaciation in the Wind River Mountains, Wyoming: Geological Society of America Bulletin, v. 59, p. 1400-1401.

———, 1965, Glaciation of the Rocky Mountains, *in* H. E. Wright, Jr., and D. G. Frey, editors, The Quaternary of the United States: Princeton University Press, p. 217-230.

———, 1976, Pleistocene stratigraphy and chronology of the mountains of western Wyoming, *in* W. C. Mahaney, editor, Quaternary Stratigraphy of North America: John Wiley and Sons, Inc., New York, p. 353-380.

Schmidt, D. L. and J. H. Mackin, 1970, Quaternary geology of Long and Bear Valleys, west-central Idaho: U. S. Geological Survey Bulletin 1131-A, 22 p.

Stewart, R. A., 1977, The glacial geology of Wildhorse Canyon, Custer County, Idaho: Lehigh University M.S. thesis, 103 p.

Umpleby, S. G., L. G. Westgate, and G. P. Ross, 1930, Geology and ore deposits of the Wood

River region, Idaho: U. S. Geological Survey Bulletin 814, 250 p.

Wigley, W. C., 1976, The glacial geology of the Copper Basin, Custer County, Idaho: a morphologic and pedogenic approach: Lehigh University M.S. thesis, 104 p.

Wigley, W. C., T. P. Pasquini, and E. B. Evenson, 1978, Glacial history of the Copper Basin, Idaho: a pedologic, provenance, and morphologic approach, *in* W. C. Mahaney, editor, Quaternary Soils: Geological Abstracts, Norwich, England, p. 265-307.

Williams, P. L., 1961, Glacial geology of the Stanley Basin, Idaho: Idaho Bureau of Mines and Geology Pamphlet 123, 29 p.

Chapter 13

Pleistocene Flood Deposits and Gravels

Late Cenozoic Gravels in Hells Canyon and the Lewiston Basin, Washington and Idaho

by

Gary D. Webster[1], Mary J. Pankratz Kuhns[2], and Gail L. Waggoner[3]

ABSTRACT

Six late Cenozoic gravels mapped in the Lewiston basin are attributable to a Snake, Salmon, or Clearwater River origin on the basis of preliminary studies of cobble lithology. The oldest, the North Lewiston Gravel, is between 12.0 and 6.0 million years in age, occurs below the Lower Monumental Member, contains 95 percent basalt clasts, and is derived from the ancestral Clearwater River drainage. The Clearwater Gravel, deposited above the Lower Monumental Member, is between 6.0 and 2.0 million years old, contains a higher percentage of nonbasaltic igneous and older metamorphic rocks, and is also derived from the Clearwater drainage. A gravel believed to be coeval with the Clearwater Gravel but derived from the ancestral Salmon River is the Clarkston Heights Gravel. The Clarkston Heights Gravel is distinguished by the abundance of red and green volcaniclastic rocks derived from the Seven Devils Group. The Clarkston Heights Gravel and the Clearwater Gravel are probably the upstream equivalent of the Middle Ringold gravels.

The Clarkston Gravel is restricted to a gravel underlying the northeastern part of Clarkston, Washington. This gravel is derived from the ancestral Salmon River and is believed to be late Pliocene or early Pleistocene in age. It is distinguished from the Clarkston Heights Gravel by the coarser cobble size and the clay interbeds. Deposits coeval with the Clarkston Gravel are believed to be present in the Snake River canyon below Clarkston.

Gravel deposits of the Bonneville Flood (14,000-15,000 years ago) formed expansion, point, and back eddy bars. The Bonneville deposits are recognized in Hells Canyon, the Lewiston basin, and lower Snake River canyon. Touchet Beds derived from the Missoula Floods (post-Bonneville deposits to 12,000 years ago) are widespread in the Lewiston basin and reported for the first time from the lower Salmon and Grande Ronde canyons.

All of the late Cenozoic gravels provide clues to the regional erosional and depositional history of the Lewiston basin.

INTRODUCTION

Gravel deposits, older than 12,000 years, are found downriver from Hells Canyon along the Snake River and Clearwater River at Lewiston, Idaho, and Clarkston, Washington (Figure 1). They are diverse in character and origin. Many have been quarried as a source of aggregate and continue to be economically significant. They are the sedimentologic key to the late Cenozoic geologic history of the area.

PREVIOUS WORK

The Snake River and Clearwater River gravels have been the subject of several studies during the past fifty years. Working in the Channeled Scablands of southeastern Washington, Bretz (1929) recognized backwater deposits of the Missoula Flood both upstream and downstream from Lewiston. MacKenzie (1942) made counts of the coarser cobbles attempting to discriminate the diverse gravels of the Lewiston area. Lupher (1945) described a "Clarkston Stage" of the Pleistocene and included sands and gravels, here considered of diverse origin and character, in one unit that he designated the Clarkston Gravels. Stearns (1962) reported gravels attributed to the Bonneville Flood at the Brownlee Dam site above Homestead, Oregon, and several localities in and downstream from Hells Canyon. Furthermore, Stearns (1962) incorrectly considered some of the backwater deposits described by Bretz (1929) in the vicinity of Lewiston to be of Bonneville

[1]Department of Geology, Washington State University, Pullman, Washington 99164.
[2]2321 Livingston, Missoula, Montana 59801.
[3]2888 Bluff St. #352, Boulder, Colorado 80301.

Webster, G. D., M. J. P. Kuhns, and G. L. Waggoner, 1982, Late Cenozoic gravels in Hells Canyon and the Lewiston basin, Washington and Idaho, *in* Bill Bonnichsen and R. M. Breckenridge, editors, Cenozoic Geology of Idaho: Idaho Bureau of Mines and Geology Bulletin 26, p. 669-683.

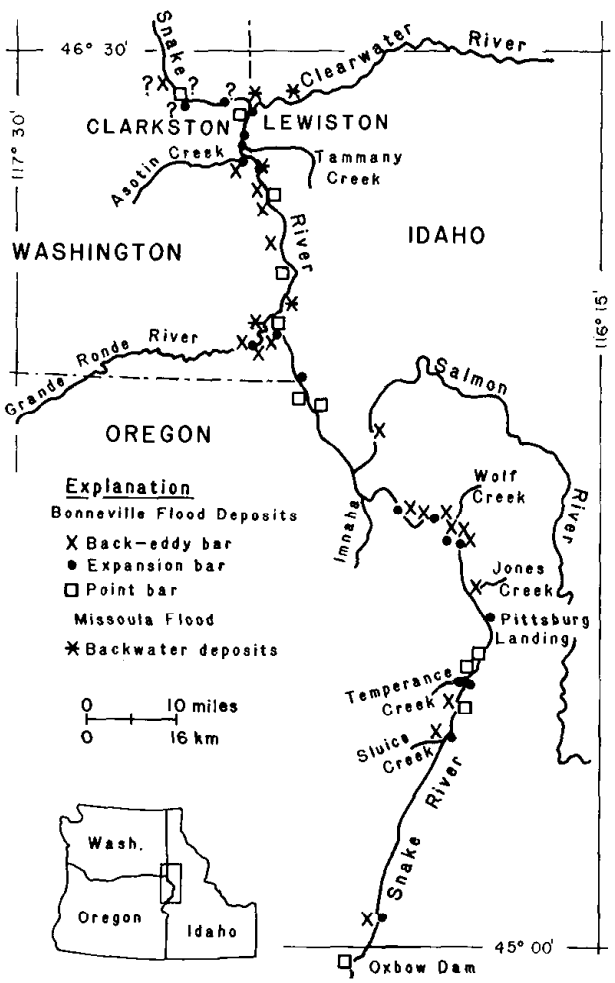

Figure 1. Index map and map showing location of Bonneville Flood and Missoula Floods deposits.

origin. Mapping the late Quaternary geology of the Lower Granite Reservoir area, Hammatt (1976) incorrectly interpreted most postbasalt alluvial deposits, except Holocene alluvial gravels and sands and early(?) Pleistocene gravel, as Missoula Flood in origin. Detailed sedimentologic studies of gravels along the lower Clearwater River valley by Kuhns (1980), on the lower Snake River canyon by Webster (1980) and Wheeler (1980), and in the Clarkston area by Waggoner (1981) provide new information permitting a revised interpretation of these gravels.

REGIONAL GEOLOGY

The Lewiston basin and Hells Canyon area lie within the most eastward extension of the Columbia Arc (Taubeneck, 1966). The arc is composed of a series of calc-alkaline volcanic and volcaniclastic units of predominately andesite composition belonging to the Seven Devils Group and associated ophiolitic sequences of Permian-Triassic age (Vallier, 1974, 1977; Avé Lallemant and others, 1980). These units are overlain by clastic sediments of Jurassic age and intruded by granites of Jurassic to Early Cretaceous age. The arc rocks probably formed southwest of their present location and were accreted to the western margin of the American Plate in the Permian-Triassic (Hamilton, 1976) or the Cretaceous (Davis and others, 1979, Avé Lallemant and others 1980). To the east of the suture zone in the Whitebird-Riggins valley, the Idaho batholith of Cretaceous and early Cenozoic age intrudes rocks of the Precambrian old continental basement and Belt Supergroup. The old continental basement rocks contain a variety of augen gneisses, orthogneisses, pelitic schists, and amphibolites. Rocks of the Belt Supergroup are metamorphosed to the amphibolite facies. Originally they were sandstones, siltstones, and impure carbonate rocks.

The Miocene age Columbia River Basalt Group filled the pre-Tertiary terrain that was deeply dissected by westward-flowing rivers (Figure 2).

The present Clearwater River system drains a large area of the Idaho batholith and older quartzite and gneiss. The Salmon River also heads in the Idaho batholith but cuts through the Seven Devils Group in Hells Canyon. All major drainages have cut deeply into the Columbia River Basalt Group.

GRAVEL STRATIGRAPHY

Gravels preceding Holocene fluvial deposits within the Lewiston basin include six recognizable units. They range in age from late Miocene to late Pleistocene (Table 1). Their stratigraphic relationships are rather complex and include the following: (1) the oldest gravel is overlain by an intracanyon basalt flow; (2) the four oldest gravels are not in direct contact with one another; (3) most gravels are laterally in contact with basalt; and (4) the two youngest gravels directly overlie or are in lateral contact with most older gravels. Recognition of each of the six gravels is based upon cobble lithologies (Table 2) and stratigraphic relationships.

NORTH LEWISTON GRAVEL

As described by Kuhns (1980), the North Lewiston Gravel crops out approximately parallel to

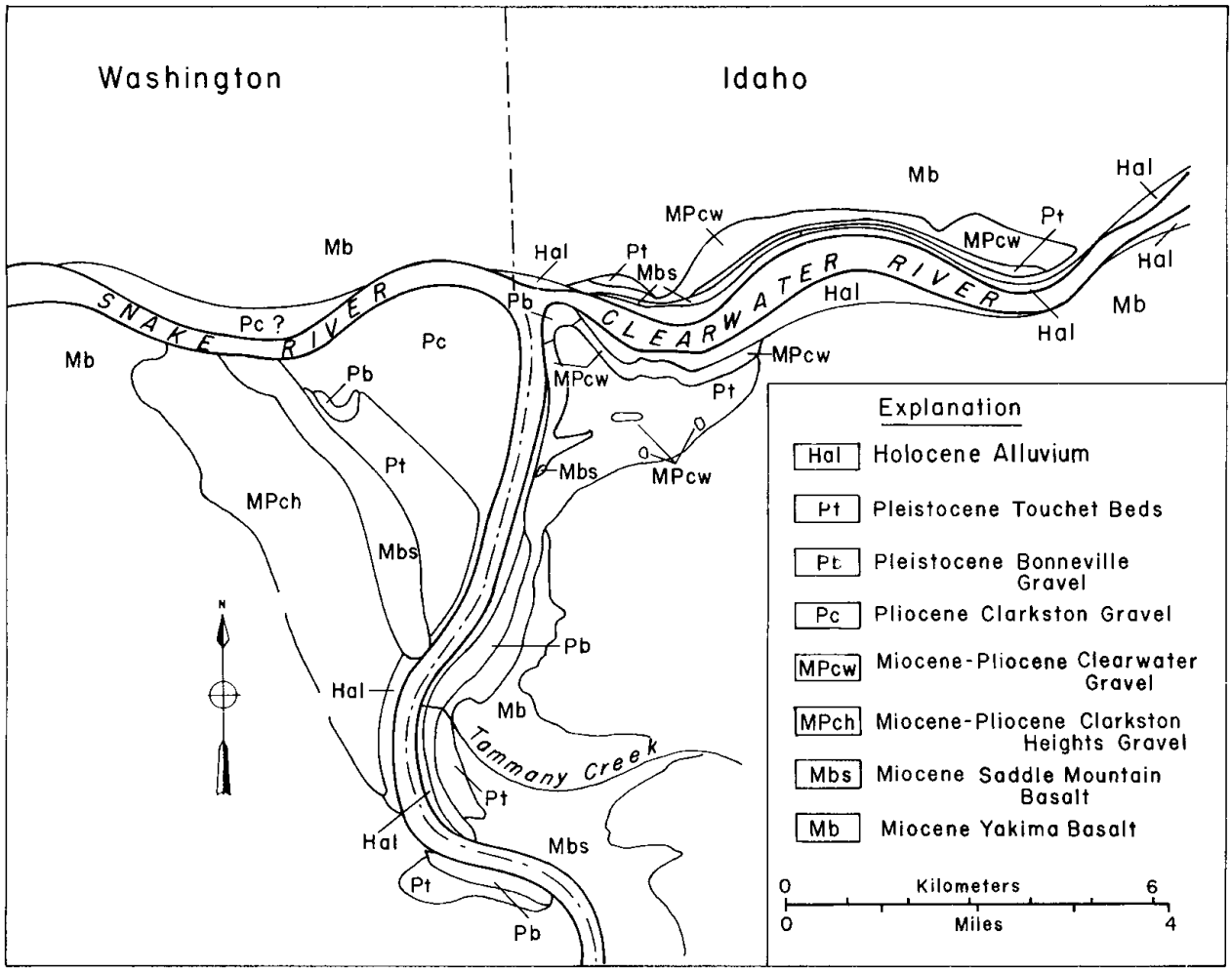

Figure 2. Generalized geologic map of the Lewiston and Clarkston area showing distribution of major gravel deposits. Basalts after Camp, 1976.

the present course of the Clearwater River in the lower Clearwater River valley. It is a fluvial gravel confined between 750 to 850 feet (229 to 259 meters) in elevation. The best exposures are found along Hatwai Road and at the base of the old Lewiston grade (Figure 3), where the gravels occur 10 to 80 feet (3 to 24 meters) above the present river level.

Cobbles of the North Lewiston Gravel (based on a count of 1,000 clasts) consist primarily of basalt clasts having approximately 95 percent subrounded basalt and only 5 percent well-rounded igneous and metamorphic rocks. Igneous lithologies present include 0.4 percent mafic dike porphyry. Metamorphic rocks inside 1.1 percent banded biotite gneiss and 0.8 percent banded gneiss.

Partially consolidated silt to medium sand-sized quartz and basalt grains constitute the characteristically oxidized, bright orange matrix. Primary matrix minerals are 40 percent quartz, 30 percent basalt fragments, 15 percent plagioclase, 4 percent potassium feldspar, 2 percent biotite, 1 percent hornblende, and a trace of olivine in the 0.0 and 1.0 phi size intervals. Traces of muscovite, augite, and magnetite appear in the 2.0 and 3.0 phi size grades. The darker appearance of this gravel is due to the abundance of basalt fragments in the cobbles and matrix.

Imbrication, which is well developed in many of the outcrops, is two directional at some localities suggesting back-eddy deposition. Other directional indicators such as cross-bedding were not observed.

The North Lewiston Gravel is at least 6 million years old because it underlies the 6 million year old Lower Monumental Member (McKee and others, 1977) of the Saddle Mountains Basalt Formation. The maximum age of these gravels is post canyon cutting which is post-Weissenfels Ridge Member (between 14.0 and 12.0 million years) to pre-Pomona

Member (12.0 million years) time (Swanson and others, 1979).

The name North Lewiston Gravel is used informally since the total extent of the unit is unknown. The gravels may be the result of aggrading conditions in the lower Clearwater River valley resulting from filling of the ancestral Snake River canyon below Lewiston by the Pomona or Elephant Mountain (10.5 million years) Members.

CLARKSTON HEIGHTS GRAVEL

The Clarkston Heights Gravel is herein informally defined as those sands and gravels extending in a northwest direction from the SE¼, sec. 8, T. 10 N.,

Table 1. Stratigraphic sequence and age of late Cenozoic gravels and basalts in the vicinity of Lewiston, Idaho. All basalt members belong to the Yakima Basalt subgroup of the Columbia River Basalt Group (Swanson and others, 1979).

Stratigraphic Unit	Age	Basalt Stratigraphy
Modern alluvium	12,000 to present	
Missoula Flood deposits	14,000-15,000 to 12,000	
Bonneville Flood deposits	14,000-15,000	
Clarkston Gravel	Late Pliocene? or early Pleistocene?	
Clearwater Gravel	Late Miocene to Pliocene (6 m.y. to 2 m.y.)	
Clarkston Heights Gravel	Late Miocene to Pliocene (6 m.y. to 2 m.y.)	Lower Monumental Member (6 m.y.)
North Lewiston Gravel	Late Miocene (12 m.y. to 6 m.y.)	Elephant Canyon Member (10.5 m.y.) Pomona Member (12 m.y.) Older basalt members

Table 2. Comparison of major rock types, given as percent of 1,000 cobbles, recognized in modern gravel bars of the Clearwater, Salmon, and Snake Rivers and ancient gravel deposits in the Lewiston basin. Several distinct lithologies are recognizable within each of the four major rock groupings. Data are probably insufficient to be statistically evaluated.

GRAVEL DEPOSIT	Columbia River Basalts	Seven Devils Group	Igneous Rocks Nonbasalt	Older Metamorphic Rocks
Slate Creek, Salmon River[1]	43.9	34.8	5.5	15.8
China Bar, Salmon River	56.3	12.0	17.8	13.9
Lochsa River[1]	---	---	31.0	65.2
South Fork, Clearwater River[1]	84.6	---	10.1	9.2
North Fork, Clearwater River[1]	22.7	---	33.9	42.6
Pittsburg Landing, Snake River	39.1	34.3	18.7	7.9
Asotin Bar, Snake River	74.3	19.5	3.8	2.4
North Lewiston Gravel[1] (Ancestral Clearwater)	95.6	---	2.2	2.2
Clearwater Gravel, lower unit[1] (Ancestral Clearwater)	53.7	---	25.8	19.7
Clearwater Gravel, upper unit[1] (Ancestral Clearwater)	58.4	---	26.3	20.2
Clarkston Heights Gravel, Loc. 1[2] (Ancestral Salmon)	57.5	16.1	16.2	10.2
Clarkston Heights Gravel, Loc. 2[2] (Ancestral Salmon)	70.8	10.3	9.1	9.9
Clarkston Gravel, Loc. 1[2] (Ancestral Salmon)	80.2	6.8	10.1	3.4
Clarkston Gravel, Loc. 2[2] (Ancestral Salmon)	58.5	12.3	19.0	9.2

[1]Kuhns, 1980
[2]Waggoner, 1981

Figure 3. North Lewiston Gravel underlying Lower Monumental Basalt; base of old Lewiston grade. Note rounded metamorphic, igneous, and basalt clasts. Lower Monumental Basalt in place in upper right corner of photograph.

R. 46 E., to the NW¼, sec. 24, T. 11 N., R. 45 E. (Washington). It is restricted to the southwest side of the northwest-trending band of Saddle Mountains Basalt flows between Clarkston and Clarkston Heights (Figure 2). Excellent exposures are present in road cuts and gravel pits along Critchfield Road to the southeast (Figures 4 and 5) and Evans Road to the northwest. The unit is named for the suburb of Clarkston Heights which it underlies. The Clarkston Heights Gravel is a minimum of 337 feet (103 meters) thick according to water well logs from the area. Lupher (1945) considered them an undesignated part of his Clarkston Gravels and reported a maximum thickness of more than 400 feet (122 meters) based on topographic relief.

Cobble lithologies in this gravel as reported by Waggoner (1981) average 64 percent basalt, 13 percent red and green volcaniclastic rocks of the Seven Devils Group, 13 percent igneous rocks (mostly granitics and porphyries), and 10 percent metamorphic rocks (mostly quartzite and gneiss). All clasts are well rounded. The matrix is a bimodal, pebbly medium-grained sand or sandy pebble which alternates vertically between sand and pebble domination. The alternating sand and pebble dominance of the matrix results in a recognizable rhythmic bedding in the upper part of the unit. Small boulders are present in the upper parts of this gravel. The matrix is partly cemented and oxide stained. The degree of weathering of the basalt and granitic cobbles is intense, many cobbles crumbling to the touch. Sedimentary structures are not common in the unit; however, imbrication and foreset cross-bedding indicate paleocurrent directions to the northwest, which is the trend of the gravel unit. Sand stringers and lenses of the same composition as the matrix sand in the gravel occur in the upper part of the unit.

The gravel is fluvial in origin. The cause of the aggradation is unknown. No glacial striations or ice-rafted erratics were found in these deposits to support a glacial origin as proposed by Lupher (1945). Lupher also speculated that the aggradation might be the result of some unrecognized downstream structural or sedimentologic feature.

The Clarkston Heights Gravel fills a canyon cut into the Pomona Member (12.0 million years) of the Saddle Mountains Basalt. It is overlain by modern loess, colluvium, and remnants of the Touchet Beds. The canyon filled by the Clarkston Heights Gravel was described by Lupher and Warren (1942) as the Asotin Canyon of the ancestral Snake River formed during the Asotin Stage of probably early Pleistocene time. However, the higher percentage of derived andesitic porphyries and older metamorphic rocks in these gravels implies an origin of Salmon River drainage rather than Snake River. Therefore, we propose that this canyon is of the ancestral Salmon and predates capture of the Snake River. If the proposal by Wheeler and Cook (1954) that the Snake River was not diverted to the north until early Pleistocene time is correct, then the Clarkston Heights Gravel is older than early Pleistocene. The Asotin Stage of Lupher and Warren (1942) must be late Miocene in age, since the intracanyon flows of the Saddle Mountains Basalt formed within the ancestral canyon.

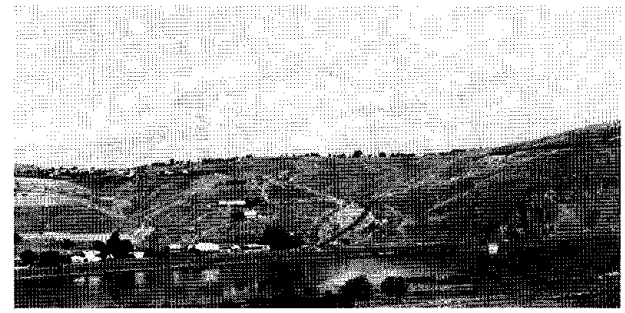

Figure 4. View to the northwest up Critchfield Road of Clarkston Heights Gravel filling ancestral Salmon River canyon. Ancestral Salmon River canyon extended from Swallow Rock (right edge of photo) to housing development on skyline (left side of photo) and from just above river level to houses on ridge crest at center of photograph.

The older age limit of the Clarkston Heights Gravel is uncertain. The Clarkston Heights Gravel overlies and must be younger than basalts of the Pomona Member (12.0 million years, McKee and others, 1977). It is here proposed that the Clarkston Heights Gravel is coeval with the Clearwater Gravel,

Figure 5. Clarkston Heights Gravel overlain by fine-grained Touchet Beds. Note imbrication in gravels, indicating a northwest current flow, and roundness of clasts. Housing excavation, north side of Critchfield Road, Clarkston, Washington.

as described below, because it is aggraded to the same elevation of 1,150 feet (351 meters), shows the same degree of deep weathering of basalt and granitoid clasts, is similarly iron stained, has a similar degree of cementation, and shows increasing sand stringers and lenses in the upper part. The ancestral Salmon and Clearwater Rivers merged immediately downstream from the northwest extent of the Clarkston Heights Gravel. Although easily separated on the basis of cobble lithologies, reflecting the different provenance of the two drainages, the number of similarities of sedimentologic features and concordance of aggradation seem to imply a coeval time of formation in response to a downstream change of base level. The Clearwater Gravel overlies the Lower Monumental Member (6.0 million years) as discussed below. If our proposal of time contemporaniety of the two units is correct, then both the Clarkston Heights Gravel and the Clearwater Gravel are between 6.0 million years and early Pleistocene in age. The age of the Clarkston Heights Gravel is certainly between 12.0 million years and 13,000 years. But the present evidence clearly favors an age between 6.0 million years and early Pleistocene.

CLEARWATER GRAVEL

The Clearwater Gravel forms a prominent terrace which in profile ranges in elevation from 800 to 1,150 feet (244-351 meters) along the lower Clearwater River valley. This gravel is well exposed in road cuts along the new Lewiston grade (U. S. Highway 95), Central Grade Road, the Northwest Aggregates quarry (SW¼NE¼NE¼, sec. 29, T. 36 N., R. 5 W.), south side of 16th Street (W½SE¼, sec. 1, T. 35 N., R. 6 W.) in Lewiston, and numerous small abandoned quarries between Lewiston and Lewiston Orchards. The Clearwater Gravel is informally recognized herein and the reference section is the exposure along the lower part of the new Lewiston grade (U.S. Highway 95) from the top of the Lower Monumental Member (NW¼SW¼, sec. 29, T. 36 N., R. 5 W., Idaho; Figure 6) to the ash bed exposed in the road cut along the north side of the runoff ramp in the NW¼NW¼, sec. 29, T. 36 N., R. 5 W. (Idaho).

As described by Kuhns (1980), the Clearwater Gravel consists of two gravel sequences separated by a sand. Maximum thickness of the lower gravel is 300 feet (91 meters), the intermediate sand 35 feet (11 meters), and the upper gravel 100 feet (30 meters). All units are light tan to yellow-brown with ferric oxide staining common. Current directions, indicated by foreset cross-bedding and cobble imbrication, show a westward flow parallel to that of the modern Clearwater River.

The lower gravel unit consists of well-rounded cobbles of approximately 50 percent basalt and 50 percent igneous and metamorphic lithologies. Igneous rock types include 6.7 percent quartz monzonite, 6.2 percent quartz latite porphyry, 4.4 percent pegmatite, 3.2 percent mafic porphyry, and 2.4 percent granodiorite. Metamorphic lithologies are 11.6 percent quartzite, 6.2 percent gneiss, and 1.4 percent argillite. The matrix is locally oxidized and generally unconsolidated. Major constituents of the matrix in the 0.0 and 1.0 phi size ranges are 60 percent quartz, 17 percent plagioclase, 6 percent hornblende, 5 percent potassium feldspar, 5 percent muscovite, 3 percent biotite, and traces of sphene, grossularite garnet, phlogopite, chlorite, and magnetite. The mineralogy becomes more diverse with decrease in grain size to 2.0 and 3.0 phi. Traces of additional igneous accessories such as augite, apatite, spessartite garnet, zircon, topaz, and tourmaline appear in the 2.0 phi fraction. This mineral suite is augmented in the 3.0 phi size range by gypsum, beryl, olivine, chromite, scapolite, calcite, serpentine, pyrite, chalcopyrite, and pyrrhotite.

The sand sequence between the upper and lower gravel units is variable in thickness but present in all outcrops where the complete section is exposed. It is quartz-rich and white on fresh exposed surfaces. It weathers light tan, red, or brown from iron oxidation. This sand commonly shows foreset cross-bedding, in many places in reverse direction to that of the imbrication and foreset cross-bedding of the gravels suggesting back-eddies and "behind the bar" development.

Well-rounded cobbles of the upper gravel unit consist of approximately 56 percent basalt and about 43 percent igneous and metamorphic rocks. Individual percentages of the igneous and metamorphic rock types include 9.7 percent quartz latite porphyry, 5.8 percent quartz monzonite, 5.8 percent pegmatite, 2.3 percent mafic dike porphyry, 2.0 percent granodiorite, 12.9 percent quartzite, and 5.7 percent gneiss. The matrix is the same composition as that in the lower gravel but generally one phi size coarser. Sand stringers similar to the middle sand unit are common at most localities. Westward current directions indicated by imbrication and cross-bedding are similar to those of the lower gravel.

Clastic dikes filled with sediment which can be followed upward into the Touchet Beds are present in some exposures of the Clearwater Gravel. Generally these are restricted to the upper gravel unit, but in the Northwest Aggregate quarry, east of the new Lewiston grade, they extend through the sand unit into the lower gravel unit. Small caliche-filled fractures, some of which show reverse offset of a few centimeters, trend north-northeast in the Clearwater Gravel. These fractures seem to be continuous from one exposure to another. A normally faulted clastic dike is exposed in the quarry west of Hatwai Creek near the eastern extent of the Clearwater Gravel. The dike has been offset about 3 inches (7.6 centimeters). The north-south fault can be traced through the gravel outcrop as a thin, bright red, oxidized band in the matrix. The Clearwater Gravel is a fluvial deposit formed in response to an unknown event which caused a temporary change in base level.

The Clearwater Gravel is deposited on top of the Lower Monumental Member (6 million years) and overlain by colluvium and Touchet Beds. A 6 inch-(15.2 centimeters) thick volcanic ash layer in a sequence of lake beds and fine alluvial sediments immediately above the Clearwater Gravel was found in the road cut for the runoff ramp at the top of the gravel exposure along the new Lewiston grade. The ash was analyzed by Rockwell International but was so deeply weathered that it could not be characterized or dated (Ann Tallman, personal communication, 1980). On the basis of intense weathering, an age greater than 35,000 years is speculated for this ash. Thus the precise age of the Clearwater Gravel is uncertain, but stratigraphic relationships confine their age between 6 million years and 35,000 years. As discussed under the Clarkston Heights Gravel, the accordant summit of aggradation of the Clarkston Heights Gravel and Clearwater Gravel, a similar degree of oxidation and cementation and degree of weathering of the clasts suggest a similar age for these two deposits.

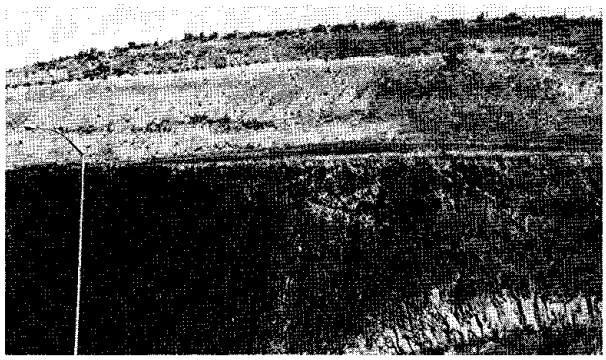

Figure 6. Clearwater Gravel overlying Lower Monumental Basalt. View to the northwest, near base of new Lewiston grade.

If the Clearwater Gravel and Clarkston Heights Gravel are time equivalent, then the 6-million-year maximum age is provided by the Lower Monumental Member and the early Pleistocene minimum age is provided by the Snake River diversion.

The similar sedimentologic characteristics of the Clearwater Gravel and Clarkston Heights Gravel are also typical of the gravels in the Middle Ringold Unit as defined by Tallman and others (1979) in the Pasco Basin and Ringold sheet gravels (probably Middle Ringold equivalents) along the lower Snake River southeast of Pasco described by Richman (1981). The Middle Ringold has been dated at 5.12 to 3.32 million years (Myers and Price, 1979). Webster (in Rigby and Othberg, 1979) considered the Ringold gravels to be of ancestral Salmon and Clearwater origin. The similarity of sedimentary features as discussed under the Clarkston Heights Gravel may be more than repetition of a sedimentary environment at different times. The Clearwater Gravel and Clarkston Heights Gravel may be coeval with the Middle Ringold. If this correlation is correct, then the change in base level which caused the aggradation may have been a base level event near the outlet of the Pasco Basin.

CLARKSTON GRAVEL

The name Clarkston Gravel is here restricted to those gravel deposits stratigraphically below the Bonneville gravel and confined to the northeast side of the Saddle Mountains Basalt which form the topographic high along the southwestern edge of Clarkston, Washington (Figure 2). This gravel underlies the city of Clarkston and exposures are rare. The best exposures are along Washington State Highway 129 at the city's eastern margin and south of U. S. Highway 12 just east of the Saddle Mountains Basalt on the western edge of the city.

Cobbles are well rounded and average 69 percent basalt, 9 percent greenstones of the Seven Devils Group, 15 percent igneous rocks (mostly porphyry and granite), and 6 percent quartzite. Small boulders are common in this gravel. Matrix sands and pebbly sands are bimodal consisting of pebbles and medium-grained sand which is uncemented. There are thin clayey interbeds, and well logs indicate a basal clay. The Clarkston Gravel is not rhythmic or cyclic like the Clarkston Heights Gravel and has a coarser average cobble size. Sedimentary structures are not common but include imbrication and foreset cross-bedding, indicating a northwest current direction.

The Clarkston Gravel is interpreted as a point bar. It might have been built either during a major flood or over a period of time by a northeastward migrating meander of the ancestral Salmon drainage. The presence of the thin clay stringers and lenses support the latter interpretation. This meander migration truncated the Clearwater Gravel on the east as shown on the geologic map (Figure 2). The Clarkston Gravel is easily distinguished from the North Lewiston Gravel and Clearwater Gravel by the presence of the red and green metamorphosed volcaniclastic rocks of the Seven Devils Group. The abundance of small boulders and thin clay interbeds distinguish them from the Clarkston Heights Gravel. Waggoner (1981) speculated that the Snake River diversion is recorded within the Clarkston Gravel based on some variation in cobble counts within the unit. Better exposures and more data are needed to verify this speculation.

Numerous gravel bars along the Snake River canyon below Clarkston including Wilma Bar, opposite Clarkston, are probably equivalent to the restricted Clarkston Gravel as suggested by Lupher (1945). These downstream equivalents were mapped by Hammatt (1976) in the Lower Granite Reservoir area, as "Scabland flood bar gravel" following the suggestion of Bretz (1929). A sedimentologic study of four of these bars by Wheeler (1980) showed that they are point, lateral, and expansion bars with the concordant upper limits between 120 and 140 feet (37 and 43 meters) above the pre-dam river level. Furthermore, he demonstrated that they were deposited by down canyon currents, proving that they are not reworked traction gravels deposited by an up canyon surge of the Missoula backwater flooding. Wheeler's (1980) cobble lithologies are also primarily Salmon River-derived.

If all of these bars are of the same origin, they require a major fill or aggradation within the ancestral Salmon River canyon preceding the diversion of the Snake River to the north. Basalt and granitic clasts, although deeply weathered, are not as intensely weathered as those in the Clearwater Gravel and Clarkston Heights Gravel. This would imply a younger age and support the suggestion that the Clarkston Gravel at Clarkston is a point bar deposited as the ancestral Salmon River migrated eastward eroding Clearwater gravels.

The age of the Clarkston Gravel is thus confined as post-Clearwater Gravel and post-Clarkston Heights Gravel and pre-Snake River diversion to the north, probably very late Pliocene or earliest Pleistocene. Lupher (1945) suggested a Pleistocene age for his unrestricted Clarkston deposits and reported glacial erratics and glacially striated cobbles in them. The Pleistocene age may be supported by Wheeler (1980) based on the discovery of sedimentary features of glacial origin on quartz sand-size grains in the deposits downstream from Clarkston. If they are glacially derived they could form either from overloading of streams during an early Pleistocene glaciation in the upper Salmon River drainage or from a catastrophic glacial discharge. However, if such glacial conditions are the cause one might expect similar deposits, presently unknown, in the Clearwater drainage. Additional study of the gravels in the lower and upper Salmon drainage and upper Clearwater drainage is needed to help solve this problem.

BONNEVILLE FLOOD DEPOSITS

The Bonneville Flood across the Snake River Plain of southern Idaho was clearly documented by Malde (1968). The age of this flood is 14,000 to 15,000 years (Scott and others, 1982 this volume). Obviously, the Bonneville Flood continued down the Snake River through Hells Canyon and the Lewiston basin to the Columbia River.

Bonneville Flood gravels are common deposits along the Snake River below Oxbow Dam (Figure 1). Webster (1980) reported expansion and back-eddy deposits of Bonneville Flood origin at several locations between Sluice Creek and Lewiston, Idaho. The Bonneville Flood deposits in the Lewiston basin are generally gray to dark gray or gray-green containing an abundance of angular to subangular Columbia Plateau basalt and Triassic Seven Devils Group volcaniclastic rock. Well-rounded pebbles and cobbles or quartzite make up a small percentage of the clasts. One-half mile above the mouth of Tammany Creek and on the western edge of Clarkston, abundant volcanic ash clasts are present in the Bonneville gravel.

On the basis of occurrence and grain size the Bonneville Flood deposits may be subdivided into three types of bars. Point bars occur on the inner

side of gentle to sharp bends in the canyon and contain gravel dominated by cobbles and small boulders. Expansion bars occur where the canyon abruptly widens. The expansion bars contain boulders slightly over 2 meters in maximum diameter and become finer downstream. Expansion bars grade into lateral bars (not designated on Figure 2) in some parts of the canyon. Back-eddy bars are present at the mouth of tributary drainages where upstream currents developed. These deposits are a mixture of gravel, generally less than 6 inches (15 centimeters) in diameter, and sand (Figures 7 and 8). In the lower part they are mostly cross-bedded and lack matrix. In the upper part the matrix is a sandy silt to clay. Sandy silt containing floating pebbles and small cobbles may dominate the sediment.

Point bars and expansion bars occur up to 120 to 200 feet (37-61 meters) above the modern flood plain. Back-eddy bars are up to 425 feet (130 meters) above the modern flood plain. They provide an upper minimal water level for the Bonneville Flood.

Although Bonneville Flood deposits in the Lewiston area have been discussed briefly by Stearns (1962) and Kehew (1977), no sedimentary analysis of these deposits was made. Lupher (1945) referred to the Bonneville Flood gravels near the mouth of Tammany Creek as reworked Clarkston Gravel between Touchet Beds and his older "Clarkston" gravels. Lupher and Warren (1942) were unaware of the Bonneville Flood and referred (Bonneville) gravels on the west side of the mouth of Ten-Mile Creek, above Asotin, to the Asotin Stage.

Most deposits mapped as scabland eddy deposits by Hammatt (1976) are Bonneville back-eddy deposits. Bonneville back-eddy bars at the mouth of Ten-Mile Creek and Couse Creek upstream from Asotin were incorrectly interpreted as Missoula Flood deposits by Bretz (1929).

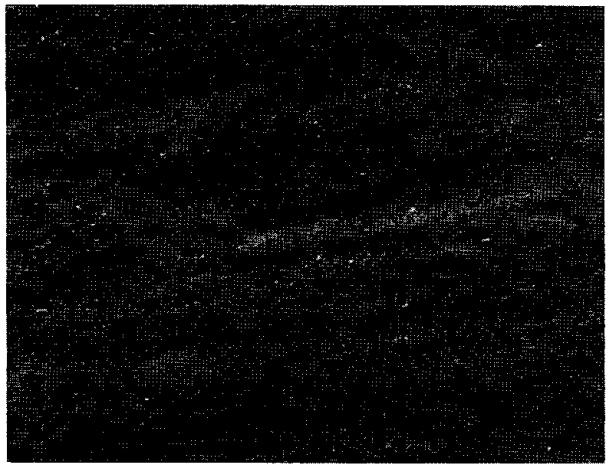

Figure 7. Bonneville gravel as exposed in west wall of intermittently used quarry at mouth of Ten-Mile Creek upstream from Asotin, Washington. Foreset cross-bedding indicates a southeast current flow in this part of the back-eddy deposit.

Figure 8. Bonneville gravel in right side of Figure 7. Note the angular to rounded surfaces of gravel, fining upward sequence, and lack of matrix in middle part of photograph.

No Bonneville Flood point or expansion bars are recognized in the Snake River canyon below Clarkston. Bonneville Flood gravel probably overlies the Clarkston Gravel in the southwestern part of the city of Clarkston, but no exposures are known showing the contact. Touchet Beds overlie the Bonneville deposits in northwestern Clarkston and upstream from the mouth of Tammany Creek.

MISSOULA FLOOD DEPOSITS—TOUCHET BEDS

Sequences of alternating medium gray and tan, thin- to medium-bedded rhythmite deposits are common in many parts of the Lewiston basin. These deposits cap the terraces that Clarkston and Lewiston are built upon. Excellent exposures are common in quarries, roadcuts, and construction excavations throughout the Lewiston basin. Each rhythmite consists of a basal medium gray basalt dominated (greater than 80 percent) pebble and granule gravel which generally has foreset or trough cross-beds indicating a current flow upstream. These gravels grade upward into fine sands and in some deposits show up-valley ripple drift overlain by planar bedding. The upper part of each rhythmite consists of very fine sand and grades upward into silt with planar laminations. Ripple drift and wavey bedding is rare. The upper surface is somewhat wavey and locally may be channeled (Figure 9). The sediments are uncemented and commonly cut by sandstone dikes. The thickness of individual rhyth-

Figure 9. Touchet Beds overlying Bonneville gravel in Atlas Sand and Gravel dump area one-fourth mile above mouth of Tammany Creek. Note the channel in the Touchet Beds filled with pea gravels of greater than 90 percent basalt. Foreset beds in Bonneville gravel indicate a northward current flow. Modern loess and colluvium at top of photograph.

mites in sequences becomes thinner upward in nearly all exposures. Sediments become finer grained upstream. Six to ten rhythmites are common in most exposures in the Lewiston area. A maximum of seventeen rhythmites occurs in the abandoned quarry one-half mile above the mouth of Tammany Creek (Figure 2), and a minimum of ten rhythmites is present in the roadcut above the junction of Joseph Creek with the Grande Ronde River. Eight rhythmites, each lacking an easily defined basal part (consisting only of medium sand), are present along the lower Salmon. The rhythmite sequences occur as discrete deposits from Riparia Bar below Little Goose Dam approximately 65 miles (105 kilometers) below Lewiston to the lower parts of the Clearwater, Grande Ronde, and Salmon River valleys. They are best developed between 850 feet (259 meters) and 1,050 feet (320 meters) but occur at elevations of approximately 1,200 feet (366 meters) at Lewiston and in the lower Grande Ronde River valley.

In the Lewiston area the rhythmite sequences were first recognized as backwater deposits of the Missoula Floods by Bretz (1929). Lupher (1945) recognized the Touchet Beds above older gravels along the lower part of the Lewiston grade. The deposits above the mouth of Tammany Creek were discussed by Webster and others (1976). Hammatt (1976) mapped them as scabland slackwater deposits in the Lower Granite Reservoir area.

The method of deposition of these units has been interpreted as backwater deposits by Bretz (1929) and slackwater deposits by Hammatt (1976). Baker (1973) considered them to be turbidites. Waitt (1980) convincingly argued for traction and suspension deposition of the Touchet Beds in the Walla Walla valley and elsewhere in the Pasco Basin. The deposits in the Snake River canyon closely resemble those of the Walla Walla area, contain similar sedimentary structures, and are believed to have formed by traction and suspension deposition.

Bretz (1928) postulated that the discharge of the Missoula Floods passed across the channeled scablands of southeastern Washington and entered the Snake River canyon at the mouth of the Palouse River approximately 85 miles (137 kilometers) downstream from Lewiston. The discharge was so great that some of the Missoula Flood waters surged up the Snake River canyon. The initial surge incorporated some of the pebbles and small cobbles from older gravel deposits and reworked them into the dominantly basalt pebble and cobble traction gravels recognized as the basal Missoula Flood deposits in the Snake River canyon. The updrainage traction sediments of each flood form the lower half of a rhythmite.

The discharge of the Missoula Flood waters was so large that it ponded at Wallula Gap resulting in Lake Lewis which flooded the Pasco Basin and surrounding areas to an elevation of 1,150 feet (350 meters) (Bretz, 1929; Waitt, 1980). Preceding the Wallula Gap ponding, hydraulic damming of the Snake River drainage occurred at the mouth of the Palouse River. The hydraulic damming at the mouth of the Palouse and the formation of Lake Lewis ponded the surge up the Snake River canyon and the normal discharge of the Snake River. The highest elevation of these hydraulically formed lakes in the Lewiston area is recognized at 1,325 feet (404 meters) by the presence of ice-rafted erratics brought in with the Missoula Flood waters (Lupher, 1940). During the period of ponding of each flood, some finer sediment carried in suspension in the upstream surge was deposited to form the upper half of a rhythmite. The duration of the ponding was short and has been estimated from perhaps a few days to two weeks (Bretz, 1959; Baker, 1973).

Although Lupher (1945) called the Missoula Flood deposits the Touchet Beds, some geologists working in this area have been hesitant to use the term. Kuhns referred to the deposits along the lower Clearwater valley as "Touchet type beds," and Waggoner (1981) called the deposits in the Clarkston area Missoula Flood deposits. Because they obviously are a Snake River canyon facies of the Pasco Basin deposits, we believe they should be referred to as Touchet Beds.

Waitt (1980) interpreted each rhythmite in the Touchet Beds to represent a single flood from the breaching of the ice dam which formed glacial Lake Missoula in western Montana. The excellent ex-

posure of thirty-nine rhythmites in the Burlingame Ditch near Touchet, Washington, is considered by Waitt (1980) to record thirty-nine floods. A maximum of seventeen rhythmites (that is seventeen floods) are present in the Lewiston basin. It is not known if all of the Missoula floods surged up the Snake River canyon to the Lewiston area. It is possible that some floods took different drainage paths across the channeled scabland and Spokane-Columbia drainage, or that some floods may have been of insufficient magnitude to extend up the Snake River canyon to the Lewiston area. Erosion and scour by subsequent floods could also possibly remove rhythmites of earlier floods. Erosion or channeling through seven rhythmites is present in the deposits at the mouth of Tammany Creek. Erosion or channeling through 1 or 2 rhythmites is seen at several localities in the Snake River canyon.

In the Lewiston basin the Touchet Beds overlie all older gravels and many of the flood basalts, including the intracanyon flows. The Touchet Beds immediately overlie the Bonneville gravel at several localities at Asotin, Lewiston, and Clarkston. Waitt (1980) considered the age of the Touchet Beds to be between 19,000 and 12,000 years old. Bonneville Flood sediments in the American Falls area of southern Idaho have recently been dated to have been deposited between 14,000 and 15,000 years ago (Scott and others, 1982 this volume). The above data suggest that the Touchet Beds are between 14,000 to 15,000 years and 12,000 years in age.

As summarized by Waitt (1980) the occurrence of the Mount St. Helens S tephra within the upper rhythmites of the Touchet Beds in the southwestern part of the Columbia Plateau establishes an age of 13,000 years for the upper part of the Touchet Beds. The St. Helens S tephra has not been found in the Touchet Beds in the Lewiston basin. It is possible that only older rhythmites of the Touchet Beds are present in the Lewiston basin.

HOLOCENE GRAVELS

Holocene gravel bars in each of the Snake, Salmon, and Clearwater Rivers above their confluences reflect the provenance of the upstream drainage basin. The Clearwater River drains a part of the Idaho batholith before entering the Clearwater embayment of the Columbia Plateau. The Salmon River also begins in the Idaho batholith, with the lower Salmon River drainage in mixed terrains of (1) western pods of the Idaho batholith, (2) major parts of the eastern bulge of the Columbia Arc containing late Paleozoic and Mesozoic volcaniclastic and carbonate rocks and Jurassic plutons, and (3) the southeastern edge of the Columbia Plateau. Sediments from the Snake River drainage come from several provenances including the Idaho batholith, northern Great Basin, Snake River Plain, and Columbia Arc before entering the Columbia Plateau. However, most of these sediments are trapped in the lakes impounded by dams built on the Snake River during the 1900s.

To better understand the gravels in the Lewiston basin, cobble counts were made upstream in each of the major drainages. Kuhns (1980) made cobble counts at three localities: (1) Lochsa River, just above the confluence with the Selway River; (2) South Fork of the Clearwater River, just above the confluence with the Middle Fork of the Clearwater River; and (3) North Fork of the Clearwater River, 35 miles (56 kilometers) above the confluence with the main Clearwater River. Webster made cobble counts at four gravel bar locations: (1) Salmon River, 1 mile (1.6 kilometers) below the mouth of Slate Creek; (2) Salmon River, one-half mile (0.8 kilometer) below the mouth of China Creek; (3) Snake River, one-half mile (0.8 kilometer) below Pittsburg Landing; and (4) Snake River, 2½ miles (4 kilometers) above Asotin.

At each locality a line was laid out across the modern gravel bar, and the first 1,000 adjacent clasts of pebble or coarser size touching the line were identified for lithology and size information. These data have been summarized into four major lithologic groups reflecting provenance. Lithologic counts from the ancient gravel deposits were then summarized, and both sets of data were compared (Table 2).

The most obvious differences in the data presented in Table 2 are the lack of Seven Devils Group lithologies in the Clearwater River drainage and the absence of Columbia River basalts in the Lochsa River drainage. A small exposure of the Seven Devils Group along the South Fork of the Clearwater River yields a few clasts of the characteristic red and green volcaniclastic lithologies, but downstream they disappear rapidly from abrasion. Although no Seven Devils Group lithologies were found in the cobble counts, a careful search of both modern and ancient gravel bars downstream of the exposure on the South Fork will yield an occasional clast. The absence of Columbia River basalts in the modern Lochsa gravels would be expected, since the Lochsa drainage is east of the Columbia Plateau.

Seven Devils Group strata are most abundantly represented in clasts in the modern gravel bars of the Salmon River at Slate Creek and the Snake River at Pittsburg Landing. Both localities are immediately downstream from outcrops of the Seven Devils

Group. Most of these rock types are greenschist facies of siltstones, claystones, and volcaniclastic rocks. The rapid decrease of these lithologies in clasts downstream is reflected in the cobble counts of both recent and ancient gravels and suggests that they are nonresistant to fluvial transport and weathering.

Dilution and loss of both nonbasalt igneous and older metamorphic rocks downstream were also noted. The Snake River drainage area has a relatively low percentage of both of these rock types. The 18.7 percent nonbasalt igneous rocks (mostly quartz diorite and diorite) at Pittsburg Landing are derived from a small pluton within 5 miles (8 kilometers) upstream. Gravels derived from the Snake River may be best characterized by low percentages of older metamorphic rocks combined with a low percentage of nonbasaltic igneous rocks.

The North Lewiston Gravel has an extremely high percentage (95.4) of basalt clasts. It is uncertain if this reflects the influence of a local tributary, or other unknown factors.

During the cobble count studies many distinct lithologies were found. The source area for many of these lithologies is not known. Reference sets are presently being compiled, and studies of cobble source areas are being initiated.

LATE CENOZOIC HISTORY

The stratigraphy of the Columbia River Basalt Group in southeastern Washington was summarized in a series of maps by Swanson and others (1980, plate 1). After the outpouring of the Umatilla Member (between 14 million and 12 million years ago), the Lewiston basin was downwarped. Downwarping in the Lewiston area produced a structural basin which drained via a canyon that was cut parallel to and a few miles to the northeast of the present Snake River canyon northwest of Clarkston, Washington. This canyon was cut into the Priest Rapids Member by the ancestral Clearwater and Salmon Rivers. The Wilbur Creek and Asotin Basalts filled this canyon, and a new canyon, the ancestral Snake River canyon, was cut to the southwest.

Downwarping and faulting continued, and the Clearwater and Salmon Rivers cut canyons to the approximate depth of the present Snake River canyon in the Lewiston basin by Pomona time (12 million years ago). The Clearwater River was in the same general position as at present. Lupher and Warren (1942) suggested that a larger stream had cut the wide canyon of lower Tammany Creek, possibly the Clearwater River. There is no gravel deposit or topographic evidence to support a Clearwater drainage into the Tammany valley. We propose that the ancestral Salmon River occupied the wide canyon of lower Tammany Creek. A gravel deposit approximately 2 miles (3.2 kilometers) southeast of Waha, Idaho, in a road cut (NE¼SE¼NW¼, sec. 15, T. 33 N., R. 4 W.) supports our proposal. This gravel occurs at an elevation of 3,800 feet (1,158 meters) and contains pebbles and small cobbles of typical modern Salmon River drainage. It is uncertain whether this gravel is an interbed or a remnant of an abandoned stream channel (V. E. Camp, personal communication, 1979). If the Salmon River occupied Tammany Creek, some unrecognized event diverted the lower Salmon River to its present course. Additional study of the gravel and Waha area is needed to resolve this issue.

Outpouring of the Pomona flow (12.0 million years ago) filled the ancestral Salmon River drainage in the vicinity of Clarkston and a new canyon was incised nearly to the depth of the present Snake River canyon, along the southwestern side of Clarkston (under the present day Clarkston Heights area). The Elephant Mountain flow should have partly filled this canyon and perhaps was the cause of the aggradation that formed the North Lewiston Gravel.

Aggradation of the ancestral Salmon River along the southwestern side of Clarkston formed the Clarkston Heights Gravel after the canyon was cut. We suggest that this occurred between 6.0 and 2.0 million years ago at the same time the Clearwater Gravel was deposited on the Lower Monumental Flow in the lower Clearwater River valley.

The ancestral Salmon River was then diverted north at Swallow Rock, opposite the mouth of Tammany Creek, probably cutting its initial canyon to the northwest along the east side of the Pomona flow, or what is today the southwestern edge of Clarkston (Waggoner, 1981). It then eroded to the northeast to the present junction of the Snake and Clearwater Rivers. The Snake River may have been diverted to the north during this time (Waggoner, 1981). We interpret the Clarkston Gravel as a point bar. Perhaps it was deposited by a large-scale flood of unknown causes, possibly glacial, after erosion of a wide flood plain by the ancestral Salmon or Snake River in the Clarkston area. With a glance at the map (Figure 2), one should observe that the Clarkston Gravel clearly truncates the Clearwater Gravel, and thus must be younger.

Approximately 14,000 to 15,000 years ago (Scott and others, 1982 this volume) Lake Bonneville overflowed through Red Rock Pass south of Pocatello, Idaho, to create the Bonneville Flood

(Malde, 1968) which proceeded down the Snake River. This flood produced a flow of 10 million cubic feet per second in the vicinity of Brownlee Dam and was at the least 410 feet (125 meters) deep (Stearns, 1962). Below Oxbow Dam, numerous expansion bars, point bars, and back-eddy deposits were formed by the Bonneville Flood.

The Bonneville gravel is overlain by the Touchet Beds deposited from the Missoula Floods. The Missoula Floods occurred between 14,000 to 15,000 and 12,000 years ago. The Touchet Beds are here recognized in the lower Clearwater, Salmon, and Grande Ronde River valleys and record at least seventeen floods.

Modern fluvial processes are eroding parts of these earlier gravel sequences and depositing gravels along the drainages at present stream level. Within the Holocene colluvium local deposits of the Mazama ash (6,600 years ago) may be found.

CONCLUSIONS

From cobble counts, sedimentologic analysis of matrix materials, stratigraphic relations, and a comparison to modern gravels in the Snake, Salmon, and Clearwater Rivers, we draw several conclusions:

1. Six distinct gravel units are recognized in the Lewiston basin area.
2. Gravels derived from the Clearwater River lack the abundant red and green volcaniclastic clasts present in gravels from the Salmon and Snake River drainages.
3. Gravels derived from the Snake River have lower percentages of the abundant quartzites and medium- and high-grade metamorphic clasts common in materials from the Clearwater and Salmon Rivers.
4. The Clarkston Gravel as defined by Lupher (1945) is restricted to a Salmon River or possibly combined Salmon-Snake River derived gravel that is younger than the Clearwater Gravel and the Clarkston Heights Gravel.
5. The Clarkston Heights Gravel is derived from the Salmon River and preceded the northward diversion of the Snake River.
6. The Clarkston Heights Gravel and Clearwater Gravel are believed to be coeval.
7. Some gravels in the Ringold Formation of the Pasco Basin are probably coeval with the Clearwater Gravel and Clarkston Heights Gravel.
8. Bonneville Flood gravel is probably the most widespread deposit in the Snake River canyon and was not recognized by the first researchers in the Lewiston basin.
9. At least seventeen Missoula Floods are recognized to have inundated the Lewiston basin.
10. Touchet Beds are reported for the first time in the lower Salmon River valley and lower parts of the Grande Ronde River valley.
11. Holocene gravels as well as the older gravels require additional provenance studies to provide answers to unresolved problems of the gravel deposits in the Lewiston basin.

ACKNOWLEDGMENTS

Geologic mapping in southeastern Washington during the summers of 1978 and 1979 by Gary Webster was supported by the Washington Division of Geology and Earth Resources. A NORCUS grant for academic year, 1979-1980, supported the work by Gail Waggoner. A grant from the Washington Division of Geology and Earth Resources supported the field work of Mary Kuhns during the summer of 1979. Appreciation is extended to Rockwell International for permission to use data from gravel studies by Webster. Discussions with Dr. Peter R. Hooper concerning the basalt stratigraphy of the Columbia Plateau greatly helped our interpretation. Diana Hatley and Betty Jo Arrasmith typed the manuscript.

REFERENCES

Avé Lallemant, H. G., D. W. Phelps, and J. F. Sutter, 1980, ^{40}Ar-^{39}Ar ages of some pre-Tertiary plutonic and metamorphic rocks of eastern Oregon and their geologic relationships: Geology, v. 8, p. 371-374.

Baker, V. R., 1973, Paleohydrology and sedimentology of Lake Missoula flooding in eastern Washington: Geological Society of America Special Paper 144, 79 p.

Bretz, J. H., 1929, Valley deposits east of the Channeled Scabland: Journal of Geology, v. 37, p. 393-427, 505-541.

———, 1959, Washington's Channeled Scabland: Washington Division of Mines and Geology Bulletin 45, 57 p.

Camp, V. E., 1976, Petrochemical stratigraphy and structure of the Columbia River basalt, Lewiston basin area, Idaho-Washington: Washington State University Ph.D. dissertation, 201 p.

Davis, G. A., J. W. H. Monger, and B. C. Burchfiel, 1979, Mesozoic construction of the Cordilleran "Collage," central British Columbia to central California, *in* Mesozoic Paleogeography of the Western United States: Pacific Section Society of Economic Paleontologists and Mineralogists, p. 1-32.

Hamilton, Warren, 1976, Tectonic history of west-central Idaho: Geological Society of America, Abstracts with Programs, v. 8, no. 3, p. 378-379.

Hammatt, H. H., 1976, Late Quaternary geology of the Lower Granite Reservoir area, lower Snake River, Washington: Geological Society of America map MC-18.

Hyndman, D. W. and J. L. Talbot, 1976, The Idaho batholith and related subduction complex: Field Guide No. 4, Department of Geology, Washington State University, 15 p.

Kehew, A. E., 1977, Environmental geology of Lewiston, Idaho, and vicinity: University of Idaho Ph.D. dissertation, 211 p.

Kuhns, M. J. P., 1980, Late Cenozoic deposits of the lower Clearwater valley, Idaho and Washington: Washington State University M.S. thesis, 71 p.

Lupher, R. L., 1940, Pleistocene history of the Lewiston basin of Washington and Idaho: Geological Society of America Bulletin, v. 51, p. 227-228.

———, 1945, Clarkston Stage of the northwest Pleistocene: Journal of Geology, v. 53, p. 337-348.

Lupher, R. L. and W. C. Warren, 1942, The Asotin Stage of the Snake River canyon near Lewiston, Idaho: Journal of Geology, v. 50, p. 866-881.

Malde, H. E., 1968, The catastrophic late Pleistocene Bonneville Flood in the Snake River Plain, Idaho: U. S. Geological Survey Professional Paper 596, 52 p.

McKee, E. H., D. A. Swanson, and T. L. Wright, 1977, Duration and volume of Columbia River basalt volcanism, Washington, Oregon, and Idaho: Geological Society of America, Abstracts with Programs, v. 9, no. 4, p. 463-464.

MacKenzie, W. O., 1942, Pebble counts in the Lewiston basin: Washington State College (University) B.S. thesis, 25 p.

Myers, C. W. and S. M. Price, 1979, Geologic studies of the Columbia Plateau, a status report: Rockwell Hanford Operation, Basalt Waste Isolation Study 4. (Available from National Technical Information Service, Springfield, Virginia.)

Richman, L. R., 1981, Sedimentary analysis of pre-Missoula gravels in the southeastern part of the Pasco Basin, Washington: Washington State University M.S. thesis, 82 p.

Rigby, J. C. and K. L. Othberg, 1979, Preliminary geologic map and report of the late Cenozoic geology of the Columbia Basin, Washington: Washington Division of Geology and Earth Resources Open-File Report 79-3, 92 p.

Scott, W. E., K. L. Pierce, J. P. Bradbury, and R. M. Forester, 1982, Revised Quaternary stratigraphy and chronology in the American Falls area, southeastern Idaho, *in* Bill Bonnichsen and R. M. Breckenridge, editors, Cenozoic Geology of Idaho: Idaho Bureau of Mines and Geology Bulletin 26.

Stearns, H. T., 1962, Evidence of Lake Bonneville Flood along Snake River below King Hill, Idaho: Geological Society of America Bulletin, v. 73, p. 385-387.

Swanson, D. A., T. L. Wright, P. R. Hooper, and R. D. Bentley, 1979, Revisions in stratigraphic nomenclature of the Columbia River Basalt Group: U. S. Geological Survey Bulletin 1457-G, 59 p.

Tallman, A. M., K. R. Fecht, M. C. Marratt, and G. V. Last, 1979, Geology of the Separation areas, Hanford Site, south-central Washington: Rockwell Hanford Operations, RHO-St-23, 133 p. (Available from National Technical Information Service, Springfield, Virginia.)

Taubeneck, W. H., 1966, An evaluation of tectonic rotation of the Pacific Northwest: Journal of Geophysical Research, v. 71, p. 2113-2120.

Vallier, T. L., 1974, A preliminary report on the geology of part of the Snake River canyon, Oregon and Idaho: Oregon Department of Geology and Mineral Industries Geological Map Series, GMS-6, 15 p.

———, 1977, The Permian and Triassic Seven Devils Group, western Idaho and northeastern Oregon: U. S. Geological Survey Bulletin 1437, 58 p.

Waggoner, G. L., 1981, Sedimentary analysis of gravel deposits in the vicinity of Clarkston, Washington: Washington State University M.S. thesis, 107 p.

Waitt, R. B., Jr., 1980, About forty last-glacial Lake Missoula jokulhlaups through southern Washington: Journal of Geology, v. 88, p. 653-679.

Webster, G. D., 1980, Bonneville Flood gravels below Hells Canyon Dam: Geological Society of America, Abstracts with Programs, v. 12, p. 159.

Webster, G. D., V. R. Baker, and C. Gustafson, 1976, Channeled scablands of southeastern Washington, a roadlog via Spokane-Coulee City-Vantage-Washtucna-Lewiston-Pullman: Field Guide No. 2, Department of Geology, Washington State University, 25 p.

Wheeler, H. E. and E. F. Cook, 1954, Structural and stratigraphic evidence of the Snake River capture, Idaho-Oregon: Journal of Geology, v. 62, p. 525-536.

Wheeler, M. T., 1980, Late Cenozoic gravel deposits of the lower Snake River, Washington: Washington State University M.S. thesis, 102 p.

Pleistocene Episodes of Alluvial-Gravel Deposition, Southeastern Idaho

by

Kenneth L. Pierce[1] and William E. Scott[1]

ABSTRACT

In southeastern Idaho, extensive gravel deposits occur on alluvial fans and along major streams. Gravel deposits of late Pleistocene age occur in each drainage; older gravel deposits form terraces or are buried by the younger gravels. Ages of these deposits are estimated from stratigraphic relations to glacial deposits, sequence relations, degree of soil development, thickness of carbonate coats on stones in soils, thickness and stratigraphy of loess mantles, and radiometric ages. These Pleistocene gravel deposits are characterized by (1) a clast-supported fabric that either is openwork or has a loose sand matrix that generally does not completely fill the spaces between clasts, (2) less than a few percent silt and clay, (3) sorting such that three-fourths of the material in a given exposure is restricted to 4 phi units in the gravel range and even better sorting in individual gravel beds, (4) subhorizontal beds decimeters thick and planar for distances of more than 5 meters, (5) a scarcity of fine-grained beds, and (6) general absence of matrix-supported beds. In contrast, Holocene alluvium is dominantly fine grained and is confined largely to upland valleys and to floodplains. Mudflow deposits are uncommon, except within the mountains and at the heads of small alluvial fans.

These late Pleistocene and older gravels were deposited by streams with sustained seasonal flows probably at least ten times larger than discharges of present streams. Glacial meltwater is only locally a factor in increased discharges because gravels in unglaciated drainages are similar in age and character to those in glaciated drainages. High flows caused by an increase in precipitation do not seem likely because during glacial times the northern Pacific Ocean, which is and was the moisture source for southern Idaho, was colder than at present. Factors thought to be responsible for markedly increased seasonal discharges are (1) a thicker cold-season snowpack resulting from climates as much as 10-15°C colder than present, (2) later and more rapid seasonal melt of this snowpack, and (3) surface runoff, rather than ground-water underflow, of most of this increase in seasonal discharge.

Stabilized rubbly colluvium on mountain slopes suggests that the periglacial conditions of the Pleistocene produced a greater supply of gravelly debris to streams. In contrast, much of the sediment now transported by streams is derived from erosion of loessial deposits that mantle much of the landscape.

INTRODUCTION

In 1974 when we started our surficial geologic studies in the Basin and Range province[2] of Idaho, we expected to find recent, widespread mudflow and flash-flood deposits forming large alluvial fans. In contrast, we determined that the alluvial fans are largely relict Pleistocene landforms, consisting of well-washed, relatively coarse-grained gravel. This gravel was deposited during discrete episodes that were probably broadly coincident with Pleistocene glacial ages. Holocene sediments are mostly fine grained and are probably largely reworked loess. They are restricted to small deposits along major drainages, where they cover late Pleistocene gravels. This contrast in almost every drainage between the gravel deposition during late Pleistocene time and the mud deposition in Holocene time documents a marked change in stream competency.

In southeastern Idaho, these aluvial gravels are areally much more extensive than glacial deposits and provide a much more visible manifestation of Pleistocene climates. In this report we give examples from sites on and adjacent to the eastern Snake River Plain that illustrate (1) the character and origin of alluvial-fan and main-stream gravels and (2) the evidence for their deposition during gravel-depositing episodes of

[1]U. S. Geological Survey, Denver, Colorado 80225.

[2]For the purposes of this report, we include the Lost River, Lemhi, and Beaverhead Ranges, which lie north of the Snake River Plain, in the Basin and Range province.

Pierce, K. L. and W. E. Scott, 1982, Pleistocene episodes of alluvial-gravel deposition, southeastern Idaho, *in* Bill Bonnichsen and R. M. Breckenridge, editors, Cenozoic Geology of Idaho: Idaho Bureau of Mines and Geology Bulletin 26, p. 685-702.

late Pleistocene and older ages. In addition, we speculate on the conditions that favored gravel deposition during these episodes and offer recommendations for future studies.

Historical observations of flash floods and mudflows on alluvial fans in the Great Basin have led to the inference that these processes are important in the construction of alluvial fans throughout the Basin and Range province. Blackwelder (1928) described the historic Willard mudflow on the alluvial fan at the mouth of Willard Canyon along the Wasatch Front, and noted that mudflow and flash-flood deposits are widespread on alluvial fans in the Basin and Range province. Clayton (1981) studied three fans in southeastern Idaho that showed evidence of late Holocene activity. Although alluvial fans whose surface is underlain by Holocene deposits do occur in southeastern Idaho, they are small and generally restricted to two settings: (1) relatively low-gradient fans of fine-grained alluvium built out onto nearly flat bottomlands of the axial drainages, and (2) very steep fans composed of bouldery deposits derived from precipitous source areas and carried down steep drainages to the fan heads.

Our conclusion that alluvial-fan and main-stream gravels were deposited by streams with sustained flows much greater than at present was first presented in a report on the Raft River Valley (Williams and others, 1974). While we continued our studies in Idaho, Funk (1976) completed a study of sedimentary characteristics of fan gravels in the Birch Creek valley and concluded that these gravels were also deposited by sustained stream flows much larger than at present.

DESCRIPTION OF GRAVEL DEPOSITS

GEOLOGIC SETTING

Quaternary gravel deposits in southeastern Idaho occur both in the basins of the Basin and Range province and on the Snake River Plain (Figure 1). These sites of gravel deposition were formed by middle to late Cenozoic extensional faulting and volcanic activity. Nearby uplifted areas contributed gravel to stream systems that deposited gravels in the basins. The timing and character of gravel deposition appear to have been strongly affected by Pleistocene climate changes. Similar changes in stream regimen in both glaciated and unglaciated drainages provide compelling evidence for climatically induced changes in Pleistocene stream discharges that were unrelated to the direct effects of glaciation.

ALLUVIAL FANS OF UNGLACIATED DRAINAGE BASINS

Raft River Valley

A 10- to 15-kilometer-wide apron of large alluvial fans covers most of the floor of the Raft River Valley, which extends 65 kilometers south from the Snake River Plain to the Utah border (Figure 1; Williams and others, 1974; Pierce and others, in press). Except for parts of the Raft River Range at the south end of the valley, the flanking ranges did not support significant glaciers in Pleistocene time.

Cottonwood Creek fan. A typical alluvial-fan sequence was deposited by Cottonwood Creek near the Raft River geothermal site about 20 kilometers south of Malta (Figure 2). The age sequence of this and other fans can be determined by (1) geomorphic relations, (2) amount of dissection by drainages heading on the fan, (3) degree of soil development, and (4) relations to faults of mid-Quaternary age. The youngest fan deposit of the Cottonwood Creek sequence forms a wedge-shaped, smooth, nearly undissected surface mantled by about 20 centimeters of eolian silt. This fan deposit heads at a distance of 6 to 8 kilometers from the front of the Jim Sage Range. The surface of the fan slopes about 1.3 degrees, and its distal portion is buried by fine-grained Holocene alluvium along the Raft River.

Borrow pits in the youngest fan gravel, 1 kilometer west of Bridge, expose more than 2 meters of gravel. The gravel has a clast-supported (stone-on-stone) fabric; the space between the stones either is filled with sand or is openwork. Fine-grained beds are rare except in soil horizons, and silt and clay are estimated to constitute only a few percent of the deposit by comparison with other gravels analyzed for grain size. We use the term well-washed to reflect this paucity of silt and clay in the gravel beds. The surface soil in this deposit is weakly developed and has similar depth of oxidation and carbonate content as do soils in deposits of the high stand of Lake Bonneville at Kelton Pass, 20 kilometers southeast of Cottonwood Creek. As these Lake Bonneville deposits have been exposed to weathering since the Bonneville Flood, which occurred 14,000 to 15,000 years ago (Scott and others, 1982 this volume), this similarity suggests a late Pleistocene age for the youngest gravels of the Cottonwood Creek fan.

Older gravels of the Cottonwood Creek fan are well exposed in a large gravel pit south of the youngest fan deposit (Figure 2). The older gravels are similar to the younger gravels in having a clast-supported framework in both openwork beds and beds with a matrix of coarse sand (Figure 3). The gravel beds contain almost no silt or clay. Most beds

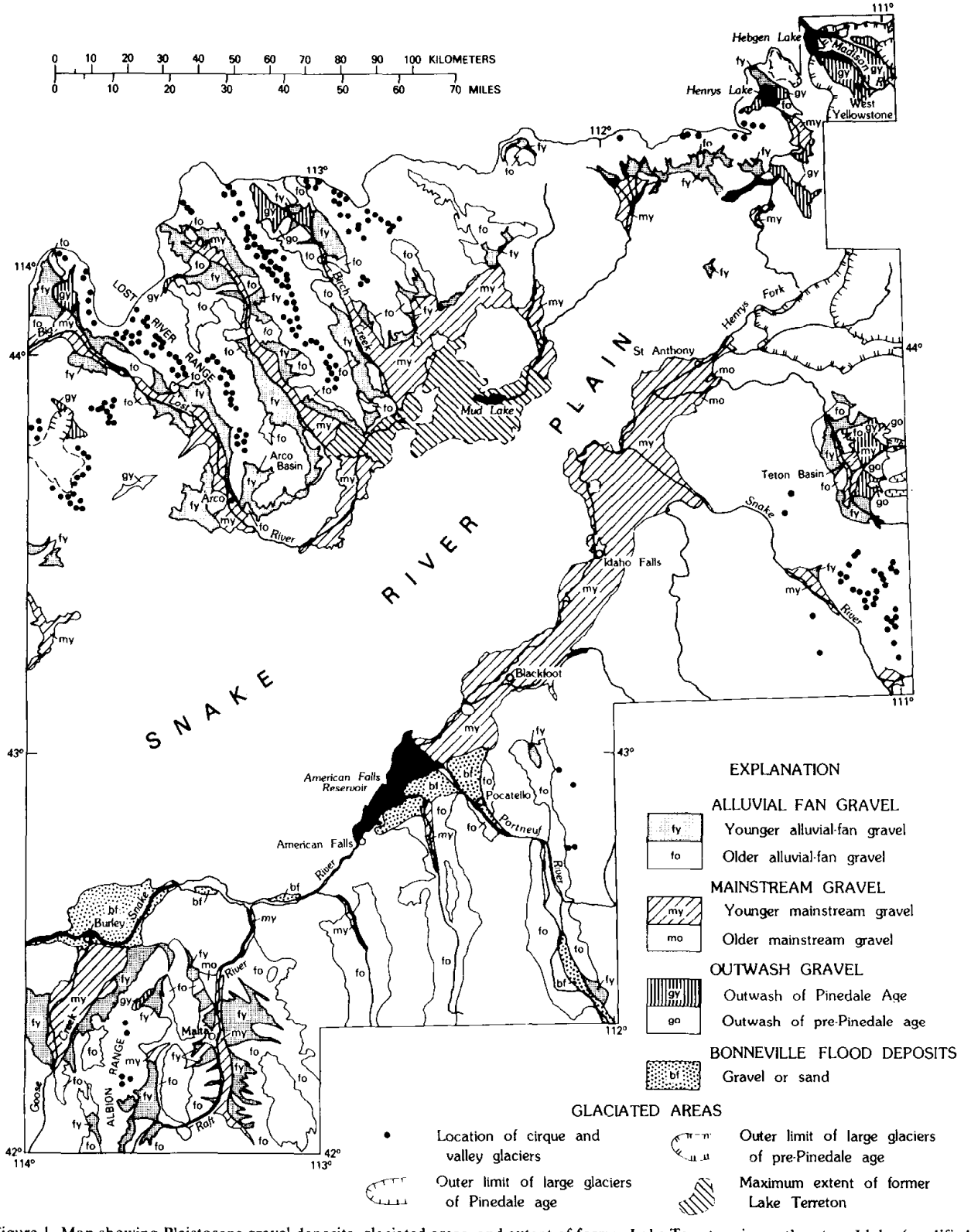

Figure 1. Map showing Pleistocene gravel deposits, glaciated areas, and extent of former Lake Terreton, in southeastern Idaho (modified from Scott, in press and Pierce, 1979).

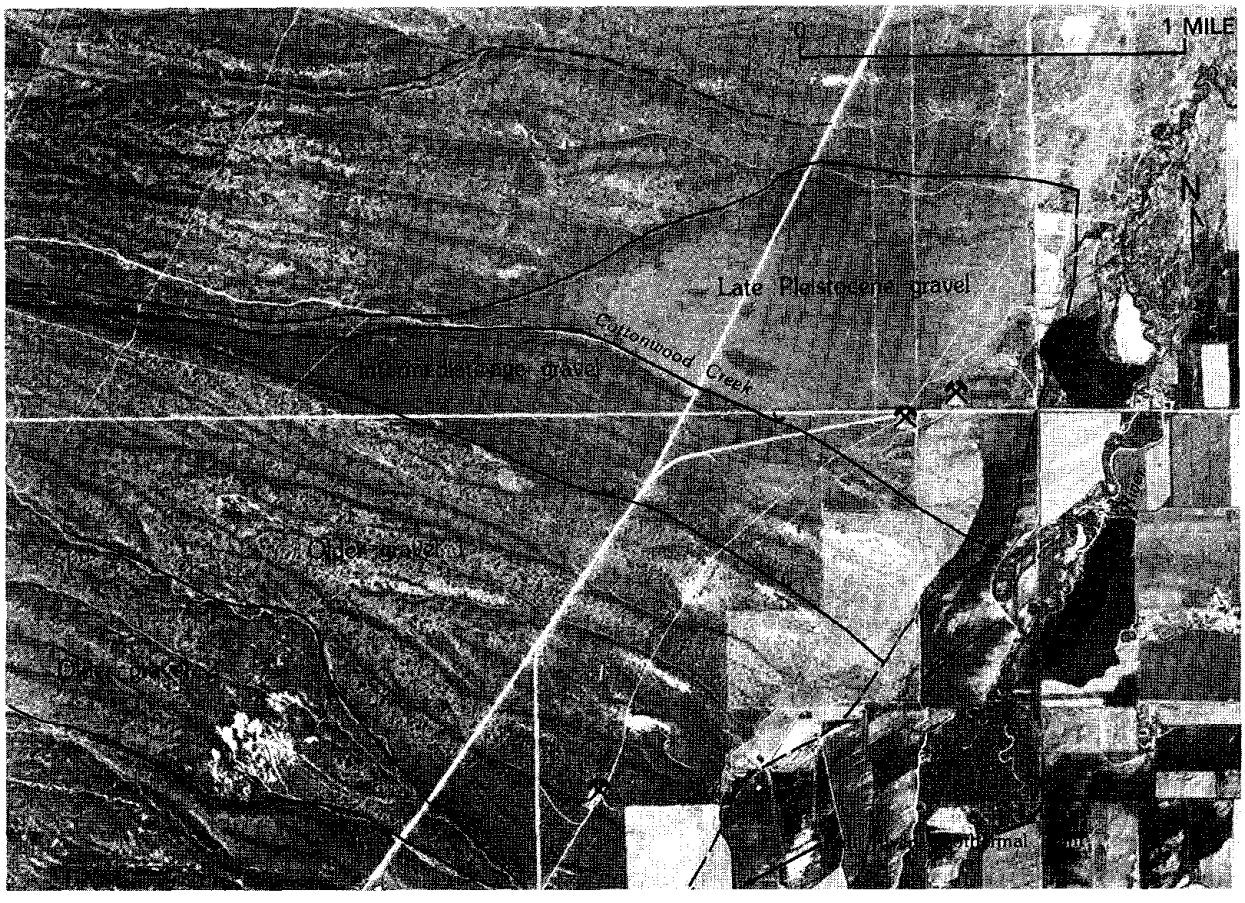

Figure 2. Vertical aerial photograph of Cottonwood Creek fan, Raft River Valley, showing contrast between smooth, wedge-shaped, late Pleistocene deposits and partly dissected older deposits. Age sequence indicated by carets, which are on younger side of contact between deposits of different ages.

are about 0.25 meter thick and are laterally continuous for more than 5 meters. Channels can be seen in cross section; one is about 2 meters wide and 0.5 meter deep. Larger channels probably exist but are difficult to trace in the gravel. Crossbedding is present in some channel deposits. Longitudinal exposures show imbrication of tabular stones. Beds with a muddy matrix were not seen. Boulders as large as 25 by 15 by 15 centimeters are present, and percussion marks are common on large stones of glassy rhyolite. The exposures show an upper gravel about 5 meters thick that partly truncates a silty, calcic soil developed in an older gravel unit.

Holocene deposits of Cottonwood Creek are largely fine grained and are confined to valleys in the Jim Sage Range and to the trench leading from the range to the apex of the youngest fan deposit (Figure 2). During the large spring runoff of 1975, Cottonwood Creek was only about 0.1 meter deep and 0.5 meter wide in the channel at the margin of the youngest fan deposit; the water was clear and was not transporting gravel.

Meadow and Sublett Creek fans. The combined fans of Meadow and Sublett Creeks on the eastern side of the Raft River Valley about 5 kilometers east of Malta (Figures 1 and 4) form large late Pleistocene alluvial fans, yet modern streamflow is generally nonexistent on these fans. These two fans cover about 125 square kilometers and were deposited by streams from the southwestern Sublett and northeastern Black Pine Ranges. Except for sand and loess dunes, the fan surfaces are flat and slope only about 0.5 degree. A loess mantle about 0.5 meter thick facilitates farming of the surface of these fans.

Particle-size analyses by the Idaho Department of Highways of samples from test holes on the fan adjacent to Interstate Highway 84 (Figure 4) show that the gravel is remarkably well washed (Figure 5). The gravel generally contains only 1 to 5 percent silt and clay. Individual samples from the test holes include several beds and have inclusive graphic standard deviations that average -2.4 ± 0.3 (in phi

units), indicating they are "very poorly sorted" (Folk, 1968), but this sorting nomenclature is not very useful in making distinctions among alluvial gravel deposits. Individual beds are better sorted than the deposit as a whole and seem to us to be as well sorted as an alluvial gravel in this environment can be. The mean grain size of the gravels decreases down-fan from about 9 ± 3 millimeters (1 S.D.; n=44) 3 kilometers from the fan head to about 5.5 ± 1 millimeters 10 kilometers farther down the fan (Figure 6). The weight percent of gravel larger than 50 millimeters in diameter decreases from about 5 percent to about 0 percent over the same distance (Figure 6).

Soils in these loess-mantled fan gravels are weakly developed. The carbonate-enriched (Cca) horizon is from 0.2 to 0.4 meter thick and locally contains a 1-centimeter-thick cemented layer. Carbonate coats on the undersides of stones in the Cca horizon at three different localities average 0.4 ± 0.3 millimeter, 0.6 ± 0.3 millimeter, and 0.8 ± 0.3 millimeter (Pierce and others, in press). This variation probably reflects differences in the time since the last activity on different portions of the fan, but the three localities are all considered to represent the last episode of gravel deposition.

No Holocene alluvial deposits were found on these two fans. Holocene alluvium of silt to silty gravel is present along the streams within the ranges, and it mantles the floors of the trenches at the fan heads (Figure 4). Stream-gauge records cover only a few years. In the 1966 water year, the maximum recorded discharge of Sublett Creek within the mountains was only 0.08 cubic meter per second (2.7 cubic feet per second), and in the 1965 and 1966 water years, no flow was recorded along Meadow Creek (Thomas, 1967, p. 65, 62).

Fans Near Southern End of Lost River Range

Although the higher parts of the central and northern Lost River Range were glaciated, the southern end of the range was not. The fan gravels in this area consist almost entirely of carbonate rocks.

Arco basin. The broad valley northeast of Arco, here called the Arco basin (Figure 1), is floored by coalescing alluvial fans that almost entirely date from the last episode of gravel deposition. The area covered by these young fan gravels is approximately 50 square kilometers; the size of the drainage basin feeding them is about 100 square kilometers. The surface of the fans is mantled by about 0.5 meter of loess. At present no perennial streams flow through the Arco basin. Carbonate coats on limestone clasts in surface soils are 1.3 ± 0.5 millimeters (1 S.D.) thick at a site near the Big Lost River and 1.0 ± 0.3 millimeter at a site near the head of the basin. These thicknesses of coats on limestone clasts are similar to those in soils in the younger fan gravels and glacial outwash of Pinedale age to the north in the Big Lost River valley (Table 1). The gravels exposed at the outlet of the basin are well washed, containing no more than a few percent silt and clay.

Alluvial fans north of Arco. Sequences of gravel deposits of small alluvial fans of various ages occur at the mouths of the unglaciated drainages on the west side of the southern part of the Lost River Range (Figure 1). At the range front, the older fans are offset by the Arco fault scarp, and younger fans have been deposited on the downdropped side of the fault. The Arco fault scarp is prominently expressed at the foot of this relatively low segment of the Lost River Range that extends for about 15 kilometers north of Arco (Malde, 1971).

The argument for Pleistocene gravel-depositing episodes is somewhat complicated in this area of small fans, because Holocene deposits of angular gravel have accumulated as pods along stream channels where the steep drainages debouch from the mountain front. Nevertheless, exposures of young fan deposits away from the fan heads generally show well-washed gravel with soils and carbonate coats indicating a late Pleistocene age. Only one mudflow deposit was noted in several gravel-pit exposures. Further north in the Lost River Valley at the base of Borah Peak, bouldery mudflows of late Holocene age occur on the surface of the Elkhorn fan (Clayton,

Figure 3. Photograph of gravel beds in older fan deposits of Cottonwood Creek, Raft River Valley. Note coarse-grained gravel beds with clast-supported framework and openwork beds. Pick head is 30 centimeters across.

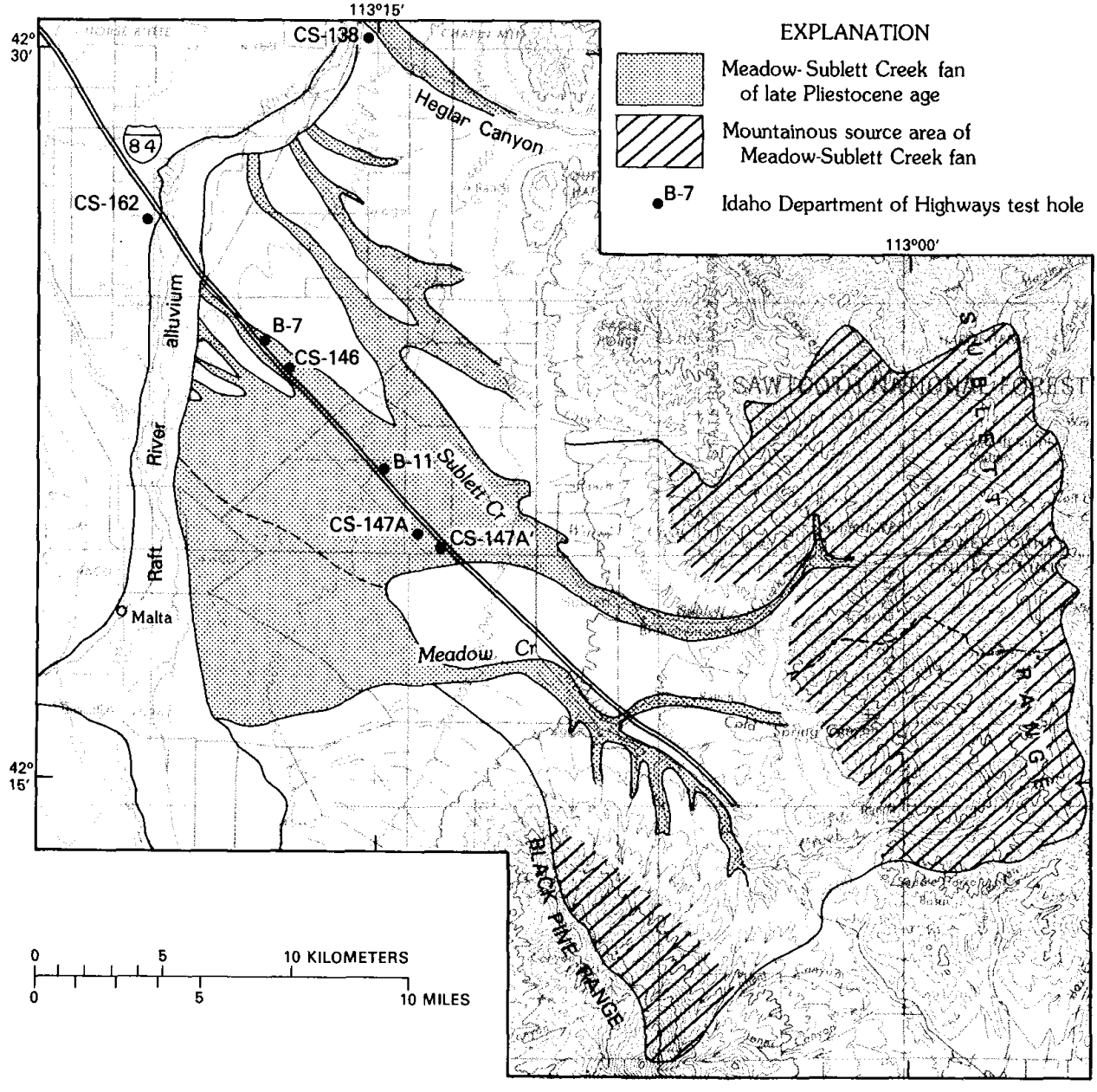

Figure 4. Map of combined alluvial fans of Meadow and Sublett Creeks, Raft River Valley, showing fan deposits of the last episode of gravel deposition.

1981, p. 34). The upper part of this fan slopes 9 degrees and the mountain front draining to the fan abruptly rises 1,500 meters within 5 kilometers of the fan head.

The best evidence that these fans are relicts of Pleistocene conditions comes from the measurement of carbonate coats on stones from the upper part of calcic horizons developed in the youngest fan gravels (section 35 fan, King Canyon fan; Table 1). The coats from the youngest fans are about 1 millimeter thick, about the same as those from outwash and moraines of Pinedale age in a similar climatic environment along Willow Creek, 70 kilometers north of Arco (Table 1). Therefore, the youngest extensive fans near Arco are probably latest Pleistocene, or Pinedale, in age (Table 1). Small deposits having weaker soils with thinner carbonate coats occur along modern drainageways (Table 1); these deposits are probably Holocene

in age.

ALLUVIAL FANS OF PARTLY GLACIATED DRAINAGE BASINS

Alluvial fans formed by gravels similar to those of unglaciated drainage basins occur downstream from mountainous source areas that were only partly covered by Pleistocene glaciers.

Ramshorn Canyon Fan

Nearly the entire surface of the Ramshorn Canyon fan in the southern Big Lost River valley (Figure 1, 20 kilometers north of Arco) was formed during the last gravel-depositing episode (Figure 7). The mean thickness of carbonate coats on stones in surface soils from five sites on this fan ranges between 1.0 and 1.3 millimeters, which suggests a Pinedale age (Table 1). Small cirque glaciers occupied less than 10 percent of the Ramshorn Canyon drainage, but during late Pleistocene time, snowmelt from the relatively high, unglaciated terrain of the basin probably contributed much more runoff than melting of the small amount of glacial ice. The vigor of the late Pleistocene streams is reflected in the pattern and size of braided channels on the fan (Figure 7). Loess of late Pleistocene age is thin or absent on the surface of the fan, but small drifts of loess are present in the lee of small fluvially undercut scarps.

Only minor Holocene deposition has occurred on this fan, primarily along a small incised channel (Figure 7). Before 1959, an earthen dam was constructed across this channel, but it was subsequently breached by the stream. A large rockslide of Holocene age has blocked the north fork of Ramshorn Canyon and prevents sediment carried by flash floods from more than half of the drainage basin from reaching the fan head.

Birch Creek Valley

Most of the alluvial fans in the western and

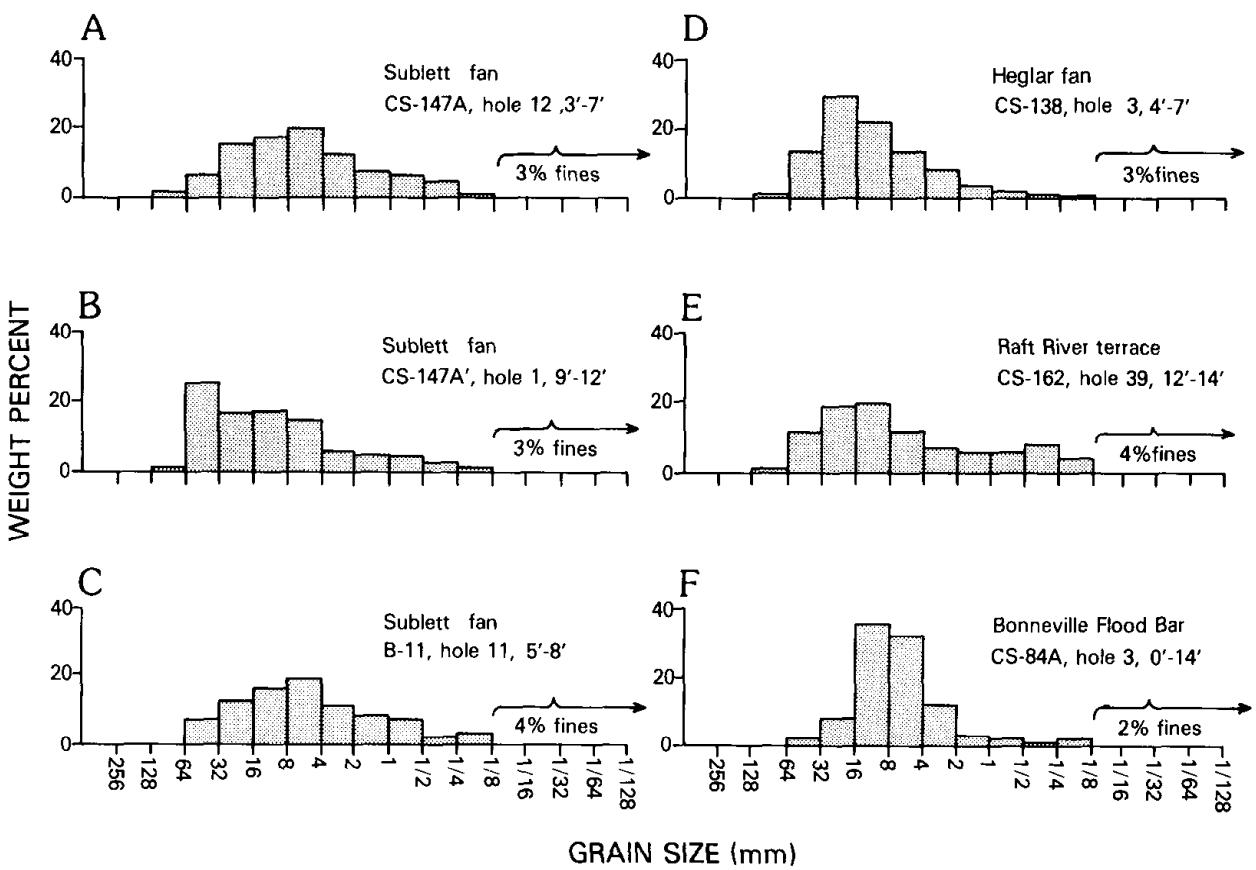

Figure 5. Particle-size distributions of bulk samples of alluvial-fan gravels, Raft River terrace gravels, and Bonneville Flood deposits, Raft River Valley. Grain-size data is derived from cumulative curves plotted from sieve data of the Idaho Department of Highways, Jerome, Idaho.

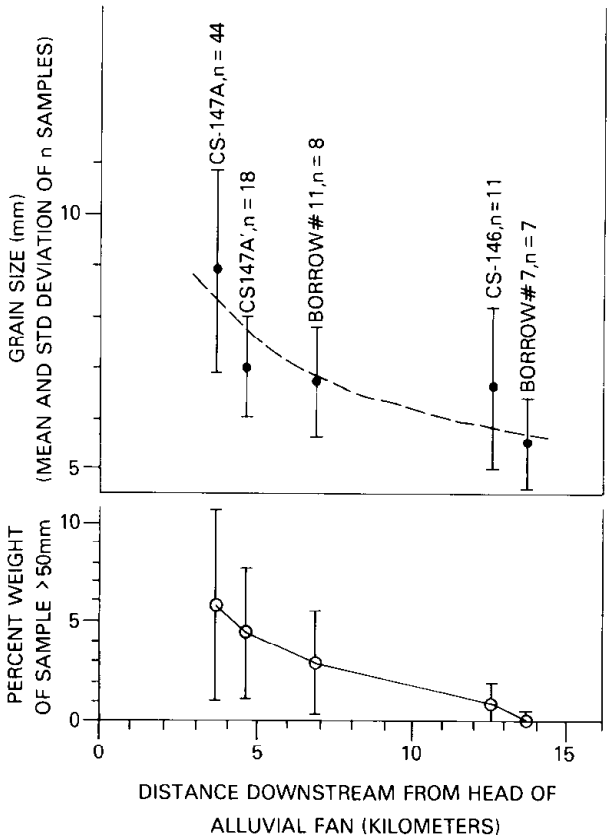

Figure 6. Plot of average grain size and weight percent of gravel coarser than 50 millimeters against distance from the fanhead for the Meadow-Sublett Creek fans, Raft River Valley, Idaho. Trend lines visually fitted. Data derived from cumulative curves plotted from sieve data of the Idaho Department of Highways, Jerome, Idaho.

northern Birch Creek valley (Figure 1) came from drainages that contained valley glaciers, some as long as 6 kilometers (Knoll, 1977). Other fans, particularly those from the southwestern Beaverhead Range, have unglaciated source areas.

Funk (1976) studied the sedimentary characteristics of the fan deposits in the valley and estimated that 90 percent of the fan deposits consist of gravel with clast-supported framework. This clast-supported gravel consists of equal parts of two facies: (A) beds averaging 0.25 meter thick of fining-upward gravel that commonly are openwork in the lower, coarser part and (B) beds of ungraded gravel averaging 0.5 meter thick that commonly have a framework filled with coarse sand.

Funk (1976, Figure 43) also noted two types of bimodal partical-size distributions (Figure 8). In his type I, the sand mode is clearly separate from the gravel mode, whereas in his type II, the two modes overlap (Figure 8). In both types about three quarters of a gravel bed is restricted to 2.3 phi units (Figure 8). Type I gravels are characteristic of braided-stream deposits (Glaister and Nelson, 1974); type II deposits are less definitive but are also characteristic of fluvial environments (Vischer, 1969). Both types result from mixing of bedload and suspended load (70 to 80 percent bedload and 20 to 30 percent suspended load) in a fluvial environment. The dominance of coarse bedload indicates transport under upper-flow-regime conditions (Funk, 1976, p. 127).

Based on the relation of facies, particle-size distributions, bedding features, and fabrics, Funk (1976, p. 130, 144) concluded that deposition of the fan gravels occurred in a high-energy, braided, fluvial system characterized by fluctuating water and sediment discharges, high-regime flow, and rapid aggradation. Deposition occurred mainly in shifting channels and bars of braided streams during waning flows after higher discharges had transported the gravel downstream. According to Funk (1976, p. 144):

> *Well-graded units with a well-developed fabric were probably deposited in bars, whereas poorly sorted units lacking a distinct fabric are most likely channel-fill deposits. Units with intermediate characteristics reflect a combination of channel and bar deposits.*

Debris-flow, flash-flood, or mudflow deposits are conspicuously absent in the alluvial-fan deposits in the Birch Creek valley, although mudflow deposits are present locally in cirques (Knoll, 1977). For the fans in Birch Creek valley, as for alluvial fans elsewhere in southeastern Idaho, the debris-flow model commonly used elsewhere in the Basin and Range province is clearly not appropriate. The alluvial-fan systems are essentially inactive under the prevailing climatic and hydrologic regimes; gravel deposition occurred under conditions of much greater sustained discharge and sediment yield than at present (Funk, 1976, p. 132, 215).

ALLUVIAL FANS OF EXTENSIVELY GLACIATED DRAINAGE BASINS

Alluvial fans downstream from extensively glaciated areas are conventionally interpreted as outwash fans of Pleistocene age. Although the outwash contribution to alluvial fans that had large glaciers in their source areas is important, the fact that unglaciated basins produced similar gravel fans, suggests that, even in glaciated drainages, factors other than outwash deposition were significant in forming gravel fans.

In the ranges north of the Snake River Plain (Figure 1), outwash locally can be traced from moraines of Pinedale age directly to large alluvial fans, such as at (1) Cedar Creek and Willow Creek in the Borah Peak area of the Big Lost River valley

(Scott, in press), (2) Bell Mountain and Spring Mountain canyons in the Birch Creek valley (Knoll, 1977; Funk, 1976, Figure 24), (3) Targhee Creek in the Henrys Lake basin (Scott, in press), and (4) West Yellowstone basin (Pierce, 1979, Figure 35). In addition to these geomorphic relations, soil development and thickness of carbonate coats on stones in Cca horizons (Table 1) suggest that these fan gravels were deposited during the last, or Pinedale, glaciation.

South of the Snake River Plain (Figure 1), outwash can be traced directly from Pinedale moraines to fan gravels at Marsh Creek on the east side of the Albion Range and at Clear Creek on the north side of the Raft River Range. The next range east of the Raft River Valley where glaciers reached the range front is the Teton Range. At the mouth of Teton Canyon, outwash forms both a fan deposit of Pinedale age and a loess-mantled fan deposit of Bull Lake age (Pierce and others, 1982 this volume, Figures 2 and 3).

MAIN STREAM GRAVELS

The main streams deposited extensive gravel fills in late Pleistocene time (Figure 1). The source areas of the Henrys Fork and of the Snake River upstream from Palisades Reservoir contained extensive glaciers; however, other main streams that deposited extensive gravel fills during late Pleistocene time have mountainous source areas in which there was little glaciation. Crude estimates of the amount of unglaciated, mountainous source areas of main streams drainages are: Goose Creek, 99 percent; Raft River, 98 percent; Big Lost River, 90 percent; Little Lost River, 95 percent; Birch Creek, 95 percent; and Snake River downstream from Idaho Falls, 90 percent. Thus, although glaciation in source areas is important to gravel deposition in some main streams, other causes must be involved.

Raft River

Deposits of the Raft River demonstrate a late Pleistocene to Holocene change in stream competency. Excavations and logs of water wells show that gravel with a clean, sandy matrix underlies 3 to 5 meters of fine-grained Holocene alluvium that floors the 1- to 3-kilometer-wide bottomland along the Raft River (Williams and others, 1974; Pierce and others, in press). The gravel probably was deposited by a

Table 1. Mean thickness of carbonate coats (in mm ± 1 S.D.) on limestone clasts from surface soils in alluvial-fan deposits, west side of the Lost River Range. Line of asterisks (*) identifies age of the youngest surface-faulting event on the Arco fault scarp (K. L. Pierce, unpublished data).

LOCATION	AGE								
	Holocene	Late Pleistocene					?	Middle(?) Pleistocene	
		A	B		B′	C			
Willow Creek									
Fan of Pinedale age		1.3 ± 0.2							
Outwash of Pinedale age		1.0 ± 0.4							
End moraine of Pinedale age		1.4 ± 0.4							
Ramshorn Canyon fan		1.2 ± 0.4			2.6 ± 1.5				
		1.3 ± 0.5							
		1.1 ± 0.4							
		1.3 ± 0.4							
		1.0 ± 0.3							
King Canyon fan		0.9 ± 0.3	1.7 ± 0.5	*	1.5 ± 0.7			6.9 ± 2.6	
		1.1 ± 0.4	1.6 ± 0.4	*	2.0 ± 0.6			6.2 ± 2.1	
			1.5 ± 0.5	*	2.1 ± 0.7				
				*	2.2 ± 1.0				
				*	2.3 ± 1.0				
Section 35 fan	0.3 ± 0.3	0.9 ± 0.4	1.7 ± 0.7	*			3.3 ± 1.3	5.0 ± 2.4	10.1 ± 5.4
		0.8 ± 0.8	1.5 ± 0.5	*			2.3 ± 1.1	5.1 ± 1.4	
			1.2 ± 0.6	*			3.2 ± 1.5		
				*			4.3 ± 2.1		
Arco basin		1.0 ± 0.3							
		1.3 ± 0.5							

large braided stream. Flanking these bottom lands are two wide belts of coalescing alluvial fans discussed previously.

The character of the main stream gravel is best seen in exposures of an older but similar gravel of the Raft River in pits north and south of the Interstate Highway 84 crossing of the Raft River (Pierce and others, in press). This gravel contains more medium and fine sand than the fan gravels and has a grain-size distribution that is more clearly bimodal (Figure 5). Mean grain size of gravel in the pits south of Interstate 84 average 7.0 ± 3.4 millimeters (1 S.D.; n=29); about 2 kilometers farther downstream it is 6.8 ± 2.0 millimeters (n=39). The cut-and-fill stratification in the sandy gravels is similar to that seen elsewhere in outwash gravels. The age of this gravel is estimated to be about 150,000 years based on the stratigraphy in the overlying loess mantle that includes two loess units and a strong buried soil developed in the lower loess unit and the upper part of the gravel (Pierce and others, 1982 this volume).

The Raft River is now a small low-gradient stream flowing between banks of fine-grained sediment; it has only minor amounts of gravel in its channel. Between 1947 and 1957, the greatest discharge of the Raft River near Bridge, Idaho, was 30 cubic meters per second (1,090 cubic feet per second) on February 5, 1951, but typical annual peak discharge is between 1.4 and 5.7 cubic meters per second (50 and 200 cubic feet per second) (Thomas and others, 1963, p. 89). The silty, fine-grained sediment that underlies the bottomlands along Raft River is Holocene in age. Carbonaceous material collected from the lower part of this fine-grained unit yielded radiocarbon ages of 8,370 ± 250 and 7,720 ± 250 years (W-3237 and W-3239; Meyer Rubin, written communication, 1975; Pierce and others, in press). A 2-centimeter-thick volcanic ash from 1.7 meters below the surface of this fine-grained unit has characteristics similar to those of the Mazama ash (R. E. Wilcox, written communication, 1975), which is about 6,600 years old. The active meander belt occupies only about one-tenth of the width of these bottomlands. Humic sediment from a depth of 2.9 meters within this belt is 680 ± 200

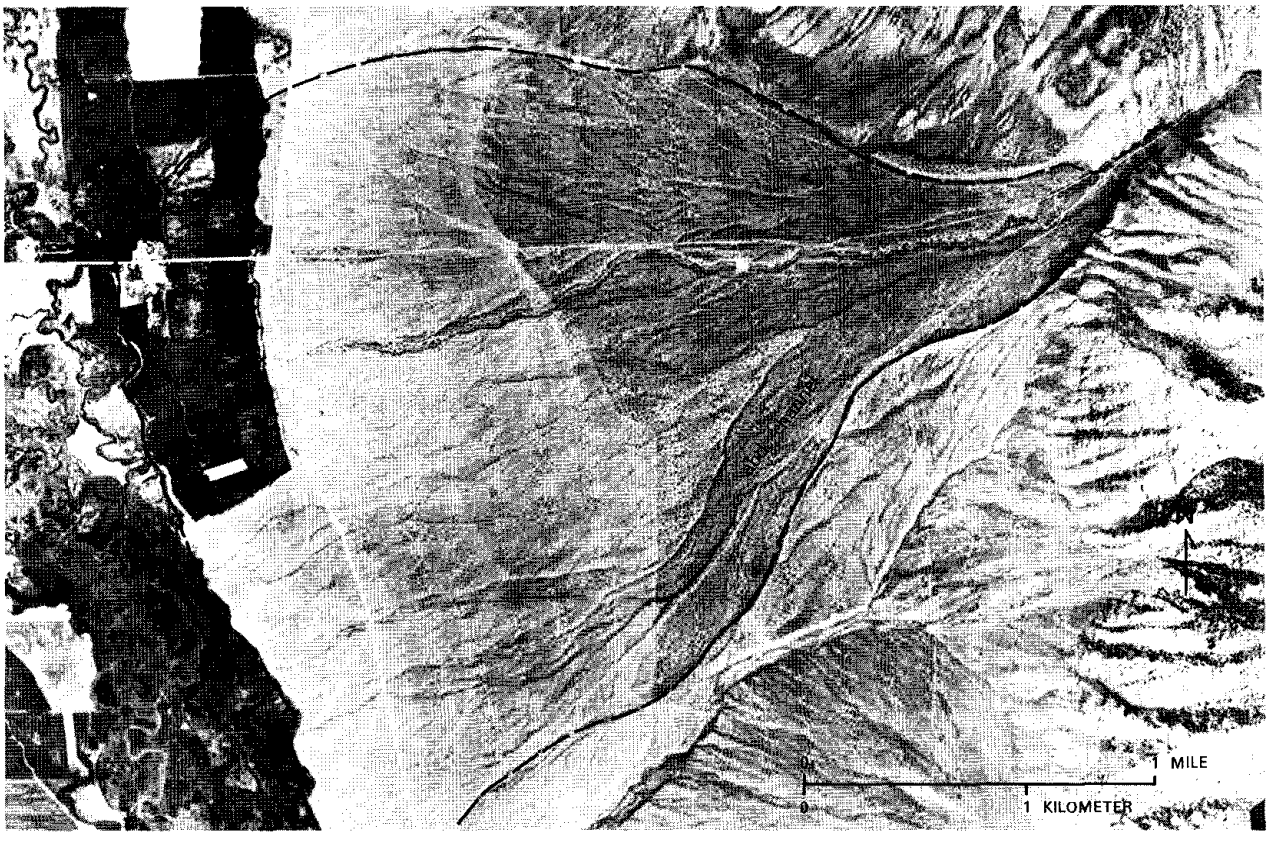

Figure 7. Vertical aerial photograph of the Ramshorn Canyon fan, Big Lost River valley. Dashed line outlines alluvial gravels of late Pleistocene age of Ramshorn Canyon with fresh surface morphology. Note preservation of braided-channel pattern. Based on thickness of carbonate coats, the conspicuous incised channel in center of photograph was abandoned near the close of the last gravel-depositing episode.

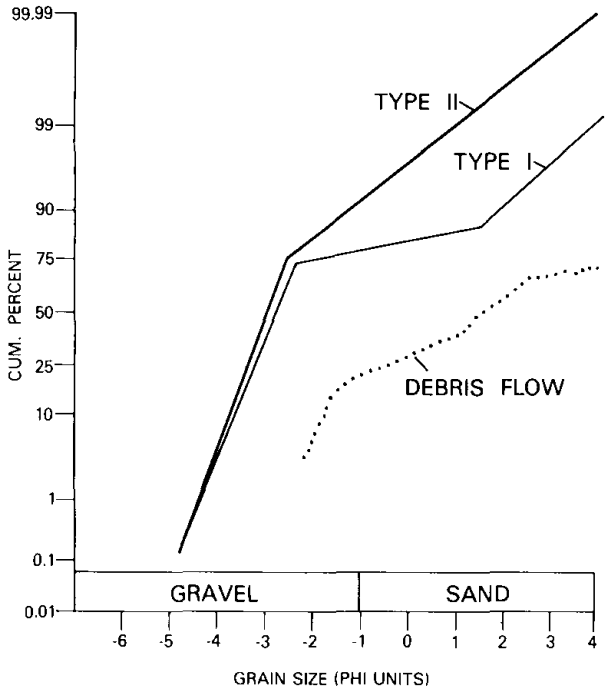

Figure 8. Particle-size distributions for the two types of gravel beds in the fans of Birch Creek valley (after Funk, 1976, Figure 43). Both distributions are bimodal. In both types, the finer fraction is sand, but in type I deposits the sand mode is more distinct from the gravel mode. For comparison, the dotted line is the particle-size distribution of a debris-flow deposit (from Funk, 1976; after Glaister and Nelson, 1974).

years old (W-3065; Meyer Rubin, written communication, 1975). These ages suggest that this fine-grained alluvium accumulated throughout the Holocene and that the underlying gravel is late Pleistocene to perhaps early Holocene in age.

In the Albion Basin to the west of the Raft River Valley, a section of dominantly fine-grained sediment was exposed to a depth of 4.5 meters by gullying of Summit Creek. Well-washed gravel is inferred to lie at a greater depth. A radiocarbon age of 9,280 ± 120 years (W-4966) from the base of this exposure provides a minimum age for the inferred change from Pleistocene gravel to Holocene fine-grained sediment deposition (Pierce and others, in press).

Snake River

An extensive gravel deposit of late Pleistocene age, about 15 kilometers wide and at least 10 meters thick, occurs along the Snake River from St. Anthony to American Falls Reservoir (Figure 1; Scott, in press). Two complimentary effects fostered its accumulation. First, American Falls Lake was dammed by the Cedar Butte Basalt 72,000 ± 14,000 years ago, resulting in elevated base levels upstream until about 14,000 to 15,000 years ago when the Bonneville Flood drained the lake (Scott and others, 1982 this volume; Bright, 1982 this volume). Second, conditions that favored deposition in other areas of nonglacial and glacial gravels at this time also existed along the Snake River. Based on the degree of soil development, the terrace marking the top of this gravel fill is Pinedale in age. Following the draining of American Falls Lake and the change in stream regimen between late Pleistocene and Holocene time, this gravel fill was incised by the Snake River and its tributaries.

Deposits thought to be the result of glacial-outburst floods from Pinedale icecaps on the Yellowstone Plateau occur beneath Egin Bench near St. Anthony and the obsidian-sand plain near West Yellowstone (Pierce, 1979, p. 48-52). These deposits consist of flat-bedded, openwork gravel composed dominantly of obsidian granules. On Egin Bench at Parker, an elongate bar 5 meters high composed of planar, inclined beds demonstrates that floodwaters were at least 5 meters deep across this 10-kilometer-wide section of the Henrys Fork valley.

Downstream from Pocatello, Bonneville Flood deposits floor large areas of the American Falls and Burley basins. Alluvial deposits that postdate the flood are limited in extent along the Snake River and its tributaries, and the flood deposits are little eroded or modified by subsequent fluvial activity. These relations suggest that the most recent episode of Pleistocene gravel deposition was mostly over by the time of the Bonneville Flood.

Big Lost River

The Big Lost River is an influent stream that flows out onto the Snake River Plain and disappears into the underlying rocks and sediments. In late Pleistocene time it transported and deposited gravel and sand much farther out onto the plain (Figure 1). During the Pleistocene, high discharges of the Big Lost River combined with flows from the Little Lost River and Birch, Beaver, and Camas Creeks to maintain Lake Terreton, a large shallow lake on the Snake River Plain (Figure 1). Upstream from Arco, the bottomlands along the Big Lost River are mantled by a meter or more of fine-grained flood-plain alluvium, presumably of Holocene age.

DISCUSSION

SYNTHESIS OF OBSERVATIONS

Gravel deposition in southeastern Idaho during late Pleistocene time occurred under conditions markedly

different from those of the Holocene, as evidenced by the contrast between widespread Pleistocene gravel deposits of fans and alluvial fills and restricted Holocene fine-grained deposits within the same drainage basins (Figure 9). According to Schumm's (1977) classification, these alluvial fans were wet fans at the time of gravel deposition; now they are mostly dry fans and receive little or no sediment.

The youngest extensive deposits of gravel are dated as late Pleistocene, probably between 25,000 and 11,000 years old, because (1) soil development in these deposits is similar to that in deposits of the last, or Pinedale, glaciation, (2) the thickness of carbonate coats on stones in soils in these deposits are similar to those in soils in deposits of the last glaciation, (3) the last gravel-depositing episode was interrupted near its end by the Bonneville Flood, which occurred about 14,000-15,000 years ago, (4) well-washed alluvial gravel deposition in the Raft River Valley and the Albion Basin had ceased by 8,000 to 9,000 years ago and fine-grained alluvium had begun to accumulate on the basin floors, and (5) these gravels are mantled by a small fraction (0.5 meter) of loess unit A that accumulated between 11,000 and about 70,000 years ago (Pierce and others, 1982 this volume).

The presence of glaciers in source areas is not particularly important for the deposition of these alluvial-fan gravels. Morphologically fresh, late Pleistocene fan deposits are present downstream from glaciated as well as unglaciated source areas. A braided channel pattern commonly is well preserved on the youngest fan surfaces (see for example Figure 7). The channel widths of the former streams have not been well defined, but for many of the alluvial fans the width was 10 meters or more. In gravel-pit exposures, beds from 0.2 to 0.5 meter thick can be traced horizontally for distances of more than 3 to 5 meters. Gravelly, braided stream deposits generally indicate abundant sediment supply and high discharges (Ore, 1964).

The fan gravels are similar in appearance, whether the source area was unglaciated, partly glaciated, or extensively glaciated. All have a clast-supported

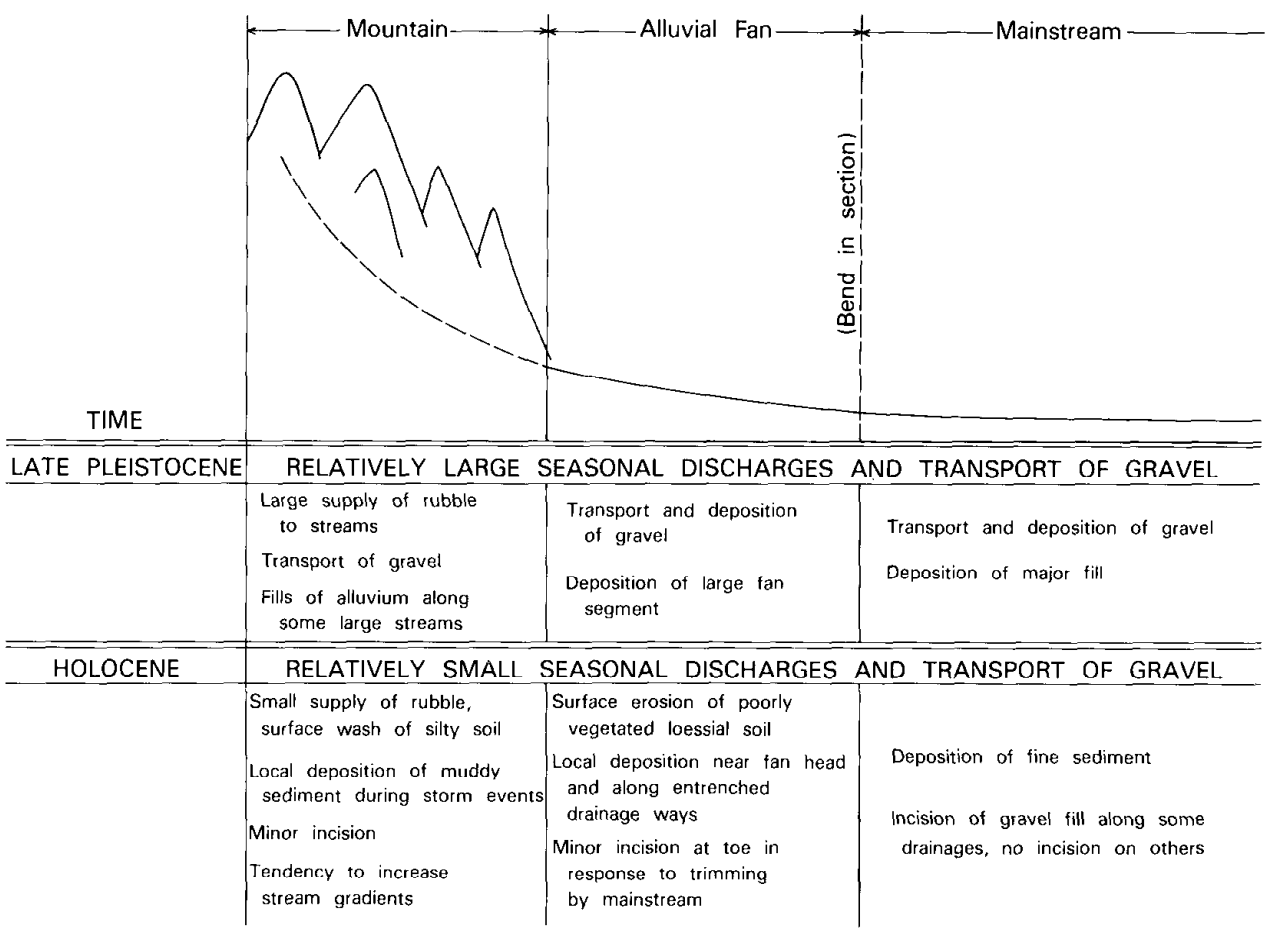

Figure 9. Model in which Pleistocene and Holocene conditions are contrasted for a drainage system in southeastern Idaho, consisting of a drainage basin, alluvial fan, and main stream.

framework and show imbrication dipping up-fan. Beds are typically from 0.1 to 0.5 meter thick and are generally planar for distances of more than several meters; low-angle cross stratification is locally discernible. Except for buried soils that separate the gravel sheets of successive episodes, beds with a muddy matrix are scarce, and silt and clay constitute at most only a few percent of the gravel beds. The abundance of loess and Holocene fine-grained alluvium in southern Idaho suggests that enough fine-grained material to form mudflows was available during times of gravel deposition as well as at present. The scarcity of fines and matrix-supported beds in the gravel suggests that final deposition was by vigorous, sustained streamflows. If debris-flow deposits, fine-grained sediments, or more poorly sorted gravels were present initially, they have been almost entirely reworked.

Standard sorting classifications were developed for sand and finer grained sediments and are not particularly useful for gravel deposits. In the Raft River Valley, samples that include several beds from the unglaciated Sublett Creek drainage have inclusive graphic standard deviations of -2.4 ± 0.3 phi units (n=16) and are classified as very poorly sorted (Folk, 1968). In the Birch Creek valley, samples from individual gravel beds of partly glacial drainages have inclusive graphic standard deviations that average -2.2 ± 0.4 phi units (n=23) and are mostly very poorly sorted (Funk, 1976, p. 103; Folk, 1968). About three-quarters of the gravel in beds from the fans of the Birch Creek valley is restricted to a range of 2.4 phi units (a factor of 5 times; Figure 8); most of the remainder is sand that is not abundant enough to fill the pore space between the gravel clasts. Analyses of samples including several different beds of the Sublett Creek-Meadow Creek fan show that about 70 percent of the particles lie within 4 phi units (a factor of 16 times; Figure 5). Thus, although these alluvial gravels are classified mostly as very poorly sorted, they probably are as well sorted as gravel can be in this environment; only beach gravels and some flood gravels are better sorted (Figure 5; Pettijohn, 1957, p. 248). Mudflow and debris-flow deposits generally are more poorly sorted, contain more silt and clay and a wider range of gravel sizes, and are matrix supported (Sharp and Nobles, 1963; Hooke, 1967; Fisher, 1971; Harmes and others, 1975, p. 153).

The last episode of gravel deposition provides a model (Figure 9) for conditions during the deposition of older, similar gravel deposits. Fan gravels having weathering characteristics and loess mantles similar to those of outwash gravels that head in moraines of Bull Lake age in Teton and Birch Creek valleys (Knoll, 1977; Scott, in press; Pierce and others, 1982 this volume) are also inferred to be Bull Lake in age. Thus, older episodes of gravel deposition appear to correlate with older periods of glaciation. However, as during the last gravel-depositing episode, a glacial source was not required for these older episodes; unglaciated drainages produced similar gravels.

Although the degree of soil development and the thickness of carbonate coats help to determine the relative age of the older gravel deposits, correlations among these deposits are much less certain than for deposits of the last episode of gravel deposition. Carbonate coats on stones from soils in fan gravels on the west side of the Lost River Range (Table 1) and from the Raft River Valley show a direct, systematic increase in thickness with age, although the rates of coat accumulation probably vary with lithology, location, and time. The thickness of carbonate coats suggests that the older fan gravels are many times the age of the fan deposits of late Pleistocene age. Gravels about 15,000 years old have coats about 1 millimeter thick on limestone clasts (Table 1; Pierce and others, in press) and about 0.5 millimeter thick on volcanic clasts. Uranium-thorium ages for carbonate coats on limestone clasts near Arco indicate that coats 2 millimeters thick are about 30,000 years old, and that coats 10 millimeters thick are about 170,000 years old (J. N. Rosholt and K. L. Pierce, unpublished data). In contrast, basalt clasts in till estimated to be about 150,000 years old east of Ashton (Pierce and others, 1982 this volume) have carbonate coats only about 3.1 ± 1.3 millimeters thick (n=32).

SPECULATIONS ON CAUSES OF GRAVEL DEPOSITION

In the Basin and Range province of southeastern Idaho, Pleistocene gravels were deposited by streams with greater discharges than present streams. Deposits have been described elsewhere in the Rocky Mountains that show a similar change in stream regimen from gravel deposition in late Pleistocene time to mud deposition in Holocene time. In the Colorado Piedmont, late Pleistocene alluvial deposits are mostly gravel, whereas Holocene alluvium is mostly silt, sand, and clay (Scott, 1965). From a hydraulic analysis of some of these gravel deposits, Baker (1974) determined that both glacial and nonglacial streams had late Pleistocene discharges an order of magnitude greater than present flows. Along streams in the basins of Wyoming, Leopold and Miller (1954) defined stratigraphic units that reflect a change in stream competency; Holocene deposits of the Kaycee Formation, and younger formations, are fine grained, whereas the Pleistocene Arvada Formation is composed of gravel. In central Utah, R. E. Anderson

(written communication, 1980) has obtained Holocene radiocarbon ages on alluvial-fan deposits that postdate more gravelly deposits of inferred late Pleistocene age. Along the East Fork River, Wyoming, studies of modern bed-load transport have shown that coarse sand and very fine pebble gravel, but almost no coarser gravel, is being transported, whereas adjacent gravel terraces show that outwash gravel was being transported in late Pleistocene time from the Wind River Range (Leopold, 1982; Meade and others, 1981; Emmett, 1980, p. 7).

The deposition of Quaternary gravels in southeastern Idaho resulted from the combined effects of the climates that prevailed under Pleistocene glacial conditions and geologic processes that produced mountainous source areas and nearby basins of deposition. That late Pleistocene gravels of glaciated and unglaciated drainages are similar argues that climatic effects other than glaciation itself were of major importance.

A simple way to explain these increased stream discharges in southeastern Idaho is to postulate increased precipitation, a mechanism that has commonly been used to explain the filling of pluvial lakes in the Great Basin. Other considerations suggest that this mechanism probably is not applicable. During the last glaciation, the north Pacific Ocean was colder (CLIMAP, 1976) than at present and therefore probably would have provided less moisture for precipitation in the western United States. Consequently, we infer that increased precipitation in southeastern Idaho during this time is unlikely. More likely, the effects of lower temperatures led to increased streamflows by decreasing the evaporation and by altering the magnitude and timing of snowmelt. With today's mean annual precipitation, pluvial Lake Bonneville could have filled to overflowing if mean annual temperatures were only about 7° C colder than at present (McCoy, 1981). Table 2 lists and briefly explains factors that would lead to sustained, seasonal stream discharges much greater than at present. Most of these factors are directly related to how much colder Pleistocene glacial conditions were, compared with the present.

Estimates of the amount of late Pleistocene cooling vary widely. A method commonly used for estimating Pleistocene temperature changes is to multiply the atmospheric lapse rate by the altitudinal difference between past and present snowlines. Such calculations yield commonly accepted estimates that late Pleistocene temperatures in the Rocky Mountains were about 6° C colder than at present (Flint, 1976). However, this simple lapse-rate calculation fails to account for precipitation gradients. If late Pleistocene precipitation and precipitation gradients were the same as at present, snowline changes suggest that mean annual temperatures at that time were 10-15° C colder than at present (Porter and others, in press; K. L. Pierce, unpublished data). Widespread permafrost conditions on the basin floors of Wyoming also suggest similar decreases of late Pleistocene mean annual temperatures (Mears, 1981).

If late Pleistocene temperatures in southeastern Idaho were 10-15° C colder than at present, the consequent changes in the timing and magnitude of peak discharges of streams might readily explain the deposition of gravel without any increase in annual precipitation (Table 2).

In the Snake River basin, snowmelt is responsible for most peak discharges (Thomas and others, 1963, p. 8). Maximum runoff of streams that head above an altitude of 3,000 meters in high, formerly glaciated terrain occurs in June, whereas that of lower altitude basins that were not glaciated occurs typically almost 2 months earlier, in late April (Thomas and others, 1963, p. 56-90). Weather records from the Yellowstone area suggest that a mean annual temperature decrease of about 10° C would delay the time when average monthly temperatures reach above freezing by about 2 months (K. L. Pierce, unpublished data). Thus, with a 10° C cooling, peak discharges from unglaciated basins in southeastern Idaho might occur about June, and peak discharges from glaciated areas might occur in July or August.

Another way to regard the effect of deferred snowmelt relates directly to lower Pleistocene snowlines. During Pleistocene glacial culminations, equilibrium-line altitudes in the western United States were about 900 meters lower than at present (Flint, 1971, p. 468; Scott, 1977; Porter and others, in press). To a first approximation, peak runoff in late Pleistocene time from unglaciated drainage basins in Idaho averaging 2,000 meters in altitude may have occurred at a similar time of year (midsummer) as that in present basins at about 3,000 meters in altitude.

In summary, colder late Pleistocene temperatures would have led to a thicker snowpack that would have melted later in the spring or summer. Because, at this time, the incidence of the sun's rays was more nearly vertical and the days were longer than earlier in the spring, melting would have occurred also at a more rapid rate, thus producing higher sustained peak discharges than at present (Table 2).

Our interpretation of the relation between alluvial-fan deposition and Pleistocene climatic cycles in southeastern Idaho differs in detail from that of Funk and Dort (1977), who concluded:

> *During a single cycle of fan development, it is inferred that erosion was the dominant process acting on the fans until the glacial climate ameliorated, because ice and snow trapped sediment in the drainage basins, effectively reducing sediment yields.*

After the ice began to recede, increased sediment loads derived from glacial drift exposed up-valley resulted in deposition of a new fan segment.

Instead, we conclude that maximum sediment supply and sediment and water discharges are directly associated with full glacial conditions. Both glacial and nonglacial source areas produced similar gravel deposits on alluvial fans in the Birch Creek valley and elsewhere in southeastern Idaho, suggesting that annual snowmelt, not the effects of deglaciation, was the key ingredient causing higher sediment and water discharges.

In addition to increased peak runoff, increased gravel supply (Table 3) was a critical factor in gravel-depositing episodes. Large differences between Pleistocene and Holocene colluvial activity are discernible within the mountains of southeastern Idaho. In mountainous areas that were not glaciated during late Pleistocene time, the slopes are extensively mantled with blocky rubble; stone stripes (Figure 10) and other forms of patterned ground occur widely. This rubble appears to be stable now, but it was last active during the colder climate of the late Pleistocene. Similar features occur on the Snake River Plain and show that periglacial conditions existed at low altitudes in southeastern Idaho at times during the Pleistocene (Malde, 1964; Fosberg, 1965).

Although little deposition of gravel has occurred downstream from the mountain fronts in Holocene time, streams within the mountains currently move some gravel. Historic and older Holocene deposits of gravelly alluvium are present along these drainages, especially at junctions between streams of different orders. Archeological studies in the Cassia Mountains show that 1-2 meters of alluvial sand, silt, clay, and fine gravel have accumulated in about the last 10,000 years, as dated by tool types and by probable 6,600-year-old Mazama ash near the middle of this fine-grained sequence (Green, 1972, Figures 7 and 8).

Furthermore, some streams that are prone to flash floods generated by intense thunderstorms have formed alluvial fans in Holocene time; however, the fans are composed largely of fine-grained sediment. For example, at the northeast end of the Raft River Valley, a fine-grained fan of Holocene age extends onto the Raft River bottoms from the mouth of Heglar Canyon (Pierce and others, in press). This young fan has blocked the Raft River resulting in the

Table 2. Factors tending to increase peak discharges of late Pleistocene streams compared with those of present and Holocene streams.

FACTOR	REMARKS
1. Cooler Pleistocene temperatures	With a mean annual precipitation of 50 centimeters, a change in mean annual temperature from 10° to 0°C would increase total annual discharge by about 4 times (Langbein, 1949; Schumm, 1965) because of decreased evaporation, transpiration, and sublimation.
2. Greater snowpack	In autumn and spring, more moisture would occur as snowfall and less would melt; thus, total water content of spring snowpack would be greater.
3. Snowmelt occurring later in the year	Later in the snowmelt season, days are longer and the incidence of the rays of the sun is more nearly vertical. Both factors would result in more rapid snowmelt and tend to concentrate snowmelt into a shorter interval of time, thus increasing peak discharges.
4. Increased surface runoff	Much of the discharge from drainage basins in southeastern Idaho is now accomplished by ground-water underflow through porous alluvial-fan and stream-channel deposits, but ground-water underflow could accommodate only a small part of any increased discharge. Before alterations by man, about 80 percent of the natural discharge from the Raft River basin was accomplished by ground-water underflow (Walker and others, 1970). If total discharge were increased fourfold and the increase was entirely manifested as runoff, surface runoff would increase twenty-fold.
5. Increased seasonally and permanently frozen ground	Runoff would increase because infiltration would be impeded by either seasonally or permanently frozen ground. Applies mainly to higher altitudes.
6. Glaciers in parts of some drainage basins	Glaciers tend to prolong peak discharges by providing a source of meltwater throughout summer. Glaciers were absent or small in many of the drainage basins that produced gravel deposits in southeastern Idaho.
7. Increased total precipitation	An increase in precipitation seems unreasonable in view of the decreased sea-surface temperatures of the late Pleistocene Pacific Ocean (CLIMAP, 1976), which is the source area for precipitation in southeastern Idaho. An actual decrease in precipitation might be likely if mean annual temperatures were as much as 10-15°C colder.

Table 3. Factors tending to increase the supply of gravel to late Pleistocene streams compared to that of present and Holocene streams.

FACTOR	REMARKS
1. Increased frost action	Frost splitting of bedrock into gravel-sized material, thereby mantling slopes of drainage basins with rubbly colluvium.
2. Increased downslope movement of rubbly colluvium	Frost climate facilitates mass movement of rubble downslope to streams. Solifluction and frost heaving were much more active than at present, especially at intermediate altitudes.
3. Diminished soil erosion	Colder climate creates greater effective soil moisture and consequently greater plant cover, which results in diminished surface erosion of the generally fine-grained soil.
4. Glaciers in parts of some drainage basins	Glaciers tend to augment the amount of both fine- and coarse-grained sediment supplied to streams.

Figure 10. Photograph of inactive stone stripe on hillslope in the Cotterel Range on the west side of the Raft River Valley. The entire upland area is mantled with rubbly colluvium that is generally stabilized by thick turf. Similar rubble mantles the source area of the Cottonwood Creek fan. This site is relatively low in altitude (2,100 meters), below the modern zone of continuous coniferous forest and near the upper limit of junipers.

formation of a marshy area above the fan. Heglar Canyon is subject to rather frequent flash floods. About 10 kilometers upstream from the mouth of Heglar Canyon, a maximum discharge of 55 cubic feet per second was recorded between 1958 and 1966 for a 20-square-kilometer drainage basin (Thomas, 1967, p. 66). A flash flood in July of 1982 flooded part of the fan and moved some gravel down an artificially straightened channel and deposited fine sand and silt on the fan surface. The gravels that were moved in the channel are interbedded with finer grained sediment and are unlike the well-washed gravels of fans of late Pleistocene age.

Under present flow conditions, streams require steeper gradients than those at present for significant gravel transport to the alluvial fans and axial drainages of the depositional basins. Holocene changes in stream profiles appear to be increasing stream gradients by deposition of alluvium along the drainages within the mountains and near the fan heads. Uplift of the mountains relative to the basins also increases gradients. Under the present climate and at present rates of deposition, erosion, and uplift, time in excess of several tens of thousands of years probably will be required for gradients to become steep enough for efficient transport of gravels out into the depositional basins. We infer that this transport might occur primarily by debris flows and mudflows generated by major storm events and thereby differ from the longer sustained streamflows inferred from the Pleistocene gravel deposits. The Tertiary fan glomerates of the western United States that have a fine-grained matrix may provide an example of what gravelly basin-fill sediments would look like that were deposited by debris flows or mudflows under present climatic conditions but on fans having gradients steeper than at present.

However, a new episode of cold climate is likely to occur (Shackleton and Opdyke, 1973; Hays and others, 1976) before the streams have sufficient time

to increase their gradients enough to transport gravel to the fans. Increased coarse-sediment supply and greatly enhanced peak discharges on the relatively low-gradient alluvial fans and axial drainages would then cause a new episode of gravel deposition.

RECOMMENDATIONS FOR FUTURE WORK

This report is a by-product of mapping and stratigraphic studies. Specific studies focused on the following aspects of gravel deposition would increase our understanding of the Pleistocene gravels of southeastern Idaho: (1) detailed comparisons of the sedimentary characteristics of alluvial fans from glaciated and unglaciated drainage basins; (2) estimation of late Pleistocene discharges by calculating velocity and discharge from the width, depth, and gradient of preserved channels and the size of transported clasts; (3) hydrologic modeling of discharges produced by snowmelt under climatic conditions appropriate for the glacial climates of the Pleistocene; (4) study of Tertiary fanglomerates and Pleistocene gravels to compare the stream regimens under which each was deposited; (5) determination of times of formation and transport of rubbly colluvium on slopes in the mountains; (6) study of present and older Holocene stream activity within the mountains; (7) dating of Pleistocene gravels older than those deposited during the last episode and comparison of times of deposition with the Quaternary climatic record; and (8) estimate rates of episodic gravel production and deposition based on volumes of gravel deposited during the last gravel-depositing episode.

REFERENCES

Baker, V. R., 1974, Paleohydraulic interpretation of Quaternary alluvium near Golden, Colorado: Quaternary Research, v. 4, p. 94-112.

Blackwelder, Eliot, 1928, Mudflow as a geologic agent in semiarid mountains: Geological Society of America Bulletin, v. 39, p. 465-484.

Bright, R. C., 1982, Paleontology of the lacustrine member of the American Falls Lake beds, southeastern Idaho, *in* Bill Bonnichsen and R. M. Breckenridge, editors, Cenozoic Geology of Idaho: Idaho Bureau of Mines and Geology Bulletin 26.

Clayton, Janine, 1981, Geomorphology of selected alluvial fans of southeastern Idaho: Idaho State University M.S. thesis, 67 p.

CLIMAP project members, 1976, The surface of the ice-age earth: Science, v.191, p. 1131-1144.

Emmett, W. W., 1980, A field calibration of the sediment-trapping characteristics of the Helley-Smith bedload sampler: U. S. Geological Survey Professional Paper 1139, 44 p.

Fisher, R. V., 1971, Features of coarse-grained, high-concentration fluids and their deposits: Journal of Sedimentary Petrology, v. 41, p. 916-927.

Flint, R. F., 1971, Glacial and Quaternary Geology: John Wiley and Sons, New York, 892 p.

Folk, R. L., 1968, Petrology of Sedimentary Rocks: Hemphill's, Austin, Texas, 170 p.

Fosberg, M. A., 1965, Characteristics and genesis of patterned ground in Wisconsin time in a Chestnut soil zone of southern Idaho: Soil Science, v. 99, p. 30-37.

Funk, J. M., 1976, Climatic and tectonic effects on alluvial fan systems, Birch Creek valley, east-central Idaho: University of Kansas Ph.D. dissertation, 246 p.

Funk, J. M. and Wakefield Dort, Jr., 1977, Quaternary climatic effects on alluvial fan systems, Birch Creek valley, east-central Idaho: Geological Society of America, Abstracts with Programs, v. 9, p. 982-983.

Glaister, R. P. and H. W. Nelson, 1974, Grain-size distributions, an aid in facies identification: Bulletin of the Canadian Petroleum Geologists, v. 22, p. 203-240.

Green, J. P., 1972, Archaeology of the Rock Creek site, Sawtooth National Forest, Cassia County, Idaho: Idaho State University M.S. thesis, 152 p.

Harmes, J. C., J. B. Southerd, P. R. Spearing, and R. G. Walker, 1975, Depositional environments as interpreted from primary sedimentary structures and stratification sequences: Society of Economic Paleontologists and Mineralogists Short Course No. 2, 161 p.

Hays, J. D., John Imbrie, and N. J. Shackleton, 1976, Variations in the Earth's orbit; Pacemaker of the Ice Ages: Science, v. 194, p. 1121-1132.

Hooke, R. L., 1967, Process on arid-region alluvial fans: Journal of Geology, v. 75, p. 438-460.

Knoll, K. M., 1977, Chronology of alpine glacier stillstands, east-central Lemhi Range, Idaho: Idaho State University Museum of Natural History Special Publication, 230 p.

Langbein, W. B., 1949, Annual runoff in the United States: U. S. Geological Survey Circular 52, 14 p.

Leopold, L. B., 1982, Geologic setting, *in* L. B. Leopold, editor, Field Trip Guidebook: American Geomorphological Field Group, 1982 Conference, Pinedale, Wyoming, p. 4-17.

Leopold, L. B. and J. P. Miller, 1954, A postglacial chronology for some alluvial valleys in Wyoming: U. S. Geological Survey Water-Supply Paper 1261, 90 p.

Malde, H. E., 1964, Patterned ground in the western Snake River Plain, Idaho, and its possible cold-climate origin: Geological Society of America Bulletin, v. 75, p. 191-208.

———, 1971, Geologic investigation of faulting near the National Reactor Testing Station, Idaho, with a section on microearthquake studies by A. M. Pritt and J. E. Eaton: U. S. Geological Survey Open-File Report, 167 p.

McCoy, W. D., 1981, Quaternary aminostratigraphy of the Bonneville and Lahonton basins, western U. S., with paleoclimatic implications: University of Colorado Ph.D. dissertation, 603 p.

Meade, R. H., W. W. Emmett, and R. M. Myrick, 1981, Movement and storage of bed material during 1979 in East Fork River, Wyoming, USA, *in* T. R. H. Davies and A. J. Pearce, editors, Erosion and Sediment Transport in Pacific Rim Steeplands: International Association of Hydrological Sciences Publication 132, p. 225-235.

Mears, Brainerd, Jr., 1981, Periglacial wedges and the late Pleistocene environment of Wyoming's intermontane basins: Quaternary Research, v. 15, p. 71-198.

Ore, H. T., 1964, Some criteria for recognition of braided stream deposits: Contributions to Geology, University of Wyoming, v. 3, p. 1-14.

Pettijohn, F. J., 1957, Sedimentary Rocks: Harper and Brothers, New York, 718 p.

Pierce, K. L., 1979, History and dynamics of glaciation in the northern Yellowstone Park area: U. S. Geological Survey Professional Paper 729-F, p. F1-F80.

Pierce, K. L., H. R. Covington, P. W. Williams, and D. L. McIntyre, in press, Geologic map of the Cotterel Mountains and the northern Raft River Valley, Cassia County, Idaho: U. S. Geological Survey Miscellaneous Geologic Investigations Map I-1450.

Pierce, K. L., M. A. Fosberg, W. E. Scott, G. C. Lewis, and S. M. Colman, 1982, Loess deposits of southeastern Idaho: age and correlation of the upper two loess units, *in* Bill Bonnichsen and R. M. Breckenridge, editors, Cenozoic Geology of Idaho: Idaho Bureau of Mines and Geology Bulletin 26.

Porter, S. C., K. L. Pierce, and T. D. Hamilton, in press, Mountain glaciation of the western United States, *in* S. C. Porter, editor, Late Wisconsin of the United States: University of Minnesota Press, Minneapolis, Minnesota.

Schumm, S. A., 1965, Quaternary Paleohydrology, *in* H. E. Wright, Jr. and D. G. Frey, editors, The Quaternary of the United States: Princeton University Press, Princeton, New Jersey, p. 783-794.

———, 1977, The Fluvial System: John Wiley and Sons, New York, 338 p.

Scott, G. R., 1965, Nonglacial Quaternary geology of the southern and middle Rocky Mountains, *in* H. E. Wright, Jr. and D. G. Frey, editors, The Quaternary of the United States: Princeton University Press, Princeton, New Jersey, p. 243-254.

Scott, W. E., 1977, Quaternary glaciation and volcanism, Metolius River area, Oregon: Geological Society of America Bulletin, v. 88, p. 113-124.

———, in press, Surficial geologic map of the eastern Snake River Plain and adjacent areas, 111° to 115° W., Idaho and Wyoming: U. S. Geological Survey Miscellaneous Geologic Investigations Map MI-1373.

Scott, W. E., K. L. Pierce, J. P. Bradbury, and R. M. Forester, 1982, Revised Quaternary stratigraphy and chronology in the American Falls area, southeastern Idaho, *in* Bill Bonnichsen and R. M. Breckenridge, editors, Cenozoic Geology of Idaho: Idaho Bureau of Mines and Geology Bulletin 26.

Shackleton, N. J. and N. D. Opdyke, 1973, Oxygen-isotope and paleomagnetic stratigraphy of equatorial Pacific core V28-238—Oxygen-isotope temperatures and ice volumes on a 10^5 to 10^6 year scale: Quaternary Research, v. 3, p. 39-55.

Sharp, R. P. and L. H. Nobles, 1963, Mudflows of 1941 at Wrightwood, southern California: Geological Society of America Bulletin, v. 64, p. 547-560.

Thomas, C. A., 1967, Peak discharges from small drainage basins in Idaho; a basic-data report: U. S. Geological Survey, Water Resources Division, Boise, Idaho, 177 p.

Thomas, C. A., H. C. Broom, and J. E. Cummons, 1963, Magnitude and frequency of floods in the United States, Part 13, Snake River basin: U. S. Geological Survey Water-Supply Paper 1688, 250 p.

Visher, G. S., 1969, Grain-size distributions and depositional processes: Journal of Sedimentary Petrology, v. 39, p. 1074-1106.

Walker, E. H., L. C. Dutcher, S. O. Decker, and K. L. Dyer, 1970, The Raft basin, Idaho-Utah, as of 1966; a reappraisal of the water resources and effects of ground-water development: Idaho Department of Water Administration Bulletin 19, 95 p.

Williams, P. L., K. L. Pierce, D. H. McIntyre, and P. W. Schmidt, 1974, Preliminary geologic map of the southern Raft River area, Cassia County, Idaho: U. S. Geological Survey Open-File Report 74-1126.

Chapter 14

Loess Deposits Southeastern Idaho

Distribution and Character of Loess and Loess Soils in Southeastern Idaho

by

Glenn C. Lewis[1] and Maynard A. Fosberg[1]

ABSTRACT

The depth of loess deposits over most of the area of south-central and southeastern Idaho is between 50 to 100 centimeters thick. The thickest loess deposits are south and east of the Snake River where depths of loess up to 36 meters have been measured. These deposits are parallel to and immediately adjacent to the Snake River.

The particle size of loess decreases with distance from the eastern margin of the Snake River Plain as indicated by a decrease in very fine sand and coarse silt and an increase in medium and fine silt. It appears that the Snake River Plain is a major source of the loess in this area. Minimum deviations to the overall trend suggest that some loess was derived from more local sources such as localized flood plains.

The calcium carbonate equivalent of the loess in the Snake River Plain varies from place to place and within a loess section. Large areas in the central Snake River Plain are underlain by a lime-silica duripan which suggests deposition and removal of loess with intervening periods when calcium was leached downward and deposited as calcium carbonate within a loess body. In the loess on the eastern side of the plain, there is no consistent relationship between the thickness of loess or annual precipitation and the calcium carbonate equivalent at the maximum zone of accumulation or in the unaltered loess.

In general, the amount of clay in the first and second clay maxima of loess sections east and south of the Snake River Plain increases with altitude and distance from the plain; however, there is no consistent relationship of the depth in the loess to the increase of clay. The presence of at least two clay maxima in most loess sections indicates more than one period of loess deposition. One loess section, described in detail, contains a buried soil, which has been named the Fort Hall Geosol, and two additional buried soils deeper in the section.

Species of clay mineral found in the coarse clay fraction are similar throughout loess deposits in southern Idaho. They consist primarily of smectite, illite, and kaolinite with lesser amounts of vermiculite and occasionally a trace of chlorite. Quartz and feldspars in the coarse clay fraction, along with high illite throughout the loess deposit, indicate relatively little weathering has taken place.

INTRODUCTION

Loess deposits in excess of 6 meters thick cover several thousand square kilometers of south-central and southeastern Idaho. Although these silty deposits constitute one of the major soil parent materials in this area, they have received little study. Most investigations of loess have been a product of agronomic, soil, geological, and ground-water surveys.

In his early work in Idaho, Russell (1902) made note of fine, yellowish white silts resembling the celebrated loesses of China and the Mississippi River Valley. He recognized that these materials were not derived from the underlying rocks and that the older lava flows are covered with fine dust whereas the younger flows are free of dust.

Early soil surveys in the southeastern Idaho area recognized eolian silt deposits (Lewis and Peterson, 1921; Baldwin and Youngs, 1925; Youngs and others, 1925; Poulson and Thompson, 1927; Youngs and others, 1928). Deposits in the Portneuf area were described as fine, floury, wind-borne material, much of which had been carried long distances and derived from a wide variety of rocks (Lewis and Peterson, 1921). Practically all of the soils of the area were thought to be modified to some extent by deposition of wind-blown material. Small areas were covered by coarser sandy material which has blown short distances, mostly from dry stream channels or exposed lava beds. In the vicinity of Burley in south-

[1]Plant and Soil Sciences Department, University of Idaho, Moscow, Idaho 83843.

Lewis, G. C. and M. A. Fosberg, 1982, Distribution and character of loess and loess soils in southeastern Idaho, *in* Bill Bonnichsen and R. M. Breckenridge, editors, Cenozoic Geology of Idaho: Idaho Bureau of Mines and Geology Bulletin 26, p. 705-716.

central Idaho (Youngs and others, 1928) the soils were recognized as being derived from fine dustlike, wind-borne materials over 6 meters thick in places.

Mansfield (1920) identified extensive deposits in the Fort Hall Indian Reservation in southeastern Idaho as volcanic ash, hill wash, etc., forming rounded hills and sloping benches. These same deposits are identified as loess in the soil survey of the Fort Hall Reservation (McDole, 1977).

Poulson and others (1943) in the soil survey of the Blackfoot-Aberdeen area in southeastern Idaho, stated that the wind-borne loess has an indefinite origin, principally from sources to the west, giving them a mixed mineralogy. These soils were described as fairly uniform with excellent moisture-holding properties.

McDole (1968, 1969) wrote a masters and doctoral thesis on the loess deposits of southeastern Idaho. His work was in the area east of Fort Hall and southwest of Pocatello. He studied some of the physical, chemical, and mineralogical properties of the loess. Some of his data is included in this paper.

The main objective of this paper is to show the aerial extent, thickness, and some properties of the loess deposits in southeastern Idaho.

GEOLOGY OF AREA

Most of southeastern Idaho lies in the northeastern part of the Basin and Range physiographic province. The mountain ranges and intervening valleys trend approximately north-south and apparently result from crustal extension and associated normal faulting during the last 10-20 million years (Williams and others, 1982 this volume; K. L. Pierce, written communication, 1981). The eastern Snake River Plain transects the trend of these ranges and basins at a high angle. Along the axis of the eastern Snake River Plain, Quaternary basaltic shield volcanoes have built up its central part, leaving the edges of the plain, lower with drainages such as the Snake River.

In Pleistocene time, the basins and the Snake River Plain have periodically been the site of both glacial and nonglacial gravel deposition (Pierce and Scott, 1982 this volume). Much of the loess in southeastern Idaho appears to have been derived by deflation of silty sediment from these flood plains and active alluvial fans.

Times of loess deposition were apparently associated with the rigorous climatic conditions of Pleistocene glaciations. Some of the ranges on the south side of the plain and most of the ranges on the north side supported small, valley glaciers (Pierce and Scott, 1982 this volume). A large ice field covered the Yellowstone-Teton area at the headwaters of the Snake River (U. S. Geological Survey, 1972). Quaternary climatic change resulted in repeated glaciation as well as other geomorphic changes. In the Yellowstone area, the last glaciation (Pinedale) occurred between 40,000+ years and 11,000 years ago; the next to last glaciation (Bull Lake) is dated at about 140,000 to 150,000 years old (Pierce and others, 1976). Although the sequence of glaciations older than the Bull Lake Glaciation has not been well dated in the Rocky Mountains, the marine, oxygen-isotope record shows that glaciations tens of thousands of years long have occurred at intervals of about every 100,000 years for more than the last 700,000 years (Shackleton and Opdyke, 1973). On the average, Quaternary environments were considerably different from the present; 90 percent of the last half a million years was more glacial than present (Emiliani, 1972).

DISTRIBUTION AND THICKNESS OF LOESS

Aerial extent of loess deposits in southern Idaho was compiled by several methods. Much of the information was derived from reports prepared by the University of Idaho and the Soil Conservation Service (SCS) for the Idaho Water Resource Board (J. C. Chugg and others, 1967-68, Special Soil Surveys of 13 Idaho Counties. Reports No. 1 through 13, U. S. Department of Agriculture (USDA), SCS, and University of Idaho). Soil survey data from published (Daniels and others, 1969; McDole, 1977) and unpublished USDA SCS Soil Surveys (Gooding County, 1969; Lincoln County, 1969; Elmore County, 1971) and unpublished field data supplied by local soil scientists from the SCS were used as major sources of data in this study. Areas not covered by soil survey literature were completed with the aid of field reconnaissance. Observations were made and field data collected on depths of the loess and nature of the underlying material throughout the study area.

A generalized map of loess thickness (Figure 1) categorizes loess deposits: shallow, 25 to 50 centimeters; moderately thick, 50 to 175 centimeters; and very thick, over 175 centimeters (Lewis and others, 1975). A minimum thickness of 25 centimeters of silty material with characteristic loess appearance was necessary before the deposit was classified and mapped as loess.

The loess depth over much of the southwestern part of the Snake River Plain and Owyhee Uplands

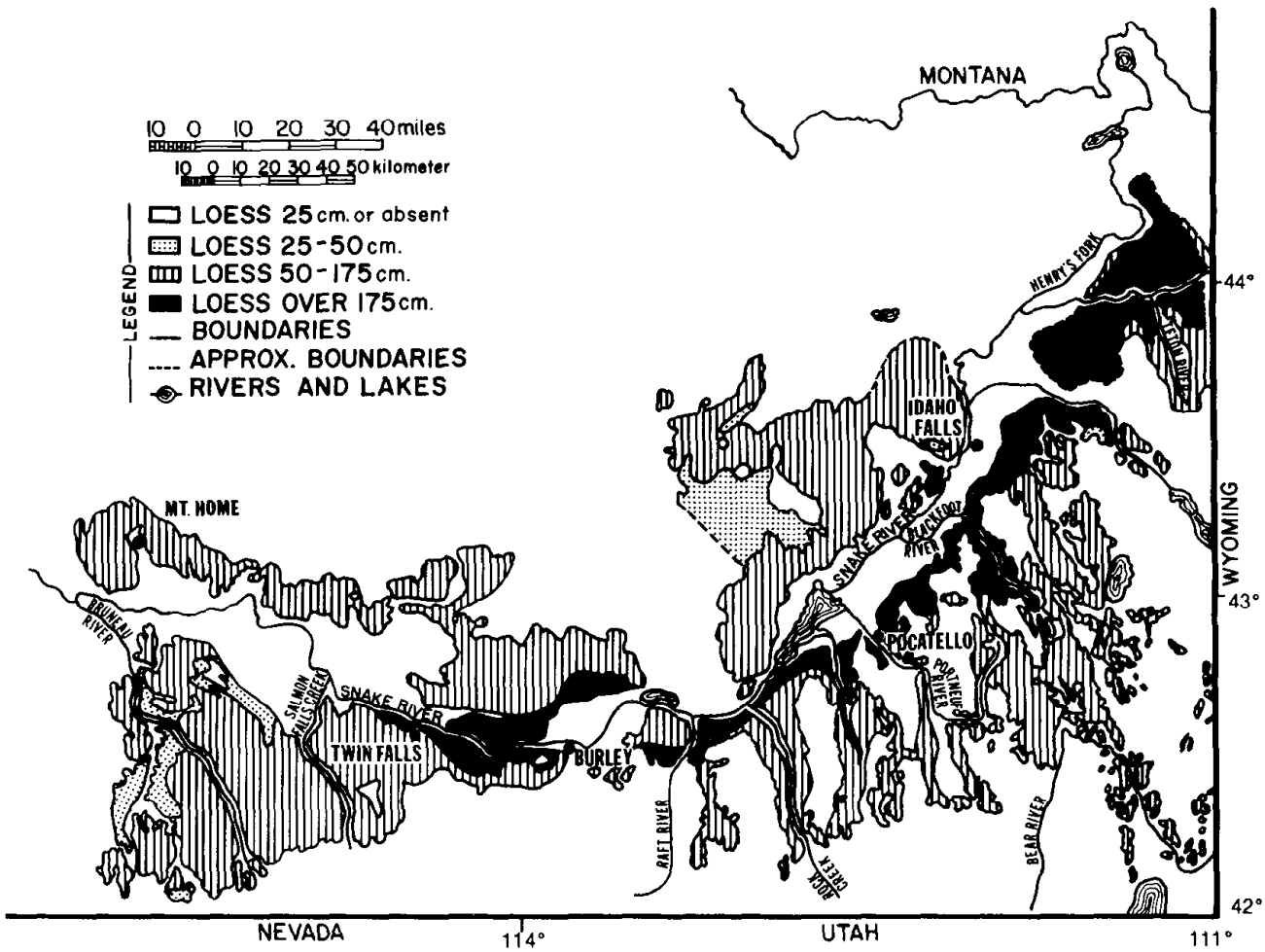

Figure 1. Areal distribution and thickness of loess in south-central and southeastern Idaho.

is less than 25 centimeters and was not shown on the map. Thus, the western limit of mapped loess (Figure 1) is in the vicinity of the Bruneau River in the Mountain Home area. Although there are small isolated areas of loess west of this boundary thicker than 25 centimeters, they are not large enough to be included on the map. These isolated areas of loess are found mostly adjacent to the Snake River in Owyhee, Canyon, and Payette Counties. There are also sizeable areas of loess deposition in western Wyoming and southwest Montana; both areas are adjacent to the Idaho deposits.

Shallow loess deposits are primarily on the area of younger basalt flows in the central part of the Snake River Plain and on the more gentle slopes in the mountain ranges adjacent to the plain. The area of loess cover may be larger than that depicted on the map in Figure 1, because the discontinuous and spotty occurrence of loess on the irregular surface of this basaltic plain made an exact boundary difficult to establish. The depth of loess indicated in Figure 1 represents the most representative loess thickness. Undoubtedly all of these older lava flows were covered with loess. In contrast, Holocene lava flows have only traces of wind-blown materials.

The thickness of loess over much of the southern Idaho study area is between 50 and 100 centimeters. This loess mantle occurs on a variety of materials including volcanic rocks, alluvium, and lacustrine sediments. In much of the western and central portion of the mapped area, the loess thinner than 1-2 meters commonly has a lime-silica duripan in the C horizon of the soil profile.

The loess mantle in the mountain valleys in the extreme southeastern part of the study area ranges from 50 to 100 centimeters thick. These north-south-trending valleys are separated from the Snake River by mountains, some of which reach elevations of 2,500 to 2,900 meters. Bright (1963) identified and named Niter loess in Gem Valley in Caribou

County, about 65 kilometers southeast of Pocatello, and suggested the source was the nearby flood plain of the Bear River.

The thickest loess deposits are east of the Snake River from the vicinity of Twin Falls (in the south-central part of the state) and extend to the northeastern corner of the study area about 100 kilometers northeast of Idaho Falls (Figure 1). One significant area lies northeast of Twin Falls on the north side of the Snake River.

Most of the very thick loess indicated in Figure 1 is considerably thicker than 175 centimeters. Well log information was used to establish loess thickness in the area between Twin Falls and Burley in south-central Idaho. Depths in this area range from 5 meters near Twin Falls to 36 meters, in lee positions, 32 kilometers east of Twin Falls. Near Burley (about 38 kilometers farther east) depths again decreased to a maximum of about 12 meters.

Maximum depth of the deposits in several areas between Raft River and the area northeast of Idaho Falls, on the eastern side of the Snake River Plain, is largely unknown. Maximum depth of loess in a section located a few kilometers southwest of Pocatello was found to be 8.5 meters. Other sites examined a few kilometers north of Pocatello showed depths of 12, 13, and 16 meters.

CHARACTER OF LOESS AND LOESS SOILS

PARTICLE SIZE DISTRIBUTION

The sampling procedure for studying the particle size distribution, as well as for other characteristics of the loess and associated soil profiles, was as follows: soils were sampled from the genetic horizons of the modern surface soil at each site. Composite samples were taken in intervals of 25 to 50 centimeters from the rest of the section. These intervals were arbitrarily selected except where distinct changes in color or other characteristics indicated natural breaks in the section.

Particle size distribution was determined on carbonate-removed samples by the pipette method as described by Kilmer and Alexander (1949).

No consistent areal pattern of particle size distribution in the loess deposits on the Snake River Plain is presently evident, either in the direction of the present prevailing winds or as a function of distance from the Snake River. Evidence suggests that this may be due to at least two factors: continuous mixing by the removal and redeposition of the loess, and multiple sources of the loess. The mineralogy of the coarse silt fraction also suggests that the wind direction was occasionally from the northwest, not from the Snake River. We are continuing our study of particle size distribution in the loess deposits on the Snake River Plain.

The particle size of loess decreases with distance from the Snake River in the terrain along the eastern margin of the Snake River Plain (Figure 1, Table 1). This will be discussed with data from loess sections along four traverses (Figure 2, Table 1).

Traverse A

Traverse A starts near the eastern margin of the Snake River Plain in the vicinity of Fort Hall and continues southeast to the vicinity of Grace. There is a decrease in very fine sand and coarse silt and an increase in medium and fine silt with increased distance from the Snake River Plain (Table 1). The decrease in particle size with distance from the plain suggests that the flood plain of the Snake River was at least part of the source of the loess.

There are some minor deviations to the overall trend. Very fine sand should be lower in section 0301 and 1504 than in 0611 since the latter is closer to the plain. Also, fine silt did not consistently increase with distance from the plain. This may suggest that the loess in traverse A was not derived wholly from the Snake River Plain. McDole (1969) postulated that the loess in sections 0611, 0301, and 1504 was derived from three different sources: the Snake River Plain and two local sources, Ross Fork Creek and Portneuf River drainages.

Traverse B

Changes in altitude as well as in distances from the Snake River Plain from Blackfoot to Garden Peak complicate the interpretations of loess particles in traverse B. Traverse B covered a distance of 8 kilometers from the plain with an elevation increase of 400 meters. The distribution of very fine sand and silts is shown in part B of Table 1. There was a small decrease in very fine sand and coarse silt and a small increase in medium and fine silt with the increase in elevation and distance from the plain. Thus, it appears that as both distance and altitude above the Snake River increase, particle size decreases.

Traverse C

Traverse C runs from west of Pocatello on the Snake River Plain to near Malad. Loess section 3611 (Figure 2) at the southern end of the traverse is

just a few miles north of the shore line of pluvial Lake Bonneville. There was a decrease in very fine sand and coarse silt and an increase in medium and fine silt with distance from the plain. This suggests that the plain was the source of the loess. Because loess section 3611 is close to the location of Lake Bonneville it could be argued that the lake constituted the source but it seems unlikely that the sources are different, since section 3611 is at the southern end of a body of loess which is continuous from the Snake River Plain.

Traverse D

Data on particle size distribution were available on four sites near the northeastern margin of the Snake River Plain (traverse D). Two of the sites are near the edge of the plain near Rexburg, and the other two sites are east near the Idaho-Wyoming border (Figure 2).

The two loess sections (3302, 3306) nearest the major rivers on the Snake River Plain had a higher content of very fine sand than those (W2015, 4101) away from the plain. The coarse silt content was also higher in the two sites nearer to the plain than at site W2015 to the east. No breakdown of the silt fractions was available at site 4101. Section 3306 is closer to the St. Anthony sand dunes than section 3302, and section 3302 is near an outwash fan from the South Fork of the Snake River, which may account for the higher amounts of very fine sand in section 3306.

Table 1. Average sand and silt size* particle distribution along four traverses on the eastern side from the Snake River Plain.

Lab. No.	Total Depth Sampled (m)	Distance from Snake River (km)	Elevation (m)	Very Fine Sand	Coarse Silt	Medium Silt	Fine Silt	Number of Samples in Section
				%				
Traverse A—Southeast from Fort Hall to Grace								
0621	10.0	20.9	1463	16.8	64.6	14.7	3.4	24
0611	7.7	30.6	1737	14.0	62.1	18.5	5.0	20
0301	7.1	41.0	1760	15.4	60.6	19.4	4.2	21
1504	6.7	47.0	1890	15.5	57.9	20.9	4.8	18
1523	1.3	78.4	1707	10.9	56.6	22.9	9.5	9
1521	2.2	89.4	1639	11.6	52.3	27.3	7.3	8
Traverse B—East from Blackfoot to Garden Peak								
0691	11.7	14.5	1433	17.9	64.2	13.8	3.2	22
0692	10.9	16.1	1554	16.9	62.4	16.6	2.8	20
0693	10.2	17.7	1646	16.1	60.8	15.8	4.4	40
0694	11.6	19.3	1798	16.8	58.1	16.9	4.9	47
0677	13.2	22.5	1829	15.8	59.9	19.0	4.8	52
Traverse C—West of Pocatello South to Malad								
3904	9.2	12.5	1737	19.6	64.0	11.2	2.1	26
3905	8.5	22.0	1743	18.2	56.4	21.2	3.4	27
3611	1.8	73.5	1585	12.0	48.3	27.1	11.4	11
Traverse D—East from Rexburg to Tetonia**								
3302	7.1	6.0	1756	18.9	58.6	17.8	3.5	11
3306	11.6	12.0	1600	31.4	52.3	18.0	3.0	-
4104	2.2	54.0	2080	11.3	-	-	-	11
W2015	8.9	60.0	2000	12.6	36.7	35.0	15.4	16

*$CaCO_3$ removed; calculated on clay-free basis
**Measured from western edge of loess deposit in the vicinity of Rexburg

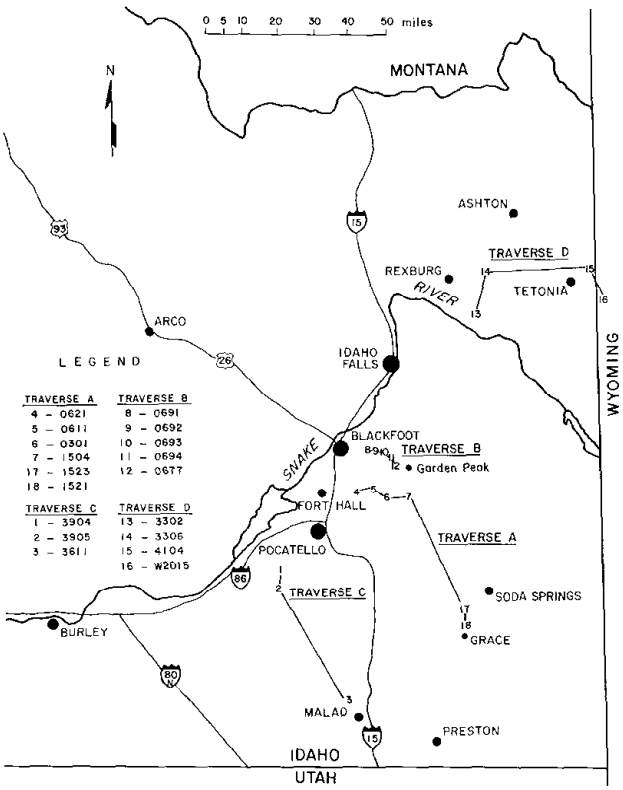

Figure 2. Location of traverses and sampling sites.

CALCIUM CARBONATE EQUIVALENT

The calcium carbonate equivalent of the loess varies both within and between loess sections. Soils of large areas in the central Snake River Plain have a lime-silica duripan which suggests cycles of loess deposition and subsequent partial removal by deflation during which calcium and silica were leached downward in the soil. In the Snake River Plain, calcium carbonate equivalents are as much as 50 percent in the zone of accumulation, although values of 20 to 25 percent are more common. In unweathered loess, carbonate content consistently ranges between 15 and 20 percent.

Data for calcium carbonate equivalent of the upper loess deposit are given in Table 2 for the four traverses. The data include the thickness of the leached zone and the carbonate content in the zone of maximum accumulation and in the unaltered loess below. These values are compared to annual precipitation, altitude, distance from Snake River Plain, and thickness of the upper deposit.

The thickness of the leached zone and the depth of maximum carbonate increases with increased precipitation as expected. The leached zone may contain some carbonates, particularly at lower elevations.

There is no consistent relationship between thickness of loess or annual precipitation and the calcium carbonate equivalent at the maximum zone of accumulation or in the unaltered loess, with the exception of section W2015. The relatively high annual precipitation of 76 centimeters at this site was apparently enough to leach out part of the carbonates during and following deposition. There did not appear to be any unaltered loess in the relatively thin deposits at sections 1504, 1523, or 3611.

More work is needed to understand the carbonate chemistry of the southern Idaho loess deposits. This discussion serves to indicate amounts present and to show the complexity of the loess deposits.

CLAY MAXIMA

Changes in clay content with depth in a loess section might indicate buried soils separating different periods of loess deposition. There is a clay maximum in the B horizon of the modern soil in all four traverses (Table 3). Below this surface soil at least one additional clay maximum is in the loess sections of traverses A, B, and C. A second clay maximum was found in section W2015 but not in the other sections in traverse D. Interpretation of the upper two clay maxima in the loess deposits of southeastern Idaho have been made by Pierce and others (1982 this volume).

The clay maximum in the modern soil can be interpreted as normal soil development. There does not appear to be a consistent relationship in traverse A between the clay content of the modern soil and the distance from the Snake River Plain. This is also true of the second clay maximum along the traverse. Also, the depth to the clay maximum is variable along the traverse. The magnitude of the second maximum is similar to the first, except for sections 1521 and 1523, where they were higher than the first.

For traverse B, clay content of the modern soil increases with distance from the Snake River Plain (Table 3). The magnitude of the second clay maxima is slightly greater than in the modern soil except for the section farthest away from the plain. Depth to the first clay maximum is variable, but the three sections farther away from the plain have somewhat similar depths to the second clay maximum.

The clay maxima in the modern soils in traverses C and D increase with altitude in the direction away from the Snake River Plain as does the second maxima in traverse C. In traverse C, the clay content of the second maxima is higher in the two sites (3905

and 3611) than in the modern soil. In traverse D, only section W2015 has a second clay maximum.

These loess sections reveal that, in general, the amount of clay increases with altitude and distance from the Snake River Plain. There is no consistent relationship of the depth to the clay along the transects. It may not be possible to compare a second clay maximum since they may not represent the same buried soil or depositional phase. This will become evident when the properties of buried soils are discussed.

CLAY MINERALOGY

X-ray diffraction patterns were made on the coarse clay fraction (0.2 to 2 μm) of samples following magnesium saturation and treatment with ethylene glycol (Jackson, 1956). In order to differentiate between vermiculite and chlorite and substantiate the presence of kaolinite, X-ray diffraction patterns were made on potassium-saturated samples. The potassium-saturated slides were heated to 500°C and rerun to differentiate between the chlorite and kaolinite. Interpretation of the X-ray patterns was based on Whittig (1965).

The clay mineral species found in the coarse clay fraction are similar throughout all the loess sections examined. They consist primarily of expanding lattice minerals (smectite), illite, and kaolinite with lesser amounts of vermiculite and occasionally a trace of chlorite. Quartz and feldspars are also found in the coarse clay fraction of most samples. Changes in amounts of these principal clay-size minerals with depth in the loess section will be discussed later.

A complete clay mineral analysis should ideally include both qualitative identification and quantitative estimation of the clay minerals present. The presence of one or more of the following characteristics in natural clay mixtures (Keller, 1962) may make rigorously quantitative expresssions of clay mineral percentages or ratios misleading: (1) inconsistencies in the chemical compositions of the clay minerals, (2) variation in the amount of amorphous (to X-ray)

Table 2. Calcium carbonate equivalent in the zones of maximum accumulation and in the unaltered loess, and thickness of leached zone as related to precipitation, altitude, distance from Snake River Plain, and thickness of upper loess.

Lab. No.	Annual Precipitation (cm)	Altitude (m)	Distance from Snake River (km)	Thickness of Upper Loess (m)	Thickness of Leached Zone (cm)	Depth to Maximum $CaCO_3$ Equiv. (cm)	Maximum $CaCO_3$ Equiv. (%)	Unaltered Sampling Interval (cm)	Loess $CaCO_3$ Equiv. (%)
			Traverse A—Southeast from Fort Hall to Grace						
0621	25	1463	20.9	>9.96	38	56	22.6	165-422	14.8
0611	33	1737	30.6	>7.67	56	81	22.9	107-315	17.2
1504	41	1890	47.0	2.03	66	97	19.7	(1)	-
1523	43	1692	78.0	2.21	89	107	32.8	(1)	-
			Traverse B—East from Blackfoot to Garden Peak						
0691	25	1433	14.5	10.67	18	61	24.1	122-457	19.8
0692	25	1554	16.1	10.92	25	38	21.1	76-381	15.1
0693	30	1646	17.7	7.87	48	48	22.6	191-343	18.0
0694	33	1798	19.3	6.50	56	81	22.8	203-381	16.6
0677	41	1829	22.5	7.32	74	124	23.1	213-345	18.1
			Traverse C—West of Pocatello South to Malad						
3904	33	1737	12.5	>9.47	23	38	27.3	76-269	17.3
3905	36	1746	22.0	4.06	53	76	30.9	94-208	15.1
3611	-	1585		2.24	86	86	28.6	(1)	-
			Traverse D—East from Rexburg to Tetonia						
3302	33	1756	6.0	>2.79	68	68	27.2	147-257	19.7
3306	36	1600	12.0	>4.57	53	94	22.2	76-152	17.0
W2015	76	2000	60.0	2.60	90	106	12.7	135-225	5.4

(1) No apparent unaltered loess present

material from specimen to specimen, (3) variability in ratios of mixing in clays that show random mixed layering, and (4) differences in the degree of postdepositional weathering of samples.

Although it is recognized that a quantitative expression of the amounts of clay minerals present in the loess is not possible, an estimate of relative amounts can be achieved by using illite equivalents (Lewis and White, 1964). Converting peak heights to illite equivalents was accomplished by dividing the smectite peak height by 4, vermiculite peak by 2, and kaolinite peak by 4, summing these along with the illite peak height, making this equal to 100 percent, and determining the contribution of each clay mineral in terms of percent.

An estimate of the relative proportions of smectite, vermiculite, illite, and kaolinite are shown in Table 4. The traverses run from the eastern edge of the Snake River Plain to the southeast, to the south, and to the east.

The expanding lattice component (smectite) appears to be decreasing with increasing distance from the Snake River Plain. Smectites occur in larger quantities in soils that have high amounts of soluble salts present, a condition more prevalent in the Snake River Plain than at higher elevations where there is more precipitation and leaching. The presence of quartz and feldspar in the coarse clay fraction, along with high illite content throughout the loess deposit, would indicate that relatively little weathering has taken place. The kaolinite content does not change significantly along the transects or between the loess sections studied. The kaolinite is probably detrital and has not changed or formed in this environment since this would require strong weathering.

PROPERTIES OF BURIED SOILS

Much work remains before the stratigraphy of the southern Idaho loess deposits can be interpreted. It

Table 3. Depth and clay content of modern and upper buried soil in loess sections.

Lab. No.	Modern Depth of 1st Maxima (cm)	Clay (%)	Upper Buried Soil Depth of 2nd Maxima (cm)	Clay (%)
	Traverse A—Southeast from Fort Hall to Grace			
0621	20-38	11.1	244-315	11.1
0611	15-30	18.6	660-709	16.9
0301	28-43	16.5	262-300	16.6
1504	66-97	19.3	277-328	19.4
1523	13-23	13.2	107-137	19.0
1521	15-25	18.5	135-157	10.8
	Traverse B—East from Blackfoot to Garden Peak			
0691	36-61	9.9	381-457	10.4
0692	38-69	10.5	381-533	12.9
0693	23-36	11.4	648-686	12.7
0694	8-23	13.1	686-711	16.6
0677	20-36	14.2	648-686	15.2
	Traverse C—West of Pocatello South to Malad			
3904	23-28	16.2	168-208	11.1
3905	33-43	20.7	455-493	28.0
3611	33-51	18.0	86-97	26.1
	Traverse D—East from Rexburg to Tetonia			
3302	173-229	5.4	-	-
3306	64-76	4.9	-	-
4101	74-132	27.2	-	-
W2015	12-36	28.0	350-370	17.1

Table 4. Estimated amounts of clay minerals in coarse clay fraction.

Lab. No.	Depth Sampled (m)	Distance from Snake River (km)	Smectite	Vermiculite	Illite	Kaolinite
		Traverse A—Southeast from Fort Hall to Grace				
0694	11.6	19.3	28	0	60	12
1523	1.3	78.4	13	0	74	13
1521	2.2	89.4	13	0	73	14
		Traverse C—West of Pocatello South to Malad				
3904	9.2	12.5	30	Tr	57	13
3905	8.5	22.0	24	9	56	11
3611	1.8	73.5	Tr	0	85	15
		Traverse D—East from Rexburg to Tetonia				
3302	7.1	6.0	22	13	50	15
3306	11.6	12.0	26	13	46	15
W2015	8.9	60.0	11	15	59	15

has been observed that buried soils are present in many of the sections studied. Stratigraphic units in the loess deposits of southeastern Idaho are discussed by Pierce and others (1982 this volume).

McDole and others (1973) reported buried soils in seven of eleven sections comprising three transects traversing the loess deposits adjacent to the Snake River flood plain near Pocatello. However, some sections did not extend through the entire depth of loess. Section 0694 gives the best expression of the greatest number of buried soils in this group. Figure 3 shows three distinct zones where maxima in calcium carbonate equivalent suggest the presence of buried soils at depths of 7, 10, and 11.5 meters. These three maxima in carbonates are stronger than the maximum present in the Cca horizon of the modern soil. Approximately coinciding with these three zones of carbonate accumulation are maxima in soluble salts (E.C.) and increases in total clay fraction. In the original auger samples, the B horizons were difficult to recognize, for they were white and enriched with secondary carbonate and other salts. The carbonate, clay, and soluble salts in these zones show magnitudes at least twice as high as the rest of the section.

There is an anomaly in the characteristic horizon sequence of these buried soils. This is the occurrence of the soluble salt maxima coincident with or above the carbonate and clay maxima. This sequence is contrary to expected horizon development as exhibited by the modern soil in the upper part of the section (Figure 3). In usual soil development, the genetic soil horizons occur with a maximum in clay nearest the surface, followed by a maximum in carbonates at a slightly greater depth and the maximum in soluble salts deeper than the carbonate maximum. Thus, since the accumulations of soluble salts occur above or coincident with the clay and carbonate maxima, it must be assumed that the accumulation of the more soluble materials was subsequent to the event that created the carbonate and clay maxima. This implies that the three buried soils in the section are each complex or polypedogenic. This is further verified by secondary $CaCO_3$ accumulation in the B horizons of buried soils in the exposed head walls of the Gay phosphate mine near the middle of traverse A, Figure 2 (Ken Pierce, 1981, personal communication).

Each of these polypedogenic buried soils reflects at least two different sets of soil-forming factors. The initial set of factors responsible for each of the buried soils formed a soil profile reflected by the accumulation of clays and carbonates. The resultant soil profile included a weakly developed B horizon and a strong Cca horizon. This soil profile reflects a degree of development at least as strong or stronger than the modern soil profile. The subsequent set of soil-forming factors, which included new deposition of materials, produced movement of more readily soluble salts and carbonates, perching these latter materials on top of the previously accumulated clay and carbonates.

Particle size analyses show the modern soil surface and buried soil zones to be higher in coarser

sands (greater than 100 μm) than the rest of the section (0694). The higher sand content is possibly the result of deflation of some of the finer loess particles during the interval of soil development. A geosol is a buried soil, having physical characteristics that are easily recognized, which can be used as a stratigraphic marker to correlate between different sites (Morrison, 1968).

The first (uppermost) buried soil with development equal to or greater than the surface soil was named the Fort Hall Geosol by McDole (1969) and McDole and others (1973). This geosol was found in seven out of ten sections in the Pocatello area. The relative increase in clay, the amount of fine clay, clay mineral types, calcium carbonate equivalent, silt, sand fractions, and total salts served to correlate this buried soil from one section to another. The Fort Hall Geosol finds its best expression in section 0694 (Figures 3 and 4) and is described as follows: The Fort Hall Geosol has 50 to 100 percent more total clay than the surface soil profile or other buried soil in the section and an increase in the fine clay fraction which is about double the increase in the coarse clay fraction. The lesser buried soils show only slight increases in both fine and coarse clay fractions.

Calcium carbonate equivalent of 32 to 34 percent in samples from the lower part of the Fort Hall Geosol is twice that of the unaltered parent loess. The calcium carbonate equivalent of the geosol also represents an accumulation of carbonates about twice the magnitude of the surface soil profile and lesser buried soils.

A slight decrease in very coarse silt occurs in the Fort Hall Geosol. The most striking anomaly in the silt fractions is seen in the amounts of coarse and medium silts. In the upper loess unit, above the Fort Hall Geosol, the amount of coarse silt is distinctly higher than the amount of medium silt. Coincident with the geosol, the relative amounts of these two fractions converge and maintain approximately equal values throughout the remainder of the sampled section.

Another identifying criterion of the Fort Hall Geosol is based on changes in the amount of very fine sand (100 to 50 μm) and coarser sands (1.0 to 0.1 millimeter) fractions (Figure 4). The very fine sand ranges from 12 percent at the surface of the geosol to a maximum of 20 percent within the geosol. The coarser sands fraction reaches a maximum of 1.3 percent in the geosol compared with less than 0.5 percent above and below the geosol.

Very fine sand reaches a maximum of 19 percent

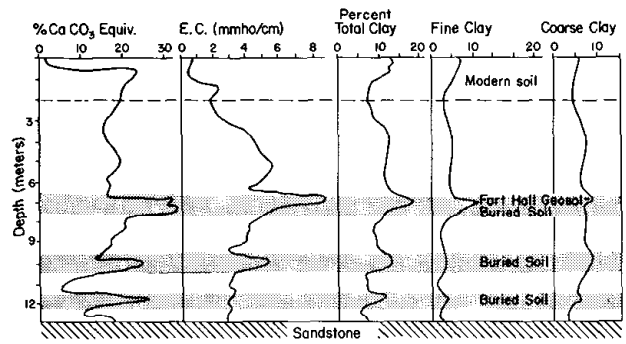

Figure 3. Calcium carbonate equivalent, soluble salts and clay in section 0694.

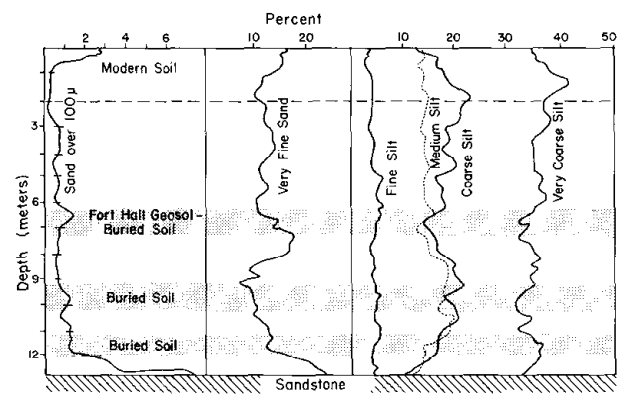

Figure 4. Sand and silt fractions in section 0694.

near the surface of the modern soil and then decreases to about 14 percent until the geosol is reached. Coarser sands reach a maximum of 2.8 percent in the upper 56 centimeters of the modern soil and then decrease to about 0.5 percent. The increase in sands in the modern soil can be explained as the removal of finer materials by water or wind erosion of the surface, leaving the coarser materials behind. The increase in sands of the Fort Hall Geosol and lesser buried soils also supports pedologic origin of these zones in the sections.

These identifying characteristics imply the nature of events which took place to form these buried soils. The initial event in the formation of the buried soils resulted in accumulations of relatively insoluble carbonates and clays. During the period of soil development deflation removed some of the finer particles from the surface of the soil and increased the percentage of sand-size particles. The Fort Hall Geosol represents a much stronger set of soil-forming factors than those responsible for the formation of the existing modern soil or the other buried soils in the section.

REFERENCES

Baldwin, Mark and F. O. Youngs, 1925, Soil survey of the Twin Falls area, Idaho: U. S. Department of Agriculture, Bureau of Soils, 52 p.

Bright, R. C., 1963, Pleistocene Lakes Thatcher and Bonneville, southeastern Idaho: University of Minnesota Ph.D. dissertation, 363 p.

Daniels, D. M., H. L. Hansen, T. W. Priest, and W. G. Perrin, 1969, Soil survey, Teton area, Idaho-Wyoming: U. S. Department of Agriculture, Soil Conservation Service, 95 p.

Emiliani, Cesare, 1972, Quaternary paleotemperatures and the duration of the high temperature intervals: Science, v. 178, p. 398-401.

Jackson, M. L., 1956, Soil chemical analysis, advanced course: Department of Soils, Univeristy of Wisconsin, 894 p.

Keller, W. D., 1962, Clay minerals in the Morrison Formation of the Colorado Plateau: U. S. Geological Survey Bulletin 1150, 90 p.

Kilmer, V. J. and L. T. Alexander, 1949, Methods of making mechanical analysis of soils: Soil Science, v. 68, p. 15-24.

Lewis, G. C. and J. L. White, 1964, Chemical and mineralogical studies on slick spot soils in Idaho: Soil Science Society of America, Proceedings, v. 28, p. 805-808.

Lewis, G. C., M. A. Fosberg, R. E. McDole, and J. C. Chugg, 1975, Distribution and some properties of loess in south-central and southeastern Idaho: Soil Science Society of America, Proceedings, v. 39, p. 1165-1168.

Lewis, H. G. and P. P. Peterson, 1921, Soil survey of the Portneuf area, Idaho: U. S. Department of Agriculture, Bureau of Soils, 52 p.

Mansfield, G. R., 1920, Geography, geology and mineral resources of the Fort Hall Indian Reservation, Idaho: U. S. Geological Survey Bulletin 713, 152 p.

McDole, R. E., 1968, Some properties of loess in the Bannock Peak transect in southeastern Idaho: University of Idaho M.S. thesis, 162 p.

———, 1969, Loess deposits adjacent to the Snake River flood plain in the vicinity of Pocatello, Idaho: University of Idaho Ph.D. dissertation, 231 p.

———, 1977, Soil survey of Fort Hall area, Idaho: U. S. Department of Agriculture, Soil Conservation Service, 97 p.

McDole, R. E., G. C. Lewis, and M. A. Fosberg, 1973, Identification of paleosols and the Fort Hall Geosol in southeastern Idaho loess deposits: Soil Science Society of America, Proceedings, v. 37, p. 611-616.

Morrison, R. B., 1968, Means of time-stratigraphic division and long-distance correlation of Quaternary successions, *in* R. B. Morrison and H. E. Wright, Jr., editors, Means of Correlation of Quaternary Successions, v. 8: Proceedings, VII Congress, International Association for Quaternary Research, University of Utah Press, Salt Lake City, Utah, p. 113.

Pierce, K. L., J. D. Obradovich, and Irving Friedman, 1976, Obsidian hydration dating and correlation of Bull Lake and Pinedale Glaciations near West Yellowstone, Montana: Geological Society of America Bulletin 87, p. 703-710.

Pierce, K. L. and W. E. Scott, 1982, Pleistocene episodes of alluvial-gravel deposition, southeastern Idaho, *in* Bill Bonnichsen and R. M. Breckenridge, editors, Cenozoic Geology of Idaho: Idaho Bureau of Mines and Geology Bulletin 26.

Pierce, K. L., M. A. Fosberg, W. E. Scott, G. C. Lewis, and S. M. Colman, 1982, Loess deposits of southeastern Idaho: age and correlation of the upper two loess units, *in* Bill Bonnichsen and R. M. Breckenridge, editors, Cenozoic Geology of Idaho: Idaho Bureau of Mines and Geology Bulletin 26.

Poulson, E. N. and J. A. Thompson, 1927, Soil survey of the Jerome area, Idaho: U. S. Department of Agriculture, Bureau of Chemistry and Soils Series 1927, no. 16, 22 p.

Poulson, E. N., L. B. Nelson, and A. E. Poulson, 1943, Soil survey Blackfoot-Aberdeen area, Idaho: U. S. Department of Agriculture, Bureau of Plant Industry in cooperation with University of Idaho, ser. 1937, no. 6, 111 p.

Russell, I. C., 1902, Geology and water resources of the Snake River Plain of Idaho: U. S. Geological Survey Bulletin 199, 192 p.

Shackleton, N. J. and N. D. Opdyke, 1973, Oxygen isotope and paleomagnetic stratigraphy of equatorial Pacific core V28-238—oxygen isotope temperatures and ice volumes on a 10^5 and 10^6 year scale: Quaternary Research, v. 3, p. 39-55.

U. S. Geological Survey, 1972, Surficial geologic map of Yellowstone National Park: U. S. Geological Survey Miscellaneous Geologic Investigations Map I-710.

Whittig, L. D., 1965, X-ray diffraction techniques for mineral identification and mineralogical composition, *in* C. A. Black, editor, Methods of Soil Analysis, Part 1—Physical and Mineralogical Properties: American Society of Agronomy Monograph 9, p. 671-678.

Williams, P. L., H. R. Covington, and K. L. Pierce, 1982, Cenozoic stratigraphy and tectonic evolution of the Raft River basin, Idaho, *in* Bill Bonnichsen and R. M. Breckenridge, editors, Cenozoic Geology of Idaho: Idaho Bureau of Mines and Geology Bulletin 26.

Youngs, F. O., A. W. Kern, and E. N. Poulson, 1925, Soil survey of the Soda Springs-Bancroft area, Idaho: U. S. Department of Agriculture, Bureau of Chemistry and Soils, ser. 1925, no. 6, 33 p.

Youngs, F. O., Mark Baldwin, A. J. Kern, and G. R. McDole, 1928, Soil survey, Minidoka area, Idaho: U. S. Department of Agriculture, Bureau of Chemistry and Soils, ser. 1923, no. 27, p. 589-902.

Loess Deposits of Southeastern Idaho: Age and Correlation of the Upper Two Loess Units

by

Kenneth L. Pierce[1], Maynard A. Fosberg[2], William E. Scott[1], Glenn C. Lewis[2], and Steven M. Colman[1]

ABSTRACT

Loess deposits in southeastern Idaho are subdivided into stratigraphic units on the basis of stratigraphic position, buried soils, and relations to other stratigraphic units. The upper unit, loess unit A, covers most of the landscape where slopes are gentle and underlying units are older than about 15,000 years. The next older unit, loess unit B, is present at stable sites where loess unit A is thick and where the underlying substratum is older than about 150,000 years. Loess units A and B seem to be consistent stratigraphic units that can be correlated over a transect 400 kilometers long. Accumulation of loess unit A ceased about 10,000 years ago, as indicated by the degree of soil development, the relation to deposits of both the Pinedale Glaciation and the Bonneville Flood, and the absence of significant loess on Holocene basalts. Loess unit A rests locally on a buried soil that is significantly better developed than the surface soil in loess unit A. A buried soil more strongly developed than the surface soil is present on glacial deposits 140,000-150,000 years old but is not present above a pumice bed correlated with a rhyolite dome 61,000 ± 6,000 years old and a basalt 72,000 ± 14,000 years old. Thus, the upper loess unit appears to have accumulated between about 70,000 and 10,000 years ago and probably correlates with the Wisconsin Glaciation. Because the buried soil on loess unit B is significantly better developed than the surface soil, it probably formed during an interval several times the 10,000 years represented by the surface soil, presumably between about 130,000 and 70,000 years ago. Loess unit B probably accumulated during an interval that ended shortly after 140,000 to 150,000 years ago and that was roughly similar in duration to that of loess unit A.

[1]U. S. Geological Survey, Denver, Colorado 80225.
[2]Department of Plant and Soil Sciences, University of Idaho, Moscow, Idaho 83843.

INTRODUCTION

Geologic studies, particularly since 1975, have yielded enough stratigraphic and age information to justify a preliminary synthesis of the age and correlation of loess deposits on and adjacent to the eastern Snake River Plain (Figure 1). We summarize here information on the stratigraphy and dating of the upper two loess units and present a correlation diagram for eleven loess sections along a 400-kilometer transect from West Yellowstone, Montana, to Gooding, Idaho. Further studies of these loess deposits and associated basalt flows and volcanic ash beds will yield additional age information, especially for loess deposits older than the upper two loess units. We limit this discussion to the two youngest loess units, because most of the available stratigraphic and dating information pertains to them. We also limit this discussion to age and correlation of the loesses, for a companion paper by Lewis and Fosberg (1982 this volume) describes the distribution, thickness, and character of the loesses in southeastern Idaho.

The stratigraphic subdivision of loess deposits is accomplished by using soils developed in the upper part of each loess unit. Depending upon the local climate, a weakly to moderately developed soil is formed in the uppermost loess (loess unit A). This soil is similar in degree of development to the soil formed in latest Pleistocene or Pinedale-age deposits in comparable environments and to that formed in Holocene time. The near absence of loess on Holocene basalts in the area shows that most of the loess is a relict deposit of Pleistocene age. Thus, both the degree of soil development and the general lack of loess deposition in the Holocene suggest a late Pleistocene age for the upper part of loess unit A. Roadcuts, mine exposures, and backhoe pits show that loess unit A generally mantles all older loess units, except along bluffs and other actively eroding areas. In multiple-unit loess sections, the

Pierce, K. L., M. A. Fosberg, W. E. Scott, and G. C. Lewis, and S. M. Colman, 1982, Loess deposits of southeastern Idaho: age and correlation of the upper two loess units, *in* Bill Bonnichsen and R. M. Breckenridge, editors, Cenozoic Geology of Idaho: Idaho Bureau of Mines and Geology Bulletin 26, p. 717-725.

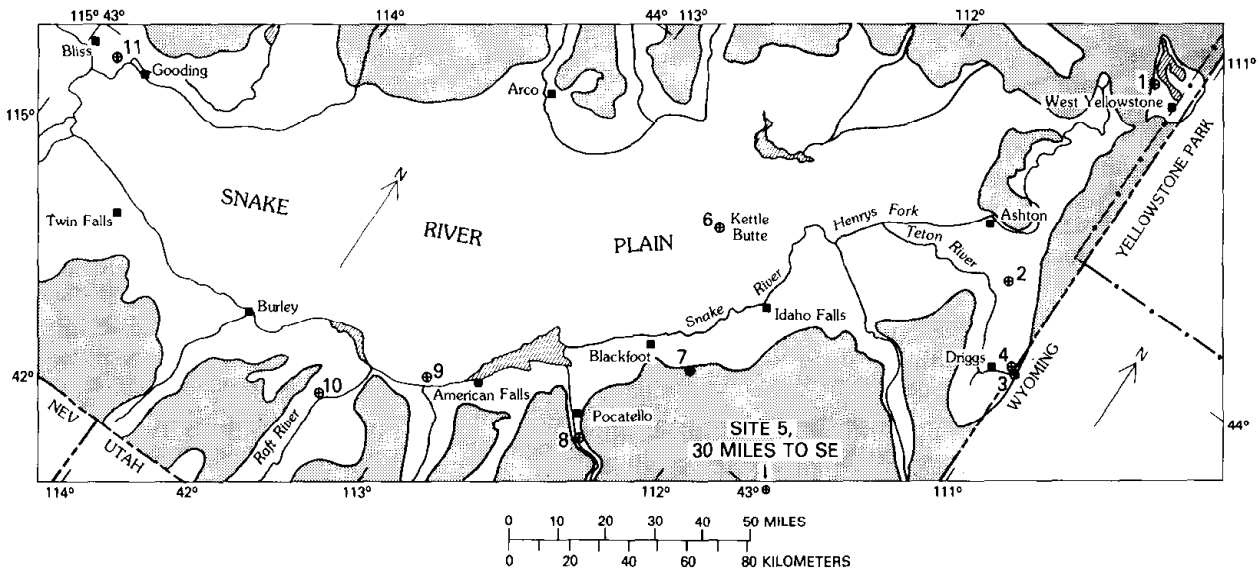

Figure 1. Location map of eastern Snake River Plain, southeastern Idaho. Numbered sites are locations of loess sections shown in Figure 2. Shading indicates mountainous areas.

base of loess unit A is marked by the top of a buried soil that is better developed than the surface soil.

The top of the next older loess unit, loess unit B, is marked by a buried soil that is better developed than the surface soil. The base of loess unit B is the top of the next deeper buried soil that is comparable to or better developed than the surface soil. Loess unit B can be recognized with confidence only in flat upland areas or in other areas where exposures suggest that no loess units have been removed by erosion.

The loess units generally do not contain datable material, although volcanic ash layers or lenses do occur locally. However, in some areas the loess units overlie numerically dated Quaternary basalts, glacial deposits, and flood-scoured surfaces, and in others the loess units overlie deposits whose relative or approximate numerical age is known. Given an increasing progression of ages for underlying units, the ages of increasingly older loess units and soils can be approximated.

Previous researchers have estimated differing ages for the loess deposits of southeastern Idaho. Bright (1967) named the loess in the Thatcher basin the Niter Loess and described stratigraphic relations suggesting it was late Pleistocene to perhaps Holocene age. McDole (1969, p. 7) deduced that the thick loess sequence and included paleosols near Pocatello dates from between 75,000 and 30,000 years ago because (1) no loess had accumulated on deposits of the Bonneville Flood, which were then thought to be about 30,000 years old and (2) none of the buried soils within the loess sequence were as strongly developed as he expected pre-Wisconsin soils to be. In contrast, Richmond (1973) concluded that the thick upper loess unit mantling glacial deposits southwest of Yellowstone National Park was of Pinedale age, which is in accord with our conclusions.

DESCRIPTION OF STRATIGRAPHIC SECTIONS

The eleven loess sections described here were selected because they provide useful information on the stratigraphy, correlation, and age of the upper two loess units along the length of the eastern Snake River Plain (Figures 1 and 2).

The best stratigraphic and age control for loess deposits comes from the West Yellowstone basin (Figure 2, site 1). Combined obsidian-hydration and potassium-argon methods date the age of glacial abrasion of obsidian in Bull Lake moraines at about 140,000 to 150,000 years old and that in Pinedale terminal moraines at about 30,000 years old (Pierce and others, 1976; Pierce, 1979). Carbon-14 and obsidian-hydration dating reveal that deglaciation of the Yellowstone Plateau occurred by about 14,000 years ago. Results of weathering-rind studies are consistent with these age assignments (Colman and Pierce, 1981).

Loess commonly overlies Bull Lake deposits in the West Yellowstone basin. At localities where the upper loess is more than 0.5 meter thick, a buried soil commonly can be distinguished below the surface soil (Figure 2, site 1; Pierce, 1979, Figure 11,

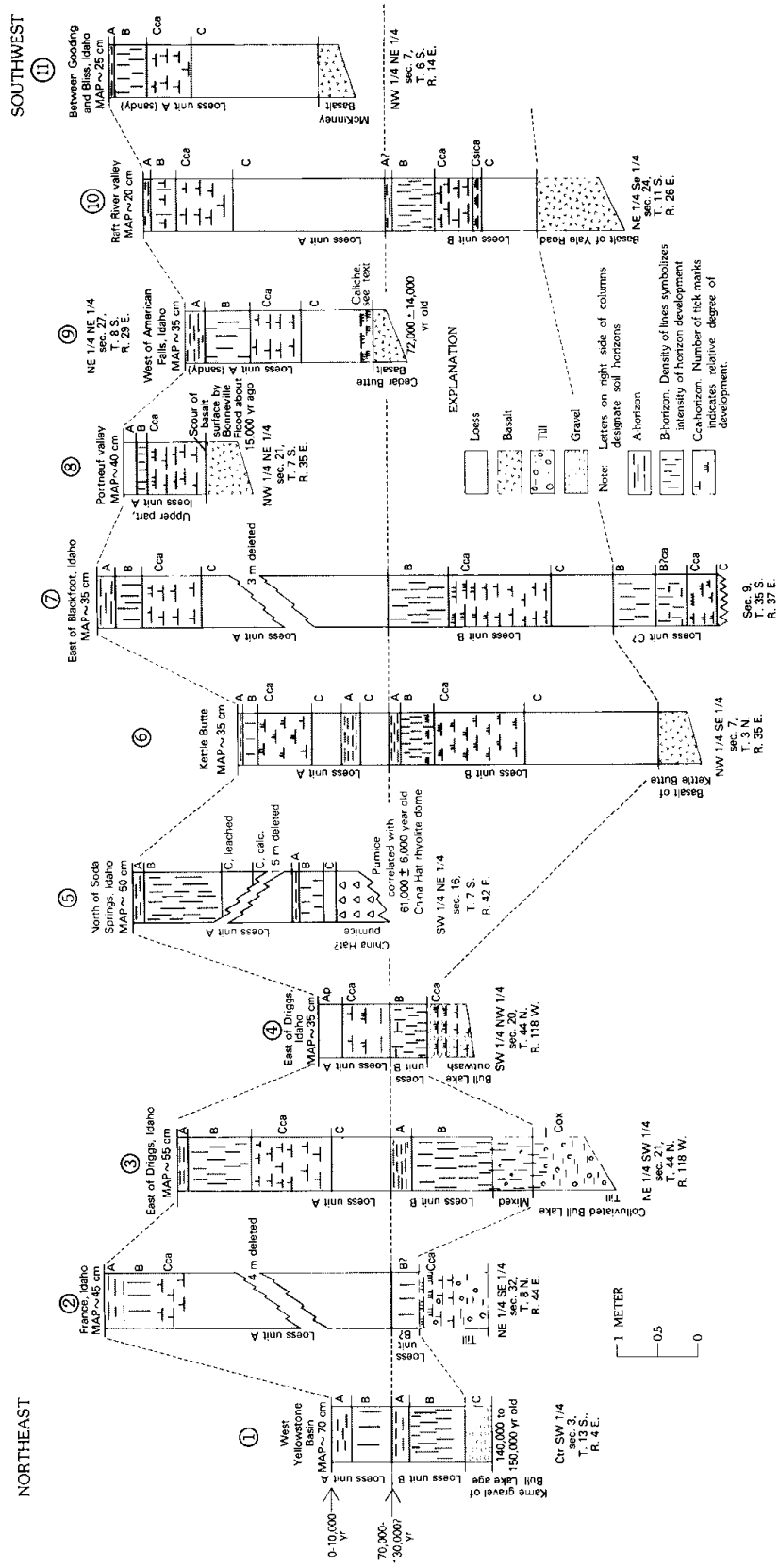

Figure 2. Stratigraphic sections along a 400-kilometer transect from West Yellowstone, Montana, to Bliss, Idaho, showing loess units, surface and buried soil horizons, and available dating of substrates for the sites shown on Figure 1. Estimates of mean annual precipitation (MAP) after Thomas and others (1963, Plate 2) and from other information.

locations 5 and 6). The loess at the ten other sites described here has about 15 percent original $CaCO_3$ equivalent, whereas the loess in the West Yellowstone basin is noncalcareous, at least in part because bedrock in the outwash source area of the West Yellowstone basin is largely noncalcareous.

Site 1 (Figure 2) is a reexcavation of a soil pit originally dug in the late 1960's by Fred Nials. The surface soil in loess unit A is weakly developed and similar to the soil on Pinedale moraines 20 kilometers to the east (Pierce, 1979, Figure 11). On the basis of sequence and soil development, loess unit A is correlated with nearby glacial deposits assigned to the Pinedale Glaciation. Loess unit A overlies a buried soil developed both in silty sediment and in the upper part of kame gravels mapped by Waldrop (1975) as Bull Lake in age. The silty sediment is also assigned a Bull Lake age, because it conformably overlies the kame gravel. This silty sediment is most likely loess altered by soil development and is here assigned to loess unit B. Compared with the surface soil, the B horizon of the buried soil has colors two chromas stronger, a thickness about 50 percent greater, and about twice as much clay (about 35 percent compared with 18 percent in field estimates by Fosberg). However, parent-material differences may complicate this comparison. Bull Lake moraines, and presumably loess unit B, are rich in basalt clasts which weather more readily than the rhyolitic material that makes up the bulk of the Pinedale moraines, and presumably loess unit A (Figure 2, site 1). Despite this parent-material difference, the development represented by the buried soil still appears to represent more time than that represented by the surface soil.

At the upper end of the Snake River Plain near Ashton, loess unit A commonly exceeds 5 meters in thickness. Carbonate has been leached from the soil in loess unit A to a depth of about 0.5 meter; the calcic horizon generally reaches only stage III and is not cemented (Gile and others, 1966). Site 2 (Figure 2) is in deep railroad cuts just northwest of France, Idaho. Here, as much as 7 meters of loess unit A overlies a buried soil developed in till and colluviated till and loess. The till was deposited by a large glacier originating in the Yellowstone-Teton area. We have not excavated and described this buried soil in detail, but it appears locally to have a calcic horizon about several tenths of a meter thick.

To the east of site 2, the loess cover thins on till that we believe is equivalent to the till at site 2. Where the loess cover is thin or absent, weathering rinds on basaltic stones in the till are about 0.9 millimeter thick, as compared with about 0.3 millimeter for rinds in the next younger till (Colman and Pierce, 1981, p. 50). Rind thicknesses on basalt stones in the West Yellowstone basin are about 0.8 millimeter in Bull Lake deposits and about 0.4 millimeter in Pinedale terminal moraines (Colman and Pierce, 1981, p. 44). Thus, both the loess-till stratigraphy and weathering rinds suggest a strong similarity between sites 1 and 2.

In the Teton Basin 8 kilometers northeast of Driggs, Idaho, loess thickly mantles moraines at the mouth of Teton Canyon (Figure 2, site 3). These moraines predate the last glaciation (Pinedale) but still retain constructional form, particularly along the bouldery lateral moraines high on the canyon walls just east of the mountain front. We agree with Edmund's (1951, Figure 7) assignment of these moraines to the Bull Lake Glaciation, although we would draw the Pinedale limit much farther down valley than he does. A combination backhoe and auger excavation, extending to a depth of 5.5 meters, exposed a well-developed buried soil beneath loess unit A. This site is relatively wet compared with the other sites, and loess unit A is leached of carbonate to a depth of 90 centimeters. At a depth of 1 to 2.6 meters in loess unit A, slightly reddened loess with a moderate, subangular, blocky structure indicates alteration, perhaps by weathering, as loess slowly accumulated on the land surface. The A horizon of the well-developed buried soil occurs at a depth of 2.6 meters. This soil and oxidized colluvium is more than 3 meters thick and is developed in loess unit B and in colluvium from the underlying Bull Lake moraines; this soil is clearly more developed than the surface soil.

Site 4 is on the outwash fan graded to the Bull Lake moraines of site 3. The loess and buried-soil sequence is similar at the two sites, although loess unit A at site 4 is thinner and the depth of leaching is less because site 4 is lower and drier. The Cca horizon of the surface soil extends down into the B horizon of the more developed buried soil, which is formed in both loess unit B and outwash of Bull Lake age (Figures 2 and 3). The calcic horizons of the buried soil include a calcic horizon with stage III development.

Site 5 is an exposure in the banks of the Blackfoot River about 20 kilometers north of Soda Springs, Idaho. At this site and additional sites to the north and east, a tephra zone with rhyolitic and basaltic pumice blocks overlain by light gray sandy pumice occurs in the lower part of loess unit A. At site 5, the tephra zone is 3.8 meters below the top of loess unit A and is 1 meter thick, containing pumice blocks as coarse as 5 centimeters. This dposit occurs 4 kilometers east of China Hat, a 275 meter high rhyolite dome of late Quaternary age. G. B. Dalrymple (written communication, 1982) obtained

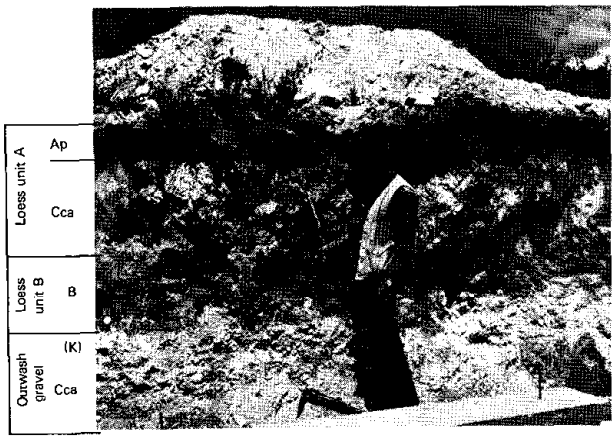

Figure 3. Loess mantling outwash gravels of Bull Lake age at loess section site 4, east of Driggs, Idaho. Cca horizon of surface soil (light-colored zone) in loess unit A overlies B horizon of buried soil developed in loess unit B. K horizon of buried soil cements outwash gravels.

a potassium-argon age of 61,000 ± 6,000 years on sanidine concentrate from a sample collected at China Hat by W. D. Leeman. At the base of the China Hat dome, rhyolitic tephra more than 8 meters thick is mantled by a mixture of pumaceous deposits and loess washed from China Hat, which in turn is overlain by the upper part of loess unit A in which the surface soil is developed. Two other rhyolite domes, Middle Cone and North Cone occur to the north of China Hat. The thickness of hydration rims on pumice from site 5 is 13.6 ± 1.3 micrometers (n =12), almost identical to the value of 13.5 ± 0.8 micrometers (n=15) determined for that on pumice from a pit at the base of China Hat, indicating that the potassium-argon date from China Hat also applies to the pumice unit at site 5.

At site 5, the surface soil has a B horizon 1 meter thick with well-developed prismatic structure, and the loess is leached of carbonate to a depth of 1.5 meters (Figure 2). This thick B horizon and deep leaching reflects the relatively high precipitation estimated to be about 50 centimeters at this site, and especially the extensive soil wetting accompanying the melting of a thick winter snowpack. The water content of the April 1 snowpack at a nearby site 100 meters higher averages 23 centimeters (Wilson and Carstens, 1975, p. 11), and local snows are deep as evidenced by a snowmobile racetrack located immediately across the Blackfoot River from site 5. At a depth of 3.25 meters, a buried soil with a B horizon about 30 centimeters thick occurs just above the China Hat tephra. Because this soil is definitely less developed than the surface soil, it does not represent the top of loess unit B, but rather a relatively minor soil in loess unit A that was formed probably not too long after the tephra was deposited.

Site 6 is on the northern flank of the Kettle Butte volcano about 30 kilometers northwest of Idaho Falls. This shield volcano is thickly mantled with loess on its northeastern, downwind side; but on the southwestern side, local outcrops of pressure ridges suggest to us an age not in excess of half a million years. At site 6, a weak soil is developed within loess unit A (Figure 2). This loess is about 2 meters thick and overlies a buried soil developed in loess unit B. The unweathered loess contains about 10-15 percent clay and 10-15 percent $CaCO_3$ equivalent. Compared with the surface soil, this buried soil is thicker, its B horizon contains 21 percent clay compared with 16 percent, and its calcic horizon is thicker and contains 58 percent $CaCO_3$ equivalent compared with 21 percent (Moody and others, 1979, site 77Ida1008). Loess unit B rests on the basalt of Kettle Butte. Based on regional studies, M. A. Kuntz (written communication, 1981) considers this basalt to be considerably younger than the basalt of Shattuck Butte, which is 15-20 kilometers to the east of Kettle Butte and is dated as 643,000 ± 57,000 years old (G. B. Dalrymple, written communication, 1980).

East of Blackfoot, R. E. McDole, M. A. Fosberg, and G. C. Lewis studied the loess and buried soils in backhoe pits and in hand-augered holes in the bottom of these pits. They named the upper loess (unit A) the Bannock Loess, and the first prominent buried soil the Fort Hall Geosol (McDole, 1969, McDole and others, 1973). Site 7 is about 300 meters above the Snake River and is plotted from the descriptions of McDole (1969, locality 0694). Unweathered loess at this site has about 7-11 percent clay and 15-18 percent $CaCO_3$ equivalent. The first buried soil (developed in loess unit B) is thicker and more developed than the surface soil, having 18 percent clay compared with 13 percent and 34 percent $CaCO_3$ equivalent compared with 23 percent (McDole, 1969, locality 0694, Tables 4 and 13). At this site, loess unit B rests on a well-expressed buried soil developed in an older loess (loess unit C?).

In the Pocatello area, the age of the upper part of loess unit A can be determined from deposits and scoured surfaces of the Bonneville Flood, which occurred between about 15,000 and 14,000 years ago (Scott and others, 1982 this volume). Site 8 (Figures 2 and 4) is on the surface of flood-scoured basalt of Portneuf Valley. Thin, discontinuous flood-gravel and broad depressions show that the basalt bench between Pocatello and Portneuf was scoured by the Bonneville Flood. As much as 1.5 meters of loess locally mantles this basalt (Figure 4), but more typically, loess thicknesses are 0 to 0.5 meter. At site 8, a typical Holocene soil is developed in the loess, indicating that it is loess unit A. In areas underlain

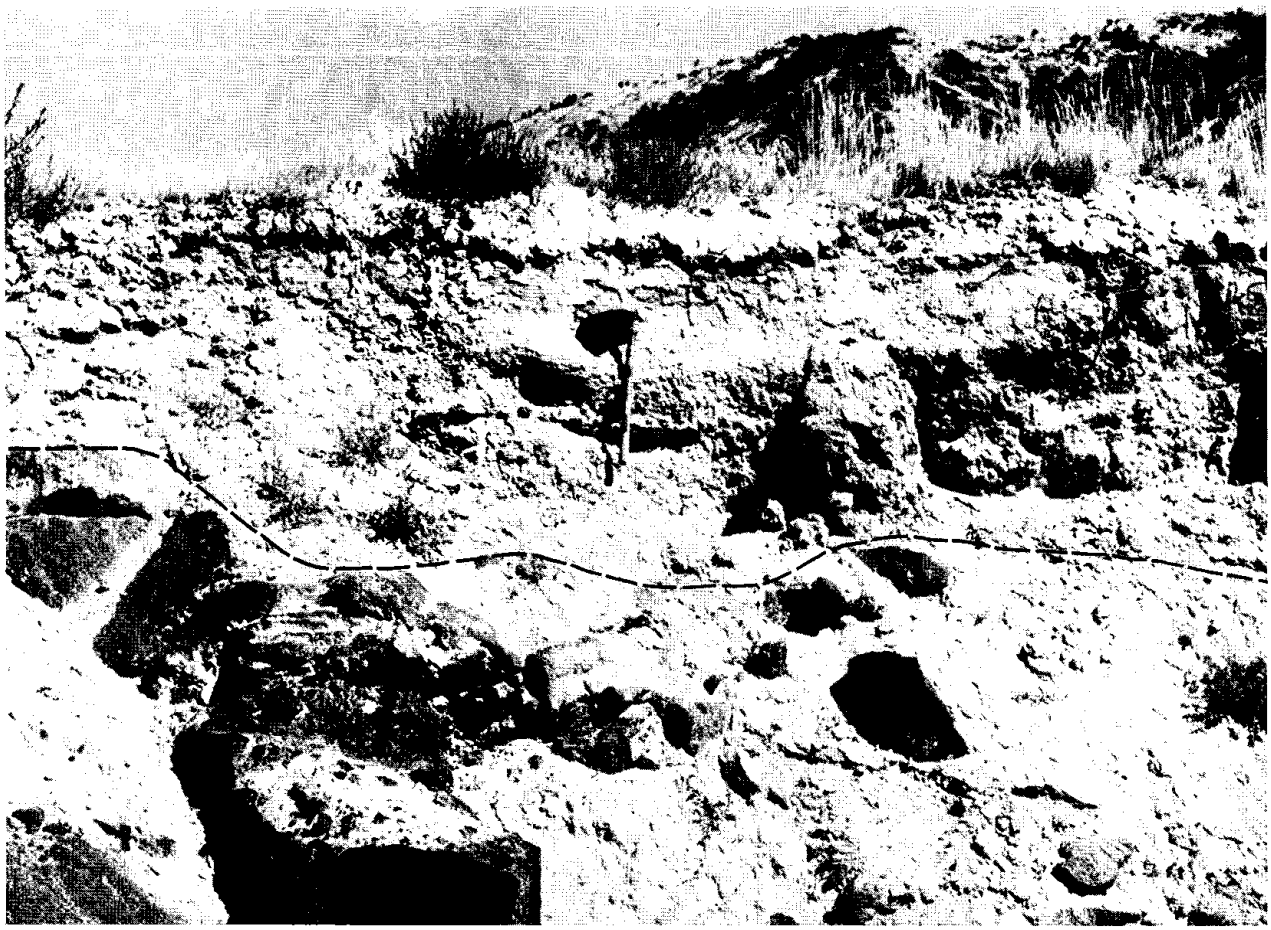

Figure 4. Loess at site 8 that accumulated on mid-Quaternary basalt after basalt was scoured by Bonneville Flood about 14,000-15,000 years ago. Loess above dashed line is about 1.5 meters thick, but loess thickness on this flood-scoured basalt and on Bonneville Flood deposits probably averages less than 30 centimeters. Exposure in roadcut along Interstate Highway 15, 0.4 kilometer northwest of Portneuf, Idaho. Entrenching tool in center of photograph is about 50 centimeters long.

by Bonneville Flood deposits or in areas scoured by the Bonneville Flood, loess unit A is roughly 10-20 percent of its full thickness in nearby localities above the level of the flood, indicating that the Bonneville Flood occurred near the end of deposition of loess unit A. The postflood loess may be disproportionately thick here relative to the interval of time during which it was deposited, because it probably accumulated quickly as sediment was deflated from flood deposits and flood devegetated areas.

The best radiometric-age control for the base of loess unit A is the potassium-argon age of the Cedar Butte Basalt, about 20 kilometers southwest of American Falls. This basalt is 72,000 ± 14,000 years old (G. B. Dalrymple, written communication, 1981; see Scott and others, 1982 this volume, for analytical results). At site 9 (Figure 2), the Cedar Butte Basalt is mantled by sandy loess 2 meters thick. This loess bears a Holocene surface soil typical for the local climate. The loess does not contain buried soils, but a zone of secondary carbonate was found on top of the basalt. No soil horizonation was observed in this caliche, and we consider it to be of vadose-water origin. Soils in this area are wetted primarily by winter and spring moisture, and drifting snow is probably important at this east-facing site. Soil water cannot move readily into the cracks in the underlying basalt until the loess is saturated to field capacity. In this semiarid area where the entire loess column would seldom exceed field capacity, most of the water is held in the loess. During the growing season, the last remaining soil water would tend to concentrate at the base of the loess. Plant roots, which are common in this zone, would withdraw water, leading to precipitation of carbonate at the base of the loess.

Site 10 (Figures 2 and 5) is one of several similar localities at the margin of the Snake River Plain in the northern Raft River valley. At these sites, one buried soil occurs in the loess succession mantling

Figure 5. Loess units A and B exposed in roadcut of Interstate Highway 86 at loess section site 10, Raft River valley, Idaho. The most clay-rich part of the B horizon of the buried soil in loess unit B occurs just above the small pit. Man in pit is sitting on top of basalt of Yale Road.

the basalt of Yale Road and the "basalt of the old railroad grade" (Williams and others, 1982 this volume). The southern part of the basalt of Yale Road is thickly mantled with loess, but the northern part is mostly blown free of loess and shows original flow-top topography. Based on our field experience, this basalt is not more than a few hundred thousand years old. Site 10 is in the dry, central part of the valley, just north of Interstate Highway 86 crossing the Raft River. The surface soil at site 10 is calcareous to the surface, displaying a weak cambic B horizon above a weakly developed Cca horizon about half a meter thick. The buried soil has stronger colors than the surface soil and contains the following features not present in the surface soil: a zone 0.5 meter thick leached of primary carbonate, an argillic B horizon with as much as 44 percent clay, and a siliceous duripan 0.5 meter thick. Roadcut exposures show that loess unit B is generally present only in topographic lows on top of the basalt of Yale Road, suggesting that the basalt was emplaced late in the time of deposition of loess unit B. The buried soil at site 10 formed in a topographic low where sediment rich in clay was washed from the adjacent slopes and soil moisture was enhanced. Thus, this buried soil shows more development than it would in a typical upland site. The basalt has not been radiometrically dated but is estimated on the basis of the two mantling loess units to be less than half the age of nearby basalt flows, dated between about 500,000 and 700,000 years old, which are mantled by at least four loess units (Williams and others, 1982 this volume).

Site 11 (Figure 2) is on the McKinney Basalt about halfway between Gooding and Bliss, Idaho. About 10 kilometers to the southwest adjacent to the Snake River canyon, the loess mantle is thick enough on the McKinney Basalt that nearly all of it can be farmed. North of this site toward the source of this basalt at McKinney Butte (Malde and Powers, 1972), original flow topography is well preserved, suggesting an age less than half a million years. The McKinney Basalt dammed the Snake River, forming a lake (Malde, 1982 this volume). Sediments are estimated to have accumulated in this lake for roughly 25,000 years (Malde, 1981, p. 35). The basalt dam impounding this lake was then breached and the Snake River canyon below Bliss was eroded (Malde, 1982 this volume), probably over a period of at least another 10,000 years prior to the time of the Bonneville Flood about 15,000 years ago (Scott and others, 1982 this volume). Thus the McKinney Basalt is probably about 50,000 years old.

At site 11, the loess is 2.5 meters thick. The surface soil is typical of a Holocene soil in this environment, having a leached B horizon 40 centimeters thick with 9-13 percent clay compared with 6-7 percent in the unweathered loess, and a Cca horizon 0.5 meter thick with 13-16 percent $CaCO_3$-equivalent compared with about 10 percent in the unweathered loess. No buried soil is present in or above the basalt at this site nor was any noted elsewhere on the McKinney Basalt, suggesting that the basalt was emplaced during the time of deposition of loess unit A.

DISCUSSION

A history of loess deposition separated by periods of nondeposition and soil development can be reconstructed from the present to more than 150,000 years ago.

During Holocene time (the last 10,000 years), loess deposition has been minimal, and the surface soil has developed in loess unit A. Little or no loess has accumulated on lava flows of Holocene age on the eastern Snake River Plain (Kuntz and others, 1982 this volume). The soil developed in loess unit A is comparable with that developed in latest Pleistocene deposits in similar climatic settings. For originally calcareous loess, this development ranges from weak profiles that are calcareous to the surface in areas with about 20 centimeters annual precipitation to profiles having argillic B horizons more than half a meter thick in areas with 50 centimeters annual precipitation (Figure 2). Calcic horizons of the surface soil are not cemented.

Based on soil development and stratigraphic relations to late Pleistocene pumice layers, glacial deposits, alluvium, and basalt flows, loess unit A

accumulated in late Pleistocene time. At site 8, local accumulations of loess unit A postdate the Bonneville Flood, which occurred about 14,000-15,000 years ago. At site 1, loess unit A is correlated in part with Pinedale moraines and outwash dated about 30,000 years old. At site 5, a coarse pumaceous tephra occurs in the lower part of loess unit A and is correlated with the emplacement of the nearby China Hat rhyolite dome, dated as 61,000 ± 6,000 years old. At site 9, the lower part of loess unit A rests on basalt 72,000 ± 14,000 years old. Thus, loess unit A appears, from the information available, to have accumulated between about 70,000 and 10,000 years ago. This interval corresponds approximately with the Wisconsin Glaciation of the midcontinental United States and with the Pinedale Glaciation of the Rocky Mountains, which is estimated to have spanned the interval between more than 40,000 and 11,000 years ago (Pierce and others, 1976).

Soils and darkened bands which may represent weak soils have been observed within loess unit A at sites 3, 5, and 6 and at other sections not described here. They represent interruptions in loess deposition or changes of rate in loess accumulation. At site 5, a buried soil that is much less developed than the surface soil occurs just above a tephra inferred to be about 60,000 years old (Figure 2). Thus, for an interval probably shorter than the Holocene (10,000 years), soil development interrupted deposition of loess unit A at some time probably much nearer 60,000 than 10,000 years ago. Additional stratigraphic studies are needed to identify and define such subdivisions of loess unit A.

Loess unit A locally overlies a buried soil developed in loess unit B. This buried soil is more developed than the post-Pleistocene surface soil, which formed in about 10,000 years. The buried soil in loess unit B is therefore estimated to have developed over several tens of thousands of years, perhaps as much as 50,000 years. Near West Yellowstone, silty sediment assigned to loess unit B overlies with apparent conformity glacial deposits assigned to the Bull Lake Glaciation and dated at about 140,000 to 150,000 years old. Loess at this site may have accumulated at the close of the Bull Lake Glaciation, so that the top of loess unit B might be only slightly younger than the glacial deposits of Bull Lake age.

At some sites where the loess is thick, the upper part of the first buried soil suggests that a soil complex is present, containing as many as three B-horizons stacked on top of each other. A soil complex is present at sites 3 and 10, as well as at other sites not described. Thus, in the time interval roughly estimated to be between about 70,000 and 130,000 years ago, thin, discontinuous deposits of loess or other fine-grained sediment may have locally accumulated on the landscape. Other areas were more stable, and soils continued to develop without interruption.

The age for the base of loess unit B is not well defined. At sites 1, 2, 3, 4, and 10, the substratum probably dates from late in the time of accumulation of loess unit B. The only dating is at site 1, where the underlying kame gravels of Bull Lake age are dated at 140,000 to 150,000 years old. A Bull Lake age for the age of the substratum at sites 2, 3, and 4 is inferred on the basis of glacial correlations. For the sections on the transect (Figure 2), the oldest part of loess unit B occurs at site 7 and probably also at site 6, but no dating is presently available.

Three of the loess sections described here are underlain by basalt flows that have not yet been radiometrically dated. The arguments made in this paper for the age of the loess can be reversed to provide estimates of the ages of the undated basalt flows. At site 6, the basalt of Kettle Butte is inferred to be somewhat older than 150,000 years, based on the similarity of the mantling loess succession with that in the West Yellowstone area. At site 10, the mantling loess sequence is quite similar to that in the West Yellowstone basin, suggesting an age of about 150,000 years for the basalt of Yale Road. And at site 11, the loess mantle is similar to that above the Cedar Butte Basalt, suggesting an age in the 50,000- to 70,000-year range for the McKinney Basalt.

Although unresolved problems remain concerning the possible desert origin of some of the loess in Idaho, the available information suggests that the bulk of the loess along the eastern Snake River Plain accumulated during glacial times and that the major sources were the flood plains of large streams and the active alluvial fans on and adjacent to the Snake River Plain (Pierce and Scott, 1982 this volume).

ACKNOWLEDGMENTS

We thank M. C. Reheis and V. S. Williams for helpful reviews of this report. The new potassium-argon age for the China Hat rhyolite dome, the Cedar Butte Basalt, basalt of Shattuck Butte, and older basalt at the mouth of the Raft River valley were determined by G. B. Dalrymple.

REFERENCES

Bright, R. C., 1967, Late Pleistocene stratigraphy in the Thatcher basin, southeastern Idaho: Tebiwa, v. 10, p. 1-7.

Colman, S. M. and K. L. Pierce, 1981, Weathering rinds on andesitic and basaltic stones as a Quaternary age indicator, western United States: U. S. Geological Survey Professional Paper 1210, 56 p.

Edmund, R. W., 1951, Structural geology and physiography of the northern end of the Teton Range, Wyoming: Augustana Library Publications, no. 23, 81 p.

Gile, L. H., F. F. Peterson, and R. B. Grossman, 1966, Morphological and genetic sequences of carbonate accumulation in desert soils: Soil Science, v. 101, p. 347-360.

Kuntz, M. A., D. E. Champion, E. C. Spiker, R. H. Lefebvre, and L. A. McBroome, 1982, The Great Rift and the evolution of the Craters of the Moon Lava Field, Idaho, *in* Bill Bonnichsen and R. M. Breckenridge, editors, Cenozoic Geology of Idaho: Idaho Bureau of Mines and Geology Bulletin 26.

Lewis, G. C. and M. A. Fosberg, 1982, Distribution and character of loess and loess soils in southeastern Idaho, *in* Bill Bonnichsen and R. M. Breckenridge, editors, Cenozoic Geology of Idaho: Idaho Bureau of Mines and Geology Bulletin 26.

Malde, H. E., 1982, The Yahoo Clay, a lacustrine unit impounded by the McKinney Basalt in the Snake River canyon near Bliss, Idaho, *in* Bill Bonnichsen and R. M. Breckenridge, editors, Cenozoic Geology of Idaho: Idaho Bureau of Mines and Geology Bulletin 26.

———, 1981, Geologic factors pertinent to the proposed A. J. Wiley Hydroelectric Project, No. 2845, Bliss, Idaho: U. S. Geological Survey Open-File Report 81-569, 75 p.

Malde, H. E. and H. A. Powers, 1972, Geologic map of the Glenns Ferry-Hagerman area, west-central Snake River Plain, Idaho: U. S. Geological Survey Miscellaneous Geologic Investigations Map I-696.

McDole, R. E., 1969, Loess deposits adjacent to the Snake River flood plain in the vicinity of Pocatello, Idaho: University of Idaho Ph.D. dissertation, 216 p.

McDole, R. E., G. C. Lewis, and M. A. Fosberg, 1973, Identification of paleosols and the Fort Hall Geosol in southeastern Idaho loess deposits: Soil Science Society of America, Proceedings, v. 37, p. 611-616.

Moody, U. L., M. A. Fosberg, A. L. Falen, and Wakefield Dort, 1979, Chemical, physical, and mineralogical analysis of soils and sediment at the Wasden site, southeast Idaho: Unpublished report submitted to the National Science Foundation, 64 p.

Pierce, K. L., 1979, History and dynamics of glaciation in the northern Yellowstone National Park area: U. S. Geological Survey Professional Paper 729-F, 90 p.

Pierce, K. L., J. D. Obradovich, and Irving Friedman, 1976, Obsidian hydration dating and correlation of Bull Lake and Pinedale Glaciations near West Yellowstone, Montana: Geological Society of America Bulletin, v. 87, p. 703-710.

Pierce, K. L. and W. E. Scott, 1982, Pleistocene episodes of alluvial-gravel deposition, southeastern Idaho, *in* Bill Bonnichsen and R. M. Breckenridge, editors, Cenozoic Geology of Idaho: Idaho Bureau of Mines and Geology Bulletin 26.

Richmond, G. M., 1973, Surficial geologic map of the Warm River Butte quadrangle, Yellowstone National Park and adjoining area, Idaho and Wyoming: U. S. Geological Survey Miscellaneous Geologic Investigations Map I-645.

Scott, W. E., K. L. Pierce, J. P. Bradbury, and R. M. Forester, 1982, Revised Quaternary stratigraphy and chronology in the American Falls area, southeastern Idaho, *in* Bill Bonnichsen and R. M. Breckenridge, editors, Cenozoic Geology of Idaho: Idaho Bureau of Mines and Geology Bulletin 26.

Thomas, C. A., H. C. Broon, and J. E. Cummans, 1963, Magnitude and frequency of floods in the United States, Part 13, Snake River basin: U. S. Geological Survey Water-Supply Paper 1688, 250 p.

Waldrop, H. A., 1975, Surficial geologic map of the West Yellowstone quadrangle, Yellowstone National Park and adjoining area, Wyoming, Idaho, and Montana: U. S. Geological Survey Miscellaneous Geologic Investigations Map I-648.

Williams, P. L., H. R. Covington, and K. L. Pierce, 1982, Cenozoic stratigraphy and tectonic evolution of the Raft River basin, Idaho, *in* Bill Bonnichsen and R. M. Breckenridge, editors, Cenozoic Geology of Idaho: Idaho Bureau of Mines and Geology Bulletin 26.

Wilson, J. A. and M. O. Carstens, 1975, Summary of snow survey measurements for Idaho (1921-1974): U. S. Soil Conservation Service, Boise, Idaho, 309 p.